

CONFERENCE PROCEEDINGS

METPLANT CONFERENCE

2023

CONFERENCE PROCEEDINGS SPONSOR



ADELAIDE, SOUTH AUSTRALIA
6 – 8 NOVEMBER 2023

www.metplant.com.au

METPLANT 2023

6 – 8 NOVEMBER 2023

ADELAIDE, AUSTRALIA

MetVal Consulting Pty Ltd

Publication No. 001



Published by:

MetVal Consulting Pty Ltd

8 Kaye Street, Fulham Gardens, SA, 5024

© MetVal Consulting Pty Ltd 2023

All rights reserved.

No part of this publication may be reproduced, stored in a retrieval system, or transmitted in any form by any means without permission in writing from the publisher.

All papers published in the volume were peer reviewed by independent reviewers before publication. The reviewing process followed was in accordance with most scientific journal guidelines and practices.

MetVal Consulting is not responsible as a body for the facts and opinions advanced in this publication.

ORGANISING COMMITTEE

Janine Herzig FTSE, FAusIMM (CP), GAICD / Convenor of MetPlant Conference Series

Dr. Shu Chen MAusIMM, GAICD

Tom Hilder MAusIMM

Aidan Giblett FAusIMM (CP)

Graham Arvidson MAusIMM (CP), MIEAust CPEng, GAICD

Neville Plint FAusIMM

Prof. Mohsen Yahyaei MAusIMM (CP)

Chris Sykes

PEER REVIEWERS

Marc Allen, Graham Arvidson, Duncan Bennett, Robert Braun, David Brimage, Shu Chen, Brian Cornish, Rodolfo Espinosa-Gomez, Aidan Giblett, Janine Herzig, Tom Hilder, Damien Krebs, Sai Wei Lam, Colin McCaughey, Joe Pease, Nick Redman, Chris Sykes & Mohsen Yahyaei

FOREWORD

MetPlant 2023, held for the first time in Adelaide, South Australia, from the 5th to 8th November, was the twelfth event in the series of conferences on Metallurgical Plant Design and Operating Strategies.

In 2023, we continued with the theme of 'World's Best Practice' that has been adopted since the beginning of the MetPlant series in 2002, presenting an update on the latest advances in metallurgical processing and plant design. Optimisation, improving processing efficiencies, case studies and design innovations continued to be popular themes and papers covered a diverse range of metallurgical unit operations and commodities. The 2023 event saw an increased focus on ESG as it relates to plant design and operation and many papers covering tailings and water management in addition to the traditional themes of comminution, hydrometallurgy and pyrometallurgy.

With the previous MetPlant Conference in 2019, the next event was originally due to be held in 2021. Following several delays and alternative scheduling due to the global pandemic and subsequent impacts on conference schedules, it was decided to move away from Perth, Western Australia and hold the 2023 event in Adelaide.

The two-stage "Call for Abstracts" resulted in more than 120 submissions, indicating that metallurgical plant design and operation remains highly relevant in the sector, within both operational and applied research fields. The criteria for acceptance of abstracts were once again very high, with around 50 abstracts initially accepted, including three keynotes. The final program featured 42 presentations, three keynote addresses and an interactive panel session.

The traditional two-day format was extended to three days in duration with a single Plenary throughout the conference per past delegate feedback.

From early in the abstract process through to the final deadlines for paper submission, it has been encouraging to have received positive responses from authors to the peer review feedback. The peer review process is essential to the MetPlant Conference framework and underpins the high quality and relevance of the event. I thank all those professionals who assisted in the peer reviewing throughout 2022 and 2023.

This year saw a record number of partners, sponsors, exhibitors, authors, and delegates all wishing to participate in MetPlant 2023. The exhibition area in 2023 was considerably larger than any in the event's history and the additional professional development events and networking functions were all extremely well attended with both the Magotteaux-sponsored Breakfast and Solvay-sponsored Conference Dinner completely sold out.

There were more than 400 Delegates from 30 different countries in attendance, which exceeded all expectations.

Bespoke, tailored partner packages were carefully negotiated resulting in several new partnering arrangements that suit the differing needs of our supporting companies. Principal Sponsor since 2002, Metso (previously Metso:Outotec) were back on board in 2023 and once again the Innovation Award was judged and presented with the support of our Innovation Partner RME Global.

It was an outstanding conference and these proceedings (and the conference recordings) really convey a snapshot of the current world's best practice, and one which will have ongoing relevance in the future and provide valuable insights to those professionals engaged in the design, specification and operation of metallurgical plants.

I thank the Proceedings Sponsor Magotteaux for their continuing support of this important resource.

I also thank the Organising Committee as well as all those who contributed abstracts, papers, posters, and presentations. Also, the reviewers, session chairs, partners, sponsors, exhibitors and, importantly, all the delegates who ensured this was the most successful event yet in terms of the exchange of ideas, experiences, and information.

Special thanks go to the CCM Team for their administrative and professional support over the past two years. Their expertise and insights were very important to the success of MetPlant 2023.

I hope you will enjoy reading these proceedings and referring back to them over time.

And I hope to see you all again in 2025 for the next instalment of the MetPlant Conference!

Janine Herzig FTSE, FAusIMM (CP) Met

MetPlant Conference Convenor

30 November 2023

SPONSORS

Innovation Partner



Principal Sponsor

Metso

Platinum Sponsor

The logo for MolyCOP consists of the word 'MOLY' in red and 'COP' in grey, with a stylized orange and grey circular graphic element between the 'Y' and 'C'.

Conference App & Gold Sponsor



Gold Sponsor



Silver Sponsor



Conference Dinner



Welcome Reception Sponsor



Breakfast Sponsor & Conference Proceedings



Coffee Cart



SPONSORS (continued)

Name Tag & Lanyards



Pre-Dinner Networking Drinks



Breakfast Sponsor



Skills Sponsor



Note Pads & Pens



Media



Session Sponsors



EXHIBITORS



The only global supplier

Cast, forged & ceramic
grinding media, mill liners
and smart tools & equipments

Maximize the recovery of valuable minerals at saleable concentrate grade with the lowest total cost of ownership & environmental impact

Low to High Chrome balls,
Forged balls, Ceramic beads

Mill liner design and supply

Unique access to Magotteaux network of experts

Deep understanding of your process to help you reduce cost and maximise revenues while lowering your environmental footprint

Mill control solutions to boost your concentrator performance: **MagoSense**, **MagoLoad**, **MagoPulp**

Laboratory equipment to support process optimization: **MagoMill** & **MagoFloat**



Grinding media
cast & forged
25 mm to 152 mm



Grinding media
& ceramic beads
0,5 mm - 60 mm



Mill liners



Smart tools
& equipments



Process optimization services and products
for abrasive and impact applications

CONTENTS

Keynote Presentations

Using a Process Digital Twin to Comply with New Sustainability Reporting Rules for Australia's Resources Sector <i>J Vagenas</i>	18
Geometallurgy - When Should Deposit Characterisation Commence? <i>K Ehrig, V Liebezeit, Y Li, B Pewkliang, E Macmillan, M Smith and S Slabbert</i>	48
We Need to Talk About Engineering <i>J Pease</i>	49

Session Papers

Case Studies and Plant Modifications I

Design and Commissioning of the Newmont Ahafo Mill Expansion <i>E Asakpo and A Giblett</i>	62
Maximising Concentrator 1 Throughput at Cadia during the SAG 20MW Gearless Motor Drive Replacement <i>C Geoghegan and C Haines</i>	70

Flotation Technology

Design of Coarse Particle Flotation Circuits for Copper Projects <i>M Pyle, G Ballantyne, G Williams, G Lane and J Concha</i>	86
Pinto Valley Mine, Copper Recovery Study with the NovaCell <i>S Morgan, P Amelunxen, B Akerstrom and L Cooper</i>	101
Concorde Cell Technology Retrofit Effect on an Existing Self-Aspirated Flotation Cell <i>M Ball, N Kupka, G Bermudez and A Yáñez</i>	116
Replacement of Sodium Ethyl Xanthate Collector at Carrapateena	124

<i>J Reinhold, S Assmann, E Brodie, J Van Sliedregt, F Burns, G Tsatouhas and J Seppelt</i>	
Application of Depressant in Copper-Nickel Separation at IGO's Nova Mine <i>A White, J Fryman, P Kittler, P Hudson, S Szabo and I Ametov</i>	135

Pyrometallurgy & Plant Trials

Flash Furnace Throat Accretion Management through Post-Combustion Oxygen Injection <i>M O'Sullivan, H Kim and K Pereira</i>	148
Carbon Inventory Management in a Carbon-In-Leach Circuit <i>O Kopa and A Paine</i>	165
Sequential t-testing in Plant Trials – A Faster Way to the Answer <i>T G Vizcarra, T J Napier-Munn and D Felipe</i>	174
Representative Measurement Using PGNAA to Digitalise Conveyed Ore Flow Quality <i>H Kurth, A Brodie, and Y Strutz</i>	187
On-line Digital Twin for Processing Plant Optimisation <i>J Moilanen, A Remes and A Grigoryan</i>	196

Mineralogy & Recovery

Mineralogy, Chemistry and Recovery: The New Century Story – Venturing into Extremes <i>P Waterhouse, C J Greet, P D Munro and D W Bennett</i>	207
Metallurgists and Modifying Factors: How Mets Can Change the World! <i>G Deans</i>	231

Case Studies and Plant Modifications II

VRM Technology: A Pragmatic Approach to Project Risk Versus Reward <i>D. Novak, D. Wall and A. Vasileff</i>	242
Implementing Sequential Flotation at Golden Grove Copper-Lead-Zinc Concentrator <i>K Tiedemann, B Rego and D Clarke</i>	256
Plant Modifications and Operating Strategies to Improve Concentrate Quality at BHP - Carrapateena <i>J Reinhold, F Burns and J Seppelt</i>	267
Converting from Single Stage to Series Ball Milling at the Newmont Tanami Operation	290

<i>A Giblett, S Hart, S Davies and A Cranley</i>	
Expansion of Mandalay Costerfield's Flotation Circuit <i>J Carpenter, H Thanasekaran, S Eibl, P Omizzolo and A Herman</i>	303
Integrated Flow Sheet Development for a Copper Operation in Central Chile <i>M Hasan, E Amini, M Maquieira, N Beaton and C Heck</i>	312

Tailings, Water & Energy Management II

Energy Savings and Carbon Footprint Reduction - Jameson Vs Conventional Copper Concentrator <i>C Anderson, G Csicsovszki, S Crane and G Ballantyne</i>	326
The Intersection of Mining and Decarbonisation: Challenges and Opportunities <i>C Meinke, R Chandramohan, K Erwin and O Olvera</i>	337
One Plant's Trash is Another Plant's Treasure; a Synergistic Approach to Novel Uses for Tailings Streams <i>R O'Donnell and J Begelhole</i>	364
First Principles Modelling of Mine Wastewater Treatment <i>K Heppner</i>	382
Optimised Process Performance Through the Modernisation of an Existing Thickener with Recent Innovations in Technology <i>A McIntosh, D Hodsdon, E Jarvie and S El-Masry</i>	404

Comminution Strategies

Fine Grinding Circuit for Magnetite Concentrators <i>S Palaniandy and H Ishikawa</i>	433
Benefits of Upgrading an HPGR with Flanged Roll Design and Advanced Mechanical Skew Control <i>J Bublitz, N Mayfield, N Elkin and B Knorr</i>	453
Improving Energy Efficiency and Reducing Carbon Footprint at the FMR Greenfields Mill Operation <i>S Latchireddi, R Latchireddi, P Fallon, B Tully, and B Hooper</i>	469
Commercialisation Pathway for Low Energy Gyratory Rolls Crusher Technology <i>M Drechsler and W Skinner</i>	486
SAG Mill Stability and Control Improvements at the Nova Nickel-Copper Operation <i>G Gomes-Sebastião and P Hudson</i>	499

Innovation & Engineering

The Future of Hybrid Lining for Large Diameter AG/SAG and Ball Mills <i>S Yaver Imam, J Bustamante, V Grover, S Abhishek, and M Sherman</i>	519
Designing Grinding Plants to Maximise Mill Availability During Relining <i>J Bohorquez, J Hodges, S Gwynn-Jones and P Van Rooyen</i>	537

Thickening and Filtration

Unlocking Increased Paste Production at Prominent Hill through Debottlenecking of the Belt Filter <i>N Curtis, O Whatnall, S Wilson, J Sum and C Samuel</i>	559
Concentrate Filter Cake Washing for Chloride Removal at Carrapateena <i>R Jones, J Reinhold, K Affleck and F Burns</i>	566
Pumping for Profit <i>R Doyle</i>	580
Slurry Pump Safety Considerations in Mineral Processing Plants <i>A Varghese, S Martins, E Lessing, G Hassan and A Karrech</i>	590
Filtered Tailings – a Copper Experience. <i>L. Vimercati and R. Williams</i>	608

Gold Processing

Real-Time Monitoring and Control of Gold Processing Plants <i>N Grigg, M Ntombela, B Wraith and A Lewis-Gray</i>	618
Ravenswood Gold Mine Expansion from 3.2 to 12 Mt/y <i>G Ballantyne, M Pyle, G Lane, A Lawry, V Jayawardana, D Jeffery, J Marx, T Mitchell and E McLean</i>	630
Evaluation of High-Shear Leach Reactor at IMK Gold Mine <i>D Prananta, A Dhayanto, W Padmonobo, R Schultz, S Flatman and M Battersby</i>	643
Refractory Gold Concentrate Treatment Hub for Toll Treating <i>L. McDonnell, R. McKechnie, K. Roche, P. Bullock and S. Nikolic</i>	668
Application of Stirred Milling in the Expansion of Martabe Gold Mine <i>M Liu, R Tanio, J Herrin and B Neilson</i>	677

AWARDS

RME / MetPlant 2023 Innovation Award Recipients

Mineralogy, Chemistry and Recovery: The New Century Story – Venturing into Extremes <i>P Waterhouse, C J Greet, P D Munro and D W Bennett</i>	207
---	-----

RME / MetPlant 2023 Innovation Award Highly Commended Recipients

The Future of Hybrid Lining for Large Diameter AG/SAG and Ball Mills <i>S Yaver Imam, J Bustamante, V Grover, S Abhishek, and M Sherman</i>	519
---	-----

MetPlant 2023 Best Paper

Maximising Concentrator 1 Throughput at Cadia during the SAG 20MW Gearless Motor Drive Replacement <i>C Geoghegan and C Haines</i>	70
--	----

MetPlant 2023 Best Paper – Runner Up

Slurry Pump Safety Considerations in Mineral Processing Plants <i>A Varghese, S Martins, E Lessing, G Hassan and A Karrech</i>	590
--	-----

MetPlant 2023 Best Presentation

Sequential t-testing in Plant Trials – A Faster Way to the Answer <i>T G Vizcarra</i>	174
---	-----

MetPlant 2023 Best Presentation – Runner Up

Flash Furnace Throat Accretion Management through Post-Combustion Oxygen Injection <i>M O'Sullivan and H Kim</i>	148
--	-----

MetPlant 2023 People's Choice – Best Presentation

<p>Maximising Concentrator 1 Throughput at Cadia during the SAG 20MW Gearless Motor Drive Replacement <i>C Geoghegan</i></p>	70
---	----

MetPlant 2023 People's Choice – Best Presentation – Runner Up

<p>Sequential t-testing in Plant Trials – A Faster Way to the Answer <i>T G Vizcarra</i></p>	174
---	-----

MetPlant 2023 Best Poster – Dual Winners

<p>CLEMENT LARTEY Developing A Flotation Predictive Model Using Pulp Chemistry Sensor Data</p> <p>RICHMOND ASAMOAH Knowing Your Pulp Chemistry Variables Improves Your Ability To Predict Copper Flotation Recovery</p>

JUDGES

Duncan Bennett, Brian Cornish, Janine Herzig, Tatiana Khmeleva, Suzanne Munro, Joe Pease, Neville Plint, Zeljka Pokrajcic, Laurie Reemeyer, John Russell, Ruth Shaw, Simon Thompson (& Delegates at the Conference for People's Choice).

PAPERS

Using a Process Digital Twin to Comply with New Sustainability Reporting Rules for Australia's Resources Sector

Presented as Keynote titled *'It is All in Scope'* at the MetPlant 2023 Conference

J Vagenas¹

1. Managing Director, Metallurgical Systems, Suite 2/101 Chalmers St, Surry Hills NSW 2010, john@metallurgicalsystems.com

ABSTRACT

Globally and in Australia, legislators, shareholders, investors, employees, and market sentiment have aligned to demand sustainability reporting transparency, particularly for energy-intensive industries like the minerals and resources sector.

Driven by the International Sustainability Standards Board (ISSB), leading European Union (EU) bodies, the U.S. Securities and Exchange Commission (SEC), and the Safeguard Mechanism in Australia, new standards will require disclosures on sustainability indicators such as greenhouse gas (GHG) emissions across Scopes 1, 2 and 3, water, energy, air quality, waste, hazardous materials, pollutants, nature-related risk factors, Product Carbon Footprint (PCF), Life Cycle Assessment (LCA) and Task Force on Climate-Related Financial Disclosures (TNFD) impacts.

The need for periodic reporting in a machine-readable digital taxonomy, scenario analysis and forward-looking statements means that data-driven technology is the only solution to meet evolving compliance standards. Manual spreadsheets simply cannot capture or process the volumes of data needed to deliver immutable, unalterable, and auditable sustainability reports.

This keynote paper explains how to leverage machine learning technology to centralise asset-wide industrial data, dynamically simulate an organisation's operations as a process digital twin, perform an asset-wide mass and energy balance, and deliver granular, finance-grade reports across sustainability indicators. It also explains how metallurgical accounting, production accounting and sustainability reporting go hand in hand for the mining and minerals industry.

Sustainability reporting is rapidly elevating to be on equal footing with financial reporting in terms of accountability and priority. The Australian Securities and Investments Commission (ASIC) is already [cracking down on greenwashing in its May 2023 report](#) with substantial civil penalties, shareholder activists demanding action by boards, and share prices and capital markets hinging on environment, social and governance (ESG) credit ratings.

Now, therefore, is the time to act, with only a short runway to prepare before new regulations take effect.

INTRODUCTION

As the world strives towards net zero, energy-intensive industries are under increasing pressure to accurately measure, report on and reduce their impact.

For the first time in Australia and across the world, legislators, shareholders, investors, employees and market sentiment have aligned to demand sustainability reporting transparency, particularly for energy-intensive industries. Businesses, consumers, staff, partners and governments are responding to this by switching to more sustainable products and services.

This new environment directly impacts the role and decisions of boards, company directors, executives, governance and risk management professionals, metallurgists, operations managers and all senior professionals in the minerals and resources sector.

To assist with an appropriate response, this paper explains

- the immediate frameworks impacting the Australian resources sector
- key sustainability indicators to measure, track and disclose
- the crucial link between metallurgical accounting, process optimisation, and sustainability reporting
- how modern digital tools enable organisations to make these disclosures accurately and at a reasonable level of assurance.

WHAT ARE THE NEW SUSTAINABILITY REPORTING RULES FOR THE AUSTRALIAN RESOURCES SECTOR?

As the Australian Government responds in line with international guidelines and regulations, a strict new era of legislated sustainability reporting and accountability will apply from 2024.

Here, the author looks at the primary international standards, starting with Australia's Commonwealth Treasury consultation paper, which is the industry's most pressing sustainability reporting change.

Commonwealth Treasury Consultation Paper

The recent Commonwealth Treasury Consultation Paper on Climate Reporting proposes to adopt ISSB standards in the 2024/2025 financial year. Large Australian companies and financial institutions will face mandatory climate-related reporting requiring limited assurance at first, with the view to broaden the scope over three years to include smaller organisations, building to a required reasonable level of assurance. Well beyond qualitative metrics, this would require granular quantitative metrics and reporting on sustainability and climate-specific indicators including GHG emissions across all scopes, climate resilience scenario analysis, climate targets and forward-looking statements to a level of detail not found in current Australian reporting practices.

The International Sustainability Standards Board (ISSB)

On 26 June 2023, The ISSB issued two international standards for investor-focused sustainability reporting. **IFRS S1** – being General Requirements for the Disclosure of Sustainability-related Financial Information, and **IFRS S2** – covering climate related disclosures. Their intention is to create a global baseline for sustainability-related financial disclosures. Both standards are based on the four pillars used in the TCFD framework; governance, strategy, risk management and sustainability-related metrics and targets - referred to in the standards as the 'core content'. The two standards are designed to disclose decision-useful information to capital markets and securities regulators and require information about all **material** sustainability-related and climate-related risks and opportunities that could reasonably affect the cash flow of an entity, access to finance and the cost of capital.

What is declared as **material** aligns with the International Accounting Standards Board (IASB) [definition](#) stating: *"Information is material if omitting, misstating or obscuring it could be reasonably be expected to influence the decisions that the primary users of general purpose financial statements, which provide financial information about a specific reporting entity."*

It is now for each jurisdiction to decide if and how they will incorporate these standards into national law or for companies to adopt the ISSB standards voluntarily.

Table 1 Summary of the IFRS Foundation Standard - IFRS S1 and IFRS S2

IFRS Standards -reporting across four 'core content' areas; governance, strategy, risk management and metrics and targets	
<p>IFRS S1: General Sustainability Disclosures (overarching principles)</p> <p>Reference: IFRS Foundation (IFRS S1)</p>	<p>IFRS S2: Climate Related Disclosures</p> <p>Themed/topic specific disclosures – Climate related</p> <p>Reference: IFRS Foundation (IFRS S2)</p>
<p>Objective of IFRS S1</p> <p>Entity needs to understand the resources it relies on and relationships along its value chain – resources and relationships are a source of value for the entity.</p> <p>A reporting entity's first step to determine what information to include in its sustainability report is an analysis to identify sustainability-related risks and opportunities.</p> <p>The second step is to consider which sustainability-related risks and opportunities are material to disclose and information that faithfully represents a sustainability-related risk or opportunity that would be relevant to the decision-making needs of the entity's primary users.</p> <p>An entity shall refer to and consider the applicability of the metrics included within the disclosure topics of the SASB standards.</p> <p>The definition of material is as per IFRS definition of materiality, meaning if omitting, misstating, or obscuring that information could reasonably be expected to influence decisions that the primary users (existing and potential investors, creditors and lenders) make based on that information.</p>	<p>Objective of IFRS S2</p> <p>The entity is required to reveal details regarding its exposure to major climate-related risks and opportunities. This will enable users of general-purpose financial reports (GPFR) to evaluate how these risks and opportunities affect the entity's financial position, performance, and cash flows, as well as its enterprise value, strategy, and business model.</p> <p>An entity must also consider the applicability of the industry-based disclosures outlined in the "Industry-Based Guidance on Implementing IFRS S2", which is based on the climate-related disclosures in the SASB standards.</p>
<p>Overview</p> <p>It is required for entities to disclose all significant information regarding sustainability-related risks and opportunities that come about from their reliance on resources and relationships. These may impact an organisation's access to cash flow, finance, or cost of capital in the short or long term.</p> <p>Examples of such risks and opportunities include their employment practices and those of its suppliers, product packaging waste, potential supply chain disruptions, control over assets such as production facilities that rely</p>	<p>Overview</p> <p>IFRS S2 identifies two types of climate-related risk:</p> <p>Physical risks:</p> <p>the physical risks from climate change, e.g., direct damage to assets, indirect effects of supply-chain disruption, changes in water availability, sourcing and quality of resources, extreme temperature changes affecting physical assets/operations/supply chain/transportation and employee safety.</p>

<p>on scarce resources, control over investments including those in associates and joint ventures, and sources of financing.</p> <p>Financial data and sustainability data need to be aligned: An entity must use the same financial data for its sustainability reporting as is used for financial reporting (to the extent that it is possible).</p> <p>For example, a resources company uses the number of units of a product it expects to produce when preparing a scenario analysis for a sustainability report. The same number of units of product should be used for financial reporting purposes.</p>	<p>Transition risks:</p> <p>risks associated with moving to a lower-carbon economy, e.g., policy, legal, technology, market and reputational risks that may carry financial implications for an entity, such as operating costs or asset impairment due to new climate-related regulations or by shifting customer demands and the development and deployment of new technology.</p> <p>The climate-related opportunities available to the entity are also in scope.</p>
<p>Core Content</p> <p>Governance: entity’s governance controls, processes, and procedures.</p> <p>Strategy:</p> <p>Organisations need to consider the risks and opportunities around sustainability that may impact their future prospects. This includes detailing their potential financial impact on their business model and value chain, and assessing how these factors may affect their strategy, decision making, financial performance and cash flows. This should be taken into account in the entity's financial planning. Additionally, this information should be disclosed to primary users to help them understand how resilient the entity's strategy and business model is in terms of sustainability risks.</p> <p>Risk management processes:</p> <p>Organisations need to be clear on how they identify, measure and prioritise sustainability risks. This includes detailing elements such as the criteria used, data sources, scope of operations covered, scenario analysis, process changes from the previous year, and how the risks are evaluated in terms of their characteristics, magnitude and probability.</p> <p>Progress metrics and targets:</p> <p>Organisations need to ensure that primary users can understand their performance regarding sustainability-related risks and opportunities. To do this they need to disclose specific industry-based metrics that demonstrate progress towards regulated targets including, milestones, interim targets, and an analysis of trends or changes.</p>	<p>Core Content</p> <p>Governance: align with IFRS S1 focused on climate.</p> <p>Strategy:</p> <ul style="list-style-type: none"> - qualitative and quantitative information for managing climate-related risks and opportunities - information on how the entity plans to achieve climate-related targets - disclose key assumptions on climate transition plans - disclose information that enables primary users to understand the resilience of the entity’s strategy and business model to climate-related changes, developments or uncertainties - climate-related scenario analysis – evaluation of climate-related risks and opportunities using various ‘what-if’ scenarios– similar to the TCFD framework - assessment of the entity’s climate resilience. - the disclosure of the scenario analysis outcomes is equally important as the disclosure of how the entity has carried out its climate-related scenario analysis. <p>Risk management:</p> <p>align with IFRS S1 focused on climate.</p> <p>Progress metrics and Targets:</p> <p>Disclosures on how an entity uses metrics and targets to measure, monitor and manage identified climate-related risks and opportunities.</p>

	<p>This includes cross-industry metrics, industry-based metrics, metrics and targets set by the entity and any targets required by law or regulation.</p> <p>Cross industry metrics – qualitative and quantitative:</p> <ol style="list-style-type: none"> 1. GHG emissions (absolute), Scope 1, 2 and 3 measured per the GHG Protocol Corporate Standard (2004) expressed as metric tonnes of CO₂ equivalent – at the parent and subsidiary/facility level for Scope 1 & 2 2. climate-related transition risks – the amount and percentage of assets or business activities vulnerable to climate-related transition risks 3. climate-related physical risks – the amount and percentage of assets or business activities vulnerable to climate-related physical risks 4. climate-related opportunities – the amount and percentage of assets or business activities aligned with climate-related opportunities 5. capital deployment – the amount of capital expenditure, financing or investment deployed towards climate-related risks and opportunities 6. internal carbon prices – the entity shall disclose how it applies a carbon price in decision-making and the price for each metric tonne of GHG emissions to access the costs of its GHG emissions 7. remuneration – disclosures on whether and how climate-related considerations are factored into executive remuneration and the percentage of executive management linked to climate-related considerations. <p>Industry-based metrics:</p> <p>In determining the industry-based metrics that the entity discloses, the entity is to refer to the “Industry-based Guidance on Implementing IFRS S2”.</p> <p>For Metals and Mining, refer to the IFRS S2 Climate-related Disclosures Appendix B Industry-based disclosure requirements, Volume B10 – Metals & Mining.</p> <p>Targets:</p> <p>An entity is required to disclose quantitative and qualitative climate-related targets it has set. For each target, the entity is to disclose:</p> <ul style="list-style-type: none"> - the metrics and approach used to set and review the target - the target objective
--	--

	<ul style="list-style-type: none"> - target application – part of the entity, specific business unit, or specific geographical region - the target period - the base period used to measure the progress of the target - absolute or intensity-based target - how the most recent agreement on climate change has informed the target. <p>Other GHG emission targets disclosures:</p> <ul style="list-style-type: none"> - whether Scope 1, 2 or 3 GHG emissions are covered by the target - gross or net GHG emissions target - if the target was informed by a sector specific decarbonisation approach - the planned use of carbon credits to offset GHG emissions – nature or technological carbon removal, the third party that will verify the credit, and other information for primary users to understand the integrity of the carbon credit.
--	---

These two standards are designed to be applied together and alongside future industry-specific standards. In time, a full suite of topic-specific IFRS Sustainability Disclosure Standards will be released, including disclosures around human capital, biodiversity, and other nature-related risk factors.

Currently, efforts are being made to establish a universal standard for ensuring sustainability-related disclosures, with ongoing work by the International Accounting and Assurance Standards Board to create ISSA 5000 as the worldwide benchmark for providing assurance on sustainability disclosures.

Although there is a high demand for a single global standard, the United States and the European Union are separately developing climate reporting systems. The ISSB has collaborated with officials from the US, Europe, Japan, and China, as well as the International Organisation of Securities Commissions (IOSCO), which includes 35 securities regulators from over 140 jurisdictions, to establish compatibility. However, there may still be some gaps. IOSCO announced on 25th July 2023 its endorsement of the ISSB standards following its comprehensive review and rapid adoption is expected in several jurisdictions.

EU's Corporate Sustainability Reporting Directive (CSRD)

The European Parliament and Council has gone even further than the ISSB. [The European Council](#) has legislated the CSRD from January 2023 and EU member states have until July 2023 to incorporate its provisions into national law. Several member states have started to transpose the CSRD into national law. The CSRD requires companies to make extensive disclosures about sustainability performance and related strategic implications. Disclosures are prescribed by the European Sustainability Reporting Standards (ESRS). In July 2023 the [European Commission](#) published the final text of its first set of ESRSs. Disclosures for some companies will be required as early as the 2024 reporting period.

How does the CSRD affect Australian resources companies?

The scope provisions of the CSRD are broad and apply to many companies operating in the EU, estimated to be nearly 50 000 in total. To assess if an Australian resources company falls within the scope of the CSRD will be complex and needs to be considered according to the EU Member State national law once the state has incorporated the CSRD.

Generally speaking, it will cover:

- Australian resources companies with securities listed on an EU-regulated market (with limited exceptions)
- Australian resources companies (listed or not) with annual EU revenues exceeding €150 million and an EU branch with net turnover of more than €40 million
- Australian resource companies with annual EU revenues exceeding €150 million and an EU subsidiary that is a large company, meeting two of the three criteria: more than 250 EU-based employees, a balance sheet above €20 million or a local revenue of more than €40 million.

Australian resources companies without direct reporting obligations under the CSRD may be asked for information by customers, suppliers, investors, or lenders because of the requirements for other entities that fall within the scope of the CSRD and are required to disclose information about their value chain, or because they are subsidiaries of EU companies with reporting obligations.

Table 2 What do in-scope Australian resource companies need to disclose?

<p>Twelve standards – reporting across four areas: (i) Governance, (ii) Strategy, (iii) Impact, risk and opportunity management and (iv) Metrics and targets</p> <p>Reference: European sustainability reporting standards – first set</p>	
<p>Two ESRS cross-cutting standards</p>	<p>Ten ESRS topic-specific standards (subject to materiality assessments)</p>
<p>ESRS 1: General requirements – double materiality concept – information that is material from either a financial perspective or an impact perspective.</p> <p>ESRS 2: General disclosures – mandatory disclosures, not subject to materiality assessments</p>	<p>Environmental</p> <p>E1: Climate change</p> <p>E2: Pollution</p> <p>E3: Water and marine resources</p> <p>E4: Biodiversity and ecosystems</p> <p>E5: Resource use and circular economy</p> <p>Social</p> <p>S1: Own workforce</p> <p>S2: Workers in the value chain</p> <p>S3: Affected communities</p> <p>S4: Consumers and end-users</p> <p>Governance</p> <p>G1: Business Conduct</p>

For future release – Sector-specific ESRs are yet to be drafted at the time of writing this paper.

The ESRs are designed to support the EU Green Deal and to align with existing sustainability frameworks in the EU such as Sustainable Finance Disclosures Regulation (SFDR) and EU Taxonomy.

The Carbon Border Adjustment Mechanism (CBAM)

In April 2023, the CBAM was introduced as part of the European Green Deal, which means EU importers of goods covered in the scope of CBAM regulation will be required to submit quarterly reports of embedded emissions within these goods to the European commission.

From October 2023, EU-impacted organisations will be expected to comply with reporting requirements across Scopes 1, 2 and 3 of emissions reporting, in advance of the full EU CBAM rollout in 2027.

CBAM goes further than reporting on an organisation's direct emissions (Scope 1), requiring measurement, and reporting on indirect electricity and other indirect emissions (Scopes 2 and 3). With Scope 3 emissions a significant contributor to energy-intensive industries, it is critical that industrial organisations have the capability to accurately calculate their indirect emissions.

CBAM and the Australian resources sector

The Australian Government's [Safeguard Mechanism Reforms Position Paper](#) in January 2023 stated that it is currently considering the option of implementing a system similar to the EU CBAM, which would allow them to levy tariffs on imported goods that are carbon-intensive such as the resource sector.

“Many stakeholders raised the issue of carbon leakage and identified a carbon border adjustment mechanism (CBAM) as their preferred approach for managing trade competitiveness impacts. Some of Australia's trading partners have proposed introducing CBAMs to help ensure trade competitiveness does not compete with decarbonisation objectives.”

“Recognising the strong stakeholder interest in the potential use of an Australian CBAM, the Government will undertake a review to explore policy options to further address carbon leakage. The review will consider CBAMs as one of the potential responses to carbon leakage that could complement Safeguard Mechanism reforms and will take into account the interests of our key trading partners.”

This was supported in August 2023 with Climate Change Minister Chris Bowen announcing that [Australia could impose a carbon border adjustment mechanism](#), as reported in the Australian Financial Review.

“The right policy settings are important to ensure a level playing field for Australian firms doing the right thing when it comes to decarbonisation. The decarbonisation task is most acute for large industrial facilities, frequently in hard-to-abate sectors and subject to competition in international markets,” he said.

An [analysis by Refinitiv](#) reported that non-EU businesses, like Australian resources companies, that operate in jurisdictions that have adopted ISSB, EU and US Securities and Exchange Commission (SEC) standards will need to be able to track, report and comply with these sustainability frameworks.

CBAM puts a price on carbon-intensive products entering the EU from October 2023, with other countries set to follow.

The Safeguard Mechanism and National Greenhouse and Energy Reporting (NGER)

The [Australian Government's Safeguard Mechanism](#) has been in place since 1 July 2016, requiring Australia's highest GHG emitting facilities to keep their emissions below a set baseline (business as usual levels, adjusted for production levels). If the facility exceeds the baseline, it must manage its excess emissions and may face a penalty if it fails to comply.

In March 2023, the Australian Government's National Greenhouse and Energy Reporting (Safeguard Mechanism) Amendment (Reforms) Rules 2023 was passed by the Australian Parliament. These reforms take effect from 1 July 2023, and require Safeguard facilities to reduce their emissions in line with Australia's climate targets.

Each covered facility is required to report its emissions annually to the Clean Energy Regulator. If a safeguard facility does not exceed its baseline for a financial year on or after a financial year commencing July 2023, it may receive Safeguard Mechanism credit units (SMCs). If they exceed their baseline for a financial year commencing July 2003 then they can:

- purchase Australia Carbon Credit Units (ACCU)
- surrender SMCs
- apply to borrow baseline from the following year (repaid with interest)
- apply to become a trade-exposed baseline-adjusted (TEBA) facility and receiving a discounted decline rate (up to 3 years)
- apply for a multi-year monitoring period (MYMP) to allow more time to reduce emissions.

How is the baseline calculated?

A [default decline rate of 4.9 percent per year. applies](#) to standard and landfill baselines (not sectorial/grid-connected electricity generation facilities). For resources companies, standard baselines will be calculated by multiplying the quantity of product that a Safeguard facility makes, by the defined emissions budget per unit of production, transitioning from facility-specific emissions intensity values to industry average values by the 2029 – 2030 financial year.

Who falls under the scope of the Safeguard Mechanism?

The Safeguard Mechanism applies to facilities that emit more than 100 000 tCO₂-e of Scope 1 (direct emissions) in a financial year. There are presently 215 covered facilities accounting for approximately 30 percent of Australia's GHG emissions.

The Safeguard Mechanism is administered through the National Greenhouse and Energy Reporting Scheme. As well as keeping emissions below the baseline, Safeguard facilities must adhere to the reporting and record-keeping requirements of the National Greenhouse and Energy Reporting.

What information needs to be recorded as part of the NGER?

As outlined by Australia's [Clean Energy Regulator](#) (CER), records of activities must be adequate to enable the CER to ascertain whether the corporation or the person has complied with its obligations under the NGER Act. This includes information that can be used to verify the relevance, completeness, consistency, transparency, and accuracy of reported data during an external audit.

Reporters are encouraged to record both the decision-making process and the details of the calculation and data analysis methods used for GHG emissions and energy production and consumption. Recommended records include but are not limited to:

- a list of all sources monitored
- the activity data used for calculation of GHG emissions for each source, categorised by process and fuel or material type
- documentary evidence relating to calculations – for example, receipts, invoices and details of payment methods
- documentation of the methods used for GHG emissions and energy estimations
- documents justifying the selection of the monitoring methods chosen
- documentation of the collection process for activity data for a facility and its sources
- records supporting business decisions and accuracy, especially for high-risk areas relating to reporting coverage (for example, applying concepts of controlling corporation, corporate group, and facility).

When facility-specific emissions factors are used, records should document the monitoring methods used and the results from the development of these emissions factors as well as information such as biomass fractions and oxidation or conversion factors.

The GHG Protocol describes other records that might be kept to maintain a high-quality and easily auditable GHG inventory.

Spotlight on Rio Tinto – Immediate impact of the safeguard reforms:

As reported in The Australian article of July 2023 [Mining giant Rio Tinto books half-year net profit of \\$US5.1 billion but aluminium assets slashed in value](#), Rio Tinto has slashed \$US1.2 billion from the value of its Australian aluminium assets on the back of the federal government's safeguard mechanism. It wrote off the value of its Yarwun alumina refinery completely due to the need to buy carbon offsets for the asset, which demonstrates the immediate and significant impact of new rules rolling out.

Biodiversity, Ecosystems and the Taskforce on Nature-related Financial Disclosures (TNFD)

Companies are required to understand the implications of biodiversity loss for their business. That is risk and opportunities to economic activities and financial assets that depend on biodiversity. For example, variability to access of feedstock, exposure to extreme environmental conditions, and/or trade and regulatory constraints.

Internationally, recognition of financial and systematic materiality of biodiversity risks is represented by the Network for Greening the Financial System, the UN Principles for Responsible Investment, the TNFD, the World Economic Forum (WEF), the Organisation for Economic Co-operation and Development, governments, and national banks.

Although not yet adopted in Australia, companies may need to disclose the risks and opportunities to the impact of the company on biodiversity, even if the risks or opportunities do not affect the company's financials.

For the Australian resources sector, the type of ecosystems service that would need to be reported would be water supply, water flow regulation, solid waste remediation & soil quality regulation, global climate regulation, rainfall pattern regulation and storm mitigation.

The TNFD has developed guidance for organisations when assessing nature-related risks and opportunities using a 'LEAP' framework.

- locate the interface with nature

- evaluate dependencies and impacts
- assess risks and opportunities
- prepare to respond to nature-related risks and opportunities and report.

The TNFD framework was published on 13 September 2023. It is expected that the Australian Government will consider the IFRS S1 Sustainability reporting standard, including nature and biodiversity issues that could apply in Australia.

WHAT DO AUSTRALIAN RESOURCE COMPANIES NEED TO MEASURE NOW TO COMPLY?

The range of new regulations rolling out globally will require a level of accuracy, detail, transparency, auditability, timeliness, frequency, scenario analysis and forward-looking statements far beyond Australian reporting practices today – and above the current capabilities within many organisations.

Depending on local jurisdictions, the new rules will require qualitative metrics and granular quantitative disclosures on a wide range of sustainability indicators such as GHG emissions across Scopes 1, 2 and 3, water, energy, air quality, waste, hazardous materials, pollutants, nature-related risk factors, PCF, LCA and TNFD impacts. These indicators will need to be reported on across the entire operation and supply chain – increasingly down to a product level in many cases.

While the full requirements will depend on location, sector and operation, Table 3 summarises the most significant changes that Australian resources companies need to measure now to comply across international (ISSB, ESRS) and national (Safeguard Mechanism Reforms 2023) reporting frameworks:

Table 3 Summary of reporting requirements for Australian resources companies

Proposed to be mandatory for first round of entities from 2024 – 2025	<ul style="list-style-type: none"> - Domestic standards will be developed by the Australian Accounting Standards Board (AASB) and designed to be aligned with the ISSB IFRS2 Standard as far as practicable. Further consultation on the standards is expected in the second half of 2023. - Climate-related financial disclosure will be required to be published in the entity's annual report. For listed entities, metrics and targets may be referenced in the directors' report and referred to in a separate report. - Limited assurance progressing to reasonable assurance will be required.
Climate-related financial information	<ul style="list-style-type: none"> - Climate-related financial information is to be disclosed using the four-pillar core content framework (also used in the TCFD) – Governance, Strategy, Risk and opportunities, Metrics and targets. - All reporting content (except Scope 1 and 2 emissions) will be subject to financial materiality.
Risks and opportunities	<ul style="list-style-type: none"> - The Treasury proposes that information about material climate-related risks and opportunities to a reporting entity's business and how the entity identifies, assesses and manages risk and opportunities need to be disclosed.
GHG Emissions – Scope 1, 2 and 3	<ul style="list-style-type: none"> - Scope 1 and Scope 2 gross, as set out by the NGER Scheme legislation. - Reporting of Scope 1 emissions, both location-based and market-based would be required using methods under NGER Scheme legislation.

	<ul style="list-style-type: none"> - Scope 3 that are material (from their second reporting year onwards). Scope 3 disclosures include upstream and downstream and are to be reported with a recognised emissions accounting framework such as the GHG Protocol) and be informed using domestic emission factors (such as the National Greenhouse Accounts Factors). Determination of boundaries for material Scope 1 emissions and the extent to which upstream and downstream value chains are represented in calculations is to be disclosed.
Industry specific standards	<ul style="list-style-type: none"> - Reporting entities would be required to have regard to disclosing industry-based metrics (where there are such metrics following a proposed consultation with members of that sector that are most relevant to their business model). - For resources companies the SASB industry-specific standards such as “Extractives & Minerals Processing” with industries coal operations, construction materials, iron & steel producers and metals and mining, are a good guide in the interim.
Scenario analysis	<ul style="list-style-type: none"> - Carry out scenario analysis (qualitative moving to quantitative), to include 2 possible future states, one of which must be consistent with the global temperature goals set out in the Climate Change Act 2022, which is to contribute to ‘holding the increase in the global average temperature to well below 2°C above pre-industrial levels and pursuing efforts to limit the temperature increase to 1.5°C above pre-industrial levels’ - As per the Australian Government’s Climate-related financial disclosure consultation paper: <i>“Entities would also report against at least one other scenario that reflects different climate future(s). This aims to help investors understand resilience of the reporting entity’s business strategy in a scenario where the world is decarbonising at a different speed. This could include a scenario reflecting the Australian Government’s commitment to reduce emissions by 43 per cent by 2030 and to net zero by 2050.”</i>
Climate resilience	<ul style="list-style-type: none"> - Disclose climate resilience assessments for each state in the scenario analysis. - Climate resilience of an entity's strategy and business model to both transitional and physical risks.
Transition planning and climate-related targets	<ul style="list-style-type: none"> - Transition plans need to be disclosed, and information about target setting, offsets and mitigation strategies. - Disclose information about climate-related targets and progress towards these targets (are they Science Based Target Initiative (SBTI) that has been verified/ validated by a third party) and how their chosen target compares to the global temperature goal set out in the Climate Change Act 2022 and Australia’s nationally determined contribution.
NGER	<ul style="list-style-type: none"> - NGER Act continues to operate alongside the domestic climate reporting regime. Under the proposed regime, more entities will need to disclose Scope 1 (absolute), Scope 2 (absolute) and Scope 3 (material) emissions. Some reporting entities may need to shift reporting readiness from the NGER date of October 31 to earlier if their annual reports are released earlier than this date.

Not yet part of the reporting landscape in Australia, however important to start preparing for:

<p>TNFD & EU Impact disclosures/nature-related risks and opportunities</p>	<p>The EU Corporate Sustainability Reporting Directive (CSRD) and the ESRS are leading the way for nature-related disclosures. Subject to materiality, companies are required to disclose biodiversity and ecosystem-related topics such as ESRS E4 Biodiversity and Ecosystems, E2 Pollution, E3 Water and Marine Resources and E5 Resource Use and Circular Economy.</p> <p>The Australian treasury consultation paper highlights the need to implement a regulatory framework for reporting in other environmental impact areas such as nature and biodiversity.</p> <p>The ISSB looks to introduce more topic-specific standards that complement the Climate Standards with the recommendation of the Task Force on Nature-related Financial Disclosures (TNFD Recommendations).</p>
<p>Product carbon footprinting (PCF)</p>	<p>PCF is the sum of GHG emissions generated by a product over the various stages of its lifecycle. Cradle-to-gate and cradle-to-grave PCF.</p> <p>PCF is based on average data from production, purchased raw materials and purchased energy. Average data will be replaced over time as supplier-specific data becomes available as legislation matures.</p> <p>Product-specific guidelines for the calculations of PCFs in the industry for comparability of products.</p> <p>CBAM requires some industries, including the resources sector to calculate total carbon emissions embedded in a product (quarterly reporting) and imposes an import tax based on the PCF of the imported goods.</p> <p>Other jurisdictions are expected to follow. For example, in the US the draft Clean Competition Act (CCA) includes 25 sectors that impose a tariff on the difference between product actual emissions and the US baseline emissions.</p> <p>The Safeguard mechanism reforms also state that new products produced by an existing Safeguard facility and products produced by a new Safeguard facility will be subject to ‘best-practice’ emission intensity values. This means if a facility can measure the PCF of each product it produces accurately, the risk of overreporting embedded emissions is significantly reduced with an opportunity to exceed the industry average value and bank some Safeguard Credit units.</p>
<p>Digital Taxonomy</p>	<p>Digital financial reporting is mandatory in 14 of G20 nations, including the US, UK, France and Germany – but not in Australia. Australian companies have had the option to voluntarily lodge digital financial reports with ASIC since 2010. Under the Corporations Act, all companies must lodge PDF and/or paper financial reports through ASIC’s lodgement portal.</p> <p>A 2019 senate inquiry recommended the Australian Government make digital financial reporting standard practice in Australia.</p> <p>As reported by the AICD, the AASB is “strongly in favour” of building a digital taxonomy for financial reporting in Australia.</p>

	<p>The ISSB has been working on a digital taxonomy in tandem with the development of IFRS S1 and IFRS S2 to facilitate digital consumption of sustainability-related financial disclosures and aims to issue the final digital taxonomy in early 2024.</p> <p>Australia's decision to make climate reporting mandatory is expected to lead to a surge in the use of digital corporate reporting, encompassing financial as well as climate and sustainability reporting.</p>
--	--

HOW CAN DIGITAL TOOLS OVERCOME THE DATA CHALLENGE?

Metallurgical accounting and sustainability reporting go hand in hand for resources companies

At the heart of finance-grade sustainability reporting and metallurgical accounting is accurate, transparent, and detailed activity data. Digital transformation for resources organisations provides the tools to accurately collect and track this information.

While data for sustainability reporting is typically collected from onsite metering or purchase records, best practice for resources facilities is to create a process digital twin of the operation and use source data to perform a granular plant-wide mass and energy balance, reconciled using dynamic simulation, that considers time dependency for batch processing.

Using a process digital twin, plant-wide data is collected, validated, simulated, and analysed across the site, to give rich insights across the operation and supply chain so the facility can report on a broad range of sustainability indicators, including Scopes 1, 2 and 3.

It enables each validated data stream to be assigned a scope, site, boundary, category/source, and data type – down to a product level – to derive the most accurate and reliable activity data throughout the resources production process.

Emissions factors are applied using internationally recognised third-party databases and the digital twin solution maintains data tables for recognised emissions factors, supplier-specific and custom emissions factors.

Activity data is the key to accurate and auditable emissions accounting

Without integrated activity data connected to a dynamic simulation that is customised to the chemistry and process dynamics of a plant, tracking inventory – and therefore associated emissions, water, and energy consumption – from start to finish is impossible.

Validated activity data streams that can be assigned a scope, boundary, category/source, and data type will derive the most accurate activity data throughout the industrial process.

Technical example A: What method delivers the most accurate activity data?

To calculate emissions of GHG, facilities often use the spend-based method as a consumption metric rather than an activity-based method. Whilst this may seem appropriate, it is not always the most accurate method of calculating emissions.

For example, the CO₂ released from neutralising acid with limestone is often calculated from the limestone addition and embodied carbon within. This is often inaccurate, and leads to overreporting of Scope 1 emissions, as at a higher pH of 4 to 6, limestone will not be entirely consumed. This means CO₂ emissions calculated through a spend-based method are higher than actual emissions.

The ideal solution to this problem is to use an activity-based method and a process digital twin, alongside the measurement of volume and acid concentration up and downstream of the dosage point. These direct measurements can be fed into the digital twin as inputs to accurately calculate the actual limestone consumption, and this consumption is reconciled against other plant information if instruments fail, or lab analyses are inaccurate.

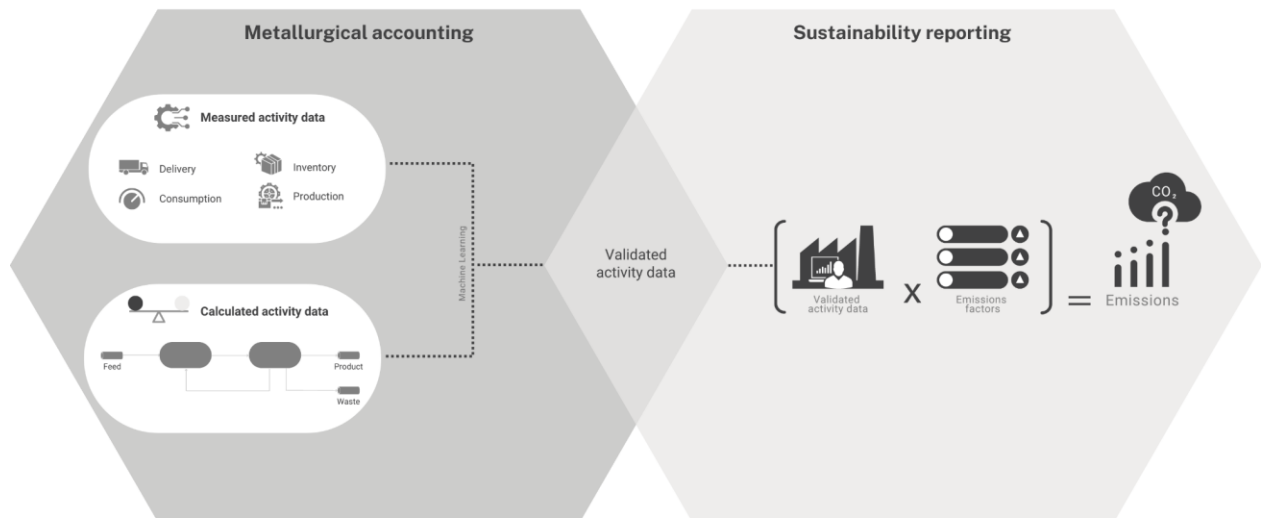


Figure 1 Sustainability Reporting, Metallurgical Accounting Using a Process Digital Twin

Using the activity-based method, a digital twin can accurately calculate CO₂ emissions without overreporting. Limestone utilisation at a higher pH could lead to only 50 percent utilisation (effectively 50 percent error) as calculated by the digital twin model, and as a result, would lead to a decrease in reported Scope 1 emissions attributed to this process by the same value.

If an organisation can accurately measure their metallurgical accounting and production reporting, then its sustainability reporting uses this data to calculate sustainability indicators across the site (Scope 1), purchased energy (Scope 2) and supply chain/other indirect emissions (Scope 3).

Technical example B: Using activity data to accurately measure Scope 2 emissions

While purchased electrical power is commonly used to calculate Scope 2 emissions, using an activity-based method is more reliable for accurate reporting.

For example, a facility in Africa was using purchased power to report on Scope 2 emissions, however analysis showed that the amount did not align with production. The plant had attempted to uncover the inefficiencies that led to the misalignment, however once a digital twin was implemented with power data incorporated into the dynamic mass balance, the site was able to uncover that electrowinning equipment was less reliable than expected and had been the cause.

In fact, 42 MWh or US\$1.5 million per year of electricity was uncovered as being purchased in excess of what was being used at the plant. In addition, the digital twin model was able to calculate the Scope 2 emissions using an activity-based method from plant information rather than the standard spend-based method. As a result, the site was over-reporting Scope 2 emissions by 7.5 percent or 8 000 t-CO₂e/y.

The mass, energy, and rate of accumulation with respect to time provide unique insights into exactly what is happening inside the processing plant at any point in time. The integration and wait times for laboratory assays and the solver calculations mean the data from these simulations are delivered within hours. Process digital twins leverage Internet of Things (IoT), big data storage and integration, machine learning and advanced database structures to deliver fast, actionable insights to stakeholders via dashboards and visualisation tools.

A process digital twin integrates with existing systems and is customisable to the plant and its processes. It automatically centralises huge volumes of data from multiple sources across the operation and supply chain and uses machine learning to validate and organise the measured (from instrumentation) and calculated (from the simulation) data.

The twin uses dynamic simulation to perform a plant-wide mass and energy balance to reconcile delivery, consumption, inventory, and production activity data. Using source data as inputs, the simulated data contextualises the measured activity data for completeness and accuracy.

This means the verified sustainability indicators are fully traceable, immutable, and unalterable, and surpass any rigorous sustainability audit tests for complete assurance.

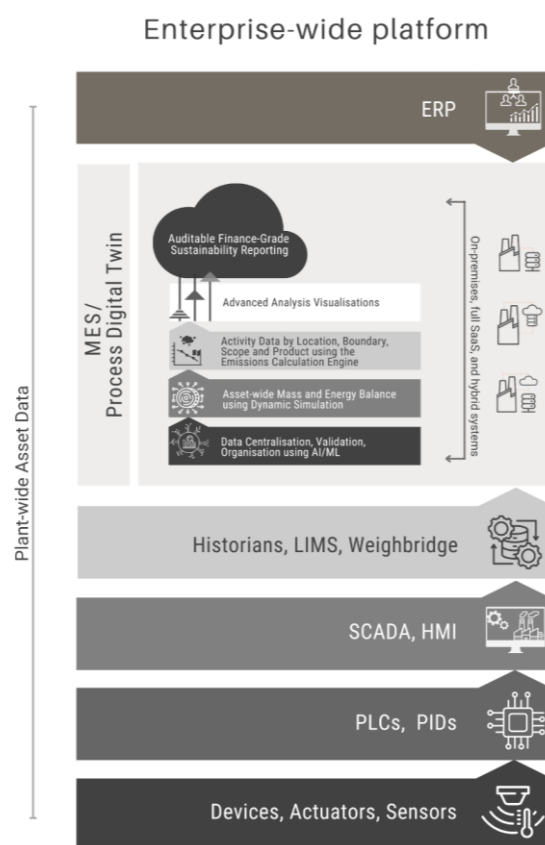


Figure 3 Enterprise-wide Platform

To understand how process digital twins work in the resources sector to deliver best-practice sustainability reporting, it can be helpful to reference the automation pyramid – a model based on the international standards ANSI/ISA 95 developed by the International Society of Automation.

Essentially, this model provides standards as to how different enterprise and control systems should work together to reduce errors, risk, and costs. It is a well-established model that is widely adopted in the resources sector.

Figure 4 provides an overview of the levels of automation for the resources sector. The automation pyramid derived from ISA 95 and adapted for the mining and minerals processing industry.

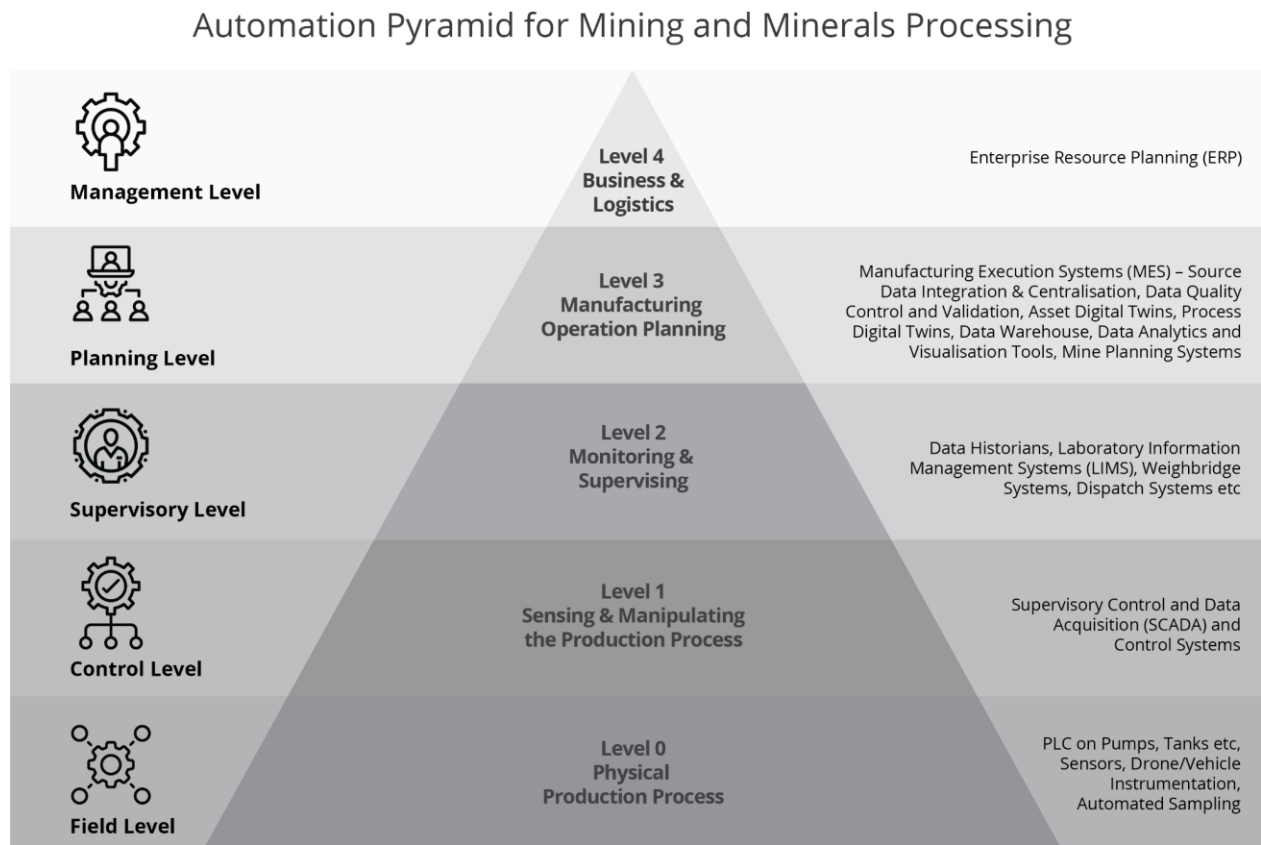


Figure 4 Automation Pyramid for Mining and Minerals Processing

Over the last ten years, innovations in digitisation – part of Industry 4.0 – have led to some incredibly advanced solutions, or digital-twin-enabled Mining/Manufacturing Execution Systems (MES), being developed for the planning level of the automated pyramid.

These fully automated digital-twin-enabled MES solutions are designed to take data from the field, control and supervisory level solutions and transform this raw data into contextualised information. The context is derived from using a detailed dynamic plant model and incorporating appropriate chemistry based on the verified flow sheet. Source-measured plant data is centralised, validated, organised, and subjected to data quality analysis, using intelligent new methods such as machine learning. Dynamic simulation technology is then used to process this data and perform a full plant-wide mass balance every hour. This provides a plant's stakeholders with a level of granularity of processing information, including constant work-in-progress inventories, directly traceable to plant data sources that was never possible.

By looking at the calculated ‘outcomes’ from the process digital twin, stakeholders can contextualise and crosscheck their measured plant data and quickly determine where problems are occurring – or where opportunities for improvement lie. All the data, such as the input data processed by the digital twin and output data calculated by the digital twin, are stored in a data warehouse. From this, authorised stakeholders can generate user-friendly data visualisations and reports. The digital-twin-enabled MES can in turn make its data available typically to a Level 4 solution, commonly an ERP solution, for overarching insights.

Scope 1, 2 and 3, and other sustainability indicators at a product level Example of an Industrial Site

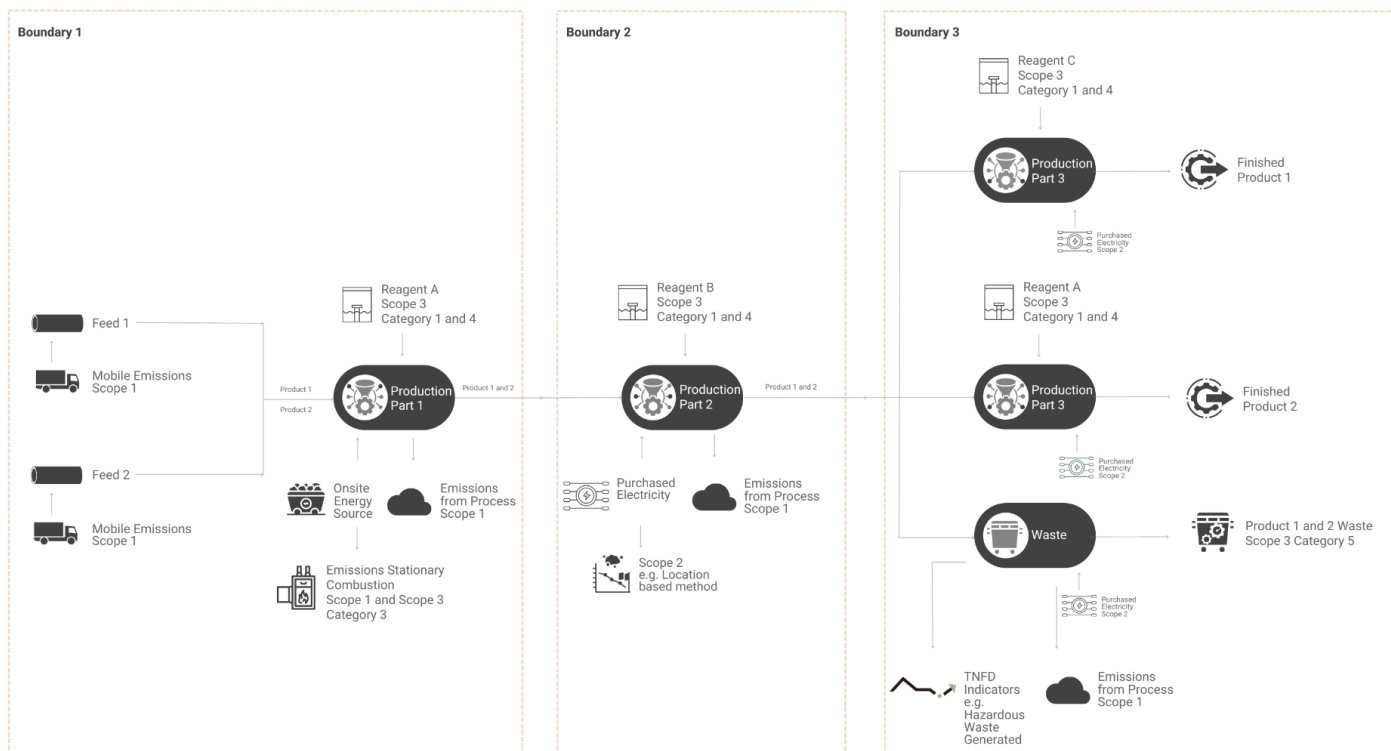


Figure 5 Using a Process Digital Twin to Calculate Scope 1, 2 and 3 and other Sustainability Indicators at a Product Level

WHY ARE DIGITAL REPORTING TOOLS THE ONLY WAY TO MEET EVOLVING REGULATIONS?

The need for regular auditable reporting in a machine-readable digital taxonomy, detailed scenario analysis, climate resilience assessments, transition planning and climate-related target setting and progress reports, means that data-driven technology is the only solution to meet evolving sustainability disclosure rules and new reporting standards.

Deploy machine-readable digital taxonomy from day one

Digital reporting taxonomy structures provide a standardised machine-readable format for sustainability reports to enable fast and consistent interpretation and comparison. In a [recent article](#), Dr Andreas Barckow, Chair of IASB supports digital taxonomy:

“Already required throughout Europe, the US and other global jurisdictions, he notes that global regulators have been ‘quite clear’ that when ISSB’s first standards are adopted within the next year, they should come with a digital taxonomy from day one.”

Delivering machine-readable data relies on consistent and automated electronic data capture, consolidation, and output.

In July 2023, the ISSB published a proposed [IFRS Sustainability Disclosure Taxonomy](#) for public comment – a digital taxonomy to facilitate digital reporting of sustainability-related financial information prepared using the ISSB standards. This enables digital tagging of information required by the IFRS standards S1 and S2. The ISSB will review feedback to deliver the final digital taxonomy early in 2024. The intention is to improve global accessibility and comparability of sustainability information for investors.

Enable automation, data quality and auditability

Particularly in the resources sector, manual spreadsheets simply cannot capture or process the volumes of data needed to deliver immutable, unalterable, and auditable sustainability reports. The biggest challenge is that siloed legacy systems and manual processes mean most organisations lack the data and digital tools to achieve this to the required levels. Often multiple spreadsheets (typically from manual data entry) and exports from other systems across the organisation are consolidated and analysed to report on sustainability indicators.

The data is raw, not validated and not contextualised. This process is laborious, open to error and data can be changed or lost and would not meet the level of assurance required from investors, company directors and other stakeholders.

Technical example C: - Using machine learning to ensure data quality

Ensuring high-quality measured data is crucial to efficient plant operation, sustainability reporting and rapid identification of issues. Manually filtering through instrument data is often far too slow and labour-intensive to be practical.

A process digital twin uses machine learning to assess the quality of measured data by taking in various types of source data, like instrument historians, weighbridge systems or laboratory data. Using historical data, the twin can identify unstable measurements and flag them to site personnel. This can indicate faulty instrumentation, poor calibrations, or other potential process issues. By considering all measured data in the surrounding equipment group, the twin can predict suggested values for measurements and flag inaccurate ones.

For example, as shown in Figure 6, a level instrument on a feed storage bin was recording inaccurate values (blue). These values were being used directly in a digital twin dynamic mass balance to calculate values (green). However, according to up and downstream instrumentation, the level instrument was not calibrated correctly, as uncovered by the data quality system indicating poor stability. Resolving this issue would allow for more accurate control of the process through more accurate feed blending.

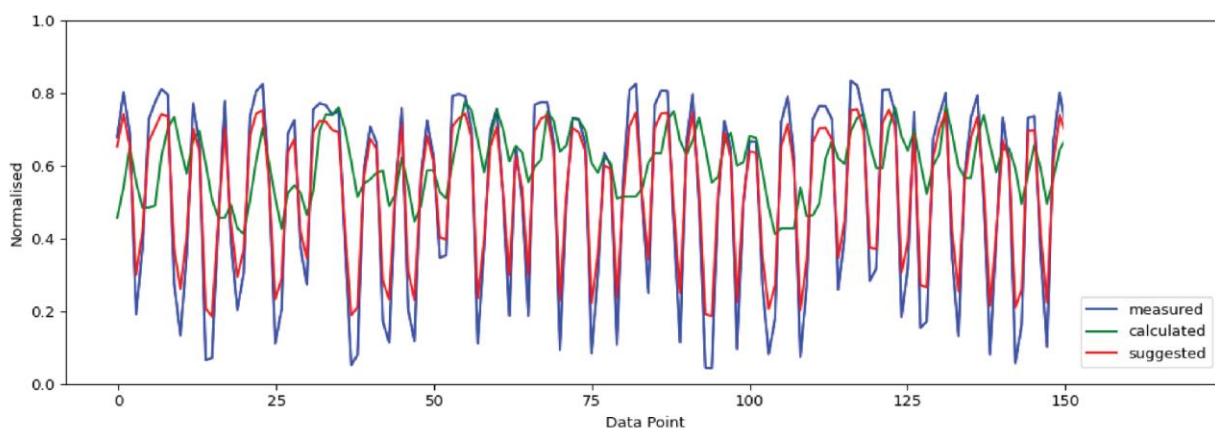


Figure 6 Unstable Measure Points

Technical example D: Using dynamic simulation to validate data and close data gaps

Often, measured data does not reflect actual plant operations due to faulty instrumentation, lack of calibrations or poor sampling. The use of a digital twin dynamic model can accurately identify not only when this measured data is faulty, but also what actual consumption/production rates and quality should be.

For example, a site in Africa had instrument-recorded mill feed rates that severely underreported the mass of feed material being fed to the circuit, resulting in inaccurate reporting of production and recovery metrics.

In Figure 7, blue is the plant-measured data and red is the digital twin calculated data. The digital twin model was able to calculate the actual consumption through the plant based on all the available data, as well as validate surrounding sources of data.

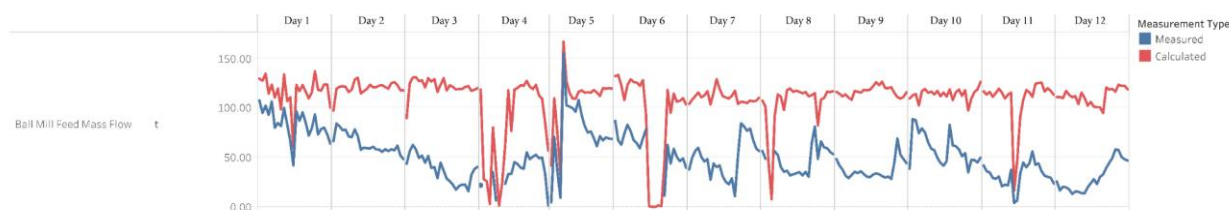


Figure 7 Ball Mill Feed Mass Flow

Through leveraging the digital twin calculated data, the site team was able to identify that this instrument was under-reading by up to 65 percent.

The digital twin is also able to calculate streams and inventories that could not be measured by the site at an hourly level. For example, the site had leach tanks that did not have instrumentation monitoring the contents of each leach tank.

Due to the complex nature of the site's leach tank operations, it was difficult for the site to predict or calculate the contents themselves. Instead, the digital twin was able to calculate not only the total content but also the product contained within each tank.

These insights allow the site to better control its leach and downstream processes through a better understanding of continuous work-in-progress inventory calculations. In Figure 8, each colour represents a different leach tank, and the mass of total metal inventory is monitored and used to monitor and control the process.

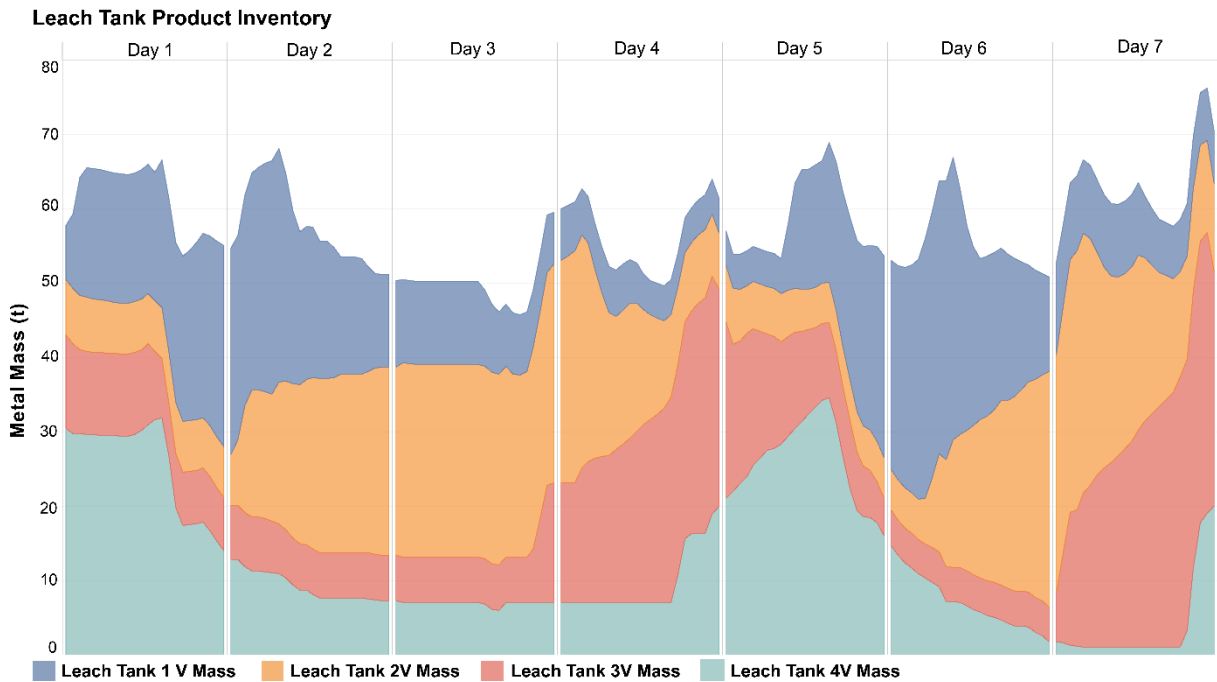


Figure 8 Leach Tank Product Inventory

Technical example E: Using dynamic simulation to validate consumption use of reagents

Using a process digital twin, the dynamic mass balance can be used to reconcile plant-measured values including plant instruments, laboratory results, deliveries of feedstocks and reagents, and final product shipments.

For example, after implementing a digital twin, a site in Africa noticed that its hydrogen peroxide reagent deliveries did not align with consumption data. This consumption data was calculated by the digital twin through process chemistry and other available plant data and the model-calculated values could not align with both figures, which triggered a review of the source data. It appeared that the delivered mass was more than double the reported consumption of peroxide.

Further investigations found that the installation of the peroxide consumption instrument was done incorrectly, resulting in the flow meter under-reading by over 100 percent. Figure 9 shows the actual peroxide consumption to final product molar ratio over time, which has declined to less than half of the original value over the period.

As this flow meter was used to control the peroxide addition into the process, it was discovered that the peroxide consumption was far more than what was actually required. In resolving this issue, the site saved US\$475 000 per year in hydrogen peroxide deliveries alone.

Not only was the site able to reduce operating costs significantly, but also reduce Scope 3 emissions associated with hydrogen peroxide production and transport, roughly equivalent to 1 000 t-CO₂e/y or around US\$100 000 per year in carbon credits within the EU.

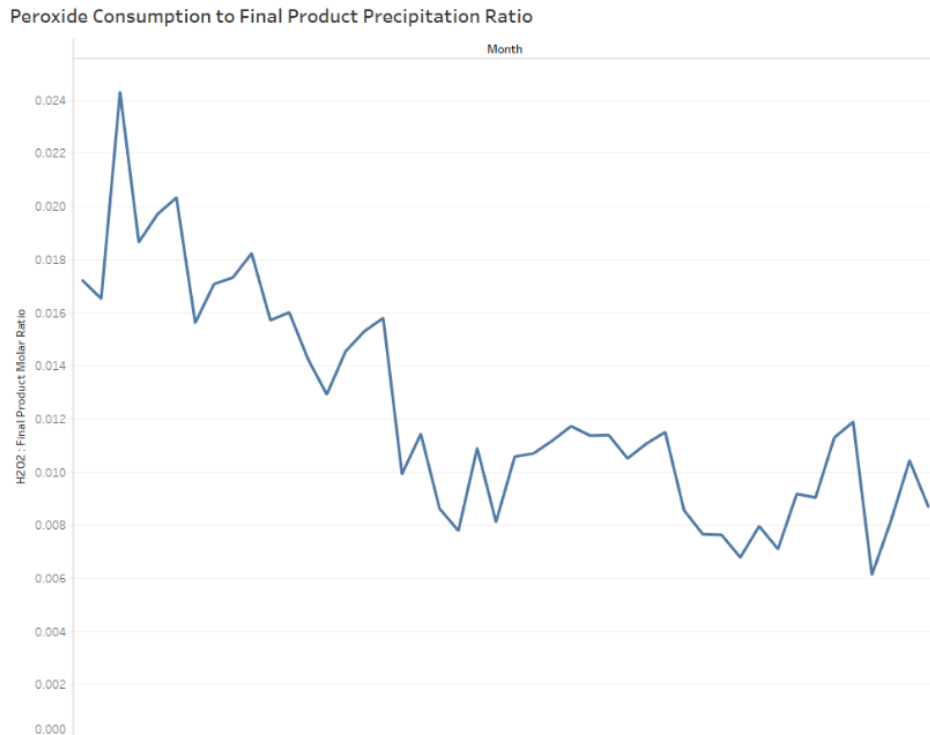


Figure 9 Peroxide Consumption to Final Product Precipitation Ratio

Track scopes 1, 2 and 3 emissions and industry-specific disclosures

Sustainability reporting requirements go further than just reporting on an organisation's Scope 1 and Scope 2 emissions with Scope 3 reporting now becoming mandatory.

Summary of Scope 1, 2 and 3 GHG emissions requirements in Australia:

- Scope 1 and Scope 2 gross, as set out by the NGER Scheme legislation
- Scope 3 that are material (from their second reporting year onwards). Scope 3 disclosures include upstream and downstream and are to be reported with a recognised emissions accounting framework such as the GHG Protocol) and be informed using domestic emission factors (such as the National Greenhouse Accounts Factors).

Industry-specific standards:

- reporting entities would be required to have regard to disclosing industry-based metrics (where there are such metrics following a proposed consultation with members of that sector that are most relevant to their business model).
- for resources companies the [SASB industry-specific standards](#) such as "Extractives & Minerals Processing" with industries coal operations, construction materials, iron & steel producers and metals and mining, are a good guide in the interim.

Technical example F: Measuring and reducing Scope 1, 2 & 3 and industry-specific disclosures/indicators

Scope 1

A process digital twin can be used to accurately calculate and/or validate Scope 1 emissions using process data and plant chemistry. For example, a facility in Kazakhstan had been recording SO₂ emissions with gas analysers, which were not working properly. The gas was fed to the acid plant, and it was assumed that there were few losses due to a lack of instrumentation that suggested otherwise.

Using the digital twin mass balance, the SO₂ analysers were identified to not be working correctly, and as shown in Figure 10 the discrepancy between the measured (blue) and calculated (red) SO₂ emissions was quantified (black).

The plant had measured 16.5 percent or 350 tonnes of acid per day lower than the model-calculated results. Over the time-period analysed, this equated to 43 000 tonnes or 26 percent of the plant-measured amount.

As the sulfur feed to the plant was determined to be accurately measured, the results indicated high sulfur dioxide losses from the stacks, equivalent to US\$21 million per year, not accounting for the risk of significant fines depending on regulatory requirements.

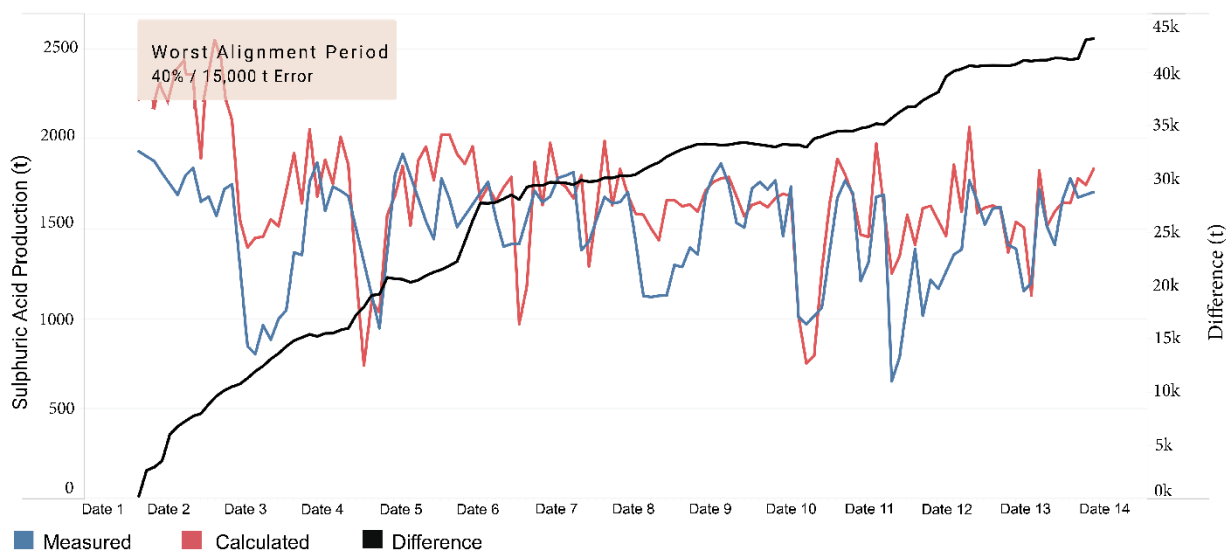


Figure 10 Discrepancy between measured (blue) and calculated (red) SO₂ emissions was quantified (black)

Scope 2

While purchased electrical power is commonly used to calculate Scope 2 emissions, using an activity-based method is more reliable for accurate reporting. For example, as detailed in *Technical example B: Using activity data to accurately measure Scope 2 emissions* a facility in Africa used an activity-based to uncover that it was over-reporting Scope 2 emissions by 7.5 percent or 8 000 t-CO₂e/y.

Scope 3

Whilst Scope 3 emissions can make up 70 to 80 percent of a site's total emissions, they are often poorly understood and misreported. A large portion of Scope 3 emissions for metallurgical facilities come from the production and delivery of reagents used within the plant, however Scope 3 emissions also come from sources that are more difficult to monitor such as business travel, delivery, use and processing of sold products and impact of waste and by-products.

These Scope 3 emissions often are calculated using a combination of unclear assumptions, default input values and formulas that cannot be easily audited, validated, or traced back to the original source.

A process digital twin can measure and trace back all these calculated values back to the source, whether it be a specific user-entered value, calculated from instrument/lab data, use a range of default inputs or a combination of these. In facilities operating in the EU (and some other jurisdictions) Scope 3 will need to be verified otherwise an industry default will apply.

Having access to this data enables organisations to meet the necessary reporting requirements, understand their operation and proactively work to reduce Scope 3 emissions.

Scope 3 Emissions

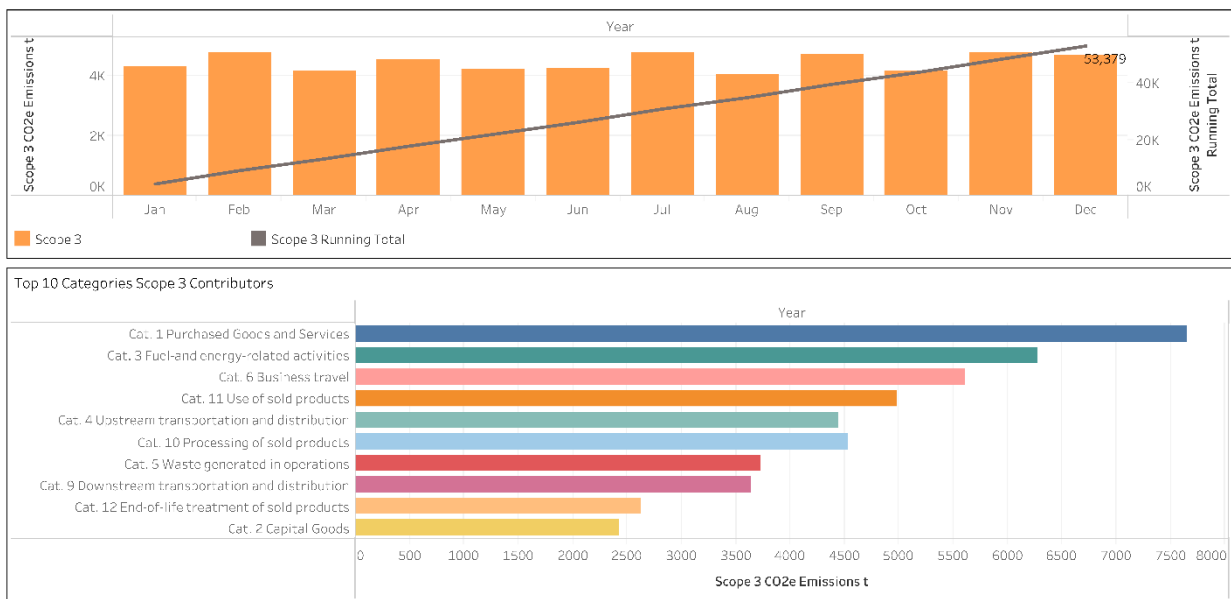


Figure 11 Scope 3 Emission calculations

Data-driven forward-looking statements using scenario analysis

Traditionally, financial statements looked at historical performance, whereas the ISSB sustainability reporting disclosure requirements are strongly future-focused, and companies will be required to use scenario analysis when assessing their climate resilience.

As summarised in Table 3 the new frameworks will mandate scenario analysis for multiple possible future states that reflect different climate future(s) and targets.

One of the biggest concerns for organisations lies in the confidence they have in the quality of their data. Digital tools – using artificial intelligence (AI) such as machine learning (ML) and artificial neural networks – automate data collection, validate, and contextualise data, and simulate and calculate

more data to close data gaps. Companies use the predictive capabilities of these models to test various future scenarios with confidence and to report on their assessment of climate resilience.

Technical example G: Using a process digital twin to calculate the material financial impact of net zero targets

By integrating multiple data sources and reconciling plant data, a digital twin can extract the data to demonstrate the financial costs of meeting reduction targets (including offsets) without the burden of manual reporting.

For example, the introduction of activity-based data in a metallurgical plant uncovered that it was purchasing 42 MWh or US\$1.5 million per year of excess electricity as a result of faulty equipment that had gone unnoticed. Refer to graphs and details in Technical examples B and F.

As a result, the site was able to save on their power consumption, but also more accurately report on their Scope 2 emissions, which was 8 000 t-CO₂e/y lower than what they had previously calculated using a less accurate method. This is approximately US\$800 000 per year worth of carbon permits (based on current EU prices).

Another site was able to reduce their Scope 3 emissions related to fuel consumption by 1000 t-CO₂e/y or US\$100 000 of carbon permits (at current EU prices) after the implementation of a digital twin. The site was able to recognise the contribution of this fuel to their overall Scope 1 emissions – which made up the bulk of the site’s carbon intensity and investigate alternative fuels as a result of the access to accurate data.

Transition planning and climate-related targets

To comply with the new reporting frameworks Australian resources companies would need to meet the following transition planning and climate-related targets:

- transition plans need to be disclosed, and information about target setting, offsets and mitigation strategies
- disclose information about climate-related targets and progress towards these targets – are they an SBTi that has been verified/validated by a third party – and how their chosen target compares to the global temperature goal set out in the Climate Change Act 2022 and Australia’s nationally determined contribution.

Technical example H: Transition planning, target setting and emissions reduction

An industrial facility needed to reduce its Scope 1 emissions sourced from neutralisation via limestone (as per details in *Technical example A*). With the help of digital tools, they discovered that over 30 percent of their Scope 1 emissions were sourced directly from the use of this reagent, not accounting for Scope 1, 2 or 3 requirements associated with the preparation, transport, and production of this reagent.

Using the digital twin and steady-state simulation, a what-if analysis is performed for the quantitative metrics around transition planning, target setting and emission reduction. This allowed for the calculations around transition planning for considering alternate flow sheets, changes to typical operating conditions, physical effects of climate on the facility, and capital and operating expenditure budgeting for planning. All results calculated can then be directly compared to actual current plant values, including Scope 1, 2 and 3 emissions. The site investigated further into alternative scenarios that could allow for alternative neutralising agents to be utilised, such as caustic.

The overall change to Scope 1, 2 and 3 emissions could be calculated from switching to caustic from limestone, accounting for changes to the process, reagent preparation and associated Scope 1, 2 & 3 emissions. The site was then able to make an informed decision on the overall change to total emissions intensity.

Nature-related disclosures

While not yet part of the reporting framework, it is important for resources organisations to start preparing for what will be needed to measure nature-related disclosures in line with the TNFD and future topic-specific ISSB and EU standards. Here is a summary of expected requirements:

- the EU CSRD and the ESRS are leading the way for nature-related disclosures. Subject to materiality, companies are required to disclose biodiversity and ecosystem-related topics such as ESRS E4 Biodiversity and Ecosystems, E2 Pollution, E3 Water and Marine Resources and E5 Resource Use and Circular Economy
- the Australian treasury consultation paper highlights the need to implement a regulatory framework for reporting in other environmental impact areas such as nature and biodiversity
- the ISSB looks to introduce more topic-specific standards that complement the Climate Standards with the recommendation of the TNFD.

Technical example I: Using a process digital twin for TNFD indicators

Global mandates are requiring facilities to monitor a range of environmental factors beyond just GHG emissions. For example, tracking the release of aqueous polluting solutes is necessary to understand the overall environmental impact of a site. While sites may measure total effluent discharge or concentration of pollutants, the level of reporting is not present at many sites to monitor and improve on the release of these pollutants.

Using a digital twin and centralised database, it is possible to calculate the release of these pollutants using a range of hourly plant data and clearly report traceable data. Digital tools can also incorporate habitat information to allow for reporting of solute emissions and report on solute release per habitat type, giving a broader picture of environmental factors. This allows personnel to quickly identify and resolve issues within the plant that may have caused unexpected spikes in pollutant discharge.

Specific aqueous species such as sulfate concentrations can be modelled within the digital twin and reported at different locations in the site to indicate effluent discharge, even if these species are not routinely measured.

Product Carbon Footprinting (PCF)

PCF is the sum of GHG emissions generated by a product over the various stages of its lifecycle: cradle-to-gate and cradle-to-grave. PCF is also expected to become something resources companies will be required to measure and report on in detail as summarised in Table 3.

Technical example J: Measure emissions down to a product level across the supply chain

Reporting emissions to a product level is becoming increasingly more important, although it remains challenging for metallurgical plants that have numerous sources of Scope 1, 2 and 3 emissions across multiple products.

Embodied carbon, as calculated by facilities, is a method commonly employed as it can be determined relatively simply with instrument and laboratory instrumentation. However, this method

is becoming inappropriate as emissions reporting legislation changes to require Scope 1, 2 and 3 emissions to be associated with these products outside of the carbon simply contained within final products.

For example, a site in Africa implemented a digital twin solution to calculate and report product-based carbon emissions. Through monitoring site activity data via a digital twin dynamic model, carbon emissions can be accurately calculated throughout the plant (even where direct measurements were not available) and allocated to the five final products that the facility exports.

This includes emissions from site activities associated with multiple products or electricity/reagent consumption at specific points in the plant flow sheet. Due to the transparency and auditability of the digital twin, the flow of data through the system can be tracked to understand how all final emissions values were obtained. Reporting is automated and simplified as well.

As shown in Figure 12, Scope 3 was a major source of emissions intensity for one of the products at the site. The site wanted to reduce the embodied Scope 3 emissions to improve overall emissions and make this final product more viable for sustainability-conscious buyers. As a result, an alternative fuel was suggested in the production process and the site was able to reduce Scope 1 emissions intensity from this source by 13.5 percent or approximately 1 000 t-CO₂e/y.

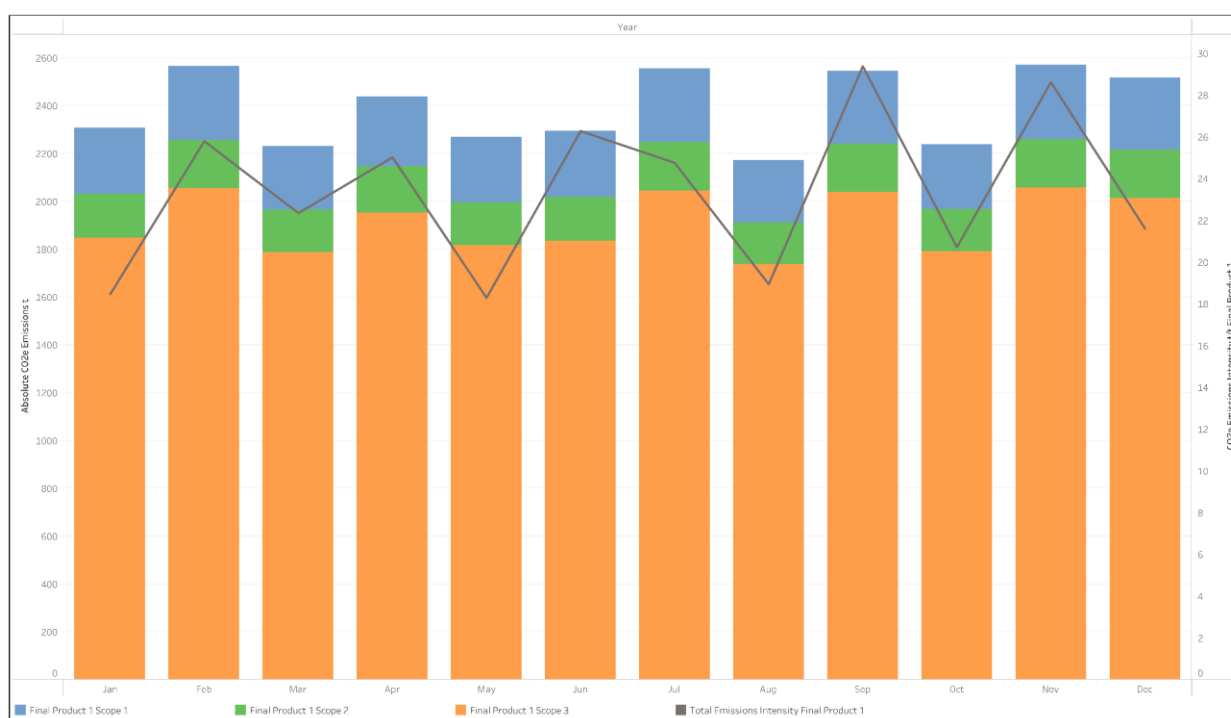


Figure 12 Measuring emissions down to a product level across Scopes 1,2 and 3

CONCLUSIONS

Rapidly evolving sustainability reporting regulations, combined with accelerating market demand for sustainable products and services, have created significant immediate and long-term implications for the energy-intensive Australian minerals and resources sector.

By outlining the latest regulations impacting the resources sector and detailing what companies need to measure and report on to comply, this paper is designed to help the preparation and

decision-making of boards, company directors, executives, governance and risk management professionals, metallurgists, operations managers, and senior industry professionals.

It explains how digital tools can be used to overcome this data challenge, concluding with the assertion that digital reporting tools are the only way to deliver the accurate and auditable disclosures necessary to meet new and emerging regulations.

Accurate measurement is the first step towards meeting compliance obligations and reducing emissions. Tracking and reporting on progress requires two essential ingredients, both of which are enabled by data-driven digital tools: finance-grade sustainability data and an auditable emissions accounting process.

Sustainability and digital transformation are two global business megatrends in recent years. Not only are they complementary, but digitisation is increasingly proven to be a path towards better business and environmental outcomes. Without digital tools, opportunities will be missed.

ACKNOWLEDGEMENTS

The author would like to acknowledge Sandra Gamble for peer reviewing the paper. Sandra has successfully completed the “Fundamentals of Sustainability Accounting (FSA) Credential” run by the SASB, now part of the International Financial Reporting Standards (IFRS) that formed the International Sustainability Standards Board (ISSB) that has been proposed by Australian treasury to be mandated here in Australia in 2024. Sandra is Chair of the Independent Pricing and Regulatory Tribunal (IPART) as well as the NSW Division Councillor for the Australian Institute of Company Directors.

REFERENCES

Australian Government Clean Energy Regulator, 2023. The Safeguard Mechanism, [online]. Available from: <https://www.cleanenergyregulator.gov.au/NGER/The-Safeguard-Mechanism> [Accessed: 4 September 2023].

Australian Government Clean Energy Regulator, 2023. The Safeguard Mechanism for financial years commencing on or after 1 July 2023, [online]. Available from: <https://www.cleanenergyregulator.gov.au/NGER/The-Safeguard-Mechanism/The-Safeguard-Mechanism-for-financial-years-commencing-on-or-after-1-July-2023> [Accessed: 4 September 2023].

Australian Government Clean Energy Regulator, 2023. Record keeping and compliance, [online]. Available from: <https://www.cleanenergyregulator.gov.au/NGER/Reporting-cycle/Complying-with-NGER> [Accessed: 4 September 2023].

Australian Government Department of Climate Change, Energy, the Environment and Water, 2023. *Safeguard Mechanism Reforms – Position Paper*. Available from: https://storage.googleapis.com/files-au-climate/climate-au/p/prj23cd662ff4387d8c254ae/public_assets/Safeguard%20Mechanism%20Reforms%20Position%20Paper.pdf

Australian Government Treasury, 2023. *Climate-related financial disclosure – Consultation paper*. Available from: <https://treasury.gov.au/sites/default/files/2023-06/c2023-402245.pdf>

Australian Securities and Investments Commission, 2023. *Report 763: ASIC’s recent greenwashing interventions*. Available from: <https://download.asic.gov.au/media/ao0lz0id/rep763-published-10-may-2023.pdf>

Directive (EU) 2022/2464 of the European Parliament and of the Council of 14 December 2022 amending Regulation (EU) No 537/2014, Directive 2004/109/EC, Directive 2006/43/EC and Directive 2013/34/EU, as regards corporate sustainability reporting, [online]. Available from: <https://eur-lex.europa.eu/legal-content/EN/TXT/?uri=CELEX:32022L2464> [Accessed: 4 September 2023].

European Commission, 2023. Corporate sustainability reporting, [online]. Available from: https://finance.ec.europa.eu/capital-markets-union-and-financial-markets/company-reporting-and-auditing/company-reporting/corporate-sustainability-reporting_en [Accessed: 4 September 2023].

European Commission, 2023. European sustainability reporting standards – first set, [online]. Available from: https://ec.europa.eu/info/law/better-regulation/have-your-say/initiatives/13765-European-sustainability-reporting-standards-first-set_en [Accessed: 4 September 2023].

Evans, N, 2023. Mining giant Rio Tinto books half-year net profit of \$US5.1bn but aluminium assets slashed in value, *The Australian*, 26 July 2023

Foster, E, 2023. Consider climate-related risks in financial statements, warns IASB, *Australian Institute of Company Directors*, [online]. Available from: <https://www.aicd.com.au/finance-governance/australian-accounting-standards/ias/consider-climate-related-risks-in-financial-statements-warns-iasb> [Accessed: 4 September 2023].

Greber, J, 2023. Bowen's 'green tariff' to shield steel, cement against carbon leakage, *Australian Financial Review*, 15 August 2023. Available from: <https://www.afr.com/policy/energy-and-climate/bowen-s-green-tariff-to-shield-steel-cement-against-carbon-leakage-20230814-p5dwew>.

IFRS Foundation, 2018. *Standards Project Summary and Feedback Statement: Definition of Material Amendments to IAS 1 and IAS 8*. October 2018. Available from: <https://www.ifrs.org/content/dam/ifrs/project/definition-of-materiality/definition-of-material-feedback-statement.pdf>

IFRS Foundation, 2023. IFRS S1 General Requirements for Disclosure of Sustainability-related Financial Information, [online]. Available from: <https://www.ifrs.org/issued-standards/ifrs-sustainability-standards-navigator/ifrs-s1-general-requirements/> [Accessed: 4 September 2023].

IFRS Foundation, 2023. IFRS S2 Climate-related Disclosures, [online]. Available from: <https://www.ifrs.org/issued-standards/ifrs-sustainability-standards-navigator/ifrs-s2-climate-related-disclosures/> [Accessed: 4 September 2023].

IFRS Foundation, 2022. *IFRS S2 Climate-related Disclosures. Appendix B Industry-based disclosure requirements. Volume B10—Metals & Mining*. International Sustainability Standards Board. Exposure Draft ED/2022/S2. Available from: <https://www.ifrs.org/content/dam/ifrs/project/climate-related-disclosures/industry/issb-exposure-draft-2022-2-b10-metals-and-mining.pdf>

IFRS Foundation, 2023. ISSB consults on proposed digital taxonomy to improve global accessibility and comparability of sustainability information, [online]. Available from: <https://www.ifrs.org/news-and-events/news/2023/07/issb-consults-on-proposed-digital-taxonomy/> [Accessed: 4 September 2023].

Philipova, E, 2023. How many companies outside the EU are required to report under its sustainability rules?, Refinitiv, [online]. Available from: <https://www.refinitiv.com/perspectives/regulation-risk-compliance/how-many-non-eu-companies-are-required-to-report-under-eu-sustainability-rules> [Accessed: 4 September 2023].

Geometallurgy - When Should Deposit Characterisation Commence?

K Ehrig¹, V Liebezeit², Y Li³, B Pewkliang⁴, E Macmillan⁵, M Smith⁶, S Slabbert⁷

1. Superintendent Geometallurgy, BHP Olympic Dam, 10 Franklin St Adelaide, kathy.ehrig@bhp.com
2. Principal Geometallurgist, BHP Olympic Dam, 10 Franklin St Adelaide, vanessa.liebezeit@bhp.com
3. Senior Geometallurgist, BHP Olympic Dam, 10 Franklin St Adelaide, yan.li@bhp.com
4. Senior Geometallurgist, BHP Olympic Dam, 10 Franklin St Adelaide, benjamath.pewkliang@bhp.com
5. Senior Geometallurgist, BHP Olympic Dam, 10 Franklin St Adelaide, edeltraud.macmillan@bhp.com
6. Lead Geoscience Data Management, BHP Olympic Dam, 10 Franklin St Adelaide, michelle.smith@bhp.com
7. Geoscience Data Management, BHP Olympic Dam, 10 Franklin St Adelaide, salomon.w.slabbert@bhp.com

ABSTRACT

Geometallurgical characterisation should commence prior to drilling the first hole. Once drill hole targeting starts, the astute exploration geologist should also be considering if viable processing options exist for the deposit style (i.e. IOCG, porphyry Cu, orogenic Au, sediment-hosted Pb-Zn, regolith-hosted ion-absorption REE, etc) and which minerals/elements are known to cause processing challenges, impact on final product quality or could be co-/by-products? It is likely that these minerals/elements may also overlap with the those which are useful for determining vectors to potential mineralisation. Hence, these elements should be part of the extended suite of elements measured on the drill core samples. Even though geologists are good at determining the presence of minerals and relative abundances in drill core, identifying the presence and abundances of some minerals, particularly the clay group of minerals, is really beyond the capability of even the best geologists. This leads to the necessity of using mineralogy measurement technology as early as practically possible in a drilling campaign.

Geometallurgical testing should commence post the discovery hole. Even with only a few mineralised samples available, the technical team (e.g. geometallurgy, geology, metallurgy, environment, mine planning) should be formulating a list of potential processing fatal flaws and commence the testing to determine if the ore properties related to the processing fatal flaws are present. As drilling continues and the project progresses through the various study phases, the number of drill core samples available will also increase. Therefore, geometallurgical testing can progressively expand to measure processing responses to the inevitable variability which exists across all ore deposits. Testing needs to be conducted on a full spectrum of possible grade ranges and mineral combinations, not just the highest grade parts of the deposit. Additionally, testing must also be conducted on tailings, mine waste and low-grade ores to determine the possible environment impacts of storing these materials on the surface.

This presentation (no paper) provides examples of this concept discussing several case studies.

We Need to Talk About Engineering

J Pease¹

1. Principal Consultant, Mineralis Consultants, Level 1, 42 Morrow St, Taringa, Queensland 4068, Australia, jpease@mineralis.com.au

ABSTRACT

The efforts of those in minerals sector to reduce emissions should include management of undesirable impurities during processing. The growing issue of arsenic in copper concentrates will be discussed. Inevitably, this requires considerations of commodity demand, comminution, fertilisers, construction, artificial Intelligence, recycling, motorcycles, desert ecosystems, and the zombie apocalypse.

Such a path inexorably leads to an uncomfortable conclusion: *we need to talk about engineering.*

ENGINEERING AND SOCIETY

My first lecture at university was “Engineering and Society”. Two comments struck me:

- The first, was that engineers saved at least as many lives as doctors because they built water storage and distribution, sanitation systems, transportation infrastructure, and chemical plants (e.g., fertilisers), that were fundamental to the improvements in life expectancy and quality of life.
- The second was a range of definitions of what an engineer does. The one that most resonated was “*An Engineer is someone who can do for 20 cents what any fool can do for a dollar*”.

I knew the last comment was pithy. The older I get the more I see it is profoundly wise. And that it extends to environmental impact, not just cost – that is, an engineer is someone who can provide what society requires for 20 units of environmental impact that what any person could do with 100 units of impact.

ARSENIC AND ORWELL

The arsenic content of traded copper concentrates has been slowly increasing. This is partly because of some new, high arsenic concentrates, but also because of increases in the baseload copper concentrate as existing major producers mine deeper. Their arsenic assay is still below smelter and penalty limits, but they produce so much concentrate that a small increase in arsenic assay means a significant increase in contained tonnes.

This problem will get worse because we need huge increases in copper production – at least double the current production rate by 2050 – to meet renewable energy targets. Many of the largest known copper deposits remain undeveloped because they are too high in arsenic – some of the copper occurs in arsenic bearing minerals like enargite and tennantite which mineral processing can’t separate from “clean” copper sulfides. They will require arsenic removal at the mine site, e.g., roasting or leaching, before sale. Only a small fraction could be blended with existing concentrates to meet smelter limits.

Anyway, blending doesn't remove any arsenic. It just dilutes it. The downstream smelter still has to remove, and safely fix and store, the increased mass of arsenic. Even if we miraculously find and develop other low-arsenic ores to meet projected 2050 demand, doubling copper production would still at least double the units of arsenic in smelter feed. More likely the arsenic units will quadruple at least - unless we do something different.

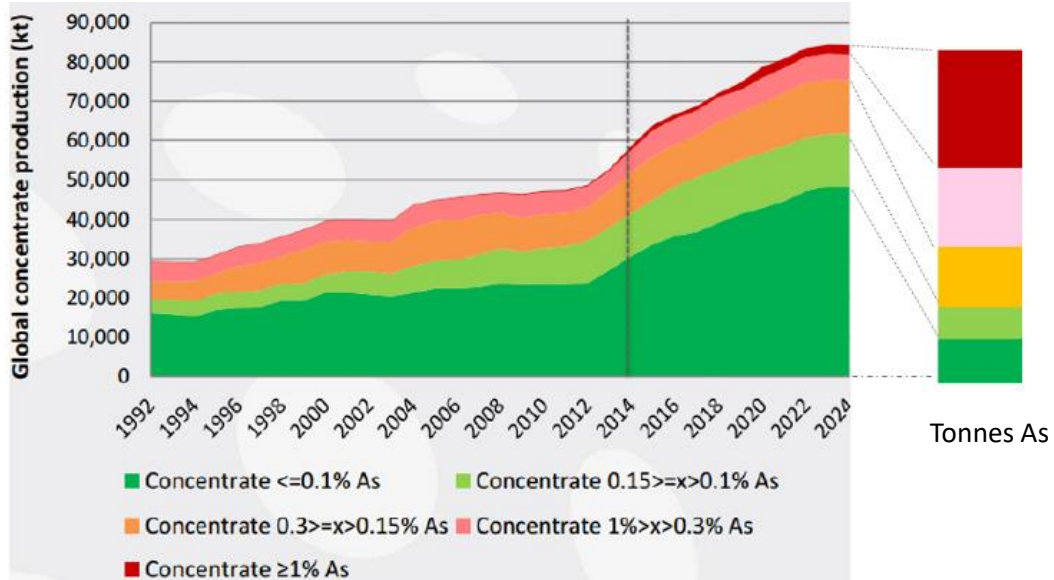


Figure 1: Arsenic content in traded copper concentrate. From Plint 2018, “Tonnes” bar added by author.

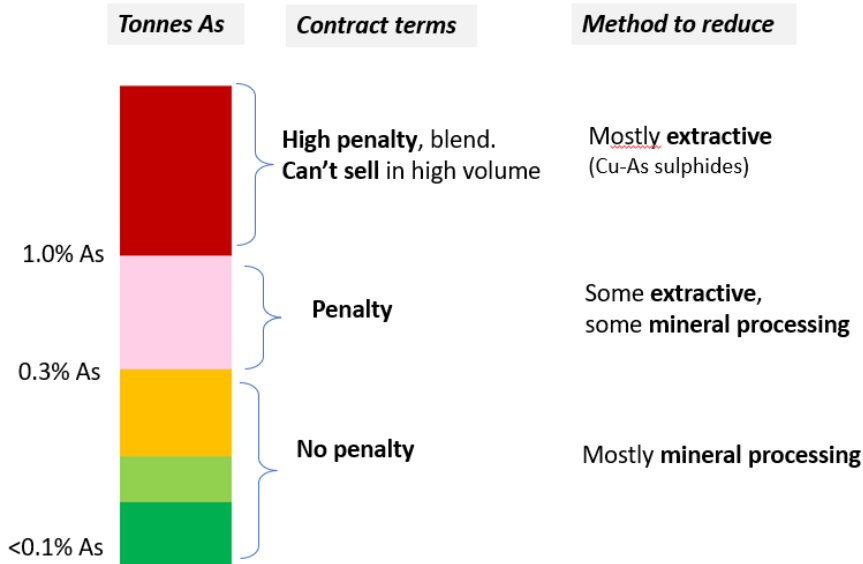


Figure 2: Contract terms and treatment options for arsenic in traded concentrates (compiled from Alvear et al 2020, concentrate contracts, and industry data, including Wood Mackenzie and Mineralis)

The arsenic in naturally occurring sulfide minerals is generally not bio-available. If we can remove it at the mine site we can dispose of it in this natural form in a remote, often arid and non-arable region. But smelting concentrate converts arsenic to bio-available compounds which need to be chemically “fixed” in a safer form. Most smelting occurs in an urbanised area or farming region.

Downstream copper smelting is dominated by China, so in the words of Police Chief Wiggum from the Simpsons, “It’s China’s problem now”.

An article in “The Economist” (2018) spoke of the consequences of impurities released during smelting:

“Tang Donghua, a wiry 47-year-old farmer... points to a chimney around 2km away that belches forth white smoke. It belongs to the smelting plant which he blames for bringing pollution into the valley. Cadmium is released during the smelting of ores of iron, lead and copper”. “China is trying to feed a fifth of the world’s population with a tenth of the world’s arable land”... “...national soil survey showed 16.1% of all and 19% of farmland (250,000km²) was contaminated... equivalent to the arable farmland of Mexico”. “Cadmium and arsenic were found in 40% of the affected land...35,000km² is so polluted that no agriculture should be allowed on it at all”. “...water along 18% of the length of China’s rivers was too polluted for use in agriculture. It is used anyway”.

We could conclude that, as much as possible, we should remove and safely store as much arsenic at the mine site. How to do that depends on the mineral occurrence of arsenic (Figure 3):

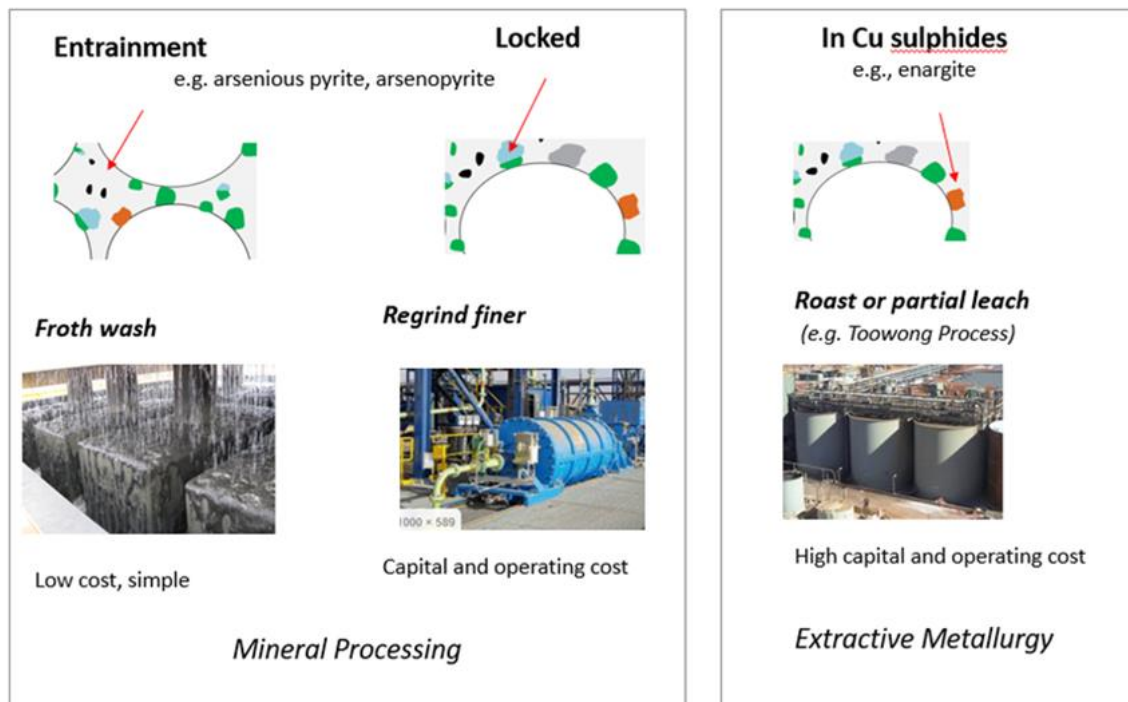


Figure 3. Options to remove arsenic at mine sites (Pease, 2019)

- For non-copper bearing minerals, arsenopyrite and arsenical pyrite, it is purely a mineral processing problem. If we regrind finer and employ good froth washing practice, we can reduce arsenic content.
- Minerals that contain both copper and arsenic, enargite and tennantite, are more problematic. To recover the copper we must recover the arsenic. This requires at least partial extractive processing on site, e.g., roasting or leaching to remove arsenic before concentrate dispatch, then securely “fix” the removed arsenic in a long-term stable form for storage near the mine site.

For ores that require the extractive processing option, the removal and storage path is more complex, but the extracted and fixed arsenic can be stored in an area that is generally remote from farming and water courses. But for those ores where mineral processing can reduce arsenic, there are few technical hurdles, only economic. Finer regrinding and better cleaning incur capital and operating cost, and if the concentrate is below the “penalty limit” (Figure 2), or can be blended below the limit, then there is no benefit from the concentrate contract.

So, a tonne of arsenic in some concentrates is a problem, while a tonne of arsenic in other concentrates is not. George Orwell (1945) may smile wryly and paraphrase “Animal Farm” to observe that *“all arsenic is created equal, but some arsenic is more equal than other”*.

Many copper producers could increase concentrate grade and reduce arsenic by finer regrinding and additional cleaning. They don’t do this because the contracts don’t reward it. Further, with good intentions, they discourage projects that increase energy consumption per unit of product. Perhaps they could reduce arsenic in concentrate, but that requires energy and they are committed to reducing the CO₂ footprint per unit of copper.

Regardless of its long-term impact, we need CO₂ to enter the food chain. We can’t say the same for arsenic. Even Mr Orwell may be surprised by our choice of which emission to address first.

ZERO EMISSIONS AND SECOND LAWS

Our companies have committed to Net Zero emissions. That is a noble objective. But it is not possible. We have to choose between Zero Emissions and the Second Law of Thermodynamics.

Producing copper – or any other commodity - requires sequential removal of every other element in the periodic table that nature so carelessly reacted, mixed and petrified with it. We have to unwind billions of years of entropy; to unscramble and un-cook the egg to recover the 1% component that we seek. That takes energy and creates waste – pretty much the other 99% of the elements in the orebody, plus all of the inputs required to unscramble them. This results in emissions including dust, noise, waste rock, tailings, slag, leach residues, fumes and off-gases. Selectively removing one emission requires extra work, which inevitably requires more energy and creates other emissions. Even recovering other payable metals is usually inefficient - we *could* produce iron and high-grade silica from copper tailings, but that would usually be wasteful of energy, materials and emissions compared with using iron ore and clean silica sand.

I know what our companies *mean* by “Zero Emissions”, but that is not what the words *say*. Yes, that observation makes me sound like an on-the-spectrum engineer. But if engineers permit the misperception that we can massively increase the world’s mineral production without similarly increasing emissions and physical footprint, then we shouldn’t be surprised when people protest about the very mines required for renewable energy.

Engineers work for society, to get the outcomes it requires with the lowest impact. Saying “Zero Emissions” when we really mean “an awful lot more emissions, but less CO₂” does not inform society on how to best balance environmental impacts. It sounds like a case of “Newspeak”, which Orwell (1949) described as *“a language designed to diminish the range of thought”*.

THE KINETICS OF SUPPLY

We have all heard the forecasts of the massive increases required in mineral supply to meet renewable energy targets. A thorough demand analysis was done by Michaux (2021), and multiple sources were reviewed by Meinke et al (2023) at the MetPlant 2023 Conference. Forecasts vary

widely depending on the assumptions made, but typically they report that in the next 27 years, copper production has to double, nickel production increase four times, and battery minerals such as lithium and vanadium must increase by around 20 times. The smallest increase, for copper, is equivalent to another 17 Escondida's or 600 Cadia's - plus more to offset the decline from existing producers.

Understandably, our mining leaders say that will be “challenging”, and will require new paradigms for exploration, discovery, permitting, government and community support, construction and ramp-up. That seems a polite way of saying that it can't happen.

Chemical engineers know that demand won't increase this quickly anyway. The forecast for each metal or mineral is made independently, assuming that all other materials are available. In reality, the whole basket will be limited to the pace of the “rate-determining-mineral”. If battery minerals don't increase by 20 times, then copper doesn't need to double. If copper doesn't double, then we can't produce the goods that need the other minerals. Whichever mineral is rate-determining will constantly vary as we develop efficiencies in use, better and longer-life batteries, and alternative technologies and materials. Nevertheless, we can be sure that all minerals cannot all advance independently on all fronts at full pace, even if we did have identified resources. Our leaders and policy makers would be wise to consider such supply kinetics when committing to the pace of change.

Meanwhile, the forecast increases in demand rarely include the number of engineers required to support the transformation in global energy and transport infrastructure, and the expansion in minerals mining and processing to support it. Just as we need to be urgently searching for new orebodies, we need to urgently train a larger cohort of engineers for the new economy.

That is, unless advances in areas like artificial intelligence (AI) can reduce the demand.

DATA AND AI

It is safe to assume that in future, most people will get most of their information from Google searches and AI queries. That puts a new responsibility on engineers. Language-based AI reads everything it finds and uses algorithms to estimate the most likely answer. Like a big version of autocorrect or autofill. Using the weight of words is fine for things that can be described by words, but not so good for things that need to make new measurements and perform complex calculations. Of course AI models can be trained for specific complex tasks – but those are not the models consulted for general public queries.

It doesn't matter if a thousand people have written that a bridge is safe – not if there is *one* good structural engineer who has recently measured and calculated that it isn't.

It was recently reported that Escondida is going to use artificial intelligence (AI) to improve its copper recovery. That will work if the AI model is specifically trained to interpret the mineralogy; to calculate the behaviour of the fundamental building blocks of performance - the mineral-size-liberation fractions. It would need to understand both how those building blocks behave *now*, and how they *would* behave for various circuit changes and operating changes. If it discounts or disregards opinions formed from inferior data or from other ores and different mineralogy. So AI will succeed if it is specifically trained on the fundamental root-causes of performance for this ore. But if it is a more general, language-based model that most people are familiar with, it could read millions of pages based on inferior data to find an inferior answer. Even if it quotes that answer with 95% certainty.

Engineers can't influence the way that most people use AI. This means we have an increased responsibility to speak and write about engineering in the public domain. Because if it isn't found by a general language-based Google or AI search, then for most people it simply won't exist.

MR 10% AND MISS 0.6%

Mineral processors scold ourselves by reporting that comminution consumes 2-3% of global electricity. The source of that number isn't clear, but it is thought the estimate was made in the 1970s and includes comminution for cement production as well as traditional "mineral processing". Steve Morrell (2023) calculated the number from more recent and comprehensive data. Using several different approaches, he estimated that mineral comminution now uses 0.6% of global electricity. The difference from the previous estimate may be due to three factors: exclusion of cement, a more extensive database, and significant increase in, and the composition of, global electricity demand. In the 1970s there were less air-conditioners, fewer appliances and no electric cars. And there was no consumption category called "data". Today data uses around 10% of global electricity¹, and is forecast to grow to 20% by 2030 (Lovel, 2018).

We don't see the energy cost of data because we don't pay for it. It is paid for by those annoying advertisements that pop up for whatever it was you recently searched for. Many data centres use renewable energy, but that is because they can – they don't need to locate near an orebody or manufacturing, a deepwater port, employment or consumption hub. Their "orebody" is energy supply, their market is virtual, so they can locate near the solar or wind farms to get first access to renewable energy. The ability to jump to the front of the queue doesn't make one industry more virtuous than another.

Information technology and data have improved our lives in many ways and can immensely improve our productivity (though parents of teenagers may disagree). But it is highly energy intensive, with more people with more phones taking higher-resolution photos and videos, shooting, sharing, storing and accumulating 10 MB and larger files "in the cloud". Just as plastic accumulates in the Pacific, and endlessly consumes energy.

When was the last time your computer suggested you store something on a hard drive rather than the cloud? Who spends Sunday afternoon deleting all but the best of the multiple sunset, scenery or social photos from their phone? Processing engineers spend their lives trying to improve comminution efficiency; so it is depressing to think that society may now use more energy storing surplus selfies, sunsets and social media posts.

¹ The estimate varies between sources. Data centre use is variously reported between 4% and 10% of global use; it isn't always clear if this is % of global energy or % of electricity. Some sources report "data centres", others as the broader "ICT". Lovel quotes ICT as % of electricity, making it comparable with the Morrell estimate for comminution. One source compares electricity with liquid fuels, saying data centre energy use is equivalent to the energy use of global aviation.

So I don't think it is inappropriate to suggest that a good engineer who knows where and how to look might find the key to improving recovery more efficiently than AI. And when the big consultancies tell us that we should use more big data to improve processing efficiency, I may not disagree, but I can't help thinking peevishly: *So, Mr 10% is telling Miss 0.6% that she needs to lose weight?*



Figure 4. The ever-expanding data lake (an artist's impression, in plastic).

THE HEIRARCHY OF BUILDINGS

If you need to build a new house, you want a good builder. You don't want his or her opinion on whether you need a new house, or need one that big, or whether you should even live in this suburb. All you want to know is: *what has to be done, how much will it cost, and how long will it take.*

If the answer is unpalatable – the cost too high, it will take too long, they will have to remove beloved trees – then you ask what options are available. Perhaps you need to scale down your plans, or live with relatives for an extra year during construction. You may not like what the builder said, but you respect the honest (and opinion-free) assessment. What you *don't* want is a builder who accepts the job without telling you that it can't possibly be done in that time or for that cost. You know that will result in an even higher price from variations, delays and aggravation.

Good engineers aspire to be like the good builder, even if the facts aren't always welcome or if it means they don't win the job. And yet...this isn't always the best outcome for society. Consider the Sydney Opera House. The good builder might have said "*It can't possibly be built for that much and it will take far longer than you think. And the acoustics won't be great.*" If we had known how long it would take and how much it would really cost, we might not have got something beautiful. Similarly, cathedrals, majestic bridges, research telescopes and spacecraft show that engineers can build beautiful things that enrich life. It's just that we spend most of our time meeting society's more prosaic needs.

That is, we mostly work at the bottom of Maslow's (1943) Hierarchy of Needs. We focus on satisfying the fundamental needs of food, shelter, water, warmth, sanitation, energy supply, materials transportation and public health. Simple shelter is a basic need, the Opera House is a higher need. It doesn't really matter if it is massively over budget and more than a decade late, so long as we still have food, shelter, and electricity for warmth and cooking.

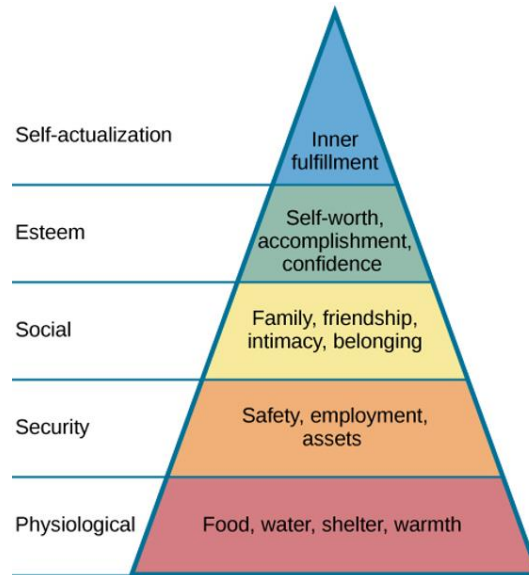


Figure 5. Maslow's Hierarchy of Needs

In wealthy societies, we have got so good at providing the basic needs that they seem to be taken for granted. No one wants to know how the sausages are made or what happens to sewerage. We quietly provide the basic needs, allowing polite society to focus on higher needs.

FOOD

Food is the most urgent human need. At the time of my first engineering lecture – not too many years before “Live Aid” - the world's population was 4.5 billion, and a significant amount faced malnutrition or starvation. In the four decades since then, population has grown to eight billion and there is less malnutrition and higher global life expectancy. That is remarkable.

This has required significant improvements and growth in farming and transportation. A critical factor was the wider application of phosphate-, potassium- and nitrogen-based fertilisers. The scientific and engineering scholar Vaclav Smil (2017 and 2022) identifies the four critical pillars of modern society - steel, concrete, ammonia and plastics. Smil calls them “pillars” because they satisfy the bulk of our “Level 1” needs for food, shelter and warmth. The close relationship between population growth and production of ammonia, the precursor to nitrate fertiliser, is shown in Figure 6.

Quite simply, without low-cost access to ammonia, we could not feed eight billion people.

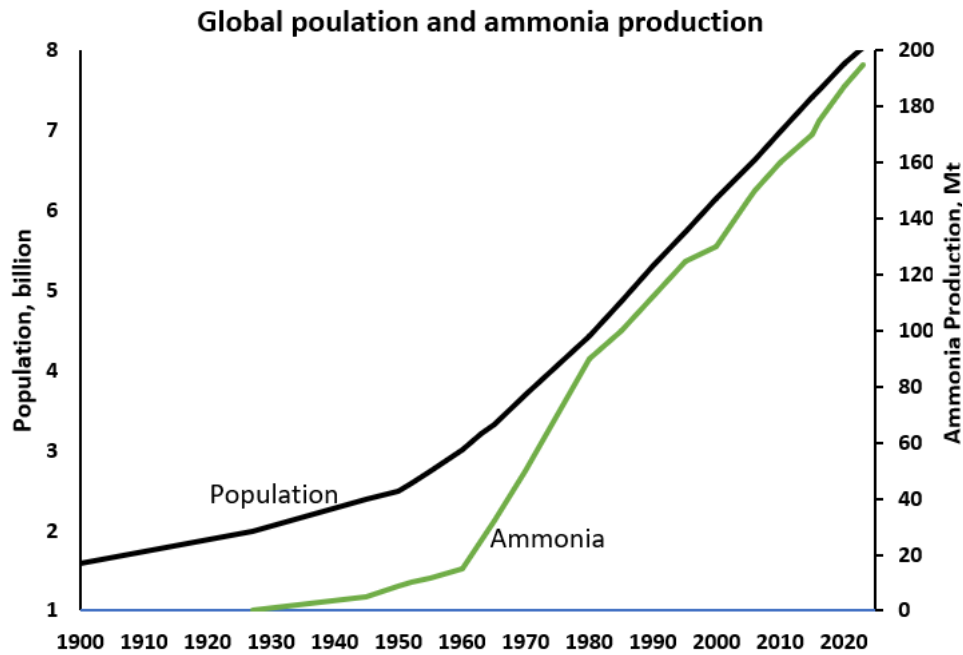


Figure 6. Global population and ammonia production (compiled from United Nations (2023) and Rowenhorst et al, 2022)

Recent reports in *pv magazine* (Carroll, 2022; Hamilton & Herben, 2022) described the installation of a “green ammonia” plant to supplement the production of an existing facility in the Pilbara region of Western Australia. The existing plant uses grid power for energy and natural gas as the feedstock for the Haber-Bosch process to combine hydrogen and nitrogen to form ammonia. The new plant will use solar power to generate and lithium batteries to store energy to hydrolyse water to create the hydrogen source for conversion. The articles showed the footprint of the current and proposed plant (Figure 7). It reported the new installation will produce 600 t/y of ammonia, at a cost of AUD 87.1M.

A more curious reporter might have researched further. The output of the existing plant (unshaded) is 840 000 t/y NH_3 compared with 600 t/y from the new (shaded) plant. So it would take 14 000 of the new plants to match existing production. That is a lot of desert ecosystem covered by a glass monoculture, and a lot of Cape York sandhills to be mined, transported, and manufactured into solar panels. There are unlikely to be significant economies of scale in the technologies employed - perhaps the opposite, since the 14 000th installation would be some distance from the hydrolysis plant, and therefore require more cabling per MW. Assuming each unit is the same cost as the first, replacing the existing plant would cost AUD 122.7 billion. That is more than the AUD 105.8 billion that the Australian government will spend on health in 2022-23 (Vines, 2023), for only a portion of the world’s fertiliser precursor. The intentions are good and the technology is interesting, but it isn’t clear that it is the **best** technology to affordably feed eight billion people with the lowest environmental impact.

It is not an engineer’s job to say which technology is the right choice; our job is to present the costs, impact and timing of different alternatives. For example, we might compare the cost and environmental impact of this installation with the same facility using nuclear energy; just as Microsoft is considering using small modular nuclear reactors to power its AI data centres (Business Today, 2023). Or using natural gas as the hydrogen source and solar energy for conversion to ammonia.

Presented with the dispassionate alternatives, society can decide the best option.



Figure 7: Yara International's proposed green ammonia plant (Carroll, 2022)

POLITICS, RELIGION AND SEX

Perhaps there was a golden age when engineering talk was welcome at social gatherings. When guests marvelled at the latest advances in public sanitation ("*You simply flush??!*"), swooned at the possibilities from international travel measured in hours rather than months, and hung off every word about machines to do their work, beaming talking movies in their homes, building affordable cars for the masses, and the prospect of space exploration.

No more. Before I learnt to hold my tongue, whenever I felt an engineering perspective would be helpful it went badly. People do not want to hear that ticking the "carbon neutral" box doesn't really reduce aircraft fuel consumption. That electric cars aren't really "zero emission". That consumption is the root of the problem - not the plastic bag it came in. That recycling isn't actually like those continuous circling arrows, it is a decreasing spiral, shaped more like a mosquito coil. Every time we unscramble the egg it consumes energy and recovery; at 75% recovery there is essentially nothing left after ten cycles. That of course recycling is good, but it doesn't provide confessional absolution for consumption.

That until alternatives are in place, we still need to use gas to produce affordable fertiliser – otherwise we can't feed eight billion people.

No matter how polite and dispassionate my words, they were always received as hostility. In a previous time we were advised to never talk about religion, politics or sex at social gatherings. Now the taboo is engineering. Indeed, when you talk about engineering, it seems you inadvertently and inappropriately spoke about two of the old taboos, and ruined any chance you might have had on the third.

Robert Pirisig (1974) referred to a similar experience in his book "*Zen and the Art of Motorcycle Maintenance*". He recounted a time when he helped some fellow travellers repair their motorbikes.

He thought it helpful to explain what he was doing so they could fix it themselves next time. Rather than gratitude, his explanation evoked anger. His companions rode bikes to feel the wind in their hair on the open road, to be at one with nature. They did not want to hear that such freedom rides on specialty alloys, high tolerance machining, and hydrocarbon fuels and lubricants. Pirsig referred to “classic” (science-based) and “romantic” notions. He noted that:

“Although motorcycle riding is romantic, motorcycle maintenance is purely classic”,

and

“This divorce of art from technology is completely unnatural. It’s just that it has gone on for so long you have to be an archaeologist to find where the two separated.”

THE LAST OF US

If engineering talk is unwelcome at social gatherings, it is especially unwelcome at home. Whatever was I thinking when I said to my children *“well, if you want to help, you could turn the lights off when you leave a room and have shorter showers”*. That did not go well, so I decided not to suggest they spend Sunday deleting obsolete photos from the cloud. I mostly now remain silent; I withdrew vocally but act locally. Every Tuesday night, under cover of darkness, I sneak outside and sift through the recycling bin, removing incorrect items placed there with good intentions and at the urging of those misleading arrowed circles. As a processing engineer, I know how hard it is to unscramble the egg, even worse when someone introduces tramp scrap to the feed. So long as my family don’t discover my nocturnal hand-sorting, we all sleep peacefully on Tuesdays, each of us content that, in our own way, we all did our bit to help.

Life is much smoother since I withdrew vocally. We enjoyed the rarity of watching a series together, at weekly intervals, rather than individual binge streaming. *“The Last of Us”* is set 20 years after the zombie apocalypse. Unfortunately, it stretched reality just a bit too far for me. Not the bit about zombie forms that suck every essence of life, even the very will to live itself, from you. No, that part isn’t a stretch for anyone who deals with corporate procurement systems. Rather, it was when the main character, Joel, risks his life and possessions to get a car battery so he can seek his brother. I knew it wouldn’t be appreciated, but I blurted *“Don’t! It is a lead acid battery that hasn’t been used for 20 years. It won’t work!”*.

Well, I was right and I was wrong. I was right that it wouldn’t be appreciated. And I was wrong about the battery. Not only did it work, but the fuel in the tank hadn’t degraded and the tyres were fine. Everything worked beautifully after 20 North American winters.

To an engineer, that is the **real** science fiction!

DOGS, DOCTORS, AND GOOD INTENTIONS

I have become discontent with my “withdraw vocally, act locally” approach. I feel obliged to do more, yet it always ends badly. I search for the right words, the right moments, the perfect tone. I practiced with my dogs. They like me. They don’t care if I am on the spectrum so long as I am on the walk.

In the manner of dogs, after they do their business they furiously scratch the ground, scattering grass, soil and pebbles in all directions – though with uncanny inaccuracy, *never* on the dropping itself. This is the moment to rehearse my recycling message: *“Girls, I really appreciate what you are doing. I can see you genuinely care and want to help. Thank you for that. Only...see how you used energy and the grass is torn up, but the dropping is untouched? Thanks for trying, but I will look after*

it". They look offended. So I get frustrated and I go too far. I always go too far. I say "well, if you really want to reduce your emissions, you could try eating less at night".

Fortunately dogs are more tolerant than people. They just look at each other with that look that I recognise so well; the one that says "He is **such** an engineer".

My sister is a doctor. She routinely delivers bad news – sometimes the very worst news – to patients. They don't get angry with her. I examined her approach: be polite, be compassionate, and be direct; nobody appreciates you drawing out or sugar-coating the message.

Well, no insights there. That approach doesn't even work with my dogs.

But finally I understood. A doctor's bad news merely questions your future existence. You don't think she is questioning your beliefs and good intentions.

ACTORS, SPORTSMEN AND ENGINEERS

We need to talk about engineering, not politics or policy. We each have our own views, but, like actors and sportsmen, we are well-advised to keep them to ourselves. Policy is not our job and not our specialty. Our job is to dispassionately develop and enumerate the options. Then society decides the best way to allocate limited resources to balance its needs with costs and environmental impact.

But there is a bias in the model. Google searches and AI queries are influenced by the weight of words. And it is much easier to write frequently and beautifully about how we think the world **should** work, rather than painstakingly researched and evidenced descriptions of how it **does** work.

WE NEED TO TALK ABOUT ENGINEERING

I have realised that I cannot talk about engineering without causing offence. I hope others have found the right words and tone, but I haven't.

But I have decided that I have to talk about it anyway. Society needs engineering more ever. The transformations proposed for the next 27 years have been compared with the scale of the Industrial Revolution – only **much** faster. The changes will need an increase in minerals supply that is unimaginable to those in the resources industry. Society has an urgent need for scientific and engineering breakthroughs, for development of arrays of options, for collecting data to inform wise policy making, and for the education and development of armies of engineers.

We are going to have to engineer the hell out of this. The pace will be frantic, the duration exhausting. We don't have time for wrong turns or poor decisions, not matter how well intended they are or how eloquently they are expressed.

And as difficult as it is, not only do we have to **do** the engineering, we simply must **talk and write** about it too. Because if it isn't found by a general Google search or AI query, then for most people it won't exist.

And if **we** don't talk about engineering, then the vacuum will be filled by others. Society will be increasingly informed by beautifully expressed opinions on **what sounds good** rather than **what works**.

And that is not a sound basis for an industrial transformation.

REFERENCES

Plint, N, "Arsenic Removal by Mineral Processing", presentation to JOGMEC International Seminar on Impurities in copper raw materials, Tokyo 2018

Alvear Flores, G, Risopatron, C, Pease, J. *“Processing of Complex Materials in the Copper Industry: Challenges and Opportunities Ahead”* JOM, The Mining, Metals and Materials Society, 2020.

Pease, J, *“Impurities in Copper Concentrates”*, presentation to Aurubis Minor Metals Symp, Lisbon 2019

Article *“The Bad Earth”* in The Economist, June 8th 2017.

George Orwell, *“Animal Farm”*, Published by Seker & Warburg, 1945

George Orwell, *“Nineteen Eighty Four”*, Published by Seker & Warburg, 1949

Michaux, S., 2021. *Assessment of the Extra Capacity Required of Alternative Energy Electrical Power Systems to Completely Replace Fossil Fuels*, s.l.: Geological Survey of Finland.

Meinke, C, Jackson, L, Erwin, K, Chandramohan, R. *“Assessing the Feasibility of Mining in Achieving Climate Change Targets Using an Energy Optimiser”*. Met Plants Conference, Adelaide 2023

Morrell, S. *“How to reduce the hard rock mining industry’s comminution carbon footprint by up to 40%”*. World Mining Congress, Brisbane June 2023.

Maslow, A *“A theory of Human Motivation”*, Psychological Review, 1941

Smil, V. *“How the World Really Works”*, Published by Penguin, 2022

Smil, V. *“Energy and Civilization: A History”*, published by MIT Press, 2017

Lovel, J. *Big Data – A big energy challenge?* Australian Energy Council, October 2018

Rowenhorst, K, Travis, A, Lefferts, L. *“1921-2021: A Century of Renewable Ammonia Synthesis”*, *Sustain. Chem.* **2022**, 3(2), 149-171; <https://doi.org/10.3390/suschem3020011>

Carroll, D. *“Yara confirms construction of Pilbara green hydrogen plant to begin in weeks”*, in pv magazine, September 16, 2022

Hamilton, S, Herben, E. *“World first certification of green ammonia plant in Australia”*, in pv magazine, October 31, 2022

Yara International website, www.yara.com/yara-clean-ammonia/

United Nations World Population Prospects/World Population 1950-2023, www.macrotrends.net

Vines, M. *“Health Overview – 2022-2023 Index”*, [Health overview – Parliament of Australia \(aph.gov.au\)](http://aph.gov.au), 2023

Dixit, P. *“Microsoft reportedly planning to use nuclear energy to power its AI data centers”*, Business Today, 26 September 2023

Pirsig, R. *“Zen and the Art of Motorcycle Maintenance”*, published by William Morrow and Co, 1974

Design and Commissioning of the Newmont Ahafo Mill Expansion

E Asakpo¹ and A Giblett²

2. Metallurgy Superintendent, Newmont Ghana Gold, Accra, Ghana.
Emmanuel.Asakpo@newmont.com
3. FAusIMM (CP Met), Director, Black Swan Metallurgy, Mindarie, Western Australia,
aidan@blackswanmet.com

ABSTRACT

Newmont Ahafo Mill Expansion project was successfully commissioned in the third quarter of 2019 and centred on the addition of a second primary crusher and a new 34 ft. diameter single stage SAG mill to complement the existing SABC circuit, commissioned in 2006. CIL circuit capacity was also increased in the expansion to accommodate the projected increase in mill throughput by over 50% to nearly 10 Mt/y. The expansion of the Ahafo processing plant will support increased gold production at Ahafo to 550 000-650 000 oz/y through to 2024, as well as reducing life of mine processing costs and supporting an extended mine life.

The comminution flow sheet selection considered both duplication of the existing SABC circuit and the addition of secondary crushing prior to selecting the final configuration. Flow sheet selection and circuit design is discussed in the context of a highly competent ore source, and the basis for the CIL circuit expansion is reviewed. The paper reviews early start up experiences and lessons learned.

INTRODUCTION

Newmont's Ahafo mine is located along the Sefwi Volcanic Belt, a northeast-southwest trending volcanic belt in Ghana. The mine is in the Ahafo region, approximately 307 km northwest from the national capital city of Accra. Mineralisation at Ahafo South occurs in two styles: Kenyasi and Subika. Kenyasi style has a metasedimentary rock footwall and a granitoid hanging wall separated by a thick zone of mylonite and cataclasite. Subika style has granitoid rocks in the footwall and hanging wall separated by mylonite zones.

Current mining and processing operations are located in the Ahafo South region depicted in Figure 1, distinct from the undeveloped Ahafo North project area. Commercial production at Ahafo began in 2006 and current operations produce over 400 000 oz of gold per year. Active mining operations at Ahafo commenced in 2006 and have historically focused on open pit mining. In November 2018, the Subika underground mine achieved commercial production, adding higher-grade, lower-cost gold production.

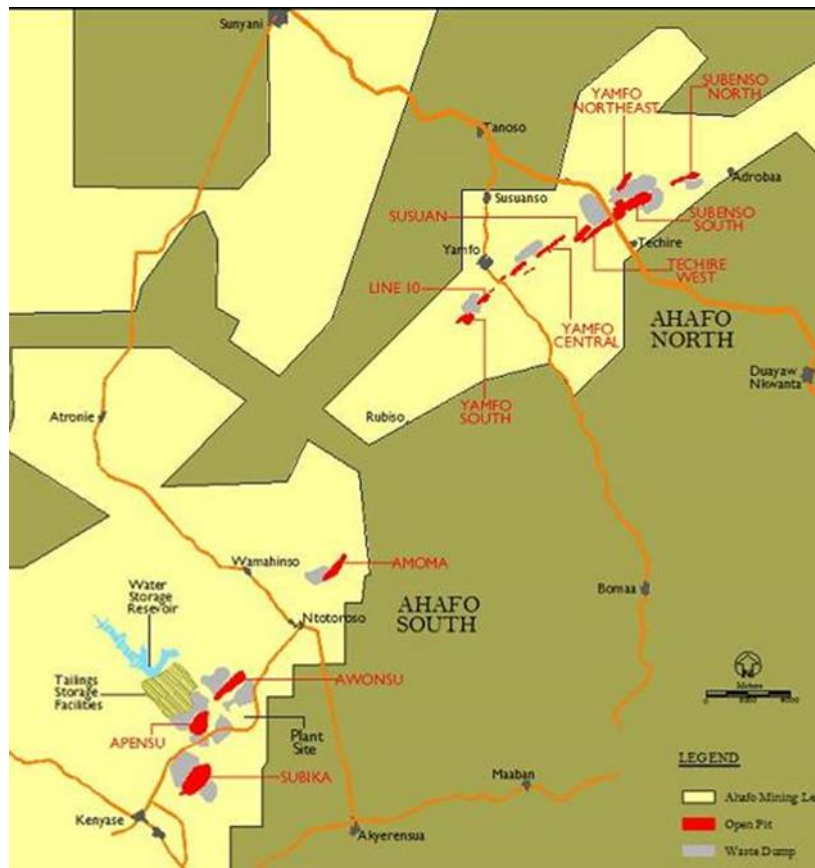


Figure 1: Ahafo South Mining Operations and Ahafo North Project Area

The recently executed Ahafo Mill Expansion was designed to maximise resource value by improving production margins and accelerating stockpile processing. The expansion supports more efficient processing of harder, lower grade ore from existing Ahafo surface mines as well as profitable development of Ahafo's highly prospective underground resource.

The Ahafo Mill Expansion has increased mill capacity by 52 percent through the addition of a new primary crusher, coarse ore stockpile, single-stage Semi-Autonomous Grinding (SAG) mill, and additional leach tanks. Installing this equipment improves flexibility as mine production fluctuates and supports higher processing volumes needed to offset the impacts of lower grades. Combined with the Subika Underground operation commencing operations in 2019, the expansion is expected to increase Ahafo's average annual gold production to between 550 000 oz and 650 000 oz a year until 2024, while reducing life-of-mine (LoM) processing costs.

OPERATIONS OVERVIEW

Open pit drilling and blasting is performed on 8 m benches using D45KS blasthole rigs and 165 mm diameter holes. The typical blast pattern in waste is 3.7 m by 4.2 m and ore is 3.5 m by 4.0 m.

The Ahafo process plant makes use of conventional gold processing methods to treat both oxide and primary ore. The mill feed currently is a mix of primary ore hauled from the Subika and Awonsu open pits, the Subika underground operation and stockpiled ore from previous open pit mining of the Apensu and Amoma pits. Processing operations are distinguished by the original (Line 1) SABC comminution circuit, and the new (Line 2) AME primary crushing and single stage SAG milling circuit. The original design capacity of the plant was 7.5 Mt/y on a 70/30 primary/oxide ore blend, decreasing to 6.0 Mt/y on 100% primary ores following the depletion of near surface oxide ore. This has been increased to 9 Mt/y with the addition of Line 2.

Subika underground and open pit ores are extremely competent and have been demonstrated to be severely SAG mill limiting ores when processed through Line 1. Early studies considered the addition of secondary crushing ahead of the SAG mill to debottleneck the grinding circuit, and large scale expansion studies considered an unconventional grinding circuit power split to recognise the requirement for a bias in the grinding circuit power split towards the SAG milling duty. Figure 3 demonstrates the competence of the Subika resource by comparison to other regional and global assets, as defined by the SMC Test drop weight index value.

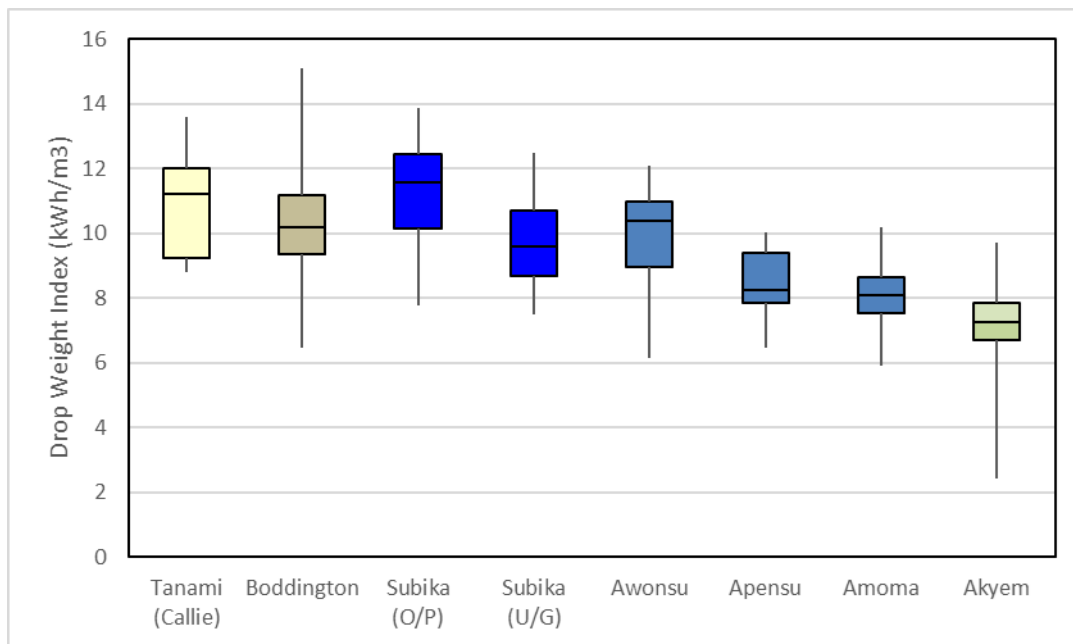


Figure 3: Database drop weight index properties for Newmont's Ghanaian and Australian resources

The option of a single stage SAG (SS SAG) mill for Line 2 was preferred on the basis of lower operating costs and higher plant utilisation than a secondary crusher based expansion. Higher project capital afforded a larger increase in overall plant capacity by comparison to pre-crushing of the SAG mill feed without the addition of further ball milling capacity, while maintaining current gold recovery levels. The SS SAG option also offered the flexibility to bleed Line 2 recirculating load (cyclone feed) into the existing Line 1 ball mill circuit when that ball mill was underutilised, allowing maximum power draw to be more readily achieved by all grinding circuit equipment.

Comminution circuit design and options analysis for the Line 2 expansion relied heavily on established site and company protocols for throughput modelling. An extensive database of key ore properties (drop weight index and Bond ball mill work index) defines ore properties utilised in power based modelling (Morrell, 2006, Morrell 2009) techniques to predict the capacity of SAG and ball mill for each ore type. Linear regression models are then fitted to the power based model outcomes for each ore type, and consequently used to predict overall plant capacity based on the feed blends specified in the mine plan. This approach has consistently predicted monthly average instantaneous milling rate to within $\pm 5\%$, and annualised rates to within $\pm 1-2\%$.

The recovery assumptions for the existing line 1 recovery models have been used since 2014. The same approach was used for compiling the recovery models for each deposit to be treated through line 2 expansion. These assumptions are,

- Head and tail grade data for each deposit and grind size interval size were plotted.
- A power-based equation was fitted through the data points to provide a formula to be used

in recovery equations.

- The power based equations were then modified to account for soluble gold losses in the CIL tail and fine carbon attrition on the processing plant

The accuracy of these models were tested with plant data obtained from the Ahafo South Mill from 2013. The data included actual ore blends and head grades of each deposit that was processed at the Ahafo South processing plant on a monthly basis and the recovery reported. It was found that the recovery models under predict the achieved recovery by more than 4%. The recovery models compiled using the approach described above were modified to include an “upscale” factor of 1.04 and was subsequently used since 2015. The basis for the 4% upscale factor has been confirmed as being the result from a change in the particle size distribution between laboratory generated leach feed and plant leach feed. Figure 4 demonstrates the accuracy of the updated recovery models using the 1.04 factor at the Ahafo South processing plant over the previous seven years.

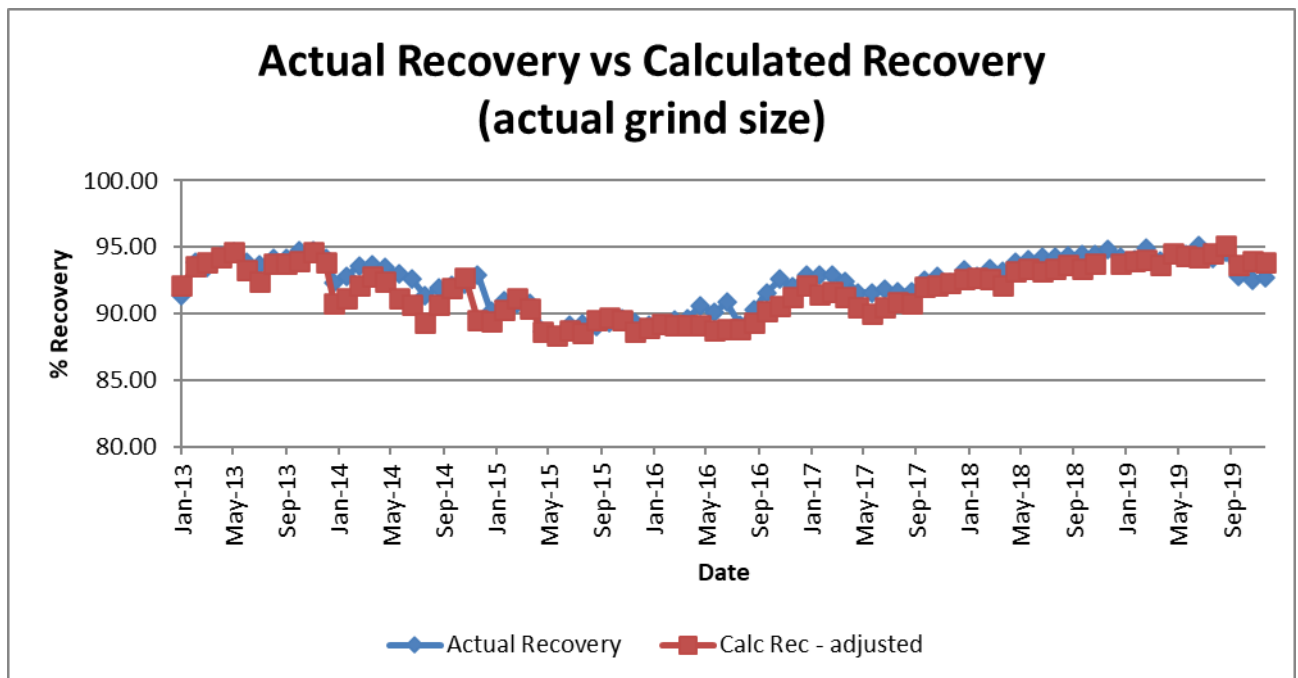


Figure 4: Modelled recovery rate versus actual performance over years 2013-2019.

The Line 2 SAG mill design leveraged a number of key features from the Line 1 circuit including turbo pulp lifters: dual pebble crushers and a double deck SAG discharge screen. At the same time the Line 2 design incorporated several changes including an integrated, reduced row shell lifter design; smaller pebble port apertures (70 mm vs 80 mm); smaller grinding media recharge sizes; smaller cyclones (20 in. vs 26 in.) and smaller pebble crushers (HP400 vs MP800). JKSimMet modelling was used extensively to support the design of the comminution circuit, leveraging the availability of existing simulation models for the Line 1 circuit and Newmont’s access to the Citic SMCC software.

The conversion from a straight ten-tank CIL circuit to a hybrid CIP circuit was supported by the use of the SIMCIL modelling program accessed through the AMIRA P420 research project website and maintained by Curtin University’s Gold Technology Group. This modelling work (Giblett, 2014) leveraged an extensive database of CIL circuit profiles for the existing plant which allowed the assessment of a wide range of operating conditions. This SIMCIL modelling exercise demonstrated current gold recovery levels could be maintained through the addition of two to three tanks, with no

value evident through the installation of additional tankage beyond that. As no material difference was evident if the tanks were installed in leach or adsorption configuration, the configuration of the new tanks as leach only vessels was preferred on the basis of lower operating costs.

COMMISSIONING

The commissioning stage consisted of separation of activities into three phases, pre-commissioning, cold commissioning, and hot commissioning. Pre and cold commissioning were performed by the EPCM (DRA Global), while hot commissioning was executed by the Newmont Owners team. Construction on the project peaked at 1200 workers during May 2019, with the last contractors and EPCM demobilising from site during December 2019. Prior to commissioning, ore was readily available on the stockpile to aid in the feeding of the new SAG mill.

The SAG mill started up without much difficulty and performed as expected with the exception of the SAG mill pebble dewatering screen, which failed shortly after the mill started. The failure was attributed to a fabrication fault and a new screen was installed a few weeks later. During start-up, the major focus of the team was to ensure that the operators were reacting appropriately to challenges and that the equipment functioned as expected. As the Line 1 SAG mill operates essentially in fixed speed mode, and the Line 2 SAG mill is equipped with a variable speed drive, the operators required some instruction on the appropriate use of mill speed to control mill weight. The training of personnel in operating Variable Speed Drive Mill without Optimisation Control System (OCS) prior to commissioning resulted in ramping up more quickly than expected and was a major success.

As the OCS was not available at the time of commissioning the commissioning team had to rely on the load cells, feed and discharge end bearing pressures and most importantly the power draw to estimate the total charge (load) and ball fillings. The metallurgical department utilised the tumbling mill power draw developed by Morrell (1993) and an in-house ball load estimation model to identify optimal operating conditions through the ramp up period. The Milltraj software was used also to guide mill speed settings to consider charge levels and toe position, to minimise the potential for liner damage during ramp up. This analysis specified the mill weight required to operate at a particular speed, for a given ball load. An example is shown graphically in Figure 5.

The first fill ball charge used was an approximately evenly weighted distribution of 3 in., 3.5 in., 4 in., 4.5 in. and 5 in. balls; in order to replicate the graded charge distribution that would be reflected by an ongoing make up charge of 4.5 and 5 in. balls.

The first ore through the SAG mill and primary crusher was achieved on the 1st and 28th of September 2019, respectively and commercial production was declared on the 15th of October 2019.

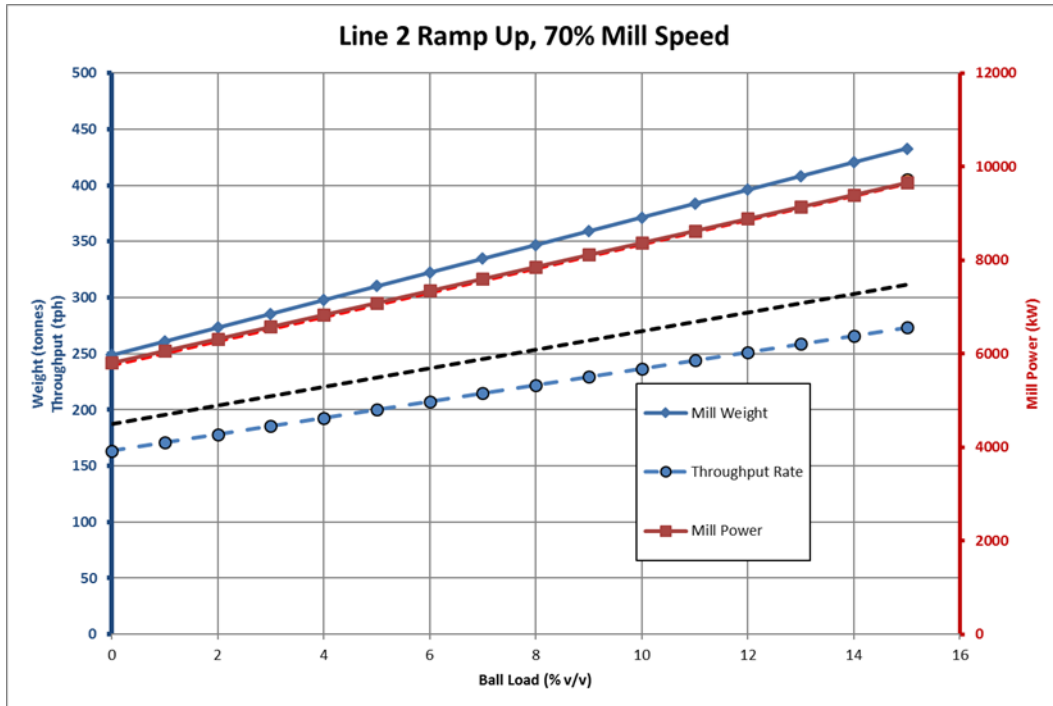


Figure 5: Sample SAG mill ramp up curve for Line 2 start-up.

RAMP UP PERFORMANCE

The ramp up of the Line 2 circuit is described in detail by Asakpo et al (2023). Early issues associated with mechanical reliability of the pebble crusher circuit and volumetric constraints of trash and interstage CIL screens were rectified in the 12 months following commissioning. At this time plant throughput rates remained constrained at 85-90% of nameplate capacity due to ongoing issues with SAG mill drive vibration at speeds above 65% of critical and low pebble crusher utilisation. After a program to diagnose and improve alignment between the motor, gearbox and pinion, the motor vibration issue was resolved in Q4 2020. This facilitated the ramp up to nameplate throughput rates from Q2 2021 onwards. Improved availability and operational control of the pebble crushing circuit from Q1 2022 allowed a product P80 of 12-13 mm to be sustained, and nameplate mill throughput rates and final grind size to be consistently exceeded as per Figure 6.

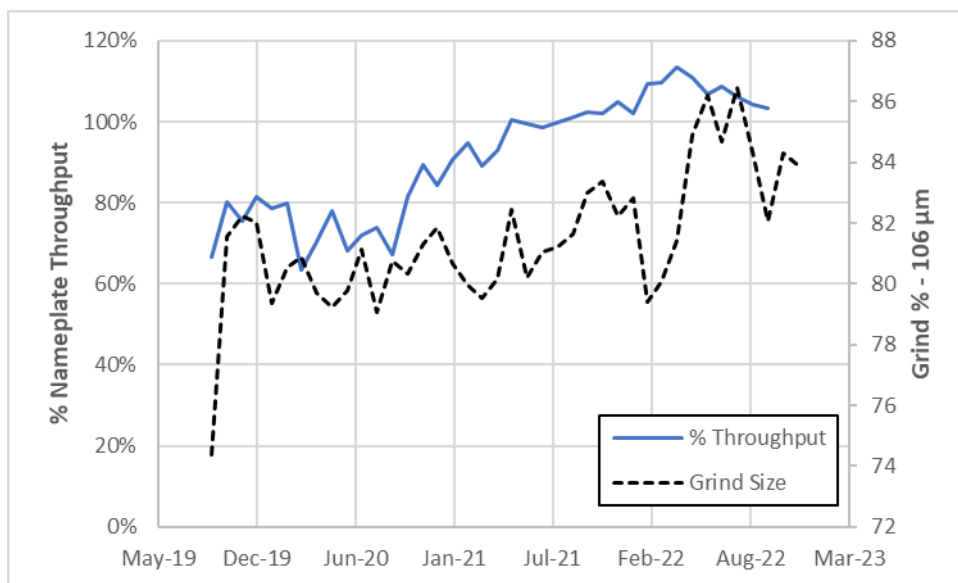


Figure 6: Line 2 mill throughput ramp up.

CONCLUSIONS

The Ahafo mill expansion project has been successfully delivered and will extend profitable production at Ahafo through to at least 2029, while further supporting the profitable development of additional resources in the Ahafo South area.

ACKNOWLEDGEMENTS

The authors acknowledge Newmont Corporation, Ahafo Mine for permission to publish this paper. The authors further recognise DRA Global for the successful execution and handover of the Ahafo Mill Expansion project. Special gratitude is also given to Francis Tenkorang and Enock Oteng Amponsah for their active involvement and tremendous effort in the compilation and analysis of plant data throughout this project. The authors also acknowledge the excellent work carried out throughout the phases of the commissioning by the entire process metallurgy, operation and maintenance team at the Newmont Corporation Ahafo Mine.

REFERENCES

- Asakpo E, Heath A and Chaffer S, 2018. Results from installing Turbo Pulp Lifter (TPL) in Ahafo SAG Mill. Mineral Engineering International Comminution 2018 Conference.
- Asakpo E, Amponsah E, Bonney-Noi S, Annandale D and Murphey K, 2023. Commissioning and optimisation of Ahafo Mill Expansion. (In press) International Autogenous and Semiautogenous Grinding Technology Conference
- Broussaud A, Legrand G, Kok D, Roux E, Guyot O and Revalor M, 2011. Integrated advanced grinding control system at Newmont Ahafo. Proceedings of International Autogenous and Semiautogenous Grinding Technology Conference, Paper 162.
- Dance A, Mwansa S, Valery W, Amonoo G and Bisiaux B, 2011. Improvements in SAG Mill throughput from finer feed size at the Newmont Ahafo operation. Proceedings of International Autogenous and Semiautogenous Grinding Technology Conference, Paper 11.
- Giblett A L, 2014. SIMCIL Modelling of the Ahafo 1X+ Project. Internal Technical Report, Newmont Corporation.
- Heath A, Chaffer S and Asakpo E, 2018. The development of optimised pulp lifter design for Ahafo SAG mill using discrete element method modelling. Proceedings of the 14th AusIMM Mill Operators Conference, pp. 578-593.
- Morrell S., 1993. The prediction of power draw in wet tumbling mills. Julius Kruttschnitt Mineral Research Centre, Department of Mining and Metallurgical Engineering, University of Queensland
- Morrell, S., 2006. Design of AG/SAG mill circuits using the SMC test. Proceedings of International Autogenous and Semiautogenous Grinding Technology Conference, Volume IV, pp. 279-298.
- Morrell, S., 2009. Predicting the overall specific energy requirement of crushing, high pressure grinding roll and tumbling mill circuits. Minerals Engineering 22 (2009) pp. 544–549.
- Van Huyssteen J and Cantor M, 2011. Continuous improvement initiatives at the Newmont Ghana Gold Limited Ahafo Mine. World Gold 2011 Conference Proceedings, pp. 129-142

Maximising Concentrator 1 Throughput at Cadia during the SAG 20MW Gearless Motor Drive Replacement

C Geoghegan¹, C Haines²

1. Specialist – Plant Metallurgy, Newcrest Mining Limited, Orange NSW 2800, Caitlin.geoghegan@newcrest.com.au
2. Superintendent - Metallurgy, Newcrest Mining Limited, Orange NSW 2800, Campbell.haines@newcrest.com.au

ABSTRACT

Concentrator 1 at Newcrest's Cadia Valley Operation is responsible for approximately 75% of Cadia's total milled production, with all material treated by the primary SAG mill within a unique HPGR-SABC circuit. In July 2021, the scheduled replacement of the Concentrator 1 20 MW SAG Gearless Motor Drive (GMD) took place. Spanning five months the SAG GMD replacement necessitated a major reconfiguration of the process circuit to maintain production during the extended SAG outage period.

The SAG GMD was installed in 1997 and had been identified as a material risk to production since 2015. Following a significant GMD winding failure event in 2015, infrastructure was installed to enable HPGR product to be re-directed from the SAG mill to one of the three secondary ball mills, thus converting the concentrator to a more conventional HPGR-ball milling circuit. This flow sheet is known as the 'SAG bypass' configuration, and prior to the SAG outage this configuration had only been in operation for a single ten-day period. In the 18 months leading up to the SAG GMD replacement, the site Metallurgical team initiated a SAG bypass throughput maximisation project, to exceed the previously demonstrated SAG bypass throughput rates. The execution of several initiatives, together with revised operating strategies, resulted in production rates far exceeding expectations. This paper examines the plant modifications and operational strategies that maximised throughput utilising a novel HPGR-ball milling circuit flow sheet.

Introduction

Newcrest's Cadia Valley Operation (Cadia) is located in the Central West district of New South Wales, 25 kilometres south of the City of Orange. The Cadia district has been an active mining area since the regional gold rush of the 1850s. Development of the Cadia Hill deposit in 1997 led to the establishment of the current Cadia Valley Operations, which has since been expanded to include the Ridgeway and Cadia East deposits. The Cadia East deposit is an orogenic porphyry Copper-Gold-Molybdenum deposit and at the time of writing the sole feed source to the concentrators.

There are two concentrators at Cadia: Concentrator 1 (formerly Cadia Hill) and Concentrator 2 (formerly Ridgeway). Both concentrators are fed from a common stockpile of Cadia East Ore. Concentrator 1 processes 75% of the ore whilst Concentrator 2 treats the remaining 25%. Concentrator 1 was constructed in 1997 and commissioned in 1998, including the world's first 40 ft SAG mill with a 20 MW Gearless Motor Drive (GMD). The commissioning challenges and repairs made to the GMD within the first decade of operation are documented (Meimaris et al., 2001) and (Gunn, 2006). The optimisation of both concentrators for processing Cadia East ore are documented by (Waters et al., 2018) and (Edmunds et al., 2021).

This paper discusses the continued operation of the Concentrator 1 circuit in a non-nominal flow sheet arrangement during the planned 40 ft GMD replacement in 2021. It examines the design philosophy, plant modifications and operational strategies executed which increased throughput to the theoretical maximum predicted by Morrell's power-based modelling approach (Morrell, 2019).

The project to replace the GMD and modifications to the non-comminution areas will not be discussed in this paper.

Background

Cadia East Ore Properties

The Cadia East mine consists of two macroblock caves (PC1 and PC2) which feed three ThyssenKrupp BK 63-75 primary gyratory crushers. The primary crushed ore is fed to the surface via an incline conveyor system at an F_{80} of 110 mm. Typical comminution parameters observed are displayed in Table 1. The belt cut parameters were used for predicting comminution energy requirements and guiding circuit assessments discussed later in this paper. The comminution data is compiled from regular monthly belt cuts on the individual crusher products and is comparable with the Feasibility Study (FS) design assumptions for Cadia East (Engelhardt et al., 2014)

Table 1 - Cadia East Ore Properties 2018-2019

	SMC Data								Bond Data			
	DWI	Mia	Mih	Mic	Axb	SG	ta	SCSE	BWI	Gbp	F_{80}	P_{80}
	kWh/m ³	kWh/t	kWh/t	kWh/t		t/m ³		kWh/t	kWh/t	g/rev	µm	µm
Belt Cut Data P95	10.3	26.2	21.1	10.9	36.2	2.9	0.3	12.3	21.4	1.1	2529	117
Belt Cut Data P50	8.9	24.1	18.9	9.8	30.9	2.7	0.3	11.3	20.3	1.1	2271	113
Belt Cut Data P5	7.8	22.1	16.8	8.7	27.3	2.7	0.2	10.6	19.2	1.0	2006	108
Cadia East Feasibility	10.0	-	-	-	27.0	2.7	-	11.3	21.5	-	-	-

Comminution Circuit Configuration

Nominal Comminution Flow sheet

The nominal flow sheet for Concentrator 1 is displayed in Figure . The nominal flow sheet is described in detail by (Waters et al., 2018). In summary, primary crushed material is reclaimed into Concentrator 1 and presents to the screening and crushing plant. Stockpile reclaimed ore is fed directly to a distribution bin which feeds two 7.3 x 4.25m double deck scalping screens with bottom deck apertures of 55 mm in closed circuit with two Metso MP1000 secondary crushers. Screen undersize combines with HPGR edge recycle and feeds to an intermediate stockpile. The intermediate stockpile is reclaimed to HPGR feed; the HPGR operates at near maximum power draw (5.6 MW), 160 bar roll pressure setpoint and operating gap of 60-70 mm to produce a P_{80} of 13-16 mm.

The HPGR product is the primary feed to the SAG mill, however the SAG also receives a bleed of primary crushed ore (~10-15%) – producing a uniquely bimodal feed, which has been documented in detail by (Waters et al., 2018). The high aspect SAG mill is 12.2 x 6.7 m in size (40 ft) and powered by a 20 MW GMD. The liner design for the SAG mill is uni-directional to optimize discharge efficiency, ball trajectory and liner life. The SAG mill product flows over a trommel with 15x35 mm apertures; trommel undersize is distributed to three parallel ball mills whilst the dewatered oversize is returned to the crushing plant. Two of the three ball mills are 9.6 MW (ML002/003) whilst the third (ML2004) is 16 MW, each in closed circuit with a cyclone bank. ML2004 (Train 3) processes nominally 35% of the SAG trommel undersize to produce a flotation feed P_{80} of 250 µm, the balance is processed via ML002/003 (Train 1 & 2) at a product P_{80} of 170 µm.

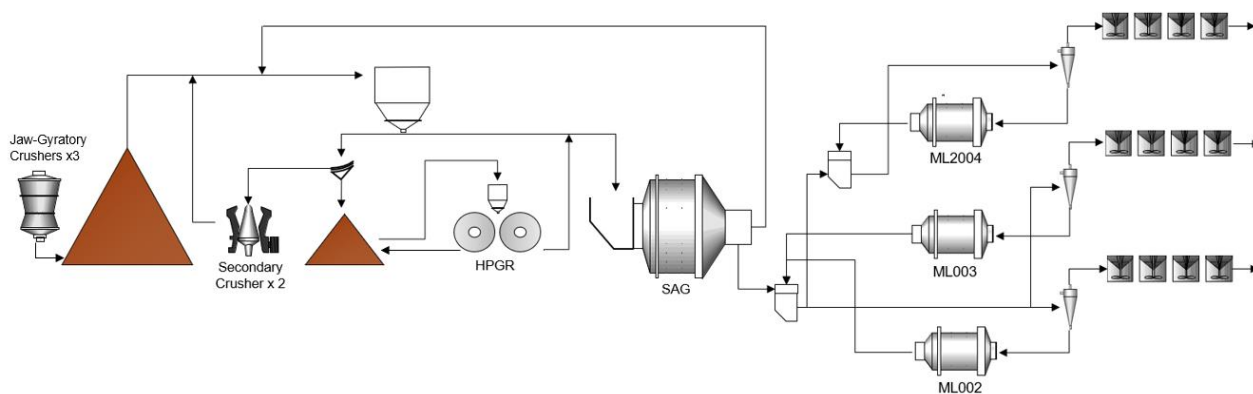


Figure 1 - Nominal Concentrator 1 Flow sheet

Non-Nominal Flow sheet (SAG Bypass Flow sheet)

In October 2015, a failure in the windings of the SAG mill GMD stator resulted in 5 weeks of downtime to Concentrator 1. The unplanned event catalysed the installation of additional conveyor infrastructure as a mitigating control to de-risk future SAG GMD issues. The additional infrastructure allows the HPGR centre product to be directed to ML2004 via a new feed chute and conveyor as displayed in Figure 2; this is referred to as ‘SAG Bypass’. The design was conceptually completed as part of the Cadia East FS, but was indefinitely deferred after being evaluated in a value engineering study. The additional infrastructure was rapidly constructed during the 2015 breakdown and completed approximately six weeks after the winding repair. Load commissioning of this equipment was not possible until 2017. In the subsequent 18 months of nominal operation an alternative discharge line for the ML2004 was designed and manufactured to allow ML2004 to be converted to an open circuit configuration, acting as a primary mill and its discharge reporting to ML002 and ML003 in a secondary grinding duty.

SAG bypass circuit load commissioning occurred in May 2017 during a second SAG GMD repair. The circuit operated for 12 hours. The maximum sustained throughput rate was 1344 t/h of Cadia Hill ore. Scats handling from the ML2004 trommel was identified as the key constraint.

The SAG Bypass configuration was operated for the second time in July 2019 during a third SAG GMD repair. The circuit operated for ten days and achieved a maximum sustainable rate of 1596 t/h of Cadia East Ore. The downstream ball milling circuits of ML002/003 were identified as the key constraint.

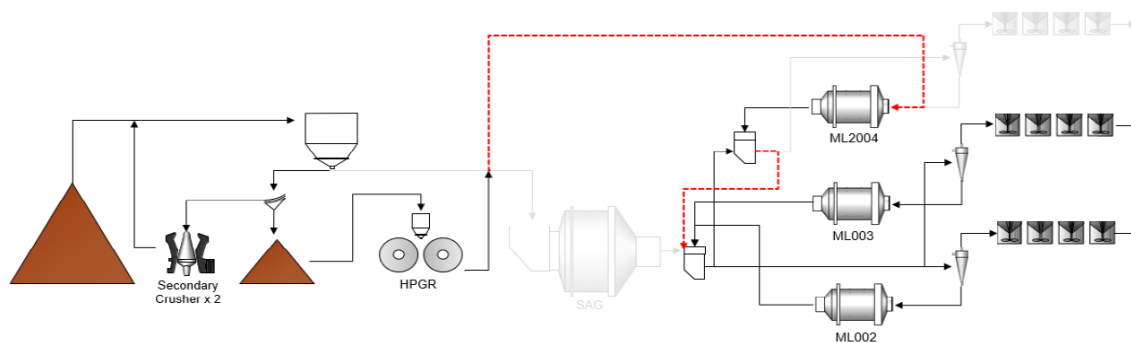


Figure 2 - Non-Nominal Concentrator 1 Flow sheet (SAG Bypass)

Table 2 below summarises the ore characteristics and circuit data during the 2017 and 2019 periods. The modelled throughput on Cadia East ore was developed using survey data from the 2017 SAG bypass trial together with Cadia East underground belt cut data from April 2016. A survey conducted during the 2019 run of SAG Bypass was used to create an accurate Concentrator 1 SAG Bypass model. This updated model underpinned the planning for the future SAG GMD upgrade outage discussed later in this paper.

Table 2 – Ore characteristics and circuit data summary during SAG bypass

	Parameter	Units	Cadia Hill Ore (2017)	Cadia East Ore (2019)
Ore characteristics	SG	t/m ³	2.7	2.7
	BWI	kWh/t	15.1	20.2
	A*b		39.8	31.0
Circuit data	Modelled throughput	t/h		1129
	Actual throughput	t/h	1344	1596

Following third SAG GMD repair in 2019 the decision was made to change the SAG GMD in 2021, three years ahead of schedule. The repair duration was forecast to be 20-weeks. A project was initiated in August 2019 to debottleneck the SAG bypass circuit flow sheet in order to maximise throughput during the 20-week outage.

Planning

Defining the Scope

The project to debottleneck the SAG bypass circuit was guided by an aspirational mission statement ‘*How can Cadia go beyond 2000 t/h in SAG bypass operation*’. This was deemed a feasible target based on the theoretical maximum throughput achievable for the given ore work index and circuit installed power as determined via the Morrell method.

The first phase of the project was a collaborative workshop held in November 2019 at Cadia. A cross disciplinary team of both external and internal stakeholders were involved across multiple days. The mix of disciplines included Cadia’s operations, engineering, metallurgy and project delivery, Newcrest group processing and external processing subject matter experts. The workshop planning was guided by learnings gathered on the 2019 operation and focused on the circuit constraints observed. Four guiding principles were defined from the observed constraints:

1. Minimise primary ball mill feed size (F_{80})
2. Minimise primary ball mill product size (P_{80})
3. Alleviate secondary milling recirculating load
4. Project implementation must have minimal impact on existing operations

The workshop explored options to address the identified constraints within two solution contexts: low capital (<AUD\$250 000) and unconstrained capital. These were then subcategorised using an impact/effort matrix assessed within the context agreed by the workshop participants. A total of 51 initiatives were identified and ranked as outputs for further work, as shown in Table 3.

Table 3 - Categorised workshop outputs

Category	No. Initiatives
Just Do	14
Potential	15
Consider	9
Reject	13
TOTAL	51

- 'Just Do' – those opportunities with a **high** value opportunity and **low** capital cost
- 'Consider' – those opportunities with a **low** value opportunity but **low** capital cost
- 'Potential' – those opportunities with a **high** value opportunity and **high** capital cost
- 'Reject' – those opportunities with a **low** value opportunity and **high** capital cost

Due to the overall project delivery schedule, all 14 'Just Do' initiatives proceeded to engineering and execution whilst all 13 'Reject' initiatives were discontinued.

The second project phase was a validation exercise on 10 of the 15 initiatives from the 'Potential' list. The validation exercise was the priority output of the workshop forward work plan and completed as a Concept Study by an independent third party with process expertise. The validation exercise examined two streams in parallel: value delivery and engineering complexity. This allowed simple throughput uplift versus schedule assessments to be made, which assisted in gating these initiatives through to engineering and execution. The value delivery stream used process modelling expertise to quantify the uplift potential of the 'Potential' initiatives. In addition, the process stress tested the uplift potential for the 'Just Do' initiatives to validate their categorisation. The engineering stream used project management and engineering expertise to determine the feasibility of an executable solution within the schedule and construction constraints. The validation exercise was completed by February 2020 and used to lock down the agreed project execution scope.

Table 4 – Category of initiatives executed

Category	No. Initiatives Executed
Just Do	10
Potential	3
Consider	3
Reject	0
TOTAL	16

Execution was the third phase of the project. Of the 51 workshop outputs listed in Table 3, only 16 initiatives proceeded through to project delivery and execution, as shown in Table 4 and Table 5. Further detailed modelling was completed on the agreed initiatives to finalise the bankable uplift and support the project business case. From March 2020 the 16 initiatives identified in Table 5 below were gated through to execution with an implementation deadline of 12 months. The

implementation deadline was set by the over-arching SAG GMD replacement project which was initially scheduled to commence on 1 March 2021.

Table 5 - Detailed of Initiatives Progressed to Execution

Category	Initiative Description	Constraint Alleviated
Just Do	Modify HPGR Edge Recycle System	Primary Ball Mill F ₈₀
Just Do	Operational Parameter Review (HPGR)	Primary Ball Mill F ₈₀
Just Do	Reduce Scalping Screen Panel Apertures	Primary Ball Mill F ₈₀
Just Do	Modify Secondary Crusher Liner Design	Primary Ball Mill F ₈₀
Just Do	Modify ML2004 Liner Design	Primary Ball Mill F ₈₀
Just Do	Increase Primary Ball Mill Media Top Size	Primary Ball Mill F ₈₀
Just Do	Correct Duty Primary Ball Mill Discharge Pump	Secondary Ball Milling
Just Do	Modify Primary Ball Mill Feed Chute	Operability
Just Do	Increase Secondary Ball Mill Media Top Size	Secondary Ball Milling
Just Do	Operational Parameter Review (Secondary Ball Mill Water Balance)	Secondary Ball Milling
Potential	Upgrade Crushing & Screening Area Conveyor Capacities	Primary Ball Mill F ₈₀
Potential	Remove Secondary Ball Mill Trommels	Secondary Ball Milling
Potential	Increase Secondary Ball Mill Power Set Point	Secondary Ball Milling
Consider	Modify Primary Ball Mill Scats Chute	Operability
Consider	Modify Primary Ball Mill Ball Retaining Ring	Primary Ball Mill F ₈₀
Consider	Modify Primary Ball Mill Discharge Pump Discharge Line to Secondary Ball Mill Hopper	Secondary Ball Milling

Circuit Modelling

Detailed circuit modelling was completed to quantify the throughput uplift attainable through implementation of the initiatives listed in Table 5 and to validate that they would bridge the gap between demonstrated rates and the >2000 t/h target.

An external third party was engaged to assist in modelling the possible process outcomes in detail. The Concentrator 1 comminution model used was originally developed in 2016 using the third party's proprietary comminution modelling techniques. The process model has since undergone periodic updates following full plant surveys, including during the 2019 SAG bypass operation, and has consistently been a robust predictor of circuit performance and identifier of throughput bottlenecks.

The specific circuit changes modelled under the SAG bypass flow sheet included:

- reduced HPGR feed top size;
- rejection of coarse particles from primary ball mill feed through HPGR edge recycle;

- increased ball mill media top sizes;
- reduced primary cyclone operating pressure;
- corrected secondary ball mill water balance; and
- a reduction in underground primary crusher Closed Side Setting (CCS).

A primary ball mill scattling rate constraint was imposed based on known materials handling capabilities.

The maximum modelled throughput rate under these circuit changes was 2281 t/h, a 685 t/h uplift over the previously demonstrated 2019 rate and well in excess of the >2000 t/h site aspiration. The modelled circuit constraint was primary ball mill scattling rate.

Table 6 - Ore characteristics and circuit data summary – 2021 model update

	Parameter	Units	Cadia Hill Ore (2017)	Cadia East Ore (2019)	Cadia East Ore (2021 Modelled)
Ore characteristics	SG	t/m ³	2.7	2.7	2.7
	BWI	kWh/t	15.1	20.2	20.3
	A*b		39.8	31.0	32.6
Circuit data	Modelled throughput	t/h	-	1129	2281
	Actual throughput	t/h	1344	1596	-

The specific circuit parameters that yielded this peak throughput are shown in Table 7 alongside the previous 2019 parameters.

Table 7 - SAG bypass circuit parameters; 2019 versus modelled 2021 operation

Parameter	Units	2019 Actual	2021 Modelled
Scalping screen panel aperture size	mm	65	45
HPGR edge recycle fraction	%	13	30
Primary ball mill media top size	mm	80	105
Secondary ball mill media top size	mm	65	80

Further reductions to scalping screen panel aperture size below 45 mm were not feasible due to the reduction in screen undersize tonnage to rates below the primary ball mill demand. Furthermore, the subsequent increase in recirculating load to the closed-circuit secondary crushers necessitated an increase to their CSS to accept the higher feed rates. Further mill media top size increases resulted in elevated circuit grind sizes for minimal change to circuit throughput rate.

The reduction to the underground primary crusher CSS (modelled from 150 mm to 100 mm) did not yield a milling rate improvement. Whilst the reduction in top size at the tighter CCS reduced the secondary crushing circuit recirculating load, it did not translate to a reduction in primary mill feed F_{80} . This is due to the multiple stages of crushing that occur prior to the primary milling circuit. Milling throughput rates are heavily dependent on the fraction of minus 10 mm material in feed, whereas modifying primary crusher gaps does not impact the size distribution in these finer fractions.

Implementation

Planning and implementation of the uplift initiatives commenced 14 months prior to the scheduled SAG GMD replacement outage.

The high impact, more complex initiatives are discussed in the following sections. These include the modifications to the HPGR edge recycle system, primary ball mill liners, primary ball mill discharge pump and piping, primary mill feed chute and the removal of the secondary ball mill trommels. All projects were managed by the site Metallurgy department, with the execution teams comprising site Reliability Engineering and Fixed Plant Maintenance departments. The physical execution of these initiatives was constrained to a 277 h plant outage that preceded the SAG bypass operation. Earlier execution was prevented by its impact on nominal circuit operation. Equally, these changes had to be reversed at the conclusion of the SAG GMD replacement. The actual implementation date was deferred to July 2021 to align with the final approved GMD replacement schedule.

HPGR Edge Recycle System Modification

The HPGR edge recycle system is designed to capture the coarse outer product material and recirculate it back to HPGR feed. The reduced compressive forces toward the edge of the rolls (Figure 3) results in coarser product towards the edge, relative to the centre of the roll.

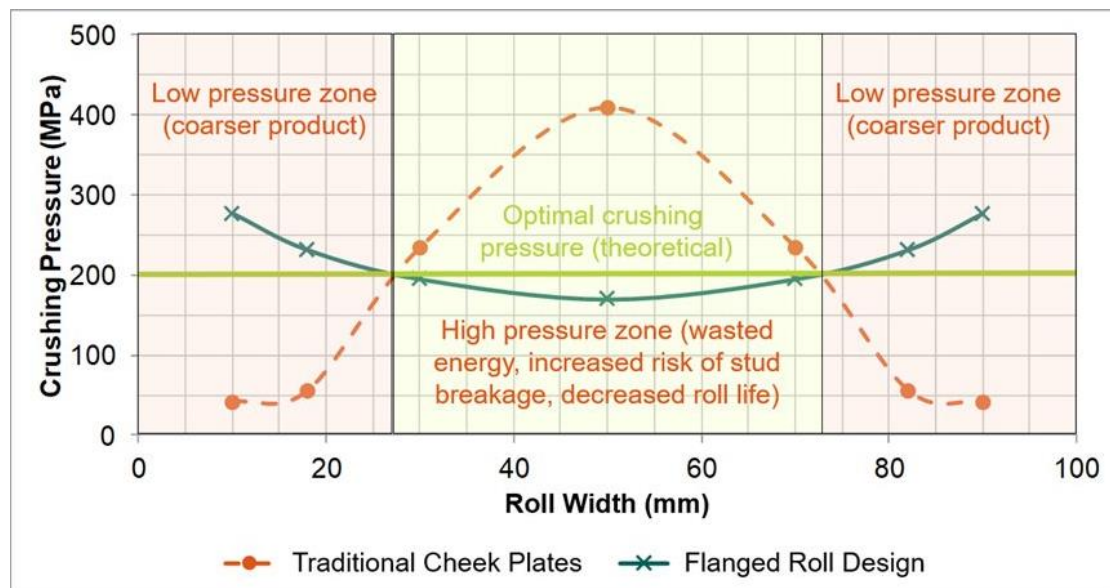


Figure 3 – HPGR pressure profile along length of roll (Metso, 2022)

The variance in particle size is marked, with P_{80} of 8 mm and 15 mm at the centre and edge respectively based on samples collected from the Cadia HPGR product. Under nominal operation the HPGR operates in open circuit (without edge recycle) at 3200 t/h to maximise SAG mill throughput.

The objective of the re-design was to maximise the quantity of edge material capture whilst maintaining the required ~2000 t/h centre product feed to the primary ball mill. This equated to 30% recycle at maximum HPGR feed rates and ensured uninhibited flow of edge product into the recycle gates.

The design change involved removal of the liner ledges directly above the edge gates and repositioning the angle of the edge chute side plate by approximately 45 degrees to increase the cross-sectional open area from above. Discrete Element Method (DEM) modelling, shown in Figure 4 below, shows the funnelling and mixing of product that occurred in the nominal set-up due to the presence of the liner ledges compared with the reduced mixing in the modified design with the ledges eliminated.

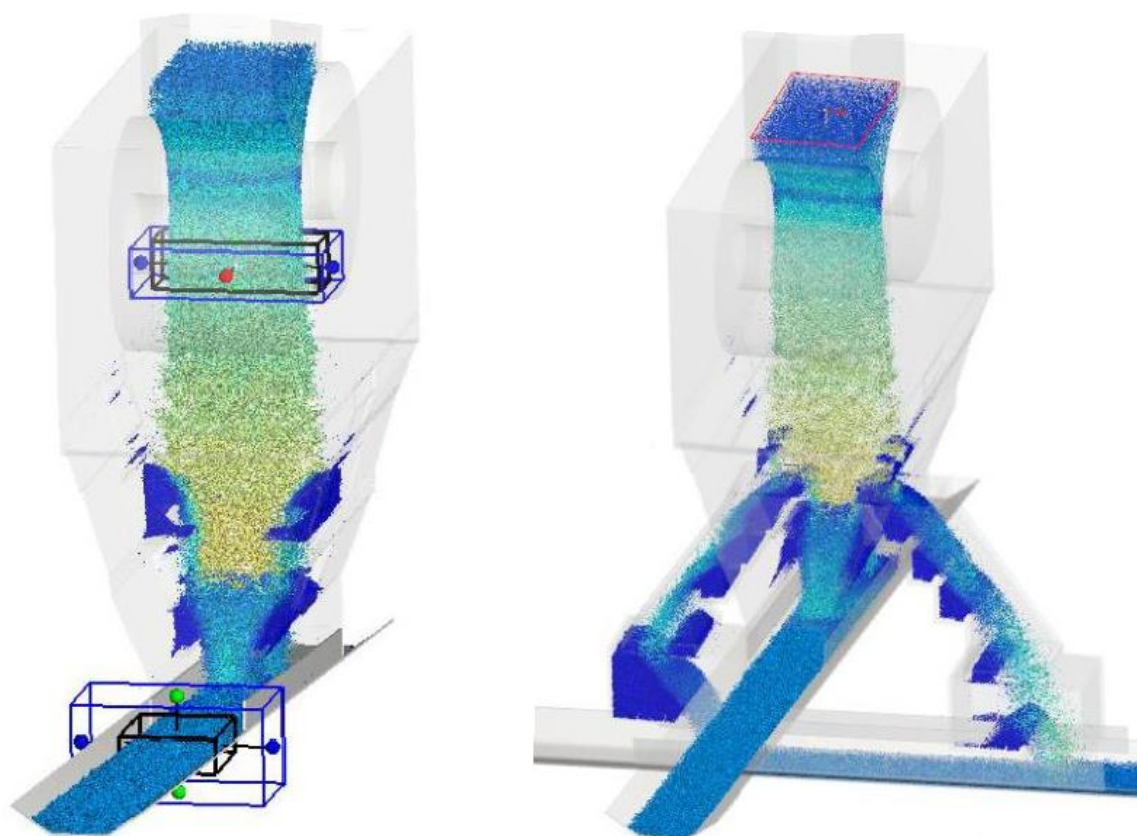


Figure 4 – HPGR edge recycle [existing design] in open circuit configuration (left) and upgraded edge recycle system at 30% recycle (right)

Primary Ball Mill Shell Liner Re-Design

A one-off, modified shell liner design was installed in ML2004 for the SAG bypass operation to cater for the different feed conditions as presented in Table 8. The objective of the design was to increase the degree of impact breakage and prevent liner damage, considering the more aggressive feed conditions and increased likelihood of mill grind-outs.

Table 8: Primary mill feed conditions; nominal and SAG bypass operation

Parameter	Units	Nominal (secondary closed circuit ball mill)	SAG bypass (primary open circuit ball mill)
F80	mm	3.2	11.7
Particle top size	mm	19	38
Media top size	mm	80	105

The new design retained the existing 'hump and bump' profile but with increased lifter height, plate height and a steeper lifter face angle. There was also a material change from white cast iron to chromium molybdenum steel to reduce the possibility of liner fractures. The DEM modelling shown in Figure 5 demonstrates the greater particle throw which was achieved using the new design which equated to a 16% increase in average impact specific energy.

Table 9 – Primary ball mill liner specifications, nominal and SAG bypass operation

Parameter	Units	Nominal (secondary closed circuit ball mill)	SAG bypass (primary open circuit ball mill)
Feed end shell lifter height	mm	175	185
Feed end shell lifter face angle	°	30	28
Total shell weight	t	381	387

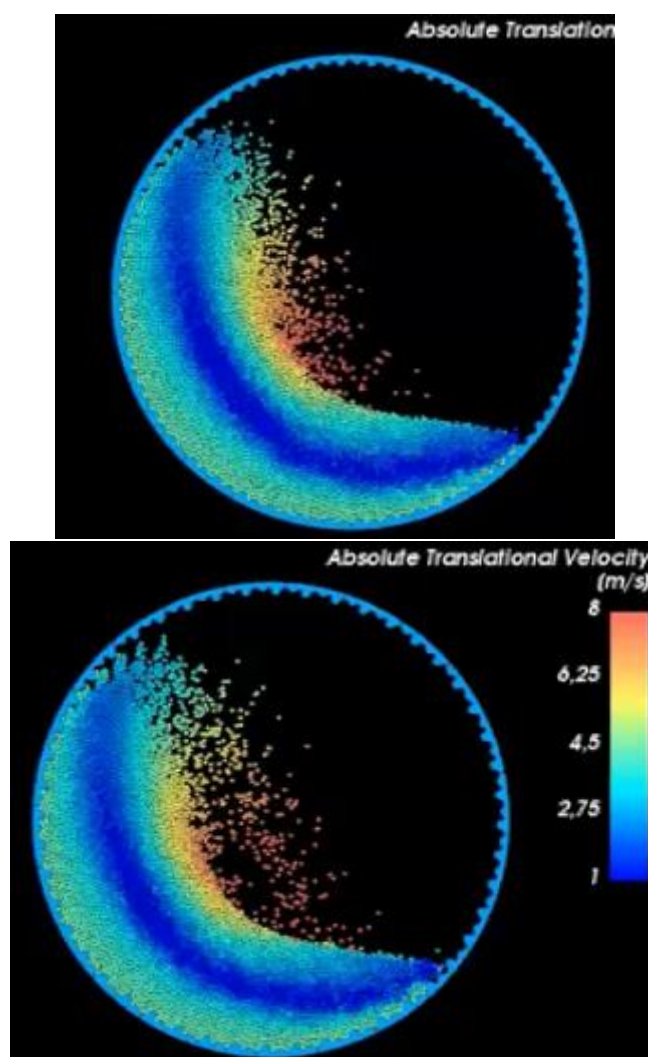


Figure 5 – Primary ball mill DEM modelling at feed end [FE] of shell, nominal design (left) and SAG bypass design (right)

Primary Ball Mill Discharge Pump Circuit Specification

The nominal Train 3 primary cyclone feed pump was oversized for the SAG bypass primary ball mill discharge duty. High water addition rates were required to satisfy the pump minimum flow requirement leading to volumetric overloading of the downstream secondary ball milling circuits. To alleviate this issue and maintain control over the circuit water balance, an alternate duty pump and piping was designed and installed. Changes included installing a Warman® MCU® 300 pump in place of the existing Warman MCR-H® 550, a reduction in suction and discharge piping diameter from 600 mm to 300 mm and de-rating of the existing pump motor from 2000 kW to 560 kW.

The pump discharge outlet into the secondary ball mill hopper was also modified to ensure equal distribution of material between the two secondary cyclone feed pumps. The prior SAG bypass operational run experienced an asymmetric split of coarse material between the two ball milling trains, which was driven by the angle at which the primary mill discharge line entered the hopper.

Removal of Secondary Ball Mill Trommels

Trommel oversize material from the secondary ball mills historically reported to a drive through sump where material was removed by a front-end loader (FEL). Under high recirculating loads, in both the nominal and SAG bypass state, slurry would report to trommel oversize and spill to the drive-through sump. When the rate of slurry discharge exceeded that which the FEL could remove, the throughput rate was constrained. Given the recirculating loads in the secondary circuit were the overall circuit constraint during the previous operational run, this modification constituted a key throughput rate uplift lever for the SAG bypass project.

This change was suitable for both the nominal and SAG bypass circuit, given that the trommel aperture sizes in the primary mills were less than or equal to that of the ball mills. As such it was implemented as a permanent change. Both trommels were removed and replaced with discharge chutes with ceramic grates at the outlet for cyclone feed pump protection. Both ball mills retained their existing trunnion ball retaining grates.

Primary Ball Mill Feed Chute Modification

The primary ball mill feed chute experienced frequent blockage events during the operational run in 2019 which resulted in activation of the chute level switch and tripping of the feed conveyor. This was temporarily mitigated using water hose set-ups but required a long-term solution for the targeted 2021 mill feed rates.

Chute DEM modelling highlighted a large static zone on the ledge of the head chute where material would build up over time. Three possible solutions were reviewed; reducing conveyor belt speed to the point where the material trajectory did not reach the ledge, increasing belt speed to reduce static zone on the ledge or removal of the ledge altogether. Changing belt speeds introduced additional project complexities and costs, therefore the partial chute modification was chosen. The rock-box portion of the chute was removed and replaced with a lip lined, sloped edge, which reduced the build-up of material that previously resulted in chute blockages.

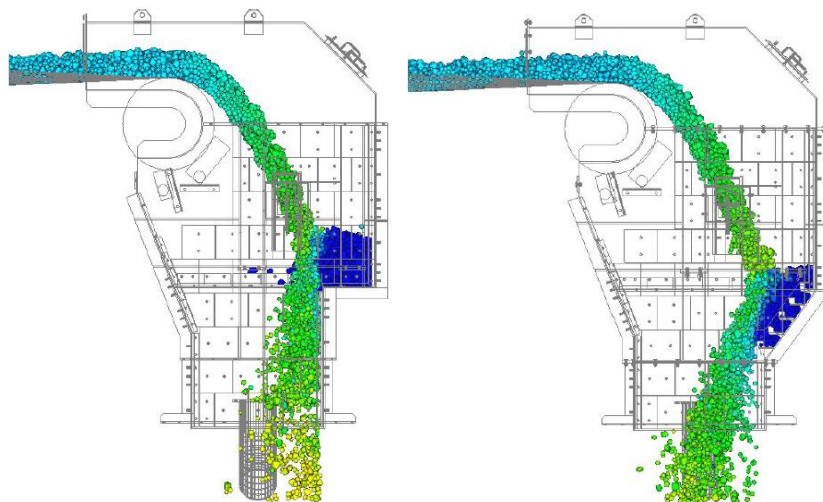


Figure 6: Primary ball mill head chute design before (left) and after (right)

Results and learnings

Throughput and Circuit Constraint

Concentrator 1 commenced a stable start-up in SAG bypass mode following the circuit conversion outage. Mill feed rates exceeded the 2019 maximum rate within two hours and surpassed the 2000 t/h budgeted stretch target within eight hours of start-up (Figure 7). A maximum, steady state rate of 2191 t/h was achieved at a 180 µm grind size. The circuit constraint was the secondary ball milling circuit recirculating load. Attempts to increase the rate beyond 2191 t/h for sustained periods resulted in cyclone roping events and overload of the secondary ball mills, characterised by rapid reductions in power draw.

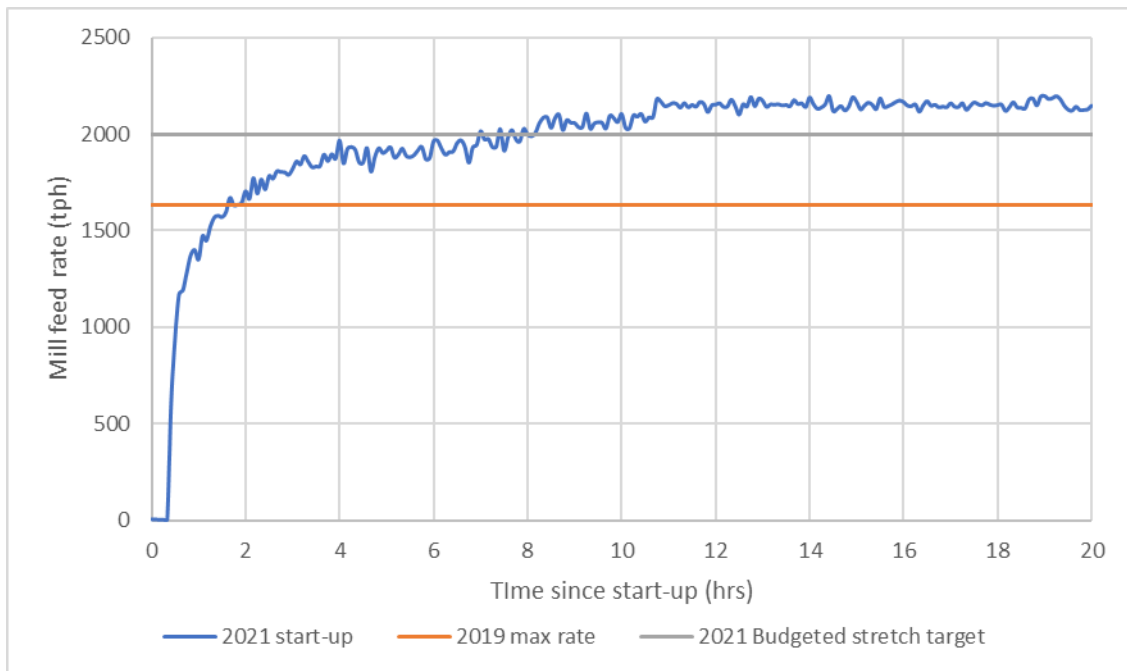


Figure 7 – 2021 SAG bypass throughput ramp-up

Primary ball mill scating rate was significantly lower than forecast, averaging 3 t/h against a modelled rate of 34 t/h. This reduction resulted in a 200-hour uplift in circuit utilisation at peak rates compared to forecast. This was due to the interaction that existed between the SAG GMD replacement crane lift load shadow and FEL route for scats removal. The schedule had assumed that rates needed to be reduced to reduce scats production during major crane lifts to avoid the FEL working under a crane load.

Operational Observations and Learnings

Screen undersize rates

The reduced secondary scalping screen apertures resulted in unsustainable HPGR feed stockpile rates during planned screen and secondary crusher outages. A 1200 t/h deficit between HPGR stockpile feed and reclaim rate was typically observed which necessitated a reduction in mill feedrates as the stockpile became depleted. As a result, larger 55 mm apertures were installed at the inclined, feed end of the screens to maintain HPGR stockpile feed rates during periods of screen and crusher duty-standby operation.

Primary mill coarse feed

During a period of unplanned HPGR downtime an attempt was made to feed coarse material from the front-end distribution bin's bleed stream direct to the mill. This material is a blend of primary and secondary crushed material with a P_{80} of 56 mm. Rates of 1000 t/h were fed to the mill. Within four hours the coarse material had lifted the steel charge and began discharging media from the mill, resulting in a ball charge loss equivalent to 3.4 MW. This incident identified the inability of the ball mill to process material of this coarser size range.

Survey Results

A circuit survey was completed mid-operation, collecting samples at the HPGR centre and edge discharge, primary mill feed and discharge, secondary ball mill discharges and cyclone feed, overflow and underflow. A comparison of the survey results against the model, 2019 operation and the SAG mill in the nominal circuit configuration is shown in Figure 8 and Figure 9.

The 2021 SAG bypass operation achieved the finest primary mill feed particle distribution, with a 40% reduction in F_{80} compared with 2019. This demonstrates the impact of the HPGR edge recycle changes and the secondary screen aperture reduction. The criticality of reducing the fraction of +1 mm particles in primary mill feed is depicted well in the trommel undersize particle size distribution shown in Figure 9. The slight inflection points in the previous SAG bypass curves above 1 mm indicate reduced breakage rates in this coarser size fraction. As expected, this contrasts with the 40 ft SAG mill (ML001) which achieves better impact breakage given its higher aspect ratio and media top size. The large shift in distribution in the +1 mm fraction of the 2021 trommel undersize results compared with 2019 were the key lever for the elevated overall throughput rates and significant reduction in total scats as it reduced transfer size to the secondary milling circuits.

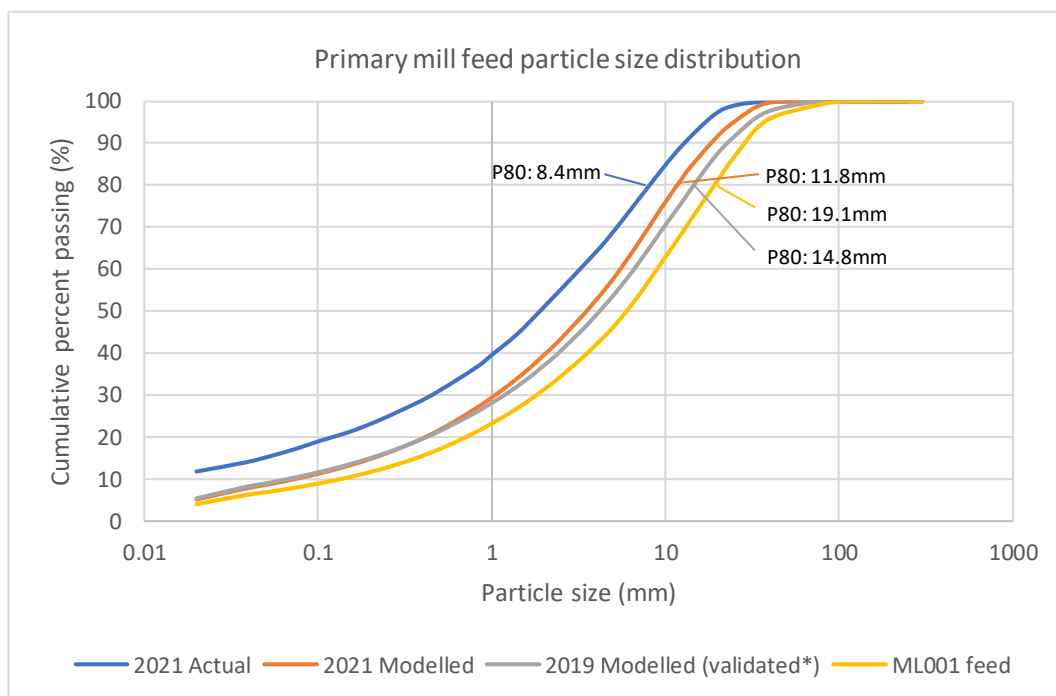


Figure 8 – Primary mill feed particle size distribution
 (*No belt cut was completed during the 2019 circuit survey, as such the post-survey validated modelled results are presented)

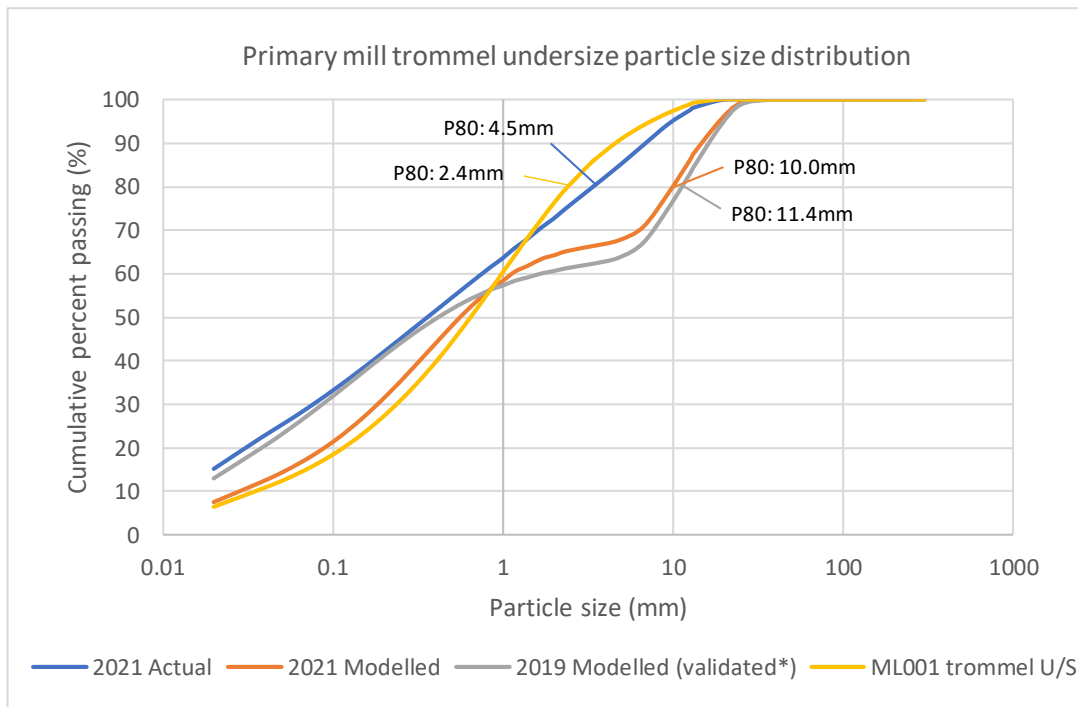


Figure 9 – Primary mill trommel undersize particle size distributions

The variance between the actual and modelled size distribution for primary ball mill feed and discharge results for the 2021 operation is pronounced. This translates to the large difference in modelled versus actual scattering rate. This is most likely attributed to the improved performance of the HPGR edge recycle system. The parabolic HPGR product size profile used in the model had been calibrated using HPGR edge product belt cuts collected in 2016 and 2019. As discussed earlier, the nominal edge recycle design resulted in funnelling and mixing of coarse edge and fine centre product material prior to capture in the edge chutes. The sizings of edge product from the 2021 survey were significantly coarser than model prediction, and conversely the centre product belt cut significantly finer than modelled. This indicates a cleaner cut of edge and centre product material with the upgraded edge recycle design, which did not align with the model.

Model Update

The model was updated using circuit survey results and Cadia East belt cut data from the 20 weeks that the SAG bypass circuit was in operation. The updated, modelled rate was 2255 t/h which was within 3% of the actual achieved steady state rate. Peak rates of 2300 t/h were demonstrated during operation, but the gradual build-up in ball mill circuit recirculating load resulted in the cyclone operational issues as discussed earlier.

The minor adjustment to the model's outputs following the survey and the alignment between actual and modelled rates were indicative of a robust circuit model.

Table 10 – Ore characteristics and circuit data summary – 2021 operation and model update

	Parameter	Units	Cadia Hill Ore (2017)	Cadia East Ore (2019)	Cadia East Ore (2020)	Cadia East Ore (2021)
Ore characteristics	SG	t/m ³	2.7	2.7	2.7	2.7
	BWf	kWh/t	15.1	20.2	20.3	20.8
	A*b		39.8	31.0	32.6	30.2
Circuit data	Modelled throughput	t/h	-	1129	2281	2255
	Actual throughput	t/h	1344	1596	-	2191

Conclusion

The successful application of the SAG bypass project uplift initiatives enabled a 37% increase in Concentrator 1 throughput rates against previously demonstrated rates. This lifted production beyond site expectations during the 20-week SAG GMD replacement. Key uplift initiatives included, but were not limited to, reduced HPGR feed top size through screen panel changes, redesign of the HPGR edge recycle system to reject coarse material from primary ball mill feed, re-design of ball mill liners to suit a primary mill duty and installation of a duty mill discharge pump to properly control the secondary ball mill circuit water balance.

The success of the project is testament to the due diligence performed to understand circuit constraints and associated operational levers, the targeted planning process and the range of expertise sought from both internal and external stakeholders.

Acknowledgements

The authors would like to acknowledge the work of Courtney Dobson and Brandon Akerstrom who both contributed towards the planning and implementation.

The authors would also like to acknowledge the contributions of Greg Lane, Matthew Pyle and Scott Munro who all contributed towards the success of this project.

References

- Edmunds, R., Wilkens, M., Akerstrom, B., & Haines, C. (2021). Debottlenecking of the Ridgeway Concentrator at Newcrest's Cadia Operation. *Mill Operators' Conference 2021*. Brisbane: AusIMM.
- Engelhardt, D., Lane, G., & Powell, M. (2014). Cadia Expansion - The impact of Installing HPGR Prior to a SAG Mill. *12th Mill Operators' Conference*. Melbourne: AusIMM.
- Engelhardt, D., Lane, G., & Powell, M. S. (2014). Cadia Expansion - The impact of Installing High Pressure Grinding Rolls Prior to a Semi-Autogenous Grinding Mill. *Mill Operators' Conference*. Townsville: AusIMM.
- Gunn, P. (2006). Problem Definition and Repair of the Rotor Pole Structure on one of the World's Largest Gearless Driven SAG Mills. *SAG Conference*. Vancouver.
- Meimaris, C., Lai, B., & Cox, L. (2001). Remedial Design of the World's Largest SAG Mill Gearless Drive. *SAG Conference*. Vancouver.
- Metso. (2022, Jan 31). *Why skewing is not beneficial for your HPGR*. Retrieved from Metso: <https://www.metso.com/insights/blog/mining-and-metals/why-skewing-is-not-beneficial-for-your-hpgr/>
- Morrell, S. (2019). Modelling approaches and their application in comminution circuit design. *World Gold 2019* (p. 1432). Melbourne: The Australasian Institute of Mining and Metallurgy.
- Waters, T., Rice, A., Seppelt, J., Bubnich, J., & Akerstrom, B. (2018). The evolution of the Cadia 40-foot SAG mill to treat the Cadia East orebody: a case study of incremental change leading to operational stability. *14th Mill Operators' Conference 2018*. Brisbane: AusIMM.

Design of Coarse Particle Flotation Circuits for Copper Projects

M Pyle¹, G Ballantyne², G Williams³, G Lane⁴, J Concha⁵

1. Head of Technical Solutions, Ausenco, 189 Grey St. South Brisbane, matt.pyle@ausenco.com
2. Director Technical Solutions, Ausenco, 189 Grey St. South Brisbane, grant.ballantyne@ausenco.com
3. Technical Consultant, Ausenco, 189 Grey St. South Brisbane, greg.williams@ausenco.com
4. Chief Technical Officer, Ausenco, 189 Grey St. South Brisbane, greg.lane@ausenco.com
5. Global Product Manager HydroFloat®, Eriez, Av. Circunvalación del Club Golf Los Incas 134, Lima, Peru, jconcha@eriez.com

ABSTRACT

The HydroFloat® cell was first implemented in a hard rock application at Newcrest's Cadia Train 3 in 2018 treating copper-gold ore. Units have since been installed and commissioned at Kennecott, El Soldado, Mogalakwena and Cadia Trains 1 and 2. Quellaveco is under commissioning at the time of writing.

The HydroFloat cell enables the recovery of coarser particles at lower liberation classes when compared to conventional flotation cells by exploiting the following mechanisms;

- particle-bubble attachment in a fluidised bed
- quiescent flotation conditions to ensure particles and bubbles remain attached
- upflow of water for hydraulically assisted flotation, and
- overflow of a liquid phase from the cell without a froth interface to minimise particle drop-back

The net result can enable coarser grind sizes, with energy savings of up to 30% for every tonne milled at similar or better recoveries. Furthermore, water consumption per tonne milled can also be reduced, and the tailings system can be redesigned to take advantage of a higher ratio of sand to fines in tailings, reduce footprint and improve tailings stability. The net improvements to recovery, coupled with reduced energy, water consumption and tailings storage, can substantially improve the economics of greenfield and brownfield copper projects.

Over the last five years, engineering and design developments have improved the operation of the cell and enabled more efficient HydroFloat circuit designs at lower cost.

This paper presents an overview of the key decisions and engineering considerations for the design of a HydroFloat Coarse Particle Flotation (CPF) circuit and integration within an existing operation or greenfield project. The paper discusses test work program design and interpretation, flow sheet configurations, classification circuit design, reagent conditioning, concentrate dewatering, regrinding and recovery of CPF concentrate to final concentrate. The paper also presents opportunities around tailings sand management and the potential benefits to tailings storage, water and power consumption and outlines the strategies to maximise the business case. The challenges related to integrating the project with conventional resource planning and business case modelling approaches is also discussed.

INTRODUCTION

Since the advent of froth flotation in 1905 at Broken Hill Proprietary Limited (BHP), grinding and flotation in concentrators has become the primary production method for a wide range of base, industrial and precious metals. Conventional froth flotation in conjunction with targeted reagent schemes is extremely effective at recovering target minerals to clean concentrates and rejecting gangue minerals at very high throughputs. The approach relies on using selective mineral reagents to make sulfide surfaces hydrophobic and then attaching those sulfide-containing particles to air bubbles in a highly turbulent regime with air addition in a flotation cell. Frothers are used to generate a stable froth at the top of the flotation cell as well as reduce the bubble size. This approach enables high target mineral recoveries particularly where liberation is greater than 5% and the particles are in the range of 10 μm to 150 μm .

At very fine particle sizes, recoveries reduce due to slower flotation rates because of less kinetic energy collisions between bubbles and particles. At coarser sizes, particles are lost due to separation of bubbles from particles due to turbulence, insufficient transport of coarser particles out of the bulk phase and into the froth phase, as well as inefficient transport of coarse particle-bubbles into the launder due to bubble breakage and particle drop-back. The impact of these phenomena are summarised by the classic size-by-size recovery curve in Figure 1.

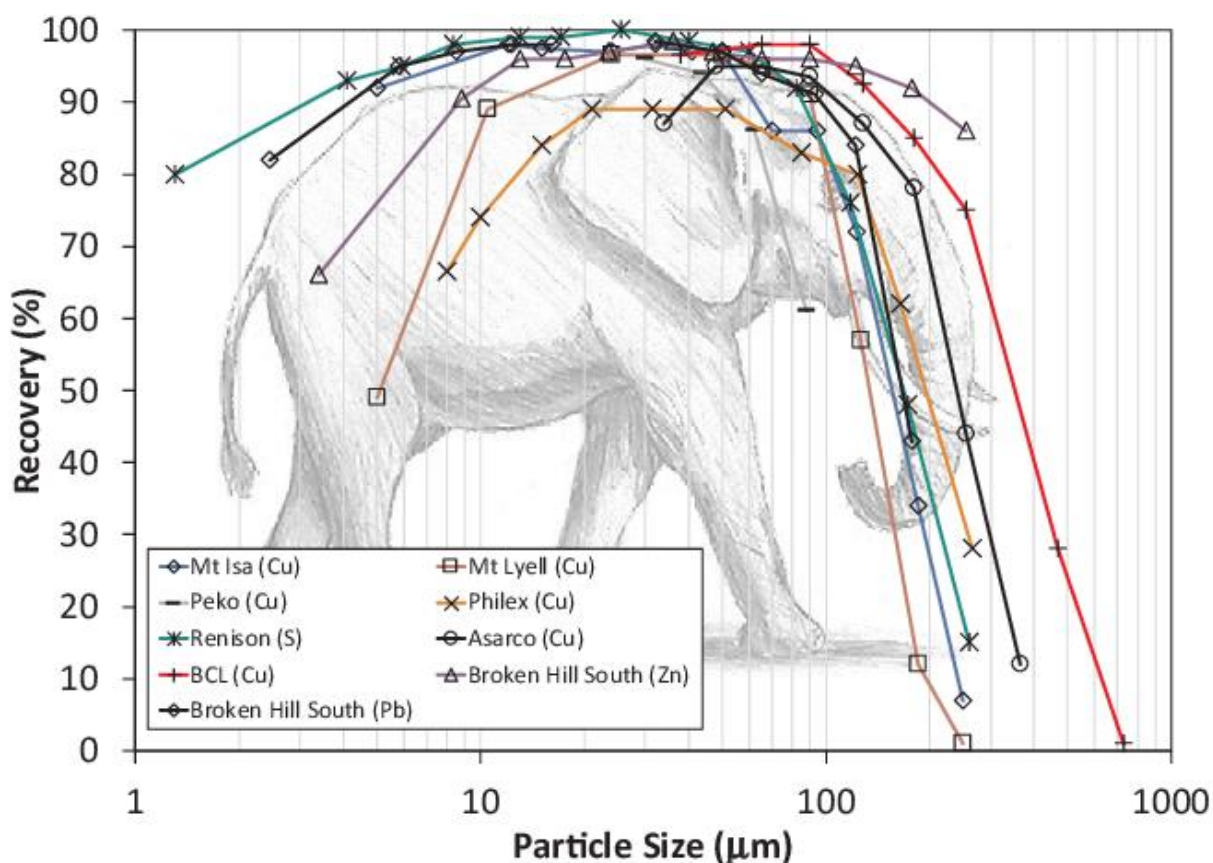


Figure 1 Flotation Elephant Curve (Lynch et al, 1981)

Whilst there are some examples of high recoveries into coarse concentrates in conventional flotation cells, further work is required to understand the specifics for why these sites achieve better coarse particle recoveries than typical sites. Mineralogy and grain structures will undoubtedly be key drivers.

Coarse particle flotation is an area of development for concentrators. There are several technologies available, including Jord NovaCell™, Eriez HydroFloat, Cidra P29 Technology™, FLSmidth coarseAIR™ and others. This paper focusses on the Eriez HydroFloat which currently has the most significant installation list.

The HydroFloat cell enables the recovery of coarser particles at lower liberation classes when compared to conventional flotation cells by exploiting the following mechanisms;

- particle-bubble attachment in a fluidised bed
- quiescent flotation conditions to ensure particles and bubbles remain attached
- upflow of water for hydraulically assisted flotation, and
- overflow of a liquid phase from the cell without a froth interface to minimise particle drop-back

The net result is improved recoveries of coarse particles. Figure 2 presents a cross section of a HydroFloat cell and Figure 3 presents typical comparison recovery by size curves for a coarse-grained copper porphyry.

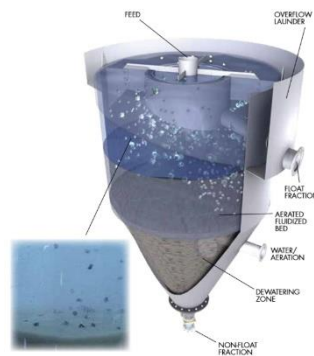


Figure 2 Eriez HydroFloat cell (courtesy of Eriez)

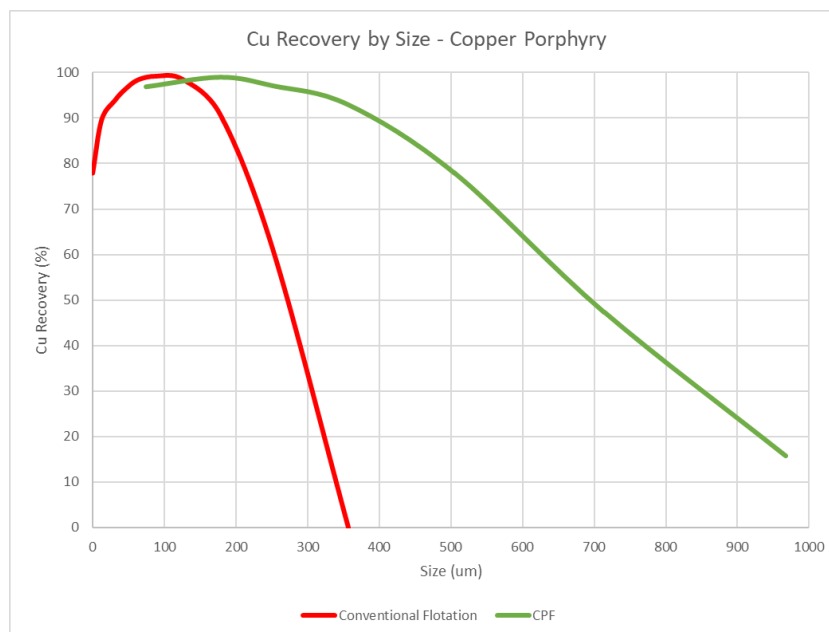


Figure 3 CPF Recovery Curve

Key projects to have implemented HydroFloat coarse particle flotation circuits include Cadia (T1/T2, T3), El Soldado, Mogalakwena and Quellaveco.

This paper outlines the test work program design and interpretation, flow sheet configurations, classification circuit design, reagent conditioning, concentrate dewatering, regrinding, tailings opportunities, business case assessments and project integration for a HydroFloat installation.

For an overview of the cell design and operation, readers should refer to papers by Arburo 2022, Carmona Franco 2015, Miller 2016, Jaques 2021, Seaman 2017, Vollert 2019 and Vollert 2023.

TEST WORK PROGRAM DESIGN AND INTERPRETATION

Conventional flotation test work programs are typically designed to determine grade-recovery curves based on grind size and liberation characteristics of the mineral. Rougher-regrind-cleaner circuits are designed to produce high grade products at high recoveries and with optimal capital and operating costs. Conditions are optimised to maximise recovery in the roughers. Regrind sizes and reagents are then tailored to achieve optimum recoveries to high concentrate grade in the cleaner circuit. Kinetic tests are used to determine the optimum flotation residence times per stage, then industrial experience is used to select scale-up factors for plant residence time from lab tests. Froth carry rates and lip loadings are selected by plant designers based on industrial experience, mineral characteristics, particle size and flotation cell type. Standard flotation tests are generally conducted with 1 kg samples in roughers, and 2 kg samples for rougher-cleaner flotation. The quantity of sample is selected to provide sufficient quantities of concentrate for testing and assaying.

The primary objective of coarse particle flotation test work is to determine the size-by-size metal and mass recovery performance of the different flotation regimes of coarse particle flotation versus standard rougher flotation. The intent is to generate size-by-size recovery curves for both conventional flotation and coarse particle flotation. These curves can then be used to model the circuit and optimise the conditions (i.e. throughput and particle size) for the project. As the project is progressing additional information is generated in the CPF test work including;

- a) grinding test work for HydroFloat concentrate.
- b) flotation cleaning test work for HydroFloat concentrate.
- c) variability test work.

The quantity of material required for test work is driven by the following factors;

- 1) the primary grind size, and the quantity of material which feeds the CPF unit after fines removal
- 2) the size of the test unit and the minimum quantity of material to achieve a stable run
- 3) the minimum quantity of material required to allow size-by-size recoveries to be determined at multiple size classes (typically four to six size classes)
- 4) generation of sufficient coarse particle flotation concentrate for subsequent test work for re-milling and flotation to final concentrate

This typically means that a single standard CPF lab test requires at least 20 kg of material at the size distribution that the project is considering. For program design with several runs allowing for some optimisation of reagents and teeter water conditions 100 kg of sample is adequate.

A typical test work flow sheet is outlined in Figure 4:

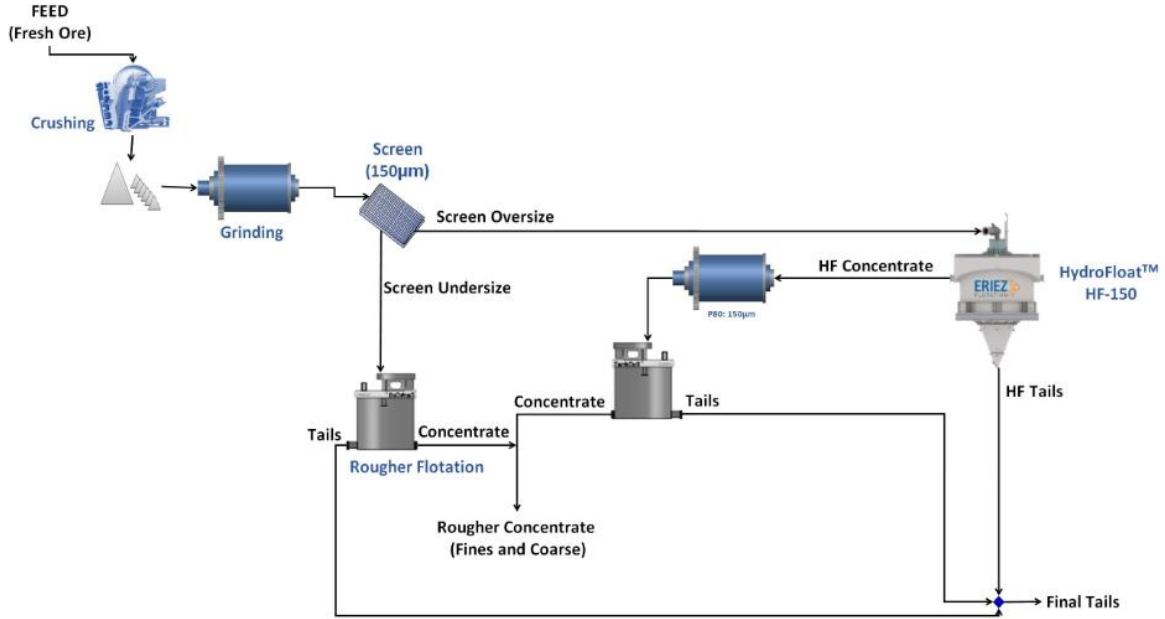


Figure 4 Simplified CPF Lab Test work Flow sheet for a coarse gangue rejection application (courtesy of Eriez)

Assays and sample quantities are indicated in Figure 5.

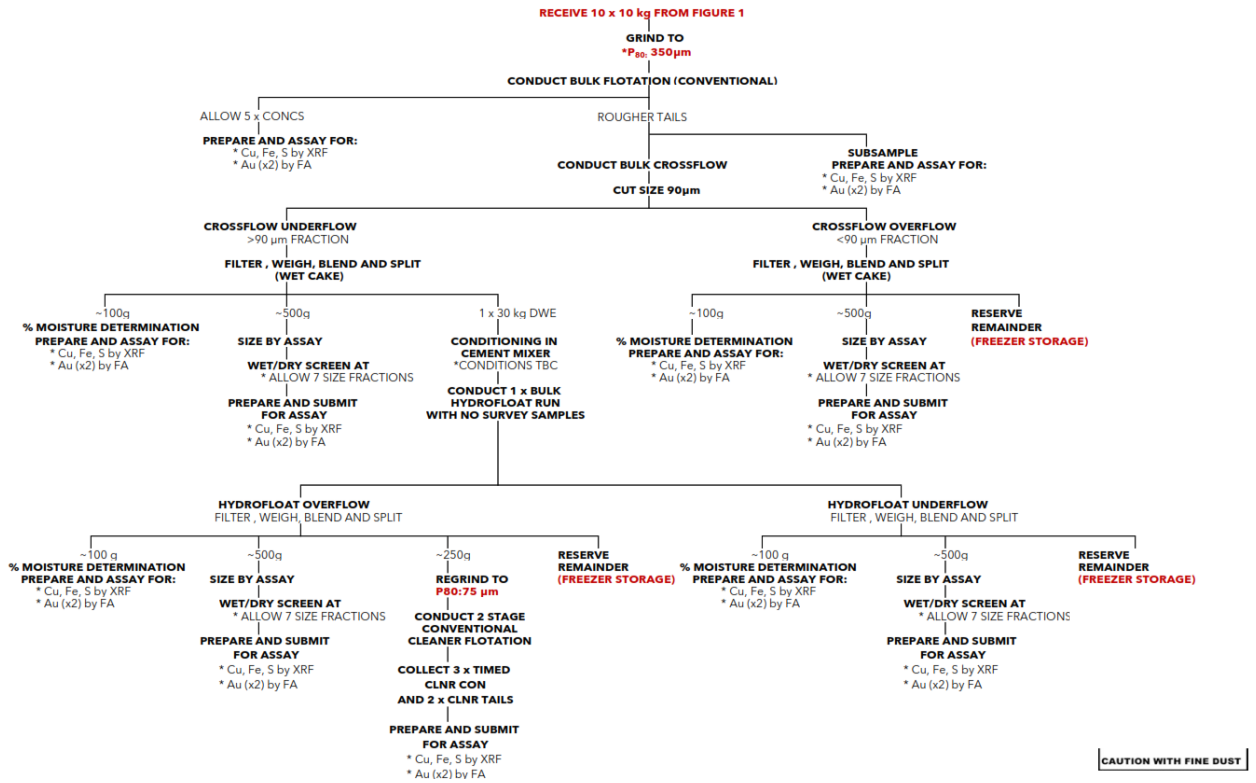


Figure 5 CPF Test work Sample Requirements for a Cu/Au project (courtesy of Eriez)

Test work should be planned to determine;

- 1) size-by-metal recovery curves for conventional flotation and coarse particle flotation
- 2) size-by-mass recovery curves for conventional flotation and coarse particle flotation
- 3) mass recovery to CPF feed and fines
- 4) optimum reagent suite and dosage rates
- 5) optimum upflow water addition (superficial velocity)

Results should be sought at the particle size distribution expected for the full size circuit. Test work can be completed in a range of flow sheet configurations, discussed in the following section, and then modelling can infer the circuit performance based on fundamental CPF response in different flow sheet configurations. This simplifies the test work procedures and can provide for more consistent results. For most projects, the objective should be to conduct testing at a coarser grind size with the ultimate objective to increase plant throughput as this generally results in the most optimum business case outcomes. Comminution modelling is required to determine the constraints in the comminution circuit and by how much the grind can be coarsened before a constraint is reached. For some projects, modifications may be required to deconstrain throughput. Increasing grind size by 150 to 200 μm from an optimum conventional flotation recovery is a sensible starting point for CPF test work, but this can be adjusted based on the project comminution constraints. Not all flow sheets and projects will be amenable to higher throughputs and coarser grind sizes, in which case increasing recovery may add value.

Test work can be completed at a range of scales. Lab and pilot scale equipment is presented Figure 6 and Figure 7.



Figure 6 HydroFloat CPF Lab Test work Unit (courtesy of Eriez)



Figure 7 HydroFloat CPF Pilot Test work Unit (courtesy of Eriez)

FLOW SHEET CONFIGURATIONS

There are four flow sheet configurations for CPF circuits as follows:

- 1) Cyclone underflow (within the grinding circuit recirculating load)
- 2) Cyclone overflow (after grinding)
- 3) Rougher flotation tailings (scavenging)
- 4) Mill classifier flow sheet

These flow sheets are outlined in Figure 8, Figure 9, Figure 10 and Figure 11.

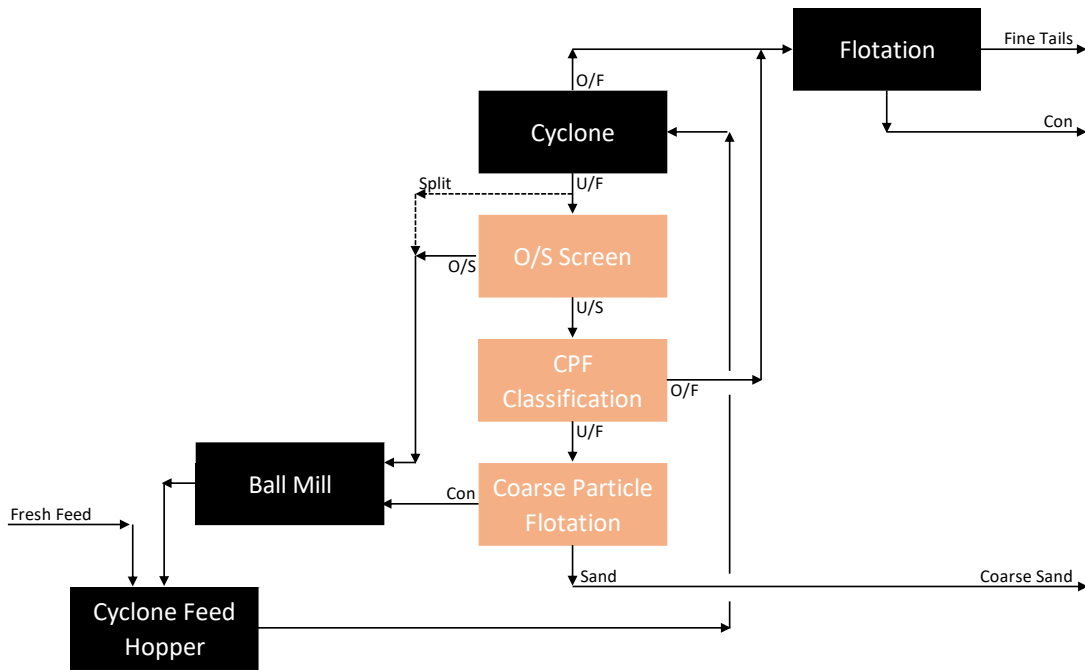


Figure 8 Cyclone Underflow Flow sheet

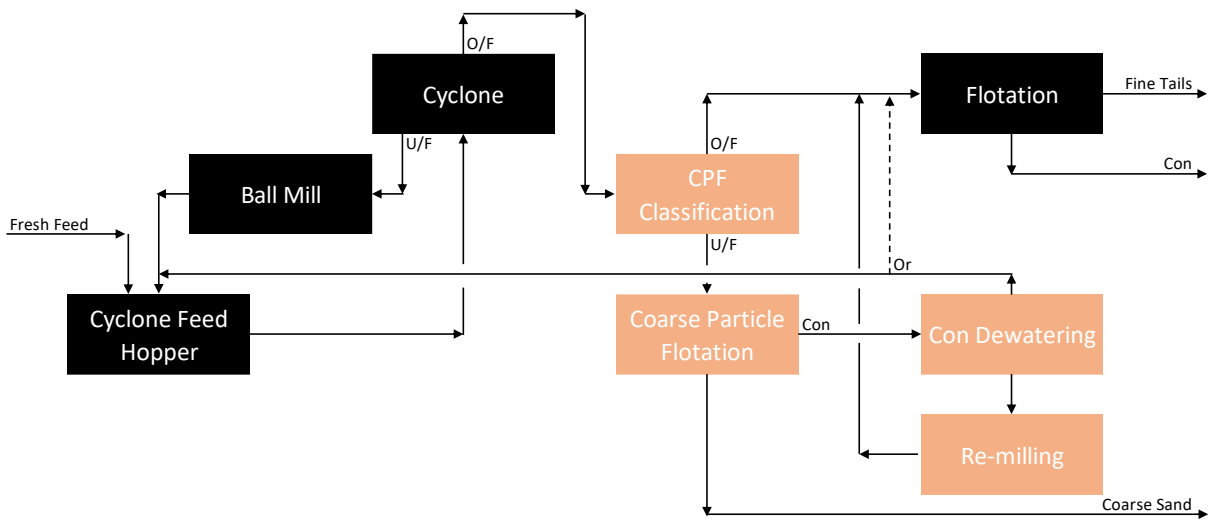


Figure 9 Cyclone Overflow Flow sheet

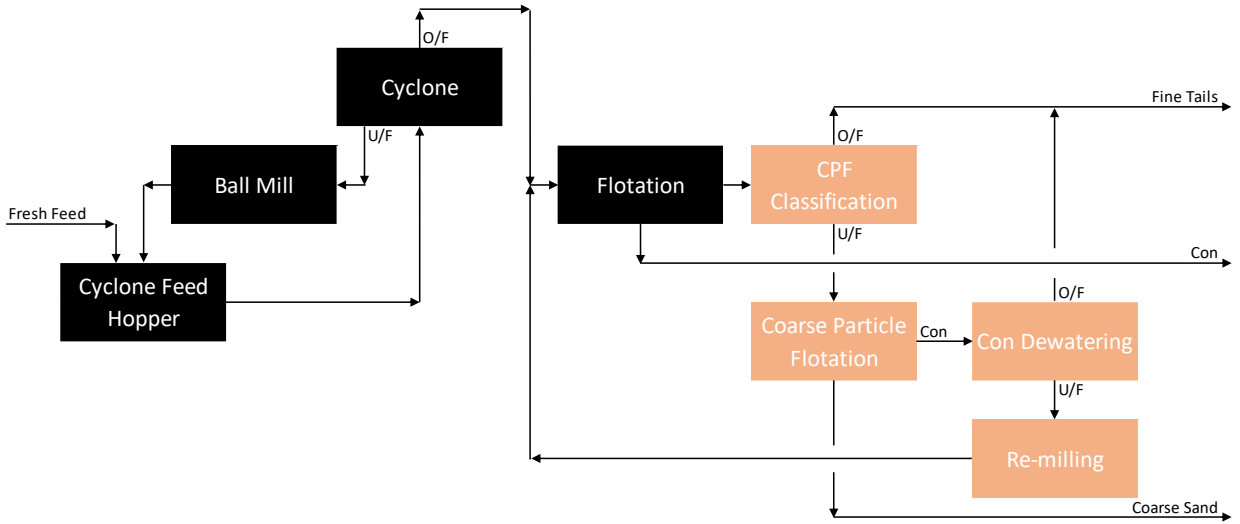


Figure 10 Rougher Tailings (Scavenging) Flow sheet

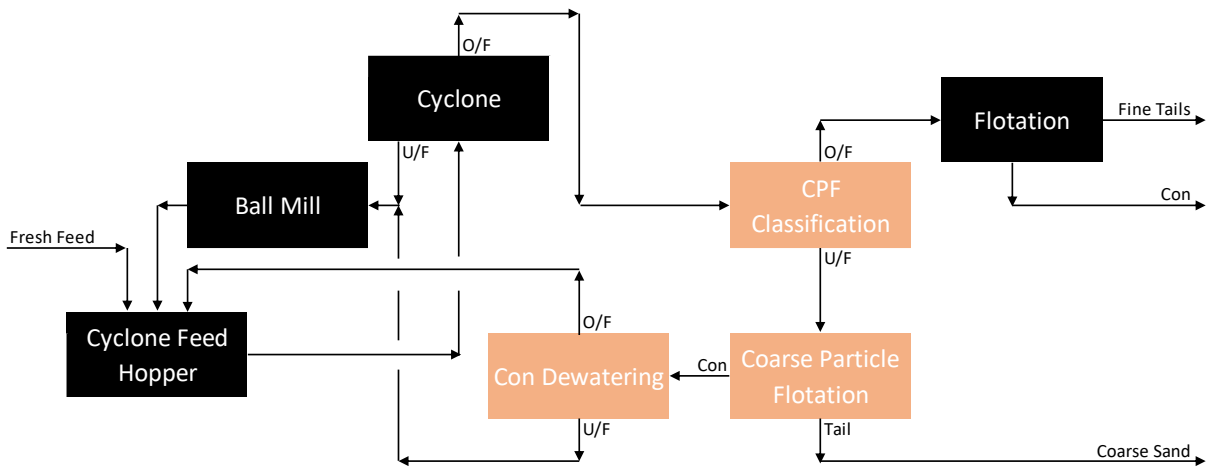


Figure 11 Classifier CPF Flow sheet

Each of these configurations have different benefits and drawbacks as outlined in Table 1.

Table 1 Circuit Configuration Considerations

	Cyclone Underflow	Cyclone Overflow	Rougher Tailings	Mill Classifier
Circuit effectiveness	Interactions with mill recirculating loads, PSD and quantity of coarse material available for recovery	Works well, however can cause water balance issues unless a thickening stage for fines is added, or water is returned to the grinding circuit	Simple for retrofitting to new or existing circuits	Simpler than cyclone underflow, but has interactions with milling circuit
Classification	Oversize protection required, adding complexity and cost to layout	Simpler than cyclone underflow, however may dilute flotation depending on circuit design. Water recycle may necessitate an additional stage of classification	Simpler than cyclone underflow, single stage classification possible.	Simpler than cyclone underflow
Water Balance	Integrated water balance with milling circuit reduces requirement to densify CPF classification overflow	Requires grinding thickener, or water recycle systems which can drive an additional stage of classification due to recirculation of fines	Water balance is managed by the tailings thickener, but hydraulic loading on thickener is increased unless water recycle system is implemented.	Water balance is integrated with grinding circuit. Has some recirculation of ultrafines (with risk of increased losses through overgrinding).
Reagent Conditioning	Limited opportunity for reagent conditioning unless a tank is added.	Limited opportunity for reagent conditioning unless a tank is added.	Can use the existing rougher bank for conditioning of PAX and diesel subject to rougher flotation regime	Limited opportunity for reagent conditioning unless a tank is added.
Flotation selectivity	Non-selective conditions required to minimise losses to sand can impact fines flotation	Non-selective conditions required to minimise losses to sand can impact fines flotation	Non-selective conditions in scavenging are unlikely to impact fines flotation, but may require reagent conditioning if a selective rougher regime is used.	Non-selective conditions required to minimise losses to sand can impact fines flotation
Demonstration at industrial scale?	No	Yes	Yes	No

CLASSIFICATION CIRCUIT DESIGN

Classification is a key component in the design of HydroFloat CPF plants. Particle size distribution requirements in the HydroFloat feed depend on mineralogy, distribution of valuable elements and gangue. In copper CPF plants, usually the feed requirement for the HydroFloat targets <10% mass

passing 106 μm , however this specification can change based on several factors. This requirement has historically been set to minimise the impact of fine particles on the fluidised bed, which can cause bed instability and recovery loss. Reducing fines also minimised unselective elution of fine particles to concentrate. However, more work is required in this area to better identify the impacts of particle size distributions on fluidised bed stability.

The early incarnations of HydroFloat circuits such as Cadia T3, Kennecott and Quellaveco use hydraulic classifiers (Crossflow Classifiers) to ensure that the fines reporting to the HydroFloat cells are minimised. Later generations of HydroFloat cells such as at Mogalakewna, El Soldado and Cadia T1/T2 have upgraded feedwells that achieve improved feed distribution and leverage similar hydraulic classification principals within the top zone of the HydroFloat cell to classify and remove ultrafines to concentrate. Concentrate dewatering screens or cyclones ensure the ultrafines, which are recovered through elutriation rather than true flotation, are ultimately discarded (in rougher tailings flow sheets) rather than returned to the process.

Newer generation CPF projects are proceeding with two stages of cyclone classification, or sand cyclones such as Weir's DE cyclone or FLS' cyclowash. These cyclones have seen adoption in tailings dam sand separation, where the objective is to maximise sand yield (recovery) whilst ensuring the fines content is less than 15% passing 75 μm . This is typically a permitting requirement to achieve safe sand material that drains water quickly and minimises the risk of high phreatic levels and instability when used for sand dam wall construction.

WATER CIRCUIT DESIGN

The HydroFloat cell and associated pre-classification processes consume a large amount of water. Water is added into the cyclone feed and sometimes into the cyclones themselves in the case of Weir DE cyclones and FLS Cyclowash cyclones in order to improve the separation efficiency. Water is also added into the cyclone underflow to achieve hydraulic transport (if necessary) and HydroFloat feed to achieve a good hydraulic feed distribution. Water is then added into the HydroFloat cell as teeter/elutriation water. Finally, water is used to dilute CPF underflow if required for transport. The water balance must therefore be appropriately designed for the circuit configuration. In some circuits, the water balance can significantly dilute the conventional rougher flotation circuit, which may negatively impact recoveries.

If a CPF plant is installed within the milling circuit or on cyclone overflow, the water addition into the HydroFloat circuit can be managed by returning dewatering cyclone overflow back to the primary cyclone feed hopper. This has the disadvantage of creating a recirculating load of fines (which misplace to primary cyclone or deslime cyclone underflow), which can cause a net increase in the amount of slimes in HydroFloat feed. This increases the risk of poor CPF performance if the CPF classification system is not adequately able to remove the slimes from CPF feed, however, this approach can reduce the water requirements of the circuit.

If CPF is installed on cyclone overflow, if water is not returned to the cyclone feed hopper, then the solids density of the classifying cyclone overflow will decrease, which may negatively impact the performance of the conventional flotation cells by reducing residence time.

If CPF is installed in a scavenging configuration, the diluted tailings stream is sent straight to the thickener and therefore there are no negative effects from the additional water, provided there is sufficient volumetric capacity in the thickener feed and process water systems.

An alternate strategy for managing the water balance is to install a dewatering cyclone overflow tank. This tank would contain most of the water from the HydroFloat circuit which reports to the dewatering cyclone overflow as well as a small quantity of misplaced ultrafines from the CPF circuit. Recycling this water to feed dilution or other process water streams within the plant can be considered but shouldn't be used for CPF elutriation water as the solids may block the teeter water

nozzles.

REAGENT CONDITIONING

A phenomenon of typical flotation is that reagents can be robbed from coarser particles by fine particles, due to their overwhelming surface area. A key consideration for CPF circuits is therefore ensuring that the coarse sulfide surfaces are suitably prepared with reagent dosing and sufficient conditioning time at the right Eh to ensure xanthates have converted to hydrophobic dixanthogen. Diesel is also typically added as a collector extender and can significantly improve the performance of the CPF cells.

For rougher scavenging, when mineralogy allows, collector can be added into the last scavenger cell to 'pre-dose' for coarse particle flotation, with additional collector and collector extender added just prior to the HydroFloat unit.

For configurations on cyclone overflow or in the milling circuit, careful thought needs to be given to the impact of adding strong and non-selective collectors early in the circuit, and the potential impact on the fine particle roughers, as there is potential to over-activate roughers in projects with complex metallurgy.

CONCENTRATE TREATMENT

Concentrate from coarse particle flotation needs to be dewatered, regrind and re-processed. CPF concentrates are typically low-grade quartz with low valuable sulfide mineral surface exposure. The power required to regrind CPF concentrates (which are mostly quartz or other competent minerals) can be significantly higher than typical flotation concentrates (which are mostly copper-bearing sulfides), so care must be taken when designing regrind circuits for this material.

The regrind size should be confirmed with test work and liberation data to balance regrind power across the circuit. The mass pull of CPF can be in the range of 10% – 20%, so it is not typically feasible to feed this material directly back into the cleaner circuit without adverse impacts on the cleaner regrind mill sizing and cleaner flotation capacities. Furthermore, stage grinding and re-floating of low grade quartz particles is more energy efficient. With the right amount of stage grinding, CPF concentrate can be returned to the conventional rougher flotation cells and achieve high recoveries. However, when there are capacity limitations, a dedicated rougher or rougher cleaner circuit for the CPF concentrate can be implemented.

TAILINGS OPPORTUNITIES

Coarsening the primary grind size presents a large opportunity to increase the fraction of 'sand' in tailings. Up to 60% of the tailings can be produced as sand rather than fines when the grind size is coarsened. Further increases to sand proportions would require improved classification and particle size distributions within the comminution circuit. Sand can either be mixed with the fines and sent to the tailings thickener, bypassed around the tailings thickener directly to the underflow distribution system, pumped separately to a TSF sand wall, or dewatered and disposed of by trucks or mechanical stacking.

Sand can be disposed into a sand structure, or co-mingled with dewatered fines to improve its handleability, co-mingled with coarse waste rock or other coarser waste streams from the process in a stable stack (Pyle, 2023).

Alternatively, sand and fines can be deposited in the form of a hydraulically dewatered stack, where sand effectively forms a filter medium for the fine tailings (Newman, 2023).

BUSINESS CASE ASSESSMENTS

To develop CPF projects, sound business case assessments are required. In the authors' experience, the maximum value from CPF projects is realised when the technology is used in conjunction with

comminution circuit assessments, and hydraulic assessments for the rest of the circuit to coarsen grind size and increase throughput. Under these conditions, throughput (and therefore revenue) can be increased by up to 30%, at similar or slightly higher total recoveries. At higher throughputs the operating cost reduces which further helps the business case for throughput based de-bottlenecking projects.

When installed to increase recovery, typically 40 – 50% of the tailings metal values can be recovered in the HydroFloat circuit. Over 90% of the recovered metal can be upgraded to final concentrate in multi-stage regrind and cleaning. Most base metal operations typically achieve recoveries of 85% or more, hence recovery improvements may only be 6 or 7% in absolute terms, which is significant but substantially less revenue than the potential throughput case. Hence the ultimate objective is generally to leverage the technology to increase throughput. Further benefits to the business case include reduced sitewide water consumption (sometimes deferring or precluding desalination or other water supply projects), reduced cutoff grade, increased reserves and more stable tailings storage options with longer project life for projects which are tailings constrained.

PROJECT INTEGRATION

A key challenge with developing CPF projects is that the value case requires changes to the mining rate, mining equipment and infrastructure, cutoff grade (and therefore ultimate pit shells), geometallurgy and throughput forecasting, process plant design and operation, water balance and tailings management. Therefore the scope of CPF projects will span all aspects of mining operations. Given the complexities this causes within most mining companies, most successful projects are justified on a recovery-only basis, but often with corporate vision to know there are longer term value cases that will be successively identified and approved organically once the technology is proven and implemented. However, this does require the engineering team to consider the long-term objectives and constraints for expansion in the circuit design.

CPF projects also do compete with conventional projects such as adding additional ball milling capacity, which is a much simpler project to justify from an operational perspective. However, adding additional grinding capacity is not necessarily the best option if the mining company is looking to improve the profitability and sustainability of its operations including reducing energy, water and producing sand for more stable tailings.

A further challenge is making project teams comfortable with the new approach of CPF. The authors are aware of projects where the technology has been rejected because lab test work has shown to be “too good”, and therefore was not trusted. Notwithstanding, a lack of metallurgical understanding around fundamental flotation principles, or conservative behaviours can lead to these conclusions and a lack of trust or scepticism of the approach. On one site, piloting, although not necessary from a test work or technical justification was a good opportunity to allow the operations team to become familiar with the approach.

When implementing CPF circuits in a brownfields environment, it is important to consider the actual circuit constraints such that latent capacity is fully utilised (at minimum additional capital) whilst at the same time key constraints are de-bottlenecked. Inefficient engineering on a conservative basis around these constraints can erode value.

From an owner’s team perspective, the project requires buy-in from all departments. This complicates the development and implementation pathway unless there is key business direction and leadership. For example, long term implementation pathways of CPF can reduce the water consumption. For projects with water limitations or high-cost water (such as Andean projects with desalination) the cost of CPF can be offset by water supply capital and operating cost savings. For other projects with tailings dam constraints, the ability to coarsen grind size and achieve more footprint-efficient tailings storage in dewatered structures is a large value driver. Most project teams tend to focus on limited scope for the concentrator only, and therefore miss long term value

opportunities around water supply, tailings, power, or ore reserves in their assessments.

There are several design decisions that can erode value from the project, so forward-thinking and experienced teams who challenge and improve the flow sheets, and fully understand the whole project context is critical to achieve successful outcomes.

SUMMARY OF INSTALLED CPF CONFIGURATIONS

Table 2 summarises installed HydroFloat circuits in hard rock applications. In addition to units shown in Table 2, there are more than 50 HydroFloat units operating worldwide treating non-sulfide ores, like phosphate, potash, lithium and coal.

Table 2 Installed CPF Configurations

Site	Commissioned	Classification	Water Balance	Duty
Cadia T3	2018	Crossflow classifiers	Tailings	Cu/Au
Kennecott	2019	Crossflow classifier	Tailings	Cu
El Soldado	2022	2 stage cyclones	Con dewatering is recycled	Cu
Mogalakwena	2022	2 stage cyclones		PGE
Cadia T1/T2	2023	2 stage cyclones	Tailings	Cu/Au
Quellaveco	Expected 2023	Crossflow classifier	Tailings	Cu

CONCLUSIONS

Coarse Particle Flotation is a step-change technology that allows for similar or greater recoveries than conventional flotation cells at particle sizes that are coarser by approximately 150 to 200 μm . This allows throughputs to be increased by up to 30% with the same milling circuit, subject to latent capacity in materials handling circuits and plant hydraulic transport. The net result can be to reduce the plant cutoff grade, reduce energy, water, and enable more stable tailings.

CPF circuit design has complexities related to the flow sheet, water balance, classification, concentrate treatment, sand handling and power supply. Business case assessments can be complex as latent capacity in the plant needs to be understood and leveraged where possible to give the most cost-effective upgrades, which means geometallurgy and robust throughput modelling which considers all key constraints is required. Furthermore, the ultimate business case spans multiple areas of plant operations, from the mine through to tailings. Ultimately, CPF technology needs buy-in from integrated owners teams with strong leadership to be able to navigate internal processes and manage CPF scope across multiple departments, to build a strong business case.

Ultimately the coarse particle flotation approach has long term potential in copper (and other hard rock applications) and the authors expect this technology will continue to see uptake in the industry, particularly for forward-thinking owners teams who can engage and drive decisions at wholistic levels in their organisations, supported by good quality engineering by those familiar with the nuances of the technology.

REFERENCES

Arbuero, K, Zuniga, J, McDonald, A, Valdes, F, Concha, J & Wasmund, E, 2022. Commissioning a HydroFloat® in a Copper Concentrator Application. In *Proceedings 11th Copper International Conference 2022* (Copper 2022, Santiago)

Carmona Franco, J, Fernanda Castillo, M, Concha, J, Chrstodoulou, L. & Wasmund, E, 2015. Coarse Gold Recovery Using Flotation in a Fluidized Bed. *Proceedings of Canadian Minerals Processors Conference*, (CIM, Toronto).

Lynch, A.J., Johnson, N.W., Manlapig, E.V. and Thorne, C.G., 1981. "Mineral and Coal Flotation

Circuits: Their Simulation and Control”, Elsevier Publishing, Amsterdam, 291 pp.

Miller, J, Lin, C, Want, Y, Mankosa, M, Kohmuench, & Luttrell, G, Miller, J, Significance of Exposed Grain Surface Area in Coarse Particle Flotation of Low-Grade Gold Ore with the HydroFloat® Technology (2016). In *Proceedings of the 28th International Mineral Processing Congress*. (IMPC, Quebec City)

Newman, P, Hydraulic Dewatered Stacking – A New Tailings Management System (2023), in *Proceeding of Tailings 2023* (Gecamin, Santiago)

Jaques, E, Vollert, L, Akerstrom, B, Seaman, B, 2021. Commissioning of the Coarse Ore Flotation Circuit at Cadia Valley Operations – Challenges and Successes, in *Proceedings 15th Mill Operators Conference 2021* (Australasian Institute of Mining and Metallurgy: Brisbane)

Pyle, M, Ballantyne, G, Lane & Meiring, S, 2023. Improving Tailings Outcomes with Next Generation Concentrators, in *Proceedings, Tailings 2023* (Gecamin: Santiago)

Seaman, B, & Vollert, L, 2017. Recovery of Coarse Liberated Gold Particles Using Pneumatically Assisted Fluidized Bed Flotation. In *Proceedings 56th Annual Conference of Metallurgists*. (COM, 56th Annual Conference of Metallurgists (COM, Vancouver).

Vollert, L, Akerstrom, B, Seaman, B, and Kohmuench, J, 2019. Newcrest’s industry first application of Eriez HydroFloat™ technology for copper recovery from tailings at Cadia Valley Operations, in *Proceedings of the 58th Conference of Metallurgists Hosting the International Copper Conference 2019*, (CIM, Vancouver).

Vollert, L, Haines, C, Downie, W, 2023. Coarse Separation – An Enabler for Improving the Sustainability of Ore Processing. In *Proceedings of the World Mining Congress 2023*. (WMC, Brisbane)

Pinto Valley Mine, Copper Recovery Study with the NovaCell

S Morgan¹, P Amelunxen², B Akerstrom³ and L Cooper⁴

1. Technology Manager - NovaCell, Jord International Pty Limited, 40 Oxley Street, St Leonards, NSW, 2065, Australia. Email: smorgan@jord.com.au
2. Senior Vice President – Technical Services, Capstone Copper, Suite 2100 – 510 West Georgia Street, Vancouver, BC, Canada. Email: pamelunxen@capstonecopper.com
3. Director – Metallurgy, Capstone Copper, 1138 N Alma School Rd, Mesa, AZ 85201, United States. Email: BAkerstrom@capstonecopper.com
4. Technical Expert – Flotation, Jord International Pty Limited, 40 Oxley Street, St Leonards, NSW, 2065, Australia. Email: lcooper@jord.com.au

ABSTRACT

The NovaCell™ is a novel froth flotation machine, invented by Laureate Professor Graeme Jameson, that recovers valuable particles over a wider particle size range. Thus, coarse and fine valuable particles that were previously lost to tailings using traditional technologies, such as mechanically agitated flotation cells, can now be recovered by one machine, potentially increasing the plant production. Targeting coarse particle recovery in the flotation circuit also allows for greater flexibility in the comminution circuit, potentially reducing the specific energy consumption, the greenhouse gas (GHG) emissions per tonne of valuable component, and improving the dewatering rates in mineral processing circuits. To investigate these NovaCell benefits, samples from an existing copper operation were studied under laboratory conditions.

In this case study, the response of plant feed and tailings material from the Pinto Valley mine, located in Arizona, USA, to NovaCell was investigated. The plant throughput is roughly 58 000 t/d, with a copper equivalent production of approximately 59 000 t Cu/y. The existing flotation circuit comprises both mechanical (self-aspirating) and column flotation cells.

The paper details the NovaCell test work and size-by-size recovery results for copper and other elements of interest. It also discusses the potential impact of the NovaCell technology as a substitute to the existing technologies at Pinto Valley mine, suggesting a significant increase in production, equivalent to approximately 15 000 t Cu/y in addition to a 15% reduction in equivalent carbon emissions per tonne of copper. Potential water consumption reductions are also discussed.

INTRODUCTION

For countries to reach their net zero emissions targets, critical minerals like copper will be essential for the clean energy transitions. However, current market forecasts indicate that the supply of copper will struggle to keep up with the future demand. For example, it is well documented that electric vehicles use more than double the copper when compared to combustion engine vehicles, and the sales of electric vehicles are steadily increasing. The International Energy Agency (IEA), founded in 1974, predicts that, based on current copper production and lead times for new mines, an accelerated transition could result in a copper supply shortfall by 2025. This would likely drive commodity prices higher and put financial pressure on consumers.

One solution would be to introduce innovative technology and processes that could enable existing copper operations to increase production and/or extend the life of their mines. However, the new technologies must be economically viable and environmentally and socially sustainable. The NovaCell is a novel froth flotation machine, invented by Laureate Professor Graham Jameson, designed to recover valuable particles over a wider particle size range than is typically achievable by conventional forced air or self-aspirating mechanically agitated flotation cells. In base metal flotation, coarse particles typically exhibit low flotation recovery due to poor liberation of the hydrophobic species. If particle attachment to an air bubble is successful, the inherent low buoyancy

of the coarse particle-bubble aggregate hinders its ability to penetrate the layer of high buoyancy fine particle-bubble aggregates collected in the froth phase. Fine particles on the other hand, with sufficient liberation, can also suffer low flotation recovery due to lack of momentum and energy resulting in poor collision efficiency with the air bubbles. Furthermore, due to their large surface area, fine particles can suffer detrimental impacts such as insufficient collector adsorption and reduced hydrophobicity from highly reactive surfaces. The NovaCell offers a solution to the mentioned challenges through the design of the particle collection and separation phases of the cell.

Figure 2 presents the process schematic of the NovaCell plant. New feed material entering the plant is combined with recycled tails. The combined stream is pumped and distributed across downcomers where particles and tiny bubbles collide in the high-shear zone ideal for fine and ultrafine particle recovery. The downcomers are designed to receive air from low pressure compressors. The advantage of the pressurised downcomers is that they can operate at higher airflows than previous downcomer designs that are naturally aspirated. The higher air flows provide more bubble surface area for fine particle attachment, thus promoting increased fine particle recovery than earlier downcomer designs.

Material exiting the downcomers enters the fluidised bed (shown as the shaded area in Figure 2). In this region, partially loaded bubbles surround particles in a low-shear environment ideal for coarse particle recovery. After attachment, both fine and coarse valuable minerals rise in the NovaCell and are collected across two product streams. A froth concentrate is collected at the top of the cell, similar to existing froth flotation technologies. A secondary recovery device, an internal cone, captures additional coarse valuable particles unrecoverable through the froth zone. The internal cone also removes the fine waste from the system; thus the stream feeds a classification circuit (represented by the cyclone in Figure 2). Here the coarse size fraction is collected as the second product. The two product streams can be combined or treated separately depending on the process requirements. Figure 2 presents magnified images of the NovaCell product streams for a porphyry copper ore. The froth product recovers particles that are more mineral rich than the screen product. The screen product generally recovers coarse particles with poor liberation of the hydrophobic species.

The NovaCell plant also produces two tails streams. The fine size fraction from the classification plant represents the fine tailings. A portion of this stream can be recycled to increase the available residence time for fines recovery, whilst the remaining material exits the system. At the bottom of the NovaCell, a second waste stream is produced which represents the coarse tailings. This stream would likely be suitable for filtration or other mechanical dewatering applications, followed by dry disposal.

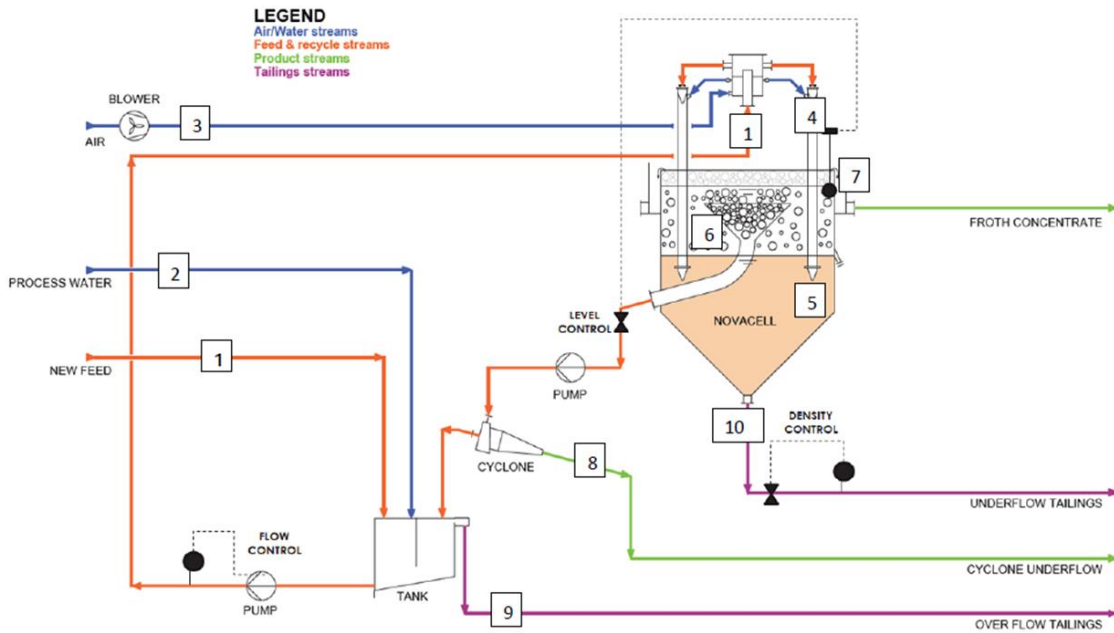


Figure 1: Process Schematic of NovaCell plant

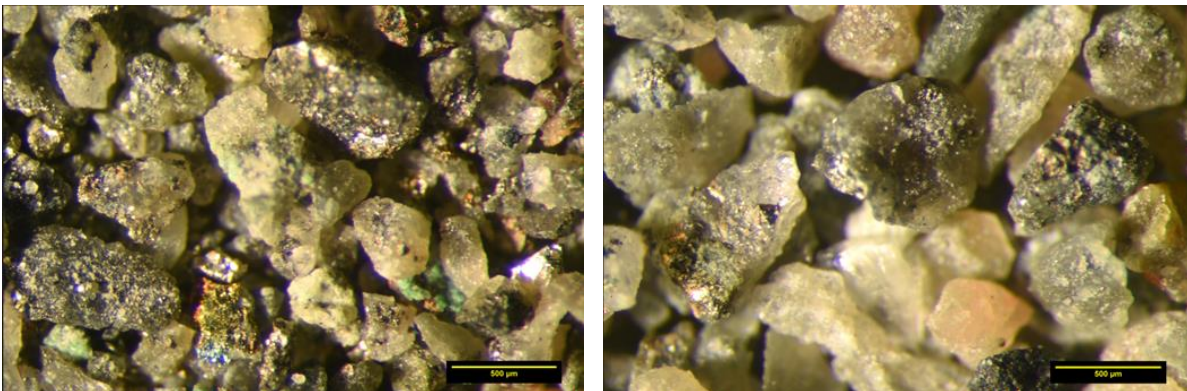


Figure 2: Magnified images of NovaCell float concentrate (left) and screen oversize (right) for porphyry copper ore

For coarse grained porphyry copper deposits, the NovaCell technology targets two principal areas to improve valuable mineral production:

- higher grinding throughput rates - by maintaining mineral recoveries at coarser flotation feed sizes, it allows operators to increase tonnage rates without significant changes to the grinding circuit.
- higher mineral recoveries – by improving the recovery of coarse and fine valuable particles, less metal is lost to the tailings dam improving recoveries and reducing environmental risks.

To date, three laboratory studies have demonstrated the potential benefits of the NovaCell technology. In copper, Jameson and Emer (2019) found that for a porphyry copper ore, the NovaCell obtained 100% recovery at particle sizes up to 300 µm. Morgan and Jameson (2022) observed similar results for a low-grade porphyry copper deposit, where the NovaCell improved copper recoveries at a P80 of 300 µm, when compared to the operating plant. In addition, the NovaCell indicated a product copper upgrade ratio was 8.4, typical of conventional rougher-scavenger circuits. In coal,

Jameson *et al.*, (2020) demonstrated that the NovaCell successfully recovered high-grade coal particles with a top size of 2 mm.

In this paper, the authors evaluate the potential benefits of the NovaCell technology with samples from the Pinto Valley mine.

CASE STUDY – PINTO VALLEY MINE

Pinto Valley Operations

Capstone Copper Corp.'s Pinto Valley mine (PVM) is an open pit porphyry copper mine in Arizona, USA. Material movement is roughly 56 000 t/d of ore to the mill, 20 000 to 25 000 t/d of dump leach material and 40 000 to 50 000 t/d of waste. The life-of-mine stripping ratio is 1.15 (leach is considered as waste in the calculation). The mine operation consumes approximately 35 000 m³ of fuel and contributes approximately 38% of PVM's carbon emissions per tonne of copper (1.6 tCO₂e per tonne of copper equivalent). Copper is primarily in the form of coarse-grained chalcopyrite (>95% of the total copper). The ore also contains some molybdenite and lesser gold and silver which contribute a minor proportion of the total revenue stream. The current planned life of mine (LOM) extends to 2039, although the company is progressing a study for a new tailings impoundment facility that will extend the LOM beyond 2039.

Pinto Valley's concentrator process flow sheet is shown in Figure 3. It consists of a crushing plant with primary, secondary, and tertiary crushing. Primary crusher product is screened, coarse material feeds the secondary crushers in open circuit and fines report to the ball mill feed. Secondary crusher product is screened, coarse product feeds the tertiary crushers in closed circuit and fines report to the ball mill feed. The nominal product size of the fine crushing plant is 10 to 12 mm (P80). The six ball mills are equipped with 4000 HP (3000 kW) motors and operated in closed-circuit with hydrocyclones to produce a flotation feed (hydrocyclone overflow) with a P80 of approximately 350 µm. The hydrocyclone overflow is directed to six rows of roughers, rougher concentrate is pumped to two regrind mills with regrind product feeding a simple cleaner circuit. The cleaners are comprised of four parallel column flotation cells with concentrate reporting to the molybdenum separation circuit or bypassing to final concentrate where, the product is filtered and trucked offsite. Column tail reports to a single cleaner scavenger bank with its concentrate in closed circuit with the column cells. Final tails comprise both the rougher tail and cleaner scavenger tail, which are thickened and deposited in a wet tailings storage facility.

Table 1: Sample characteristics of Feed Ore Sample

Particle Size (µm)	Copper		Feed Distributions	
	Feed Grade (%)	Variation from Bulk Grade	Mass	Copper
-600+500	0.03	-82.8%	13.8%	2.4%
-500+425	0.07	-63.3%	7.9%	2.9%
-425+300	0.09	-55.0%	15.7%	7.1%
-300+212	0.12	-36.9%	11.6%	7.3%
-212+106	0.20	3.9%	16.4%	17.0%
-106	0.35	83.1%	34.6%	63.3%
Total	0.19		100.0%	100.0%

Pinto Valley's copper sulfide mineral texture is considered coarse grained with a typical chalcopyrite liberation profile illustrated in Figure 4.

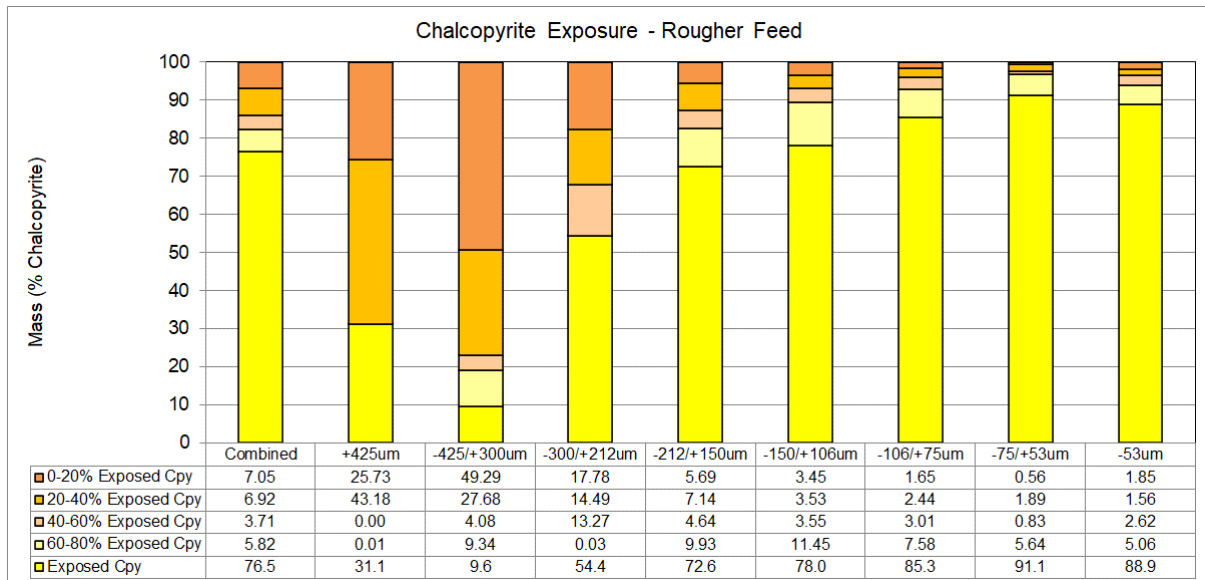


Figure 4: Typical liberation characteristics of the Pinto Valley feed ore.

Plant Rougher Tails

The PVM rougher tails sample delivered for the NovaCell test work was collected ahead of the tailings thickeners. During the sampling period, the plant was operated at reduced throughput, and therefore the P80 was finer than normal, at 212 µm. The chemical analysis of the PVM rougher tails sample contained 0.03% Cu, 34.6 ppm Mo and 0.6% Fe. Table 2 details the size-by-size elemental assays for the PVM rougher tails, including the relative variation of each size fraction from the bulk tails grade.

Table 2: Size-by-size elemental assays of Rougher Tailings Sample

Particle Size (µm)	Copper		Molybdenum		Iron	
	Feed Grade (ppm)	Variation from Bulk Grade	Feed Grade (ppm)	Variation from Bulk Grade	Feed Grade (%)	Variation from Bulk Grade
-425+300	950.4	202.2%	40.7	17.8%	0.3	-49.9%
-300+212	647.3	105.8%	38.7	11.9%	0.3	-53.4%
-212+106	308.6	-1.9%	34.7	0.4%	0.3	-48.3%

-106+53	128.0	-59.3%	14.3	-58.5%	0.4	-26.0%
-53	209.2	-33.5%	39.0	12.8%	0.9	50.0%
Total	314.5		34.6		0.6	

Table 3 details size-by-size mass and elemental distributions for the PVM rougher tails. Copper shows the highest distribution to the coarse size fractions, with around 40% of the copper in the +212 μm size fractions. In comparison, molybdenum and iron were approximately 20% and 8%, respectively. Iron presents the highest distribution to the fine size fraction, with around 70% of the iron in the -53 μm size fraction. Of interest is the relatively low sulfide content in the +53-106 μm size fraction, where conventional mechanical flotation cells are generally efficient at recovering valuable particles.

Table 3: Size-by-size mass and elemental distributions of Rougher Tailings Sample

Particle Size (μm)	Distributions			
	Mass	Copper	Molybdenum	Iron
-425+300	6.7%	20.3%	7.9%	3.4%
-300+212	10.4%	21.4%	11.6%	4.8%
-212+106	21.9%	21.5%	22.0%	11.3%
-106+53	14.5%	5.9%	6.0%	10.7%
-53	46.5%	30.9%	52.4%	69.7%
Total	100.0%	100.0%	100.0%	100.0%

A typical liberation profile of the Pinto Valley tailings stream is illustrated in Figure 5. This demonstrates that most of the liberated species across the intermediate size fractions are recovered successfully by the conventional flotation technology currently employed by the site.

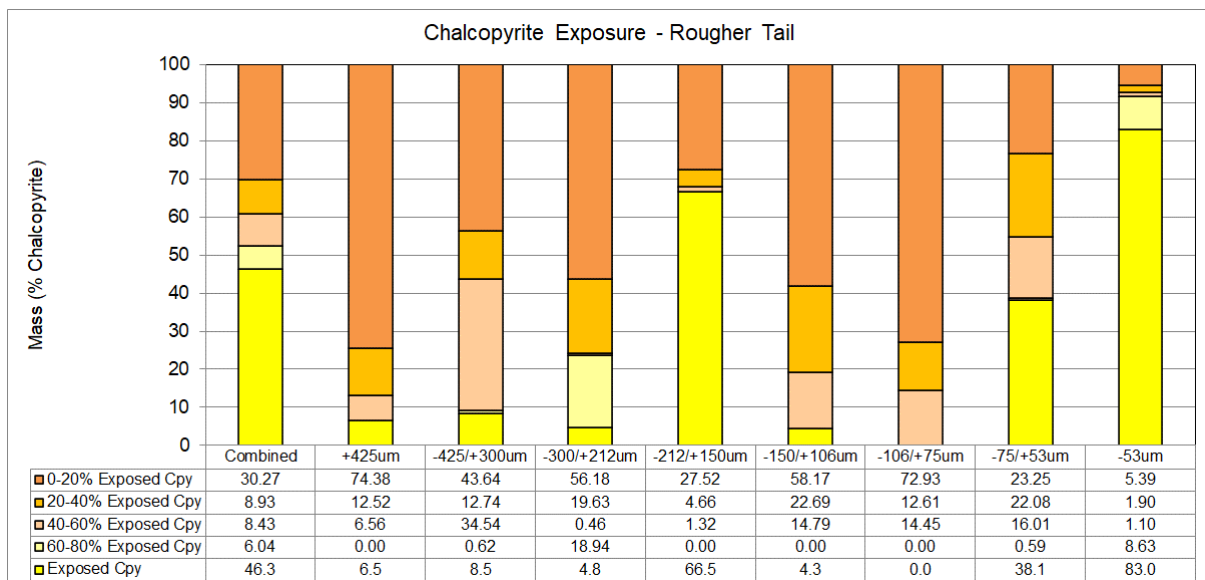


Figure 5: Typical liberation characteristics of the Pinto Valley tailings stream.

Test Conditions

The NovaCell laboratory test work was conducted in the small-scale rig (Figure 6) at the University of Newcastle. Table 4 details the operating parameters for both samples tested.

Table 4: Summary of NovaCell operating parameters.

Test Parameter	Unit	Value	
		Feed Ore	Rougher Tailing
Grind Size (P80)	µm	480	212
Column Diameter	mm	100	140
Screen Aperture	µm	300	212
Slurry Feed pressure	kPa (gauge)	200	200
Air Pressure	kPa (gauge)	100	100
Collector (PAX)	g/t	95	80
Frother (MIBC)	ppm (vol)	30	40
Feed density	(% w/w)	25%	25%
pH (Lime)	-	9.0	9.0
Eh (NaHS)	mV (Ag/AgCl)	-70	-70
Sample Feed Mass	g	6100	6500

The NovaCell products collected were the froth concentrate and screen oversize material. Both the products and remaining cell contents (defined at tails) were filtered and screened. For the feed ore sample screening was done at 500, 425, 300, 212 and 106 µm, whilst the rougher tailings material, being finer, was screened at 425, 300, 212, 106 and 53 µm.

All size fractions were submitted to an external laboratory for chemical analysis. The feed sample was analysed for copper only, whilst the plant tailings material was analysed for copper, molybdenum and iron.

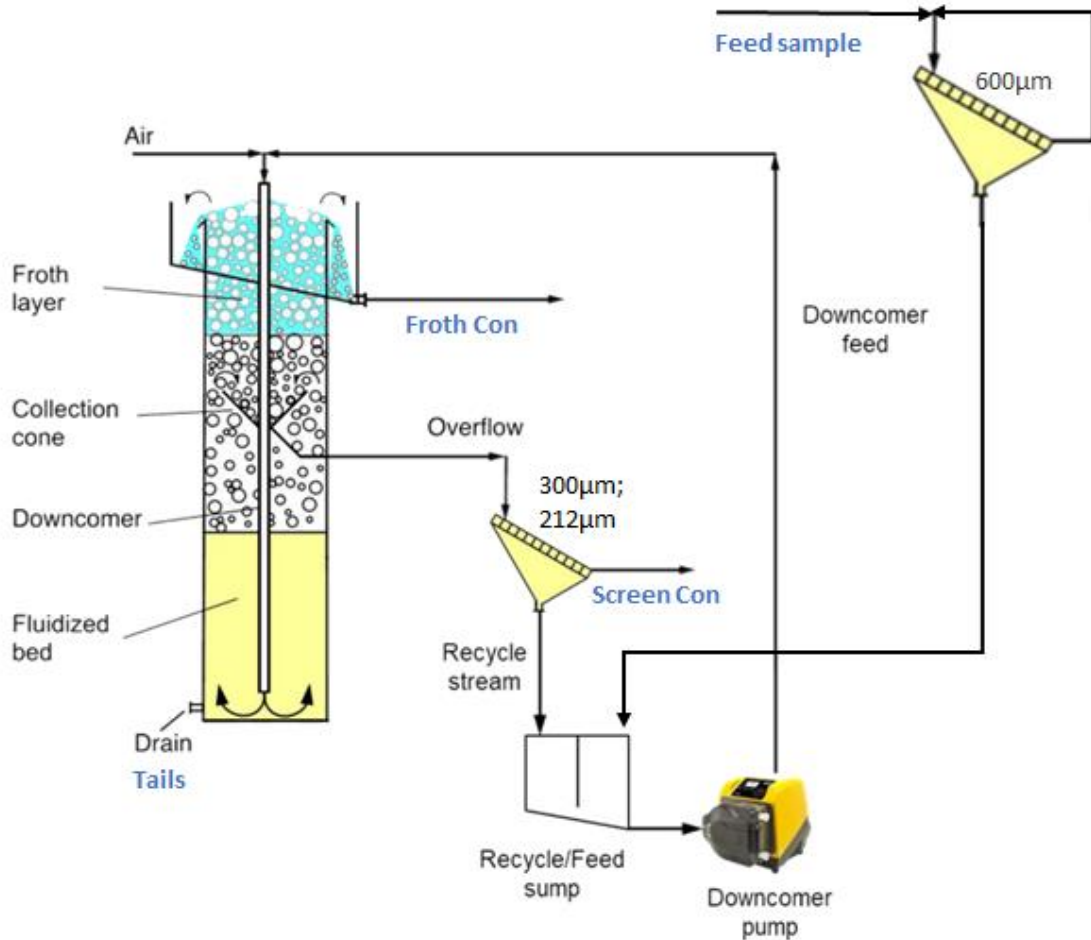


Figure 6: Schematic of NovaCell small-scale rig in batch mode

Test Results

Feed Ore

At a grind size (P80) of 480 μm , the NovaCell achieved a copper recovery of 94% from the PVM feed ore sample (Table 5). Majority of the copper was recovered to the froth concentrate at 90%, with the screen concentrate indicating 4% only. The combined concentrate mass pull was 6.0% and the combined product grade was 3.0% Cu. The product upgrade ratio (i.e. product grade/feed grade) was used to reflect mineral selectivity, and indicated an upgrade ratio of 15.8.

Currently, the Pinto Valley mine produces a flotation feed size (P80) of 343 μm , and the copper recovery in the rougher circuit is 88 – 90% (typical). The mass pull target is 5 – 8% and the product grade is 4 – 6% Cu (typical).

Table 5: NovaCell Results on Feed Ore Sample

Element	Recovery			Upgrade Ratio		
	Froth Con	Screen Con	Total	Froth Con	Screen Con	Total
Cu	90%	4%	94%	18.3	3.8	15.8

These results suggest that the NovaCell is effective at achieving a high overall copper recovery at relatively coarse flotation feed grind sizes.

Size-by-size Recovery

The size-by-size copper recoveries for the NovaCell is presented in Table 6.

The results confirm that the NovaCell can recover copper bearing particles across all the size fractions tested. It was highly efficient at recovering copper bearing particles in the -300 µm size fractions, achieving +90% copper recoveries. In the -500+300 µm size fractions, the copper recoveries were closer to 80%, and in the -600+500 µm size fraction the copper recovery dropped to 58%.

The product upgrade ratio for most of the size fractions were relatively consistent. However, the highest value achieved (41.6) was in the coarsest size fraction, suggesting that the coarse particles were very mineral rich. The lowest value achieved (9.5) was in the finest size fraction, which was likely caused by entrainment of fine waste material.

Table 6: NovaCell size-by-size copper recoveries on Feed Sample

Particle Size Range (µm)	Feed Grade (%Cu)	NovaCell Product (Froth + Screen concentrate)			
		Mass Pull (% of Total Feed)	Product Cu Recovery (%)	Product Grade (% Cu)	Product Upgrade Ratio
-600+500	0.03%	0.2%	58%	1.3%	41.6
-500+425	0.07%	0.3%	83%	1.4%	20.8
-425+300	0.09%	0.8%	83%	1.4%	16.4
-300+212	0.12%	0.5%	93%	2.6%	21.6
-212+106	0.20%	0.7%	96%	4.7%	24.2
-106	0.35%	3.5%	96%	3.3%	9.5
Total	0.19%	5.9%	94%	3.0%	15.8

Plant Rougher Tailings

At a grind size (P80) of 212 µm, the NovaCell yielded a copper recovery of 55% from the PVM rougher tailings (Table 7), with 44% from the froth concentrate and the other 11% from the screen concentrate. The combined product grade was 0.4% Cu, resulting in a calculated copper upgrade ratio of 12.6. The overall molybdenum recovery was 48%, with a product grade of 383 ppm Mo and upgrade ratio of 11.0. The overall iron recovery was 21%, with a product grade of 2.9% Fe and upgrade ratio of 4.7.

Table 7: NovaCell Results on Rougher Tailings Sample

Element	Recovery			Upgrade Ratio		
	Froth Con	Screen Con	Total	Froth Con	Screen Con	Total
Cu	44%	11%	55%	13.0	10.9	12.6
Mo	44%	4%	48%	12.9	4.2	11.0
Fe	20%	1%	21%	5.7	1.2	4.7

The results were achieved at a relatively low concentrate mass recovery of 4.4%. This is important because high mass recoveries can potentially overload regrind circuits, or otherwise require additional regrind equipment. In summary, the results suggest that the NovaCell was able to recover economically significant amounts of copper and molybdenum minerals from the PVM plant rougher tailings while maintaining selectivity and thereby limiting the likelihood of inefficiencies in downstream processing.

Size-by-size Recovery

The size-by-size recovery for copper, molybdenum and iron are presented in Table 8, Table 9 and Table 10, respectively. For copper, the size-by-size recovery results indicate that the NovaCell achieved relatively good recoveries in the fine size fractions, but the major improvement was observed in the intermediate and coarse size fractions. This may be attributed to the higher copper grades in the coarser size fractions compared to the bulk tails grade, likely a result of the reduced efficiency of the existing PVM mechanical cells at coarser size classes.

For molybdenum, the results indicated consistent recoveries in the fine and intermediate size fractions, with a decrease observed in the coarsest size fraction. This may be due to the molybdenum mineral texture and shape in the coarser size fractions.

Table 8: NovaCell size-by-size copper recoveries on Rougher Tails Sample

Particle Size Range (µm)	Feed Grade (%Cu)	NovaCell Product (Froth + Screen concentrate)			
		Mass Pull (% of Total Feed)	Product Cu Recovery (%)	Product Grade (% Cu)	Product Upgrade Ratio
-425+300	0.10%	0.3%	62%	1.22%	12.8
-300+212	0.06%	0.6%	71%	0.83%	12.8
-212+106	0.03%	0.6%	52%	0.62%	20.0
-106+53	0.01%	0.2%	46%	0.50%	38.9
-53	0.02%	2.8%	45%	0.16%	7.5
Total	0.03%	4.4%	55%	0.39%	12.6

Table 9 : NovaCell size-by-size molybdenum recoveries on Tails Sample

Particle Size Range (µm)	Feed Grade (g/t Mo)	NovaCell Product (Froth + Screen concentrate)			
		Mass Pull (% of Total Feed)	Product Mo Recovery (%)	Product Grade (g/t Mo)	Product Upgrade Ratio
-425+300	40.7	0.3%	31%	259.6	6.4
-300+212	38.7	0.6%	50%	354.5	9.2
-212+106	34.7	0.6%	48%	626.8	18.5
-106+53	14.3	0.2%	44%	695.0	37.7
-53	39.0	2.8%	51%	333.3	8.6
Total	34.6	4.4%	48%	382.5	11.0

Table 10: NovaCell size-by-size iron recoveries on Tails Sample

Particle Size Range (µm)	Feed Grade (% Fe)	NovaCell Product (Froth + Screen concentrate)			
		Mass Pull (% of Total Feed)	Product Fe Recovery (%)	Product Grade (% Fe)	Product Upgrade Ratio
-425+300	0.30%	0.3%	25%	1.6%	5.2
-300+212	0.28%	0.6%	23%	1.2%	4.2
-212+106	0.31%	0.6%	13%	1.6%	5.2
-106+53	0.45%	0.2%	19%	7.6%	15.8
-53	0.91%	2.8%	22%	3.3%	3.7
Total	0.60%	4.4%	21%	2.9%	4.7

Potential NovaCell Impact at Pinto Valley Mine

Higher grinding throughput rates

Various studies undertaken internally and externally by Pinto Valley mine have shown that the throughput bottleneck for the plant is the fine crushing plant. With minor capital investment and equipment modifications, an upper limit of 70 000 t/d can be achieved. Beyond this capacity, a larger investment is required, and the capital cost increases significantly. For this reason, the tonnage increase was fixed at 70 000 t/d.

To estimate the impact on grind size at the higher tonnage, surveys were collected around the mills and operating efficiency was determined based on the Bond model. Note that at PVM, the Bond work index decreases as the closing screen size aperture increases, i.e. the ores become “softer” when the grind is coarser (Figure 7). This is a secondary benefit of coarse grinding at Pinto Valley; however, this has not been considered in this analysis.

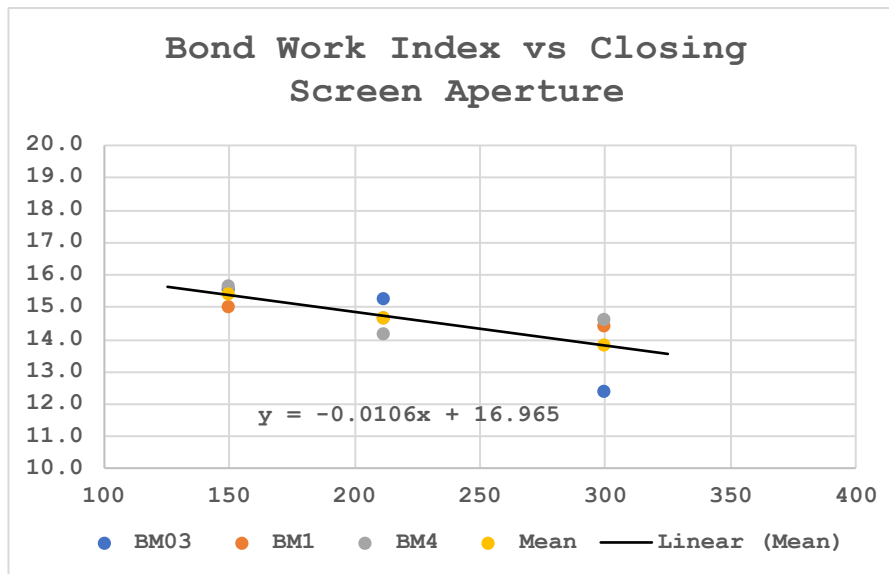


Figure 7: Bond Work Index kWh/t versus Bond test closing screen size for three samples of Pinto Valley ore

Increasing the tonnage from 58 000 t/d to 70 000 t/d at a nominal life-of-mine Bond work index of 16 kWh/t would result in an increase in the mill feed F80 from 12.5 mm to 14.5 mm and an increase the flotation feed P80 from 343 µm to 480 µm. Simulations were performed based on size-by-size kinetics measured on samples of rougher feed collected in the plant. Flotation kinetics for the

coarser grind were estimated using AminFloat, a steady-state phenomenological modeling platform configured with size-by-size collection rate (k_c) and maximum recovery (R_{max}) measured with a Full Kinetics Test (FKT), a laboratory flotation test procedure that can provide collection zone kinetics independent of froth zone effects. The results, shown in Figure 8, are compared with the performance of the Pinto Valley plant roughers (six parallel rows of 11 Wemco 164's, with some variations between rougher rows) and the NovaCell. It is expected that the area between the bottom curve ("PVM Mechanical Roughers") and the middle curve ("Laboratory FKT") is total chalcopyrite lost in the plant due to froth recovery effects in the Wemco cells; i.e. coarse particle drop-back from the froth zone. The area between the middle curve ("Laboratory FKT") and the top curve ("NovaCell") is equivalent to the improvement due to the fluidized bed effects in the NovaCell; i.e. the effect of the internal cone mechanism.

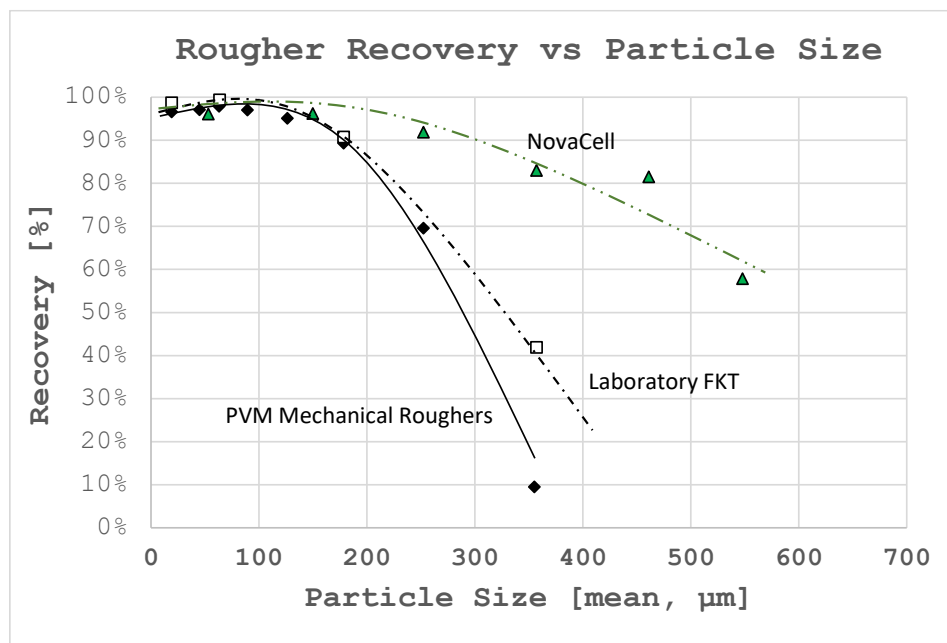


Figure 8: Size-by-size chalcopyrite recovery in the PVM mechanical rougher cells, a laboratory kinetics test in a Denver 5.0L cell, and in the NovaCell.

The simulator and NovaCell test results were used to estimate the metallurgical recovery for the 70 000 t/d throughput scenario. The circuit configuration consists of a single NovaCell treating the tailings of each of the six rougher banks. The concentrate from the NovaCell is returned to the ball mill circuit for further grinding. The fine and coarse tailings streams are combined and report to the existing thickeners.

The results indicate that for Pinto Valley's coarse-grained, fast-floating ores, the overall recovery would increase because the beneficial impact of the NovaCell is sufficient to offset the loss due to reduced liberation at the coarser grind. The coarser grind would result in a reduction of 3.7% copper recovery and 7.5% molybdenite in the existing rougher flotation circuit, but this would be offset by the coarse particle recovery achieved in the NovaCell. Overall, it is predicted that an increase in metal recovery would be achieved, of approximately 5% (absolute) for copper and 17.8% for molybdenum. Table 11 summarizes the predicted economics of the NovaCell operation at Pinto Valley mine and were calculated for a simple ten-year period and based on US\$3.50/lb Cu and US\$11.79/lb Mo.

The capital costs were determined based on simple assumptions, summarised as follows:

- US\$40M for mine fleet increase, based on the net present cost of a leased fleet sized for the current stripping ratio.
- US\$60M direct installed cost for six NovaCell circuits treating each of the rougher tails
- 1.42 installed cost multiplier for owners costs, indirect costs and contingency .

This capital cost allowance also includes minor costs incurred in debottlenecking the fine crushing plant. Downstream major equipment have already been assessed and can handle the higher throughput, but minor equipment (pumps, etc.) have not been assessed yet and these potential upgrades are not included in the above cost estimate. Lastly, the Novacell concentrate is assumed to be recycled back to the ball mills for further grinding; a separate study will be to evaluate the installation of a dedicated regrind mill for this material.

The operating costs were estimated based on current Pinto Valley milling costs. Mine operating costs were assumed to be constant per tonne of material moved. No change in the cutoff grade or mine plan was considered.

Table 11: Conceptual level economics of NovaCell operation at Pinto Valley mine

Parameter	Units	Base Case	NovaCell
Tonnage	t/d	58 000	70 000
Grind Size (P80)	µm	343	480
Copper Recovery	%	85%	90%
Water Consumption	m ³ /t	0.43	0.43
Capital Cost	US\$	\$0	-\$126,200,000
Capital Intensity	US\$/t/d		\$10,517
Total Copper Production	t/y	57 802	73 149
Total Molybdenum Production	t/y	394	630
Copper Equivalent Production	t/y	59 130	75 269
Incremental Revenue	US\$	\$0	\$124,528,000
	US\$/t	\$0	\$4.87
Operating Cost	US\$/t	-11.92	-10.76
	US\$	\$161,013,000	\$241,691,000
After-tax Earnings (21%)	US\$		\$335,938,000
NPV (10 Yr, 8%)	US\$		
IRR	%		63%
GHG	TCO _{2e} /tCuEq	4.27	3.62

The economics suggest that the NovaCell technology presents a compelling opportunity to significantly increase the metal production, by approximately 15 000 t/y of equivalent copper², with a payback period of less than two years. Furthermore, because the increased production is achieved at higher throughput and coarser grind, it does not require a commensurate increase in the energy consumption of the Pinto Valley concentrator. For this reason, the CO_{2e} per tonne of equivalent copper production is estimated to drop from 4.27 t to 3.62 t, amounting to a 15% reduction in equivalent carbon emissions per tonne of copper equivalent.

² Equivalent copper production is calculated based on \$3.50/lb Cu and \$11.79/lb Mo.

CONCLUSIONS

The technology benefits of the NovaCell have been investigated on feed ore and rougher tailings samples from Pinto Valley Mine. On the feed ore sample, the NovaCell demonstrated high overall copper recoveries at relatively coarse flotation feed grind sizes (P80) of 480 µm. In addition, the NovaCell recovered a significant proportion of the coarse valuable particles to the froth concentrate. On the rougher tailings sample, the NovaCell was able to recover economically significant amounts of copper and molybdenum minerals while maintaining selectivity and thereby limiting the likelihood of inefficiencies in downstream processing.

The potential impact of the NovaCell technology at Pinto Valley Mine suggested a significant increase in metal production, by approximately 15 000 t/y of equivalent copper and a 15% reduction carbon emissions per tonne of copper equivalent.

Based on the NovaCell test work results and predicted economic benefits, Pinto Valley mine has decided to investigate the technology further at site. A NovaCell pilot plant trial is planned for Q1 2024, and the results are expected to be published in future technical papers.

Other planned future work includes:

- Evaluation of a dedicated regrind and cleaner circuit for the Novacell concentrate, instead of returning the concentrates to the ball mills.
- Detailed liberation studies on Novacell product streams, and analysis of Novacell flotation kinetics with the aim of developing a scale-up model that does not require piloting.
- Evaluation of filtration or other dewatering technology on the coarse Novacell tailings.

ACKNOWLEDGEMENTS

The authors would like to acknowledge Professor Graeme Jameson, Joshua Sovechles and Kitty Tang from Hunter Process Technologies (HPT) for their assistance in conducting the NovaCell test work. We would also like to thank the Pinto Valley metallurgical teams for providing the samples for the NovaCell test work.

The authors acknowledge the funding support from the Australian Research Council for the ARC Centre of Excellence for Enabling Eco-Efficient Beneficiation of Minerals, grant number CE200100009.

REFERENCES

Capstone Mining Corp., "2021 Sustainability Report." www.capstonecopper.com

https://capstonecopper.com/wp-content/uploads/2022/12/Capstone_2021_SustainabilityReport.pdf

Jameson, G.J., and Emer, C., 2019. Coarse chalcopyrite recovery in a universal froth flotation machine, *Minerals Engineering* 134, pp 118-133

Jameson, G.J., Cooper, L., Tang, K.K., and Emer, C., 2020. Flotation of coarse coal particles in a fluidized bed: The effect of clusters, *Minerals Engineering* 146, pp 2-13

Morgan, S., and Jameson, G.J., 2022. Improving mill throughputs, with coarse and fine particle flotation in the NovaCell™ in *Proceedings IMPC Asia-Pacific 2022*, pp 1101-1117

Concorde Cell Technology Retrofit Effect on an Existing Self-Aspirated Flotation Cell

M Ball¹, N Kupka², G Bermudez³, A Yáñez⁴

1. Services BA, Process Metallurgy Manager, Metso Finland, Rauhalanpuisto 9, 02231 Espoo, Finland, michelle.ball@mogroup.com
2. Minerals BA, Senior metallurgist, Metso Finland, Rauhalanpuisto 9, 02231 Espoo, Finland, nathalie.kupka@mogroup.com
3. Services BA, Product Director Flotation, Metso Canada, 5045 South Service Road, Burlington, ON L7L 5Y7, Canada, guillermo.bermudez@mogroup.com
4. Minerals BA, Product Manager Concorde Technology, Metso Finland, Rauhalanpuisto 9, 02231 Espoo, Finland, alejandro.yanez@mogroup.com

ABSTRACT

Fine and ultrafine particles present challenges for recovery due to their slow kinetics and associated long residence times. However, the need to recover these particles increases as ore bodies become more complex. The Concorde Cell™ was developed with the specific objective to overcome these challenges for any flotation application. Slurry introduction at the top of a Concorde Blast Tube™, being equipped with forced-air injection and maintained under pressure, allows for the slurry to reach supersonic speed within the Blast Tube, reverting to sub-sonic conditions when discharged into the cell tank, thereby generating a shockwave before striking against an impingement bowl. This novel development opens new possibilities for retrofitting into existing self-aspirated pneumatic flotation cells.

This report summarises the Concorde Blast Tube upgrade of a self-aspirated pneumatic flotation technology at an industrial application. Pilot scale studies were conducted benchmarking the Concorde Cell to the self-aspirated pneumatic cell already installed in the plant, leading to the subsequent replacement of this technology with the Concorde Cell. The metallurgical performance of both flotation cells at pilot and industrial scale are discussed in detail.

INTRODUCTION

In mineral processing applications, fine to ultrafine particles are generally understood as being smaller than 20 to 30 µm (Drzymala et al., 2020; Hassanzadeh et al., 2019). Flotation usually operates most efficiently when particle size is between 10 and 150 µm (Shergold, 1984). As such, in comparison to these coarser particles and for the same percentage of solids, fine to ultrafine particles have higher specific surface area, higher water film surface area, lower mass, lower momentum and higher surface energy (Nguyen & Schulze, 2003).

Such particles tend to float more slowly but they are more easily entrained (Feng & Aldrich, 1999; Trahar, 1981; Wang, 2016). Much longer residence times are therefore required to achieve similar recoveries to average-sized particles. As a consequence, the flotation of fine to ultrafine particles is more difficult and usually exhibits lower performance. Yet, with the declining grain size of ore bodies and more and more disseminated minerals, the ability to recover these particles is becoming important for the flotation of ores in general, but especially for metals critical to the green and digital transition. Today, a plant regrind closing size of 4 to 5 µm can be considered economically viable (Michaux, 2021).

Smaller bubbles and a higher shear-rate in the flotation cell can increase the flotation rate of fine to ultrafine particles (Nguyen & Schulze, 2003). These two considerations have driven the development

of the Concorde Cell by Professor Jameson of the University of Newcastle (Jameson, 2010). The Concorde Cell is a pneumatic high intensity forced air flotation type of technology (Metso , 2021). Unlike agitated flotation, pneumatic flotation involves mixing the air and the pulp in a continuous stream, thereby separating contact and froth treatment zones.

Test work at pilot and industrial scales with the Concorde Cell was performed and benchmarked against the self-aspirated pneumatic flotation technology (SAP). This article presents the metallurgical performance of the Concorde Cell against the SAP, in a metallurgical coal application.

METHODS

Technology description

Fine and ultrafine particles present challenges for recovery due to their slow kinetics and associated long residence times. However, the need to recover these particles increases as ore bodies become more complex. The Concorde Cell was developed with the specific objective to overcome these challenges for any flotation application. Slurry introduction at the top of a Concorde Blast Tube, being equipped with forced-air injection and maintained under pressure, allows for the slurry to reach supersonic speed within the Blast Tube, reverting to sub-sonic conditions when discharged into the cell tank, thereby generating a shockwave before striking against an impingement bowl.

This novel development opens new possibilities for retrofitting into existing self-aspirated pneumatic flotation cells. An upgrade from an SAP to a Concorde Cell mainly consists in keeping the tank and auxiliary equipment while removing the existing downcomers and replacing them with a set of Concorde Blast Tubes.

Test work

Pilot test work was conducted at Hunter Process Technologies (HPT) under the guidance of Prof. Graeme Jameson, in Newcastle (NSW), Australia. Figure 1 shows the pilot unit that was used for the test work. This equipment is mobile and can be transported to mine sites for test work, alternatively test work can also be conducted in a laboratory.



Figure 1 – Concorde Cell at pilot scale in industrial environment

RESULTS AND DISCUSSION

Pilot Scale Testing

Metallurgical coal samples for laboratory test work were provided by an industrial metallurgical coal washing plant located in the Bowen Basin, Queensland, Australia. Two streams from the operating full-scale SAP, the “fresh feed” and the “pumped feed”, were investigated at pilot scale. The fresh feed comes directly from the desliming cyclone overflow stream. This stream contains no reagents, whether diesel (collector) or MIBC (frother). The pumped feed is composed of the fresh feed and a portion of tailings that is recycled back to the feed of the SAP and as such, contains some reagents. About 22% (w/w) of the pumped flotation feed consists of the tailings in the laboratory test work, and about 29% in the industrial plant.

Figure 2 and Figure 3 show the yield-ash curves and the combustibles recovery against ash content for the fresh feed and the pumped feed in the Concorde Cell and the SAP. The results are similar for the fresh feed experiments, with the Concorde Cell arguably producing a marginally cleaner concentrate with an ash content lower by 0.1 to 0.4% compared to the SAP. The difference between the two technologies is more pronounced near the knee of the curve, with the Concorde Cell producing 6% more yield and recovering 7% more combustibles.

In the case of the pumped feed, there is a significant difference between the concentrates of the two devices. Over a wide range of yields and combustibles recovery, the Concorde Cell ash content was in average about 1.5% lower than the corresponding SAP values. The ash content in the product remains higher than in the fresh feed runs, even when taking into account the ash content in the feed. Froth washing was applied in the fresh feed runs to reduce entrainment and produce a cleaner concentrate as done in column flotation. These results show that froth washing did help decrease the ash content with limited impact on the yield. In general, the wash water demand in coal flotation is about 1.5 times the water flow reporting to the froth to achieve a high level of performance (Laskowski et al., 2007).

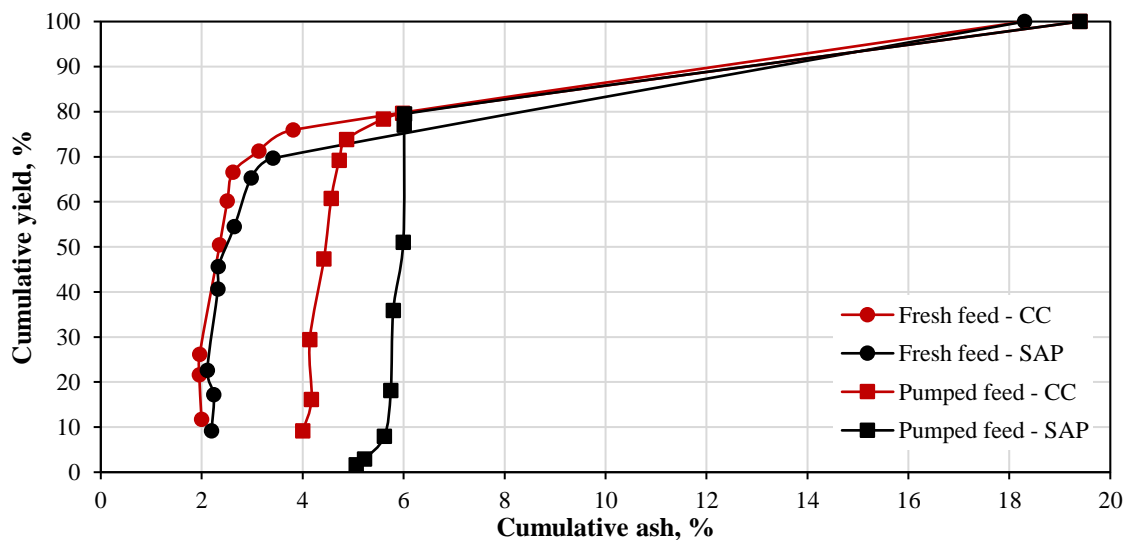


Figure 2 – Cumulative yield against cumulative ash for the fresh feed and the pumped feed in the Concorde Cell (CC) and the SAP

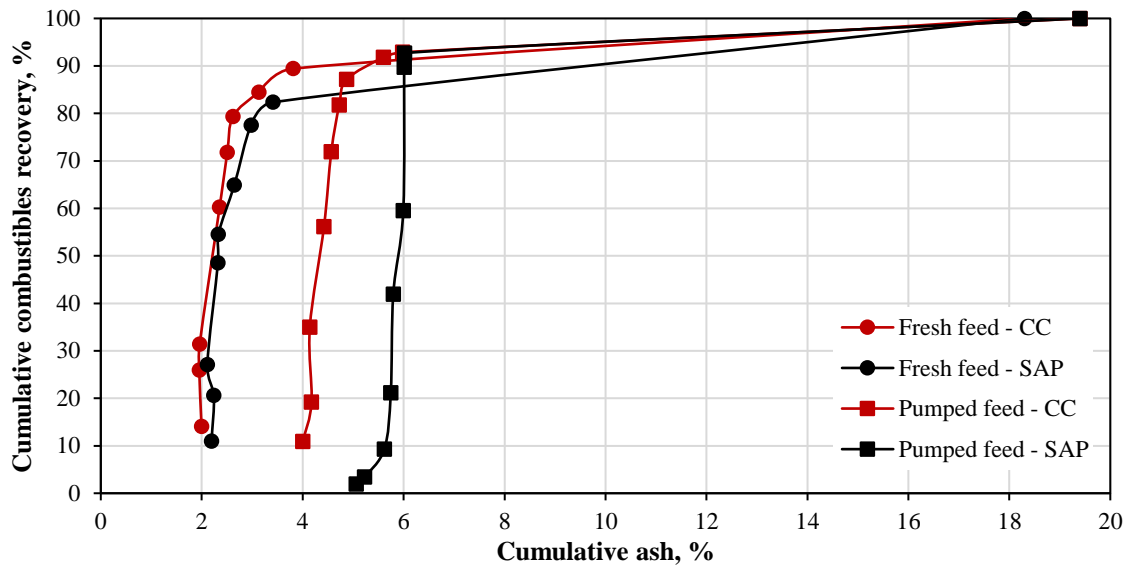


Figure 3 – Cumulative combustibles recovery against cumulative ash for the fresh feed and the pumped feed in the Concorde Cell (CC) and the SAP

Figure 4 shows the cumulative yield against flotation time only for the pumped feed as these runs were conducted without stepwise reagent addition. It is clear that the flotation rate in the Concorde Cell is significantly faster than in the SAP. The yield increases almost linearly, which suggests that some factor limited the recovery in the SAP and most likely the bubble carrying rate. There is most likely insufficient bubble surface area available to capture the coal in the SAP compared to the Concorde Cell. As the latter was designed to produce finer bubbles, it can be assumed that the bubble surface area flux is larger in the Concorde Cell than in the SAP, allowing the Concorde Cell to achieve higher yields and combustibles recovery for a given ash content. Furthermore, the high shearing rate most likely contributes to maintaining the low ash content despite the high yield, by preventing mechanical entrainment of the ash through high dispersion and high energy dissipation in the cell.

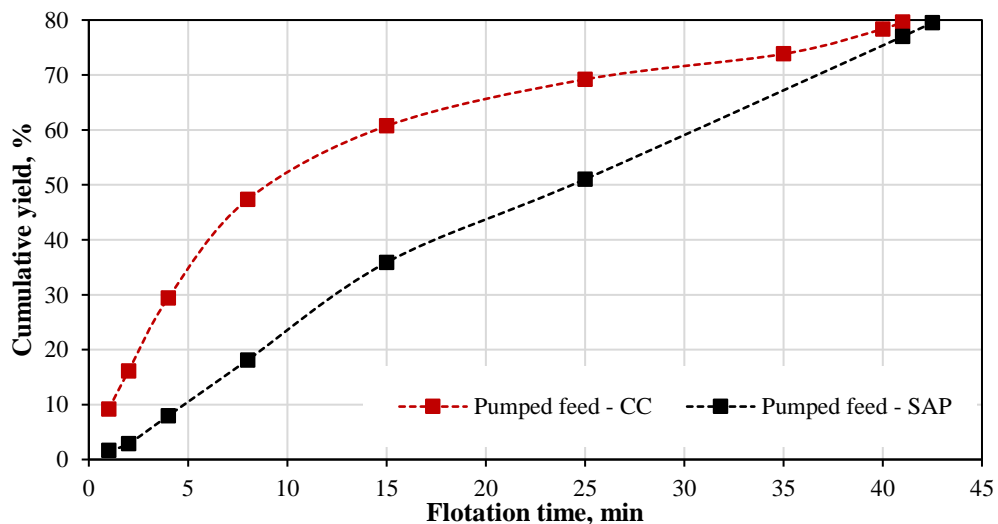


Figure 4 – Cumulative yield against flotation time for the pumped feed

Industrial Scale Testing

The Concorde Cell results at pilot scale led to the replacement of the SAP with the Concorde Cell in the metallurgical coal washing plant mentioned (Figure 5 and Figure 6). Metso conducted a sampling campaign on the Concorde and SAP cells to gain understanding on the metallurgical performance of both cells at industrial scale. Three individual sampling rounds were completed on the feed, tailings, and the concentrate streams of both units. Additionally, fresh feed to flotation, SAP feed, Concorde feed, pumped feed, combined tails, and combined concentrate were analysed on a size-by-size basis. The SAP was operated with froth washing whereas the Concorde Cell was not (due to mechanical issues with the washwater system).



Figure 5 – Fully installed and operating Concorde Cell in the metallurgical coal washing plant



Figure 6 – Concorde Blast Tubes and impingement bowls inside the existing SAP flotation tank

Table 1 and Table 2 present the balanced average results of the three rounds of sampling for the SAP and the Concorde Cell respectively. The yields are much lower compared to that in the pilot scale as the metallurgical coal washing plant operates at a limited amount of recycle. This was selected to increase the throughput of the cells in the plant, but ultimately influence the yield with a lower amount of recirculation through the system of a single particle. Over the three sampling rounds, the Concorde Cell pulled on average 4.8% more mass to concentrate than the SAP at the same ash content, and this despite the fact that only the SAP was operated with froth washing during the survey. The ash content in both feeds is almost identical. As such, the SAP produces lower yield, expected due to froth washing, but does not compensate with a cleaner concentrate. To identify the

source of the performance difference, a size-by-size analysis was conducted.

Table 1 – SAP balanced average results

Stream	Yield, %	Ash content, %	Ash recovery, %	Average %solids
Feed	100.0	26.26	100.0	2.2
Conc	54.7	6.08	12.65	18.1
Tails	45.3	50.6	87.4	1.1

Table 2 – Concorde Cell balanced average results

Stream	Yield, %	Ash content, %	Ash recovery, %	Average %solids
Feed	100.0	26.55	100.0	2.3
Conc	59.5	6.07	13.61	18.5
Tails	40.5	56.6	86.4	1.2

The particle size distributions of the fresh feed, and the feeds, concentrates and tailings of the Concorde Cell and the SAP were analysed. They show that between 75 and 80% of the feed particles are in the -45 µm size fraction and that the particle size distributions (PSDs) are similar for the respective streams of the Concorde Cell and the SAP. Figure 7 displays the ash content of the various streams around the Concorde Cell and the SAP while Figure 8 plots the yield to the concentrates of the two cells. Figure 5 shows that in the bulk (unsized) data, the ash contents of the concentrates are identical but in the size fractions, ash is higher for the Concorde Cell except in the critical size fraction of -45 µm, where it is slightly lower, despite the higher yield and the absence of wash water. Figure 6 shows that for every size fraction, the Concorde Cell produces a higher yield than the SAP especially in the fines, -63 µm and -45 µm, where the yield is higher by 5 and 11% respectively. As such, the Concorde Cell outperforms the SAP consistent with the pilot scale tests, but the industrial scale reveals that this improved metallurgical performance is driven by the performance of the fine size fraction. This confirms that the unique features of the Concorde technology – finer bubbles, a high shear-rate high energy dissipation environment, the sonic shockwave – do recover the otherwise unrecovered coal value.

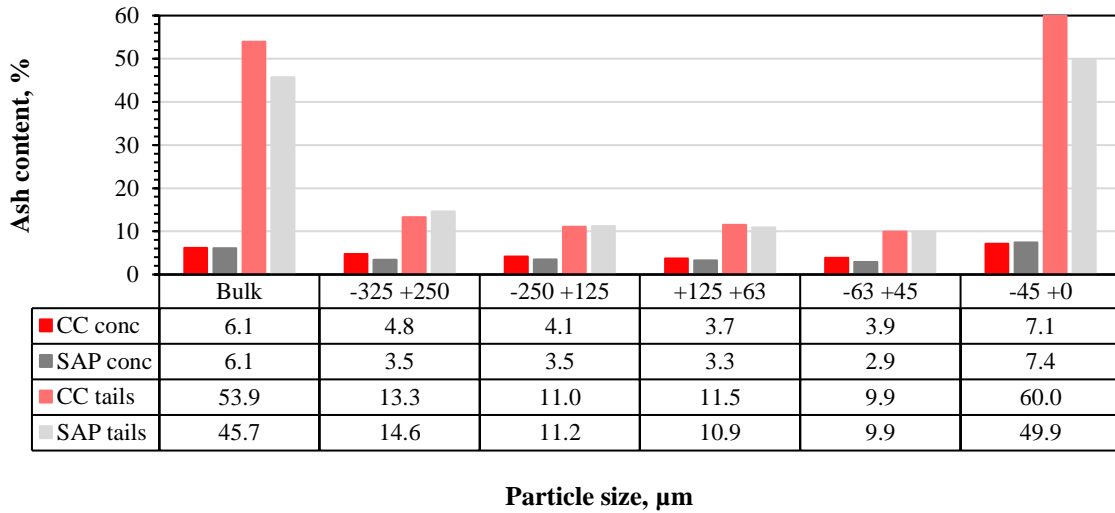


Figure 7 – Ash content by particle size for the different streams of the Concorde Cell (CC) and the SAP

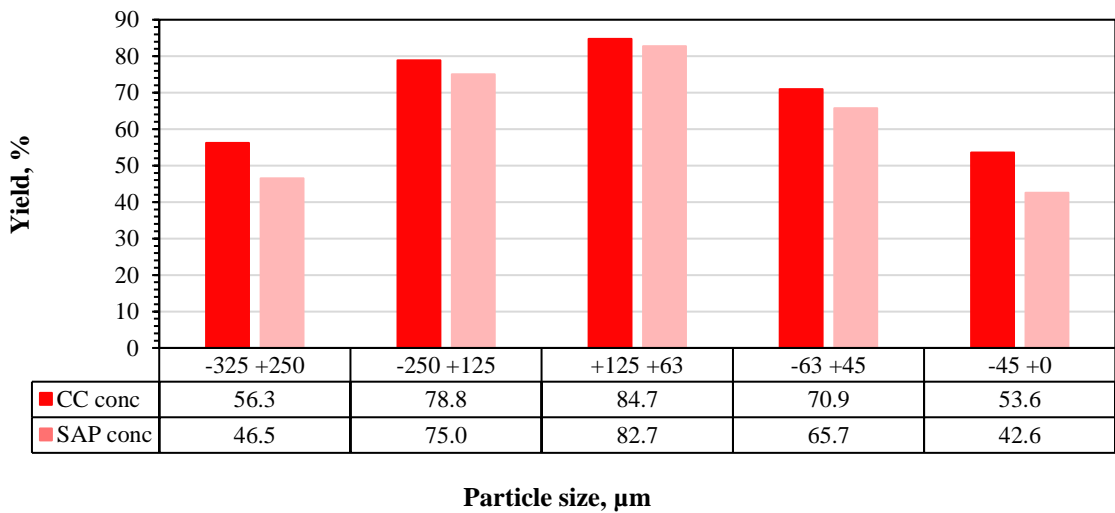


Figure 8 – Yield by particle size for the concentrate of the Concorde Cell (CC) and the SAP

CONCLUSIONS

The Concorde Cell is an enhanced pneumatic flotation technology. With its shockwave-induced high shear rate and finer bubbles and its high energy dissipation, the Concorde Cell provides a very favourable environment for the recovery of fine particles. Slurry introduction at the top of a Concorde Blast Tube, being equipped with forced-air injection and maintained under pressure, allows for the slurry to reach supersonic speed within the Blast Tube, reverting to sub-sonic conditions when discharged into the cell tank, thereby generating a shockwave before striking against an impingement bowl. This novel development opens new possibilities for retrofitting into existing self-aspirated pneumatic flotation cells.

Test work at pilot and industrial scales with the Concorde Cell was performed and benchmarked to SAP cells. In both scales evaluated, the Concorde Cell consistently outperformed the SAP.

In most cases, the Concorde Cell provides faster kinetics and a higher grade. In the case of metallurgical coal, at pilot scale, the Concorde Cell provided higher yields than the SAP thanks to the faster kinetics. At industrial scale, the Concorde Cell pulled on average 4.8% more mass to concentrate than the SAP at the same ash content, and this despite the fact that only the SAP was operated with froth washing during the survey. A size-by-size analysis of the streams revealed that for every size fraction, the Concorde Cell produces a higher yield than the SAP especially in the fines, -63 μm +45 μm and -45 μm , where the yield is higher by 5 and 11% respectively. As such, the Concorde Cell outperformed the SAP consistent with the pilot scale tests. The sized analysis of the industrial scale test reveals that this improved metallurgical performance is driven by the fines.

This confirms that the unique features and scalability of the Concorde technology – finer bubbles, a high shear-rate high energy dissipation environment, the sonic shockwave – do recover the otherwise unrecovered coal value.

REFERENCES

- Drzymala, J, Bednarek-Gąbka, P, & Kowalczyk, P B, 2020. Simplified empirical and phenomenological evaluation of relation between particle size and kinetics of flotation. *Powder Technology*, 366, 112-118. <https://doi.org/https://doi.org/10.1016/j.powtec.2020.02.041>
- Feng, D, & Aldrich, C, 1999. Effect of particle size on flotation performance of complex sulfide ores. *Minerals Engineering*, 12(7), 721-731. [https://doi.org/https://doi.org/10.1016/S0892-6875\(99\)00059-X](https://doi.org/https://doi.org/10.1016/S0892-6875(99)00059-X)
- Hassanzadeh, A, Azizi, A, Kouachi, S, Karimi, M, & Celik, M S, 2019. Estimation of flotation rate constant and particle-bubble interactions considering key hydrodynamic parameters and their interrelations. *Minerals Engineering*, 141, 105836. <https://doi.org/https://doi.org/10.1016/j.mineng.2019.105836>
- Jameson, G J, 2010. New directions in flotation machine design. *Minerals Engineering*, 23(11), 835-841. <https://doi.org/https://doi.org/10.1016/j.mineng.2010.04.001>
- Laskowski, J S, Luttrell, G H, & Arnold, B J, 200). Coal Flotation. In M. Fuerstenau, G. J. Jameson, & R. H. Yoon (Eds.), *Froth flotation - A century of Innovation* (pp. 611-633). Society for Mining, Metallurgy and Exploration.
- Metso, 2021. *Concorde Cell™ - Recover the unachievable ore value*. Metso. Retrieved 12.10.2023 from <https://www.metso.com/portfolio/concorde-cell/?r=3>
- Michaux, B, 2021. *Advancement of Mineral Processing Simulation Platforms for the Integration of Water Quality – Process Performance Interactions in Water Management Systems* [PhD, TUBAF]. Freiberg, Germany.
- Nguyen, A V, & Schulze, H J, 2003. *Colloidal Science of Flotation* (1st. Edition ed.). CRC Press. <https://doi.org/https://doi.org/10.1201/9781482276411>
- Shergold, H L, 1984. Flotation in Mineral Processing. In K. J. Ives (Ed.), *The Scientific Basis of Flotation* (pp. 229-287). Springer Netherlands. https://doi.org/10.1007/978-94-009-6926-1_7
- Trahar, W J, 1981. A rational interpretation of the role of particle size in flotation. *International Journal of Mineral Processing*, 8(4), 289-327. [https://doi.org/https://doi.org/10.1016/0301-7516\(81\)90019-3](https://doi.org/https://doi.org/10.1016/0301-7516(81)90019-3)
- Wang, L, 2016. *Entrainment of Fine Particles in Froth Flotation* [University of Queensland]. Australia.

Replacement of Sodium Ethyl Xanthate Collector at Carrapateena

J Reinhold¹, S Assmann², E Brodie³, J Van Sliedregt⁴, F Burns⁵, G Tsatouhas⁶ and J Seppelt⁷

1. Senior Metallurgist - Plant, BHP Carrapateena, Pernatty, South Australia, 5173. Email: jacqueline.reinhold@bhp.com
2. Technical Manager – Mining, InterChem, 20 Harper Street, Abbotsford, VIC 3067, Email: sassmann@interchem.com.au
3. Metallurgist - Plant, BHP Carrapateena, Pernatty, South Australia, 5173. Email: eve.Brodie@bhp.com
4. Metallurgist - Plant, BHP Carrapateena, Pernatty, South Australia, 5173. Email: jessica.vanSliedregt@bhp.com
5. Superintendent - Metallurgy, BHP Carrapateena, Pernatty, South Australia, 5173. Email: fraser.burns@bhp.com
6. Business Manager – Mining, InterChem, 20 Harper Street, Abbotsford, VIC 3067, Email: gtsatouhas@interchem.com.au
7. Processing Manager, BHP Carrapateena, Pernatty, South Australia, 5173. Email: joe.seppelt@bhp.com

ABSTRACT

Carrapateena is a copper–gold deposit hosted in a brecciated granite complex located in the Gawler Craton, South Australia. The deposit is currently mined using the sub-level cave (SLC) mining method, with future mining to incorporate a block cave beneath the sub-level cave. The ore is processed by a conventional sulfide flotation concentrator, producing a copper gold silver (Cu-Au-Ag) concentrate with chalcopyrite and bornite as the main copper-bearing minerals.

In 2021, the then OZ Minerals engaged InterChem to investigate alternative collectors to Sodium Ethyl Xanthate (SEX), which had been utilised as the primary collector in the concentrator since commissioning. Although xanthates are commonly used collectors, their limitations can include lower selectivity against gangue minerals, OH&S concerns relating to classification as spontaneously combustible Dangerous Goods (Class 4.2) under the Australian Dangerous Goods Code, and dosage inefficiency resulting in higher reagent costs. Therefore, drivers for the project were to improve selectivity for copper whilst maintaining or improving flotation performance and product quality, improving Carrapateena’s safety and risk profile by the removal of xanthates from site, and optimising dosage to target reduction in overall reagent costs.

This paper outlines the process followed to investigate a variety of reagents to replace sodium ethyl xanthate in the Carrapateena concentrator and the final selection. It will discuss the method of introducing the chosen collector into the plant across numerous stages with official implementation and cessation of xanthate usage as of 2023, as well as ongoing geometallurgical test work to review its performance on future ore.

INTRODUCTION

Carrapateena is a copper–gold deposit, located 460 km north of Adelaide, South Australia. Sulfide mineralisation hosted within the hematite breccias of Carrapateena is a combination of dominantly fine-grained disseminated to medium-grained blebby chalcopyrite with a discrete high-grade zone of bornite; rare chalcocite, digenite, and covellite in hematite breccias. The initial Sub-Level Cave (SLC) footprint focuses mining activities on a bornite-chalcopyrite dominant core of the resource. Further expansion to full Block Cave (BC) operation is presently under development and will expand mining activities into an increasing portion of chalcopyrite and chalcopyrite-pyrite domains.

The sulfide flotation concentrator produces a Cu-Au-Ag concentrate for sale to copper smelters. Construction of the concentrator was completed in late 2019, with slurry commissioning in Q4 2019, and the first concentrate produced and filtered in December that same year.

Throughout 2021 and 2022, the concentrator flotation and regrind circuits were expanded and reconfigured to provide greater capacity and flexibility to uplift concentrate quality through improved rejection of non-sulfide gangue (NSG).

As mining progresses to deeper sections of the orebody, the mill feed will see an increase in the proportion of chalcopyrite and pyrite. The Carrapateena concentrator was initially designed to operate in a bulk flotation strategy, with no need to reject the minor pyrite present in the flotation feed to achieve target concentrate quality. With the future change in feed sulfide mineralogy, the incorporation of sulfide gangue rejection minerals, specifically pyrite, will become increasingly important.

In 2021, Carrapateena engaged InterChem to investigate alternative collectors to Sodium Ethyl Xanthate (SEX), which has been utilised as the primary collector in the concentrator since commissioning. SEX is also the primary collector at the near-by and similar Iron Oxide Copper Gold (IOCG) flotation concentrators at BHP Prominent Hill and BHP Olympic Dam. Although xanthates are commonly used collectors, their limitations can include lower selectivity against gangue minerals, OH&S concerns relating to their classification as spontaneously combustible Dangerous Goods (Class 4.2) under the Australian Dangerous Goods Code, and dosage inefficiency resulting in higher reagent consumption and cost.

Key objectives of this investigation were to identify collector(s) with the potential to improve selectivity of copper against pyrite, whilst maintaining suitable metal recovery performance, improving the plant safety and risk profile by removing xanthates from site, and optimising dosage to target a reduction in overall reagent costs.

This paper describes the process followed to investigate a variety of replacements to SEX, the final selection, the stages of implementation and the cessation of SEX usage as of 2023.

REAGENT SCREENING PROGRAMME

To identify an appropriate xanthate replacement, a reagent screening programme was completed at the Carrapateena metallurgy laboratory.

This programme was completed in two stages. First a broad range of ~20 collector chemistries were investigated, including various thionocarbamates (TC), modified thionocarbamates, mercaptans, dithiophosphates (DTP), and several blends thereof. It was envisaged that this initial stage would identify a shortlist of collector chemistries deemed to be most suitable for a low Cu:S Carrapateena ore, and to inform more detailed testing of these collectors in a second stage of reagent screening.

Broad reagent screening

In the first stage, the feed material was ore from the Carrapateena SLC with a lower than typical Cu:S ratio of 0.87 specifically chosen to highlight the pyrite depression performance of the screened collectors. Test procedure involved 2 kg charges of flotation feed being freshly ground in a rod mill to the process plant design target P80 size of 75 μm . All flotation tests were conducted in a 5 L flotation cell, using a kinetic rougher flotation procedure producing four concentrates and tailings.

Carrapateena process water was used throughout the test work. The dosage of the alternative collectors tested was generally kept constant or slightly increased relative to SEX in order to give a favourable flotation response.

From the initial stage, three alternative collectors (DS0065, DS0071 and DS0074) from the DTP and TC chemistry families were chosen to take forward. Improved metallurgical performance was achieved compared to that of SEX as presented in Figure 1. Improvements in Cu and Au recovery and concentrate grade were observed, alongside improved selectivity for Cu against Fe and S, indicating selectivity against pyrite.

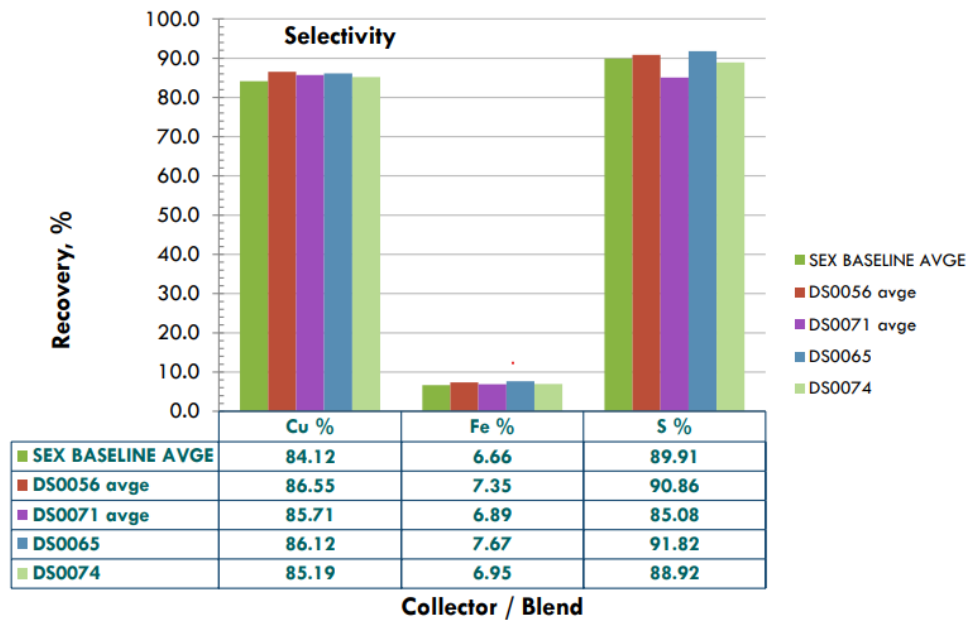


Figure 1: Stage #1 Alternative Collector Screening Selected Results

Focused reagent screening

Testing in the second stage was conducted on a second ore composite that was blended from drill core to provide a representative view of future ore characteristics and flotation performance. Testing again involved 2 kg charges of flotation feed being freshly ground in a rod mill to a P80 size of 75 μm . An initial rougher flotation stage was completed in a 5 L flotation cell. This stage was extended to regrind and cleaning tests to understand impacts on final concentrate grades. The rougher concentrate was regrind to the process plant design target P80 size of 20 μm in a lab stirred media mill. Three stages of dilute cleaning tests were completed on the regrind product. SEX was replaced by the alternative collectors in both the rougher and cleaning stages.

The results from the rougher tests indicated that the three Interchem collectors achieved comparable copper recovery and grade in comparison to those achieved with SEX, as well as higher Au recovery (up to +3.1%) and Au grade (up to +1.3 ppm).

The results (Figure 2) from cleaner tests indicated that DS0065 and DS0071 collectors have the best potential to outperform SEX including higher copper recovery (up to +2.3%) and concentrate grade (up to +4.1%) post regrind. DS0065 and DS0071 also achieved similar improvements in selectivity for Cu against S, and Fe in comparison to SEX in the cleaner tests.

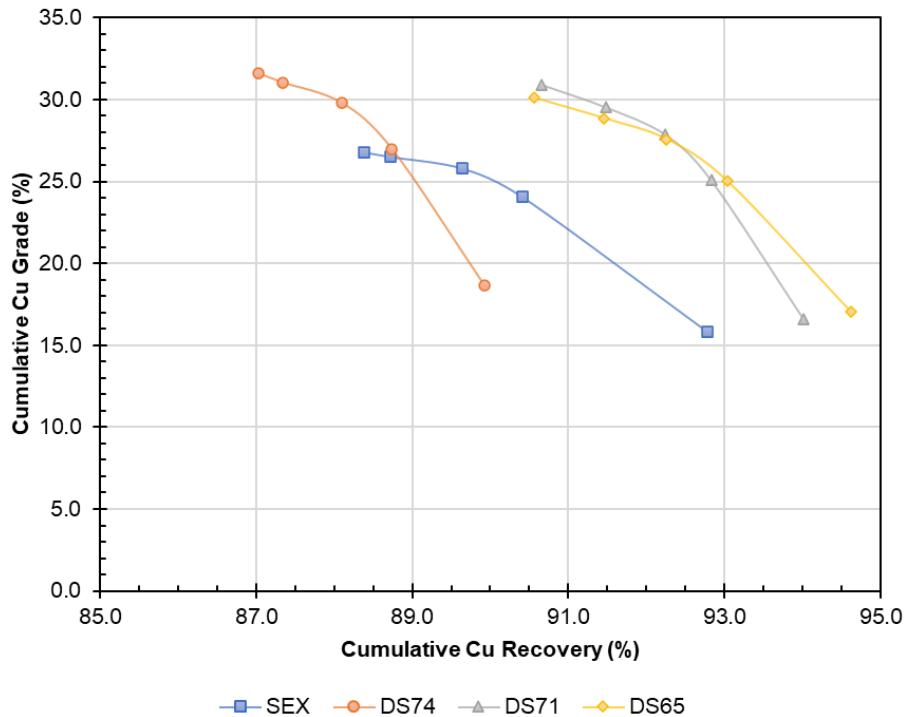


Figure 2: Stage #2 Alternative Collector Screening Results

Based on the results from this phase of flotation test work, it was determined that the DTP (dicresyl, diethyl) blend, DS0065, now commercially known as INTERCOL C4450, was the highest performing reagent. This collector was taken forward to full plant trials as described below.

Further variability testing

To build supporting data that improved concentrate grade by using C4450 over SEX in ores with dominant pyrite mineralogy, further comparative laboratory flotation tests were conducted. This work was completed concurrent to the full plant trials so as not to delay full implementation. Test procedures were similar to those used during the 2nd stage of reagent screening. Ten additional lower Cu:S composites were developed from drill core samples.

Presented in Figure 3 is a summary of the final concentrate grade for both C4450 and SEX against the flotation feed Cu:S ratio, which is the known driver for concentrate grade variation at Carrapateena. Throughout this testing, C4450 demonstrated on average a 2.3% increase in concentrate Cu grade without any observed impact on Cu recovery.

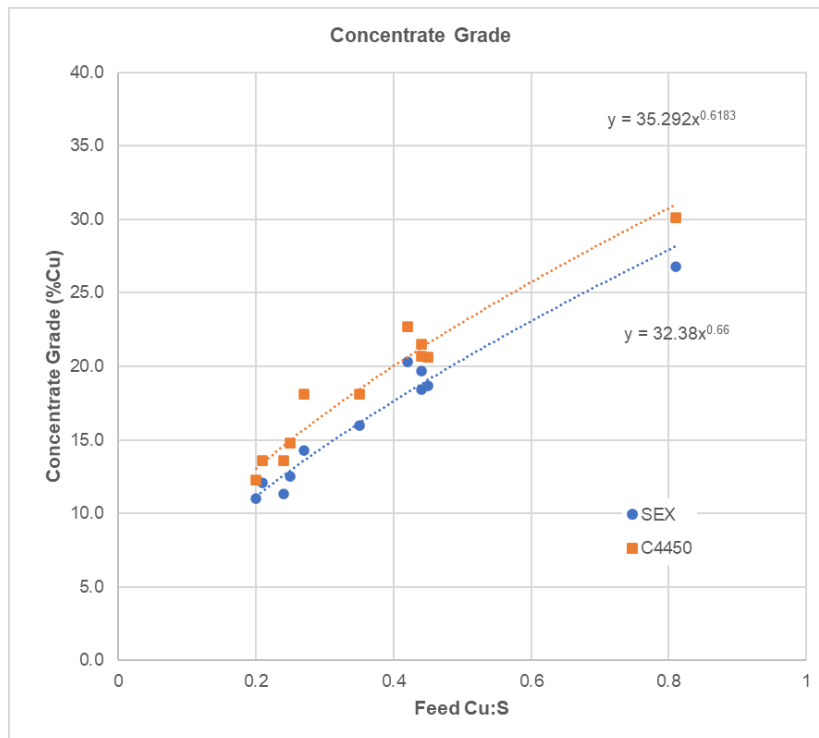


Figure 3: Variability Alternative Collector Screening Results

PLANT TRIALS

The plant trial of C4450 was carried out in two stages. An initial sighter trial was conducted to confirm circuit operability wasn't affected, and to conduct shakedown testing of trial dosing arrangements and dosing locations. Subsequently a structured long-duration on-off trial was established to develop a thorough understanding of the metallurgical performance at plant scale.

Sighter trial

Prior to implementing a full plant trial, a two-day sighter trial was conducted in the plant in early February 2022, which demonstrated that SEX can be replaced with C4450 without any significant disturbance to circuit operation.

During this stage, the trial reagent dosing pumps and control logic were commissioned and tested. Final dosing locations were confirmed and dosing setpoint ranges were established based on froth appearance and stability. The trial showed a lower dosage of C4450 was required compared to SEX to maintain copper recovery without resulting in visible overcollection in the cells. An initial 30% dosage reduction was recommended to the operations team when swapping from SEX to C4450 for the duration of the subsequent longer term trial.

Long term trial

The trial was performed using an on-off shift-by-shift (12 hr) basis, where C4450 replaced SEX as the primary flotation collector. A trial planner detailing the timeline for swapping between SEX and C4450 was updated and distributed as required based on the trial progress. Other flotation reagents were also maintained as-is throughout the trial, with only SEX being replaced. This was inclusive of Interchem INTERFROTH F228 frother on an as-needs basis across the circuit, INTERCOL C6096 being dosed to ball mill feed, and Solvay Aerophine 3418A being dosed to the third rougher cell.

C4450 was dosed in the same locations as the standard SEX set up: the rougher conditioning tank, the third rougher cell, the scalper Jameson feed box and the head of the first cleaner. A secondary dosing set up enabled seamless transitions between the two reagents. The transitions aligned with the collection of the shift composite samples at approximately 3pm/3am as per the on-off trial planner.

This trial dosing system was integrated into the plant process control system allowing consistent dosing philosophy across both SEX and C4450. Both collectors were dosed based on target ratios of grams of collector to tonnes of Cu, set by the flotation technicians, and as calculated by the control system as determined from copper grade readings from the Metso on-stream analyser (OSA).

The trial continued for 244 shifts between March and July 2022; the data from 96 shifts were usable (48 pairs). 148 shifts were disregarded due to plant instability and downtime, regrind mill downtime, or due to OSA downtime (which affected generation of shift composites and dosing flow control).

Throughout the trial, weekly collection of duplicate flotation feed samples was completed. Laboratory “hot” flotation tests were performed of these sample pairs, with one sample being dosed with SEX and the other with C4450.

Plant trial results

Overall performance

Headline analysis of the plant trial results, displayed in Table 1 as averages across each data set, indicated no significant variance is seen in recovery or concentrate quality for similar feed Cu grade and Cu:S, and was achieved with a reduction in reagent consumption.

Table 1: SEX vs. C4450 Plant Performance Comparison

	C4450	SEX
Dose Rate (g/tCu)	570	837
Copper Feed Grade (%)	1.40	1.40
Copper Concentrate Grade (%)	43.3	43.2
Feed Cu:S	1.56	1.57
Concentrate Cu:S	1.75	1.73
Copper Recovery (%)	93.4	93.2
Gold Recovery (%)	85.2	85.1
Silver Recovery (%)	83.5	82.8

Recovery assessment

Trial data was analysed using the comparison of regression lines for SEX and C4450 considering the:

- Feed grade vs. recovery for copper and gold; and
- Feed copper to sulfur ratio vs. copper concentrate grade.

At Carrapateena, flotation recovery is a known function of head grade, while concentrate copper grade is a known function of the feed copper to sulfur ratio, both of which vary regularly based on the sulfide mineralogy blend.

Analyses of the regression lines in the form of t-tests at the 95% confidence level were completed to determine the statistical significance, as shown in Figure 4.

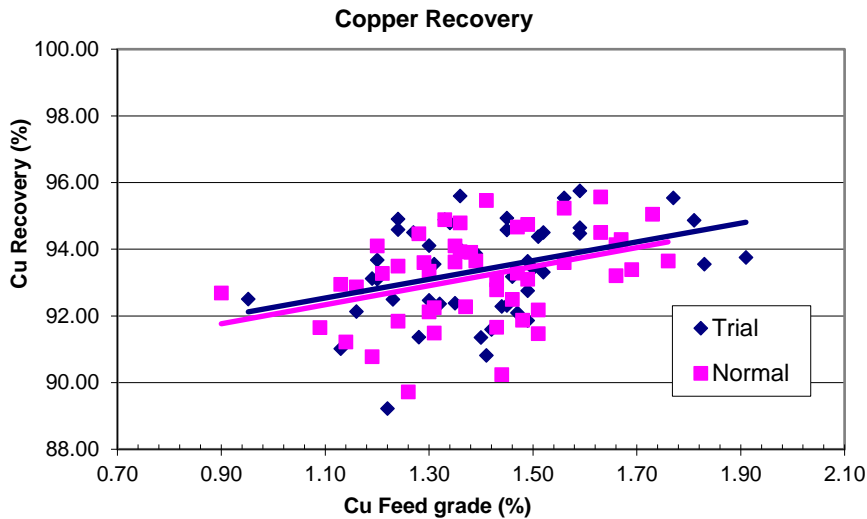


Figure 4: Cu Recovery (%) vs. Cu Feed Grade (%)

Cu recovery vs Cu feed grade regression lines are vertically offset by 0.19%, indicating C4450 results in an improved recovery of 0.19% +/- 0.5% irrespective of the feed grade. However, the statistical significance of this difference is negligible.

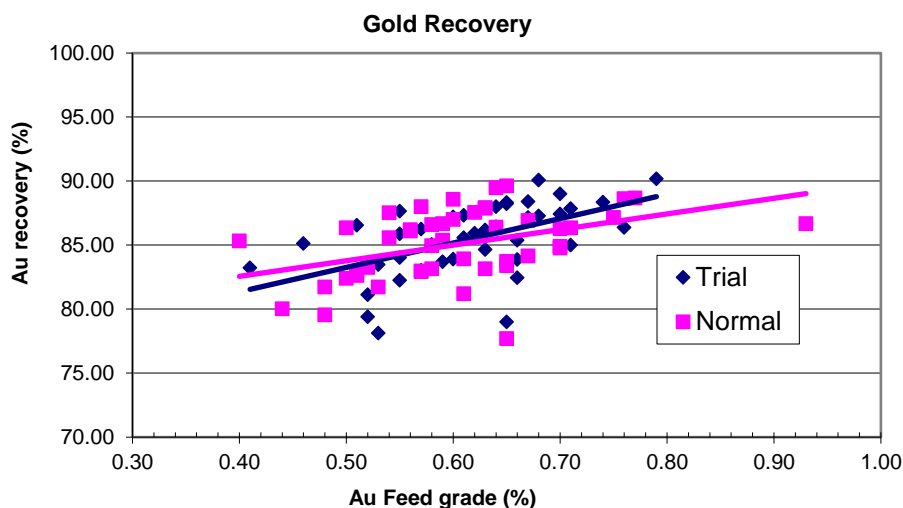


Figure 5: Au Recovery (%) vs. Au Feed Grade (%)

As shown in Figure 5, Au recovery vs Au feed grade regression lines are vertically offset by 0.25%, indicating the C4450 change has increased Au recovery by 0.25% +/- 1.0% irrespective of the feed grade. However, the statistical significance of this difference is also negligible.

Concentrate grade assessment

Concentrate Cu:S vs feed Cu:S regression lines are vertically offset by 0.034 indicating the C4450 change has improved concentrate Cu:S by 0.034 +/- 0.029 irrespective of the feed Cu:S. The separation is statistically significant. The follow-on consideration from this is a comparison of the concentrate Cu grade for a feed Cu:S as shown in Figure 6 and Figure 7, which proved to be not statistically insignificant.

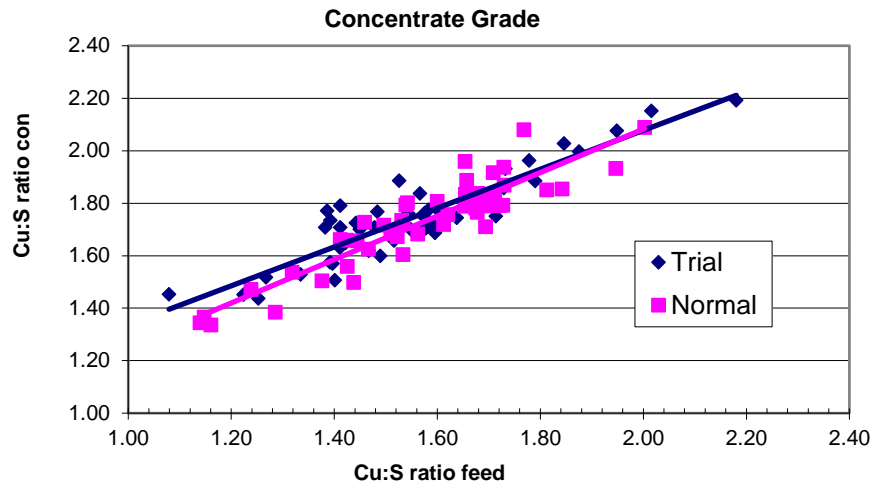


Figure 6: Concentrate Cu:S vs. Feed Cu:S

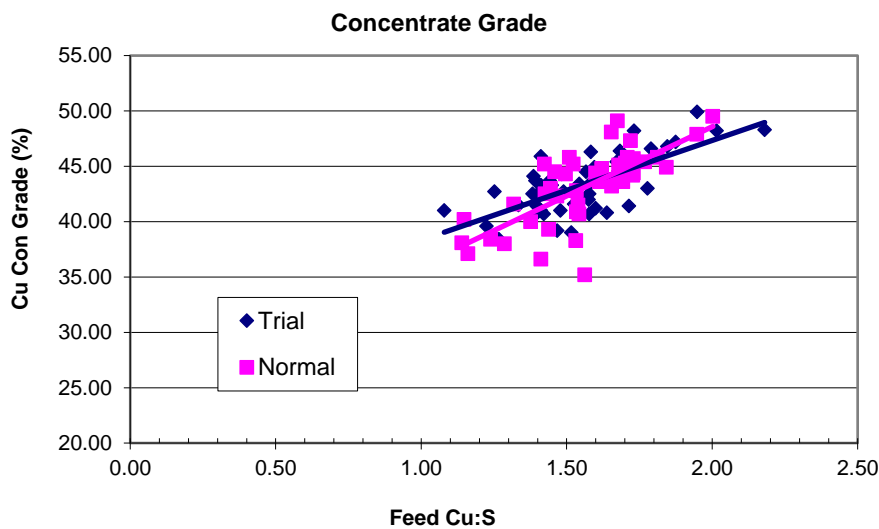


Figure 7: Cu Concentrate Grade (%) vs. Feed Cu:S

Dosage rate assessment

Due to the higher cost point of C4550, the necessary dosage to achieve equivalent or improved plant performance as with SEX was an important aspect of the trial outcome. Initial laboratory flotation tests and the sighter trial had suggested a decrease of 30% in collector dosage could be achieved with C4550.

In review of the plant trial, a statistically significant difference in the C4450 dosage rate was observed with a 32% reduction (571 g/t Cu) compared to SEX (837 g/t Cu); aligning well with pre-trial expectations.

Data indicates the SEX usage during the trial was lower than historical trends. Comparing the dose rate of C4450 during the trial to the historical SEX usage, a decrease of 43% was observed.

The average of these two values, 37.5%, was taken forward as the assessed collector dose rate reduction.

Laboratory rougher hot flotation tests

For the duration of the plant trial, laboratory flotation (hot float) tests on plant samples comparing SEX and C4450 were conducted. These tests aimed to compare the two reagents using a live plant sample, whilst eliminating any disturbances from the plant. Duplicate float feed samples were collected from the flotation feed sample pump and brought back to the metallurgy laboratory. The samples were then floated using a 5 L lab scale flotation cell, using the standard Carrapateena rougher hot float test procedure with either SEX or C4450 as the collector. A total of 38 hot floats were performed (19 pairs) during the trial and the preceding month.

The results were compared using a paired t-test comparing means at 95% confidence. No statistical differences were noted for Cu and Au recoveries. Likewise, there were no differences in Cu, Au, Si, Fe or S grades in the rougher concentrate (without regrind cleaning).

Plant trial performance summary

The results achieved in the plant trial and accompanying hot float laboratory tests overall indicated that C4450 maintained existing plant performance when replacing SEX, despite a 30% decrease in collector consumption.

The improvement in pyrite rejection performance displayed in the reagent screening tests was not replicated in the plant trials. This is likely a result of the difference in feed mineralogy between the laboratory test work and feed to the plant during trial. The samples selected for the screening test work had a lower Cu:S ratio of 0.20-0.90, whereas the plant trial feed Cu:S ratio ranged from 1.14 to 2.20, averaging 1.56. As there was minor pyrite in the feed during the trial, the same extent of improvement in concentrate grade due to improved selectivity against pyrite was also not observed.

TRANSITION DECISION

Final assessment of plant performance from the combined test work and plant trials concluded is that C4450 can match SEX Cu recovery performance, and when significant pyrite is present in the ore, will provide an increase in final Cu concentrate grade. It was assessed that this performance was obtained with a 37.5% decrease in reagent dosage on a grams of collector per kg of Cu basis.

As SEX is a commodity product and C4450 is a speciality collector, there exists a price difference between the two, with C4450 being the more expensive on a per unit mass basis. Considering the observed decrease in C4450 reagent use, an economic assessment was made on the expected cost movement involved in the transition.

Relative cost comparisons between SEX and C4450 were made considering the assessed dosing rate of and difference in reagent unit price. It is expected that the transition would largely be a cost neutral proposition, with the increase in unit pricing being offset by the lower consumption rates. This analysis disregarded savings related to the removal of the requirement for reagent SEX mixing processes.

SEX is delivered to site as bagged and boxed solids pellets. The pellets are prepared for dosing to the flotation circuit by first being dissolved in a dedicated mixing tank by the plant operation technicians. This regular task is time consuming, especially with the due care and diligence required to safely manage the spontaneously combustible hazard of SEX.

Conversely C4450 is delivered to site as liquid and is dosed neat without the need of dilution or mixing activities. Thus, operational activities to resupply storage tanks are undertaken with both reduced frequency and duration.

Considering the above, a decision to transition the Carrapateena processing plant to C4450 was made on the basis of:

- Maintaining plant flotation circuit performance on current ores;
- Offering a pathway to concentrate grade improvements on future ores through improved pyrite rejection;
- removing a hazardous substance from site and eliminates time-consuming reagent dissolution and mixing task;
- a cost neutral transition.

POST TRANSITION REVIEW

A permanent transition was made to C4450 in January 2023 after enabling the necessary supply logistics. Flotation performance after the transition largely aligned with that seen during the early 2022 plant trials, as shown in Figure 8, potentially with improved consistency of Cu recovery.

Reagent dosage reductions largely exceeded expectations, in particular the first rougher cell by ~49% across the first month of the transition, as shown in Figure 9. The permanent transition also enabled optimised dosing positions within the flotation plant.

Previously SEX and 3418A were co-dosed to rougher cell 3. After the transition to C4450, it was identified that overcollection and poor froth stability was occurring at this cell, and as such, subsequent staging of the reagents, was shifted to rougher cell 4, which greatly improved operational stability.

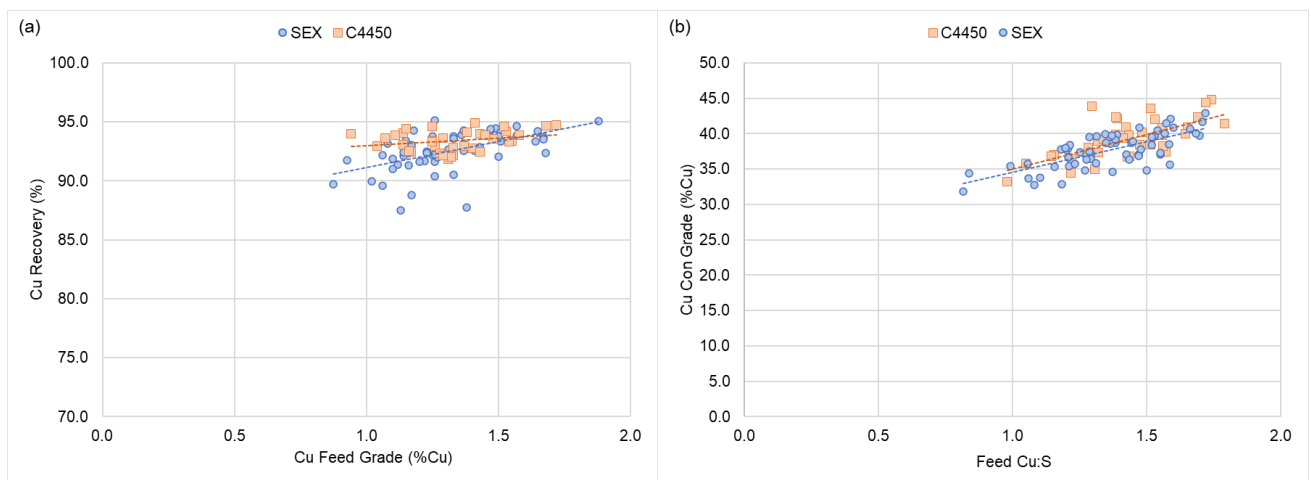


Figure 8: Post Implementation Performance: (a) Cu Recovery (%) and (b) Cu Concentrate Grade (%)

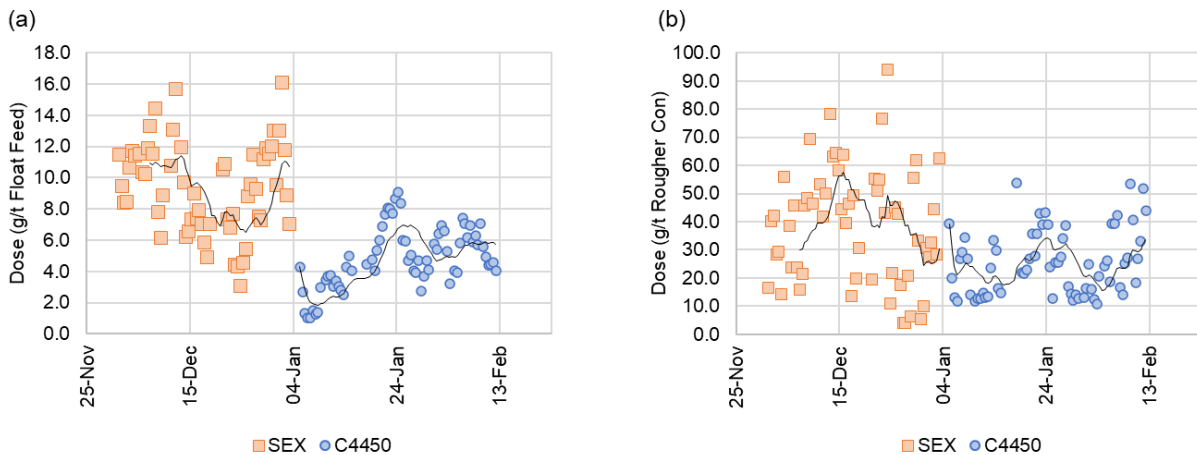


Figure 9: Post Implementation Performance: (a) Rougher cell 1 dose rate and (b) Cleaner 1 dose rate

CONCLUSIONS

The three drivers of this investigation were to: improve future product quality by improving selectivity against pyrite, maintain copper recovery and eliminate the use of xanthates to reduce safety risks and manual tasks within the concentrator.

The trial and laboratory test work demonstrated that C4450 can match SEX Cu recovery performance, and when significant pyrite is present in the ore, will provide an increase in final Cu concentrate grade. C4450 can accomplish this at lower reagent consumption rates, and considering the costs associated with SEX and C4550, do so from a cost neutral position.

It was recommended that a permanent change be made to C4550 as the primary collector in the copper concentrator. Even though there was no change to current plant performance or costs, the material benefits lay in the reduced effort and safety risks associated with mixing and storing SEX onsite.

The permanent transition from SEX to C4450 usage occurred in January 2023. Flotation performance post transition is aligned with the expectations stemming from the earlier trials, with potential upside to be realised on dose rate reductions.

ACKNOWLEDGEMENTS

The authors would like to acknowledge the Carrapateena Processing Team who have all played a part in the successful implementation of the program and without which, it would not have been successful.

References

OZ Minerals, Carrapateena Block Cave Access Declines now underway. ASX Release, 3 December 2021,

https://www.ozminerals.com/ArticleDocuments/362/20211203_CarrapateenaBlockCaveDecline_ASXRelease.pdf

OZ Minerals, Carrapateena produces first copper concentrate; operational ramp up outlined ASX Release. 20 December 2019

https://www.ozminerals.com/ArticleDocuments/368/191220_Carrapateena_First_Concentrate.pdf

Application of Depressant in Copper-Nickel Separation at IGO's Nova Mine

A White¹, J Fryman², P Kittler³, P Hudson⁴, S Szabo⁵ and I Ametov⁶

1. Project Metallurgist, IGO, Nova Mine, email: Aaron.White@igo.com.au
2. Plant Metallurgist, IGO, Nova Mine, email: Jacob.Fryman@igo.com.au
3. Senior Metallurgist, IGO, Nova Mine, email: Paul.Kittler@igo.com.au
4. Senior Metallurgist, IGO, Nova Mine, email: Paul.Hudson@igo.com.au
5. Technical Sales Engineer, Solvay, email: Sylvia.Szabo@solvay.com
6. Regional Technical Manager, Solvay, email: Igor.Ametov@solvay.com

ABSTRACT

Laboratory flotation testing conducted at the Nova Operation in June 2020 indicated that AERO® 7261A depressant was capable of replacing the triethylenetetramine (TETA) - sodium sulfite system in the sequential Cu-Ni flotation circuit. A plant trial, subsequently conducted in May-June 2021, demonstrated that AERO 7261A depressant was a viable replacement for TETA in the copper flotation circuit, although the addition of sodium sulfite was still necessary for optimum performance. This paper details the plant trial methodology, the analysis of the plant trial data and the overall outcomes of the AERO 7261A depressant plant trials.

INTRODUCTION

The IGO Limited (IGO)-owned Nova Nickel Operation is located in the Fraser Range, approximately 160 km East-North-East (ENE) of Norseman in Western Australia. The Nova concentrator processes massive sulfide ore from the Nova and Bollinger ore deposits to produce high-grade copper and nickel concentrates by differential froth flotation. The major copper-bearing mineral is chalcopyrite, while the nickel is predominantly hosted in pentlandite. The flotation separation of chalcopyrite from pentlandite and pyrrhotite (the major iron-bearing mineral) is facilitated with a synergistic combination of TETA and sodium sulfite.

A method for the differential flotation of copper and nickel from Ni-Cu sulfide ores from the Sudbury region was developed in the mid-1990s and published in detail in 1996 (Kelebek *et al*, 1996). The method exploits the natural, collectorless floatability of chalcopyrite, but in the presence of sulfur dioxide as a pyrrhotite and pentlandite depressant and diethylenetriamine (DETA) as an effective chelating agent of activating ions. The mechanism behind the observed flotation selectivity involves deactivating of pyrrhotite by DETA and depression of pyrrhotite and pentlandite by sulfur (IV) oxy species, such as sulfite, bisulfite, metabisulfite and sulfurous acid. These species are formed as a result of complex equilibria of sulfur dioxide in aqueous solutions (Weil, 1983). It was hypothesized that sulfur (IV) oxy species destroy sulfur-rich hydrophobic surface layers and form hydrophilic entities on the surface of pyrrhotite and pentlandite. This depressant action does not affect the recovery of chalcopyrite and, in fact, is enhanced in the presence of DETA.

Later, Kelebek and Tukul (1999) demonstrated that DETA may be replaced with TETA, while sulfur dioxide can be successfully substituted with sodium metabisulfite (SMBS). SMBS dissolved in water converts to sodium sulfite (Na₂SO₃) which can also be used as sulfur dioxide replacement.

TETA, which is a more powerful chelating agent than DETA, has a lower vapour pressure, and hence presents a lower possibility of personnel exposure to the chemical in a plant environment. The major challenges with the TETA-sodium sulfite system are the high cost of TETA and its occupational health and safety (OHS) risks. TETA belongs to a Dangerous Goods class of materials as it is harmful to

sulfite for the differential flotation of chalcopyrite and pentlandite. The addition rates of TETA and sodium sulfite in the rougher circuit are typically 50 g/t and 100 g/t respectively, while in the cleaner circuit the dosages of TETA and sodium sulfite are correspondingly 80 g/t and 160 g/t.

THE PLANT TRIAL

Methodology

Laboratory Screening

Screening of various Solvay reagents was conducted in the Nova laboratory in June 2020, using simple rougher-scavenger flotation tests only on copper rougher feed (CRF). A two-stage approach was taken, with an initial screening of four depressants at dosages of 40-100 g/t, before the two best performing reagents (in terms of Cu-Ni selectivity, copper grade and copper recovery) were utilised for the next phase of testing. Tests were completed in random order. AERO 7261A was selected for a plant trial due to its ability to match the performance of the TETA-sodium sulfite combination in terms of copper recovery, grade and Cu/ Ni selectivity. The optimum dosage of AERO 7261A was found to be 75 g/t. Given the results of this test work, the assumption was made that the same reagent scheme could be effectively used in a subsequent cleaning stage. Potential complications from sulfide oxidation/ sample aging and rougher concentrate combination also contributed to the decision to only conduct rougher-scavenger work in the laboratory.

Plant Commissioning

Following the selection of AERO 7261A for a plant trial, safety and operational risk assessments were completed and temporary dosing systems to the copper rougher and cleaner banks were installed. A week-long pre-trial commissioning run was conducted in April 2021 to elucidate the general effect of AERO 7261A on the flotation circuit performance and determine the optimal depressant dosage. The commissioning run also aimed to identify and fix any operating issues with the trial equipment. Personnel from Solvay were deployed to site to assist in the smooth operation of the copper circuit during the preliminary run, as well as to maintain detailed activity logs for future reference. During this period, it was established that AERO 7261A was able to successfully replace both TETA and sodium sulfite in the copper rougher flotation circuit, in line with the laboratory rougher test results. However, in the copper cleaner circuit AERO 7261A was ineffective as a lone depressant. It was found that to maintain the nickel grade in the final copper concentrate below the specification limit, addition of sodium sulfite was required at around 250 g/t (with respect to plant feed). This was determined following an increase of AERO 7261A dosage up to 200 g/t in the cleaner circuit, with nickel contained in copper concentrate still ~0.3% above target. AERO 7261A was therefore staged down and sodium sulfite addition increased until nickel suppression was sufficient.

After refinement of the reagent dosages during the pre-trial commissioning run, the optimal dosages selected for the commencement of the plant trial were found to be as follows:

- Copper rougher circuit: 10 g/t AERO 7261A and no sodium sulfite
- Copper cleaner circuit: 30 – 40 g/t AERO 7261A and 250-300 g/t sodium sulfite.

While the original intention was to replace both incumbent reagents with AERO 7261A, the replacement of TETA (the more hazardous and expensive reagent) was considered sufficient enough to deem the commissioning run a success. The reasoning for the requirement of sodium sulfite in the cleaning circuit was unclear and requires further investigation.

Plant Trial

The full plant trial was conducted during May-June 2021, with Solvay personnel again on site for the entire duration for assistance and optimisation. On the advice of Solvay, the trial was structured as blocks of six trial shifts (ON) and six baseline shifts (OFF), with each shift being 12-hours duration. AERO 7261A dosing was utilised for trial periods, while baseline periods featured the original TETA-

sodium sulfite dosing scheme. Each block consisted of three days, with the first shift in each block considered to be a transition shift and therefore not included in the trial results.

Sampling for the trial included the collection of shift composites and copper flotation circuit surveys. Shift composites were comprised of a number of cuts taken pneumatically at designated intervals throughout a 12-hour shift by the on-stream analyser (OSA) for the copper and nickel circuit feeds and concentrates, as well as the two nickel tailings streams. Circuit surveys were conducted over half-hour periods with cuts taken at 10-minute intervals, with the addition of intermediate tails and concentrate streams for circuit mass balancing purposes. 16 surveys were completed over the course of the trial to provide a more detailed picture of the operation and performance of the copper circuit under each reagent scheme. For each shift, copper recovery and concentrate grades were calculated from the assays of shift composites. These grades and recoveries formed the basis for statistical analysis.

For the first month of the trial, covering the first four blocks of trial shifts, the performance of the copper circuit under trial conditions, compared to baseline conditions, could be summarised as follows:

- Copper recovery was higher by ~1.5%
- Nickel recovery to the copper concentrate was also higher
- The nickel grade of the copper concentrate was higher, often above the allowable threshold

Analysis of plant survey results available at that time showed that both copper and nickel flotation in the copper cleaners was much faster under trial conditions and that the last cells of the cleaner-scavenger bank were contributing little to copper recovery but were recovering nickel which harmed concentrate quality. The operating response was to run much deeper pulp-froth interface levels (for improved froth drainage and reduction of entrainment), lower air flow rates in the copper cleaner cells and drop out the last of the copper cleaner-scavenger cells. In this way, copper recovery was maintained but nickel recovery was reduced such that the copper concentrate was now within specification. An additional impact of these operating conditions was that recovery of non-sulfide minerals (as measured by MgO and SiO₂ assays) was significantly reduced and their grades in the copper concentrate decreased.

For the last two weeks of the trial, covering the final two blocks of trial shifts, the performance of the copper circuit under trial conditions, compared to baseline conditions, could be summarised as follows:

- Copper recovery was higher by ~0.5%
- Nickel recovery to the copper concentrate was similar to the baseline
- MgO recovery to the copper concentrate was significantly decreased
- The copper and nickel grades of the copper concentrate were very similar under trial and baseline conditions, and both were within specification

Results

The shift composite plant trial data from the last two weeks of the trial was analysed using a least squares effect leveraging statistical model. This statistical model is available within the JMP software package routinely used by Solvay. Average copper feed grades for the baseline and trial periods used in the statistical analysis were 2.15% and 2.08% respectively.

Copper Final Concentrate Copper Grade and Recovery

The outcomes of the least squares statistical analysis of copper final concentrate (CFC) Cu grade as a function of Cu in the copper rougher feed (CRF) are presented in Figure 2.

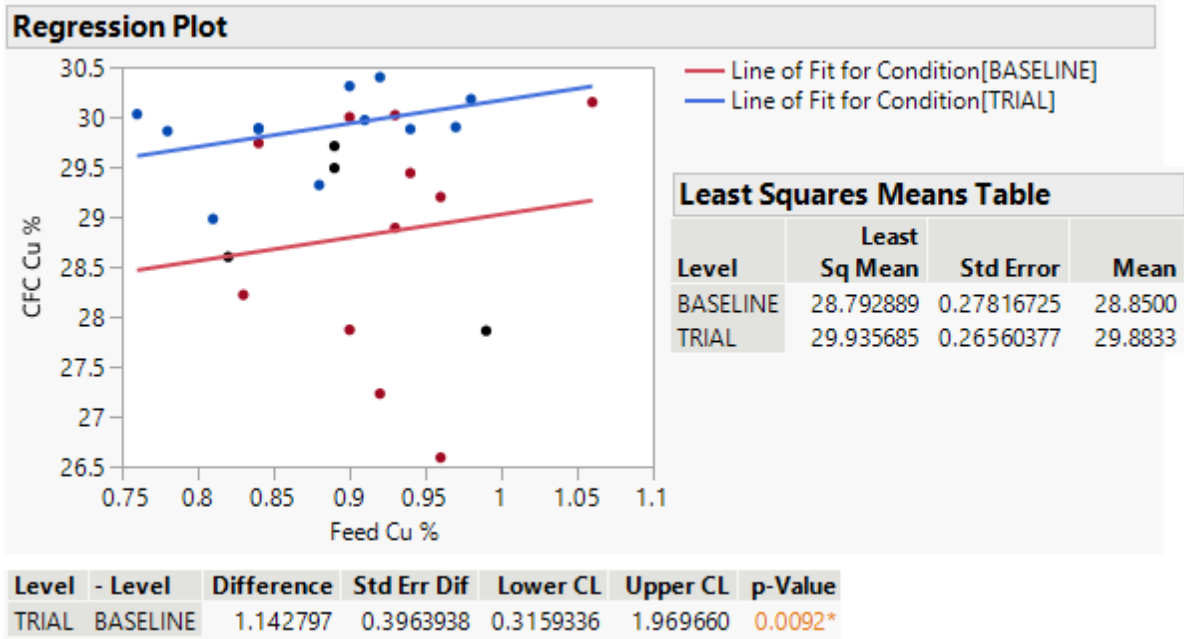


Figure 2: The least squares analysis for Cu grade in the copper final concentrate (CFC) as a function of Cu in the copper rougher feed (CRF). Black dots correspond to the transition days and are excluded from the analysis

The analysis suggests that during the AERO 7261A periods the mean CFC Cu grade was 1.03% higher compared to the baseline conditions (TETA-sodium sulfite). The least square mean was 1.14% higher, and the result was statistically significant at 99.1% (1-p-Value).

The results of the least squares statistical analysis of copper final concentrate (CFC) Cu recovery as a function of Cu in the copper rougher feed (CRF) are shown in Figure 3.

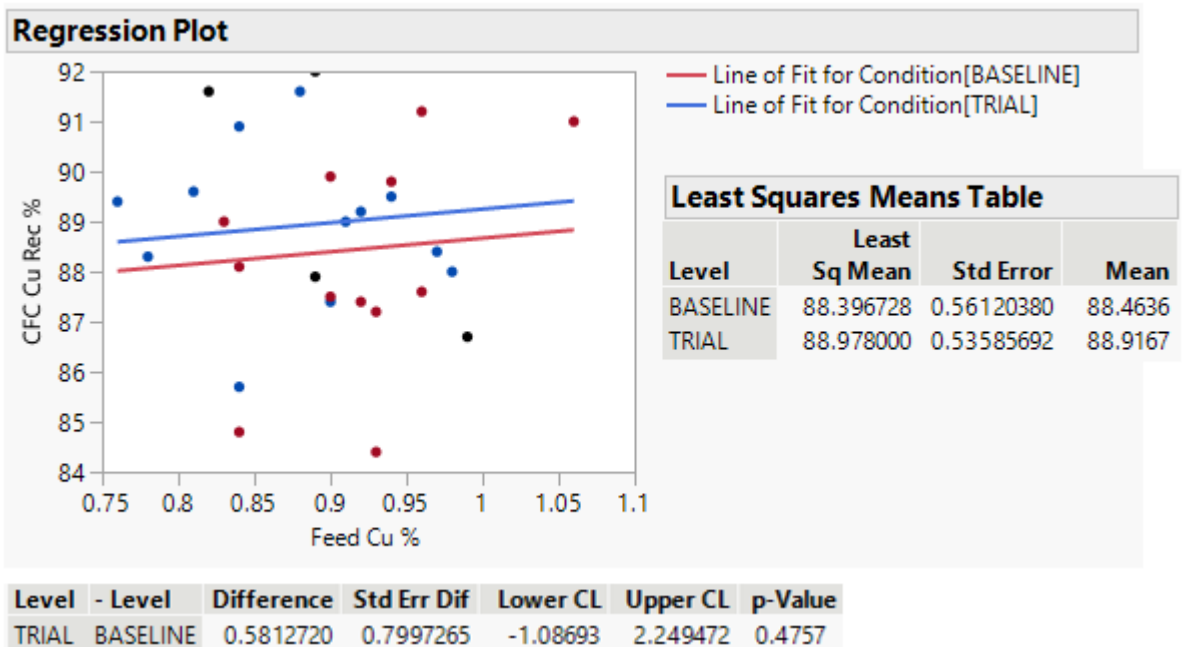


Figure 3: The least squares analysis for copper final concentrate Cu recovery as a function of Cu in the rougher feed (CRF). Black dots correspond to the transition days and are excluded from the analysis

According to the analysis, during the AERO 7261A periods the mean copper final concentrate Cu recovery was 0.45% higher compared to the baseline. The least square mean was 0.58% higher, however at only 52% confidence and, therefore, not statistically significant.

Copper Final Concentrate Nickel Grade and Recovery

The results of the least squares statistical analysis of copper final concentrate (CFC) Ni grade as a function of Ni in the copper rougher feed (CRF) are shown in Figure 4.

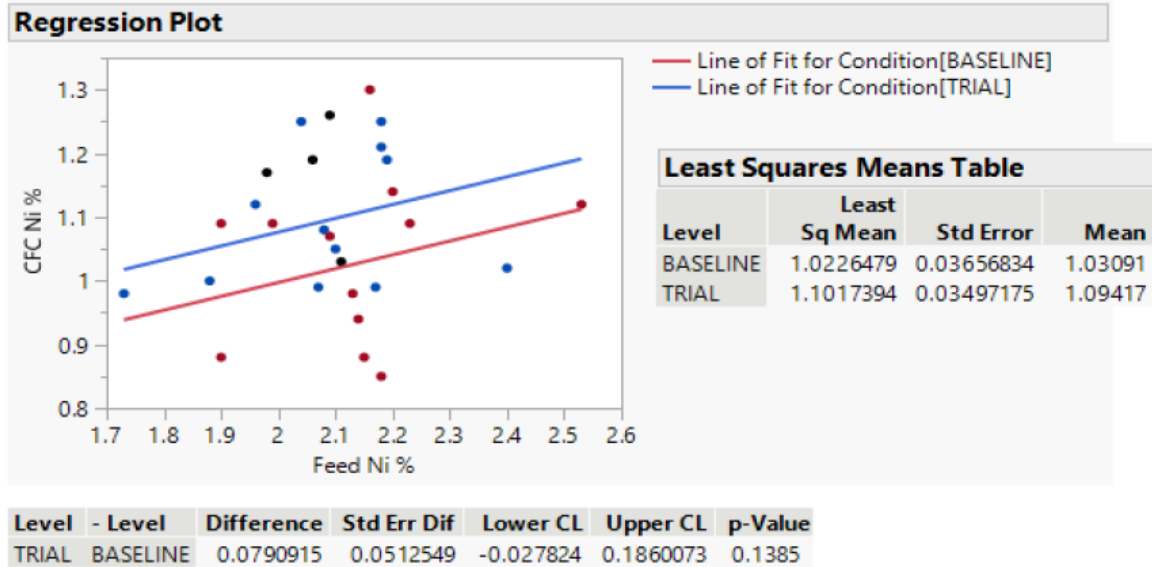


Figure 4: The results of the least squares statistical analysis of copper final concentrate (CFC) Ni grade as a function of Ni in the copper rougher feed (CRF)

According to the analysis, during the AERO 7261A periods the mean copper final concentrate Ni grade was 0.06% higher compared to the baseline. The least square mean was 0.08% higher, although at 86% confidence did not meet the minimum threshold required to be considered statistically significant (90%).

Nickel Final Concentrate Nickel Grade and Recovery

The least squares analysis results for the nickel final concentrate (NFC) Ni grade as a function of nickel in the copper rougher feed (CRF) are shown in Figure 5.

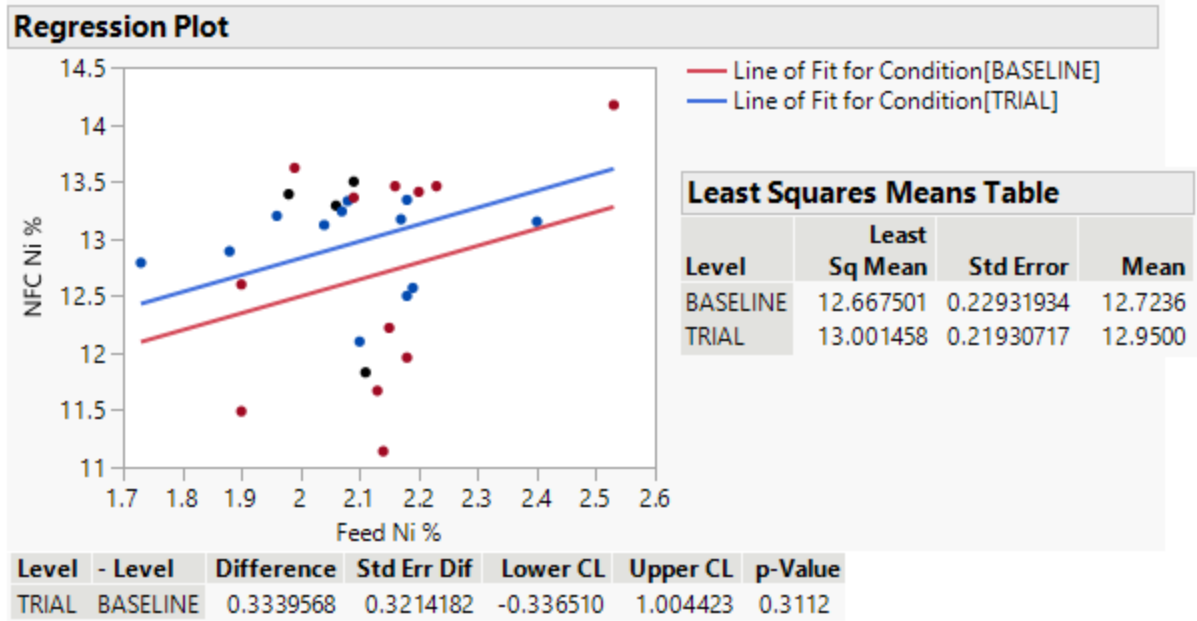


Figure 5: The least squares analysis for Ni grade in the nickel final concentrate (NFC) as a function of Ni in the copper rougher feed (CRF). Black dots correspond to the transition days and are excluded from the analysis

The least squares model suggests that a marginally higher (0.33%) nickel final concentrate (NFC) Ni grade was achieved during the AERO 7261A trial periods. The difference was not statistically significant, i.e., the confidence level was only 69% (p-Value was 0.3112).

The least squares analysis results for the nickel final concentrate (NFC) Ni recovery as a function of nickel in the copper rougher feed (CRF) are shown in Figure 6.

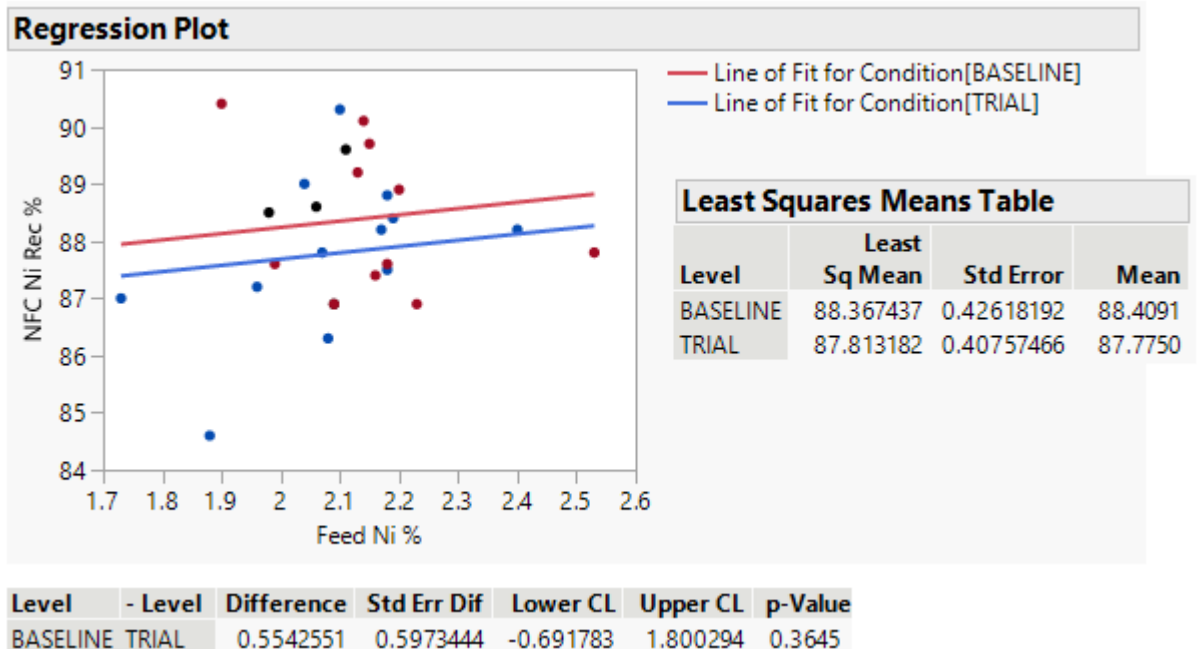


Figure 6: The least squares analysis for nickel final concentrate (NFC) Ni recovery as a function of Ni in the copper rougher feed (CRF). Black dots correspond to the transition days and are excluded from the analysis

The analysis shows that during the AERO 7261A trial periods the mean nickel final concentrate Ni

recovery was 0.55% lower compared to the baseline. The p-Value was 0.3645 indicating that the difference is not statistically significant, i.e., the confidence level was 63.5%.

Effect of AERO 7261A on Co, Fe, S MgO and SiO₂ in Copper and Nickel Final Concentrates

The least square analysis of grades and recoveries of Co, Fe, MgO, S and SiO₂ in the CFC and NFC streams are summarised in Tables 1 and 2.

Table 1: The least square analysis of CFC Co, Fe, MgO, S and SiO₂ grades and recoveries.

Stream	CFC grade				CFC recovery			
	Baseline	Trial	Diff.	p-Value	Baseline	Trial	Diff.	p-Value
Co	0.0338	0.0362	-0.0025	0.198	1.188	1.228	-0.040	0.60
Fe	29.98	30.78	-0.8	0.0019	3.47	3.30	0.170	0.13
MgO	0.812	0.467	0.345	0.0001	0.353	0.189	0.164	0.0001
S	32.62	33.93	-1.31	0.002	7.02	6.89	0.13	0.54
SiO ₂	2.71	1.32	1.39	0.0003	0.239	0.108	0.131	0.0005

The least squares analysis outcomes for CFC presented in Table 1 show the following:

- A slightly (0.0025%) higher Co grade was observed for the trial period, however, at only 80% confidence. The difference in Co recovery, 0.04%, was not statistically significant (p-Value was 0.6).
- Although statistically significant (p-Value 0.0019), the 0.8% difference in CFC Fe between the trial and test conditions was low in magnitude as the CFC Fe grade was ~30%. The difference in CFC Fe recovery was also of low magnitude, i.e. only 0.17% at 87% confidence.
- A statistically significant lower MgO grade and recovery were achieved during the AERO 7261A trial periods. A 0.345% difference in MgO grade represents a 42.3% decrease in grade during the trial period, while a 0.164% decrease in MgO recovery corresponds to a 46.5% decrease.
- A 1.31% statistically significant higher S grade during the trial periods was observed, however taking into account the 24-32% S grade range the difference was of low magnitude. The observed difference in S recovery was not statistically significant.
- Both SiO₂ grade and recovery were lower, by 1.39% and 0.131% respectively, during the AERO 7261A trial periods, with the difference being statistically significant.

The least squares analysis outcomes for NFC are presented in Table 2.

Table 2: The least square analysis of NFC Co, Fe, MgO, S and SiO₂ grades and recoveries in NFC

Stream	NFC grade				NFC recovery			
Element	Baseline	Trial	Diff.	p-Value	Baseline	Trial	Diff.	p-Value
Co	0.4718	0.485	-0.0133	0.31	87.85	87.42	0.43	0.63
Fe	42.19	42.54	-0.35	0.17	25.91	24.82	1.09	0.26
MgO	1.319	1.165	0.154	0.15	3.07	2.51	0.56	0.07
S	31.88	32.47	-0.59	0.52	36.33	35.59	0.74	0.52
SiO ₂	4.62	3.81	0.81	0.013	2.15	1.65	0.50	0.02

The least squares analysis outcomes for NFC show that:

- The difference in both NFC Co grade and recovery during the baseline and trial periods was not statistically significant, i.e. p-Values were 0.31 and 0.63 respectively.
- The difference in both NFC Fe grade and recovery during the baseline and the trial periods was not statistically significant either, namely p-Values were correspondingly 0.17 and 0.26.
- Lower grade and recovery were achieved during the AERO 7261A trial periods, i.e. a 0.154% difference in MgO grade and 0.56% decrease in MgO recovery.
- The difference in both NFC S grade and recovery during the baseline and the trial periods was not statistically significant.
- Both SiO₂ grade and recovery were lower, by 0.81% and 0.5% respectively during AERO 7261A trial periods (with both differences being statistically significant), however the magnitude of the difference was not substantial compared to the SiO₂ grade and recovery values.

Thus, AERO 7261A did not provide any substantial effect on CFC and NFC grades and recoveries of Co, Fe, MgO, S and SiO₂.

Survey Summary

A comparison of the circuit performance between the trial and baseline using data gathered from the surveys conducted is displayed in Table 3.

Table 3: Comparison Data from Circuit Surveys

Sample	Baseline (TETA/ Sodium Sulfit)	Trial (AERO 7261A)
Feed Grade		
Cu%	0.93	0.91
Ni%	2.24	2.22
MgO%	7.72	7.64
Copper Final Concentrate		
Cu Recovery %	85.6	87.8
Ni Recovery %	1.16	1.46
MgO Recovery %	0.26	0.21
Grade Cu%	29.7	29.7
Grade Ni%	0.96	1.20
Grade MgO%	0.69	0.55

Both conditions featured very similar feed grades, with variation managed through the provision of a two-month duration of the trial and three day ON/ OFF periods. The results were analysed and presented as a function of feed grade, with no mineralogical results available at the time of writing. Feed grades were reasonably similar to those used in laboratory testing (0.87% Cu, 2.1% Ni). The surveys display similar results to the findings from the shift composite statistical analysis, with copper and nickel recovery higher, and MgO recovery lower, with the addition of AERO 7261A as compared to baseline conditions.

AERO 7261A in Cu Circuit Process Water

As AERO 7261A is a water-soluble, modified polyacrylamide-based polymer, a concern was raised about a potential AERO 7261A build-up in the Cu circuit process water. The decision was made to collect process water samples during the TETA/sodium sulfite and AERO 7261A periods and analyse them for total organic carbon (TOC). It was anticipated that a build-up of AERO 7261A in process water would manifest itself in the higher concentration of TOC, which could lead to issues with selectivity in the flotation circuit.

The copper scavenger tail (CST) samples collected during the trial sampling campaigns were filtered, with the filtrate then analysed for TOC by an external laboratory.

The results of the TOC analysis of process water are presented in Table 4.

Table 4: TOC analysis of the copper scavenger tail (CST) filtrate samples

Sample	Conditions	TOC (ppm)
1	TETA/Na ₂ SO ₃	56
2	AERO 7261A/Na ₂ SO ₃	26
3	TETA/Na ₂ SO ₃	69
4	AERO 7261A/Na ₂ SO ₃	19
5	TETA/Na ₂ SO ₃	28
6	AERO 7261A/Na ₂ SO ₃	27
7	AERO 7261A/Na ₂ SO ₃	23
8	TETA/Na ₂ SO ₃	53
9	AERO 7261A/Na ₂ SO ₃	20
Average	TETA/Na ₂ SO ₃	52
Average	AERO 7261A/Na ₂ SO ₃	23

The results show that during the TETA/Na₂SO₃ periods the process water TOC concentration was more than two times higher than during the AERO 7261A periods, i.e. on average 52 ppm and 23 ppm, respectively. The higher TOC value during the TETA/Na₂SO₃ periods may be explained by the mechanisms by which TETA/sodium sulfite and AERO 7261A depress pentlandite.

TETA is a powerful chelating agent for metal ions including copper, nickel, iron and other ions. It is believed that TETA forms metal complexes with activating ions (Cu²⁺ and Ni²⁺) in solution as well as removes these ions from the mineral surface. Sodium sulfite then acts as a depressant. TETA remains in process water and contributes to TOC.

AERO 7261A is a water-soluble polymer, which has been originally formulated to depress pyrite and pyrrhotite. Evidently, AERO 7261A is also an effective pentlandite depressant. The AERO 7261A depression mechanism is believed to selectively and reversibly adsorb on mineral surfaces, rendering them hydrophilic. That is, although a water-soluble polymer, AERO 7261A is not expected to remain in process water and should not greatly contribute to process water TOC. The difference in TOC values recorded is unlikely to be a direct function of the molecular weight of the two reagents. While the molecular weight of AERO 7261A is proprietary information (not disclosed by the manufacturer), the small molecular weight of TETA would suggest that higher TOC levels would be expected from the use of AERO 7261A on this basis.

INDICATIVE ECONOMIC BENEFITS

An assessment of the indicative economics of AERO 7261A usage compared to the previous reagent scheme is displayed in Table 5:

Table 5: Indicative Economic Comparison of TETA-Sodium Sulfite versus AERO 7261-Sodium Sulfite

Baseline conditions	TETA	Sodium Sulfite	Total
Unit Price AUD/kg	\$8.58	\$0.60	
Usage Rate g/t	93	220	
Unit Reagent Cost AUD/t	\$0.80	\$0.13	\$0.93
Annual Cost* AUD	\$1 265 812	\$209 398	\$1 475 210
Annual Usage* t	149	352	
Trial conditions	AERO 7261A	Sodium Sulfite	Total
Unit Price AUD/kg	\$3.91	\$0.60	
Usage Rate g/t	50	300	
Unit Reagent Cost AUD/t	\$0.20	\$0.18	\$0.38
Annual Cost* AUD	\$310 131	\$285 543	\$595 674
Annual Usage* t	80	480	
Potential Annual Savings AUD			\$879 536

*Based on processing 1.586 Mt/y

Significant cost savings, in excess of \$800 000 per year, are indicated by the adoption of AERO 7261A based on nominal flotation circuit performance during the plant trial. The cost of nickel depressants per tonne of ore would be decreased from \$0.93 to \$0.38, mostly driven by AERO 7261A only being one quarter of the cost of TETA. As the value of nickel revenue vastly outweighs the reagent costs, the economic benefits of AERO 7261A use are highly dependent on the impact of its use on nickel recovery. Given the relatively short nature of the “optimised” section of the trial, further assessment

of the economic impact of nickel losses is to be conducted during general operation and future blocked trials.

CONCLUSIONS

An AERO 7261A Depressant plant trial, conducted at the Nova Operation in May-June 2021, demonstrated that AERO 7261A is a viable replacement for TETA in the copper flotation circuit. During the plant trial, AERO 7261A provided a 1.1% higher CFC Cu grade at a comparable Cu recovery and did not negatively affect the nickel circuit performance. AERO 7261A also did not have any substantial effect on CFC and NFC grades and recoveries of Co, Fe, MgO, S and SiO₂.

Based on the outcomes of the plant trial, AERO 7261A is now being commercially used at the Nova Operation. The potential economic benefits of replacing TETA with AERO 7261A are estimated to be in the order of \$800 000 per annum; however, continued statistical analysis of circuit performance and repeat block trials will allow IGO to ensure that it remains the superior reagent post changeover.

ACKNOWLEDGEMENTS

The authors would like to express their gratitude to IGO Limited, the Nova Operation management, metallurgical team, laboratory and processing plant operators for their support of this project.

REFERENCES

- Kelebek S, Wells P F and Fekete S O, 1996. Differential flotation of chalcopyrite, pentlandite and pyrrhotite in Ni-Cu sulfide ores. *Canadian Metallurgical Quarterly*, 35(4): 329-336
- Kelebek S and Tukul C, 1999. The effect of sodium metabisulfite and triethylenetetramine system on pentlandite–pyrrhotite separation. *International Journal of Mineral Processing*. 57(2):135-152
- Liao X, Chen Y and Chen J, 2022. Application of macromolecular organic polymer S-7261A in arsenic removal by flotation of refractory mixed copper ore. *Minerals Engineering*, 182: 107560
- Weil E D, 1983 Sulfur compounds. In: Mark, H.F., Othmer, D.F., Overberger, C.G., Seaborg, G.T. & Grayson, N., eds, *Kirk-Othmer Encyclopedia of Chemical Technology*, 3rd ed., Vol. 22, New York, John Wiley & Sons, pp. 107–167.
- Yoon R H, Chen X, Nagaraj D R, 1997. Comparison of different pyrrhotite depressants in pentlandite flotation. In: Finch, J.A., Rao, S.R., Holubec, I. (Eds.), *Proceed. Processing of Complex Ores. Mineral Processing and the Environment*. Sudbury, Ontario, CIM: Montreal, pp. 91–100.

Flash Furnace Throat Accretion Management through Post-Combustion Oxygen Injection

M O'Sullivan¹, H Kim² and K Pereira³

1. Senior Metallurgist – Smelter Production Support, BHP, Olympic Dam
Email: mark.osullivan@bhp.com
2. Flash Furnace Metallurgist – Smelter Production Support, BHP, Olympic Dam
Email: helen.kim@bhp.com
3. Flash Furnace Metallurgist – Smelter Production Support, BHP, Olympic Dam
Email: kassandra.baldi@bhp.com

ABSTRACT

The Olympic Dam flash furnace smelts high copper bearing concentrates directly to a blister copper & high copper fayalite slag. During operation, the section between the flash furnace and waste heat boiler, known as the “throat”, progressively builds up with a solid precipitate from the process. This is referred to as “accretion” and is typically a mixture of spinel (CuFe_2O_4 & Fe_3O_4), delafossite (CuFeO_2), cuprite (Cu_2O) and tridymite (SiO_2).

Removing throat accretion requires flash furnace downtime. If the build-up is too large in size, its removal methodology changes and can expose operators to hazardous environments, ie exposure to acidic dusts, hot furnace gases and significant manual handling risks. Historically, the flash furnace was required to be taken offline every two days for an hour to allow for the safe and efficient removal of throat accretion.

The flash furnace offgas consists of primarily SO_2 , N_2 with small amounts of O_2 & CO_2 and “dust” (entrained particles containing a mixture of Cu, Fe and SiO_2 with minor concentrations of Al_2O_3 and CaO). The offgas phase equilibria can be described through the Cu-Fe- O_2 - SiO_2 system. A review into this system indicated that an increase in oxygen partial pressure ($p\text{O}_2$) would result in both:

- fully oxidised slag with no metallic copper present – forming a more brittle accretion with less metallic properties
- increased liquidus temperature – decreasing the extent of accretion formation.

Oxygen was injected into the settler freeboard through non-operational fuel oil burners to provide the process sufficient oxygen ($p\text{O}_2$ between $10^{-1.5}$ and 10^{-3} atm) to create optimal throat accretion forming conditions. Consistent injection of sufficient oxygen has resulted in the reduction in throat accretion size.

INTRODUCTION

Olympic Dam Smelter Overview

The Olympic Dam smelter consists of a flash furnace for primary copper smelting via the “direct-to-blister” process, an electric furnace for slag cleaning of high copper containing slags and two anode furnaces for fire-refining blister copper to anode copper. The flash furnace is a typical Metso design with a reaction shaft where the sulfide particles react with oxygen, settler where the bath and fluxing reactions take place and the uptake shaft where the off gas and entrained particles are vented from the furnace. The blister copper and slag form two immiscible layers that are periodically tapped from the furnace via separate tapholes.

The furnace offgas contains a mixture of gases (primarily SO_2 , N_2 with small amounts of O_2 & CO_2) and dust particles (entrained particles containing a mixture of Cu, Fe and SiO_2 with minor concentrations of CaO and Al_2O_3). These dust particles collect and build-up at the throat (interface between the flash furnace and waste heat boiler) resulting in the requirement for the furnace to be brought offline so robotic rock breakers can mechanically remove the build-up.

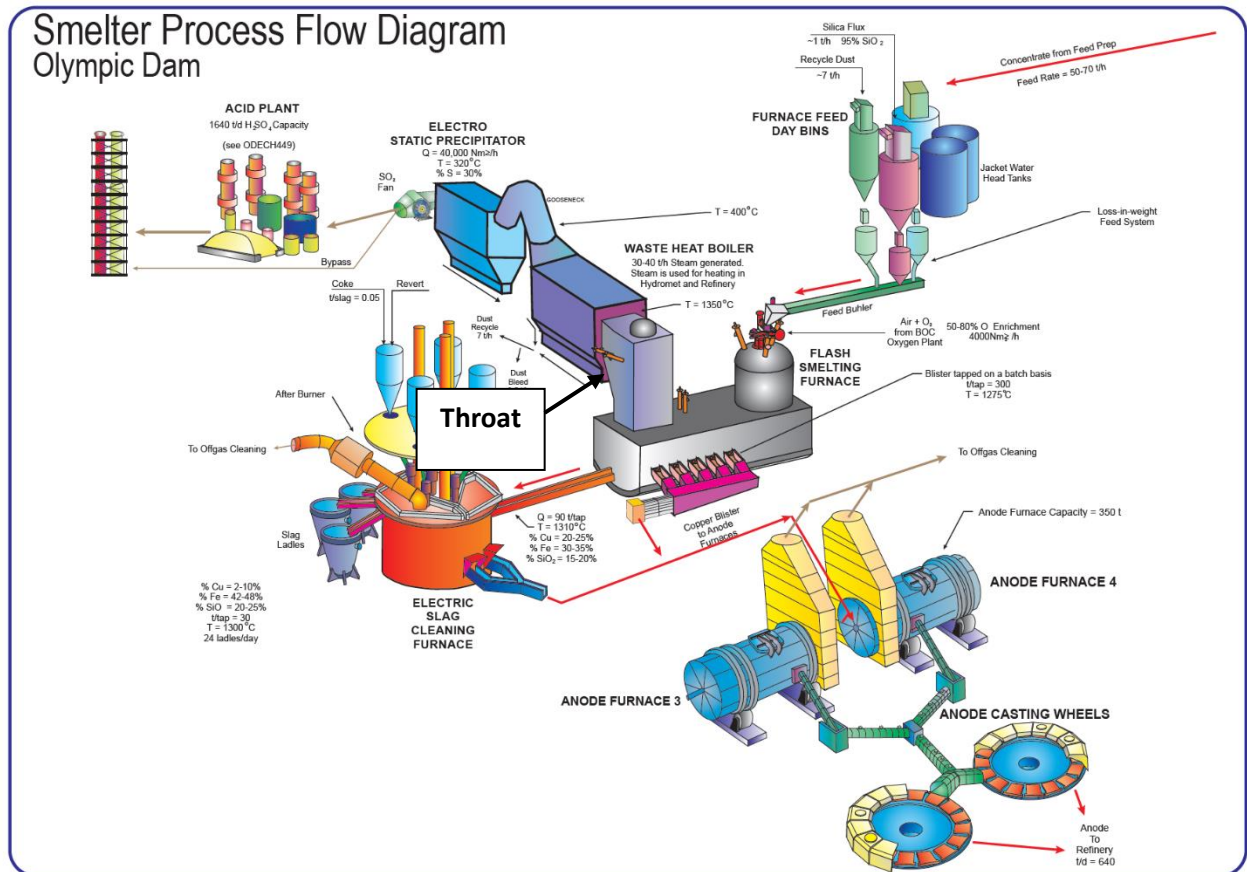


Figure 1 – Olympic Dam smelter process flow diagram

THROAT ACCRETIONS

Accretions formations between the uptake shaft and waste heat boiler cause considerable operational and maintenance issues in many flash furnaces throughout the world. At Olympic Dam they have proven especially difficult, requiring more frequent removal than other operations. The accretions are a mixture of spinel (CuFe_2O_4 & Fe_3O_4), delafossite (CuFeO_2), cuprite (Cu_2O) and tridymite (SiO_2) (Hall, et al., 2002).

Accretion growths with undesirable size and shape can result in significant production downtime and expose operators to manual handling risks. At Olympic Dam, the accretions are qualitatively defined by size (small, medium or large) and by shape (conventional or sheet), as shown in Figure 2.

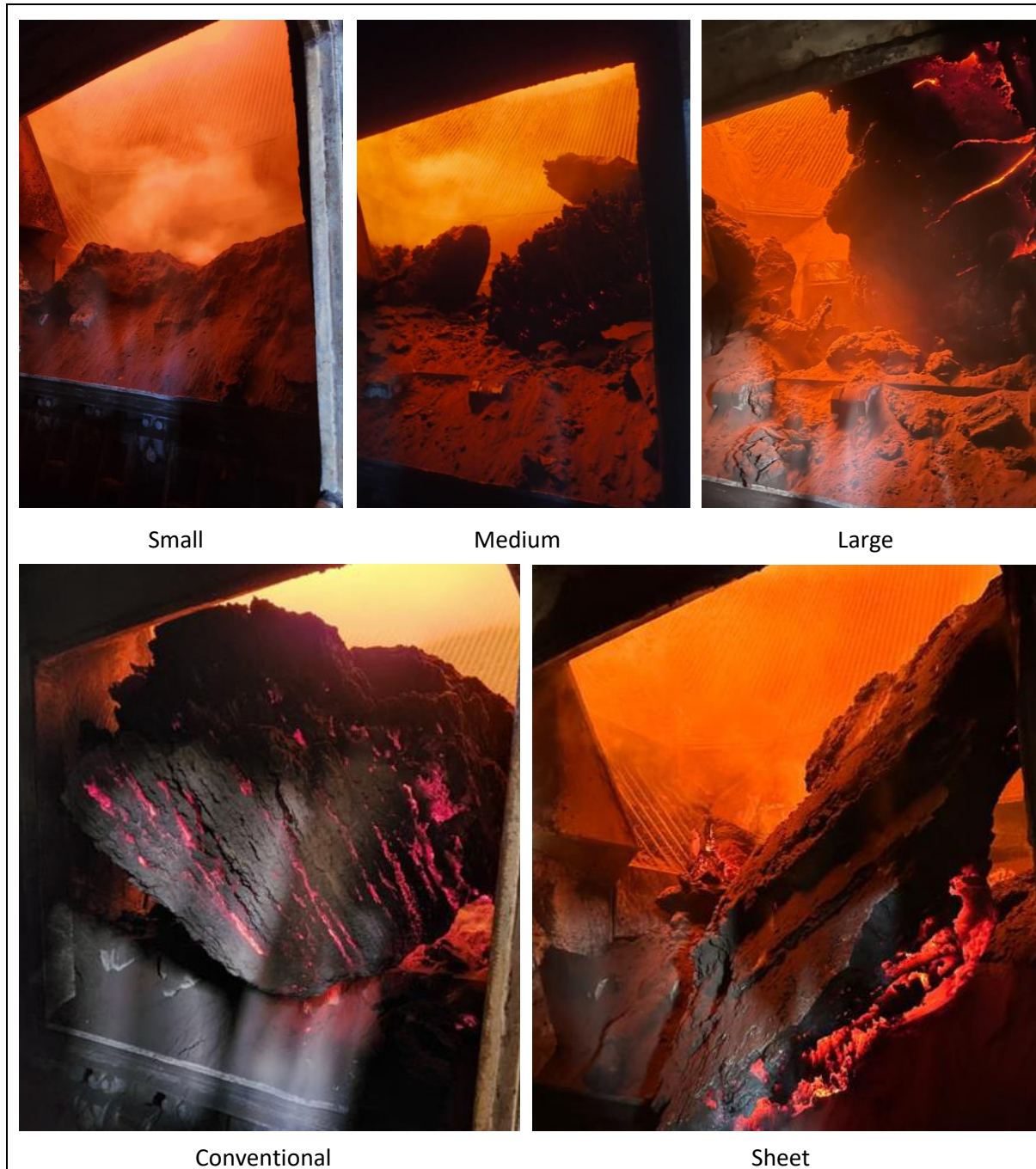


Figure 2 – Throat accretion categorisation size and growth type (conventional or sheet)

THERMODYNAMICS & PHASE EQUILIBRIA

Concentrate Feed and Uptake Shaft Dust Composition

Dust is smelted concentrate particles that are small enough to be entrained in the offgas stream, and therefore, the flash furnace dust composition is a direct result of the feed composition. Increases in the copper content in feed result in a decrease in iron content in dust. The dust Cu:Fe ratio is typically between 1.6 and 2.6. The relationship between concentrate and uptake shaft dust composition (Cu, Fe, SiO₂ and Cu:Fe ratios) is displayed in Figure 3. Concentrate compositions are obtained routinely from the feed system for operational process control, whereas uptake shaft dust samples have been collected on an ad hoc basis, by allowing dust to deposit on a steel bar inside the furnace.

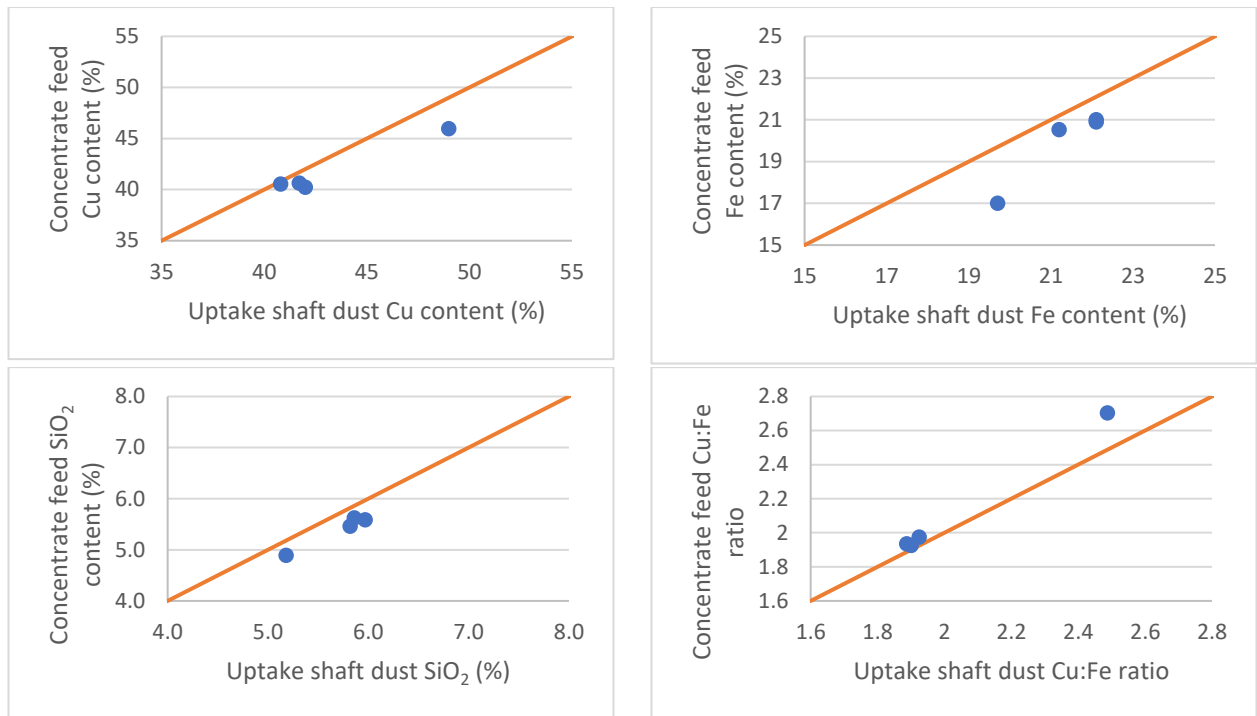


Figure 3 – Flash furnace uptake shaft dust versus concentrate Cu, Fe and SiO₂ content & Cu:Fe ratio

Thermodynamics & Phase Equilibria

The flash furnace off gas thermochemical system can be described simplistically through the Cu-Fe-O system, first described by Elliot & Luraschi (1976) in Figure 4, where L₁ is liquid copper, L₂ is liquid slag and S.S. is a spinel, either Fe₃O₄ or CuFe₂O₄ depending on iron content of the system. This shows the influence of temperature, oxygen partial pressure (pO₂) and dust composition on the resulting phase formations.

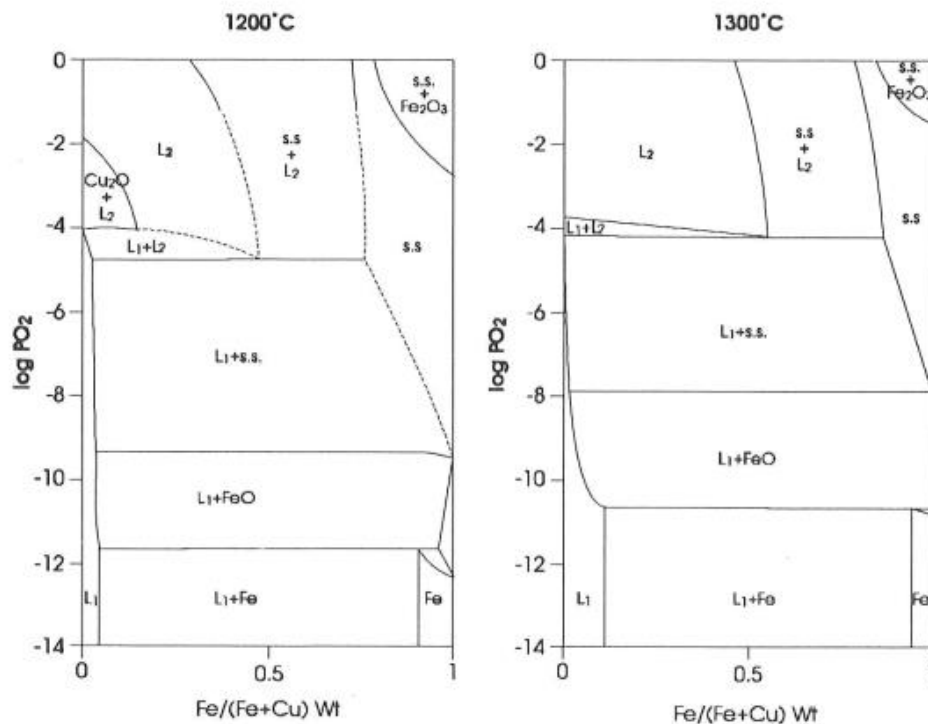


Figure 4 - Cu-Fe-O phase diagrams for 1200 °C & 1300 °C (Elliot and Luraschi, 1976)

The influence of SiO_2 on the liquid phase boundaries was not evaluated by Elliot and Luraschi (1976), however, the concentration is high and variable enough to influence the phase equilibria. Hence, thermodynamic modelling accounting for the impacts of SiO_2 was completed using FactSage 8.2. Figure 5 presents the relationship between $p\text{O}_2$ and temperature for various dust compositions. The Olympic Dam smelting process operates at relatively high oxidising conditions to produce blister copper directly from concentrate ($p\text{O}_2 = \sim 10^{-4.8}$ atm).

The location of the liquid regions in the Cu-Fe- O_2 - SiO_2 system is primarily a function of:

- temperature – an increase in temperature results in an increase in liquid fraction of system
- gaseous phase conditions – $p\text{O}_2$ between 10^{-2} & 10^{-4} atm results in a decrease in liquidus temperature
- Cu content of the dust – increase in Cu results in a decrease in liquidus temperature
- Fe content of the dust – increase in Fe results in an increase in liquidus temperature
- SiO_2 content of the dust – increase in SiO_2 results in decrease in liquidus temperature.

Characteristics of operation with conditions above a $p\text{O}_2$ of $10^{-4.5}$ atm:

- lower liquidus temperatures (between 1150 °C & 1250 °C)
- primary phase field transitions from spinel to delafossite at higher Cu contents (Cu:Fe > 2.4)
- all liquids in slag phase.

Characteristics of operation with conditions below a $p\text{O}_2$ of $10^{-4.5}$ atm:

- very high liquidus temperatures (>1350 °C)
- formation of liquid copper metal.

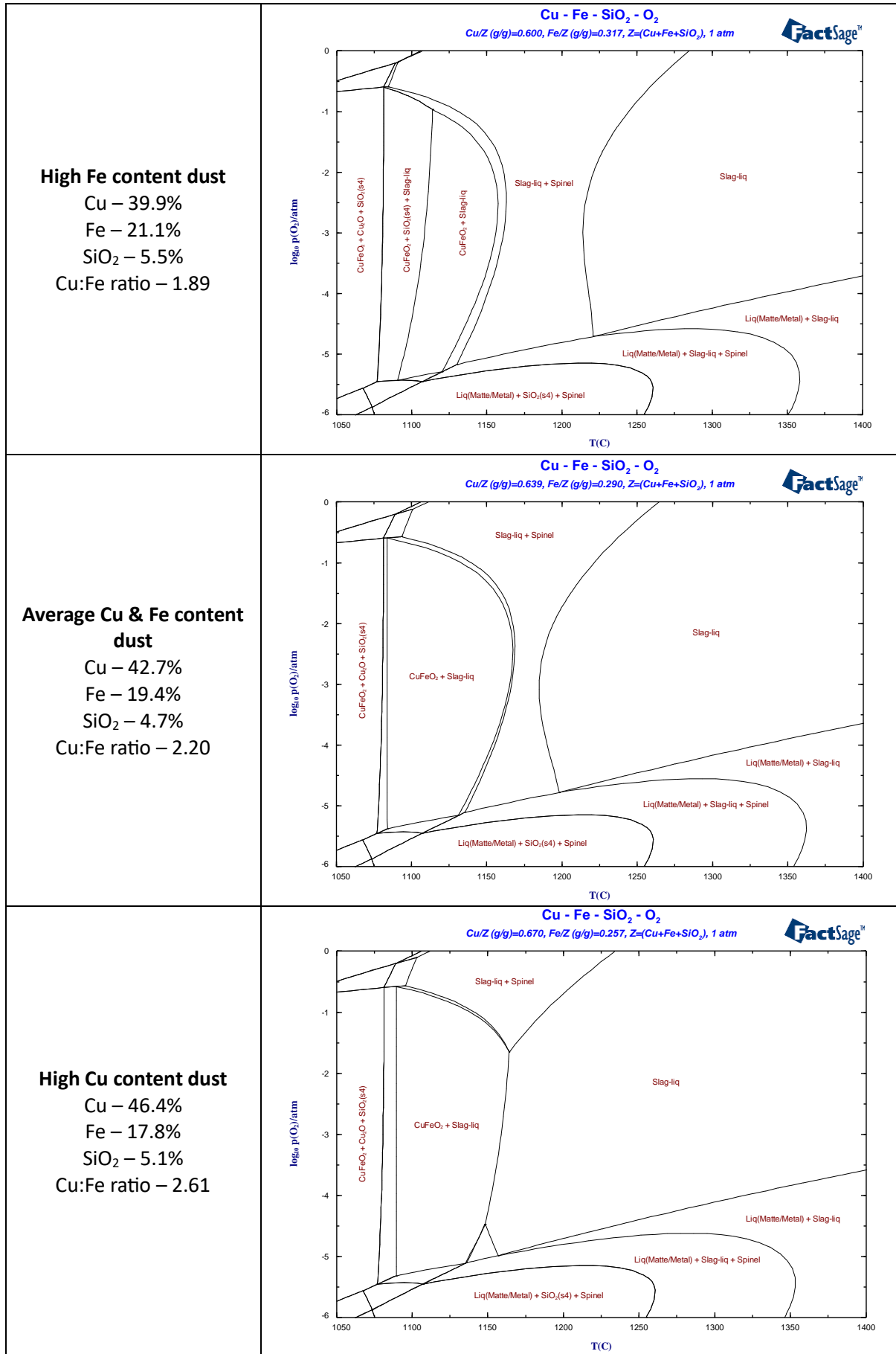


Figure 5 – Phase diagrams for various dust compositions

The liquidus phase boundaries from these three phase diagrams versus pO₂ for both FactSage and polynomial estimations has been translated in Figure 6. The flash furnace operating pO₂ for slag and blister chemistry control is presented as “smelting pO₂”. The entrained dust leaving the reaction shaft will be in a similar oxidation state, therefore, any adjustments to dust pO₂ must be done relative to this oxidation state.

The resulting dust liquid temperature polynomial regression was:

$$Liquidus\ Temp = 6.86 \log[O_2]^2 + 44.71 \log(O_2) - 1.69[Cu:Fe] - 4.32[Cu\%] + 11.21[Fe\%] - 8.97[SiO_2\%] + 1271.59$$

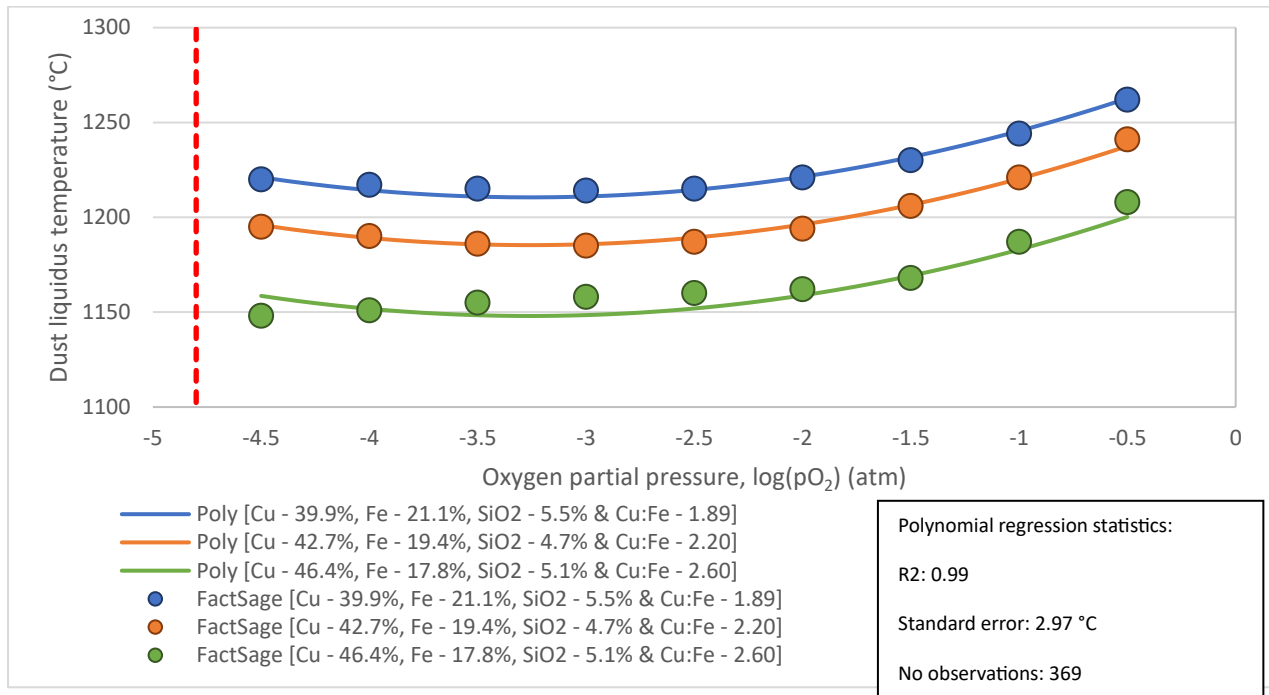


Figure 6 – Dust liquidus temperature for varied dust compositions (polynomial estimated & FactSage)

The impact of composition (Cu, Fe and SiO₂) and pO₂ on the dust liquidus temperature was evaluated through the FactSage 8.2 equilibrium module for conditions outlined in Table 1.

Table 1 - Operational and composition range modelled in FactSage 8.2

Component	Minimum	Maximum
pO ₂ (atm)	10 ^{-4.5}	10 ^{-0.5}
Cu (%)	37.8	46.4
Fe (%)	17.7	22.9
SiO ₂ (%)	4.0	5.9
Cu:Fe ratio	1.65	2.60

Partial pressures outside of the provided range was excluded for the following reasons:

- < 10^{-4.5} atm – The rapid increase in spinel liquidus temperature results in difficulty with data regression

- $> 10^{-0.5}$ atm – Conditions not reasonably achievable in current operational set-up, ie will require settler gas composition of >50 vol% O_2 .

SETTLER OXYGEN INJECTION

Following a review of the phase equilibria, it was proposed to add oxygen to the settler freeboard to drive the equilibrium to:

- oxidise all the metallic copper to produce an iron silicate slag which is much more brittle than a spinel and copper mixture
- increase the liquidus temperature to reduce the size of the accretions that are formed.

This was achieved by using non-operational fuel oil burners (between the reaction and uptake shaft) as injection ports for oxygen enriched air. The flash furnace is equipped with 11 fuel oil burners (three in the reaction shaft, six in the settler roof and two in the settler sidewall). During normal operation the fuel oil burners are used to assist with heat balance management to achieve target slag and blister temperatures. During flash furnace downtime, the burners are used to retain heat in the furnace to minimise thermal cycling. This set-up is shown in Figure 7.

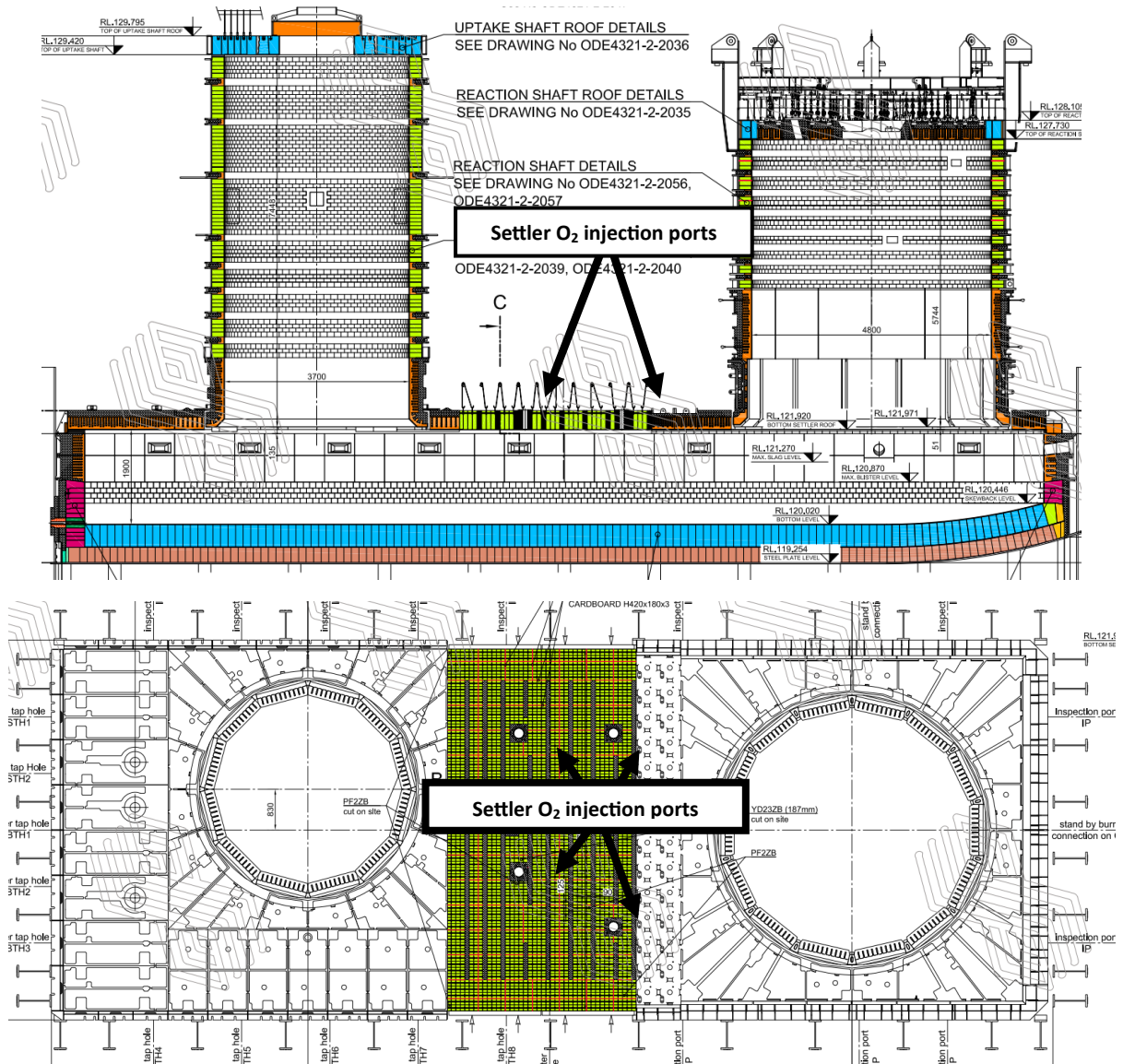


Figure 7 - Schematic of the flash furnace and settler oxygen injection location

Dust Temperature and pO_2 Measurements

Temperature and pO_2 measurements of the dust were taken at approximately the uptake shaft midpoint. A modified celox probe with both oxygen and temperature outputs was wired into a data logger for data collection. Standard Electronite celox probes (with the caps removed) were used to measure both electromotive force (EMF) and temperature. The EMF and temperature signals were converted to pO_2 via the equation below (Collins, 1995).

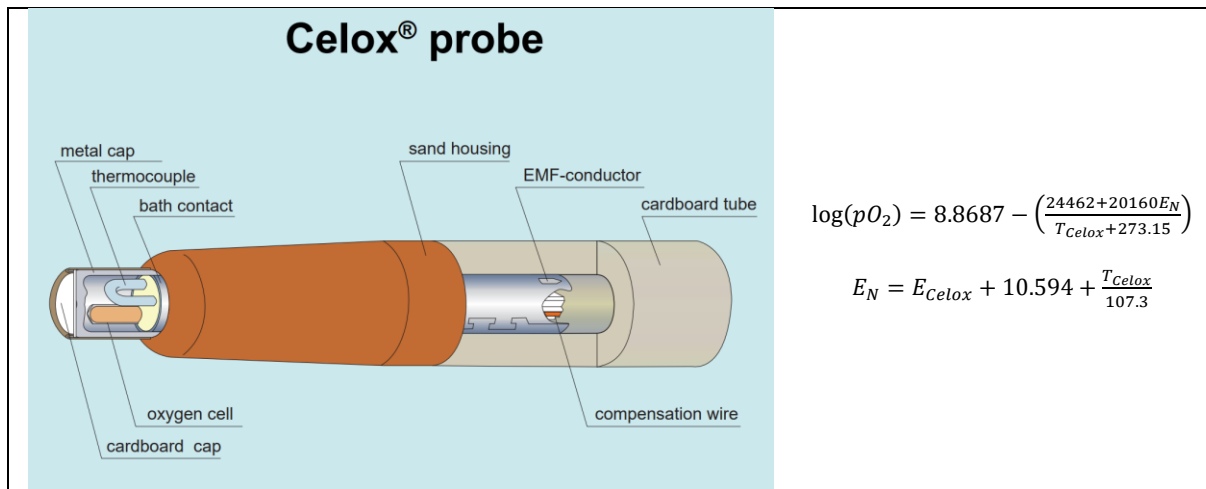


Figure 8 – Schematic of celox probe (Maes, 2012) and pO_2 equation (Collins, 1995)



Figure 9 - Uptake shaft temperature and oxygen measurement & celox probe before & after

The relationship between oxygen flow rate and measured pO_2 is presented in Figure 10. An increase in settler oxygen results directly in an increase in pO_2 . The variability in pO_2 is the result of a fundamental characteristic of flash smelting. Previous work has demonstrated that between 70 - 80% of the sulfur in concentrate is eliminated in the reaction shaft. The total required oxygen is bound to the particles, however, due to the variability in particle sizes; larger particles are under oxidised whereas smaller particles are over oxidised (Collins, 1995).

In the slag bath, these particles react with each other towards equilibrium, however, the dust particles that are entrained in the offgas stream do not have the opportunity equilibrate. Therefore, the pO_2 variability at the exit of the reaction shaft will likely be similar to the pO_2 variability at the exit of the uptake shaft. Consequently, it is not possible to achieve a target pO_2 but rather a pO_2 range.

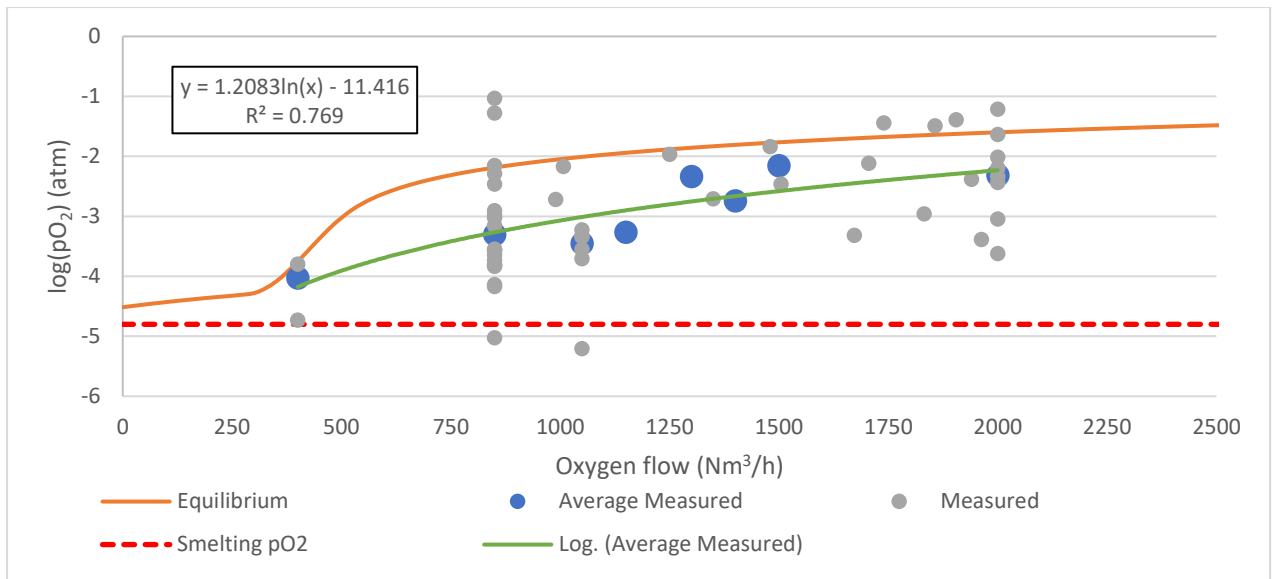


Figure 10 - Settler oxygen injection flow versus dust oxygen partial pressure (greater than 75 t/h)

Gas and dust temperature in the uptake shaft ranged from ~1200 °C to ~1340 °C. Figure 11 displays the measured temperatures with an average of ~1270 °C.

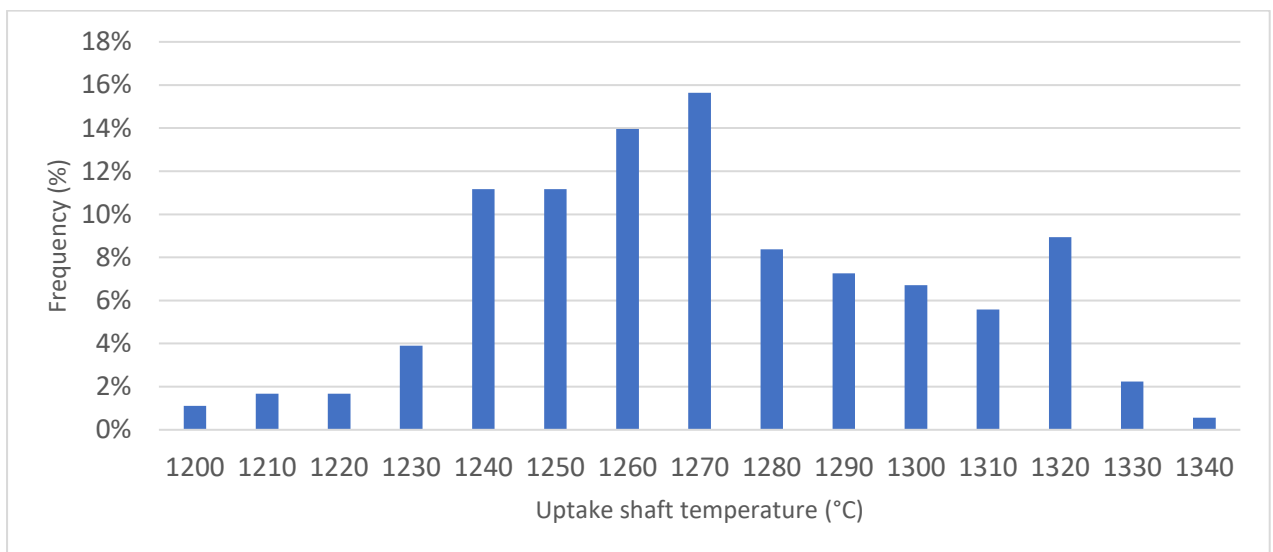


Figure 11 - Histogram of measured uptake shaft temperatures at 75 t/h

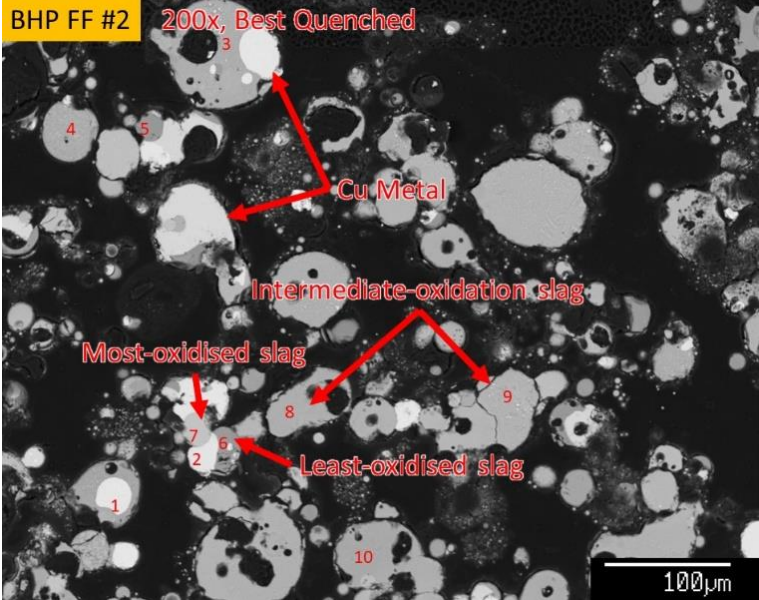
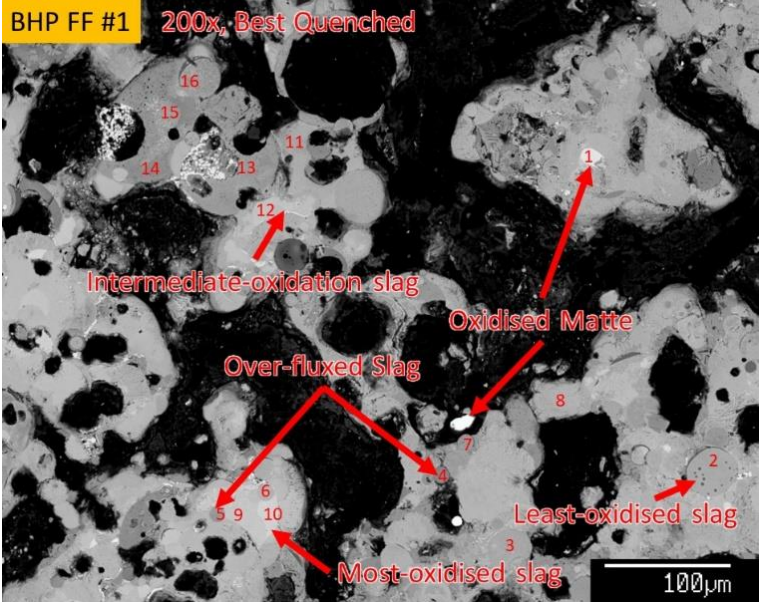
Dust Microstructure Analysis

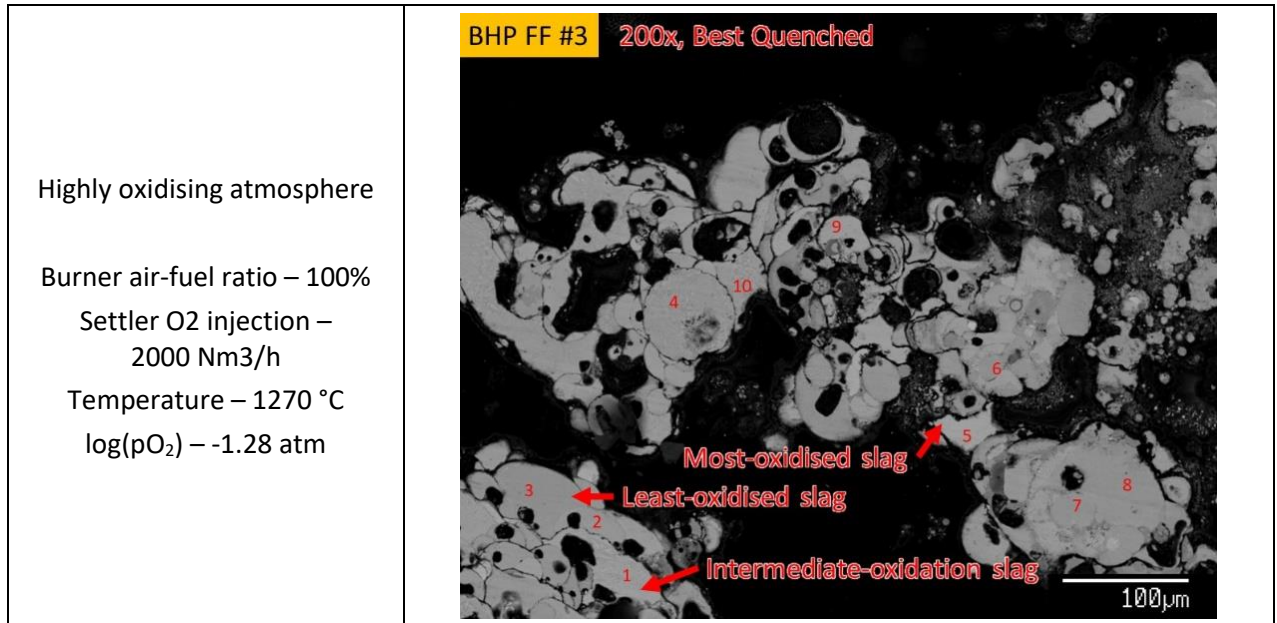
Quenched samples of flash furnace dust were sent to the University of Queensland's Pyrometallurgy department for analysis of dust microstructure using scanning electron microscope (SEM) and electron probe micro-analyser (EPMA). The quenched dust samples were mounted in epoxy resin for the EPMA analysis using the JEOL 8200 SuperProbe in wavelength dispersive x-ray spectrometer (WDS) mode. SEM operated at 15 kV, 20 nA with 0-10 μm spot size). Three furnace conditions were tested to evaluate the effect of oxygen injection of the dust phase assemblage (reducing, oxidising and highly oxidising).

All three samples measured were completely fluid with no solid precipitate measured and consisted of a wide variety of slag compositions with the highly oxidised case appearing more homogenous. There was no miscibility gap at the composition and operating conditions, therefore the presence of various slags indicated that the system was not at equilibrium. Moreover, at equilibrium the reducing atmosphere conditions should have solid spinel precipitate. This further indicates the system is not at equilibrium.

The micrographs of the quenched dust samples are presented in Table 2.

Table 2 – Micrographs of quenched flash furnace dust samples at different operating conditions



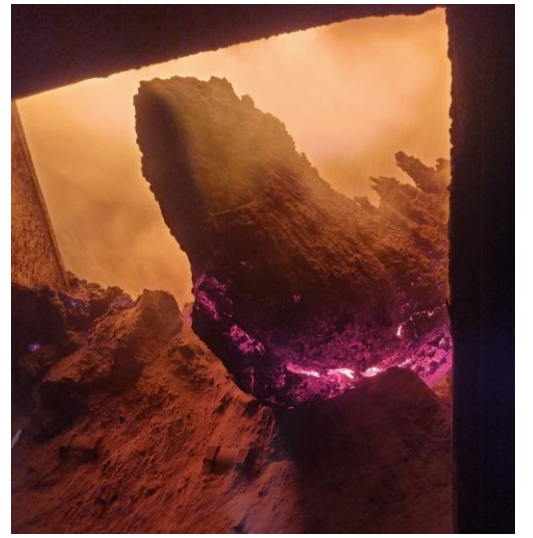

Furnace Condition	High Magnification Micrograph of Best-Quenched
<p>Reducing atmosphere</p> <p>Burner air-fuel ratio – 90%</p> <p>Settler O₂ injection – 0 Nm³/h</p> <p>Temperature – 1290 °C</p> <p>log(pO₂) – -6.24 atm</p>	<p>BHP FF #2 200x, Best Quenched</p> 
<p>Oxidising atmosphere</p> <p>Burner air-fuel ratio – 100%</p> <p>Settler O₂ injection – 700 Nm³/h</p> <p>Temperature – 1293 °C</p> <p>log(pO₂) – -4.13 atm</p>	<p>BHP FF #1 200x, Best Quenched</p> 



Effect on Accretion Growth

A general trend can be observed in the resulting accretion growth when subjected to different operating conditions. This is illustrated in Table 3.

Table 3 – Various accretion growths with the associated differing operating conditions

	
Date 18 th of May 2022 Accretion Size Very large Accretion Type Conventional Atmosphere High reducing Estimated log (pO₂) -7 to -8 atm Feed Cu:Fe 2.21 Liquidus Temperature 1270 – 1322 °C	Date 9 th of December 2022 Accretion Size Large Accretion Type Conventional Atmosphere Oxidising Estimated log (pO₂) -3.69 atm Feed Cu:Fe 2.32 Liquidus Temperature 1173 °C
	
Date 25 th of March 2023 Accretion Size Medium Accretion Type Conventional Atmosphere Oxidising Estimated log (pO₂) -2.45 atm Feed Cu:Fe 2.23 Liquidus Temperature 1188 °C	Date 10 th of March 2023 Accretion Size Small Accretion Type Conventional Atmosphere Oxidising Estimated log (pO₂) -2.51 atm Feed Cu:Fe 1.78 Liquidus Temperature 1231 °C

The relationship between dust liquidus temperature versus accretion size was analysed for comparable smelting run times. Figure 12 shows large accretion growths have coincided with periods of low liquidus temperature and highly reducing conditions.

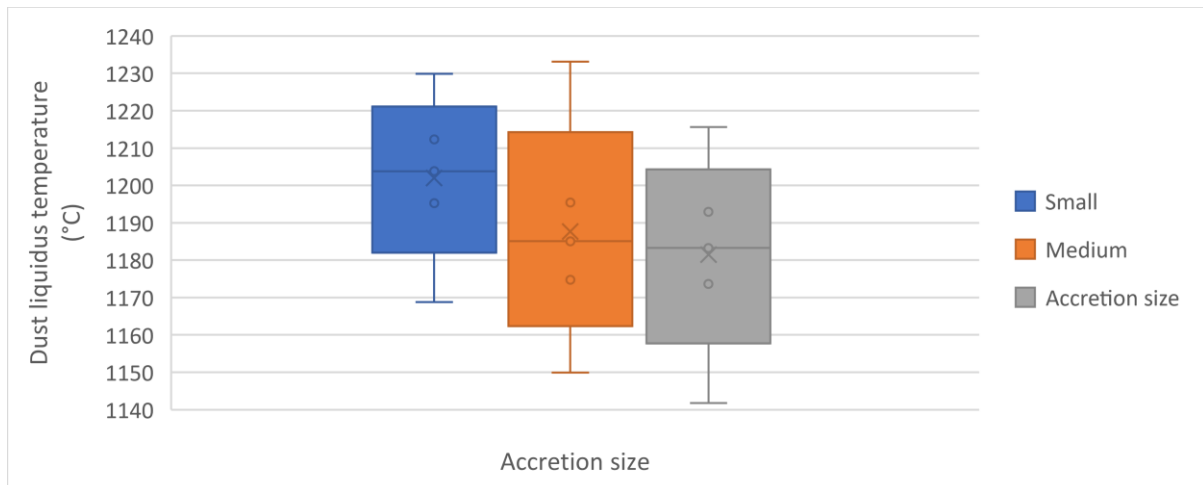


Figure 12 – Effect of liquidus temperature on throat accretion size (average feed rate > 68 t/h & concentrate smelted 2000 to 4000 t).

Effect on Inspection Frequency

The flash furnace is internally inspected for water leaks from cooling elements at a maximum frequency of four daily. During these inspections, various other tasks are completed opportunistically to avoid additional downtime, such as throat and concentrate burner cleaning. However, the requirement to clean the throat build-up drives the inspections to historically occur at a reduced frequency, ie two daily.

The flash furnace metallurgist and smelting production supervisor completing the inspections will determine the time until the next inspection. This decision is typically based on the size of the throat accretion, but may also be impacted by planned downtime (ie shutdowns) or internal/external maintenance requirements.

Figure 13 details the typical recommended and actual frequencies of inspections. Initially after the introduction of oxygen in the settler freeboard, a decrease in the recommended frequency was observed indicating a decrease in accretion size. This allowable increase in operational time was not fully realised due to external factors such as unplanned plant downtime. Plant downtime, depending on the duration (ie expected >60 minutes) will generally trigger an opportunist inspection.

Between April and September 2023, a change in accretion growth shape to “sheet-like” was observed. This resulted in the requirement to inspect the furnace at a higher frequency. The initial theory around oxygen injection was to aim to operate with a more liquid dust (ie lowest liquidus temperature) based on previous work by George-Kennedy (1993) and Hall et al (2002). This theory has since been challenged and refined, and the benefits initially seen during the oxygen injection trial are now believed to be due to:

- full oxidation of the liquid copper to form a brittle iron silicate slag
- increase in liquidus temperature resulting in a decrease in accretion size.

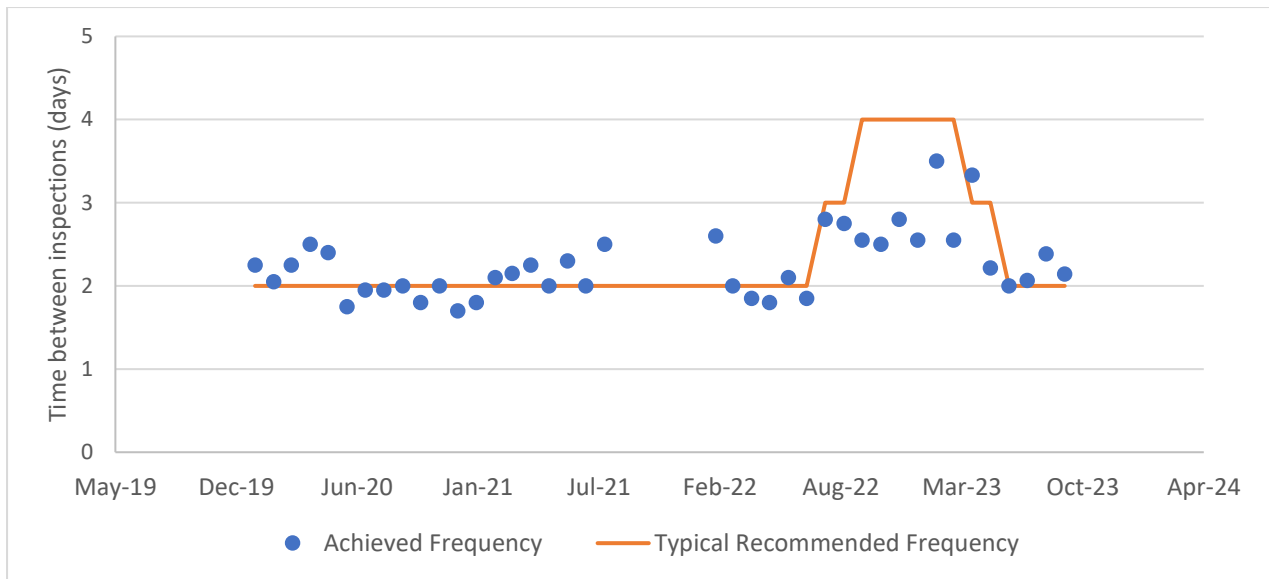


Figure 13 – Effect of average dust liquidus temperature on throat accretion size

CONCLUSIONS

An investigation into the dust particle phase equilibria indicated that modifications to the off-gas composition would change the phase equilibria and produce the following favourable accretion forming conditions:

- full oxidation of the liquid copper to form a brittle iron silicate slag
- increase in liquidus temperature resulting in a decrease in accretion size.

Analysis into the Cu-Fe-O₂-SiO₂ system indicated that targeting a dust liquidus temperature of 1210 °C would result in smaller more manageable accretions. This is currently being trialled by modifying the target settler oxygen injection flow rates based on the expected concentrate feed assay.

A reduction in throat accretion size was temporarily achieved by modification of the dust phase equilibria, allowing for a reduction in inspection frequency from two daily to three daily. However, since then, changes in feed chemistry have made it difficult to achieve dust liquidus temperatures above 1210 °C. This has aligned with increased difficulties in removing throat accretion build-up and hence a deviation back to two daily inspection frequencies. Further work is required to be completed to further specify uptake shaft accretion formation mechanisms.

ACKNOWLEDGEMENTS

The authors wish to thank BHP Olympic Dam for permission to publish this paper, the PYROSEARCH (University of Queensland's pyrometallurgy department) for their tireless work investigating, defining and categorising high temperature pyrometallurgical systems which has allowed for accurate predictions of pyrometallurgical systems, the BHP smelter technical team for efforts collecting and analysing measurements and samples, smelter process control team for supporting the coding required to execute oxygen injection, smelter production & control team for safely embedding oxygen injection into daily operations and executing proposed operational strategies, smelter electrical maintenance team for building bespoke measuring equipment to enable collection of process data and Olympic Dam laboratory team for supporting analysis of non-routine samples.

REFERENCES

Collins, D, 1995. Reactions in the Shaft of the Olympic Dam Flash Furnace, Masters thesis, University of Melbourne, Wollongong.

Elliot, J and Luraschi, A, 1976. Phase Relationships in the Cu-Fe-O-SiO₂ System, 1100 to 1350°C, in *Proceedings Copper Symposium TSM-AIME 1976*, pp 90 – 114.

George-Kennedy, D, 1993. Developments in Direct-to-Blister Flash Smelting of High Grade Concentrates at Olympic Dam, in *Proceedings of the Seventh International Flash Smelting Congress 1993*, pp 179 – 185.

Hall, T, Jorgensen, F, Solnordal, C and Wright, S, 2002. Accretion Formation and Sulphation Chemistry, Olympic Dam, CSIRO Minerals.

Maes, R, 2012. Celox® for on-line process control in modern steelmaking. Available from:
<https://www.heraeus.com/media/media/hen/doc_hen/sensors_and_probes/celox-online.pdf>
1/7/2023

Carbon Inventory Management in a Carbon-In-Leach Circuit

O Kopa¹, A Paine²

1. Morobe Consolidated Goldfields Limited, Papua New Guinea, Plant Metallurgist, Harmony Gold, omega.kopa@harmonyseasia.com
2. Molycop, Product Manager Gold Processing, adrian.paine@molycop.com

ABSTRACT

Morobe Consolidated Goldfields Limited (Harmony Gold), the developer and operator of Hidden Valley Gold and Silver mine in Papua New Guinea have over the past two years (2021/2022), evaluated the benefits of installing six of Mintek's online carbon concentration meters (C² Meters) in their Carbon-In-Leach (CIL) circuit. The C² Meters developed by Mintek and supplied by Process IQ (now Molycop) use the principle of ultrasonic attenuation to determine the carbon concentration in CIL tanks in real-time, providing a reliable measurement for use in an automated carbon management strategy.

Manual sampling of the non-homogenous mixture of carbon in a CIL tank is challenging, and measurement accuracy is influenced by a variety of factors such as the sampling method, position and frequency of measurement, operators' errors, and inconsistencies during sampling. In addition, the time between manual samples dictates the rate at which decisions can be made on moving carbon between tanks, to achieve the desired carbon profile and prevent excessive soluble gold losses to the tailings stream. On the other hand, the continuous measurements from the C² Meters mitigate the sources of error and provide a more accurate and repeatable real-time estimate of the total carbon inventory in the tanks.

Significant benefits were achieved from improving the carbon management in the CIL circuit, namely reduction in soluble gold and silver losses to the CIL tails as well as reduction in carbon fines generations.

Real-time measurements of carbon concentrations in the CIL tanks provided an opportunity to automate the carbon management strategy. Previously, the carbon concentration measurements were done manually on four-hourly intervals to monitor and manage carbon in CIL tanks. The control room operator (CRO) manually inputs the measured carbon concentration data into the distributed control system (DCS) and activates the carbon forwarding sequence from the main control room. After commissioning of the C² Meters, manual entry of carbon concentration was eliminated, and manual sequencing of carbon movement was replaced with an automated system. The integration of the existing manual controls into automatic controls was a significant upgrade initiated and implemented onsite, which was one of the main driving forces behind optimising metal recoveries and carbon management in the CIL circuit.

INTRODUCTION

The Hidden Valley Gold and Silver mine is situated in the Morobe Province, 90 km south-west of Lae, Papua New Guinea's industrial hub. They operate a conventional gravity circuit, a CIL circuit and a Merrill-Crowe circuit for extracting gold and silver. Both gold and silver are extracted from gravity and CIL, with pregnant solution from both reporting to the Merrill-Crowe circuit for zinc precipitation before going to smelting.

In 2020 Harmony Gold Limited made a decision to invest in the purchase of six C² Meter units for installation in the carbon-in-leach circuit at its Hamata Process Plant.

The measurement of the carbon concentration is traditionally undertaken manually. This practice can lead to time-consuming and often inaccurate measurements. Furthermore, it can lead to poor carbon management in the CIL circuit and loss of recoverable solution gold/silver into tailings.

Furthermore, the carbon concentration measurement obtained manually can be largely influenced by factors such as sampling method, position and frequency as well as operators' sample handling error and inconsistencies during sampling. By employing a machine to measure the carbon concentration, it is possible to reduce the number of error sources providing more accurate and reliable results.

Due to the non-homogeneity of carbon in the CIL tanks, the continuous high-frequency measurements from an online carbon concentration meter provides a better estimate of the total carbon inventory in the tank.

The carbon concentration meter (C² Meter) is explicitly designed to measure and provide continuous online monitoring of the carbon concentration in the slurry tanks. The accurate measurement of this variable for managing carbon inventory is a critical parameter in the efficient operation of the Carbon-in-Leach (CIL) circuit.

Integrating accurate high frequency carbon concentration readings into an automated carbon inventory management system can have significant benefits, such as:

- maintaining a consistent carbon profile in the CIL circuit and enabling the implementation of an efficient carbon movement strategy
- effectively managing of events such as carbon transfer to the CIL circuit, carbon transfer between tanks, and carbon recirculation between the CIL circuit and elution
- preventing over- or under-transferring of carbon from one tank to the other
- determining if there is carbon leakage or short circuiting between tanks
- compensating for variability in equipment performance
- maintaining a consistency in the process, independent of operator's experiences
- automatically detecting if carbon transfer pumps are not functioning properly.

The carbon meter operates based on the principle of ultrasound attenuation. There is a relationship between the carbon concentration and the attenuation of a high frequency ultrasonic signal passed through a slurry containing carbon. On the transmitter side of the probe, an electrical voltage is converted to an ultrasonic signal which sends sound waves through the slurry or the slurry-carbon mixture. On the opposing side, the resultant attenuated waves are detected by a receiver and then converted back to an electrical signal. By knowing the relative density (information that can either be entered manually or calculated by another C² Meter unit or read in from online density probe/meter), the controller can calculate the degree of attenuation between the transmitted and received signal and correlate it to the carbon concentration.

INSTALLATION AND COMMISSIONING

The installation of the C² Meters was completed in October 2021, and the instruments' commissioning, and calibration were finished in November 2021. The installation was straightforward and completed by Hidden Valley personnel with remote off-site assistance from Process IQ. Commissioning was also completed off-site by Process IQ due to restriction in travelling to site caused by the COVID-19 pandemic.

There are seven CIL Tanks at the Hamata Processing Plant on which six C² Meter units were installed successfully. Currently, six tanks are used as active CIL Tanks, while the final tank (TK7) is used as an

INOC Tank for cyanide destruction and TK6 switches between being used as a CIL or INCO Tank, respectively. Currently, six of the units installed are fully operational.

The C² Meter probes were mounted on metal plates used as anchor points. They were then inserted into the respective tanks adjacent to the manual sampling point and immersed 1.5 m below the surface of the slurry as shown in Figure 1.



Figure 1: C2 Meters control panel, and probe installation

Several factors were considered during the installation of the probes:

- probes installed away from carbon forwarding pump's suction point
- probes installed away from discharge points of the carbon forwarding pump
- probes installed away from Elution barren carbon discharge point
- probes installed to be submerged 1.5 meters below slurry surface
- probes installed away from sump pump discharge points
- probes installed several meters away from feed receiving zones, especially on CIL TK1 and CIL TK2 (fresh feed receiving tanks).

Integration

All C² Meter output signals were connected to the plant Distributed Control System (DCS). Trends of the online carbon measurements were setup on the DCS interface and also on the mine's PI system where live data can also be viewed from desktops and laptops. The high frequency measurement data from the C² Meters are shown in the PI trends in Figure 2.

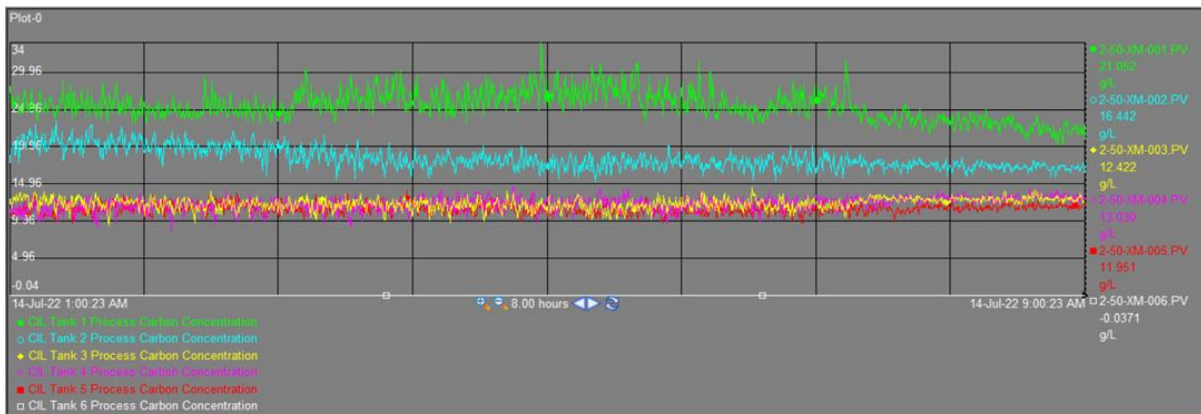


Figure 2: High frequency carbon concentration trends

Factors Affecting Readings

The most important factor affecting the C² Meter carbon concentration reading is the slurry's relative density (RD). Ideally one C² Meter probe should be used as a reference probe positioned in a carbon-free tank to compensate for changes in density. In the leach circuit at Hidden Valley there was no suitable location to install the reference probe and it was therefore decided that densities would be entered manually by the operator after taking grab samples. It was expected that this wouldn't have a significant effect on the readings as the variability in the densities were very low.

Another parameter influencing the carbon concentration reading is the feed flow into the tank as well as tank turbulences. This was found to have an actual effect on the carbon concentration reading where the carbon moves around the tank in pockets. Having a real-time measurement was an important benefit of the C² Meter and essential for correcting the effects of this behaviour. A filtered reading from the C² Meter provides a more accurate representation of the carbon content of the entire tank than what could be achieved with spot-samples and can easily be implemented as part of a control strategy.

Due to the measurement technique of the C² Meter, it is possible that the measurement can be affected by foreign materials, giving inconsistent or no readings. These foreign media can be grinding media or beads, clay, grit, pebbles etc. Typically, the most problematic area is the first slurry tank for large particles and beads, especially when the inlet screen is faulty. Larger particles are removed by the sieve together with the carbon in the first tank but it's not possible to remove smaller particles which can also influence the measurements.

Scale forming on the C² Meter measurement probes was another factor influencing the readings. These coatings are mostly caused by lime and are easily removed through frequent cleaning with 3% HCl solution as part of routine maintenance.

Performance

A good correlation was found between manual carbon measurements and online C² Meter readings, with minimal variance as shown in Figure 3. It must be borne in mind that the manual method is influenced by factors such as position and depth of the sampling, type of sampler used as well as number of samples taken. In this comparison only one manual grab sample per time instance was used for comparison, which is not a true representation of overall carbon concentration in the tank due to the dynamic behaviour of the slurry and carbon caused by agitation and density differences.

Furthermore, the C² Meter readings obtained for the comparison were extracted from the mine's PI system. This reading is a filtered measurement covering a period of time whereas the manual sample is an instance in time.

There is also the influence of the manual density input into the analyser, as discussed earlier, which can also influence the C² Meter reading. Despite all these factors, a good correlation was observed between the manual and online readings, as shown in Figure 3.

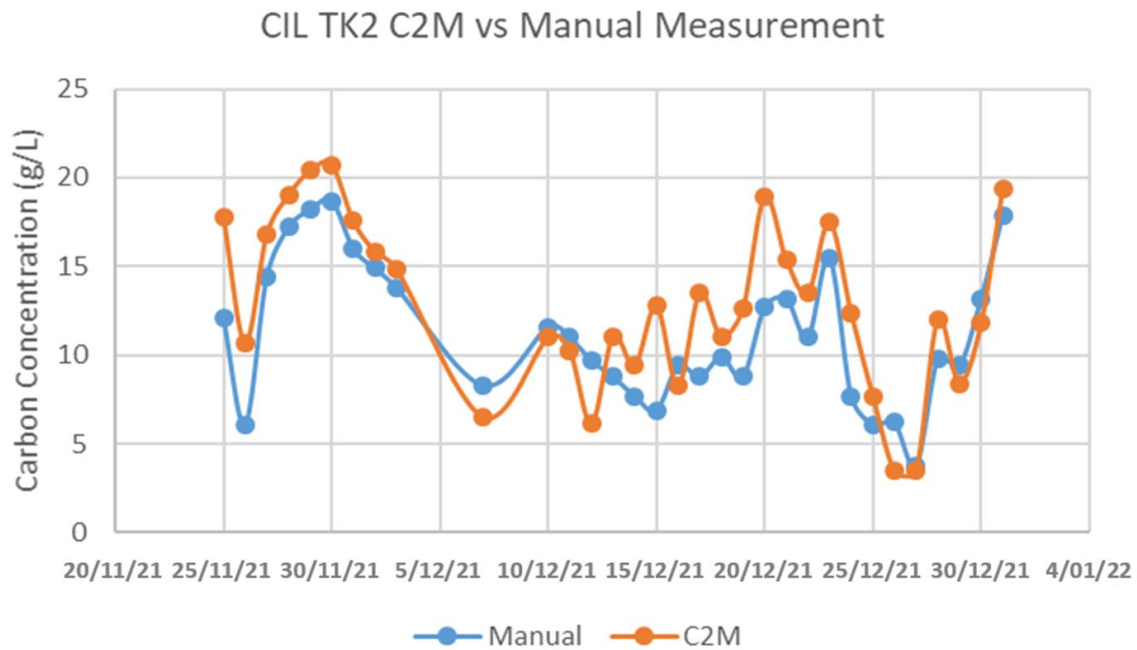


Figure 3: Carbon C2M vs Manual Measurements (g/L)

Carbon Forwarding Sequence Integration and Automation

The carbon forwarding sequence integration and automation followed the installation and commissioning of the C² Meters. Prior to the project, the carbon forwarding sequence was manually operated by control room operators through the Distributed Control System (DCS) user interface. Thus, integration of this existing manual control into automatic controls was a key driver behind optimising carbon management in the circuit. A switch was created in the control loop as a standby system to switch between manual and automatic in the event there were issues with the carbon forwarding pump(s) and/or the carbon meters. High and low carbon concentration limits, as well as a target setpoint for each tank were some of the inputs into the controller, which define the desired carbon profile through the circuit and when carbon forwarding pumps would switch on or off.

The carbon movement control philosophy introduced at Hidden Valley followed the modified push method described by Smit (2015). The main objective of this control philosophy is to move the carbon up the circuit in small increments rather than in one cycle. This essentially allows more time for carbon to be loaded with a higher concentration of gold and silver before being transferred to elution from CIL TK1.

The highest carbon concentration is maintained in the front-end tanks to ensure that adsorption of most of the dissolved gold and silver is happening concurrently with leaching. Higher concentrations

also ensure that there is sufficient carbon available in the front tanks for harvesting (Woollacott et al., 1990).

Since there was good carbon management in the CIL circuit and sufficient carbon as per target in CIL TK1 & CIL TK2 (carbon harvest tanks), the frequency of elution carbon stripping was maintained. Before the installation of C² Meters, budget elution strips were at 1.5 - 2.0 strips in a 24-hour period. However, with the installation of C² Meters elution carbon stripping went up to 3.0 - 4.0 x strips within 24-hours period which was double, and a great result achieved thus far.

RESULTS

Gold Solution losses

With the C² Meters installed and the carbon movement controller implemented, one of the most significant benefits from this project was the consistent overall improvement in gold recovery. This was achieved by reducing the gold-solution-losses through improved carbon-in-circuit management. The implementation of Mintek's carbon control philosophy along with the real-time carbon concentration readings from the C² Meters played an important part in achieving the benefits in reducing the gold in solution losses. This was through maintaining an effective and consistent carbon profile in the CIL circuit.

The data in Figure 4 shows that, starting from May 2021 the average gold in solution losses reduced from around 0.027 ppm with a standard deviation of 0.013 to around 0.016 ppm with standard deviation of 0.01, when comparing before and after installation. The changes helped to bring more consistency to the process and prevent periods when the gold in solution losses would spike above 0.03 ppm.

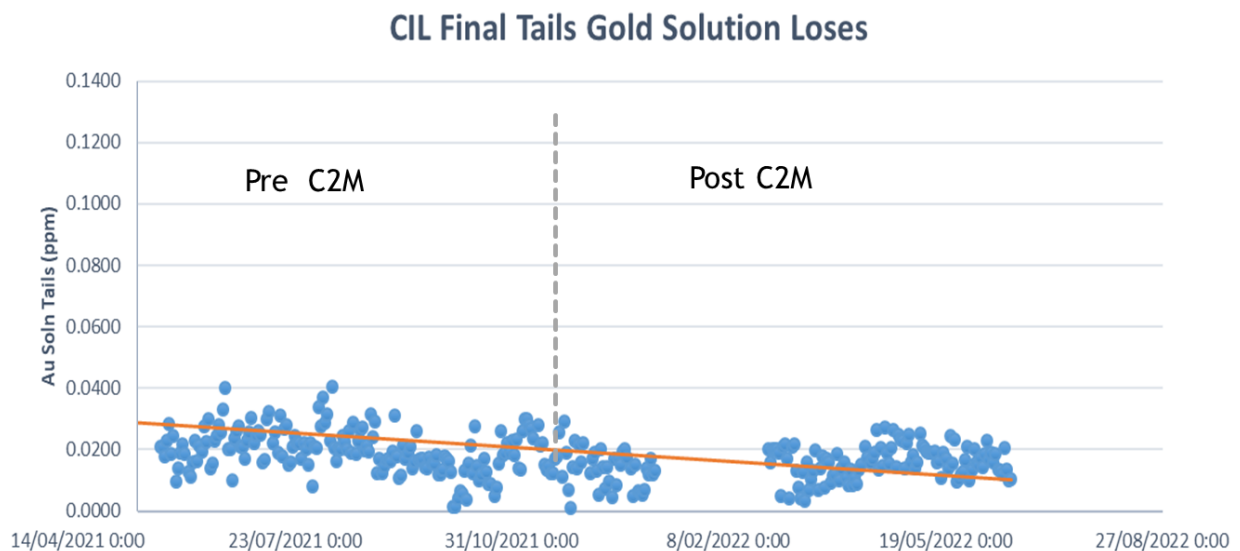


Figure 4: Overall gold-in-solution losses

Silver recovery

There was also a 5% improvement in the overall silver recovery. The graph in Figure 5 shows the average silver recovery before and after C² Meter installation.

It is expected that, through additional refinements in the carbon movement controller, solution gold losses in tailings could drop further to below 0.01 ppm for silver and 0.005 ppm for gold due to a more consistent process.

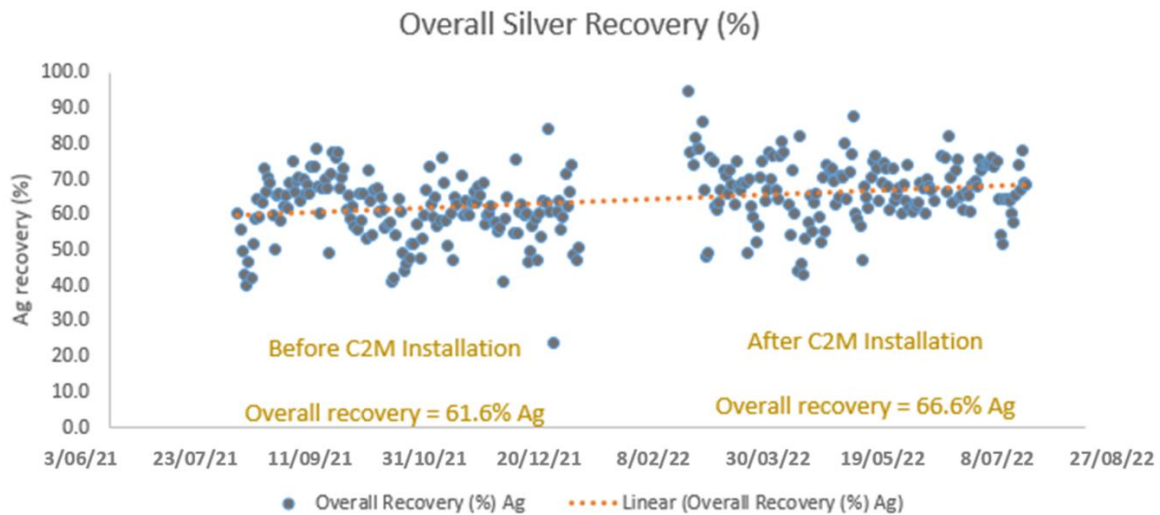


Figure 5: Overall silver recovery trends

New carbon addition rate

The new carbon addition rate as shown in Figure 6 was measured over a three-month period from March 22 to June 22 as part of the evaluation process. The addition rate dropped from around 0.45 kg/t to under 0.05 kg/t, which is equivalent to an 89% reduction.

It is most likely that the initially high carbon addition rate was due to unknowingly overloading the circuit with too much carbon. Knowing how much carbon is in the tanks as well as managing the carbon inventory throughout the circuit is essential for preventing carbon overcrowding in any given tank. Before the trial, the lack of frequent and reliable carbon inventory data often leads to carbon build up in the front end of the circuit with very little knowledge of what was happening in the back end.

The creation of carbon fines in a gold circuit is largely caused from attrition between carbon particles in the circuit. This problem is exacerbated when there are excessive amounts of carbon in any of the tanks. Attrition occurs mostly in the CIL/CIP tanks due to agitation, as well as during carbon regeneration. Attrition also occurs during carbon transfer, screening, and elution, described by Kale (2019). The generation of carbon fines leads to gold loss as fines contain a high concentration of gold, which escape the carbon screens and reports to the tailings.

Although not quantifiable, it is expected that using less carbon in the circuit reduced overcrowding and the amount of fines generated in the circuit, and are therefore also aiding in lower gold and silver losses.

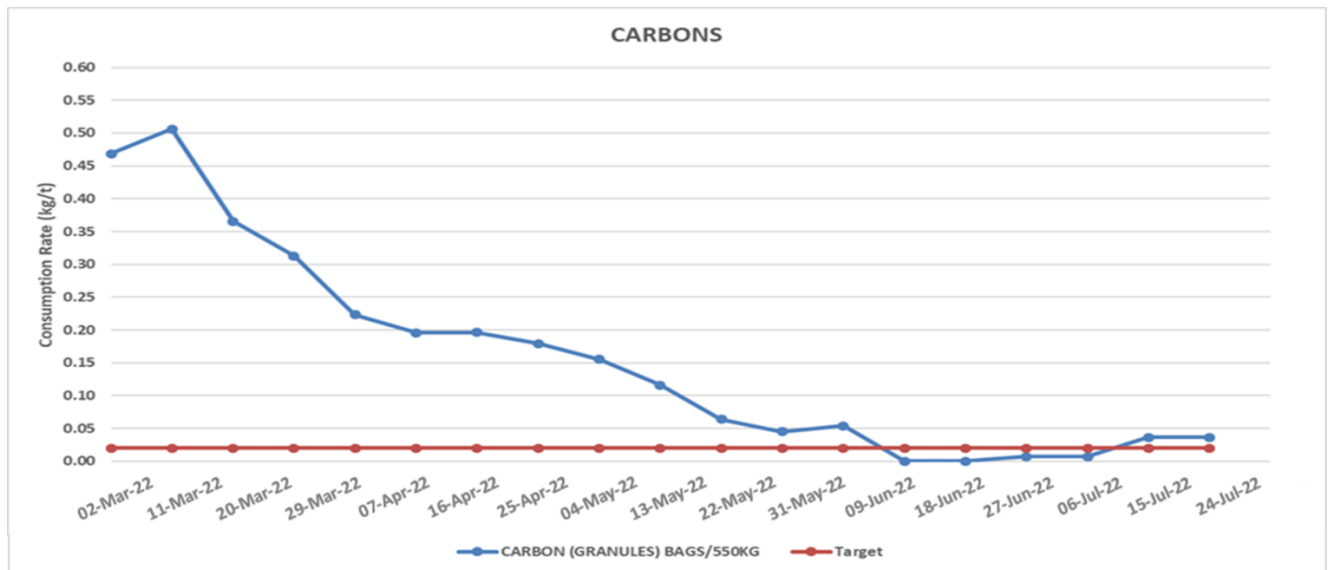


Figure 6: New Carbon Addition Rate (kg/t)

CONCLUSIONS

The project has delivered considerable benefits to the plant thus far, with significantly more gold and silver being recovered. The instruments are performing reliably and accurately. Some of the project highlights include:

- effective carbon management in CIL circuit
- consistent back-to-back stripping at elution circuit
- more efficient use of operators' time, both in the field and in the control room
- reduction in new carbon addition rate
- reduction in gold solution losses
- increase in silver recovery
- the project payback period was less than three weeks.

It was calculated that over a 12-month period, the estimated improvement to the bottom line due to reduced gold losses is around A\$5 000 000.

To ensure that the C² Meters continue to be reliable, they should be cleaned and calibrated every three months. Further improvements can be made to the measurements by providing the C² Meters with an online density reading.

ACKNOWLEDGEMENTS

The authors wish to acknowledge the continued support and encouragement given by work colleagues and the leadership team leading up to this paper. In particular, the author expresses gratitude to Michael Kretschmann, Joe Kikako, Imae Iofa and Adrian Paine from Molycop. Without their support and encouragement, the work would have not come this far.

REFERENCES

Kale, A, Study on attrition of carbon particles during regeneration of activated carbon, pp 196 (World Gold Conference 2019: Perth, Australia).

Steward, P, 2004. Insights from Simulation of a CIL/CIP Circuit, pp 439-440. (MetPlant Conference 2004: Perth, Australia).

Smit, HS, 2015. Carbon concentration measurement and control in a counter-current carbon adsorption circuit – update on recent installation at a Witwatersrand gold plant, pp 322 (World Gold Conference 2015: Johannesburg, South Africa)

Woollacott, LC, Stange, W and King, R.P, 1990. Towards more effective simulation of CIP and CIL processes. The modelling of adsorption and leaching. The South African Institute of Mining and Metallurgy, University of Witwatersrand, Transvaal. *Journal of the South African Institute of Mining and Metallurgy*, 90 (10): 275-276

Sequential t-testing in Plant Trials – A Faster Way to the Answer

T G Vizcarra¹, T J Napier-Munn², D Felipe³

1. Senior Process Specialist, JKTech Pty Ltd, 40 Isles Road Indooroopilly QLD Australia 4068, t.vizcarra@jktech.com.au
2. HonFAusIMM, Emeritus Professor, Julius Kruttschnitt Mineral Research Centre, 40 Isles Road Indooroopilly QLD Australia 4068, t.napier-munn@uq.edu.au
3. MAusIMM, Process Specialist, JKTech Pty Ltd, 40 Isles Road Indooroopilly QLD Australia 4068, d.felipe@jktech.com.au

ABSTRACT

It has long been established that the best way for a metallurgist to undertake a plant trial comparing two process conditions is to run the trial as a sequence of short duration pairs, each pair incorporating the 'on' and 'off' conditions in random order. The results are then analysed using a paired t-test. The number of pairs required, and therefore the duration of the trial, can be calculated from a formula which includes the expected difference in performance between the two conditions, the expected standard deviation of the data, and the choice of decision-making risks. This, however, sometimes leads to trials of long duration.

This paper proposes the use of a modified sequential paired t-test for mineral processing plant trials of this kind. The principles of such tests have been known for many years but for some reason are rarely applied. Rather than generating the number of paired results prescribed by the sample size formula and then carrying out the t-test, sequential testing involves inspecting the results after each data pair is acquired and terminating the trial when one of two pre-calculated boundaries has been reached, concluding either that an improvement has been achieved, or not.

The paper explains how to apply the method and demonstrates this in a number of real case studies. It is shown that in most cases this leads to a significant decrease in the number of pairs required to achieve a statistically robust decision, and thus a reduction in the duration and cost of the trial. It is therefore recommended that sequential paired t-testing be adopted in place of conventional paired t-testing in plant trials.

INTRODUCTION

Process improvement initiatives in mineral processing plants will typically culminate in some type of a plant trial, where the effect of the change (reagent, process control, equipment or technology, etc) is tested in a full-scale production environment. Most metallurgists will, at some point in their early careers, learn the hard way that these types of experiments are very different to their laboratory-based analogues, in that the prevailing conditions of the production plant are difficult to hold constant. Unlike laboratory experiments, in which process variables can be closely controlled, plant trials are subject to largely uncontrollable changes in variables such as throughput, ore mineralogy, and operator practice, leading to unplanned variations in daily concentrator performance during, and even prior to, the commencement of the trial.

Such variability will usually camouflage any real effects of a tested change, and in so doing exacerbate the risks of poor decision-making after the trial has ended. Given that implementing changes often entails increased costs, whether in higher OPEX, CAPEX (or both), one of the key objectives of plant trials is to mitigate the risks of proceeding with changes that not only are potentially expensive but could also lead to no benefit or could perhaps even be detrimental to overall performance. The problem confronting production metallurgists is that, if a change has the potential to improve circuit performance by (say) 2% - a magnitude typical of optimisation efforts and often worth millions of dollars per year in extra metal production – how can one know whether or not the tested change has 'worked', especially when the range of day-to-day concentrator

performance can be in the order of 10-20%, as in Figure ?

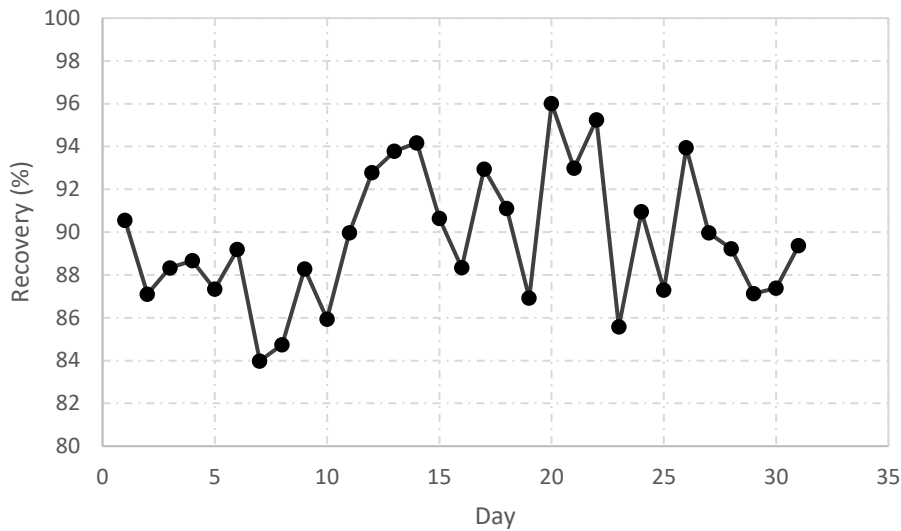


Figure 1 – Typical example of highly variable concentrator metal recovery data.

The answer, perhaps surprisingly, is ‘easily’, with the correct experimental design, followed by analysis using robust statistical methodologies. There are a range of experimental designs to choose from, depending on the context and the objectives of the experiment, with some discussed in detail in Napier-Munn (1995) and Napier-Munn (2014), as well as in a range of case studies in the mineral processing literature (Long et al., 2012; Napier-Munn and Meyer, 1999; Napier-Munn, 2008; Seaman et al., 2012; Vizcarra et al., 2018). Common to these experiments is in the ability of the ensuing analysis to disentangle the effect of the trial variable(s) from the effect of interfering variables and background experimental error (‘noise’). Such experiments circumvent the problems of uncontrollable production variables swamping the effect of the trial variable. However, a key requirement is adherence to the statistical criteria underlying the experimental designs.

For the common case of comparing two conditions (eg. new vs. old reagent, equipment ON vs. equipment OFF), the best type of experiment is the *paired trial*. This type of experimental design has become ubiquitous in mineral processing, as the resulting data is compatible with the paired t-test, a simple yet powerful analytical procedure that can detect small differences in seemingly overwhelming noise. However, the design of an appropriate paired trial can sometimes prescribe durations that are quite long (e.g. months in cases where the expected benefit of the change is small or the experimental error is large). This paper discusses an adaptation of the paired trial, called sequential testing, which has shown promise in reducing the required duration of paired experiments. An overview of the conventional paired trial and t-test is given and compared to the sequential approach. Case studies are described to illustrate its application in mineral processing, showing that experimenters can reach conclusions faster, and with the same level of risk mitigation as that provided by conventional t-testing.

REVIEW OF PAIRED TRIALS

The requirements of the paired t-test dictate the manner in which its input data is generated in the first place. The paired t-test interrogates *differences* within pairs, which are otherwise comparable in the sense that apart from the trial variable, all other variables are held nominally ‘constant’. In a mineral processing context, almost everything changes dynamically over time, and nothing is ever ‘constant’. However, adjacent time-periods always have the best chance of being similar, and

therefore comparable, given a sufficient trial length (number of pairs).

In a practical sense, this means that comparisons can take place between shift results from (for instance) Monday and Tuesday. This is because ore type, throughput, circuit conditions etc. are most likely to be ‘similar’ within this confined time-block. By the same reasoning, comparisons are not undertaken between shift results from Monday and the following Friday, as they are too far apart in time to warrant a fair comparison.

In the context of (say) reagent testing, if the baseline reagent is tested on Monday, the trial reagent would then be tested on Tuesday, and the difference in recovery within this pair of days is what would be subjected to the paired t-test.

It should be recognised that interfering variabilities and uncontrolled changes *within a given time-block* may still camouflage the effect of the trial condition. The approach to overcome this is to undertake the switch between baseline and trial conditions a sufficient number of times so that the effect of the trial can be observed through these variabilities. This is equivalent to generating a sufficiently large sample size (a concept most metallurgists would be familiar with) so that the statistics of the resulting dataset is reliable, and representative of the notional underlying population. Another requirement is the need to ensure that within each time-block, the order of the baseline vs. trial variable is random, as a further guard against any systematic biases that may take place in the background over time. These concepts are illustrated in Figure 2, which shows the first 5 time-blocks (pairs) of data in an example paired trial. The order within each pair can be determined by tossing a coin.

Time-block	1		2		3		4		5	
Day	Mon	Tue	Wed	Thu	Fri	Sat	Sun	Mon	Tue	Wed
Condition	Baseline	Trial	Baseline	Trial	Trial	Baseline	Trial	Baseline	Baseline	Trial

Figure 2 – Structure of example paired trial, with randomisation of the condition in each time-block.

The final step in designing a paired trial is then to determine the size of the dataset that is needed, and therefore the total duration of the trial. This is discussed in the next section.

SAMPLE SIZE FORMULA – NUMBER OF PAIRS REQUIRED

One of the major objectives of any trial is to minimise the risks of arriving at an incorrect conclusion, and to do so with the minimum amount of data that is necessary to collect. In paired trials, the decision will be whether to accept the new condition (e.g. purchase and commission the new equipment for on-going production) or whether to revert to baseline conditions if the new condition has been deemed ineffective or uneconomic to implement long-term. The risks that the business will need to protect itself against in this context are expressed as probabilities, and are twofold:

- the risk of concluding that the trial condition leads to an improvement, when it does not (designated as α)
- the risk of concluding that the trial condition does not lead to an improvement, when in fact it does (designated as β), a lost opportunity.

In statistical parlance these are respectively termed ‘type 1’ and ‘type 2’ errors, also referred to colloquially as ‘false positives’ and ‘false negatives’. The sample size, and so the duration of the trial, is partly determined by the level of risk which one is willing to accept for each. A typical threshold is less than 5% (i.e. to ensure at least 95% confidence in a result) though this is arbitrary and can otherwise be selected depending on the consequences of being wrong in either case. These concepts underlie the sample size formula for a paired t-test (Cochran and Cox, 1966):

$$n = \frac{(z_{\alpha} + z_{\beta})^2 s^2}{D^2} \left(\frac{f + 3}{f + 1} \right) \quad (1)$$

where:

n = number of pairs required

z_{α} = normal deviate at a confidence level of α (e.g., 1.96 for a common choice of 95%)

z_{β} = normal deviate at a confidence level of β

s = expected standard deviation of paired differences

D = desired difference to detect

$f = n_{\text{approx}} - 1$, where $n_{\text{approx}} = (z_{\alpha} + z_{\beta})^2 s^2 / D^2$.

The variable D is a professional decision, frequently the minimum improvement of interest (e.g. the minimum change in recovery that would justify long-term implementation of the new reagent or equipment being tested). Key also is the expected standard deviation, s , which represents the prevailing variability in the process which the trial must overcome. This is usually estimated from historical plant data. If the noise in the system is large, then larger sample sizes are required to give the t-test sufficient power to detect differences which may otherwise be camouflaged in this noise. This is illustrated in Figure 3 which shows the number of required pairs at different ratios of D/s .

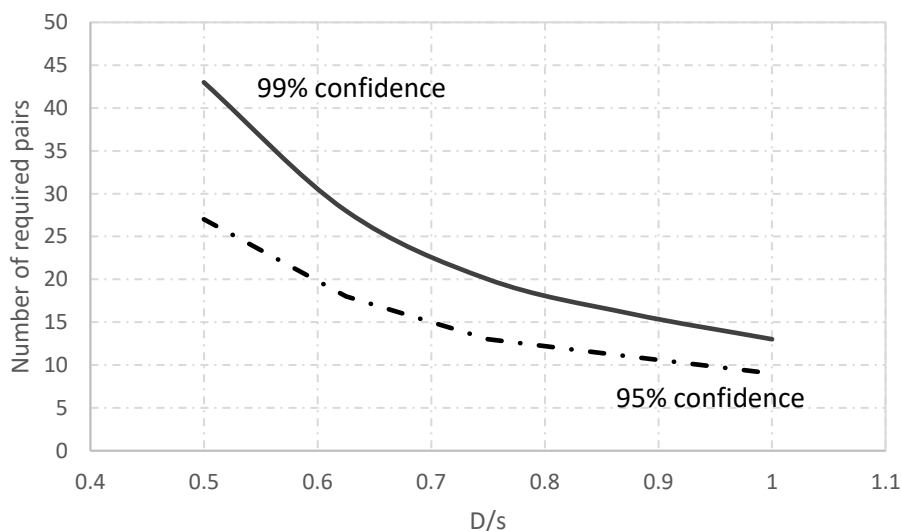


Figure 3 – Number of pairs required for different D/s ratios at 99% and 95% confidence levels (one-sided test, $\beta = 0.2$ for both trends).

If the difference is the same magnitude as the noise ($D/s = 1$) then the required sample size is between ~10-15, depending on the level of confidence desired. However, as the noise becomes progressively larger and D/s diminishes, the required sample size increases significantly. At $D/s = 0.5$ (common in mineral processing trials), 27 pairs are required for a 95% level of confidence (i.e., constraining the risk of a false positive to 5%). Assuming that the baseline vs. trial condition switches on a daily basis, this equates to a trial duration of almost 2 months. If 99% confidence is required

(which might be necessary in cases where the risk of a false positive has severe consequences, such as in equipment trials where CAPEX is at stake), this demands 43 pairs, or a trial length of almost 3 months. It should be highlighted that the trends in Figure 3 are for a relatively relaxed β risk (the risk of a ‘missed opportunity’) of 20%. If there is a desire to minimise the chance of the trial failing to detect a real difference which might indeed be lurking in the variability of the data, this would entail even larger sample sizes and correspondingly longer trials.

Note that the full number of pairs must be generated before the t-test is applied. Some experimenters will undertake the t-test after each pair is complete and stop the test if and when a significant difference emerges. This is not a valid practice and is not a sequential test as described in this paper. Sufficient tests must be completed to give time for the result to emerge, whether positive or negative. A significant improvement as determined by the t-test may well manifest itself before the designated number of tests is completed. However it is possible for that improvement to disappear again as the trial proceeds to the end point as determined by Equation (1), and so the trial should not be considered complete until the requisite number of pairs has been accumulated.

REVIEW OF THE PAIRED T-TEST

The power of the paired t-test arises from its analysis of differences within data pairs, rather than the native data itself. For data which are correlated in time (often the case for mineral processing data), the standard deviation of these differences is frequently less than that of the original data, giving the paired t-test a greater ability to detect changes in highly variable datasets. Hypothesis testing with the paired t-test is discussed in detail in Napier-Munn (2014), but at a high level the approach involves:

- comparing the magnitude of the change against the experimental variability, represented by the statistic, t . The larger this number, the greater the difference compared to experimental error, and the more evidence there is of a real change in circuit performance
- benchmarking the experimental t-statistic against the null hypothesis distribution (H_0) which assumes that there is no difference between the baseline and trial conditions
- if t is ‘similar’ to the H_0 distribution, then H_0 is accepted, and the conclusion is that there is insufficient evidence for the efficacy of the trial condition; experimenters are forced to conclude that there is no difference in the absence of data to show otherwise
- if t is significantly ‘different’ to the H_0 distribution, then H_0 is rejected and the alternative hypothesis (H_1) is accepted, with the conclusion being that the trial condition leads to a real change.

These concepts are illustrated in Figure 4 which shows the H_0 distribution centred on a mean difference of 0 (i.e.. the change between baseline and trial conditions if H_0 was true), and two experimental t-values. One of these aligns closely with the H_0 peak and represents a case where the difference between baseline and trial conditions is not significantly different; the conclusion would be that the trial has not resulted in any change to circuit performance.

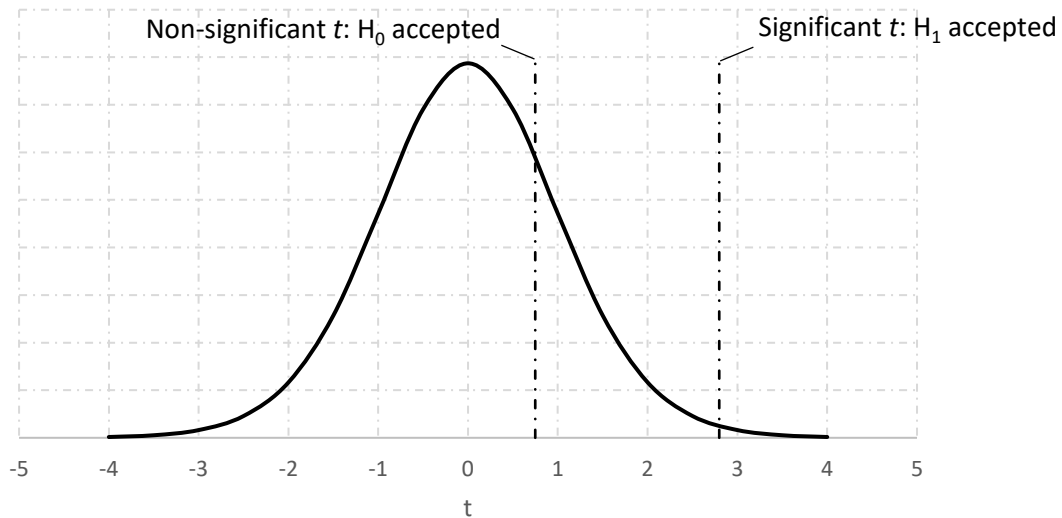


Figure 4 - Null hypothesis testing with the t-statistic.

The second of these lies much further away from the H_0 peak, representing a scenario where the experimental difference between baseline and trial conditions is large relative to experimental variability. For a one-sided test (often the case with plant trials) the area under the histogram ('P-value') to the right of each line represents the risk of a type 1 error (i.e.. a 'false positive'). For the left line, it is 23%, while for the right line, it is 0.6%.

Thus, in the second case the probability of this experimental result occurring under conditions where H_0 is true is so small, that H_0 must be rejected and H_1 accepted; that is, the conclusion is that the trial condition leads to a real change to circuit performance and is not simply an artefact of experimental error. As previously discussed, it is common to conclude that a real change has occurred if the type 1 error (P-value) has been reduced to less than 5%, providing at least 95% confidence that a change has indeed occurred.

The approach for undertaking a paired trial is therefore to:

1. use Equation () to determine the total length of the trial
2. randomise the order of the baseline vs. trial condition within each time-block
3. execute the trial as per the prescribed design
4. use the paired t-test to analyse the results
5. implement the change if H_1 is accepted, or revert to the status quo if H_0 is accepted, depending on the calculated value of P.

There is often a temptation to terminate the trial as soon as a P-value less than the chosen α has been reached. However, implicit in the described approach is that the sample size is sufficiently large for the P-value to have meaning (i.e.. that Equation () has been adhered to). This is a key difference between traditional t-testing and sequential t-testing, in which trials may be terminated early if prescribed by the results of the sequential analysis. This is discussed in the next section.

SEQUENTIAL T-TESTING

Sequential testing is not a new concept; it was developed in the 1940s as part of wartime efforts to improve Allied industrial productivity (Box et al., 1956; Wald, 1947). It initially found application in manufacturing but has since been applied to other disciplines such as forestry (Fowler and O'Regan, 1974), psychology (Schnuerch and Erdfelder, 2020), and clinical monitoring (Bartholomay, 1957; Spiegelhalter et al., 2003).

Sequential testing involves analysing trial data as each new pair is generated using further considerations of the alternative hypothesis. As demonstrated in this section, this often leads to a shorter trial. In sequential testing, t is compared not just against the H_0 distribution (as in Figure 4), but also a notional H_1 distribution, discussed in Cumming (2006). The heights of each distribution at the experimental t -value are used to generate a likelihood ratio (LR), which is the key metric in the sequential test. This is illustrated in Figure 5, where the likelihood ratio for this experimental result is defined as $0.244 / 0.013 = 18.8$.

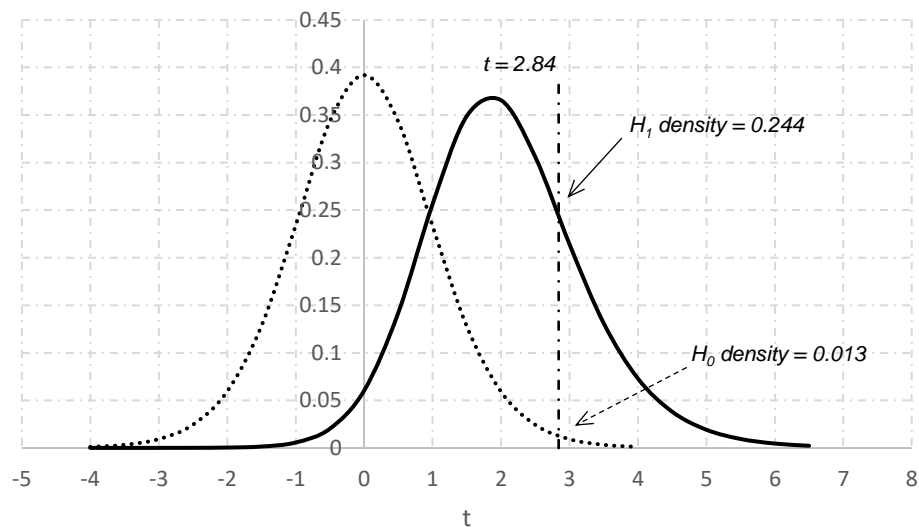


Figure 5 – Example H_0 and H_1 distributions compared with experimental $t = 2.84$.

The LR is plotted after the generation of each paired result. When the trend crosses either an upper or lower boundary (defined by $(1 - \beta)/\alpha$ and $\beta/(1 - \alpha)$ respectively), signifying regions where either H_1 or H_0 should be accepted, then the trial can be terminated. If the LR trend is within the boundaries, the trial remains inconclusive and must continue. The example in Figure 6 shows the sequential LRs during an ON/OFF trial of a flash flotation cell in a Pb/Zn concentrator. For $\alpha = 0.05$, $\beta = 0.2$ and $D/s = 0.5$, the test could have terminated after 14 pairs with H_1 accepted. This compares to $n = 27$ calculated by the classical sample size formula in Equation (), a ~50% reduction in required sample size. The mean recovery improvement was $1.4 \pm 1.1\%$ (95% confidence interval), shown in Figure 6b with the vertical reference line at 0% to illustrate the type 1 error risk ($P = 0.007$).

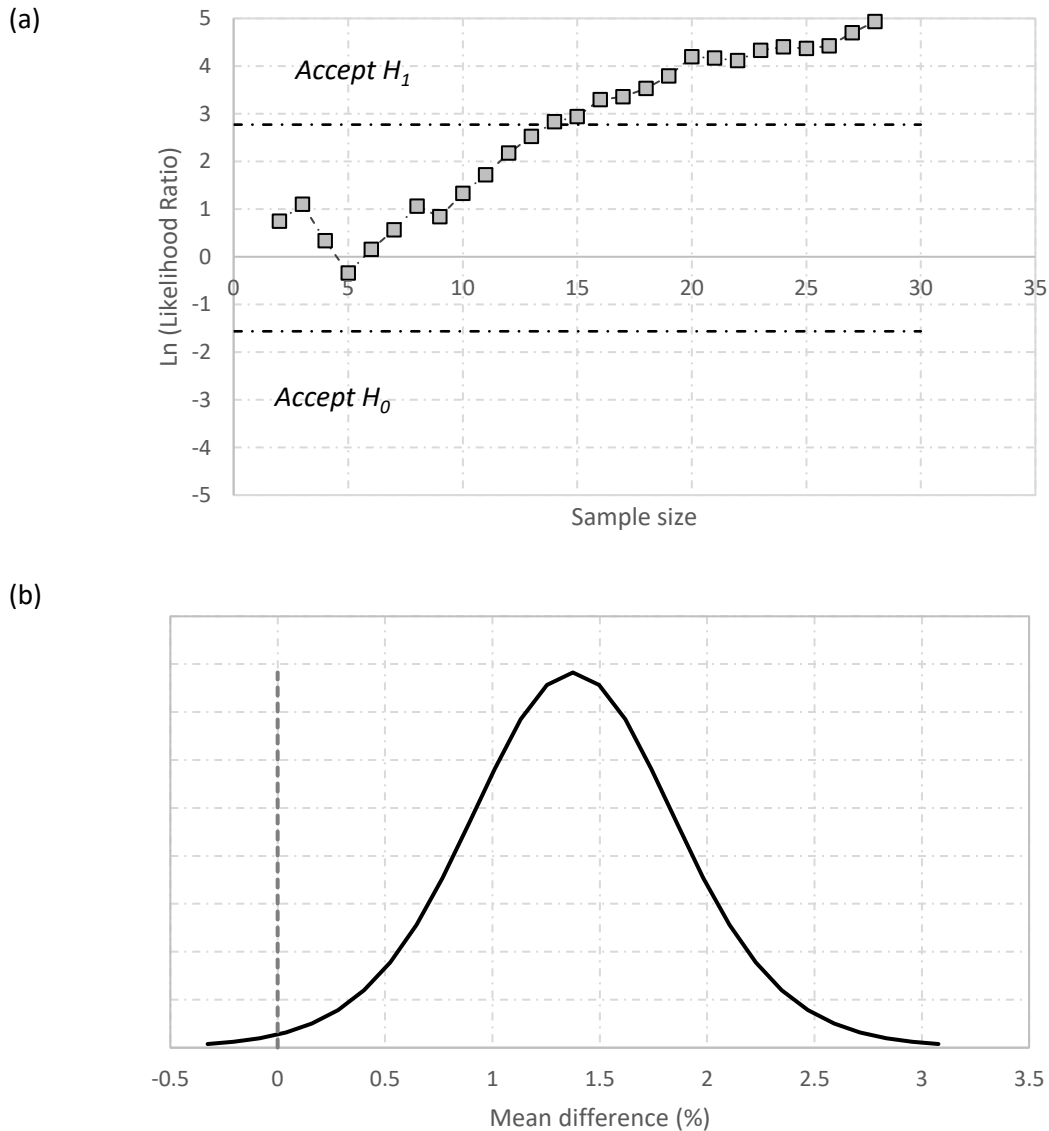


Figure 6(a) – Example sequential test results ($\alpha = 0.05$, $\beta = 0.2$ and $D/s = 0.5$) of a flash flotation cell trial; (b) mean recovery improvement (reference line = 0%).

A similar result was obtained for the trial of a flotation magnetic conditioning device, where for $\alpha = 0.05$, $\beta = 0.2$ and $D/s = 0.5$, the test could have terminated after 14 pairs with H_1 accepted. Again, for these inputs, Equation () prescribes that 27 pairs must otherwise be used in the paired t-test for adequate control of type 1 and 2 errors. The mean recovery improvement was $4.9 \pm 3.8\%$ (95% confidence), shown in Figure 7b ($P = 0.007$).

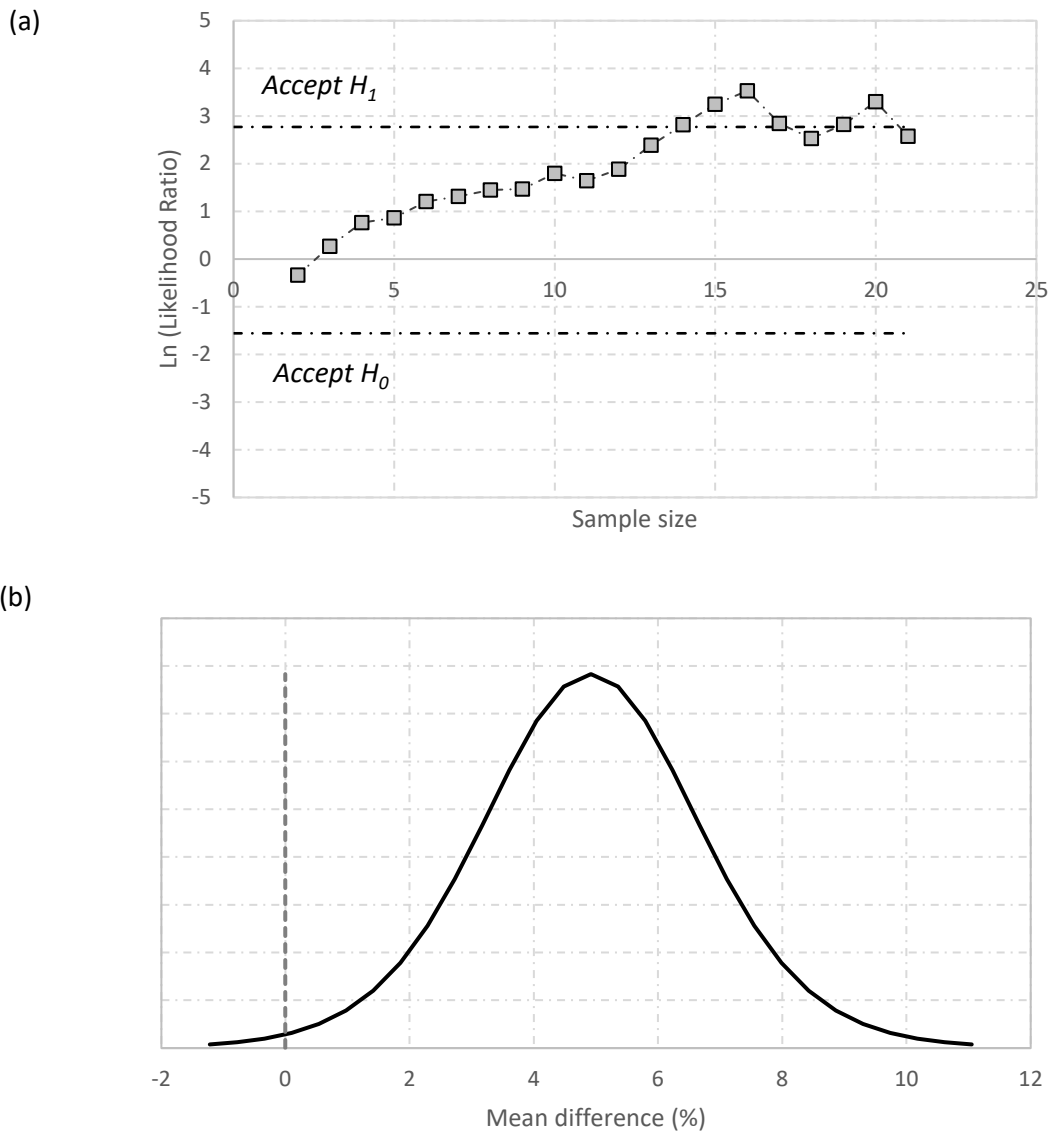


Figure 7 - Example sequential test results ($\alpha = 0.05$, $\beta = 0.2$ and $D/s = 0.5$) from a trial of a flotation magnetic conditioning device; (b) mean recovery improvement (reference line = 0%).

Figure 8 shows results from a gold flotation reagent trial in which Equation () prescribed 157 pairs - a 10-month trial using daily ON/OFF pairs. This long duration was a result of the historical variability in plant recovery (and indicated that the trial probably should not have been undertaken in the first place). The expected benefit in gold recovery was 2% as determined from laboratory testing. However, it was clear that this benefit vanished when the reagent was trialed in the plant. The sequential results indicated that the test could have been terminated after 48 pairs (approximately 3 months), with the conclusion that the new reagent should not be implemented. This is reinforced in Figure 8b, which shows the experimental mean recovery difference distribution closely aligning with the 0% reference line. In this case, as the sequential test decision lines were constructed with $\beta = 0.2$, the risk of a type 2 error (the opportunity cost of concluding there is no improvement whereas in fact there is such an improvement) was 20%. That risk can be reduced of course, to give the test a better chance of detecting any real differences that may be lurking in the data, but at the cost of a longer trial.

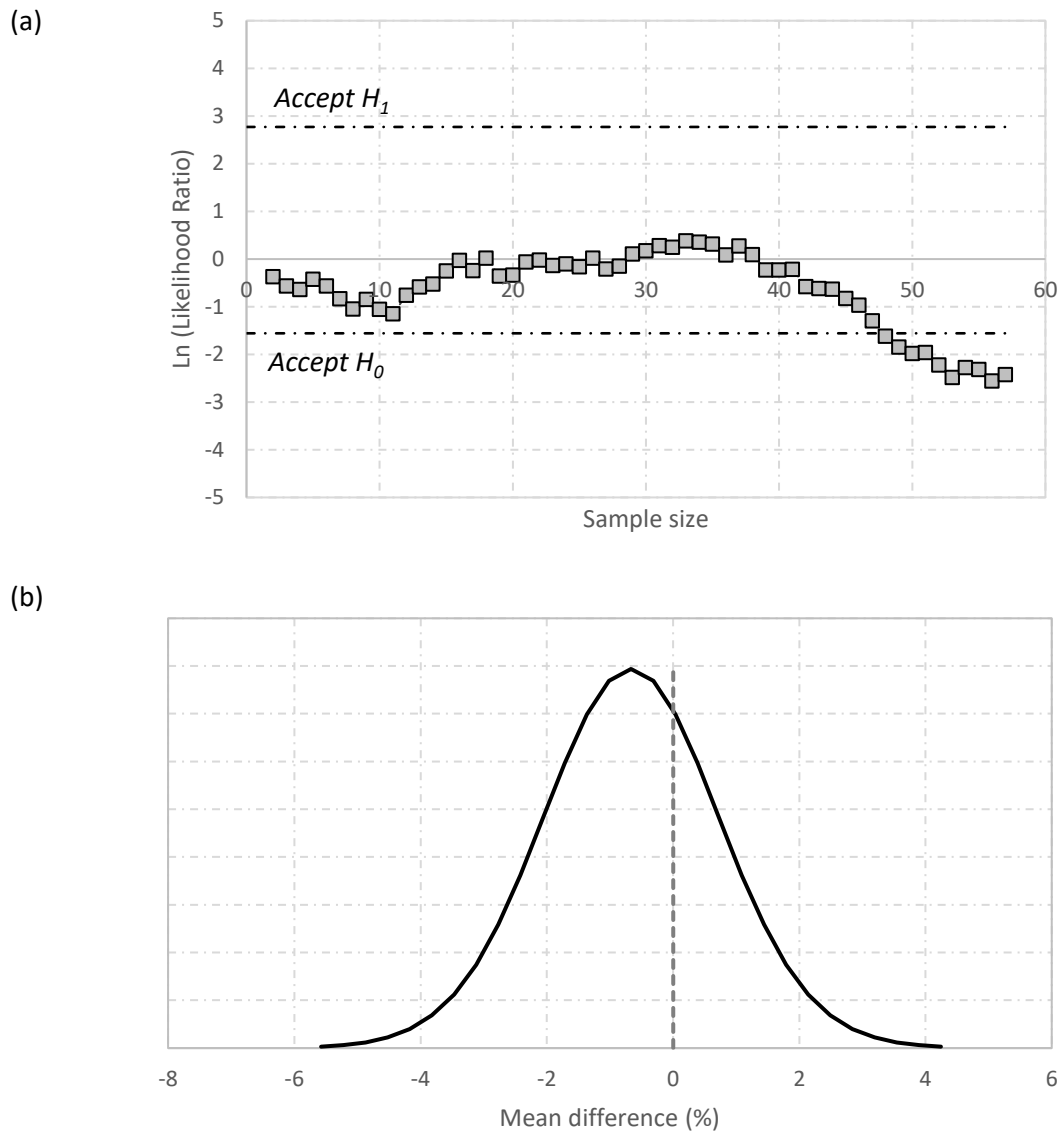


Figure 8 – Example sequential test results ($\alpha = 0.05$, $\beta = 0.2$ and $D/s = 0.2$) from a gold collector trial; (b) mean recovery improvement (reference line = 0%).

While these ad-hoc use cases were encouraging, a more comprehensive validation of the sequential test was undertaken by generating synthetic baseline and trial recoveries each of known mean, standard deviation, and correlation between successive days (to simulate similar time-based correlations in actual plant data which are harnessed by the paired t-test). The sequential test routine was executed until a conclusion (either correct or incorrect) was reached, and the results stored. This routine was then iterated and repeated 1000 times, so that the distribution of sample sizes of the 1000 synthetic trials could then be compared to the sample size formula.

An example is shown in Figure 9, for a known recovery difference of 2% between synthetic baseline and trial populations, and a standard deviation of differences = 4%. Type 1 and 2 errors were controlled to 5% each. Equation () prescribed that 46 pairs were required to control to these risks, but of the 1000 simulated sequential tests, the vast majority (87%) required smaller samples to reach a conclusion, typically between ~15-30 pairs. Of the 1000 simulated trials, the sequential test made an incorrect conclusion (i.e.. failing to detect a real difference that was indeed there) in 3% of cases. This aligned closely with the defined tolerance for the type 2 error ($\beta = 5\%$).

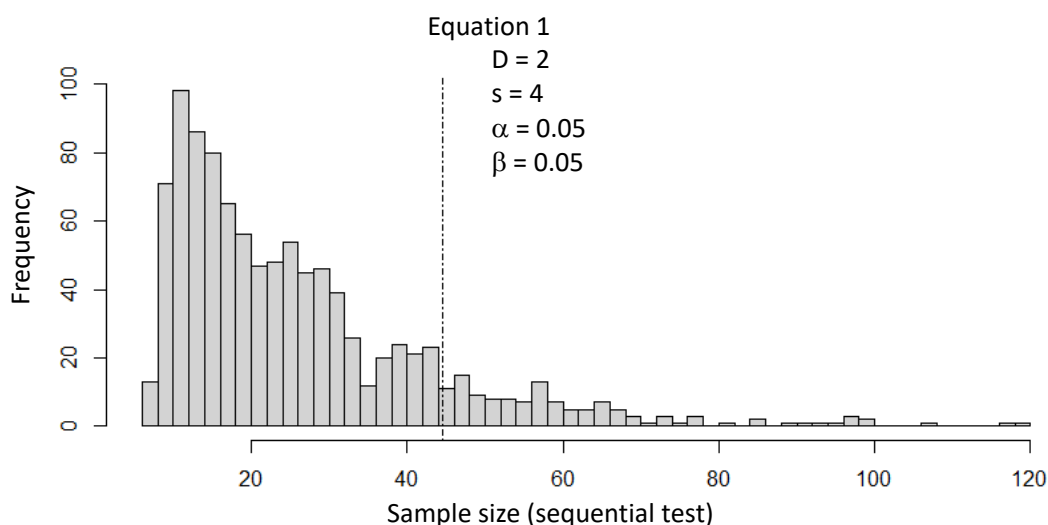


Figure 9 – Distribution of sequential test sample sizes for a validation test case. The sample size formula prescribed $n = 46$, shown with the vertical reference line. The mean and median sample sizes were $n = 27$ and 22 , respectively. The parameters shown were used both in Equation (1) and the execution of the 1000 simulated sequential t-tests.

Though not reported here, similar results were obtained in test cases of various combinations of mean differences, standard deviations, α and β values. Sample size reductions of this magnitude (up to 75%) have also been reported elsewhere (Schnuerch and Erdfelder, 2020). It is now recommended that sequential testing be used as a preferred method for paired-trial analysis as it can control the risk of incorrect conclusions with the same efficacy as traditional paired t-testing, and mostly in significantly reduced timeframes.

There are instances, illustrated in Figure 9, where the sample size can exceed that prescribed by Equation (). However, in practice, the trial can be stopped at the limit prescribed by Equation () and the results then analysed with traditional paired t-testing. Equation () can thus be used to determine the maximum expected length of the trial, with subsequent planning (and expectation-management amongst site stakeholders) based upon that duration. Once the trial proceeds, the results can be analysed daily using the sequential methods described in this paper, and terminated once a conclusion is reached. In most instances, this would be prior to the sample size prescribed by Equation (1).

CONCLUSIONS AND RECOMMENDATIONS

Sequential t-testing is a powerful technique to control the risks of type 1 and 2 errors with the same efficacy as the conventional paired t-test, while concurrently reducing the required sample size to do this compared to the traditional sample size formula. In practice, it is recommended that:

1. the traditional sample size formula is used to dictate the maximum length of a plant trial
2. baseline vs. trial conditions are applied to the plant in a randomised order, as they would be for a traditional paired trial
3. sequential analysis as described in the paper is used to analyse the results after each time period (e.g., shift or day)
4. the trial concludes once the sequential analysis terminates, or the trial duration has reached that prescribed by the sample size formula if the sequential analysis has not yet terminated by then. Results can then be analysed with a traditional paired t-test
5. all the relevant statistics are quoted when reporting the result: the 'effect' (magnitude of

mean difference), the confidence intervals on the effect (including a lower confidence interval or worst-case value where a process improvement is being sought), and the confidence with which one or other hypotheses can be accepted or rejected.

Sequential testing can be undertaken in the freely available software package *R* using the *sprtt* add-in (Steinhilber, 2021) available from (<https://cran.r-project.org/web/packages/sprtt/index.html>).

ACKNOWLEDGEMENTS

Meike Steinhilber (now at the University of Mainz) is thanked for useful discussions on the topic.

REFERENCES

- Bartholomay, A.F., The sequential probability ratio test applied clinical experiments. The New England Journal of Medicine, 1957, **256(11)**, 498-505.
- Box, G.E.P., Connor, L.R., Cousins, W.R., Davies, O.L., Himsworth, F.R., Sillitto, G.P., *The design and analysis of industrial experiments*. 1956, Oliver and Boyd, London.
- Cochran, W.G., Cox, G.M., *Experimental designs*. 2nd edn. 1966, John Wiley & Sons.
- Cumming, G., 2006. How the noncentral t distribution got its hump, In *7th International Conference on Teaching Statistics*. International Association for Statistical Education (IASE) and International Statistical Institute (ISI), Salvador, Brazil.
- Fowler, G.W., O'Regan, W.G., 1974. One-sided truncated sequential t-test: application to natural resource sampling, Pacific Southwest Forest and Range Experiment Station, Forest Service, U.S. Department of Agriculture.
- Long, G., Taylor, S., Lumsden, B., 2012. Statistical Plant Trials – Efficiently Combining Concentrate Grade and Metal Recovery Results, In *11th Mill Operators Conference*. Australian Institute of Mining and Metallurgy.
- Napier-Munn, T.J., Detecting performance improvements in trials with time-varying mineral processes – Three case studies. *Minerals Engineering*, 1995, **8(8)**, 843-858.
- Napier-Munn, T.J., *Statistical Methods for Mineral Engineers: How to Design Experiments and Analyse Data*. 2014, Julius Kruttschnitt Mineral Research Centre.
- Napier-Munn, T.J., Meyer, D.H., A modified paired t-test for the analysis of plant trials with data autocorrelated in time. *Minerals Engineering*, 1999, **12(9)**, 1093-1100.
- Napier-Munn, T.J., 2008. Some practical problems in running statistically valid plant trials, and their solution, In *MetPlant*. Australasian Institute of Mining and Metallurgy, Perth.
- Schnuerch, M., Erdfelder, E., Controlling Decision Errors With Minimal Costs: The Sequential Probability Ratio t Test. *Psychological Methods*, 2020, **25(2)**, 206-226.
- Seaman, D.R., Lauten, R.A., Kluck, G., Stoitis, N., 2012. Usage of Anionic Dispersants to Reduce the Impact of Clay Particles in Flotation of Copper and Gold at the Telfer Mine, In *11th Mill Operators Conference*. AusIMM, Hobart.

Spiegelhalter, D., Grigg, O., Kinsman, R., Treasure, T., Risk-adjusted sequential probability ratio tests: application to Bristol, Shipman and adult cardiac surgery. *International Journal for Quality in Health Care*, 2003, **15(1)**, 7-13.

Steinilber, M., 2021. sprtt: An R Package for Sequential Probability Ratio Tests Using the Associated t-Statistic. Heidelberg-University.

Vizcarra, T.G., Hart, M.G., Karbowiak, A.T., Napier-Munn, T.J., 2018. Getting the most from existing processes: using cleverly designed experiments to optimise the line 3 AG mill at Boyne Smelters Limited, In *14th AusIMM Mill Operators' Conference*. Australasian Institute of Mining and Metallurgy, Brisbane.

Wald, A., *Sequential analysis*. 1947, John Wiley, Oxford, England.

Representative Measurement Using PGNAA to Digitalise Conveyed Ore Flow Quality

H Kurth¹, A Brodie², and Y Strutz³

1. Chief Marketing Officer & Minerals Consultant, Scantech International Pty Ltd, 143 Mooringe Avenue, Camden Park SA 5038, h.kurth@scantech.com.au
2. General Manager Marketing, Scantech International Pty Ltd, 143 Mooringe Avenue, Camden Park SA 5038, a.brodie@scantech.com.au
3. Technical Manager, Scantech International Pty Ltd, 143 Mooringe Avenue, Camden Park SA 5038, y.strutz@scantech.com.au

ABSTRACT

Average ore grades for most commodities are declining and processing costs are increasing. Mining companies look to technologies for improved sustainability: reducing energy, water, and reagent consumption, tailings generation and Green House Gas (GHG) emissions. There has been little focus on the main asset: the orebody. Ore quality variability affects metal recoveries by up to 10 - 15%. Measurement is required in order to manage ore quality effectively. Major mining companies have recently begun to see value in sensing ore quality in real time to better understand its implications and assess potential benefits. Real time measurement to digitise conveyed flow quality using proven technologies has been implemented with minimal risk.

High performance Prompt Gamma Neutron Activation Analysis (PGNAA) has been used successfully in the minerals sector for over twenty years for representative, continuous, real time multi-elemental measurement of conveyed flows in over a dozen commodities. The technique is suitable for primary crushed rock and is unaffected by particle size, belt speed, mineralogy, dust, layering and moisture content.

Recent developments include direct measurement of gold in conveyed ore using GEOSCAN-GOLD. Measurement times have reduced with smaller parcels being measured at good precision allowing decisions to be taken with a high degree of confidence. The technology has been successfully applied in bulk ore sorting where increases in ore grade have been recorded and 5 to 20% of the mined ore is rejected as waste. The diverted coarse waste has saved up to 20% of GHG emissions in comminution, mainly due to elimination of milling, with only minor metal losses.

The paper presents multi-elemental data's utility in improving ore blending, diverting waste from plant feed, enabling feed-forward control for process operators, and facilitating ore reconciliation and metal accounting. It showcases successful installations with gold, copper, and iron ore examples and discusses risk reduction strategies for assessing and implementing this technology.

INTRODUCTION

Global demand for critical metals and minerals is increasing as technologies used in decarbonisation rely on larger quantities of embedded metals and have more frequent replacement requirements (e.g., wind turbines, solar panels, and batteries). This approach requires high levels of resource inputs that may not be fully recyclable and hence causes additional consumption of metals and minerals at higher demand levels than previously required.

Existing higher-grade resources are being depleted and lower grade resources are being mined but these require much larger throughput rates to achieve economies of scale at acceptable financial returns. Throughput rates eventually plateau as maintenance and operating costs rise disproportionately to product revenues. An alternative to mining and processing larger tonnages at lower quality is to apply technologies that assist with pre-concentration.

Improving process feed quality has many benefits as diverted material that is uneconomic to process may be discarded as coarse waste and a proportion of this may be segregated as clean waste that has additional value for other uses, such as for aggregate or for civil earthworks applications by the mining company or nearby communities. Measurement technologies are needed to determine the value of small parcels of mined material so that segregation can occur before further cost and resources are expended on the material. Comminution is a large component of processing cost and consumes significant energy, media and water. Avoiding unnecessary comminution and downstream processing becomes a financially beneficial outcome for material that generates little if any product value. Savings in resources include water, power, reagents and equipment wear and tear (maintenance cost). Any material not processed also avoids the generation of GHG and fine tailings. This may extend a tailings dam life and postpone planned costs creating a saving for the operation. The paper discusses the various benefits available and how these have been quantified in different commodities.

MEASUREMENT TECHNOLOGY

Real time measurement to digitise conveyed flow quality using proven technologies has been implemented at many sites. High confidence in decisions on material quality can be made when there is high confidence in the performance of a measurement technology. Ideally measurement should be representative, precise and timely to maximise potential benefits. High performance Prompt Gamma Neutron Activation Analysis (PGNAA) has been used successfully in the minerals sector for over twenty years for representative, continuous, real time multi-elemental measurement of conveyed flows in over a dozen commodities. The technique is suitable for primary crushed rock and unaffected by particle size, belt speed, mineralogy, dust, layering and moisture content.

High performance PGNAA utilises a source of neutrons beneath the conveyed flow and elemental nuclei in the conveyed material capture neutrons and release gamma energy responses unique to each element. These spectral responses are accumulated over a measurement period of 30 seconds to two minutes using an array of high specification detectors enabling the proportion of each element in a conveyed parcel to be determined and reported (Figure 1). High performance PGNAA is the most representative analysis available to the minerals industry resulting in many elements from carbon onwards in the periodic table to be measured at high precisions over short measurement times to low levels of detection. Recent developments include direct measurement of gold in conveyed ore using GEOSCAN-GOLD (Balzan et al, 2022).

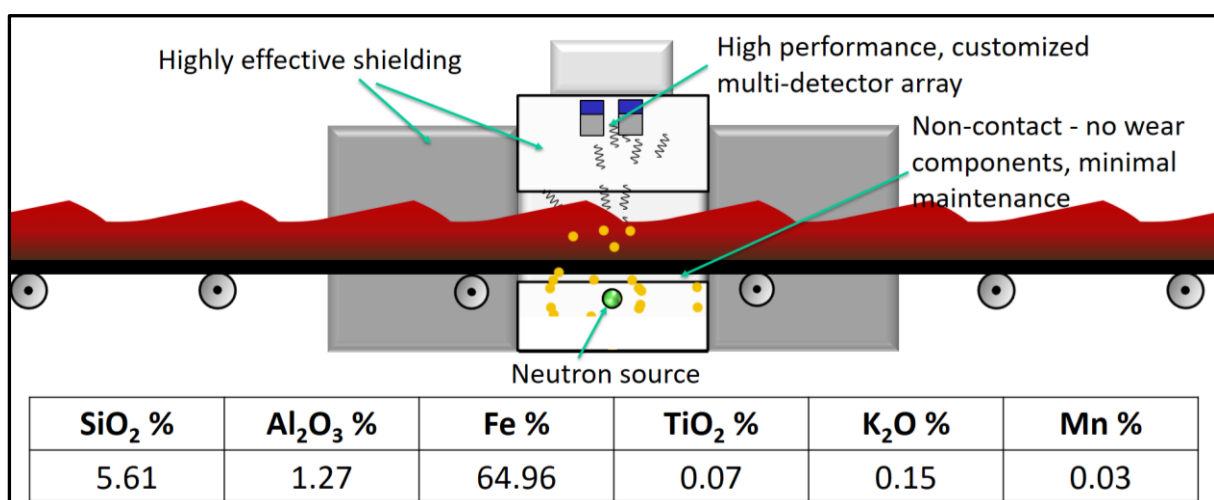


Figure 1 - Cross-section through GEOSCAN high specification PGNAA analyser showing main

components and an example of elemental results for a two-minute measurement increment

Other advanced capabilities include measurement on conveyors in underground settings. Normally FRAS (fire resistant, anti-static) rated conveyors contain chlorine compounds which can prevent lower specification analysers from measuring the conveyed flow quality. The high performance GEOSCAN has been successfully implemented on multiple conveyors in underground locations. It is also the only technology of its type suitable for measuring potash ore and product as it can easily distinguish the sodium, potassium, magnesium and chlorine in the material. Other unique capabilities of this system include measuring phosphorus in iron ore to 0.01% P.

APPLICATIONS AND BENEFITS

The high performance GEOSCAN technology has been successfully applied in many different applications and is customised to the data requirements for each. Measurement data can be used at a single location, for example after a primary crusher, for multiple concurrent uses. Some of these may involve instantaneous responses to the quality or in determining an average quality over a longer timeframe, such as compositing multiple results, depending on the intended use of the data and the benefits available.

Bulk sensing for diversion (bulk sorting)

Conveyed material can be measured at full production flows and unbiased measurement data provided to enable quality control. Shorter measurement time provides a higher level of selectivity, but it has been shown that some technologies (that do not provide representative measurements) used for even shorter measurement times actually increase the amount of misallocated material. Shorter measurement times are only more beneficial if accompanied by high measurement precisions (Kurth, 2022 and Scott et al, 2020). This highlights the need to customise the measurement solution to the application.

Iron Ore

The technology measures quality of bulk commodities such as coal, bauxite, manganese, phosphate rock and iron ore. Elements measured routinely in iron ore include iron, aluminium, silicon, manganese, titanium, phosphorus, potassium and sodium. Calcium and magnesium are also measured when needed. Bulk sensing in iron ore has resulted in many benefits throughout processing circuits but a major benefit has been the diversion of product quality material to avoid unnecessary processing. At Assmang Khumani operations in South Africa iron ore quality on overland conveyors between two mines and a beneficiation plant is measured and diverted as needed (Matthews and Du Toit, 2011). An average of one third of their annual mine output is direct shipping quality and diverted to bypass the jig plant saving US \$5 M/y in jig plant costs. Approximately 8 kg of the 12 kg CO₂ e/t full processing emissions are saved for this material, or some 40 000 t CO₂ e/y in addition to the processing cost saving. Utilising analysers for the bypass application was considered in the original plant design so a smaller plant was able to be built with the same planned output capacity at a significantly lower capital cost. The initial and ongoing savings have been benefitting the operation for over fifteen years.

Copper

Some elements respond particularly well to high performance GEOSCAN and can be measured to very low precision. Copper is one of these and precisions of 0.02% Cu have been achieved at multiple sites for 30 second measurement increments such as New Afton in British Columbia (Nadolski et al, 2018). Some ore types are considered relatively homogeneous (e.g., porphyry copper) and therefore potential for upgrading through bulk sorting has been suggested as being quite low. The basis for these assumptions has been grade data from blocks of many hundreds or thousands of tonnes predicted using geostatistical methods using assays from widely spaced assayed drill core intercepts in an orebody block model. Measured parcels are typically up to tens of tonnes and much higher variability has been seen at the measured parcel size than that predicted from

block models. Bulk ore sorting has been successfully applied to mines extracting porphyry copper ores. Copper ore grade variability occurs at different scales, and this can be utilised for bulk ore sorting to increase ore grade and quality consistency in plant feed (Figures 2 and 3).

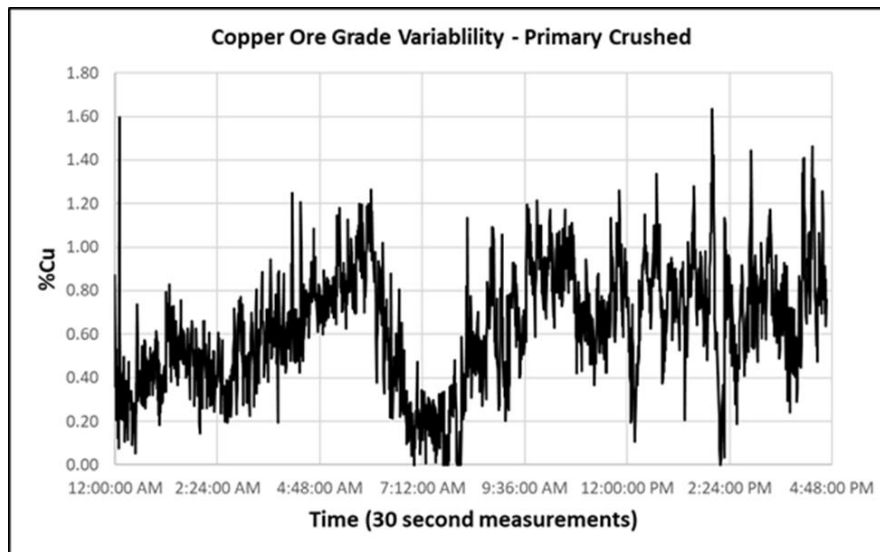


Figure 2 – Copper ore grade variability from each 30 seconds of conveyed flow from a block cave mine (Scantech)

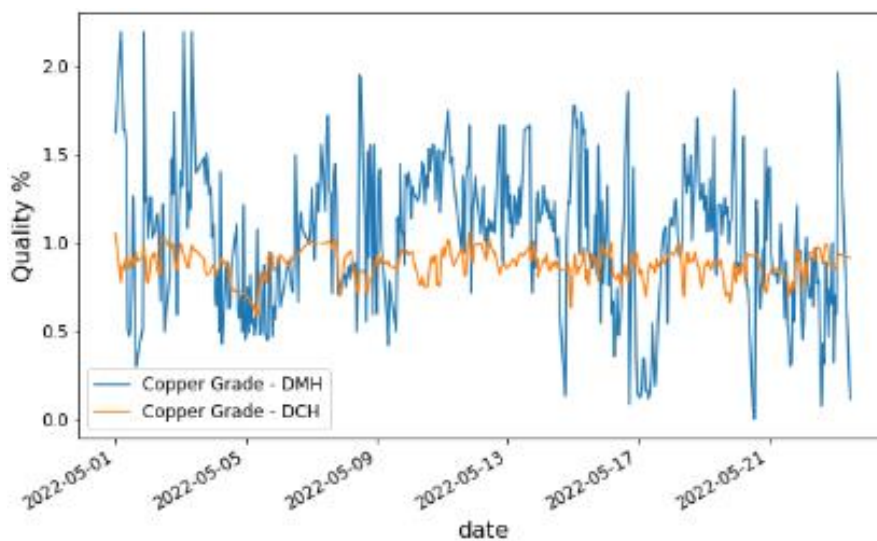


Figure 3 – Copper ore grade variability at Ministro Hales and Chuquicamata (Navarrette et al, 2022)

Bulk ore sorting at a copper mine in Chile resulted in increases of 20%+ in copper grade with 5-20% of the mined ore being rejected as waste. Copper ore processing can produce 32 kg CO₂ e/t. The diverted coarse waste has saved up to 20% of GHG emissions, mainly due to not being milled, with only minor (up to 2.5%) metal losses. Savings of over 40 000 t CO₂ e/y are achieved at an ore processing rate of 1200 t/h where 14% of the mined ore is discarded at waste. Figure 4 shows an example installation in a bulk sorting application.



Figure 4 – High specification GEOSCAN analyser generating representative, multi-elemental data used in a base metals bulk ore sorting plant for 30 second parcel diversion.

A diversion system (Figure 5) can utilise a screen to divert material to the waste stacker if grade by size analysis indicates that fines are predominantly above cut-off grade. The screen is raised or lowered to divert each 30 second parcel of flow as needed with fines always falling to the ore stacker side. The bulk sorting systems are designed to meet the requirements for each application and can be scaled according to required flow rates. Designs can cater for mobile plants as well as permanent installations.



Figure 5 – Example of a diversion system used in a copper ore bulk sorting plant for ore flows of 500 t/h (Hillyer, 2019)

Ore blending

Multi-elemental data used to improve ore blending in process feed has resulted in many benefits including:

- Control of copper metal in leach circuit feed to prevent overloading and copper losses to discard (Arena and McTiernan, 2011),
- Control of additives in copper leach feed, e.g., pyrite additive to copper carbonate ore in feed to a ferric leach process (Balzan et al, 2016),
- Improvements in metal recoveries of up to 15% through a more consistent process feed quality (Goodall, 2021).

In ore blending applications the measurement need not be over very short parcels to be effective and longer measurement times of five minutes have been utilised to prevent more frequent responses to higher ore variations seen in shorter increments. Blending can be beneficial on product material such as mineral concentrates to dilute a deleterious component prior to loading onto a train or ship. Blending of coal and iron ore is common to ensure average shipment quality is near the required specification and to enable adjustment through blend changes if quality varies from the target.

Blending is used in additive control prior to blast furnaces in the iron making process where sinter basicity is determined from measurements of multiple elements and limestone dosing adjusted to a target ratio. High performance GEOSCAN has been particularly beneficial in this application as it measures elements such as aluminium and magnesium that low specification systems are unable to measure effectively (Balzan, 2022).

Feed forward control

Measurement of the material flow after the primary crusher allows multi-elemental data to be visible by process operators well before the ore enters processing operations. These can be relatively simple processes of beneficiation or more complex processes such as flotation, leaching or smelting. A good understanding of the ore and waste mineralogy and the process sensitivity to changes in feed quality allow process operators to adjust process settings to optimise process efficiency. This may include the application of geometallurgical data to correlate feed quality with process performance outcomes. Some elemental data can be utilised for non-measurable parameters such as ore hardness which can be used to control mill feed rate.

Other compositional variations may be present that indicate high clay content or other deleterious material such as talc in a copper flotation process feed (through Mg measurement). Feed forward control can be used to control mass flow as well as reagent dosing (depressants or other flotation chemicals depending on the parameter affected). Acid addition is a typical reagent that requires proportioning to feed quality, particularly acid-consuming gangue content in a leach feed (Balzan et al, 2016) or for phosphate rock composition variation in phosphoric acid reactor feed. Such reagent adjustments have been shown to increase process performance (recoveries) by a few percentage points as normal process inefficiencies due to the absence of timely, representative and precise data are avoided.

Changes in ore type detected through continuous monitoring of run of mine ore enables beneficiation plant operators to optimise responses and ensure maximum process recovery for each ore type. Patel (2014) discusses the feed forward application where lead-zinc ore is measured in feed to a dense medium separation plant at Mount Isa Mines so that density cut points can be modified to suit changes in feed quality. Matthews and Du Toit (2011) discuss the benefits in measuring beneficiation feed to predict upgrade factors for different ore types and these are verified by utilising analysers on the jig product streams and discard flows.

Metal Accounting and Ore Reconciliation

The representative and precise multi-elemental measurement data provided for primary crushed conveyed flows is ideal for feedback to the mine to allow ore reconciliation to the mine schedule and block model. It represents the actual ore supplied from the mine to the process operation feed. It is the most effective way to quantify the quality of mined material as it is not dependent on sampling coarse flows and associated hazards.

This data is the most representative and precise to utilise for metal accounting for the process operations. When used for ore blending or bulk sorting the analyser data will be able to represent the material flow to the crushed ore stockpile or directly to the mill if measured after the crushed ore stockpile. Matthews and Du Toit (2011) discuss the application of analyser data for elemental balance at the Khumani iron ore operations as all relevant conveyed flows, including discard flows, contain analysers and belt weighers to quantify tonnages and grades.

In gold ores the GEOSCAN GOLD is able to measure elements as proxies for gold if they are present over each thirty seconds of flow and it can measure gold directly as an element. Direct gold measurement requires a longer measurement time, and this varies from five to ten minutes in successful installations to date (Balzan et al, 2022). The nature of the gold mineralisation determines the suitability of proxy elements. Gold measurement allows a previously unattainable level of metal accounting to be performed.

Technology risk reduction

The main requirements after safety are generally performance and maintenance (equipment and calibration). High performance GEOSCAN has proven successful in many commodities in the minerals sector and many published papers attest to its success as outlined in the applications detailed previously. Technology need not present a risk to mining companies and a proven analyser product provides significant confidence in the data it generates when regularly maintained. Flexible configurations and customised calibrations ensure the optimal solution is provided for each application.

Risk can be further reduced through test work on samples from sites which determine the initial calibration. The performance estimates supplied are compared to those achieved on site within an initial three-to-six-month period in most cases. Most performances should be achieved within a very short implementation timeframe. Financial security is usually linked to performance achievement.

Analysers are installed during planned maintenance shutdowns to avoid interruptions to normal production, and they do not interfere with conveyed flows. The main risk for many end users of measurement technologies is how to benefit from the data generated. The risk can be reduced by engaging with a vendor with broad and successful implementations in the same industry that can share application successes and understands the relevance of the data. The analyser vendor cannot necessarily control how much benefit the end user derives but should be accountable for the performance of their analyser.

CONCLUSIONS

The mining industry's demand for increased resource efficiency and reduced environmental impact drives the need for innovative technologies. The Scantech GEOSCAN on-belt analyser technology has shown significant benefits across various mineral processing applications. The use of real-time, multi-elemental analysis has proven successful in optimising material diversion, controlling additives in processing, and implementing feed-forward controls, thereby enhancing overall operational efficiency.

The findings in this paper underline the high specification GEOSCAN analyser's ability to increase ore grade by up to 20% through bulk sorting, reduce GHG emissions, improve process recovery by 10 to

15% through ore blending, and provide valuable data for ore reconciliation and metal accounting. These benefits, combined with customised analyser configurations and calibrations, offer a compelling solution to the mining industry's sustainability and efficiency challenges.

However, the potential of such technology is not fully tapped. Future research could explore more diverse applications and further optimise the use of data generated by on-belt analysis. While the technology has proven successful in numerous situations, a broader understanding of its applications and benefits will contribute to more sustainable and efficient practices in the mining industry.

ACKNOWLEDGEMENTS

The authors wish to acknowledge permission of Scantech International Pty Ltd to publish this paper and acknowledge customers who have published their own papers on the successful implementation of the technology.

REFERENCES

- Arena, T and McTiernan, J, 2011. On-belt analysis at Sepon copper operation, in *Proceedings MetPlant 2011*, pp 527-535 (The Australasian Institute of Mining and Metallurgy: Melbourne).
- Balzan, L A, 2022. Improved stability in control of sinter feed basicity by using GEOSCAN real time on-belt analysis, in *Proceedings AISTech 2022 — Proceedings of the Iron & Steel Technology Conference*, 16–18 May 2022, Pittsburgh, Pa., USA. DOI 10.33313/386/161. pp 1388-1394 (© (2022 by the Association for Iron & Steel Technology).
- Balzan, L, Jolly, T, Harris, A, and Bauk, Z, 2016. Greater use of Geoscan on-belt analysis for process control at Sepon copper operation, in *Proceedings XXVIII International Mineral Processing Congress*, (Canadian Institute of Mining, Metallurgy and Petroleum: Quebec).
- Balzan, L A, de Paor, A, Doorgapershad, A and Fitcher, W, 2022. The end of the rainbow: real time direct gold analysis in run of mine ore at Newcrest's Telfer mine using GEOSCAN analysis, in *Proceedings of International Mineral Processing Conference – Asia Pacific 2022*, pp 1140-1149 (The Australasian Institute of Mining and Metallurgy: Melbourne).
- Goodall, W, 2021. Understanding what is feeding your process: how ore variability costs money, in *Process Mineralogy Today*, March 10, 2021. Available from: <https://minassist.com.au/understanding-what-is-feeding-your-process-how-ore-variability-costs-money/> [Accessed: 26 May 2023].
- Hillyer, L, 2019. Mining Automation – Mine Smarter, Load Quicker & Ore Sorting, presentation to Future of Mining Australia 2019, (Aspermont Ltd). Available from: <https://www.youtube.com/watch?v=2NJ3HhphJc4/> [Accessed 26 May 2023].
- Kurth, H, 2022. Ore quality measurement and control using Geoscan-M PGNA real time elemental analysis, in *Proceedings International Mining Geology Conference 2022, Brisbane, Australia and online*, pp 338-345 (The Australasian Institute of Mining and Metallurgy: Melbourne).
- Matthews, D, and du Toit, T, 2011. Validation of material stockpiles and roll out for overall elemental balance as observed in the Khumani iron ore mine, South Africa, in *Proceedings Iron Ore Conference 11-13 July 2011 Perth, WA*. pp 297-305 (The Australasian Institute of Mining and Metallurgy: Melbourne).
- Nadolski, S, Klein, B, Samuels, M, Hart, C J R, & Elmo, D, 2018. Evaluation of cave-to-mill opportunities at the New Afton Mine, in *Proceedings of the 50th Annual Canadian Minerals Processors Operators Conference, Ottawa, Ontario, 23-25 January 2018*. (eds: Danyliw, B, Cameron, R, and Zinck, J) pp 270–281 (Canadian Institute of Mining, Metallurgy and Petroleum, Montreal).

Navarrete, M, del Rio, P, Aravena, P, Soto, A, Valido, J C, and Allende, J, 2022. Stockpile Modeling and Ore Traceability with Advanced Analytics at DMH, paper presented to MineriaDigital2022 - 9th International Congress on Automation, Robotics and Digitalization in Mining (Gecamin).

Patel, M, 2014. On-belt elemental analysis of lead-zinc ores using prompt gamma neutron activation analysis, in *Proceedings XXVII International Mineral Processing Congress 2014*, Gecamin: Santiago, Chile, chapter 17.

Scott, M, Rutter, J, du Plessis, J, and Alexander, D, 2020. Operational deployment of sensor technologies for bulk ore sorting at Mogalakwena PGE Mine, in *Proceedings Preconcentration 2020*, (The Australasian Institute of Mining and Metallurgy: Melbourne).

On-line Digital Twin for Processing Plant Optimisation

J Moilanen¹, A Remes² and A Grigoryan³

1. Director – Digital Solutions, Metso Finland Oy, Rauhalanpuisto 9, 02230 Espoo Finland, jari.moilanen@metso.com
2. Technology advisor – process modelling and simulation, Metso Finland Oy, Rauhalanpuisto 9, 02230 Espoo Finland, antti.remes@metso.com
3. Corporate Manager Processing, Dundee Precious Metals Inc., Bacho Kiro 26, 3rd floor, Sofia, 1000, Bulgaria, Armenak.Grigoryan@Dundeeprecious.com

ABSTRACT

Digital twin technologies developed for the mining industry create new insights into the material flows and metallurgical processes. This provides an opportunity to optimise the operations of processing plants over the full production chain to manage impacts of variability in the feed materials, metallurgical processes, and the business environment. Digital twins with AI algorithms for automatic adaptation of physical process models are reliable for solving resource efficiencies and optimising emission footprints in daily operations. Recipe matching to variable ore types allows for significant savings in energy, water, and chemical utilisation per unit of product. With the ability to test run any process configuration and operating strategy before execution, the risk of environmental, financial or safety issues is greatly mitigated.

Increased knowledge and situational awareness of the process allows for better decision making and planning within the plant, resulting in better recovery and process optimisation. Transparent tracking of material flows from the mine to the processing and refining plants with online material balances provide operations with information about material flows. In addition, online material balances provide operations with cross validation of data to ensure quality of sensor data, health of assaying equipment and practices.

This paper describes a case study where a modern science-based metallurgical digital twin was developed and deployed for the Dundee Precious Metals Inc Ada Tepe minerals processing plant in 2022. The case study discusses the key learnings and critical points in the ways of working in a digital twin project. The paper further discusses the site's technical architecture with existing systems for process control and IT infrastructure. The impact on selected key performance indicators (KPIs) on metallurgy, sustainability and economy are also reviewed. Furthermore, the paper examines the future potential of metallurgical digital twins to deliver more sustainable solutions by reducing the mining industry's carbon and environmental footprint, as well as increasing the resilience for energy, water and materials.

INTRODUCTION

On-line process simulation of material flows and metallurgical processes allow mining operations to ensure they use resources in an optimal way while considering both the impacts and constraints of current and future states. Production recipe matching to variable ore types allows for significant savings in energy, water, and chemicals per produced ton of product. Increased knowledge from the process dynamics allows the users to better understand how the processes interact and influence each other e.g., with various ore types (Takalo et al, 2021).

This feedback enables the operators to make informed decisions, resulting in better recovery and process optimisation. With the ability to simulate scenarios on control actions and operating strategy before execution, the risk of impaired production can be understood and mitigated, and as an outcome environmental, financial and safety issues can be addressed. These scenarios on alternative operating strategies may reflect the impact of process inputs that cannot directly be controlled such as ore type or cost of energy, but also the results of active controls to optimise Key

Performance Indicators (KPIs). Typical KPIs are summarised in Table 1.

Table 1 – Typical KPIs

Metallurgy	Economy	Sustainability
Production volume	Revenue & profitability, Net Smelter Return (NSR)	Use of energy
Concentrate grade & mineral recovery	Cost structure	Use of chemicals
Material mass balances	Resources efficiency	Water footprint
Losses in tails	Performance results for block of ore	Carbon footprint
Penalty elements		Life Cycle Assessment (LCA)

With digital twin technologies these KPIs can be monitored on-line, or they can be predicted as a simulation scenario. Figure 1 presents scenarios of control strategies A and B with their respective impact on grade of the concentrate. It is important to note that the usefulness of these predictions for operative decisions depend on how well the underlying process model describes the process dynamics without bias. Quality of process model is discussed in the following chapters.

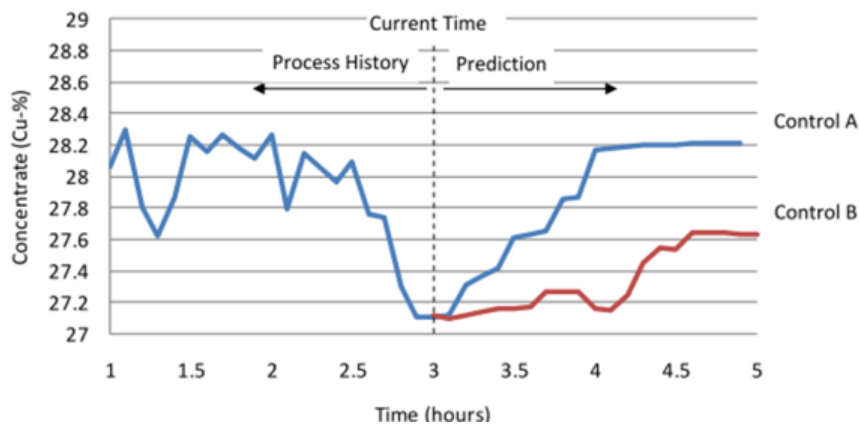


Figure 1 – Predicted scenarios of control actions by a digital twin that can help operators to select optimal control strategies.

This increased knowledge allows for better decision making within the plant or at a remote location, resulting in better operational performance and safety, and process optimisation. Improved situational awareness on processes and the operational state of process equipment opens an opportunity for effective support of operations from remote locations and facilitates the development and operation of future autonomous processing plants.

PERFORMANCE REQUIREMENTS FOR A PLANT DIGITAL TWIN

Unbiased reliability of the underlying process models is critical to the usefulness and value of digital twins for on-line monitoring and future scenario predictions. Off-line simulation models without connectivity to process data easily lose their capability to represent the current state of the process which also leads to erratic predictions of the future, as presented in Figure 2.

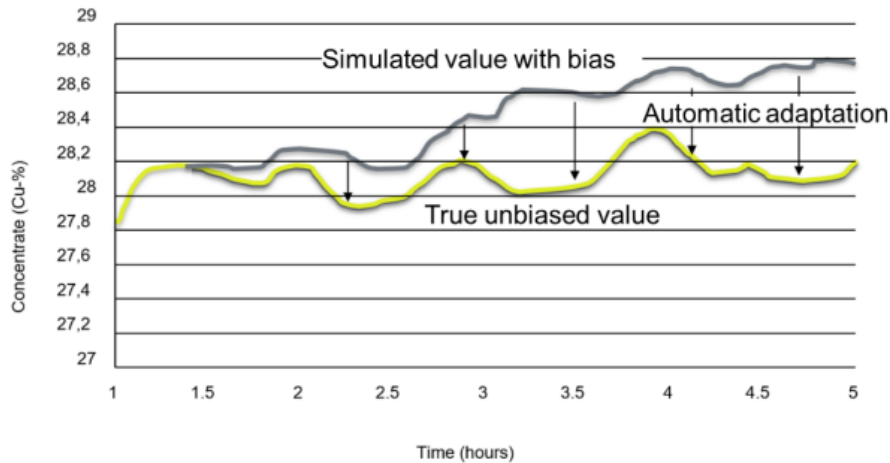


Figure 2 – Correction of simulation error with automated model adaptation

The usual reasons why the simulation models may be biased are changes in the process operating state that, at worst, invalidate the calibration and functioning of the models. These changes may be slow, as in the case of equipment wear, changes in fundamental inputs to the process such as ore characteristics, quality of process water, or seasonal fluctuation of ambient temperature. Alternatively, the changes may be abrupt because of sudden changes in the ore feed, the use of alternative process flow sheet connections or planned or unplanned shutdowns of the key equipment.

Reliable and unbiased process models can be achieved with automated adaptation and learning from on-line sensors and process history data; hence the accuracy of the process models is related to the quality and amount of sensor data available. It is important to measure not just performance, but also the factors that determine performance. However, some of the critical determining factors cannot yet be measured on-line – e.g., mineral grain size and texture, contamination of surfaces in flotation or changing distribution of target element between different minerals. It may be possible to compensate with human input (e.g., geometallurgical feedback) or by developing soft sensors, or proxies and algorithms that correlate other measurements with the underlying measure.

Good housekeeping of sensors, instruments and onstream analysers (OSAs) is important for ensuring the accuracy and repeatability of measurements. In addition to online data laboratory assays can be used for model adaptation. Furthermore, the laboratory assays provide an opportunity for simulation models to detect faulty measurements or biased assays. A specific model parameter adaptation algorithm minimises any sudden modelling errors and drifting divergence due to any changes in the operating state as discussed earlier. Figure 3 presents the operating principle of the automated model adaptation. As a practical example in mineral flotation, on-line elemental assays are continuously applied to detect changes in the ore floatability, and flotation kinetic rates of minerals are automatically adapted by an automated algorithm to reflect the changes in the ore feed. On-line adaptation enables the physical models of digital twins to continuously track the process and adjust to changing conditions for unbiased predictions. In case of changes in the process flow sheet it is enough to update the underlying physical model to reflect the changes, and the process model is readily available for scenario predictions.

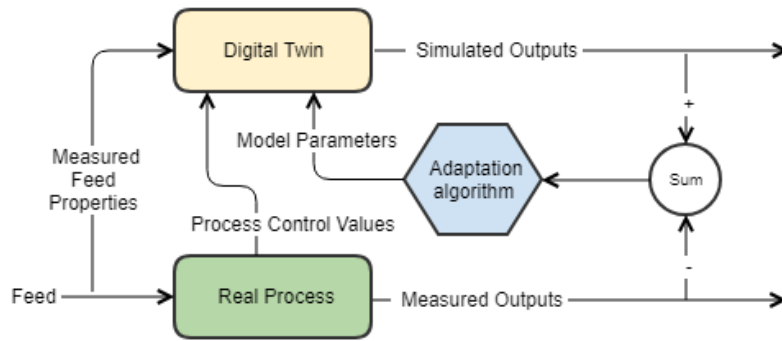


Figure 3 – Principle of automated model adaptation of a digital twin.

The adaptation framework of an industrial digital twin and aspects such as data quality, cost functions, various methods and parameter selections are discussed in Koistinen et. al (2020). In addition, studies have already indicated that physics-based flotation models can efficiently be adapted if information-rich data sets are available. One type of adaptation framework for physics-based models utilises a stochastic global optimisation algorithm in moving time windows (Ohenoja et al., 2020). Also, (Oosthuizen et al, 2021) presented how the key flotation process model parameters, including dynamic mass balances, static froth flotation models and empirical relations, can theoretically be estimated from the online measurements. In addition, a procedure where the flotation kinetic model parameters were paired with selected grade on-line assays and then individually tracked with recursive estimation methods, has been proven for mineral flotation models (Pietilä, Kaartinen and Reinsalo, 2013, Kaartinen et al., 2013).

DEVELOPMENT AND DEPLOYMENT OF A DIGITAL TWIN AT DUNDEE PRECIOUS METALS ADA TEPE GOLD CONCENTRATOR

Dundee Precious Metals Inc. (DPM) is a Canadian-based, international gold mining company engaged in the exploration, development, mining and processing of precious metal properties. DPM's current operations are in Namibia and Bulgaria, with exploration in Bulgaria, Ecuador and Serbia. Ada Tepe, commissioned in 2019, is the first greenfield mine in Bulgaria in the last 40 years. The Ada Tepe mining operation has open-pit mining, with some of the processes including crushing, milling, flotation, dewatering, and filtering circuits. The tailings from the process plant are stored at an Integrated Mine Waste Facility (IMWF). The concept of the IMWF is to place thickened tailings into cells constructed from mine rock. Rehabilitation of the slopes is being performed during operation compared to conventional tailings. The mine produces high grade gold concentrate which is then transported for further treatment in a smelter. Figure 4 presents a simplified plant flow sheet.

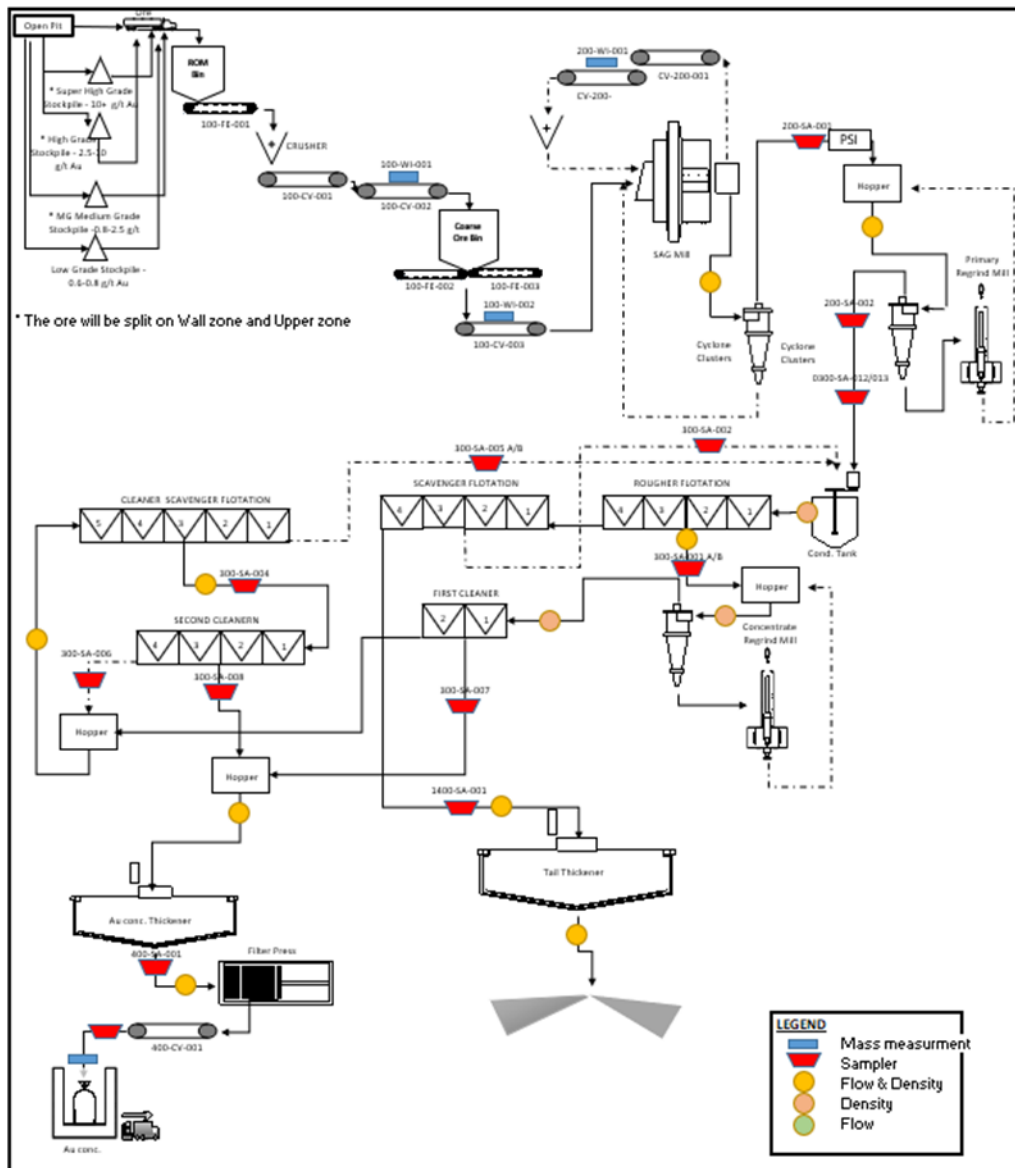


Figure 4 – Simplified flow sheet of Ada Tepe concentrator.

At Ada Tepe plant process optimisers are used for optimal process control. A Model Predictive Control (MPC) based grinding optimiser covers the grinding circuit with a SAG and VertiMills and ensures consistent grind size (P80 32-36 μm) for flotation feed. Consistent grind size in the flotation feed is the key parameter for plant performance. The flotation circuit uses flotation optimisers as well for maximising recovery and consistent process control. Optimisers in the dewatering section take care of turbidity of thickener overflow with optimal flocculant dosage and underflow density control that are critical for the IMWF feed. The limits of targeted KPIs and input parameters of process optimisers can be adjusted by simulating the process within the digital twin by what-if scenarios. This process can be automated and linked to the process optimisers, which is a logical next step for Ada Tepe mine.

Digital twin project in phased approach

As part of a larger digitalisation project to employ model predictive process optimisers for process control, DPM investigated digital twin technologies. The process started by exploring how the digital twin is expected to add value, what it can do, and finally, what benefits are available with a digital twin in operation. Findings of the benefits are summarised in Table 2. Cross departmental contributions from different organisational levels came to a common view on targets, highlighting

multiple sources of benefits to the operations. Furthermore, it was clear from the beginning how the digital twin would be used by the plant operators, metallurgists, and production planning teams.

Table 2 – Identified benefits of a metallurgical digital twin for the DPM Ada Tepe mine

Digital twin adds value by:	Digital twin capability:	Operations with a digital twin may:
making operation systematic across working shifts	follows plant material and water balance	prevent overly high circulating loads and mass pulls
allowing faster reaction to issue to minimise impact of events where and when required	provides grade and recovery targets for Advanced Process Control	prevent exceeding of dewatering capacity
evaluating options for de-bottlenecking eliminating unnecessary changes in the process	indicates process limits and bottlenecks	improve Au recovery, avoiding losses
better understanding of process dynamics	provides plant economic performance vs a theoretical index	Assist to maintain Au grade target
		avoid penalty elements in the concentrate

The actual digital twin project started with building the digital twin for a sulfide flotation operation consisting of static and dynamic flotation models with live data connection for the digital twin. As is typical for digital twin implementation, the project was split into phases. In the first phase, a static model of the flotation process was created with an actual process flow sheet. Attention at this phase was on defining the process connections and mass balances with related process performance data that form the basis for the process model. The data was readily available from process test campaigns, and the data was used for validating the current process flow sheet.

In the second phase, the static process model was converted to a dynamic model with equipment hold-ups to allow for time dependent simulations. Finally in the third phase, the created digital twin simulation model was connected with live plant data for effective model adaptation. The focus on data connectivity in establishing a cyber secure communication link was achieved by the use of industry standards and best IoT practices that accommodate to existing modern infrastructure for Information (IT) and Operational Technologies (OT).

IT infrastructure for data connectivity

The digital twins handle and produce potentially sensitive data and may contain information of current operations and future plans that cannot be shared with unauthorised parties. At a technical level, the selected option was to fully integrate the digital twin and its connectivity with the corporate IT policies and practices where the cyber security design principles are already applied. In the installation the digital twin application runs in Microsoft Azure cloud, as presented in a schematic diagram in Figure 5. Running the digital twin in cloud offers better scalability with cloud resources for computationally intensive process simulation compared to local installation on site, as well as safe access for effective maintenance and support. Plant data from the Process Control System (PCS) is

accessed via on-site OPC server, data routing I/O service software and firewalls. Cloud-end connectivity is handled with an IoT Hub of the cloud.

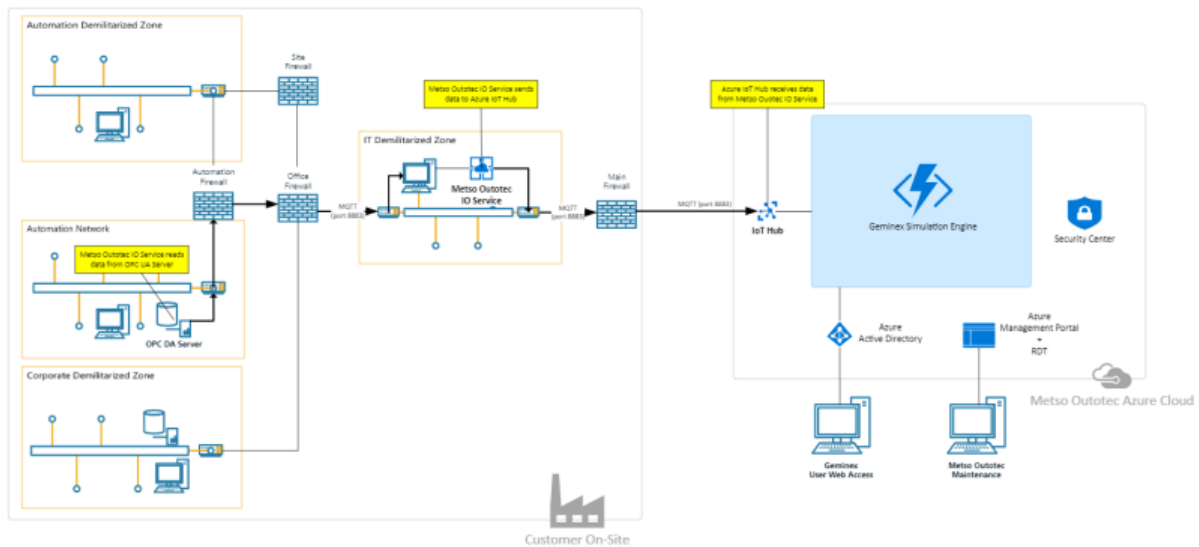


Figure 5 – Schematic architecture of a cyber secure connection from the edge to cloud to the digital twin.

Design of user interface and simulation cards

For effective buy-in for operational use, the user experience (UX) and user interfaces play a key role. Customer journey mappings with end users in large and small organisations suggest that the process flow sheet is commonly a preferred way of navigating the sources of information and presenting the results. This may be due to similar flow sheet like user experience for the operators and plant metallurgists with process control system displays and plant design documentation. Figure 6 presents the developed operator interface for the sulfide flotation where the plant operators and metallurgists can monitor the flotation performance in real time.

The digital twin complements traditional measurements with a set of soft sensors. The soft sensors are inferred from the first principle process models and algorithms of the digital twin. The soft sensors provide the metallurgists and operators with an opportunity to delve into the performance of each unit process and the circuit with information that is not available on-line such as floatability of mineral particles, mineral content in particle size fractions or dynamic materials balance of the flotation circuit. Figure 6 presents a digital twin display with soft sensors for flotation cell specific solids contents, metals recoveries and grades, stream flowrates and P80 particle size fractions. Furthermore, the soft sensors can be communicated to plant control systems for closed loop control, and soft sensors as virtualised measurements can cross validate the actual instrument readings. Important for the usefulness of the process model and the soft sensors is that they respond in a realistic way for each ore type that drive the performance of the plant. This is achieved by calibrating the kinetic model parameters based on laboratory studies, and further adapted automatically to changing conditions, as discussed earlier.

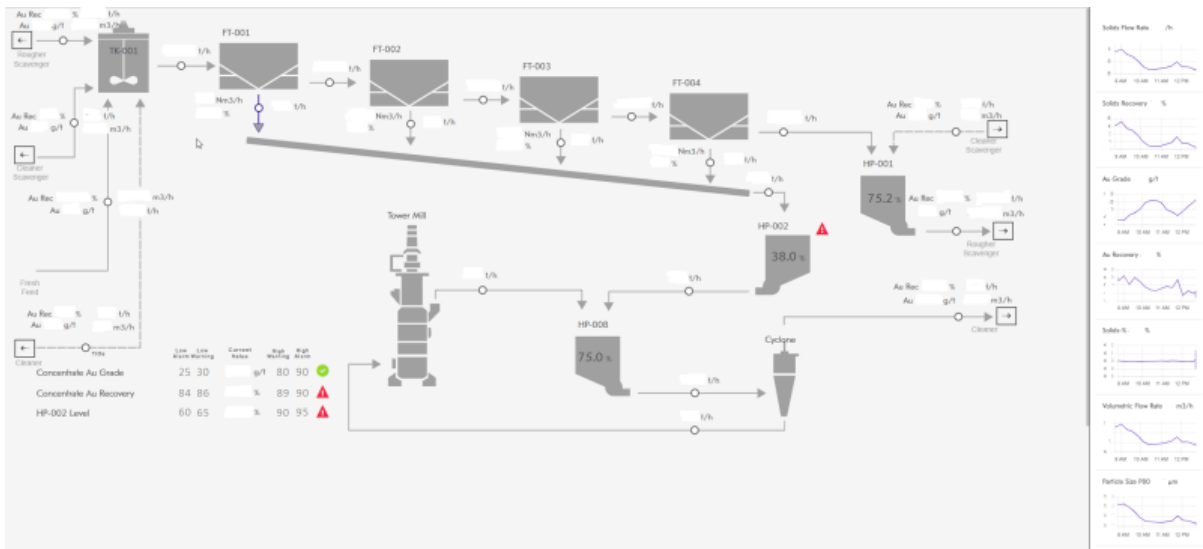


Figure 6 – Monitoring view of a digital twin for flotation with measurements and soft sensors such as equipment specific solids contents, metals recoveries and grades, stream flowrates and P80 particle size fractions. All production values have been removed from screenshot for confidentiality.

In addition to real time monitoring the digital twin provides the metallurgists with an opportunity to test the outcomes of alternative processing parameters. The scenarios are built by scenario cards, as presented in Figure 7 for the cleaner flotation. With the scenario predictions the metallurgists can find optimal processing parameters for each shift to reflect the ore blend available.

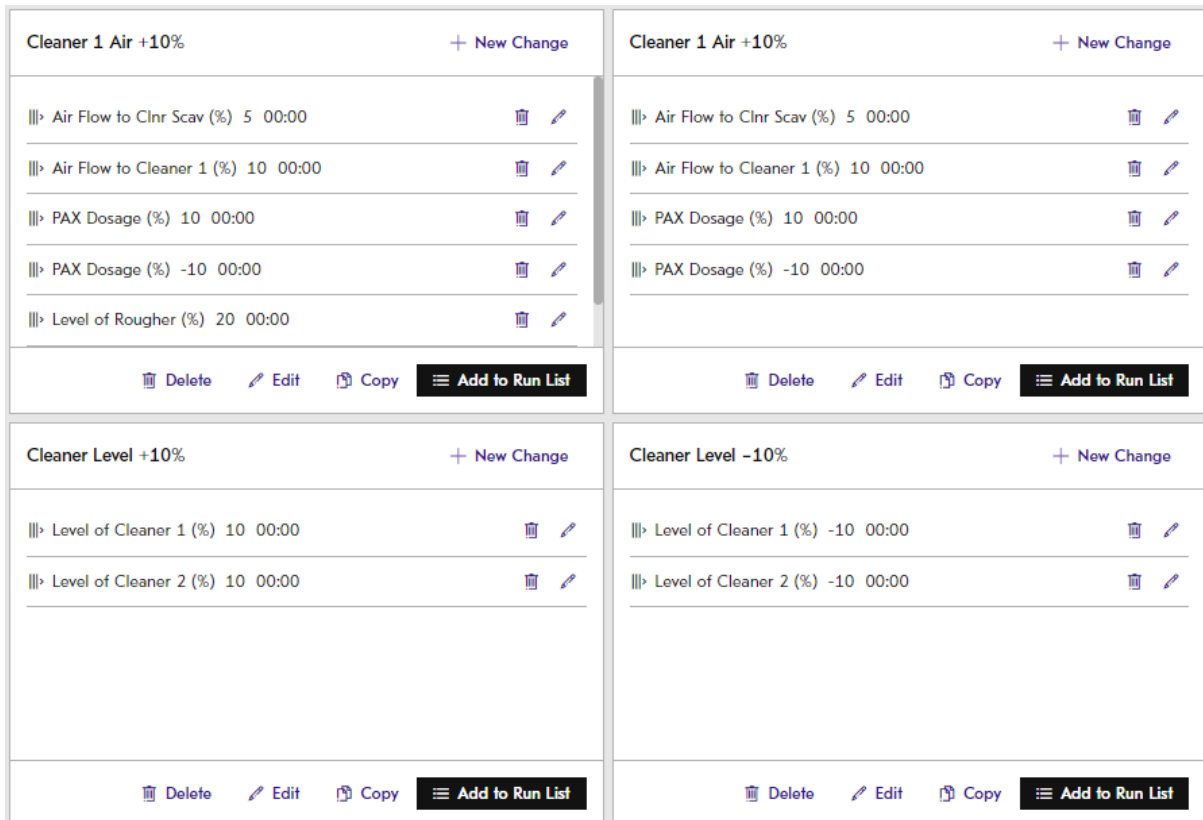


Figure 7 – Library of simulation cards for alternative parameters for cleaner flotation. Simulation cards are easy to build as needed by the metallurgists.

Benefits of digital twin project

The digital twin is used for plant optimisation on a daily basis, and it needs to integrate seamlessly with advanced process control (APC) process optimisers. The digital twin predictions will give a set of alternative operating targets and finds an optimum for each process area optimiser. Finally, for example in flotation, the control froth speed, aeration, levels, and reagent dosages are manipulated with parameter settings in the process control systems.

Ada Tepe currently uses the digital twin for previously determined what-if scenario simulations at the beginning of every shift and makes the data available to operators for decision making. This allows the operators to learn how the key performance parameters will change when adjusting the flotation reagents, slurry levels of flotation cells or throughput with the existing ore feed. In addition, the operators can check the impact of other parameter settings with what-if simulations as needed.

Most of the local workforce at Ada Tepe has no prior experience in mining and mineral processing, and automation greatly assists the young and unexperienced workforce. The implemented digital twin helps increase the confidence of operators in general, as well as delivering assurance with any proposed changes to process parameters. Trial and error scenarios are tested and fully understood in simulation before implementation in the live production environment.

At Ada Tepe one of the KPI's is compliance to predicted recovery generated by Recovery Model. The Recovery Model is a regression formula generated with past actual data, and it is used for production budgeting and forecasting. Figure 8 presents the difference between actual and predicted gold recovery by the Recovery Model from the beginning of January 2021 until May 2023. The Recovery Model is a fixed formula used for production planning and predicts the plant throughput and gold grade before each displayed period. A positive trend on compliance to the Recovery Model can be observed from the chart after commissioning of the digital twin in the beginning of year 2022. This suggests better understanding of the process and implications of changes in processing parameters. This has contributed to reaching the production targets, and eventually higher gold recovery.

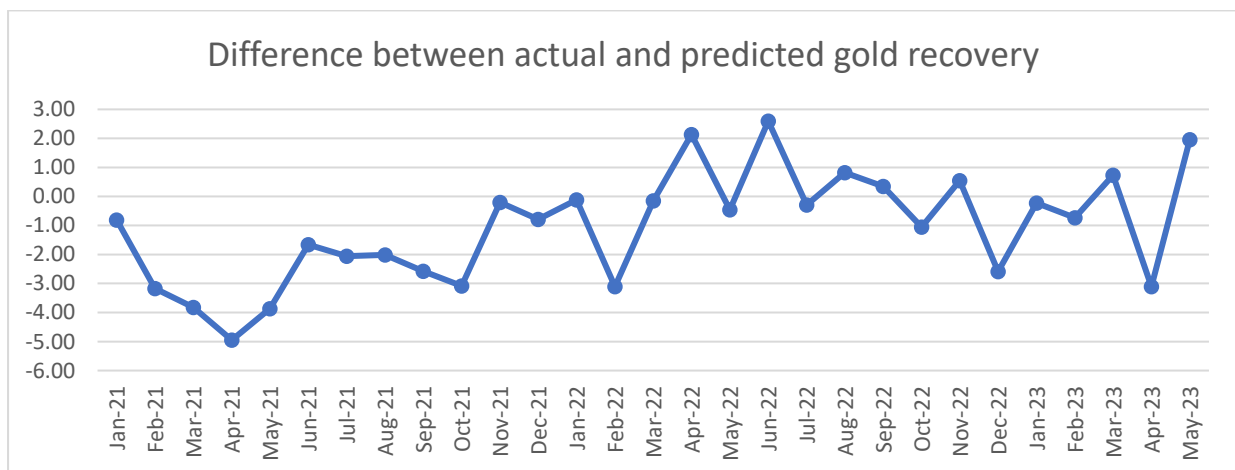


Figure 8 – Difference between actual and predicted gold recovery by the Recovery Model for production planning and budgeting

CONCLUSIONS

Typical key drivers for the digital transformation and implementation of digital twins in the mining industry relate to Environmental, Social and Governance (ESG) criteria such as energy efficiency and the use of water, as well as operational productivity by matching the processing strategy with

available ore types for increased metals recovery and process throughput. Digital twins contribute to these by allowing operations to make decisions based on a complete overview of material flows and blends. By improving resource efficiencies and subsequently reducing emission footprints with accurate models, the digital twin technologies assist safe, sustainable, and more economical operations. Furthermore, improved situational awareness of processes and the operating condition of process equipment opens an opportunity for effective support to operations from remote locations. It may also facilitate the development and operation of future autonomous processing plants, assuming that the fundamental influences on performance can be adequately measured or inferred.

It was recognised that the key characteristic of a successful digital twin project was that development should be end-user directed to address the operational constraints and preferences, rather than developer driven. The subject-matter expertise in metallurgy of the supplier of the Technology was identified as an important factor for success.

At Ada Tepe the digital twin helped increase the confidence of inexperienced process plant operators. It also delivered accurate predictions of any proposed changes to the plant. Trial and error scenarios were tested and fully understood in simulation before implementing the changes in the live production environment. Better understanding and management of the process contributed to reaching the production targets and higher gold recovery. Furthermore, the simulation by the digital twin gives a complete view of process status, as well as visibility to areas where corrective actions are required.

Metallurgical digital twins have clear potential to help the mining industry to achieve greater production efficiency, better recoveries of valuable minerals, use less energy per produced ton of product, and reduce environmental footprint of the operations. In the future, processing plants will require even more resilience to cope with constraints with energy and water, as well as more complicated feed materials. Development of modern technologies to address this resilience requires a high level of control and optimisation of the full operation, provided by the metallurgical digital twins.

ACKNOWLEDGEMENTS

The authors would like to acknowledge Dundee Precious Metals Inc Ada Tepe and Chelopech and Metso for professional support for the project.

REFERENCES

Kaartinen, J., Pietilä, J., Remes, A., Torttila, S. Using a Virtual Flotation Process to Track a Real Flotation Circuit, IFAC MMM 2013 International Symposium - Control, Optimization and Automation in Mining, Minerals and Metal Processing, San Diego, California, USA, 25-28 Aug. 2013.

Koistinen, A., Ohenoja, M., Tomperi J. and Ruusunen, M., Adaptation framework for an industrial digital twin, SIMS Conference on Simulation and Modelling SIMS 2020, 22-24 Sep. 2020, Virtual Conference, Finland

Ohenoja, M. et al. (2020) 'Model Adaptation for Dynamic Flotation Process Simulation', in 2020 7th International Conference on Control, Decision and Information Technologies (CoDIT). 2020 7th International Conference on Control, Decision and Information Technologies (CoDIT), pp. 183–188. doi:10.1109/CoDIT49905.2020.9263863.

Oosthuizen, D.J., le Roux, J.D. and Craig, I.K. (2021) 'A dynamic flotation model to infer process characteristics from online measurements', Minerals Engineering, 167, p. 106878. doi:10.1016/j.mineng.2021.106878.

Pietilä, J., Kaartinen, J. and Reinsalo, A.-M. (2013) 'Parameter estimation for a flotation process tracking simulator', IFAC Proceedings Volumes, 46(16), pp. 122–127. doi:10.3182/20130825-4-US-2038.00048.

Takalo, V-P., Remes, A., Liipo, J., Digital tool set to improve the economic value and metallurgical response of different ore types and their blends, CIM 2021 Convention, Virtual Event, May 5, 2021.

Mineralogy, Chemistry and Recovery: The New Century Story – Venturing into Extremes

P Waterhouse¹, C J Greet², P D Munro³ and D W Bennett⁴

1. Processing and Pipeline Manager, New Century Resources, Queensland, pwaterhouse@newcenturyresources.com
2. Manager Minerals Processing Research, Magotteaux Australia Pty Ltd, South Australia, Christopher.greet@magotteaux.com
3. Principal Consultant, Mineralis Consultants Pty Ltd, Queensland, pmunro@mineralis.com.au
4. Principal Consultant, Mineralis Consultants Pty Ltd, Queensland, dbennett@mineralis.com.au

ABSTRACT

New Century Resources Ltd commenced processing the 77.3 Mt of Century 3.0% zinc tailings in August 2018 following a comprehensive sampling and testing program. Plant re-commissioning followed a staged approach, with tailings hydraulic reclamation capacity increasing concurrently with progressive refurbishment of flotation capacity. Plant metallurgical performance did not match expectations from the laboratory test work, in particular zinc recoveries and zinc concentrate grades were lower than anticipated. The causes for the lower zinc recovery and concentrate grade included a lack of cleaner flotation capacity, particularly in the second cleaner stage immediately following ultrafine milling (UFM) of the first cleaner concentrates. To increase cleaner flotation capacity and therefore increase cleaner block zinc recovery, the second cleaner feed was redirected to an existing and refurbished B22/6500 Jameson Cell in a cleaner scalper duty in May 2021. After commissioning, the Jameson Cell achieved very little and no changes to cell settings (pressures, flows) or reagents made any significant difference to mass recovery or zinc recovery.

Investigation into the causes of the poor Jameson Cell performance determined that regrinding the UFM cyclone underflow to a P_{80} of 4.5 μm to liberate sphalerite from silica created pulp/surface chemistry conditions that severely impeded sphalerite flotation. This phenomenon was noted in the second cleaner, with flotation not really starting until half-way down the bank. Further, a size reduction to 80 percent passing 4.5 μm increased the sphalerite particle surface area by a factor of approximately ten. Therefore adding “normal” quantities of activator and collector were insufficient to activate and recover the ultrafine sphalerite.

Laboratory tests addressing each critical part of sphalerite flotation (liberation, pulp chemistry and reagent addition) separately did not improve zinc recovery at all. It was not until all three parts were satisfied did the sphalerite flotation response improve. This paper describes the Century tailings process development and challenges created in ultrafine particle flotation after pulp chemistry changes induced by ultrafine regrinding.

INTRODUCTION

The Century operations shown in Figure 1 are located at Lawn Hill in far north-west Queensland and commenced production of lead and zinc concentrates in November 1999. Mining and processing continued with mean annual production of 475 000 t of zinc and 50 000 t of lead in concentrates until 2016, making Century one of the largest zinc mines in the world. The zinc concentrate had a low iron and silica content compared with other large sedimentary exhalative (SEDEX) lead-zinc-silver operations of the Mt Isa Inlier (Mt Isa, Hilton, George Fisher, Lady Loretta, Dugald River, and

McArthur River). This was to provide a low leach residue feedstock mainly for the then affiliated Budel zinc smelter in the Netherlands.

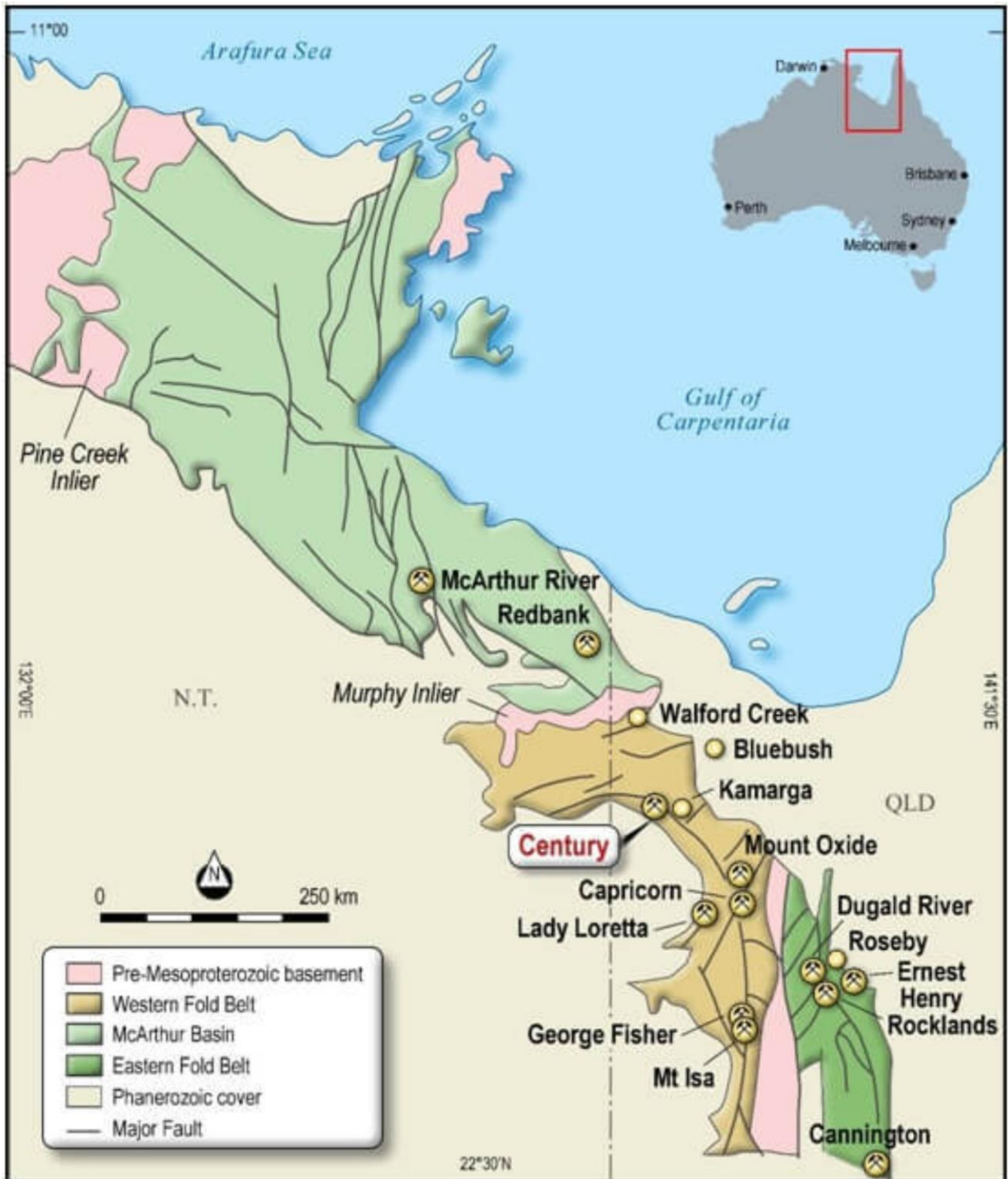


Figure 1: Century operations location

The original Century operation featured open pit mining, and a nominal 7 Mt/y process flow sheet consisting of primary crushing, SAG and ball milling with a P80 48 to 60 μm product reporting to flotation. The flotation section consisted of carboniferous gangue removal by pre-flotation, lead flotation to produce lead concentrate, and zinc flotation including ultrafine milling (UFM) to a P80

6.5 µm before final zinc cleaning to produce zinc concentrate. The products were transferred in slurry form via a 304 km underground pipeline to the port facility at Karumba (Burgess et al, 2003). Century produced 77.3 Mt of tailings at 3.0% Zn and 12 g/t Ag before shutting down in 2016.

Retreatment of tailings had been studied before closure and was done in earnest by New Century Resources after acquiring the operations from MMG in 2017. Laboratory metallurgical test work on sampled tailings and the results of a pilot plant run at ALS Metallurgy indicated that a 50 – 52% Zn zinc concentrate with less than 7.5% SiO₂ was achievable at 50 - 53% zinc recovery by hydraulic tailings reclaim, bulk flotation, regrinding and multi-stage cleaning. Zinc concentrate product would re-use the existing thickening, slurry pipeline, and Karumba facilities.

Tailings retreatment commenced in August 2018. The strategy used for the Phase 1 capacity ramp-up to 8 Mt/y throughput was based on the hydraulic mining starting with one water cannon and approximately half of the total rougher-scavenger and cleaner tank-cell flotation capacity at approximately 3 Mt/y. Each additional water cannon commissioned added a similar capacity. The initial flotation circuit refurbishment and ramp-up focused on bringing all cleaner circuit capacity on-line, before re-commissioning the second half of the rougher and scavenger capacity. The refurbishment and ramp-up was completed in March 2020, and throughput was increased to target the Phase 2 design of 12 Mt/y. This progressive ramp-up created significant challenge for the operators with mis-matched rougher-scavenger and cleaner capacities. The overall circuit was unbalanced and became cleaner- capacity limited as the throughput increased over 9 Mt/y.

The discrepancy between laboratory flotation test results and plant performance was a bugbear not only for the process development work but for operating plant improvement work. Positive results in the laboratory were often not replicated in plant operations. This limited confidence in investment to improve plant performance. The reasons for the variable and misleading results were not understood until the pulp chemistry issues were mastered.

Additional cleaner flotation capacity in an existing B22/6500 Jameson Cell was available, originally used in a carbonaceous gangue pre-flotation duty in the previous operation. Laboratory tests using the standard Glencore Technology Jameson Cell “mimic” procedure on cleaner 2 feed (after UFM) sample demonstrated potential for recovering approximately 50% of the cleaner feed zinc into a 50% Zn product. This would nearly double effective cleaning capacity, allowing throughput to be increased while maintaining zinc recovery. Accordingly, the Jameson Cell was commissioned in May 2021 in this cleaner scalping duty. It was unsuccessful in this duty recovering virtually no sphalerite. New Century Resources initiated a program to determine the reasons for this failure, leading to (a) an understanding of the detrimental pulp chemistry conditions caused by the UFM and the subsequent reactivity of the very fine mineral particles generated, and (b) the requirements for flotation of sphalerite and other sulfide minerals in these conditions.

MINERALOGY

The important minerals in the Century tailings are sphalerite, galena, silver minerals, pyrite, carbonaceous gangue, and silicates (mainly quartz and muscovite). The sphalerite is commonly in composites with silicates and very fine (<1 µm) carbonaceous gangue. The carbonaceous gangue (kerogen) is important for processing and concentrator quality as it is naturally hydrophobic. Silver mineral (typically in the form of freibergite) distribution closely follows galena based on a reasonable correlation between lead and silver assays, although some silver also occurs as an impurity in sphalerite (Waltho et al, 1993). Semi-quantitative mineragraphy conducted by McArthur Ore Deposit Assessments provides a good image in Figure 2 highlighting the challenges of the Century tailings.

Sphalerite liberation in the +8 μm fraction is poor and much of the sphalerite and silicate gangue is “diseased” with very fine carbonaceous gangue.

Each of these minerals has a different flotation rate constant as will the composite classes for each mineral particle size fraction. Fine mineral particles (less than 10 μm) such as treated at Century generally have a low flotation rate constant leading to a minor difference in flotation rate of sphalerite relative to other hydrophobic particles.

The Century tailings consist of a mixture of minerals previously exposed to flotation processing. Simply stated, the current plant feed consists of material that had either floated into a discard stream or reported to tailings. Liberation was therefore understood to be critical for the tailings retreatment to be successful, otherwise the minerals could be expected to respond similarly the second time around when being re-processed.

**Century Tailings Sp
SCAN**

Fine + CS5

April 2013

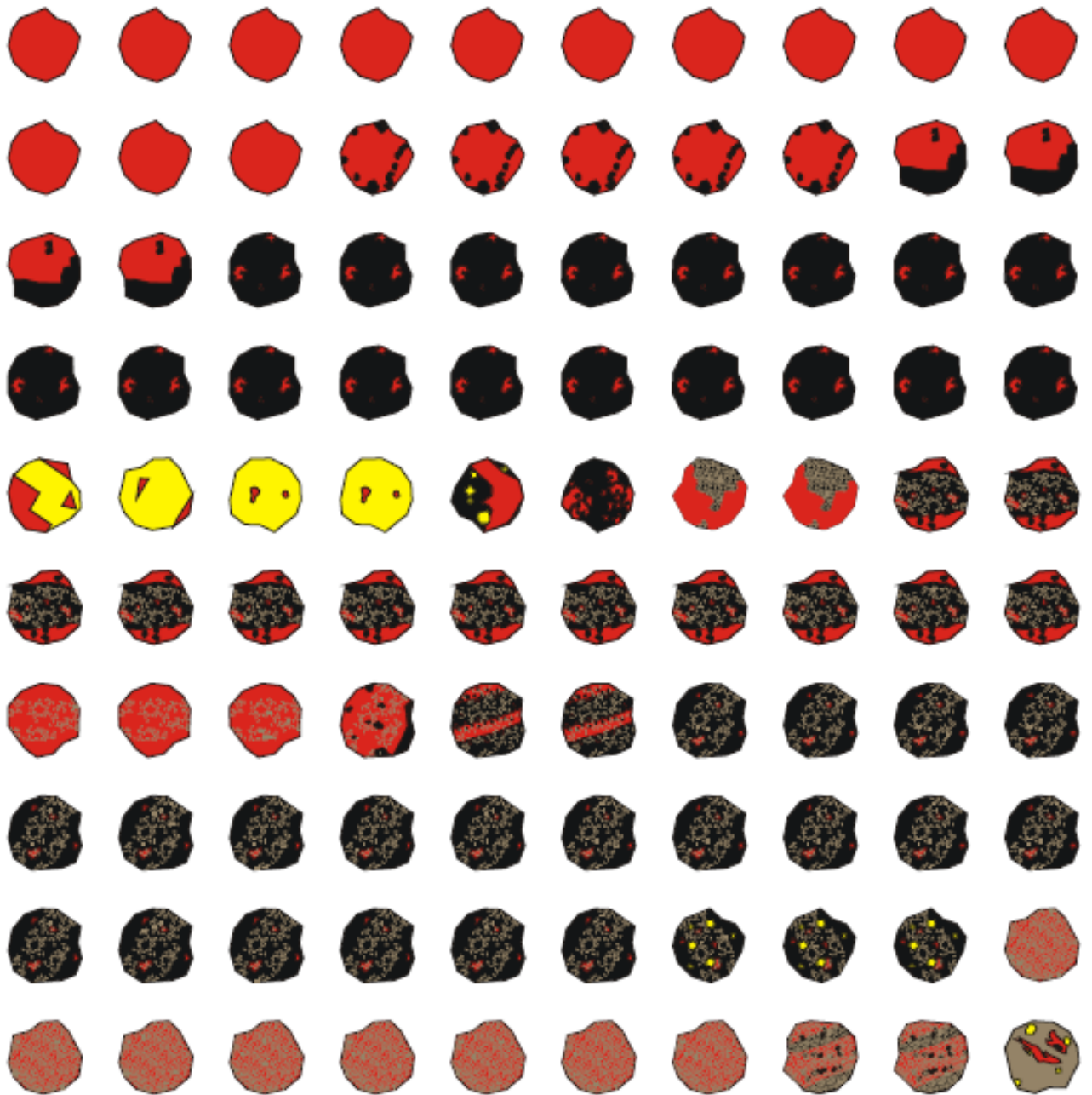


Figure 2: McArthur Ore Deposit Assessments particle map for a +8µm fraction of a Century tailings sample

PROCESS DESCRIPTION

The following description is for the 2018 concentrator design before changes made to improve metallurgical performance with increasing throughput. Tailings are reclaimed at a nominal rate of 9 Mt/y as a slurry from the storage facility by hydraulic mining as shown in Figure 3 (New Century Resources website, 2022). The screened slurry is pumped to surge tanks at the Century concentrator.



Figure 3: Tailings hydraulic mining

The surge tanks' slurry feeds first stage hydrocyclones, with overflow reporting to rougher flotation and underflow reporting to a 6.7 MW ball mill. Ball mill discharge reports to second stage hydrocyclones, with overflow reporting to rougher flotation and underflow returning to ball milling. The 2018 grinding design was modified to maximise the solids reporting to the ball mill rather than normal size reduction circuit practice of targeting a product size to flotation. This is because the zinc recovery benefit from "scrubbing" the tailings solids is greater than the benefit from increased sphalerite liberation; a common requirement for sulfide tailings retreatment (Munro et al, 2021).

All conventional flotation cells at Century are 100 m³ tank cells, except for one 200 m³ cell in a scavenger duty. Rougher and scavenger flotation is in two parallel banks at natural pH using copper sulfate activator, sodium isobutyl xanthate collector and MIBC frother. Rougher and scavenger residence time is approximately 65 minutes. Rougher and scavenger concentrates report to two parallel cleaner 1 banks and scavenger tailings are thickened before discharge to the Century pit. Cleaner 1 banks tailing reported to final tailings, and cleaner 1 banks concentrate reports to the UFM circuit. The UFM circuit consists of 2" and 3" hydrocyclone packs, with a design cut point of approximately 5.5 µm, and hydrocyclone underflow distributed to Stirred Mill Detritors (SMD). Hydrocyclone overflow and SMD discharge report to a surge tank, Tank 26 (equipment number TK 26 on flow sheets). Tank 26 discharges to three stages of cleaning in parallel banks of cleaners 2, 3, and 4, with tailings from each stage reporting back to the previous stage. Concentrates from the two cleaner 4 banks is final concentrate at 46 – 48% Zn and less than 8% SiO₂.

Final concentrate is thickened to 37% solids in a 37 m diameter thickener before discharge to concentrate storage tanks, and transport to the Karumba concentrate facility via positive displacement pumps and the 304 km pipeline.

A simplified process flow diagram at the completion of planned ramp-up in March 2020 is presented in Figure 4.

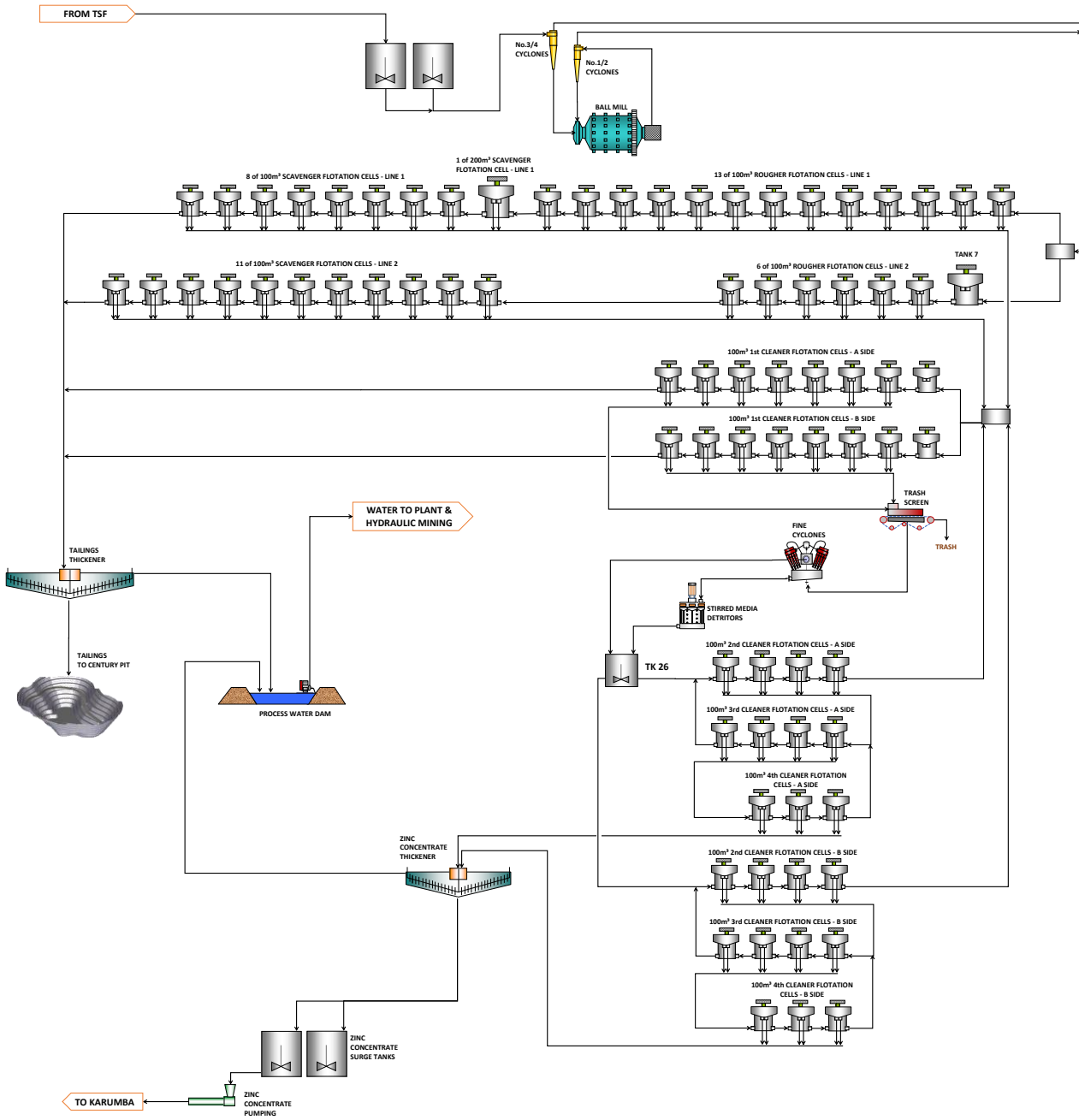



Figure 4: Century Dam tailings retreatment simplified process flow diagram March 2020

CHEMISTRY

The metallurgical results achieved during operations were below those from the laboratory bench scale and pilot plant test work. Of note, the lead grade in concentrate was more than double the expected 3%, and this impacted concentrate zinc grade which stabilised at 48% Zn compared with the expected range of 51 – 54.5% Zn. Zinc recovery was also significantly below expectations, and only when half the rougher-scavenger capacity with all of the cleaner capacity was operating at an annualised throughput of 8 Mt/y in August 2019 did plant performance approach laboratory performance with a mean 50.5% zinc recovery from August 2019 to January 2020.

Review of the possible causes for these differences suggested that the partial drying of tailings samples to allow compositing for testing may have preferentially oxidised galena and prevented it from floating, a situation which does not occur in processing. Yu et al (2009) provides the rest potential data for sulfide minerals in Table 1, including the important Century sulfide minerals pyrite, sphalerite, and galena.

Table 1: Sulfide mineral rest potential value

Mineral	Rest Potential (V,SHE)		
Pyrite	0.66	Most Noble	
Arsenopyrite	0.66		
Marcasite	0.63		
Chalcopyrite	0.56		
Sphalerite	0.46		
Covellite	0.45		
Bornite	0.42		
Galena	0.40		
Argentite	0.28		
Stibnite	0.12		
Molybdenite	0.11		Least Noble

It was often noted during operations that plant results could not be reliably mimicked in the site laboratory.

The site metallurgical improvement plan used data from mineralogical studies and laboratory test work, which showed that improved sphalerite liberation by decreasing cleaner feed P80 to 4.5 μm and washed-froth cleaner scalping could provide a significant increase in metal production. This would allow increased throughput while maintaining or improving zinc concentrate grade and zinc recovery. The mass and grade distribution data by size for a final concentrate sample is shown in Table 2, showing the significant benefit due to liberation in zinc and gangue element assay between the +4.5 μm and -4.5 μm fractions.

Table 2: May 2020 final concentrate mass and element department by size

Size Fraction	Mass %	%Zn	%Pb	%Fe	%SiO ₂
+4.5µm	28	37.2	7.2	7.36	11.1
- 4.5µm	72	52.6	4.3	1.15	5.94
Total	100	48.3	5.3	3.01	7.31

The results from a mimic Jameson Cell test on a cleaner feed sample from Tank 26 is presented in Table 3.

Table 3: Jameson Cell in “cleaner scalper” duty simulation test result

Product	% Mass	% Zn	Zn Recovery %	SiO ₂
Cleaner 3 Con 1-4 (Jameson Cell Concentrate)	29.4	49.8	50.5	3.94

The test results supported the investment case to refurbish and commission the B22/6500 Jameson Cell in a cleaner-scalper duty in May 2021, with the flow diagram presented in Figure 5. The performance of the Jameson Cell during commissioning was well below expectations, to the point where it really wasn't adding any value at all. A review of the cell operating conditions confirmed that it was operating within normal physical parameters but that very little sphalerite was floating, giving perhaps only 5 – 10% zinc recovery into a 45% zinc concentrate. Changes to copper sulfate and xanthate collector additions, wash water addition and feed density had no effect on performance. Turning the wash water off entirely decreased concentrate grade by approximately 10% Zn absolute demonstrating the efficacy of washed froth cleaning but did not increase zinc recovery, suggesting that the cell was not even operating on a flotation grade-recovery curve.

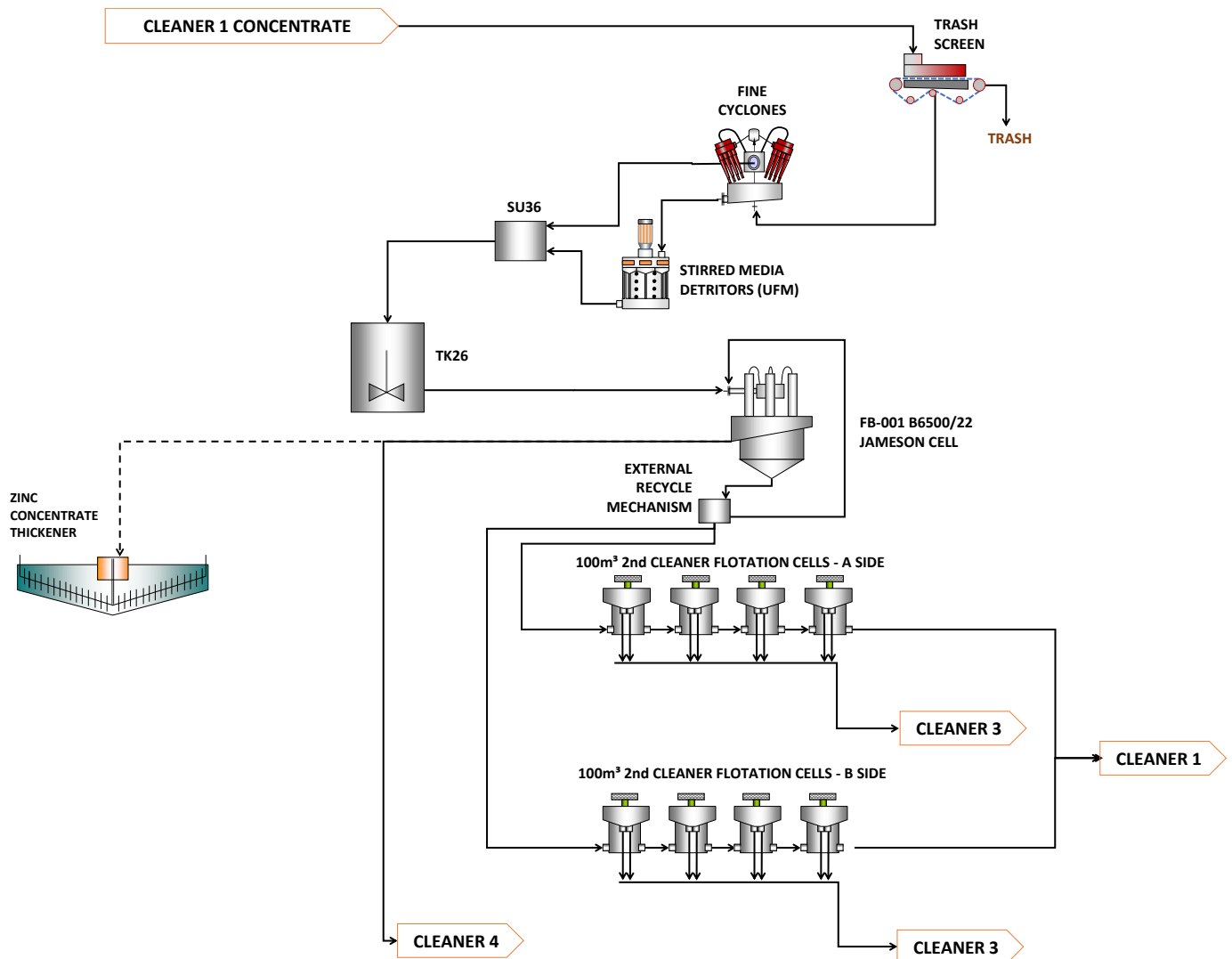


Figure 5: UFM and Jameson Cell simplified flow diagram

Pulp chemistry measurements were taken around the UFM circuit and the cleaner circuit, including pH, Eh, and dissolved oxygen (DO) and compared with the conditions required for sphalerite flotation;

- pH slightly below neutral to alkaline
- Eh greater than 0 mV SHE
- DO greater than 3 ppm.

The sample pulp chemistry conditions at Tank 26 appeared to be suitable on first readings with a pH of 6.7, approximately +200 mV SHE potential, and a DO of 4.5 ppm. However, it was noted that sample DO dropped rapidly over two minutes to less than 2 ppm.

This indicated that the pulp oxygen demand was not satisfied, and the conditions precedent for sphalerite to float were not met. Samples taken at the Jameson Cell gave a similar result. The UFM hydrocyclone overflow and underflow samples showed that oxygen demand in these streams was satisfied, but the UFM discharge samples showed a very high oxygen demand. The results from a DO survey are presented in Figure 6, showing that UFM discharge and cleaner 2 feed have less than 3ppm DO, compromising sphalerite flotation.

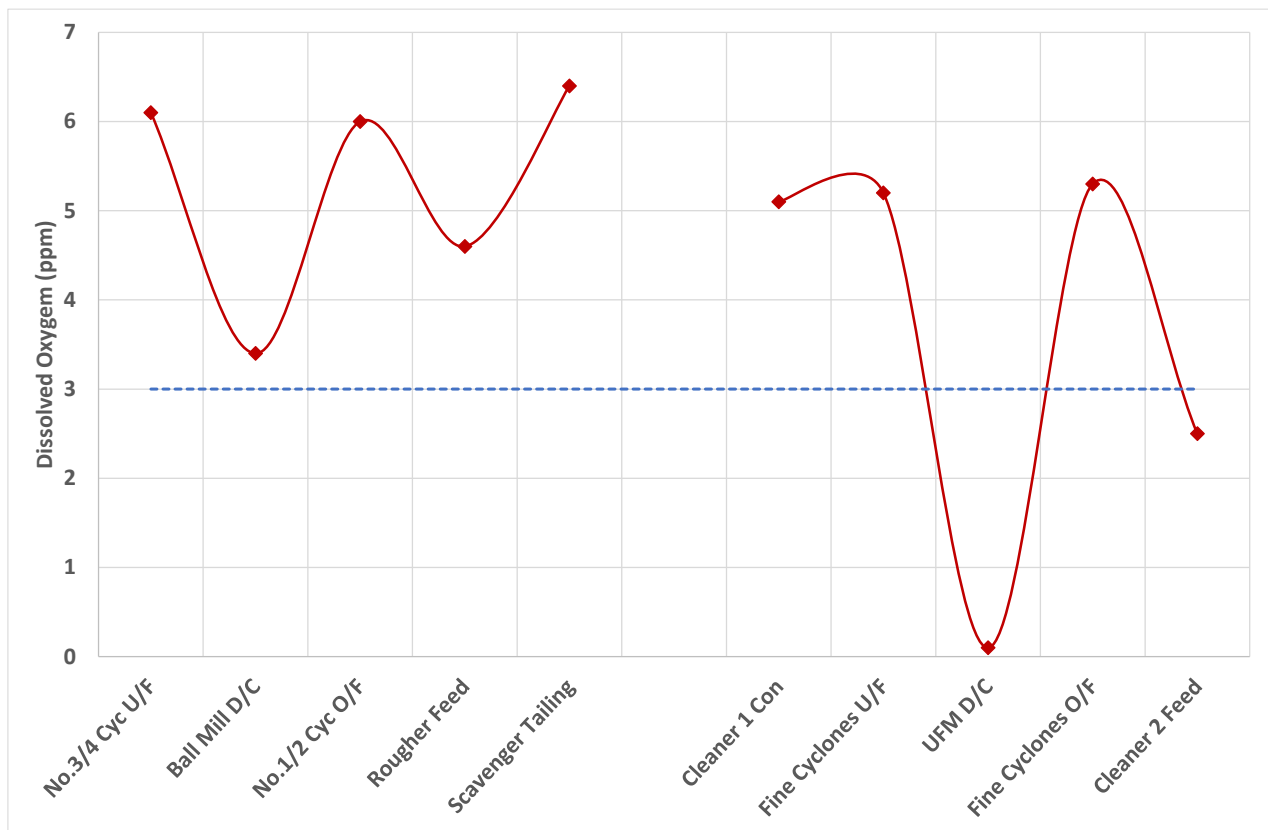


Figure 6: DO survey results

The conclusion was that the UFM discharge was the likely cause of poor sphalerite flotation performance due to the unsatisfied oxygen demand, and even mixing with UFM hydrocyclone overflow and a residence time of 65 minutes in Tank 26 did not provide enough aeration to increase DO for the whole stream to respond appropriately in the Jameson Cell.

CLEANER 2 OPEN CIRCUIT TRIAL

Cleaner 2 froth characteristics also seemed to tell a story; the froth appeared weakly mineralised in the first two cells of both of the parallel banks compared with the last two, suggesting that the pulp oxygen demand was slowly being satisfied down the bank and sphalerite flotation wasn't really getting going until late in the bank. The cleaner 2 tailings were reporting back to cleaner 1 feed before regrinding, so a cleaner 2 open circuit trial (cleaner 2 tailings to final tailings) was conducted in October 2021 to measure the impact of this closed circuiting on metallurgical performance. The simplified flow diagram showing closed and open circuit configuration is presented in Figure 7.

Dissolved oxygen profiles taken during the trial graphed in Figure 8 showed that recirculating cleaner 2 tailings was feeding pulp with a high oxygen demand back into cleaner 1. This compromised cleaner 1 performance with 8% lower zinc recovery in closed circuit as shown in Table 4. This lower recovery translated to a recirculation of 7.2 tph Zn back from cleaner 2 to cleaner 1.

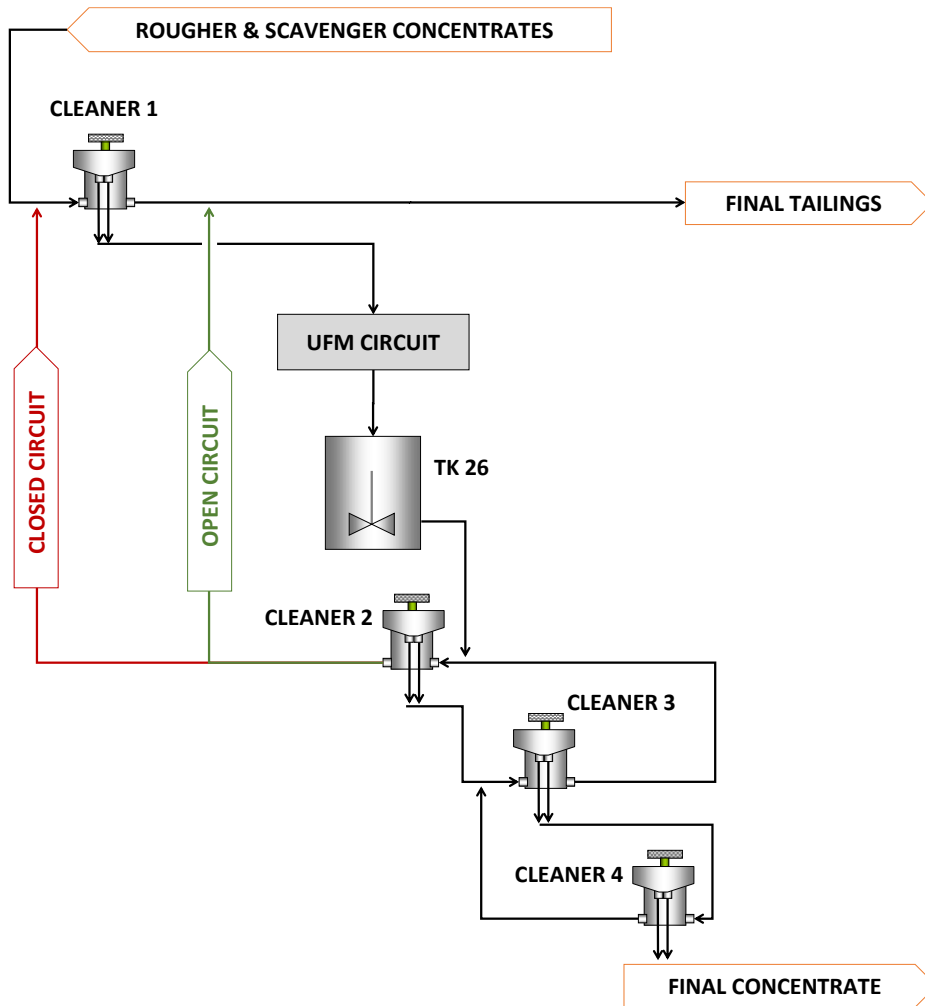


Figure 7: Cleaner 2 closed and open circuit configurations

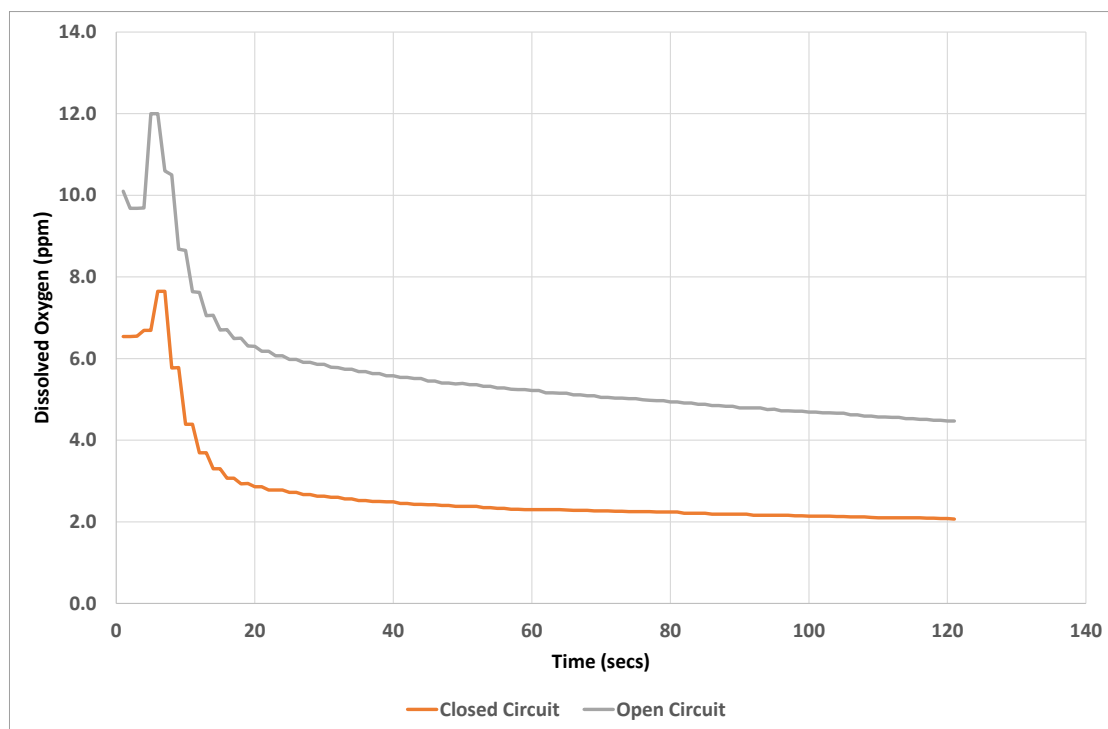


Figure 8: Cleaner 1 concentrate dissolved oxygen profile – closed and open circuit

Table 4: Cleaner 2 open circuit trial results

Circuit Configuration	Recovery (%)			
	Zn	Pb	Fe	Si
Cleaner 1 - Closed Circuit Cleaner 2	83.2	83.5	36.1	37.2
Cleaner 1 - Open Circuit Cleaner 2	91.0	89.5	51.9	48.6
Difference (Closed – Open)	-7.8	-6.0	-15.8	-11.4
Cleaner 2 - Closed Circuit Cleaner 2	61.4	51.1	29.3	25.8
Cleaner 2 - Open Circuit Cleaner 2	65.7	63.5	19.8	18.6
Difference (Closed – Open)	-4.3	-12.4	+9.5	+7.2

PLANT PULP CHEMISTRY MEASURES AND LABORATORY TEST WORK

Plant pulp chemistry

Multiple pulp chemical measurements of the three process streams of interest (hydrocyclone overflow, the UFM discharge and Tank 26 discharge) were collected between 17 to 19 December 2021. The pH, pulp potential (Eh), dissolved oxygen (DO) and temperature for each of the process streams are presented in Figure 9. The mean Eh-pH curve for this data appears in Figure 9, and the oxygen demand (OD) data are provided in Figure 10.

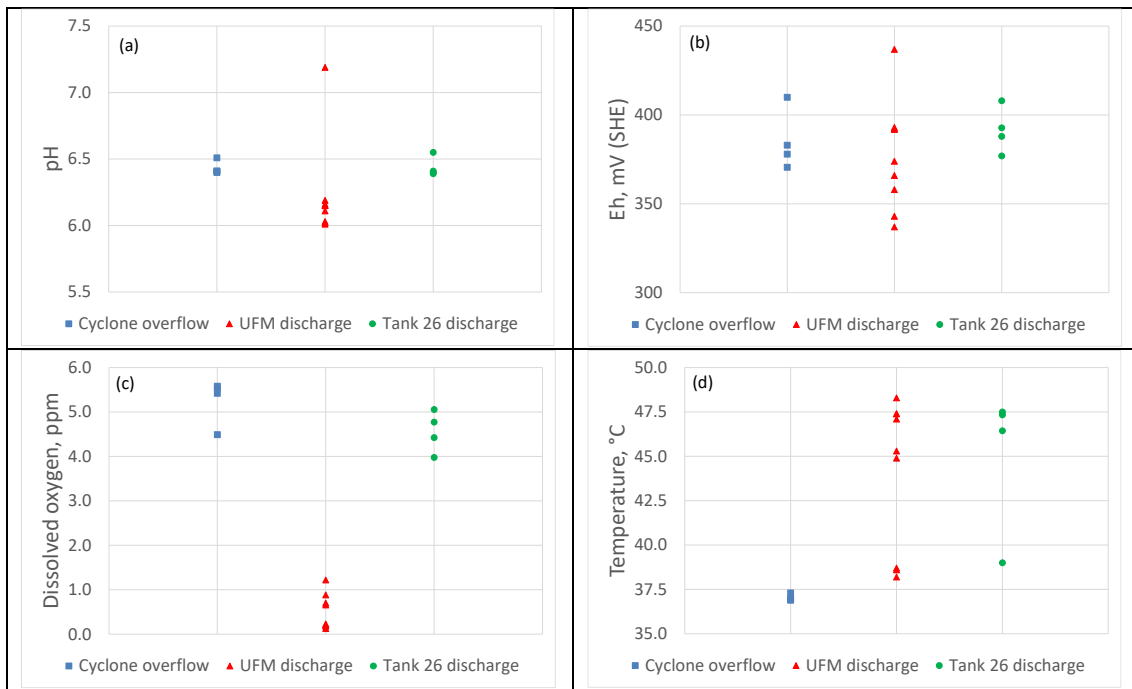


Figure 9: (a) pH; (b) Eh; (c) dissolved oxygen; and (d) temperature data for the hydrocyclone overflow, UFM discharge and Tank 26 discharge.

The first thing to note is that there is considerable scatter in the data. That is, the pulp chemical parameters do not stay constant, but vary markedly. This can be attributed mostly to changes in the mineralogy with time.

The pH through the circuit was slightly acidic (Figure 9(a)). There were subtle variations in the pH between each process stream; however, the UFM discharge appears to operate at a marginally lower pH compared with the hydrocyclone overflow and Tank 26 discharge.

The Eh throughout the circuit is oxidising (Figure 9(b)), typically around 375 ± 50 mV (SHE), with subtle variations. The data suggests that the UFM discharge tends to have a slightly lower Eh, but only marginally. Essentially, the pH and Eh in this part of the circuit do not vary greatly when examined individually, however when plotting the Eh-pH curve (Figure 10) the line is nominally perpendicular to the water-oxygen line indicating that oxidative reactions are occurring.

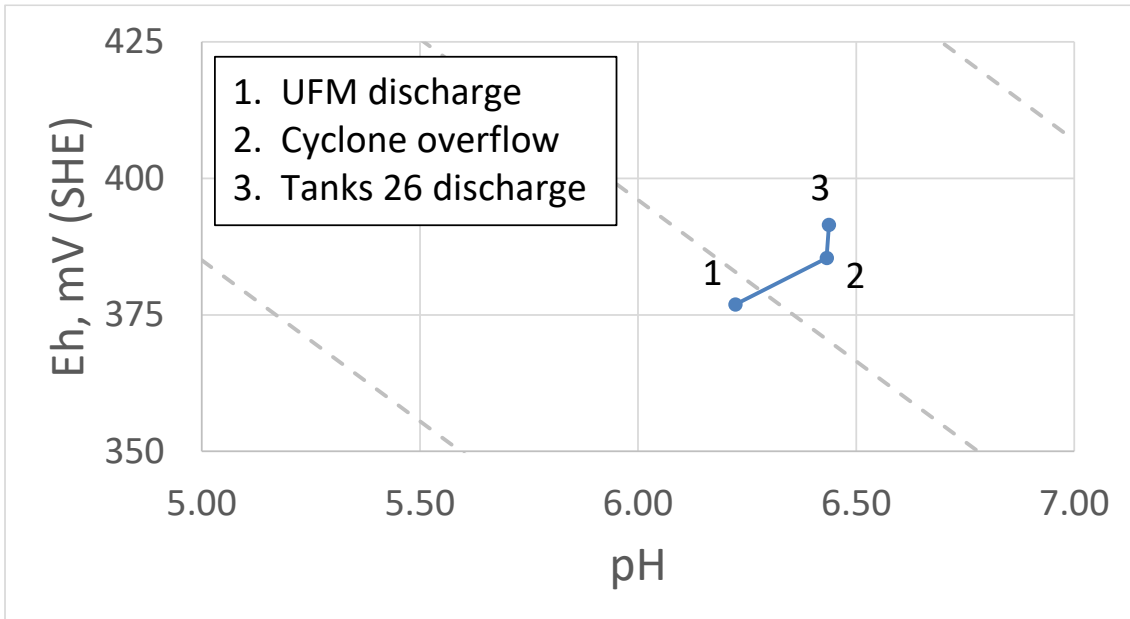


Figure 10: The Eh-pH curve

The dissolved oxygen content of the pulp showed significant variation (Figure 9(c)), with the hydrocyclone overflow having the highest readings at around 5.0 ppm. In contrast, the UFM discharge had a mean dissolved oxygen concentration of 0.5 ppm. Tank 26 discharge dissolved oxygen concentration was nominally 0.5 ppm lower than that reported for the hydrocyclone overflow.

An examination of the oxygen demand data (Figure 11 essentially says that the reactivity of the hydrocyclone overflow pulp is low (mean of 0.23 min^{-1}). However, the oxygen demand of the UFM discharge was considerably higher (mean of 3.98 min^{-1}). The increased reactivity in the UFM discharge is related to a number of factors. First and foremost, as the grinding process reduces the particle size (and increases the surface area) the reactivity of the pulp will increase, and secondly as the only oxygen entering the regrind mill is in the hydrocyclone underflow (mill feed) as it is consumed and not replaced so the oxygen demand is driven higher. The oxygen demand of Tank 26 discharge was also high (0.92 min^{-1}). It is apparent that the pulp chemistry of the UFM discharge when mixed with the hydrocyclone overflow has a marked impact on the reactivity of the Tank 26 discharge.

Pulp temperature while not strictly a pulp chemical parameter does influence the solubility of oxygen in the aqueous phase. That is, as the temperature increases the solubility of oxygen in water decreases. This will influence the Eh, the dissolved oxygen and oxygen demand. The pulp temperature will be influenced by seasonal variations, differences in ambient temperature between day and night, the dissipation of energy during grinding, as well as the oxidation of sulfide minerals (for example, the oxidation of pyrite is an exothermic reaction and will increase the temperature of the pulp). It is apparent in the data presented in Figure 9(d) that the pulp temperature of the UFM discharge was 5 to 10°C higher than the hydrocyclone overflow. It is also evident that the pulp temperature of Tank 26 discharge is nominally the same as the UFM discharge.

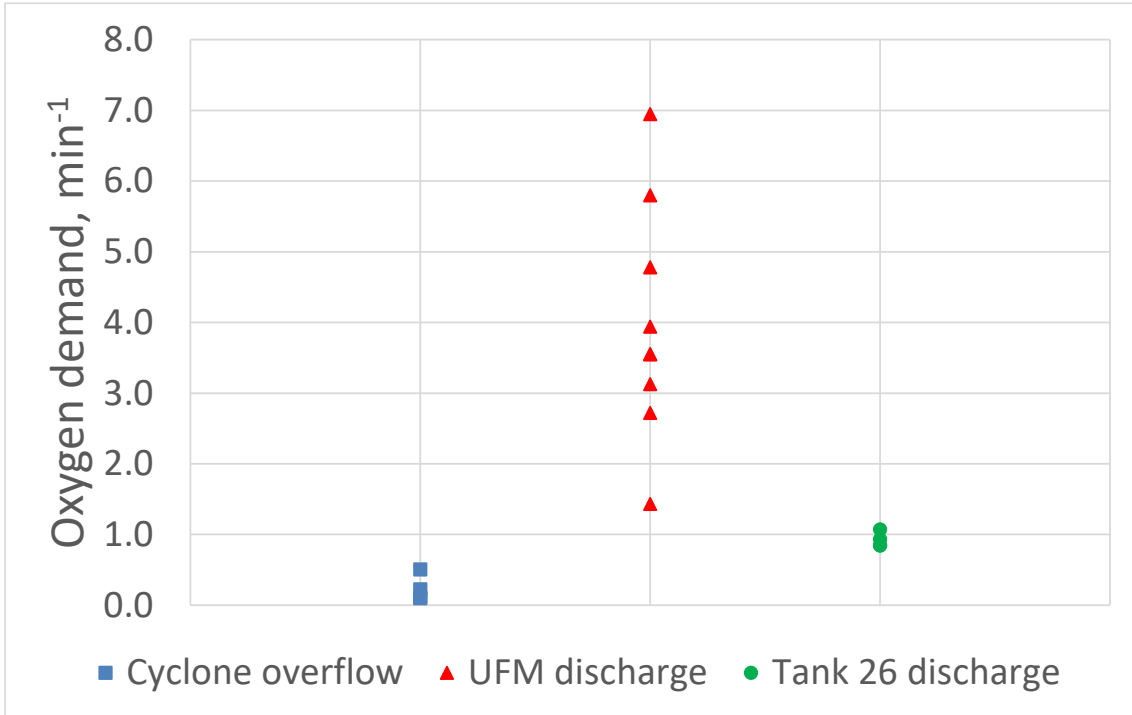


Figure 11: Oxygen demand data

Can the UFM discharge oxygen demand be reduced?

Historic data (Figure 12) indicated the zinc grade/recovery curve for the UFM discharge is inferior to that generated for the hydrocyclone overflow. The pulp chemistry data clearly shows that the UFM discharge oxygen demand is significantly higher than the hydrocyclone overflow, and this is likely to be a contributing factor to the poor sphalerite flotation reported for the UFM discharge. Therefore, a focussing question is: Can the UFM discharge oxygen demand be reduced?

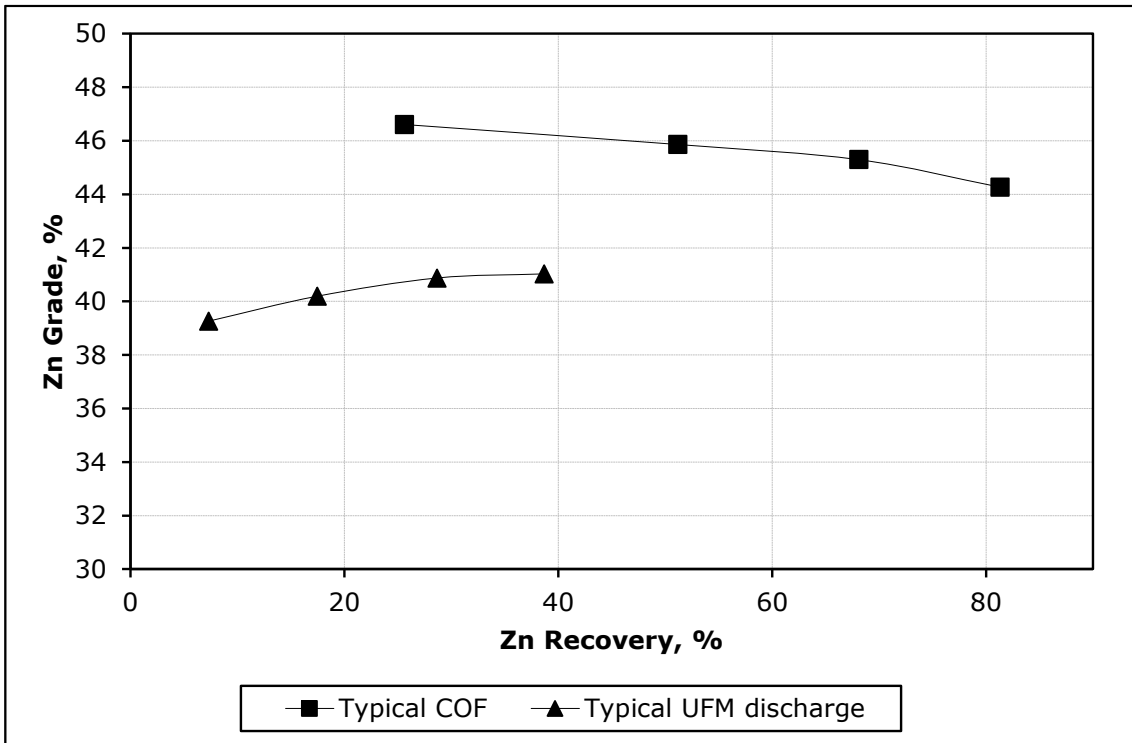


Figure 12: Typical zinc grade/recovery curves for the hydrocyclone overflow and UFM discharge

Two aeration tests were completed, and the results are presented in Figure 13. The first point to note is that the oxygen demand of the pulp at time zero was significantly higher than that measured in the plant at the UFM discharge. For example, on 17 December the plant UFM discharge was 1.43 min⁻¹, and this had increased to 4.60 min⁻¹ after collecting the sample, walking it to the laboratory and transferring it to the flotation cell. This indicates that the pulp exiting the UFM is very reactive and “hungry” for oxygen, consuming what little oxygen that was in the pulp during the journey from the plant to the laboratory.

The second point to note is that as the aeration time increased the oxygen demand decreased, and after nominally 60 minutes of aeration the oxygen demand approached that measured in the hydrocyclone overflow. It is also evident that aeration increased the dissolved oxygen content of the pulp, but even after 60 minutes the dissolved oxygen concentrate of the UFM discharge was significantly lower than that measured in the hydrocyclone overflow (Figure 14). This suggests that there may be a need to aerate the pulp for a longer period of time.

Ultimately, this work has demonstrated that the addition of oxygen in some form can significantly reduce the oxygen demand of the UFM discharge.

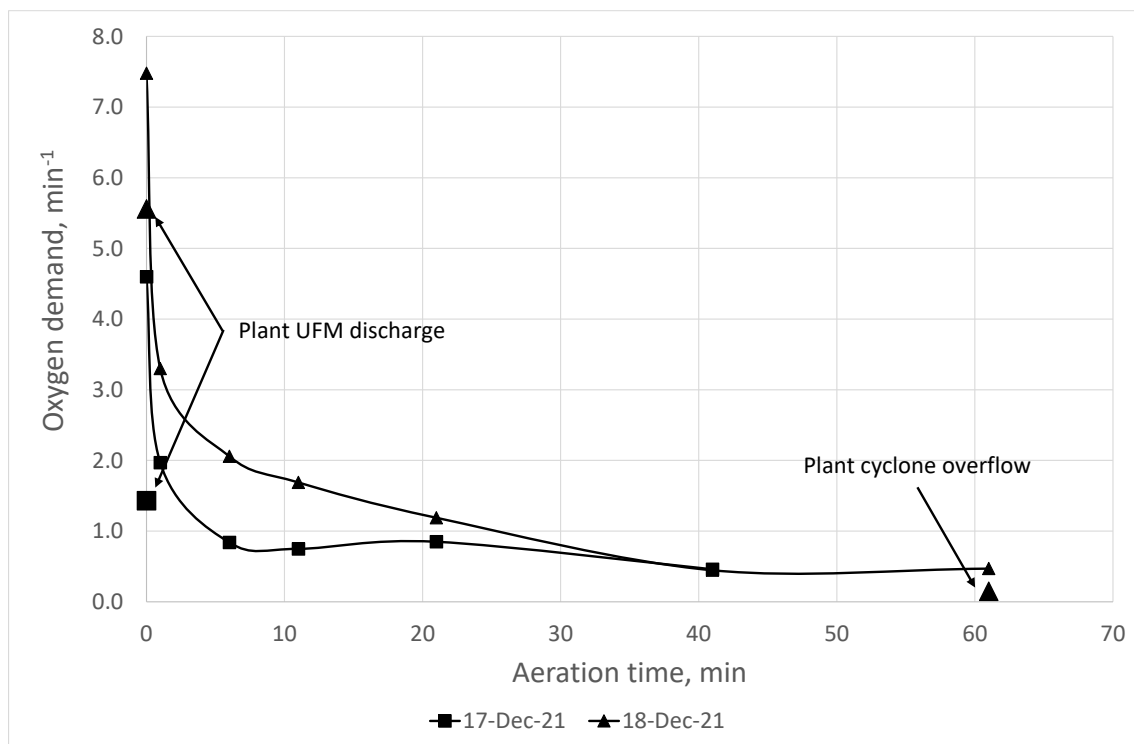


Figure 13: Aeration time versus oxygen demand for the UFM discharge

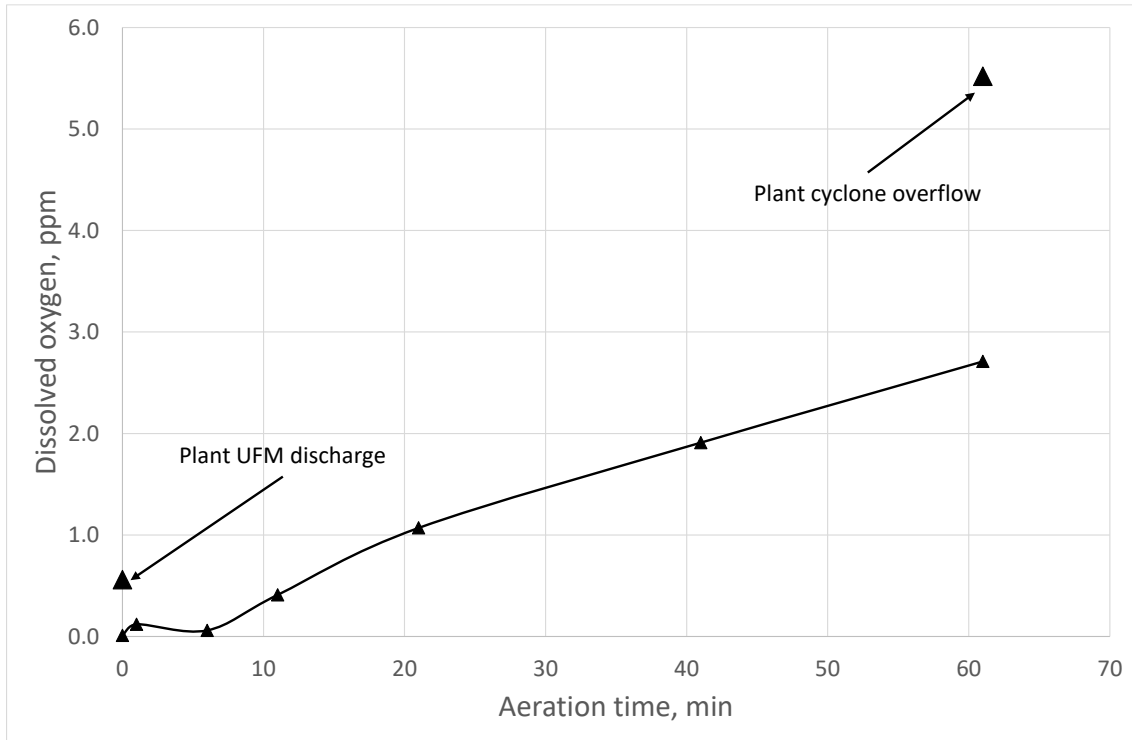


Figure 14: Aeration time versus dissolved oxygen concentration for the UFM discharge

UFM discharge sphalerite flotation response

Based on the pulp chemistry observations a series of flotation tests were completed investigating the effect of aeration and higher reagent additions on sphalerite flotation from the UFM discharge. Conditions tested were:

1. As received (391 g/t CuSO_4 + 174 g/t SIBX);
2. Aeration for 60 minutes (391 g/t CuSO_4 + 174 g/t SIBX);
3. Higher reagents (1184 g/t CuSO_4 + 526 g/t SIBX); and
4. Aeration for 60 minutes plus higher reagents (1235 g/t CuSO_4 + 549 g/t SIBX).

These tests were completed at the as received pulp density (nominally 30% solids) as a reliable, reproducible method for diluting this stream to the same percent solids as the hydrocyclone overflow without adversely effecting pulp chemistry has not been developed.

The plant pulp was transferred to the 5 L flotation cell, and conditioned for two minutes to homogenise it. During this time, the oxygen demand of the pulp was measured. For aeration tests the agitator speed was set at 300 r/min prior to introducing air at 5 L/min for the prescribed period of time. The pulp was then conditioned with copper sulfate, collector and frother before increasing the impellor speed to 500 r/min and turning the air on to 7 L/min for flotation. Four timed concentrates were collected after 0.5, 1.5, 3.0 and 5.0 minutes for a total of 10 minutes. Process water was used to maintain the pulp level in the flotation cell.

The feed grades for the four tests are provided in Table 5. The feed grades did vary marginally, given that the four samples were collected at different times through the day. However, the variations are considered minor therefore a comparison of the tests is valid.

Table 5: Test feed grades

Test	Zn %	Pb %	C %	IS %	SiO ₂ %
As received	25.99	5.78	4.94	8.27	27.47
Aeration	25.32	5.98	4.93	8.93	27.48
High reagents	26.34	5.28	5.02	8.08	27.68
Aeration and high reagents	26.15	4.99	5.05	8.44	27.70

An examination of the pulp chemistry measurements during the flotation tests revealed that the pH and Eh were reasonably similar, and did not vary markedly between tests. However, the dissolved oxygen did display some movement. The UFM discharge dissolved oxygen concentration for all four tests was nominally the same at 0.2 ppm (Figure 15). Following aeration, the dissolved oxygen content had increased to at least 2.4 ppm, but decreased to zero after conditioning with reagents just prior to flotation in all cases. By the end of flotation, the dissolved oxygen levels had increased to over 4.0 ppm.

It was interesting to note that even after aerating the pulp for 60 minutes, the dissolved oxygen concentration dropped to zero following conditioning with reagents. This suggests that simply bubbling air through the pulp is not an effective means of introducing oxygen to the pulp to reduce the oxygen demand.

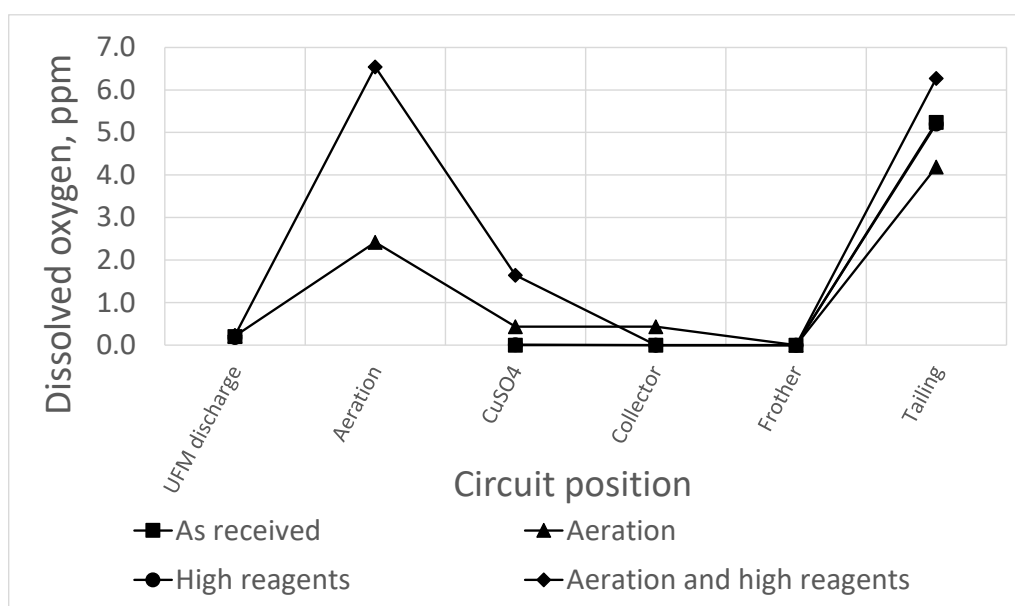


Figure 15: The dissolved oxygen profile for the flotation tests

The zinc grade/recovery curves are presented in Figure 16, with the iron sulfide (IS) and silica selectivity curves reproduced in Figure 17 and Figure 18. The zinc recoveries at 30.2% Zn concentrate grade are provided in Table 6, with the zinc concentrate grade and diluent recoveries at 43% zinc recovery reported in Table 7.

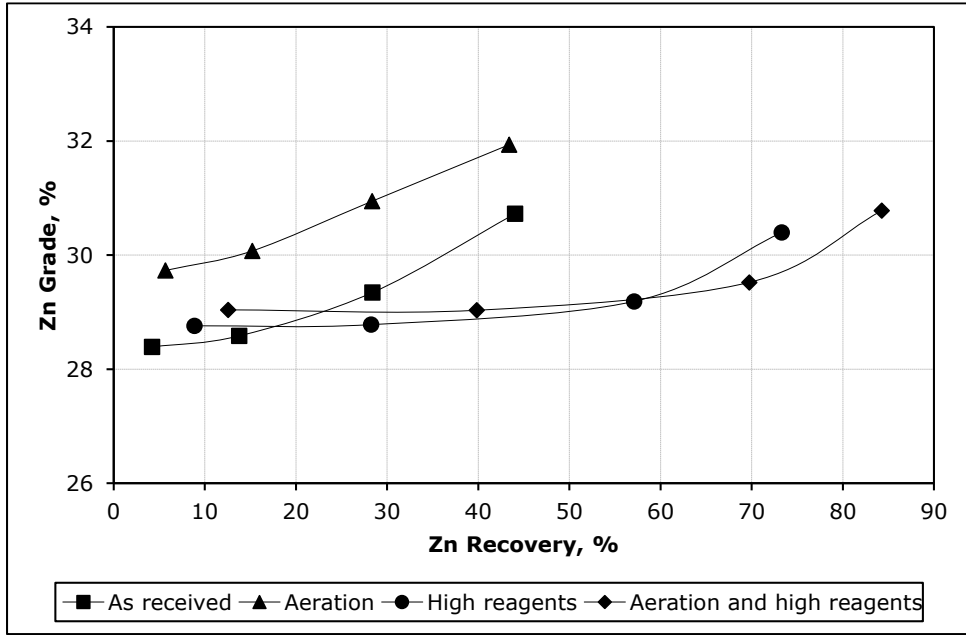


Figure 16: Zinc grade/recovery curves

An examination of Figure 16 reveals that aerating the as received pulp shifted the zinc grade/recovery curve up to higher concentrate grades. For example, at 43% zinc recovery the zinc concentrate grade increased by 1.3% Zn (Table 7). This increase in zinc concentrate grade can be attributed to improved selectivity for sphalerite against iron sulfides (Figure 17). However, simply aerating the pulp did not improve the zinc recovery.

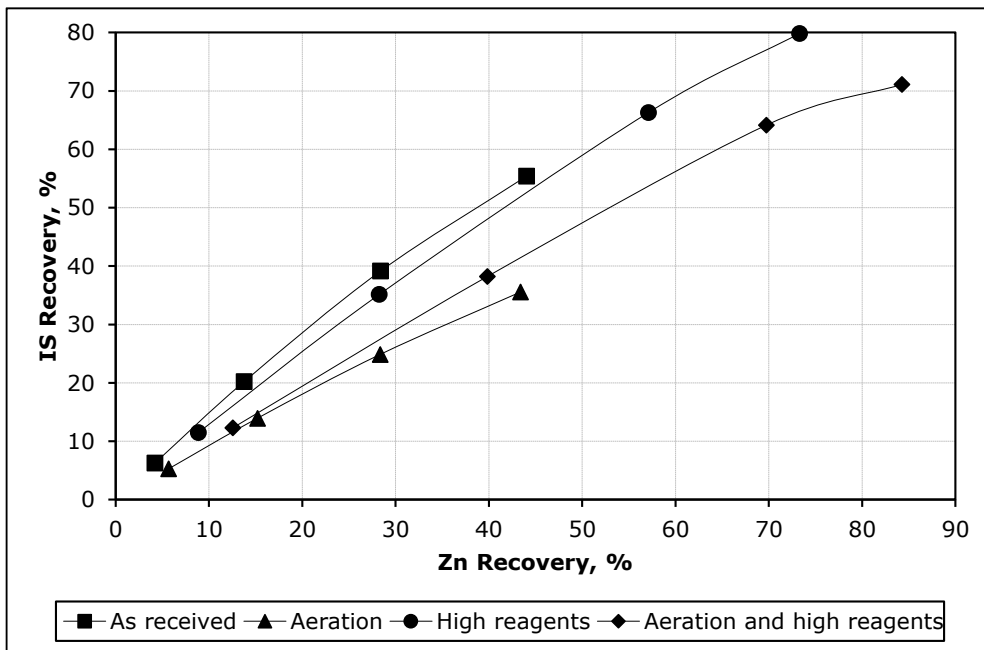


Figure 17: Zinc-iron sulfide selectivity curves

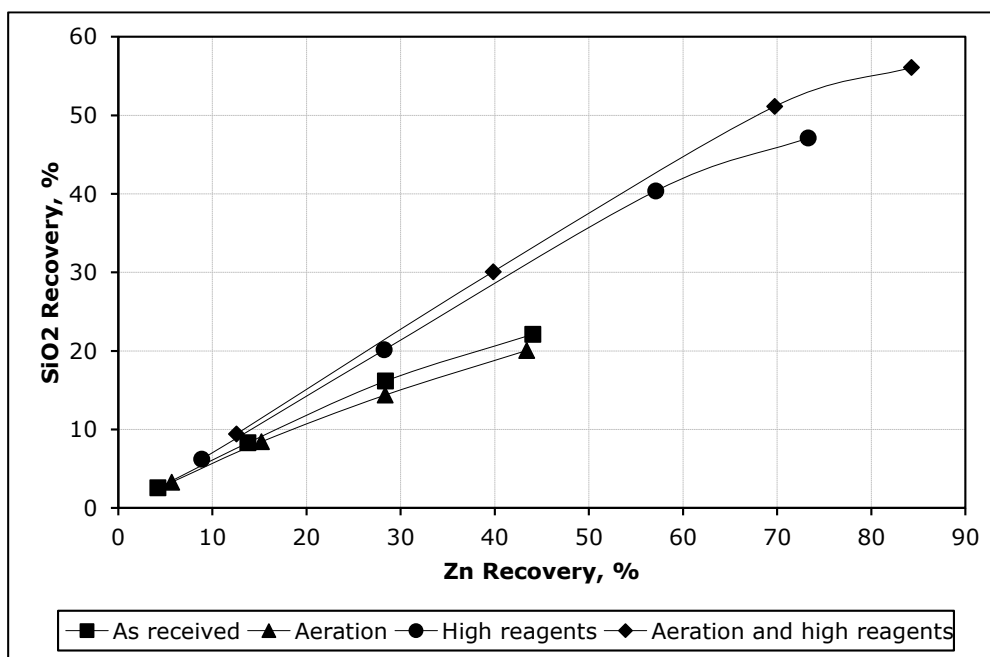


Figure 18: Zinc-silica selectivity curves

Table 6: Zinc recovery at 30.2 percent zinc concentrate grade

Test	Zn recovery, %
As received	38.1
Aeration	17.1
High reagents	70.6
Aeration and high reagents	77.6

Table 7: Zinc concentrate grade and diluent recoveries at 43 percent zinc recovery

Test	Zn grade, %	Diluent recovery, %			
		Pb	C	IS	SiO ₂
As received	30.6	64.5	34.8	54.4	23.2
Aeration	31.9	63.3	34.5	35.3	21.8
High reagents	29.0	54.5	36.7	51.1	31.2
Aeration and high reagents	29.1	48.6	37.5	41.0	33.1

The addition of considerably more copper sulfate and collector did result in as significant shift in the zinc recovery. That is, at 30.2% Zn zinc concentrate grade the zinc recovery increased from 38.1% (for the standard test) to 70.6% when more reagent was added (Table 6). This increase in recovery was accompanied by a deterioration in zinc concentrate grade as more silica was recovered. This is unsurprising given the intimate intergrowths of sphalerite and silica in the Century ore body.

The combination of aeration and the higher reagent addition produced another step change in zinc recovery. At 30.2% Zn concentrate grade, the zinc recovery was 77.6% compared with 38.1% for the standard test (Table 6). The zinc concentrate grade was again lowered; however it is apparent that the aeration step led to an improvement in selectivity for sphalerite against the iron sulfides, but this was off-set by a deterioration in the selectivity against silica. This is further emphasised when the zinc and silica grade are plotted against one another (Figure 19). There is a strong linear relationship between the two providing additional evidence that sphalerite and silica are strongly associated. This inevitably means that any increase in zinc recovery will be accompanied by an increase in silica

recovery unless adequate liberation is achieved (i.e., a P_{80} of 5 μm or less (Munro, 2021)). Added to this, the zinc grade/recovery curves for the higher reagent addition tests are reasonably flat giving further weight to the notion that liberation is also a problem.

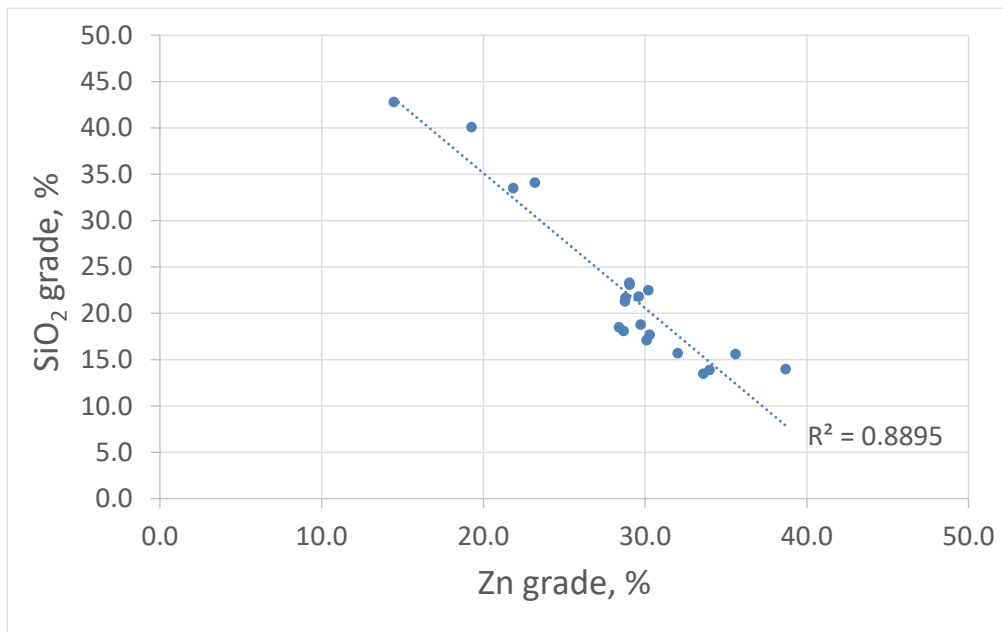


Figure 19: Zinc versus silica grade relationship

Points to note

The following points are worth keeping in mind when considering flotation of the UFM discharge:

1. Re-grinding will increase the pulp temperature, and at these higher values (e.g., +45°C) it is likely that the xanthate collector will start to decompose.
2. Time-of-Flight Secondary Ion Mass Spectrometry analysis undertaken by the University of South Australia on samples of UFM feed and discharge indicated that surfaces of sphalerite particles leaving the UFM had a lower concentration of copper than the feed.
3. Re-grinding to the desired P_{80} value to liberate the silica from the sphalerite (typically around the 5 μm mark) will see a significant increase in the surface area.
4. The large surface area and high temperatures of the pulp generated during re-grinding will produce very low dissolved oxygen concentration, which will have a number of influences:
 - a. The oxygen content of the pulp may be too low for collector adsorption;
 - b. There is insufficient oxygen in the pulp to react with pyrite, passivate its surface and render it hydrophilic. This would lead to loss in selectivity and lower zinc grades.
 - c. High oxygen demand values (i.e., the pulp is very reactive).

These four points suggest that the UFM discharge requires additional copper sulfate and collector for the sphalerite to float.

Liberation is key, particularly liberation of silica from sphalerite. If liberation is not achieved it is likely that for every 1% abs. increase in zinc recovery there will be about 0.6% increase in silica recovery, based on the limited data set collected for these flotation tests presented in Figure 20. Therefore, routine mineralogical analysis is required to understand the locking characteristics of the sphalerite and silica, as well as confirm the target regrind size.

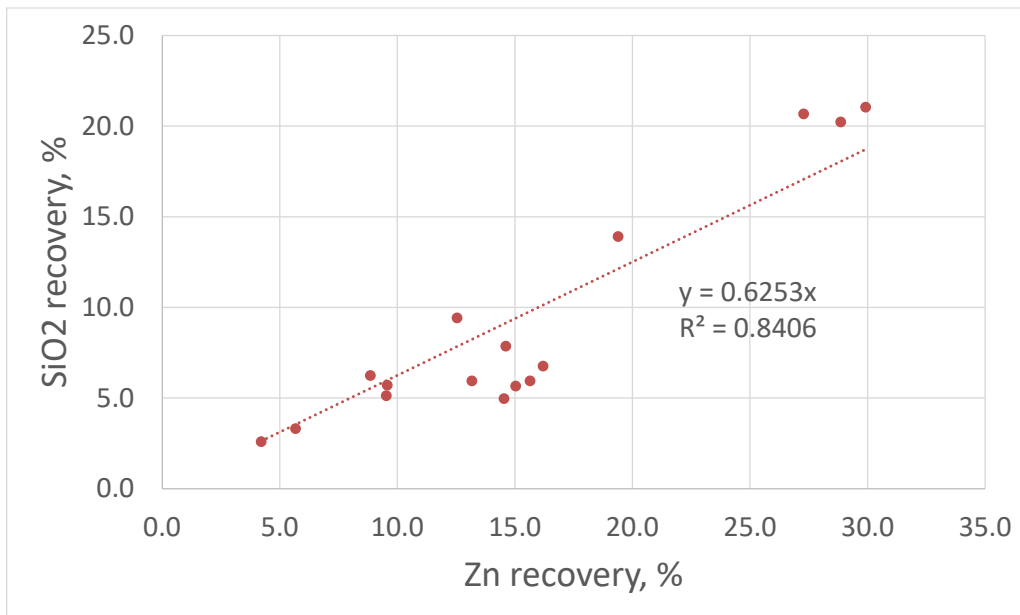


Figure 20: Zinc recovery versus silica recovery relationship for the flotation tests conducted in this study.

CONCLUSIONS

The following conclusions can be drawn from this study:

1. The plant pulp chemistry surveys confirmed that oxygen demand of the UFM discharge is markedly higher (3.98 min^{-1}) than that of the hydrocyclone overflow (0.23 min^{-1}), and Tank 26 discharge is between these extremes (0.92 min^{-1}).
2. The addition of oxygen either by aeration or the addition of dilute hydrogen peroxide did bring the oxygen demand of the UFM discharge down to a value like that reported for the hydrocyclone overflow.
3. In terms of sphalerite flotation compared to the base case:
 - a. Aeration for 60-minutes did increase zinc concentrate grade; attributable to an improvement in selectivity against iron sulfides. However, the zinc recovery did not increase.
 - b. Increasing the copper sulfate and collector did increase the zinc recovery markedly (greater than 30%), but the zinc concentrate grade remained low due to poor selectivity against iron sulfides and silica.
 - c. Combining aeration and the higher reagent additions increased the zinc recovery by a further 7%, but the zinc concentrate grade remained low. The selectivity against iron sulfide had improved but this was off-set by the poor selectivity against silica.
 - d. The zinc grade/recovery curves are comparatively flat suggesting that sphalerite/silica liberation is an issue.

The work strongly suggested that a three-pronged approach was required to improve the zinc recoveries following regrinding:

1. The particles must be reground to adequately liberate the sphalerite from the silica (and other gangue species), to improve the zinc concentrate grade;
2. The pulp chemistry must be adjusted using some form of oxygen to improve collector adsorption, but also oxidise the iron sulfides, which will lift the zinc concentrate grade; and
3. Add sufficient copper sulfate and collector to increase the zinc recoveries.

The aforementioned items 1 and 3 were already possible with existing equipment leaving item 2 as the key to achieving the conditions required for a step-change in Century metallurgical performance. In December 2022 a Hyperjet air injection system was installed in Tank 26 as part of an experimental program to satisfy UFM product oxygen demand before cleaner flotation. A photograph of the Hyperjet system is shown in Figure 21, with optimisation work ongoing at time of publication.



Figure 21: Tank 26 Hyperjet system

REFERENCES

1. New Century Resources website <https://newcenturyresources.com/century-mine-project/>, accessed 8 December 2022.
2. Burgess, F., Reemeyer, L., Spagnolo, M., Ashley, M., Brennan, D., *Ramp Up of the Pasminco Century Concentrator to 500 000 tpa Zinc Metal Production in Concentrate*, pp153-163, in *Proceedings Eighth Mill Operators' Conference*, Townsville 2003 (AusIMM: Melbourne).
3. A.E. Waltho, S.L. Allnut, A.M, Radojkovic, *Geology of the Century Zinc Deposit*, p125, *Proceedings International Symposium – World Zinc '93* (AusIMM: Melbourne)
4. *Electrochemistry of Flotation of Sulfide Minerals*, Y.Hu, W.Sun, D.Wang, Tsinghua University Press, 2009, p62.
5. Munro, P., Barnes, K., Bennett, D., *Tales of Tails – Values from Liabilities?*, p273 in *Proceedings Mill Operators' Conference 2021*, Brisbane, (AusIMM: Melbourne)

Metallurgists and Modifying Factors: How Mets Can Change the World!

G Deans¹

1. Director, Modifying Factors, Level 2, 70 Hindmarsh Square, Adelaide SA 5008
email: Geoff.Deans@modifyingfactors.com

ABSTRACT

There is little controversy or debate around the proposition of why or what natural resources are essential to enable the transition to a decarbonised society.

For these valuable metals to be useful, they first need to be extracted and purified from the naturally occurring compounds in the earth's crust, or by using existing recycled materials, in a such a way that the impacts are understood and acceptable. A material challenge the resources sector is collectively facing is how the process of project development and resource extraction can be realised in a way that is acceptable to crucial stakeholders. These stakeholders include, but are not limited to, governments, communities, investors, lenders, insurers, auditors and regulators.

As the resources are fixed, the potential impact of Modifying Factors (mining, processing, metallurgical, economic, infrastructure, marketing, legal, environmental, social and governance factors) can have a material effect on the attributes of a Mineral Reserve (JORC, 2012) and overall project viability.

The opportunities and challenges for the resources sector are material as the transition away from fossil fuels occurs. By extension our dependence on mineral resources will increase, with demand for many critical minerals expected to grow multifold by the middle of this century (United Nations, 2023). In order to realise the value and utility of these minerals, they must be first economically extracted, processed and sold.

WHY 'METS' MATTER!

Metallurgists or 'Mets' are the crucial innovators and creators of the new technologies and processes that will underpin the adaptability and improvement of mineral processing. To de-risk and optimise the required pipeline of projects 'first principles' or scientific thinking is required to do more with less. Metallurgists are tasked with mitigating the 'transition risks' created by changes in the regulatory landscape, stakeholder risk acceptance, investor expectations, consumer pressures and preferences by devising flow sheets that enable substantial reductions in waste, particularly waste rock, and tailings, whilst decreasing energy and water consumption. The consequences of the processing infrastructure and technology selections to the risk profile, impact profile and value proposition of a project are material, with the impacts underpinning the life of mine performance across the financial, technical, environmental and social domains.

Resources, Reserves and Reasonable Prospects for Economic Extraction

Whilst each orebody, project and context are unique, there are a common set of 'factors' for consideration that will directly, indirectly and cumulatively influence the prospects for economic extraction. Globally, these are defined as 'Modifying Factors' and underpin asset 'cut-off grade' assessments and demonstrating the preconditions (pathway to delivery) *and* considerations (price, quality, and quantity) required to report an Ore Reserve. These factors are defined by CRIRSCO as the Committee for Mineral Reserves International Reporting Standards and are reflected in the National

Reporting Organizations standards and reporting templates that provide the global common definition for Modifying Factors (CRIRSCO, 2019, Figure 1).

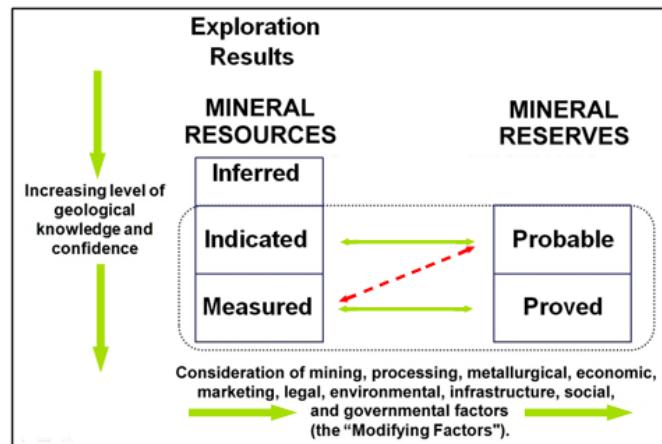


Figure 1 - The CRIRSCO International Reporting Template (2019)

The CRIRSCO Standard Guidelines (2019) state that ‘the effect of any of a Modifying Factor on the likely viability of a project and/or on the estimation and classification of the Mineral Reserves must be fully explained’. This is reflected in the ‘if not, why not’ principle of The Australasian Code for Reporting of Exploration Results, Mineral Resources and Ore Reserves or the ‘JORC Code’ (2012). The CRIRSCO Standard (2019) also states that ‘Mineral Resource estimates must have reasonable prospects for eventual economic extraction’. To enable an assessment of ‘reasonable prospects’ a project can define a ‘design criteria’ that reflects the explicit goals that a project must achieve in order to be successful. A materiality assessment that assesses each Modifying Factor as independent consideration is important, but in practice, Modifying Factors do not behave in isolation. There are dynamic trade-offs and feedback loops between factors that will influence multiple factors concurrently creating multi-factor risk. Multi-factor risk can materially influence the net impact on the project design criteria and in turn, overall prospects for economic extraction.

Impact trends – more minerals, more waste, more impacts

A consequence of this projected global demand for minerals is an intensification of mining activities and an increase in associated land disturbance (Valenta et al, 2023). In the domain of the four metals needed in many batteries: copper, lithium, manganese, and mine waste volumes, waste rock and tailings are likely to rise ‘exponentially’ (Valenta et al, 2023). This projected increase in project developments will lead to more intrusions into existing natural ecosystems and social structures, resulting in more interactions and more impact pathways. These interactions highlight the concurrent overarching trends of ‘complicated’ (systems and rules based) and ‘complex’ (global, non-linear and fluid) that frame the major challenge the global minerals sector is now collectively facing; specifically, *how* technically and economically viable resources can demonstrate ‘reasonable prospects for economic extraction’ when reconciled with the impacts from ‘Modifying Factors’.

Case study - Complex Orebodies and Global Copper

Copper is currently responsible for the largest mining footprint and the largest amount of mine waste worldwide (Valenta et al, 2023) and is shown in shown in Figure 2. Copper is responsible for the largest quantity of tailings, with 40% of global stored tailings, according to corporate disclosures recorded by Franks et al. (2021). If this trend continues, the total amount of mining waste generated by the mining sector over the 2020-2050 period could be in the order of 2000 Gt of tailings and

waste rock. Tailings generation over the next three decades could amount to US\$1.6 trillion in additional storage costs (using Cox et al.'s 2022 estimation of US\$2.29/t). In short, to realise the value from the copper deposits storage of water, rock and tailings will be required as a precondition of development. This expanded footprint exacerbates mining-induced pressures on the local context, affecting land, water, and other resources connected to livelihoods (Owen and Kemp, 2019). The associated cultural, economic, and ecological value destruction can be devastating, particularly for land-connected peoples such as Indigenous or agrarian communities (Owen et al., 2022).

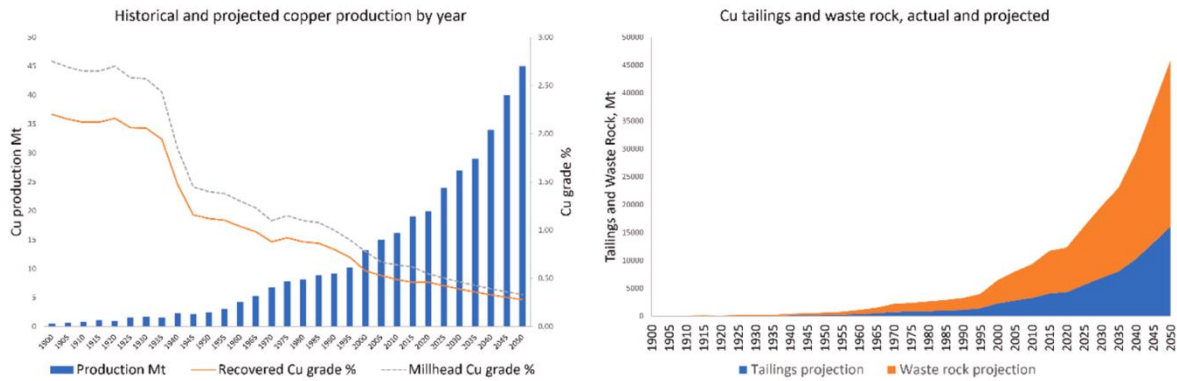


Figure 2 Valenta et al (2023) Copper Historical and Projected Copper Tailings and Waste Rock

The materiality of direct, indirect and cumulative impacts from Modifying Factors is becoming clearer. Valenta et al, (2019) examined and analysed 308 global copper projects and assessed that of the top forty copper deposits globally by tonnage (Figure 3), providing context around the materiality of the associated modifying factors and highlighting likely future trends stating that:

The current stock of known, undeveloped copper orebodies is characterised by its complexity. Copper mines of the future will be lower grade, deeper, and larger footprint operations (Prior et al., 2012). These mines will consume more energy (Norgate et al., 2007), water (Norgate and Lovel, 2004), generate more waste (Mudd, 2009), and produce more deleterious elements, such as arsenic (Schwartz et al., 2017). Additionally, copper mines of the future are more likely to be located in remote and ecologically sensitive areas (Duran et al., 2013; Vidal et al., 2013), on the lands of indigenous or tribal peoples, and in jurisdictions characterised by corruption and poverty (Rogich and Matos, 2008). Projects with these characteristics are likely to stimulate concerns from stakeholder groups, leading to increased scrutiny at the regulatory approvals and project permitting phases of project development. In this paper, we propose an expanded definition of the term “complex orebodies”. Valenta et al, (2019, p816).

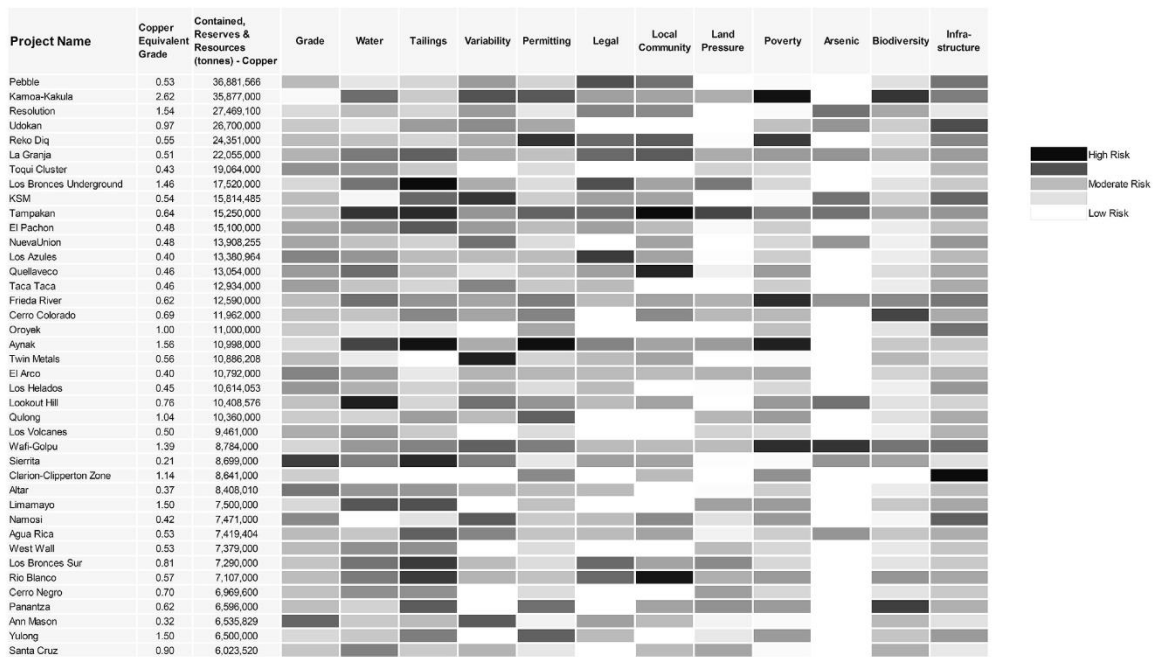


Figure 3 Global Top 40 Copper undeveloped deposits (in 2019) by tonnage. R.K. Valenta et al.

The work of Valenta et al, (2019) highlights that complex orebodies have common factors, or Modifying Factors, that can constrain projects in unique configurations, for unique consequences. This work also highlights the opportunity for Modifying Factors to provide a ‘lingua franca’ or ‘common language’. Currently ‘listening without hearing’ is a conundrum that curbs proactive identification, analysis and assessment of constraints and informed decision making. A common language can enable a ‘common way of thinking’ to enable a diverse range of internal and external stakeholders can align consultation and engagement around the impact pathways that underpin and define effective risk management.

Risk Management: Inputs and outputs

Mineral resources projects are defined by orebody knowledge factors including but not limited to commodities, location, depth and geometallurgy. Maximising orebody value and project value is driven by cause-and-effect relationships between the ‘input factors’ (e.g. cost of capital, cost of materials, labour, energy, licenses and agreements) and ‘output factors’ (e.g. technical performance, production rates, marketing, sales, royalties, taxes and fees).

To proactively assess and manage the risk of not ‘meeting or exceeding the project Design Criteria’, defined as ‘the endorsed project objectives that reflects the explicit goals that a project must achieve in order to be successful’ (Massachusetts Institute of Technology, 2023), the risk appetite and acceptable consequences for all crucial stakeholders must be defined. These goals commonly reflect a range of performance metrics that are influenced by financial, social, political and stakeholder factors such as Environmental, Social and Governance, or ‘ESG’ performance expectations and disclosures.

In practice, risks to projects and stakeholders are realised via common ‘impact pathways’ between Modifying Factors. These pathways can be sequenced to reflect a system of operation; specifically ‘input factors’ and ‘output factors’ that influence the level of certainty in achieving the project Design Criteria (Figure 4).



Figure 4 Modifying Factors, impact pathways and Design Criteria-Tie (Deans,G. 2023)

Systems approach: infinite impacts, finite impact pathways

As part of project studies, metallurgists and project teams, will trade-off factors such as land, power, water and cost to optimise project value. These are data driver decisions that define *what* needs to be achieved. In practice, *how* factors are traded-off will create interactions. The interactions can be sequential or concurrent, direct, indirect or cumulative. The interactions can create 'friction' and unintended impacts that may amplify multiple risks concurrently, leading to multi-factor risks. These interactions, as demonstrated by Valenta et al. (2019) and Franks et al. (2014) can result in heightened uncertainty and risk for project proponents and stakeholders alike. As the impacts are manifested from multiple dynamic factors and the materiality defined by stakeholder values and risk acceptance, baseline assessments, or static impact assessment model are quickly outdated. The development of 'knowledge bases' provides the ability for systematic analysis, assessment and transparent reporting of 'impact pathways' can enable contextualisation of the risks to enable more agile, integrated and informed risk based decision making.

Managing Change

Resource project development takes time, with the global average being more than 16 years from the discovery to production (IEA 2023 & Statista 2023). In practice, over these time horizons there will be macro and micro changes in the operational, economic, regulatory and societal contexts that are reflected in the considerations for Modifying Factors. Many changes will alter the input assumptions and influence the impact pathways for projects. To proactively manage impacts that enable or constrain future economic extraction a key consideration for project planning is understanding and assessing the effect and consequence of interactions between Modifying Factors over the project lifecycle.

Tailings Storage Facility Development - Contextualised Design, suitability considerations and multi-factor impacts

As mining developments dynamically interact with existing local contexts, producing risks and impacts in both directions (L'ebre et al., 2022), there are numerous 'suitability considerations' to consider for adapting mine planning to local social, cultural, political, economic, and ecological conditions (Valenta et al (2023)). How project proponents analyse and assess these considerations is crucial but complex as common 'impact pathways' can produce multiple impacts concurrently. Considerations specific to land access, as a precondition for development provides a practical example of this complexity.

As different 'stakeholders' will place unique values and hold different risk appetites to common impacts, 'multi-factor impacts' underpin 'multi-factor risk'. This is straight forward in theory but complex in practice as represented in Figure 5 for the selection, design and development of a Tailings Storage Facility (TSF). These factors are material considerations for Metallurgists as an approved Tailings Storage Facility is a precondition of many mining operations. and provides a case study of the relationships between impacts and impact pathways. An expanded example is represented in Figure

5 -where Modifying Factors represent common 'impact pathways' between project proponents and their crucial stakeholders.

Modifying Factors – Example - Tailings Storage Facility (TSF)

Multi-Factor Risk Factors – Impact Pathways that influence NET risk and value

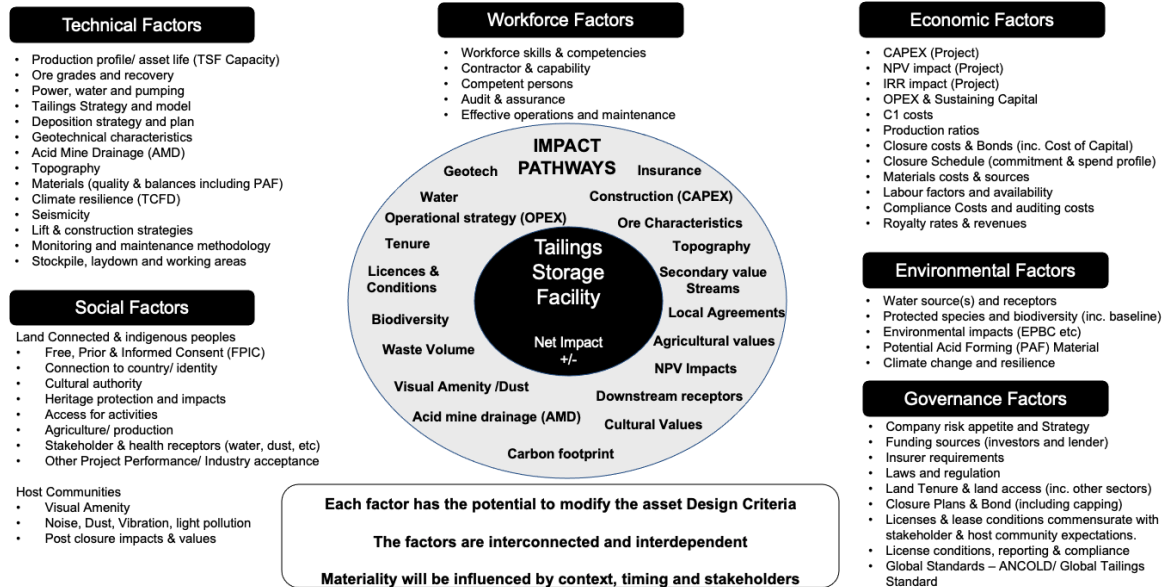


Figure 5 Example of Modifying Factors and 'impact pathway' considerations for the development of a Tailings Storage Facility (Deans, 2023)

Critically, whilst intuitive, it is not explicitly assessed through traditional impact assessments increasing uncertainty. Many of which are subject to change overtime. In a complex and integrated project, the traditional 'impact assessment' framework and methodology (Source, Pathway, Receptor) narrows the focus of the 'impact' the 'Receptor' specific to the model scope, often omitting the multi-factor impact considerations. This is demonstrated through Figure 5 – whereby multiple impact pathways can and will concurrently influence multiple modifying factors.

An Outside View and why does this matter?

It is generally understood that mineral and energy developments profoundly transform environments, communities and economies in a way that can generate social conflict (Davis and Franks 2014). Environmental, Social and Governance (ESG) standards and disclosures provide a more detailed lens for stakeholders such as investors, insurers, lenders and regulators to inform decision making. Traditional risk orientations are threat-focused and seek to restrict or contain stakeholders, serving to identify opportunities to define and develop shared value opportunities to facilitate and expedite development. This is an 'inside view' or project centric orientation to project development and is illustrated in Figure 6.



Figure 6 Inside and Outside View adapted from Kahneman, D. (2011)

Risk increases when external factors, be they 'inputs' or 'outputs' (or the outside view) is not adequately assessed and considered, leading to a 'decide-announce-defend' development orientation. Where the scientific method is not applied, internal and external views are decoupled from the project. The reasons for myriad, but commonly the professional competence applied to analysing and understanding socio-economic and socio-political circumstance does not match the financial and technical competence (Harvey, 2017). Davis and Franks (2014) provide an empirical sample of how this decoupling can manifest, citing 50 extractive projects globally in the past decade where 20-30% have been delayed, suspended or curtailed because of some form of social conflict (Figure 7). Their seminal conclusion is that the apparent cause of conflict and suspension was not the actual cause; rather many project proponents failed to identify underlying issues that were not, for various reasons, brought into the open. Project proponents ended up treating symptoms instead of addressing root causes. The impacts and interdependences of multi-factor risks increases uncertainty and risk. Risks from Modifying Factors can result in delays, cost overruns, rework and even project abandonment.

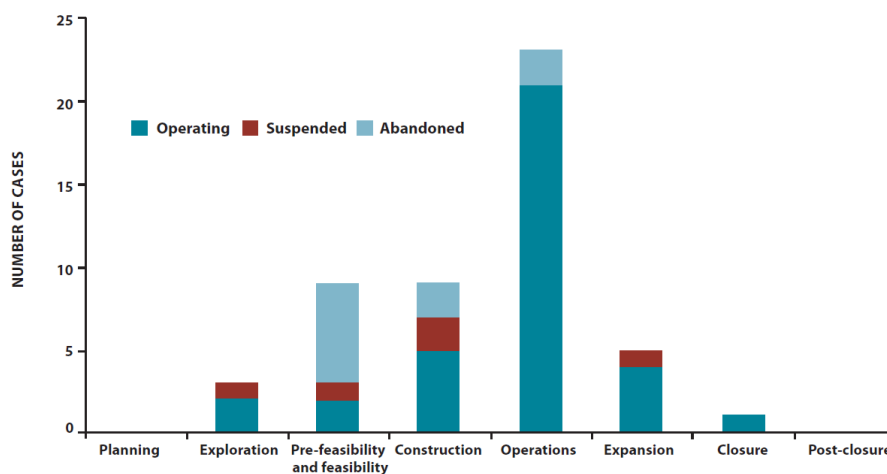


Figure 7 - Cases of company-community conflict: Project Phases (n=50) - Franks et al (2014)

The emergence of multi-sector risk

As other sectors such as renewable energy, agriculture and civic infrastructure seek to grow concurrently to meet global megatrends, so will the competition for resources within *and* between sectors located in common, jurisdictions, common geographies with common stakeholders.

There is increasing global and local competition for the critical inputs (power, water, land, labour etc) between sectors in common jurisdictions and geographies. Over time, it is reasonable to anticipate that the complexity and materiality of multi-factor risks that influence complex orebodies (ibid, 2019) will increase in intensity and frequency. Furthermore, some compounding of impacts is already being experienced through common classes of infrastructure such as high voltage power transmission lines (Macdonald-Smith, A. 2023).

Potential interactions of modifying factors within *and* between projects that cross sectors include power infrastructure, water infrastructure, transport infrastructure, mining, minerals processing, economic jurisdictions, project valuation, legal frameworks, topographic constraints, cumulative environmental and social impact acceptance, regulatory conditions, shareholder investment criteria, climate resilience, and insurer and lender conditionality. Critically, unlike other sectors such as manufacturing, resource projects are defined by their resource characteristics that reduces flexibility.

What to do? Natural factors and human actors – Constraints based design

Companies and project proponents that can proactively and effectively reconcile their Design Criteria, with the minimum acceptable impact profiles and performance expectations of their crucial stakeholders will reduce the risk of ‘surprises’ and the likelihood for material rework.

The use of Modifying Factors that is focused on ‘impact pathways’ provides a common language creates provides greater transparency impacts from which risk appetites and risk acceptance can be moderated and assessed. A common acceptance of impacts (perceived or real) and their potential pathways (Figure 5) is essential to enable development, underpins continuity of production and enables expansions and a future growth pipeline.

Context based design allows project proponents to identify, assess and understand the material constraints that may otherwise prevent project development. Once constraints are understood, project proponents can optimise the pathways to achieve the acceptable design criteria. This approach to design flow reduces the risk of rework whilst increasing the asset’s physical and economic resilience to external factors.

Why Mets Matter!

Risk is uncertainty of outcome. In many cases risk cannot be eliminated, but it can be reduced to a range that is ‘acceptable’ or corresponds to the defined risk appetite. As Valenta, et al (2023) highlight, given the amount of mine waste expected to be generated under a business-as-usual mining scenario, it is critical that alternative pathways are implemented to reduce waste generation in each step of the extraction process. This is both an efficiency opportunity and a material factor reducing impacts and inputs that are pre-conditions and or considerations for development.

While metallurgists play a pivotal role in optimising recovery of the ore reserves to maximise economic return in the short and long-term, they also have a material influence and impact on the inputs (power, water, land etc) and outputs (waste properties and quantity) required; or Modifying Factors. ESG considerations are can be classified as Modifying Factors with sustainability outcomes, informed by the performance of the asset or project relative to peers, or as assessed by external standards, principles and frameworks.

When, where and how minerals are sourced and the management of the waste streams has a direct and material impact on the project's ability to achieve the Design Criteria, achieve financial close and make a commitment to construction. A critical attribute of reserve extraction that differs from other sectors is that deposits are fixed and defined by geological characteristics and once exhausted or no longer of economic value, the project will finish. Therefore, companies need to optimise their plans and performance in the context and characteristics of their operation to enable continuity of production while retaining optionality for future growth. This means factors around water sources, infrastructure requirements, materials balances and tailings designs need to be optimised technically and economically to deliver the optimal possible outcome. This means value and valuation models need to consider the net impact to the project budget, schedule and value. A work package specific model, managed in isolation can focus on the optimal *technical* solution, rather than the optimal *overall* solution.

CONCLUSIONS

In a project development there is an inherent tension between the 'technically feasible' and 'optimal possible'. There are many factors material to project development that are outside the control of the project proponent but the path to greater project acceptance is clear. To develop and operate mining projects in a way that meets or exceeds the project design criteria *and* is acceptable to crucial stakeholders, project proponents need more metal with less waste, less inputs and less impacts.

Uncertainty around the impacts associated with Modifying Factors is multifaceted but can be characterised common impact pathways resulting in dynamic risk profiles and consequences. We live in a complex and dynamic world.

There is growing complexity in assessing the potential impacts required to provide guide decision making and in the context of the resources sector provide reasonable transparency of the material project specific factors that influence Reserve Reporting.

Critically, there are intensifying competing priorities and competition within *and* between sectors. Getting to financial close and constructing projects to enable value realisation is important. How projects are developed and how decisions are made will define stakeholder perceptions and project legitimacy. Reconciling *what is possible* with *what is required* is essential to de-risk development and to optimise outcomes. Metallurgists materially inform the design, delivery, and operation of processing and non-processing infrastructure; their decisions directly impact where, when and how critical and common resources are used.

Metallurgists and their teams have an important role to positively influence the impact pathways by investing in alternative extractive processes that reduce input requirements and reduce waste.

Valenta, et al (2023) highlight that beneficial reduction outcomes include:

- smaller volumes and footprint area,
- lower toxicity and chronic contamination, and
- lower risk of catastrophic tailings dam failure.

JORC Code (2012) encourages best practice estimation methods and promotes the principles of transparency, materiality and competence. The complexity in providing transparency and assessing project specific factors that influence materiality increases for Reserve Reporting when multiple modifying factors interact. By reconciling 'inside' needs with the 'outside' suitability considerations of the host context, project proponents can gain and communicate greater confidence in being able to design and deliver the optimal acceptable outcome. Just as there are inherent

factors, constraints and thresholds for processing recovery based on ore characteristics, so will there be for the necessary inputs and outputs that underpin a project.

These factors can be the difference between a resource becoming a reserve!

REFERENCES

- CRIRSCO (2019). CRIRSCO International Reporting Template November 2019. URL: https://www.crirSCO.com/docs/CRIRSCO_International_Reporting_Template_November_2019.pdf
- Davis, R, & Franks, D. (2014). "Costs of Company-Community Conflict in the Extractive Sector." Corporate Social Responsibility Initiative Report No. 66. Cambridge, MA: Harvard Kennedy School.
- Deans, G. (2023). Modifying Factors Website. URL: www.modifyingfactors.com Accessed 22/08/2023
- Deans, G. Longbottom. M. (2019). "No Assumptions, No Surprises" AusIMM Tailings Conference Paper. AusIMM
- Duncan, R. (2019). What If What You Think You Know Just Ain't So? Forbes Online, May 31, 2019. URL: <https://www.forbes.com/sites/rodgerdeanduncan/2019/05/31/what-if-what-you-think-you-know-just-aint-so/?sh=2ff74d6d355e> Accessed 12 August, 2023
- Edmans, A. (2023) The End of ESG* London Business School, CEPR, and ECGI Financial Management.
- Harvey, B. (2017) "Social Performance – A new professional discipline". Published in the AusIMM Bulletin August, 2017.
- International Energy Agency (IEA) (2023) URL: <https://www.iea.org/reports/critical-minerals-policy-tracker/promoting-exploration-production-and-innovation>
- Kahneman, D. (2011). "Thinking, fast and slow". Farrar, Straus and Giroux.
- Macdonald-Smith, A. (2023). 'Green Energy Way Off Pace for 2023'. 23 August 2023 issue of Australian Financial Review. Accessed 24 August, 2023
- Macdonald-Smith, A. (2023). Brolga and bat ruling a 'death knell' for Victorian wind farm. Australian Financial Review, 4 August, 2023. URL: <https://www.afr.com/companies/energy/brolga-and-bat-ruling-a-death-knell-for-victorian-wind-farm-20230801-p5dt2l>. Accessed 12 August, 2023
- Massachusetts Institute of Technology. (2023) Design Criteria Definition. URL: <https://www.mit.edu/course/21/21.guide/designcr.htm>
- Manalo, P. (6 Jun, 2023) 'Discovery to production averages 15.7 years for 127 mines'
- URL: <https://www.spglobal.com/marketintelligence/en/news-insights/research/discovery-to-production-averages-15-7-years-for-127-mines> Accessed 12 August, 2023
- McKinsey - <https://www.mckinsey.com/capabilities/strategy-and-corporate-finance/our-insights/daniel-kahneman-beware-the-inside-view>
- Valenta, R.K., Kemp, D., Owen R.J., Corder, G.D. and Lebre, E. (2018). Re-thinking complex orebodies: Consequences for the future world supply of copper. Journal of Cleaner Production 220. Pages 816-826, ISSN 0959-6526
- Rick K. Valenta, Éléonore Lèbre, Christian Antonio, Daniel M. Franks, Vladimir Jokovic, Steven Micklethwaite, Anita Parbhakar-Fox, Kym Runge, Ekaterina Savinova, Juliana Segura-Salazar, Martin

Stringer, Isabella Verster, Mohsen Yahyaei, Decarbonisation to drive dramatic increase in mining waste—Options for reduction, *Resources, Conservation and Recycling*, Volume 190, 2023, 106859, ISSN 0921-3449,

The Australasian Code for Reporting of Exploration Results, Mineral Resources and Ore Reserves ('the JORC Code') (2012). URL: <https://www.jorc.org/>

University of Queensland, Sustainable Minerals Institute (2023). "What does a Metallurgist do exactly?" – URL:: <https://study.uq.edu.au/stories/what-does-metallurgist-do-exactly>

United Nations, (2008) United Nations Declaration on the Rights of Indigenous Peoples and Free, Prior and Informed Consent, GA Res 61/295, UN Doc A/RES/61/295 (13 September 2007)

VRM Technology: A Pragmatic Approach to Project Risk Versus Reward

D. Novak¹, D. Wall², A. Vasileff³

1. Principal Engineer, GPA Engineering, 121 Greenhill Rd, Unley SA, David.Novak@gpaeng.com.au
2. Lead Metallurgical Process Engineer, GPA Engineering, 121 Greenhill Rd, Unley SA
Dean.Wall@gpaeng.com.au
3. Process Metallurgical Engineer, GPA Engineering, 121 Greenhill Rd, Unley SA
Anthony.Vasileff@gpaeng.com.au

Abstract

The mining industry is working to enhance its Environment, Society and Governance (ESG) credentials, tackling challenges such as energy footprint reduction and decarbonisation, environmental stewardship of tailings, water and mine closure, all within the overarching constraint of cost pressures. Vertical roller mills (VRMs) have the potential to be a significant contributor to the improvement of virtually all of these ESG characteristics; however, a low appetite for risk has often inhibited the uptake of new technology in the mining industry. An opportunity exists for the industry to change the technology evaluation process to focus on a broader, pragmatic risk versus reward profile in order to capitalise on the benefits of this innovative technology.

Most mineral processing plants rely on wet grinding, utilising equipment such as SAG and ball mills to promote liberation of minerals from ores. The process inherently has high electric power intensity and utilises significant amounts of water as the medium for the grinding process. Many industries outside of traditional mineral processing have utilised alternate grinding processes such as HPGRs and VRMs for dry grinding of feedstock. In these applications, dry grinding has historically been selected for multiple reasons, such as production of a final dry product, energy savings and water management. However, challenges like dust management and particle size classification are associated with smaller size fractions, due to high recirculating loads and materials transport systems.

The adoption of VRMs and similar technology in mineral processing offers many clear advantages to ESG project outcomes. However, the traditional risk/reward impact on the larger project outcomes, such as net present value (NPV) and internal rate of return (IRR), does not tend to present a favourable case. This paper highlights the pragmatic adoption of VRMs as an innovative technology into minerals processing flow sheets for their financial and ESG benefits, whilst facilitating a framework for the identification and evaluation of techno-economic risks and benefits for the overarching project.

Introduction

The volatile nature of commodity markets places large downward pressure on the primary producers, the miner and mineral processor. Changes in supply and demand can result in unprecedented price swings that lead to the 'boom and bust' periods experienced in the mining industry. Following a string of recent global downturns, companies have generally succeeded at becoming leaner and more efficient (Deloitte, 2016). However, these efficiency gains only get so far, where further improvements can only be gained by meaningful innovation leading to step change improvements (Deloitte, 2016).

The mining industry acknowledges the need for innovative technologies and practices to drive the next wave of productivity. In parallel, there is increasing push from investors and Government to enhance Environment, Society and Governance (ESG) credentials in areas such as energy reduction, decarbonisation, water consumption and mine closure. The reality is, however, that mining companies are slow to action innovative projects and/or herald ESG stewardship due to risks unique to the industry (eg grade uncertainty, commodity price swings, geopolitics). For a company to commit to an innovative idea or project, the project must be sufficiently de-risked and it must be demonstrated with sufficient confidence that a return on investment can be realised, hopefully at a level exceeding that for a more conventional project.

Vertical roller mill (VRM) technology offers the mining industry a host of economic benefits for comminution while also having the potential to improve virtually all ESG areas. Most notably, as demonstrated in other industries, VRMs have improved project NPV and IRR, reduced energy consumption (as compared to SAG and ball mills), reduced water usage, simplified process flow sheets and facilitated the ease of integrated waste landforms commonly or historically referred to as 'dry stacking of tailings.' To date, only a few examples of VRM applications in the mining industry have transpired (Jankovic et al, 2016).

While these outcomes should be achievable more broadly in mining, adoption of the technology needs careful consideration with the process of de-risking beginning in the early study stages. At pre-feasibility study stage, various project options in terms of size, configuration, process flexibility, layout, location are developed and assessed to allow the option with the best risk and economic profile to progress to feasibility. Despite the engineering effort that goes into these studies, financier and investor decisions are typically only based on the fundamental determinants, such as total deposit, head grade, AISC, NPV, IRR, and risks.

It is common when evaluating new technologies during pre-feasibility or feasibility to add a notional contingency factor (5-20%) on top of the capital cost estimate. This may be excessive and could be enough to prevent further evaluation of these alternative technologies, with the project deciding to progress down the "safer" conventional route. The authors believe that careful and targeted consideration of VRMs in a few key areas will assist in de-risking the technology for mining projects and enable more appropriate contingency factors. These key areas for consideration are: (1) operational readiness & spares management, (2) wear rate testing, (3) contracting strategies, (4) project team diversity, and (5) investment cost profile.

This perspective paper is a summary of the authors' observations, empirical data and anecdotal evidence for the positive adoption of VRMs in the mining industry, with the aim to provide some independent pointers for VRM technology adoption outside of the key technology providers. It provides a brief technical overview of VRM's and their history in other industries, followed by a presentation of key risks and benefits associated with the technology. Using this background information as a starting point, the authors then provide recommendations for areas worthy of additional attention, including proposed changes to the project evaluation process.

Please note that the application of the VRM technology as presented within this paper is highly dependent on the specific flow sheet and ore properties of the project - thorough metallurgical testing and evaluation is required to support the selection of the technology.

VRM Technology Overview

Technical Overview

The basic mechanism in a VRM involves the use of a rotating horizontal table with a small number of angled grinding wheels with an in-built air classification system directing oversize material back down to the grinding table or to an external recycle stream. The grinding principle involves both compression grinding, like in high-pressure grinding rolls (HPGR), together with shear force grinding due to the opposing grinding faces. This in turn provides a low specific grinding power requirement. The key differentiators between VRM and mining industry HPGR technology is the mechanism of grinding, by the addition of shear force and an inbuilt sealed air-classifier. A schematic of the key VRM components is shown in Figure 1.

Operating History

The VRM technology has been used since the early 1900s in the cement/pulverised coal/slag grinding industries (Jankovic et al, 2016) due to their high drying capacity, low energy consumption, compactness and reliability in operation (Simmons et al, 2005). VRMs in these raw material industries have been subject to a number of improvements and upgrades. The most notable of these is the option to install the classifier outside of the mill housing, leading to a dramatic reduction in fan energy requirements. Other areas of enhancement include in situ hard facing of roller wear liners and the use of longer-lasting materials for table and roller surfaces to reduce downtime and maintenance (Ito et al, 1997).

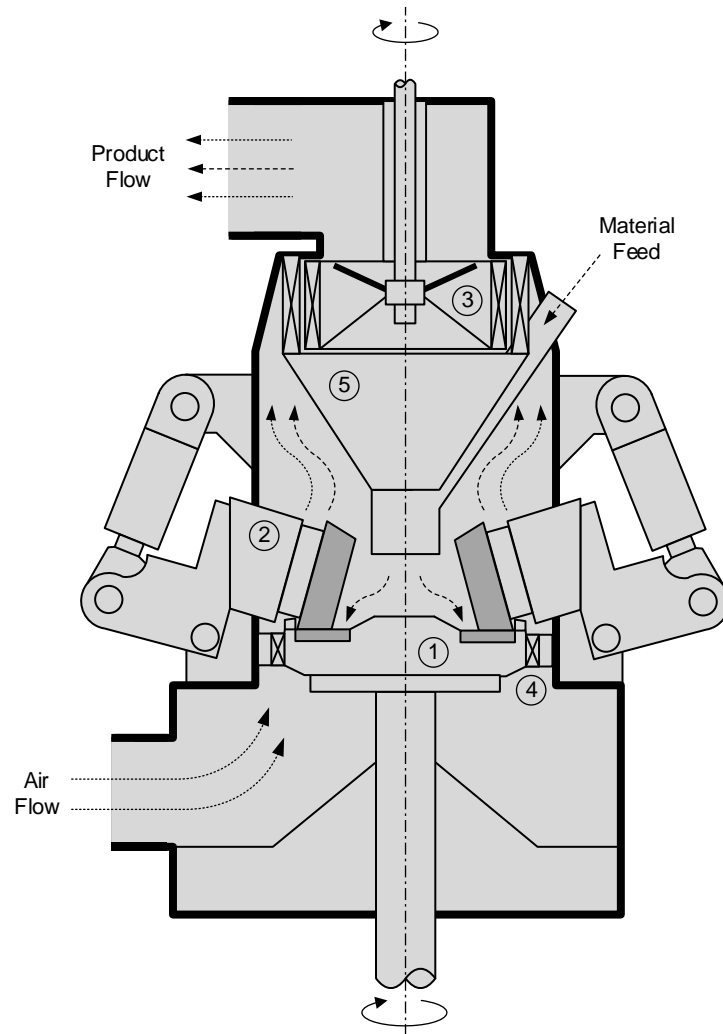


Figure 1. Schematic of a typical Vertical Roller Mill depicting (1) rotating grinding table, (2) horizontal grinding rack and rollers, (3) dynamic air classifier, (4) louver ring and (5) grid cone.

Adoption in Mining

Traditionally, the mining industry has used a wet processing route for comminution via semi-autogenous grinding (SAG) mills and ball mills for primary grinding applications and then utilising ultrafine grind technologies (such as tower mills, ISA Mills, SMDs and others) for finer particle comminution applications like concentrate regrinding. The use of dry grinding and air classification, initially through the use of HPGRs, began in the 1990s after this technology was introduced to the cement industry in the 1980s.

The adoption of VRMs in the hard rock mining industry has been the subject of academic discussion since the 2000s, followed by the use of the technology in phosphate ore grinding at Foskor in 2012 (Gerold et al, 2012). Increasing energy costs, plus water reduction targets due in part to water scarcity, mean that VRMs are now under consideration in contexts where the benefits of the technology have the most impact. This is particularly the case for magnetite processing (in combination with dry magnetic separation) and in remote mine sites where power and water supply present significant economic challenges.

Benefits & Risks of Vertical Roller Mills

The following section outlines both the major benefits and prevailing risks related to the adoption of the VRM technology in a hard rock mining setting. The purpose of this information is to illuminate areas that warrant additional attention during the definition stages of a project. This can be used to quantify the potential benefits for inclusion in financial models, or to understand what challenges remain.

Benefits

The primary benefit of the VRM technology is the potential to provide a significantly improved NPV as compared to conventional comminution alternatives. Despite (in some cases) higher initial capital investment in a VRM, operating costs are typically dramatically lower for reasons as presented below. This is mainly due to power consumption for grinding shown to be significantly lower than traditional SAG/ball mill combinations (Boehm, 2015). Overall, this has been shown to translate into an economic benefit as compared to traditional wet-grinding circuits (Swart et al, 2022; Jankovic et al, 2016).

Energy Consumption

The grinding mechanism of a VRM relies on compression and shear between the rollers and grinding table. Grinding energy is, therefore, typically utilised more efficiently in the particle bed as compared to the random particle-media collisions experienced in a ball mill (Boehm, 2015). Results have shown that this typically results in energy savings of up to 30% (Jankovic et al, 2016). The authors note that anecdotal evidence indicates that VRM energy savings greater than 40% for the combined grinding and air classification unit operations have been demonstrated in pilot test work as to an equivalent SAG and ball mill with wet classification. Hence thorough metallurgical testing is required specific to the relevant orebody, in order to fully evaluate the potential opportunity.

Total comminution energy is a combination of the grinding power demand and the product classification power demand. It is important to note that the VRM air classification energy is high when compared to traditional wet classification. The classification energy typically approaches 50% of the total power demand. However, it is important to note the combined energy demand for the VRM grinding circuit, inclusive of air classification is significantly less than that for an equivalent wet grinding circuit inclusive of the wet classification system. It is also noted that ball mills become less efficient when targeting finer product, which is when the energy savings of a VRM become more significant (Swart et al, 2022).

Energy Demand Management

VRM technology provides a very fast response time to steady state operation in producing a target particle size distribution, typically minutes to hours in duration as compared to ball mills, which typically take from many hours to days to reach steady state operation. This unique feature offers the potential for flexible power demand through fast turndown/ramp up, which offers broader electrical supply options, such as renewables and battery energy storage systems (BESS). This enhances renewables penetration, with one project evaluated approaching 80% based on the lowest levelised cost of electricity. Thorough electrical engineering consultation in conjunction with operational considerations may provide energy solutions that further improve a project's NPV.

Process Efficiencies

The different grinding mechanism employed by the VRM also enables process efficiencies that can be used to optimise the design of the rest of the flow sheet, as well as the design and selection of individual equipment items. A key aspect of the VRM is the creation of a 'steep' particle size distribution, relative to other grinding technology options (Reichart, 2015). This supports the

phenomenon of enhanced grinding efficiency, as well as a reduction in the generation of ultrafine particles that can negatively impact filtration, thickening and other unit operations.

The positive impact of dry grinding by VRM on downstream flotation is also notable (Katzmarzyk et al, 2019). The mechanisms for this differ across different applications, but the VRM tends to produce particles with 'rougher' surface characteristics and micro fractures at grain boundaries. This has been shown to result in higher oxidation reduction potential (ORP) measurements which indicates higher surface reactivity for reagent adherence (Katzmarzyk et al, 2019).

Coarse Particle Rejection

Some VRM units air classification systems ('air swept') are capable of producing a coarser middlings stream, often referred to as 'grits,' that can then be subjected to a dry separation technique for the mass rejection of gangue material. This beneficiated stream can then be blended back into the main VRM feed stream. This operation has a number of potential benefits:

- Higher feed rates for fresh ore material
- Reduced sizing of downstream process and product handling systems
- Creation of a relatively coarse dry waste stream.

The authors are familiar with flow sheets of this nature being tested and recommended for magnetite concentrate projects, utilising both VRM's and dry, low intensity magnetic separation (DLIMS) technology. We are also aware of significant work being undertaken in the development of magnetic separation technologies for the separation of ultra-fine (less than 50 microns) magnetite particles from gangue in magnetite ore. The use of dry gravity separation techniques could also enable the realisation of these benefits for other ore types.

Geostable Tailings Enablement

A key shift that has occurred across the mining industry is the move away from tailings dams towards dewatered tailings landforms, sometimes referred to as 'integrated waste landforms' or 'dry stacking.' This practice involves the creation of a geostable landform from waste material, with minimal moisture content present in the source material.

The failure of numerous traditional upstream tailings dams, particularly in South America, means that regulatory approval of new dams is no longer possible in many jurisdictions. As a result, the requirement for different tailings disposal methodologies, particularly those that are both low risk and fit-for-purpose, is growing rapidly.

The VRM technology has the potential to enable the selection of this type of tailings deposit, particularly through the generation of a dry, coarse grits reject stream that can be combined with a finer, dewatered tailings stream and waste rock as needed. This blended engineered material has superior geotechnical stability, allowing for the creation of taller, consolidated landforms that reduce the overall footprint required for tailings disposal. It also has positive impacts in terms of waste rock oxidation and dust suppression (Wanninayake & Dixon, 2023). Additionally, the targeted generation of a grits stream also reduces the amount of material fed to the next stages of the process, and reduces the size and cost required for tailings dewatering equipment.

The approvals process of tailings facilities may be facilitated by the utilisation of the VRM technology due to the abovementioned ESG credentials. It may also have additional benefits on the project specific financial metrics, such as NPV, in reduced closure costs and rehabilitation costs. However, these will need consideration of project design criteria.

Water Stewardship

Dry grinding technologies, such as VRMs, have the obvious benefits of not requiring water to operate. In the case of the VRM, water consumption is especially low, given the compact nature of the technology where no water is required for cooling or dust mitigation. The project benefits associated with reduced water consumption can be significant, especially for operations where water access is limited and/or costly, or in places where ongoing water security presents a risk to the project. This also leads to a reduction in water treatment infrastructure.

Unit Capacity, Turndown & Ramp Up

VRMs are designed as scaled units capable of effective throughputs in the order of 1000 dry t/h of feed in a single unit (Lynch & Rowland, 2005). An example of a typical VRM turntable with rollers suitable for 1000 dry t/h is shown in Figure 2. The key driver to the throughput of the VRM is the recirculation rate of coarse particles that are rejected by the air separator (Altun et al, 2017).



Figure 2. Internal view of a VRM for approximately a 1000 t/h duty (Image courtesy of Mining Technology, 2023)

Turndown is possible by reducing the number of active rollers in operation or when maintenance is required for roller tyres. This turndown facility is a useful attribute when utilising renewable energy or during periods of high unit power cost. It may also present opportunities for targeted energy savings when material is being mined from sections of the orebody that are known to have favourable grinding conditions.

The nature of the VRM and its grinding/separation mechanisms mean that the time required to achieve steady state operation is relatively short. The authors understand that this ramp up time is typically less than one hour, sometimes significantly so, but the specifics of this are linked to individual applications. This indicates that the impact of suboptimal operating conditions following

downtime events is much less than in traditional milling circuits, which has the potential reduce requirements for buffer capacity both upstream and downstream.

Risks

The section below aims to highlight some of the known or perceived risks that relate to the application of the VRM technology, with a focus on technical design risks outside of the VRM unit itself, often referred to as the balance of plant.

Feed Material Presentation

The VRM feed stream requires careful screening to prevent foreign material entering the grinding table and causing damage to the main wear surfaces. A careful investigation is required to facilitate tramp material removal, which poses a greater risk on applications such as magnetite ore.

Additionally, the VRM grinding circuit requires dry feed material of typically less than 3% w/w moisture. If higher incoming moistures are expected, a hot gas dryer is required to dry the feed material prior to entering the grinding table, attracting additional CAPEX and OPEX.

The VRMs also require a maximum feed particle size of no greater than 5% of roll diameter. The design, selection and performance monitoring of upstream crushing processes are therefore essential to successful application of the VRM.

Wear Rates

The VRM has known drawbacks, notably the grinding surface wear rates, which have been addressed over time by the cement industry (Ito et al, 1997). Like any grinding mill, VRMs perform optimally when wear surfaces and geometry are within defined tolerance. However, abrasive wear over time will affect these geometric tolerances which results in increased wear rates. More unique to VRMs, the hard, abrasive materials that present in the VRM feed have the propensity to build up on the grinding table over time and increase wear rates this way. Industry experience has shown that VRMs are most suitable for applications where the wear rate is 10 g/tonne or less due to implications on maintenance costs (Jensen et al, 2010).

Fortunately, VRM machines rolls and grinding tables have similar wear surface structures to HPGR rolls and the mining industry has spent many years addressing the types of wear materials suitable for use in HPGRs, such as metal matrix composites. This knowledge should be readily transferrable to VRM tyres, enabling faster penetration of VRMs into the mining industry.

Product Transport

The fine, dry material produced by the VRM presents several challenges from a materials handling perspective. This system requires careful integration into the facility design for footprint and functionality considerations, particularly as traditional belt conveyors are unlikely to be suitable due to the liquified flow nature of the ultrafine dry particles.

The cement industry typically uses pneumatic conveying in these applications, while en-masse conveyors and bucket elevators are utilised by the grain industry. Both technologies come with capacity restrictions, as standard units currently produced by vendors may not always be available in sizes required by some higher capacity mining projects. Additional challenges that accompany highly mechanical equipment like the en-masse systems is more complex maintenance. It is possible to split or divert these dry streams should this type of flexibility be required in high-capacity circuits, however, materials handling engineering together with plant layout considerations are important to address early in project development.

From the authors' experience with these projects, it is suggested that immediate repulping of VRM product material tends to be the most effective option to enable efficient transport and storage via standard slurry pumping and agitated tanks. However, this choice may compete with the water reduction goals of the project and so requires detailed consideration.

Dust Management

Any process involving handling of dry material presents a risk of dust generation. While the VRM unit itself is self-contained during normal operation, all associated equipment (especially transfer points, storage vessels or repulp tanks) will require significant consideration for dust management. This is particularly important when the use of water to mitigate dust generation is not an option.

Furthermore, the potential for the build-up of silica material inside the VRM unit means that any maintenance activities in this area may require a number of controls to be in place, thereby increasing the time and complexity of the works.

An additional risk for some specific applications comes in the form of the creation of a hazardous area in and around this circuit, due to creation of an explosive dust environment. This issue is a known consideration for regrind applications involving the VRM in downstream iron ore processing.

Foundation Design

Design of concrete foundations and associated civil works is a key consideration for any comminution project, as this can represent up to 40% of the total installed cost of the project. In the case of the VRM, the height of the unit and elevated centre of gravity presents specific challenges to civil engineering design.

The foundation design, whilst site specific to geotechnical conditions, is considerable, factoring static, dynamic and vibrational loads. Attention needs to be given to shear forces in the footings and the constructability of large mass footings, potentially up to 2000m³ for the larger VRM units. This presents additional complexity to the construction stage of a project.

A review of technology provider data, geotechnical conditions and civil engineering review is considered valuable at the early stage of a project to ensure project cost and schedule contingencies can be kept to a minimum.

Technical and Operational Expertise

The application of a new technology like the VRM, especially one whose performance is directly tied to the success of the overall project, requires a significant amount of investment in experienced, adaptable technical and operational personnel. However, there are several competing aspects that the mining companies need to consider:

- Current operational/maintenance expertise exists primarily in a different industry (cement/industrial minerals) – one that tends to be located near cities and/or ports
- Many of the drivers that encourage the adoption of the VRM technology are linked to remote locations (limited water, expensive energy)
- Technical knowledge tied to a few vendors, most without a permanent local support presence in Australia and other global mining areas
- Initial project development work completed by senior technical staff within mining companies, many of whom do not wish to transition to site-based technical roles.

Technology Evaluation

Key Areas for Consideration

VRM technology providers have only recently focused on marketing to the global mining industry, with one of the more recent installations being the phosphate hard rock grinding project for Foskor in South Africa in 2012 (Gerold et al, 2012). This means that the broad body of evidence and experience base that influences technology selection is yet to be developed. As a result, any potential VRM applications are heavily dependent on the evaluation processes applied to each specific project, and the engineers and executives tasked with these activities.

Operational Readiness & Spares Management

Given the limited VRM operating experience within the mining industry, proper specification of operational readiness requirements early in the study and design phases will be essential to achieving effective ramp up and realisation of the project objectives. It is also envisaged that during the early phases, knowledge sharing with the cement industry could prove beneficial and enable effective training programs for VRM operators. To this point, investment in training of personnel will be key to operational success.

Spares inventory will become a key aspect to the successful integration of the technology. The practice of spares holding – where traditionally competing operations and vendors will share key spare parts – has proven valuable to the mining industry, particularly in remote areas. This practice has yet to evolve for VRM's in the mining industry. However, there may be some existing versions of this in the cement industry that can be expanded upon. Given the lack of other operating sites available to share parts, criticality risk reviews of the major spares will also become crucial. Therefore, it is advised that critical spares are also identified and specified accordingly in the early project phases.

Wear Rate Testing

Mining projects will typically have higher particle density and abrasion indices than cement or industrial minerals. The heavier particles will impact the wear rates experienced within the VRM, particularly in the classification system. The level of wear expected within these units has not been published broadly for mining applications, with assessments being targeted to the more established cement industry (Jensen et al, 2010). As a result, it is expected that projects seeking to utilise VRM technology will need to conduct their own investigation of wear rates on key components, ideally with support from selected vendors and specialist engineers. It is anticipated that this knowledge will then begin to build and disseminate across the industry as more VRM installations occur.

Contracting Strategies

The complexity of adopting a new technology like the VRM means that the project will typically require greater input from the owner's team. Therefore, typical Design and Construct or EPC-style contracts, where much of the risk/responsibility is shifted to a large services provider, may not be best placed to ensure a positive project outcome. A consultative and collaborative style contract strategy with a carefully selected technology provider should provide better project outcomes.

It is important to note that a high level of vendor involvement outside of their area of expertise should be undertaken with caution, particularly for materials handling system design and power system integration. In the authors' experience, opportunities for optimisation and value engineering were not considered under this type of engagement.

Project Team Diversity

The development of a minerals processing flow sheet will typically utilise a metallurgist as the key person selecting the technology and study direction. This can mean that significant focus is placed on

defining specific technical and cost metrics that are directly related to the application of the technology, rather than the broader project. In the authors' experience, other engineering disciplines and similar project stakeholders require a greater early input to ensure successful project evolution. Particularly, early involvement from civil/structural, mechanical, materials, materials handling and electrical disciplines should be sought.

Investment Cost Profile

The VRM is a compact unit, making the footprint of the installation smaller and reducing the civil engineering costs when compared to a traditional milling circuit. Savings are also made due to the method of construction of the two systems. Ball mills are typically built at the supplier's factory and transported to the mine site in large componentry. In contrast, the VRM is built onsite, avoiding difficult logistical issues and associated costs, however, site-based expertise and costs would be greater for remote mining projects in the authors' opinion.

However, given the lack of actual VRM installed cost data for mineral processing plants and subsequent learnings to be developed, the authors opinion is that the equipment and installation costs are similar or slightly higher for a VRM than a comparable ball mill system, reflecting greater componentry count of the system, which includes items such as the rollers, table and the hydraulic system. Civil, electrical and mechanical installation costs are also increased due to the increased requirement for feed material presentation and materials handling infrastructure. Although, it is important to note that in a number of feasibility studies the overarching total project investment cost has been found to be considerably lower due to lower operating costs, such as power and water.

The power demand profile is an area not typically considered in early-stage project development. Recent work undertaken by the authors has seen a significant step change improvement to the project NPV, when the power system is engineered in conjunction with the VRM demand profile.

Traditional estimate methodology used to support studies and final investment decisions (FID) are likely lacking to properly evaluate adoption of a VRM for mining applications, especially if ESG considerations are not properly accommodated. The result is potentially an overestimation of contingency due to the inadequate identification of risk and allowance for controls. It is expected that through careful engineering and project management in the key areas identified herein, contingency allowances can be reduced to appropriate levels so that an equitable project evaluation can occur.

Proposed Evaluation Methodology

The risk profile with all technologies changes over time and mining executives need to take the courage to adapt to new innovative solutions. They will need to empower the engineers and metallurgists to complete an evaluation of the VRM technology for their specific application. It is acknowledged that this is maybe a challenging task given that adoption of the technology and its application in mineral processing applications is in its early stages. However, the authors believe that this is best achieved by undertaking a criticality risk review which essentially comprises a gap analysis that compares the variables to existing VRM applications or existing similar technologies, such as HPGRs.

The methodology suggested in this paper is divided into the executive team and technical team for the evaluation and development of a VRM solution.

1. Executives – while executives may focus on the positive NPV and IRR for a specific project, a broader vision requires the following:

- a. Courage – for the selection of the technology into the flow sheet, based on in-depth engineering assessment
 - b. Financial and social licence to operate value – development of a risk versus reward for the deployment of the technology within the broader tailing’s strategy
 - c. Engagement and empowerment of an appropriate technical team – this includes not only metallurgists but also other SMEs such as, but not limited to, tailings, dust, materials handling, materials engineers, civil/structural engineers and electrical engineers
 - d. ESG targets – corporate social responsibility, water usage, water security, energy reduction, ease of integrating renewable power into the energy mix
 - e. Contracting strategy eg EPCM and owners’ team to be fully integrated with technology providers, constructors and specialist consultants
 - f. Contingency allocation – careful engineering to reduce the contingency allowance so that an equitable project evaluation can take place.
2. Technical personnel – a technical team comprising a breadth of knowledge in the following key subject matter areas is required (typical of more traditional wet grinding circuit evaluations):
- a. Dry materials handling – specifically ultrafine dust transport at high tonnage rates, inclusive of storage and buffer systems
 - b. Logistics expertise of large and specialist componentry for shipping, warehouse and spare parts management
 - c. Maintenance planners – engaged early in project delivery to ensure plans are in place for accessing critical spares
 - d. Electrical engineers – experienced in deployment of high voltage power and integration with renewables to take advantage of the VRM’s ability to ramp up and down quickly. This is to effectively match the load demands with power supply security and lowest levelised cost of power. Remote mine locations are better suited to VRM’s due to the flexible load profile
 - e. Materials specialists – to develop wear rate models for the grinding surfaces together with the classifier system
 - f. Tailings specialists – to consider the application into the flow sheet for geotechnically stable tailings deposition
 - g. Infrastructure specialists – whilst site selection is typically limited due to orebody

location, choices around infrastructure to support the project development is suggested, eg access to national electrical grids versus developing fit for purpose mine site micro-grids.

The inclusion of VRM technology into a mineral processing flow sheet may, in many circumstances, substantially improve the financial metrics of the project. However, a broader range of corporate benefits may be realised, such as the ease of integrating renewable power sources, reducing water consumption and more socially acceptable tailings deposition. To effectively capture all the potential benefits and address the risks, the level of detail traditionally used to support the FID (typically AACE Class 3) is insufficient. The above methodology, such as the use of non-typical subject matter experts and independent third-party reviewers, should be considered to provide targeted definition in key areas required for broader project evaluation.

CONCLUSION

The VRM technology has the potential to dramatically improve mining project financial metrics, such as NPV and IRR, together with enhancement of ESG credentials in areas such as renewable power integration, water and energy use reduction, and more socially acceptable tailings deposition. Widespread adoption of VRMs in mineral processing is highly probable, providing early adopters gain timely success; however, sufficient due diligence is key to measuring the risk versus reward profile for this innovative technology. Classical project development studies are not the most appropriate method for the selection of the VRM technology into a mining project due to broader key project drivers.

De-risking the VRM technology while sensibly evaluating the broad range of positive NPV contributors for mining projects will enable more equitable assessment when comparing to more conventional equipment. The key areas for assessment include:

- Operational readiness and spares management
- Wear rate assessments and testing
 - To inform careful feed presentation and fine product materials handling design suitable for high-capacity mineral processing plants
- Contracting strategies
- Project team diversity, beyond traditional subject matter experts
- Investment cost metrics for power, water and tailings management
 - Understanding power demand profiles and the positive contribution of flexible power supply systems.

Some areas of VRM technology adoption review will require greater attention when implemented into a mineral processing plant compared with traditional industry usage, eg wear rates from certain feed minerals/ores due to higher specific gravities and silica as examples. Project studies from a wider subject matter experts and multi-discipline engineering approach, beyond typical strong metallurgical focus, will prove to be very valuable in facilitating positive mining project financial and technical outcomes.

ACKNOWLEDGEMENTS

The Authors would like to thank Ms. E. Potezny and Mr E. Higginson for their help in research and data collection for the paper.

CONFLICT OF INTEREST DECLARATION

The Authors declare that they have no known competing financial interests or personal relationships that could have appeared to influence the work reported in this paper.

REFERENCES

- Altun, D, Benzer, H, Gerold, C and Schmitz, C, 2021. Predicting the grinding energy of VRM depending on material characterization, *Minerals Engineering*, 171, 107095.
- Boehm, A, Meissner, P, and Plochberger, T, 2015. An energy-based comparison of vertical roller mills and tumbling mills, *International Journal of Mineral Processing*, 136, 37–41.
- Deloitte, 2016. *Innovation in Mining* (Deloitte Touche Tohmatsu Limited: Melbourne).
- Gerold, C, Schmitz, C, Stapelmann, M and Dardemann, F, 2012. Latest Installations and Developments of Loesche Vertical-Roller-Mills in the Ore Industry, in *Proceedings International Mineral Processing Conference 2012*, pp 24–28 (International Mineral Processing Council: New Delhi, India).
- Ito, M, Sato, K and Naoi, Y, 1997. Productivity increase of the vertical roller mill for cement grinding, in *Proceedings IEEE/PCA Cement Industry Technical Conference 1997*, pp 177–194 (Institute of Electrical and Electronics Engineers: Hershey, PA, USA).
- Jankovic, A, Özer, C, Valery, W and Duffy, K A, 2016. Evaluation of HPGR and VRM for dry comminution of mineral ores, *Journal of Mining and Metallurgy A: Mining*, 52, 11–25.
- Jensen, L R D, Friis, H, Fundal, E, Møller, P, Brockhoff, P B and Jespersen, M, 2010. Influence of quartz particles on wear in vertical roller mills. Part I: Quartz concentration, *Minerals Engineering*, 23, 390–398.
- Katzmarzyk, J L, Silin, I, Hahn, K M, Wotruba, H, Gerold, C and Stapelmann, M, Investigation on flotation behaviour of a copper sulfide ore after dry grinding by Loesche vertical roller mill, in *Proceedings International Copper Conference 2019* (Conference of Metallurgists: Vancouver, BC, Canada).
- Lynch, A J and Rowland, C A, 2005. *The History of Grinding*, pp 84–89 (Society for Mining, Metallurgy, and Exploration, Inc. (SME): Colorado).
- Mining Technology, 2023. Loesche - Grinding Mills for Ores and Minerals [online]. Available from: <<https://www.mining-technology.com/contractors/crushers/loesche/>> [Accessed 13/09/2023].
- Reichart, M, Gerold, C, Fredriksson, Adolfsson, G and Lieberwirth, H, 2015. Research of iron ore grinding in a vertical-roller-mill, *Minerals Engineering*, 73, 109–115.
- Swart, C, Gaylard, J M and Bwalya, M M, 2022. A Technical and Economic Comparison of Ball Mill Limestone Comminution with a Vertical Roller Mill, *Mineral Processing and Extractive Metallurgy Review*, 43(3), 275–282.
- Simmons, M, Gorby, L and Terembula, J, 2006. Operational experience from the United States' first vertical roller mill for cement grinding, in *Proceedings IEEE Cement Industry Technical Conference 2005*, pp 241–249 (Institute of Electrical and Electronics Engineers: Kansas City, MO, USA).
- Wanninayake, A and Dixon, T, 2023. Feasibility study of co-disposal of tailings and mine waste rock, in *Proceedings Mine Waste and Tailings Conference 2023*. p 14 (Australasian Institute of Mining and Metallurgy: Brisbane, Australia).

Implementing Sequential Flotation at Golden Grove Copper-Lead-Zinc Concentrator

K Tiedemann¹, B Rego², and D Clarke³

1. MAusIMM, Group Principal Metallurgist, Develop Global, West Leederville WA 6007, kurt.tiedemann@develop.com.au
2. MAusIMM, Senior Metallurgist, 29 Metals Golden Grove, Yalgoo WA 6635, brandon.rego@29metals.com
3. MAusIMM, Senior Metallurgist, 29 Metals Golden Grove, Yalgoo WA 6635, dale.clarke@29metals.com

ABSTRACT

The Golden Grove Concentrator is located within the Murchison region of Western Australia. The Processing Plant treats ore mined from multiple polymetallic orebodies. Historically, ore treatment campaigns depended heavily on cleanly segregating copper ores from lead/zinc ores during mining. The concentrator only had sufficient residence time and capability to produce two concentrates sequentially. As mining progressed, mixed copper/lead/zinc zones became more prevalent, with ore classification becoming reliant on copper to lead ratio to identify segregation and processing route. This resulted in payable metals misreporting to a stream where they were an unwanted diluent, and generally, no payment was realised.

In 2021, an additional copper flotation circuit was commissioned. This facilitated the sequential production of three separate concentrate streams. This improved metal recovery and concentrate quality from mixed mineralised zones and simplified the mining requirements. The retrofit to the brownfields operation required creative solutions to balance metallurgical, operational and maintenance-friendly considerations to achieve the final project requirements.

INTRODUCTION

The original Golden Grove processing plant was commissioned in 1990 with the original flow sheet using sodium dichromate to separate the chalcopyrite and galena prior to the sphalerite flotation process. This was abandoned, and campaign treatment of copper ore in the form of chalcopyrite-bearing material and zinc ore in the form of chalcopyrite, galena and sphalerite-bearing material became the norm. For almost 30 years, the mineralisation of the targeted ore bodies allowed them to be treated as two separate ore types, optimising metal recovery and concentrate quality by configuring the flotation circuit to treat in campaigned operation. Golden Grove ores are quite coarse-grained and well-liberated at a primary grind of approximately P_{80} 106 μm . As a result of this, a regrind stage is only used in the triple sequential circuit for zinc bearing composites scavenged late in the circuit.

In 2018, the ore bodies became harder to segregate, and chalcopyrite became more associated with sphalerite. Campaign milling was further refined into three campaign types, copper only ore, lead-zinc ore and copper-zinc ore. The latter still contained amounts of galena in the feed, but due to the reduction in flotation residence time with treatment rates having increased from 0.6 Mt/y to >1.4 Mt/y, there was limited capacity to produce separate copper and lead concentrates. It became necessary to maximise recovery of the chalcopyrite and galena in a mixed bulk concentrate prior to sphalerite flotation to avoid invoking treatment penalties in zinc concentrate. For this reason, the elemental ratio of Cu:Pb in the feed would remain unchanged in the concentrate stream by maximising both recoveries concurrently.

The method implemented to deal with high and low copper-content zinc ores without any capital investment was to classify ore based on Cu:Pb elemental ratio. Mill feed was blended to achieve less than 1.0 Cu:Pb ratio material as lead-zinc ore and material >4.0 Cu:Pb ratio as copper-zinc ores.

The material in the middle ground was blended into either classification based on predominate feedstocks at the time.

This strategy was hindered when the assigned mined and stockpile grades were drastically different from what was presented to the processing plant, affecting concentrate quality and plant stability. There was also valuable material reporting to either a non-payable or low-payable product.

With the life of mine geochemistry indicating the mixed feed zinc ore was here to stay, a suite of treatment options was investigated, with the final selection resulting in an additional reagent and flotation module being added to the existing plant. This maximised value with the ore, debottlenecked mining processes, and improved circuit flexibility and mill utilisation. This paper reviews the investigations, considerations, and outcomes for converting the Golden Grove processing plant to operate a three-stage sequential flotation circuit.

Where “clean” copper-only ores can be mined and delivered, these remain a separate campaign as they typically contain much higher pyrite content, which reduces sphalerite flotation performance. The copper concentrate from the sequential flow sheet is blended with the copper concentrate from the copper-only ore for sale.

OPPORTUNITY

The modifications to the flotation and dewatering circuits had two primary goals:

- 1) Increase the available flotation capacity for Cu recovery when treating Zn ores. The three available rougher and scavenger banks available prior to zinc flotation had only 20 min of residence time at 200 t/h, resulting in between 5-10% copper recovery loss.
- 2) Create a circuit capable and flexible enough to produce three products. However, this came with a trade-off. The strategy was not to make three separate concentrates, all targeting high recovery and grade; the objective was to maximise Cu and Zn grade and recovery and minimise the amount of Pb contained in both.

Mineralogical analysis showed that, on average, the Zinc concentrate produced during Cu/Zn campaigns contained 8-10% chalcopyrite. 70% of the chalcopyrite present was fully liberated and expected to be recovered to the copper concentrate had there been sufficient flotation capacity. Laboratory flotation tests on copper circuit tailings supported the hypothesis.

An improvement of 4.5% Cu recovery and >1.5% Zn recovery for Zn ores (as much as 5%), with associated payables in both concentrates, were modelled using the 2020 life of mine plant with an increased NSR value of \$23.3 M AUD over a five-year period. Other additional benefits sum up to approximately \$16.7 M AUD per annum based on 2020 modelling and financials as shown in Table 1.

Table 1 - Summarised expected benefits of triple sequential flotation.

	Increased Cu and Zn recovery	Improved concentrate payables	Plant availability (0.5% increase)	Improved mining rates (NSR)	Improved ore NSR (Cu + Pb + Zn)	Annual Expected Benefit
Annualised value \$M	4.7	4.4	1.5	2.5	3.6	16.7

FLOW SHEET DEVELOPMENT

Historical test work carried out as part of a feasibility study for a new ore source achieved very good selectivity in the four-product flow sheet with the use of SMBS for galena and sphalerite suppression. This, however, seemed to be only suitable to small zones for that specific ore source and could not be consistently replicated.

After testing an extended range of conditions and reagents, tapioca dextrin significantly improved selectivity between chalcopyrite and galena in the copper flotation stage. Rejected schemes assessed in the laboratory included increased temperature, activated carbon, altered pH, bulk flotation, reverse flotation, dichromate and SO₂ injection.

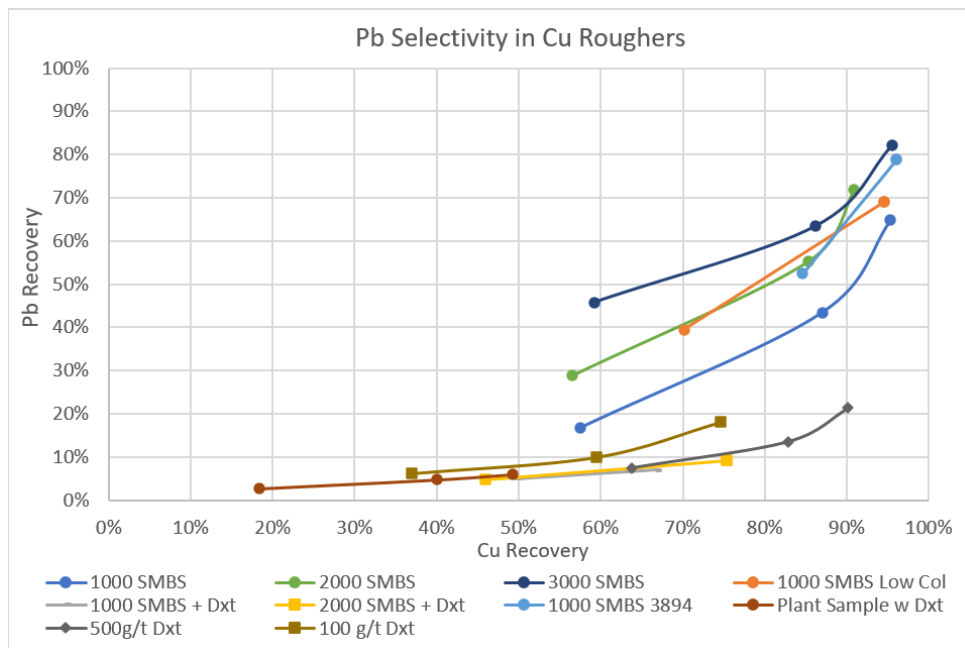


Figure 1 - Pb selectivity curves for laboratory Cu rougher tests.

Validation of the Cu-Pb separation process at the plant-scale was completed during a Cu-Zn ore campaign in November 2019 by incorporating SMBS and dextrin into the flotation feed via dosage into the SAG mill. This demonstrated that a clean copper concentrate could be produced, and the lead was reactivated for recovery prior to Zn flotation. This provided sufficient proof of concept for the project to proceed.

Further variability work was completed by performing flotation test work on samples of flotation feed and process water taken from the plant while milling Zinc ore.

PLANT DESIGN DEVELOPMENT

The historical copper rougher and scalper flotation circuit consisted of 1 x Dorr Oliver DO300 and 2 x DO600 flotation cells, providing 160m³ of volume and approximately 21 minutes of residence time at 210 tph with gas hold up of 15%. Plant performance indicated that there was insufficient capacity to produce a copper concentrate followed by a lead concentrate sequentially using the existing equipment. Further testing was performed on copper circuit tailings via additional flotation time in a laboratory cell. This confirmed that with additional flotation time, additional copper was recovered at an acceptable scavenger grade, indicating that an increase in residence time would benefit recovery.

Flotation surveys have consistently shown that the first copper rougher can produce saleable copper concentrate grade in a single stage. To take advantage of this, the plant design was orientated around using a rougher scalper configuration to produce a large portion of the final concentrate at the front of the circuit. The key criteria used to select the rougher scalper cell were: compact footprint but capable of high throughput, high upgrade performance, easily integrated wash water, and the ability to act in either rougher or scalper duties. Both the Glencore Technology Jameson cell and Eriez StackCell were identified as potential options for the required duty.

The StackCell was piloted on live plant streams to validate its potential use in a rougher scalper duty. It was found that the cell consistently produced a high-grade concentrate which did not require any additional cleaning. The successful results gathered during the pilot plant trial, combined with the compact footprint of the StackCell meant it was well suited to the rougher scalper duty.

Testing for the scale up and sizing of the Jameson cell was carried out using the procedure supported by Glencore which uses multiple stages of cleaning in a laboratory cell. This test work was completed on slurry samples and process water taken from the plant in order to most closely mirror the plant conditions.

With the rougher scalper and final cleaning flotation equipment selected, it was proposed that conventional flotation cells or tank cells be considered for the remaining scavenger duties. With the limited space available, tank cells provided the best configuration for this specific installation. Error! Reference source not found. Error! Reference source not found. shows the simplified CuPbZn flotation flowsheet (McKernan 2020).

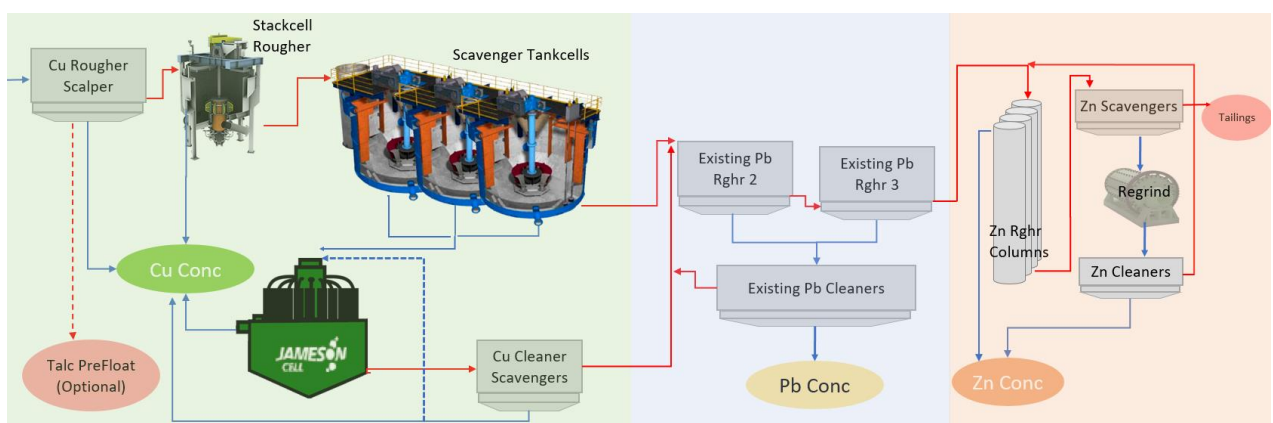


Figure 2 - Simplified Copper, Lead, Zinc sequential final flow sheet.

Additional supporting infrastructure was required to aid in treating the concentrate produced. This included an additional concentrate storage tank prior to filtration, a dextrin mixing and dosing system and consideration of additional sample pumps and OSA integration. A concentrate clarifier was re-purposed to a thickener duty to handle the additional concentrate stream, and two standby

GL&V Agidisc filters were moved to the copper concentrate filtration duty.

GENERAL ARRANGEMENT

Being a 30-year-old brownfield processing plant, the Golden Grove infrastructure is tightly integrated together, making real estate for any expansion at a premium. An area located next to the existing copper and lead flotation building was selected which still allowed maintenance access to the existing low-pressure blower shed (Figure 3).



Figure 3 - Key equipment and buildings within the processing plant.

The existing flotation building, the blower shed, and major process and water pipe corridors formed the boundary for the new installation. With the intention of maximising flotation residence time within the available footprint, three 70 m³ tank cells were selected for primary scalping duty. In addition to this, the pre-existing DO300 was incorporated into the new Cu circuit so that it could be run as either the first Cu rougher, or if required it could perform a talc pre-float function.

INTEGRATION INTO OPERATING PLANT

In addition to the new footprint, four new pump sets and hoppers were installed under the existing flotation building, and a train of unused Metquip BQ80 cells was repurposed to scavenge the tailings from the Jameson cleaner. These cells were included in the flow sheet as a precaution if the Jameson did not capture all the gold presented to it from the scavenger cells.

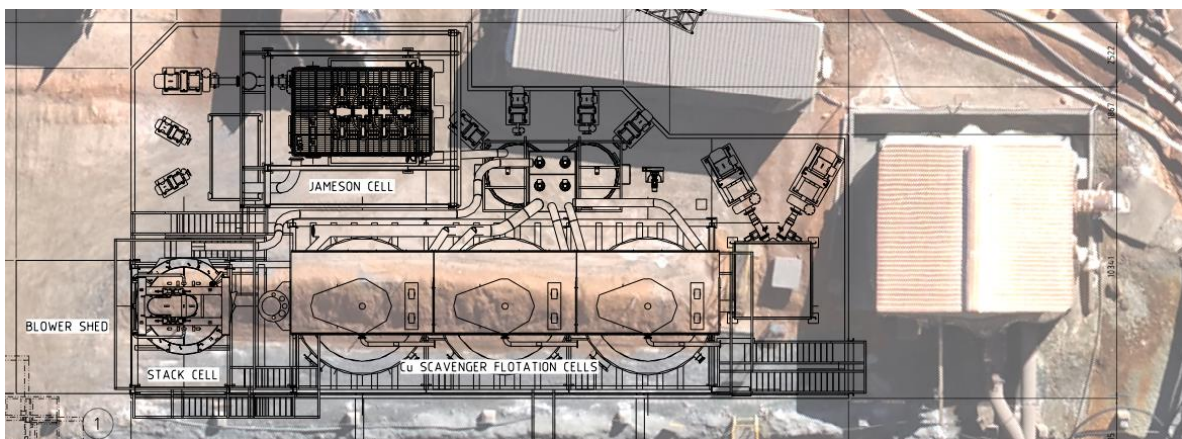


Figure 4 - General Arrangement overlap of new equipment – 180 degree rotated view of Figure 3.

The new circuit has 35 min of rougher and scavenger residence time at 210 t/h, with 380 m³ slurry volume. Converting the first DO300 cell to Cu duty left the subsequent stage for Pb flotation with a reduced 128 m³ of capacity. A review of the life of mine ore grades indicated this is sufficient capacity for lead recovery prior to zinc flotation.

Installation and tie-ins occurred in a staged approach to limit the impact on the operating plant, with slurry commissioning commencing in March 2021 on copper-only ore and then sequential zinc ore in April 2021.

COMMISSIONING

Commissioning of the new equipment was carried out on a copper-only campaign. This was to assist the mill operators and metallurgists so that they weren't trying to address both operational and metallurgical issues at the same time. The circuit was bypassed after a week's operation to allow any modifications to be made to address issues that were identified.

Significant data was collected by way of metallurgical surveys during the commissioning of the new circuit. An indicator of selectivity was the Cu:Pb ratio in the feed and concentrated in each node in the circuit. This is shown in Figure 5 with the grey 1:1 parity line to highlight axis scale differences. Chalcopyrite naturally shows faster flotation kinetics than galena does, so this is not a holistic representation of the effects of reagents and conditions.

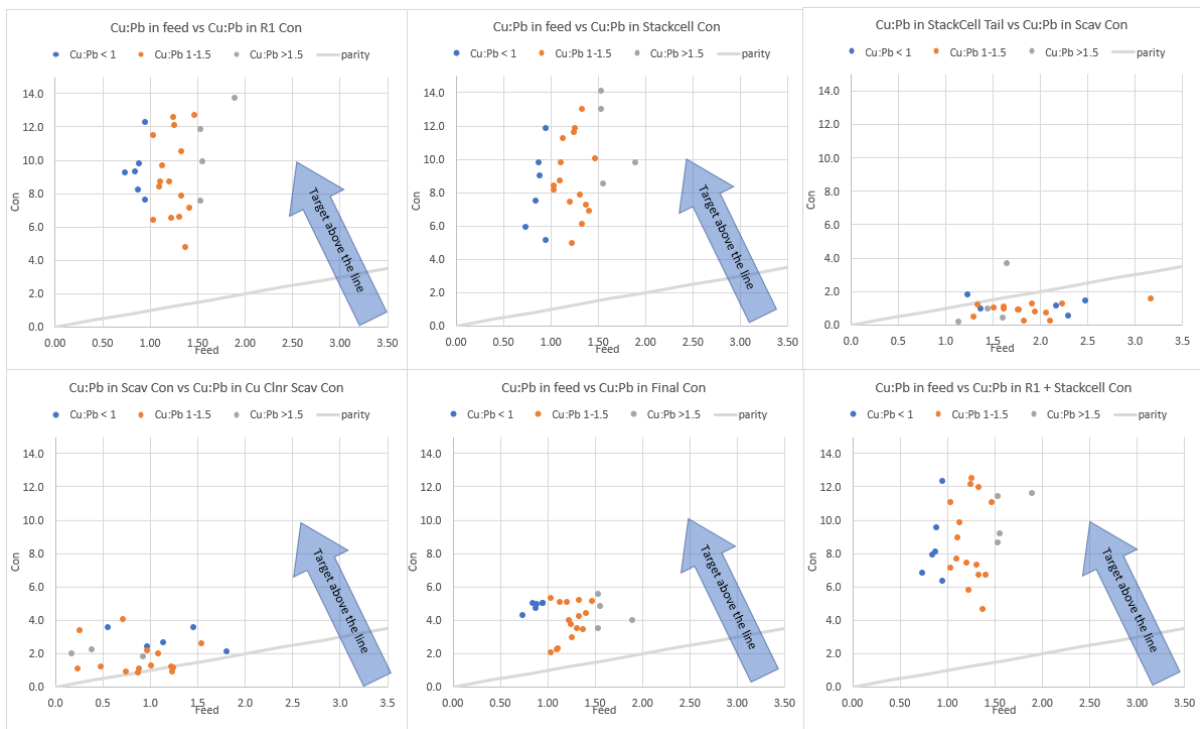


Figure 5 - Selectivity between Cu and Pb throughout the circuit in first months of commissioning.

Lead flotation in the subsequent flotation stage was enabled by the addition of Aerophine 3418A without any detriment to performance from the prior circuit configuration.

The reagent conditions for the historical circuit and the new flow sheet are shown in Error! Reference source not found..

Table 2 - Flotation Conditions Prior and Post Modification

	CuZn/PbZn (bulk flotation)	CuPbZn (sequential flotation)
Rougher pH	Natural (7.0-8.0)	9.0 – 10.5
Collector	RTD-609 and 3418A	RTD-609 dosed in Cu circuit only with 3418A dosed in Pb circuit
Depressant	SMBS	SMBS + Dextrin

It was found that initial elevated dosages of dextrin between 500-1000 g/t ore slowed the flotation kinetics of both Cu and Pb and caused downstream issues in the zinc flotation circuit. The froth became sticky and heavy and, even with increased air rates, could not achieve the required froth carry rates to meet recovery targets. The initial laboratory test work and plant validation trials had indicated that higher dosages of dextrin would be required to achieve the required separation, however, reducing the dextrin dosage to below 100 g/t ore was just as effective. Further, the flotation's selectivity improved as pH increased from approximately 7-8 to 9.0-10.5.

The effect of SMBS on Golden Grove ores does not have the consistent effect on galena suppression it does in other sequential operations. Very early work on the use of SMBS to depress galena showed promise on some ore bodies with SMBS only at 2-3 kg/t dosages but were not able to be replicated across all ore samples. SMBS is, however, consistently effective for both pyrite and sphalerite rejection in chalcopyrite and galena flotation.

It was found that a staged addition was beneficial if both dextrin and SMBS were further dosed prior to the scavenger circuit to maintain the selectivity between Cu, Pb and Zn.

The rougher-scalper approach is a success, with 45-60% of the copper concentrate recovered from the first two flotation devices in the flow sheet. The DO300 cell and StackCell account for five minutes of the flotation time in the whole circuit. Figure 6 shows the results of 25 surveys around the circuit during commissioning and includes testing a range of operating conditions.

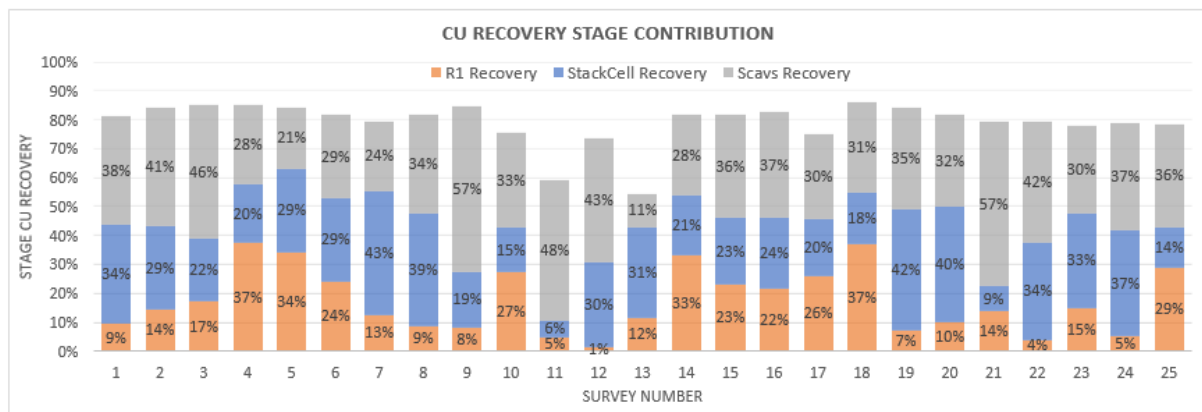


Figure 6 - Stage recovery in Cu flotation circuit inclusive of stress testing operating limits.

The circuit design was designed to treat up to 260 t/h or ore at a grade of 4.3% copper in line with an extreme LOM scenario. Valving and pipework design allows the option to redirect streams so that flotation cells can be turned off, bypassed or reported to a cleaning stage rather than directed to the final concentrate in reduced mass pull conditions.

The sequential circuit produces a clean copper concentrate, regardless of Cu:Pb ratio in the feed as can be seen in **Error! Reference source not found.** Ores that previously would have little or no value assigned to the copper component typically recover 40-60% of the copper metal previously lost to a non-payable stream or tailings.

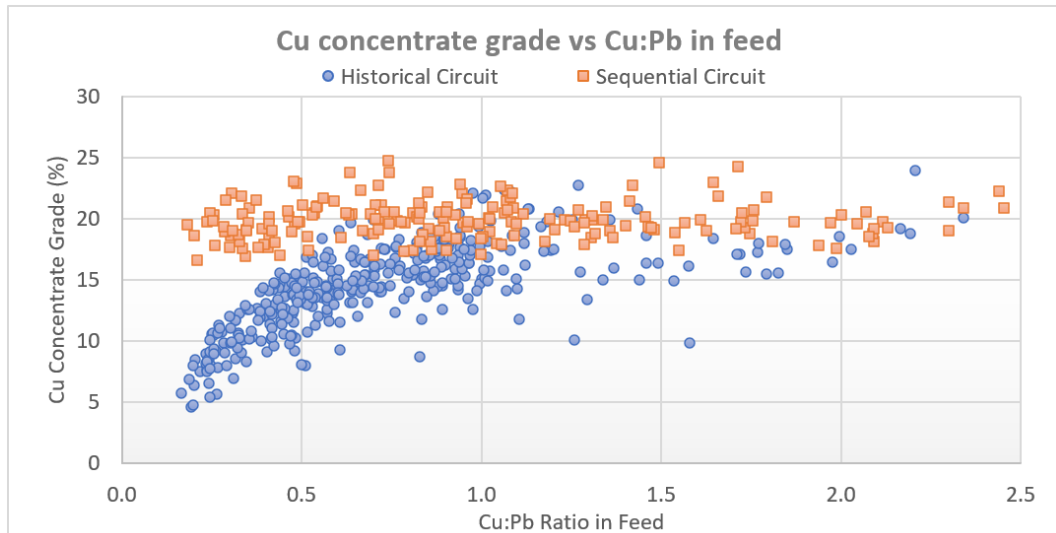


Figure 7 - Cu concentrate grade of sequential circuit versus historical.

FLOW SHEET OPTIMISATION

Prior to the plant upgrade, four to six hours of mill downtime was necessary to allow for the crushed ore stockpile to empty and for flotation and dewatering circuits to be flushed prior to acceptance of the new ore type during a campaign change (McKernan 2020). With the reconfiguration of plant due to the triple sequential upgrade, the transition process from copper only to complex zinc and vice versa has been optimised, so as to not require any plant downtime (**Error! Reference source not found.**). This has resulted in an average increase in plant availability of 0.82% versus the previous bulk circuit, a significant improvement above even the expected gain of 0.5% for the project.

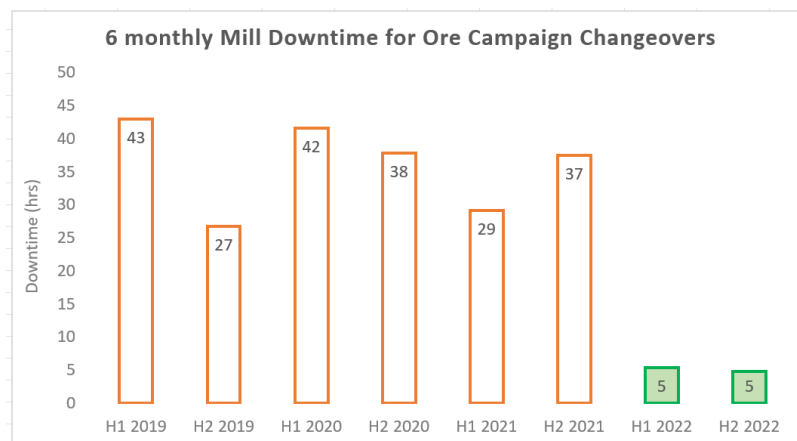


Figure 8 - Reduction in mill downtime due to sequential flow sheet optimisation.

Optimisation work on the reagent scheme, chemical conditions and circuit configuration has further improved the selectivity of the flow sheet. It was identified that at higher pH, dextrin dosages could be reduced without affecting selectivity between copper and lead. **Error! Reference source not found.** shows that reduction in dextrin dosing rates to less than 100 g/t have been possible since commissioning. However, when the dextrin is turned off completely there is a relatively fast, undesirable, increase in lead recovered to the copper circuit.

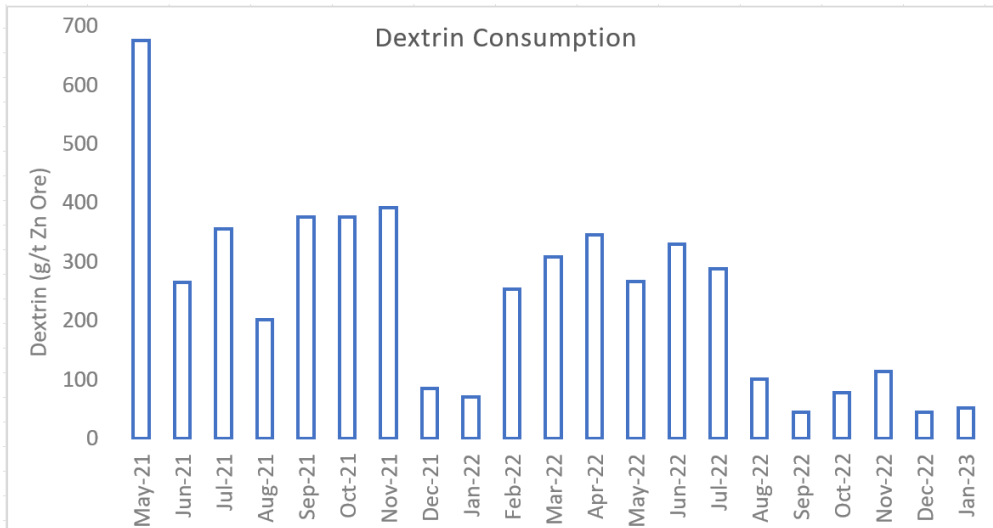


Figure 9 - Reduction in dextrin dosage rates since commissioning.

The optimal copper roughing pH range for the sequential circuit has been found to be between 9.5 to 10.2. Below this, there is less effective copper/lead separation, while above it impacts lead recovery to lead concentrate. By comparison, the Golden Grove ores have relatively high pyrite content with the Cu-only flow sheet operating at pH between 9.5-10.5 (still producing final concentrate grade from the first rougher) and cleaning at between 10-11.

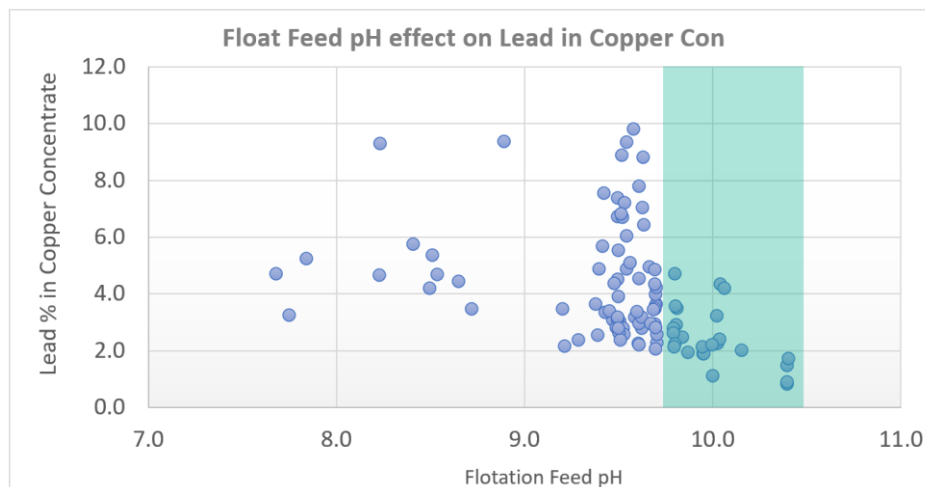


Figure 10 - Cu:Pb selectivity at increasing dextrin and pH ranges.

The optimised circuit is effective in keeping lead grade in copper concentrate below 5% at most Cu:Pb feed ratios except for instances of very low Cu:Pb ratio (very low copper in feed to plant) as shown in **Error! Reference source not found.** There is little requirement to stockpile filtered copper concentrate due to high lead content and blend with cleaner copper concentrate before it is able to be sold, which was occasionally required prior to the circuit changes.

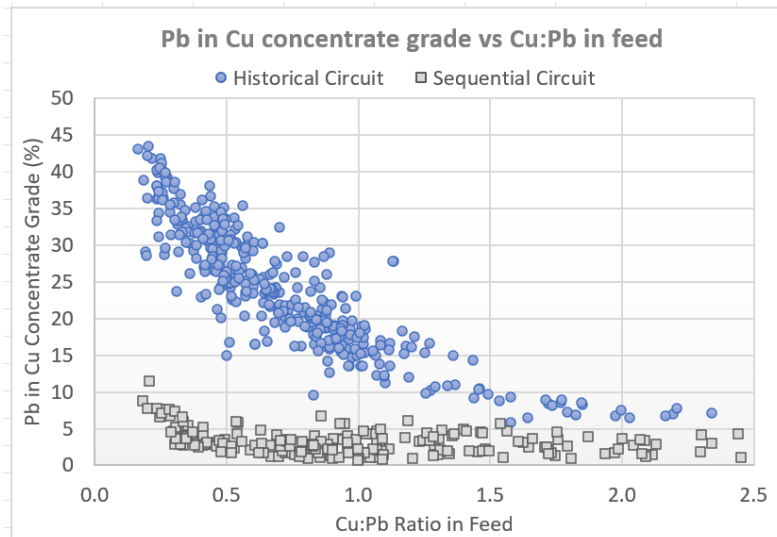


Figure 11 - Pb deportment to Cu concentrate pre and post upgrade.

The improved selectivity allows for ores that were previously classified as lead-zinc based on feed ratio to be reclassified as copper-lead-zinc. The ability to recover the copper previously reporting to lead concentrate to a copper concentrate has resulted in an increase in payability by \$4.5m annually, based on approximately 450 t of copper metal that does not misreport to lead concentrate.

A suite of automation projects has been completed to date, including integrating automated reagent dosing into the circuit. The copper collector is a good example of tangible benefits in plant performance. Dosing of the copper collector is based on g/t of copper metal in feed, calculated from the live mill feed weigher and the Courier On-Stream Analyser. **Error! Reference source not found.** shows an uplift of almost 1.5% copper recovery over the period of 1.5 years (See, 2022). Payable metal recovery models are routinely validated and updated into the geological and block models, which have had an effect on increasing the Golden Grove mineable reserve.

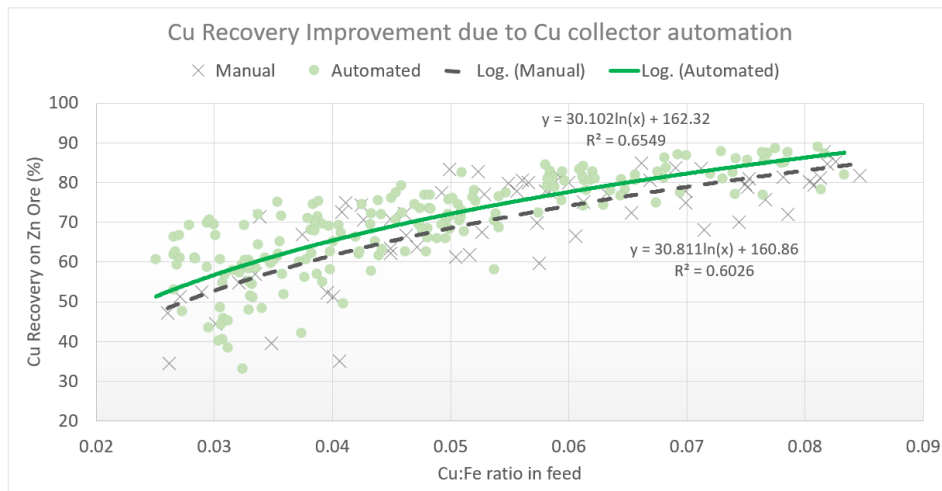


Figure 12 - Cu Recovery uplift (Zn ore) due to reagent addition automation.

Further optimisation projects are planned to deal with elevated talc in the feed through completing the talc pre-float modifications, as well as making pipework and pumping changes to alternate between Zn and Cu Scavenger regrind duty as dictated by ore mineralogy. When used on the Cu circuit, the regrind product will be directed to the Jameson Cell for improved fines recovery rather than the existing conventional cells.

CONCLUSIONS

The upgrades to the Golden Grove Concentrator to facilitate a triple sequential flotation flow sheet were ultimately a success. The plant now has the flexibility to produce clean copper, lead and zinc concentrates, and is also able to produce saleable concentrate from lower and mixed feed grades that were previously inaccessible.

The brownfields footprint required equipment selection to minimise installation area, but also maximise performance. The additional reagent addition and conditions work well within the new flowsheet and have resulted in improved operability and production.

ACKNOWLEDGEMENTS

The authors wish to acknowledge the keen attitude and support of the Processing, Laboratory, Mechanical and Electrical teams at the Golden Grove concentrator. With everyone working together and going above and beyond the project was implemented with speed and better than anticipated results.

The authors would also like to acknowledge the tireless efforts put in by the metallurgy team over the years to find a suitable flow sheet that would achieve the results needed. No rock was left unturned.

REFERENCES

Kittler, P, 2017, *GG TN 179 Flotation of Hougo hanging-wall samples - effect of feed Cu_Pb ratio on concentrate grade*, Golden Grove Technical Report.

McKernan, E, 2020, *GG TN 239 Metal Losses Due to Campaign Changeovers*, Golden Grove Technical Report.

McKernan, 2020, *GG TN 248 Triple Sequential Upgrade Summary*, Golden Grove Technical Report.

See, H, 2022, *GG TN 265 RTD Automation Analysis*, Golden Grove Technical Report.

Plant Modifications and Operating Strategies to Improve Concentrate Quality at BHP - Carrapateena

J Reinhold¹, F Burns² and J Seppelt³

1. Senior Metallurgist - Plant, BHP Carrapateena, Pernatty, South Australia, 5173. Email: jacqueline.reinhold@bhp.com
2. Superintendent - Metallurgy, BHP Carrapateena, Pernatty, South Australia, 5173. Email: fraser.burns@bhp.com
3. Manager - Processing, BHP Carrapateena, Pernatty, South Australia, 5173. Email: joe.seppelt@bhp.com

ABSTRACT

Carrapateena is a copper–gold deposit hosted in a brecciated granite complex, located 460 km north of Adelaide, South Australia. The Kokatha people are the traditional owners of the land. The deposit is currently mined using the sub-level cave (SLC) mining method, with future mining to incorporate a block cave footprint beneath the SLC.

The copper mineralogy present is chalcopyrite and bornite. Deleterious non-sulfide gangue (NSG) minerals are present as ultrafine intergrowths (<5 µm) in both host iron oxide breccia and valuable sulfide minerals. A flotation concentrator produces a high-grade Cu-Au-Ag concentrate, with trace smelter deleterious NSG minerals.

The concentrator, as commissioned in 2019, consisted of a rougher flotation bank, a High Intensity Grinding (HIG) mill for rougher concentrate regrind, a Jameson cell as a cleaner scalper, and a three-stage conventional cleaning circuit. Jameson cell and conventional third cleaner concentrates were combined to form the final Cu-Au-Ag concentrate.

Regrind to a notional 20 µm target is critical to liberate sulfide grains sufficiently for cleaning. Jameson Cell froth washing reduces entrainment of NSG present as slimes to the flotation concentrate. However, the conventional Cleaner circuit did not have that functionality and as such slimes reported to the third Cleaner concentrate. Insufficient installed HIG mill power impeded regrind to a finer target of 15 µm, as required by some ore types.

Following commissioning, the installation of a second Jameson Cell in the conventional Cleaner circuit resulted in all final concentrate undergoing froth washing; installation of a second HIG mill expanded regrind capacity, enabling finer regrind targets to be achieved.

With the completion of a second Jameson Cell and a Cleaner circuit reconfiguration, a staged approach was taken to optimise individual unit operations for both copper recovery and NSG rejection. Two different operating strategies were established and a longer term trial conducted, which confirmed the effectiveness of these operating strategies and circuit modifications.

This paper gives an overview of the process to optimise the Carrapateena flow sheet to improve concentrate quality by rejecting NSG, including the installation and commissioning of the second Jameson Cell, Cleaner circuit reconfiguration, expanded regrind capacity and the creation of flexible operating strategies.

INTRODUCTION

Carrapateena is a copper–gold deposit, located 460 km north of Adelaide, South Australia. The deposit is currently mined using the sub-level cave (SLC) mining method, with future mining to incorporate a block cave footprint beneath the SLC.

The copper mineralogy present at Carrapateena is chalcopyrite and bornite, hosted in an iron oxide breccia; which is typical of IOCG deposits located in South Australia. A sulfide flotation concentrator produces a Cu-Au-Ag concentrate for sale to copper smelters. Construction of the concentrator was completed in late 2019, slurry commissioning began in Q4 2019 with the first concentrate produced and filtered in December that same year.

Throughout 2020 and 2021, the concentrator flotation circuit was expanded and reconfigured to provide greater capacity and flexibility to address and improve concentrate quality, and to reduce the department of deleterious NSG-sulfide gangue minerals to the concentrate. This paper describes the Carrapateena concentrator, the development of this circuit reconfiguration, and subsequent optimisation work that created the flexible operating strategies now employed, plus details of additional expansions underway to further the same aims.

Mineral Resource And Mine Description

The Carrapateena Mineral Resource, at the time of writing, is 950 Mt with a grade of 0.56% Cu, 0.25 g/t Au and 2.7 g/t Ag. The Carrapateena deposit is an Iron Oxide Copper-Gold (IOCG) mineralised zone characterised by semi-coincident gravity and magnetic anomalies, enclosed in Donnington Suite granitoids and overlain by approximately 470 m of post mineralisation unconformably overlain with sediments of the Stuart Shelf. Below the unconformity, the mineralisation has a rough cylindrical shape with a footprint of 500 m diameter and a vertical extent of approximately 2000 m.

The Carrapateena Breccia Complex (CBC) that hosts the mineralisation is a brecciated granite complex and can be described as a combination of weakly to strongly altered polymictic to massive, locally mineralised hematite-sericite-quartz breccias with clasts and fragments of granite and other meta-sedimentary materials. Various dykes are also found within the deposit. Alteration assemblages are hematite, sericite, chlorite, carbonate and silica; clearly fitting the hematite end member, ‘classical’ IOCG alteration.

Sulfide mineralisation hosted within the hematite breccias is a combination of dominantly fine-grained disseminated to medium-grained blebby chalcopyrite with a discrete high-grade zone of bornite, rare chalcocite, digenite, and covellite in hematite breccias. Pyrite is extensive around the fringes of, and at depth, within the CBC.

With the resource located at depth, underground mining is used to exploit the resource. An initial Sub-Level Caving (SLC) operation mined its first ore in Q1 2019 and fully ramped up to the design rate of 4.25 t/y in Q4 2020. The initial SLC footprint focuses initial mining activities to an initial bornite-chalcopyrite dominant core of the resource. Further expansion to full Block Cave (BC) operation is presently under development and will expand mining activities into an increasing portion of chalcopyrite and chalcopyrite-pyrite domains.

Process Plant Description

As the Carrapateena process plant has not previously been described by others, a detailed description is provided in this paper.

SLC ore is primary crushed underground in a 450 kW ThyssenKrupp KB 54x67 to a nominal P80 size of 100 mm. Primary crushed product is conveyed to the surface where it is stockpiled on a coarse ore

stockpile (COS) with nominal total capacity of 60 000 t and live capacity of 12,000 t. Two 75 kW Metso 1.2 m x 7.1 m apron feeders reclaim the coarse ore for grinding. A Metso VisioRock system is located on the grinding circuit feed conveyor. This provides an online circuit feed sizing.

The grinding circuit is a conventional SABC circuit, which is comprised of a $\varnothing 8.5 \times 4.57\text{m}$ single pinion 7.0 MW Metso SAG mill and $\varnothing 6.71 \times 4.57 \text{m}$ EGL dual pinion 9.5 MW Metso ball mill. The ball milling circuit is closed by a cyclone pack consisting of twelve Weir Cavex 500CVX cyclones, fed by a duty/stand-by pair of 560 kW Weir Warman 350TU-MCR cyclone feed pumps. A deviation from the Prominent Hill flow sheet, on which Carrapateena is based, is the addition of pebble crushing due to Carrapateena more competent ore. A 220 kW Metso HP3 cone crusher performs this duty at nominal CSS of 10 mm. The grinding circuit nominally produces flotation feed at a P80 size of $75 \mu\text{m}$ at a nominal rate of 500 t/h.

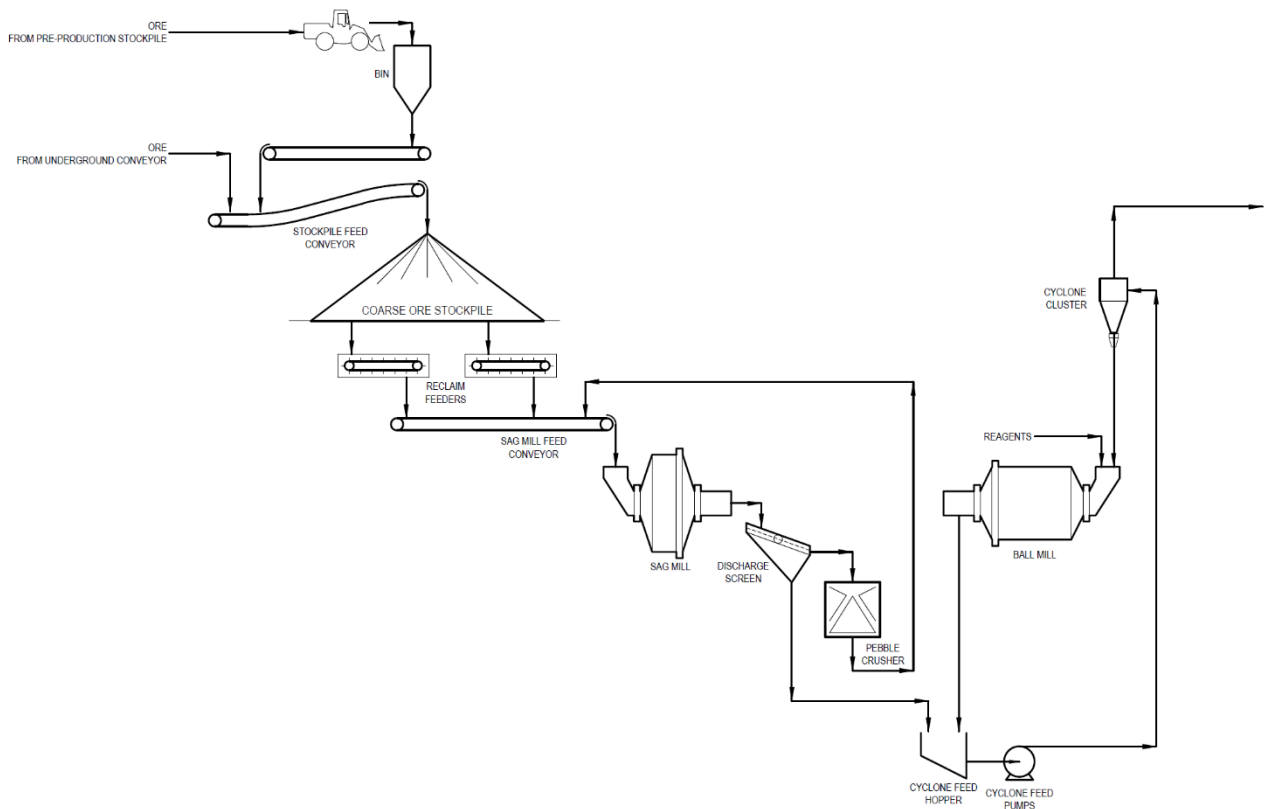


Figure 1: Carrapateena Grinding Circuit Flow sheet - Commissioned

The flotation circuit commences with a roughing stage of five Metso e130 tank cells. Rougher tails report to the final tailings thickener. Rougher concentrate proceeds to the regrind circuit where a hydrocyclone pack consisting of twelve Weir Cavex 150CVX cyclones, cut at a nominal $20 \mu\text{m}$. Underflow proceeds to a single regrind mill – a 1,600 kW Metso HIG1600/900 – producing a nominal mill product size of $20 \mu\text{m}$. A 4.0 SG ceramic media blend of 2.5 mm and 4.0 mm is used as the grinding media. A risk of deleterious element deportment to the final concentrate was noted in the design, due to varying metallurgical performance of certain ore types. Therefore, sufficient regrind capacity was allowed to reduce the regrind mill product size to $15 \mu\text{m}$ at the nominal design rates.

The regrind mill product, combined with the hydrocyclone overflow, feeds a E4232/10 Mark IV Glencore Technology Jameson Cell in a cleaner scalper duty. Cleaner scalper concentrate reports directly to the final concentrate. Cleaner scalper tailings proceed to three stages of conventional

mechanical cleaning comprising of six Metso e50 cells, four e20 cells and three e20 cells in cleaner one, two and three respectively. Cleaner one is operated in an open-circuit configuration, with tailings reporting to final tailings. Cleaners two and three are operated in a closed-circuit configuration, with the tailings of each reporting back to the proceeding stage. Feasibility test work supported that these three stages of mechanical cleaning would be sufficient to produce quality concentrate. The concentrate from cleaner three, combined with the cleaner scalper concentrate, produces the final copper-gold concentrate.

Sodium Ethyl Xanthate (SEX) is the primary collector and is stage-dosed throughout the rougher and post-regrinding to the cleaner scalper and cleaner one at total nominal rate of 25 g/t. Isopropyl ethyl thionocarbamate (IPETC) is a secondary collector and is dosed to the ball mill feed chute at nominal rate of 3 g/t. The collector suite is focused on bulk sulfide recovery, without active pyrite depression. High copper final concentrate grades (35-45% Cu) are maintained due to the presence of bornite in the sulfide mineralogy. A weak alcohol-based frother is dosed as required throughout the flotation circuit.

The flotation circuit is equipped with an extensive Metso automation package consisting of online copper analysis via a Courier 6X SL, online particle sizing of primary cyclone overflow and regrind mill discharge with a PSI500, and FrothSense cameras located on each cell in the rougher and first cleaner stages. These are essential for later development of operational strategies.

The copper concentrate is dewatered first by a 15 m Metso high-rate thickener to nominal underflow density of 65% w/w, and then by a filtered by Metso VPA2040-32/40 vertical plate filter press to a nominal filter cake moisture of 9% w/w. Cake washing with fresh water during filtering removes remnant process water containing high levels of salinity from the filter cake. A 580 m³ concentrate storage tank provides 24-hour surge capacity between the thickener and filter press. Concentrate is hauled by road train to Whyalla for shipment of concentrate to smelters.

Flotation tailings are dewatered first by a 27 m Metso high-rate thickener, to nominal density of 60% w/w solids. A pumping train, consisting of six 220 kW Weir Warman 8/6 AHPP high pressure centrifugal pumps arranged in series, transfers the thickened tailings slurry between 7.5 km and 11.8 km to sub-aerial discharge spigots within a dedicated tailing storage facility. This pumping facility has since been upgraded with the addition of a further three 220 kW Weir Warman 8/6 AHPP pumps to the existing centrifugal pumping train, and installation of a parallel 2,000 kW MHWirth triplex single-acting piston diaphragm pump to undertake the primary tailings pumping duty.

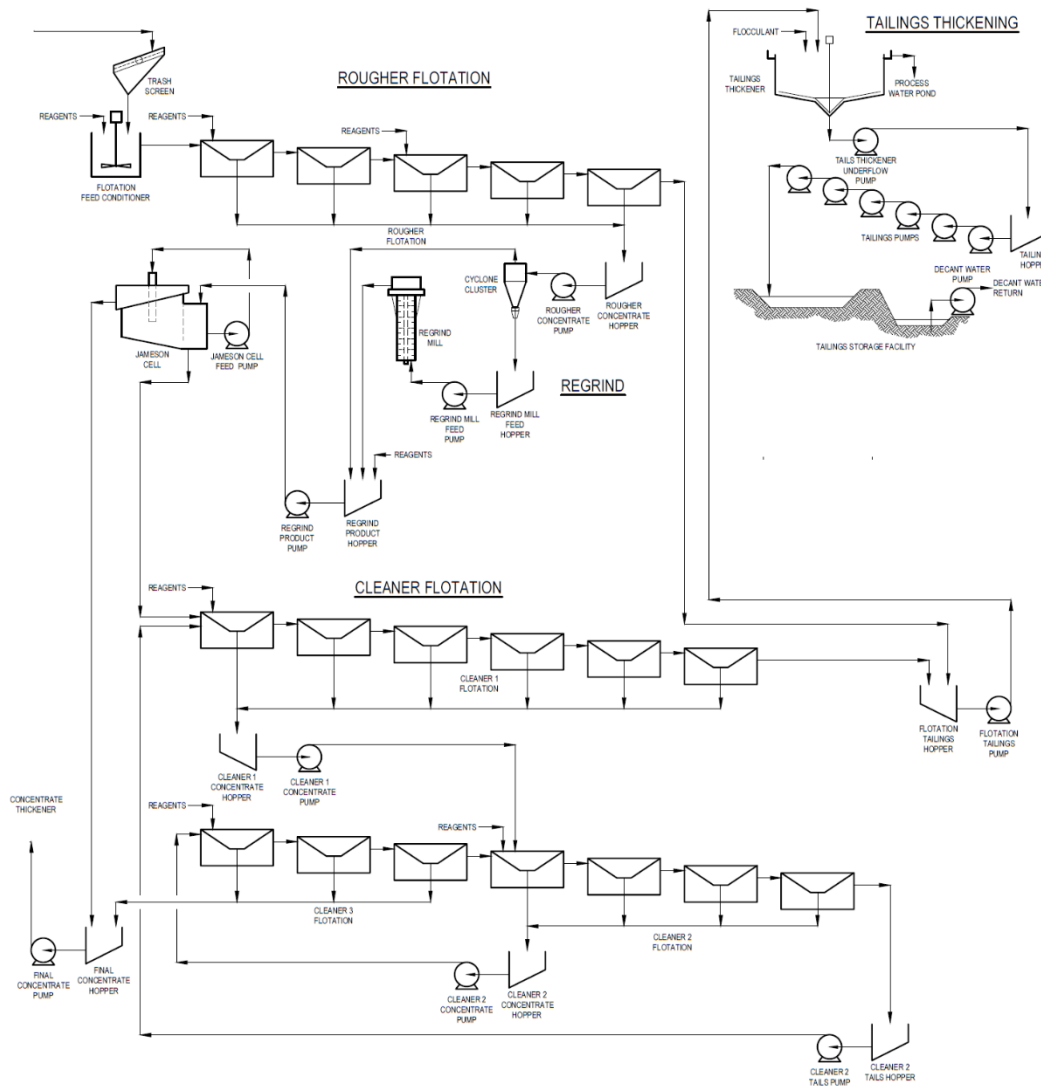


Figure 2: Carrapateena Flotation Circuit Flow sheet - As Commissioned

FLOTATION CIRCUIT CHALLENGES

The key requirement of the Carrapateena flotation circuit is to reduce the final concentrate NSG mineral grades to maximise concentrate quality opportunities for the Carrapateena product.

Given the similarities of the IOCG deposits between Carrapateena and Prominent Hill, the Prominent Hill flow sheet was selected as basis for feasibility test work and ultimately the design of the Carrapateena process plant. The Prominent Hill circuit was designed considering the need for high flotation selectivity against and rejection of NSG to produce a quality concentrate. Additionally, early Prominent Hill optimisation learnings were included in the base design of Carrapateena.

NSG for Carrapateena is dominated by haematite (Fe_2O_3) and silica (SiO_2) that form the host breccia. Further, the two deleterious non-sulfide minerals of note are fluorite (CaF_2) and uraninite (UO_2). Mineralogical assessment of laboratory flotation products, presented in Figure 3, highlighted both sulfide-gangue binary composites and ultrafine gangue entrainment as key contributors to final concentrate deleterious non-sulfide mineral content. The assessment also highlighted that rougher regrind product size will be critical to reduce the department of deleterious minerals to the final concentrate. Subsequent mineralogical assessments, shown in Figure 4, have supported the importance of ultrafine regrind, indicating that these minerals present with an average mineral grain

size of 8 μm . At this ultra-fine grain size, these minerals provide a significant entrainment rejection challenge which forms the focus of this paper.

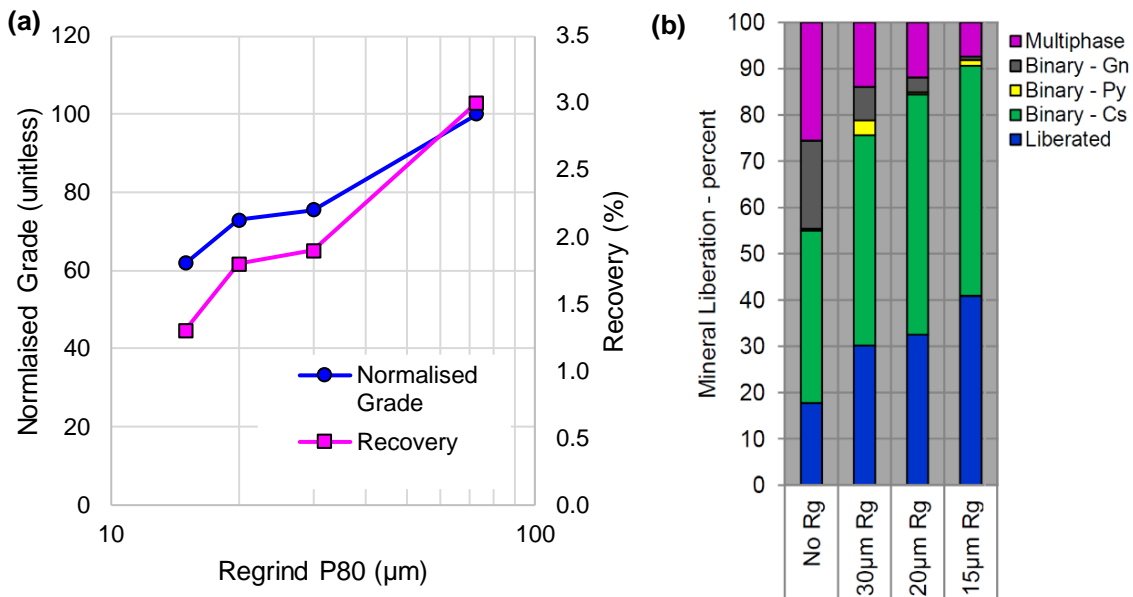


Figure 3: Laboratory Regrind P80 Response Tests (a) Normalised Deleterious NSG Mineral Grade and Recovery to Final Concentrate (b) Deleterious NSG Mineral Carriers in Concentrate

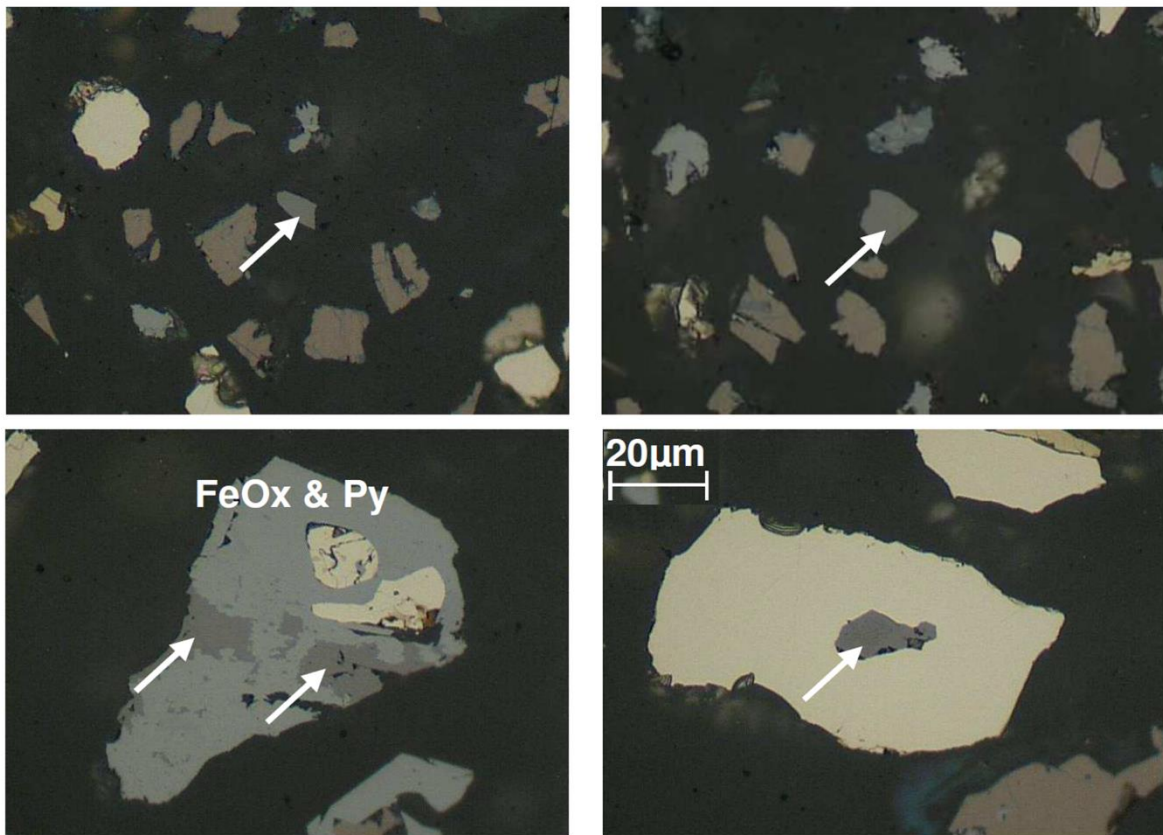


Figure 4: Deleterious Non-Sulfide Mineral Grains (Arrowed) Observed in Carrapateena Final Concentrate – Both Liberated and Locked

FLOTATION CIRCUIT MODIFICATIONS TO BUILD FLEXIBILITY

Late 2018 and early 2019 saw the onboarding of the metallurgical leadership for the concentrator operations team. A fresh view of the design of the cleaner circuit highlighted several opportunities to further enhance the value of the operation. Through engagement of engineering company Engenium and metallurgical consultancy Mineralis, a cleaner circuit expansion and reconfiguration was developed based on the mineralogical understanding that:

- deleterious elements are present primarily as fine-grained NSG
- ultrafine rougher concentrate regrind is required to liberate deleterious NSG minerals from copper sulfides
- subsequent Cleaner flotation operation must minimise entrainment recovery of liberated, ultrafine NSG.

The reconfiguration intended to provide:

- equipment to 100% froth wash the final concentrate
- recycle of a composite rich stream for targeted further ultrafine grinding
- froth crowding to stably increase scavenger froth depths to reduce down the bank entrainment
- optionality to release high NSG recirculating loads to tails when required
- additional flotation capacity to accept both expanded plant throughput and very dilute operation of the Cleaner banks.

This was justified on new metallurgical modelling; existing metallurgical assumptions, the proposed process plant design documents, and Net Smelter Return (NSR) analysis.

Cleaner Circuit Reconfiguration Description

The preferred upgraded Cleaner circuit flow sheet was established in Q2 2019 and was taken forward to detailed design throughout remainder of 2019. Construction commenced in Q3 2020 and commissioning in Q1 2021. While the reconfiguration centred around transfer of the cleaner three duty to a Jameson cell for improved NSG rejection with froth washing, the project saw extensive changes throughout the cleaner circuit. Changes to unit operations are highlighted in Figure 5.

Cleaner One, originally six e50 tank cells, was split with the creation of Cleaner One Scavenger bank formed by the last two e50 cells. Cleaner One concentrate continues to report to Cleaner Two. Cleaner One scavenger concentrate recycles to the regrind circuit after classification. The recycling of Cleaner One scavenger to regrind aims to apply additional grinding power specifically to slower floating composite particles in the regrind circuit product. The scavenger concentrate reports to a new deslime pack of eight Weir Cavex 150CVX cyclones, cutting at a nominal 8 μm . This cut size is significantly finer than the regrind cyclones to drive composites to the regrind mill feed, and is aligned with average deleterious NSG mineral grain size as indicated by the mineralogy.¹¹

Deslime cyclone underflow combines with regrind cyclone underflow at the regrind mill feed hopper. Deslime cyclone overflow combines with regrind cyclone overflow and regrind mill discharge to form Cleaner 1 Jameson feed.

The fourth Cleaner One cell was provisioned with the required valving to direct its concentrate between either the Cleaner One concentrate launder or the Cleaner One Scavenger concentrate launder. This provided ability for the Cleaner One bank capacity to flex with feed grade or mineralogy changes.

The Cleaner Three duty transferred to a new Glencore Technology E2532/6 Jameson Cell. Cleaner Three Jameson concentrate combines with Cleaner One Jameson concentrate to form a fully froth washed final concentrate.

Cleaner Three tailing reports to a Cleaner Three scavenger bank, formed by three e20 tank cells (original Cleaner Three bank). Cleaner Three scavenger concentrate recycles to Cleaner Three Jameson feed and this bank mass pull can be flexed to main maintain block recovery or manage ultrafine NSG recirculating loads.

Cleaner Two bank remained unchanged; however Cleaner Two tailings was provisioned with the ability to open circuit to final tailings, providing an additional route to release recirculating loads of ultrafine NSG as required.

Numerous pump motor and pulley upgrades were completed to enable the new flow sheet and higher volumes associated with increased dilution water throughout the flotation circuit.

Extensive froth crowding was installed at Rougher cells 4 and 5, and at the entirety of both Cleaner One Scavenger and Cleaner Three Scavenger banks. This improved operation at increased froth depths in these low mineral-loaded duties. This enabled aggressive down-the-bank mass pull profiles to drive NSG entrainment rejection.

To de-risk operating the HIG1600 at higher media charge levels required for full power draw, which anecdotally could lead to higher elutriation losses of media, a media safety screen was installed on the regrind mill discharge stream, and an internal media classifier was installed on the mill's grinding rotor.

To support the physical process modifications, a significant automation effort applied to the flotation circuit. The FrothSense camera system was utilised to provide a total bank and down-the-bank profile control of mass pull at the Roughers, Cleaner One and Cleaner One scavenger. Regrind size is controlled by PSI500 manipulating the regrind mill power draw. OSA copper readings allowed creation of Cleaner One Jameson and Cleaner Three Jameson recovery controllers to prevent unselective over recovery at the critical final stage unit operations. Process water additions were automated to allow operators to select flotation densities.

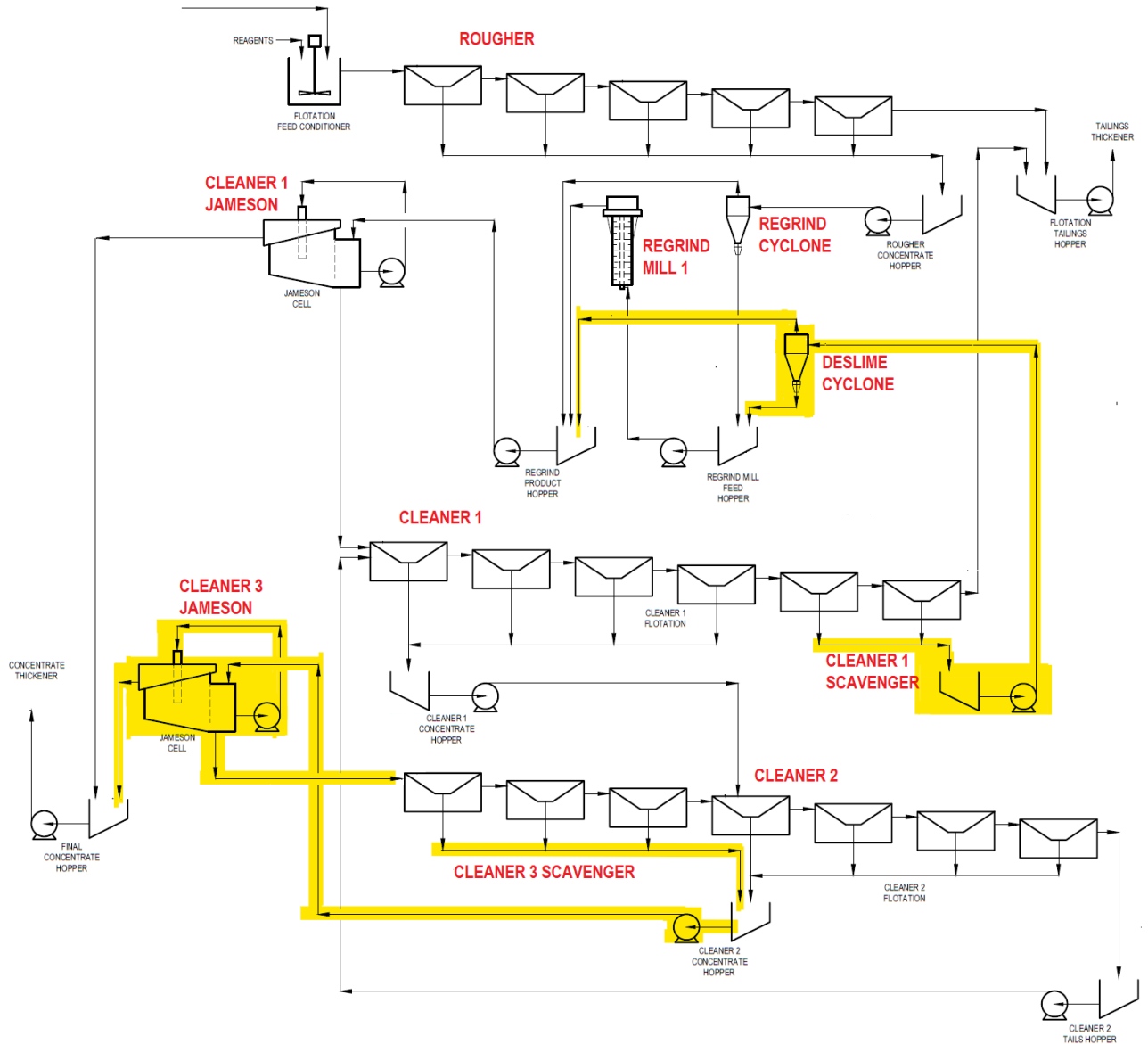


Figure 5: Carrapateena Flotation Circuit Flow sheet - Reconfigured

DEVELOPMENT OF FLEXIBLE OPERATING STRATEGIES

After reconfiguration of the Carrapateena Cleaner circuit in Q1 2021, an NSG rejection operating strategy was developed based on the mineralogical understanding that deleterious elements are present primarily as ultrafine-grained NSG minerals; that ultrafine rougher concentrate regrind is required to liberate these minerals from copper sulfides; and subsequent Cleaner flotation operation must minimise entrainment recovery of liberated, ultrafine deleterious NSG minerals.

Typical flotation practice to minimise entrainment recovery includes multiple stages of cleaning, froth washing and operation at dilute cell density. The NSG rejection strategy aimed to exploit specific modifications introduced in the cleaner reconfiguration that directly related to these traditional methods in addition to other operational changes. The tactics employed within the operating strategies are given in Table 1.

Table 1: Initial Copper Recovery and NSG Rejection Strategy Outline

Operating Strategy	NSG Rejection	Recovery Focus
When	Expected higher content of deleterious NSG minerals in flotation feed	Normal operations
Intent	Fully liberate and aggressively reject entrainment	Sufficiently liberate and target recovery
Tactics	Finest regrind P80	Standard regrind P80
	Reduced mass pull at mechanical cells	High mass pull at mechanical cells
	Steeply decreasing froth velocity profiles	Decreasing froth velocity profile
	Limit Jameson Cell recovery	Highest Jameson Cell recovery
	Low scavenger recirculating loads	High scavenger recirculating loads
	High wash water rates	Normal wash water rates
	Dilution cleaning - lower % solids	Increase flotation residence time - higher % solids
Impact	Increasing concentrate quality	Increasing copper recovery

The plant was separated into unit operations with each tactic described in Table independently evaluated at relevant unit operations for its effectiveness to reject NSG. These development surveys were assessed with the optimum conditions for each operation brought together for a full plant trial in Q2 of 2021.

To measure the extent of NSG rejection, the recovery of silica was used as a proxy for the entirety of NSG. Additionally, the upgrade ratio is also monitored as a key metric for deleterious elements, where the upgrade ratio is given as the grade in concentrate divided by grade in flotation feed.

Mechanical Flotation Cells

The tactics applied to mechanical flotation cells were changes in mass recovery and froth velocity profiles in the rougher bank and Cleaner One bank, with recirculating loads in the Cleaner One scavenger and Cleaner Three scavenger banks also considered.

Bank Mass Recovery and Recirculating Loads

A reduction in mass recovery target for a given feed was trialed from the rougher, first Cleaner, and first Cleaner scavenger banks to reject NSG. To achieve this, the target concentrate flow was reduced. Using PID controllers, this concentrate flow rate target is fed back to the froth velocity controllers for each cell that manipulate each cell pulp level and air addition. To investigate mass recovery and recirculating loads, the froth velocity profiles with each bank were maintained at the standard operation values for these trials, and the concentrate flow rate targets were adjusted.

The trials were completed on the basis that a decrease in mass recovery from the rougher and first Cleaner resulted in no discernible difference in copper recovery but did decrease in NSG recovery. There was limited impact on the rougher deleterious element upgrade ratio.

For the first Cleaner scavenger however, it was identified that the mass recovery could be significantly reduced from the previous operational norm. The flow target could be reduced by 50% without impact on the copper recovery. The reduced flow rate target became the operational norm

for the Recovery Focus strategy, and a further decrease was assessed for the rejection of NSG. Further reducing the first Cleaner scavenger mass recovery target did not have a significant effect on the NSG recovery instead only a negative impact on copper recovery.

The first Cleaner and first Cleaner scavenger flow rates have a significant impact on the presence of a recirculating load in the cleaning circuit. By reducing the flow rates, less NSG reported to the following Cleaner stages with less opportunity to report to the concentrate. Despite lower flow rates not having a direct impact on the individual trials, the impact on the overall strategy would be assessed in the plant trial.

Bank Froth Velocity Profile

Down-the-bank surveys completed on the Roughers and Cleaner One identified a considerable proportion of NSG recovery was from the last cells of the roughers and Cleaner banks. Moving progressively down the bank, the concentrate had a lower copper grade and higher levels of NSG. To make use of this observation for the NSG rejection strategy, the mass recovery of each cell was decreased significantly down the end of the bank. To achieve this, FrothSense cameras were essential in providing a measurement of froth velocity into to the launder.

A target velocity was fed into the air addition and pulp level controllers of each cell to maintain that velocity over the course of the trial. The target velocities were set as a ratio to the first cell. A ratio of 1 on the second cell would indicate the second cell velocity target is equal to that of the first cell. A 0.25 ratio would indicate the second cell velocity target is 25% of the first. The first cell velocity was determined by a mass recovery controller. During testing velocity profiles, the overall mass recovery of the bank was maintained.

In the case of the roughers, all concentrate mass was recovered off the first four rougher cells in the NSG rejection strategy with the last cell ratio being set at 0. This resulted in a decrease in copper recovery of 2% and an increase in NSG rejection. The deleterious NSG upgrade ratio decreased from 1.63 to 1.34 and recovery from 12% to 11%. There was no change in Si recovery.

This same process was repeated for the first Cleaner bank. By reducing the froth velocity ratios down the back end of the bank, the deleterious element ratio decreased from 1.36 to 1.15 and recovery from 12% to 10%. Similarly, no change was noted to Si recovery and a 2% loss of copper recovery was observed across the bank.

The resultant strategy was to significantly reduce the froth velocity and as such mass recovery at the back end of each of the rougher, first second, second, third and third scavenger banks to achieve the best NSG rejection. The effect of this strategy and impact on other unit operations would then be considered in the overall plant survey.

Jameson Cell

Recovery Limit

Following the circuit reconfiguration, a series of surveys were taken from the Cleaner Three Jameson where a range of operation parameters were considered to investigate their effect on the copper and NSG rejection of the cell. Those considered were wash water rates, the presence of lip extenders that reduced lip length, pulp level, and air addition rate. A change in lip length would alter mass recovery from the cell which had been identified in the mechanical cells as a possible method to reduce NSG entrainment. The pulp level and wash water rates would alter the extent of froth washing to displace the water and entrained particles contained in the froth.

It was determined that air addition had the greatest effect in NSG rejection. This supports the deleterious NSG presence as ultra-fines being carried across to the concentrates a result of

entrainment. The high air rate does not allow for the wash water, even at higher wash rates, to effectively displace the slurry in the froth to draw the entrained particle down towards the tails. The lip extenders resulted in no significant change to copper recovery or NSG rejection, whilst the other two conditions, wash water and slurry level, did have some effect.

Copper and NSG selectivity curves were developed for both Cleaner One Jameson and Cleaner Three Jameson. These curves, presented in Figure 6, resulted from the numerous surveys of each cell across a wide matrix of air, pulp depth, and froth wash water conditions. An observation from both cleaners was an increase in stage copper recovery resulted in an increase in the stage deleterious element recovery. Of note was an inflection point in the trend at ~75-85% copper recovery where the slope of the deleterious element recovery greatly increased for a given percent in copper recovery. Operation of the Jameson Cells beyond this limit saw significant loss of selectivity against NSG.

A target stage copper recovery, as measured online by the plant OSA, was taken forward as the primary target for the operation of Jameson Cells. When operating with a Recovery Focus strategy, Cu recovery would be limited to ~75% to align with the selectivity curve's inflection point, similar to the approach outlined by Seaman et. al. for the Jameson Cells installed at the Telfer Gold Mine. When operating for NSG rejection, this stage recovery target would be lowered to minimise unnecessary NSG entrainment, within the limit of maintaining an acceptable Cleaner circuit recovery.

The effectiveness of this strategy and its impact on other unit operations would then be assessed in the overall plant trial.

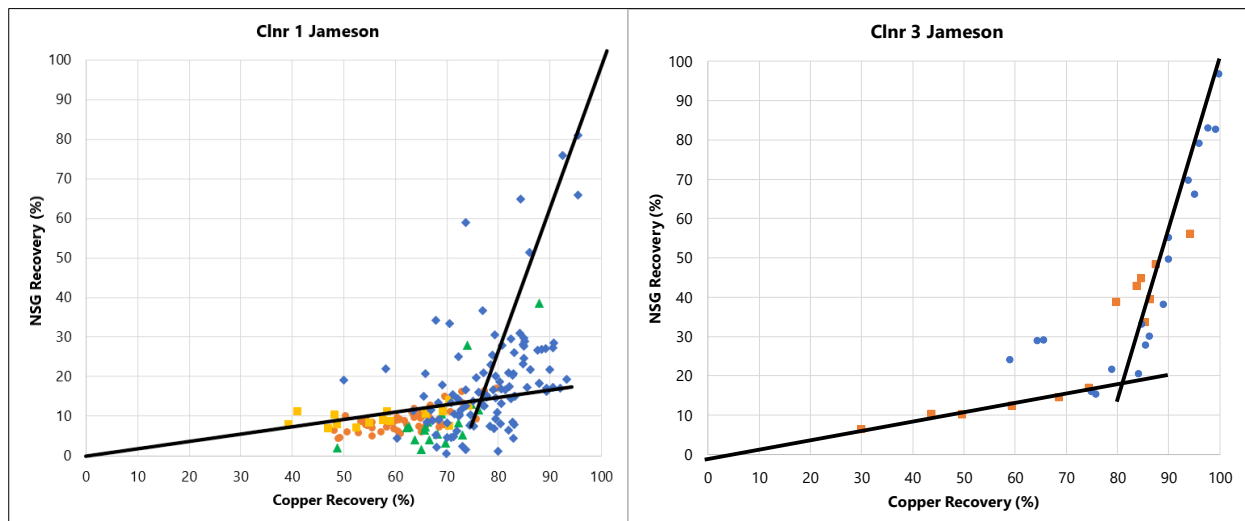


Figure 6: Jameson Cell Copper – NSG Selectivity Curves

Dilution Cleaning

Operating flotation cells, especially mechanical cells with low pulp densities, is a traditional method to reduce NSG entrainment. However, operation at low densities increases volumetric flow rates and reduces flotation residence time. The circuit reconfiguration provided an opportunity to build in capacity to allow dilution cleaning. The addition of flotation capacity with the new Jameson Cell and the upgrade of numerous pumps, allowed operation of Cleaner Two and Three circuits at low densities below 10% solids w/w.

Further, the operation of Jameson Cells requires a continuous feed flow to the distributors. During periods of lower fresh feed flow to the cells, a greater proportion of tailings slurry will re-enter the

feed box through a port and thus recirculate within the cell. The slurry level and hence recirculating load within the cell is controlled through release of tailings through dart valves.

During the early stages of operation, prior to completion of the reconfiguration work, it was identified that the Cleaner One Jameson Cell dart valves were often below 5% open position. The tailings and rejected NSG is ultimately given multiple passes in the cell as it recirculated to maintain slurry level. Similarly, this was observed upon commissioning of the Cleaner Three Jameson Cell. The addition of greater dilution water to the Jameson Cells was pursued after consultation with Glencore Technology to reduce the recirculating load and the NSG entrainment in the concentrate due to high residence times and recirculation within the cell.

Several low-density surveys were completed to assess the effect of dilution water. Increasing dilution water was provided to the Cleaner Three Jameson feedbox until a circuit constraint (ultimately Cleaner Two tails pumping capacity) was reached and identified. This constraint was reached at ~30 m³/h of water addition.

PLANT TRIAL ASSESSMENT OF OPERATIONAL STRATEGIES AND MODIFICATIONS

Following the investigations required to set the tactics at each individual unit operation, an extended full plant trial of the developed NSG rejection strategy was conducted. The full plant trial was conducted of a period of seven days in May 2021.

The aims of the plant trial were to:

- quantify the impact of the strategy of NSG rejection and copper recovery at the plant level
- confirm the interoperability and compatibility of the individually identified tactics and identify any synergistic or deleterious interactions not observed during the isolated development surveys
- assess the ability of the plant to sustain the strategy, such as: management of recirculating loads over extended periods; process control limitations; impacts on froth handling and transport; and surfacing of unforeseen plant bottlenecks.

Final Strategy Selections

Table 2 presents the operating tactics selected for use. Notably, a strategy adjustment, highlighted in bold, was made mid-trial in response to incoming plant assays that indicated sustained rougher recovery losses. The primary adjustment was the reintroduction of a consistent, extremely slow mass pull from the last rougher cell. Going forward in this paper, results from these two periods are presented separately as NSG Rejection and Balanced strategies.

Table 2: NSG Rejection Strategy Trials – Operating Tactics

Operating Tactics		Recovery Focus 1 May DS-22 May NS	NSG Rejection 23 May NS-27 May DS	Balanced 27 May NS-1 Jun DS
Regrind	Mill discharge P80	20	20 µm	20 µm
	Regrind product P80	17-18 µm	17-18 µm	17-18 µm
	Regrind cyclone pressure	120 kPa	120 kPa	120 kPa
	Deslime cyclone pressure	140 kPa	140 kPa	140 kPa
Mechanical cell mass pull	Rougher	160	140 m ³ /h	140 m ³ /h
	Cleaner 1	80	30-40 m ³ /h	30-40 m ³ /h
	Rougher – Cell 5	Pulling	Dropped out	Lapping

Down the bank velocity profiles	Rougher velocity ratios	1.00 / 0.75 / 0.65 / 0.40 / 0.40	1.00 / 0.75 / 0.65 / 0.25 / 0.00	1.00 / 0.75 / 0.65 / 0.25 / 0.10
	Cleaner 1 – Cell 4	Pulling	Lapping	Lapping
	Cleaner 1 velocity ratios	1.00 / 0.80 / 0.40 / 0.40	1.00 / 0.80 / 0.40 / 0.20	1.00 / 0.80 / 0.40 / 0.20
Jameson Cell recovery	Cleaner 1 Jameson recovery target	75%	60%	60%
	Cleaner 3 Jameson tails grade target	15-25% Cu	25-35% Cu	25-35% Cu
Scavenger recirc loads	Cleaner 1 Scavenger mass pull	30 m ³ /h	15 m ³ /h	15 m ³ /h
	Cleaner 3 Scavenger air	4.5/4.5/3.0 m ³ /min	4.5/3.0/3.0 m ³ /min	4.5/3.0/3.0 m ³ /min
Froth washing	Cleaner 1 Jameson	60 m ³ /h	75 m ³ /h	75 m ³ /h
	Cleaner 3 Jameson	40 m ³ /h	45 m ³ /h	45 m ³ /h
Dilution cleaning	Cleaner 1 Jameson density	15% solids	15% solids	15% solids
	Cleaner 3 Jameson dilution water	15 m ³ /h	30 m ³ /h	30 m ³ /h

Plant Trial Results

The plant trial was assessed on the ability of the strategy to improve concentrate quality, and the resultant recovery impact required to achieve the quality improvement.

Shift deleterious NSG upgrade ratios were determined for the whole plant, and of the rougher and Cleaner blocks separately. These results are presented in Figure 7 (a). Leading into the trial, the rejection ratio for the month of May averaged 0.78. Upon commencement of the NSG rejection strategy, an immediate drop in the deleterious element ratio for both plant and the cleaner block were observed. Throughout the trial period, the deleterious element ratio for the plant averaged 0.61. After the strategy adjustment to a balanced setting on the 27 May dayshift, deleterious NSG ratios remained low, but with greater variability.

Shift deleterious NSG recoveries were similarly determined for the whole plant, and for the rougher and Cleaner blocks separately. These results are presented in Figure 7 (b). Leading into the trial, deleterious element recovery for the month of May averaged 2.3%. Once the NSG Rejection strategy was implemented, an immediate drop in the deleterious NSG recovery for both the plant and the Cleaner block were observed. Throughout the trial period, this recovery for the plant averaged 1.6%.

The deleterious NSG ratio for the rougher block did not reduce with either of the implementation of the NSG Rejection strategy, or the adjustment to a Balanced strategy when rougher cell five was returned to operation. Despite the unchanged rougher deleterious NSG ratio, rougher recovery was observed to reduce with implementation of the NSG Rejection strategy. The combination of lower recovery and an unchanged (or potentially increased) upgrade ratio is likely an artefact of the rougher deleterious NSG recovery having larger components due to true flotation in copper sulfides composites prior to regrind. It may also be the result of the recovered copper sulfide composites holding a higher deleterious NSG grade than the bulk remainder of entrained NSG rejected during the strategy.

Further, variation in the achieved upgrade ratio and recoveries increased during the balanced stage of the trial. This is potentially due to the variable froth stability in rougher cell 5 complicating the ability to hold this cell in a very low mass pull condition. At the time of the trial, the planned rougher froth crowding had not yet been installed.

With reduced deleterious NSG ratios and recovery for the plant, it follows that the grades in concentrate were observed to reduce across the trial. Leading into the trial, grades in final

concentrate for the month of May averaged a normalised, unitless value of 80, in comparison throughout both stages of the trial, the grade in final concentrate averaged a normalised value of 59. Figure 7 (c) presents the grade in the final Cleaner One Jameson and Cleaner Three Jameson concentrates by shift. The largest grade reduction occurred at the Cleaner Three Jameson, indicating the operating changes employed in the mechanical Cleaner circuit and at Cleaner Three Jameson appeared to drive most of the rejection achieved by the strategy.

To confirm the mechanism of greater deleterious NSG mineral rejection, a representative composite of final concentrate was compiled for each stage of the NSG rejection trials. These two composites underwent QEM*SCAN mineralogical analysis. Figure 8 presents the distribution of deleterious NSG minerals across each liberation class in these composites, against the distribution by liberation class derived from similar mineralogical analysis on monthly final concentrate composites, for the period April 2020 to February 2021.

There is a clear reduction in the amount of NSG deporting to the 100% liberated class, and elevated distribution of these minerals across the remaining partially liberated classes. This confirms that the deleterious NSG rejection had been achieved, as intended, by reducing the recovery of liberated NSG minerals. Liberated mineral grains remain the largest form of deleterious NSG in the concentrate; however, this material is often sub-micron in particle size and highly resilient to rejection by normal flotation means and standard entrainment reduction methods.

Figure 9 (a) presents the final concentrate copper grades for May 2021 against the flotation feed Cu:S ratio, which is the leading indicator of final concentrate grade. During NSG Rejection trials, final concentrate copper grades exceeded the pre-trial Recovery Focus performance by ~3% Cu on average. With the NSG Rejection operating strategy focused on entrainment reduction, an improvement in copper concentrate grade is an expected outcome. More prevalent NSG minerals (iron oxide and silicates) are expected to be better rejected alongside the targeted deleterious NSG species. Figure 7 (d) presents the anticipated reduction of concentrate silica grade that drove the observed copper grade increase.

Figure 9 (b) presents the copper recovery by shift for the whole plant and against flotation feed Cu grade. The initially prescribed NSG Rejection strategy impacted copper recovery for the plant by ~2-3%. The primary recovery loss was observed to be occurring at the rougher block. Given good NSG Rejection performance observed at that time, the operating strategy was adjusted to a Balanced setting, allowing the fifth and last rougher cell to pull concentrate – albeit in a restricted “lapping” condition - which was a step back from the normal Recovery Focus operation. This change was made on 27 May dayshift, with an immediate impact seen on the rougher block recovery forward from that date.

As presented in Figure 9 (b), plant copper recovery during the Balanced strategy was largely indiscernible from total plant recovery prior to the commencement of the trial. A small Cleaner circuit recovery loss was incurred across both NSG Rejection and Balanced strategies. No specific changes to the strategy were made to address this loss, as it was both an expected outcome and assessed as required to achieve the desired deleterious NSG rejection. Thus the impact of this loss on whole plant recovery was not significant.

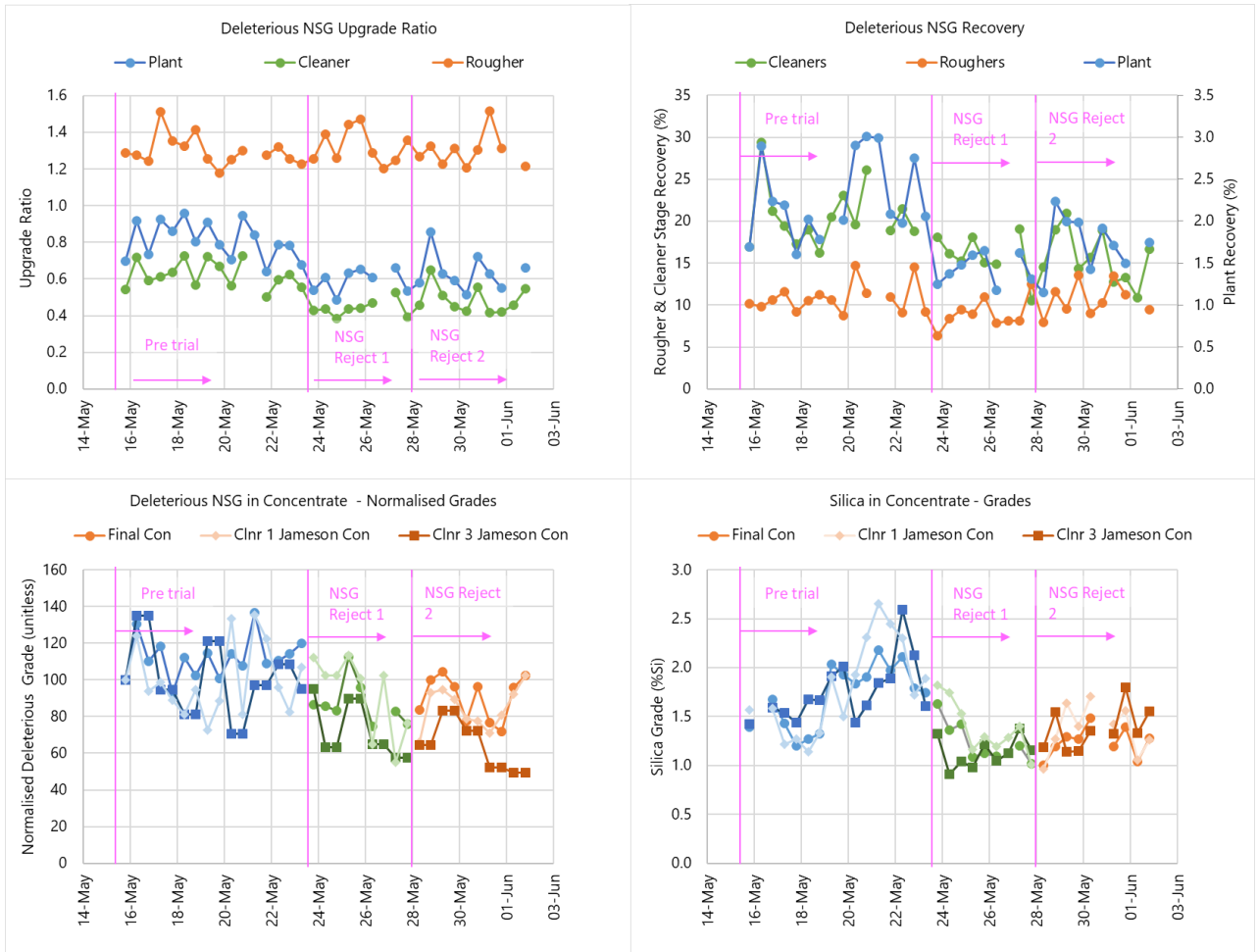


Figure 7 Full Plant Trial - (a) NSG Upgrade Ratios (b) NSG Recoveries (c) Normalised NSG Concentrate Grade (d) Si Concentrate Grade

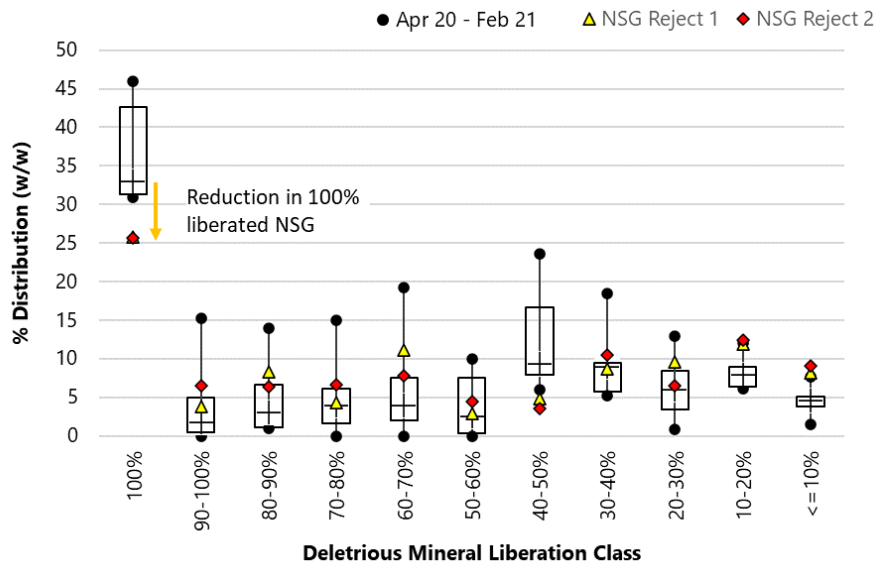


Figure 8: Deleterious Mineral Liberation in Concentrate – Typical Operation and NSG Rejection Trial

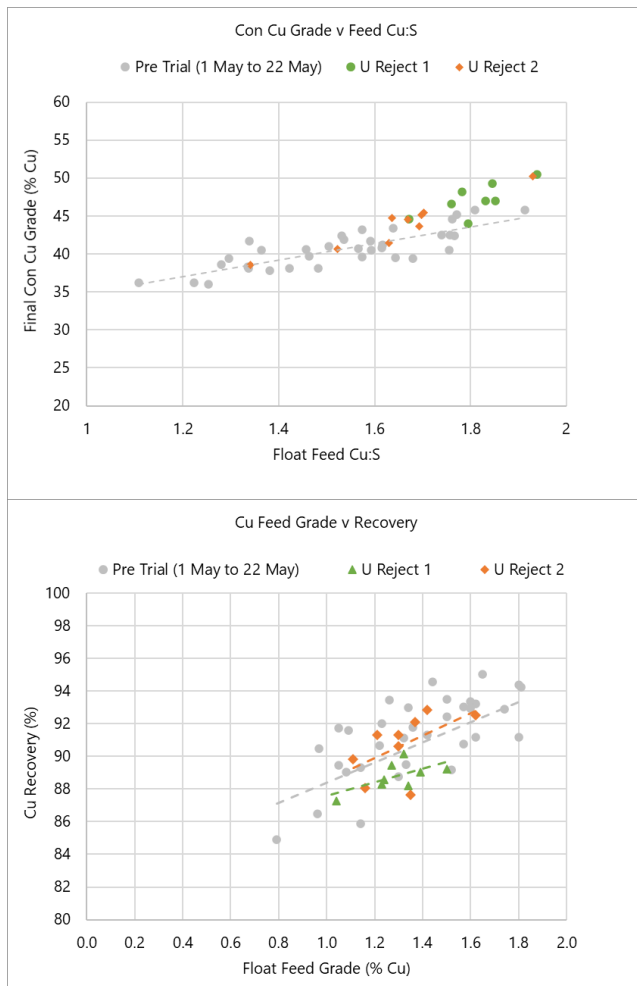


Figure 9: Cu Response to NSG Rejection Trial (a) Cu Concentrate Grade (b) Cu Concentrate Recovery

Assessment of Impact on Plant Performance

Following operating strategy development and full plant trials, a post investment review (PIR) was conducted. The PIR assessed the plant performance improvements achieved by the reconfiguration. The assessment was based on data from both trials, and from ongoing plant performance trends before and after the circuit reconfiguration.

The PIR did not attribute a single recovery or grade improvement figure, but instead outlined a new improved operating envelope that was underpinned by the flexible operating strategies.

Figure 10 presents this operating envelope for both (a) NSG rejection ratio v Cu recovery and (b) concentrate Cu grade v Cu recovery. The envelope is bracketed by two endpoints of:

- when operating for NSG Rejection, a 20% decrease in the NSG upgrade ratio and +3% Cu grade increase were achieved, at the baseline circuit recovery
- when operating with a Recovery Focus, a +1.2% Cu grade and +1.2% Cu recovery was achieved at the baseline circuit NSG rejection ratio.

Further, gold recovery was found to have greatly improved in the range of +0.5% to +3.9%, dependent on the operating strategy.

The PIR additionally highlighted opportunities to further improve NSG rejection, such as greater froth crowding and the need to critically assess the expansion of regrinding capacity to allow finer sizes.

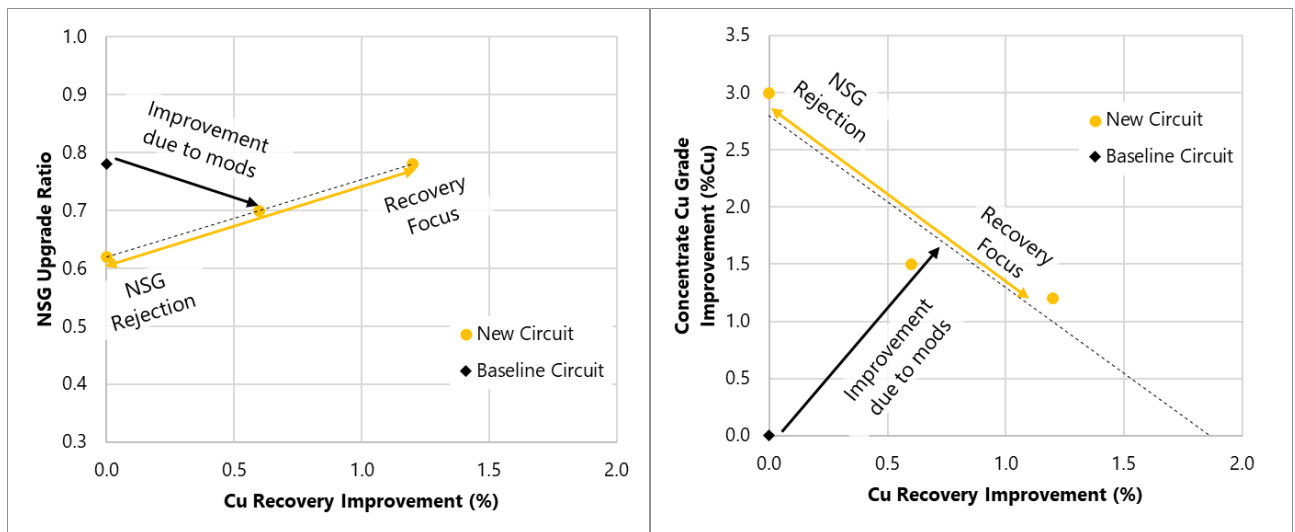


Figure 10: New Operating Envelope – (a) NSG Upgrade Ratio and (b) Concentrate Grade

FUTURE MODIFICATIONS TO EXPAND REGRIND CAPACITY

Future ore test work indicates that regrind sizes as fine as 10 μm may be required on some ore types to achieve sufficient liberation of deleterious NSG minerals from the copper sulfides. The regrind mill typically operates at a target of 20 μm , resulting in a Cleaner block feed particle size of $\sim 17\text{-}18 \mu\text{m}$ once the regrind product is recombined with the regrind cyclone overflow.

Consequently, a critical debottlenecking concern for Carrapateena is regrind capacity; specifically regrind power to achieve target sizes for future ores. It is anticipated that regrind capacity may become fully utilised through:

- Increased rougher concentrate tonnages, driven by:
 - Higher concentrator feed sulfide mineral grades,
 - Lower concentrator feed Cu:S ratio, and
 - Increasing concentrator feed rates.
- Coarsened rougher concentrate particle size, driven by a coarser primary grind size at higher concentrator feed rates.
- Future ores requiring a finer than current regrind product size to sufficiently mitigate the deleterious NSG deportment to final concentrate.

Assessment of Installed Regrind Capacity

To understand fully the specific grinding energy (SGE) (kWh/t) requirement over the anticipated operating envelope, a trial of reducing the regrind mill product size target was undertaken in December 2020. The regrind mill target product size was progressively stepped finer, with an evaluation period allowed between each step. The trial lasted 10 days, with the target size reduced from 20 μm to 15 μm and then to 10 μm .

To achieve the grind size target, the process control system monitors the mill discharge P80 as measured by the PS1500 and manipulates the SGE of the mill to control the discharge P80 to the target. The SGE is maintained by manipulating the HIG mill rotor speed such that the required power is drawn for the prevailing mill feed tonnage. Throughout the trial the mill was operating at the typical feed density of 38-40% solids w/w. Media loading is balanced based on required power, maximum mill filling, and rotor speed.

The SGE during this period increased from 38-40 kWh/t to ~55 kWh/t (varying between 50 and 60 kWh/t). The regrind mill overall power draw increased from ~800 kW to ~1200 MW with peaks close to the full installed power of 1600 kW.

It is worth noting that the mill did not achieve the finest 10 μm setpoint and full mill power draw, as it was limited by the control system's maximum allowed SGE limit. The finest achieved grind size was ~12 μm . Additional power draw and a finer grind size would have been achieved if this limit was relaxed, however that additional extent would be limited by the allowable slurry exit temperatures which are controlled to maintain regrind mill shell liner material integrity. Despite this, sufficient data was collected to develop a plant scale SGE v P80 signature relationship, that largely agreed with results produced by a HIG5 test mill under laboratory conditions, as presented in Figure 11.

Using the trial signature plot, a sensitivity analysis was performed to predict the required mill power across the forward production estimates. It became evident that at times, at the higher forward concentrator milling rates, additional regrinding power will be required and the capacity of the existing mill will be reached, particularly whenever a regrind size of 10-15 μm is required.

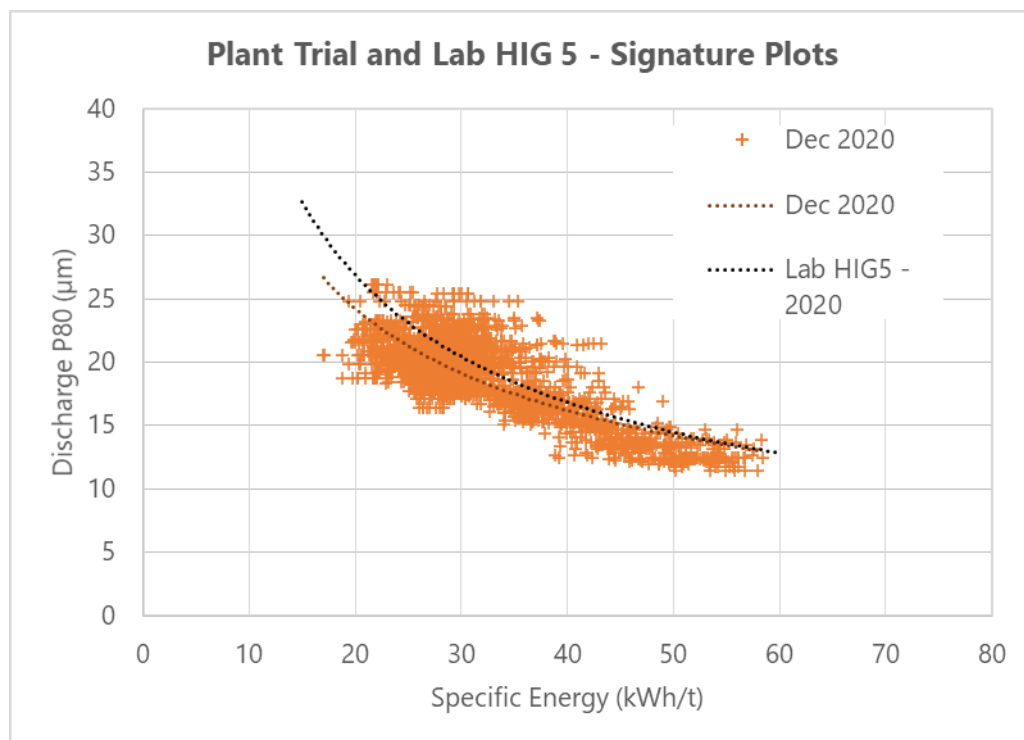


Figure 11: Regrind Capacity Plant Trial – Achieved Signature Plot v Lab HIG 5 Test work

Regrind Capacity Expansion

With the need for additional regrind capacity confirmed, an engineering study assessed several options to apply the additional regrind capacity within the circuit. Two options were specifically reviewed in detail. Firstly, installation of a smaller HIG700 dedicated to Cleaner One scavenger concentrate regrind to relieve the HIG1600 of this duty, thereby allowing greater capacity for rougher concentrate regrind. Secondly, installation of a duplicate HIG1600 in parallel to the existing HIG1600, such that the existing regrind duty is shared between both mills.

Duplication of the HIG1600, with the flow sheet as presented in Figure 12, was the option selected to take forward to detailed design and construction, a decision driven by:

- Commonality of mill spares (both consumable wear liners and capital driveline spares)
- Increased maintenance strategy flexibility, downtime of one regrind mill covered, in part, by the latent turn up capacity of the remaining online mill.
- Reduced circuit complexity for operations.
- 10 µm regrind case unlikely to be achieved by a single mill in the rougher concentrate regrind duty.

As detailed design and engineering progressed, the regrind expansion modification scope was confirmed and new plant layout as shown in Figure 13) finalised to include:

- Upgrade of the rougher concentrate pump to allow capacity for sufficient regrind cyclone dilution water to achieve a finer cyclone cut size. No changes to the regrind cyclone cluster was assessed as necessary for the finer cut size other than changes to internal component dimensions (spigots and vortex finders).
- Relocation of the regrind and deslime cyclone clusters to a new common platform local to both mills, reducing pumping duties, launder requirements and allowing increased regrind mill feed and product hopper residence times.
- New regrind mill feed hopper, common to both mills, fitted with an agitator to mitigate risks of PSD segregation between mill feeds.
- New 1600 kW Metso HIG 1600/900.
- New regrind mill discharge media safety screen dedicated to the new mill.
- New regrind mill product hopper located in a position to all gravity launder flow from both mills.

At the time of writing, major construction activities for the described regrind expansion are underway with commissioning scheduled in Q3 2022.

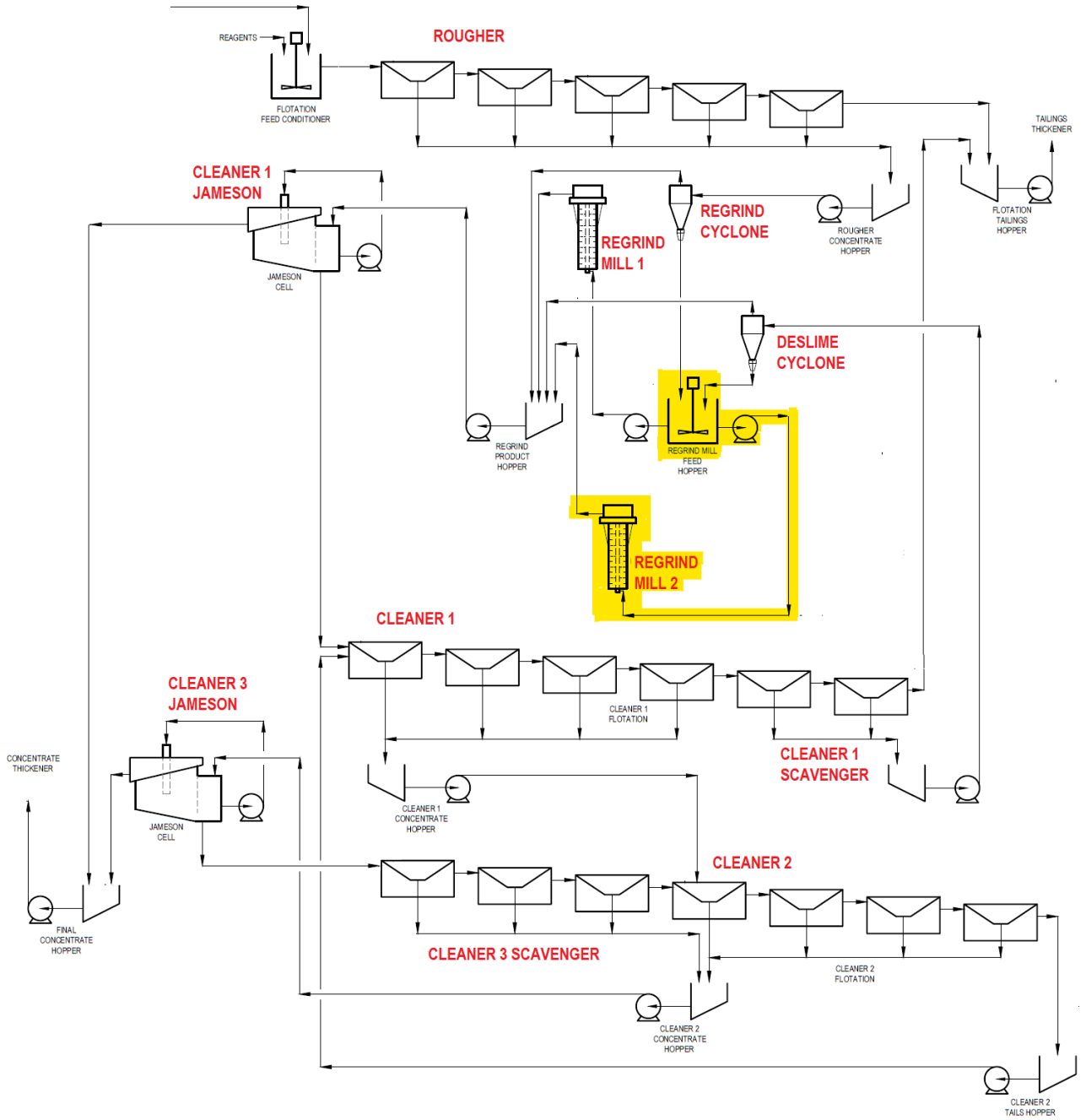


Figure 12: Carrapateena Flotation Flow sheet – Regrind Capacity Expansion

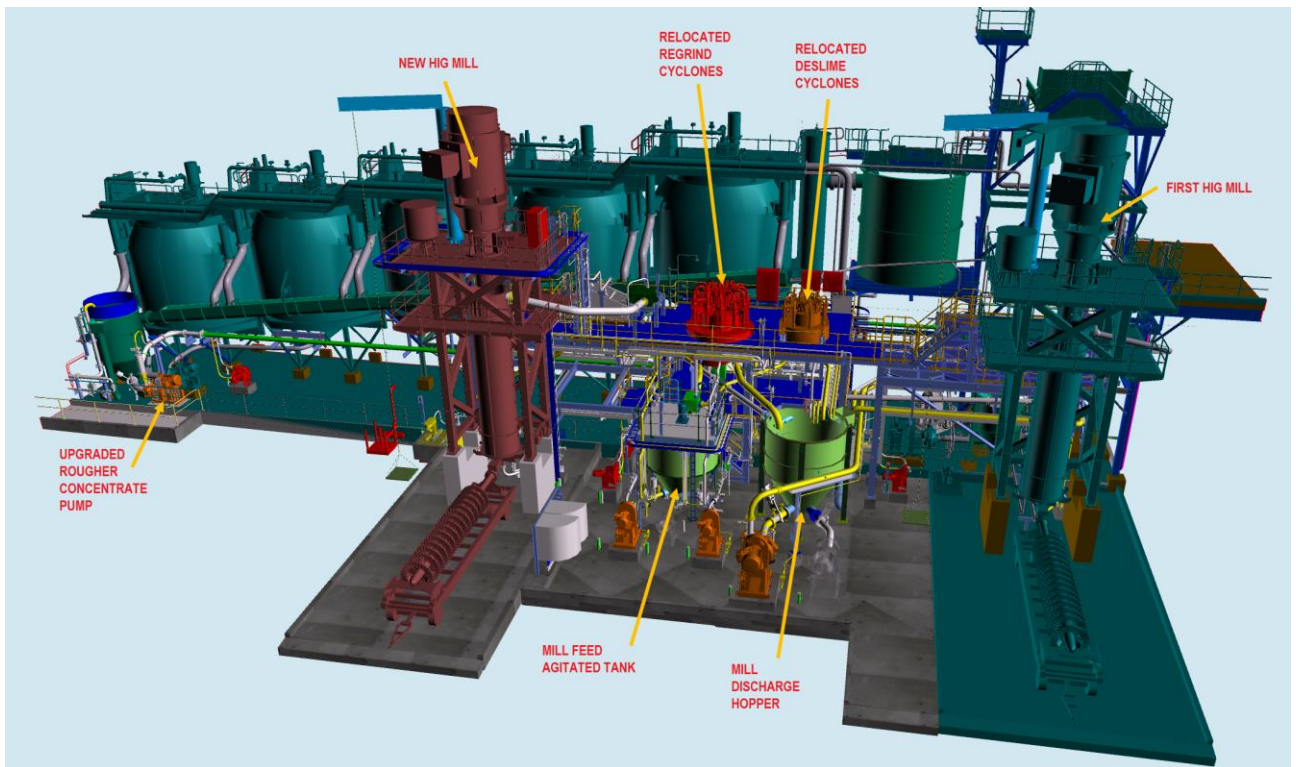


Figure 13: Regrind Capacity Expansion – 3D Model

CONCLUSIONS

The changes implemented to the Carrapateena flotation flow sheet achieved the project objectives and significantly enhanced the metallurgical performance of the circuit. The ability for the plant team to take an agile approach to rapid project development assisted with early implementation of changes following ore commissioning of the concentrator circuit and to develop a high-quality outcome focused on product quality, customer requirements and maximising business value.

It is the view of the authors that the improvements should be reviewed as a package of implemented actions contingent on each other. In isolation, the mechanical equipment, flow sheet, instrumentation, process control, and operating strategy changes would not have yielded the benefit achieved. The systematic approach of utilising quantitative mineralogy, data analysis, sound metallurgical principles, high quality instrumentation, and calibration all coupled with the above physical changes ensured a robust and sustainable project that will continue to deliver business value.

ACKNOWLEDGEMENTS

The authors would like to acknowledge the Carrapateena Processing Team who have all played a part in the successful implementation of the program and without which, it would not have been successful. Also, the support of Carrapateena management in championing innovation, acting with agility and for supporting the project team to enable the change early in the mine life.

REFERENCES

OZ Minerals, Carrapateena produces first copper concentrate; operational ramp up outlined, ASX Release, 20 December 2019,

https://www.ozminerals.com/ArticleDocuments/368/191220_Carrapateena_First_Concentrate.pdf

OZ Minerals, Growth projects strengthen Mineral Resources and Ore Reserves, ASX Release, 16

November 2021

<https://www.ozminerals.com/ArticleDocuments/362/20211116-2021SummaryOfMineralResourceAndReserveStatements-ASXRelease.pdf>

Sawyer, M., Geology of Carrapateena, OZ Minerals Internal Report, 2014, Unpublished.

OZ Minerals, First Quarter Report 2019, ASX Release, 12 April 2019,

https://www.ozminerals.com/ArticleDocuments/368/190412_ASX_Release_-_OZL_Q1_2019_Report.pdf

OZ Minerals, Carrapateena mine production ramp-up complete, ASX Release, 4 December 2019

https://www.ozminerals.com/ArticleDocuments/364/201204_ASX_Release_Carrapateena_Ramp_Up_Complete.pdf

OZ Minerals, Carrapateena Block Cave Access Declines now underway, ASX Release, 3 December 2021

https://www.ozminerals.com/ArticleDocuments/362/20211203_CarrapateenaBlockCaveDecline_ASXRelease.pdf

K E Barns, P J Colbert, P D Munro, Designing the Optimal Flotation Circuit - The Prominent Hill Case, Proceedings of the Tenth Mill Operators' Conference 2009 pp 173 – 182, Australasian Institute of Mining and Metallurgy

P J Colbert, P D Munro, G Yeowart, Prominent Hill Concentrator - Designed for Operators and Maintainers, Proceedings of the Tenth Mill Operators' Conference 2009 pp 23 – 32, Australasian Institute of Mining and Metallurgy

P Woodward, N Muhamad, T Ly, Optimisation of the Prominent Hill Flotation Circuit, Proceedings of the MetPlant Conference 2013 pp 431 – 444, Australasian Institute of Mining and Metallurgy

Mineralogical Assessment of The Carrapateena Test Products – Report KM3788, ALS Metallurgy Kamloops 2013, Kamloops, British Columbia

Characterization of Dilutants, Sweetener & Penalty Elements in Carrapateena Final Con – Report 21/32, Advanced Mineral Technology Laboratories 2021, London, Ontario

Seaman, D R, Burns, F, Adamson, B, Seaman, B A and Manton, P, Telfer processing plant upgrade - The implementation of additional cleaning capacity and the regrinding of copper and pyrite concentrates, Proceedings 11th AusIMM Mill Operators' Conference 2012 pp 373-382, Australasian Institute of Mining and Metallurgy

Converting from Single Stage to Series Ball Milling at the Newmont Tanami Operation

A Giblett¹, S Hart², S Davies³ and A Cranley⁴

1. FAusIMM (CP Met), Black Swan Metallurgy, Black Swan Metallurgy, Western Australia, aidan@blackswanmet.com
2. FAusIMM, Director Processing, Newmont Australia, Western Australia, steven.hart@newmont.com
3. FAusIMM, Director Processing, Newmont Australia, Western Australia, scot.davies@newmont.com
4. FAusIMM, Metallurgy Superintendent, Newmont Tanami Operations, PO Box 8020, Alice Springs, 0871, andrew.cranley@newmont.com

ABSTRACT

The Granites Gold Mine commenced operations in 1986 as a 300 000 t/y single stage ball milling, gravity/cyanidation plant. The process plant underwent a series of upgrades between 1989 and 2003 changing the flow sheet configuration initially to SABC and then back again to single stage ball milling at an ultimate capacity of 2.85 Mt/y. Following the completion of open pit mining and the exhaustion of open pit ore stockpiles, milling circuit capacity reduced to 2.3 Mt/y on the harder underground ore, with the grinding circuit often being mine constrained since that time. The configuration of the process plant prior to 2017 did not incorporate a leach feed thickener, which required grinding circuit classification efficiency to be compromised by high density operation to maintain adequate slurry viscosity in the downstream leach/CIP circuit.

The Tanami plant was expanded in 2017 to increase the plant capacity to 2.6 Mt/y, concurrent with the installation of a second decline to boost underground mine production. The process plant expansion included the addition of a secondary 4.8 m x 7.1 m EGL, (2.7 MW) variable speed ball mill to operate in series with the existing 5.5 m diameter x 9.3 m EGL, (4.7 MW) fixed speed Metso shell supported ball mill. A leach feed thickener was also installed to decouple the grinding and leach circuits. Ore transfer between the two mills is managed by a combination of flat-bottomed 400CVXFB cyclones producing a primary COF P80 around 250 µm and a bleed of primary gravity circuit tailings to the secondary mill cyclone feed hopper.

This paper discusses the performance of the expanded grinding circuit since commissioning and compare the performance of the grinding circuit processing underground ore in both single stage and series milling configuration.

INTRODUCTION

The Tanami gold mine is located in the remote Tanami Desert of Australia's Northern Territory, 540 km northwest of Alice Springs. The site is located on Aboriginal Freehold Land and is managed by the Central Desert Aboriginal Land Trust for the Traditional Owners of the region, who are from the Warlpiri language group. Newmont has fully owned and operated Tanami since 2002 as a Fly-in, Fly-out (FIFO) operation in one of Australia's most remote locations.

The site infrastructure is split between The Granites and Dead Bullock Soak (DBS) operational areas, which are separated by a 42 km paved haul road. The Granites includes the processing plant, power station, tailing storage facilities, airstrip, accommodation village and associated support facilities. DBS includes facilities for the support of the underground mine, including a power station, refrigerated ventilation facilities, workshops, stores, offices and an accommodation village.

Ore is recovered from the underground operations at DBS, incorporating the Callie and Auron orebodies as well as the Federation and Liberator deposits, which will be brought on-line over the next few years. Proven and probable reserves at the Tanami Operations as of 2022 stand at 5.66 Moz (Newmont, 2023). All ore is hauled to the surface using ~60 t capacity articulated trucks.

Ore is tipped onto a Run in Mine (RIM) pad located near the mine portal into ore parcels representing one week production periods. This allows the mine to reconcile production with the processing team through the batching of weekly production through the mill. Figure 1 shows the underground deposits at DBS in long section.

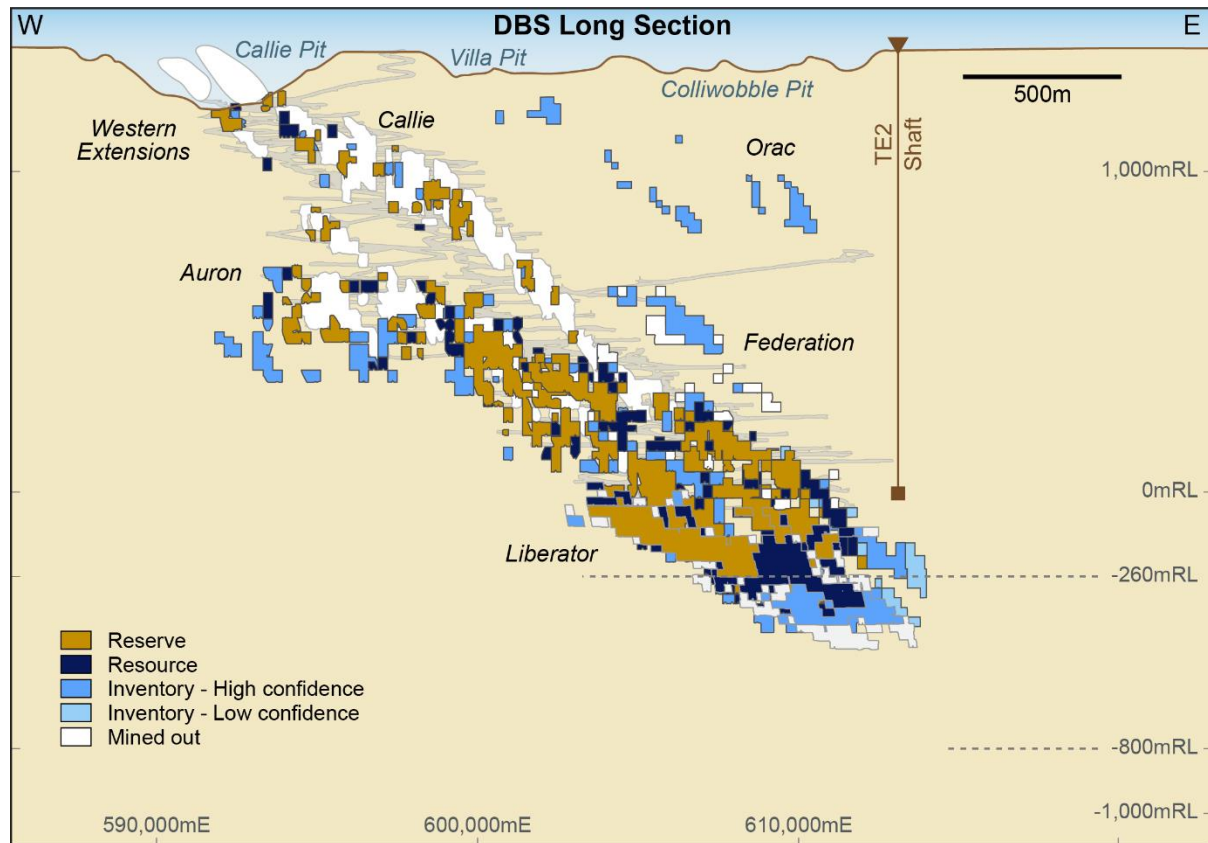


Figure 1: Long Section of DBS showing underground deposits.

PROCESSING OPERATIONS

The Granites Gold Mine commenced operations in 1986, processing 300 000 t/y of open pit ore using a three-stage crush, single stage ball mill, gravity, leach and carbon adsorption flow sheet. A series of plant upgrades occurred from 1989 to 2003 as described by Giblett et al. (2014) to increase plant capacity to 2.85 Mt/y on blends of open pit and underground ore. The plant flow sheet from 2003 onwards utilised a 5.5 m diameter by 9.3 m long (4.7 MW) shell supported overflow ball mill operating in single stage, grinding to nominally 80% passing (P_{80}) 170 μm .

From late 2009 milling rates declined due to the depletion of open pit ore stockpiles (which were predominantly oxides), with the mine delivering a feed blend of 80–90% underground ore progressing to 100% underground ore from late 2011. As the operation transitioned to 100% underground ore feed blend, the mill capacity was predicted to reduce to 2.3 Mt/y at the nominal grind size target of 80% passing 170 μm . Since December 2012, the plant has processed a blend of Auron and Callie underground ore. Average ore characteristics are summarised in Table 1.

Figure 2 shows the average monthly throughput rate from 2008 to 2023, with the switch to 100% primary (UG) ore and commissioning of the new circuit identified. The decline in throughput rate as the mine moved from surface to underground operations is clear, driven by both harder ores as well as limited mine production. Figure 3 presents the longer term trend of annual plant production.

Table 1: Tanami Ore Types, Comminution Properties

Ore Source	Dwi	Axb	WiBM	WiRM	Ai
Auron	10.3	28	20.7	23.9	0.09
Federation	10.8	27	22.0	24.8	0.09
Liberator	10.5	27	21.2	24.2	0.05
Callie	10.9	27	16.9	19.4	-

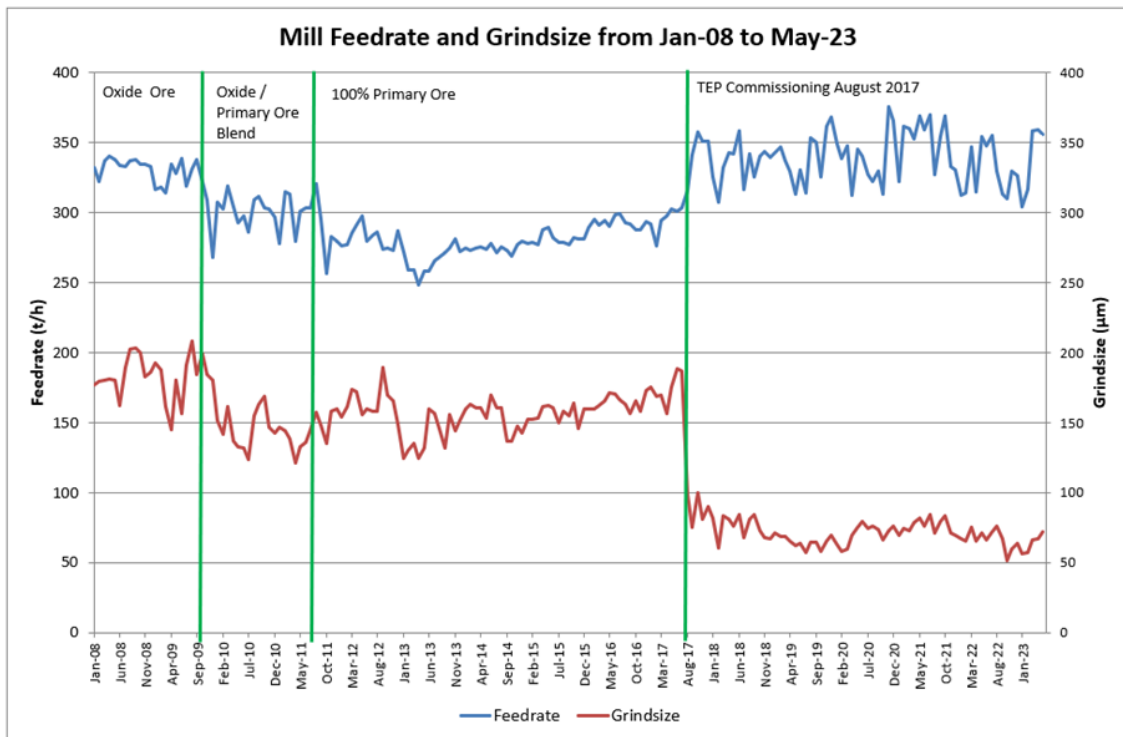


Figure 2: Historical Milling Rates

In order to boost mine production rates, the Tanami Expansion Project (TEP) was initiated which included building a second decline for a section of the underground mine (to allow a circular truck route to be established to increase productivity) and adding incremental capacity in the processing plant. The second decline was completed in mid-2016, providing a step change in mining rates ramping up to 2.6 Mt/y (312 t/h), and plant upgrades were substantially complete by June 2017. The process plant expansion achieved commercial production in August 2017 and included the following key components:

- A second ball mill to allow the annual average throughput to be increased from 2.3 Mt/y up to 2.6-2.8 Mt/y.
- Classification and efficiency improvements due to the installation of a pre-leach thickener.
- Wet plant upgrades, such as sampling stations, a tailings deslime circuit for paste filter plant feed preparation and a tailings filter plant installation.
- An upgraded gravity concentration circuit to maximise gravity gold recovery.
- Expanded electrowinning capacity enabling gravity and leach gold to be recovered separately.

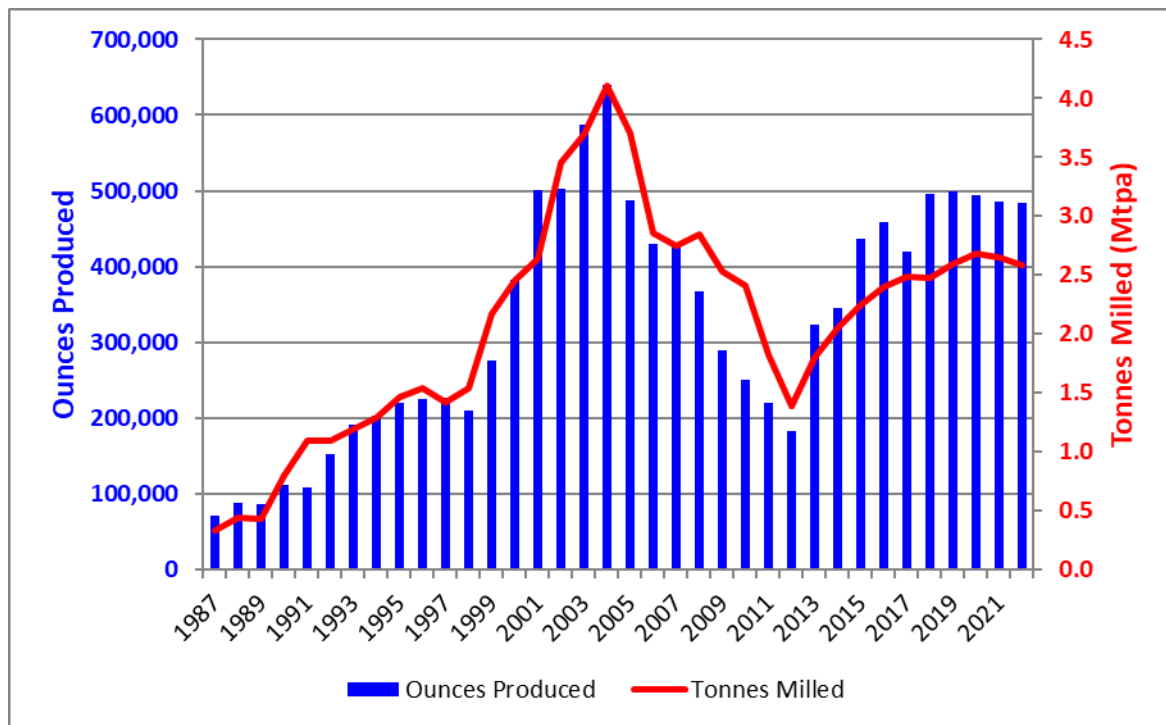


Figure 3: Annual Production

PROCESS OVERVIEW

Underground ore is transported 42 km by side tipping road trains to The Granites processing plant site run of mine (ROM) pad adjacent to a contract crushing plant. The 3-stage crushing circuit reduces ROM ore to a P_{80} of 10 to 12 mm delivering it to a 3500 tonne capacity Fine Ore Bin (FOB).

Crushed ore is recovered from the FOB via two apron feeders and then ground in a 5.5 x 9.3 m EGL (4.7 MW) primary overflow ball mill, operated in closed circuit with a hydrocyclone distributor consisting of ten 400CVXFB Weir Warman Cavex Flat Bottom cyclones. Quicklime is added to the mill feed conveyor via a screw feeder located beneath a lime silo. Trommel oversize is discharged into a scats bay and periodically recycled back to the ball mill via an emergency feeder located adjacent to the ore bin.

The primary ball mill circuit cyclone overflow combined with a bleed from the primary gravity circuit tailings is reverse fed to a 4.8 m diameter x 7.6 m flange to flange (2.7 MW) grate discharge secondary ball mill. The 2.7 MW ball mill motor has a variable frequency drive fitted with the intent being to vary the mill rotational speed (and volumetric filling) depending on throughput rate requirements caused by ore supply limitations from the mine. This mill is in closed circuit with ten 400CVX10 Weir Warman cyclones. The grind size from the grinding circuit is typically within a P_{80} range of 50 μm to 80 μm , when both the primary and secondary ball mills are operating. The cyclone overflow is sampled via an automated, cross-stream sampler and reports to a pre-leach thickener ahead of the leach/CIP circuit.

Gravity recoverable gold is recovered from the grinding circuit in two distinct circuits. The primary milling gravity circuit consists of a 30 in Knelson concentrator, receiving feed from the 3 mm DSM screened undersize of the underflow of a dedicated 400CVXFB cyclone located within the primary grinding circuit hydrocyclone distributor. A second primary gravity concentrator (40 in Knelson) was installed along with a feed screen as part of the TEP expansion, however this is not currently operated due to commissioning issues that have yet to be resolved.

Previously a spirals and tabling circuit worked in parallel to the 30 in Knelson Concentrator. A dedicated 400CVXFB cyclone fed a 3 mm DSM screen, with the screen undersize feeding ten Mineral Technologies MG4CF triple start rougher spirals. Rougher spiral concentrate fed three Mineral Technologies HG10S 5 turn triple start cleaner spirals, with cleaner spiral concentrate being further concentrated by two #12 half size Wilfley tables operated in series. This circuit was turned off in April 2021 due to structural corrosion.

The secondary grinding gravity circuit comprises a split of the secondary mill cyclone underflow, which is fed to a single 40 in Knelson concentrator. Concentrates from the 30 in and 40 in Knelson concentrators are processed in a CS4000 Acacia Reactor which is operated on a daily batch cycle. Electrowinning of the Acacia pregnant solution is carried out in a dedicated 18-cathode electrowinning cell.

The milling circuit can be operated in primary / secondary configuration (as planned), or in primary configuration (if the secondary ball mill shuts down). The primary ball mill is operated at lower throughput rates when the secondary mill is offline to ensure grind size is not excessively compromised.

Cyclone overflow from the grinding circuit gravitates over a vibrating trash screen for the removal of plastic material and then reports to the Pre-leach thickener ahead of the leach circuit. The pre-leach thickener targets 50% solids slurry density to feed the leach/CIP circuit (which is the maximum allowable for the tanks).

The leach circuit consists of three 1500 m³ tanks and one 600 m³ tank. Cyanide is added to the head of the circuit with a top up to the third leach tank. A sodium cyanide level of 160 to 180 g/m³ is maintained within the first and third tanks of the leach circuit, with tailings exiting the CIP plant at 60 to 100 g/m³ sodium cyanide. Oxygen can be injected into all four leach tanks via the shaft of the tank agitators. Oxygen is produced on site from three by two tonnes per day (tpd) pressure swing adsorption (PSA) plants.

The CIP circuit consists of seven 600 m³ adsorption tanks fitted with air agitated vertical wedge wire inter-tank screens. Carbon movement is via Weir Warman recessed-impeller pumps. Carbon concentrations are maintained at 8-10 g/l in each tank, depending on whether there are six or seven tanks online due to maintenance inspection requirements.

Final loaded carbon is removed from the head of the adsorption circuit at a normal rate of two 3.4 t batches per day. Elution is carried out via an Anglo American Research Laboratories (AARL) process. Electrowinning is carried out in an 18-cathode electrowinning cell. Loaded stainless steel wool is high-pressure cleaned, and the gold sludge concentrate is vacuum filtered, dried, and smelted in a conventional tilting furnace. Eluted carbon is regenerated in an Ansac horizontal rotary kiln operating continuously.

Residue from the CIP circuit is treated in a tailings thickener that targets 60% solids before being pumped to the Tailings Storage Facility. Destruction of cyanide on the CIP tail is achieved by injecting Caro's Acid into the tailings thickener underflow line, with weak acid dissociable cyanide concentrations (CN_{WAD}) being less than 45 g/m³. The total leach and adsorption residence time is approximately 22 hours.

As part of the TEP, a deslime section and filter plant were installed to process a portion of the CIP tailings slurry. This circuit comprises a cluster of 14 x 250 CV20XV Weir Warman Cavex cyclones and a 158 m² Jord vacuum filter belt. Up to 120 wt/h of filter cake produced from the filter belt is discharged onto a conveyor belt and radial stacker feeding a 10 800 t capacity stockpile for use in mine backfill. Once the material has dried to between 10-12% it is loaded and backhauled to the mine using the trucks that deliver ore to the processing plant. Due to changes in the target specification of the filtered material for paste backfill, the deslime cyclones have not been utilised

since January 2021.

The process flow sheet overview is presented in Figure 4.

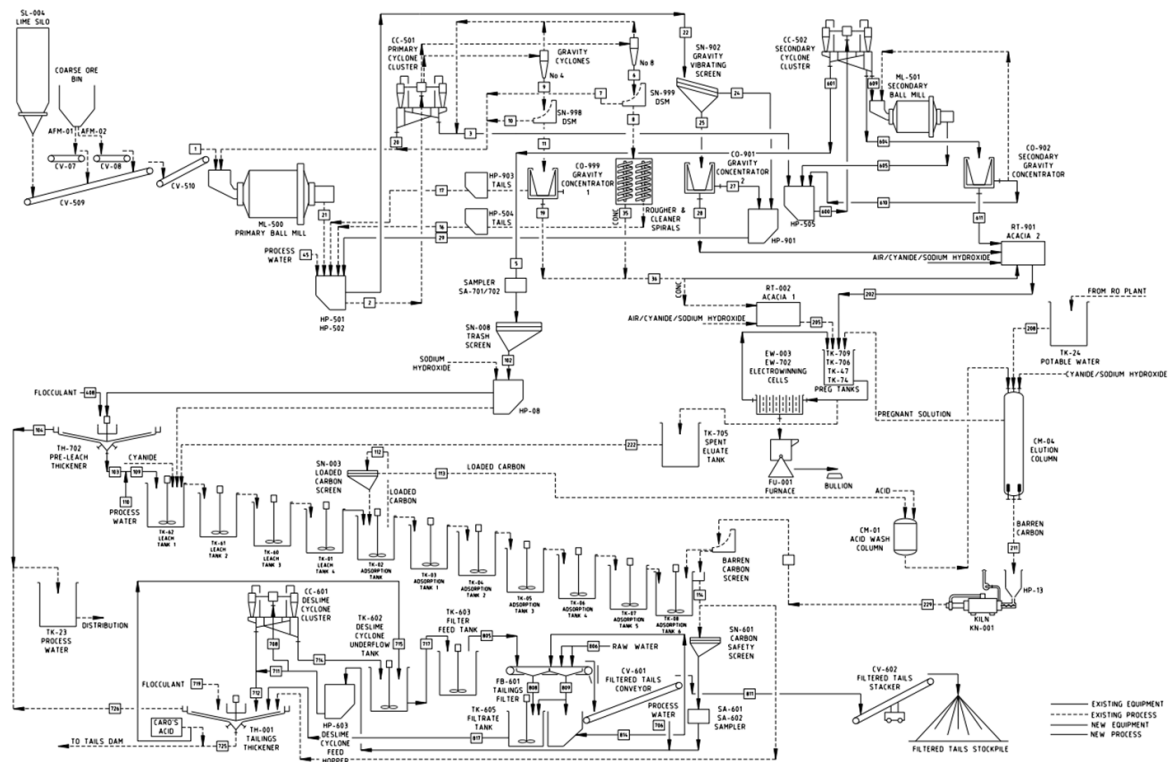


Figure 4: The Granites Process Flow sheet

Milling Circuit Upgrade, Mill Selection and Design Basis

The incremental nature of the TEP expansion (18% increase in milling rates) simplified the flow sheet options to series or parallel milling utilising either stirred mills or additional ball milling capacity. The structural viability of existing foundations of the previously decommissioned secondary ball mill (4.5 m × 7.6 m, mill #3) supported the addition of ball milling capacity. While the size of the existing Mill 3 foundations exceeded the immediate requirements for the TEP expansion, reusing them allowed a comparable total capital spend compared to pouring new foundations to locate a smaller mill, and also allowed for future expansion planning up to a known target at the time of 3.2 Mt/y. Future expandability was a favourable concept given the perceived upside underground potential at Tanami at the time of the study and plans for the installation of a shaft as the mine developed deeper. Figure 5 shows an aerial view of the plant area and the location of the old secondary ball mill and foundations.

Power-based modelling performed identified that a new 1.5 MW ball mill would achieve the TEP target milling rate at a grind size of 125 µm while a 2.7 MW ball mill matching the existing Mill 3 foundations would allow upside capacity to 3.5 Mt/y at a coarser grind size P₈₀ of 160 µm. Given the comparable capital cost, potential for future expansion and Newmont's expectation that running the larger mill in grate discharge configuration would be efficient at low tonnage rates, the larger ball mill was selected as the preferred option, along with a variable speed drive. The intent was to operate the mill at reduced volumetric filling of between 22% to 27% ball charge and critical speeds of around 60%, drawing between 1500 kW and 1800 kW during the initial ramp up.

Parallel ball milling was discounted given the layout of the operation and difficulty getting an appropriate distribution of workload to two parallel ball mills of unequal size. This left the team with the preferred option of series ball milling and solving for one issue only, that being how to drive a

coarser product from the primary ball mill to feed the secondary milling circuit, and hence not constrain the overall productivity. This was achieved by selecting flat bottomed cyclones in the primary cyclone cluster as well as redirecting gravity tailings from selected primary mill gravity circuits to the secondary ball mill as required to balance the grinding workload between the two milling stages.



Figure 5: Granites Plant Aerial View Prior to TEP

Milling Circuit Performance and Grinding Efficiency

The pre-leach thickener was commissioned on 7th July 2017 and the secondary ball mill and gravity circuits were brought online in early August. Commercial production was achieved during the third week of August following two weeks of continuous operation at the design average of 309 t/h, and consistent operation up to the maximum target of 340 t/h. Sustained operation beyond this was feasible but limited by ore supply from the mine at the time. It was clear from the outset that the series ball milling configuration could meet and exceed the TEP targets (In October 2017 a throughput record was set that held until March 2023). Although commissioning occurred swiftly, there were a number of operational challenges encountered during the first years of operation. Key among these were:

- The primary gravity 40 in Knelson Concentrator could not be operated as planned due to

the gravity tails hopper design and return pumps not being able to deliver slurry back to the primary ball mill discharge hopper without significant water additions being made. These water additions impacted the primary mill water balance, and furthermore slumping in the hopper (caused by build-up of solids followed by sudden release) prevented its ongoing use. As the overall gravity recovery process still achieved 65% to 75% gold recovery without this unit operating, the primary Knelson concentrator has not been brought back into service but will be as future upgrades to the circuit are made (allowing the 30 in Knelson Concentrator to be retired).

- The automatic secondary ball mill ball charging system did not operate as planned and required a significant amount of redesign to ensure the safe addition of grinding media could be made. The system comprised an electromagnet installed on an overhead travelling hoist which would pick the media up from a bunker at ground floor, hoist it to a point high in the mill building, travel horizontally and then discharge it into a chute which fed the secondary ball mill feed chute. Containment of grinding media, limit and position switch reliability, hoist performance led to several challenges, however the backup system of kibble additions meant that this rarely impacted production.
- Although the primary milling circuit was intended to be operated with a cluster of ten Cavex flat bottomed cyclones, the team realised that an unplanned stoppage of the secondary ball mill could lead to the primary ball mill being stopped (and resultant full plant outage), as the grind size from the flat bottom cyclones was potentially much coarser than the leach circuit could tolerate. Given the circuit had been designed to allow the secondary ball mill to be bypassed and the operation to continue using primary ball milling only, it was necessary to only change four of the cyclones to flat bottom cyclones and ensure that the remaining six conventional cyclones were available to be operated if required. As two of the cyclones fed the primary gravity circuits at all times, these were retained as conventional in either milling configuration, with four flat bottom cyclones operating in primary secondary ball milling mode, switching to four conventional cyclones for primary ball milling operation if and when required. This transfer happened quite regularly during commissioning and resulted in greater uptime than otherwise possible (all be it at slightly reduced throughput rates when primary ball milling alone). Attempts to operate both types of cyclones at the same time proved ineffective with continual blocking of the conventional cyclones.
- Following commissioning and with more operating data available from the flat bottom cyclones, the Team realised that the flat bottom cyclones could still operate satisfactorily with the Primary ball mill only online (at reduced rates of 250-300 t/h). As a result, the conventional cyclones were removed, and the plant now operates with a full cluster of ten flat bottom cyclones.
- The secondary ball mill was installed with internal grates, in part because the mill was sized for future mill expansions to 3.2 Mt/y rates, and based on modelling only part of the installed power was required initially to reach the targeted 2.6 Mt/y. The first set of ball mill grates (12 mm x 30 mm openings) initially operated well, with inspections showing no sign of pegging, or throughput hold up inside the mill. However, as operations continued through the first year, an increased level of pegging was noted, with square (irregularly shaped) grinding media jamming in the grate openings as shown in Figure 6. Depegging of the grates was necessary to prevent slurry hold up within the mill, and spillage at the feed end of the mill indicated that flow was restricted. The cause of pegging was traced back to a lack of relief on the grate openings with the initial supply, a basic error but one that went unchecked during detailed design. A new grate design was developed and manufactured, such that by the first change out of grates (approximately 18-months after commissioning) the new parts were available on site. A relief angle was installed in the grate opening with

the 12 mm slot opening relieved to 23 mm over the 75 mm depth of the grate. Figure 7 compares the difference in the amount of pegging observed in service for the two grate designs.



Figure 6: Original OEM supplied grates after 12-months operation (80% pegging in some areas)



Figure 7: Comparison between original grates (left) and modified design (right) after similar operating hours.

- Toward the end of life of the second set of secondary mill grates (early 2021), thinning of the rib area between grate openings resulted in flexion of the rubber which caused large diameter media to escape from the mill. Given that the mill was in secondary duty, it was charged with 30 mm diameter balls. Hence it didn't take much for near new media to be ejected from the grate once the rib had worn down after approximately 20-months of service. A steep increase in grinding media consumption was noted, and for a period, 40 mm diameter balls were sourced to make up fresh additions to the mill. As a result of this, the design was again modified to increase the rib thickness between each grate from 9 mm to 16 mm (when new). These changes in combination are expected to see the life of the grates extend well beyond two years.
- The original project design was expected to achieve a final product grind size P_{80} of 125 μm at the 2.6 Mt/y rate, improving on the existing baseline processing rate of 2.3 to 2.5 Mt/y at a grind size P_{80} of 160 to 180 μm (and at times coarser). As a result of the Secondary mill installation and improved classification efficiency (resulting from the pre-leach thickener installation), the operation achieved a P_{80} of 60 to 70 μm at the target throughput rate. The recovery improvement expectation of 1.6% has been exceeded, with overall gold recovery

for the operation increasing from 95.5% to around 98.0% as per Figure 8.

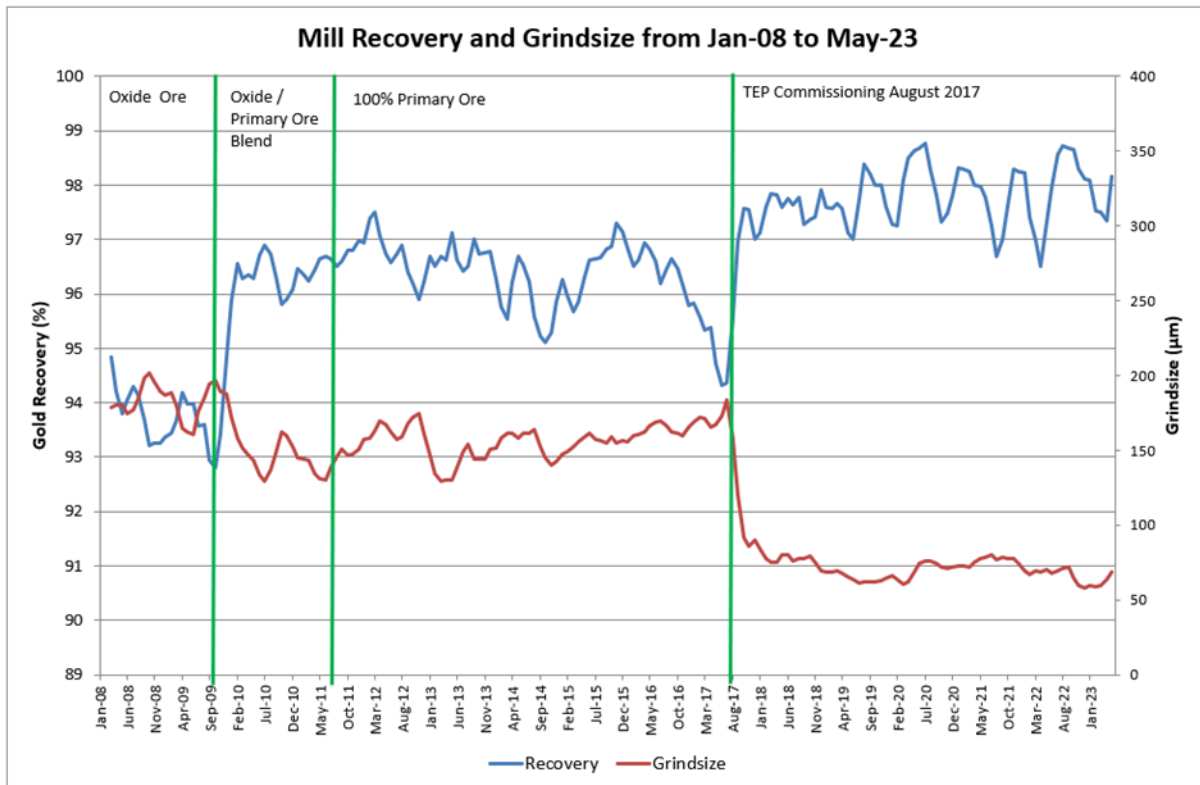


Figure 8: Plant gold recovery and grind size

MILL SURVEYS AND CIRCUIT EFFICIENCY

The Tanami operations and metallurgy team executed a grinding circuit survey in August 2018 to assess input ore properties, circuit operating conditions and performance. At the time of the survey the plant was operated at the design throughput rate of 340 t/h. Hardness data was generated on primary crusher product and primary ball mill feed samples to support energy efficiency analysis consistent with the methods of the Global Mining Guidelines Group (GMG 2021a, 2021b). This analysis, summarised in Table 2, demonstrated that the performance of the secondary ball mill was contributing to an overall efficiency benefit of approximately 20-30% relative to the benchmark methods of Bond and Morrell. The Morrell-based assessment was more definitive in that the primary mill performance was well aligned with expectations, and that the overall circuit efficiency gain was attributable to the secondary mill. The Bond based assessment was less favourable to the primary mill, although the assessment of the secondary mill was comparable to the Morrell analysis.

An additional two surveys were performed in 2020 at a slightly elevated milling rate (350 t/h), and these surveys incorporated Bond ball mill work index (WiBM) tests conducted at both 212 and 106 µm closing screens, with the latter screen size more relevant to the actual plant grind size. The reduction in Bond work index at the finer product grind, while material, was not sufficient to explain the significant improvement in milling efficiency observed for the secondary ball mill. It does, however, highlight the importance of conducting the ball work index test at the appropriate closing screen size.

Table 2: Tanami milling energy demand relative to benchmark methods.

Assessment	2018 Survey	2020 Survey 1	2020 Survey 2
Primary Mill (Morrell)	99%	109%	108%
Primary Mill (Bond)	119%	122%	125%
Secondary Mill (Morrell)	37%	50%	48%
Secondary Mill (Bond)	44%	53%	52%
Circuit (Morrell)	70%	76%	72%
Circuit (Bond)	82%	88%	86%

The surveys confirmed that ore properties were consistent with the plant expansion design basis (Table 3) and not the cause of the significant difference in predicted grind size (P_{80} 125 μm) and actual (P_{80} 60-70 μm) grind size. Secondary ball mill power draw had increased to 2300 kW at the time of the surveys, much closer to the installed capacity of 2700 kW due to increased ball charge and speed.

Table 3: Design vs measured ore properties.

Property	TE1 Design	2018 Survey	2020 Survey 1	2020 Survey 2
DWi, kWh/m ³	9.8	10.3	9.3	9.3
WiRM, kWh/t	23.7	24.9	22.8	23.0
WiBM, kWh/t (212 μm)	19.3	19.5	19.2	19.6
WiBM, kWh/t (106 μm)	-	-	17.8	18.3
Specific Gravity	2.87	2.84	2.85	2.82

A summary of key performance indicators from the two surveys is presented in Table 4. Despite a coarser feed size distribution than the TEP design basis, the final product grind size was much finer than expected and doesn't align with Bond or Morrell predictions, despite equivalent specific energy consumption (Figure 9).

Table 4: Design vs survey operating conditions

Property	TE1 Design	2018 Survey	2020 Survey 1	2020 Survey 2
Feed t/h	340	344	353	352
Mill Feed F80, mm	8.2	10.7	10.1	10.1
Primary Mill kWh/t	12.9	14.2	13.6	13.6
Primary Mill T80, μm	244	260	288	285
Secondary Mill kWh/t	7.1	5.3	6.2	6.1
Secondary Mill P80, μm	125	69	67	68

Levin test work on the primary cyclone overflow and combined primary mill transfer stream (incorporating gravity tailings stream flow) was also performed in an attempt to better define the energy requirements of the secondary grinding stage. The Levin derived estimates of closed-circuit secondary grinding power were on average 40% higher than those achieved in the plant, demonstrating little improvement in predictive accuracy relative to the conventional power-based model estimates.

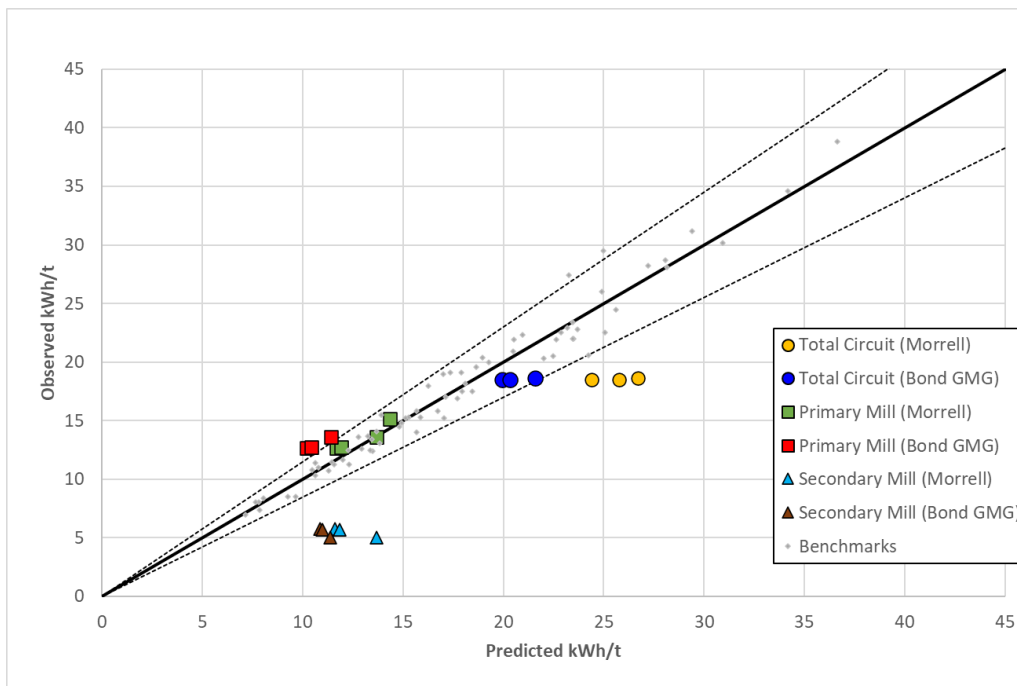


Figure 9: Specific energy comparison

The performance of the series ball milling configuration has consistently outperformed design expectations since commissioning in 2017, an outcome that mill survey and model analysis attributes to the high efficiency of the secondary ball mill. The oversized nature of the secondary ball mill has allowed a grate discharge configuration of the mill and generally low speed (<75% of critical) operation, in addition to the advantage of small diameter grinding media which is known to improve the efficiency of fine particle grinding. The combination of these benefits has delivered an overall circuit efficiency benefit of 15-25%.

Conclusions

As the Tanami comminution circuit transitioned from surface oxide and underground basement ores to 100% underground ores, throughput of the operation dropped from 2.8 Mt/y to 2.3 Mt/y rates. As underground mine production increased, the throughput of the mill recovered some of this

capacity but at the expense of grind size and recovery, particularly given the lack of a pre leach thickener ahead of the CIP circuit, and requirement to maintain tank densities within a very tight range.

The conversion to a series milling configuration and introduction of pre leach thickening to improve cyclone classification efficiency as a part of the Tanami Expansion project (TEP) in 2017 has allowed the circuit to meet and now exceed the design expectation with throughput rates regularly achieving a 2.8 Mt/y rate, and only limited by ore supply from the mine and contract crushing plant capacity in recent years.

This has been accompanied by a reduction in grind size from a P_{80} of 170 μm prior to the upgrade to nominally 65 μm , and a corresponding increase in gold recovery from 95.5% to 98.0%. The grind realised has substantially exceeded the TEP design basis of 125 μm and has provided a significant recovery benefit to the operation. The high efficiency of the grate discharge secondary ball mill has been consistently evident in operating data and validated through well designed and executed grinding circuit surveys and power-based modelling.

ACKNOWLEDGEMENTS

Newmont Corporation and the Newmont Tanami Operation are acknowledged for providing permission and support to publish this paper. The valuable contributions of many operations and project team members to the success of the project are acknowledged, particularly Neil Ireland, Brendan Parker, Ian Edwards, Abbas Manesh and Sharyn Thacker.

REFERENCES

Giblett, A., Cranley, A. and Thacker, S., 2014. Three Decades of Gold Production at the Newmont Tanami Operations. 12th AusIMM Mill Operators' Conference, Townsville QLD.

Global Mining Guidelines Group (GMG), 2021a. Determining the Bond efficiency of industrial grinding circuits. <https://gmgroup.org/guidelines-and-publications/>

Global Mining Guidelines Group (GMG), 2021b. The Morrell method to determine the efficiency of industrial grinding circuits. <https://gmgroup.org/guidelines-and-publications/>

Newmont Corporation, 2017. Tanami Expansion Project Adds Profitable Production and Extends Mine Life. <https://www.newmont.com/investors/news-release/news-details/2017/Tanami-Expansion-Project-Adds-Profitable-Production-and-Extends-Mine-Life/default.aspx>

Newmont Announces Increased 2022 Mineral Reserves of 96 Million Gold Ounces and 68 Million Gold Equivalent Ounces (February 23, 2023) https://s24.q4cdn.com/382246808/files/doc_financials/2022/sr/Newmont-2022-Reserves-Release_Final.pdf

Newmont Corporation, 2018. Tanami Operations, 43-101 Technical report.

Newmont Corporation. Newmont Regional Operating Statistics (2014-2022). https://s24.q4cdn.com/382246808/files/doc_financials/2022/q4/Newmont-Full-Year-and-Fourth-Quarter-2022-Operating-Statistics_Final2.pdf

Expansion of Mandalay Costerfield's Flotation Circuit

J Carpenter¹, H Thanasekaran², S Eibl³, P Omizzolo⁴ and A Herman⁵

1. Flotation Process Engineer, Eriez Flotation, 21 Shirely Way Epping VIC 3076, jcarpenter@eriez.com
2. Technical Sales Director, Eriez Flotation, 21 Shirely Way Epping VIC 3076, homiet@eriez.com
3. Metallurgist, Mandalay Resources Costerfield Operations, McNicols Lane Costerfield VIC 3523, s.Eibl@mandalayresources.com.au
4. Plant Manager, Mandalay Resources Costerfield Operations, McNicols Lane Costerfield VIC 3523, P.Omizzolo@mandalayresources.com.au
5. Flotation Process Engineer, Eriez Flotation, 21 Shirely Way Epping VIC 3076, anggah@eriez.com

ABSTRACT

Eriez Flotation and Mandalay Resources have worked together to increase mill throughput and improve the recovery of fine gold and antimony at the Costerfield site in central Victoria. The scope of this expansion included increasing the capacity and flexibility of the flotation circuit and recovering additional gold from the flotation tailings.

To meet the challenge of limited real-estate, Eriez commissioned two different flotation technologies to expand both the up-front and back-end of the existing flotation circuit. Eriez StackCell[®] technology was implemented as a pre-rougher stage in order to reduce the load on the existing flotation circuit. The innovative two-stage StackCell[™] design features a high-shear contacting chamber and quiescent separation chamber and improves recovery of fine particles and slow floating minerals with a 75-85% reduction in flotation volumetric requirement.

For Mandalay Resources, the StackCell pre-rougher enabled production of an immediate final concentrate, reducing the load on the downstream conventional cells. The StackCell's high-capacity and compact design was ideal to fit into a small footprint without major modifications to existing layouts. Installing two cells in series had the benefit of providing increased residence time and capacity to handle surges and future variations in ore blends and grind sizes. Two flotation columns, utilising Eriez' unique CavTube[™] sparging systems, were installed to treat the plant final tailings. The objective of this was to recover the fine gold-bearing particles lost in conventional flotation, producing a concentrate to blend with that from the existing circuit.

This paper recounts the project from the early testing phases through to the commissioning and successful integration of the units into the Costerfield flotation circuit.

INTRODUCTION

Over the last 30 years, most equipment suppliers have offered ever-increasing unit sizes and larger flow rates with fewer unit operations to reduce the cost of mechanical flotation equipment (Mankosa, 2018). Here, the cost benefits are gained only via the efficiencies of scale. This approach is usually used mainly due to the industry's familiarity and experience with conventional flotation technology. The well-established scale-up method for conventional cells allows practitioners to estimate the equipment capital cost based on simple laboratory test work. However, this method is usually unsuitable for de-bottlenecking and expanding an existing flotation circuit, especially when a very limited real-estate allocation becomes the restriction.

According to the well know "elephant curve" in Figure 1, lower flotation recovery can be observed at both very fine and very coarse particles (Lynch et al., 1981). For fine particles, the flotation rate is a

function of the local fluid turbulences, which relates to the efficiencies of the bubble-particle collision increase with kinetics energy (Williams and Crane, 1983). In fact, a significant number of particles was lost to the final tailing and about 85% of the losses were in the size fractions of below 50 microns and coarser than 150 μm . As a result, an alternative technology that can recover the particle loss at both ends of the size fraction is needed to minimise the particle loss at the final tail stream.

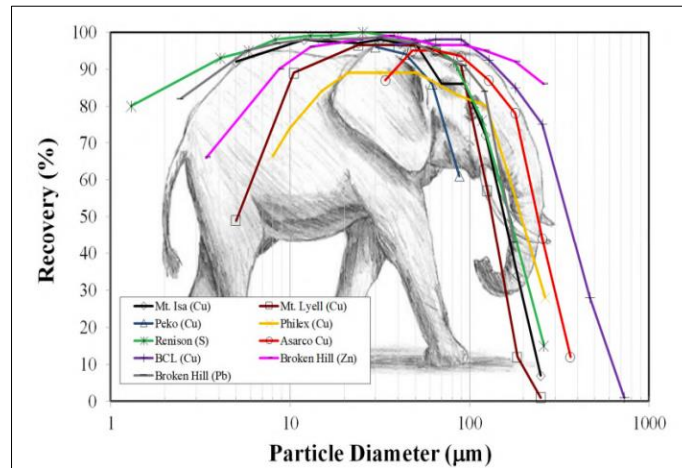


Figure 1: The typical recovery vs particle size curves for the conventional flotation cell. (Lynch et al., 1981)

Mandalay Resources, which owns the Costerfield Mine, contacted Eriez Flotation Division (EFD) to explore the possibility of increasing the flotation circuit's capacity and flexibility while recovering additional gold from the final tail stream. The Costerfield Mine is located within the Costerfield mining district in Victoria. It consists of a large, disseminated gold-antimony orebody, first crushed by a primary mobile crusher, followed by primary and secondary ball mills. The ore is then treated in pre-rougher, rougher, scavenger and cleaner flotation circuits, as shown in Figure 2. The gold-antimony flotation concentrate is shipped to a smelter in China via the port of Melbourne.

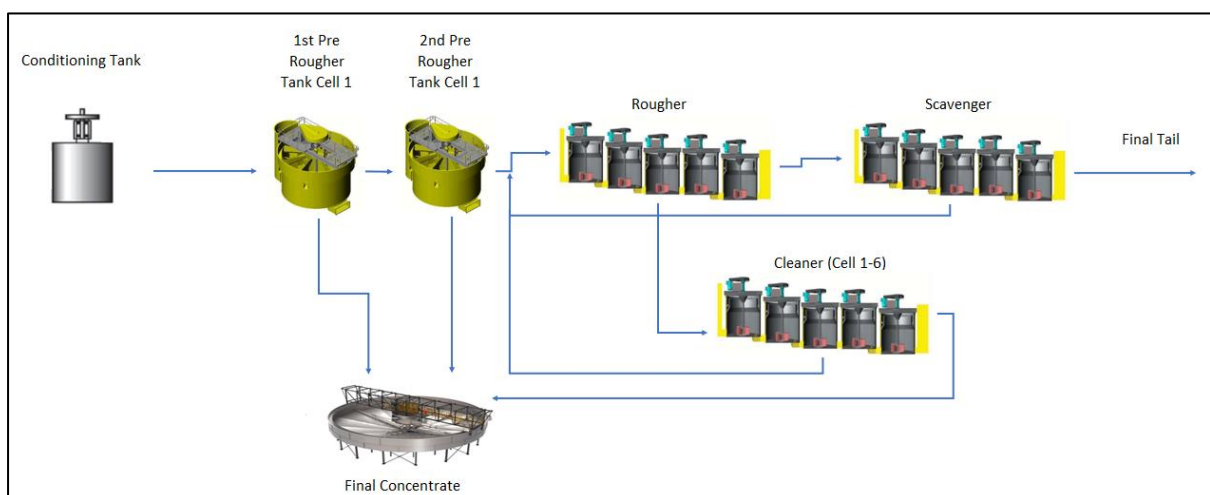


Figure 2: The simple flow diagram for the existing Mandalay Resource's Costerfield flotation circuit.

The majority of gold losses in the tails at Costerfield occur in the ultra-fine fractions, with as much as 46% of the total gold lost to flotation tailings in the -11 μm fraction. Most of this ultra-fine gold is free gold but is lost to tails due to the incapability of the conventional flotation cells to float the fine gold. After successful pilot campaigns, two StackCells and two cavitation flotation columns were installed

at both ends of the existing flotation circuit, as shown in Figure 3. This paper aims to discuss the early pilot test work of both StackCell and the cavitation flotation column. After that, the benefits and circuit improvements after the successful integration of both technology into the Costerfield flotation circuit are briefly discussed.

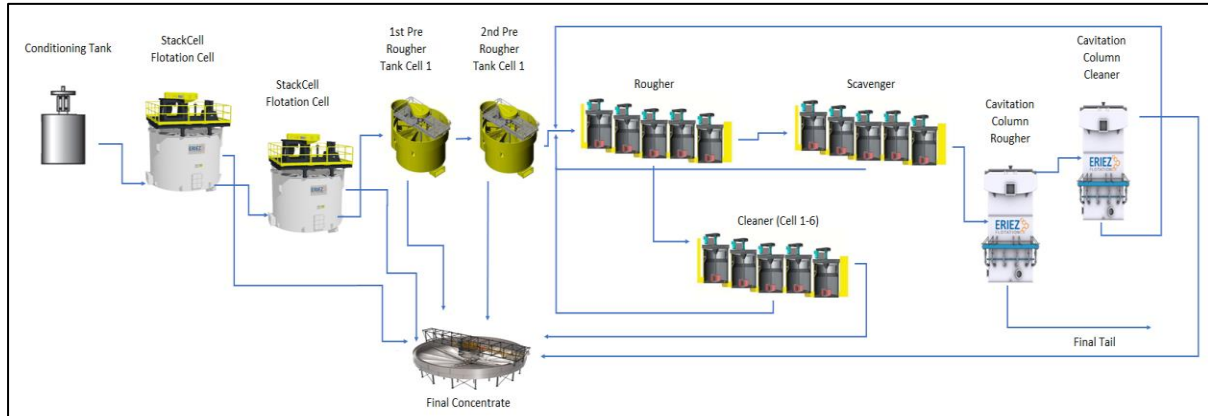


Figure 3: The new configuration for Mandalay Resources' Costerfield flotation circuit incorporating Eriez StackCells and Eriez cavitation flotation columns.

THE IMPLEMENTATION OF STACKCELL TO THE FLOTATION CIRCUIT

Eriez Flotation Division (EFD) designed the StackCell technology to provide a more efficient flotation option by decoupling the particle contacting zone with the phase separation process. The StackCell focuses the energy input to enhance the fine recovery by improving the flotation kinetics towards the “sweet spot” of the elephant curve. Subsequently, the size of the unit can be reduced significantly while maintaining a similar capacity and metallurgical performance as current conventional flotation cells. The implication of applying the StackCell technology has many advantages, including a more than 40% reduction in energy consumption and a significant reduction in plant height, footprint, and foundation loads.

Figure 4 shows the general illustration of a typical industrial-sized StackCell. Generally, a single StackCell consists of two tanks, one inside another. The internal tank is equipped with a stator-rotor assembly and capped with a spinning lid, which facilitates bubble-particle contact. The slurry feed is fed from the bottom of the internal tank and mixed with air in a high intensity mixing environment. This causes the time required for the bubble-particle attachment to occur in mere seconds. After that, the aerated slurry flows into the outer separation chamber through the gap between the internal tank and the spinning lid. The outer separation chamber provides an ideal environment for separating the froth from the slurry. In addition, the lack of mixing at the outer separation chamber maximises the use of wash water to hydraulically reject entrained particles from the froth concentrate.

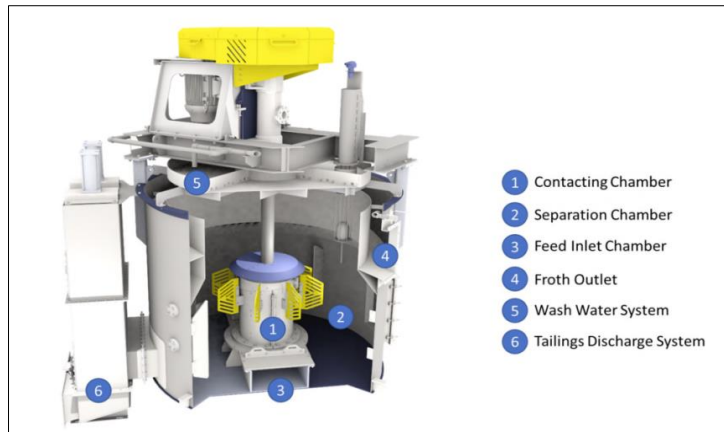
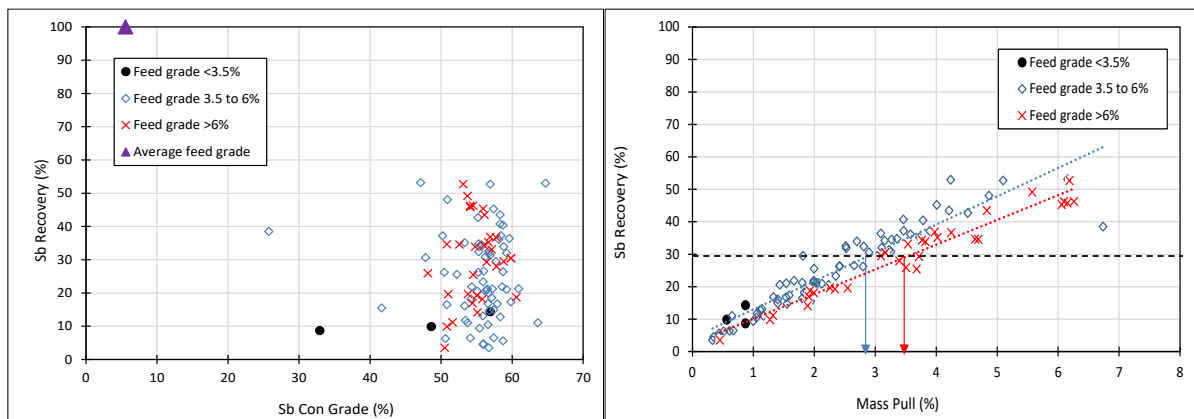


Figure 4: The general illustration of the typical industrial-sized StackCell.

The StackCell pilot test work was performed to study the feasibility of implementing the StackCell as a pre-rougher stage to reduce the load on the existing flotation circuit. The target concentrate grade for antimony was set at between 52% to 55% Sb. Figure 5 (a) shows the plot for the antimony recovery against the antimony grade at the concentrate stream. Note that the data points were plotted at three feed grades ranging from < 3.5%, 3.5 to 6% and > 6%. It can be observed that the concentrate grades of the StackCell were maintained at 50% to 60%. In addition to that, the average antimony grade at the concentrate for the StackCell was 55%, slightly higher than the plant's average antimony grade of 54.2%. The results showed that the StackCell was able to achieve the target antimony concentrate grades. Subsequently, the StackCell comfortably achieved stage recovery of 20% to 30%, contributing to an overall plant recovery of 97%. Figure 5 (b) shows the plot for the antimony recovery against the mass pull. It can be observed that the recovery increases as the mass pull increases. For example, at 30% recovery, the mass pull for the feed grade of 3.5% to 6% was 2.9%, while the mass pull for the feed grade of > 6% was 3.5% respectively.



(a)

(b)

Figure 5: The plot from the pilot test work for (a) the plot for the antimony recovery against the antimony grade at the concentrate stream and (b) the plot of the antimony recovery against the mass pull

Meanwhile, StackCell was able to recover the gold from the feed. Figure 6 (a) shows the plot for the gold recovery against the gold grade at StackCell concentrate. Three feed grades were evaluated here, which were < 6 g/t, 6 g/t to 8 g/t, and > 8 g/t. It can be observed that the gold grade in the concentrate was maintained at 30 g/t to 50 g/t. The StackCell achieved an average gold concentrate of 40.65 g/t,

higher than an average plant gold grade of 37.8 g/t. Overall, the StackCell was able to achieve 10% to 20% stage gold recovery, contributing to the plant's gold recovery of 86.7%. Figure 6 (b) shows the graph for the gold recovery against the mass pull. Like antimony, the gold recovery increases as the mass pull increases. For example, at 30% recovery, the mass pull for feed grade of < 6 g/t, 6 g/t to 8 g/t, and > 8 g/t were 4%, 5.5% and 6%. The results suggest that a higher feed grade requires higher mass pull.

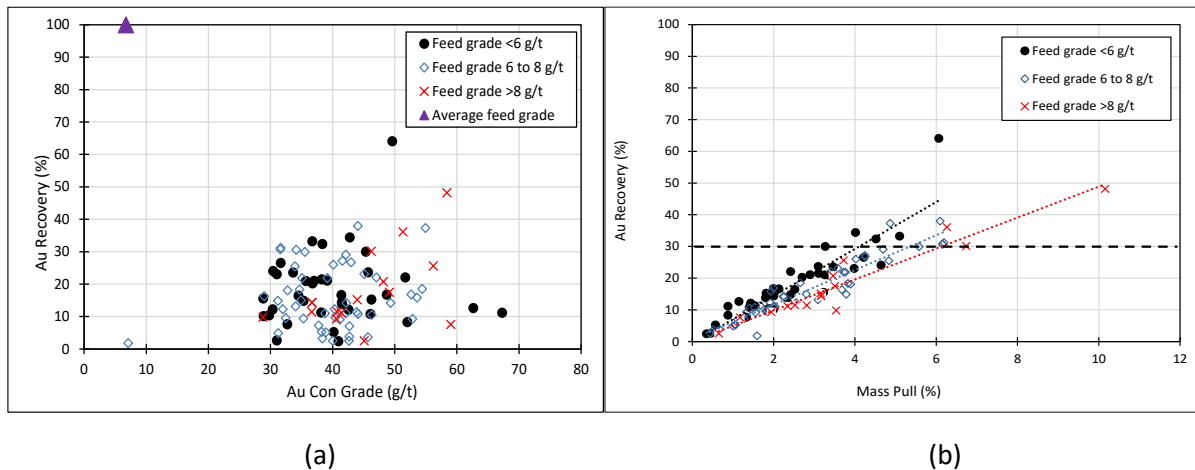


Figure 6: The plot from the pilot test work for (a) the gold recovery against the gold grade at StackCell concentrate, and (b) the graph for the gold recovery against the mass pull.

After successful pilot test work campaigns, Eriez commissioned two different flotation technologies to expand the existing flotation circuit's up-front and back end, as shown in Figure 3. At the up-front of the existing flotation circuit, Eriez commissioned two StackCells as a pre-rougher stage. The StackCell pre-rougher enabled the production of an immediate final concentrate, which reduced the load on the current downstream conventional cells. This subsequently increased the flexibility for the maintenance of the whole flotation circuit, and the circuit could remain in operation if one of the flotation cells broke down. Meanwhile, the StackCell's high capacity and compact design were ideal to fit into the existing plant without majorly modifying the existing layout. Moreover, installing two StackCells in series increased residence time, the capacity to handle surges, and future variations in ore blends and grind sizes.

THE APPLICATION OF CAVITATION FLOTATION COLUMN FOR GOLD RECOVERY

Eriez Cavitation Flotation Column has several metallurgical benefits; it mainly has the ability to provide superior separation performance compared to the conventional mechanical flotation process, is excellent for reducing the entrainment in the froth and has low capital and operating cost (Murdoch et al., 1991). The general flow and features of the Cavitation flotation column are shown in Figure 7. The feed slurry enters the column at one or more feed points located in the upper third of the column body and descends against a rising swarm of fine bubbles generated by the CavTube sparging system. The particles attached to the bubbles rise to the top of the column and eventually reach the interface between the pulp and the froth. The froth depth can be adjusted and predetermined via an automatic controller that regulates the opening of the tailing valve. Once the particles are transferred into the froth, it then carried into the float launder via mass action.

The EFD CavTube sparging system can efficiently generate a large number of micro-bubbles per unit area for a given airflow. This causes the probability of bubble-particle contact to increase significantly, which has a direct bearing on the capacity. The micro-bubbles are generated by circulating the slurry from the lower section of the column through a set of in-line, parallel CavTube spargers, in which compressed air is injected. Apart from generating micro-bubbles, the CavTube also has a long wear

life. In fact, unlike other dynamic sparging systems, the Cavitation Tube has no direct impingement on the slurry flow, which, when coupled with robust materials of construction, ensures a long service life.

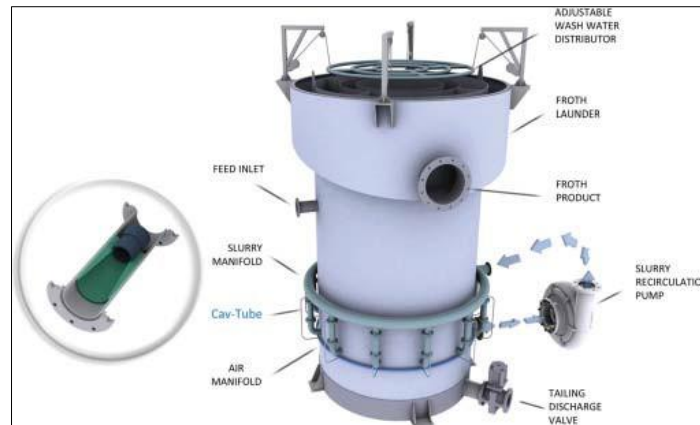


Figure 7: the general diagram of the Eriez Cavitation Flotation Column.

The feasibility of applying the Eriez Cavitation Flotation Column to recover gold from the final tail stream was tested onsite on a pilot test work. The aim of this test work is to show that the Eriez flotation installation can produce a product of around 60 g/t from this tailings stream. Initial estimates from the site indicate the plant tailings to have an average gold grade of 1.5 g/t. Eriez installed two cavitation pilot columns next to the existing final tailing stream to achieve this.

The gold recovery versus gold grade results for both flow sheets (with and without recycle) are shown in Figure 8 (a). The Eriez cavitation tube columns were able to achieve gold grades of 50 – 55 g/t at a recovery of 67% when using the tails recycle set-up. The same gold grade was achieved without any recycling but at a lower recovery of 50%. Most of the gold grades achieved without the recycle stream were higher than those with the recycle tails. Figure 8 (b) shows a linear relationship with the gold recovery increasing as the mass pull increases.

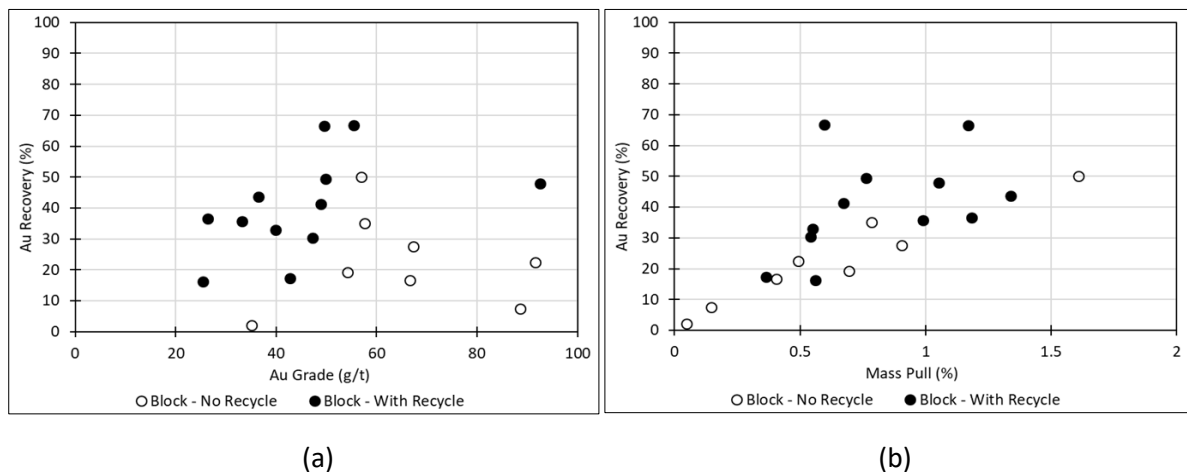


Figure 8: The plot for (a) gold Recovery versus Gold Grade and (b) the effect of Mass Pull on the Gold Recovery

Two Eriez cavitation flotation columns were installed at the back end of the flotation circuit to recover additional gold from the final tailing stream after a successful pilot test work campaign. The final tail of the existing circuit was fed into the cavitation flotation column rougher. The concentrate of the cavitation flotation column rougher was further processed to the cavitation flotation cleaner to produce the final concentrate. Meanwhile, the tail stream from the cavitation flotation column rougher became the new tail stream and the tail stream from the cavitation flotation cleaner was

recycled back to the rougher flotation cell.

The industrial-sized installation aimed to achieve a target concentrate of 45 g/t of gold and block recovery of 30%. The gold block recovery versus the final concentrate grade is plotted in Figure 9 (a). A lot of scatters were observed in this graph, covering concentrate grades of 40 – 160 g/t and recoveries of 5 – 80%. This could be due to the “gold nugget effect” affecting the representative sampling when performing the assay but a detailed mineralogical study would be required to support this hypothesis. In addition to that, this period of testing was primarily optimisation, so this wide range of results is understandable given the range of conditions used and alterations in the feed grade. Having said that, the target performance of 45 g/t at an average 30% recovery has been achieved in these surveys. Towards the end of the commissioning work, the gold grades at the tail stream continuously decreased, as shown in Figure 10.

The block gold recovery as a function of the column block mass pull is shown in Figure 9 (b). The total mass pull of the column circuit is very low, with the majority of surveys showing less than 2%. From 0 – 2%, the trend shows a linear increase in recovery as the mass pull increases. Above a mass pull of 2%, there is a sharp break away from this trend, albeit with only 3 data points.

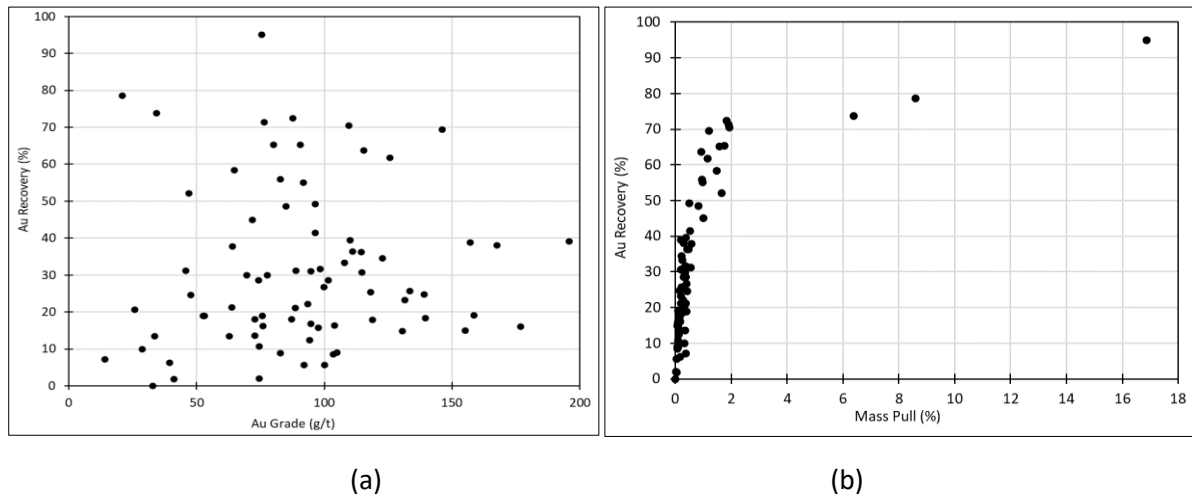


Figure 9: the plot from the pilot test work for (a) column block gold recovery vs concentrate grade, (b) Block gold recovery as a function of block mass pull.

The Eriez column installation has been commissioned to produce a saleable gold product from the plant flotation tails. As such, a key indicator of the performance of the column is the gold grade of the final tails stream. Figure 10 shows the gold grade of the final tails throughout the commissioning period. Over this period, there are many ups and downs, corresponding to different operating conditions and changes within the plant. Overall, there was a clear downward trend in the plant tail's grade as the project progressed. The gold grade decreased from 0.90 g/t at the start of the commissioning work to 0.60 g/t at the end of the commissioning work, indicating the level of gold being recovered from the plant tails in the columns.

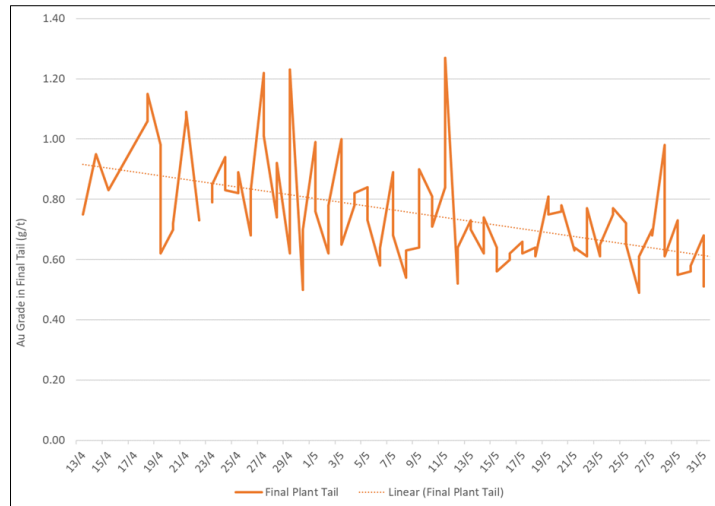


Figure 10: Gold grade in the plant final tails over the course of column commissioning

The Eriez column performance must also consider the assay results of antimony. The block antimony recovery is plotted as a function of the final concentrate antimony grade and block gold recovery in Figures 11 (a) and 11 (b), respectively. As with the gold, there were considerable scatters in the antimony grade versus the recovery plot, as shown in Figure 9 (a). Moreover, the antimony concentrate grades range from 0 - 60% and recoveries from 0 - 90%. Figure 11 (b) shows that the recoveries of gold and antimony are very closely related and follow a 1:1 trend.

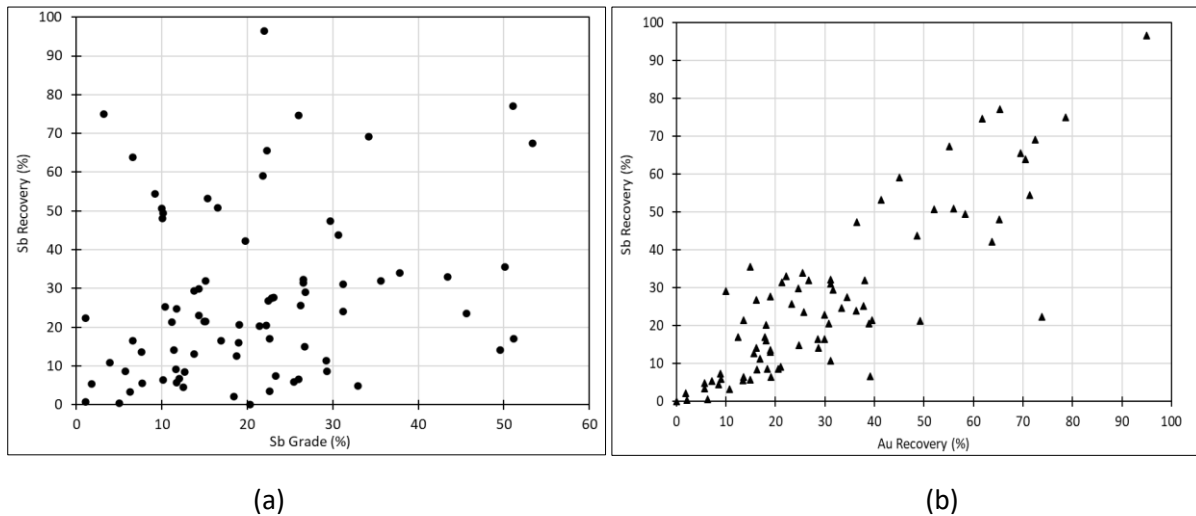


Figure 11: The plot from the pilot test work for (a) antimony block recovery versus antimony grade in final concentrate and (b) Antimony block recovery as a function of the block gold recovery.

CONCLUSIONS

Eriez Flotation Division has commissioned StackCells and cavitation flotation columns at the up-front and the back end of the existing flotation circuit as part of the expansion project to increase the circuit flexibility and to recover additional gold from the tail stream after a series of successful pilot test work campaigns. The outcome of the pilot test work and industrial-sized commissioning are concluded as follows:

- The StackCell technology implemented as a pre-rougher stage was able to produce an immediate final concentrate. It proved to help to increase the circuit's maintenance and operation flexibility and, at the same time, reduce the load on the downstream conventional flotation cells. The high capacity and compact design of the StackCell were ideal to be

implemented when only limited real-estate space was available without major modifications to existing layouts.

- Implementing the Eriez cavitation flotation columns has proved beneficial in recovering additional gold from the final tail stream from the existing conventional flotation circuit. It was able to achieve the target concentrate of 45 g/t of gold and block recovery of 30%. The gold grade at the final tailing was monitored throughout the commissioning period. It clearly showed that the gold grade decreased from 0.90 g/t to 0.60 g/t at the end of the commissioning work, indicating the level of gold being recovered from the plant tails in the columns.

ACKNOWLEDGEMENTS

The authors would like to acknowledge the tremendous contributions of the industrial participants involved in this work. These contributions, in terms of time, manpower, expertise and willingness to trial new technology, are gratefully acknowledged.

REFERENCES

Lynch, A.J., Johnson, N.W., Manlapig, E.V. and Thorne, C.G., 1981. Mineral and Coal Flotation Circuits – Their Simulation and Control, Developments in Mineral Processing Series, Elsevier Scientific Publishing Company, New York, NY.

Mankosa, M.J., Kohmuench, J.N., Christodoulou, L., and Yan, E.S., 2018. “Improving Fine Particle Flotation using the StackCell™ (Raising the Tail of the Elephant Curve),” Minerals Engineering, Vol 121, June 2018, pp. 83-89.

Murdock, D J, Tucker, R J and Jacobi, H P, 1991. Column cells versus conventional flotation: A cost comparison, *Column 91, Int Conf on Column Flotation*, Sudbury, 2-6 June.

Williams, J.J.E, and Crane, R.I., 1983. “Particle Collision Rate in Turbulent Flow,” International Journal of Multiphase Flow, Volume 9, No. 4, pp. 421-435

Integrated Flow Sheet Development for a Copper Operation in Central Chile

M Hasan¹, E Amini², M Maquieira³, N Beaton⁴ and C Heck⁵

4. Metallurgical Specialist, Digital Solution, Orica Australia, 72 Newmarket Street, Windsor QLD 4030 Australia, maruf.hasan@orica.com
5. Manager – Technical Services, Digital Solution, Orica Australia, 72 Newmarket Street, Windsor QLD 4030 Australia, eiman.amini@orica.com
6. Manager – Technical Services, Teck Resources Limited, Alonso de Córdova 4580, Piso 10 Las Condes, Santiago, Chile, miguel.becerra@teck.com
7. Senior Manager - Technology (IES), Digital Solution, Orica Australia, 72 Newmarket Street, Windsor QLD 4030 Australia, nick.beaton@orica.com
8. Metallurgical Superintendent, Carmen de Andacollo, Teck Resources Limited, Camino a Chepiquilla s/n, Andacollo Región de Coquimbo, Chile, christian.jara@teck.com

ABSTRACT

The Orica Digital Solutions team has recently developed a mine-to-concentrate flow sheet for the Teck Resources Carmen de Andacollo (CdA) operation using the Integrated Extraction Simulator (IES), a cloud-based platform designed to predict and optimize the performance of mining value chains. A combination of industry-standard phenomenological and Artificial Neural Network (ANN) models was used or developed for the blasting, comminution, and flotation circuits, respectively. The flow sheet was then used for life of mine (LOM) performance simulation, and the results were written back to the resource block model (block model conditioning) for various scenarios. The simulation scenarios, such as standard and less intensive blast designs, as well as the installation of a HPGR in the crushing circuit, were tested. Three levels of grinding circuit product sizes were also assessed in the study, in conjunction with the other scenarios. Finally, 3.6 M simulations were conducted in under a minute through the development of a MetaModel from the IES flow sheet.

The simulation results showed that the less intensive blast design had a minimal impact on plant throughput and metal production. However, installing a HPGR in the crushing circuit increased metal production by 10.6% at the optimum grind size. The paper outlines the steps involved in developing the integrated flow sheet and how it was used to generate bankable outcomes that can be used by CdA management to choose the scenario that maximizes their production over the remaining LOM.

INTRODUCTION

The concept of mine to concentrate or value chain flow sheet is an extension of the well-established mine to mill optimisation strategy. The mine to concentrate flow sheet goes beyond the blasting and size reduction process by evaluating the impact of each mining operation on the final metal production rate throughout the lifespan of a mine. The production of a mineral commodity is a comprehensive process that involves extracting the ore from the earth's crust (e.g., blasting), liberating the minerals through size reduction (e.g., comminution), and subsequently separating the valuable minerals from the gangue minerals (e.g., predominantly flotation). Traditionally, these three processes were treated as isolated operations, with each process optimised independently and without considering the entire value chain. As a result, potential economic benefits, as well as opportunities for energy and water savings, were often overlooked or not fully understood. This approach of standalone optimisation was primarily due to the absence of integrated software platforms in the past.

Integrated Extraction Simulator (IES) is a next-generation software for mineral processing simulation. It serves as a cloud-based simulation and optimisation platform, specifically designed to predict and optimise the performance of mineral processing operations. IES seamlessly integrates various units of

operation, such as drilling and blasting, crushing, grinding, and flotation. As a result, it enables the generation of realistic predictions for concentrator performance across different operational scenarios. IES incorporates a variety of simulation models, primarily inherited from the JKMRC (Julius Kruttschnitt Mineral Research Centre) at The University of Queensland plus customised phenomenological and machine learning models added to the platform later. The integrated flow sheet of IES offers a unique feature of having three distinctive options for simulating different aspects of a mining operation.

- *mass simulation* – This is most useful when running several simulations to detect the simultaneous effect of a wide range of variables on the circuit performance. Mass simulation is also helpful when used for design purposes and in constraint-based simulations. The mass simulation is mainly used to support throughput determination for various scenarios.
- *optimisation* – This can be used to minimise, maximise, or seek a performance goal when it is feasible to define and consider circuit limitations—that is, in constraint-based optimisation.
- *sensitivity analysis* – This allows to investigate the impact of desired variables that can vary in a range (e.g., ore competence) on target parameters (e.g., throughput) under pre-defined constraints.

The IES has already been utilised in several studies to evaluate the impacts of ore characteristics and operating conditions on the process plant performance. These studies include assessing the effects of differential blasting, feed fragmentation, grind size, and grade department on plant throughput and metal recoveries (Amini et al, 2020; Carrasco et al, 2019; Koh et al, 2023), investigating the influence of preconcentration on net present value (NPV), water consumption, and energy consumption (Scott and Amini, 2020), examining the effects of pre-treatment technologies in the mining value chain (Amini and Beaton, 2020; Amini et al, 2020), and exploring the effects of grade engineering in the mining value chain (Keeney et al, 2020).

The Orica technical services developed a mine-to-concentrate flow sheet using the IES platform. In this process, a combination of industry-standard phenomenological models and Artificial Neural Network (ANN) models were used or developed for blasting, comminution, and flotation circuits. The flow sheets were employed to condition the resource block model in twelve simulation scenarios, aiming to assess the impact of grind size, blast design, and the addition of HPGR in the crushing circuit on the metal production rate. The paper describes the procedure used to develop the operationally integrated flow sheet and explains how it was utilised to generate bankable outcomes. These outcomes were used by the mine operational team to determine the scenario that maximises production for the remaining life of the mine (LOM).

CONFIGURATION OF THE VALUE CHAIN FLOW SHEET

The value chain flow sheet was developed using the methodology provided by Amini and Beaton (2020). A brief description of developing the value chain flow sheet is detailed following.

- data collection and cleaning
 - data were collected and grouped into four categories 1. ore characteristics, 2. equipment specifications, 3. process operation condition, and 4. performance response.
 - clean the data based on non-operational time, “0” and “negative” value
 - average out the data on a monthly basis.
- mine to mill flow sheet development, model implementation, and validation

- develop baseline mine to mill flow sheet by integrating blasting, crushing, and grinding operation
 - implement prior developed JKSimMet process models (calibrated through plant survey) into the IES platform
 - assess and fine-tune the model response with the average operational data
 - identify the process constraints and set up the flow sheet optimiser to apply them to the flow sheet
- flotation flow sheet development using a machine learning model
 - flotation model development to determine flotation process response with the change in ore characteristics and mine to mill conditions
 - implement the flotation flow sheet in the IES environment
- value chain flow sheet development
 - develop the value chain flow sheet by integrating flotation and mine to mill flow sheet using IES embedded flow sheet feature

An integrated base case flow sheet was developed following the above methodology as shown in Figure . The integrated flow sheet comprises a complex crushing circuit with four separate lines, a conventional semi autogenous ball mill crusher (SABC) circuit, and a flotation circuit encoded with a machine learning model.

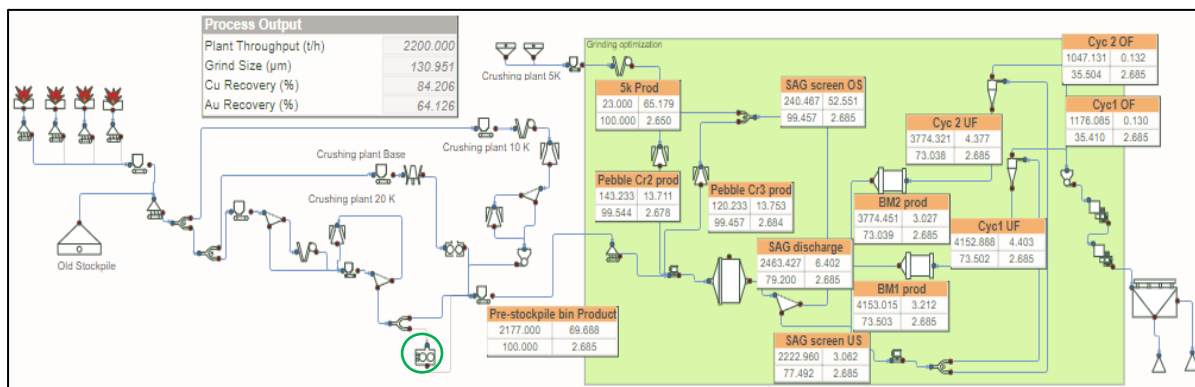


Figure 1 – Integrated flow sheet of a Copper operation in the Central Chile

Flow sheet model description

The flow sheet within IES consists of a combination of phenomenological and empirical models, necessitating calibration using survey and process data gathered during operations. The key process models for the flow sheet are described as follows.

Kuz Ram Fines Blast Model

The original Kuz Ram model, proposed by Cunningham (1983), is widely recognised as one of the most commonly used models for estimating fragmentation resulting from blasting. This model is based on the Kuznetsov and Rosin-Rammler equations. However, a notable limitation of this model is its tendency to underestimate the quantity of fines produced. To address this issue, the 'Crushed Zone Model' was developed at JKMR (Kanchibotla et al, 1999), known as the 'Kuz Ram Fines Blast Model' in IES. One advantage of this model, compared to the original Kuz-Ram model, is its increased sensitivity of the fine particle size distribution (PSD) to rock mass strength and explosive performance characteristics.

The mining operational team was studying the impact of a less intensive blast design in three different domains of the mine throughout the LOM scenario. The objective was to minimise the adverse effects of blast vibration on the nearby town. The blast design for both the base case and less intensive blast was formulated within the IES using the Kuz Ram Fines Blast Model. The disparity between the base case and less intensive blast design was quantified in terms of the loading factor (g/t), as presented in Table 1.

Table 1 – Comparison of Base Case and Less Intensive Blast Design

Domain	UCS (MPa)	Loading Factor (g/t)		Mean Fragmentation Size, X50 (mm)	
		Base Case	Less Intensive	Base Case	Less Intensive
4	over 80	401.5	299.6	91.5	108.4
5	20-40	302.4	289.0	83.1	84.8
7	60-80	323.3	301.5	72.4	77.1

Primary Crushing Model

The primary crushing circuit is composed of three crushing lines: the base, 20K stream, and 10K stream. The base crushing circuit incorporates a cone and roll crusher, the 20K crushing circuit comprises a jaw and cone crusher, and the 10K crushing circuit includes a jaw, secondary cone, and tertiary cone crusher. The crusher operation in each circuit was described using the Andersen and Whiten Crushing model (Whiten, 1972 and Andersen and Napier-Munn, 1988).

Primary Grinding – SAG Milling

The variable rates model (Morrell et al, 2001) was utilised to describe the operation of the semi-autogenous mill (SAG) mill in the flow sheet. The Variable Rates SAG mill model incorporates the dimensions and operating conditions of the mill, as well as ore-specific hardness parameters (A, b, and ta) and the throughput of a base case condition. These parameters are used to determine the machine-specific breakage rates at various particle sizes. By combining these breakage rates with a population mass balance model, the SAG mill performance can be predicted for a given feed size distribution and ore hardness. The predicted SAG mill performance includes throughput, volumetric total load, particle size distribution (PSD), and power draw.

The variables that were used to fine-tune the SAG mill model were:

- SAG feed % solids
- Drop Weight Index (DWi) – converted to A, b, and ta values
- SAG feed sizes
- plant throughput
- SAG % critical speed (SAG mill Speed)

Secondary Grinding – Ball Milling

The ball milling operation in the flow sheet was described using the perfect mixing ball mill model developed by Whiten (1976). The 'Perfect Mixing Model' enables the scaling of breakage rates from baseline conditions to a variety of different operating conditions for which performance is projected.

Classification – Hydrocyclone

The Nageswararao model (1978) was employed to characterise the operation of the hydrocyclone in the flow sheet. This model combines the cyclone dimensions with the operating conditions through a series of regression equations to determine the classification efficiency curve. The classification efficiency curve is used to predict the size distributions and flow rates of the two product streams from the hydrocyclone.

Flotation Model

There was a lack of available phenomenological models for the flotation process to predict recovery and metal production based on changes in blasting and comminution operating conditions, such as blast fragmentation, throughput, and grind size. To address this, a machine learning flotation model was developed (Koh et al, 2022) and implemented in the IES flow sheet to calculate flotation response with variations in blasting and comminution operating conditions.

The machine learning model was built using IES ModelNet package. Training and validation of the model utilised operational data from the site spanning 2018 to 2021, totalling 1033 data records. The machine learning model accurately predicts flotation response by considering changes in ore characteristics and operating conditions in the blasting and comminution process. The model receives relevant information, such as comminution grind size and throughput, through the connecting stream to incorporate it into its predictions.

Figure 2 depicts a comparison among the actual Cu recovery, the machine learning (ML) model, and the Geomet model (currently used by the mine for recovery prediction). The figure illustrates that the machine learning-based flotation model achieves a close prediction of Cu recovery compared to the actual values, outperforming the Geomet model.

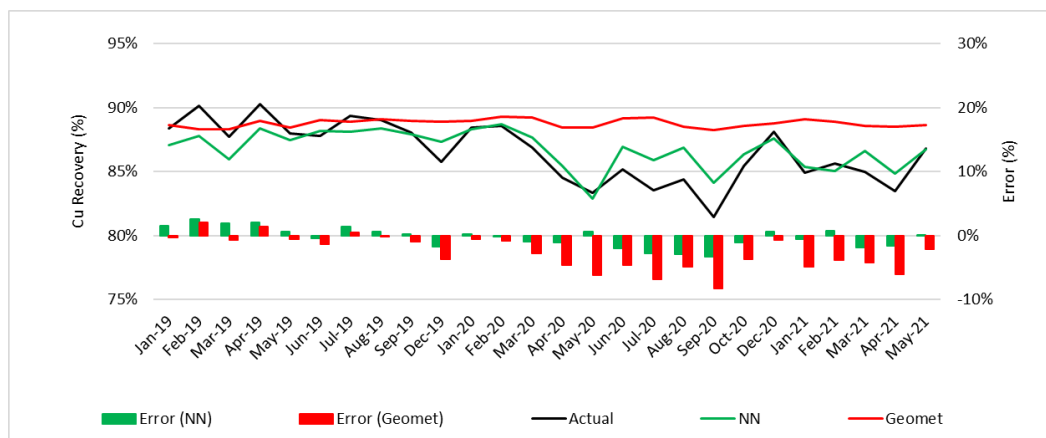


Figure 2 –The flotation circuit Cu recovery (monthly average)

Flow sheet constraint manager

IES offers the capability for users to optimise flow sheet simulation results according to their defined parameters. This functionality allows users to easily define optimisation boundaries by dragging, dropping, and resizing a subset box on the flow sheet. The equipment and streams within the subset can provide attributes as parameters that can be adjusted, as well as constraints that can be applied to the optimisation function.

The Constraint Manager within IES enhances simulation accuracy by allowing users to define operating ranges for equipment settings as parameters and establish processing targets as constraints. In the

integrated flow sheet of the mining operation, the Constraint Manager was utilised to manage throughput potential. By setting limits on the SAG mill load, cyclone pressure, and final grind size, the maximum achievable throughput was calculated under these constrained conditions. This approach utilised the fine-tuned flow sheet to deliver more realistic simulation results.

Flow sheet fine-tuning

The flow sheet fine-tuning was carried out to address the process variability observed in the Copper mining operation and develop a predictive flow sheet to handle future variability. The variabilities in the operation are illustrated in Table 2, showcasing the range of operational data. This variability serves as a justification for fine-tuning the equipment models within the flow sheet. By refining the models, it was possible to enhance the predictability and accuracy of the simulation result.

Table 2 – Variation in operation data

Variable	Min	Max	15 th Percentile PI Data	85 th Percentile PI Data
Estimated SAG DWi Value	7.99	10.12	8.31	9.14
Estimated SAG A Value	74.55	80.88	75.57	78.08
Estimated SAG b Value	0.34	0.47	0.39	0.44
Estimated SAG ta Value	0.25	0.32	0.28	0.31
BWi (kWh/t)	13.55	15.34	14.15	14.94
SAG Mill Product % Solids	74.91	80.39	76.78	79.86
SAG Mill Fractional Speed	0.69	0.75	0.71	0.73
Throughput (t/h)	2074.8	2448.1	2154.8	2364.8
SAG Power (kW)	12134.1	13977.6	12445.6	13496.2
Total Ball Mill Power (kW)	25551.0	28008.4	25925.9	27404.9
Cyclones 1 Pressure (psi)	6.8	9.2	7.9	8.7
Cyclones 2 Pressure (psi)	7.0	9.5	7.9	9.0
Cyclone Overflow P80 (µm)	127	160	136	150
Flotation Feed P80 (µm)	123	143	128	138

Figure 3 depicts the comparison between the predicted throughput generated by IES and the actual values over a two-and-a-half-year period. It is important to note that plant throughput is influenced by various factors, some of which are not considered in the models, particularly when throughput is constrained by events occurring upstream or downstream of the comminution circuit. Despite these limitations, the predictions generally exhibit a reasonable alignment with the observed trends for the variables accounted for in the model. The average absolute error, indicating the deviation between predicted and actual values, was found to be 1.04%.

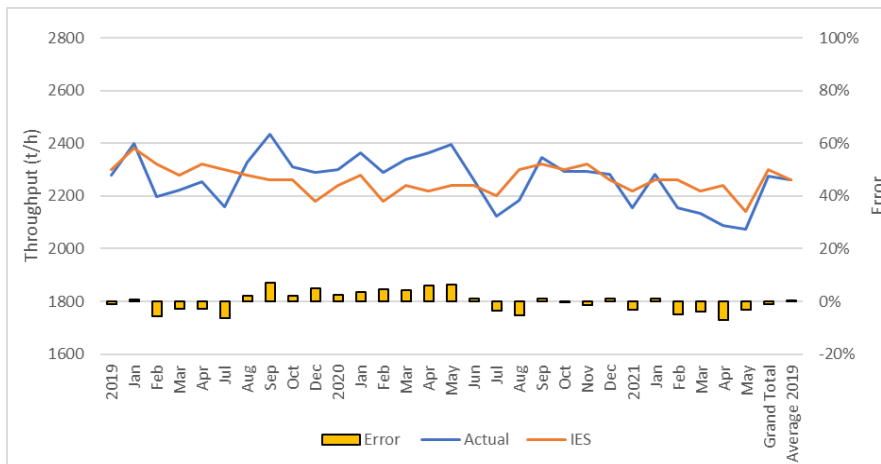


Figure 3 – Actual and IES predicted plant throughput from Jan 2019 to May 2021

The combined cyclone overflow P80 and IES predicted P80 is shown in Figure 4. The average absolute error was 1.3%.

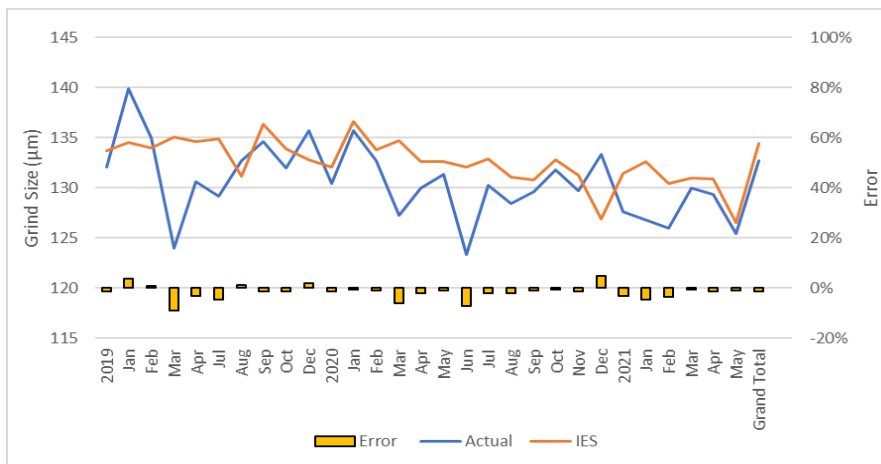


Figure 4 – Cyclone overflow P80 actual vs simulated

LIFE OF MINE SIMULATION

The fine-tuned and validated value chain flow sheet was utilised for short-, medium-, and long-term optimisation scenarios. In the long-term optimisation strategy, the mine metallurgical team primarily assessed two scenarios. The first involved modifying the blast design for the remaining LOM, while the second scenario involved evaluating the impact of incorporating a HPGR in the 20K crushing circuit to enhance the efficiency of processing harder rock. These two scenarios were tested using block data developed through geostatistical modelling, representing the LOM, and utilising the integrated flow sheet. The operational team provided a total of 310 589 block data points for simulating the metal production under the two alternative scenarios and comparing them with the baseline operation. Each block data point included coordinates, blast fragmentation data (fracture frequency, point load index, uniaxial compressive strength (UCS), ore characteristics data (DWi and BWi), and elemental grade and recovery (Geomet) data. The mass simulation was conducted at four conditions listed as follows:

- standard blast design (Base Case)
- less intensive blast design
- HPGR in the 20K crushing circuit (refer green circle in Figure)
- Cyclone P80 size (100 µm, 130 µm and 155 µm)

The mass simulation of the block model followed the flow diagram depicted in Figure 5. Initially, the block data was filtered, and subsequently, a representative subset of the block model was chosen for primary simulation. The results obtained from the primary simulation were utilised to create a neural network based (NN) MetaMode following the methodology provided by Koh et al, (2021). This MetaModel was developed to predict plant throughput and metal recovery.

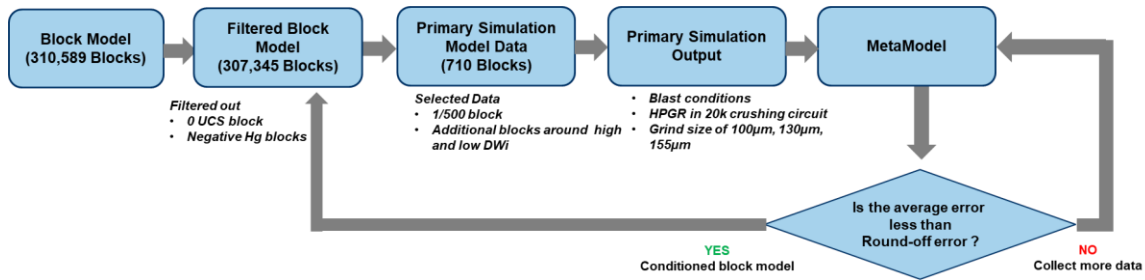


Figure 5 – Life of Mine simulation flow chart

After its development, the flow sheet MetaModel was employed to condition the block model. The significant advantage of using the MetaModel over the IES phenomenological model is that it requires considerably less simulation time and cost to condition the block model. In the process of conditioning the block model, a total of 3.6 M simulations were conducted, which would have taken approximately 800 server days using the IES phenomenological model. However, by utilising the MetaModel, the same simulation was completed in minutes. Figure 6 displays the IES flow sheet surrounding the MetaModel.

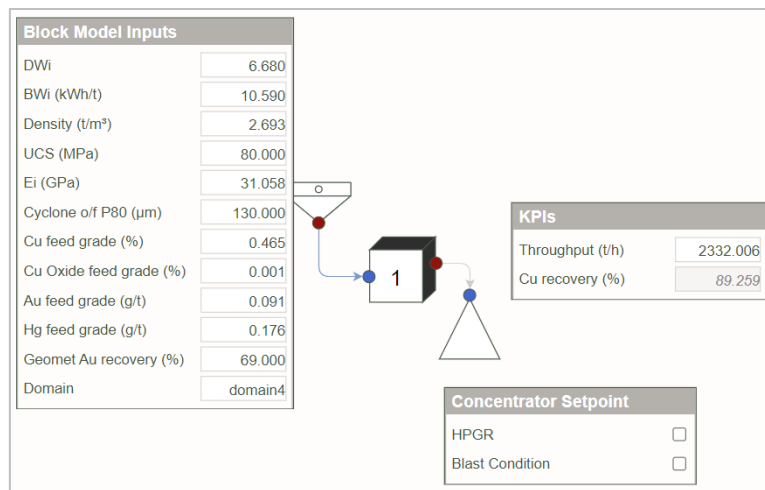


Figure 6 – IES MetaModel flow sheet

The validation of the MetaModel, in comparison to the actual performance, is presented in the parity charts illustrated in Figure 7. The results for the throughput prediction errors are as follows: 0.44% for the training dataset, 0.46% for the validation dataset, and 0.47% for the test dataset. These values indicate the level of deviation between the predicted throughput values by the MetaModel and the actual performance data.

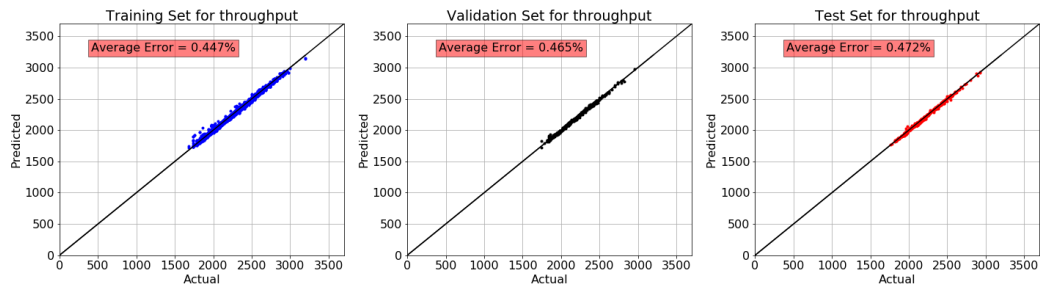


Figure 7 – Parity chart for flow sheet MetaModel

FLOW SHEET APPLICATION AND DISCUSSION

The output of the LOM simulation was used to condition the block model by writing the results back into it in 12 different simulation scenarios. The conditioned block model can then be utilised for future planning and strategy assessment. An example of the conditioned block model is provided in Figure 8.

xcentre	ycentre	zcentre	catg	lith	minzone	dwi	Axb	b	A	ta	bwi (kWh/t)	density (t/m3)	Cu Grade (%)	Cu Oxide (%)	Cu Recovery	Au Grade (ppm)	Au Recovery	Hg Grade (ppm)	UCS (Mpa)	Ei (Gpa)	Domain
98995	52175	855	1	4	1	4.2	64.2	1.08	59.7	0.63	14.0	2.6	0.89	0.001	0.87	0.13	0.69	0.10	60.0	45.0	7
99005	52175	855	1	2	1	4.2	64.2	1.08	59.7	0.63	16.0	2.6	0.46	0.001	0.85	0.12	0.68	0.10	60.0	45.0	7
99015	52175	855	1	4	1	4.2	64.2	1.08	59.7	0.63	14.0	2.6	0.85	0.001	0.87	0.11	0.69	0.12	60.0	45.0	7
99005	52175	855	4	1	4.2	64.2	1.08	59.7	0.63	14.0	2.6	0.79	0.001	0.87	0.16	0.69	0.03	80.0	45.0	4	
98985	52175	855	1	4	1	4.2	64.2	1.08	59.7	0.63	14.0	2.7	0.40	0.001	0.87	0.12	0.69	0.05	80.0	45.0	4

Condition 1		Condition 2		Condition 3		Condition 4		Condition 5		Condition 6		Condition 7		Condition 8		Condition 9		Condition 10		Condition 11		Condition 12	
S-No HPGR-100		280-No HPGR-100		S-HPGR-100		280-HPGR-100		S-No HPGR-130		280-No HPGR-130		S-HPGR-130		280-HPGR-130		S-No HPGR-155		280-No HPGR-155		S-HPGR-155		280-HPGR-155	
tph	Recovery	tph	Recovery	tph	Recovery	tph	Recovery	tph	Recovery	tph	Recovery	tph	Recovery	tph	Recovery	tph	Recovery	tph	Recovery	tph	Recovery	tph	Recovery
1934	0.92	1932	0.92	2067	0.91	2041	0.91	2225	0.89	2223	0.89	2339	0.88	2323	0.88	2492	0.87	2474	0.87	2600	0.86	2593	0.86
1872	0.92	1868	0.92	2007	0.93	1977	0.93	2111	0.93	2111	0.93	2223	0.92	2218	0.92	2364	0.92	2358	0.92	2473	0.92	2460	0.92
1919	0.92	1915	0.92	2055	0.90	2028	0.91	2211	0.89	2208	0.89	2310	0.88	2483	0.86	2464	0.86	2600	0.85	2581	0.85		
1911	0.92	1912	0.92	2067	0.91	2053	0.91	2210	0.91	2217	0.89	2354	0.89	2458	0.89	2458	0.89	2600	0.88	2600	0.88		
1967	0.92	1972	0.92	2112	0.92	2102	0.92	2262	0.91	2274	0.91	2398	0.90	2405	0.90	2489	0.91	2493	0.91	2600	0.90	2600	0.90

Figure 8 – Block model conditioning

A further assessment was conducted on the simulated output data by comparing the average metal production across different life of mine scenarios. Specifically, the assessment compared the base case blast scenario with less intensive scenario. The findings indicated that adopting the less intensive blast design would result in a reduction of average metal production to less than 1% (refer to Figure 9) compared to the base case or standard blast design used for processing the blocks. The impact of the change in fragmentation size, caused by the alteration in blast design, was mostly absorbed by the robust crusher circuit and did not significantly affect the performance of the grinding and flotation circuit (refer to Figure 10). The result suggests that it is possible to modify the current blasting design to a less intensive blast design with minimal reduction in metal production. This change would have several advantages, including minimising the adverse effects of vibrations on the nearby town and reducing overall blasting costs.

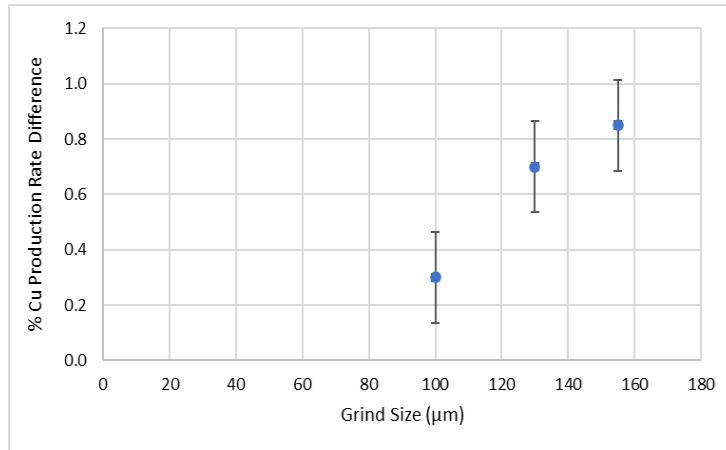


Figure 9 – Base case blast and less intensive blast design avg. Cu production rate difference at the different grind size

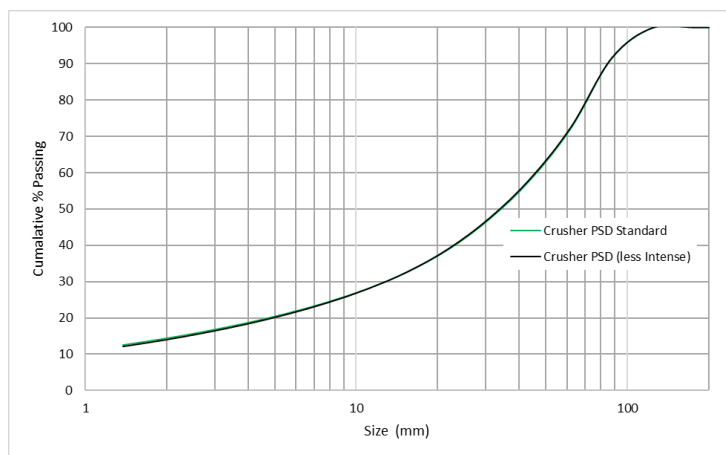


Figure 10 – Crushing circuit product size in different blast design

The simulation results showed the inclusion of a HPGR in the crushing circuit will lead to a substantial improvement in the metal production rate. The results demonstrate an increase in Cu production rate ranging from 5% to 13% at various grind sizes, as illustrated in Figure 11. The incorporation of the HPGR has resulted in a significant reduction in the product size of the crushing circuit, leading to an increase in metal production, as shown in Figure 12.

The obtained outcome will be instrumental in calculating the economical indexes to evaluate installation of the HPGR in the crushing circuit throughout LOM.

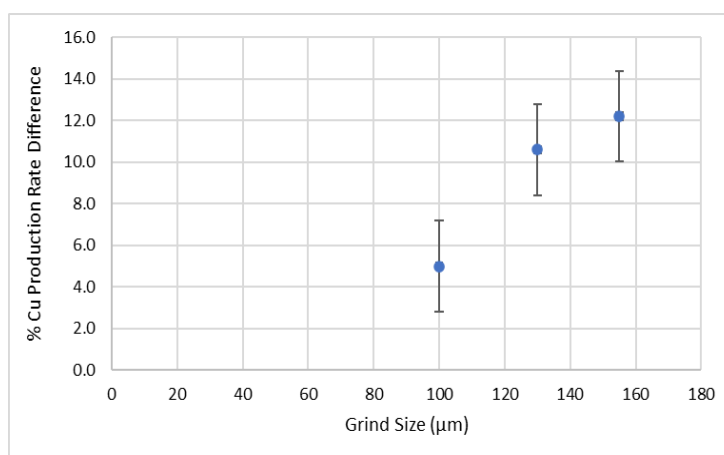


Figure 11 – Increase in Cu production rate at standard blast design with HPGR in the 20K crushing circuit

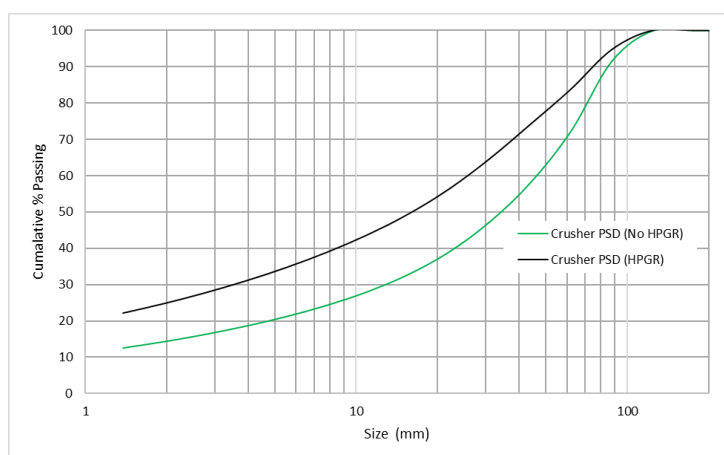


Figure 12 – Crushing circuit product size with and without a HPGR (at the base case blast scenario)

CONCLUSION

The Orica Digital Solutions technical services has successfully developed a comprehensive value chain flow sheet for a copper mine in Central Chile, integrating various operations such as blasting, crushing, grinding, and flotation. Each operation along the operation vale chain was modelled. Industry-standard phenomenological models were used for blasting and comminution process units. For the flotation operation, a machine learning predictive model was specifically developed to forecast elemental recovery and grade based on changes in ore properties.

The validity of the flow sheet was established by looking into two years of operational data. Subsequently, the validated flow sheet was used to conduct mass simulations to predict metal production over LOM. The mass simulation considered two blasting conditions (base case and less intensive), the inclusion of a HPGR in the 20K crushing circuit, and three grind sizes (100 µm, 130 µm, and 155 µm). The results from the mass simulation indicated that changing the blasting design from the base case to a less intensive option resulted in an insignificant reduction of plant throughput, less than 1%. However, incorporating the HPGR in the 20K crushing circuit demonstrated a notable increase in Cu production rate, ranging from 10% to 13% at the grind sizes of 130 µm to 150 µm.

The developed flow sheet offers valuable opportunities for short to medium-term plant optimisation work without disrupting ongoing operations. It enables effective crisis management during short-term operational challenges, such as restoring plant throughput during equipment downtime by utilising the flow sheet. Additionally, it facilitates short-term optimisation efforts, such as identifying process bottlenecks, quantifying constraints, and optimising the energy balance of the comminution circuit for a new orebody by striking a balance between SAG and ball mill operations to maximise metal production. Furthermore, the flow sheet supports medium-term optimisation analysis, including optimising the blending of the stockpile and fresh ore for improved performance.

ACKNOWLEDGEMENT

The authors would like to thank Orica for giving permission to publish the paper.

REFERENCES

Abadi, M., Barham, P., Chen, J., Chen, Z., Davis, A., Dean, J., & Yu, Y. (2016). Tensorflow: A System for Large-Scale Machine Learning. In Proceedings of the 12th USENIX Symposium on Operating Systems Design and Implementation. Savannah, USA.

Amini, E., Becerra, M., Bachmann, T., Beaton, N., & Shapland, G. (2020). Development and Reconciliation of a Mine Operation Value Chain Flow sheet in IES to Enable Grade Engineering and Process Mass Simulations for Scale-Up and Strategic Planning Analysis. In SME Annual Conference and Expo, Arizona, February 23-26, 2020.

Amini, E., & Beaton, N. (2020). Development of mine operation value chain flow sheets fine-tuned and constraint based on the process information (PI) data to evaluate proposed operation strategies and ore pre-treatment technologies. In Preconcentration Digital Conference, November 17-18, 2020.

Andersen, J.S., & Napier-Munn, T.J. (1988). Power prediction of cone crushers. In Proc. 3rd Mill Operators' Conference, AusIMM.

Carrasco, C., Gahona, M., La Rosa, D., Shapland, G., Beaton, N., & Amini, E. (2019). Augmenting Traditional Mine to Mill with Cloud-Based Simulation and Reconciliation Capabilities. In SAG Conference, Vancouver, 17-19 January 2019. Chollet, F. (2015). Keras. Retrieved from GitHub repository: <https://github.com/fchollet/keras>

Chollet, F. (2015). Keras. Retrieved from GitHub repository: <https://github.com/fchollet/keras>

Cunningham, C.V.B., (1983). The Kuz–Ram model for prediction of fragmentation from blasting. Proceedings of 1st International Symposium on Rock Fragmentation by Blasting, Lulea, pp 439–454.

Kanchibotla, S.S., Valery, W., & Morell, S. (1999). Modelling fines in blast fragmentation and its impact on crushing and grinding. In Proceedings of the Explo 1999 conference. Carlton, Victoria: AusIMM p. 137–44.

Keeney, L., Beaton, N., Scott, M., La Rosa, D., Amini, E., Rutter, J., & Faramarz, F. (2020). The integration of mine to mill and grade engineering at Anglo American's Los Bronces Mine using IES. In Preconcentration Digital Conference, November 17-18, 2020.

Koh, E.J., Amini, E., Maquieira MB., Heck CJ., McLachlan GJ., & Beaton, N. (2022). An Automated Machine learning (AutoML) approach to regression models in minerals processing with case studies of developing industrial comminution and flotation models. Minerals Engineering, 189, 107886. ISSN 0892-6875. <https://doi.org/10.1016/j.mineng.2022.107886>.

Koh, E.J., Amini, E., Watkins, R., Mayhungu, E., & Bergmann, C. (2023). Maximising Value at a Platinum Group Metals Concentrator by Development of an Integrating Comminution and Flotation Flow sheet. In *comminution 2023*, Cape Town, South Africa

Koh, E.J., Amini, E., McLachla, C.J., & Beaton, N. (2021). Utilising a deep neural network as a surrogate model to approximate phenomenological models of a comminution circuit for faster simulations. *Minerals Engineering*, 170, 107026. ISSN 0892-6875.

Morrell, S., Valery, W., Banini, G., & Latchireddi, S. (2001). Development in AG/SAG Mill Modelling. SAG Conference, Vancouver, pp. 71-84.

Nageswararao, K. (1978). Further developments in the modelling and scale-up of industrial hydrocyclones. PhD thesis, The University of Queensland.

Scott, M., & Amini, E. (2020). Quantifying economic and environmental impacts of preconcentration. In *Preconcentration Digital Conference*, November 17-18, 2020.

Whiten, W.J. (1972). The simulation of crushing plants with models developed using multiple spline regression. *J.S.A. Inst. Min. Met.*, 72, 257-264.

Whiten, W.J. (1976). Ball mill simulation using small calculators. *Proc. AusIMM*, No 258, June 1976.

Energy Savings and Carbon Footprint Reduction - Jameson Vs Conventional Copper Concentrator

C Anderson¹, G Csicsovszki², S Crane³ and G Ballantyne⁴

1. Glencore Technology, Senior Metallurgist, 180 Ann St, Brisbane Qld 4000, chris.anderson1@glencore.com.au
2. Glencore Technology, Principal Metallurgist, 180 Ann St, Brisbane Qld 4000, gabor.csicsovszki@glencore.com.au
3. Ausenco, Process Engineer, 189 Grey Street, South Brisbane QLD 4101, Sam.Crane@ausenco.com
4. Ausenco, Director Technical Solutions, 189 Grey Street, South Brisbane QLD 4101, Grant.Ballantyne@ausenco.com

ABSTRACT

Traditional concentrator design involves the use of large mechanical cells of up to 630 m³ to provide sufficient residence time for flotation of ever lower grade ore bodies. Increasingly, companies are required to release Environmental Social Governance (ESG) disclosures for projects and demonstrate savings in both Scope 2 and Scope 3 emissions. However, very few benchmarks of emissions in flotation and regrind circuits are available in publications.

An alternative approach using the Jameson Concentrator has previously been demonstrated at New Britannia, Philex and Ozernoye which combines both IsaMill and Jameson Cell technology into a full-concentrator flow sheets to drastically reduce footprint, power, operating cost (OPEX) and capital cost (CAPEX) requirements. However, the benefits in terms of Scope 2 and 3 emissions have yet to be determined.

This paper presents a comparative case study between the Jameson Concentrator and a conventional copper concentrator. Each design is compared on a consistent basis in terms of plant footprint, power consumption, height, and Scope 2 and 3 carbon emissions.

The results demonstrate that the Jameson Concentrator approach results in savings in power consumption and footprint. In addition, both Scope 2 and Scope 3 emissions are reduced both during construction and during operation. It was found that the carbon savings during operation of the plant outweighed the emissions savings during construction by several orders of magnitude.

INTRODUCTION

As emissions of greenhouse gases (GHG) around world continue to grow, mining companies are under increasing pressure to innovate new methods of production which lower emissions, and drive towards net-zero production. In fact, mining operations generate 2-3% of CO₂ worldwide (Legge et. al., 2021), so they clearly have a responsibility to reduce emissions. According to climate scientists, global carbon dioxide emissions must be cut by as much as 85 percent below 2000 levels by 2050 to limit the global mean temperature increase to 2 °C above pre-industrial levels (Metz et. al., 2007). Achievement of this goal will require leadership and innovation from all companies, including technology suppliers, Engineering, Procurement and Construction Management (EPCM) and operators, in the mining sector in general, to lower the carbon footprint so that the commodities as an example, which are essential to a zero-carbon future, are produced.

The World Resources Institute (WRI) divides emissions into three categories as shown in Figure 1. Scope 1 consists of direct emissions from owned or controlled sources (e.g. diesel powered mining equipment). Scope 2 emissions consist of indirect emissions from the generation power consumed by the operation, and Scope 3 consist of all other indirect emissions that occur in a company's value chain (e.g. steel, concrete, reagents and grinding media). Copper producers generated 97 Mt of CO₂

equivalent in 2018, of which concentrators contributed almost a third. Flotation is responsible for about 20% of energy and emission intensity (Sykes et al., 2007). In addition, the energy intensity of concentrators becomes exponentially higher with lower grade ore bodies (Northey et al., 2013).

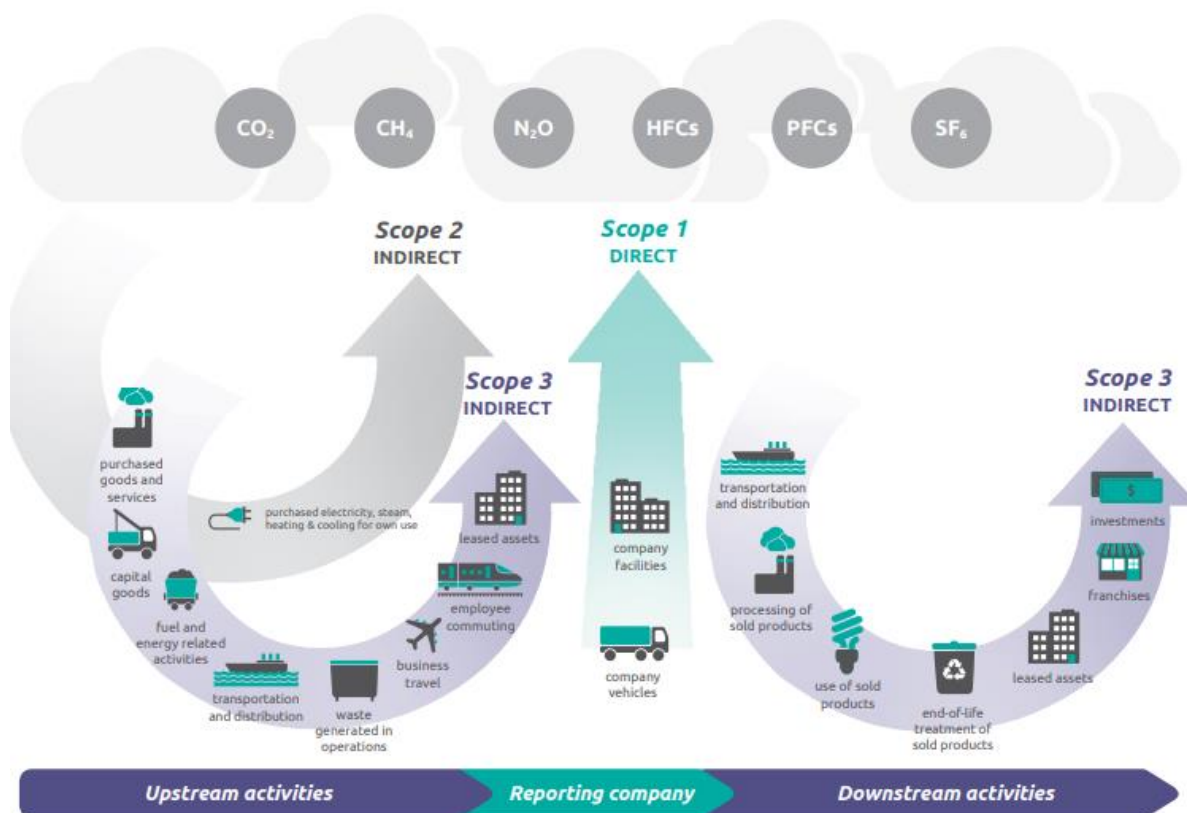


Figure 1: Overview of the GHG Protocol Scopes and Emissions across the Value Chain (Protocol, 2011)

To cut carbon emissions, mining companies have typically divested coal assets and the most visible and largest operators have set grandiose carbon emission targets for Scope 1 and 2 emissions. The copper miner giant, Codelco, uses solar power at one of its operations in Chile while BHP and Fortescue Metals are investing in renewable energy as a few examples. However, energy-efficient new technologies can also be a large contributor to Scope 1 and 2 emissions (Ballantyne et al. 2023).

The Jameson Concentrator is a combination of high-intensity Jameson flotation cells for minerals separation and IsaMill fine grinding to achieve acceptable mineral liberation. The high efficiency of Jameson Cells typically translates into fewer cells in each duty and a reduced number of cleaning stages, which significantly decreases concentrator footprint and power consumption (Anderson, 2022).

The following discussion investigates the extent to which applying the Jameson Concentrator approach can reduce GHG emissions, both during construction of the plant and during its operation.

BASIS OF ASSESSMENT

Ausenco, a global engineering company and frontrunner in delivering sustainable projects in the mining industry, undertook a comparative Class 4 (AAE) engineering study to determine the capital and operating cost differences between a Jameson Concentrator, offered by Glencore Technology, and a conventional plant for a major copper project. Furthermore, the study identified the differences in carbon emissions between the Jameson and conventional concentrator over the 15-

year life of mine (including Scope 2 and 3 emissions) – including a high-level understanding of the carbon associated with the production of concrete and steel.

The study was nominally based on a recent copper concentrator project in North America to provide a basis for the mineralogy and ore characteristics, with a throughput of 14 Mtpa. The study included the following objectives:

- To capture the savings in steel and concrete between the Jameson and conventional concentrator,
- To identify the differences in environmental impact including but not limited to carbon footprint between the Jameson and conventional concentrator over the 15-year life of mine (including Scope 2 and 3 emissions) – including a high-level understanding of the carbon associated with the production of concrete and steel.

Design Basis

Each option was based on the following design basis.

Table 1: Plant Design Basis

Item	Units	Value
Plant design capacity	Mt/y	14.0
Life of mine (LOM)	years	15
Operating availability	%	91.3
Feed grade, average	%Cu	0.39
Feed grade, max for design	%Cu	0.79
Metal recovery, design	%	91.0
Concentrate grade, nominal	%Cu	26.0
Ore specific gravity	t/m ³	2.73
Feed size, P ₈₀	µm	75
Regrind size, P ₈₀	µm	40
Specific grinding energy	kWh/t	7.8
Media Consumption (Vertical Mill - Steel Media)	g/kWh	6.5
Media Consumption (IsaMill - Ceramic Media)	g/kWh	8.0

Flow sheets and mass balances were developed for both the conventional and Jameson Concentrator circuits. A preliminary 3D model was developed for each option, with preliminary material take-offs (MTOs) for bulk earthworks, concrete, steel and platework developed based on the 3D model, as well as reference projects in Ausenco's database.

Battery Limits

Battery Limits for the trade-off study were as follows:

- Feed to rougher flotation (excluding conditioning tanks)

- Media addition (bag splitter)
- Flotation tailings – discharge of the flotation tailings stream to tailings thickener
- Final concentrate – final concentrate stream reporting to concentrate thickener
- Process water to concentrator – considered as a flanged connection within 5 m of the flotation and regrind circuits.
- Gland and raw water supply – considered as a flanged connection within 5 m of the flotation and regrind circuits.
- Plant air and instrument air – considered as a flanged connection within 5 m of the flotation and regrind circuits.
- Flotation reagents – addition points within conventional and Jameson concentrators.

Key Input Assumptions

The following rates were assumed for carbon emissions:

Table 2 Summary of GHG emission equivalents

Parameter	Units	Value	Source
Steel	kgCO ₂ e/ kg	1.89	Hammond & Jones, 2008
Concrete	kgCO ₂ e/ kg	0.14	Hammond & Jones, 2008
Steel (media)	kgCO ₂ e/ kg	1.82	Hammond & Jones, 2008
Ceramic (media)	kgCO ₂ e/ kg	0.97	Calculation
Electrical energy	kgCO ₂ e/ kWh	0.389	ClimeCo LLC, 2023

Conventional Circuit Design

The conventional circuit design is summarised in Figure 2. The head feed is processed in a bank of five 630 m³ tank cells, with the concentrate sent to a closed-circuit vertical stirred regrind mill to reduce the particle size from 80% passing 75 µm to 80% passing 40 µm. The regrind circuit product is sent to a three stage cleaner circuit comprised of seven 70 m³ tank cells, with the cleaner tails reporting to a cleaner-scavenger consisting of five 70 m³ tank cells. The circuit is designed to produce a 25.77% Cu product at a nominal recovery of 91.0%.

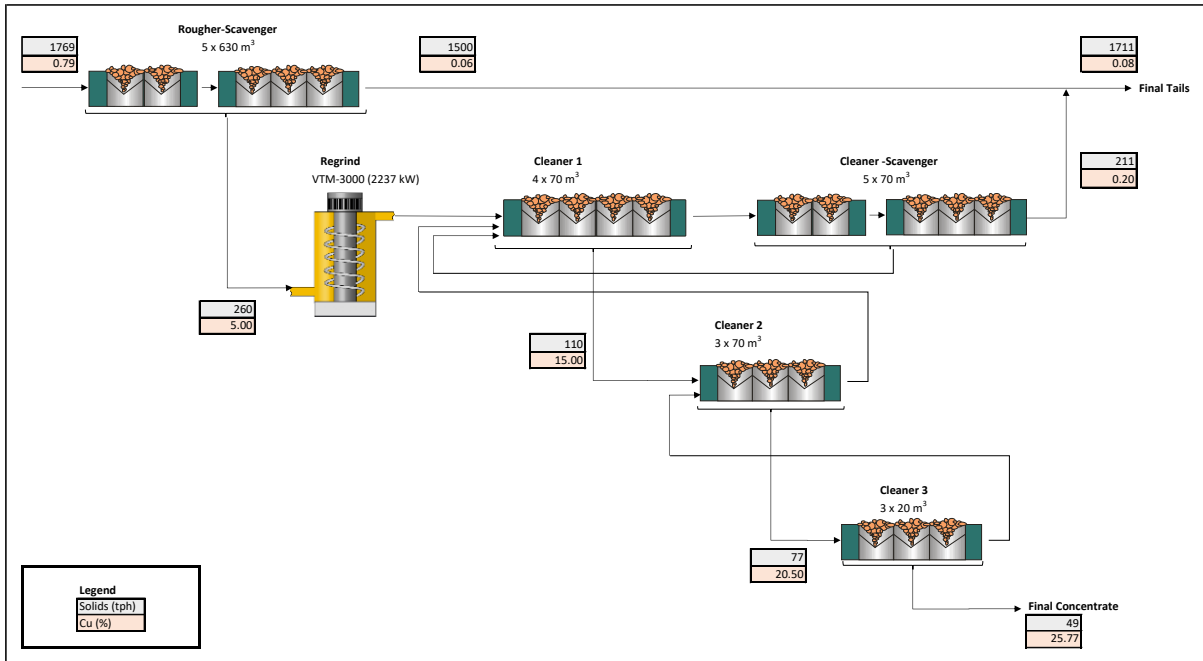


Figure 2: Simplified Flow sheet – Conventional Circuit

The plant layout for the conventional circuit is shown in Figure 3. The layout is based on a flat terrace arrangement with a focus on minimising the step height between successive cells, as well as the final tails sump to keep the building height to a minimum. Cognisance is given to crane access for agitator removal during maintenance.

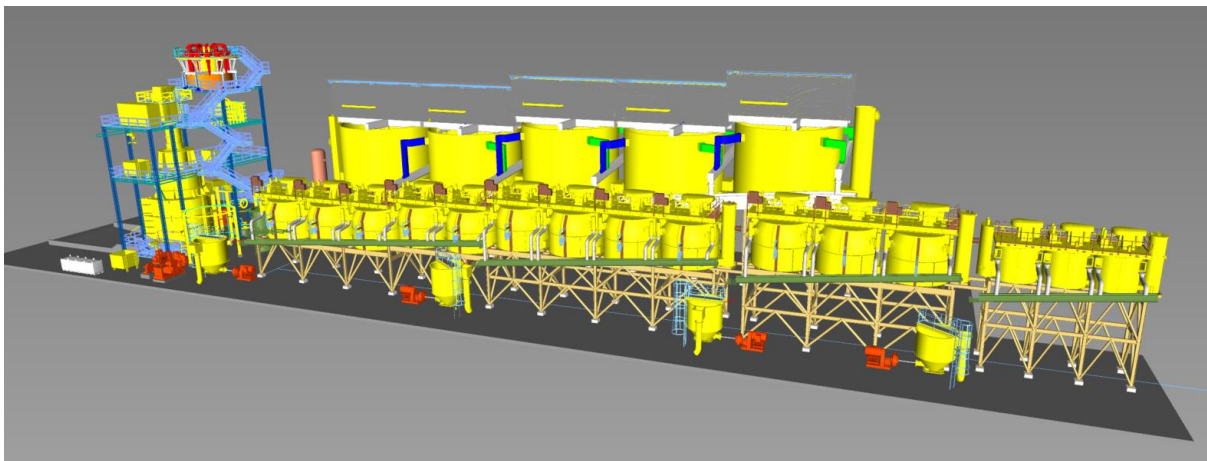


Figure 3: Plant Layout - Conventional Circuit

This plant layout results in the following quantities in terms of concrete and steel:

Table 3: Preliminary Quantities – Conventional Circuit

Quantity	Units	Value
Footprint (L x W x H)	m	120 x 32 x 25
Structural Steel	t	426
Equipment Steel	t	662
Concrete	t	10 391

The power consumption for the conventional circuit option is summarised in Table 4

Table 4: Power Consumption Summary – Conventional Circuit

Area	Units	Conventional Circuit
Flotation	GWh/y	30.1
Regrind Mill	GWh/y	7.7

Jameson Concentrator Design

Head feed is processed in a rougher-scalper Jameson Cell which is operated with a deep froth and high wash water rate to generate a final concentrate grade. Typically, rougher-scalper Jameson Cells can achieve between 60-80% recovery in this duty depending on the liberation of the material. The tails of the rougher-scalper is processed in a scavenger Jameson Cell which is operated at a low froth depth and high air rate without wash water in order to generate a high mass pull and low tailings grade.

The regrind mill operates in open-circuit with a cyclone and is sized as an M7500 primarily due to the high volumetric flow rate. The low specific grinding energy of 7.8 kWh/t means that the mill will only draw 729 kW under nominal conditions and 1131 kW under design mass pull conditions. 5 mm ceramic media is used to reduce the feed from an F_{80} of 75 μm to a P_{80} of 45 μm .

The regrind product to feed a B4500/12 Jameson Cell which operates with a deep froth and high wash water flow rate to scalp out the newly liberated material and produce a final concentrate. The remaining middlings particles in the tailings of the cleaner-scalper are fed to the cleaner-scavenger Jameson Cell. This cell is set up to run aggressively without wash water, with low froth depth and high air rate to drive a high mass pull and low cleaner tails grade. The resulting concentrate is passed to a smaller E2514/3 Jameson Cell, which operates with high froth depth and wash water to produce a concentrate from the middlings material, which can be blended into the final concentrate.

A key feature of the resulting circuit is that each cell has been given only one function in the circuit: either grade-focussed, or recovery-focussed. This means that each cell can be set up with appropriate operating conditions and can make use of the Jameson Cell's tails recycle mechanism to absorb a wide range of feed fluctuations to maintain overall circuit stability despite any fluctuations in feed grade and mass pull.

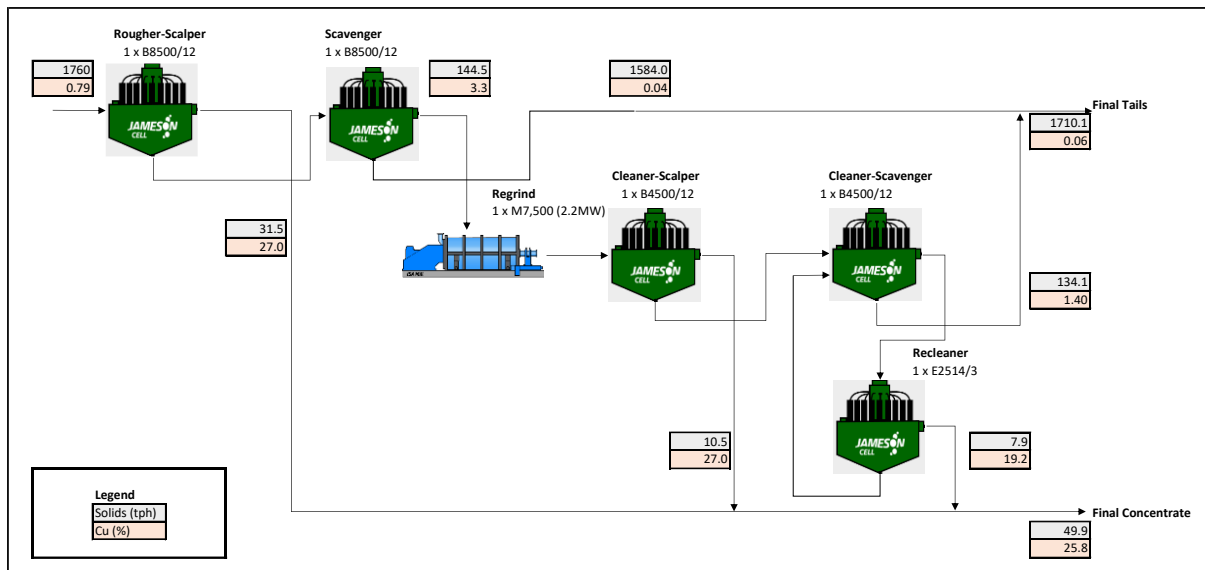


Figure 4 Simplified Flow sheet – Jameson Concentrator

The plant layout for the Jameson Concentrator is shown in Figure 4. Once again, the layout is based on a flat terrace arrangement, where the height of the structure is driven by the feed into the bottom of the Jameson Cell, as well as the height of the tails sumps into which the Jameson Cells discharge. The larger rougher-scavenger Jameson Cells are supported on concrete, whereas the smaller Jameson Cells in the cleaners are supported on a steel structure. Cognisance is given to pump and valve access for maintenance. Unlike conventional cells, the Jameson Cells do not require frequent overhead crane access. Maintenance on the downcomer and slurry lens can be done by hand, while the cells are operating.



Figure 5: Plant Layout - Jameson Concentrator

This plant layout results in the following quantities in terms of concrete and steel.

Table 5: Preliminary Quantities – Jameson Concentrator

Quantity	Units	Value
Footprint (L x W x H)	m	45 x 41 x 18
Structural Steel	t	87
Equipment Steel	t	155
Concrete	t	5679

Due to the fewer equipment in the flow sheet, the Jameson Concentrator required 846 t less steel and 1963 m³ less concrete compared with the equivalent conventional concentrator.

The power consumption for the conventional circuit option is summarised in Table 6.

Table 6: Power Consumption Summary – Jameson Concentrator

Area	Units	Jameson Concentrator
Flotation	GWh/y	18.5
Regrind Mill	GWh/y	5.8

COMPARISON OF GREENHOUSE GAS EMISSIONS

The GHG emissions for both option is compared in Figure 6.

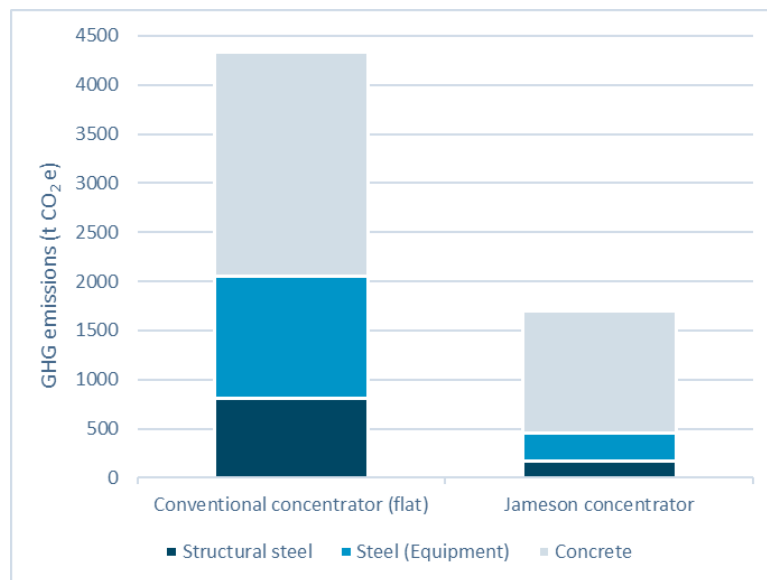


Figure 6: Comparison of Conventional and Jameson Concentrator Construction GHG Emissions

The increase in footprint and structure required in the conventional flotation circuit option resulted in 2.5 times the GHG emissions in the construction phase than the Jameson cell circuit.

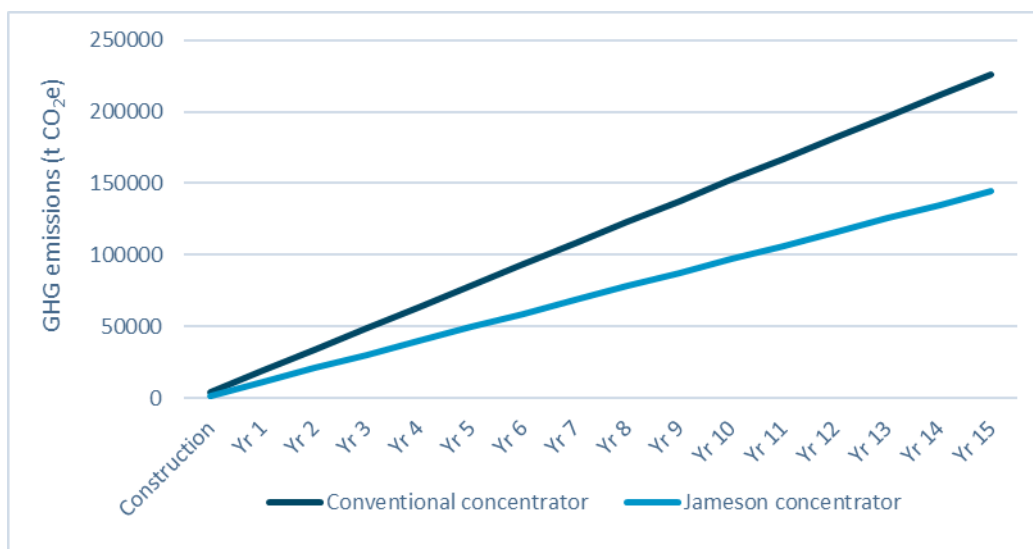


Figure 7: Comparison of Conventional and Jameson Concentrator Total GHG Emissions

The annual Scope 2 emissions, associated with electricity required in the conventional circuit resulted in a 59% increase when compared to the Jameson Cell circuit. This increase was predominantly related to the agitation power required in the tank cells.

Interestingly, operational emissions far outweigh construction emissions by two orders of magnitude. In fact, the plant produces emissions equivalent to the construction emissions every three to four months in the case of a conventional concentrator and every two months for the case of a Jameson Concentrator. This suggests that efforts to reduce GHG emissions should be focussed on reducing operational emissions as a priority.

CONCLUSIONS

A trade-off study between a conventional circuit and a Jameson Concentrator circuit has been conducted to an AACE Class 4 level. The results demonstrate that the Jameson Concentrator approach results in savings in power consumption of 35% which has a significant impact both on operating cost and on GHG emissions during operation of the plant. Due to fewer equipment in the flow sheet, the Jameson Concentrator required 78% less steel and 19% less concrete compared with the equivalent conventional concentrator.

In terms of GHG emissions, the Jameson Concentrator approach resulted in a 61% reduction in emissions during construction and 42% during operations. Interestingly, the GHG emissions over the life of mine far outweighs the emissions savings during construction by two orders of magnitude. This demonstrates that reduction of the total kWh/t processed is critical to reducing the carbon footprint of future metallurgical plants.

REFERENCES

Anderson, C., Csicsovski, G., Stieper G., How the Jameson Concentrator Drives Reduced Energy Consumption and Smaller Footprint. Proc. of 18th International Conference on Mineral Processing and Geometallurgy. Procemin Geomet 2022.

Ballantyne G, Pyle M, Foggatto B, Martin K and Lane G (2023) 'The Impact of Greenhouse Gas Emission Costs on the "True Economics" in Comminution Trade-Off Studies'. *SAG 2023 Conference, Vancouver, Canada*.

ClimeCo LLC, 2023, <https://carbonfund.org/calculation-methods/>, [Retrieved 28/08/2023].

Hammond, G.P. and Jones, C.I., 2008. Embodied energy and carbon in construction

materials. *Proceedings of the Institution of Civil Engineers-Energy*, 161(2), pp.87-98.

Legge, D.C. Müller-Falcke, H., Naucér, C., and Östgren, E., 2021. Creating the zero-carbon mine. *McKinsey & company*. <https://www.McKinsey.com/industries/metals-and-mining/ourinsights/creating-the-zero-carbon-mine> [Retrieved April 23, 2022].

Metz, B., Davidson, O.R., Bosch, P.R., Dave, R. and Meyer, L.A., 2007. Summary for policymakers. *Climate change*.

Northey, S., Haque, N. and Mudd, G., 2013. Using sustainability reporting to assess the environmental footprint of copper mining. *Journal of Cleaner Production*, 40, pp.118-128.

Protocol, G.G., 2011. Corporate value chain (Scope 3) accounting and reporting standard. *World Resources Institute and World Business Council for Sustainable Development, Washington*,

Sykes, C., Brinson, A., Tanudisastro, G., Jimenez, M. and Djohari, J., 2020. Zero emission copper mine of the future. *Zero Emission Copper Mine of the Future*.

The Intersection of Mining and Decarbonisation: Challenges and Opportunities

C Meinke¹, L Jackson², K Erwin³, R Chandramohan⁴

1. Operations Optimisation, Senior Process Consultant Ausenco, 401 9th Ave Suite 1430 Calgary AB , connor.meinke@ausenco.com
2. Operations Optimisation, Process Consultant, Ausenco, 1200 – 1050 West Pender Vancouver Canada, landon.jackson@ausenco.com
3. Operations Optimisation, Global Technical Director, Ausenco, 1200 – 1050 West Pender Vancouver Canada, rajiv.chandramohan@ausenco.com
4. Operations Optimisation, Lead Process Consultant Ausenco, 1200 – 1050 West Pender Vancouver Canada, kevin.erwin@ausenco.com

ABSTRACT

In the face of the climate crisis, a shift to a low-carbon economy is critical in preventing the loss of life and significant economic damage. However, the decarbonisation transition presents unique challenges, primarily concerning the supply and demand of critical minerals essential for technologies like electric vehicles, renewable energy storage, and hydrogen production. Certain “green” technologies require a significant increase in global mineral demand to be implemented even though they are pivotal in the fight against climate change. In particular, the high demand for batteries may stretch resource availability and production to its limits. This paper delves into the extraction constraints and emphasises the potential impacts if the demand for critical mineral resources surpasses the capabilities of the sector.

This paper presents optimisation solutions aimed at curbing the inevitable increase in mineral extraction. The goal is to manage its rate while adhering to supply and demand requirements based on confirmed and accessible mineral resources. The paper proposes the following practical strategies:

- the preferential use of electric bikes over electric cars to lessen the demand for minerals
- prioritising nuclear and hydroelectric power to reduce the dependence on battery-intensive renewable energy sources
- scaling up hydrogen capacity to offer an alternative solution for widespread electrification.

The paper also advocates for policy tools such as carbon taxes and renewable incentives which can play a vital role in reducing carbon production and achieving a balanced economic evaluation of technological alternatives in the field of energy generation.

Canada and Australia can play a leading role in the global shift towards a low-carbon economy. The paper offers strategic recommendations aimed at implementing policies that would effectively decrease the expected demand for minerals, aligned with achieving climate targets. These include enhancing key mining operations, fostering nuclear projects, instituting a comprehensive carbon tax system, expanding natural gas pipeline networks, and initiating partnerships with hydrogen vehicle manufacturers. Despite the complexities inherent in this transition, the paper concludes that with strategic planning and investment, nations like Canada and Australia can lead the global migration towards sustainable energy and transport systems, which will help lower the world's carbon footprint.

INTRODUCTION

The urgency of climate change necessitates a swift transition to a low-carbon economy (IPCC, 2022). This monumental shift involves moving from traditional fossil fuel-based systems towards renewable energy sources and sustainable transportation alternatives. Although such a transition is considered vital in alleviating the detrimental impacts of climate change, it presents significant resource availability and sustainability challenges. A major challenge is the balance of critical minerals supply and demand, essential for manufacturing renewable energy technologies and electric vehicles.

Researchers from various disciplines have explored the predicament of diminishing mineral resources and escalating demand for renewable energy. For instance, Wang et al. (2023) from The Breakthrough Institute meticulously analysed the total metal demand needed for power generation under different temperature mitigation scenarios. Their study underscores a potentially significant surge in the production of certain materials, such as neodymium, fiberglass, dysprosium, solar-grade polysilicon, and tellurium, to fulfil the growing demand for the manufacture of renewable sources of energy. Their research highlights the need for ramping up mineral production and fostering public policies that support mineral resource development for clean technologies. They acknowledge that recycling contributes to the solution but will have limitations in meeting the escalating mineral demand.

Mills (2019) provided an economic perspective on the green transition. Through comparisons of energy outputs from identical investments in natural gas and solar, the author showed that natural gas outperformed solar photovoltaics (PV) cells (used for solar electric panels) by 600%. Mills brought attention to the hidden costs associated with renewable energy, stemming from the need to balance the electrical power grid due to the erratic electrical outputs of power generated using solar PV, thermal, and wind turbine technologies. Mills (2019) illustrated the exorbitant costs associated with battery storage when compared with natural gas and warned of the slowing growth in renewable technologies, stressed the need for the substantial mining rates required for battery materials, and the relatively minor impact of electric vehicles on global petroleum demand. Considering all these challenges, Mills believes that hydrocarbons will remain the world's principal energy source for the foreseeable future.

Michaux's (2021) analysis conducted at the Geological Survey of Finland (GTK), presents an in-depth understanding of the impending metal crisis linked with decarbonisation efforts. It shines a spotlight on the massive volume of metals and minerals required to establish a low-carbon future. Michaux (2021) underlines the magnitude of the task ahead - transforming over 99% of the global vehicle fleets from fossil fuel-based vehicles to Electric Vehicles (EVs) and transitioning about 85% of our power generation from hydrocarbon-based to renewable energy sources.

Adopting a unique bottom-up approach, Michaux's report underscores the physical material requirements for this transition, contrasting the typical top-down method centered mainly around estimated costs and CO₂ footprint metrics (Michaux, 2021). His report evaluates the feasibility of the new global ecosystem and the long timescales involved in mineral extraction and the manufacturing cycles from invention to commercialisation.

Michaux's (2021) comprehensive analysis concluded that a vast number of additional power plants are required to fulfil non-fossil fuel electrical power needs, highlighting the practical limitations of such an expansion. It further explored the requirements of various non-fossil fuel systems as solutions to balance the demand, where each solution showcased clear advantages and disadvantages compared to each other and existing fossil fuels. One significant aspect of Michaux's (2021) report highlights the importance of the material requirements for energy transition (i.e., moving away from fossil fuels), such as the mass of lithium-ion batteries needed for electric vehicles. Michaux's research suggested a potential shortfall in global reserves is imminent to support the quantity of batteries required for the energy transition; emphasising the need to rethink the EV

battery solution to be less mineral-intensive.

Overall, Michaux's (2021) analysis suggests that a significant reduction in societal demand for all resources will be necessary, highlighting that the existing renewable energy sectors and EV technology systems could merely be stepping stones to a different, and more sustainable solution. Michaux's work thus underscores the need for innovative solutions, realistic resource and timeline planning, and a comprehensive understanding of global energy demand and supply.

This paper presents optimised scenarios for decarbonisation that remains within the constraints of the available mineral resources and feasible production expansion timelines. The investigation is guided by the following crucial questions:

1. How much mineral resource is necessary for vehicles (both electric and hydrogen powered), power generation and battery storage in a low-carbon future?
2. What is the availability of these critical minerals based on proven resources and how much does production need to increase by?
3. What government policy decisions reduce total mineral resource demand?

In addition to the detailed analysis and scenarios provided in this paper, an interactive bespoke website is introduced, called Ausenco Energy InSite. This tool allows users to estimate the total metal demand under various circumstances and manipulate the variables discussed in the analysis, creating custom scenarios. This tool serves as an essential resource for stakeholders and decision-makers, offering a hands-on exploration of the complex dynamics between metal demand, decarbonisation efforts, and the potential constraints on resources. Examples of the global metals supply and demand in mining sectors in Canada and Australia are presented to demonstrate the tools effectiveness.

Key inputs to the paper and optimisation development

The analysis assumptions used in this paper are:

- sectors such as building heating, steel manufacturing, cement production, and other industrial systems will successfully achieve decarbonisation.
- common minerals/materials like iron, aluminum, and sand are not considered, even though their production rates are anticipated to rise
- the energy and metal demands from vehicles hinge on the distribution of vehicle types (whether hydrogen, EV, or electric bikes), the metal required per kWh of installed battery capacity/engine size, the distance vehicles travel, and their efficiency on a kWh/km basis, and the weight and kilometers travelled by long-haul vehicles
- energy demands for decarbonising power systems and industry are determined by current emissions, the power necessary to replace industries like steel manufacturing, and the current power distribution
- upon establishing the energy demand, the distribution of renewable energy is selected. This choice guides estimates for the total minerals required for those systems and the battery capacity needed for renewables
- the total metal demand is a composite of the minerals required to build EVs, hydrogen vehicles, power plants, and the battery facilities for the power plants.

Key critical minerals used for EVs, power generation, and batteries

Key minerals used for battery and power generation are shown in Table 1 as percentages of either battery mass or installed power.

Table 1 Basis for mineral demand for batteries and power generation systems.

Metal	Electric ¹ vehicles	Stationary NMC batteries ²	Offshore wind ¹	Onshore wind ¹	Solar PV ¹	Hydroelectric ¹	Nuclear ¹
	kg/kWh battery	kg/kWh battery	t/MW installed	t/MW installed	t/MW installed	t/MW installed	t/MW installed
Copper %	17.9	11.9	51.9	28.5	41.3	100.0	27.9
Nickel %	13.4	2.3	1.6	4.0	-	-	24.6
Manganese %	8.3	0.1	5.1	7.7	-	-	2.8
Cobalt %	4.5	0.6	-	-	-	-	-
Lithium %	3.0	2.5	-	-	-	-	-
Graphite %	22.3	24.0	-	-	-	-	-
Chromium %	-	-	3.4	4.6	-	-	41.5
Zinc %	0.034	-	35.7	54.1	0.4	-	-
Rare Earth Metals %	0.2	-	-	-	-	-	-
Silicon %	-	-	-	-	57.8	-	-
Others %	0.1	-	-	-	0.5	-	1.8
Non-Critical %	30.3	50.1	2.3	1.1	-	-	1.4
1. (IEA, 2022a) 2. (Michaux, 2021)							

Analysis approach and optimiser development

Figure outlines the approach to metal optimisation: blue items represent inputs, green items signify intermediate results, and yellow items indicate the final metal demand. This approach follows the framework outlined in the Key inputs to the paper and optimisation development section. The analysis can be scaled to any level (local, country, global, etc), provided that the necessary information is available utilising the Ausenco Energy InSite website; however, this paper performs the analysis on a global scale.

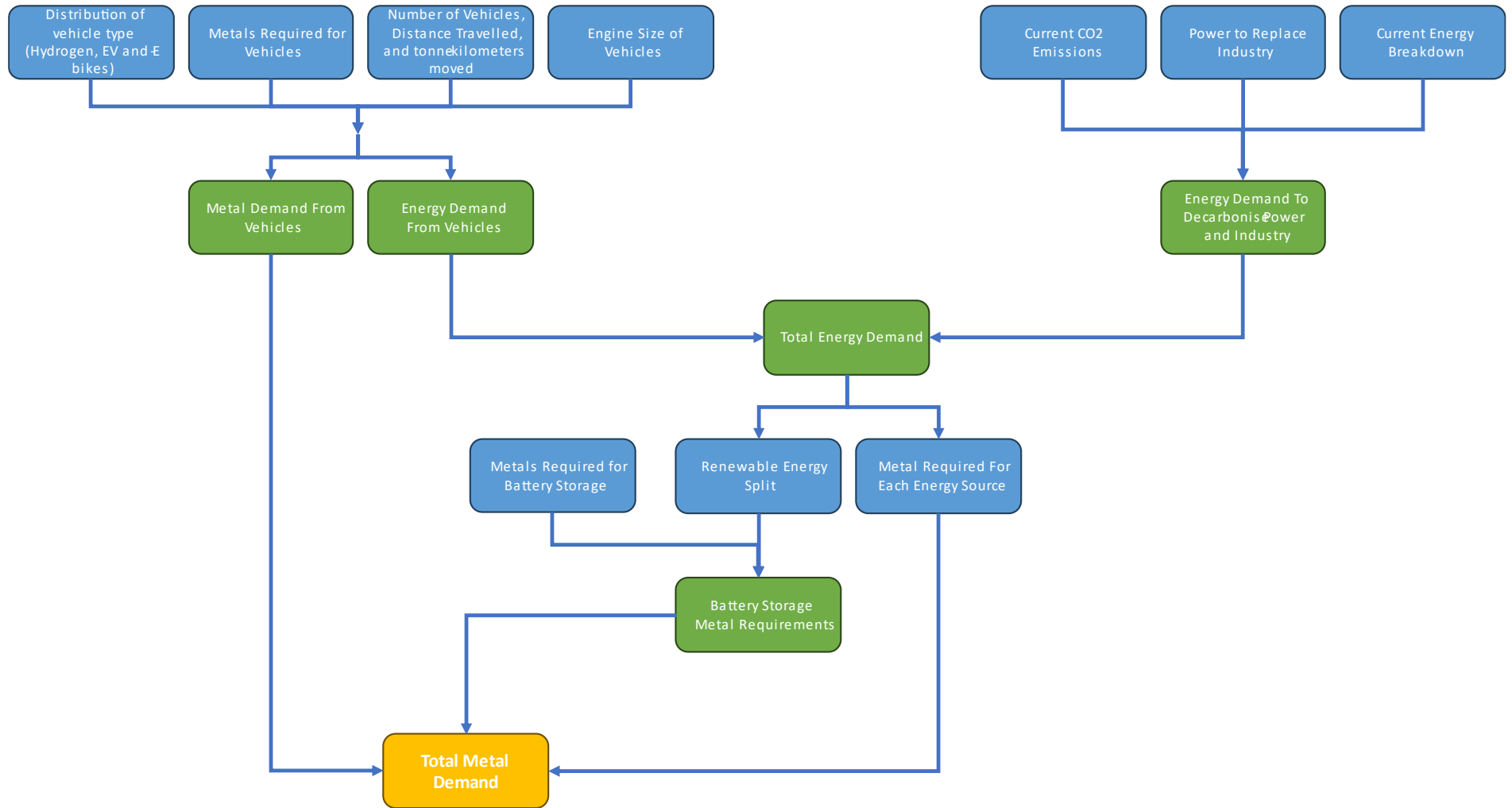


Figure 1 - Optimisation Analysis Flow sheet

ESTABLISHING THE BASELINE

According to the United Nations climate action mandate, the world needs to transition away from non-renewable sources to renewables to meet the 2050 climate action goals. (United Nations, n.d.). Secondary to the climate action goal is whether the mining industry can expand production at the rate required to meet the demand by the year 2050. Current climate models suggest that nearly complete reductions in CO₂ emissions are required by 2035 to restrict global temperature rise to 1.5°C. However, challenges present themselves due to the continually increasing CO₂ emissions (excluding the unusual years of the COVID-19 pandemic) and logistical difficulties associated with altering global systems.

The primary concern revolves around the capability of the mining industry to provide the necessary material swiftly enough to meet the 1.5 °C target, illustrated in Figure 2. The total demand for minerals, discussed in detail in the following sections, will determine the rate at which these materials must be extracted. Several key factors must be considered in the context of decarbonisation:

- the development of most mines takes between 10 to 15 years (from the initial drill hole), to market and raising funds for project development and design, construction and commissioning. (IEA, 2022c)
- power plants typically require up to 3-10 years for installation depending on the technology (from design to construction and commissioning) (IEA, 2022c)
- industrial scale decarbonisation cannot commence until these plants have been established and there is a sufficient supply of materials to sustain them.

Considering these constraints, to achieve the 1.5°C target within the next 12 years (from 2023), virtually all the minerals necessary for decarbonisation would need to be extracted immediately after the mining development time. The feasibility of this will depend on the total demand for minerals and the necessary increase in production. If meeting this demand is deemed impractical or impossible, the 2.0°C case allows a more gradual increase in production, in line with several countries' 2050 net-zero targets. In this scenario, a 27-year period is assumed (2023 - 2050). However, taking into account the optimistic assumption of a ten-year time frame for project development, the actual time frame to produce the necessary minerals decreases to 17-years shown in Figure 2.

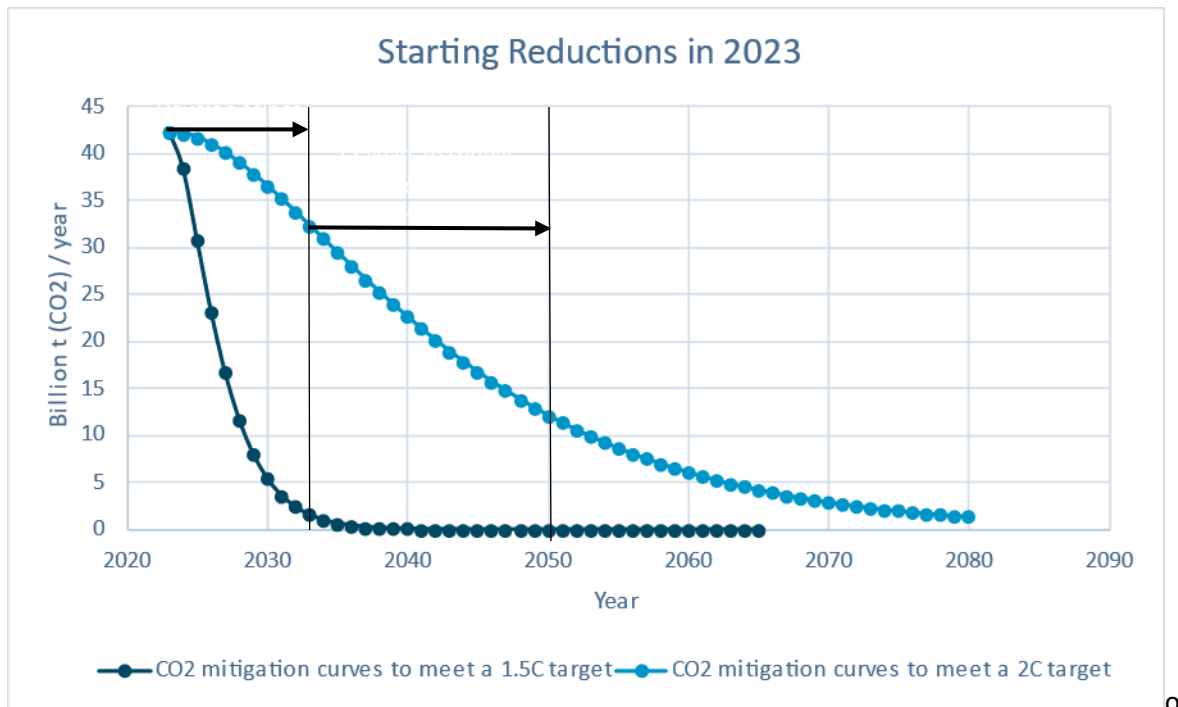


Figure 2 - Allowable CO₂ production per year to achieve 1.5 °C and 2.0 °C targets (Our World in Data, 2019)

The Current Status - Mineral Production, Resources and Reserves

Table 2 (US Geological Survey, 2023) illustrates the current mineral production rates (kt/y), reserves (kt), and resources (kt) of the most critical minerals for decarbonisation.

As illustrated in Table 2 it becomes clear that at the current rates of production, reserves of key metals like copper and nickel may be depleted in around 40 and 30 years, respectively. However, it's important to note that new reserves and resources continue to be discovered and added, influenced significantly by the value of the commodity. Thus, the critical factor is not solely the size of the total reserve or resource but the production rate and the agility with which it can be ramped up to meet the evolving demands.

Table 2 Current metals and minerals production (kt/y), world reserves (kt) and world resource (kt)

Minerals	Current production (kt/y)	Reserve (kt)	Resource (kt)	Reserve time left (y)
Copper	22 000	890 000	2 960 000	40
Nickel	3300	100 000	200 000	30
Manganese	20 100	1 700 000	11 300 000	84
Cobalt	190	8300	16 700	43
Chromite	42 200	560 000	11 440 000	13
Molybdenum	255	12 000	8000	47
Zinc	13 000	210 000	1 690 000	16
Rare earths	300	130 000		433
Silicon	9150	Large	Large	N/A
Germanium	0.1	2.5	2.5	36
Lithium	130	26 000	63 000	200
Graphite	1300	330 000	470 000	253
Uranium	59	8070	15 647	136
Lead	4550	85 000	1 915 000	18
Vanadium	105	5382	57 618	51
Zirconium	1400	68 000		48
Platinum	0.19	70	15	368
Palladium	0.21	70	15	333

The Current Status – GHGe by Industry

Figure 3 represents the annual greenhouse gas emissions (GHG) estimated at 50 Gt CO_{2eq} in 2019 (Ritchie, et al., 2020) and surging to as high as 58 Gt CO_{2eq} by 2022 (Kharas, et al., 2022). 72% of emissions come from electricity generation. This analysis does not directly consider agriculture, as its connection with the minerals industry is not significant. Nonetheless, it's vital to consider that additional power capacity would be required if high-power systems like lab-grown meat become commercially viable, or if desalination plants are adopted widely. Hence, this paper primarily concentrates on strategies to mitigate the other 40.6 Gt CO_{2eq}.

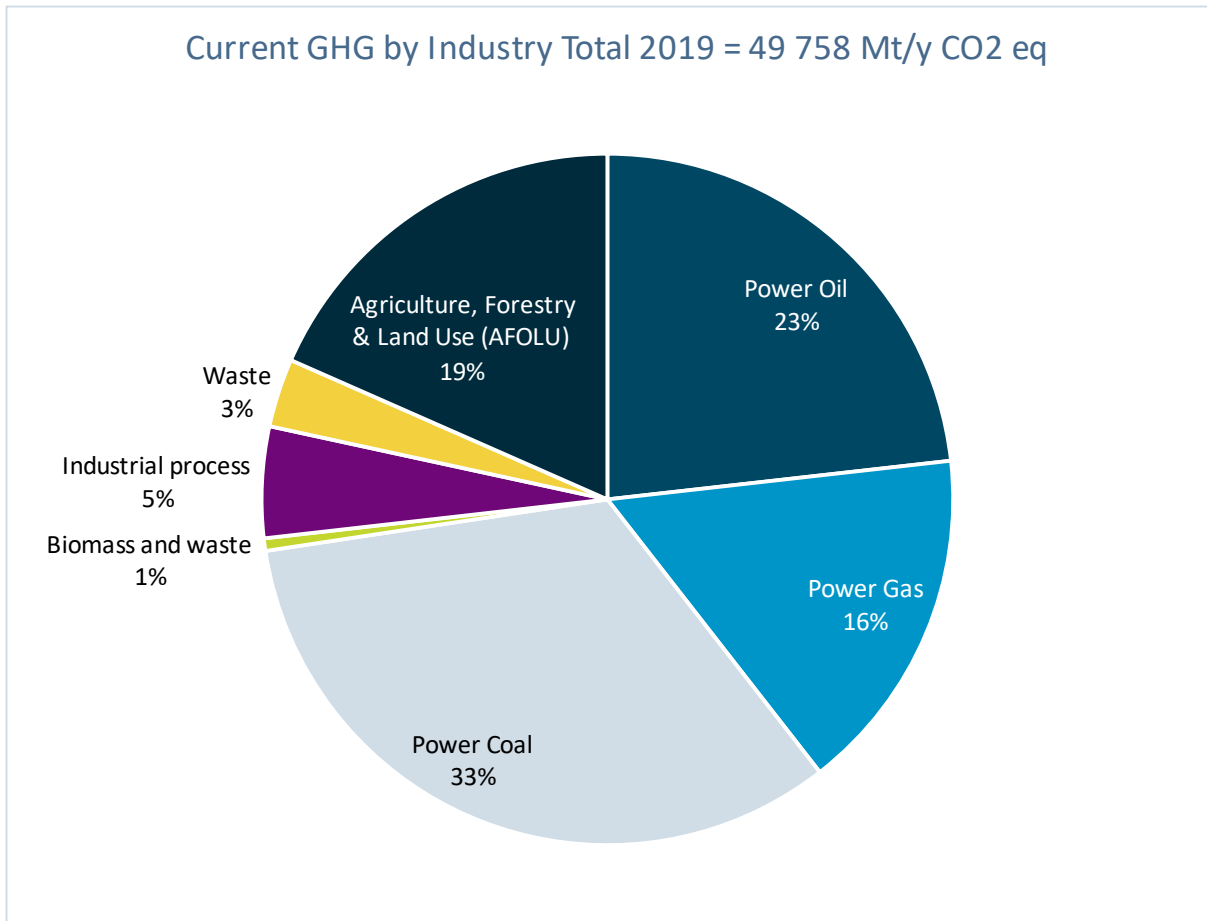


Figure 3 - Green House Gas Emissions by industry showing % make up and Mt CO_{2eq}/y produced by each industry.

The Current Status – Global Electrical Power Generation

Global electric power is predominantly generated by carbon-intensive industries. The largest step towards achieving decarbonisation would be to replace the 17 400 TWh/y of carbon-based energy. The current global breakdown of electrical power generation is shown in Figure 4.

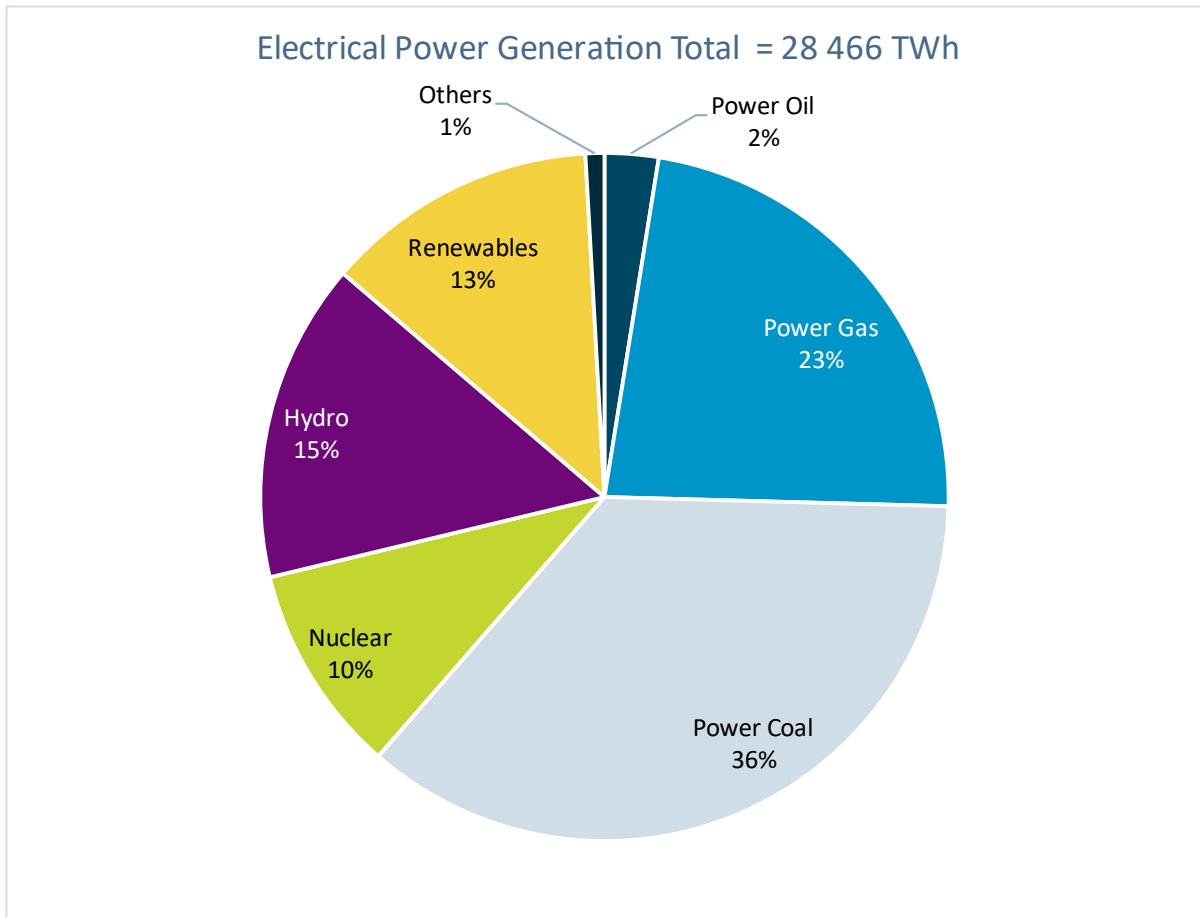


Figure 4 - Global electricity generation by source

ARE THERE ENOUGH MINERALS AND ENERGY SUPPLY TO SUPPORT NET ZERO TARGETS BY 2050?

Michaux (2021) completed an in-depth analysis of the total metal demand required for decarbonisation and electrification. The analysis determined that the total mineral requirements to decarbonise the global economy is dictated by:

1. The calculation of the number of transportation vehicles that must be replaced and the associated increase in grid power demand from both electric and hydrogen-powered vehicles.
2. The need to replace existing carbon-based power technologies, such as coal-burning plants.
3. The expansion of power storage systems, contingent on power storage duration due to solar and wind intermittency, and the materials that can be used.

Electric Vehicles (EVs) excel in short-range travel applications due to their high energy efficiency, lower emissions, and regenerative braking, which recovers a lot of energy in stop-and-go traffic. Electric motors perform better for short distance propulsion in passenger vehicles, grid-connected buses, light-duty vehicles, motorcycles, and bicycles. The limited range of EVs, due to current battery technology constraints, and the need for frequent recharging, make them less suited for long-distance and heavy-duty applications.

Hydrogen vehicles can either be fuel cell electric drive (FCEV) or hydrogen internal combustion engines (H₂ICE). This study assumes the use of FCEV to show the impact on PGM demand. They are more suitable for heavy transportation than EVs because of hydrogen's high energy density per unit

of weight (15 kWh/kg vs 0.23 kWh/kg (Michaux, 2021)). Hydrogen functions better in applications such as Class 8 heavy commercial vehicles (HCV) trucks, long-distance rail, and maritime shipping. Hydrogen, due to its high energy density per unit of weight, can deliver the necessary power for these applications without significantly adding to the vehicle's weight. The refueling process for hydrogen vehicles, which is similar to conventional refueling, along with its long-range capabilities, make it an attractive solution for these heavy-duty applications.

Battery (200-300 Wh/kg) technology would need to continue improving at its current exponential rate until 2043 to match the current drive energy density of hydrogen (15 000 Wh/kg) or 2035 for gasoline (3100 Wh/kg). Battery density does not necessarily have to match hydrogen to be competitive in shorter ranges, but hydrogen's energy density advantage becomes more pronounced in long-haul transportation where the lower energy density of batteries significantly impacts weight and volume considerations.

How Many Electrical Vehicles Do We Require – Light Vehicles

Table 3 summarises the global electrical vehicle strain on battery production and energy systems (Michaux, 2021). It provides a stepwise estimate of the additional grid power required, resulting in an additional 6310 TWh of new power being required by the grid and an additional 642 Mt of batteries needing to be produced.

Table 3 Summation of worldwide electrical vehicle strain on battery production and energy systems (Michaux, 2021)¹

Vehicle	kWh / vehicle (installed battery)	Million vehicles required	Efficiency (kWh/km)	Tkm travelled	TWh perfect efficiency	Efficiency [Grid to Drive] (%) ²	TWh	Mt – Li-Ion batteries ³
Passenger Vehicles	68 ⁴	695	0.19	5.4	1030	67	1530	206
Buses & Delivery Trucks	227	29	1.32	0.80	1060	67	1580	29
Commercial Vans, Light Trucks	153	601	0.31	7.9	2130	67	3180	402
Motorcycles	22 ⁵	62	0.09	0.16	15	67	22	6
Total	-	-	-	14.3	4230	-	6310	642
<ol style="list-style-type: none"> 1. Based on Simon Michaux estimates – unless otherwise referenced 2. Includes drive losses and power line losses 3. 0.23 kWh/kg battery 4. (Electric Vehicle Database, 2023) 5. (Toll, 2019) 								

The impact of EVs on power and mineral demand can be significantly reduced through efficient use of transport. For example, converting passenger vehicles to buses would reduce the grid demand by ~1250 TWh due to higher passenger efficiency (50 passengers per vehicle vs 1.5 for passenger vehicles). Further, if internal combustion engines (ICE) vehicles were instead replaced with E-bikes, the total weight of batteries required would reduce from 206 Mt to 2.0 Mt, a substantial reduction, though this would necessitate significant social change and city design adjustments.

Transitioning to Hydrogen Fueled Vehicles – Heavy Transport

Hydrogen vehicles have some notable drawbacks when utilised as transportation systems

- most hydrogen is derived from steam methane reform (SMR), which releases CO₂
- low-carbon methods, such as electrolysis, are energy inefficient, requiring ~50 kWh/kg for separation from water and an additional 2.5 kWh/kg to compress to 700 bar for fuel cell use, plus additional power for transportation bringing to total to nearly 58 kWh/kg. (Michaux, 2021)
- dependence on several rare earth metals and platinum (~0.26 g/kW (Heraeus, n.d.) based on installed motor size)
- hydrogen's atomic size poses significant challenges in terms of transportation, as it can cause embrittlement of pipelines and tanks not specially designed for it. This is due to hydrogen's ability to seep between molecules, weakening their bonds. Repurposing existing natural gas pipelines for hydrogen transport is therefore not straightforward.

Table 4 provides an estimate of the total power required to produce 200 Mt/y of hydrogen to power long haul industries resulting in an additional power load of 11 600 TWh.

Table 4 Total power and hydrogen needed per year to transition long distance vehicles from diesel/fossil fuel to hydrogen¹

Vehicle / Industry	k Vehicles	Billion tonne-kilometers (Tkm)	TWh/Billion units	TWh ⁴	Mt – H ₂
Class 8 HCV Trucks	29 000	-	0.26	7500	130
Rail Transport ²	110	9 400	0.11	1070	18
Maritime Shipping ³	120	72 100	0.041	2980	52
Total Production	29 230	81 500	-	11 600	200

1. Based on Simon Michaux estimates - GTK unless otherwise stated
 2. Includes all kinds of rail (freight and passenger)
 3. Includes all maritime shipping (small to very large vessels)
 4. Includes inefficiency of creating H₂ by electrolysis and compression into tanks – total power required by H₂ production (58 kWh/kg) including 10% losses

Table 5 outlines the total tonnes of PGMs needed in long-haul vehicles to catalyse the hydrogen reaction in fuel cells. Both tables are reproductions of Simon Michaux's work (Michaux, 2021). Class 8 HCV trucks require the most hydrogen power and metal production followed by maritime shipping then rail transport.

Table 5 Tonnes of PGMs required¹

Vehicle / Industry	kWh / Fuel Cell ²	Mt – H ₂	t PGM ^{3,4}
Class 8 HCV Trucks	370	130	2800
Rail Transport ²	2400	18	70
Maritime Shipping ³	40 500	52	1230
Total Production	-	200	4100

1. Based on Simon Michaux estimates – GTK unless otherwise stated
2. Platinum in fuel cell driven by power required by engine
3. Small amount compared to vehicles of platinum, palladium and rare earth metals are required to produce the hydrogen needed
4. Platinum can be replaced with palladium in fuel cells

If all light vehicles transitioned to hydrogen, total PGM demand to build the first generation of vehicles would increase from 4.1 kt to 26 kt, and addition grid power demand would also rise due to hydrogens production inefficiency from electrolysis (green hydrogen) from 6 300 TWh to 15 400 TWh excluding heavy transportation. However, some of the metal demand could be offset by recycling catalytic converters in ICE vehicles, which typically contain 5-14 g of platinum and palladium per vehicle. This could replace 9-19 kt (Waste Advantage, 2021) of the required metal.

How Much Power Generation is Required?

The overall power demand to decarbonise the economy is estimated in Figure 5. This figure shows the cumulative increase in global energy demand, indicating a total grid power of 48 460 TWh. However, this need is partially met by existing renewable and nuclear energy, leaving an additional 37 730 TWh of power that needs to be generated. Notably, hydrogen vehicles require nearly twice as much power as electric ones due to the substantial energy expenditure necessary for the production of green hydrogen via electrolysis. The replacement of non-renewable power is a sizable task, whereas industrial processes demand relatively less power. The current annual power requirements stand at approximately 2 800 TWh (BP, 2022) of which renewables and nuclear energy contribute 10 700 TWh.

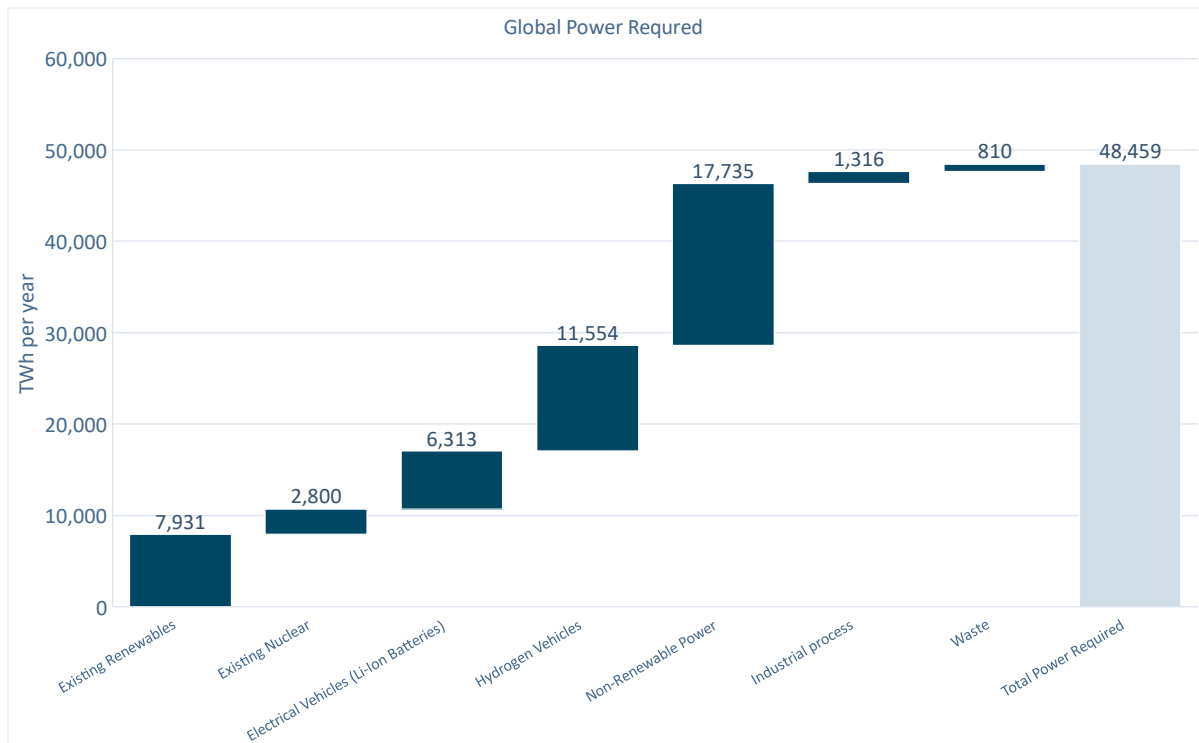


Figure 5 - Total power required to replace carbon emitting sources.

The balance of energy between solar, wind, hydroelectric (hydro), and nuclear sources impacts the total mineral demand. Solar and wind energy generation lead to the highest mineral demands, followed by nuclear, and then hydro. However, there are not substantial differences in mineral demand between these power systems. Key minerals required for renewables include zinc, copper, and silicon, while nuclear power primarily uses copper, chromium, and nickel. Hydro, despite having the lowest metal demand mainly for copper, cannot be solely relied upon due to geographical constraints and significant environmental impact.

Importantly, the suitability of these renewable power sources is highly region-specific. For instance, the efficacy of solar power significantly depends on the region's sunlight exposure, wind energy depends on wind patterns, and hydro power depends on the availability of water bodies and mountains. Conversely, non-renewable power sources are less region-specific but contribute considerably to greenhouse gas emissions. Therefore, a thoughtful combination of these resources, based on regional specifics, will be crucial in achieving the decarbonisation targets. The currently targeted energy split to meet global energy demand is presented in Figure 6.

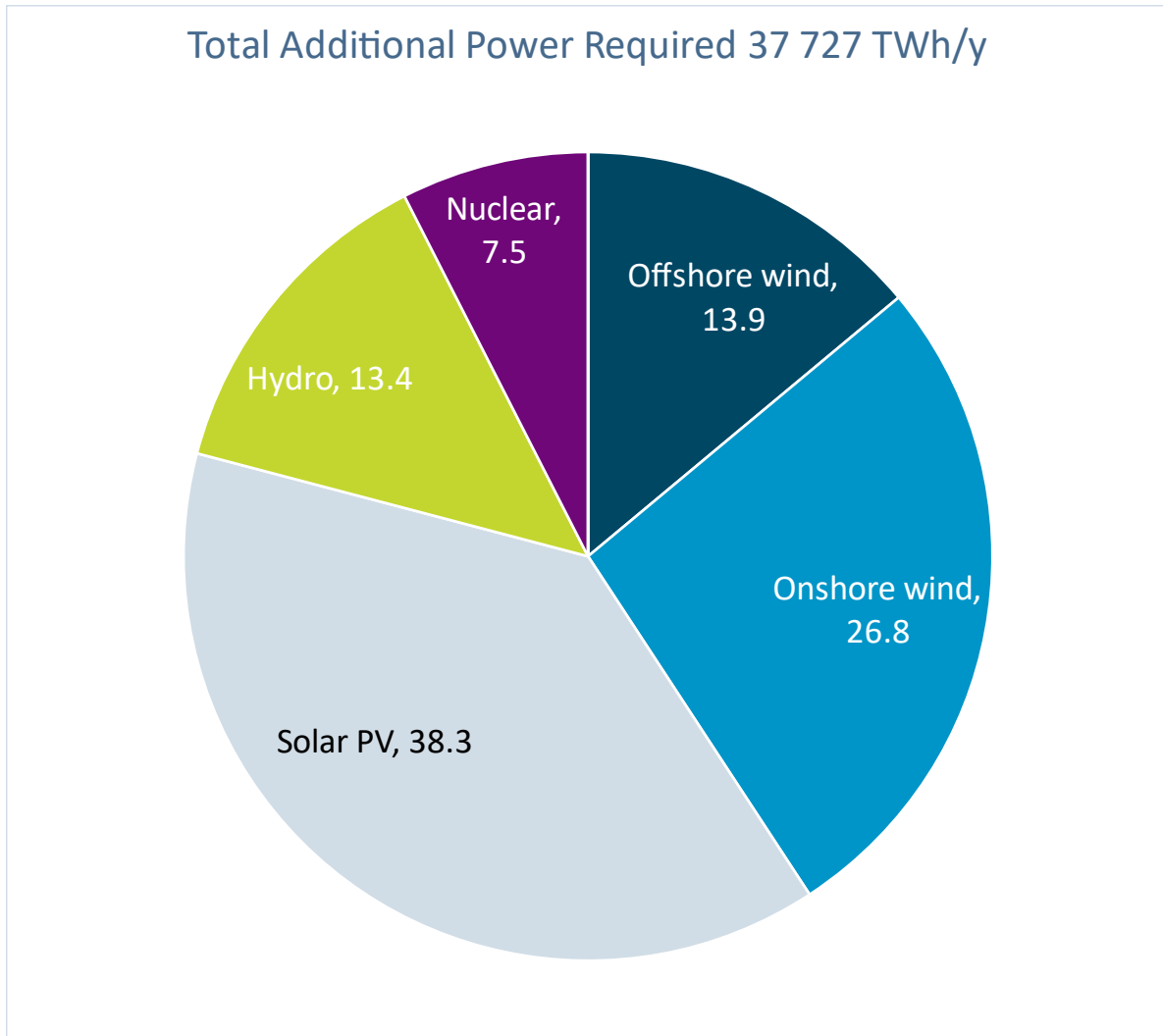


Figure 6 - Breakdown of New Power Requirements (Michaux, 2021)

How can we store energy?

To adequately install renewable energies like solar and wind a certain amount of surge capacity is required to compensate for the intermittency of their power output. Currently that fluctuation is handled by natural gas facilities. Storing the energy in some form of battery system will be required to minimise the use of fossil fuels.

The duration of battery storage required to support renewable energy is a contentious subject, with estimates varying significantly. The lowest estimate is 2 days, while the highest is up to three months (or 84 days (Michaux, 2021)). These estimates largely depend on the location of the power plant and the environmental factors that effect it.

The number of battery facilities were estimated using storage capacities of two, 28, and 84 days. Assuming that only the highest capacity battery facilities were being installed, which is equivalent to Moss Landing, which can store 2 330 MWh. With 85% storage efficiency considered, the intermittent renewable demand is 35 kTWh/y, which is then divided by the total storage capacity time. The results for NMC [Nickel Manganese Cobalt], lead, and salt batteries are shown in Table 6. Other battery technologies are possible such as pumped storage and hydrogen but are currently impractical as a global solution due to the geographic requirement of pumped storage and the inefficiency of green hydrogen production.

Table 6 Battery metal weight comparison

Capacity (days)	TWh	Number of facilities	NMC battery 270 Wh/kg (kt battery) ¹	Lead battery 50 Wh/kg (kt battery) ¹	Salt battery 160 Wh/kg (kt battery) ²
2	193	82 955	715 873	3 865 717	1 208 036
28	2706	1 161 374	10 022 228	54 120 033	16 912 510
84	8118	3 484 122	30 066 685	162 360 100	50 737 531
1. (May, et al., 2018) 2. (Wood Mackenzie, 2023)					

Although NMC batteries have the higher energy density, the battery storage facility weight doesn't hinder facility development, unlike electric cars which operate more efficiently with higher density batteries as they need to carry the weight of the car and the battery. Therefore, NMC batteries are the worst choice in this case, as they are most reliant on critical minerals. Lead batteries, predominantly dependent on lead, would exhaust most of the world lead reserves to build enough facilities (Table 2). So, for storage battery systems, salt batteries, primarily relying on sodium and aluminium, are the preferred options due to the abundance of these materials. However, even with just two days of capacity 82 950 battery facilities would have to be built which might prove prohibitive regardless of mineral requirements. Many facilities are still being built with NMC batteries instead of salt, such as the Oneida Energy Storage plant in Canada (Leggate, 2023) and the Liddell Battery plant in Australia, (Parkinson, 2022).

Other technologies will likely be necessary instead of batteries, for example natural gas plants with carbon capture, or small nuclear reactors that can quickly ramp up and down. Improved energy conversion for hydrogen storage will also be needed. Pump storage systems could be adopted in some areas but not all.

Establishing the Base case minerals required to achieve NetZero targets

Whether there is enough metal to transition to a renewable economy depends largely on the storage capacity required for renewables. Based on current reserves and resources, there is sufficient metal to decarbonise the economy assuming only two days of NMC storage is required as shown in Table 7. However, time is a limiting factor. Based on practical timelines, it is unlikely that the mining industry can provide this much material to limit global warming to 1.5°C. The results in Table 7 provide the "base case" scenario and the world current metal demand trajectory.

Table 7 shows the contributions of each sector to the total metal demand. Electrical batteries and NMC battery storage account for nearly 90% of all the decarbonising mineral demands. This would require significant increases in mining production for several critical minerals. Existing cobalt resources and reserves would be expended, copper production would need to increase by 80%, equivalent to 18 more Escondida Mines (Escondida represents ~4.5% of world copper production) or 180 Highland Valley Copper Mines. To fuel the battery demand lithium and graphite production need to ramp up significantly. Note that uranium is shown in kt/y as it is continuously expended while the other minerals are shown as totals to build the necessary systems.

Table 7 Base Case Metal Demand

Metals	Electrical vehicles	Hydrogen vehicles	Power plants	NMC battery storage 2 day capacity 193 TWh	Additional required mineral total	Current production	Increased production cases		Reserve + Resource	
	kt	kt	kt	kt	kt	kt/y	1.5 °C (% Increase)	2.0 °C (% Increase)	kt	% required
Copper	115 099	-	42 535	144 022	301 656	22 000	1371%	81%	3 850 000	8%
Nickel	86 324	-	2208	28 399	116 932	3300	3543%	208%	300 000	39%
Manganese	53 006	-	3913	-	56 919	20 100	283%	17%	13 000 000	0%
Cobalt	28 775	-	-	6878	35 653	190	18 765%	1104%	25 000	143%
Chromite ore	0	-	3163	-	3 163	42 200	7%	0%	12 000 000	0%
Zinc	216	-	27 325	-	27 542	13 000	212%	12%	1 900 000	1%
Rare earths	1082	-	403	-	1484	405	366%	22%	-	-
Silicon	0	-	26 528	-	26 528	9150	290%	17%	-	-
Lithium	19 255	-	-	30 451	49 706	130	38 235%	2249%	89 000	56%
Graphite	143 441	-	-	290 657	434 098	1300	33 392%	1964%	800 000	54%
Uranium (kt/y)	0	-	157	-	157	59	265%	16%	23 718	1%
Lead	0	-	-	-	0	4550	0%	0%	2 000 000	0%
Others	671	-	223	-	894	1655	54%	3%	88 000	1%
PGM	0	4.1	-	-	4	0.4	1009%	59%	170	2%
Total	447 870	4.1	106 455	500 407	1 054 736	118 040	-	-	34 075 888	-
Total %	42.5%	0.0%	10.1%	47.4%	-	-	-	-	-	-

CANADA VS AUSTRALIA MINERAL PRODUCTION

Table 8 shows the comparison of Canada and Australia's mineral reserves to meet total decarbonisation demand. Of the over 300 000 kt of copper that will be needed, Canada's reserves (7600 kt) only represent 2.7% while Australia's large copper deposits could provide nearly 35% of the copper required. Canadian deposits represent 12.5 y of production while Australia's represent 23.8 y. Canadian uranium however is very high grade and low cost making it more competitive in the near term (IAEA; NEA, 2020).

Table 8 Canadian and Australian Mineral Contribution to Decarbonisation

Metals	Minerals for decarbonisation (US Geological Survey, 2023) (IAEA; NEA, 2020)		
	Global requirement (kt)	Canada (% reserves)	Australia (% reserves)
Copper	249 716	3.0	38.8
Nickel	106 690	2.1	19.7
Manganese	56 919	-	474
Cobalt	33 172	0.7	4.5
Chromite ore	3 163	-	-
Zinc	27 542	6.5	4 234
Rare earths	1 484	55.9	283
Silicon	26 528	-	-
Lithium	38 724	2.4	16.0
Graphite	329 276	-	-
Uranium (kt/y)	157	1 254	2 384
Lead	0	-	-
Others	894	-	-
PGM	4.1	-	-

Although there are sufficient reserves for all the critical minerals, the significant time to develop each mine, and the number of new mines required to meet the metal demand is daunting. So, reducing the total demand should be prioritised, along with increasing mining production and exploration, particularly in any country that wants to be a larger player in the decarbonisation economy, such as Canada or Australia.

For example, Canada's energy consumption comes from three primary sources, natural gas, refined petroleum products (RPPs) and natural gas liquids (NGLs), which together account for approximately 60% of Canada's energy demand share (Canada Energy Regulator, 2021). Canada's large reserves of natural gas and oil, 10% of world's reserves, contribute to the heavy focus on fossil fuel consumption and storage but also provides opportunity to transition to a net zero economy (IEA, 2015). Coal remains below 5% of the energy consumption with hydro-electric, nuclear and other renewable

sources making up the remainder of the balance. Achieving Net Zero CO₂ emissions in Canada would require a hydrogen and nuclear transition in the short term. Canada's large uranium deposits would act as a steady supply of energy with steam methane reforming (SMR) with carbon capture and storage (CCS) responding to disturbances in energy demand. This stable base load of power would allow the development of additional hydro and other renewable energy sources such as 'green hydrogen' as well as adequate storage facilities in the form of hydro pumping and hydrogen storage.

Australia's economy has an even larger reliance on fossil fuel energy than Canada. Nearly 40% of Australia's energy consumption is from coal and 56% is from oil and gas (Geoscience Australia, 2023). The large coal deposits, 14% of total world reserves, and accessibility to oil and gas imports are major contributors to this composition of energy supply (Worldometer, 2023). A Net Zero CO₂ energy transition in Australia would require utilisation of its vast uranium supply and development of nuclear energy generation while phasing out its reliance on coal. Otherwise, Australia should target other renewable opportunities such as hydro, wind and solar. Storage of such energy would require significant investment in salt battery storage or hydro-pumping, which Australia has numerous low-cost potential sites (Blakers, et al., 2020).

OPTIMISATION CASES

There are opportunities to reduce mineral demand from the base case to make achieving Net Zero CO₂ by 2050 a more feasible goal. To achieve such a feat, the projected demand for battery minerals must be reduced as they represent 90% of forecast decarbonisation mineral demand. Meanwhile, power plants represent the other 10% and hydrogen powered vehicles will strain PGM supply. As many authors have shown before, meeting power plant demand is feasible through mostly renewables when only considering the requirements of the power plants themselves (Wang, et al., 2023).

1. The battery requirement for electrical vehicles, which represent 42.5% of projected metal demand, can be reduced by:
 - a. Improving battery energy density
 - b. Reducing the number of vehicles being produced
 - c. Producing different kinds of vehicles
2. Hydrogen vehicles require a small but significant metal group (PGMs). Replacing electrical with hydrogen vehicles would significantly reduce projected demand for all other critical minerals while substantially increasing demand on PGMs.
3. It is argued above that battery facilities are unfeasible due to sheer number and minerals required. Therefore reducing the share of energy produced from renewables in favour of nuclear or hydro-electric will reduce the projected battery demand.
 - a. Producing salt-based storage facilities instead of NMC storage facilities would reduce forecast total critical metal demand by 47.4%

To optimise the analysis, several constraints were developed:

- 1) Nuclear power must have at least 40 years of operation
- 2) Hydropower depends on location and cannot exceed 15% of global power demand.
- 3) Battery capacity was assumed to be fulfilled by sodium-based systems.

Actions to Reduce Metal Demand

Four main actions were investigated to reduce metal demand and the results of each action are shown cumulatively in Table 9. It is assumed that NMC batteries are not pursued as a long-term strategy and are instead replaced by salt batteries or other technologies.

Action 1 – Maximise Hydroelectric and Nuclear Power

Increasing the share of nuclear and hydroelectric (hydro) power reduces the total mineral use for power plants by 6%. This is reduced significantly further if NMC batteries are used for renewable storage. The main advantage of focusing on nuclear and hydro power is the reduced requirement for battery storage and a steadier energy flow to the grid.

Action 2 – Minimise electric cars

There are many ways to reduce the number of electric vehicles used. One potential solution is to instead produce electric bikes (E-bikes), as they require 100x less metal to produce compared with EVs, while providing a similar outcome. As EVs can be less effective for long distance travel, E-bikes are a simpler and cheaper alternative that significantly reduces battery metal for a similar outcome, but with much shorter manufacturing times. Most EV owners also possess an internal combustion vehicle to compensate for these shortcomings (Davis, 2021). This redundancy poses significant problems, not only due to the metal demand required to manufacture an EV but also because the CO₂ emissions produced during the construction of an EV are higher than those generated by ICE vehicles (IEA, 2022b).

This outcome would require a rethinking of most North American style cities to be built more densely and reduce city sprawl to reduce car use overall. For rapid decarbonisation, adoption of E-bikes would be the fastest solution to reduce mineral demand. Shifting from personal EV vehicles to E-bikes reduces the total metal requirement by 25.6%.

Action 3 – Replace electric vehicles with hydrogen powered vehicles

Replacing the remaining electric vehicles such as buses and light-duty trucks with hydrogen powered vehicles has the greatest impact on reducing mineral demand, with a decrease of 50.3%. But it significantly increases the demand on PGMs and electrical power. Hydrogen powered vehicles could replace personal EVs but, like EVs, they also incur long lead times and high production costs. Further, hydrogen power requires a significant increase in power supply to produce green hydrogen on a large scale. Since there is not a current substantial hydrogen economy there would be an even higher lead time to development. However still from a mineral reduction perspective, pursuing a hydrogen-based economy rather than EVs produces the best outcomes for reducing overall mineral demand.

Action 4 – Utilise blue hydrogen

Hydrogen can be produced by exploiting natural gas and carbon capture technology. Hydrogen can be produced through numerous ways incurring different CO₂ emissions and different costs, including: (IRENA, 2020) (S&P Global, 2023)

1. grey hydrogen is produced by steam methane reform (SMR) or coal gasification and has the highest carbon footprint (~1.3 \$US/kg hydrogen)
2. blue hydrogen is produced like grey but includes carbon capture and storage (CCS), reducing atmospheric CO₂ emissions to 5-15% those of grey hydrogen (~2.0 \$US/kg hydrogen)
3. turquoise hydrogen involves the pyrolysis of natural gas, producing solid carbon black that is easier to store than CO₂(~6.0 \$US/kg hydrogen)
4. green hydrogen is produced through renewable means, like electrolysis, biogas, and anaerobic digestion. (~14 \$US/kg hydrogen)

Steam methane reform without carbon capture requires 97% less power input than SMR with CCS (blue) and electrolysis (green). (ZAPANTIS, 2021)

Even with carbon capture there are environmental concerns with continuing to use natural gas due to fugitive gas emissions, energy reductions, and because SMR-CCS methodologies don't fully eliminate total emissions. Some experts (Howarth & Jacobson, 2021) argue against blue hydrogen and advocate for the immediate transition to green hydrogen, which minimises CO₂ emissions. However, green hydrogen requires much more electrical power and therefore more minerals, while natural gas conversion technologies are already proven and widely available. Therefore, from a mineral minimisation perspective a mixture of blue and green hydrogen would be the best solution in the short term.

Longer term solutions should apply increasing carbon taxes on blue, and turquoise hydrogen to help green hydrogen be more competitive and encourage better carbon capture techniques, though acknowledging that green hydrogen will increase power and mineral demand, resulting in other environmental impacts and higher non-CO₂ emissions.

Therefore Action 4 to utilise blue hydrogen, while not perfectly carbon neutral, would further reduce projected total mineral requirements by an additional 14.0%, which results in a total reduction in the projected mineral demand, due to a decreased power demand and a near total reduction in battery demand for vehicles.

Actions 1 to 4

The combined implementation of actions 1-4 provides the best outcome in terms of minimising mineral production but not necessarily for reducing CO₂ when action 4 (blue hydrogen) is included. There is a substantial power increase when replacing electric vehicles with green hydrogen (10 000 TWh/y), while using blue and turquoise hydrogen production methods reduces the power consumption from the base case by 17 000 TWh/y and 27 000 TWh/y from action 3.

Table 9 Mineral Minimisation Cases – (Salt Battery Storage)

Metals	Base case	Action 1: minimising power plant minerals	Action 2: E-bikes	Action 3: replace electric vehicles with H ₂	Action 4: blue / turquoise - H ₂ production
Copper	157 634	143 452	107 011	39 242	7 911
Nickel	88 533	89 646	62 316	3 777	2 469
Manganese	56 919	55 575	38 793	3 568	692
Cobalt	28 775	28 775	19 665	0	0
Chromite ore	3163	5269	5269	5890	4104
Zinc	27 542	16 562	16 494	23 418	3069
Rare earths	1 484	1 323	980	345	45
Silicon	26 528	16 014	16 014	22 872	3141
Lithium	19 255	19 255	13 159	0	0
Graphite	143 441	143 441	98 027	0	0
Uranium	157	474	474	474	474
Lead	0	0	0	0	0
Others	894	804	592	191	25
PGM	4.1	4.1	4.1	26	26
Total	554 329	520 595	378 798	99 803	21 956
% Change	-	6.1%	25.6%	50.3%	14.0%
% Cumulative Change	-	6.1%	31.7%	82.0%	96.0%
TWh/y	37 727	37 727	36 219	46 814	20 669
kt metal / TWh	14.7	13.8	10.5	2.1	1.1

Table 9 shows the mineral minimisation cases, illustrating that minimising power plant minerals, substituting E-bikes for cars, replacing electric vehicles with H₂, and leveraging blue/turquoise H₂ production dramatically decrease the overall mineral requirements. In the optimised scenario, nuclear power would produce nearly 70% of the power, with hydro at 15% and renewables accounting for the rest.

POLICY

The outcome of the present analysis, as well as its potential practical application, will inevitably be shaped by policy decisions. Even though the optimisation models may appear straightforward, their actual implementation poses significant challenges. This section elaborates on several such challenges and suggests potential solutions, emphasising the importance of expanding the mineral extraction to ensure the successful deployment of low-carbon technologies.

The Massachusetts Institute of Technology (MIT) has developed a software tool referred to as "EN-ROADS" (MIT Management Sustainability Initiative, 2023) that allows the simulation of various policy decisions affect on climate change. This tool provides an estimate of their effectiveness if such policies were enacted in a specific year (2023 for this example). If no action is taken, climate change is projected to increase global temperatures by 3.3°C by the year 2100. The minimum temperature

increase allowed by these models is 1.2°C by 2100, which represents the warming that has already occurred.

The implementation of a carbon tax emerges as the single most effective solution for reducing the projected increase in global temperatures, with a potential reduction of 0.8°C at a rate of \$250/t-CO₂. This substantial impact is primarily attributed to the straightforward way the tax affects all sectors of industry, creating incentives to reduce carbon emissions by the most efficient means available (MIT, 2022). Additional measures such as further taxing carbon-based power sources and subsidising renewable energy and nuclear power could result in a combined decrease of 0.7°C compared with the “do nothing” case. Enhancing efficiency in buildings and industry, as well as further electrification, could contribute to a further reduction of 0.5°C. Reductions in methane production and other heat-trapping gases could further lower temperatures by 0.4°C, which is a significant consideration if the use of blue and turquoise hydrogen is pursued.

A critical factor to consider is the trade-off between cost, the reduction of CO₂ emissions and mineral removal. For instance, a low-cost electric car is priced around 40 000 CAD, while a good electric bike costs approximately 3500 CAD. In circumstances where an electric bike can practically replace an electric car—and by extension, an internal combustion engine (ICE) car—it could do so at a tenth of the cost and with a hundredfold reduction in resource use, resulting in a larger CO₂ reduction per unit. Therefore, it can be much more effective from a mineral and CO₂ perspective to occasionally use an ICE vehicle rather than produce a new EV, given that shorter distances are better suited to electric bikes while longer journeys are more efficiently undertaken by hydrogen vehicles, leaving little justification for personal electric vehicles.

Several mineral reducing policies and comments are provided below:

Adoption of nuclear energy and expansion of hydroelectric

- adopting nuclear energy has been a struggle due to significant social resistance, and permitting for nuclear energy along with waste deposition has been challenging
- Canada and Australia could be leaders in the nuclear industry by exploiting their uranium resources. Canada has the highest-grade deposits worldwide in the Athabasca Basin. Australia has lower grade deposit but twice the reserves of Canada.
- many of the cost overrun and installation time concerns could be mitigated by collaborating with South Korean and Japanese commissioning teams that consistently install plants in three to five years (Jhoo, 2016).
- expand hydroelectric utilisation where applicable.

Minimise car use, and encourage public transport, genuine ride sharing, bicycle use and E-bike use.

- various measures that can encourage bike ridership include wide cycle-safe lanes, clear signage, segregation from motor vehicles where possible, use of high-quality material for cycle lanes, and so on. (Hull & O’Holleran, 2014)
- cities in Canada and Australia were designed with cars in mind, making it difficult to choose other modes of transportation. Developing public infrastructure that competes with cars in regard to safety and speed could substantially minimise mineral demand
- the decision to drive a car instead of transit or biking is largely due to the lack of good

infrastructure, driving is done by default because it's fastest, providing safer and faster options than driving induces demand for other transportation systems. (Buehler, et al., 2016)

Action 3: Hydrogen vehicles for long distances

- hydrogen vehicles are still in their early stages, and a wide hydrogen distribution system does not yet exist, expanding production is very important to reducing metal demand.
- incentivising companies to build blue and turquoise hydrogen facilities and working with car manufacturers to create low-cost hydrogen powered vehicles can encourage their use.

Action 4: Blue and turquoise hydrogen economies

- incentivising the production of blue and turquoise hydrogen would speed up the adoption of hydrogen as a gasoline replacement more effectively than electric vehicles or waiting for green hydrogen to meet scale demand.

CONCLUSIONS AND RECOMMENDED PATH FORWARD

The path towards a low-carbon economy is a formidable challenge, made even more complex by the anticipated resource constraints. The data clearly indicates that batteries, particularly for electrical vehicles and renewable storage, are the primary limiting factors to decarbonisation due to their significant impact on global mineral demand.

Reducing CO₂ emissions from energy production has the most substantial effect on global temperatures. Enacting robust policies such as applying high taxes and subsidies in this category could potentially result in a 1.5°C reduction from the predicted levels without intervention. However, it's worth noting that power generation only accounts for 10% of the total minerals required for decarbonisation.

Conversely, the reduction of battery use in electric vehicles and renewable energy storage could mitigate up to 90% of the mineral demand associated with decarbonisation. By concentrating on non-battery-intensive solutions, such as nuclear and hydroelectric power, we can notably diminish the demand for battery storage. Incorporating salt-based batteries further reduces the mineral requirements of storage systems. Likewise, a shift towards hydrogen-powered vehicles for long-distance transportation and E-bikes for short commutes can result in the lowest possible metal requirement for a decarbonised economy.

To implement the current base case globally would require the following:

- 37 700 TWh of power added to the grid (a 133% increase)
- 9000 additional power plants of the largest size, necessitating 106 Mt of critical minerals
- replacement of small duty vehicles with electric vehicles, requiring 448 Mt of critical minerals
- replacement of transportation vehicles with hydrogen-powered vehicles, necessitating 4.1 Mt of PGMs and 200 Mt/y of hydrogen
- substantial increases in critical mining development over the next decade to provide enough metals by 2050
- 82 000 large-scale battery facilities, based on the two-day storage scenario, installed by 2050

Despite all these measures, limiting warming to 1.5°C by 2035 seems unachievable and even keeping it within 2.0°C by 2050 is highly challenging.

While this base case scenario poses significant hurdles, the path towards carbon reduction will greatly depend on the strategies chosen. This analysis highlights the critical need to reduce mineral

demand as a primary strategy for addressing these challenges.

Encouragingly, transitioning to electric bikes instead of electric cars would result in a 25% reduction in global metal demand. Further, by prioritising nuclear and hydroelectric power, battery demand in renewables can be decreased substantially. Meanwhile, drastically expanding hydrogen capacity can result in over a 50% reduction in mineral demand, given its reliance on PGMs.

Canada and Australia are well-positioned to play a leading role in this low-carbon transition. Key strategic actions should include:

- expanding mining operations and exploration for critical metals such as copper, zinc, nickel, uranium, and PGMs
- developing more nuclear projects to replace existing coal and natural gas power plants, while exploiting vast uranium resources
- establishing a comprehensive carbon taxing structure to incentivise blue and turquoise hydrogen production and encourage a shift towards green hydrogen production through carbon taxes
- expanding natural gas pipeline network in place like Alberta and British Columbia to facilitate the rapid scale-up of hydrogen production capacity
- collaborating with manufacturers of hydrogen-powered vehicles to stimulate production and make hydrogen vehicles competitive alternatives to ICE vehicles.

These steps, although not exhaustive, are critical starting points for this complex and nuanced transition. Achieving a sustainable, low-carbon economy will necessitate ongoing innovation, policy adaptation, and international cooperation. Yet, with strategic planning and investment, Canada and Australia have the potential to emerge as leaders in the global shift towards sustainable energy and transportation systems.

ACKNOWLEDGEMENTS

Acknowledgement to Adrienne Leung and Majurran Vimalan for their contribution to development of the optimisation website. Acknowledgement to Grant Ballantyne for his review of the paper.

REFERENCES

- Argonne National Laboratory, 2010. *Life-Cycle Analysis Results of Geothermal Systems in Comparison of Other Power Systems*, s.l.: Center for Transportation Research.
- Blakers, A., Stocks, M. & Lu, B., 2020. *Australian electricity options: pumped hydro energy storage*, s.l.: Australian National University.
- BP, 2022. *Statistical Review of World Energy*. [Online]
Available at: <https://www.bp.com/en/global/corporate/energy-economics/statistical-review-of-world-energy.html>
[Accessed 08 01 2023].
- Buehler, R., Götschi, T. & Winters, M., 2016. *Moving toward active transportation: how policies can encourage walking and bicycling*, s.l.: University of Zurich.
- Canada Energy Regulator, 2021. *Canada's Energy Futures 2021*, s.l.: Government of Canada.
- Davis, L., 2021. *Energy Institute At HAAS*. [Online]
Available at: <https://energyathaas.wordpress.com/2021/09/20/three-facts-about-evs-and-multi-vehicle-households/>
[Accessed 13 06 2023].
- Electric Vehicle Database, 2023. *Useable battery capacity of full electric vehicles*. [Online]
Available at: <https://ev-database.org/cheatsheet/useable-battery-capacity-electric-car>
[Accessed 15 05 2023].
- Geoscience Australia, 2023. *Australia's Energy Production, Consumption and Exports*, s.l.: Australian Government.

- Heraeus, n.d. *PGM Market Analysis*. [Online]
Available at:
https://www.heraeus.com/media/media/hpm/doc_hpm/precious_metal_update/en_6/20181031_PGM_Market_Analysis.pdf
[Accessed 18 03 2023].
- Howarth, R. & Jacobson, M., 2021. How green is blue hydrogen?. *Energy Science & Engineering*, 9(10), pp. 1676-1687.
- Hull, A. & O'Holleran, C., 2014. Bicycle infrastructure: can good design encourage cycling?. *Urban, Planning and Transport Research*, 2(1), pp. 369-406.
- IAEA; NEA, 2020. *Uranium 2020, Resources, Production and Demand*, s.l.: OECD.
- IEA, 2015. *Oil and Gas Reserves*, s.l.: s.n.
- IEA, 2022a. *Minerals used in clean energy technologies compared to other power generation sources*. [Online]
Available at: <https://www.iea.org/data-and-statistics/charts/minerals-used-in-clean-energy-technologies-compared-to-other-power-generation-sources>
[Accessed 15 04 2023].
- IEA, 2022b. *In the transition to clean energy, critical minerals bring new challenges to energy security*. [Online]
Available at: <https://www.iea.org/reports/the-role-of-critical-minerals-in-clean-energy-transitions/executive-summary>
[Accessed 02 05 2023].
- IEA, 2022c. *The Role of Critical Minerals in Clean Energy Transition*, s.l.: World Energy Outlook Special Report.
- IPCC, 2022. *IPCC Sixth Assessment Report*, s.l.: IPCC.
- IRENA, 2020. *Green Hydrogen: A guide to policy making*, Abu Dhabi: International Renewable Energy Agency.
- Jhoo, D., 2016. *South Korea is second-fastest nuclear plant-building country*. [Online]
Available at: <https://www.scmp.com/news/asia/article/2027347/south-korea-second-fastest-nuclear-plant-building-country>
[Accessed 05 05 2023].
- Kharas, H. et al., 2022. *Tracking emissions by country and sector*. [Online]
Available at: [https://www.brookings.edu/blog/future-development/2022/11/29/tracking-emissions-by-country-and-sector/#:~:text=Global%20greenhouse%20gas%20emissions%20\(GHG,reachin%2062%20GT%20by%202030.](https://www.brookings.edu/blog/future-development/2022/11/29/tracking-emissions-by-country-and-sector/#:~:text=Global%20greenhouse%20gas%20emissions%20(GHG,reachin%2062%20GT%20by%202030.)
[Accessed 19 02 2023].
- Leggate, J., 2023. *ENR: Canada's Largest Battery Storage Facility Planned in Ontario*. [Online]
Available at: <https://www.enr.com/articles/56480-canadas-largest-battery-storage-facility-planned-in-ontario#:~:text=A%20major%20battery%20storage%20project%20in%20Canada%2C%20said,Oneid a%20Energy%20Storage%20site%20in%20Haldimand%20County%2C%20Ontario.>
[Accessed 27 June 2023].
- May, G., Davidson, A. & Monahov, B., 2018. Lead batteries for utility energy storage: A review. *Journal of Energy Storage*, pp. 145-157.
- Michaux, S., 2021. *Assessment of the Extra Capacity Required of Alternative Energy Electrical Power Systems to Completely Replace Fossil Fuels*, s.l.: Geological Survey of Finland.
- Mills, M., 2019. *THE "NEW ENERGY ECONOMY": AN EXERCISE IN MAGICAL THINKING*, s.l.: Manhattan Institute.
- Ministry of Energy, 2021. *Alberta Hydrogen Roadmap*, s.l.: Government of Alberta.
- MIT Management Sustainability Initiative, 2023. *Climate Interactive*. [Online]
Available at: <https://en-roads.climateinteractive.org/scenario.html?v=23.6.1>
[Accessed 12 06 2023].
- MIT, 2022. *Carbon Pricing*. [Online]
Available at: <https://climate.mit.edu/explainers/carbon-pricing>
[Accessed 25 05 2023].
- Our World in Data, 2019. *CO2 reduction needed to keep global temperature rise below 1.5 C*.

[Online]

Available at: <https://ourworldindata.org/grapher/co2-mitigation-15c?time=2000..2100>

[Accessed 15 01 2023].

Parkinson, G., 2022. *Renew Economy: AGL gets green light for 2GWh big battery at Liddell coal plant*. [Online]

Available at: <https://reneweconomy.com.au/agl-gets-green-light-for-2gwh-battery-at-liddell/>

[Accessed 19 March 2023].

Ritchie, H., Roser, M. & Rosado, P., 2020. *CO₂ and Greenhouse Gas Emissions*. [Online]

Available at: <https://ourworldindata.org/co2-and-greenhouse-gas-emissions>

[Accessed 12 03 2023].

S&P Global, 2023. *Cold Decemeber boosts hydrogen production costs, as market price indications emerge*. [Online]

Available at: <https://www.spglobal.com/commodityinsights/en/market-insights/latest-news/energy-transition/011723-cold-december-boosts-hydrogen-production-costs-as-market-price-indications-emerge#:~:text=Hydrogen%20production%20via%20steam%20methane,December%202022%20at>

[Accessed 12 02 2023].

Stubbles, J., 2000. *Energy Use in the US Steel Industry: An Historical Perspective and Future Opportunities*, Washington, DC: US Department of Energy.

Toll, M., 2019. *Electrek*. [Online]

Available at: <https://electrek.co/2019/11/05/new-2020-energica-electric-motorcycle-more-battery/>

[Accessed 03 06 2023].

United Nations, n.d. *For a livable climate: Net-zero commitments must be backed by credible action*.

[Online]

Available at: <https://www.un.org/en/climatechange/net-zero-coalition>

[Accessed 15 06 2023].

US Geological Survey, 2023. *Mineral Commodity Summaries 2023*, Virginia: USGS.

Wang, S. et al., 2023. Future demand for electricity generation materials under different climate mitigation scenarios. *Joule*, 7(2), pp. 309-332.

Waste Advantage, 2021. *How to Recycle a Catalytic Converter*. [Online]

Available at: <https://wasteadvantagemag.com/how-to-recycle-a-catalytic-converter/#:~:text=Although%20the%20quantities%20vary%20by,%2C%201%2D2%20grams%20rhodium>

[Accessed 16 05 2023].

Wood Mackenzie, 2023. *Sodium-ion update: A make-or-break year for the battery market disruptor*.

[Online]

Available at: <http://www.woodmac.com>

[Accessed 05 02 2023].

Worldometer, 2023. *Australia Coal*. [Online]

Available at: <https://www.worldometers.info/coal/australia-coal/>

[Accessed 28 June 2023].

ZAPANTIS, A., 2021. *BLUE HYDROGEN*, s.l.: Global CCS Institue.

One Plant's Trash is Another Plant's Treasure; a Synergistic Approach to Novel Uses for Tailings Streams

R O'Donnell¹, J Begelhole²

1. MAusIMM, Senior Project Metallurgist, Glencore Zinc
2. MAusIMM, Senior Project Metallurgist, Glencore Mt Isa Mines

ABSTRACT

The Mount Isa Mines (MIM) copper concentrator has been supplying the on-site copper smelter with silica flux for decades. The silica-rich stream is sourced from the tails of the flotation circuit which would otherwise be directed to one of the backfill plants, or the tailings dam. This synergistic approach to the use of tailings not only provides the smelter with low-cost flux material but also allows for an increase in copper recovery by reusing tailings.

The production of silica flux from tails began in the 1990s and the process has gone through several iterations over time and different concentrator streams have been used as flux sources. Changes in ore mineralogy as well as smelter requirements have driven various modifications and upgrades of this circuit, intending to produce the highest quality silica flux possible. The success of the silica circuit is highly dependent on the silica grade of the ore and in recent years this has declined to the extent that the silica circuit was no longer a viable source of flux.

In 2020 the silica circuit was upgraded to include a reverse flotation stage to further increase the upgrade of silica in the tails. However, consistently low flux quality drove the search for a new source of silica to meet smelter demand. Tailings from a new ore type, Black Rock Cave (BRC), were found to be a suitable source of flux and modifications to the silica circuit were made to utilize this stream.

This paper reviews the history of the circuit operation as well as the novel approaches that have been taken to produce a high-quality product from a waste stream and how these changes impact downstream operations.

INTRODUCTION

Mount Isa Mines is one of the longest-running mining operations in Australia and currently operates multiple mines, process plants and smelters to produce copper, lead and zinc products. There are two processing plants on site: copper and lead-zinc. This paper will focus on the former, and the synergies that lie between the on-site copper concentrator and the copper smelter.

Copper has been processed on site since the 1940s, with many changes in the operation since this time. In the 1960s the on-site Black Rock Open Cut was developed to process the highly weathered, clay rich, oxide copper ore. Due to processing difficulties this deposit was shortly abandoned until 2020 when sub-level caving commenced. Since the 60s, most of the feed to the copper processing stream has originated from two on-site copper underground mines and processed through on-site concentrators. The current copper concentrator configuration has been running since 1973 and has historically been the main feed source for the on-site copper smelter. The commissioning of the copper ISASMELT™ in the 1990s and the development of the Ernest Henry Mine, brought about significant changes in the requirements for copper production, including an increase in silica flux.

Mount Isa Mines is located 900 km inland from Townsville and due to its remoteness, is self-sufficient in many aspects of its operations. Where possible, consumables are minimized if alternatives can be found on-site. Examples of this include the use of fly ash and lead slag as a partial cement replacement in the backfill, as well as an integrated process water system that encompasses the use of mine water, surface water as well as thickener overflows and water reclaimed from the tailings dam.

Background

The use of the ISASMELT for copper production began at MIM in the late 1980s, after the technology was originally developed on-site for lead production in partnership with the CSIRO. The ISASMELT is used in the primary smelting stage at the MIM copper smelter. The furnace has a very quick reaction time, with much of the smelting occurring in the gas phase above the bath. At the feed port, the flux (silica) and concentrates are introduced into the furnace and oxygen-enriched air and fuel are injected down the lance. The concentrates, flux, oxygen, and fuel, react above the bath to produce matte and slag. The matte contains the copper, and the slag is comprised of the non-valuable elements such as iron and silica.

Silica is highly important in the smelting process as it is needed to create the fayalite slag which removes iron and other elements from the concentrates. Silica flux also lowers the melting point of the slag, which means less energy is required for the process and it reduces the risk of solidifying in the furnace. It also lowers the density of the slag, which allows for better separation of the slag and matte in the next stage of the smelting process, in turn reducing copper losses.

River sand, or mined silica, is conventionally used for flux and the higher the purity of the flux product, the less additional energy needs to be used to melt it due to the lower volume. Contaminants in flux can also have other deleterious effects on the smelting and downstream processes. For example, magnesia (MgO) can increase slag viscosity, resulting in increased copper losses due to poor settling of the matte and slag phases. Due to the remoteness of the MIM copper smelter, as well as the size of the operation, importing river sand or mining silica to use as flux is a cost-intensive exercise. For these reasons, an alternative source of silica flux was investigated.

The onsite copper concentrator predominantly processes ore from the Mount Isa copper mines, Enterprise and X41, which consist of chalcopyrite, hosted within silica-dolomite altered and variably brecciated Urquhart shales. In the 1990s, the feed to the copper concentrator typically contained 3.5% copper and 60-70% silica. Consequently, the tailings of the copper concentrator are rich in silica, and it was proposed that these could be used as a source of flux for the smelter.

Since the commissioning of the ISASMELT, there have been several iterations of the silica circuit depending on the smelter's requirements and the feed coming into the concentrator. As the silica was sourced from concentrator tails streams, the quality of the flux product was directly proportional to the amount of silica in the ore being processed at the time and as such, did not always result in a consistent high-grade flux product. The silica flux grade requirements from the smelter have varied over the years, but the goal has always been to produce the cleanest product possible, ideally with a silica grade of over 80%. Based on historical mineralogy, it was found that the coarse size fractions of the scavenger tails stream (>100 µm) were the highest in silica and for the most part, this was used as the basis for flux supply to the smelter.

The silica flux produced by the concentrator has always been blended into the concentrate before filtration, a method termed "pre-fluxing". Due to the relative ease of mixing slurries compared to dry products, the silica would be well dispersed throughout the concentrate, creating a homogenous product. The pre-fluxed concentrate is produced in a semi-batch process whereby the silica is dosed into agitated concentrate stock tanks after thickening, before filtration. The flux dosage varies depending on the silica grade of both the concentrate, and the flux, as well as the fluxing target set by the smelter. The target varies based on the concentrates being blended at the time and the use of pre-flux allows for additional silica to be dosed into the "own-mine" concentrate to account for deficits in third-party concentrates. This results in the MIM pre-fluxed concentrate having a silica content of anywhere from 14% to 25%. Finally, trim silica is added to the dry final blend concentrate to allow the smelter a tighter control of the flux content of the product entering the furnace.

The use of a recycled stream for flux has many benefits, but also some drawbacks. Besides cost, the main benefit of this circuit is reducing the volume of tailings reporting to the tailings storage facility,

as well as a small increase in recovery of copper units. The production of pre-flux silica accounts for over two million tonne reduction in the overall final tails volume over its 30-year life. Despite the removal of the coarse size fraction by the silica system, there is no significant impact on the thickening and deposition of the tails, due to the relatively small reduction in final tails volume. Another benefit of using a tailings stream for flux production is that the particle size of the flux is much finer than what would be obtained from river sand or a crushed product, which is generally measured in millimetres compared to microns. This finer particle size allows for a better distribution of silica through the concentrate, as well as a quicker melting time due to the smaller particle size.

The drawbacks of the silica circuit are related to the reduction of grade control compared to buying a flux product. Not only is more flux required when a lower grade product is created, thus increasing the volume, and lowering the overall copper content of the concentrate, but the other diluents present can often cause great issues in the furnace chemistry. The primary example of this is MgO (contained within talc and dolomite) which results in a more viscous slag, requiring higher temperatures which consequently shorten the brick life of the furnace. Talc or dolomite entrainment into the flux is the largest hurdle the circuit must overcome and has led to many changes to operating practices and circuit configuration over the years.

The Silica Circuit History

The silica circuit has been in operation at the MIM copper concentrator for the last 30 years. Although it has gone through many iterations in this time, the operating principle has always been the same: to recover the highest-grade silica stream in the plant. This usually entails the recovery of the coarse size fraction of a tailings stream as silica is hard relative to the other minerals present in the ore, resulting in a coarser grind size. Removing the fines has the added benefit of rejecting the low grade (and MgO containing) fines. In the early 1990s, the initial requirements of the silica circuit were: to produce a flux grade of greater than 85% silica and less than 2.6% MgO, at a rate of 60,000 tonnes per annum.

The first silica circuit was used during the commissioning of the copper ISASMELT furnace in 1990. This circuit comprised of a cyclone to remove the fine portion of the scavenger tails, and a set of pilot scale flotation cells to remove any remaining floatable material (including sulphides and naturally floating non-sulphide gangue like talc). Only xanthate was used as a collector and methyl isobutyl carbinol (MIBC) as a frother. The tails of the reverse flotation were directed straight to the final concentrate pump box before thickening. This circuit was able to achieve the smelter's fluxing requirements of 60 000 tonnes per annum at a grade of 82.6% silica. Although high, the grade was still short of the initial target set by the smelter. This circuit was operated based on run hours. The smelter would let the concentrator know if the flux target had been reached, and if not, the circuit would be run for longer. The control was rudimentary and unreliable due to frequent sanding events.

In 1993, the reverse flotation circuit was decommissioned and replaced with a "silica composite flux" circuit. Instead of using the scavenger tail, the circuit would use the reground scavenger concentrate which is naturally high in copper composited with silica. As per the previous circuit, a cyclone was used to reject the fines fraction, and the coarse fraction was then passed over a micro-screen, and no flotation step was used. The micro-screen removed the fine pyrite fraction, as excessive iron can also be an issue for the smelter. The control of this circuit was also based on run hours. From historical reports, the cyclone and the micro-screen combination were able to produce a 79% silica grade.

Due to poor circuit control when fluxing directly into the final concentrate pump box based on run hours, a fluxing system was built at the concentrator in 1994, which allowed the silica to be stored and then dosed into the concentrate pump box in a controlled manner. In this iteration of the system, the scavenger tails were again used, but without flotation of the non-silica gangue. Despite the addition of better control for silica dosing, other issues arose such as bogging of the concentrate thickeners due to the coarse silica that was being added to the concentrate before thickening.

In 1996, the circuit was again upgraded, this time due to the addition of the Ernest Henry Mine (EHM)

concentrate being processed at the smelter. The EHM concentrate has a low silica grade of 2% when compared to the MIM copper concentrate silica grade of 9%. The silica deficit of the EHM concentrate, coupled with the increase in concentrate tonnage, effectively doubled the fluxing requirement, initiating significant changes to the silica dosing system. The flux was still produced at the concentrator, but a new storage and dosing system was built at the concentrate dewatering plant, affording the smelter further control of the silica content of the furnace feed. The silica was added post-thickening and before filtration, which avoided bogging the thickeners but still allowed the silica to be blended in slurry form. The new dosing system allowed for 125 000 t/y of flux to be produced at a grade of ~79% SiO₂.

In 1999, the micro-screen was removed from the silica circuit due to maintenance difficulties. It blocked often and caused significant spillage and downtime and was seen as more hassle than it was worth. After the removal of the micro-screen, the silica circuit comprised of a single cyclone, the overflow reporting to tails and the underflow being pumped to the dosing system. This configuration would be kept unchanged for the following 20 years, until gradual drifts in feed mineralogy forced changes to the system to keep up with smelter requirements.

The grade of the silica flux produced is directly correlated to the silica grade of the ore entering the concentrator. Over the years, the ore has become progressively more dolomitic, which has consequently reduced the silica content and increased the MgO. The dilution of the flux with deleterious gangue is a double-edged sword. More flux is required to make up the deficit, but this consequently increases the MgO content of the pre-fluxed concentrate. In 2017, the concentrator's pre-flotation cleaning circuit had to be bypassed regularly to reduce the MgO content of the final concentrate, reducing overall plant copper recovery by up to 2%. Despite the concentrate grade being within smelter specifications (for copper as well as MgO), a lower MgO grade in concentrate had to be targeted to allow for the increase that would occur during pre-fluxing. The pre-flotation cleaning circuit is the main lever for MgO rejection from the concentrate, whilst minimising recovery losses. For this reason, discussions about milling silica from the onsite quarry began.

The onsite quarry is an alternate source of silica at Mount Isa Mines and is typically used to produce "fine" trim silica (<2 mm) for addition to the ISASMELT furnace feed, and coarse silica (>40mm) for addition to the converters. In 2018 the auxiliary circuit suspended the operation of copper recovery from slag recycle streams and began milling mined silica for the smelter. This exercise cost over \$30/t of flux to produce and resulted in the loss of the copper usually recovered from the scavenger tails silica circuit. At this point, the silica in the concentrator feed had reduced to less than 40%, with the maximum upgrade of the silica via cyclone to between 50-60%. During times of low silica in the feed, silica milling was continued until an alternative source could be found.

Silica Reverse Flotation

In 2018, laboratory test work was conducted on samples of silica cyclone underflow and it was determined that a flux grade of 80% silica could be achieved if additional flotation processes were used to reject gangue. This brought about the revival of reverse flotation of the silica product, intending to float the non-silica gangue, to upgrade the stream as much as possible. The main difference between this reverse flotation circuit and the one used in the early '90s is that a fatty acid collector was included in the reagent scheme to float dolomite and decrease the MgO in the final product. Based on the initial laboratory results, the silica content of the scavenger tail was upgraded from 58% to 80%, with a decrease in MgO from 3.7% to 1.8%. The downside is that the copper which was usually recovered in the scavenger tail stream was also floated, reducing the flux grade from 0.19% to 0.15% copper.

Based on the success of the laboratory flotation work, a reverse flotation circuit was commissioned in 2020. Surplus flotation banks were refurbished and repurposed for the silica circuit, with the existing cyclopack to be used as a pre-concentration step. Figure shows the process flow diagram for the

reverse silica flotation circuit. Approximately 40% of the scavenger tail is rejected via the cyclones, significantly reducing the volume to be treated through flotation. The cyclone underflow is then dosed with reagents, which include two types of collectors: sodium isobutyl xanthate, and a specialty fatty acid collector. MIBC was found not to be required due to the residual frother in the tailings stream. The froth is sent to the final tails and the high silica tailings from the flotation banks are pumped up to the silica storage and dosing system at the concentrate dewatering plant.

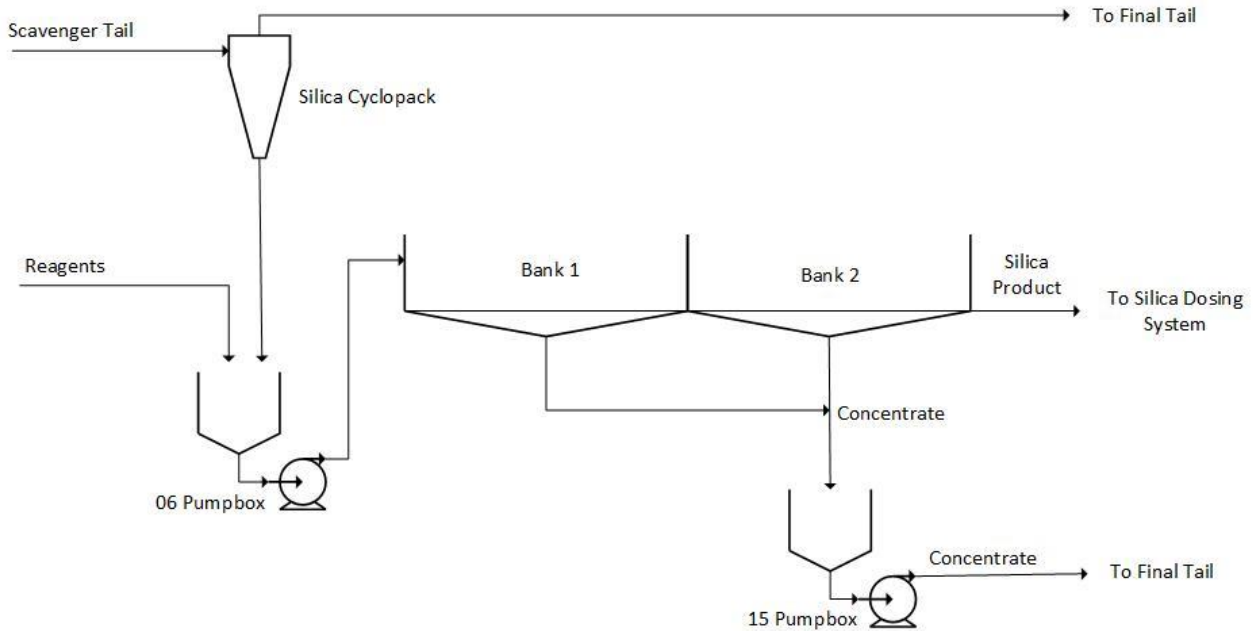


Figure 1: Silica Reverse Flotation Process Flow Diagram

From the test work, the new reverse flotation circuit looked promising. However, it should be noted that test work was completed on a relatively good set of samples that contained minimal talc. During the commissioning of the circuit, the 80% silica target obtained in the laboratory could not be consistently achieved in the plant and the MgO in the flux product was much higher than expected. Samples were collected to compare the results obtained in the laboratory to those in the plant, result shown in Table 1.

Table 1: Comparison of Laboratory and Plant Data for Reverse Flotation

Element	Lab Test work			Plant Operation		
	Scavenger Tail Grade (%)	Reverse Float Product (%)	Upgrade	Scavenger Tail Grade (%)	Reverse Float Product (%)	Upgrade
SiO ₂ (%)	58	80	1.38	52.33	72.04	1.38
MgO (%)	3.7	1.8	0.49	8.25	4.87	0.59
Cu (%)	0.19	0.15	0.79	0.17	0.25	1.46

Table 1 shows the silica content of the test work feed samples was higher than the plant equivalent, which enabled a higher quality flux to be achieved. However, the upgrade ratio of silica in both the laboratory and plant cases is the same. In short, the circuit is performing within its design parameters, but the low silica content of the ore is still having a detrimental effect on the quality of the flux material, despite the addition of the reverse flotation stage.

Although the quality of the flux improved compared to performance with just the single cyclone stage,

the production of flux below the target silica grade is still problematic for the smelter. Every 10% reduction of silica in the ore, equates to the displacement of 30,000 tonnes of concentrate per annum that could otherwise be processed at the smelter. This is equivalent to a 3-4% reduction in the smelter's concentrate consumption. The increase of MgO in the silica flux is also managed at the concentrator, requiring detrimental changes to circuit operation which reduce copper recovery to achieve the MgO target of the pre-flux concentrate. With the ongoing decline of silica feed grades, and the knowledge that this would further drop over the life of mine, investigations began to determine if there was a way to produce the 80% silica flux that the smelter requires without having to resort to milling mined silica.

Black Rock Tail as Silica Flux

In April of 2020, an additional circuit was commissioned to allow the processing of the Black Rock ore from a newly developed sub-level cave beneath the historical open cut. In August 2020, it was found that the silica content of Black Rock Cave (BRC) tailings stream was considerably higher in SiO₂ than the scavenger tails of the main circuit. While still mined on the MIM lease, the BRC ore exhibits very different mineralogy from that of the X41 and Enterprise ores. BRC ore is a weathered deposit located closer to the surface. The deposit predominantly contains chalcocite and native copper rather than chalcopyrite, as well as a high clay content. However, there are still significant amounts of silica present in the coarse fractions of the tails which also have a much lower MgO content.

Laboratory flotation tests were conducted to determine if the tailings could be upgraded to produce a viable flux product. The outcome was positive, and BRC tails were found to produce a superior flux to the main circuit scavenger tail stream. The BRC silica grade is also expected to increase over the life of mine, when compared to the X41 and Enterprise ores. Another benefit is that the MgO content is five times lower, and the copper content in tails is much higher due to the poor floatability of native copper and oxide copper minerals. This would result in a significant increase in copper units whilst producing a better-quality flux, a win for both the smelter and concentrator. Table 2 shows a comparison of the different silica flux products that were being considered at the time.

Table 2: A Comparison of Different Silica Flux Products

Comparison of Different Silica Flux Products			
Product	SiO ₂ (%)	Cu (%)	MgO (%)
Treated* Scavenger Tail	72.04	0.25	4.87
Trim Silica	91.8	0.624	0.52
BRC Tail	72.8	0.66	0.95

* Treated indicates processing through the reverse silica flotation circuit

In March 2021, a pipework diversion was installed, allowing a portion of the BRC tails streams to be directed through the reverse flotation circuit. A small trial was conducted which found that a marginal improvement in silica grade could be obtained by floating the BRC tail, however, the concentrate froth was tenacious, which resulted in pumping difficulties due to the large amount of ultra-fine clays in the stream. Significant copper losses were also sustained when floating the BRC tail. It was determined that cyclone separation of the stream to remove the ultrafine material would be the better approach.

Four composites of BRC tail samples were sent for cyclosizing and XRD to understand the mineral size associations in the stream. The samples were selected to ensure that ores with varying head grades were captured to determine if there was any significant variation in mineralogy. The results of the cyclosizing found that the mineral distribution of the tails was very similar, with more copper reporting to tails for the higher head grade samples. The results also found that 20% of the material by mass was in the -C5 size fraction (<10.1 µm) where clays are a significant source of silica along with quartz. In

the larger size fractions the clay component is much lower, and quartz becomes the dominant silica component. The results of the size by mineralogy analysis are shown in Figure 2.

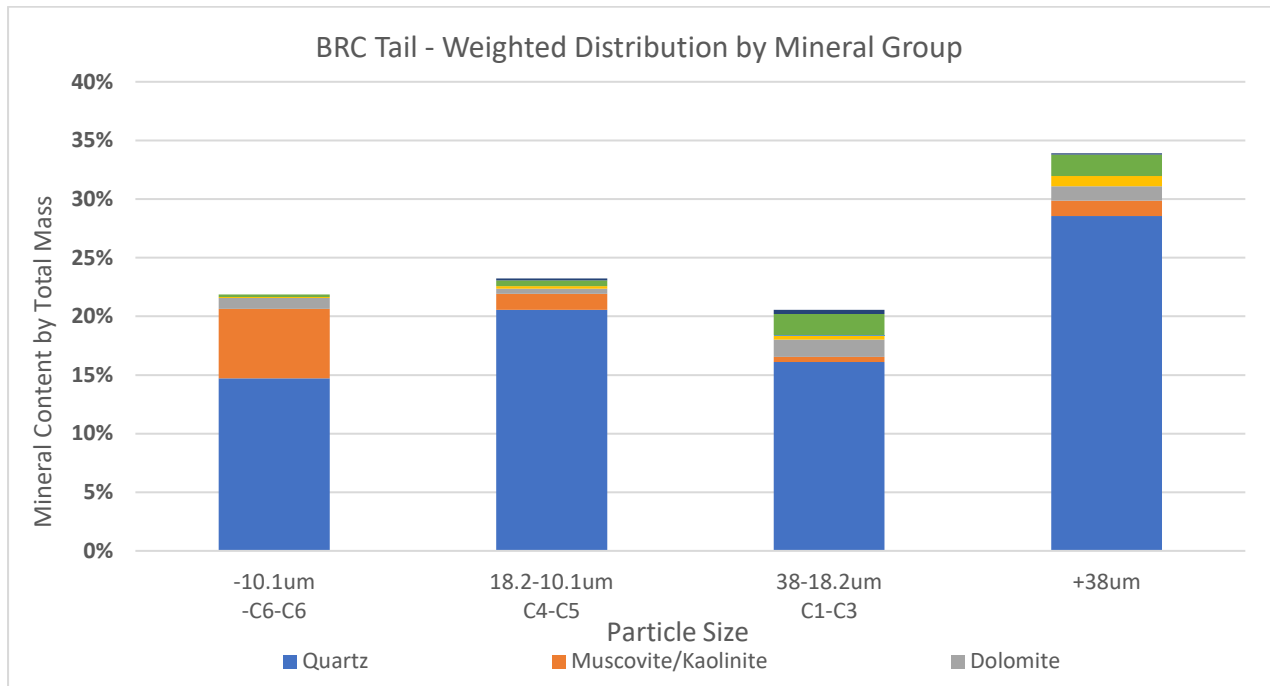


Figure 2: Size by Mineralogy of BRC Tails

Size by assay as well as cyclone modelling concluded that a marginal upgrade of silica could be achieved by cycloning, however, the real benefit lay in the increased copper recovery. A significant quantity of the copper contained within the BRC tail is native copper, particularly in the coarser size fractions. This mineral is not effectively recovered in the flotation circuit, but fortunately will report to the cyclone underflow due to its higher specific gravity. Approximately 60% of the copper in the BRC tail can be recovered via the cyclones at a 15 μ m cut size, with a silica upgrade of 5-10% relative. The following graph shows the weighted size distribution of copper minerals in the BRC tails.

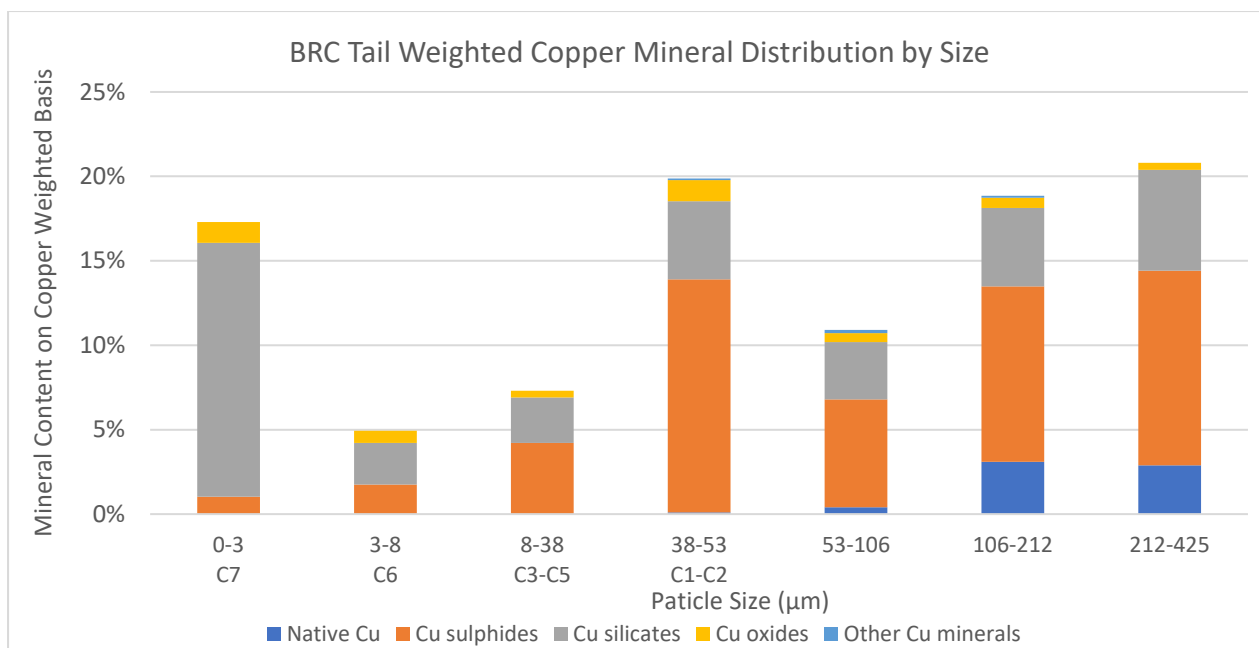


Figure 3: Copper Mineralogy of BRC Tails

The rejection of MgO through cyclones is not as selective as flotation, but still allows for an increase in the concentrator MgO threshold due to the significantly lower MgO content of the BRC tails compared to the scavenger tail. On a practical level, this translates to an increase in the amount of MgO allowable in the copper concentrate, by reducing the MgO contained within the pre-flux silica. This subsequently allows for less rejection of chalcopyrite in the pre-flotation stage. The copper recovery of the main flotation circuit can thus be increased by reducing the mass rejected in the pre-flotation cleaning circuit. The production of a cleaner flux product is therefore beneficial for both the smelter and concentrator. The removal of the reverse flotation stage also reduces reagent costs by up to \$800 000 /y due to the high cost of the fatty acid collector.

Cyclone modelling conducted by Weir showed that the current cyclones installed in the silica circuit were fit for purpose and could be used to process the BRC tails stream at a fixed throughput with minor alterations. Higher cyclone pressures and smaller vortex finders were recommended to achieve a cut size of 15µm. Further reductions in cut size would require additional smaller cyclones to be installed and modifications to the distributor. It was decided that the existing equipment with minor modifications would be trialed first to determine if it was a success, before investing capital in a new cyclone configuration. The other benefit to using the existing equipment is that the scavenger tails from the main flotation circuit can still be used if required. This is particularly important, as the BRC ore is campaign processed along with magnetic converter slag (referred to as Mags) through the auxiliary circuit which impacts the availability of the silica flux.

One of the main constraints for this project was CAPEX minimization and as such, no upgrades to equipment such as pumps and cyclones were considered. Only minor equipment changes were included in the project scope to enable the use of the silica circuit for BRC tails processing. Significant pipework modifications were required, as the BRC circuit is located several hundred meters from the silica circuit. The pipework design needed to be flexible enough to allow for the use of both BRC and scavenger tails as feeds to the silica circuit, without compromising the operation of either circuit.

A design criterion was created, which considered the existing equipment available for the silica circuit to process BRC tails and the upper and lower limits in terms of flow and density. Due to the nature of the circuit set-up, the BRC tails report to either the final tails pump box or to the silica circuit, the stream cannot be split. At the time of the study, the mill throughput was identified as one of the major

constraints and had to be capped at 45t/h, to avoid overwhelming the silica circuit. As per the design criteria, 45t/h was believed to be the upper operating limit of the existing equipment being repurposed for this project.

Commissioning and Adjusting to Business Strategy Changes

Between August 2022 and May 2023, scavenger tails were the source of feed to the silica circuit, however, during this time, there were three periods where BRC was trialled with the inclusion of Mags (trial 1, trial 2 & trial 3) and two stages where no mags were part of the feed blend.

The installation of the new pipework to connect the BRC circuit to the silica system commenced in July 2022, with the first stages of the circuit commissioning starting in September of that year. The initial results from the first operation of the silica circuit with BRC tails (trial 1) were delivering reasonable performance, however, the business was challenging the 'believed' limited throughput rates. By the time the new silica circuit was operational, the mill throughput target had been increased to 70 t/h, with a feed blend of BRC and Mags being processed, with the expectation that in 2023 the mill would be processing 75 t/h in order to achieve the production requirements. Mags are high in iron, particularly magnetite, with a significant copper content that is blended into the BRC feed to improve copper recovery.

During the silica cyclone modelling, the initial recommendation by Weir was to install 44 mm spigots and 60 mm vortex finders to allow the cyclones to operate at a lower cut point, with both CVX250 cyclones in operation. This configuration, coupled with an increase in mill throughput, led to significant spillage when the silica circuit was operational. It caused several pump boxes to overflow and highlighted other issues with shortcomings in the downstream silica circuit pipework. As a short-term solution (trial 2), the cyclone set-up was changed to 60 mm spigots and 70 mm vortex finders to accommodate the increased volume. This modification allowed for the increased throughput whilst reducing spillage, but also compromised the metallurgical performance of the cyclones for flux production resulting in lower quality flux and poorer copper recovery.

The only way to operate the silica cyclones with the recommended cyclone set-up (44 mm spigots and 60 mm vortex finders) was to have an extra cyclone added to the cluster to manage the increased plant throughput. The business recognized this constraint, and an additional cyclone was installed in April 2023.

A third trial (trial 3) was designed to scope both cyclone setups to ensure that the silica and copper upgrades were still acceptable with the changes that were required to be made to facilitate the increased throughput. While performing the trial, a feed blend with Mags occurred, which consisted of nine buckets of BRC and one bucket of Mags, equating to approximately 17% Mags by mass. Figure 4 shows the effect of Mags on the grade of the silica flux;

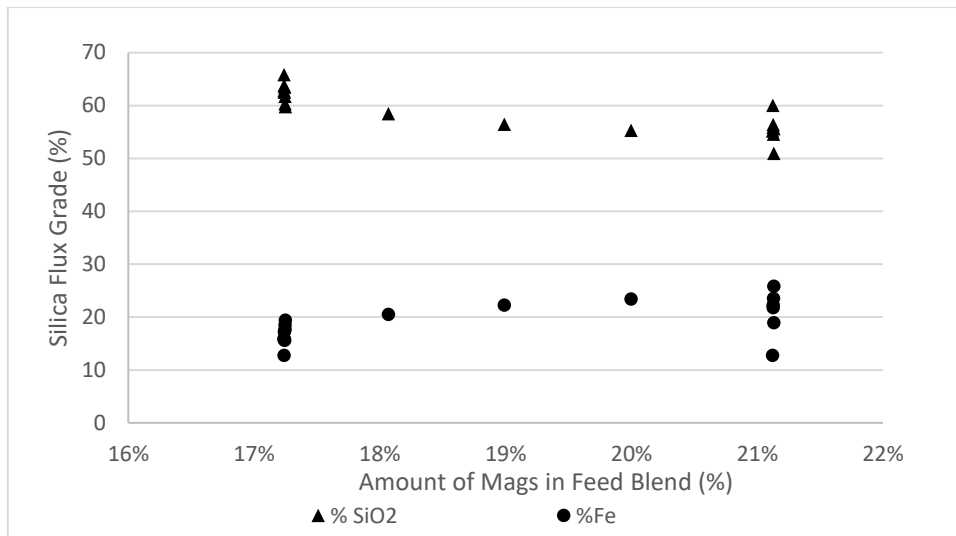


Figure 4: Effect Mags on Silica Flux Grade

The additional iron contained of Mags resulted in a significant amount of iron being present in the silica flux product due to dense magnetite preferentially reporting to the silica cyclone underflow. Not only does iron in the silica product displace all other minerals, thus diluting the grades (particularly for silica), it also breaches the smelter's iron limits in the concentrate. The high iron in flux cannot be rectified without substantial changes being made to the silica circuit, which would require a significant capital upgrade. The only way to reduce the amount of iron in the silica flux without modifying the circuit is to remove it from the blend.

Figure 5 demonstrates the SiO₂ grade of the silica stock tank over time in which these trials were occurring. In the periods of late September and early November 2022 (trials 1 and 2), Mags were blended into the BRC feed, negatively impacting the silica grade. Figure 5 also shows the cyclic nature of the scavenger tails product, which increased in silica grade over the month of December 2022 and into January 2023, although historically the average SiO₂ grade of the flux is only 60% - 70%. The scavenger tail SiO₂ grade decreased again from January 2023 through to the end of March 2023. BRC tails was processed with no Mags in the blend in January 2023 and again in April 2023, with a resultant flux grade of approximately 75% - 78% SiO₂.

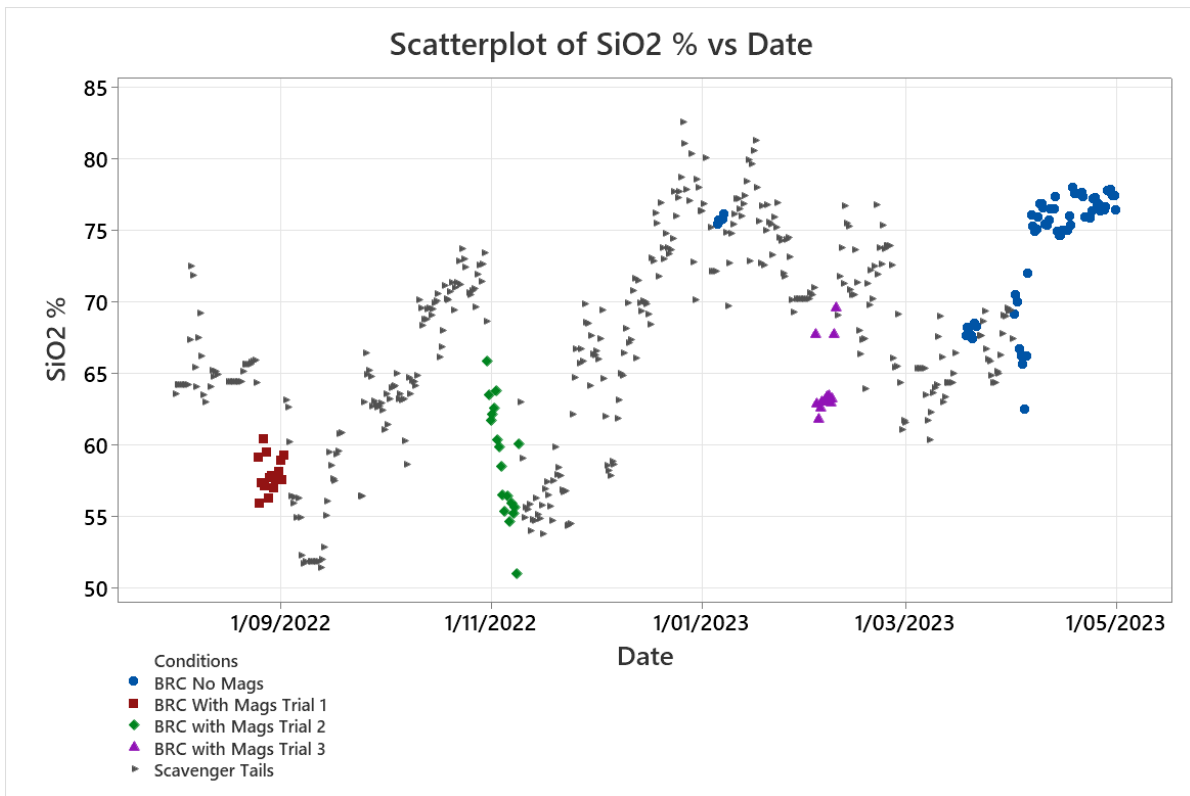


Figure 5: Chart of silica grade produced between August 2022 and May 2023

Figure 6 shows the iron grade of the silica flux during the period of August 2022 to May 2023. The figure clearly shows when Mags is blended in the BRC feed as it significantly increased the Fe content in the silica flux. This elevated the iron content from 5 to 18.8% Fe on average during this trial. During the period where BRC tails was used with no Mags in the feed blend in January 2023, there was a slight increase in Fe grade, however, to the extent that it will have a negative impact on the copper smelter.

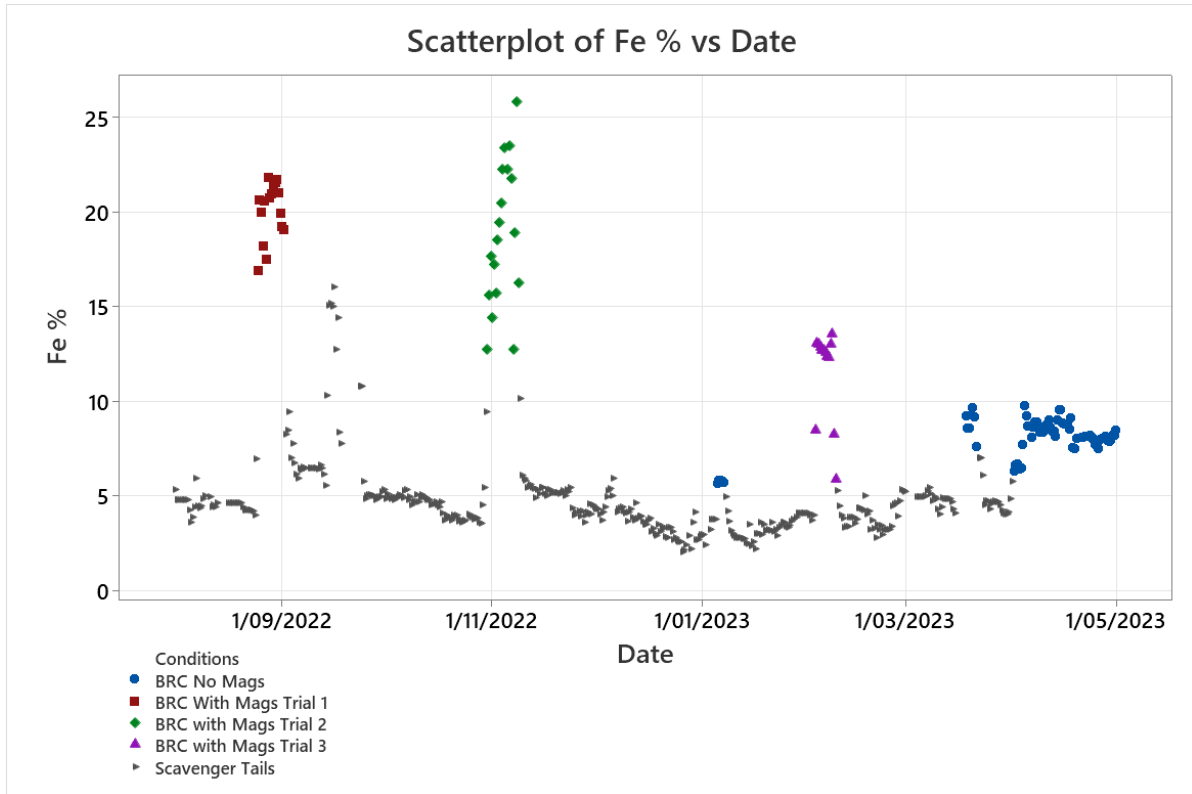


Figure 6: Chart of iron grade produced between August 2022 and May 2023

Figure 7 highlights the increase in copper grade when BRC is used as the feed source, irrespective of the presence of Mags in the feed blend. When BRC was blended with Mags at the end of September and at the start of November 2022, the copper grade increased from approximately 0.3% Cu when scavenger tails are used as the feed source to 0.95% Cu when BRC tails was used with Mags in the feed blend. When BRC (no Mags in the feed blend) was used as the feed source in January 2023, there was an increase in copper grade compared to the scavenger tails with copper grade almost doubling from approximately 0.3% Cu to 0.58% Cu. In April 2023, when BRC (No Mags) was used as the feed source for the silica flux, there is a significant increase in Cu units, which has a positive impact on the total revenue for the project.

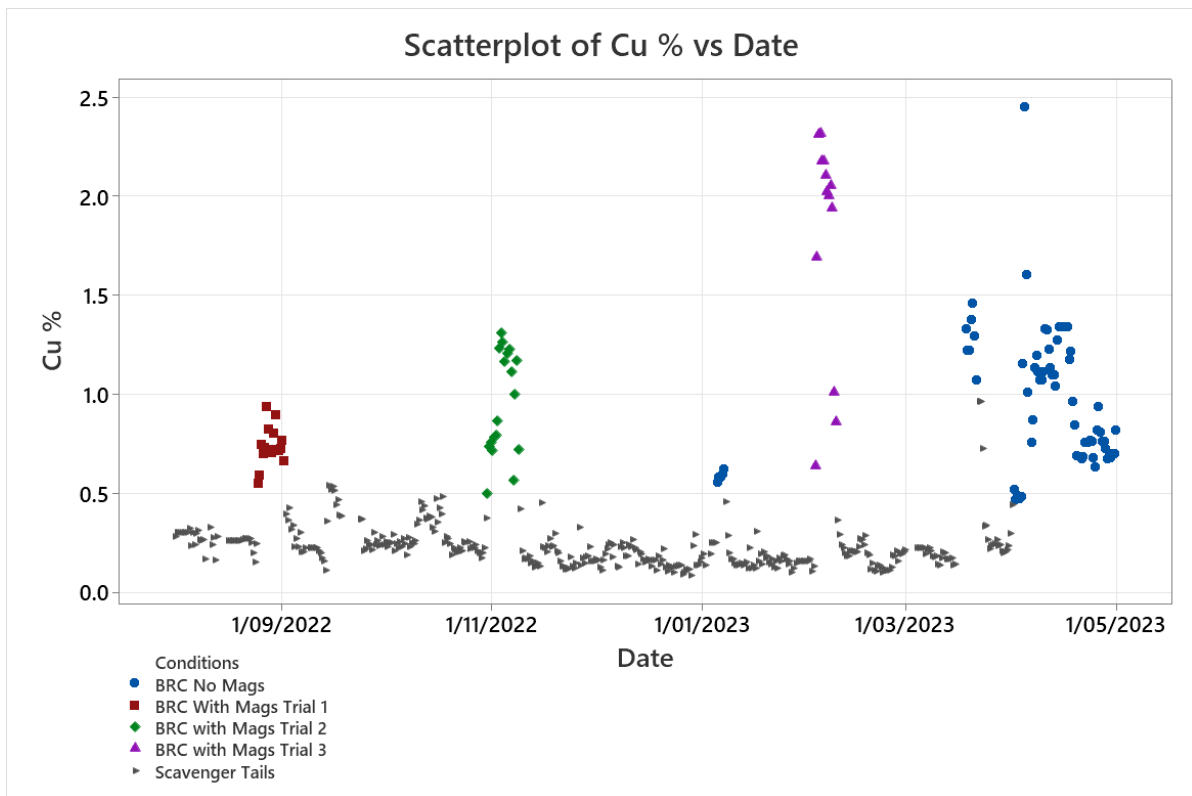


Figure 7: Chart of copper grade produced between August 2022 and May 2023

Figure 8 shows a significant reduction in MgO when BRC is used, compared to using scavenger tails as the silica flux feed source. This is regardless of the addition of Mags being blended into the feed or when BRC was used with no blending. As mentioned, this is a major positive for the smelter chemistry and performance as it reduces the slag viscosity and heat requirements and reduces copper loss to slag.

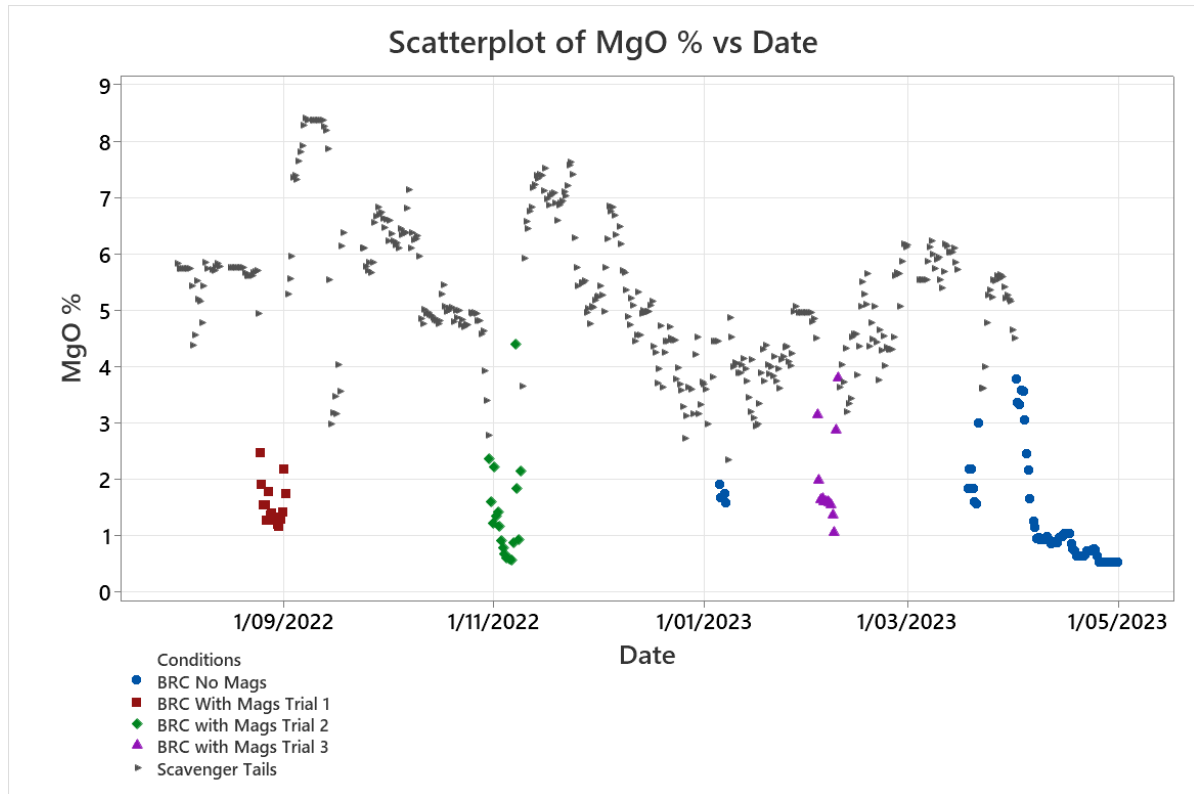


Figure 8: Chart of MgO grade produced between August 2022 and May 2023

Statistical Comparisons : Scavenger Tail Vs BRC Tail

For visual simplicity, only two months were compared for the purpose of this paper. Even though a simplified version has been presented, the analysis has been completed on the entire data set, which represents a conservative approach. December 2022 and April 2023 were the two months chosen for comparison as a single feed type was processed continuously for the duration of these months. Due to the nature of the silica system being a batch process, it is difficult to obtain periods of continual processing.

The two elements that most impact the smelter returns are the grades of silica and copper. The higher the silica grade in the silica flux, the lower the volume to the smelting process which allows more third-party concentrates to be processed. This has a secondary effect which isn't quantified in this paper as the battery limit for this study was the concentrator product. However, it is worth mentioning that the smelting process is a batch feed process, meaning that the lower amount of silica required due to higher quality, the more copper can be processed over any given period. So inadvertently, this process in the concentrator has increased the efficiency of the copper smelter as the smelter is throughput limited.

Figure 9 shows that the silica grade has increased when using BRC. With the higher silica grade produced, this equates to approximately 11 000 fewer tonnes of silica flux required by the smelter per annum. It also shows that the specifications of the product produced was much more stable during the BRC period which helps the smelter calculate the silica requirements in the smelter feed blend.

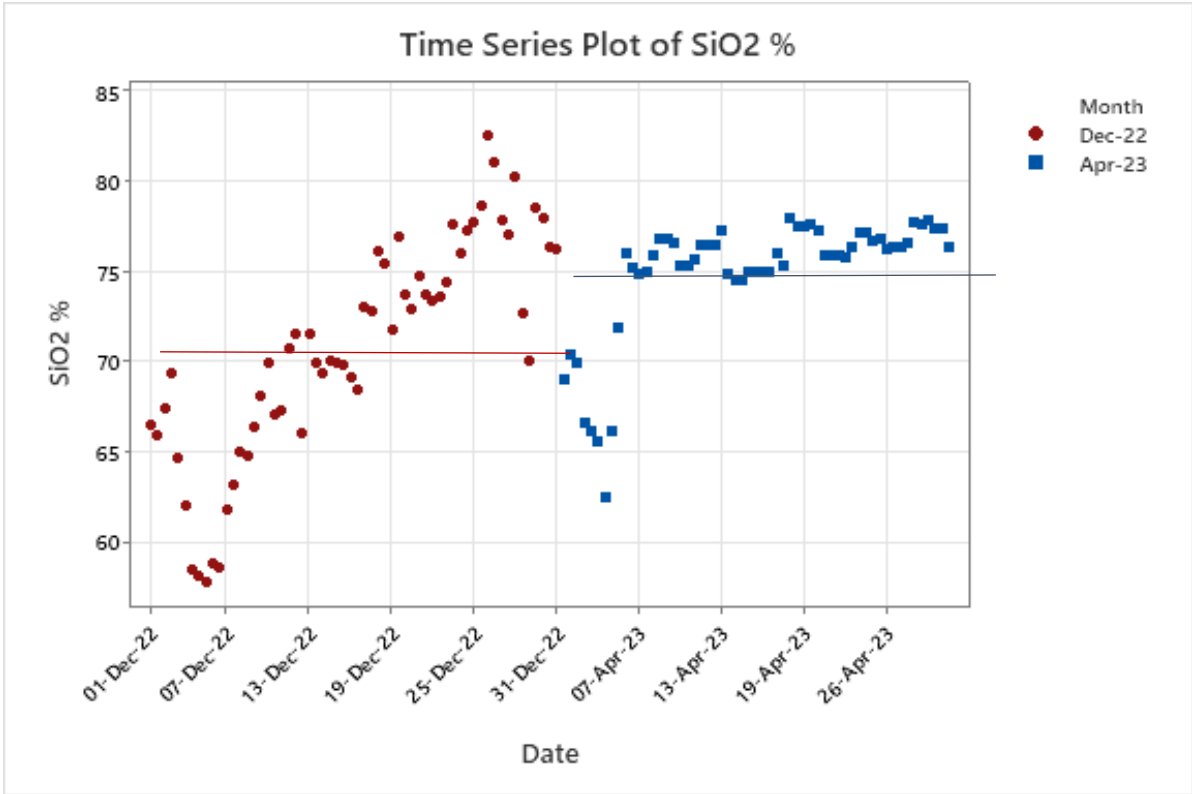


Figure 9: Time series plot highlighting the increase in SiO₂%

Figure 10 is a histogram comparing silica in the flux product when BRC is used compared to the scavenger tails. It not only shows the mean silica grade is higher when using BRC, but the standard deviation is much lower which enables the smelter to have greater confidence in the silica quality when they are producing slag chemistry models.

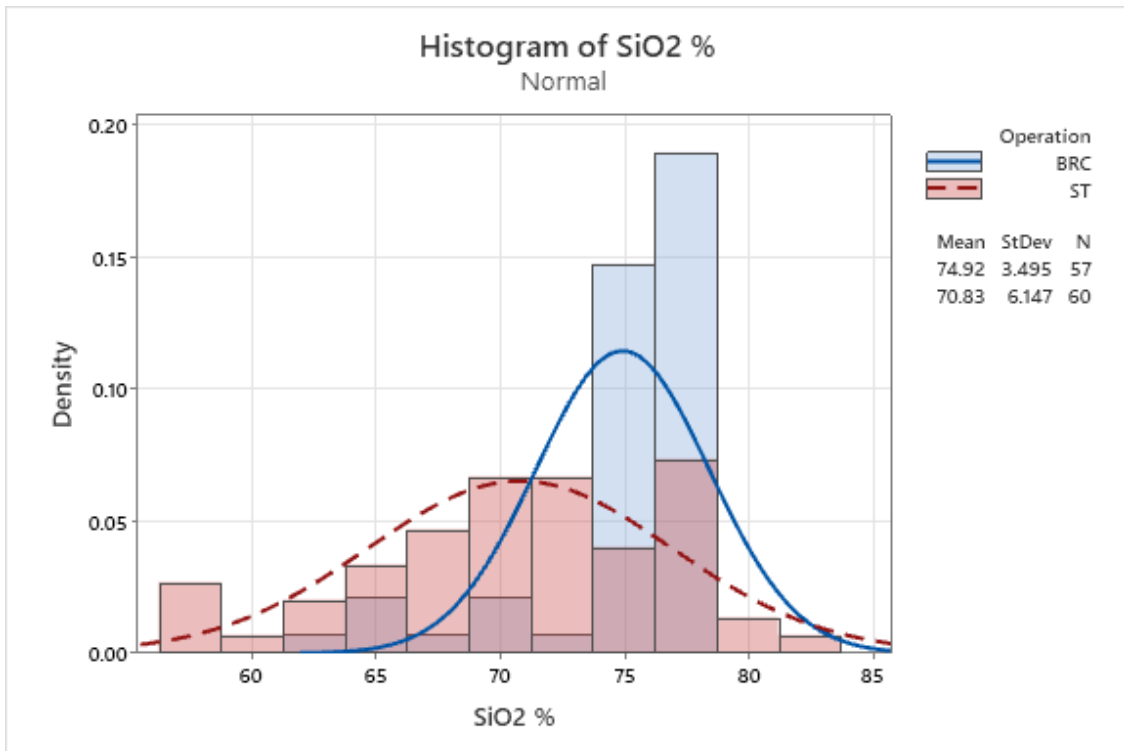


Figure 10: Histogram chart comparing SiO₂%

Figure 11 shows that using BRC as the feed to the silica flux circuit increases the copper units reporting to the smelter. As copper is not critical to the smelting process, the variability of the copper in the silica flux isn't an issue. However, the increased grade of copper in the silica flux means there is a corresponding increase in copper metal production. According to the smelter's 2023 flux forecast, the increase in copper metal by changing the source will be approximately 714 t. Overlaid on the chart is the mean for the respective periods.

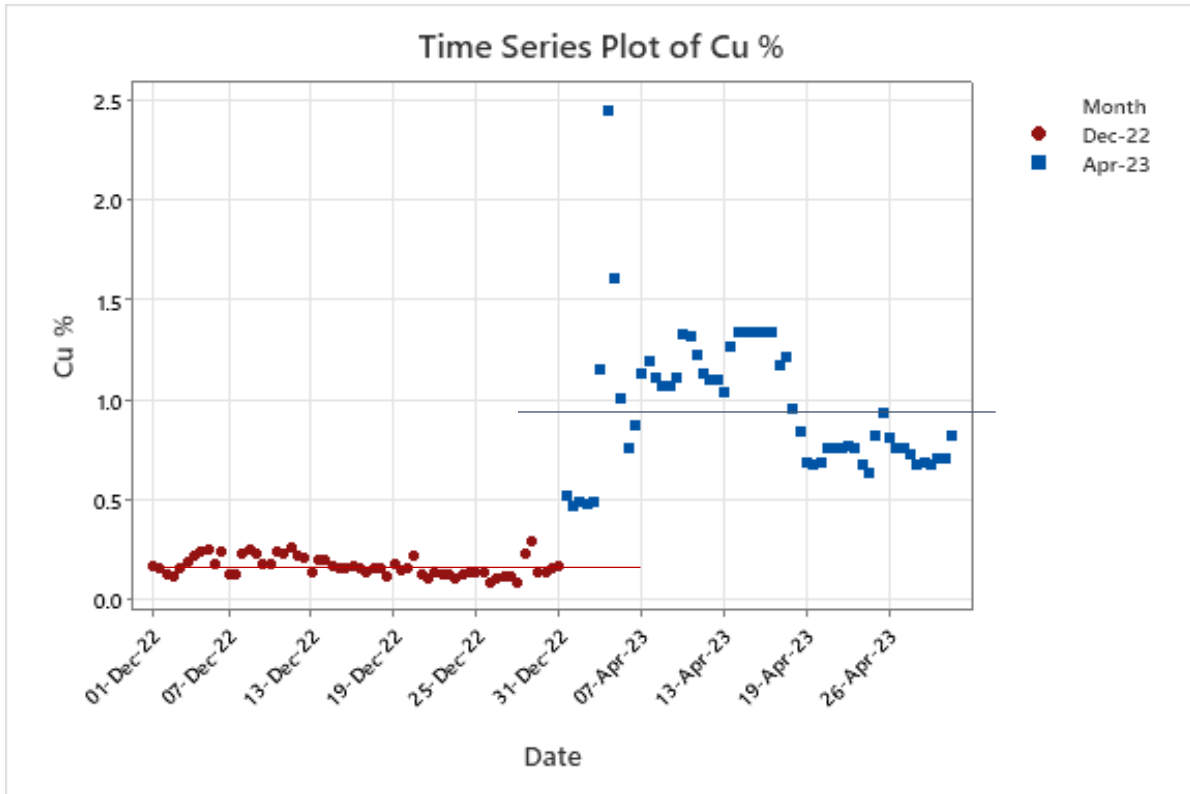


Figure 11: Time series plot highlighting the increase in copper units when BRC is used

Figure 12 is a histogram comparing Cu% in the silica flux product when BRC is used compared to using Scavenger Tails. This is an increase of 0.8% Cu that is now reporting to the smelter.

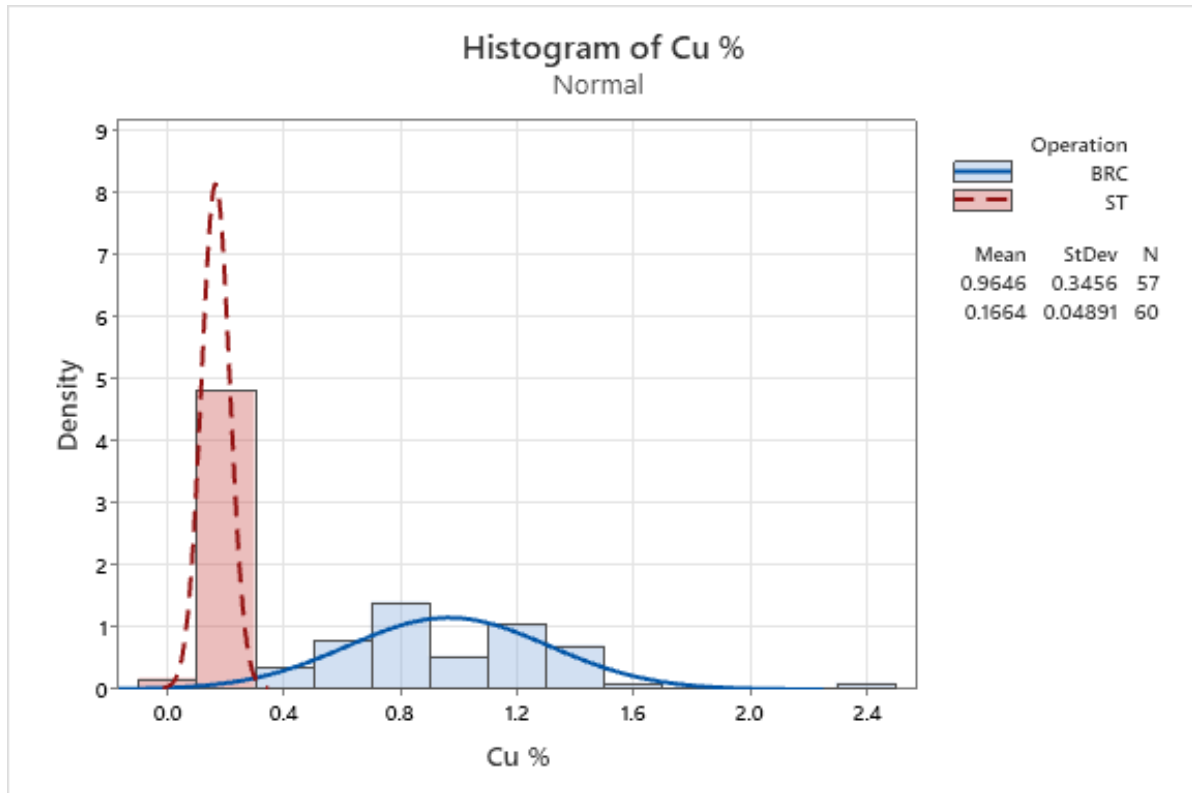


Figure 12: Histogram chart comparing Cu %

Revenue Generation

There are three factors that impact the NET revenue¹ of the product when comparing the use of scavenger tails and BRC as feed sources for flux production. Figure 13 shows the changes to revenue, OPEX and unit cost production of silica between the two main sources: scavenger tail and BRC tail. Increased copper recovery, higher silica flux grade and a reduction of operational costs have all been experienced with the use of BRC tails as a flux. The revenue figures shown in Figures 13 & 14 are only related to the copper concentrator and do not include the increased smelter returns that a higher-grade silica flux product can deliver. As previously mentioned, a change in silica flux grade of 10%, equates to 30 000 tonnes per year of concentrate which has the potential to significantly impact the volume of third-party concentrates that can be treated through the smelter.

When considering the financial drivers for this project, the first consideration is the increase in copper content in the silica flux product. The BRC ore mineralogy shows there is a higher amount of oxide copper minerals and native copper present compared to that of X41 and Enterprise ores. Because of this, there is a higher amount of copper that is not recovered by the flotation circuit, and consequently higher copper losses to tails in this circuit. The benefit of using cyclones as part of the silica flux production is that a portion of the native copper that was once lost to tails can now be recovered and sent to the copper smelter by the flux production.

The second financial driver is the increased quality of silica flux being produced. Simplistically, the higher the grade of silica that is produced, the less silica flux is required to be used by the copper smelter, therefore significantly increasing the opportunity for third-party concentrate consumption. The third driver is the ability to reduce operational costs. The largest cost saving generated is due to eliminating the requirement for reverse silica flotation. When using BRC tails as the feed source, there is no requirement for using reverse silica flotation to gain an upgrade to the flux product.

The reverse silica flotation circuit used for the scavenger tails required the use of fatty acid, xanthate, and additional power for the agitators. By changing feed source to BRC tails, these costs are eliminated. The costs of reagents and power are significant, totalling \$889 206 /y. Due to the elimination of reagents and reduction in power, the unit cost has been reduced by over \$14 /t of Silica flux produced. When considering the reduction of operational costs and increased revenue generated, the NET revenue for the project is over \$8.4 M/y.

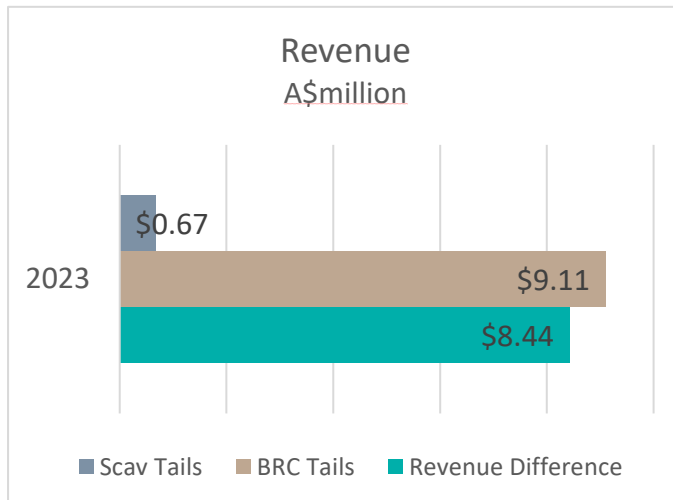


Figure 13: Chart showing revenue generation comparison.

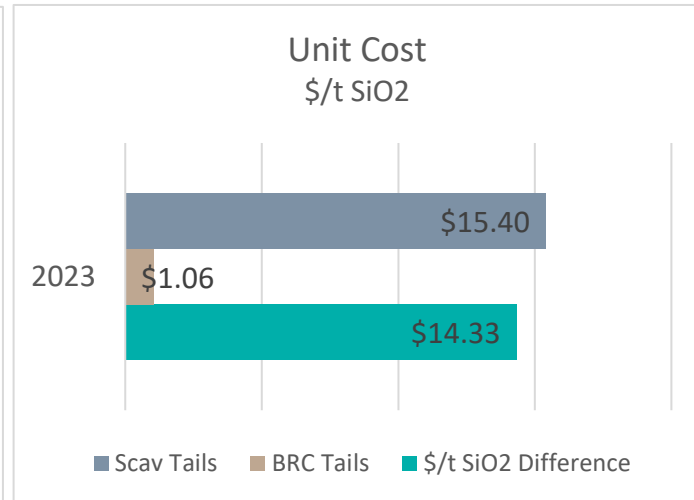


Figure 14: Chart showing unit cost reduction

CONCLUSIONS

The MIM silica circuit is an innovative approach to the production of a value adding stream from tailings. The benefits of the silica system are difficult to quantify due to the downstream impacts on the smelter, particularly when poor flux grades result in the modified operation of the concentrator and/or the smelter. Smelter production is intrinsically linked with copper concentrate supply, but the added integration of a flux system that is highly dependent on concentrator feed mineralogy further complicates the ownership and direction of both plants. The complexity associated with this type of system in terms of the operational impact on both assets involved should be seriously considered if contemplating similar activities. The risk lies in the silo effect that many operations find themselves in, where communication breakdown can have serious impacts on processes that span multiple plants. Despite these impacts, for MIM this integrated system has benefitted the copper concentrator's metal recovery overall and flux supply for the smelter has always been assured.

The ability of a concentrator to selectively upgrade certain minerals is highly dependent on the feed mineralogy, and this is where the biggest vulnerability of the silica circuit lies. Gradual changes to the long-term mineralogy of the ore have led to developments in circuit modifications and increased flexibility in the pursuit of the highest quality flux grade. Changes to business strategies, as well as feed sources for the concentrator, have led to rapid decision-making when considering the implications for downstream assets. Being able to pivot quickly and stay flexible has allowed the business to maintain an integrated approach between the assets as well as remain as self-sufficient as possible considering the remote location.

The silica system has supplied flux, almost continuously, to the copper smelter for over 30 years which provides considerable operating cost benefits to a smelter that is located 900 km from the closest seaport. Besides consumable cost savings and the increased copper recovery associated with the silica system, the added benefit of reducing tailings volume is another important aspect that should not be forgotten. In conclusion, a process that converts tailings to a value-adding product, such as the silica system, may increase the operating complexity of integrated assets but brings with it many benefits, including more sustainable operation and a measurable reduction in the final tailings footprint.

First Principles Modelling of Mine Wastewater Treatment

K Heppner¹

1. SysCAD, Sr. Process Simulation and Software Development Engineer, Saskatoon SK,
kevin.heppner@syscad.net

Abstract

In this paper, the author presents a first principles thermodynamic approach to modelling of water treatment. The conventional ferric sulfate and slaked lime treatment of mining wastewater is simulated via PHREEQC calculations embedded within a SysCAD process simulation model. Multicomponent, multiphase co-precipitation and adsorption models are employed for the removal of typical contaminants including aluminium, nickel, molybdenum, arsenic, uranium, and sulfate. Surface complexation of both ferrihydrite and gibbsite secondary minerals are considered in the adsorption model. The resulting model is used to optimise a multi-stage raffinate water treatment process to meet environmental regulations while minimising tailings volume and treatment cost. Ryan and Alfredson (1976) reported on neutralisation test work done on a raffinate stream from a mine in Australia. This work was used as the basis to characterise the raffinate feed stream. A sensitivity analysis is employed to identify potential risks associated with common operational upset conditions and mitigation strategies are proposed.

Introduction

Remaining competitive in today's challenging regulatory environment requires a fundamental understanding of the chemical processes impacting a mine wastewater treatment process. Depending on the contaminants, a series of different treatment steps involving hundreds or thousands chemical reactions may be required to treat the water. To model complex water treatment plants, it is advantageous to use free energy minimisation to calculate chemical equilibrium at various points in the process. This work presents a first principles approach to modelling the removal of arsenic, molybdenum, nickel, aluminium, and various other metals in the treatment of solvent extraction raffinate using lime and ferric sulfate. Competitive adsorption to both ferrihydrite and alumina surfaces are considered, along with precipitation of numerous secondary minerals. The SysCAD process simulation software is used with the SysCAD-PHREEQC interface using the minteq.v4 database.

Uranium Ore Processing

Conventional processing of uranium ore to produce a uranium ore concentrate involves wet grinding, leaching with sulfuric acid and oxidant, solid/liquid separation with washing to minimise soluble loss, solvent extraction and stripping, and product precipitation, drying, and in some cases, calcining. A high-level block flow diagram of a conventional uranium ore processing facility is shown in Figure 1. Reagents and water consumption are intentionally not shown to simplify the diagram.

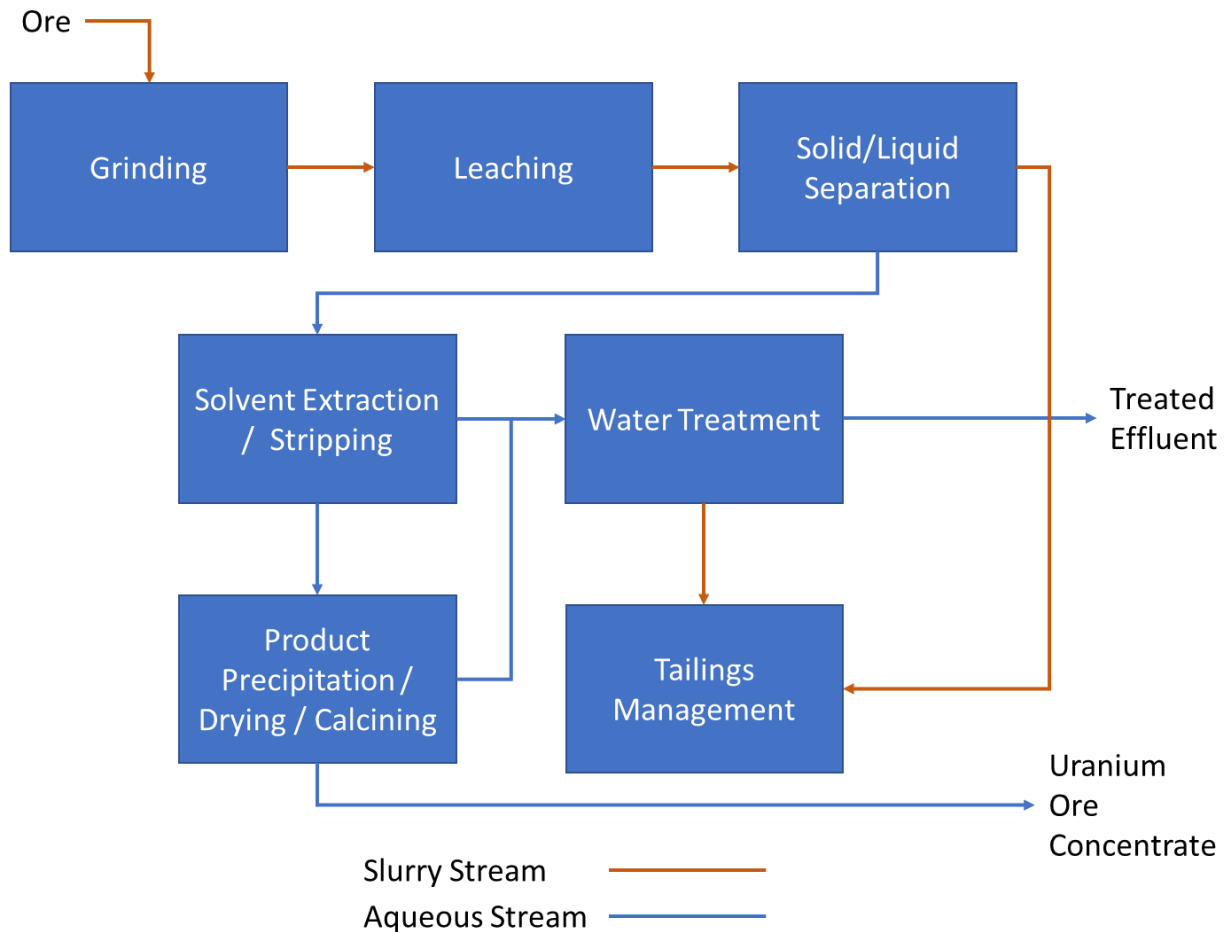


Figure 1 - Simplified uranium ore processing facility block flow diagram

Water treatment is required for treatment of solvent extraction raffinate, spent organic solvent regenerant, precipitation barren solution (in the case of strong acid stripping), and other site water sources. Conventional water treatment involves the treatment of combined waste streams with slaked lime slurry and ferric sulfate reagent. This is typically done over a series of precipitation tanks to allow sufficient residence time and to separate process conditions. For example, it is common to maintain low pH conditions at the front of the circuit to promote removal of carbonates. Carbonates are detrimental to the subsequent removal of uranium in the second stage of the water treatment circuit.

A typical water treatment flow sheet is shown in Figure 2 as a SysCAD model flow sheet.

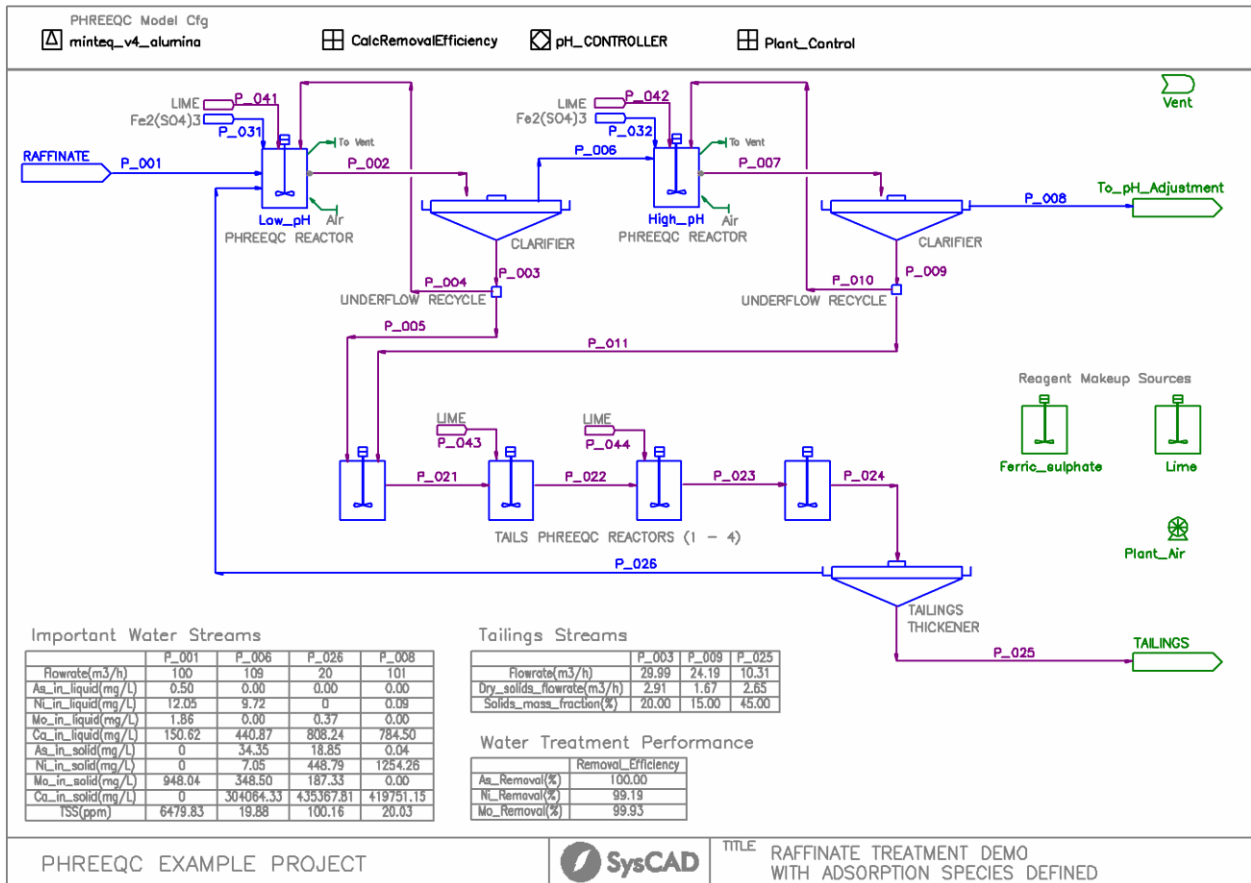


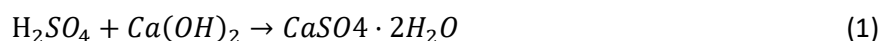
Figure 2 - SysCAD model of conventional two-stage water treatment circuit

It is important to understand the functions of the three circuits:

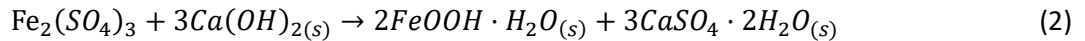
1. The first circuit operates at a low pH, typically in the range of 3.5 – 5. This is for the removal of metallic oxyanions, aluminium, and iron. Metallic oxyanions adsorb to freshly formed ferrihydrite and alumina and are removed from the circuit. These conditions also promote the removal of sulfate as gypsum.
2. In the second circuit, additional lime is added to raise the pH between 9 – 11. This is done to remove metals as hydroxides. Additional ferric sulfate may also be added if required to promote further adsorption of various ions. Metal removal here includes the removal of nickel, uranium, copper, and residual aluminium.
3. Finally, the tailings circuit is intended to create a geochemically stable tailings product for long term storage in a licensed tailings management facility.

Model Theory

Treatment of mining-impacted waters containing sulfuric acid and sulfate metal salts typically involves neutralisation using slaked lime and approximately 45% by mass ferric sulfate solution. Sulfuric acid reacts with lime to form gypsum (or anhydrite depending on temperature) by the following reaction:

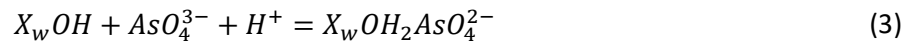


Ferric sulfate reacts with lime to form hydrous ferric oxide:



Ferrihydrite acts as a sorbent for metallic oxyanion species such as arsenate, molybdate, selenite, etc. at pH around 3.5 - 5. Dzombak and Morel (1990) developed a two-layer diffuse layer model that has been widely used to describe sorption to hydrous ferric oxide surfaces. In this model, strong and weak sorption sites exist which have different binding mechanisms for species. A significant collection of equilibrium data is available in PHREEQC databases (United States Geological Survey, 2021) for common contaminants of potential concern (COPCs).

An example of a sorption reaction is given below. Here, a weak sorption site reacts with arsenate to form an adsorbed species in acidic conditions:



Model Implementation

The two-layer model of Dzombak and Morel is available in the software package PHREEQC. SysCAD supports seamless integration of PHREEQC thermodynamic calculations via an embedded interface. Sophisticated mapping algorithms are employed to transfer information from streams in the SysCAD software to PHREEQC for thermodynamic calculations. These methods are fully defined elsewhere (SysCAD help documentation links listed in references). The SysCAD-PHREEQC interface supports calculation of:

- speciation within the aqueous phase including activity coefficient calculations
- secondary mineral solubility, i.e. minerals that are formed in the water treatment circuit
- simultaneous adsorption to multiple surfaces, e.g. co-adsorption of COPCs to hydrous ferric oxide and alumina
- ion exchange with other materials such as clays or specialised resins.

The connectivity of SysCAD with external thermodynamic packages is illustrated in Figure 3 and Figure 4. Stream information is passed from SysCAD to an external thermodynamic package via a mapping algorithm that links SysCAD chemical species to chemical species within the thermodynamic package. More information on model configuration and species mapping is available on the SysCAD online documentation (SysCAD, 2023).

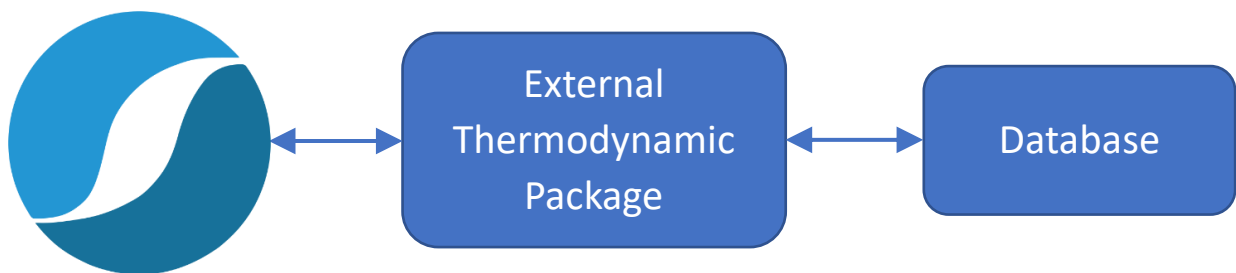


Figure 3 - Connectivity between SysCAD and external thermodynamic package

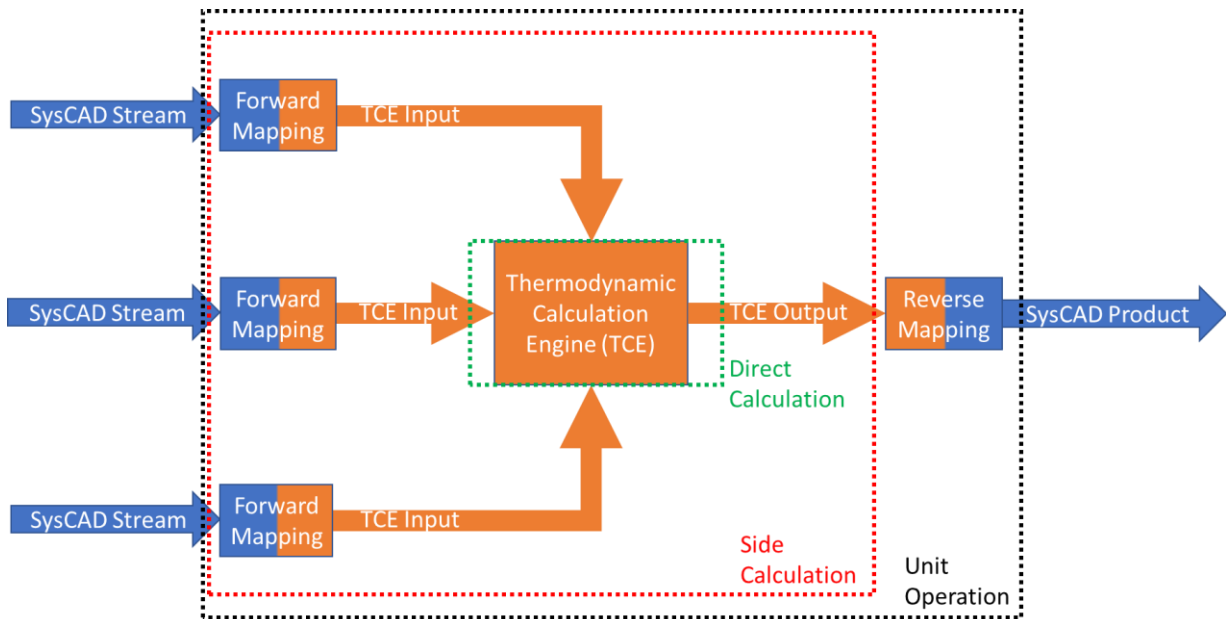


Figure 4 - Species mapping between SysCAD and external thermodynamic package for different unit operation types

Sorption model parameters

Sorption to ferrihydrite and alumina were considered in this model. Parameters for these models were obtained from Dzombak and Morel (1990) and Goldberg (2002), shown in Table 3.

Table 3 - Adsorption surface parameters used in the model

Sorbent	Surface Area per Mole	Moles of Sites per Mole	Reference
Alumina	51 500 m ² /mol	0.197 (only one site type)	Goldberg (2002)
Ferrihydrite	53 300 m ² /mol	0.005 (strong) 0.2 (weak)	Dzombak and Morel (1990)

The minteq.v4 database contains adsorption data for many elements to hydrous ferric oxide. Details on this database are available in a report developed by HydroGeoLogic, Inc. (1998).

Reactions and data for the adsorption of arsenic and nickel to alumina were taken from Goldberg (2002). These reactions and $\log_{10} K$ values were added to the minteq.v4 database as a modification.

Hydrous ferric oxide and alumina sorption sites were calculated from summing up the total ferric oxyhydroxide and alumina species formed during precipitation. Ferric precipitates contributing to sorption included only oxyhydroxide and hydroxide minerals. Alumina precipitates included alumina oxides and hydroxides, as well as AlOHSO₄. This was included based upon observations from Robertson (2017).

More information on the diffuse layer model is available in the original reference (Dzombak and Morel, 1990).

Water Treatment Process Simulation

In this example, a raffinate from a typical ore processing plant is fed to the water treatment circuit. It is treated in a two-stage ferric lime water treatment process. Ferric sulfate and lime are both added in stages to promote removal of deleterious elements. The combined stream is then treated with additional lime to generate an engineered tailings product for final containment in a licensed facility.

Raffinate feed chemistry

Raffinate data used in the analysis is presented in Table 4. This raffinate assay was selected due to its high iron and aluminium content. It also contains significant amounts of other elements such as copper, nickel, vanadium, and phosphate. The molybdenum assay in the raffinate was not reported by Ryan and Alfredson (1976), and thus, a typical concentration of 5 mg/L was assumed.

Neutralisation test work data from Ryan and Alfredson (1976) at pH 4 was used to calculate the fraction of iron in the raffinate present as ferrous ions. By doing a PHREEQC calculation of the neutralisation process to pH 4, the ferric to ferrous ratio of the raffinate was adjusted until the amount of residual iron predicted by PHREEQC in the treated raffinate matched the reported experimental results. It was calculated that 11.5% of the iron was present as ferrous ion based upon this method. It is expected that raffinate will contain both ferric and ferrous ions due to leaching circuit conditions as well as contact of leach liquor with reducing agents present in the solvent extraction reagents.

Table 4 - Raffinate assay used for water treatment plant analysis (Ryan and Alfredson, 1976)

EOC	Feed Concentration (mg/L)
Al	1 840
As	<0.5 ³
Ba	<0.05 ³
Ca	150
Cu	80
Fe	2 300
Mg	1 880
Mn	7
Ni	23
Pb	2.3
Si	540
U	3.8
V	26
Zn	7
Cl	360
P	280
SO ₄	26 300
Mo	5 (assumed)

Process flow diagram and baseline analysis

The flow sheet of a SysCAD model for this two-stage process is presented in Figure 2. Each circuit is represented as a single neutralisation tank. It is recognised that most neutralisation circuits will employ multiple tanks in series to allow for sufficient residence time for the reactions to take place, as well as for the staged addition of lime to avoid scaling issues. Because this is an equilibrium model, and carbonate degassing was not considered, there was no advantage to representing multiple tanks. As such, the process was simplified.

³ The detection limit value was used in the simulation as an input value.

Low pH treatment

The acidic mining wastewater contains numerous contaminants including arsenic, molybdenum, nickel, aluminium, and iron sulfates with sulfuric acid. In the first stage treatment process, slaked lime slurry is added to the process to achieve a terminal pH of between 3.5 – 5 over a series of neutralisation tanks. Ferric sulfate is also added based upon molar ratio of total iron to arsenic and vanadium. This results in the formation of predominantly ferric oxyhydroxides, aluminium hydroxides, and gypsum. Ferric and aluminium hydroxides at this pH readily adsorb oxyanion species such as molybdate, arsenate, sulfate, phosphate, vanadate, and other species. The competitive adsorption of each of these species is considered in this model, along with coprecipitation of other minerals, such as nickel molybdate. The treated stream leaving the reaction tank is sent to a clarifier where a thickened slurry containing the precipitated contaminants is produced. A portion of this slurry is recycled to the front of the process for precipitation seeding. The balance of the slurry is sent to tailings treatment. The treated overflow from the clarifier proceeds to high pH treatment.

High pH treatment

In this stage, a mixture of ferric sulfate and lime is added to the influent low pH clarifier overflow. Slaked lime is added such that the terminal pH is between 10 – 11. Ferric sulfate is again added to achieve a target ratio of total iron to dissolved contaminants. At these conditions, and with the addition of ferric sulfate, nickel hydroxide is formed along with ferric hydroxide, gypsum, and other minerals. For this raffinate, it was found that a 15 Fe : 1 V molar ratio was required to remove the vanadium to acceptable levels.

Tailings treatment

This circuit receives slurry from both the low and high pH circuits. Lime is added to the treated slurry prior to thickening and disposal. The tailings thickener underflow reports to a licensed tailings management facility while the overflow is sent back to the front of the water treatment circuit. In this analysis, the focus is on the treatment of raffinate. However, in a typical operating mine site, water generated from the consolidation of tailings over time is collected and returned to the water treatment circuit. Along with other site water sources, this results in a complex mixture of water streams which a water treatment circuit must be equipped to treat.

Operational considerations

A ferric lime water treatment process presents challenges which require both operational and design controls to ensure reliable operation. The process relies upon accurate measurement of pH, which requires frequent probe cleaning and calibration. Because slaked lime is used to remove sulfates, these circuits are often operated in supersaturated gypsum conditions. This results in equipment scaling issues which can, over time, significantly reduce the residence time of neutralisation tanks, reduce flow capacity in pipes, damage pump seals, etc. Furthermore, the effectiveness of these circuits depends on effective solid liquid separation in clarifiers and sand filters. To address these issues, process enhancements are often introduced, such as:

- in-circuit recycling of clarifier underflow to promote seeding
- introduction of air into tanks for enhanced mixing (e.g. Pachucas or mixed tanks with air spargers) and recycle of solution
- filtration/polishing for removal of entrained solids from clarifier overflow
- upcomers in tanks to enhance residence time and reduce channeling.

These modifications also impact the circuit chemistry. For example, the recycle of underflow causes changes in the pH of the tanks receiving the underflow, while the addition of air to tanks affects the tank redox potential. These types of effects can be modelled when using a comprehensive

thermodynamic model such as that employed in this work. Such effects can be very important for the removal of redox sensitive contaminants of potential concern, such as arsenic and selenium.

PHREEQC model selection

The suitability of the PHREEQC software for modelling of treatment of uranium milling raffinate and geochemical controls on uranium mine tailings is well established by Robertson et al. (2014), Liu and Hendry (2011), Moldovan (2006) and others. The minteq.v4.dat database was selected for this work because it contains all of the required species. It uses the Davies equation for activity coefficients and thus is sufficient for dilute solutions encountered during the neutralisation of sulfuric acid raffinate with slaked lime.

Baseline simulation

Table 5 gives the pH conditions that were selected as baseline operating conditions. These were selected based upon review of neutralisation test work reported in Ryan and Alfredson (1976), Robertson et al. (2014), and Liu and Hendry (2011) and are typical for this type of water treatment circuit.

Table 5 - pH setpoints used in the water treatment circuits

Circuit	Terminal pH
Low pH circuit	4
High pH circuit	11
Tailings treatment circuit	10

In addition, clarifier performance was also incorporated into the analysis. A nominal clarity of 20 mg/L total suspended solids in the low pH and high pH thickener overflows was assumed. The tailings thickener overflow clarity was assumed to be 100 mg/L. The tailings thickener is expected to have a slightly higher entrained TSS in the overflow due to its primary function of tailings consolidation.

The tanks were modelled with air addition to ensure fully oxidising conditions. This was accomplished by ensuring that oxygen was in excess in the calculation. This ensured that iron was fully oxidised, and therefore maximised the generation of ferric hydroxide. This was done in the model by ensuring that excess oxygen was present in the vent streams from the low and high pH reaction tanks.

Results of the baseline simulation are presented in Table 6. The baseline condition simulation predictions compared favourably to guideline limits obtained from various sources (Government of Canada Justice Laws Website, 2023; Environment and Climate Change Canada, 2016). Thus, these process parameters were deemed suitable for use as a baseline simulation.

No tuning of the thermodynamic model was done for this work. The only modification involved suppression of formation of crystalline oxides, such as Fe_2O_3 for example, in favour of amorphous oxide hydroxide minerals, such as $\text{FeO}(\text{OH})$, which are expected to form at these conditions. The database is used as-is to provide an estimate of the performance of the water treatment plant assuming chemical equilibrium. It is important to understand the inherent limitations associated with using an equilibrium assumption and use model results appropriately.

Analysis of the solids in the low pH, high pH, and tailings circuits provides insight into the roles of these circuits. Table 7 presents the distribution of elements in the secondary mineral and surface complexation phases for each of the major solids streams in the process. Each phase adds up to

100%, i.e. the sum of the secondary mineral or the sum of the surface complexation elemental distribution adds to 100%. This is calculated from many minerals and surface complexation species.

The secondary minerals formed in the low pH treatment circuit, given in Table 7 (a), are predicted to be comprised predominantly of calcium sulfate with aluminium and iron oxyhydroxide secondary minerals. The elemental distribution of surface complexation species on the alumina and ferrihydrite surface is also shown. The high concentration of phosphate in the feed solution and its affinity for sorption results in a significant fraction of available ferric oxide surface sites being occupied by phosphate. Arsenate, molybdate, and sulfate are other sorbed anions of note. Cation adsorption also occurs to a limited extent, including calcium, copper, and lead.

The high pH circuit tailings solids are presented in Table 7 (b). The secondary minerals formed in this circuit are predominantly calcium sulfate with magnesium, iron, and aluminium hydroxides. The formation of copper, nickel, uranium, vanadium, and zinc hydroxide is also calculated. Ferric sulfate is added to this circuit to further enhance removal of vanadium (added at a molar ratio of 15 Fe : 1 V). Analysis of the surface complexation elements indicate the sorption of arsenate and vanadate alongside cations such as calcium, magnesium, nickel, lead, and zinc.

The final tailings solid stream is presented in Table 7 (c). The tailings are a combination of the low pH and high pH solids streams, adjusted with lime addition to pH 10. Thus, the tailings consist predominantly of aluminium, iron, and magnesium hydroxides with various hydroxides of other metals. Calcium molybdate, calcium sulfate, basic calcium phosphate, and barium arsenate are also predicted to form. Surface complexation species are predominantly adsorbed cations alongside sorption of arsenate, molybdate (to a limited extent), sulfate, and vanadate. It is anticipated that neutralisation of low pH solids results in the desorption of molybdate, which is offset by the formation of calcium molybdate.

Table 6 - Results of baseline simulation

Parameter	Baseline
Low pH circuit	
pH	4
Clarifier UF (%sol)	15
Clarifier OF (ppm)	20
High pH circuit	
pH	11
Clarifier UF (%sol)	15
Clarifier OF (ppm)	20
Tailings Circuit	
pH	10
Thickener UF (%sol)	45
Thickener OF (ppm)	100
Effluent	
Flow (m ³ /h)	101
Al (mg/L)	0.53
As (mg/L)	3.74E-7
Ba (mg/L)	3.13E-3
Ca (mg/L)	788
Cl (mg/L)	334
Cu (mg/L)	0.08
Fe (mg/L)	0.47
Mg (mg/L)	2.3
Mn (mg/L)	7.48E-4
Mo (mg/L)	3.32E-3
Ni (mg/L)	0.10
P (mg/L)	0.03
Pb (mg/L)	2.90E-4
SO ₄ (mg/L)	458
Si (mg/L)	3.48E-3
U (mg/L)	2.68E-3
V (mg/L)	0.01
Zn (mg/L)	0.30
Tailings Flowrate (m³/d)	247
Reagent Usage (dry, t/d)	
Lime as Ca(OH) ₂	54
Ferric sulfate	4.3

Table 7 - Predicted elemental distributions in secondary minerals and surface complexation

Element	Content (%)	Element	Content (%)	Element	Content (%)
Secondary Minerals		Secondary Minerals		Secondary Minerals	
Al	5.5	Al	0.12	Al	3.0
Ba	1.39E-4	Ca	18	As	2.46E-5
Ca	13	Cu	0.34	Ba	6.77E-5
Cl	1.08E-4	Fe	2.4	Ca	19
Cu	0.01	H	2.5	Cu	0.13
Fe	7.0	Mg	8.6	Fe	4.5
H	1.7	Mn	1.26E-3	H	2.2
Mn	0.02	Ni	0.03	Mg	2.9
Mo	0.02	O	54	Mn	0.01
O	54	P	0.14	Mo	7.95E-3
P	0.01	S	14	O	54
Pb	3.16E-3	Si	0.02	P	0.45
S	17	U	0.01	S	14
Si	1.3	Zn	0.03	Si	0.70
Surface Complexation		Surface Complexation		Surface Complexation	
As	0.05	As	3.18E-4	As	0.08
Ba	1.04E-7	Ba	1.97E-5	Ba	1.53E-5
Ca	2.31E-3	Ca	38	Ca	12
Cu	0.05	Cu	8.59E-3	Cu	0.06
H	4.2	H	0.28	H	1.9
Mg	1.56E-6	Mg	0.45	Mg	14
Mn	5.27E-8	Mn	2.55E-10	Mn	1.61E-8
Mo	1.12E-6	Mo	7.25E-7	Mo	9.57E-3
Ni	0.01	Ni	5.1	Ni	2.0
O	72	O	42	O	65
P	24	P	5.05E-10	P	1.29E-6
Pb	1.87E-3	Pb	0.11	Pb	0.20
S	0.18	S	1.47E-3	S	0.17
V	1.40E-9	V	13	V	2.6
Zn	3.65E-5	Zn	0.07	Zn	1.1

(a) Low pH

(b) High pH

(c) Tailings

Solid secondary minerals and adsorption species are determined by the PHREEQC model. This allows for insight into the possible mechanisms of mineralogical control for COPCs. The predicted mineralogical controls for baseline conditions are provided for selected elements in Table 8.

Table 8 - Mineralogical controls for selected deleterious elements

Element	Low pH (pH 4)	High pH (pH 11)	Tailings (pH 10)
As	Adsorption	Adsorption	Barium arsenate, adsorption
Mo	Adsorption, copper molybdate	Limited adsorption (not well controlled at high pH)	Calcium molybdate, adsorption
Ni	Limited adsorption (not well controlled at low pH)	Nickel hydroxide, adsorption	Adsorption
Cu	Copper molybdate, limited adsorption	Copper hydroxide, adsorption	Copper hydroxide, adsorption
Pb	Lead phosphate chloride, limited adsorption	Lead hydroxide, adsorption	Adsorption
Zn	Limited adsorption (not well controlled at low pH)	Zinc hydroxide, adsorption	Adsorption

It is noted that mineralogical controls will be a function of raffinate feed chemistry as well as process conditions, and thus, these predictions are specific to the water treatment case being analysed.

Equilibrium model limitations

It is recognised that the assumption of equilibrium may not be valid in some cases. It is known that reaction kinetics may play an important role for lower temperature processes, such as water treatment. Thus, predictions from an equilibrium model should be considered as semi-quantitative. They are useful for identifying trends, and when used appropriately, can be very important for determining where additional test work is required to better understand a water treatment process.

Modelling is a tool to support process design and operation which can be used in conjunction with test work and/or plant data. For example, knowledge of equilibrium and comparison to actual plant data provides very useful insight into the state of a water treatment process. Equilibrium predictions provide a theoretical maximum for the process from which kinetic parameters can be derived based upon a combination of test work, pilot plant and real plant data. As a result, removal efficiencies of contaminants predicted by an equilibrium model may exceed actual water treatment plant performance.

It is notable that the PHREEQC interface with SysCAD allows for adjustment of saturation indices of precipitates. These factors can be used as a tuning factor to account for supersaturation resulting from kinetics.

Simulation of upset conditions

The following upset conditions were simulated to understand the potential variability of effluent quality and volume with typical upset conditions. These upset conditions included:

- deviations in pH of the low, high, and tailings neutralisation circuits

- increase in total suspended solids of the low and high pH clarifier, and tailings thickener overflow
- increase/decrease of the low and high pH clarifier, and tailings thickener underflow solids content
- increase in levels of contaminants to the water treatment feed
- change in oxidation level (set by the addition of air to each reaction tank).

These upset conditions can occur in a real plant due to malfunctioning or improperly calibrated pH probes, sudden changes in flowrates causing clarifier bed upsets, channelling of clarifier liquid into the underflow, changes in ore chemistry and/or upstream process upsets, and plugging of air spargers. By performing sensitivity analysis, one can determine a priori operational controls and ancillary equipment required to ensure reliable operation.

Due to the number of sensitivity analysis runs being performed in this work, each of the above scenarios are discussed separately in the following subsections.

Effect of pH

The effect of pH is presented in Table 9. In this set of scenarios, deviations of pH from setpoint were tested to determine the effect on process key performance indicators for the circuit. The pH of the low pH, high pH, and tailings circuits were adjusted in sequence from their nominal setpoints to see the effect on effluent quality, tailings volume, and various other plant performance indicators. The results are summarised below:

- Decrease in LPT pH: A significant impact on molybdenum removal is seen. This is because the low pH circuit plays a significant role in the removal of molybdenum via adsorption.
- Increase in LPT pH: The removal efficiency of arsenic and molybdenum is significantly improved at higher pH. This is due to improved adsorption efficiency in this pH range and increased precipitation of iron and alumina at higher pH. This indicates a higher pH than 4 is advantageous for this circuit.
- Decrease in HPT pH: Going from pH 11 to 10 in the high pH circuit reduces the effluent concentration of nickel and aluminium. This is due to the amphoteric nature of these metals at pH > 10.5. Thus, moving to a pH of 10 – 10.5 may be advantageous for this circuit.
- Increase in HPT pH: Increasing the pH to 12 in the high pH circuit results in significant solubilisation of aluminium, and thus, this pH is not suitable.

Based upon this sensitivity analysis, it is seen that:

- tight pH control is very important for effective removal of COPCs
- the optimal pH profile is likely around 4.5 for low pH treatment and around 10.5 for high pH.

Effect of clarifier/thickener overflow total suspended solids (TSS)

The effect of clarifier/thickener overflow TSS is presented in Table 10. Clarifier performance can be affected by flow dynamics, flocculent dosage, fines content in the feed, and other factors. As a result, it is important to understand the effect of overflow TSS deviations from expected values to characterise the robustness of a water treatment process. The following observations can be made:

- Maintaining stable, efficient operation of the low pH circuit clarifier is very important for control of molybdenum.
- The high pH circuit clarifier is important for the control of uranium, aluminium, copper, nickel, and zinc.

Based upon this sensitivity analysis, potential operational upsets in the clarifier would be likely to pose issues for treatment of this raffinate. Thus, additional controls such as secondary filtration for TSS removal, sufficient surge capacity (both for stable flow and for contingency storage of off-spec effluent), and other measures to ensure stable operation may be required.

Effect of clarifier/thickener underflow solids

The effect of clarifier/thickener underflow solids is presented in Table 11. The clarifier/thickener underflow affects the water balance rather than the treated water chemistry. As tailings solids content decreases, more pore water is entrained with the tailings, which reduces the total effluent flowrate. Furthermore, the low pH and high pH clarifier underflow density affects flows throughout the circuits.

Table 9 - Effect of pH on water treatment plant performance

Parameter	Baseline	Decrease LPT pH	Increase LPT pH	Decrease HPT pH	Increase HPT pH	Optimal pH
Low pH Circuit						
pH	4.0	3.0	5.0	4.0	4.0	4.5
Clarifier UF (%sol)	15	15	15	15	15	15
Clarifier OF (ppm)	20	20	20	20	20	20
High pH Circuit						
pH	11	11	11	10	12	11
Clarifier UF (%sol)	15	15	15	15	15	15
Clarifier OF (ppm)	20	20	20	20	20	20
Tailings Circuit						
pH	10	10	10	10	10	10
Thickener UF (%sol)	45	45	45	45	45	45
Thickener OF (ppm)	100	100	100	100	100	100
Effluent						
Flow (m ³ /h)	101	101	101	100	101	101
Al (mg/L)	0.53	0.71	0.50	0.08	5.1	0.16
As (mg/L)	3.74E-7	5.99E-7	3.28E-7	3.56E-7	4.45E-7	3.14E-7
Ba (mg/L)	3.13E-3	3.04E-3	3.29E-3	3.14E-3	2.68E-3	3.22E-3
Ca (mg/L)	788	800	787	738	1015	769
Cl (mg/L)	334	334	333	335	334	333
Cu (mg/L)	0.08	0.07	0.06	0.07	0.13	0.07
Fe (mg/L)	0.47	0.42	0.50	0.49	0.47	0.49
Mg (mg/L)	2.3	2.1	2.4	53	1.7	7.0
Mn (mg/L)	7.48E-4	6.02E-3	5.20E-4	2.89E-4	0.02	1.91E-4
Mo (mg/L)	3.32E-3	0.01	2.64E-3	3.30E-3	3.31E-3	2.67E-3
Ni (mg/L)	0.10	9.47E-3	0.09	0.07	0.54	0.06
P (mg/L)	0.03	3.86E-3	0.04	0.03	0.03	0.03
Pb (mg/L)	2.90E-4	1.66E-3	1.68E-5	1.43E-4	0.02	3.72E-5
SO ₄ (mg/L)	458	453	458	506	425	465
Si (mg/L)	3.48E-3	3.32E-3	3.68E-3	3.48E-3	5.60E-3	3.59E-3
U (mg/L)	2.68E-3	2.38E-3	2.80E-3	4.25E-3	2.51E-3	3.12E-3
V (mg/L)	0.01	0.01	0.02	0.01	0.01	0.02
Zn (mg/L)	0.30	0.30	0.30	0.07	4.8	0.12
Tailings Flowrate (m³/d)	247	247	246	245	247	246
Reagent Usage (dry, t/d)						
Lime as Ca(OH) ₂	54	54	54	54	55	54
Ferric sulfate	4.3	4.4	4.2	4.3	4.3	4.2

Table 10 - Effect of clarifier/thickener TSS on water treatment plant performance

Parameter	Baseline	Increase LPT OF	Increase HPT OF	Increase Tails OF
Low pH Circuit				
pH	4.0	4.0	4.0	4.0
Clarifier UF (%sol)	15	15	15	15
Clarifier OF (ppm)	20	500	20	20
High pH Circuit				
pH	11	11	11	11
Clarifier UF (%sol)	15	15	15	15
Clarifier OF (ppm)	20	20	500	20
Tailings Circuit				
pH	10	10	10	10
Thickener UF (%sol)	45	45	45	45
Thickener OF (ppm)	100	100	100	500
Effluent				
Flow (m ³ /h)	101	101	101	101
Al (mg/L)	0.53	0.55	1.1	0.53
As (mg/L)	3.74E-7	8.67E-6	8.55E-6	3.77E-7
Ba (mg/L)	3.13E-3	1.03E-3	3.19E-3	3.25E-3
Ca (mg/L)	788	788	873	788
Cl (mg/L)	334	334	334	334
Cu (mg/L)	0.08	0.07	1.7	0.08
Fe (mg/L)	0.47	0.50	12	0.47
Mg (mg/L)	2.3	2.2	43	2.3
Mn (mg/L)	7.48E-4	8.62E-4	8.26E-3	2.94E-3
Mo (mg/L)	3.32E-3	0.07	3.32E-3	3.32E-3
Ni (mg/L)	0.10	0.01	0.35	0.10
P (mg/L)	0.03	0.03	0.69	0.03
Pb (mg/L)	2.90E-4	2.87E-4	3.22E-3	2.90E-4
SO ₄ (mg/L)	458	458	523	458
Si (mg/L)	3.48E-3	0.01	0.08	3.50E-3
U (mg/L)	2.68E-3	2.60E-3	0.06	2.68E-3
V (mg/L)	0.01	0.01	0.36	0.01
Zn (mg/L)	0.30	0.30	0.44	0.30
Tailings Flowrate (m³/d)	247	247	245	247
Reagent Usage (dry, t/d)				
Lime as Ca(OH) ₂	54	54	54	54
Ferric sulfate	4.3	4.3	4.3	4.3

Table 11 - Effect of clarifier/thickener underflow solids on water treatment plant performance

Parameter	Baseline	Reduce LPT UF solids	Increase LPT UF solids	Reduce HPT UF solids	Increase HPT UF solids	Reduce Tails solids	Increase Tails solids
Low pH circuit							
pH	4.0	4.0	4.0	4.0	4.0	4.0	4.0
Clarifier UF (%sol)	15	10	20	15	15	15	15
Clarifier OF (ppm)	20	20	20	20	20	20	20
High pH circuit							
pH	11	11	11	11	11	11	11
Clarifier UF (%sol)	15	15	15	10	20	15	15
Clarifier OF (ppm)	20	20	20	20	20	20	20
Tailings circuit							
Ph	10	10	10	10	10	10	10
Thickener UF (%sol)	45	45	45	45	45	35	55
Thickener OF (ppm)	100	100	100	100	100	100	100
Effluent							
Flow (m ³ /h)	101	101	101	101	101	97	103
Al (mg/L)	0.53	0.53	0.52	0.53	0.52	0.52	0.53
As (mg/L)	3.74E-7	4.05E-7	3.59E-7	4.04E-7	3.67E-7	3.62E-7	3.81E-7
Ba (mg/L)	3.13E-3	3.27E-3	3.05E-3	3.35E-3	3.09E-3	3.10E-3	3.15E-3
Ca (mg/L)	788	788	788	788	788	788	788
Cl (mg/L)	334	334	335	334	335	335	334
Cu (mg/L)	0.08	0.08	0.08	0.08	0.08	0.08	0.08
Fe (mg/L)	0.47	0.48	0.47	0.47	0.47	0.47	0.47
Mg (mg/L)	2.3	2.3	2.3	2.3	2.3	2.3	2.3
Mn (mg/L)	7.48E-4	1.14E-3	8.03E-4	2.64E-3	8.03E-4	7.60E-4	7.53E-4
Mo (mg/L)	3.32E-3	3.35E-3	3.30E-3	3.34E-3	3.31E-3	3.30E-3	3.33E-3
Ni (mg/L)	0.10	0.10	0.10	0.10	0.10	0.10	0.10
P (mg/L)	0.03	0.03	0.03	0.03	0.03	0.03	0.03
Pb (mg/L)	2.90E-4	3.00E-4	2.83E-4	2.99E-4	3.38E-4	2.85E-4	2.94E-4
SO ₄ (mg/L)	458	458	458	458	458	458	458
Si (mg/L)	3.48E-3	3.79E-3	3.33E-3	3.68E-3	3.40E-3	3.38E-3	3.55E-3
U (mg/L)	2.68E-3	2.70E-3	2.68E-3	2.68E-3	2.68E-3	2.68E-3	2.68E-3
V (mg/L)	0.01	0.01	0.01	0.01	0.01	0.01	0.01
Zn (mg/L)	0.30	0.30	0.30	0.30	0.30	0.30	0.30
Tailings Flowrate (m³/d)	247	246	247	247	247	342	186
Reagent Usage (dry, t/d)							
Lime as Ca(OH) ₂	54	54	54	54	54	54	54
Ferric sulfate	4.3	4.0	4.5	4.4	4.3	4.3	4.4

Effect of feed contaminant levels

The effect of feed contaminant levels is presented in Table 12. For molybdenum and uranium, the increase of contaminant levels results in an increase in the effluent concentration, as expected. In the case of aluminium, solubility control as $\text{AlOH}(\text{SO}_4)$ in the low pH circuit and $\text{Al}(\text{OH})_3$ in the high pH circuit resulted in no change in aluminium concentration in effluent. Note that this change did increase the total tailings volume. In the case of arsenic, a decrease in arsenic is seen. However, this is because the ferric sulfate dosage is tied to the arsenic concentration in raffinate in this process simulation model, and thus, the arsenic concentration decreased. Note as well that the tailings flowrate increased significantly due to increased ferric sulfate dosage.

Effect of oxidation level

Oxidising conditions are generally beneficial for the removal of many COPCs in a ferric lime water treatment circuit, although there are exceptions. Baseline simulations (and all other simulations to this point) were conducted with ample air provided to each reaction tank to ensure fully oxidising conditions. This was done by adding enough air that excess oxygen was measured in the vent from each tank. The effect of air addition is observed by turning it off. A significant increase in uranium, copper, manganese, and iron in the final effluent is observed when no air is added. The model predicts a net benefit of having air addition in the process.

Table 12 - Effect of raffinate contaminant levels on water treatment plant performance

Parameter	Baseline	Increase Mo	Increase U	Increase Al	Increase As
Raffinate Chemistry					
Mo (mg/L)	5.0	10	5.0	5.0	5.0
U (mg/L)	2.8	2.8	10	2.8	2.8
Al (mg/L)	1 840	1 840	1 840	3 000	1 840
As (mg/L)	0.50	0.50	0.50	0.50	1.0
Effluent					
Flow (m ³ /h)	101	101	101	100	101
Al (mg/L)	0.53	0.53	0.53	0.52	0.53
As (mg/L)	3.74E-7	3.74E-7	3.74E-7	3.79E-7	7.49E-7
Ba (mg/L)	3.13E-3	3.12E-3	3.13E-3	2.89E-3	3.13E-3
Ca (mg/L)	788	788	788	788	788
Cl (mg/L)	334	334	334	335	334
Cu (mg/L)	0.08	0.07	0.08	0.07	0.08
Fe (mg/L)	0.47	0.47	0.47	0.45	0.47
Mg (mg/L)	2.3	2.3	2.3	2.2	2.3
Mn (mg/L)	7.48E-4	7.48E-4	7.59E-4	7.40E-4	7.53E-4
Mo (mg/L)	3.32E-3	6.19E-3	3.32E-3	3.54E-3	3.31E-3
Ni (mg/L)	0.10	0.10	0.10	0.10	0.10
P (mg/L)	0.03	0.03	0.03	0.03	0.03
Pb (mg/L)	2.90E-4	2.90E-4	2.98E-4	3.08E-4	2.94E-4
SO ₄ (mg/L)	458	458	458	458	458
Si (mg/L)	3.48E-3	3.49E-3	3.48E-3	3.31E-3	3.49E-3
U (mg/L)	2.68E-3	2.69E-3	9.15E-3	2.56E-3	2.68E-3
V (mg/L)	0.01	0.01	0.01	0.01	0.01
Zn (mg/L)	0.30	0.30	0.30	0.30	0.30
Tailings Flowrate (m³/d)	247	247	247	258	247
Reagent Usage (dry, t/d)					
Lime as Ca(OH) ₂	54	54	54	54	54
Ferric sulfate	4.3	4.3	4.3	4.4	4.4

Table 13 - Effect of air addition on water treatment plant performance

Parameter	Baseline	No Air
Low pH circuit		
pH	4.0	4.0
Clarifier UF (%sol)	15	15
Clarifier OF (ppm)	20	20
High pH circuit		
pH	11	11
Clarifier UF (%sol)	15	15
Clarifier OF (ppm)	20	20
Tailings circuit		
pH	10	10
Thickener UF (%sol)	45	45
Thickener OF (ppm)	100	100
Effluent		
Flow (m ³ /h)	101	101
Al (mg/L)	0.53	0.52
As (mg/L)	3.74E-7	3.45E-7
Ba (mg/L)	3.13E-3	3.05E-3
Ca (mg/L)	788	787
Cl (mg/L)	334	334
Cu (mg/L)	0.08	0.98
Fe (mg/L)	0.47	0.65
Mg (mg/L)	2.3	2.2
Mn (mg/L)	7.48E-4	0.06
Mo (mg/L)	3.32E-3	3.42E-3
Ni (mg/L)	0.10	0.10
P (mg/L)	0.03	0.04
Pb (mg/L)	2.90E-4	2.06E-4
SO ₄ (mg/L)	458	458
Si (mg/L)	3.48E-3	3.40E-3
U (mg/L)	2.68E-3	0.05
V (mg/L)	0.01	0.01
Zn (mg/L)	0.30	0.30
Tailings Flowrate (m³/d)	247	246
Reagent Usage (dry, t/d)		
Lime as Ca(OH) ₂	54	54
Ferric sulfate	4.3	4.4

Conclusions

Thermodynamic analysis of a water treatment plant was carried out using the PHREEQC interface in SysCAD. This model allows for the incorporation of precipitation of secondary minerals as well as adsorption to multiple sorption types, in this case alumina and hydrous ferric oxide. The model was used for a typical ferric lime treatment process for raffinate, the composition of which was obtained from test work available in the open literature (Ryan and Alfredson, 1976).

The use of sensitivity analysis allows for virtual testing of a proposed water treatment process. To test the robustness of the process, typical operational upsets include pH deviation, clarifier

overflow/underflow solids content variability, feed composition changes, and oxidation level were introduced. Based upon this, the following conclusions can be made:

- pH must be tightly controlled for effective removal of deleterious elements. Based upon analysis of the trends, a pH of 4-5 for the low pH circuit and a pH of 10-11 for the high pH circuit would be recommended for further testing.
- Optimal clarifier performance is crucial for control of deleterious elements in the final effluent. There was significant sensitivity of several COPCs on clarifier performance, and thus, for this particular raffinate, secondary filtration and/or contingency surge and storage capacity may be required to guarantee process performance.
- Changes in feed chemistry have an expected effect on performance. It is important to closely monitor the feed chemistry of the raffinate and make process changes to ensure consistent effluent quality. Such changes include increase of ferric sulfate reagent addition and adjustment of pH targets, as appropriate.
- Oxidation level is very important for removal of many of the COPCs as well as for optimal reagent consumption. It is therefore prudent to ensure effective operation of air spargers during operation of the water treatment plant. It would be prudent to have oxidation reduction potential monitoring in the water treatment process.

A comprehensive chemical equilibrium model is a powerful tool to understand trends in a water treatment process. It is understood that results from this analysis show trends from which observations can be made. As with any model, results require verification/validation against test and pilot plant data. However, a rigorous model such as the one employed in this work provides insight into areas of concern in a process which can help to guide further investigation. In conjunction with test work, pilot plant, and operating data, it can provide information on chemical kinetics, optimal process setpoints, and many other insights. Importantly, it can identify potential areas for concern in a process where additional test work and/or design considerations may be required.

References

- Dzombak, D.A. and Morel, F.M.M. (1990) "Surface Complexation Modeling – Hydrous Ferric Oxide", John Wiley & Sons.
- Environment and Climate Change Canada (2016) "Federal Environmental Quality Guidelines – Vanadium" [online], Available at: <https://www.ec.gc.ca/ese-ees/default.asp?lang=En&n=48D3A655-1>, Accessed: June 2023
- Goldberg, S. (2002) "Competitive Adsorption of Arsenate and Arsenite on Oxides and Clay Minerals", *Soil Sci. Soc. Am. J.* 66(2):413–421.
- Government of Canada Justice Laws Website (2023) "Metal and Diamond Mining Effluent Regulations" [online], Available at: <https://laws-lois.justice.gc.ca/eng/regulations/sor-2002-222/FullText.html>, Accessed: June 2023
- HydroGeologic, Inc. (1999) "Diffuse-Layer Sorption Reactions for use in MINTEQA2 for HWIR Metals and Metalloids" [online], Available at: <https://www.epa.gov/sites/default/files/documents/SUPPLE2.PDF>
- Liu, D.J. and Hendry, M.J. (2011) "Controls on 226Ra during raffinate neutralization at the Key Lake uranium mill, Saskatchewan, Canada", *Applied Geochemistry* 26(12): 2113-2120.

Moldovan, B. (2006) "Fate and Transport of Arsenic in Uranium Mine Tailings: Rabbit Lake Mine", PhD Thesis (unpublished), University of Saskatchewan, Saskatoon, Canada.

Robertson, J., Shacklock, K., Frey, R., Gomez, M. A., Essilfie-Dughan, J. E. and Hendry, M.J. (2014) "Modeling the Key Lake uranium mill's bulk neutralization process using a pilot-scale model", Hydrometallurgy 149: 210-219.

Robertson, J.M. (2017) "Geochemical Characterization of Aluminum and Magnesium Secondary Mineral Phases in Uranium Mill Tailings", PhD Thesis (unpublished), University of Saskatchewan, Saskatoon, Canada.

Ryan, R.K. and Alfredson, P.G. (1976) "Liquid Wastes from Mining and Milling of Uranium Ores – A Laboratory Study of the Treatment Methods", Australian Atomic Energy Commission.

SysCAD (2023) "SysCAD Documentation" pages related to PHREEQC [online], Available at: https://help.syscad.net/PHREEQC_Model_Configuration, https://help.syscad.net/PHREEQC_Reactor, https://help.syscad.net/TCE_Species_Mapping, Accessed: June 2023

United States Geological Survey (2021) "PHREEQC Version 3" [online], Available at: <https://www.usgs.gov/software/phreeqc-version-3>, Accessed: June 2023

Optimised Process Performance Through the Modernisation of an Existing Thickener with Recent Innovations in Technology

A McIntosh¹, D Hodsden², E Jarvie³ and S El-Masry⁴

2. Senior Product Manager - Thickening, Metso, Australia, andrew.mcintosh@metso.com
3. Process Engineer, West Cliff Coal Preparation Plant, South32, David.Hodsden@south32.net
4. Senior Design Engineer, Metso, Australia, edward.jarvie@metso.com
5. Technical Support Expert, Metso, Australia, sherif.el-masry@metso.com

ABSTRACT

Thickeners and clarifiers are used in mineral processing for solid liquid separation. Water is recovered for reuse within the plant. Thickened underflow is collected from the thickener for further processing or placement in a tailings storage facility where the stability of that material is of high importance for environmental and safety reasons.

One aspect critical to thickener performance is the feed system. That is where the incoming feed slurry is received, conditioned, and mixed with flocculant which enhance the materials' settling characteristics. Superior feed system design enables thickeners to be operated at high unit area loading rates and deliver improved process performance; high underflow density and optimal water recovery. For this reason, the thickener feed system has been referred to as 'the heart of thickener performance' (Triglavcanin, 2008).

In today's world, water is becoming an increasingly scarcer and more valuable resource in most locations where minerals processing occurs. The importance of reliable, high-performing thickener technology, therefore, continues to grow.

Another important consideration is that, as society moves towards circularity and reducing waste, the reuse of existing installed equipment through modernisation and upgrades is growing in importance in the world of minerals processing.

These demands drive thickener suppliers to invest in research and development and strive to create industry-leading technologies to achieve more sustainable thickener designs that take technical performance to the next level.

This paper discusses recent innovations in thickener feed system design. Following extensive research and development, including validation through modelling and test work, this innovative design was implemented during recent upgrades of existing thickeners. These upgrades enabled the existing equipment to be repurposed to operate at higher capacity, while achieving improved process performance.

Implementation of a recent upgrade is discussed in detail - including before and after operational results of thickener performance at site.

INTRODUCTION

The West Cliff Coal Preparation Plant (WCCPP) was opened in 1976 and is owned and operated by Illawarra Metallurgical Coal Operations (a subsidiary of South32). It is located 25 km northwest of Wollongong and 75 km south of Sydney, near the town of Appin in New South Wales, Australia.

The operation of the WCCPP is tied to the underground mine at Appin that produces premium quality hard coking coal used for steelmaking. As a by-product, a small amount of energy coal is also produced.

WCCPP is one of two washeries operated by South32 Illawarra Metallurgical Coal, the other being the Dendrobium Coal Preparation Plant in Port Kembla.

WCCPP was built in 1975 and initially designed to process 2 Mt of run of mine (ROM) coal per annum (mtpa). Production has increased over time, with a 2008 snapshot showing that processing had reached 3 Mt (a 50% production increase). Production at time of publishing is around 4-4.5 Mt/y, which is greater than double the initial nameplate capacity.

Following processing at WCCPP, coal is transported by road and rail to Port Kembla in Wollongong where it is used by the BlueScope Port Kembla Steelworks or distributed overseas through the Port Kembla Coal Terminal.

WCCPP uses thickeners for solid/liquid separation (dewatering). Namely in coal product (flotation concentrate) thickening and tailings thickening duties. Water is recovered for reuse within the plant, whilst thickened underflow is collected from the thickeners for further processing before going to market (as a product) or tailings storage. Performance of the thickeners directly affects the plant's water and energy consumption as well as the processes adjacent to the thickeners.

This paper discusses an upgrade of the existing coal product thickener which took place in late 2022.

EXISTING 24.4M COAL PRODUCT THICKENER

This section introduces the existing thickener before the upgrade and describes challenges presented due to its age and the condition of components, and opportunities to improve thickener process performance.

24.4m Coal Product Thickener

West Cliff's coal product thickener is 24.4 m internal diameter and was originally supplied and installed during the year 1975, making it 47 years old at the time of upgrade in 2022. The original supplier of the thickener is no longer in the business of supplying or upgrading thickeners.

Existing Thickener Components and Condition Before Upgrade

The thickener was a centre column style thickener with a half-length access bridge from the tank periphery to the thickener's central drive / maintenance area, as shown in Figure 1. The bridge also supported instrumentation, control and electrical cabling, as well as air and water services.



Figure 1: Existing WCCPP coal product thickener before upgrade (emptied)

The existing thickener showed signs of wear and tear consistent with 47 years of operation, signalling the need for an overhaul and refurbishment. The thickener tank is a steel wall / concrete floor construction. The steel tank walls were assessed as part of the upgrade pre-works and determined to need significant repair or replacement works in the near future.

The thickener rakes and drive cage were also assessed to be in need of refurbishment.

Thickener process duty before upgrade

The main slurry feed stream to the thickener is flotation concentrate which is received from the flotation circuit via the overflow from Concentrate Thickening Cyclones. The thickener also receives filtrate and cloth wash streams from the horizontal belt filters.

Process loading to the thickener had increased significantly over time; in line with plant total throughput increases and various upgrades, including addition of a flotation circuit in 2010.

Data on the original thickener design process loadings was not available. However, data from site informs that at the time of proposing the upgrade during 2019 the thickener was receiving nominally 50 dt/h solids feed rate. This was proposed to increase to a nominal 120 and maximum 143 dt/h solids feed rate after the upgrade in line with the WCCPP overall processing capacity.

From a process design perspective, certain critical components such as the thickener feed system and overflow launders would experience hydraulic loadings beyond the original duty for which they were designed in the proposed future operating conditions. This meant acceptable process performance could not be realistically expected if the existing design of critical internal components was maintained at the increased loading.

By today's standards the existing 24.4 m diameter tank is considered an appropriate size for the upgrade duty. The slurry feed rate and dry solids feed rate at the nominal upgrade duty resulted in an internal liquor rise rate of 2.6 m/h and a solids-loading rate of 0.26 t/m²/h. Those loadings are

within the typical sizing recommendations for this thickening application.

Thickener Overflow and Process Water Reuse

Thickener overflow reports to the thickener overflow sump via an open overflow launder and is reused as process water within the WCCPP. As such, the quality of the thickener overflow is important to flotation circuit recoveries and a certain minimum standard of overflow water quality must be achieved. Excessive froth loading on the existing thickener limited flotation reagent dosing due to its effect on overflow quality and created product spillage risk during thickener froth out events.

Thickener Underflow

The underflow from the thickener reports to the three horizontal belt filters via dual underflow pumps (in duty/standby configuration). The pumps and piping are housed in an access/underflow tunnel ('caisson') beneath the concrete thickener floor. The horizontal belt filters further dewater the coal product after thickening.

Sites specification for the thickener underflow density before and after the upgrade was minimum 35% solids by weight (% solids w/w). Acceptable underflow quality was routinely achieved prior to the upgrade.

Flocculant Dosing

WCCPP uses an anionic flocculant at a concentration of approx. 0.22%w/v which is the 'as received' concentration from the flocculant make up plant.

Flocculant dosage to the thickener was not varied with the thickener feed rate. This is uncommon in thickener operation and presented an opportunity to optimise flocculant consumption.

A feedwell sampling and slurry settling rate measurement instrument was fitted to the bridge. Typically, this instrument is used in the automated thickener process control regime to control flocculant dosing by measuring the settling rate of flocculated samples taken from the feedwell. This determines if the flocculant dose is optimised for both the feed rate and physical characteristics of the material currently being fed to the thickener.

The feedwell sampling and slurry settling rate measurement instrument had not been functional for an undetermined period of time. This instrument was therefore not used in the thickener control. Rather, flocculant addition was manually controlled and generally maintained at a constant flow rate.

Increase or decrease to flocculant dose rate were made manually based upon operator visual observations of the bed level via a series of taps positioned vertically on the thickener sidewall. When opened those taps provide operators visual feedback on solids concentration at different heights within the thickener, as the material flows from the taps.

Thickener Drive and Risks Associated with Parts Availability.

The existing drive was a multi-pinion geared slewing bearing style drive mounted on the central drive / maintenance platform on top of the existing centre column. It is understood that the drive had previously been upgraded at some stage during the thickener's life however details of that upgrade were not available.

A major concern noted by South32 prior to the upgrade was the risk posed by possible failure of the thickener drive. Due to age of the thickener, drive replacement parts had become unavailable. This was deemed to present a critical risk to WCCPP production in the future. This key concern initially prompted site to consider upgrading this thickener.

Thickener Feedwell Design Prior to Upgrade

The existing feedwell was somewhat typical of 'conventional' feed system designs at the time the thickener was constructed. It featured an open-bottom design with a perforated annulus at the discharge zone, as can be seen in Figure 2.



Figure 2: Original thickener feedwell (prior to upgrade)

It was apparent that increases in plant loading over time resulted in flows to the thickener that exceeded the original design duty of the existing feedwell. Additionally, the existing feedwell design is relatively outdated by today's standards.

Existing Thickener Upstream Feed Arrangement

The feed slurry stream was gravity fed from the cyclone overflow hopper directly to the thickener feedwell. The elevation between the cyclone overflow hopper and the thickener feedwell was approximately 4000mm over a relatively short span (refer figure 3).

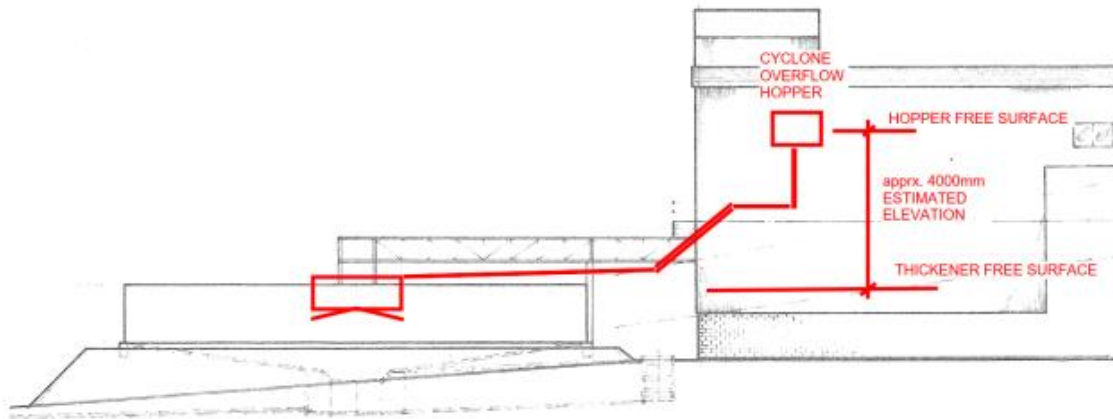


Figure 3: Schematic showing thickener upstream feed arrangement, note the significant elevation drop to thickener.

The significant fall in the pipework over a relatively short span created a high energy launder flow stream that reported to the thickener feedwell inlet at an estimated velocity of 5.5 m/s. In best practice this should be avoided as the high velocity causes feed slurry to present to the thickener feedwell with high hydraulic energy and turbulence. This generates significant froth and excess shear energy which can damage flocculated aggregates. This is detrimental to flocculation, gravity settling and overall thickener process performance.

Froth Management before upgrade

The existing thickener was fitted with several froth suppression elements to manage the froth present on the thickener surface. This included duckbill sprays mounted on one side of the bridge; a 'spilling weir' water curtain on the opposite side of the bridge; feedwell froth suppression sprays; and a rotating froth boom spanning between the feedwell and overflow froth baffle at the tank wall. This configuration is shown in Figure 4.

Froth on the thickener surface was consistent with industry expectation for a relatively challenging coal flotation thickener application. However, operators noted that at times when excessive froth accumulated during process upsets in the flotation circuit, it could take considerable time to be brought back under control. The impact of froth on the thickener surface and its negative impact on plant process water quality along with the risk of uncontrolled product spillage was determined to be a limitation to further optimising performance in the flotation circuit through increasing flotation reagent dosing.

A circumferential froth baffle was supported from the tank wall to prevent froth from discharging into the overflow launder. WCCPP operations installed a cut-out in the froth baffle close to the overflow discharge point, allowing accumulated froth to discharge into the overflow. This was understood to have been a solution to excessive froth build up resulting from the inability to manage froth accumulation within the thickener. This compromised overflow clarity but mitigated the risk of solids building up in the overflow launders and potentially uncontrolled product spillage from the thickener.



Figure 4: Existing Coal Thickener Before Upgrade of bridge and froth management, note the waterfall style froth suppression curtain on the left-hand side of the centre well and rotating froth boom

Key Drivers for the upgrade in summary

South32 project documentation summarised key drivers for the upgrade as:

- existing thickener approaching end of serviceable life
- upgrade thickener components to suit increased WCCPP production capacity
- improved reliability
- common wear/spare parts with tailings thickener as far as practicable
- upgrade thickener features and technology
- reduce froth and solids carry over in overflow liquor stream
- improved thickener performance and controllability

UPGRADE DESIGN AND IMPLEMENTATION

The West Cliff Coal Product Thickener upgrade was implemented in three phases namely:

- scoping and feasibility
- detailed engineering
- supply and Installation.

The sequence and execution of each phase is critical to the equipment performance and the overall project success and satisfaction of all stakeholders. After a review of upgrade implementation options Metso was selected as the preferred technology partner to implement the thickener upgrade and tie-in scope described in the following sections. South32 WCCPP and Metso worked closely as a project team to achieve the project objectives.

Phase One – Scoping and Feasibility

The Scoping and Feasibility phase is primarily focused on identifying project motivations, requirements, and goals to formulate a targeted solution. The Feasibility component addresses both technical and commercial aspects through early engineering, clear definition, and pricing.

Stakeholder Discussions and Project Mapping

Early discussions and project mapping meetings involved representatives from the South32 project execution team, WCCPP operations personnel and technical and project delivery representatives from Metso. These parties mapped out key considerations including:

- the end owners' key project drivers
- South32 and Metso project delivery processes
- project execution methods, scheduling, and sequencing
- supply strategies and preferences
- technical specifications
- equipment process design criteria
- operational requirements and feedback from existing equipment operation
- technical equipment requirements and configurations

Thickening Test work

Dynamic thickener test work is a highly valuable and low-cost method of assessing thickener performance across a range of both current and future operating conditions. Test work enables correct thickener configuration, definition of operating parameters and benchmarking of expected performance. (Arbuthnot, 2008),

Samples of thickener feed slurry were carefully collected upstream of any chemical dosing equipment to provide representative samples of feed the upgraded thickener is required to process. Plant process water was also collected. All samples were transported to the Metso laboratory in Perth, Western Australia.



Figure 5: - 99 mm Diameter Lab Scale Thickener used for laboratory dynamic thickener test work.

During the thickener test work the slurry samples were prepared to reflect the future design operating conditions of the thickener. The feed slurry solids concentration was adjusted, and the lab scale test unit (see Figure 5) is operated at rise rate and solids loading rates reflective of the design operating conditions of the full-scale thickener at the specified upgrade duty.

The dynamic thickener test work parameters were:

- feed solids loading rate 0.26t/m²/h
- feed solids concentration 11%w/w
- liquor rise rate 2.30 m/h
- flocculant dose 40g/t (Magnafloc 10)

The slurry characteristics measured during testing informing that the material flocculated optimally at feedwell densities up to 12% solids w/w. The test work showed that the material tested could achieve an operating underflow density of 47.3% solids w/w and an improvement in overflow clarity was feasible in the full-scale thickener after upgrading.

Process Design Criteria

Coal processing plants tend to experience relatively large variations in plant feed rates and coal recovery, noting that these plants commonly process material from various seams, with variations in ROM physical properties.

This presents challenges when defining the operating process envelope. The thickener upgrade was specified to operate with relatively large variations in solids feed rate (dtpH) and feed slurry solids concentration.

The design criteria nominated a maximum thickener feed density of up to 16.6% solids w/w. Thickener test work indicated that feed solids concentrations above 12%w/w would be difficult to process and that a feed slurry dilution system would have been required. These systems utilise

liquor from the surface of the thickener to reduce the solids concentration in the feedwell.

It was identified that modifications could be made to the plant flow sheet to re-route the low solids concentration filtrate return and cloth wash return streams from the coal product filters to a new thickener feed tank. This modification facilitated dilution of the thickener feed stream from the maximum 16.6%w/w down to 10.3%w/w feed solids concentration thus mitigating the need for a dilution system within the thickener. This simplifies the thickener configuration and operation.

Metso and WCCPP process engineers produced a conservative envelope of process design data scenarios with consideration of thickening test work results, current WCCPP operating conditions and future operations at WCCPP upgraded capacity. These scenarios were captured in a Project Process Design Criteria document.

Clearly defining and agreeing the Project Process Design Criteria document at this early stage is an important step in ensuring the upgraded equipment will meet the performance expectations of all stakeholders, and in de-risking subsequent project stages.

The South32 – Metso project team agreed on three process scenarios to define the overall design operating envelope for the WCCPP Coal Thickener upgrade:

- current operation (2 of 3 modules)
- nominal design (3 of 3 modules)
- max design (3 of 3 modules, at maximum solids loading and volumetric flow rates)

Assessments of Existing Equipment Condition

WCCPP had conducted routine asset integrity assessments of the existing Coal Thickener, including visual inspections and ultrasonic thickness testing. This good record of historical assessments allowed for rates of degradation to be estimated as an input into the planning of the upgrade works.

Options for repairs due to the poor condition of the existing upper tank wall and launders were considered. However, the existing tank overflow system also had insufficient capacity for the nominated upgrade duty. To reduce shutdown site works and schedule, a solution of replacing the complete upper tank wall section including overflow launders was decided upon. This satisfied the requirement for wall repairs as well as achieving the required overflow capacity increase.

Full replacement of the existing bridge, rake drive and raking mechanism was agreed upon as the most economical solution to the general poor condition of those existing structures and the issues with end of life / parts availability with the existing drive unit.

It was decided to replace the existing centre column style bridge and drive combination (which featured a relatively complex and outdated multi pinion drive) with a modern full span bridge type design that features a rake drive with a single planetary gearbox. This substitution is a cost-effective upgrade solution for older centre column thickeners as it offers benefits including:

- utilising a rake drive with lower cost commercially available modern planetary gearbox configurations (these were not available when the original drive was designed)
- full span bridge provides improved maintenance access
- full span bridge provides improved safety when a second point of egress is required
- full span bridge design presents opportunity to complete tie-ins such as external bridge supports while the thickener is still in operation, prior to the shut down for the upgrade works. This eliminates complicated works to repair or replace a centre column during a shutdown window.

Scope Definition and Scope Split

Whilst the work scope was primarily driven by South32's focus towards asset end of life management, and upgrade to ensure reliability, availability and processing capacity, Metso's experience with Coal concentrate thickening enabled identification of significant potential performance improvements with relatively minor additions to the scope of works. Examples are modifications to the upstream feed hydraulic system within the washery, and the inclusion of a large external thickener feed tank.

The project team defined the thickener upgrade scope as:

- new full span truss bridge complete with hydraulic power unit, rake drive and 300mm rake lift system
- new thickener instrumentation including marshalling panel, rake speed sensor, rake torque sensor, rake height sensor, feedwell sampling and slurry settling rate measurement instrument and ultrasonic bed level instrument
- new feed system complete with Metso's Reactorwell™ advanced feedwell design, feedpipe, flocculant dilution and dosing system and froth suppression spray system
- new external feed tank
- new rake mechanism complete with low torque rake arm profile, rotating froth booms and underflow discharge cone scraper
- replacement of the top 1100 mm tank wall section complete with froth baffle, overflow launder and discharge system and replacement bridge stools to suit new bridge

This scope of work is indicated in Figure 6.

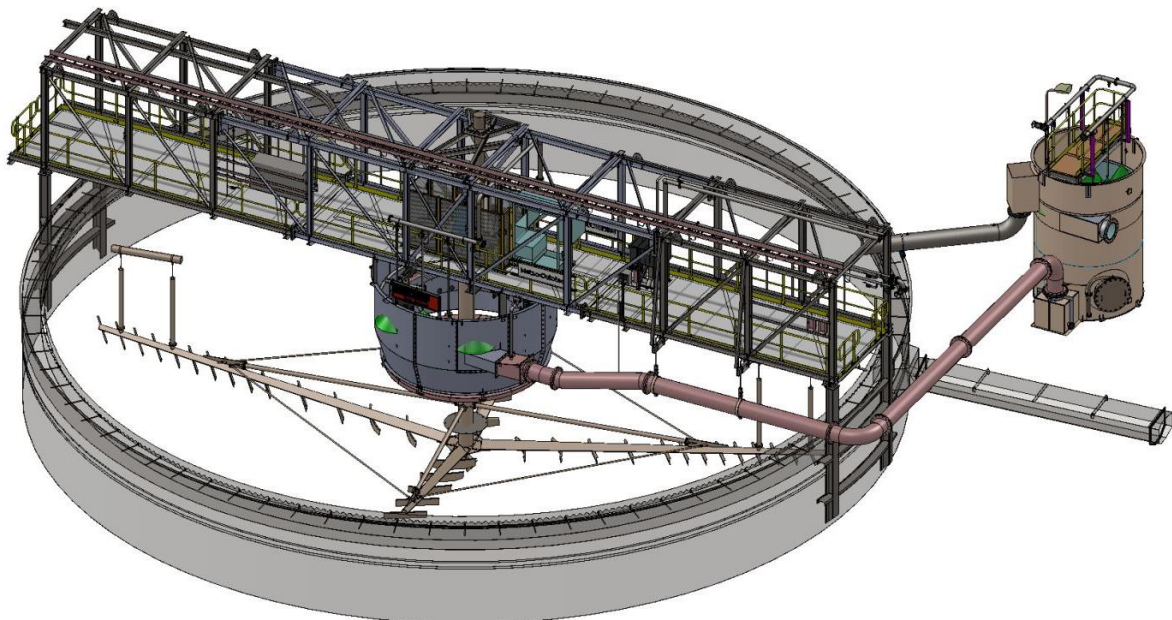


Figure 6: 3D model of new upgraded equipment (View looking Northeast)

The project team worked closely to identify and include additional components such as air and water services and walkway lighting in the equipment supply package to aid in the equipment operability, minimise site installation works and mitigate the need for ad-hoc post installation modification.

Phase Two – Detailed Engineering

Detailed engineering was then carried out to convert the concepts into detailed designs and fabrication drawings sufficient for final design and stakeholder reviews and ultimately fabrication, delivery and installation planning.

3D Laser Scanning

Limited original fabrication information, undocumented as-built modifications and installation tolerances all pose significant design and installation risk for brownfields projects. The most effective method to manage design and installation risk for integration of existing equipment is to utilise 3D laser scan survey and building information modelling (BIM) techniques. This provides an accurate representation of the current state of existing infrastructure that can be interrogated, reviewed and shared between multiple stakeholders.

Figure 7 shows a view generated from the 3D laser scan data showing the existing thickener including half-length thickener bridge and ring gear drive system supported on central support column, and the complexity of the plant piping and interfaces. This gives a good indication of the level of detail and usefulness of information captured using this technology.

The 3D laser scan was a critical step in the project allowing fast, accurate and well considered engineering designs along with buildability and installation planning.



Figure 7: View generated from 3D laser scan data showing pre-upgrade thickener with half-length bridge

Integration of Thickener Feed System with Plant

Feed slurry presentation to the thickener feedwell is critical to any thickener's performance. Entrained air or froth and excessive slurry velocity significantly reduce the performance of thickener feed systems and can lead to excessive wear rates.

Often the characteristics of the feed slurry at the thickener inlet are determined by the upstream hydraulic and piping arrangement. Careful consideration of the upstream layout is important, not only for the thickener performance but also to ensure modifications within the thickener equipment package do not adversely affect the upstream hydraulic system – for example causing upstream equipment, tanks and launders to overflow or spill.

The existing thickener arrangement at the WCCPP had many features which resulted in poor

thickener feed characteristics at the feedwell. The feed slurry presented to the thickener as high velocity launder flow with significant volumes of froth and air entrained in the slurry stream. This caused surging, burping and splashing and created significant volumes of froth that were difficult to manage within the thickener.

Metso completed a detailed review of the upstream hydraulic arrangement from the thickener inlet flange up to the cyclone overflow hopper. It was agreed that an alternative piping route and the installation of a feed de-aeration tank external to the thickener was required to ensure the best thickener upgrade performance and maintainability.

Feed System Optimisation

While WCCPP were generally satisfied with the existing coal thickener process performance, Metso had identified that improvement in the feed system arrangement and components would significantly enhance thickener performance.

Benefits of the new feed system arrangement primarily relied on careful transport of the feed slurry from the washery building down into the thickener, significant froth management improvements, more advanced preparation and dosing of flocculant, including Metso's Floc-Box secondary dilution just before the feedwell, and the implementation of Metso's latest technology advancement - the Reactorwell. These features are shown in Figure 8.

Key expected benefits from upgrading to best practice designs and the best available modern thickening technology were:

- reduced flocculant consumption
- reduced froth loading
- increased flotation reagent dosing flexibility
- improved overflow clarity and reduced recirculating load in washery
- improved thickener operational stability and reduced operator intervention
- reduced wear rates and maintenance

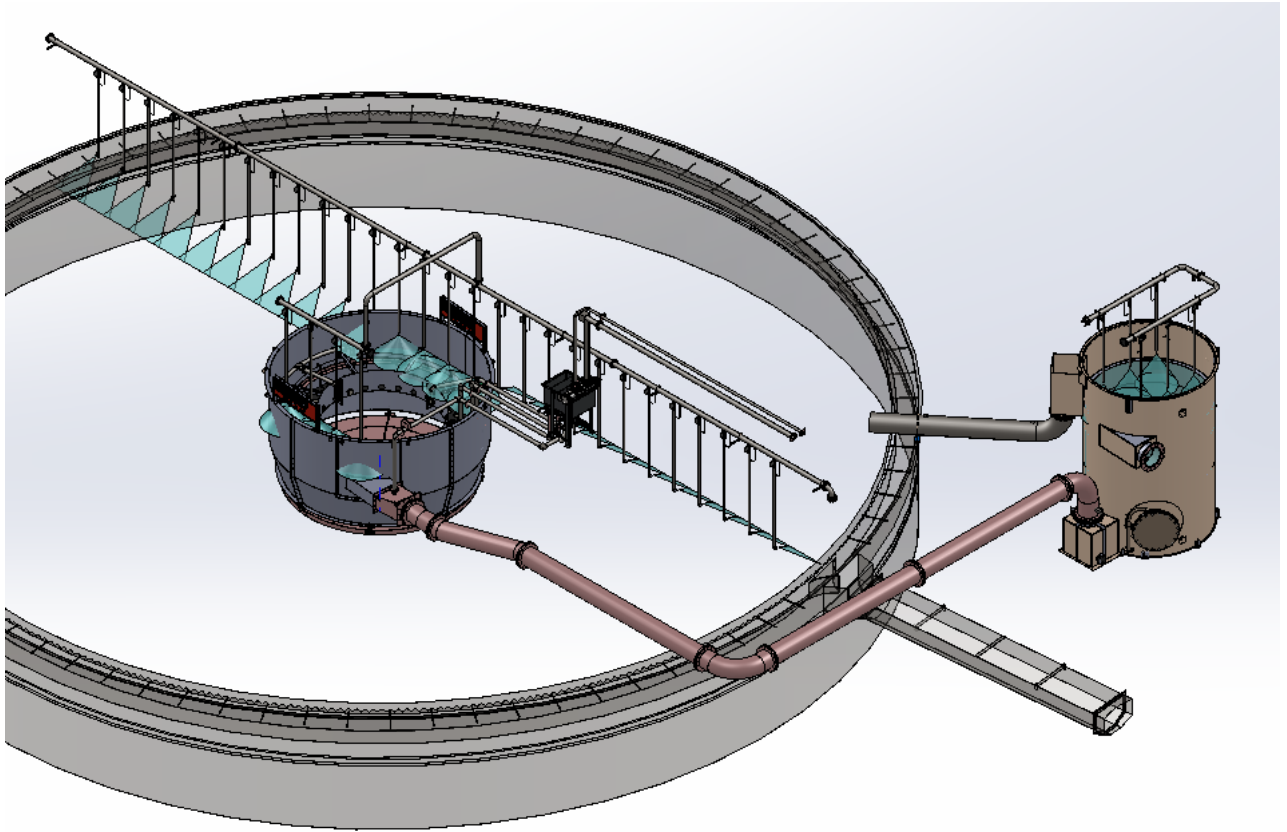


Figure 8: Upgrade feed system & froth management components. Including Reactorwell, external feed de-aeration tank & froth suppression sprays (bridge, drive & raking mechanism omitted for clarity)

External Feed De-Aeration Tank

The new external feed de-aeration tank is a key component that is highly effective at dissipating excessive feed hydraulic energy, separating and knocking down froth and conditioning the feed stream to achieve ideal slurry presentation to the thickener feedwell.

This tank also provides an effective location to perform dilution of the feed slurry by combining two low solids streams from the coal product filters to achieve the required feed concentration at the feedwell for optimal flocculation. Combining these streams in this location also enables good mixing of the multiple streams upstream of the thickener feedwell.

The feed tank is relatively large with an internal diameter of 3 m, overall height of 4.4 m and nominal residence time in the order of 60 s. Typically, achieving high residence times in a gravity slurry system is difficult due to the risk of solids sedimentation. However, the coal thickener feed slurry has a low settling velocity (in the order of 1 m/s) due to the combination of the low solids density of coal, low feed solids concentration and particle size which affords greater design flexibility.

The low settling velocity allows many tank design features that are highly favourable for managing feed slurries with high volumes of froth. A tangential slurry inlet at the free surface provides the optimal method of feed energy dissipation without creating additional froth loading. The bottom outlet nozzle sits below the thickener free surface, meaning that the feed tank is not free draining to the thickener. This ensures short circuiting does not occur, and that the discharge remains as full pipe flow being submerged well below the thickener free surface minimising entrained air and froth.

The relatively large residence time and surface area maximise froth separation and froth knock down by the froth suppression sprays.

The feed tank tangential inlet is highly advantageous for slurry handling however design reviews identified that this feature also concentrates high wear rates at the inlet area. To manage anticipated high wear rates the feed tank was fitted with a ceramic tile wear protection system. Ceramic tile lining is not common in thickener feed systems however South32's experience is that it will provide a long wear life and reduce operating costs over the equipment life.

The feed tank is designed for safe and effective maintenance including upper and lower maintenance platforms and a manhole through the tank sidewall. Wear rates in the downstream slurry system will be significantly lower because of the energy dissipation in the feed tank. South32 assessed this to be substantially beneficial to operations since the maintenance occurs in this accessible feed tank. This is significantly simpler than maintenance of the suspended feedpipe and feedwell within the thickener.

Metso Reactorwell Technology

This upgrade was the first installation of the new Metso Reactorwell technology in Australia. Metso identified this application as an excellent candidate for the novel technology and shared research and development presentations and modelling demonstrating benefits of the new design to key South32 stakeholders early in the project.

Like many mining operations, South32 operates in a sensitive environmental area and are cognisant of the importance of optimising water management and recovery through employing best technologies and practices. It was also identified that Reactorwell has potential to operate at reduced flocculant dosing rates presenting an opportunity to minimise carbon footprint (in addition to operational cost reduction). After careful review and consideration South32 agreed to adopt this new planet positive technology in the upgrade.

The new Reactorwell design retains some features of Metso's previous generation feedwell designs; namely a section for mixing and energy dissipation; a section for aggregate growth and solids distribution; proven gravity dilution systems; and a closed bottom design.

As can be seen in Figure 9, in addition to the proven design features the Reactorwell features a unique feed inlet trough populated with multiple slurry nozzles to form a slurry distribution system. This system transforms the rotational energy of the incoming feed into vertical flows to create an evenly mixed lower energy zone outside of the feed trough where flocculation and aggregate growth occur. Viduka et al (2021) discuss in detail how this trough design introduces a new mode of mixing compared to previous feedwell technology and is the most advanced feature of the Reactorwell design.



Figure 9: 3D rendering of the new Metso Reactorwell technology.

As discussed in Heath (2010), Computational fluid dynamics (CFD) modelling techniques are employed (Figure 10) in the assessment and development of thickener feedwell technologies to optimise the feedwell design and achieve balance between the multiple functions of the thickener feedwell including:

- controlling and utilising kinetic energy in the feed slurry coming to the feedwell from the upstream plant
- balancing the energy in the feedwell to achieve 'zones' of high and lower energy in different areas of the feedwell as required for efficient mixing of flocculant and to subsequently promote aggregate growth
- controlling the flow of supernatant liquor in the thickener into the feedwell to ensure that the correct solid concentration is achieved, and that uncontrolled dilution does not occur
- effective solids hold up to achieve adequate mixing and aggregate formation whilst preventing short circuiting of un-flocculated material
- even distribution of well flocculated aggregates out of the feedwell to ensure utilisation of the full area inside the body of the thickener.

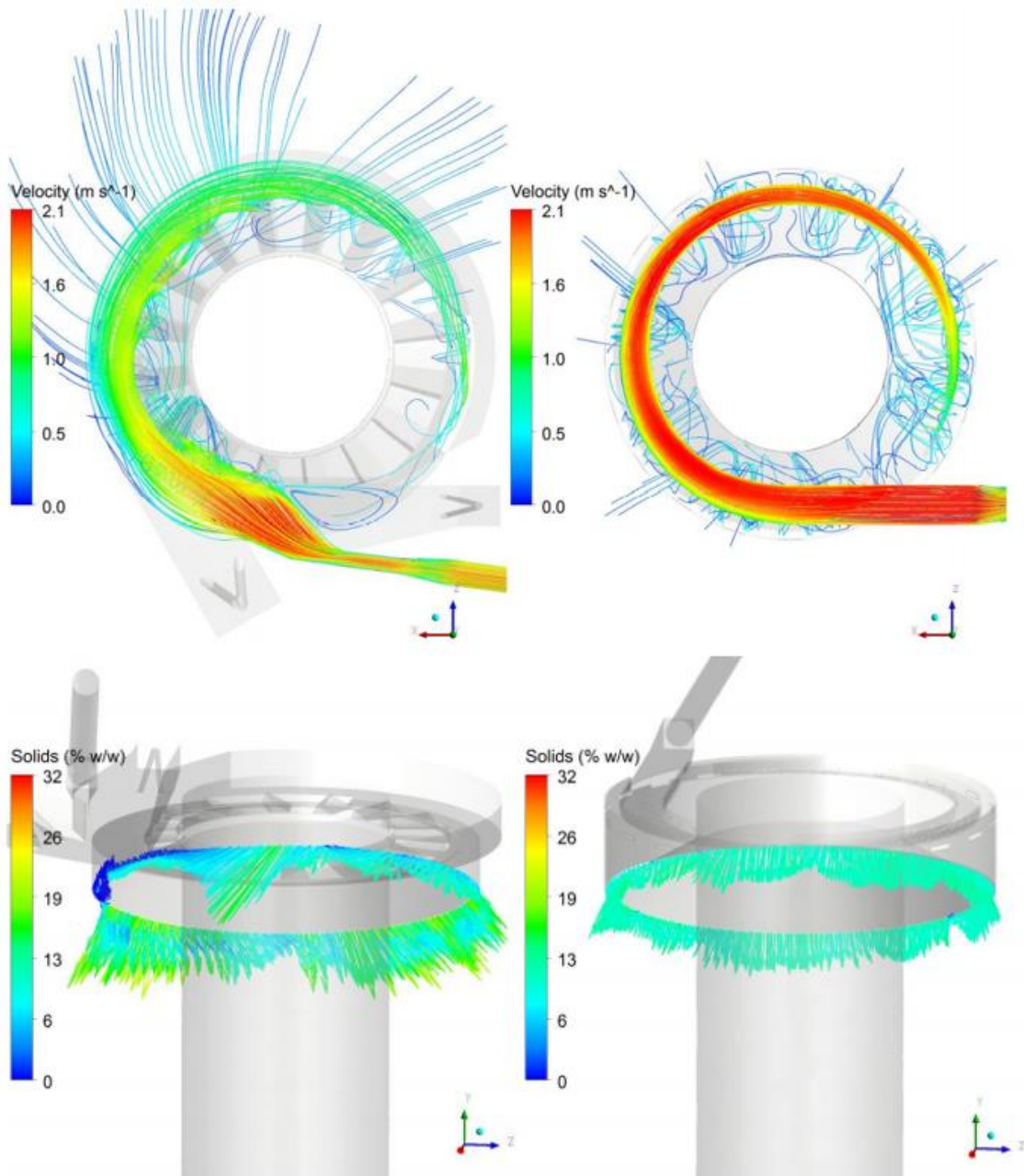


Figure 10: Computational Fluid Dynamics (CFD) modelling of relevant design parameters during the Reactorwell research and development process. **Top left** – Velocity streamlines after 45 seconds in previous feedwell design. **Top right** – New Reactorwell velocity streamlines after 45 seconds, note velocity (red) is maintained through inlet trough. **Bottom left** – Outlet symmetry in previous feedwell design. **Bottom Right** – New Reactorwell outlet symmetry, note distribution is far more homogenous.

Froth Management

Despite the best efforts in design and slurry handling it was expected that moderate volumes of residual froth would accumulate in the feedwell and on the thickener surface from time to time depending on the operation of the flotation circuit and feed material characteristics.

Based on extensive experience with thickener froth management systems Metso designed an effective spray arrangement which features high volume full cone spray nozzles in the external feed tank and the feedwell; locations where the froth is contained in a small area without mechanical transport by booms or similar.

On the thickener surface the froth is less contained and is mechanically transported by rotating froth booms. In that area inclined flat fan sprays were used to provide more concentrated froth destruction as the froth that is pushed by the booms passes under the bridge mounted sprays.

The system is designed with access and fittings to enable easy maintenance of each individual spray nozzle while in operation.

Integration of Thickener Overflow System with Plant

The specified upgrade duty resulted in increased volumetric overflow rates. This necessitated assessment of the existing overflow system. The overflow is discharged from the Thickener free surface through a gravity flow hydraulic system with multiple hydraulically coupled sub-systems down to the process water tank (hopper). Overflow liquor is discharged from the process water tank through a pump.

Each of the coupled sub systems has a high probability of interacting with each other and must be assessed both in isolation and as part of the complete hydraulic system to ensure satisfactory operation. This multi-system assessment included:

- thickener overflow weir
- thickener overflow launder
- thickener overflow nozzle
- overflow duct between thickener and overflow sump/hopper
- overflow hopper.

The existing plant layout afforded very minimal excess gravity head (elevation) between each of the hydraulic sub systems. This is typical of a processing plant where throughputs have increased, and process water storage volumes have been maximised already, with the highest possible storage tank operating levels. Increasing the flow rate capacity of the existing overflow hydraulic system required development of more complex non-standard hydraulic system elements; as is often the case with brownfields upgrades of gravity hydraulic systems.

Site walkthrough and 3D scan reviews identified relevant plant interfaces and highlighted physical constraints such as:

- level of thickener could not be raised due to adjacent structures
- elevation drop between thickener overflow outlet and overflow hopper was minimal, allowing no scope to increase overflow piping/duct work sizes or gradients
- overflow duct to overflow hopper passed through the washery building allowing little scope for modification of geometry, elevation and gradient
- overflow hopper diameter and height are very small, modification without impacting pump control and performance was not feasible.

To increase the volumetric flow rate of the existing overflow hydraulic system the following modifications were implemented:

- new thickener overflow weir and launder
- new thickener overflow outlet complete with an energy conserving flow diverter

Integration of Thickener Underflow System with Plant

The increased throughput on the Coal Thickener also results in higher volumetric underflow rates.

An assessment of the expected volumetric underflow rates and their discharge from the thickener was necessary to ensure sufficient discharge capacity is available. Sufficient discharge capacity is required to avoid thickener solids inventory accumulating faster than it can be discharged, and overloading the thickener. This can manifest in thickener “bogging” events where the rake is unable to rotate due to solids build up, resulting in expensive downtime and clean out of the tank contents.

Operating scenarios in the Project Process Design Criteria were reviewed alongside data from test work including anticipated underflow densities and underflow rheology measurements. A summary of the expected operational requirements for a range of underflow solids concentrations and thickener solids loadings was produced. South32 assessed the expected operational requirements against the existing underflow discharge system empirical operational data to perform a “by difference” assessment of the capacity of the existing system.

It is noted that the resulting underflow nozzle discharge velocity would be considered high at the highest volumetric discharge scenarios. Typically, the underflow withdrawal arrangement would be modified to reduce this velocity and avoid risks such as rat holing of material inside the thickener, excessive nozzle wear rates and pump suction losses.

In this case, due to the expected low frequency of operation at these high volumetric flow rates it was decided that modification to the system would be delayed and addressed as part of a future upgrade of the underflow discharge and pumping system.

Spares Commonality with Existing Equipment

South32 had previously engaged Metso to upgrade the WCCPP Tailings Thickener and were highly motivated to pursue commonality between the Tailings and the new Coal Thickeners, with primary focus on the drive unit, wear parts and spares inventory.

Commonality of mechanical arrangements was also seen as beneficial to operations and maintenance.

The thickening test work identified that the Coal Thickener rake drive duty required significantly less torque than the Tailings Thickener duty. A lower torque drive arrangement was proposed for the Coal Thickener upgrade, however, the project team identified benefits in selecting a drive with commonality to the Tailings Thickener.

This allowed for a reduction in spares inventory and de-risked maintenance operations.

Design Collaboration and Reviews with Operational Personnel

The upgrade design process captured unique and valuable feedback from WCCPP plant operations personnel. Multiple design reviews were held where detailed 3D models were overlaid into 3D laser scans of the existing plant and equipment as indicated in Figure 11.



Figure 11: Laser scan images showing before upgrade arrangement versus final upgrade design models.

This facilitated design modifications and scope inclusions that accommodated site specific operational procedures; lessons learnt from previous projects; simplified installation; and minimised post installation modification by site personnel. Operator specified features incorporated into the upgrade scope included:

thickener bridge walkway extended to full length and full width to improve access for overflow launder clean out

- thickener bridge extended to provide monorail load landing area facilitating load transfer from overhead monorail to site mobile crane
- service air and service water headers along full length of the bridge with multiple hose points
- electrical cable tray and routing to simplify installation works
- electrical field start/stop and isolators to simplify installation works
- additional instrumentation to reduce reliance on operator manual checks, including rake

- speed sensor and ultrasonic bed level instrument
- positioning feed tank and inlet pipework to regain safe access within the washery building.

This process and stakeholder input was critical to the upgrade success and satisfaction of all stakeholders.

Design for Installation and Supply Strategy

Designing equipment for ease of installation is essential in upgrade projects where shutdown durations must be minimised and installation risks that might cause schedule overruns should be designed out where possible. The project team worked closely to consider installation sequencing, methodology and resourcing and ensure upgrade installation works were completed according to the planned shutdown schedule.

Metso standard thickener designs were adjusted to improve installation including:

- adjustment of bridge height to match existing walkway levels
- supply of piping with short pipe spools and additional length (green) for trimming on site, with loose flanges at one end for site welding
- adjustment of piping interface flanges to match existing plant pipe routes.

To minimise the installation site works the project team agreed to fully fabricate and paint the top wall segment in a workshop relatively close to site and split into as large piece as possible for road transport and handling.

The replacement tank wall top section was designed for ease of fit up and simplified welding. Site surface protection was limited to the weld margins only and a high-quality tank shell weldment was achieved.

The design and orientation of the external feed tank was carefully considered to greatly simplify installation works. The tank was positioned to enable re-use of an existing concrete plinth as the support footing. Additionally, inlet and outlet piping routes were simplified by limiting runs to have bends in a single plane. Existing steel structures were utilised to provide structural pipe supports.

Phase Three – Fabrication, Supply and Installation

The final phase of the upgrade is materialising the scoping and design work into tangible results for the owners and operators through fabrication, purchasing, QA, installation and commissioning.

Fabrication and Supply Considerations for Shutdown Works

Fabrication and procurement quality and scheduling is critical for upgrade projects where shutdown timeframes are limited, and any quality problems can cause duration overruns or installation compromises.

Project procurement and quality management best practices were employed to mitigate project risks, including:

- Project procurement and quality management plans
- Installation test plans
- NDT testing
- Fabrication hold points for QA and witnessing
- Factory Acceptance testing

In addition to these practices trial assembly of the fabricated modules and procured equipment was

an essential step to ensure successful installation. This provided valuable opportunity for witnessing and inspection of the equipment by the designers and installation team, with critical interfaces cross checked against field surveys prior to the shutdown.

Fabrication Planning to Optimise Cost And Schedule

Early project scoping and cost estimate definition was based upon utilising Metso's well-established fabrication and quality management base in China. Metso executes a large volume of thickener fabrication through workshops in China, where a significant in-house project and quality management presence has been set up over the last two decades.

Chinese fabrication is well known for being cost effective. This presents other project quality benefits as the scale of the fabrication workshops and effective labour costs enables more complete trial assemblies of fabricated components.

Additionally, a significant portion of procured components are sourced from, or can be readily freighted to China. This enables benefits of workshop trial assembly of those components with the fabricated components.

While Chinese based fabrication was generally more favourable, South32 had identified an opportunity to carry out installation of the replacement upper tank wall and launder sections during an earlier shutdown if those components could be delivered early. This was achieved by manufacturing those tank wall segments at a fabrication shop that was close to site.

The 'local' fabricator had a good working relationship with WCCPP and was also engaged as the installation contractor. This relationship and elimination of the fabricator/installer project interface was considered beneficial to the project and shutdown planning.

Installation and Shutdown Safety

Any site shutdown activities must be carefully considered and managed so that works can be completed safely and without injury. The South32 - Metso project team and site installation contractors shared a strong commitment to safe work.

In addition to the more common risks associated with planning and completing site works, the project team identified the following risks specific to the Thickener upgrade:

- large mobile cranes performing heavy lifts adjacent to multiple overhead conveyor gantries
- elevated fire risk due to the presence of coal dust and residue along with hydrocarbon reagents
- multiple contractor work groups interacting closely due to shutdown time constraints
- limited original as built drawings and equipment masses were available for demolition planning
- isolation and lock outs across multiple work groups with the requirement for frequent energisation/isolations
- hazardous materials including coal and coal dust and potential for interaction with lead based paints and asbestos due to the age of the WCCPP

Installation Works

Minimising plant outages is a key objective in planning site works to be completed during a plant shutdown. The thickener upgrade was estimated to require a shutdown in the order of seven to ten days, depending on the inclusion of night shifts. South32 could not readily accommodate that shutdown duration.

It was therefore decided to split the installation over two shorter duration shutdowns along with increased pre-works while the plant was operating.

The first shutdown was utilised to upgrade the tank wall top section complete with overflow discharge system. The first shutdown was scheduled for a duration of five days and utilised five day shifts and five night shifts.

Activities in the first shutdown included:

- tank draining and cleaning of accumulated solids
- tank wall surveys
- marking of cut lines
- demolishing and removal of original tank wall top section
- lifting into place of wall panels complete with overflow launder sections
- temporary welding in place
- final welding was completed after confirming satisfactory fitting of all sections
- non-destructive testing of welds
- blasting and application of surface protection
- the new thickener overflow discharge chute was installed and the existing overflow hopper modifications made.

The first shutdown was successfully completed in five days and four hours.

Prior to the second shutdown many pre-works and installation tasks were completed while the WCCPP was operational. This reduced the duration of the second shutdown. Five day shifts were utilised to complete a number of tasks including:

- Installation of new bridge mounting stools
- Modification of existing pipe routes, cable trays and washery building cladding to facilitate installation
- Installation of the new external feed tank, feed tank support structure, and sections of new piping
- Pre-assembly of new Reactorwell, new rake mechanism and the new thickener bridge

The second shutdown was utilised to perform the majority of the thickener component upgrades and included significant demolition and installation works. The second shutdown was scheduled for five days, also utilising day and night shifts.

Activities in the second shutdown included:

- tank draining and cleaning
- demolition and removal of existing bridge, feed system, rake mechanism, rake drive system and central support column
- lifting of the complete pre-assembled rake mechanism into the thickener and placement onto hardwood dunnage
- lifting of the Reactorwell over the rake mechanism driveshaft and set down atop of the rake mechanism on dunnage
- the pre-assembled bridge was lifted as a single assembly onto the bridge stools.
- The new internal feed system and rake mechanism components were then lifted into their final positions and fastened in place as shown in Figure 12.
- fit out of the remaining minor components including rake drive, flocculant dosing system, froth suppression system, instrumentation, wiring and termination.
- Finally, plant tie ins for the piping and access walkways were completed and the equipment readied for dry commissioning.



Figure 12: Coal Product Thickener at completion of installation.

The second shutdown was successfully completed in five days, with an unrelated extension to the WCCPP shutdown of one day providing additional time to complete non-critical commissioning tasks.

The total shutdown duration for the upgrade was in the order of ten days. It should be noted that separation of the works into two shutdowns incurred additional duration due to additional isolation, clean out, preparation and mobilisation tasks.

Commissioning

Dry and wet (process) commissioning were completed according to Metso standard procedures and checklists.

It is worth noting that in Metso's experience wet commissioning of a thickener after upgrading is typically less complex compared to new plant since the majority of the existing plant systems remain unchanged. However, it remains important to methodically work through the steps to bring the thickener back into operation as quickly and successfully as possible.

Overall commissioning proceeded to plan and was deemed successful. However, there were unexpected challenges setting up and integrating the new feedwell sampling and slurry settling rate measurement instrument. Initially this was due to incorrect voltage to the instrument and other electrical and instrumentation (E&I) integration issues. However, once those issues were resolved difficulties were encountered with the vacuum suction and settling of a representative sample of this relatively light and froth prone feed material. At time of writing the South32 – Metso project team are continuing to work through these challenges with support from the instrument supplier.

OBSERVATIONS AND PERFORMANCE DATA AFTER COMPLETION OF UPGRADE

Immediately following commissioning of the upgrade, WCCPP's process and operations team deemed the upgrade to be a success. The following were noted regarding thickener performance after upgrade:

- underflow density consistently meets specification
- the thickener is operating at lower flocculant dosing rates compared to before the upgrade
- froth reduction and improved overflow clarity (refer Figure 13 showing upgraded thickener in operation)
- at times when there is an upset in the flotation circuit, the upgraded thickener is able to recover quickly from frothing events
 - this presented an unanticipated benefit in that site has been able to optimise flotation recoveries by being able to increase reagent dosing without process water quality becoming an issue (as was the case pre-upgrade)
- site is no longer needing to add make up water to improve overall water quality in the circuit
- like for like spares with the Tailings Thickener
- improved, safer access to thickener feed well compared to the original design
- Improved and safer plant access due to re-routing of the thickener feedpipe inside the washery building.

It should be noted that due to commissioning challenges with the feedwell sampling and slurry settling rate measurement instrument, at the time of writing that instrument is not utilised in the flocculant addition control loop as intended. Flocculant addition is currently set and tuned manually, as it was pre-upgrade.

It is believed that there is opportunity to further optimise and decrease flocculant dosing once this control loop is commissioned.



Figure 13: Thickener operating after upgrade, note overflow clarity and low levels of froth on thickener surface.

Analysis of Before / After Upgrade Data

Analysis of the plant distributed control system (DCS) data along with field sampling before and after upgrade supports the reported improvements in operation of both the Coal Thickener and Flotation circuit post upgrade.

The improved functionality of the new feed system to deal with the coal flotation product efficiently and produce consistent performance is reflected evidently in two key elements.

Firstly, the step change decrease in the flocculant dosing observed in the DCS data analysis presented in figure 14.

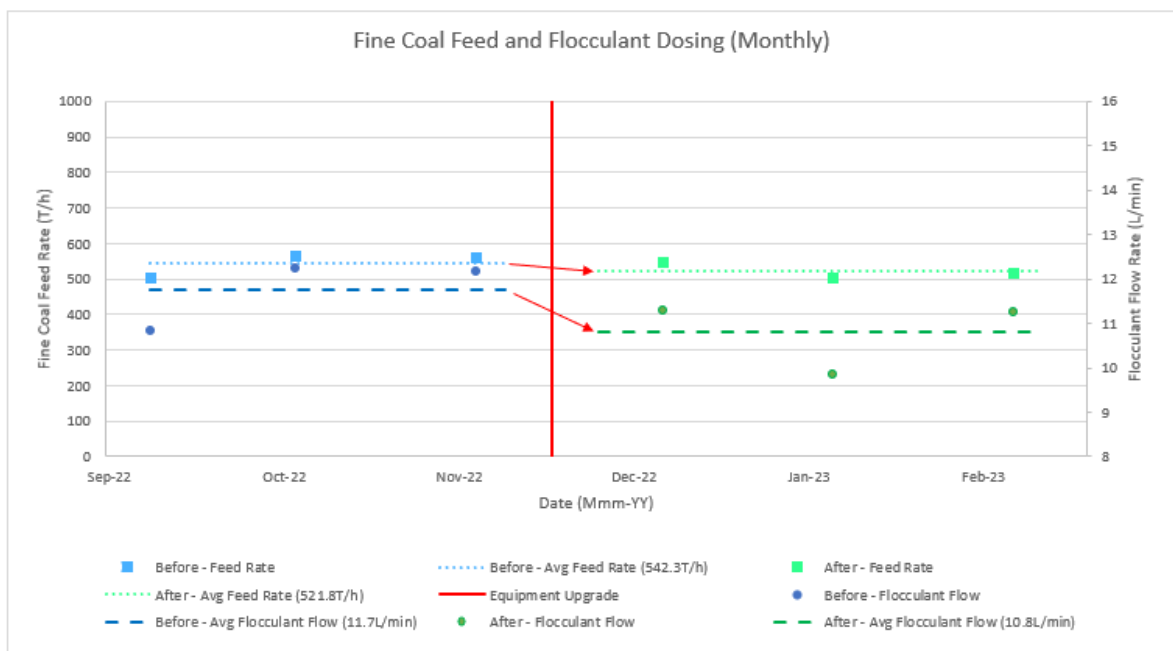


Figure 14: DCS data analysis demonstrating comparable feed rate with step change reduction in flocculant dosing after upgrade

The authors note that flocculant consumption is typically analysed on a grams of flocculant consumed per dry tonne of thickener feed solids (gpt) basis. However, due to the instrumentation arrangement and data availability this was not possible. These graphs are included to show trends to support sites observed improvement in flocculant utilisation.

Secondly, the improved overflow clarity as demonstrated through field sampling and lab analysis of the samples. Overflow clarity is equally important by improving the quality of the process water in reducing the recirculating fine solids in the plant thus improving the washing efficiency. This can be observed in Figure 15 depicting a reduction in concentration of total suspended solids in the overflow.

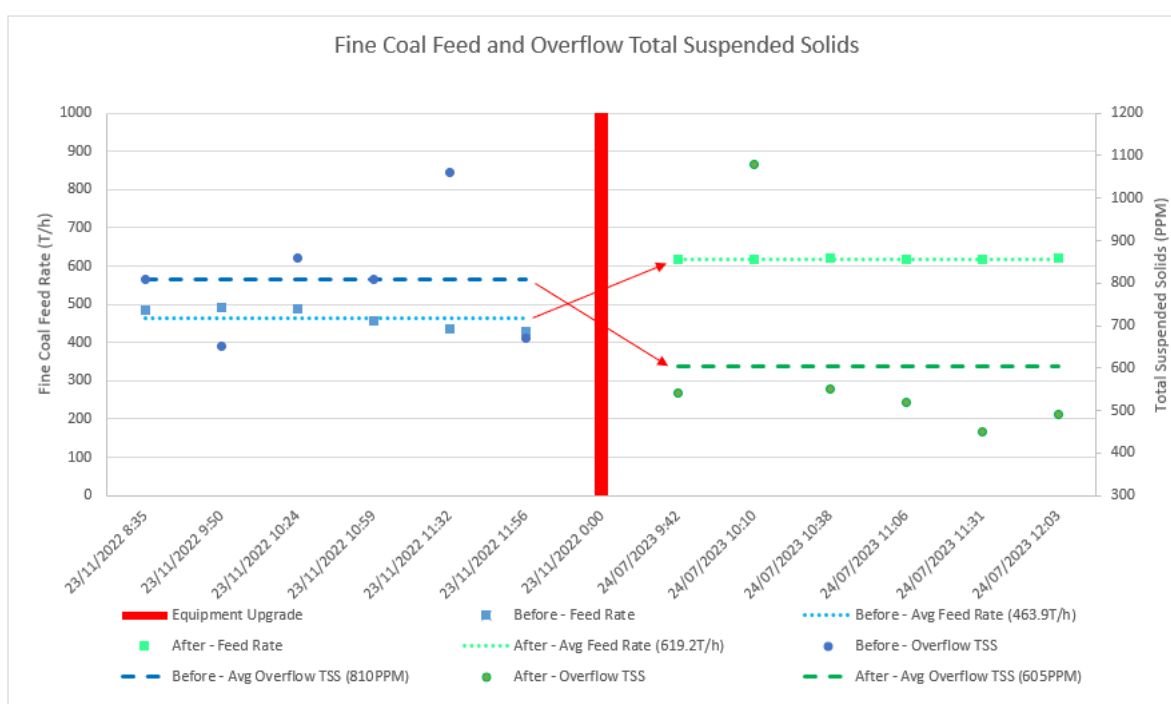


Figure 15: Field sampling and lab analysis of Thickener overflow total suspended solids (TSS) combined with DCS data for feed rate demonstrating increased feed rate with step change reduction in overflow TSS after upgrade.

Thickener underflow density or solids concentration is a key metric of thickener performance. To achieve satisfactory downstream filtration performance the underflow solids concentration must exceed 35% solids (w/w). Operations have reported that underflow solids concentration is satisfying this requirement and lab analysis of field samples confirmed a solids concentration exceeding 40% (w/w).

Benefits to flotation yield

The improved froth management on the thickener has enabled optimisation of the flotation circuit through increased flotation reagent dosing rates without thickener froth out events occurring. Analysis of the flotation yield rates for comparable feed ash content identified an improved trend in the flotation circuit after the Coal Thickener upgrade. Figure 16 shows the improved flotation yield trend line that corresponds to the observed improvement in flotation circuit operation enabled by the thickener upgrade.

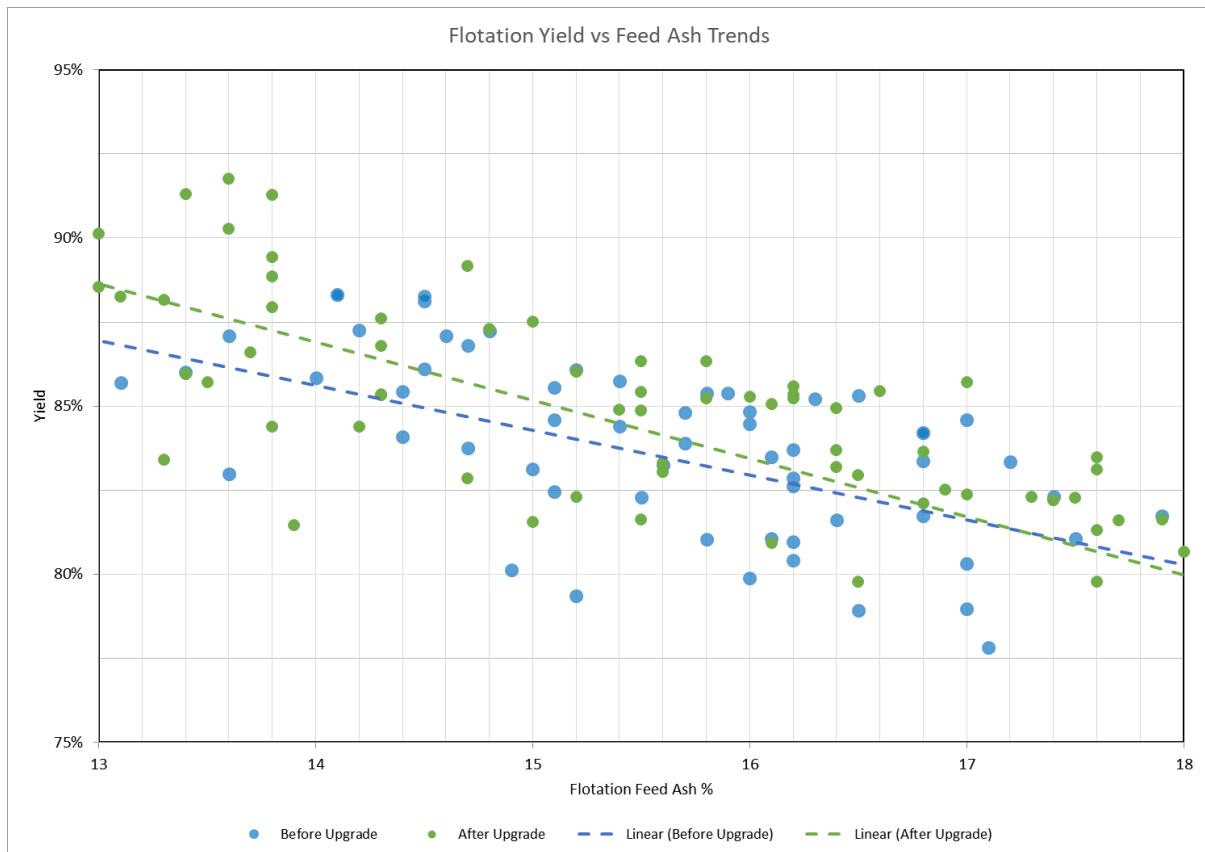


Figure 16: Improved trend in flotation Yield vs. feed ash resulting from improved coal thickener froth management after upgrade.

CONCLUSIONS

This paper demonstrates the thickener performance benefits that were realised, as well as improvements to adjacent processes, through the successful implementation of the coal product thickener upgrade at the West Cliff Coal Preparation Plant.

Underperforming thickeners are common in many processing plants, particularly in concentrate thickening duties where existing poor feed system designs and reagents dosed in flotation circuits can present significant challenges to achieving optimal performance.

Opportunity exists to maximise process performance through upgrades that harness the latest technological developments to bring critical internal components such as the thickener feed system up to today's high levels of performance.

Retrofitting with latest technologies also enables more socially and environmentally friendly processing through factors such as reducing embedded carbon via reduced flocculant consumption and improving water quality and reuse.

These upgrade options should be investigated when considering maintenance and reliability driven improvements which become necessary with the passing of time and aging of installed equipment.

A holistic approach is required for these upgrades, noting that upstream considerations such as feed presentation from the plant as well as impacts on adjacent processes must be considered in the upgrade process.

ACKNOWLEDGEMENTS

The authors would like to thank the entire team involved in the complete upgrade process - from scoping to completion of installation and commissioning. The authors specifically acknowledge Tim Pratt, Richard Emery, and Phil Brown from the South32 West Cliff project team for their roles in driving this project to success.

REFERENCES

Arbuthnot, I, 2008. Sizing paste thickeners from pilot and laboratory data, in *R Jewell, AB Fourie, P Slatter & A Paterson (eds), Paste 2008: Proceedings of the Eleventh International Seminar on Paste and Thickened Tailings*, pp. 97-102 (Australian Centre for Geomechanics: Perth)

Heath, AR & Triglavcanin, RA, 2010. Advances in thickener feedwell design via CFD modelling. *XXV International Mineral Processing Congress (IMPC 2010)*, (Brisbane September 2010).

Triglavcanin, RA 2008. The Heart of Thickener Performance, in *R Jewell, AB Fourie, P Slatter & A Paterson (eds), Paste 2008: Proceedings of the Eleventh International Seminar on Paste and Thickened Tailings*, pp. 63-81 (Australian Centre for Geomechanics: Perth)

Viduka, SM & Henriksson, B 2021. Thickener feedwell internal trough slurry distribution method, in *AB Fourie & D Reid (eds), Paste 2021: 24th International Conference on Paste, Thickened and Filtered Tailings*, pp. 71-78 (Australian Centre for Geomechanics: Perth)

Fine Grinding Circuit for Magnetite Concentrators

S Palaniandy¹ and H Ishikawa²

1. MAusIMM, Global Product Manager, Nippon Eirich Co. Ltd., U4 119 Gardens Drive Willawong QLD 4110 Australia, samayamutthirian@nippon-eirich.com
2. Senior Technical Officer, Nippon Eirich Co. Ltd., Gojinsha Meieki 3 Bldg. 3-9-37 Meieki, Nishi-ku, Nagoya, Aichi: 451-0045 Japan, ishikawa.hidemasa@nippon-eirich.co.jp

ABSTRACT

The steel-making industry is moving towards a low-emission process that requires high-grade ore or pellets. Direct reduced (DR) iron is one of the ways to reduce carbon emissions during steel production. Pellet for DR requires 66% iron content which is higher than the blast furnace-grade pellet. Lower grade ores such as magnetite, typically around 30 – 40% iron head grade, can be upgraded to 69% iron content, suitable for low-emission steel making. These magnetite deposits require fine grinding down to 20 – 25 μm to liberate the magnetite particles and produce a concentrate with 69% iron. For the last 15 – 20 y, gravity-induced stirred mills such as the TowerMill have been used for the fine grinding duty.

Although the technology is well established, there are still opportunities to improve the circuit design based on the learnings from the current operating circuits, especially for highly variable ores. For example, the mill feed configuration, grinding media size, agitator tip speed, classification choice, and configuration (hydrocyclone and/or fine screen) are some of the variables that can be considered in addition to the grinding power requirement.

Fine grinding circuit audits show that there are opportunities to improve the grinding efficiency by 10 - 15% if the circuit is designed considering these operating variables during the circuit design phase. Customised TowerMill design according to project requirements optimises layouts that reduce the steel and concrete requirement. The TowerMill circuit produces a narrow product size distribution, an essential criterion for long-distance slurry pipeline transportation. The tight top size control and minimal ultra-fines generation minimise the wear in the pipe and enhance the pumping process, as well as the dewatering at the port.

This paper discusses the TowerMill circuit design based on the experience gained from a current operating site and recent developments in the TowerMill design that will help to configure circuits to produce high-grade magnetite concentrate.

INTRODUCTION

A shortage of high-grade iron ore presents a significant hurdle for steelmakers who are trying to reduce their carbon emissions. Steel accounts for seven percent of energy sector carbon dioxide emissions. Direct reduced (DR) iron is one of the ways to reduce carbon emissions during steel production. The DR-grade pellet requires 66% Fe content which is higher than the blast furnace-grade pellet. If the global steel industry follows the path to net zero emissions by 2050, then the demand for DR-grade pellets will increase drastically.

Options to resolve this matter include ramping up the mining of higher-grade ores, if available, advancement in green steel-making technology that can use a lower grade ore or concentrating the iron in lower grades ores such as magnetite, which is typically around 30 – 40% iron head grade. Although magnetite has a lower iron content, the magnetic properties within the ore make it easier to concentrate through multiple stages of magnetic separation. Comminution is an important step in magnetite processing to liberate and separate the magnetite from the gangue. Typically, the magnetite concentrator grinds down to 22 – 35 μm for liberation to achieve the required concentrate grade, which is considered energy intensive. Rejecting the gangue (silica) after each grinding stage

through a magnetic separation is common. The gangue rejection helps to reduce the grinding power requirement in the subsequent comminution stages as the feed rates reduce. Usually, the concentrator adopts two or three grinding stages depending on the liberation size that offers maximum gangue rejection.

The concentrators aim for 35 – 50% mass rejection after the first stage of grinding. For example, the Karara Mining concentrator was designed to remove 32% of the mass in the rougher magnetic separation stage and another 30% at the intermediate magnetic separation stage. In this case, only 38% of the mass will be flowing into the fine grinding circuit that is energy intensive for further liberation. The cleaner magnetic separation removes another 11% of the mass after grinding in the TowerMill. This staged gangue rejection offers grinding power reduction in the downstream separations compared to grinding down to liberation size in a single stage followed by single-stage separations. Table 1 shows the magnetite project specifications in Australia. In general, all projects are targeting large plant feed rates up to 10 000 t/h and finer grind sizes between 25 – 35 μm to achieve the concentrate grade of around 65 – 67% Fe.

The comminution energy requirements in these plants are huge, therefore technology selection is crucial including the circuit design. For example, the Hawsons project has an extremely low head grade of 14% Fe aimed to grind down to 25 μm liberation size to achieve the targeted concentrate grade of 69% Fe. The Hawsons ore is competent with an A x b value of 53 but soft for grinding with a Bond ball mill work index of 6.3 kWh/t with a closing screen of 53 μm (Koenig and Broekman K, 2011). The lower Bond ball mill index value is a major advantage for the Hawsons project as the grinding energy requirement will be corporately lower.

Table 1: Magnetite projects specifications in Australia

Project	Plant feed rate (t/h)	Head grade (% Fe)	Concentrate grade (% Fe)	P80 (μm)
Karara	2625	34.0	65	35
WA-3	7950	30.4	67	25
Sino Iron	9396	30.0	65	32
WA -1	1563	32.0	67	32
WA -2	2482-	30.7	67	32
Hawsons	9927	14.0	69	25

All the previously mentioned projects require fine grinding for the liberation of magnetite particles. Besides liberation size, ore variability is another challenge that needs to be considered during the circuit.

REVIEW ON MAGNETITE CIRCUIT DESIGN AND POTENTIAL APPLICATION OF STIRRED MILL

In general, there are three types of magnetite circuits i.e. two stages, three stages, and four stages of grinding circuits. The four stages grinding circuit is mainly implemented in Russia and Commonwealth of Independence (CIS) countries where these plants were developed during the Soviet Union era with a primary rod mill and followed by three stages of ball mills with magnetic separation in between the grinding mills. Recently these plants were undergoing modernisation by implementing stirred mills to

replace the third and fourth stage grinding due to their ability to achieve a finer grind size down to 22 μm and energy efficiency. In other parts of the world, two or three grinding stages are more common. For example, the Sino Iron project Pilbara region was designed with two grinding stages. The autogenous (AG) mill is used for primary grinding and, the secondary grinding is carried out in a ball mill circuit that grinds down to 32 μm . Karara Mine is a magnetite project in mid-west Western Australia that was designed for three stages of grinding, where the primary grinding is carried out in high-pressure grinding rolls (HPGR). The secondary grinding is in the ball mill and the tertiary grinding is carried out in the TowerMill circuit. The FMG Iron Bridge project has an innovative comminution circuit design where the primary and secondary grinding is being carried out using HPGR. The secondary grinding HPGR is closed with an air classifier to produce 100 μm product to the intermediate magnetic separation. The vertical stirred mill is used for fine grinding of intermediate and cleaner magnetic separation. The choice of grinding stages depends on the grind size that is required to remove the gangue minerals. The RMS concentrate is ground in the vertical stirred mill. The choice of the grinding stage depends on the liberation size and amount of material that can be rejected in that separation stage.

ORE VARIABILITY AND CHALLENGES IN FINE GRINDING CIRCUIT DESIGN

Ore variability is a major challenge in any grinding circuit design (Bueno et. al., 2015). In general, the grinding circuit is expected to be flexible and cope with ore with feed variation and produce a consistent product for the separation stage. This includes the variation in ore hardness, feed grade, and feed size. For example, Figure 1 shows the cumulative frequency of the Bond ball mill work index with a closing screen of 75 μm . The Bond ball mill work index values exhibit a wide range from 14 to 24.4 kWh/t, which is considered moderate to very hard. The choice of percentile for designing the grinding mill is essential to cope with the variability and minimise the risk of under-sizing the mill. The main question here is how a fine grinding circuit in a magnetite plant (either secondary or tertiary stage grinding) will cope with such hardness variation, as this value greatly impacts the capital expenditure project. For example, the increase in power was calculated for 12 Mt/y magnetite circuit where the primary mill is AG mill, and the secondary mill is TowerMill technology.

The transfer size is 460 μm at 80% passing, and the targeted grind size is 32 μm . Four Bond ball mill work indexes were considered for the 50th, 80th, 94th, and 98th percentile, as shown in Figure 1. The power requirements were 7175, 9019, 11 428, and 12 504 kW, respectively, after considering the reduction in circuit feed rate (from ore to RMS concentrate) and the gravity-induced stirred mill efficiency factor. A power increase from 26 – 71% is realised based on the choice of the percentile. This aspect directly impacts the project's capital expenditure as the number of mills and all the auxiliary equipment, such as the slurry pumps, hydrocyclone, steel/concrete instrumentation, and installation. A consistent feed to the plant (in terms of ore hardness, feed size, and grade) through mine planning and blending of ores will help to design the plant at an optimum capital expenditure with operational flexibility.

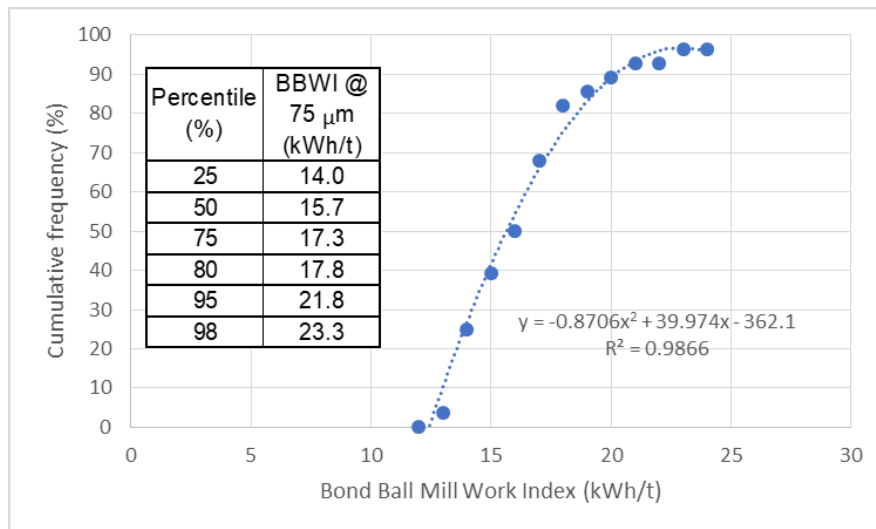


Figure 1: Cumulative frequency of Bond Ball Mill work index for magnetite ore

Meanwhile, the feed size determines the technology selection in the secondary or tertiary grinding in a magnetite concentrator. For example, if an autogenous mill is used as primary grinding with a transfer size around 250 – 400 μ m (at 80% passing), then it is of utmost importance to select a grinding technology that can cope with the long tail of particle size up to four or six millimetres. A technology selection based only on the 80% passing exhibits a higher risk as the particle size distribution especially when the feed has a long tail at the coarser end from the 80% to 100% passing. Figure 2 shows the particle size distribution of a primary autogenous (AG) mill circuit hydrocyclone overflow. Although the 80% passing size is 260 μ m, the top size ranges up to 4.75 mm. In this case, choosing the appropriate stirred milling technology that can cope with the top particle size is essential. Besides that, it is important to consider the additional power required to comminute these long tail particles from 80 to 100% passing sizes.

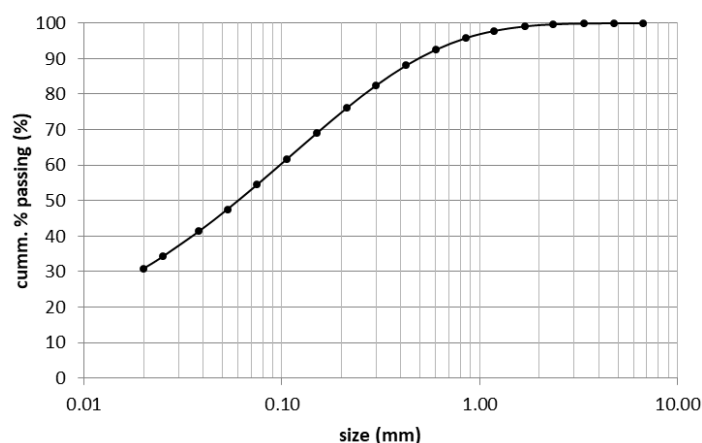


Figure 2: Particle size distribution of primary AG mill hydrocyclone overflow

Here, the stress intensity imparted by the grinding media must break the largest particles. Equation 1, Equation 2 and Equation 3 show the models for media stress intensity in the vertical stirred mill proposed by Jankovic (2001). Among the operational and design variables that affect the media stress

intensity are grinding media size (d_{GM}), grinding media density (ρ_{GM}), stirrer tip speed (v_t), the diameter of mill (D), the diameter of stirrer (D_s), density of slurry (ρ), coefficient of friction (μ), and ratio between horizontal and vertical media pressure (K). Here the stress intensity is used for comparison purposes and not as an absolute value.

$$SI_{tot} = SI_{GM} + SI_g$$

Equation 1

$$SI_{GM} = d_{GM}^3 * \rho_{GM} * v_t^2$$

Equation 2

$$SI_g = K * d_{GM}^2 * \frac{(D - D_s) * (\rho_m - \rho)}{4 * \mu}$$

Equation 3

Based on the stress intensity equations presented, the fraction of grinding media and gravitational stress intensities was analyzed. The analysis shows that eighty percent of the stresses are contributed by the gravitational stress intensity meanwhile another twenty percent is contributed by grinding media. Based on this analysis, it can be deduced that the main grinding work is done by the gravitational stresses meanwhile, the grinding media stress intensity is used fine tuning to achieve the targeted grind size when coping with ore variability. For TowerMill, the density and size of grinding media are constant as it uses the 20 mm steel media. Screw rotational speed is the only operating variable to manipulate the grinding media stress intensity. Here, the variable frequency drive (VFD) controls the main drive motor to adjust the speed, hence the mill's power draw.

Nippon Eirich has installed one unit of 1750 HP TowerMill in regrinding duty at the Haile Gold Mine in South Carolina, United States of America (Palaniandy et al., 2021). This mill is installed with a variable frequency drive that allows varying the screw stirrer rotational speed. Four circuit surveys were carried out in 2019 to evaluate the circuit' at different screw rotational speeds (Palaniandy et al., 2021). The data from this survey was reanalysed to evaluate the impact of stress intensity towards grinding efficiencies at coarse and fine particle sizes. The Bond operating work index represents the coarse particle size grinding efficiency meanwhile, the grinding efficiency at fine particle size is represented by the size-specific energy at 25 μ m marker size. Figure 3 shows the effect of stress intensities (gravitational and grinding media) on the grinding efficiencies. In general, the operating work index and size-specific energy decrease as the stress intensity increases, indicating grinding efficiency increases. This exercise has created insights for the TowerMill operation, especially to cope with ore variability by adjusting the speed. The authors agreed and acknowledged that increasing speed will reduce the wear life of the screw liners, but the enhancement of performance contributes to the profitability of the operations.

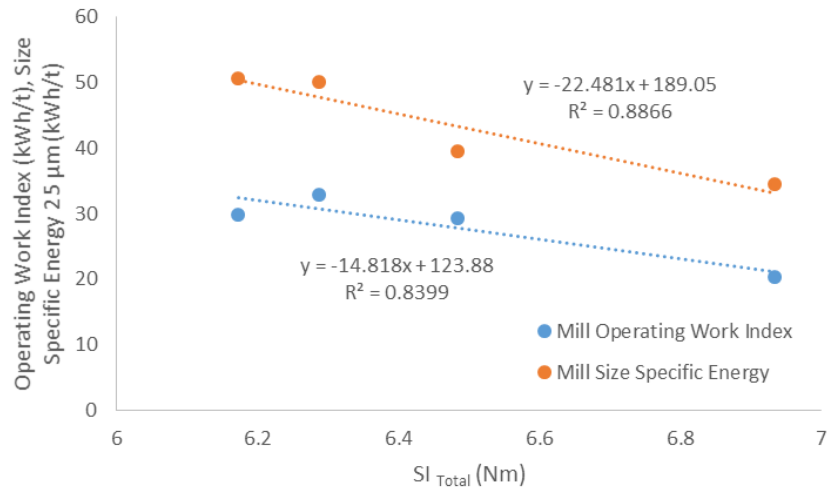


Figure 3: Operating work index and size-specific energy as a function of stress intensity

The ability to cope with coarse feed size and adjust the stress intensity is important when grinding the rougher magnetic concentrate (RMS) and intermediate magnetic concentrate (IMS). Typically the RMS and IMS will pick up the particles even if it has a small fraction of magnetite. These are the particles that exhibit the long tail from 80 to 100% passing as shown in Figure 2. The ability of the grinding technology to comminute the coarser particles and operates flexibly is the key to achieving the recovery and grade of the magnetite concentrate.

CONSIDERATION DURING CIRCUIT DESIGN AND OPERATIONS

Ore characteristics such as feed size (F80, F98, etc.), product size (P80, P98, etc.), and ore hardness are taken into consideration when determining the power requirement. Typically, the TowerMill grinding test will be carried out to determine the specific energy requirement. Based on the *grinding test* material, the performance guarantee is given on the circuit throughput and particle size at eight percent passing. Sometimes, samples are not available for the grinding test, here, the specific energy will be determined using the database and benchmark the value against the global database of a particular commodity such as the magnetite. Other ore characteristics, such as Bond Ball Mill Work Index, will be considered during the benchmarking.

Besides the ore characteristics, the choice of primary and/or secondary grinding duty also plays an important role in designing the circuit. Each grinding technology has its characteristics in terms of product size distributions. Figure 4 shows the circuit product particle size distribution of three different grinding technologies, i.e. HPGR, AG mill, and ball mill. The HPGR closed with a three millimeters screen, and the AG mill closed with hydrocyclone is operating on primary grinding duty meanwhile the ball mill is operating on secondary grinding duty. The authors acknowledge the differences in the particle size at 80% passing is different due to its grinding duty but it is important to evaluate the overall particle size distribution that affects the grinding performances. The HPGR has a coarse top size of up to 3 mm but at the same time, it consists of 30% of the finished product. Meanwhile, the AG mill circuit product has a top size of 4.75 mm and consists of 20% of the finished product. Similar observation for the ball mill circuit product as well where there is almost 60% of the finished product. In this case, a reverse closed-circuit configuration is preferred to scalp the finished product before the grinding. It is important to consider such observation for an efficient grinding circuit design.

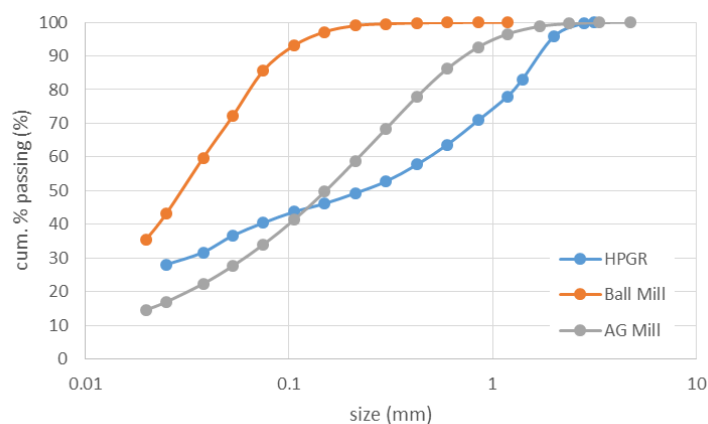


Figure 4: Particle size distribution circuit products from AG mill, HPGR and ball mill

The considerations during the circuit design can be divided into several categories such as

- Flow sheet design
- Process - Optimum screw rotational speed, grinding media size, classification technology – hydrocyclone, fine screen, coarse classifier and mill feed configuration
- Layouts
- Mechanical design such as the lubrication unit cooling method
- Maintenance practice
- Control and monitoring systems including sensors and ball charging for power control

The following section will discuss the design aspects from the flow sheet design and process in magnetite concentrators based on the authors' global experiences.

FLOW SHEET DESIGN

The TowerMill circuit flow sheet design depends on the grinding duty, energy demand, water requirement, feed and product size, reduction ratio, capital and operational expenditures. Recently the evaluation of CO₂ generation in comminution circuits is becoming important. For example, the secondary or tertiary grinding circuit can be designed in parallel, series, or one circuit with two or more mills closed with one hydrocyclone cluster. Although all three circuit designs have the same duty, their operations, maintenance, availability, operational flexibility, capital, and operational expenditures are different. The decision on a circuit design should be based on its ability to achieve productivity, product quality, and the lowest total cost of ownership for a profitable operation. This section will present and review three possible circuit designs in the magnetite concentrator for parallel and series circuits.

As mentioned in the earlier section, the grinding stages depend on the liberation of magnetite from the gangue minerals and the potential removal of these gangue minerals. Typically, a 30% rejection is expected for economical stage separation. For example, the Sino Iron project has adopted two stages of grinding (autogenous mill and ball mill) with a transfer size of 180 μ m. The mass rejection in the rougher magnetic separation stage is approximately 50%. Karara Mining, another magnetite project in the mid-west Western Australia, adopted three stages of grinding (HPGR-Ball mill-TowerMill) with transfer sizes of 4 mm and 55 μ m respectively. Approximately 30% of masses is being rejected in rougher and intermediate magnetic separation stages.

It is important to carry out a grinding test to determine the specific energy requirement accurately and more importantly, it is essential to use the rougher concentrate before designing the circuit as the

feed to the secondary or tertiary grinding circuit are the concentrate from the magnetic separator. The specific energy value is not accurate if the plant feed (without magnetic separation) is used for the grinding test as this is not the actual representation of the actual feed to the circuit. This is an important step as there are operating variables such as the ball size, mill feed configuration and screw rotational speed that can be optimized to potentially reduce the specific energy consumption specifically for the circuit in series. The following section will discuss on a magnetite project study in Australia and all the consideration that was taken for the secondary grinding circuit design.

Grinding Test

Nippon Eirich has carried out the NE-024 TowerMill grinding test on this rougher concentrate for this sample. The primary grinding circuit is an autogenous mill therefore, its circuit product has a long tail from 80 to 100% passing, as shown in Figure 5 (a). The top particle size is 4.75 mm meanwhile, there is almost 40 % of the finished product in the feed. Meanwhile, Figure 5 (b) shows the specific energy as a function of P80 for the rougher concentrate that is used to determine the grinding-specific energy requirement. The specific energy required to reduce from F80 = 300 to P80 = 32 μm is 9.58 kWh/t. The grinding media size used during the test was 20 mm.

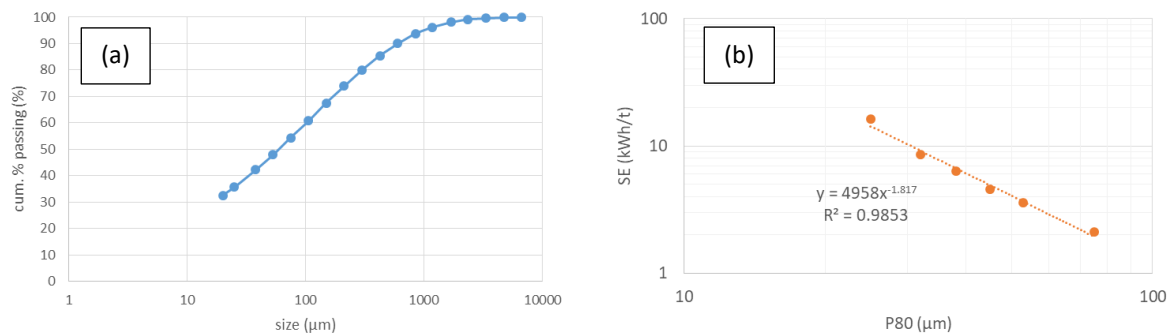


Figure 5: (a) Feed particle size distribution (b) Specific energy as a function of P80.

In this section, two flow sheets design options were discussed for a grinding duty to reduce the particle size from 300 μm to 32 μm . The feed rate to the circuit is 600 t/h and the Bond ball mill work index of the ore is 18 kWh/t (the closing screen used was 75 μm).

- Option 1 – Two circuits in parallel with each circuit grinding 300 t/h circuit feed
- Option 2 – Two circuits in series grinding with a feed rate of 600 t/h

Figure 6 and Figure 7 show the circuit flow sheet for two options with their respective mass and water balances. In Option 1, there are two TowerMill circuits closed with a cluster of hydrocyclone. The circuit feed was divided equally into these two circuits and the circuit products combined to feed the cleaner magnetic separation stage. These two circuits are identical and receive a 300 t/h circuit feed rate. Based on the circuit feed rate and specific energy requirement, the power draw of the TowerMill will be 2876 kW. The main drive motor will be operated with a variable frequency drive. The 15-inch diameter hydrocyclone was chosen to close this circuit. There will be ten hydrocyclone units in the cluster, with nine units in operations and one spare unit. Four 16 x 14 slurry pump units were chosen for the hydrocyclone feed pump for both circuits. One slurry pump will operate, and the other will be on standby duty. Both slurry pumps will be equipped with a 200 kW motor.

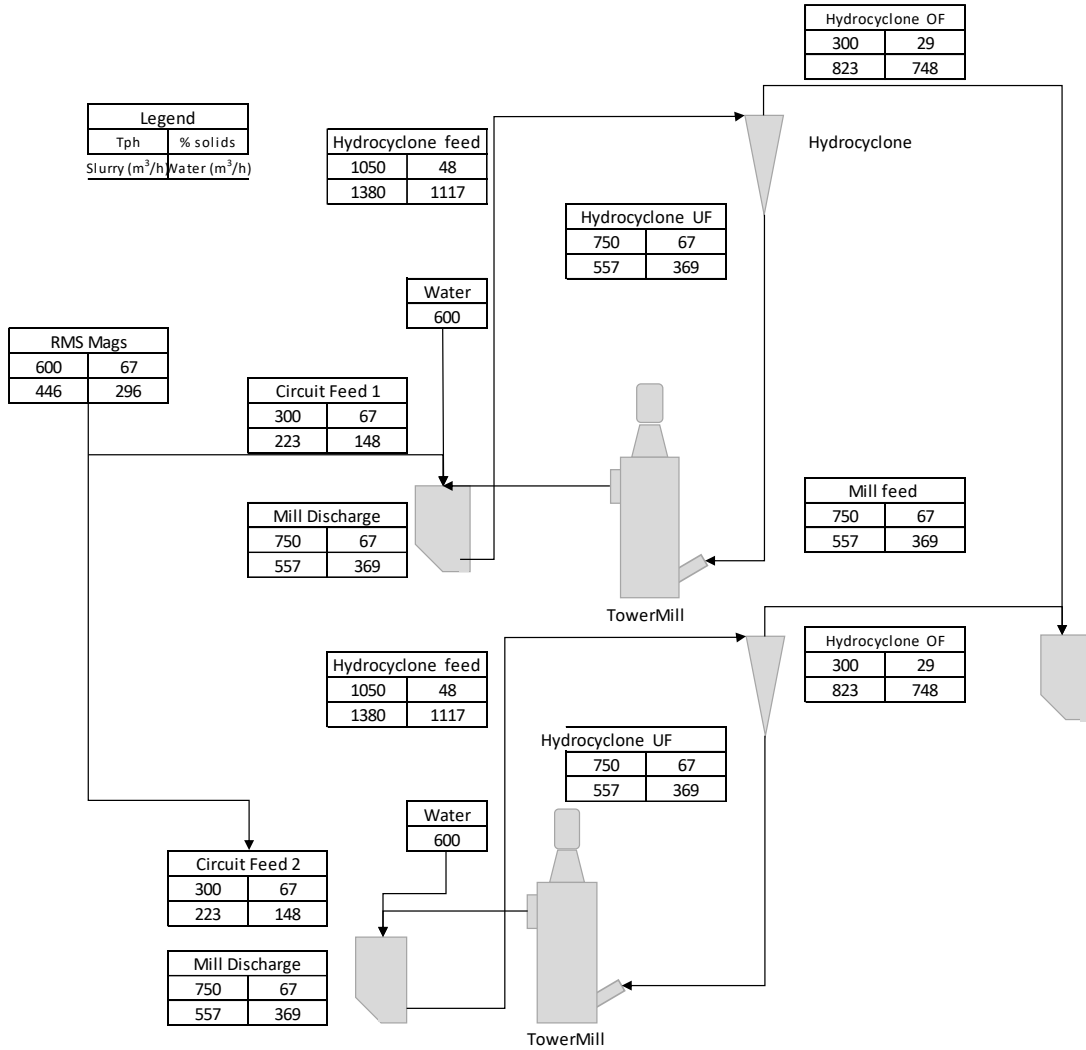


Figure 6: Option 1 - Two circuits in parallel with each circuit grinding 300 t/h circuit feed

In Option 2, two TowerMill circuits will be operating in series. The first circuit is operating for a coarser grinding duty reducing the feed size reducing from 300 μm to 45 μm at 80% passing size. The second circuit will be reduced from 45 μm to 32 μm at 80% passing. In this case, a transfer size of 45 μm was chosen. Table 2 summarizes the specifications of the Option 2 proposal.

Table 2: Specific energy and power requirement for Circuit 1 and 2

Circuit	Circuit feed rate	F80 (μm)	P80 (μm)	Specific energy (kWh/t)	P (kW)
1	600	300	45	5.16	3096
2	600	45	32	4.43	2656

Furthermore, there is an option to further reduce the specific energy requirement in Circuit 2 by using a smaller grinding media size as the feed size is 45 μm . In this case, a 15 mm grinding media is proposed for this grinding media. Table 3 shows the specific energy and power requirement for Circuit 2 with 15 mm grinding media. A specific energy reduction of 31% was realized with a smaller grinding media

in Circuit 2. The overall circuit-specific energy reduction is around 14% with a combination of grinding media size i.e., 20 mm in Circuit 1 and 15 mm in Circuit 2.

The TowerMill in Circuit 1 can be operated with a direct online start motor as the power should be maxed out to achieve 45 µm or lower at 80% passing. Meanwhile, Circuit 2 can be operated with a VFD for operational flexibility to cope with ore variability. For example, if a 2610 kW motor is installed in the Circuit 2 TowerMill, the power margin is 1.42 which is sufficient to cope with variabilities either ore hardness, feed size, or throughput.

Based on the circuit feed rate and specific energy the mill power draw ranged between 4926 – 5752 kW. Four units of 18 x 16 slurry pumps were chosen for the Option 2 circuit. The slurry pumps are equipped with a 400 kW motor. The circuits will be closed with two clusters of 20 units of 15-inch hydrocyclone (18 units operating and two units of spares).

Table 3: Specific energy and power requirement for Circuit 2 with 15 mm grinding media

Circuit	Circuit feed rate	F80 (µm)	P80 (µm)	Specific energy (kWh/t)	P (kW)
2	600	45	32	3.05	1830

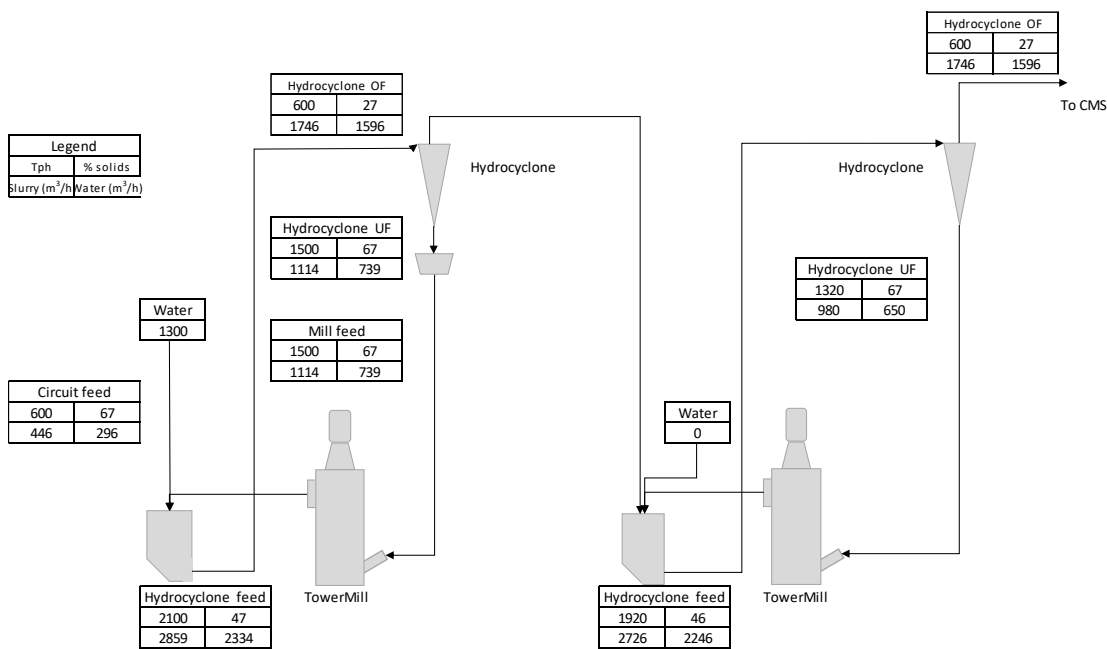


Figure 7: Option 2 – Two circuits in series grinding with a feed rate of 600 t/h

DESIGN AND OPERATIONAL VARIABLES CONSIDERATIONS FOR THE TOWERMILL CIRCUIT

This section will discuss the design and operational variables that should be considered in designing a TowerMill circuit. Among the variables are mill feed configuration, grinding media size, screw agitator rotational speed, use of coarse classifier and classification choice (either hydrocyclone or fine screen).

These variables have strong influences on the performances of the circuit, capital and operational expenditures. Besides that these variables have impacts on CO₂ emissions as well.

Mill feed configurations

The authors have discussed the impact of mill feed configuration in several technical papers since 2017 (Palaniandy et. al., 2017, Palaniandy et. al., 2018). There are two options to feed the TowerMill i.e., top or bottom feed. Figure 8 shows the top and bottom feed ports at the mill shell. The choice of top and bottom feed configuration depends on the feed size distribution, reduction ratio and circuit product size. If the feed particle size distribution has a long tail at the coarse end as shown in Figure 5 (a), then the bottom feed configuration is preferred. The high pressure at the bottom of the mill will efficiently comminute the coarser particles. The authors have conducted a full circuit survey at Karara Mine to compare the differences in grinding efficiencies of top and bottom feed (Palaniandy et. al., 2017). Table 4 summarizes the performance of the TowerMill circuit with top and bottom feed configurations. As the circuit feed top size is 1.18 mm, the bottom feed configuration is more efficient compared to the top feed based on lower values of bond operating work index, size-specific energy at 35 µm, and circulating load. Typically, the bottom feed can be gravity fed from the hydrocyclone underflow launder if the gravity head is sufficient. Gravity bottom feed is the best option to feed the TowerMill cost-effectively at higher grinding efficiency.

If the mill feed requires pumping due to insufficient gravity head, then a pump box is required in between the hydrocyclone underflow launder and mill feed nozzles. This design further add to the circuit design complexity as there will be additional operating variables such as water addition for level control, mill feed slurry density, etc. Previously, the author audited a bottom feed circuit with a pump box between the hydrocyclone underflow launder for a concentrate regrind. The main issue was that the mill feed became too dilute, i.e., 40 – 45% solids (w/w), due to water addition at the mill feed pump box for maintaining the sump level. Therefore, thorough consideration is necessary before designing such a circuit.

Conversely, the design with a mill feed pump box has its advantages if the ore is highly variable in terms of grade, especially in regrinding duty. If the feed rate fluctuates drastically due to grade fluctuation, then it is recommended to have a pump box to feed the mill. This will ensure a consistent mass flow rate into the mill hence the particles will have a sufficient residence time in the grinding zone. One of Nippon Eirich's customers has designed their circuit with the mill feed pump box to minimise the mill feed mass flow rate fluctuation.



Figure 8: Mill feed configuration – top and bottom

Table 4: Performance of TowerMill circuit with top and bottom feed configuration (Palaniandy et. al., 2017)

Mill Feed Configuration	Top	Bottom
Bond Wi (kWh/t)	14.2	9.9
SSE at 35 μm (kWh/t)	55.0	27.6
Circulating load (%)	185	122

Conversely, if the circuit feed has a narrow particle size distribution and the circuit is designed for low reduction ratio grinding duty, then top feed configuration is preferred. For example, for a grinding duty with $F_{80} = 55 \mu\text{m}$ with a top size of $100 \mu\text{m}$, grinding down to $35 \mu\text{m}$ at 80% passing, then this duty can be done with top feed.

Generally, the choice of top or bottom feed also depends on the space availability and layouts. In some projects, the top feed was chosen due to constrain in layouts. In this case, the specific energy requirement is adjusted accordingly to cope with this circuit design.

Grinding media size

The typical choices of grinding media size for TowerMill are 12.7, 15, 20 and 25.4 mm. There are examples where a 38 mm grinding media is used in the TowerMill. The choice of grinding media depends on the top particle size in the circuit feed. The general rule of thumb, the grinding media should have sufficient stress intensity to comminute the largest particles in the feed. Almost 80% of the TowerMill applications use the 15 and 20 mm grinding media for the secondary, tertiary and regrinding duty. There are applications for ultrafine grinding duty to produce circuit product below $20 \mu\text{m}$ that uses 12.7 mm. For example, the TowerMill in Mount Isa Mine zinc retreat circuit uses 12.7 mm grinding media to produce a circuit product of $12 \mu\text{m}$. Meanwhile, the 38 mm grinding media was used in a TowerMill for phosphate ore secondary grinding duty.

As mentioned in the earlier section, the grinding media size plays an important role in grinding efficiency. There is a possibility of reducing the specific energy requirement by using a smaller grinding

media provided it can comminute the largest particle in the feed. The authors have evaluated the grinding media size of grinding efficiency in TowerMill on magnetite ore. Table 5 shows the summary of the TowerMill circuit performances with 17 and 20 mm grinding media at Karara Mine. Both circuits' specific energies and feed sizes are similar. The TowerMill with 17 mm grinding media shows lower circulating load, operating work index and size-specific energy. This exercise shows that smaller grinding media has improved the grinding efficiency in the TowerMill.

Table 5: Effect of grinding media size on the TowerMill circuit performances

TowerMill No.	1	2
Circuit feed rate (t/h)	373	367
F80 (μm)	62.7	63.9
Grinding media diameter (mm)	20	17
SE (kWh/t)	2.94	3.00
Circulating load	106	71
Mill Operating work index (kWh/t)	30.8	25.2
SSE at 35 μm (kWh/t)	22.6	20.2

The enhancement of grinding efficiency is contributed by the increase in specific surface area for the smaller grinding media. The total surface area of the 17 and 20 mm grinding media are 7139 and 6088 m² respectively. The total surface area of the grinding media increased by 17% when the diameter was reduced from 20 to 17 mm which increases the probability of particles being nipped and comminuted.

There is a small difference in terms of the costs. For example, the 15 mm grinding media is \$ 100 more expensive than the 20 mm but the efficiency that it contributes reduces the overall circuit operating costs. Table 6 shows the operating cost comparison for circuit Option 2 as shown in Figure 7. As mentioned in the previous section, there is a possibility to use the 15 mm grinding media in the Option 2 flow sheet for the second TowerMill circuit. Based on the specific energy values presented in Table 2 and Table 3, the energy and grinding media costs were evaluated. Table 6 shows the operating costs when the Option 2 circuits use only 20 mm and a mix of 20/15 mm. The mixed grinding media 20 mm (in Circuit 1) and 15 mm (in Circuit 2) for Option 2 exhibit lower specific energy consumption. In this case, the energy and grinding media cost are lower when the grinding media selection is optimized based on its grinding duty. The authors understand that there will be additional logistics at the site to handle two different sizes of grinding media, but the example shows an annual savings of almost \$ 2 million which is significant for a profitable operation. Therefore, it is worth selecting the optimum grinding media size for a given operation. Besides that, the reduction in energy and grinding media consumption will help to reduce CO₂ emissions. The impact of CO₂ emission will be discussed in the following sections.

Table 6: High-level operating cost comparison (energy and grinding media)

Grinding media sizes in Option 1 and 2 (mm)	20 + 20	20 + 15
Circuit feed rate (t/h)	600	600
Specific energy (kWh/t)	9.59	8.21
Availability (%)	92	92
Annual operating hours (h)	8059	8059
Annual energy consumption (kWh)	46372637	39699619
Energy Cost (\$/kWh)	0.27	0.27
Annual energy cost (\$)	12520612	10718897
Grinding media consumption (g/kWh)	22	22
Annual grinding media consumption (t)	1020	873
Grinding media cost (\$/t)	1300	1400
Annual grinding media cost (\$)	1326257	1222748
Total cost (\$)	13,846,869	11,941,645
Cost/tonne (\$/tonne)	2.86	2.47

Note: The high level operating cost comparison in this table is only for energy and grinding media only.

Screw stirrer rotational speed and amount of grinding media

The power draw in the TowerMill is dictated by the amount of grinding media and screw rotational speed. The use of variable frequency drive is becoming more common in TowerMills to aid the start-up and operational flexibility. Although VFD contributes to capital expenditure, its superiority towards operational flexibility is notable. The VFD is used in the main drive motor to control the screw stirrer rotational speed and offers flexibility to cope with ore variability. Most of the recent TowerMill installations are with VFD for operational flexibility. The authors have conducted the TowerMill circuit audit by varying the screw rotational speed and evaluating its impact towards grindability (Palaniandy et. al., 2021). The results show that the screw stirrer's rotational speed can be operated between 50% - 100% speed without losing its grinding efficiency. It is important to note that a minimum stirrer speed is required to maintain grinding media stress intensity for efficient comminution. This operational flexibility offers additional power when grinding harder ore and the ability to turn down the power when the circuit is treating comparatively softer ore. For example, Circuit 2 TowerMill in Option 2 (refer to Figure 7) has a power margin of 42%. If the circuit is treating high-grade ore or harder ore, then there is additional power in the circuit that can be used to achieve the targeted grind size of 32 μm to the cleaner magnetic separation by adjusting the screw rotational speed.

Besides the screw rotational speed, the amount of grinding media in the mill also can be varied by adding or removing the grinding media from the mill shell. This is the traditional way of controlling the power draw before the application of VFD. Figure 9 shows the TowerMill power draw as a function of the amount of grinding media in the mill shell and screw rotational speed. Typically, such plots with their mathematical model are developed during circuit commissioning and provided to the control room operator. The operators can use this graph to estimate the screw rotational speed or amount of

grinding media to achieve a certain value of power draw. The mathematical model can be embedded into the control system for more sophisticated TowerMill power draw control.

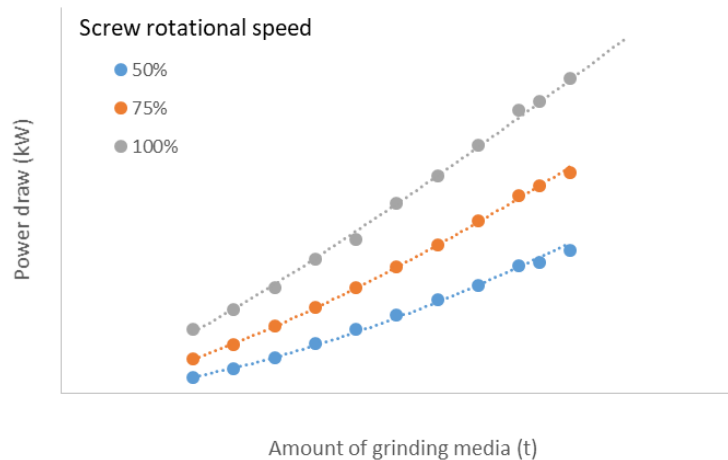


Figure 9: Power draw as a function of the amount of grinding media and screw rotational speed

Choice of classifications technology

Classification is the most crucial operation in any grinding circuit and the type of classifier dictates the quality of grinding circuit products. Hydrocyclone has been a preferred technology and widely as the classifier to close the TowerMill circuit. Almost 98% of the TowerMill circuit is closed with hydrocyclone. This technology is preferred as it is comparatively cheaper, requires smaller space, easy operation and maintenance plus its performance is generally acceptable by the industry standard. Although the hydrocyclone is widely used, this technology has its disadvantages as well. The classifications in a hydrocyclone are influenced by particle size and density and the density effect is severe in magnetite concentrator.

The density effect becomes more pronounced when the magnetite particles are liberated from the gangue silica. Magnetite particles have a higher density compared to silica. Particles with different densities experience misplacements in a hydrocyclone. For example, the coarser silica particles with lower density report to the hydrocyclone overflow stream meanwhile the high density fine magnetite particles report to the hydrocyclone underflow stream. These coarser silica particles in the hydrocyclone overflow stream coarsen the overall grinding circuit product particle size distribution. This phenomenon creates a situation where the grinding circuit is assumed to not achieve the guaranteed particle size at 80% passing. Conversely, the fine magnetite particles are recycled back to the TowerMill resulting in an over-grinding situation.

An assay-by-size exercise was carried out on the circuit audit sample to investigate the impact of multicomponent minerals on grinding and classification in a TowerMill circuit. Figure 10 shows the efficiency curves of a single component, magnetite, and silica of a 15" hydrocyclone from that circuit. It can be deduced that magnetite and silica have different cut sizes. The d50c value for magnetite and silica were 35 μm and 58 μm respectively. The 80% passing size of magnetite and silica in the hydrocyclone overflow stream were 36 μm and 61 μm respectively. The combined single-component particle size was 44 μm . The density effect affects the overall particle size distribution of the circuit product. The question is the necessity for additional grinding power to reach the targeted grind size as in reality the additional grinding energy will be used to comminute the gangue mineral, silica.

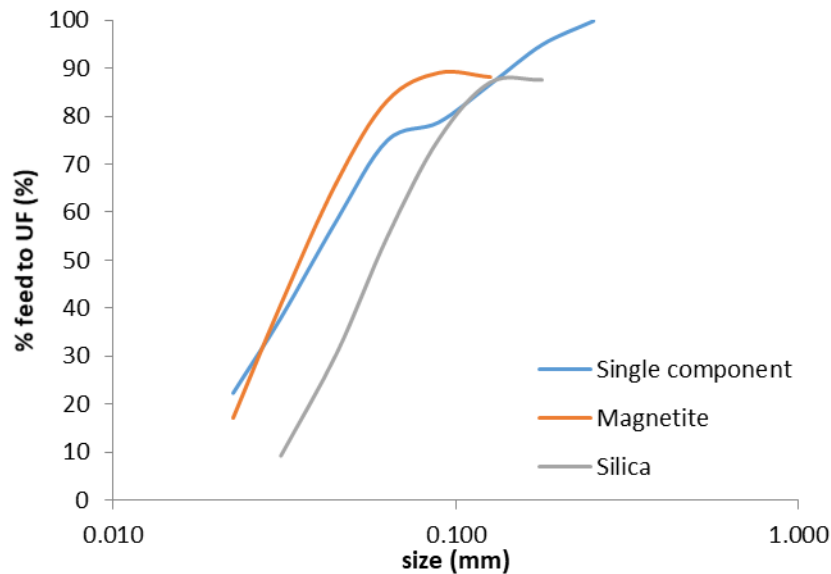


Figure 10: Efficiency curve of a single component, magnetite and silica

Alternatively, fine screens can be an alternative solution to eliminate the density effect. Reja et.al. (2023) reported that their fine screen has 25 – 35% higher classification efficiency compared to hydrocyclone plus there is a potential to increase the mill capacity up to 20%. Besides, improving the classification efficiency, the fine screens are also used to enhance the Fe content in the concentrate by scalping the coarser particles i.e., + 53 or + 106 μm particles. For example, the original design of the Karara Mining concentrator consists of a 100 μm fine screen on the intermediate magnetic separator (IMS) concentrate stream. The screen oversize is recycled back to the ball mill and the undersize that has upgrades in terms of Fe content is further ground in the TowerMill circuit before the cleaner magnetic separation. The main function of the fine screen is to enhance the Fe grade for the subsequent processes and to selectively grind the particles that have magnetite and enhance the recovery.

As per the previously mentioned examples, the fine screen in a magnetite concentrator can be used to enhance the concentrate grades and improve the classifications of hydrocyclone by installing it at the cleaner magnetic concentrate stream. For example, the circuit Option 1 and 2 products flow to the cleaner magnetic separator. The CMS concentrate flows into a 53 or 63 μm fine screen. Similar to the fine screen application at Karara Mining, the screen undersize will have a higher Fe content (enhancing grade), and the screen oversize (that might contain magnetite) will be recycled back to the TowerMill circuit for further liberation and recovery. Additionally, there is a possibility of some liberated coarse silica that contains magnetite flowing through the TowerMill circuit in Options 1 and 2 without passing through the grinding mill. The fine screen in the CMS concentrates stream can capture these coarse particles that might contain magnetite and recycle them back to the TowerMill circuit.

Hybrid classification is another example to enhance classification efficiency, especially for slurry pumping. Typically, the circuit product specifications for slurry pumping are stringent, especially on the top size. Hybrid classification by combining hydrocyclone and screen is used to achieve the specification required for slurry pumping. A TowerMill installed in a magnetite circuit in the Pan Zhi Hua area in China is using hybrid classification to control the top particle sizes. Figure 11 shows a simplified flow sheet of the TowerMill circuit for slurry pumping. In China. The 75 μm fine screen is

installed in the hydrocyclone overflow stream. The screen undersize will flow to the pumping station meanwhile the + 75 μm particles are recycled back to the mill. The hybrid classification ensures a narrow circuit product size distribution.

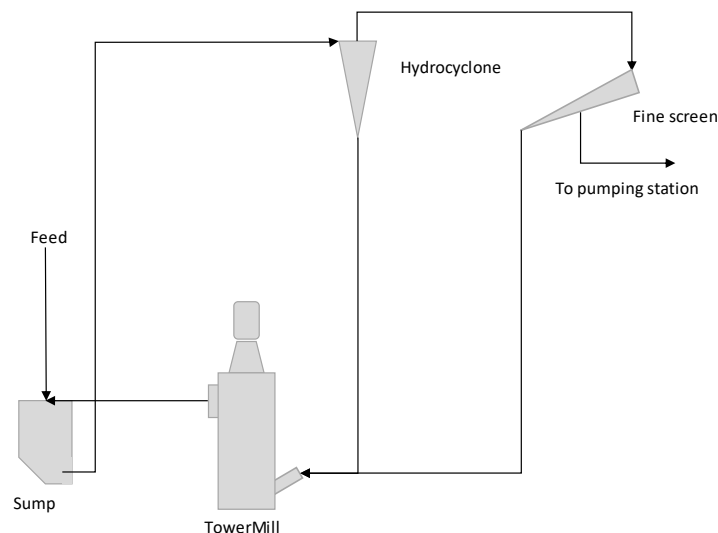


Figure 11: TowerMill circuit flow sheet for slurry pumping preparation

Classification in magnetite concentrators is an essential duty for recovery and grade control. Choosing the appropriate classification technologies is important to achieve productivity and product quality. Besides that, capital and operational expenditure consideration is essential in choosing the classification technology for a profitable operation. Especially with fine screen, the area requirement is big, especially for high throughput plants and its initial investment is higher compared to hydrocyclone. Therefore, hybrid classification such as the setup shown in Figure 11 is considered a good solution as it requires a smaller number of screens compared to screen-only classifications.

CAPITAL AND OPERATIONAL EXPENDITURE OF OPTION 1 AND 2 TOWERMILL CIRCUIT

Based on the learnings presented earlier in the paper, the capital and operational expenditure were calculated for the circuit flow sheet Option 1 and 2 as shown in Figure 6 and Figure 7 respectively. The capital expenditure considers the costs for all the main equipment in the circuit such as the TowerMill, VFD, hydrocyclone, hydrocyclone feed pumps, sumps and instrumentations (flow meter and density meter). The scope of supply for TowerMill includes the control cabinet and all related terminal boxes. Meanwhile, electricity, grinding media, screw liners, and maintenance labour are considered for operational expenditures.

The capital cost for all of the supply mentioned is around US\$10 M for both circuits with Option 2 a slightly higher value around seven percent as shown in Table 7 as the number of hydrocyclones is more in Option 2 and a larger hydrocyclone feed pump. Table 8 shows the operating expenditure comparison for both options which includes electricity, grinding media, screw liners, and maintenance labour. Option 2 shows a lower operating expenditure which is mainly attributed to energy and grinding media savings. The operating cost per ton for Circuit Option 1 and 2 are US\$3.17 and US\$2.96 respectively.

Figure 12 shows a high level of cumulative operational expenditure for a 15-year circuit operation based on a 4% annual cost escalation. The operating cost savings is approximately US\$21 M. Based on

these analyses; Circuit Option 2 offers a better total cost of ownership. Besides that, the additional power available in the second TowerMill offer a great advantage to cope with ore variability.

Table 7: CAPEX comparison for Options 1 and 2.

Circuit	Option 1 (20 mm + 20 mm)	Option 2 (20 mm + 15 mm)
CAPEX fraction	1	1.07

Table 8: OPEX comparison for Option 1 and 2

OPEX Item	Option 1	Option 2
Annual Energy cost (USD)	13 434 525	12 633 763
Annual grinding media cost, liner and labour (USD)	1 907 857	1 678 601
Annual OPEX (USD)	15 342 383	14 312 364
Annual throughput (t/y)	4 835 520	4 835 520
OPEX (USD/t)	3.17	2.96

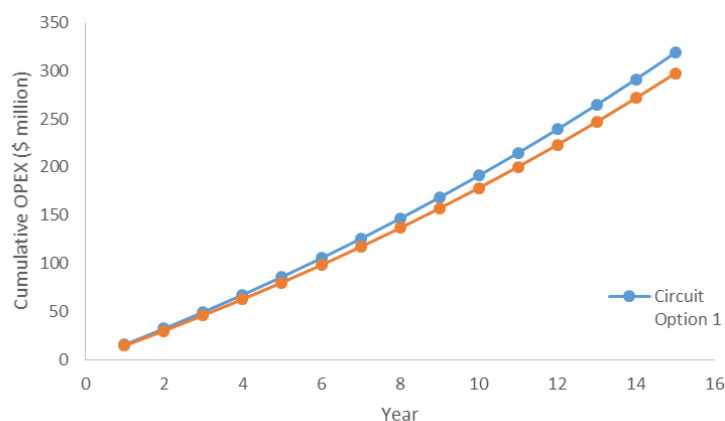


Figure 12: Cumulative operating expenditure for the period of 15 years

CARBON EMISSIONS COMPARISON

Carbon emission is becoming important in the mining industry. In general, mining companies are looking for technologies that have lower CO₂ emissions to fulfil the net zero carbon emission by 2050. Stirred mills such as the TowerMill are considered energy efficient compared to the tumbling mills. Besides technology selection, the flow sheet selection also plays an important role in carbon emissions. Selecting an appropriate circuit configuration will ensure lower emissions. Carbon emissions for circuit options 1 and 2 were analysed. The carbon emission due to electricity and steel consumption was taken into consideration. The CO₂ generation for electricity and grinding media is taken as 0.556 kg CO₂/kWh of electricity generated and 2.3 kg CO₂ emitted per kg of steel balls consumed (Morrell,

2022). The CO₂ emission for circuit Option 1 and 2 are 7.1 and 6.2 kg/t-of ground ore. Table 9 shows the comparison of CO₂ emissions for Circuit Option 1 and 2. The CO₂ emission due to electricity generation (TowerMill and pumps) and steel consumption (grinding media was taken into consideration. This analysis indicates that energy is the main contributor towards CO₂ emissions. Circuit Option 2 emits lower CO₂ compared to Option 1 due to lower energy consumption and grinding media consumption. This comparison concludes that circuit flow sheet design contributes to lowering CO₂ generation.

Table 9: Comparison of CO₂ emission

Circuit	Option 1	Option 2
Annual CO ₂ emission contributed by energy (t)	28 561	27 539
Annual CO ₂ emission contributed by grinding media (t)	5608	2 343
Annual circuit throughput (t/y)	4 835 400	4 835 400
CO ₂ emission per t of ore ground (kg/t-of ground ore)	7.1	6.2

FLOW SHEET SELECTION

Table 10 shows the summary of the comparison of circuit options. As discussed, the capital expenditure is almost similar for both circuits. Circuit Option 2 offers a lower operating expenditure and carbon emission compared to Circuit Option 1. There is little logistic effort in handling two different sizes of grinding media and a greater number of hydrocyclone for maintenance. Conversely, Circuit Option 1 offers simplicity in terms of design, operation and maintenance as the parallel are identical. Based on these factors, the owners project team or the engineering companies can select the best option depending on the overall project requirement.

Table 10: Summary of circuit options comparison

Circuit	Option 1	Option 2
Capital expenditure (million USD)	10	10.7
Operating expenditure (USD/t)	3.17	2.96
CO ₂ emission per ton of ore ground (kg/t-of ground ore)	7.1	6.2
Maintenance effort		Slightly higher
Logistics effort		Slightly higher

CONCLUSIONS

This paper presents the TowerMill circuit design based on the authors' global experiences working on various magnetite projects. The magnetite circuit can be designed for two or three stages of separation depending on the magnetite liberation size and amount of gangue minerals rejections. Ore variability in terms of ore hardness and feed size distribution is one of the challenges in designing the magnetite concentrator. Vertical stirred mills such as the TowerMill have been adopted for secondary and tertiary grinding duty due to their energy efficiency and operational flexibility. Its capability and wide range of feed size distribution have enabled the technology to be after the AG, SAG or HPGR.

This paper has reviewed two TowerMill grinding circuits – parallel and series for a 600 t/h secondary grinding duty in a magnetite concentrator. The grinding test indicates a specific energy value of 9.59 kWh/t to reduce the feed from 300 µm to 32 µm but with a TowerMill circuit operating in series, there is a potential of reducing the specific energy by 15% through operational condition changes. The

application of VFD for the TowerMill enables the changing in operational conditions by turning the power up or down by varying the screw rotational speed.

Choice of grinding media is critical as there is the possibility to reduce the energy requirement by using the appropriate grinding media size for a given grinding duty. The mill feed configuration also contributes towards the grinding efficiency whereas the bottom feed configuration exhibits higher grinding efficiency. The choice of classification technology is crucial. The hydrocyclone is more popular due to its cost-effectiveness, simplicity and easy operation but the main disadvantage in magnetite application is the density effect. Hybrid classifications that combine hydrocyclone and fine screens are a cost-effective solution that offers a high classification efficiency.

The circuit flow sheet with the series arrangement offers a lower operating expenditure and CO₂ emission compared to the parallel one. Moreover, both flow sheet options have a similar capital expenditure. Although the circuit comparison was done for a secondary grinding duty, a similar methodology can be used to evaluate the TowerMill design and operating condition in a tertiary grinding circuit. This paper has discussed the important aspects and guidelines that need to be considered in designing the secondary and tertiary TowerMill grinding circuit that are relevant to the owners project team and engineering companies.

ACKNOWLEDGEMENTS

The authors would like to thank Nippon Eirich for allowing this paper to be published.

REFERENCES

- Bueno, M. Foggiatto B. and Lane G. (2015). Geometallurgy applied in comminution to minimize design risks. Proceedings of The 6th International Conference on Semi-Autogenous and High-Pressure Grinding Technology (SAG 15). Vancouver, Canada. 1-19.
- Koenig R. L. and Broekman K. T.(2011). Development of the Hawsons Low-Grade Magnetite. Proceedings of the Iron Ore 2011 Conference. Perth, Western Australia. 633-638.
- Morrell S. (2002). Helping to reduce mining industry carbon emissions: A step-by-step guide to sizing and selection of energy-efficient high-pressure grinding rolls circuits. Minerals Engineering. 179. 107431.
- Palaniandy, S. Spagnolo, M. Halomoan, R. Zhou, H and Ishikawa H. (2017). Fine grinding circuit process improvement at the Karara Mine concentrator. Proceedings of Metallurgical Plant Design and Operating Strategies – Worlds Best Practice (MetPlant 2017). Perth, WA. 101 – 120.
- Palaniandy, S. Halomoan R. and Ishikawa H. (2018). Shifting the comminution workload from the primary ball mill to TowerMill circuit. Proceedings of 14th AUSIMM Mill Operators' Conference 2018. Brisbane, QLD.
- Palaniandy, S. Carr, D. Johns J. and Williams N. (2021). Installation, commissioning, operation and performance review of TowerMill at OceanaGold Haile Gold Mine, South Carolina. Proceedings of AUSIMM Mill Operators' Conference 2021. Brisbane, QLD.
- Reja, Y. Zhang, B. Jain, A. and Makola C. (2023) A simple methodology to predict improvements in capacity of closed grinding circuits. Proceedings of the 13th International Comminution Symposium (Comminution '23). Cape Town, South Africa. 1 – 17.

Benefits of Upgrading an HPGR with Flanged Roll Design and Advanced Mechanical Skew Control

J Bublitz¹, N Mayfield², N Elkin³ and B Knorr⁴,

6. Julian Bublitz, Global HPGR Product Specialist, Metso, Perth, WA

7. Nick Mayfield, Senior Manager Grinding R&D Program, Metso, York, PA, USA

8. Nathan Elkin, R&D Process Engineer, Metso, York, PA, USA

9. Brian Knorr, VP Concentrator Technologies, Metso, York, PA, USA

ABSTRACT

The flanged roll technology has been shown to significantly improve the performance of high-pressure grinding rolls (HPGRs). The flanged roll design diminishes the edge effect. The technology is proven with the HRC3000 (HRC), the largest HPGR in the world, which has been operating since 2014. To reduce the footprint and installation cost for the HRC, a new concept was developed – the Advanced Mechanical Skew Control (AMSC) system. As part of the design validations, a HPGR with 2.4 m roll diameter has been upgraded with the Metso flanged roll design and an AMSC retrofit package. To unlock the significant benefits of the flanged roll design, the AMSC holds the key; providing a reliable solution to mechanically control the crushing forces while eliminating any excessive skew events. The effects and reactions of the AMSC have been measured and recorded using load sensing pins, providing operational data to prove the efficiency of the AMSC and to validate the FEA models for both the upgrade kit and AMSC designs.

This paper discusses the effect of flanged rolls in a 2.4 m HPGR, and how this technology supports the demand to plant performance and efficiency improvements to meet future targets regarding increased throughput projections. It shows the direct comparison between HPGRs with and without flanged rolls in the same grinding circuit. The paper further highlight the immediate and direct response of the Advanced Mechanical Skew Control, while validating the reliability and effectiveness of this system. Finally, the paper discusses flow sheet applications for flanged rolls and the follow-on benefits to downstream grinding circuit equipment.

INTRODUCTION

The successful utilisation of HPGR technology in a growing range of applications within the mining industry has been a major development in recent years. The ability to confidently incorporate HPGR technology into energy efficient and sustainable comminution circuit designs provides new options to plant designers that didn't exist only a decade ago.

However, HPGR performance can be further improved. Traditional HPGR designs are known for an inefficiency called the edge effect. The edge effect describes a condition of impaired comminution performance at the edges of the tyres due to a reduction in crushing pressure (Morley, 2010; Van der Meer, 2010). This effect is caused by the interaction between the ore and tyre surfaces (in motion) and the cheek plates (relatively static). The edge effect is a result of lower pressure at the edges of the rolls and therefore creates a coarser product particle size distribution (PSD). The coarser PSD either leads to increased circulating load, in closed circuit applications, or in open circuit applications to a coarser material reporting to the downstream equipment. The pressure drop at the edges of the rolls further leads to an uneven wear profile, described as a "bath tub" (Morley, 2006), while the higher pressure in the centre of the tyre increases the risk of stud breakage (Hart *et al*, 2011). Accurate modelling (Morrell *et al*, 1997) and scale-up work (Van der Meer, 2010) could address and describe the inefficiency, but did not offer a solution to improve the HPGR performance.

In 2014, the Metso HRC high pressure grinding rolls were launched, successfully implementing the flanged roll design into an industrial HPGR application. The HRC has proven its increase in energy

efficiency and throughput, and pioneered the industry acceptance of flanges as superior grinding technology (Mular, 2015).

In addition to the process benefits associated with the flanged roll design, the comminution performance and overall HPGR circuit efficiency are also improved via a reduction in the edge effect (Knorr et al, 2015). -An extension in service life is achieved as a result of more uniform wear across the width of the rolls, and the larger wear mass of the flanges in combination with movement at similar velocity as the material through the high-pressure zone.

Following the initial implementation of flanged rolls, the application of the flanged HPGR design has remained an area for continued development with an emphasis on demonstrating the process benefits of flanges and the continued improvement of the overall equipment design to reduce total cost of ownership.

The flanges are part of the advanced technology used in the latest HRC evolution. This innovation included a design to allow for incorporation of the unique aspects of the flanged roll HRCe HPGR into a retrofit upgrade kit available for existing traditional installations. This upgrade allows for the improvement of comminution performance in existing installations to increase circuit capacity and reduce specific energy requirements.

Retrofit Upgrade Kit Components

A more extensive discussion of the upgrade components, operating principles, and design criteria can be reviewed in Knorr *et al*, (2023). The complete upgrade kit, as shown in Figure 1, and the sub-components, as tabulated in Table 1, incorporate the key technological components of the Advanced Mechanical Skew Control (AMSC) for controlling skew.

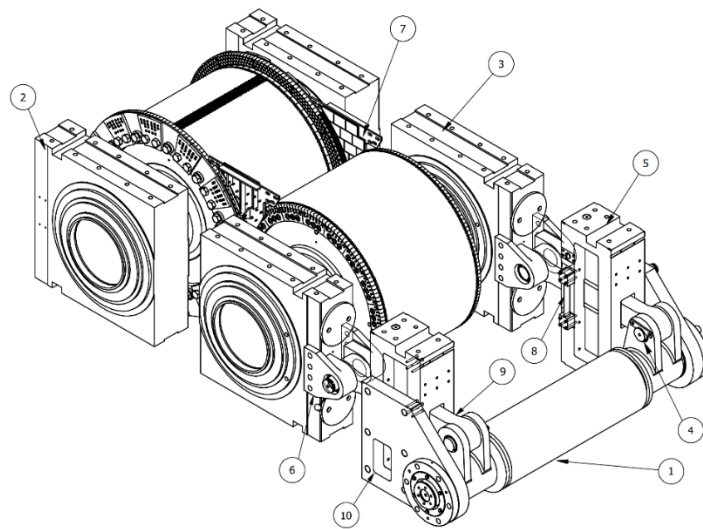


Figure 1- Retrofit Kit with Advanced Mechanical Skew Control in isometric view (Knorr et al, 2023)

Table 1- Retrofit Kit Item Description

Item	Description	Item	Description
1	Load Distribution Tube	6	Bearing Housing Brackets
2	Flanged Roll Assembly	7	Feed Chute Side Liners (Cheek Plates)
3	Non-Flanged Roll Assembly	8	Hydraulic Bypass Lines
4	Load Sensing Pins	9	Push-Pull Links
5	Vertical Pressure Columns	10	Pressure Column Brackets

Modifications to components of the existing machine were necessary for the installation of flanged rolls and AMSC into the customer's HPGR including:

- Bearing housings
- Vertical pressure columns
- Feed chute frame
- Installation of scrapers
- Lower cross section of the machine frame at the fixed roll end.

Bearing Housings

The bearing housings for the floating roll have been modified to allow the installation of brackets to connect the push-pull rods to the housings as shown in Figure 2.

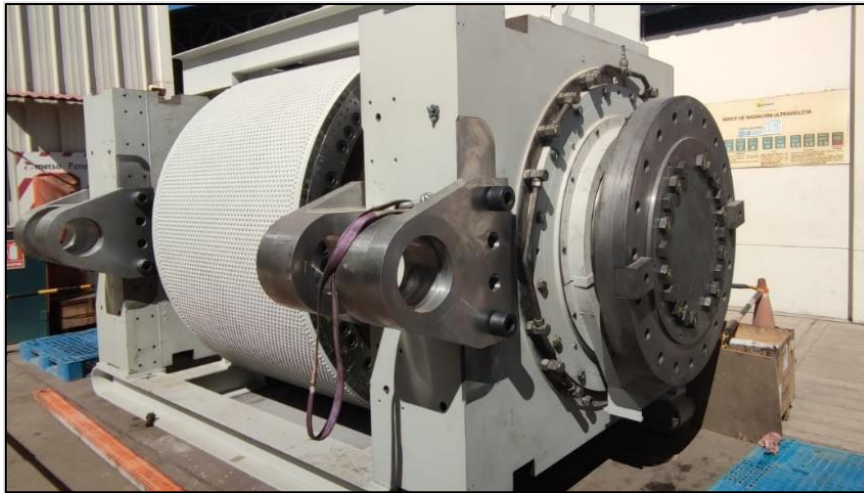


Figure 2 - Installation of AMSC brackets to the floating roll bearing housings (Knorr et al, 2023)

Vertical Pressure Columns

A set of existing pressure columns has been modified for AMSC installation. A hole has been machined through the columns and the internal hydraulic lines received a bypass line to allow the push-pull links to run through the pressure columns centre. The outer faces have been machined, with holes drilled and tapped to install the brackets onto the outboard side of the columns.

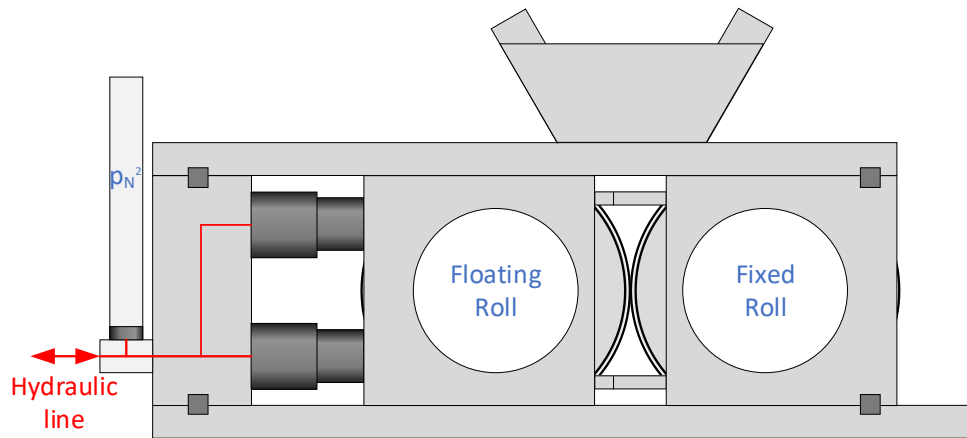


Figure 3 - Hydraulic line integrated into the standard pressure column (Knorr et al, 2023)

The standard columns have the hydraulic line integrated into the columns, as shown by the red lines in Figure 3. It was necessary to install a bypass line for the hydraulic connections and to re-position the piston accumulators. The piston accumulator had to be moved from the end face of the vertical pressure columns to the upper inboard side of the columns. The resulting AMSC assembly is shown in Figure 4.



Figure 4 - Advanced Mechanical Skew Control Assembly (Knorr et al, 2023)

Feed Chute Frame

Modifications to the feed chute frame are required to allow for the larger diameter of the flanges, which now protrude over the fixed roll surface. The cheek plate brackets have been modified to install the new feed chute side liner design.

Scrapers

A multitude of scrapers have been installed to remove the packing on both ends of the flanged roll. Scraper brackets have been installed inside the HPGR to support the scrapers.

Lower Cross Section of the Machine Frame at the Fixed Roll End

The protrusion of the flanges over the roll surface makes it necessary to cut slots into the lower cross section of the machine frame at the fixed roll end to allow the flanged roll to slide into the machine frame during the roll change.

Operating Principle

The AMSC has been designed to control skewing within defined tolerances. This provides reliable

protection when operating flanged rolls, eliminating the risk of interference or excessive forces between the floating roll's edge blocks and the fixed roll's flange segments during a major skewing event. The push-pull links are connecting the bearing housings with the load distribution tube. This is creating a direct force transmission between the housings on either side of the HPGR.

Skewing events are detected by the linear position transducers, measuring the positions of the floating roll bearing housings on either side, and the load sensing pins in the push-pull link connection at the Load Distribution Tube (LDT) clevises, recording the related reaction forces.

Validation of the operating principle using load sensing pin data is discussed further in the paper.

AMSC Design Criteria

Crush-On and Crush-Out situations have the highest potential to cause sudden, uneven loading between both rolls due to partial coverage of material between the rolls. These severe skewing events are difficult or even impossible to control with conventional hydraulic controls. Figure 5 visualises such an event.

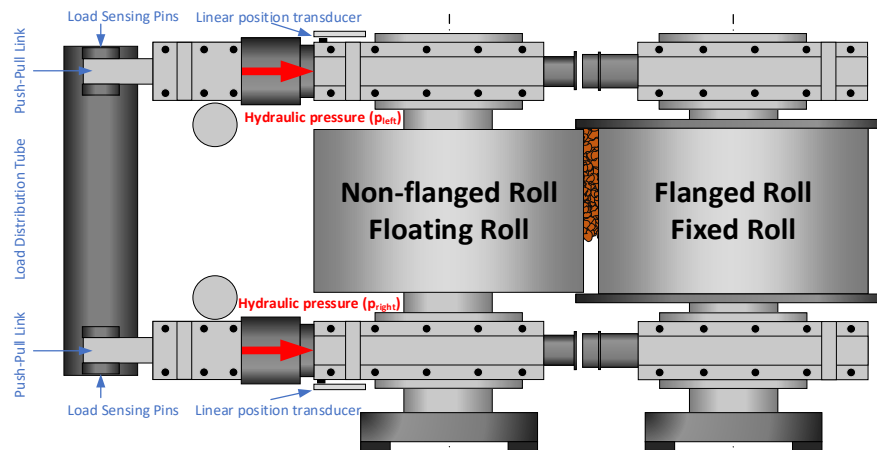


Figure 5 - Uneven load scenario due to partial feed coverage across the width of the roll (Knorr et al, 2023)

Uneven load situations have been simulated with various load conditions, e.g., a 70:30 skewing load scenario as shown in Figure 6. The reaction forces are immediately transferred via the load distribution tube.

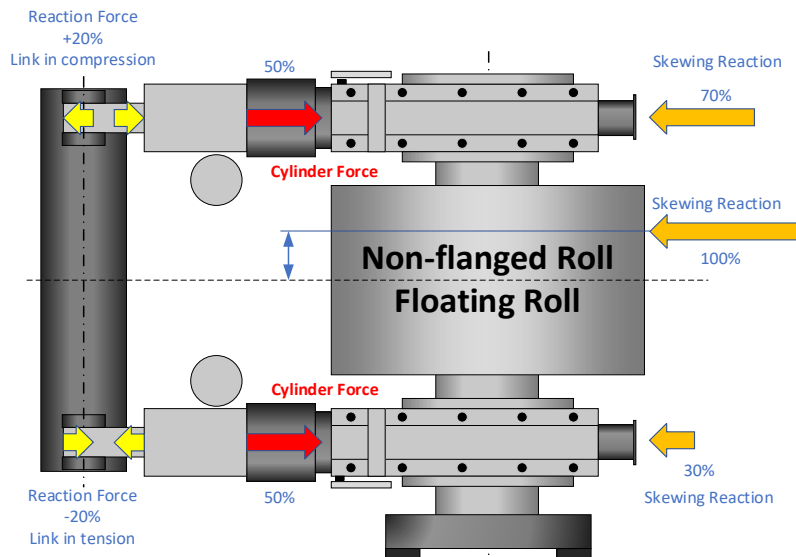


Figure 6 - Skewing load simulation with a 70% / 30% scenario (Knorr et al, 2023)

Utilising the retrofit kit components to control skew, therefore enabling the use of flanged technology, is the next phase of flanged roll performance validation. This critical validation exercise follows previous works at the pilot and industrial scale and proves the effectiveness of the AMSC system for both retrofitting existing machines and for the next generation of HPGRs, the HRCe.

SITE VALIDATION DATA

Pilot scale flange performance validation

The first demonstration of flanged roll technology in an operational environment was completed at Freeport McMoran's (FMi) Morenci Concentrator using a 740 mm x 400 mm pilot HRC machine. The full details of this work are covered in Knorr *et al*, (2015b).

The flow sheet consisted of a truncated feed arrangement using one vibrating screen to scalp the incoming fresh feed and a second vibrating screen to close the HRC circuit. The plant feed was taken from the crusher product feeding the Morenci concentrator. Downstream from the HRC circuit was a 650 HP VertiMill (VTM) in a secondary grinding duty prior to rougher flotation.

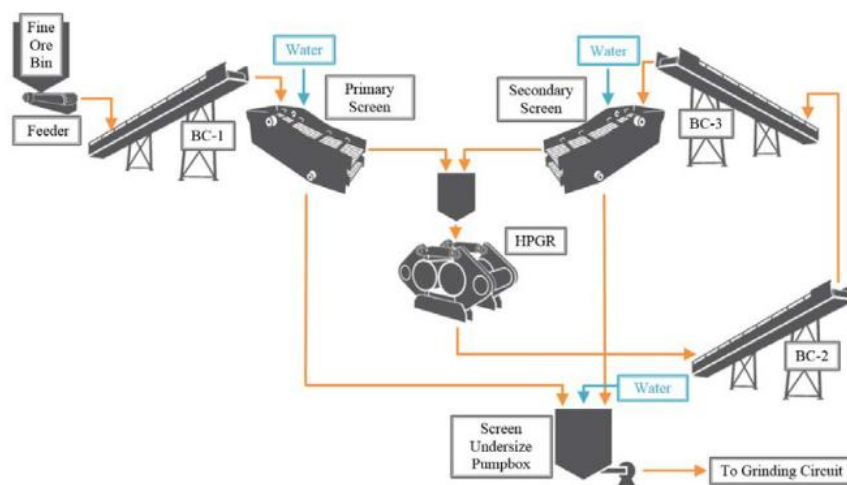


Figure 7: Morenci Pilot Plant circuit flow sheet (Knorr, 2015)

The primary process testing program consisted of 22 total tests with varying specific force set points and closing screen apertures to evaluate the performance of the flanged roll. A secondary testing

series, focusing on the reduction in edge effect from the flanges, was also executed via 12 additional tests. Knorr et al, (2015a) provides additional detail on the test plans, consequences of edge effect, and implications for large scale operations.

At this pilot scale, the observed benefits of the flanged roll were proven by reducing the circuit specific energy consumption by 13.6%, lowering the circulating load by 24%, and increasing throughput by 19%.

Table 2: Balanced test results summary for all twelve tests of the “edge effect” matrix (Knorr, 2015)

Test #	Cheek plate / flange - wear	Specific force (N/mm ²)	Specific throughput (t·s/m ³ -hr)	Net circuit specific energy (kW·hr/tonne)	Circulating load (%)	Force acting angle (deg)
Z1B	Cheek plates - new	3.49	178.5	2.82	107%	2.7
Z2B	Cheek plates - new	4.49	215.6	3.04	111%	2.6
Z3A	Cheek plates - half worn	4.51	213.5	3.34	124%	2.6
Z4A	Cheek plates - half worn	3.49	203.9	2.82	135%	2.7
Z5A	Cheek plates - fully worn	3.50	210.7	2.81	122%	2.7
Z6A	Cheek plates - fully worn	4.49	223.4	3.05	114%	2.6
Average cheek plate results			207.6	2.98	119%	2.7
Z7A	Flanges - new	3.50	231.6	2.67	93%	3.1
Z8A	Flanges - new	4.51	240.0	2.72	87%	2.9
Z9A	Flanges - half worn	3.49	279.8	2.35	102%	3.1
Z10A	Flanges - half worn	4.51	239.7	2.65	80%	2.9
Z11A	Flanges - fully worn	4.49	236.6	2.71	78%	2.9
Z12A	Flanges - fully worn	3.50	256.5	2.35	102%	3.1
Average flanged tire results			247.4	2.57	90%	3.0

In parallel with the performance evaluations of the flanged roll, the pilot HRC was utilised for development and validation of all mechanical components for the machine. This was primarily focused on the flange and edge protection, stud selection, cheek plates, etc. The learnings from component failures, iterations, and ultimately successful designs were used to directly influence the engineering decisions for the HRC3000 machine at the FMi Metcalf Concentrator.

HRC3000 – full scale flange performance validation

The first validation of flanged roll technology in an operational environment at large scale was completed at the FMi Metcalf Concentrator with the design, supply, and commissioning of the HRC3000. A thorough account of this work is captured within Herman *et al*, (2015).

Unlike the previous pilot studies, due to the nature of the production environment, there is no opportunity to conduct flange on/off trials with the HRC3000. Also, due to the flow sheet design, there is only one single HPGR unit and therefore no opportunity for a side-by-side trial of flanges vs. cheek plates. However, despite this reality, the scale up from the pilot machine to the HRC3000 has been validated with respect to specific throughput, operating gap, and circulating load.

Table 3: Observations of HRC3000 at Morenci operation (Knorr, 2015)

	Prediction based on flanged-tire pilot plant	HRC™3000 observations
Specific throughput (t·s/m ³ -hr)	276	275-325
Operating gap (mm)	99	93-112
Circulating load (%)	58-85	45-55

Despite early challenges during commissioning, as documented in Mular et al, (2015), the HRC3000 edge protection and flange design have proven to be long lasting and reliable. At the time of writing,

the machine has been running for over nine years and continues to set the bar for flanged roll service life. Confidence in the designs for flanged roll and non-flanged edge protection have enabled the AMSC retrofit kit to be introduced as a low-risk optimisation step for existing sites to experience the benefits of operating a flanged HPGR.

AMSC retrofit kit

The first trial components of the AMSC retrofit kit were installed on a single HPGR in a concentrator plant consisting of eight HPGRs. This provided the first large scale side by side trial of flanged and standard HPGR configurations, as documented in Knorr et al, (2023).

Flow sheet

The eight total machines are divided into two parallel lines of four HPGRs each. Each line discharges onto a common discharge conveyor for all four machines (preventing easy sampling for each product). The product conveyors feed vibrating wet screens with the screen undersize reporting to downstream milling. The wet screen oversize is recycled back to the HPGR ore bins via a transfer point on the fresh feed conveyor.

The ore bins above the HPGR feed hoppers are filled via tripper car that discharges material simultaneously into both lines of HPGRs as it moves from one end of the HPGR building to the other. This combination of all recycled material being transferred onto the fresh feed conveyor and subsequent splitting by the tripper car into both lines of HPGRs results in all eight machines theoretically receiving the same feed PSD. However, it is plausible that some segregation occurs between the ore bins and down through the HPGR feed hoppers.

Sampling campaign and sample points

The performance of the AMSC retrofit kit was validated by collecting plant operating data during a sampling campaign of the key streams within the circuit. The survey focused on four HPGRs in a single line, including the HPGR which was operating with the retrofit kit. During the survey, the feed ore was reported by the mine operators to be representative of typical feed stock from the mine. In preparation for the survey, the ore bins were reportedly supplied with consistent material and maintained at an adequate fill level for the upcoming survey work.

The sampling was executed by first stabilising all four units in the line, then stopping the unit with the flanged retrofit kit installed and allowing the flanged unit product to clear the product conveyor. The three standard units were then crash stopped, locked out, and sampled. The feed conveyor to each machine could be sampled individually, while the products were combined in one bulk sample on the product conveyor.

Next, the flanged machine was individually brought online and operated until stable conditions were achieved throughout the circuit. This machine was crash stopped and sampled individually for feed and product.

Process performance results

The steps for analysing the performance of the standard and flanged machines consisted of validating the operating data, normalising the results, and simulating the circuit performance. Simulation was required due to constraints with sampling around the wet screens (no samples were possible of oversize or undersize), which restricted the ability to directly evaluate circulating load and circuit specific energy consumption. The operating data during the surveys demonstrates that the standard and flanged machines were operating under same general conditions, i.e., specific force, roll speed, and hopper level.

Parameter	Units	1st Survey (Standard Roll)	2nd Survey (Flanged Roll)
Feed Rate	tph	3478	3495
Power	kW	5117	5510
Specific Force	N/mm ²	4.0	3.9
Roll Speed	m/s	2.9	3.0
Gap	mm	57	56
F80	mm	30.9	27.7
P80	mm	16.6	12.0
Specific Energy	kWh/t	1.5	1.6

Visually, during the survey execution, the product on the discharge conveyor was observed to be noticeably finer when operating the flanged machine vs. the standard machines. This was validated with the PSD results from the laboratory as shown in Figure 8.

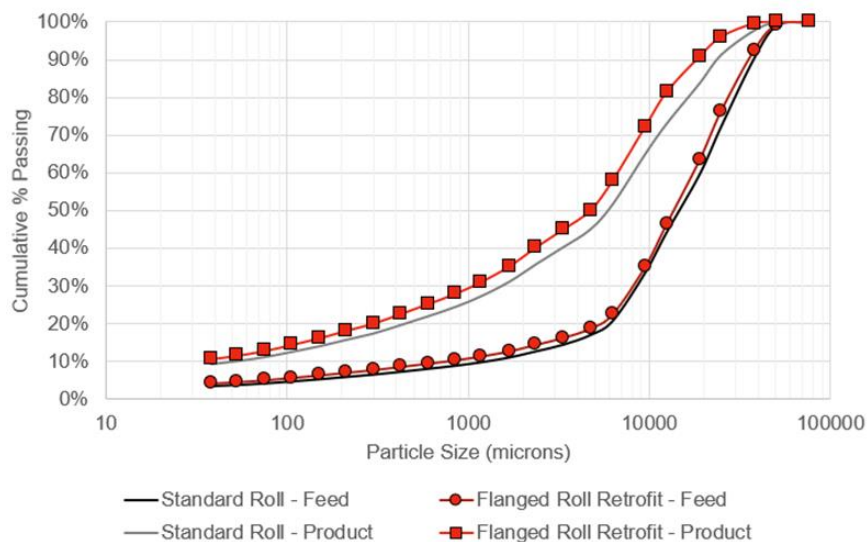


Figure 8: HPGR survey feed and product particle size distributions (Knorr, 2023)

As expected, and shown in Table 4, the power draw with the flanged roll was higher than the standard, resulting in slightly higher specific energy across the unit. Additionally, despite best efforts to obtain comparable feed competencies for the survey, laboratory analysis via Packed Bed Test (PBT) was required to confirm any differences in ore characterisation which could affect the results. The PBT results demonstrated that the feed material to the flanged and standard machines were approximately the same, especially at the typical specific energy level that the machines normally operate.

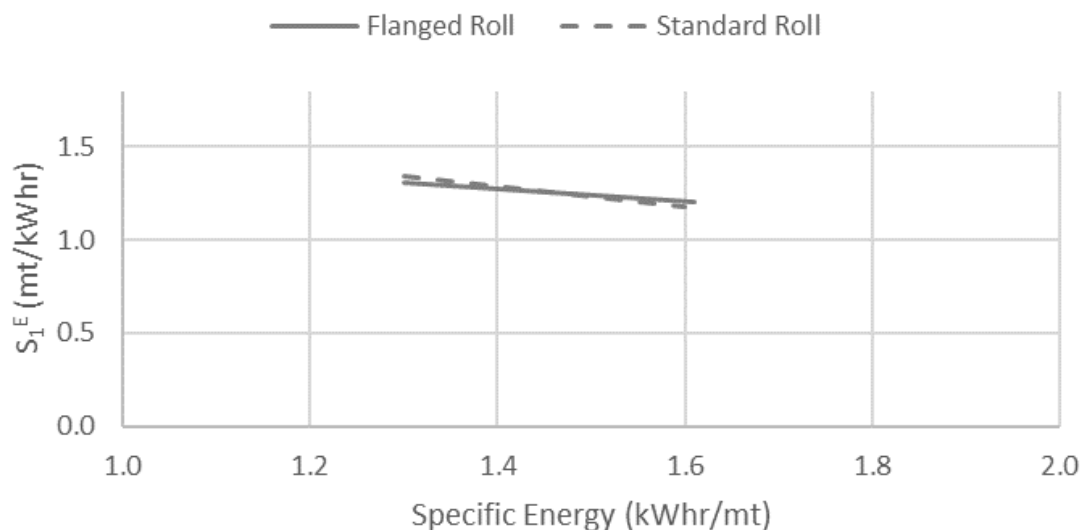


Figure 9: Competency variation as derived from Packed Bed Test Data (Knorr, 2023)

The specific energy level of 1.42 kWh/t was selected for circuit simulation to adjust for any impacts to the survey results due to the slightly higher specific energy for the flanged unit. This specific energy level aligns with the typical operation of this concentrator plant. Partition curve parameters for the wet screens were assumed due to lacking any measured data from the operation during the survey. The simulations were completed at three different aperture settings on the wet screens, resulting in a range of total circuit capacity increases from 6.1 – 7.4%.

Using the normalisation and analysis method, this increase in circuit capacity is directly attributable to the flanges and is independent of ore characterisation or other variables in the operation as shown in Table 5.

Table 5: Simulated results across a range of closing screen sizes (Knorr, 2015)

Wet Screen Aperture	Roll Configuration	Resulting Circ. Load (%)	Circuit Capacity Change (+/-%)
10mm	Standard	72.7%	
	Flanged	62.8%	+6.1%
8mm	Standard	91.4%	
	Flanged	79.2%	+6.8%
6mm	Standard	118.3%	
	Flanged	103.3%	+7.4%

Mechanical performance and AMSC performance validation

Knorr et al, (2023) details the strong mechanical performance of the flanges, edge components, and AMSC system. The components were in operation for 217 days, processing almost 13 Mt of ore, with over 4000 crushing hours. During this trial period, the major components of the upgrade kit performed well and according to the design expectations. Continued improvement processes have been initiated around the scraper design.

To directly validate the action of the AMSC system, load sensing pins were installed in the load distributor. These load sensing pins are also standard issue within the HRCe design. The pins continuously collected data during operation, crush on, and crush out events.

The observed load data during operation correlated strongly with the predicted load distribution from the FEA simulations which were done during the design phase. This data not only validates the design methods, but also proves the AMSC system effectiveness for managing biased load within the HPGR and controlling skew to within allowable limits for flanged operation.

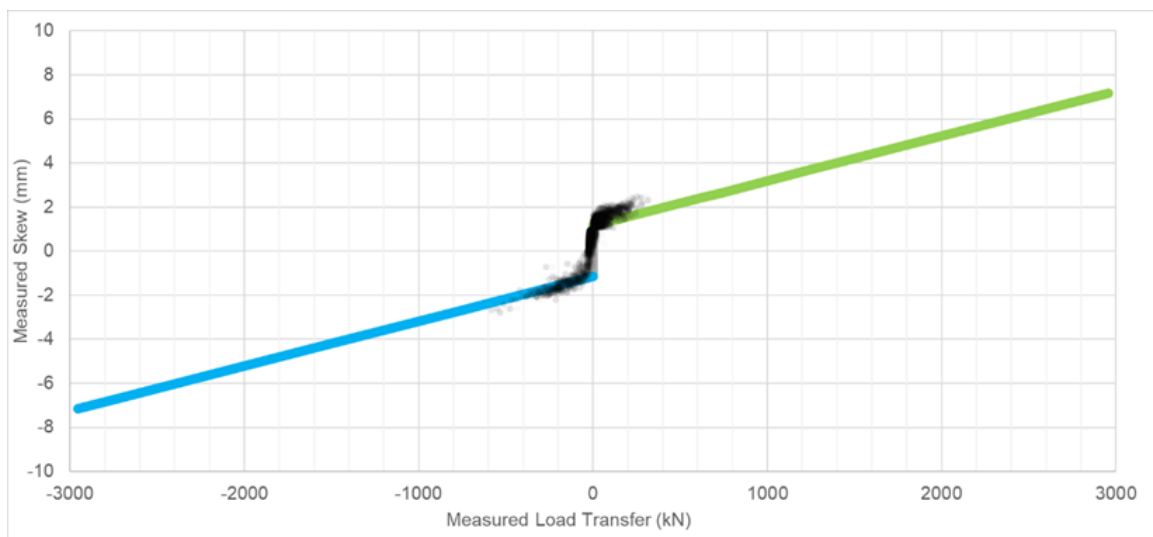


Figure 10: Measured skew vs. measured load transfer (Knorr, 2023)

Historical skew events on this machine (defined as > 10 mm) aligned with expectations for typical HPGR operation, with skew being most notable during crush on and crush out events as the material stream between the rolls is difficult to fully maintain across the roll width. This machine also registered high skew events during normal operation under steady state, highlighting the need to control the magnitude of skew within acceptable limits such that the flanges do not contact the non-flanged edge segments, as shown in Figure 11. There are additional benefits to controlling the skew as even a standard machine can suffer from high skew event trips which result in unplanned downtime, machine damage, or premature wear.

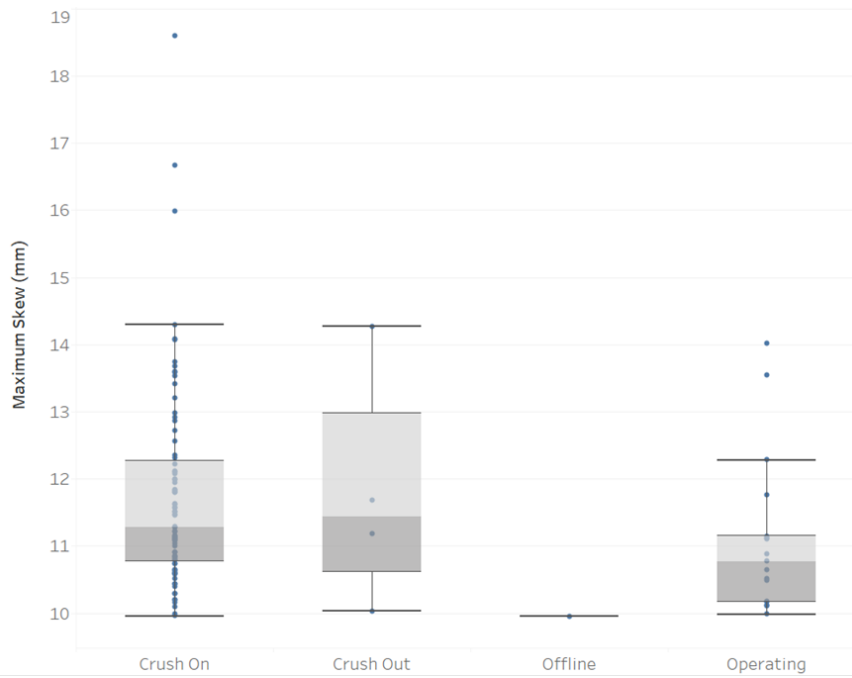


Figure 11: Historical major skew events on the standard HPGR – pre retrofit kit installation (Knorr, 2023)

During the trial, specific skewing events were studied to further validate the limited magnitude of the machine skew due to installation of the AMSC system. A typical start up sequence is shown in Figure 12 where the material is first introduced to the rolls as they rest on the shim pack at idle speed. The maximum measured skew as the rolls nipped and reached the operating gap was 3.6 mm with a load distribution force of 694 kN.

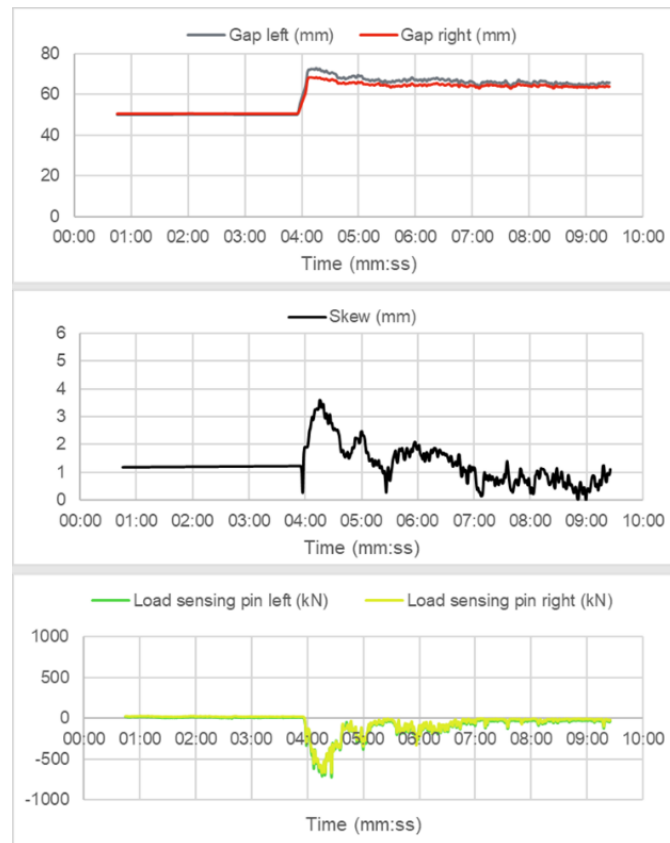


Figure 12: Skew event during crush on sequence (Knorr, 2023)

Similar performance was observed during shutdown sequences and normal operation. During one upset condition while shutting down, the machine closed to the starting gap of 50 mm and then quickly opened due to a (hypothesized) slug of material entering the crushing zone from the feed hopper. The AMSC limited skew in this condition to a gap of 3.8 mm and 796 kN of load distribution force as shown in Figure 13. During an upset condition while under stable operation, a skew event was limited to 5 mm and 1109 kN of load distribution force as shown in Figure 14. It is hypothesized that this skew event was caused by unstable ore and segregation in the ore bins and HPGR feed hopper.

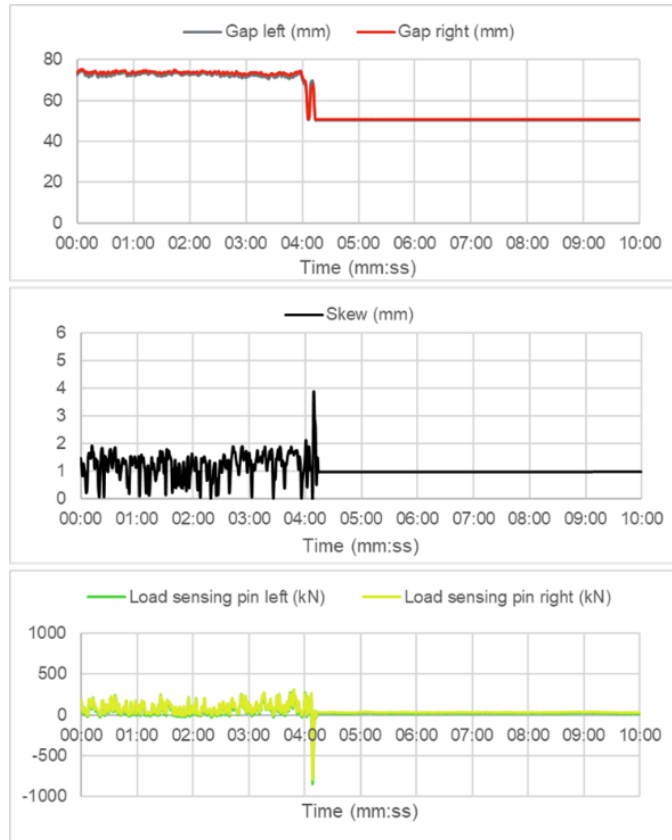


Figure 13: Skew event during crush out sequence (Knorr, 2023)

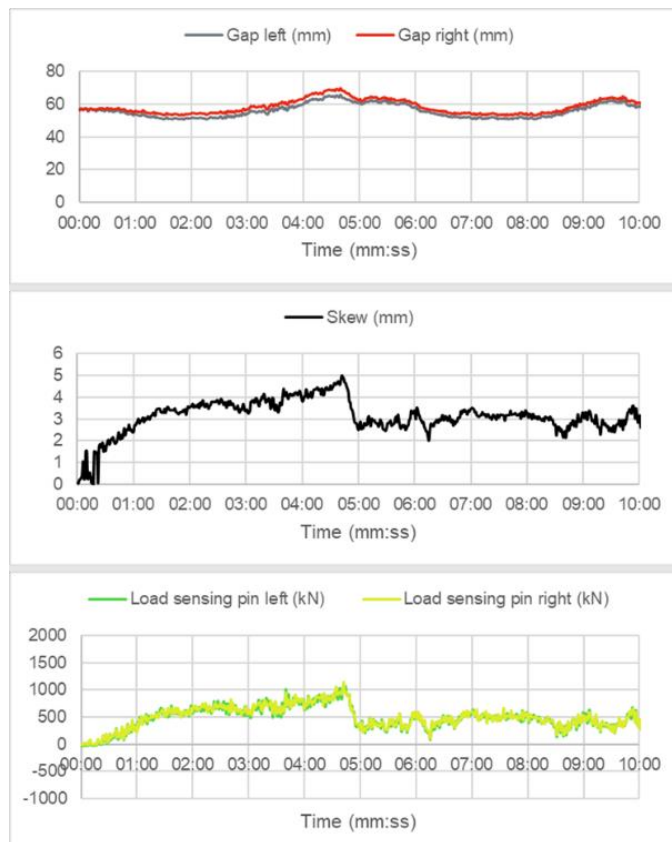


Figure 16: Skew event during typical operation (Knorr, 2023)

The process and mechanical performance validations for the installed base of flanged rolls should give confidence to the plant operator when considering this technology on its technical and economical merits. The flanged benefit can also extend beyond the HPGR by creating a series of follow-on effects for downstream classifiers, mills, and other circuit equipment.

FLOW SHEET APPLICATIONS

One of the design challenges for an HPGR circuit has been the complexity of the installation of auxiliary equipment needed to implement the improved efficiencies made available by the HPGR technology. In a greenfield installation, considering the reduction of circulating load expected with a flanged roll installation due to the reduced edge effect, the size or quantity of screens may be able to be reduced. In applications where the condition of the material being processed prohibits classification and the HPGR is therefore installed in an open circuit configuration, such as iron ore pelletising preparation, a benefit is observed from the more equalised feed PSD across the width of the roll (Rodriguez *et al*, 2021).

Installing the flanged roll upgrade into a brownfield HPGR application without modifying classification infrastructure, instead provides the ability to increase circuit capacity without overloading existing conveying. Alternatively, the classification screens can be adjusted to a smaller aperture to reduce the HPGR circuit product size. Considering this approach of reducing the transfer size (d80) can help unload the power requirements of downstream ball milling processes, thereby increasing overall plant energy efficiency.

The reduction in d80 that can be achieved by utilising a flanged roll configuration on the HPGR circuit continues to drive the potential for downstream circuits to transition directly to vertical stirred mills. If the d80 can be reduced to the 1-3 mm range with top size control at 6 mm, the Metso VTM has demonstrated to reduce milling circuit specific energy consumption by 15% as compared to ball milling circuits (Houde & Boylston, 2019). This resulting option of an HRCE circuit direct to VTM circuit can provide considerable energy savings compared to a traditional SAG / Ball Mill circuit. In fact, the reduction in circulating due to reduced edge effect from installing flanges onto an HPGR with limited skewing enables other HPGR circuit configurations to become increasingly economically feasible, particularly in cases where energy and water costs are high; this may lead to implementing a fully dry grinding circuit (Lind *et al*, 2019).

A comminution circuit flow sheet recently adopted for a new concentrator plant in South America represents the most enduring technology currently available. Conventional horizontal mills have been replaced with the combination of the HRCE HPGR and VTM grinding mills to achieve better energy efficiency. This flow sheet is expected to save 25% of installed power compared to a conventional HPGR/ball mill circuit and over 40% compared to a conventional SABC circuit.

CONCLUSIONS

In addition to previous validation work demonstrating the benefits of flanges on Metso's HRC HPGR, ranging from pilot scale to the largest HPGR operating in the world, the continued evolution of HPGR technology for limiting skewing to allow for the installation of flanges onto the fixed roll has been demonstrated successfully on an upgraded 2.4 m roll diameter traditional HPGR. During the first phase of the trial, the Advanced Mechanical Skew Control system performed as designed to maintain skew well below the acceptable limits required to allow for the operation of a flanged roll without the concern of flange to non-flanged roll interference.

Upgrading a traditional non-flanged HPGR with the AMSC and flanged roll has unlocked the benefits of flanges including improved size reduction, lower circulating load, and circuit SEC.

This continued validation of skew control and flange operation highlights the potential benefits for considering implementation of flanged roll HPGRs in a variety of flow sheet designs and upgrade projects with targets to improve capacity for any given size of HPGR and to be more planet positive

with regards to energy and water consumption. The next phase of the trial on the 2.4 m roll diameter HPGR is planned for late 2023 with emphasis on scraper performance improvements and full roll life cycle process and wear performance evaluation.

REFERENCES

Herman, V, Harbold, K, Mular, M, & Biggs, L, 2015. Building the World's Largest HPGR - The HRC 3000 at the Morenci Metcalf Concentrator, in *Proceedings SAG Conference 2015*.

Houde, M, & Boylston, A, 2019. Design, Construction and Operating Experience of the SAG-Tower Mill Circuit at SEMAFO's Boungou Mine in Burkina Faso, in *Proceedings SAG Conference 2019*.

Hart, S, Parker, B, Rees, T, Manesh, & McGaffin, I, 2011. Commissioning and ramp up of the HPGR circuit at Newmont Boddington Gold, in *Proceedings SAG Conference 2011*.

Knorr, B, Herman, V, & Whalen, D, 2015a. A Closer Look at Increasing HPGR Efficiency Via Reduction in Edge Effect, *SME Annual Meeting 2015*.

Knorr, B, Elkin, N, Mayfield, N, Mular, M A, & Whalen, D, 2015b. Pilot study of various HPGR circuit arrangements and crusher configurations, in *Proceedings SAG Conference 2015*.

Knorr, B, Bublitz, J, Elkin, N, 2023. Upgrading a 2.4-meter HPGR with AMSC and Flanged Roll Design, in *Proceedings SAG Conference 2023*.

Lind, P, Murray, K, Boylston, A, & Arce, I, 2019. Reducing Energy and Water Consumption Through Alternative Comminution Circuits, in *Proceedings SAG Conference 2019*.

Morley, C, 2006. High Pressure Grinding Rolls – a technology review, in *Advances in Comminution, Society for Mining, Metallurgy, and Exploration, Inc, Colorado*, pp 15–39.

Morley, C, 2010. HPGR-FAQ, in *The Journal of The Southern African Institute of Mining and Metallurgy*, 110: 107–115.

Morrell, S, Lim, W, Shi, F & Tondo, L, 1997. Modelling of the HPGR Crusher, *SME Annual Meeting 1997*

Mular, M A, Hoffert, J R, & Koski, S M, 2015. Design and Operation of the Metcalf Concentrator Comminution Circuit, in *Proceedings SAG Conference 2015*.

Rodriguez, V A, Barrios, G K P, Bueno, G, & Tavares, L M, 2021. Investigation of Lateral Confinement, Roller Aspect Ratio and Wear Condition on HPGR Performance Using DEM-MBD-PRM Simulations, in *Minerals 2021*, 11:801.

Van der Meer, F, 2010. High Pressure Grinding Rolls Scale-up and Experiences, in *Proceedings IMPC 2010*.

Improving Energy Efficiency and Reducing Carbon Footprint at the FMR Greenfields Mill Operation

S Latchireddi¹, R Latchireddi¹, P Fallon², B Tully² and B Hooper¹

1. EEMS Australia, Unit 19/12-16 East Victoria Park WA 6101, Australia, slatchireddi@eemillsolutions.com
2. FMR Greenfields Mill Operation, Coolgardie, WA 6429, Australia, paulf@fmrinvestments.onmicrosoft.com

ABSTRACT

Comminution is energy intensive and a major contributor to the carbon footprint of the resources sector. Morrell (2022) estimated that the global installed motor capacity of ball mills is approximately 67.6 billion kWh - 58% of the total estimated annual global comminution electricity consumption. More than a century ago, in 1914 (Van Winkle, 1918), it was well demonstrated that Marcy open-ended grate discharge ball mills are more energy efficient compared to Hardinge overflow ball mills. However, overflow mills have become dominant due to the inability of trunnion-based grate-pulp lifter discharge ball mills to reproduce the expected performance of open-ended grate discharge mills because of internal material transport issues.

The invention of the dual chamber pulp lifter, energy efficient pulp lifter (EEPL), which eliminates the internal material transport issues, namely flow-back and carry-over, and hence ensures efficient grinding conditions, thus allows the trunnion-based grate-pulp lifter ball mills to operate like open-ended grate discharge ball mills. This has generated research interest to understand and demonstrate the century old proven benefits of open-ended grate discharge mills.

Comprehensive laboratory and pilot mill studies undertaken at the University of Utah have once again demonstrated the significant energy savings of open-ended grate discharge mills compared to overflow mills, which have led to successful industrial installations.

This paper summarises the results from three implementations between 2015 and 2022, at copper, magnetite, and gold milling operations. This paper further discusses the energy savings and other benefits observed at the most recent (2022) implementation at FMR Greenfields Mill Operation in Australia. All three operations have demonstrated energy savings of over 25%, in addition to an increase in throughput.

After successful conversion of one out of three overflow mills (one primary and two secondary mills), specifically secondary Mill#2, at the Greenfields Mill Operation in March 2022, the plant is operating with one primary mill and one secondary mill instead of two secondary mills; demonstrating the ability of one grate discharge mill to do the work of two overflow mills, in addition to saving 510 kWh of motor power and decreasing grinding media consumption by 19.7%. Electrical energy savings alone remove 2268 tonnes of CO₂ emissions per annum (22% of the operations emission) besides reducing 244 tonnes of CO₂ emissions per annum due to reduction in media consumption.

In the next phase of the project, FMR Greenfields Mill Operation will review the upgrade of the primary Mill#3 from an overflow mill to an EEMS discharge system based on the results of the Mill#2 grate conversion. This is expected to further increase power savings by ~300 kWh, decrease the total carbon footprint by 3869 tonnes (35.2% of total), and provide circuit flexibility when toll treating different ore types.

INTRODUCTION

The most energy efficient breakage system would be one where particles leave the energy field as

1. NET revenue is referring to the total dollar value minus all the expenses. All the economics in this section are referring to NET values, all expenditures are not included in this report.

soon as they become of product size, so that the energy is used to break coarser particles. In tumbling mills, free falling or tumbling rocks and balls transfer the energy to break particles and a special discharge arrangement is required to facilitate the internal material transport of product sized particles out of the breakage field. The efficiency of product removal depends on the design of the discharge mechanism.

In its Technical Brochure No 101, The Mines and Miners Supply Company USA (1942), reported that the quest for an efficient discharge mechanism started as early as 1912 when Mr. Frank Marcy stated that 'rapid change of mill content is necessary for high efficiency'. However, overflow mills are preferred due to their simplicity of design and operation, where it has been a well-accepted practice to increase the circulating load to attain rapid material displacement in mill contents and avoid over grinding.

Literature on overflow and grate discharge mechanism

The first true comparative tests between overflow and grate discharge mechanisms in ball mills were carried out in 1914, when the Marcy open-ended ball mills (Figure 1) were successfully tested against Hardinge's conical overflow ball mills at Inspiration Consolidated Copper Concentrator (Van Winkle, 1918). The comparative tests conducted over 3 months at Inspiration have amply demonstrated the advantages of open-ended grate discharge mills when compared to overflow mills in terms of lower energy consumption per tonne and significantly higher productivity of up to 35%.

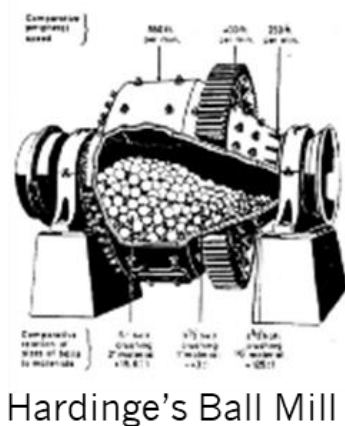


Figure 1: Hardinge and Marcy open ended ball mills.

Increase in mill diameter to more than 3m and, many mechanical and operational challenges with open-ended or grate-only mills, led to the development of the modern grate discharge mill design, consisting of a grate and pan or pulp lifter as shown in Figure 2. The two conventional pan lifter designs – radial and curved or spiral type, were developed in the 1930s and have since been predominantly used in autogenous grinding (AG), semi-autogenous grinding (SAG) and Ball mills.

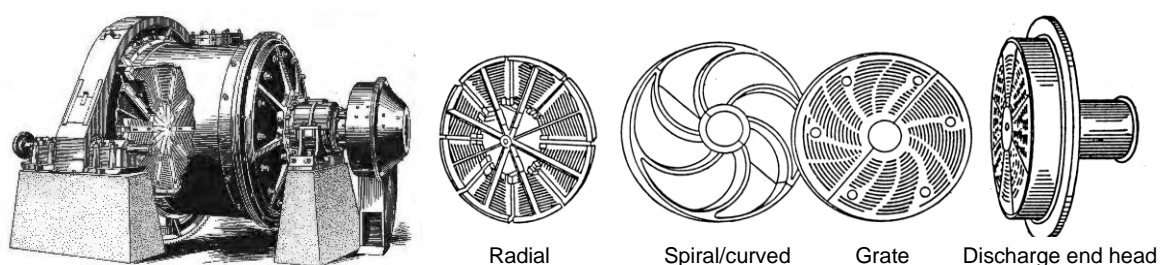


Figure 2: Grate discharge ball mill and different discharge systems. (Taggart, 1940).

Although the addition of pulp lifters on top of the grates facilitated the use of simpler trunnion support, the arrangement did not produce similar improvements in throughput and energy savings as observed in open-ended grate mills. The high cost of maintenance could not be justified compared to overflow mills; hence ball mills have moved predominantly to the overflow design. McIver and Makni (2022) have recently summarised the performance comparisons of grate ball mills verses overflow ball mills and mentioned that a grate discharge has never been reported to have had a negative effect on milling efficiency, and grate discharge provides ball milling efficiency greater than an overflow discharge.

The poor performance of grate discharge mills with radial pulp lifters is attributed to the presence of excessive slurry and curved or spiral pulp lifters were tried as alternative, but the problem could not be eliminated (Mokken et al, 1975). Subsequently, Rowland & Kjos, (1975) reported that if there is an excessive amount of slurry, i.e. more than the volume of voids in the grinding media, it affects grinding efficiency. Morrell and Kojovic, (1996) observed a reduction in power draw of SAG mills operating with a slurry pool and mentioned that it adversely affects the mill grinding capacity. Songfack and Rajamani (1999) reported that the main bottleneck in trying to improve the efficiency of current grinding circuits is the lack of understanding of the mechanism of material transport in grinding mills. Unfortunately, there was no published data, either to substantiate the previous claims or to understand what relationship exists between the load carrying capacity of pulp lifters and mill performance, until late 1990.

Material transport through mills and development of Energy Efficient Pulp Lifters (EEPL)
Extensive research carried out by Latchireddi S (1996, 2002, 2003a, 2003b) on grate discharge mills with different designs of grate and pulp lifters, radial and curved, has identified the inherent process issues as **flow-back** and **carry-over** of slurry, resulting in a large slurry pool inside the grinding chamber as illustrated in Figure 3.

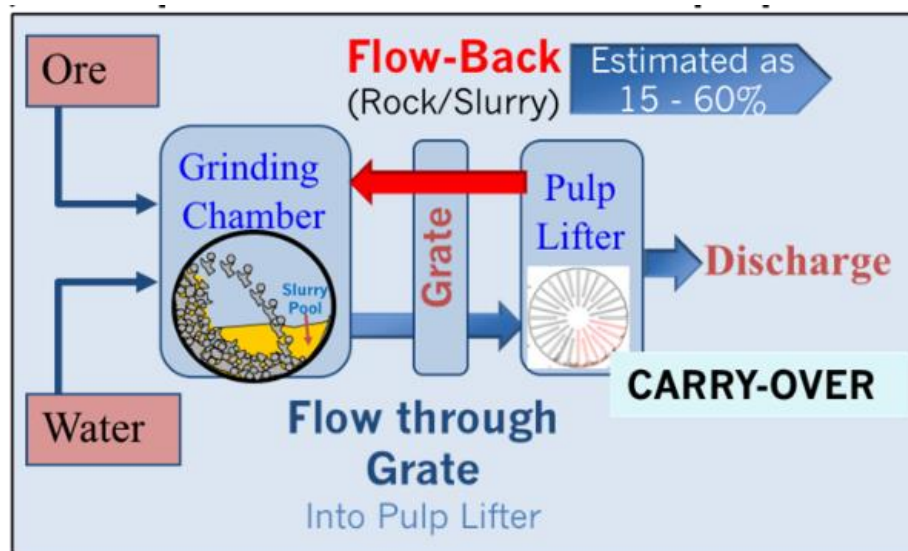


Figure 3: Material transport in mills with radial or curved pulp lifters (Latchireddi S, 1996, 2002).

To overcome these inherent issues, Latchireddi S and Latchireddi R (2016) developed a novel pulp lifter design called EEPL which is more advanced and efficient compared to its predecessors. The EEPL designs eliminates flow-back and carry-over and allows mills to operate as open-ended grate discharge mills (Figure 4). EEPL designs have been successfully operating at several AG/SAG mill operations around the world, and consistently delivering significant energy savings and increases in

productivity.

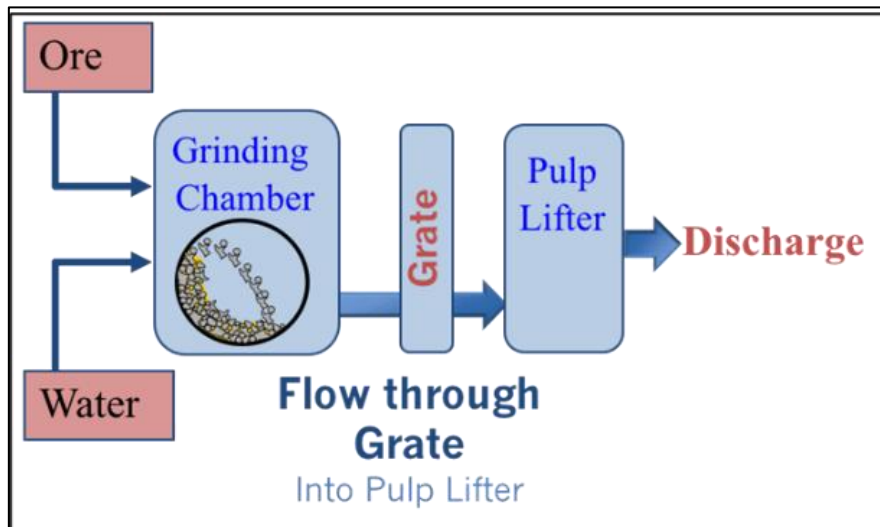


Figure 4: Material transport with EEPL in mills (Latchireddi S and Latchireddi R 2016).

Research at University of Utah

Successful operation of EEPL in AG/SAG mills prompted studies to apply the same design to ball mills to eliminate the large body of slurry and ensure efficient grinding conditions. To understand the process advantages of grate discharge ball mills compared to overflow mills, extensive experimental investigations were carried out in a pilot mill (Figure 5) at the University of Utah by Prof Rajamani and team (Latchireddi R et al, 2015 and Latchireddi R, 2017) during 2011-2017, which was equipped with load cells and a torque sensor.



Figure 5: The pilot ball mill with interchangeable discharge end (overflow and grate discharge).

The findings of this research are summarised as follows:

- The grate discharge mill demonstrated a lower energy requirement of ~40% to achieve the same product size when compared to overflow mills.
- A significantly lower particle residence time in the grate discharge mill, compared to the overflow mill, implied a quicker and more efficient transport of product-size particles, thus providing potential for breakage of new particles.
- The higher particle residence time in the overflow mill suggested inefficient material transport, with particles spending more time in the mill.
- Variation of product size with respect to mill speed and percent solids concludes that grate mills can be effectively used to vary product size using both control variables.
- In an open-ended grate mill, slurry volume is effectively 100% of charge void space, thereby allowing all particles to pass through the cascading media before exiting the mill, which leads to efficient breakage of particles.
- The slurry pool in overflow mills is estimated to be 270% to 300% of the charge void space, where a significant proportion of the grinding energy is utilised against buoyancy and drag forces and not directly for comminution.
- The excessive slurry pooling in overflow mills promotes movement of slurry over the ball mass, resulting in short circuiting of some of the feed to the discharge, causing inefficient comminution.

Industrial application of research findings

Application 1

The first application of the research findings was carried out at Sandfire Resources' Degussa Copper operation, whose grinding circuit was designed as a SAG and ball (SAB) circuit, with the SAG mill in closed circuit with primary cyclones, and pebbles circulating to the SAG mill feed, to produce particles P_{80} 180 μm going forward to an overflow ball mill (but supplied with a grate discharge option). The ball mill is in closed circuit with cyclones to produce particles P_{80} 45 μm . The grinding circuit operated as expected until the mill feed shifted to more competent ore in 2013, which limited throughput and resulted in high pebble circulation and production of a large proportion of ultra fine particles ($-10 \mu\text{m}$) that adversely affected flotation performance.

To overcome these issues, several conventional techniques were implemented but with limited success. EEMS were then engaged to develop a holistic model and identified poor material transport and inefficient charge motion as the critical issues. In 2015, Sandfire successfully implemented the EEMS modified design of SAG shell liners to generate optimal charge motion and the patented EEMS energy efficient pulp lifter (EEPL) to overcome the material transport issues in both the SAG mill and ball mill, in addition to replacing the SAG circuit cyclones with a 2 mm aperture vibrating screen and adding a pebble crusher as shown in Figure 6. The operational data of the EEPL discharge system compared with the design data of ball mill in overflow configuration are presented in Table 1 (Knoblauch et al. 2015).

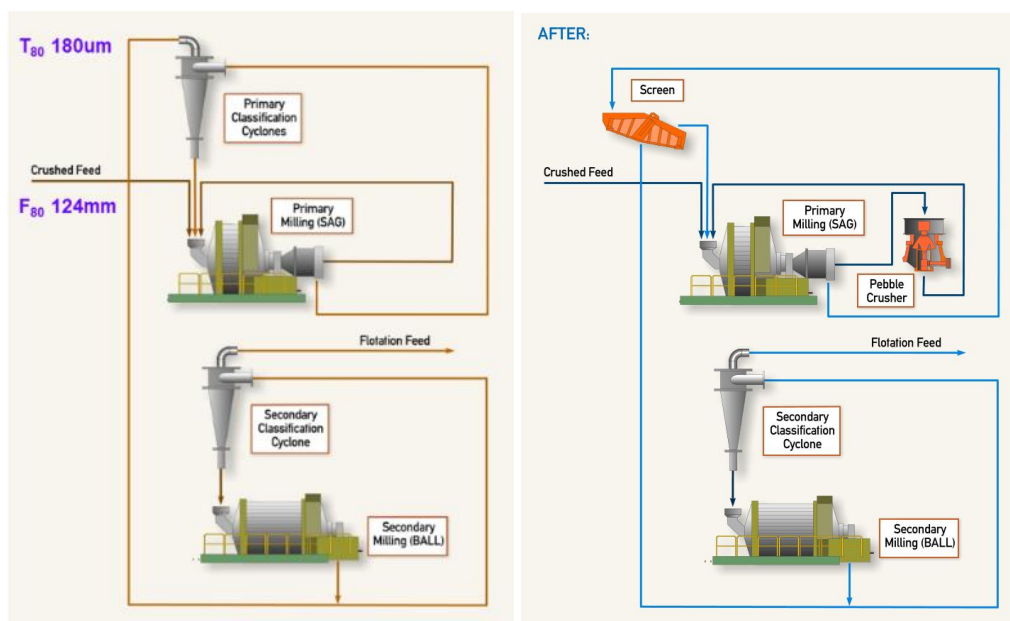


Figure 6: Degrusa grinding circuit before and after modification.

Table 1: Operational results of ball mill at Sandfire Resources Degrusa operation.

Parameter	Overflow (design)	Grate-EEPL (after)	Benefit against Overflow
Mill Size	4.7 m x 7.5 m 2800 kW	4.7 m x 7.2 m 2800 kW	
Ball Charge, % volume	28	16	-42.8%
Throughput, t/h	187	236	+26.2%
Feed Size, F ₈₀	180 µm with cyclones	1300 µm with 2 mm Screen	
Product Size, P ₈₀	45 µm	45 µm	
Power draw, kW	2321	1690	-27.2%
Specific Energy, kWh/t	12.4	7.2	-42.2%

A summary of the observations includes:

- an observed 42.2% energy saving, confirming the pilot mill test results of 40% energy savings with open-ended grate discharge compared to overflow mills.
- the EEPL discharge system appeared to allow an overflow ball mill to operate like an open-ended grate discharge mill.
- a grate mill is capable of handling coarser feed to produce the same product size.
- at the Degrusa ball mill, 40% of motor power remains available to achieve more throughput and finer grind, so a second ball mill was not required for future expansion to process 287tph.

Application 2

Iron pipe manufacturer Jindal Saw, identified an opportunity at its magnetite ore processing plant where ore is processed in parallel ball mills before beneficiation in rougher wet magnetic separators in closed circuit with cyclones to produce a final product of P₈₀ 74 µm. A schematic process flow

diagram of one line of four parallel lines in Plant B is shown in Figure 7.

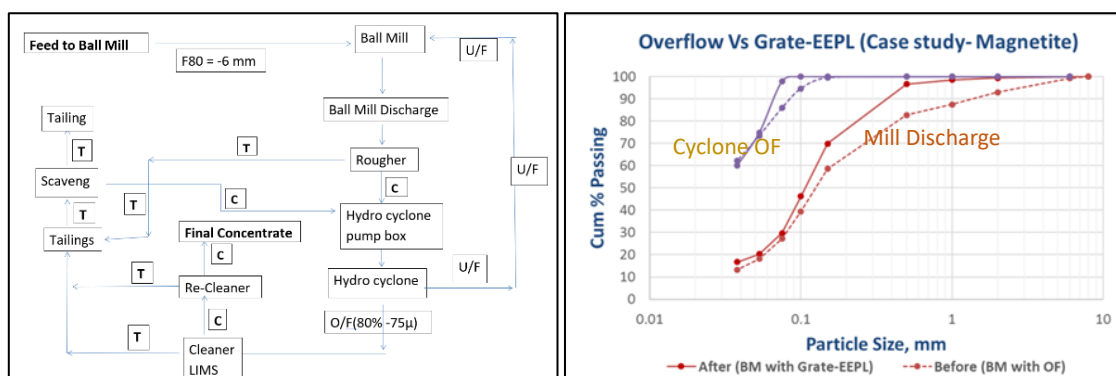


Figure 7: a) Jindal Saw grinding circuit flow diagram and b) Size distribution of mill discharge and cyclone overflow.

Line-6 of the four (lines 5, 6, 7 and 8) was first selected to convert from overflow to grate discharge by installing the patented EEPL discharge system with the primary objective of saving energy. A comprehensive grinding survey of Line-6 was carried out, followed by holistic modelling to predict the performance of a grate mill with the EEPL discharge system. Modelling estimated energy savings of around 30% as well as an increase in throughput by 10-20%. All mill internals, shell, and discharge liners were modified to suit the grate discharge process. The Line-6 ball mill was commissioned in July 2019 and Table 2 summarises the mill performance before and after installation.

Table 2: Operational results of ball mill at Jindal Saw operation.

Parameter	Overflow (before)	Grate-EEPL (after)	Benefit against Overflow
Mill Size	4.57 m x 8.08 m 2800 kW	4.57 m x 7.7 m 2800 kW	
Ball Charge, %vol	28	14	-50%
Throughput, t/h	128	159	+24%
Feed Size, F ₈₀	3520 µm	3520 µm	
Product Size, P ₈₀	74.0 µm	74.2 µm	
Power draw, kW	2214	1490	-32.6%
Specific Energy, kWh/t	17.3	9.4	-45.6%

Consistent energy savings have once again proven the research findings and ability of the patented EEPL discharge technology to operate ball mills as open-ended grate discharge mills.

A summary of the observations is as follows:

- Consistent energy saving of >45%.
- A 24% increase in ball mill throughput.

Considering the consistent energy savings and higher throughput, two more mills (Line-5 and Line-7) have been converted to grate discharge with EEPL technology.

The advantage of an increase in throughput while reducing energy (kWh/t) has significant ramifications for the industry; no longer will mill constrained operations need to sacrifice throughput, the primary grind, and recovery, and operations that are ore-supply-limited can reduce their energy costs and carbon emissions.

FMR GREENFIELDS MILL OPERATION

Background

The FMR Greenfields Mill Operation located near Coolgardie was founded in 1892, when gold was discovered in the area known as Fly Flat by prospectors Arthur Bayley and William Ford. Gold exploration and processing continued to occur sporadically at the Greenfields site until the Greenfields Processing Site was constructed in 1987 by Coolgardie Gold NL to process ore from the Baileys Underground Mine with a nameplate capacity of 250,000 t/y, with the 500 kW ball mill being the sole mill. In 1994 throughput was doubled to 500 000 t/y with the installation of the 875 kW ball mill and a third upgrade to 900 000 t/y occurred in 2008 by adding the 1325 kW ball mill.

During the majority of toll milling campaigns the Greenfields Mill Operation treated low to moderate grade ores which meant that the plant had sufficient downstream capacity to handle an increased throughput rate. This was where the opportunity was identified to potentially improve the grinding efficiency and throughput and therefore increase the revenue generated through toll milling. Alternate options were discussed as to how to utilise the efficiency gains, including maintaining the existing throughput rate and grinding finer to increase recovery on certain ores, and maintaining the existing grind and increasing throughput. A decision was taken to turn off the 500 kW ball mill to realise significant maintenance and operational cost savings.

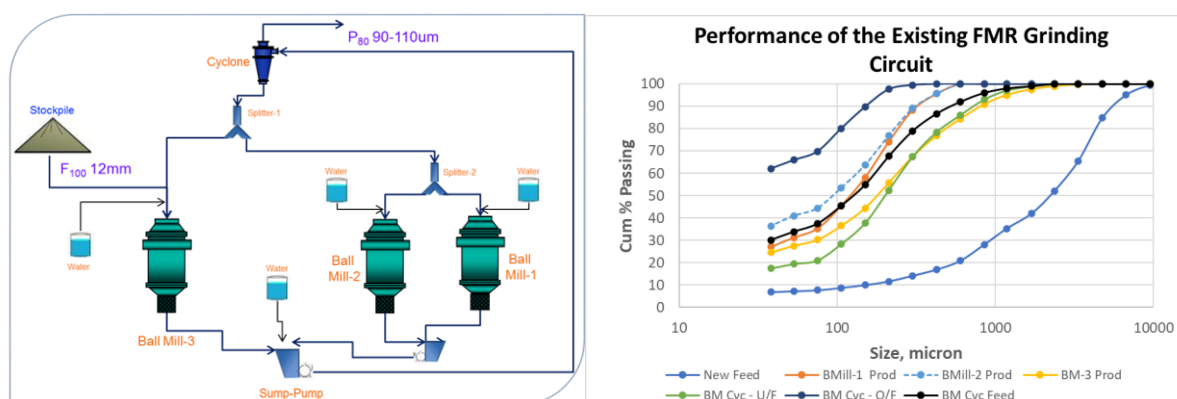


Figure 8: a) Greenfields Mill Operation grinding circuit flow diagram and b) Grinding survey size distribution data.

The FMR grinding circuit at the Greenfields Mill Operation was treating about 2 800 dry tonnes per day using 3 overflow balls mills – 1325 kW (Mill#1 - 3.8 x 6m), 875 kW (Mill#2 - 3.32 x 5.18m) and 500 kW (Mill#1 - 2.7 x 4.8m), all in one closed circuit with new feed of F₈₀ 6-10 mm going into the Mill#3 (Figure 8). The Bond work indices (BWi) and product size varies with the ore treated in the toll treatment facility.

FMR Greenfields Mill Operation reached out to EEMS Australia with the objective of improving the grinding efficiency of the toll treatment facility to increase the plant throughput. An initial plant visit and grinding survey was carried out in October 2019 and the results were sent to EEMS for analysis and modelling in January 2020. Following is a summary of the data analysis, EEMS's holistic modelling results and the plant operating results.

EEMS modelling and simulation results with EEPL technology

EEMS carried out holistic modelling of the FMR Greenfields Mill Operation grinding circuit using the design, process, and operational data provided along with the particle size distribution (PSD) and percent solids data from grinding surveys.

The major issue in each existing overflow ball mill was the presence of a large slurry pool well above discharge trunnion level, which:

- Absorbs a significant amount of grinding energy.
- Exerts buoyancy force on media, thus reducing grinding efficiency.
- Reduces probability of particle breakage as illustrated in the Discrete Element Modelling (DEM) charge motion and transport simulations (Figure 9).

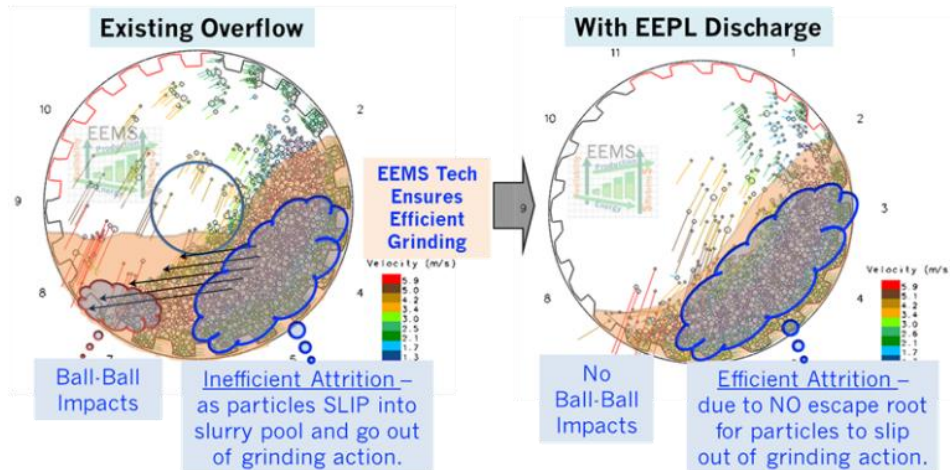


Figure 9: Charge motion in Mill#2 a) with overflow and b) with grate-EEPL discharge.

The EEMS design, consisting of optimised patented EEPL discharge system and shell liners, eliminates all material transport issues and ensures efficient grinding conditions for particle breakage by:

- providing a smooth cascading motion with efficient attrition without the excess slurry, which results in efficient grinding while ensuring all particles pass through the grinding media.
- ensuring optimal grinding conditions to significantly improve particle breakage rates and allow efficient material transport.
- producing a steeper particle size distribution which then improves classification efficiency and reduces the circulating load.

EEMS holistic modelling results and recommendations

The holistic modelling for FMR Greenfields Mill Operation grinding circuit converting Mill#2 from overflow to grate-EEPL discharge, together with a chart showing the comparison of Mill#2 discharge PSD, are given in Figure 10.

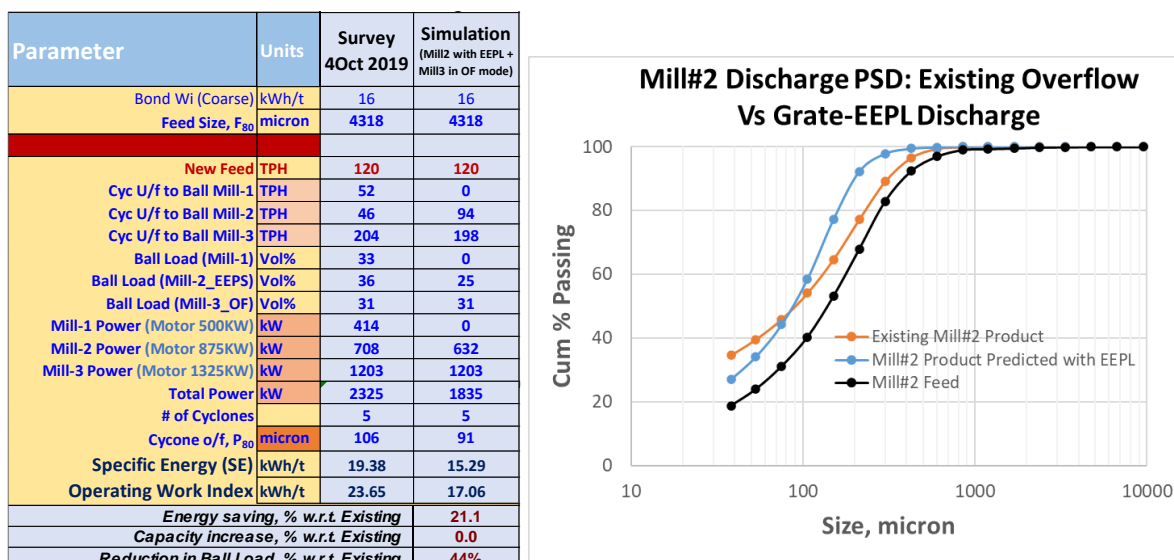


Figure 10: a) Modelling and simulation results and b) comparison of Mill#2 product PSD.

The key benefit of converting Mill#2 from overflow to grate discharge with EEPL technology is that the FMR Greenfields Mill Operation grinding circuit will have surplus capacity to utilise as and when required. Important process advantages noted from the installation are as follows:

- capacity to allow Mill#1 to be completely bypassed and reduce operational costs.
- Mill#2 will be able to do the work of both Mill#1 and Mill#2 as overflow mills, demonstrating the ability of the grate-EEPL system to double the grinding capacity for the same product size, while saving 70 kWh of motor power, and observing a 31% reduction in ball charge in Mill#2.
- reduction in plant specific energy to 15.29 kWh/t (from 19.38 kWh/t), leading to a 21.1% decrease in plant energy requirements.
- improved breakage of +150 μm particles, as all particles must trickle through the tumbling grinding media.
- relatively lower fines generation, as the finer particles discharge faster than the coarse particles and present for classification.

The following stagewise recommendations were given to FMR for implementation to realise the stated benefits.

Stage-1: Convert Mill#2 to grate-discharge with EEPL technology and completely bypass Mill#1, reducing energy requirements by 21.1% as well as saving power, operating, maintenance, and media consumption costs associated with Mill#1.

Stage-2: Convert Mill#3 to grate-discharge with EEPL technology to increase total energy savings to 36% and increase grinding capacity.

Stage-3: Upgrade classification circuit to handle the extra grinding capacity created.

Implementation of Stage 1-converting Mill#2 from overflow to EEPL grate discharge system

The custom designed EEPL discharge pulp lifters and grates were made of chrome-moly steel while the shell and feed head liners were made of rubber. Conversion of Mill#2 from overflow to grate-EEPL discharge occurred in April 2022.

After installation, the circuit started in the pre-installation configuration with all three mills in operation. Shortly after start-up the feed to Mill#1 was gradually diverted to Mill#2 while observing the Mill#2 product size and adjusting the ball charge as required. Mill#2 ball charge volume started

at 15% and gradually increased to 21% until Mill#1 was completely bypassed. The proportion of cyclone underflow was also increased towards Mill#2, however no quantitative estimation was done. Mill#2 discharge end with grate-EEPL system is shown in Figure 11 together with the grates after 3 and 4 months of operation.



Figure 11: a) Mill#2 with grate-EEPL discharge end and b) worn steel grates after 3 months c) worn rubber grates after 4 months.

While the rubber liners have worn at the expected wear rate, taking into consideration the increased mill productivity, higher wear rates were observed on the steel grates. This prompted steel grates to be replaced with rubber grates, which improved grate life. Alternative designs are being considered to further improve the life of grates. Pegging of both steel and rubber grates has not been an issue.

Pre and post grinding survey data

Grinding surveys were carried out before and after installation of EEPL grate discharge system in Mill#2 to assess the performance of the overall comminution circuit with details given in Figure 12.

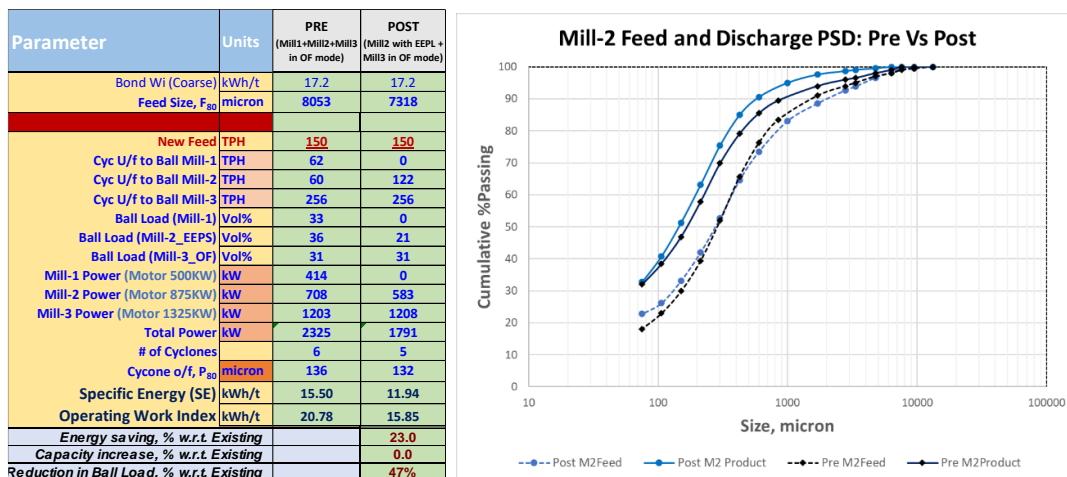


Figure 12: a) Pre and post survey data b) Pre and post comparison of Mill#2 feed and product PSD.

Comparing the pre and post grinding survey data shown in Figure 12, the following observations were made:

- Savings of 534 kWh of motor power from secondary grinding mills (Mill#1 and Mill#2) has decreased the plant specific energy from 15.50kWh/t to 11.94kWh/t – a reduction by 23%.
- Although mill feed and product size from the pre and post grinding surveys of 2022 (Figure 11) are significantly different to the 2019 survey (Figure 10), the observed plant energy savings (23%) matched well with the predicted energy savings (21.1%), which illustrates the predictive capability of the EEMS holistic modelling approach.

- The PSD of Mill#2 product post installation shows higher breakage of coarser particles as predicted in the simulation (Figure 10), which indicates a fundamental advantage where particles cannot bypass the tumbling media, (unlike in overflow ball mills due to presence of a large slurry pool) which increases particle breakage rates.

Pre and post operational data

The daily operational data of pre (January 2021 to March 2022) and post (April 2022 to Apr2023) conversion of Mill#2 from overflow to EEPL grate discharge system has been compared to evaluate the performance of FMR Greenfields grinding circuit.

Comparison of plant throughput:

Operational results since April 2022 have amply proven that the conversion of the overflow ball mill to a true open-ended grate mill using EEPL technology enables a significant increase in mill capacity for the same grind size. In addition to doubling Mill#2 capacity, diverting a higher proportion of cyclone underflow towards Mill#2 has also helped increase plant capacity by 10% from 0.935 Mt/y using Mill#1+Mill#2+Mill#3 to 1.025 Mt/y using Mill#2+Mill#3 (Figure 13).

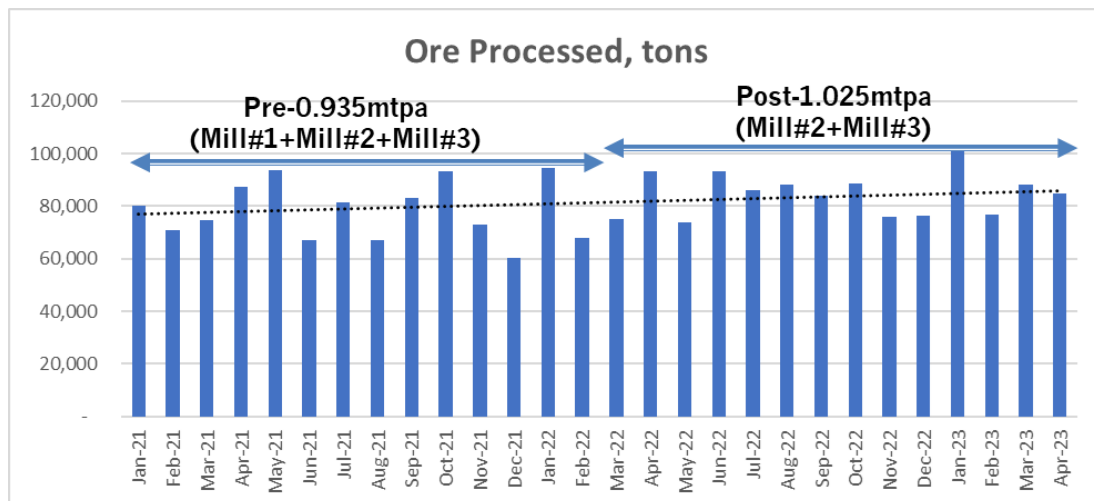


Figure 13: Pre and post comparison of plant throughput.

Comparison of plant power consumption:

Pre and post data of daily plant power draw and daily plant specific energy are plotted in Figure 14 which clearly shows the power savings since implementation of the grate-EEPL system in Mill#2 with plant power draw decreased from 2315 kWh to 1805 kWh – a saving of 510 kWh on average since April 2022, which reduced the plant specific energy by 22% from 19.07 kWh/t to 14.44 kWh/t while doing the same or more grinding without Mill#1.

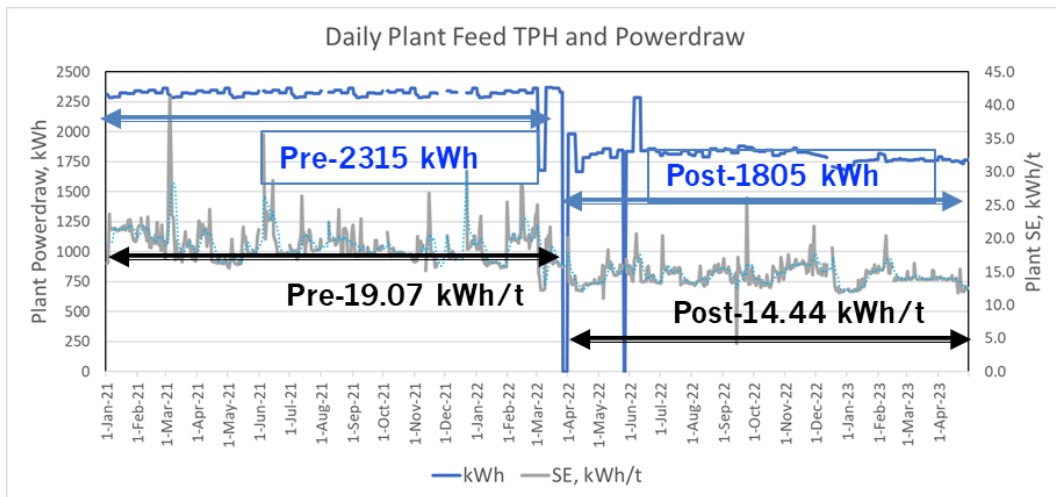


Figure 14: Pre and post comparison of plant power draw and plant specific comminution energy.

Comparison of feed and product size:

Effective utilisation of ball action and quick migration and removal of the finished product enables grinding of particles with high energy efficiency, and this too can grind coarser particles, which is evident from Figure 15, where the daily plant data of feed (F_{80}) and product (P_{80}) size are plotted for pre and post operating conditions. It is visible from Figure 15 that the product size gradually increases with increase in feed size before conversion, whereas finer product is generated after conversion of Mill#2 to grate-EEPL discharge.

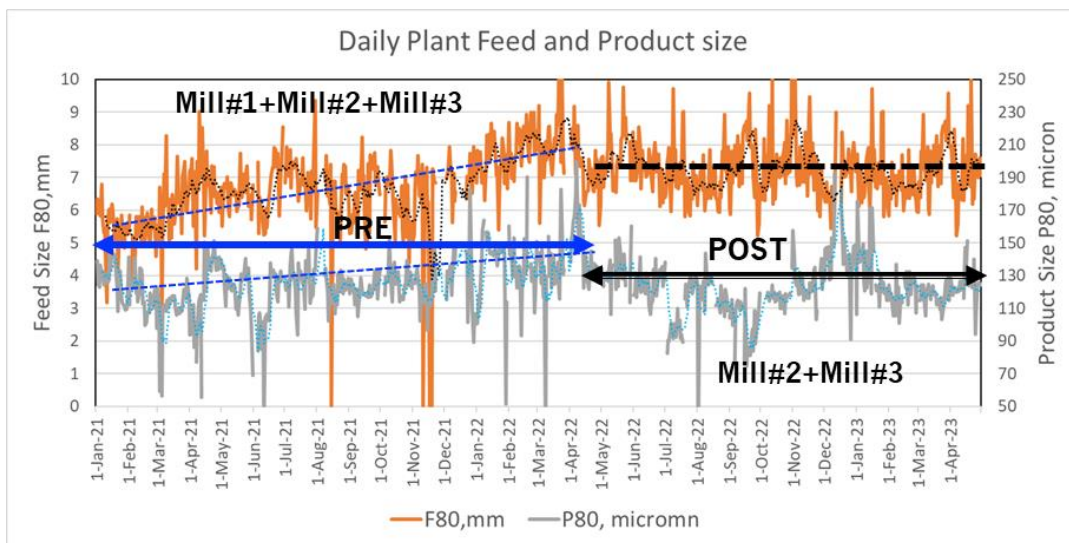


Figure 15: Pre and Post comparison of plant feed and product sizes.

Comparison of ball wear:

The plant media consumed in 12 months before conversion of Mill#2 was 875 t to process 0.935 Mt of ore, while used 769 t of media and processed 1.025 Mt of ore. In contrast to the general concern of higher ball wear and ball breakage, media wear decreased from 936 g/t to 751 g/t (a 19.7% reduction) as shown in Figure 15, while processing more tonnes. Lowering the media consumption also leads to a reduction in carbon footprint by 2.3 kg CO₂ per kg of steel ball consumption (Morrell 2022), and it is estimated to further reduce CO₂ emissions by 397 t/y to process 0.935 Mt/y of ore in post operational scenario. Similar observations were made at Jindal Saw and Degussa, where hi-chrome media is used.

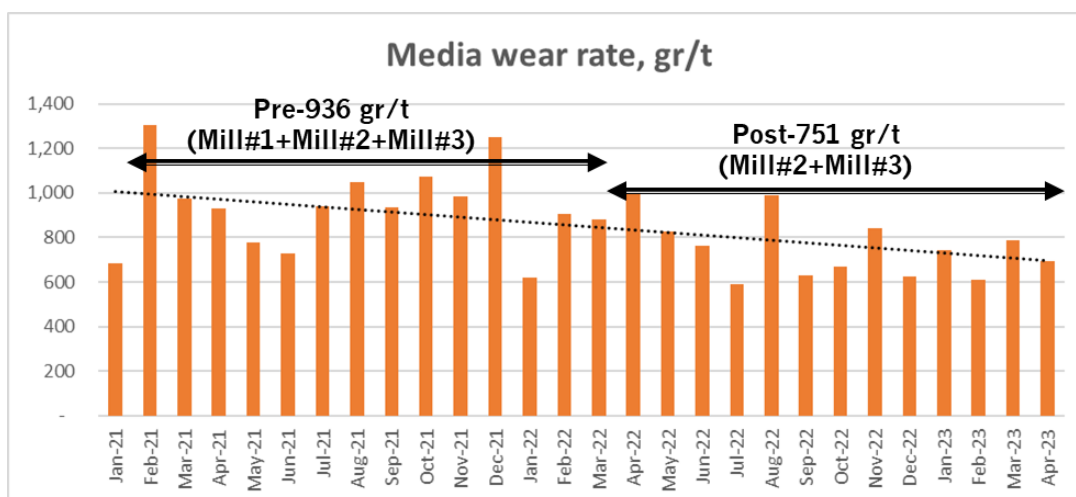


Figure 16: Pre and post comparison of media consumption.

ENERGY EFFICIENCY AND CARBON FOOTPRINT

A major contributor to the carbon footprint of the mining industry is comminution and the pressure to significantly improve comminution energy efficiency is intense. Morrell (2022) recently estimated the annual electricity consumption of AG/SAG and ball mills as 116.5 billion kWh (TWh) with 48.9 billion kWh being consumed in AG/SAG mill circuits and 67.6 billion kWh in ball mill circuits. Considering a global emissions rate of 0.556 kg CO₂/kWh of electricity generated and a total of 2.3 kg CO₂ emitted per kg of steel ball consumption, Morrell (2022) estimated the total annual CO₂ emissions from AG/SAG and ball mills as summarised in Table 3 including the potential reduction in CO₂ emissions of the mining industry using High Pressure Grinding Rolls (HPGR) technology.

Table 3: Estimated global CO₂ emissions from AG/SAG-ball mill circuits and potential savings using HPGR-ball mill technology (Morrell 2022).

Estimated Global Data	Units - per year	AG/SAG-Ball Mill
Electricity consumption	TWh	116.5
CO ₂ from electricity generation	Mt	64.8
Steel ball consumption	Mt	6.5
CO ₂ from steel ball manufacture	Mt	15.0
Total CO ₂ emissions	Mt	79.8

Consistent operation of ball mills over the last few years after converting from overflow to open-ended grate discharge with EEPL technology has demonstrated a significant increase in energy efficiency with a considerable reduction in specific energy consumption, as predicted and observed in both laboratory and pilot scale tests carried out at the University of Utah (Latchireddi R, 2017).

CO₂ emissions are estimated using the specific energy (kWh/t) values and the throughput operated after converting an overflow mill to a grate discharge using EEPL technology for each of the case studies and summarised in Table 4.

Table 4: Estimated CO₂ emissions from case studies based on specific energy consumption and absolute power savings from converting overflow to grate discharge with EEPL Technology.

Based on Specific Energy (SE) consumption	Copper (Degruusa)		Magnetite (JSW)		Gold (FMR)	
	Before (Overflow)	After (EEPL)**	Before (Overflow)	After (EEPL)**	Before (Mill#1+Mill#2)	After (Mill#2-EEPL)**
# of Mills	1	1	3	3	2	1
Bwi, kWh/t	14.3	14.3	15.5	15.5	17.4	17.4
Ball Load, Vol%	33	18	32	16	36	21
Throughput, TPH	187	236	128	159	122	122
Motor Power, kW	2800	2800	2800	2800	1300	825
Power Draw, kWh	2321	1690	2214	1492	1122	612
Sp Energy, kWh/t	12.412	7.161	17.297	9.384	9.221	5.016
%Energy Savings wrt Overflow		42.3	-	45.7	-	45.6
Tonnes of CO ₂ Emmissions wrt specific energy@tph**	13,029	7,517	12,233	6,636	5,004	2,722
Reduction in CO₂ Emmissions, tonnes/yr		5,512		5,596		2,282
%Reduction in Carbon Footprint		42.3		45.7		45.6
** throughput attained with EEMS is taken for estimation of CO₂ emmissions						
Based on absolute power savings	Copper (Degruusa)		Magnetite (JSW)		Gold (FMR)	
	Before (Overflow)	After (EEPL)	Before (Overflow)	After (EEPL)	Before (Mill#1+Mill#2+ Mill#3)	After (Mill#2-EEPL+ Mill#3)
Power Draw, kWh	2321	1690	2214	1492	2315	1805
Tonnes of CO ₂ Emmissions per Year from Electricity	10,324	7,517	9,848	6,636	10,297	8,029
Reduction in CO₂ Emmissions, tonnes/yr		2,807	-	3,211	-	2,268
%Reduction in Carbon Footprint		27.2	-	32.6	-	22.0

An example of estimating CO₂ emissions for the FMR (Gold) case is provided following:

Reduction of CO₂ emissions based on the specific energy:

- Base case in overflow = 122 tph x 9.221 kWh/t x 8000 hr x 0.556 kg)/1000 = 5004 t CO₂ per annum.
- With EEMS = (122 tph x 5.123 kWh/t x 8000 hr x 0.556 kg)/1000 = 2780 t CO₂ per annum.

Reduction of CO₂ emissions based on the absolute power savings:

- Absolute motor power savings per hour = 2315-1805 = 510 kWh
- Reduction in CO₂ emissions per annum= 510kWhx 8000 hr x 0.556 kg) /1000 = 2,268 t

Considering the absolute motor power savings realised at each of the operations, without considering the increased throughput, the estimated annual reduction in carbon footprint in tonnes of CO₂ emissions are given in Table 4, which shows an average of 27.3% reduction in carbon footprint. This illustrates that the global carbon footprint from ball mills can be reduced to the tune of 10.26 Mt of CO₂ emissions per year from a total of 37.58 Mt (58% of 64.8 Mt) of CO₂ emissions generated from global power consumption of ball Mills.

CONCLUSIONS

Successful operation of numerous ball mills installed at copper, iron, and gold operations, after converting overflow ball mills to open-ended grate mills using EEPL discharge technology, has illustrated the benefits observed early in the twentieth century when the Marcy open-ended grate discharge mill was compared against Hardinge's conical overflow mill at Inspiration Hills Copper Mine (Van Winkle, 1918).

Since successful conversion of one secondary overflow mill at the Greenfields Mill Operation in March 2022, the plant has been operating with one primary mill and one secondary mill and not needing to utilise a second secondary mill, demonstrating the magnitude of attaining high throughput in open-ended grate discharge mills compared to overflow mills.

Following comparison of one-year of post-operational data with one year of pre-operational data, the following observations were made:

- a reduction of 510 kWh in electricity consumption, which reduced specific energy of the secondary grinding circuit by 45.6% and overall plant specific energy by 22%
- saving of 510 kWh (4.08 million kWh per annum) electrical energy reduces a total of 2268 t of CO₂ emissions per annum.
- a decrease in grinding media consumption by 19.7% that further reduces the CO₂ emissions by 397 t/y for processing 0.935 Mt/y.
- increased plant capacity by 10% from 0.935 Mt/y to 1.025 Mt/y
- a sharper product size distribution with coarser feed product
- an ability to use percent solids to control product size.

FMR Greenfields Mill Operation is considering the upgrade of the primary Mill#3 from an overflow to an EEPL discharge system based on the results of the Mill#2. This is expected to save more energy, further reduce the operations carbon footprint, and provide circuit flexibility when toll treating different ore types.

Converting overflow ball mills to open-ended grate mills using EEPL discharge technology can result in:

- improved revenue by increased throughput with a lower carbon footprint
- direct power savings with real reductions in carbon emissions
- direct media cost savings
- no requirement to sacrifice the primary grind (and recovery) in mill-limited operations.

ACKNOWLEDGEMENTS

The authors would like to express their sincere gratitude to all the individuals and organisations that have contributed to the publication of this research paper. First and foremost, they thank the (late) Professor Dr. Rajamani, for his invaluable guidance and support throughout the research process. His expertise and insights were instrumental in shaping the direction and focus of this research.

The authors extend their heartfelt gratitude to their guru and mentor Dr. Morrell for giving the research topic to work on transport through grate and pulp lifters for their PhD at JKMRC.

The authors are also grateful to FMR Greenfields Mill Operation in Western Australia and JSW at Bhilwara, Rajasthan, India for providing support and operational data. Without their support, it would not have been possible for this project to be completed.

REFERENCES

- Knoblauch, J., Hooper, B and Latchireddi, S., 2015. Commissioning of Sandfire Resources Copper Processing Plant at DeGrussa, Western Australia. Paper 62, SAG 2015 Conference, Vancouver 2015.
- Latchireddi, R., 2017. Study of grate discharge and overflow ball mills - differences, scale-up and model validation, Ph.D. Thesis, University of Utah, USA.
- Latchireddi, S., 2002. Modelling the performance of grates and pulp lifters in autogenous and semi-autogenous mills, Ph.D. Thesis, University of Queensland, Australia.

- Latchireddi, S., 2006. A New Pulp Discharger for Efficient Operation of AG/SAG Mills with Pebble Circuits. Proc. SAG 2006, Vancouver, Canada.
- Latchireddi, S., and Latchireddi R, 2016. US10668477, Pulp Lifter (Energy Efficient Pulp Lifter- EEPL is the trade name).
- Latchireddi, S. and Morrell, S., 2003a. Slurry flow in mills: Grate-only discharge mechanism part-1, Minerals Engineering, 16(7), 625-633.
- Latchireddi, S and Morrell, S, 2003b. Slurry flow in Mills: Grate-Pulp lifter discharge mechanism part-2, Minerals Engineering, 16(7), 635-642.
- Latchireddi R., Rajamani R. K., and Latchireddi S., 2015. Overflow versus grate discharge ball mills: an experimental investigation, CMP 2015.
- Marcy Mills-One easy Step, 1942. The Mines and Miners Supply Company USA, Technical Brochure No 101.
- Mclvor, R.C., and Makni, S., 2023. The effects of discharge design on wet ball milling performance, SME Annual Meeting Feb 2023, Denver, Preprint 23-057, 1-5.
- Mokken, A.H., Blendulf, G.K.I. and Young, G.J.C., 1975. A study of the arrangements for pulp discharge on pebble mills, and their influence on mill performance. J.S. African IMM, May, 257-289
- Morrell, S., 2022. Helping to reduce mining industry carbon emissions: A step-by-step guide to sizing and selection of energy efficient high pressure grinding roll circuits, Minerals Engineering, 179, 1-26.
- Morrell, S. and Kojovic, T., 1996. The influence of slurry transport on the power draw of autogenous & semi-autogenous mills. Autogenous and semi-autogenous grinding technology, Vancouver, Eds: Mular, Barratt and Knight, xii-xvi University of British Columbia : 378-389.
- Rowland, C.A and Kjos, J.M. (1975) Autogenous and semi-autogenous mill selection and design, Australian Mining, September, 21-35
- Songfack, P., Rajamani, R., 1999. Hold-up studies in a pilot scale continuous ball mill: dynamic variations due to changes in operating variables. Int. J. Miner. Process. 57, 105.
- Taggart, A.F., 1945. Handbook of Mineral Dressing, John Wiley and Sons, Inc. New York : 5(78)-5(80)
- Van Winkle, C. T., 1918. Recent tests of ball mill crushing, Transactions of The American Institute of Mining Engineers, New York Meeting 1918, Vol-LIX,227-248

Commercialisation Pathway for Low Energy Gyratory Rolls Crusher Technology

M Drechsler¹ and W Skinner²

1. Director, CBSM Mining Services Pty Ltd, Adelaide SA 5167, mark@cbsmmining.au
2. Research Professor, Future Industries Institute, University of South Australia, Mawsons Lakes SA 5095, William.Skinner@unisa.edu.au.

ABSTRACT

Comminution accounts for over 5% of global energy consumption and an innovative Gyratory Rolls Crusher (GRolls™) technology has been developed in South Australia to reduce energy and water consumption, providing dry and wet crushing from ~20 mm to 20 µm fractions without media, replacing up to two stages of size reduction. The GRolls is a compression-based particle size reduction device, designed to generate fine and ultra-fine products from coarse feeds, by simultaneously applying pulsed compression and shear forces to a packed particle bed. The breakage mechanisms initiated by these forces include impact breakage, inter-particle compression, induced tensile failure and particle shear forces generated by a gyrating roll.

The paper presents the commercialisation pathway of the GRolls technology, from “proof of concept” to laboratory scale Alpha prototype and upscaled 3-5 t/h Beta prototype for a pilot plant. A systematic progression of laboratory scale testing of a wide range of feed materials through the Alpha prototype was undertaken to confirm the “proof of concept” design and identify the many design variables and operational configurations that affect the GRolls crushing and energy performance. The test results were evaluated against some of the currently available comminution solutions such as the High Pressure Grinding Rolls (HPGR) and Vertical Rolls Mill (VRM) that the sector is moving towards to provide more economical dry comminution and a progression towards partial to fully dry process flow sheets.

The commercialisation pathway has confirmed the broad performance range and energy consumption of the GRolls which could be modularised in the near future to support new and existing low grade mining operations including critical minerals, potentially unlocking resources located in remote areas restricted by limited water and power infrastructure.

Introduction

Comminution is the reduction of solid materials from large to smaller particle sizes by crushing, grinding or milling. Comminution for mining accounts for approximately two percent of the total global power consumption and generates similar levels of greenhouse gas emissions (Engeco, 2021). In a typical mining operation comminution circuits may account for around 25% of its power consumption, with power accounting for around 10% of operating costs and grinding consumables (media) accounting for up to 30% of operating costs. In cement production, grinding accounts for nearly 70% of their operating power cost (ECRA, 2015), and a similar level of global power consumption to mining.

Mine operators are seeking continual capital and operating cost reductions to stay competitive, increasing power efficiencies from their comminution circuits and lower water demands to meet stricter regulatory requirements, higher environmental sustainability and community expectation levels (Luukanan, 2020). Mining operations are also becoming more remote as global resources are exhausted, with new lower grade mining operations generally having limited access to water and power infrastructure.

The International Energy Agency (IEA) identified in their 2022 report “The Role of Critical Minerals in Clean Energy Transitions” the following mining industry trends which will impact on meeting Net Zero targets by 2050:

- Declining ore quality and more complex ore bodies
- Industry takes 17 years on average from discovery to production
- Many mineral deposits in areas of “high water stress”
- Production of many critical minerals needs to increase many fold
- Environment, Social & Governance (ESG) imperatives will drive energy efficiency production.

Energy efficient crushing technology currently extends down to around the 1-10 mm particle size, below which attrition and grinding circuits are used to achieve fine grind sizes below 100 µm. Grinding equipment such as ball mills, semi-autogenous grinding (SAG) mills, autogenous grinding (AG) mills and stirred media mills can account for a large portion of the mine operations power requirements, are wet processes and use media. The mining sector is moving towards greater use of HPGR and VRM to provide more economical dry comminution and a progression towards dry process flow sheets. The ability to undertake mineral processing using dry circuits reduces the amount of water needed for processing and concentration, which could lead to the elimination of tailings storage facilities that cover large surface areas and reduce the risk of catastrophic failures.

An example is the new flow sheet developed for the OZ Minerals (now BHP) West Musgrave copper nickel deposit in Western Australia, where dual VRM’s replace traditional SAG and ball mill circuits prior to flotation and separation circuits. The dry flow sheet has eliminated the need for media, improved flotation recovery and reduced power consumption by 15% sufficiently for the project to be powered by 70% renewable energy sources (OZ Minerals, 2020). The Grange Resources Southdown project in Western Australia has developed a Prefeasibility Study also based on dual VRM’s for a dry magnetite flow sheet (David et al, 2023).

Concept Design

In 2017 a concept for Gyrotory Rolls Crusher (GRC) technology was developed in Adelaide Australia by Mr Chris Kelsey based on his over 60 years’ experience in the mining industry. The GRC technology was developed to meet industry need for comminution units capable of operating in both dry and wet conditions, and reducing coarse feed (i.e. up to 20 mm) into fine and ultra-fine particle sizes (e.g. less than 100 µm), appropriate for first stage beneficiation. The commercialisation pathway for the GRC technology is described in more detail in Drechsler and Skinner (2023).

The GRC technology is a unique combination of load mechanisms designed to generate fine and ultra-fine products from coarse feeds, by simultaneously applying pulsed compression and shear forces to a packed particle bed (Figure). The breakage mechanisms initiated by these forces include impact breakage, inter-particle compression, and particle shear forces generated by a gyrating roll – thus inducing and enhancing particle tensile failure. Cyclic compression is generated as the gap is closed between the rollers due to the eccentric shaft, and steady compression is generated as the material is drawn through the gap. The shearing forces are generated due to particles moving across the opposing faces of the rollers and due to the relative cyclic gyrotory motion of the rollers. At most locations between the rollers all of these mechanisms can happen simultaneously.

The GRC technology consists of a “v” profiled main rotating roll and an opposing gyrotory roll with an intermeshing “v” profile (Figure 2). The main rotating roll is driven through a gearbox, while the gyrotory roll is mounted on a shaft with an eccentric off-set to generate the gyrotory motion. The gyrotory roll is engaged and free to rotate in mesh with the main driven roll as feed enters the crusher. The gyrotory motion generates a high frequency pulsing action which initiates shearing particle breakage. The combination of main roller rotation speed and oscillation frequencies are targeting to achieve around 10-100 impacts of the oscillating roller for each rotation of the driven roller (around 4° to 36° of rotation).

A laboratory scale (Alpha) GRC unit was designed and built (see Figure 3 and Figure 4) to confirm the

concept design and undertake multi-commodity feed material trials.

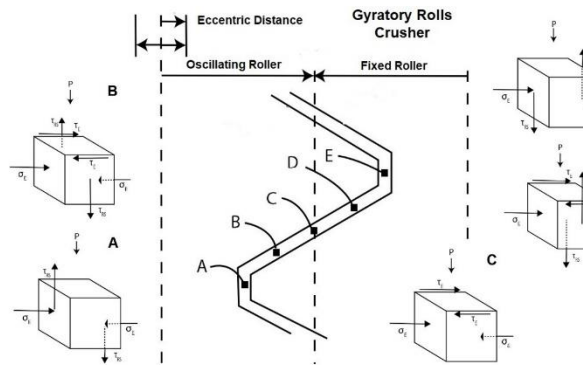


Figure 1: GRC Crushing Chamber Loads

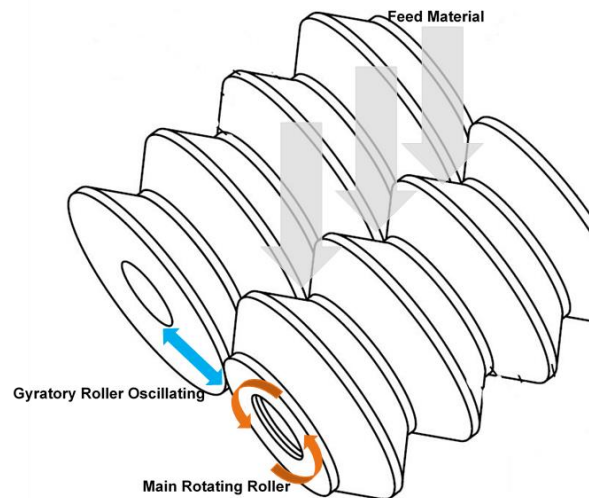


Figure 2: Concept Design of GRC



Figure 3: Roller configuration for GRC



Figure 4: Laboratory scale GRC GRolls400 unit

Concept Validation Testing

The first set of laboratory testing was conducted on a dry silica sand (<400 μm) feed material under different unit configurations and operating conditions to validate the concept design and provide essential baseline data to improve the laboratory scale unit. The concept design testing confirmed that the crushing technology can achieve size reductions in dry testing as hypothesised and modifications to the frame, bearings, drive and feed systems were applied based on test data.

As a result of the concept design testing, the Gyratory Rolls Crusher technology and GRolls trademark are now protected by various international patent and Australian trademark applications and registrations.

Systematic Testing

Systematic laboratory scale testing on silica sand, slag, limestone (- 20 mm and - 9.5 mm) and magnetite ore (- 10 mm) feed materials under different configurations was conducted over a three-year period to demonstrate and validate the impressive size reductions for a range of dry feed

materials. Testing conditions were documented and photographic/video recordings undertaken of all tests conducted. The feed and discharge materials were analysed using laser sizing unit and sieves to determine the size reduction performances, with independent particle size distribution testing conducted on all feed materials and validating the laser sizing data of discharge materials.

A summary of the grading performance of the GRolls is presented in Figure 5 which clearly demonstrates the large and consistent size reduction performance over a range of feed materials. The range of percentage fines (<75 µm) generated during a single pass ranged from 19% to 38%. Limestone (specific gravity of 2.65 g/cm³) and magnetite ore (specific gravity of 3.38 g/cm³) materials of a very similar feed size generated very similar product gradings as shown in Figure 6 even though they have very different densities and hardness properties.

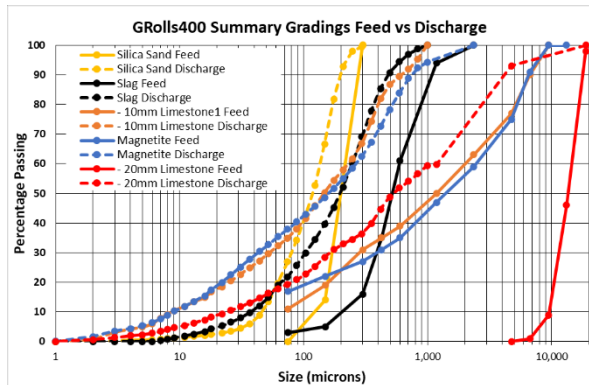


Figure 5: GRolls Gradings Summary Feed vs Discharge

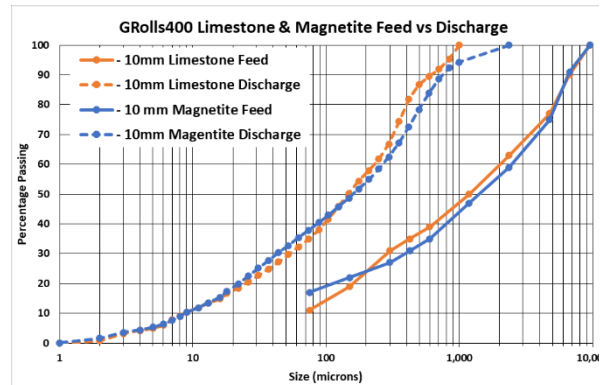


Figure 6: GRolls comparison Limestone vs Magnetite Feed

The magnetite ore material was tested as different size fractions (- 10 mm and - 3 mm) which resulted in very similar discharge curves and 38% <75 µm (Figure 7), with further testing achieving 46% <75 µm. The - 10 mm magnetite result is further compared in Figure 8 against published data from a similar magnetite ore processed by a HPGR presented in Baawuah et al (2020), showing the very impressive 38% <75 µm result for the GRolls against 18% for a HPGR. Subsequent improvements to the Alpha unit have resulted in an even higher result of 46% <75 µm for magnetite.

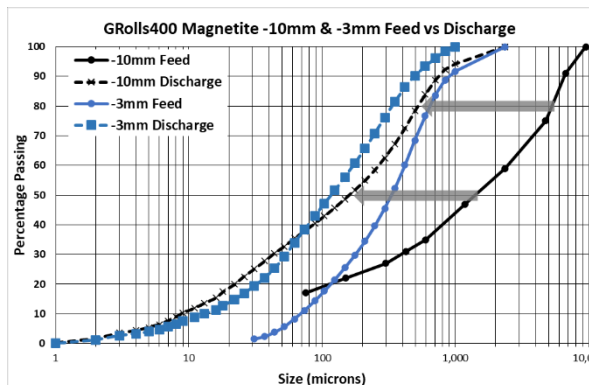


Figure 7: GRolls Magnetite -10 mm vs -3 mm comparison

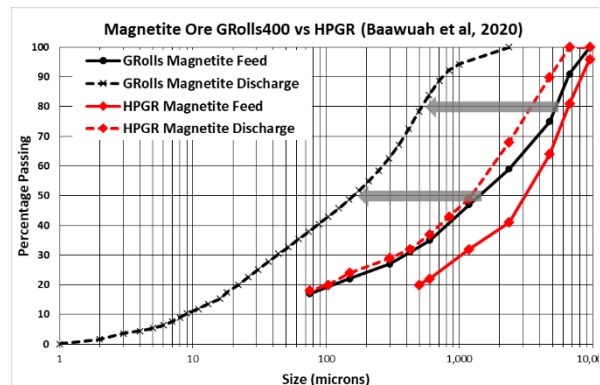


Figure 8: Magnetite Ore Comparison GRolls vs HPGR

The limestone material was further tested varying the size fractions, with 29% to 38% <75 µm generated from feed with fines which ranged from maximum size of 2.36 mm to 10 mm (Figure 9), whilst 20% to 25% <75 µm generated from feed with no fines ranging from maximum sizes of 9.5 mm to 20 mm (Figure 10). The + 2.36 mm - 9.5 mm limestone was passed through the GRolls unit a second time and recorded 63% passing 75 µm (Figure 10).

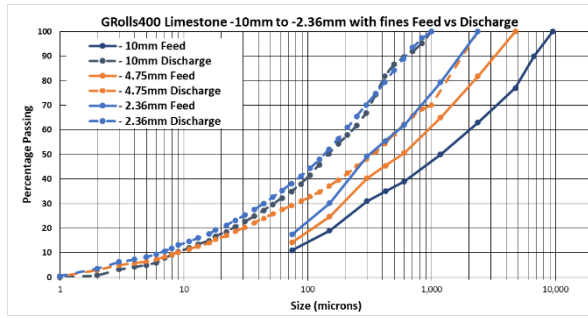


Figure 9: GRolls – 10 mm to – 2.36 mm feed comparisons

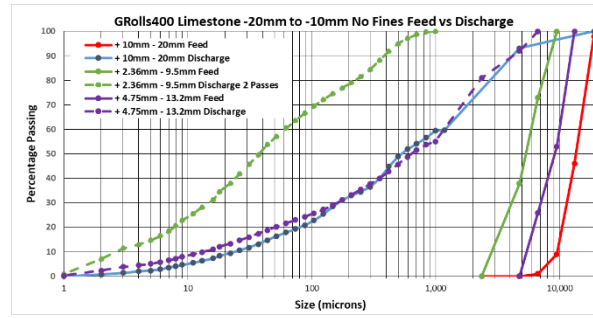


Figure 10: GRolls – 20 mm to – 10 mm feed comparisons

Another measure of the crushing performance is assessed by using reduction ratios, being the ratio of feed (F) particle size to the product (P) particle size. In this study, the 80% reduction ratio (RR80) and 50% reduction ratio (RR50) were used to estimate and compare the GRolls performance over the range of feed materials. The RR80 and RR50 were estimated using Eqs. (1) and (2), respectively.

$$RR80 = \frac{F80}{P80} \quad (1)$$

$$RR50 = \frac{F50}{P50} \quad (2)$$

Where F80 and P80 are the 80% passing feed and product particle sizes, respectively, whilst F50 and P50 are the 50% passing feed and product particle sizes, respectively.

Figure 11 demonstrates that the GRolls laboratory unit can achieve very high reduction ratios (RR80 of 10 to over 30) of dry coarse feed materials from 2 mm to 20 mm in size, whilst still achieving high reduction ratios for dry feed materials less than 2 mm (RR80 of 1.8 to 2). The percentage of minus 75 μm fraction in all tests were over 19%, with the majority exceeding 30% for both fine and coarse feed materials.

A suite of limestone materials was tested, ranging from 2 mm up to 20 mm in size, with the highest reduction ratio RR80 exceeding 17 achieved for a minus 9.5 mm material. The testing showed lower reduction ratios when coarser feed materials greater than 10 mm were tested, but still achieving an impressive 5 to 6 times RR80. The testing showed lower reduction ratios RR80 of around 2 for feed materials less than 3 mm.

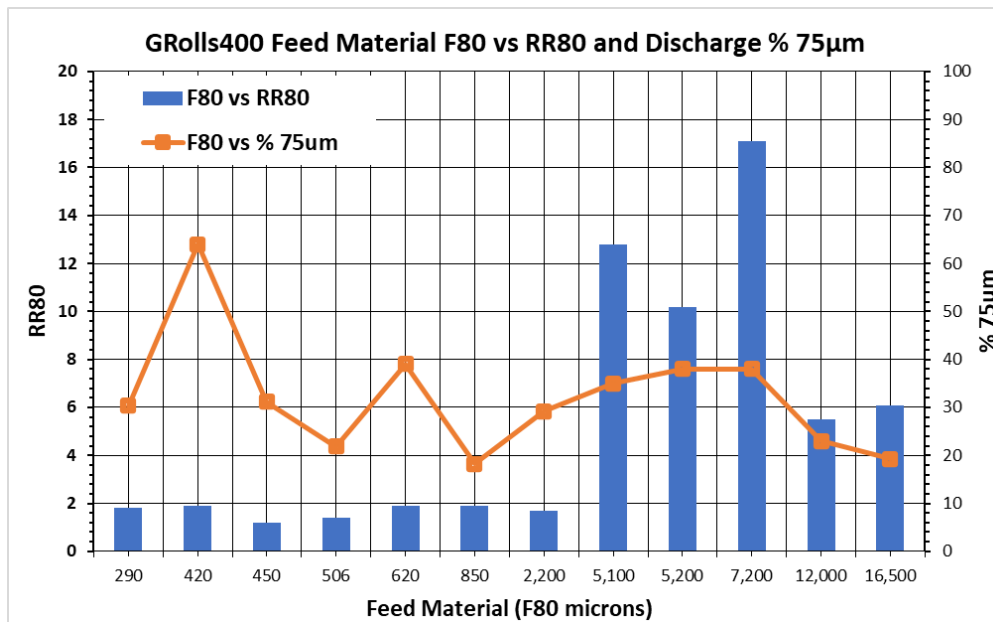


Figure 11: GRolls F80 vs RR80 and % 75 μm

The testing demonstrated that even for very coarse feed materials the GRolls was able to generate a high proportion of fines (20-46% <75 μm) in a single pass, and around 50-64% <75 μm after two passes, with high reduction ratios RR80 between 1.8 and 17.

Energy Efficiency Testing

Laboratory testing included recording the power consumption of the Alpha GRolls unit with different baseline feed materials to determine initial energy consumption and validate the concept of the GRolls being energy efficient.

The Net Specific Energy (NSE, kWh/t) was determined based on the difference between the no load and power draw during processing of the feed material, as per Eq. (3).

$$NSE \text{ kWh/t} = \frac{\text{Gross power draw (kW)} - \text{No load power draw (kW)}}{\text{Circuit tonnage (t/h)}} \quad (3)$$

The Size-Specific Energy ($SSE_{(75\mu\text{m})}$, kWh/t) is the energy consumed in a comminution process to generate particles less than 75 μm (Ballantyne et al., 2015), as per Eq. (4).

$$SSE (75\mu\text{m}) \text{ kWh/t} = \frac{NSE \text{ (kWh/t)}}{\% < 75 \mu\text{m generated} / 100} \quad (4)$$

The Bond operating work index (W_{i0}) was calculated as per Eq. (5)

$$W_{i0} = \frac{NSE \text{ (kWh/t)}}{\left(\frac{10}{\sqrt{P_{80}}} - \frac{10}{\sqrt{F_{80}}} \right)} \quad (5)$$

where P_{80} is the 80% passing size of product in μm, and F_{80} is the 80% passing of feed in μm.

The initial energy consumption test results are presented in Table 1.

Table 1: Summary of GRolls Energy Studies

Feed Material		GRolls Dry Trials					
		Silica Sand	Lead Zinc Slag	Limestone -9.5mm	Limestone 9.5 – 20mm	Magnetite Ore Feed	Magnetite Ore Re-Feed
F80	μm	290	850	5,100	16,500	5,200	620
F50	μm	230	510	1,180	14,500	1,400	320
F20	μm	184	320	160	10,500	140	110
F<75μm	%	0	5	11	0	17	11
NSE	kWh/t	3.5	3.3	4.8	8.0	9.0	5.9
SSE _(75μm)	kWh/t	11.7	17.6	13.8	41.4	23.8	15.1
W _{io}	kWh/t	17.5	35.9	10.2	69.7	29.7	37.1
P80	μm	160	446	265	2,700	510	320
P50	μm	114	271	125	520	160	110
P20	μm	64	125	31	78	22	32
P<75μm	%	30	18.2	35	19.3	38	39
RR80	Reduction	1.8	1.9	19.2	6.1	10.2	1.9
RR50	Ratio	2.0	1.9	9.4	27.9	8.8	2.9

Note F = feed material, P = product discharge single pass

The GRolls energy results are compared to magnetite ore testing for the HPGR (Baawuah et al, 2020), VRM and AG/Ball mill testing (David et al., 2023). The GRolls Net Specific Energy (NSE) of 9.0 kWh/t is lower than AG/Ball milling (23.2 kWh/t), comparable to a VRM at 6.9 kWh/t and higher than the HPGR at 1.6 kWh/t. The GRolls reported very large size reductions (RR80) generating over twice the fines content (%<75 μm) which results in significantly lower recirculation loads and low overall energy consumption for tertiary and quaternary dry comminution circuits.

Main Drive Testing

Laboratory testing was conducted to determine the effect of varying the speed of the main drive on the crushing performance. Baseline limestone feed minerals of minus 9.5 mm and 9.5 mm to 20 mm fractions in a single pass, and a second pass (9.5-20 mm refeed) were tested over a large range of main drive speeds, as shown in Figure 12 to Figure 14.

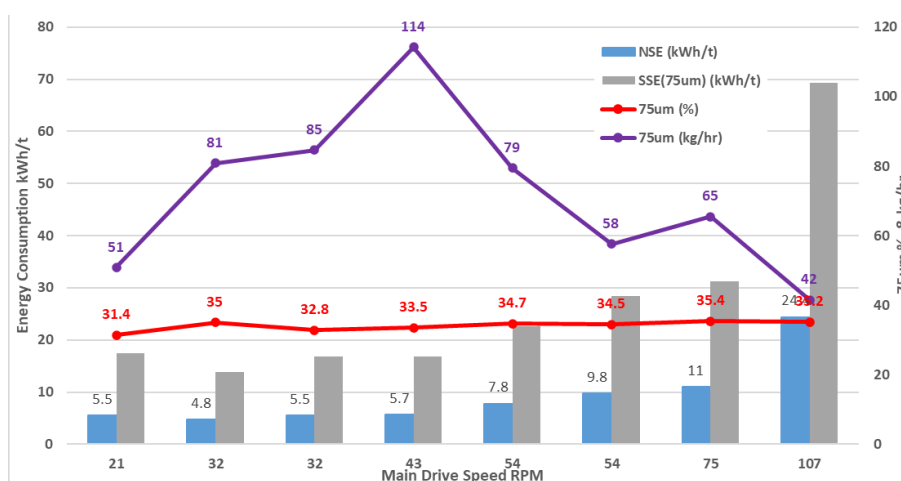


Figure 12: Limestone -9.5mm Main Drive Speed Trials

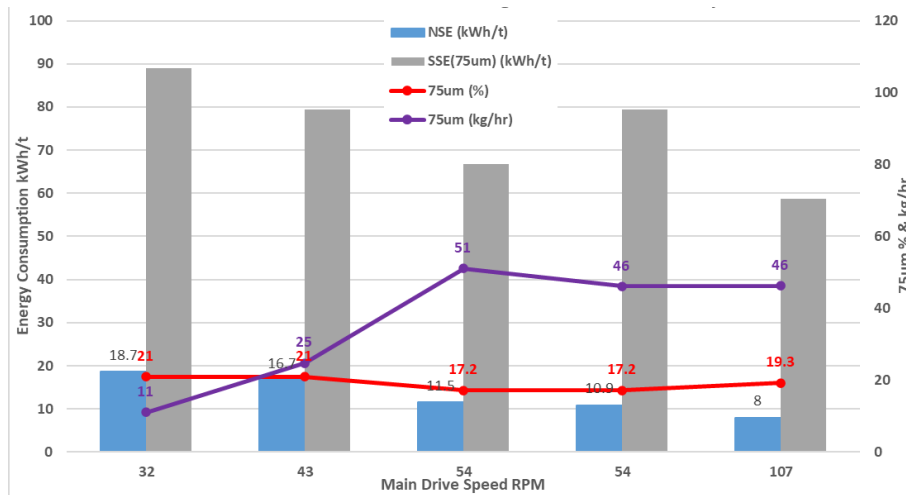


Figure 13: Limestone 9.5-20mm Single Pass Main Drive Speed Trials

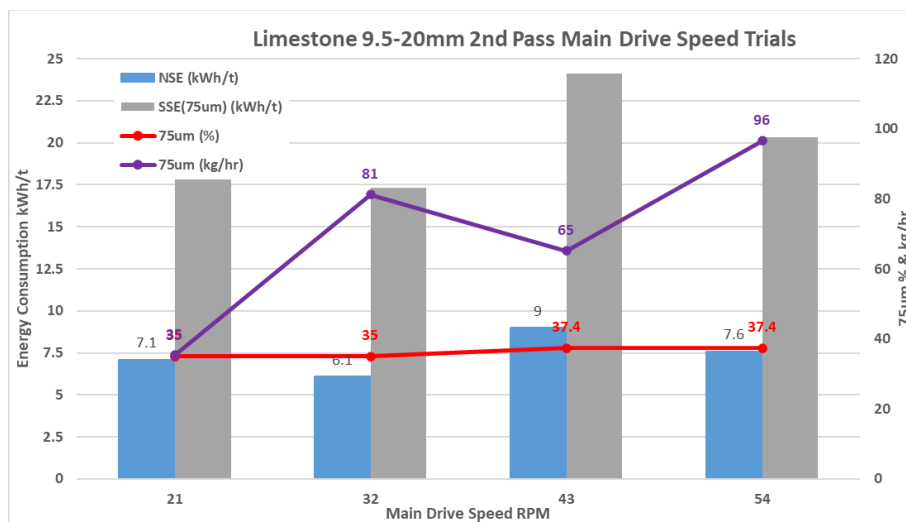


Figure 14: Limestone 9.5-20mm Second Pass Main Drive Speed Trials

The testing showed the main drive speed had a significant influence on the power consumption and production rate, and it was different for each feed material. Figure 12 shows that the power consumption increased by a factor of around five and productivity rates decreased when the speed was increase from 21 rpm to 107 rpm for a minus 9.5 mm feed material, with a similar trend for second pass materials (Figure 14). For the coarse aggregate feed material (Figure 13) the opposite occurred with power consumption dropped and productivity increased for the higher drive speeds.

This testing program demonstrated a testing program comprising many small samples (5-10 kg each) tested through the GRolls under different unit configurations can provide significant data to assess process scenarios to optimise dry plant configurations and generate samples for mineral processing testing.

Dry vs Wet Feed Materials

Laboratory testing of wet feed materials was undertaken to confirm the applicability of the GRolls technology to wet mining processes. Minus 3 mm limestone was fed as a 33-34% solids (w/w) slurry into the Alpha GRolls unit to simulate a mining wet process circuit requiring tertiary/quaternary re-grind. The test conditions included processing the same feed material dry and twice as a slurry, collecting in a discharge bin and sampling the dry and two wet discharge materials for particle size distributions.

The dry processing test was (Figure 15) conducted at a rate of around 300 kg/hr which produced comparable results to previous testing using an air classification system. Due to the size of the slurry pump the wet testing (Figure 16) was conducted at around 1 200 kg/hr (four times the dry test rate).



Figure 15: GRolls Dry – 3 mm limestone feed material



Figure 16: GRolls Wet 33% solids (w/w) slurry – 3 mm limestone feed material

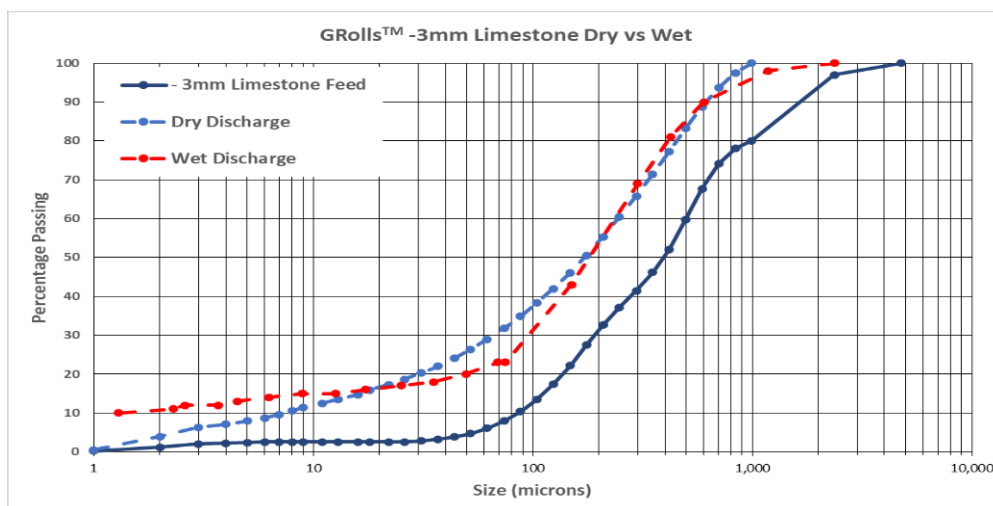


Figure 17: Gradings of GRolls dry vs wet test

Results presented in Figure 17 and Table 2 show comparative size reductions (RR80 and RR50) for the slurry coarse fractions at the very high feed rates. The % fines generation (<75 μm) was slightly less for slurry (23%) compared to dry processing (32%); however the overall rate of product fines generation was much higher due to the higher feed rates.

Table 2: GRolls Dry vs Wet Test Results

CBSM Wet Test Results		R17-T1	R17-T2
		Dry	Wet
F80	µm	1,000	1,000
F50	µm	400	400
F20	µm	110	110
F<75µm	%	7.8	7.8
Rate	kg/hr	327	1,200
% solids	% w/w	100%	33%
P80	µm	460	420
P50	µm	175	185
P20	µm	30	50
P<75µm	%	31.9	23.0
	kg/hr	104	276
RR80	Reduction Ratio	2.2	2.4
RR50		2.3	2.2

When compared to the flat rolls of the HPGR, the GRolls has chevron shaped rolls which contains and directs the slurry into the crushing chamber. Wet processing is not possible with HPGR units and VRM units, whilst possible, have had limited success in wet processing. Similar to dry testing results, the amount of fines generation is highly dependent on the slurry feed rate, with slower slurry feed rates expected to achieve improved % fines (<75 µm) generation.

Development and Research Applications

The laboratory GRolls unit will continue to be used in ongoing laboratory testing programs on various feed materials and applications to build a comprehensive test work database as a key element of Intellectual Property of the GRolls technology. The testing will include assessing further modifications and improvements to frame, bearings, load applications, feed and discharge systems, as well as different lining options.

The University of South Australia will be engaged to undertake broad Research and Development (R&D) related to GRolls energy consumption and post-comminution processing flow sheet consequences and benefits. This R&D will be led by Professor William Skinner of UniSA's Future Industries Institute. Key research investigations will include, liberation benefits afforded by high compression and shear, subsequent impact on beneficiation (wet, dry), dry comminution chemistry benefits (e.g. avoidance of inadvertent activation, improved leach kinetics, etc.) and potential for fully dry processing of commodities. This R&D will be pursued through various engagements, including advanced analysis of products via projects within the ARC Centre of Excellence, and which may include activities with many mining industry participants using the GRolls involved in a current submission for Copper for Tomorrow Cooperative Research Centre (CfT CRC, <https://www.copperfortomorrow.com.au/>) if awarded.

Commercial Applications

The GRolls units will target replacing or augmenting wet or dry tertiary/quaternary comminution units for the global mining and cement industries to provide improved energy and water efficiencies resulting in lower capital and operating costs (Figure 18).

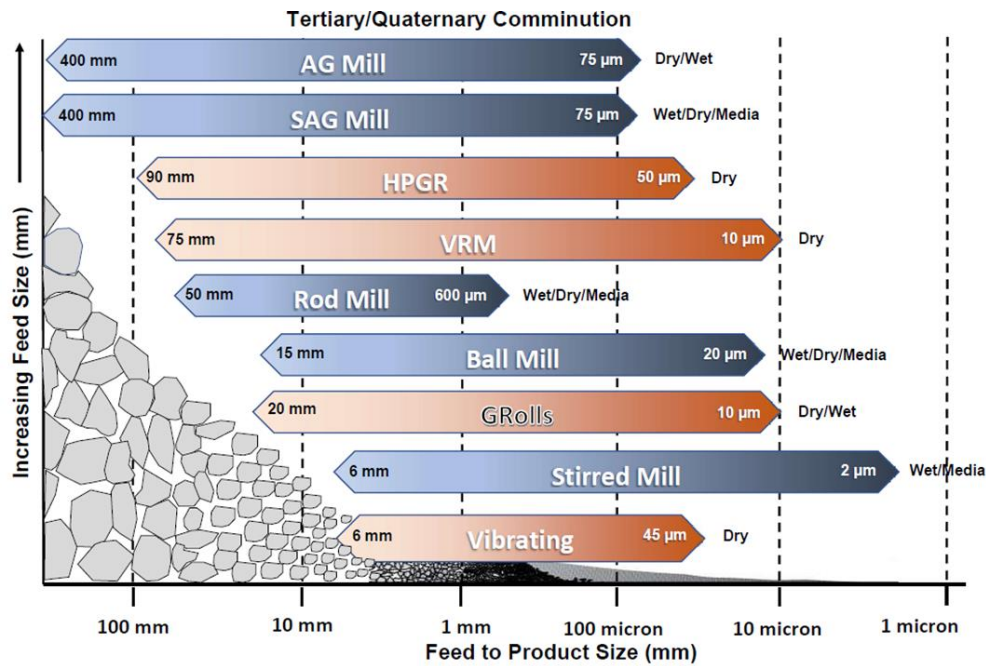


Figure 18: Tertiary & Quaternary Comminution Technologies

The GRolls technology is planned for commercial applications in the next year with small lab scale (<1 tph) and pilot plant scale (3-5 tph) units, followed by progression through to 25 tph units and 75-100 tph units. The lab and pilot scale GRolls units will be mobile and able to travel to remote mineral resource locations or academic testing facilities for testing bulk, chip and drill core samples through test equipment that closely replicate operational performances and thereby reducing project risks. These small GRolls units could also reprocess old tailings at their in situ moisture content for winning rare earths and other critical minerals.

GRolls pilot plants could be established at critical mineral resources as part of proving the resource, with the number of GRolls units incrementally increased as part of a staged establishment and subsequent expansion of a critical mineral operation. Small GRolls units for mobile plants or small pilot/modular plant units can incrementally augment existing process flow sheets to reduce bottlenecks, improve performance of existing equipment and provide smaller quantities of specialist/niche products if needed. Opportunities may be realised in processing small, satellite deposits in brownfield operations, without transporting additional tonnages to existing concentrators. Progression from smaller units to larger units can increase augmentation or replace existing flow sheet equipment as well as be installed within new dry or wet processing circuits. Replacing re-grind with “re-crush” using a GRolls prior to cleaning circuits engenders further energy savings and may also further improve recovery rates.

The GRolls can be operated dry or wet, therefore can be applied to all mineral process flow sheets, providing energy and water efficiencies, modularisation to match renewable energy sources and incremental performance improvements, from feasibility studies through to full operation. The GRolls technology can provide significant competitive advantages to our customers as the design is simple, scalable and robust which will allow units to have low manufacture costs whilst achieving power savings, increased fines generation and flow sheet flexibility.

The GRolls can also be applied to the cement industry as well as waste recycling applications.

Conclusions

A concept for a GRolls technology that can operate in both wet or dry process conditions whilst reducing coarse feed into fine and ultra fine particle sizes with low recirculation rates has been

progressed through extensive laboratory testing. These results confirm that the GRolls can achieve final product sizes less than 75 µm in a few passes with lower recirculation loads resulting in lower power consumption, without media and could eliminate at least one stage of quaternary comminution in a mining circuit. This would achieve a simplification of the mineral processing flow sheets for many mining operations, reduce power and grinding media consumption, dramatically reduce the amount of water used, stored and consumed during the process and eliminate high risk tailings storage.

The GRolls technology will provide benefits to the following applications:

- Dry tertiary and quaternary comminution circuits to:
 - reduce power and water consumption
 - eliminate media and improve recovery grades
 - augment processing capacity with smaller modular units
- Wet re-grind circuits for lower power consumption and eliminating media
- Crush dry, moist or wet tailings, fly ash, slags or other valuable waste materials
- Mobile crusher for laboratory, exploration, pilot plant studies or integration into modular process trains.

Laboratory GRC units can process both dry and wet feed materials, testing 5-10kg samples under numerous crushing configuration scenarios to replicate possible mineral processing flow sheets whilst generating fine grained samples for intensive mineral liberation testing.

Acknowledgements

The authors wish to acknowledge Mr Christopher George Kelsey, the inventor of the GRolls technology, who sadly passed away in December 2022 prior to him seeing the successful completion of the commercialisation pathway for his innovative crushing technology.

The authors acknowledge the technical and financial support of CBSM Mining shareholders.

The authors also wish to acknowledge the support of the South Australian government through the Department of Energy and Mines and their ThinkingCriticalSA incentive program and the support of the ARC Centre of Excellence for Enabling the Eco-Beneficiation of Minerals, grant number CE200100009.

References

- Baawuah, E., Kelsey, C., Addai-Mensah, J., Skinner, W., 2020. Comparison of the performance of different comminution technologies in terms of energy efficiency and mineral liberation. *Minerals Engineering* volume 156 106454.
- Ballantyne, G., Mainza, A., Powell, M., 2015. Using comminution energy intensive curves to assess efficiency of gold processing circuits. In: *World Gold*. 29 Sept – 1 Oct. Johannesburg, South Africa, Southern African Institute of Mining and Metallurgy, pp. 1-10.
- David, D., Stanton, C., Gerold, C., Schmidtz, C., Baaken, S., and Everitt, M., 2023. Pilot testing and Plant Design Comparison of Dry VRM Milling plus Magnetic Separation with AG and Ball Milling plus Magnetitic Separations for Grange Resources Southdown Ore. In prep, *Comminution23* conference proceedings, special issue of *Minerals Engineering*.
- Drechsler, M. and Skinner, W., 2023. Commercialisation pathway for a low energy wet/dry Gyratory Tolls Crusher comminution technology. In prep, *Comminution23* conference proceedings, special issue of *Minerals Engineering*.
- ECRA, 2015. ECRA future Grinding Technologies Project – Report about Phase 1. European Cement

Research Academy, Technical Report TR 127/2015.

ENGECO, 2021. Mining Energy Consumption 2021.

International Energy Agency, 2022. The Role of Critical Minerals in Clean Energy Transitions. World Energy Outlook Special Report.

Luukkanen, S., Tanhua, A., Zhang, Z., Canales, R.M., Auranen, I., 2022. Towards waterless operations from mine to mill. Minerals Engineering Volume 187 107793.

OZ Minerals, 2020. West Musgrave Pre-Feasibility Study – a low carbon, long life, low-cost mine. ASX release, 12 February 2020.

SAG Mill Stability and Control Improvements at the Nova Nickel-Copper Operation

G Gomes-Sebastião¹ and P Hudson²

1. Executive Director, Improve IO Pty Ltd, 5/74 Kent Way, Malaga, WA, greg.gomes@improveio.com.au
2. Senior Metallurgist, IGO Nova Pty Ltd, 85 South Perth Esplanade, WA, paul.hudson@igo.com.au

ABSTRACT

Strategies introduced at IGO's Nova operation have improved stability and control in the SAG milling circuit. These strategies relate to the development of a prediction model for SAG mill media volume (ball charge), and improvements to the SAG mill charge weight (total load) controller.

Prior to these improvements, poor control over SAG media charge volume and charge weight had resulted in process instability, downtime and overall reduced throughput.

Media overcharging and lack of control was tackled by development of a power-based model and a media consumption rate model of the SAG mill. These models are used to control media addition rates on a day-to-day basis to target the desired media charge.

Control of the SAG mill charge weight was improved by incorporating modelled disturbance inputs into the existing PID loop. The disturbances included were derived from an online mill feed particle size distribution measurement and a proxy for ore density/hardness, both of which were determined to be significant predictors of future mill weight changes. The issue of reducing mill weight resulting from liner wear over the reline cycle, rather than changes in actual charge weight, has also been compensated for using an adjustment to the mill weight setpoint based on measured liner consumption rates.

Following the introduction of these improvements, the issues resulting from overcharging and unstable weight control have greatly diminished resulting in improved overall throughput, reduced average SAG specific energy (kWh/t) and greater downstream stability within the flotation circuit. These models and controllers require occasional re-calibration but have proved robust over time.

INTRODUCTION

The Nova deposit was discovered in July 2012, with development of the current operation commencing in January 2015. Following a successful construction and commissioning phase, the operation commenced commercial production in July 2017, and reached its nameplate production rate in the December 2017 quarter.

The site has encouraged continuous improvement and although the plant was commissioned with the latest available technology, personnel continually strive for system and process improvements. This paper discusses a continuous improvement program centred around the operation and control of the SAG mill. A systematic approach was taken to clearly identify the problems and incrementally resolve these to increase efficiency, improve stability and reduce wear. The results of each of the incremental changes were evaluated to determine the effectiveness of the solution. This systematic approach aided in identifying changes that were of little to no benefit or changes that added complexity rather than improving the system.

The implemented systems are designed to accommodate for failures and compensation of various inaccuracies in components that may occur during live control. This allowed large changes to operating philosophy to be made without negatively impacting production on the site.

NOVA GRINDING CIRCUIT OVERVIEW

To contextualise the improvements implemented to the SAG mill operation and control, a brief overview of the comminution circuit is provided.

Run of Mine Feed Characteristics

The following description of the plant setup has been extracted from the paper written by Gomes-Sebastiao, et al, 2018. Nova-Bollinger (Nova) is a typical magmatic segregation deposit containing an assemblage of nickel, copper and iron-bearing sulfides (predominantly pentlandite, chalcopyrite and pyrrhotite respectively), with pyrrhotite being the dominant sulfide gangue mineral. A degree of variability exists within the Nova ore deposit, with six ore types classified in the PFS (prefeasibility study) according to lithology and mineralogical composition. Variation in ore supply from the mine necessitates good ROM (run-of-mine) stockpile management to minimise the variation in metallurgical responses stemming from variations in the relative abundance of ore types fed to the plant. Ore blending at Nova is based on a target nickel feed grade through the blending of ROM stockpiles that are classified according to grade.

Comminution Circuit Design

The Nova comminution circuit has a conventional primary crush followed by SAB flow sheet design, with key components described in Table 1.

Table 1 – Comminution circuit components

Circuit	Equipment	Flow path
Primary crushing	C120 Metso jaw crusher	Discharge to surge bin & mill feed
Primary milling (open circuit)	6.1 m \varnothing x 3.55 m Outotec SAG mill (variable speed drive)	Discharge to cyclone feed hopper
Secondary milling & classification (closed circuit)	4.7 m \varnothing x 6.25 m Metso ball mill (variable speed drive) 8x 400CVX cyclones	Discharge to cyclone feed hopper Overflow to flotation feed

The comminution circuit produces flotation feed to sequential copper and nickel flotation circuits via single stage crushing and a two-stage milling circuit (semi-autogenous grinding mill and ball mill). The flotation feed target is 80% passing 106 to 125 μm depending on liberation requirements to achieve optimum flotation performance. The comminution circuit was designed with the intent to provide the flotation circuit with a stable feed.

The discussion on the flotation circuits is beyond the scope of this paper, but for clarity the copper flotation circuit consists of rougher, scavenger, cleaner and cleaner scavenger circuits. The same is true for the nickel circuit consisting of rougher, scavenger, cleaner and cleaner scavenger circuits. With the nickel flotation circuit having higher capacity than the copper circuit.

INTEGRATED ADVANCED CONTROL SYSTEMS

Process automation at Nova was addressed early in the prefeasibility study (PFS) and included the adoption of advanced process control (APC) platforms and an extensive network of measurement devices. The APC platform interfaces with the underlying programmable-logic-controller (PLC) systems and is capable of adjusting controller set points and/or outputs depending on the operating mode selected by the user. The APC system is typically used for making higher level control decisions but also has an extensive range of tools that can be used for more advanced stabilisation strategies. Having an APC platform on site allowed the fast adaptation and trial of new strategies on the SAG mill.

SAG Mill Control Problems

Having operated the SAG mill for several years, various areas for improvement were identified from historical data. Firstly, the torque on the SAG mill motor ran close to its limits. The SAG mill motor is controlled by a Siemens Harmony drive, this drive has built in protection that will slow the motor down when the torque limit is exceeded. These events would cause subsequent losses in throughput and instability in the flotation circuit affecting recovery with manual intervention from the control room operator required to reduce load in the SAG mill by reducing or stopping mill feed.

Review of the design criteria for the mill demonstrated that the SAG mill should not operate this close to its torque limits. Analysis of the drivers that cause high torque events were reviewed and it was determined that having tighter management of the mill media charge would greatly assist in reducing the number of high torque events.

Reviewing historical data on SAG mill weight control demonstrated that there were multiple periods of high variability. This often-required manual intervention from the operating crew to stabilise the mill. The feed to the mill had previously been stabilised using a model predictive controller for the mill feeders. This strategy worked well, and it can be shown that the mill feed was stable and not the cause of the instability in the mill. The variability in the mill weight must therefore be related to variation in feed characteristics of the ore. In order to increase the mill stability and provide an automated solution it was determined that online measurement of feed particle size prior to the SAG mill was necessary. Additional instrumentation was sourced and implemented provide measurements for this purpose and are discussed in this paper.

Media charge control

The metallurgical team performed extensive work to monitor, predict and optimise the volume of grinding media in the SAG mill, motivated by past issues with low throughput, high torque faults (on the mill's variable speed drive) and shell liner failures caused by overcharging the mill. Prior to this work, the solution to low SAG throughput had usually been to increase media addition with little regard for the volume of media within the mill.

Following a complete reline of the SAG mill, the team measured the media volume in the mill using the cord method on a fully ground out mill, and subsequently measured the total charge (media plus rocks) following a crash-stop of the mill. These measurements, along with the mill dimensions, operating speed, and power, were used to calibrate a power model of the mill, as described by Napier-Munn et al (1996).

Over several weeks of operation, the team recorded the media addition and ore throughput, and then re-measured the media charge following a full grind out to produce a calculation of steel media consumption on a g steel/t ore treated basis. This consumption rate formed the basis of a 'live' media charge estimate that enabled the metallurgy team to vary the media addition rate and target a desired ball charge volume with a reasonable degree of accuracy. Relevant data for this live calculation was logged and queried using the OSIsoft PI historian.

The model is periodically re-assessed, and small adjustments made based on crash stop measurements (using the power model to estimate rock and filling) or following a complete grind out and accurately measuring media filling (usually following a mill reline).

The team also noted that a fixed volume of media takes up a different volume % within the mill over the life of the mill shell liners, due to the increasing internal diameter of the mill. This factor was measured based on new and worn liners and ore throughput across a whole reline cycle. It has been included in the live media volume prediction model, ensuring that the estimate is more accurate across the reline cycle. The implementation and upkeep of this method has resulted in stable operation, and the ability to control and optimise the media charge as desired. Since its introduction,

there have been no further issues with VSD torque protection faults or failure of internal liners.

SAG mill circuit controllers

The changes to the control of the SAG mill feed and weight controller took place in conjunction to the work that was completed to control the volume of media in the SAG mill. The two sets of work complemented each other to promote stability in the SAG mill.

The control is divided into several sections, namely, the feed to the SAG mill, the control of the SAG speed, the water addition to the SAG mill feed and the control of the ball mill discharge circuit.

Control of mill feed rate

In the APC setup the main control loops for the feed to the SAG mill are model predictive controllers which contain first order models for each of the apron feeders. Using a simple step test on the apron feeder speed and monitoring the weightometer readings, the following first order models were derived.

The model used for the primary feeder is:

$$\frac{6.5 e^{-32s}}{75s + 1}$$

The model used for the e-feed (emergency stockpile feeder) is:

$$\frac{3.4 e^{-15s}}{45s + 1}$$

When a feeder starts up, there is a 300 second delay where the speed of the apron feeder will be held at a constant value. This allows the dynamics of the modelled feed rate to come in line with the actual feed rate on the belt. Therefore, for the first five minutes after a feeder is started the control will hold a constant value. The start-up speed is established using an experimentally derived offset value and the gain derived from the controller model.

The APC controllers are setup to monitor the state of the apron feeders, so that the operator does not need to switch to manual control when changing between the primary feeder and the e-feeder. The feed rate controller in the APC system has been setup to accept a maximum feed rate setpoint of 240 t/h. When both feeders are off and the controller is in APC mode, the output of the control block will be 0% (apron feeders are still in motion in the field). When a single apron feeder starts up and the other is not running, the output of the controller will immediately jump to an appropriate value.

The SAG mill at Nova runs as a mill with a fixed feed rate and variable speed. The feed rate to the mill should therefore be constant for normal operation and specified by the operator. When the controller is in APC mode it runs the feed rate setpoint at a constant value, however this mode contains a safety controller which will reduce the feed rate to the mill when the mill weight setpoint is 3 t (2.5 t when on e-feed) above the specified weight setpoint. This is a protection for the mill to prevent it from being overloaded.

This safety controller utilises a PID style limit controller for setpoint adjustment, this means that the further over the mill weight setpoint the SAG mill is the more the feed is reduced. Additionally, the longer the mill weight setpoint is over the limit, the more the feed rate will reduce as well. Once the mill weight begins to reduce, then the feed rate will gradually increase back to the operator specified setpoint. The rate at which the controller reacts can therefore be tuned and has been helpful in adjusting the system response where feed has been reducing unnecessarily. This safety controller will only reduce the feed rate setpoint down to 140 t/h. If the mill is still overloading at 140 t/h (which is highly unlikely), then there is something wrong with the equipment and the operator must

take action to prevent further damage to the plant's infrastructure.

Operator usage of SAG feed control

The SAG feed controller interface is both on the crushing and grinding page of the SCADA (supervisory control and data acquisition). The feed controller is labelled WIC11213 (weight indication controller in area 112, control loop number 13) and shown in Figure .

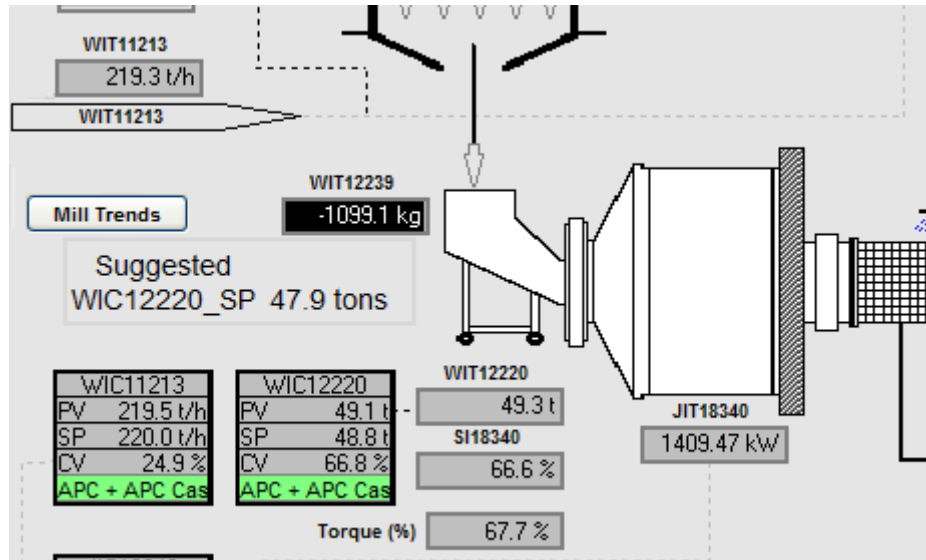


Figure 1 - WIC11213 interface on SCADA grinding page

Rock size analyser

By observing the process from the control room, it was noted that a visual change can be seen in the ore before a fluctuation in the mill weight occurred. There is a CCTV (closed-circuit television) system used on site that allows the control room operator to monitor certain parts of the plant and in particular the feed that is on the conveyor to the SAG mill. The visual difference on the ore can be described as a change in the amount of fine material that is present. An increase in fine material would indicate to the operator that the mill weight was likely to decrease, with the converse being true as well. It can be clearly seen in Figure 2 that there is a difference in the percentage of fines, this is what the operators were able to remark on.

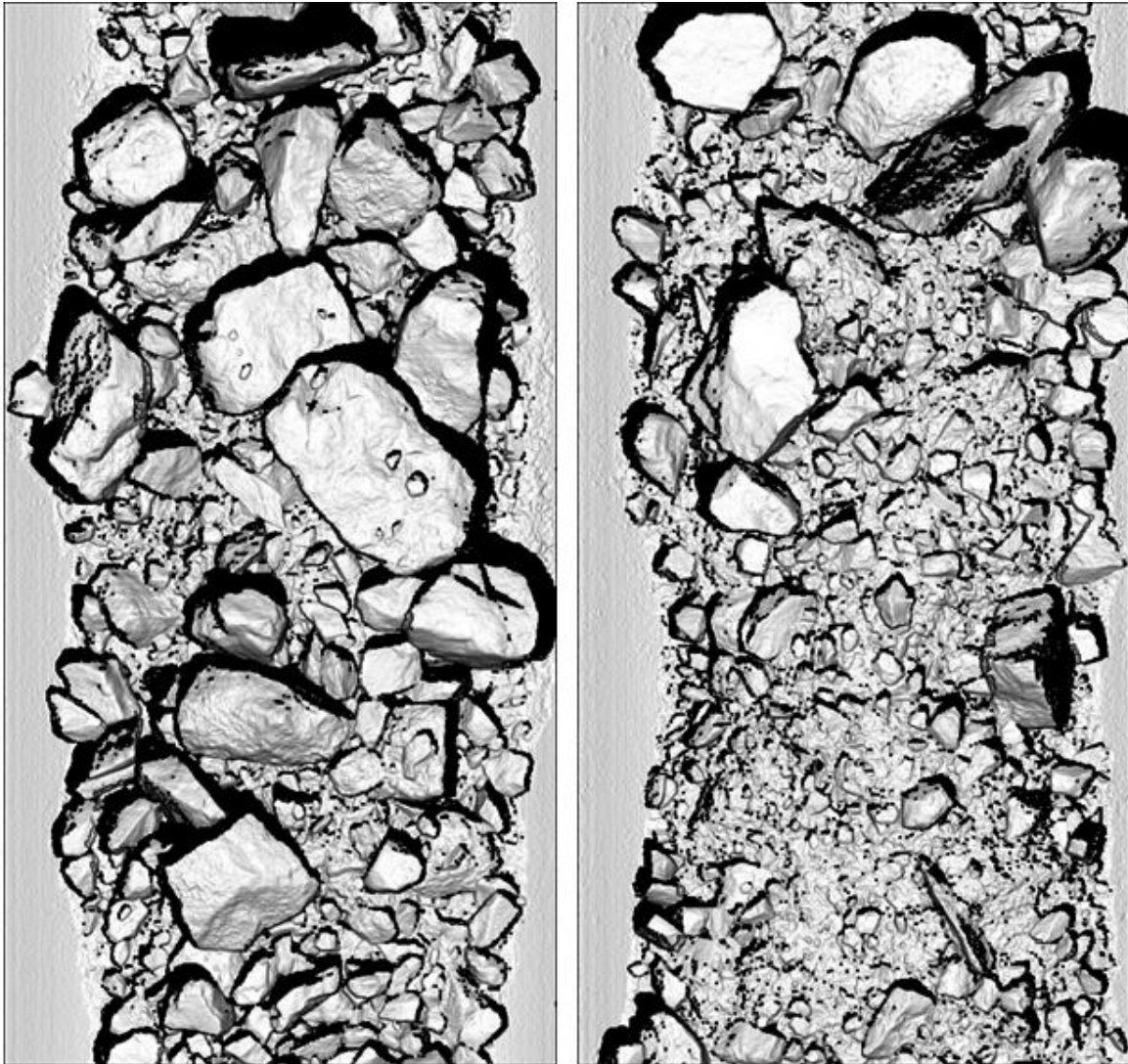


Figure 2 – Coarse material on left, fine material on right (images from IGO Nova site)

Given that the reaction of mill weight vs the visual inspection of rock size distribution showed a strong correlation the decision was made to automate the process to obtain better control of the mill and reduce the operator input required. For this reason, several vendors were engaged for information on trialling an online rock size distribution instrument. The following factors were considered when selecting an instrument:

- Ease of installation
- Technical support
- On-going costs and maintenance required
- Technology used

It was found that the majority of instruments that were available in the market at the time (2017/18) utilised 2D images. Few offered systems that obtained a 3D scan of the material on the belt. Having called several sites it was found that the 2D systems were considered to be “mostly accurate”, but the image processing was not readily able to distinguish fines that were lumped together from larger rocks. From research and white papers released, 3D scans used for size distribution showed the potential to more accurately identify lumped fines and measure smaller rock sizes to obtain more accurate size distributions.

For the reasons previously mentioned a decision was taken to contact Optimization (formerly MBV Systems) and Innovative Machine Vision, who developed the 3DPM system. As there were no reference sites available in Australia at the time, it was not possible to obtain reviews and references within Australia. A paper was however presented at a technical conference on the use of the system at Boliden Mines in Sweden, Thurley, et al (2018). For this reason, it was requested that the instrument be trialled for a 3-month period before purchase. Remote commissioning of the instrument was also arranged with Optimization to reduce the risk and cost associated with a trial.

Having the rock size distribution enables one to see how the ore broke up when passing through the crushing circuit, softer material produces more fines and harder materials produce less fines. Having this live data allows one to derive some conclusion on how easily the ore would break up in the mill. The raw data shown in Figure 3 shows the variations in mill weight vs rock size distribution before the control strategies were implemented:

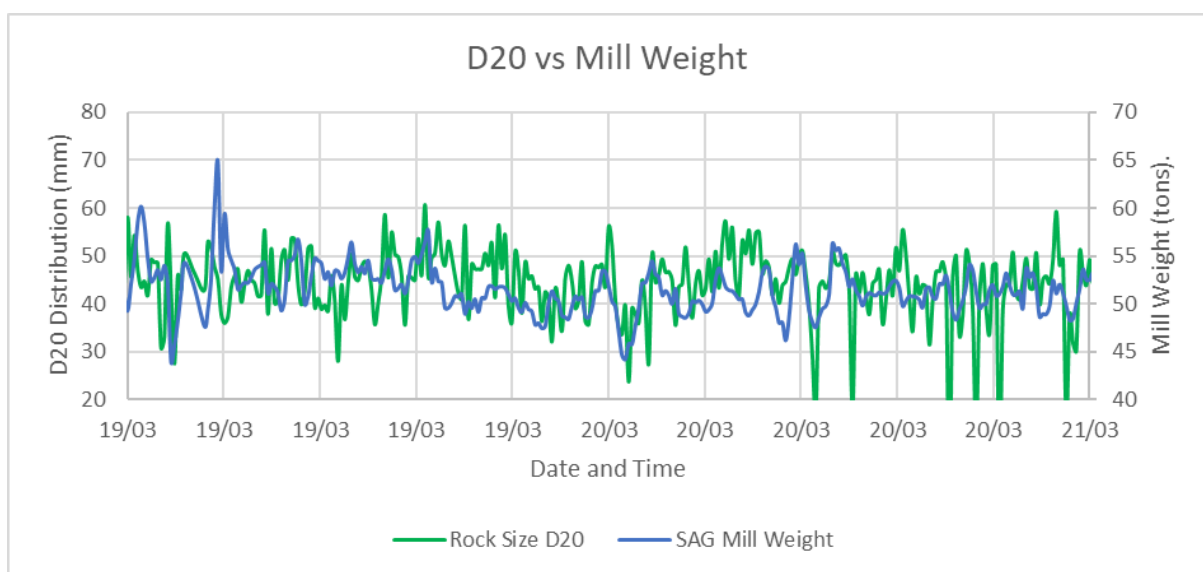


Figure 3 - Rock size distribution D20 vs mill weight

The correlation between the mill weight and the D20 for Figure 3 is 0.1611. However, the rock size analyser is located just after the weightometer on the feed belt, which is a substantial distance from the SAG mill. The feed conveyor to the mill runs at a fixed speed, with the amount of material being delivered onto the belt being variable. For this reason, the time that material takes to travel from the rock size analyser to the SAG mill was assumed to be constant. This time delay was measured several times and repeatedly shown to be 110 seconds.

By time delay compensating the data (software time compensation) shown in Figure 3, the data correlation increases to 0.2436. For the data period specified it is known that the SAG mill speed is not running at a fixed speed during this time, but rather adjusting speed to compensate for weight fluctuations. This would then dampen the correlation between the data sets, for this reason the correlation of 0.2436 was taken to be a strong enough correlation to attempt to utilise the D20 in the SAG mill speed controller.

The instrument installation was completed above the conveyor that feeds the SAG mill and located approximately 2 metres after the weightometer. The installation and remote commissioning were both completed with minor hardware changes made to suit the site conditions. The data also showed a strong correlation with the mill operating measurements. For these reasons it was decided to purchase the instrument after the trial had completed. The instrument has been running reliably

for the last 5 years with only minor maintenance required on the computer parts (additional cooling fan in enclosure and replacement of ethernet card). The instrument is an active part of the mill control strategy on an on-going basis.

Bulk density approximation

As discussed in the previous section the SAG mill weight controller was adjusted to receive a feed forward signal from the rock size analyser, which adjusts the SAG speed based on changes in the D20 fraction (fines in the ore). To further improve stability, an additional feed forward signal was introduced using the feed rate/feeder speed ratio data.

Based on experience at a previous sulfide flotation site, it was known that a relationship may be established between the feed tph and the feeder speed as a proxy for the plant feed grade. The relationship was based on the linear relationship between the weight and volume of ore delivered by the apron feeder. With higher-grade ore having higher density, it requires a lower speed to deliver the same feed rate. This same relationship was observed at Nova, and work was conducted to approximate the density of the ore, given that ore with a higher density and require more energy for comminution. Density increases are related to sulfide content, most of which is Fe Sulfide (pyrrhotite). Sulfides are both softer (require less grinding energy input) and more dense than oxide gangue minerals. Thus higher iron (proxy for sulfide) content results in higher density and softer ore. Fe is a better indicator of this than Ni, as the ratios of Ni:Fe change with Ni head grade.

To determine the ore density without installing additional equipment, several assumptions were made to utilise the available resources. It was assumed that for a fixed speed, the apron feeder delivering material onto the feed conveyor would deliver a fixed volume of material. By dividing the throughput measured on the weightometer by the speed of the apron feeder, a proxy for density was calculated. The ratio, inverted as speed/feed rate, was used to directly adjust the mill speed in response to changes in feed grade, instead of in reaction to changes in weight.

Figure 4 illustrates the ratio and mill speed data collected at 1-minute intervals over a 1-hour period, although the data was validated over a larger period. The average ratio was calculated each minute, and the cumulative sum of differences was plotted. The results, as shown in Figure 4, showed a delay of approximately 5 minutes between the cumulative ratio falling and the mill speed falling in response to the change in weight, with a resulting change in speed of about 8% per 0.04 change in cumulative ratio.

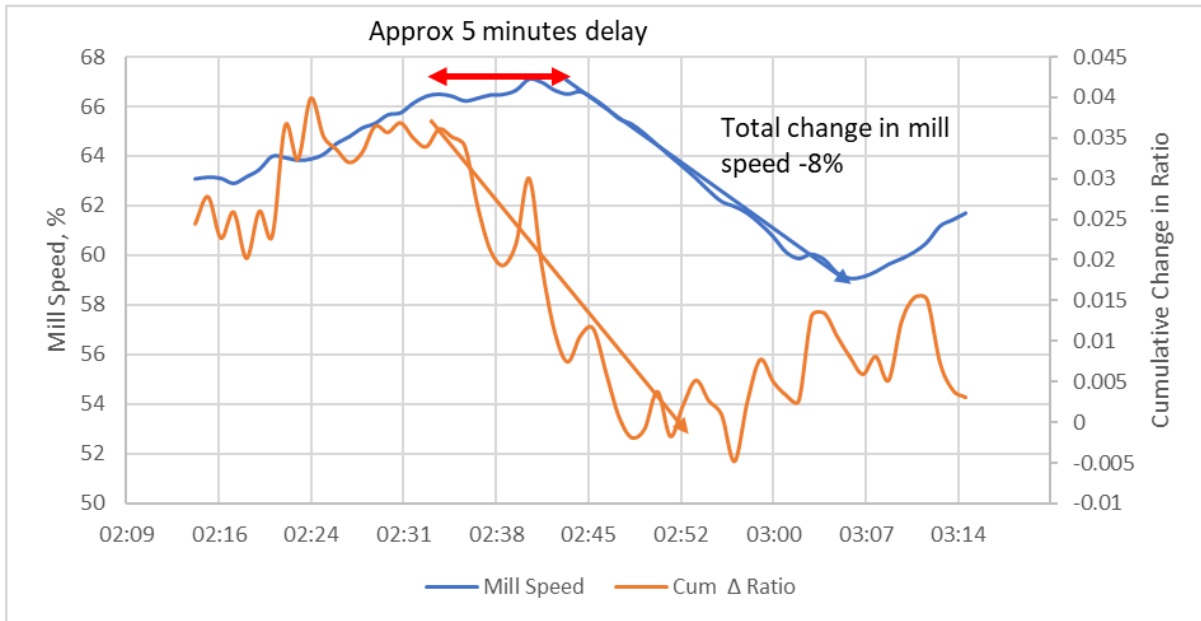


Figure 4 - Change in mill speed vs changes in the feed density proxy

SAG mill weight control

The SAG mill speed control (WIC12220) is setup as a conventional PID feedback loop. There are however two feed forward components that have been added to this loop which have greatly enhanced the control of the SAG mill as previously discussed. Because of the control actions based on the feed forward components, the PID loop has been tuned with a small gain and long integral time which makes the action from the feedback loop slow to react.

The first feed forward components are based on the quantity of fines in the feed to the SAG mill which is measured by the 3DPM rock size analyser D20 (size passing under 20% distribution). The other feed forward component is based on a proxy for the density of the feed to the mill where the volume of material delivered by the apron feeder is taken to be constant for a given speed and therefore the density of the material should be proportional to the feed rate divided by the apron feeder speed. The derivation of these components and their relation to the SAG mill was discussed in the previous sections.

Error checking and filtering is applied to the feed forward component calculations. If the measurements' fault, then the values passed to the PID loop as feed forward component will simply retain their last known good value. A measurement fault in this context means that the values have not updated for more than 60 seconds or are outside of their normal bounds. This means that the SAG mill speed will vary based only on the feedback loop for the PID controller. Since the PID controller has been tuned with both feed forward components, the PID alone will respond very sluggish and will not be able to tightly control the mill weight. There are two feed forward components, and the control can utilise these independently but having only one of the components will mean the controller tuning will be poor.

The controller has also been setup so that the mill speed will not decrease speed as rapidly as it can increase. This approach reinforces the stability of the mill, as the mill possesses a greater intrinsic capability to recover from low weight conditions in comparison to high weight conditions. This is accomplished by having a "limit controller" override the normal control whenever the mill speed is requested to decrease at a high rate of change. The limit controller is simply a PID with a slow response, the normal PID controller is prohibited from going below the limit controller.

The various parts of this controller were implemented in stages, including stages where strategies

were trialled and removed. The following stages have been identified as being most significant for the controller changes:

- A. Simple PID loop in PLC. No feed forward components or other interactions, only a single input, single output (SISO) system.
- B. The D20 measurement from the 3DPM was incorporated into a MPC controller.
- C. The MPC controller was removed and a PID loop with a single feed forward component was added that utilised the D20 from the 3DPM.
- D. Compensation was added to adjust the mill weight setpoint to account for liner wear (discussed in next section)
- E. The feed forward component for the ore density proxy was added to the control loop.

The functional diagram, shown in Figure 5, illustrates the final running controllers configuration for the SAG mill weight controller.

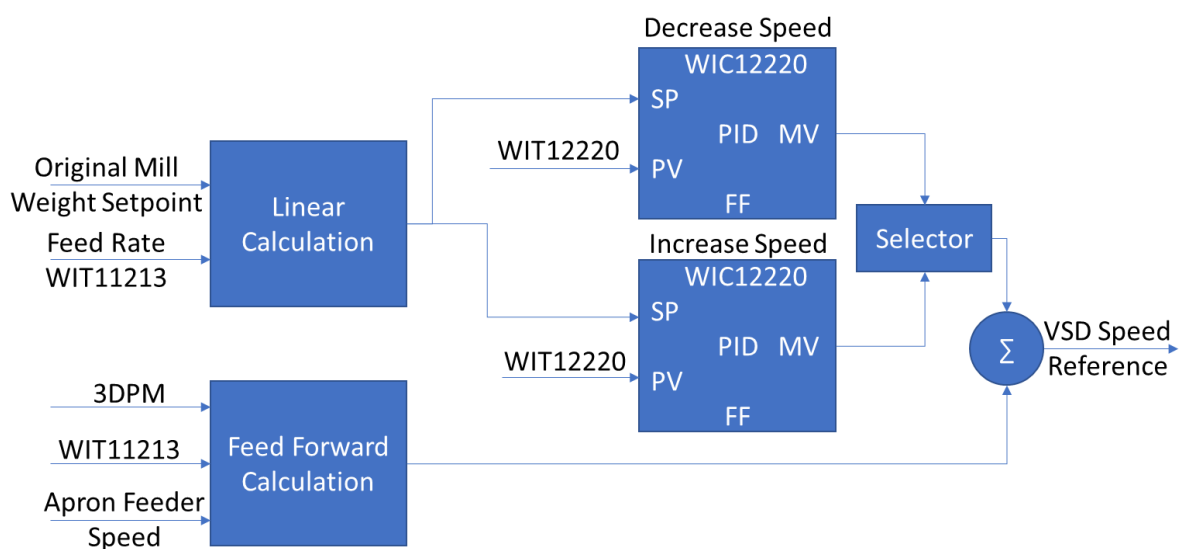


Figure 5 - Functional diagram for SAG mill speed control in APC mode

SAG mill weight setpoint

In an ideal situation the SAG mill weight setpoint is set so to maintain a constant/optimal fill volume. Since the internals of the SAG mill change over time (e.g. wearing of the liners), the SAG mill weight needs to be adjusted so that the fill volume is maintained.

To assist the processing team in setting the mill weight setpoint, a continuous calculation will reduce the mill weight setpoint as material is processed by the mill. This adjustment to the setpoint only takes place when the operator grants the APC permission to alter it. Since there may be times when this adjustment is not running an all-time monitor is kept running and displayed for use. When a re-line occurs, the metallurgical team has access to adjust the suggested mill weight setpoint.

The rate at which the setpoint is reduced has been determined by the IGO metallurgical team and is a linear formula based on historical data of production throughputs and liner wear rates. The mill weight setpoint is dropped by 31.2 kg (actual wear rates excluded from this paper) per 1000 tonnes of ore processed. The mill weight setpoint can also be manually adjusted when liners are replaced (or as determined by the metallurgical team), this is accomplished through a graphical interface setup on the process control system.

Loading grinding media

An additional feature was implemented to reduce disturbances when grinding media is added. This is because grinding medium is added in batches of 1.8 to 2.0 t, this abrupt addition of media results in a corresponding fluctuation in the mill weight. A button was added on the SCADA grinding page that was to be used by the operator when balls are going to be loaded into the SAG mill.

Pressing the aforementioned button does the following:

- Creates a record of when balls are loaded
- Reduces the mill weight setpoint (internal to the controller logic) by two tonnes for ten minutes
- Once the ten-minute time expires the mill weight setpoint would gradually be increased to its value prior to pressing the button

By reducing the mill weight setpoint the controllers will increase the mill speed (and drop feed if required) so that the mill is better able to handle the sudden surge of weight that occurs when grinding media is loaded into the mill.

This part of the controller worked well if the button is pressed 10 minutes prior to the balls being loaded. However, this is reliant on human interaction to trigger the system at the correct time. Due to inconsistencies with the use of this button, it was not included in the final control solution. The other improvements made to the control system enable it to sufficiently cope with the surge in introduced weight when grinding medium is added.

SAG mill feed water

The feed water to the SAG mill (FIC12200) can be run in several modes, the following gives a description of each:

- Auto – The setpoint is specified in the flow control block and the valve (VLV) is altered to maintain the specified flow rate.
- Ratio: The user will specify the percent solids required in the mill. The controller will then calculate the required water flow based on the amount of material being fed to the SAG mill.
- APC+APC Cas: Works the same as Ratio mode, with a few exceptions. When the feed to the SAG mill is dropped abruptly, the controller will use the feed rate setpoint for up to 20 minutes to calculate the water flow rate required rather than using the actual feed rate to the mill. This reduces disruptions if the feed to the mill is temporarily disrupted. Additionally, if the SAG torque measurement is above 77%, additional water will be added to the SAG mill in attempt to flush more material out of the mill and reduce the mill weight.

Additional pre-processing control actions

To enhance system performance, several auxiliary features have been integrated into the control system to address exceptional scenarios such as blockages or start-ups.

To maintain a stable operational environment, the system is programmed to limit the speed of both the primary and emergency apron feeders to 55% of their maximum capacity if the belt feed rate falls below 60 t/h for more than five seconds. This limitation helps to prevent excessive winding of the apron feeders during instances of material underloading or non-passage through the weightometer. Additionally, upon the re-establishment of material feed on the belt, the maximum apron feeder speeds are restricted to 55% for a duration of five minutes.

A single controller has been employed in the PLC setup, and the same output is directed to two separate apron feeder outputs with a 4-20 mA output. To ensure seamless transitions between the

feeders, which can operate simultaneously in the field, the APC logic has been configured to switch between the primary and emergency stockpiles feeders smoothly by using a model predictive controller.

The signals from the rock size analyser are passed through a stochastic filter as described by Baas, D. and Mikhael, G.L. (2018). This filter decreases the impact that outlier measurements have on the control actions, while allowing the system to react appropriately to changing conditions. This is particularly helpful for measurements that have an update rate that is relatively slower than other measurements in the plant. The rock size analyser provides updates every 15 seconds and has multiple outliers due to the variable nature of the ore which influences the manner in which it is delivered from the feed bins.

RESULTS

A full two years of data was used for the analysis of the results from 2019-11-01 until 2021-11-01. The following stages, as discussed in the paper, have been compared to determine the effect that each change had on the performance of the SAG mill stability:

- A (01/11/2019 to 1/03/2020): Simple PID loop in PLC. No feed forward components or other interactions, only a SISO system.
- B (1/03/2020 to 6/04/2020): The D20 measurement from the 3DPM was incorporated into a MPC controller.
- C (6/04/2020 to 25/01/2021): The MPC controller was removed and a PID loop with a single feed forward component was added that utilised the D20 from the 3DPM.
- D (25/01/2021 to 23/03/2021): Compensation was added to adjust the mill weight setpoint to account for liner wear (discussed in next section)
- E (23/03/2021 to 01/11/2021): The feed forward component for the ore density proxy was added to the control loop.

The following timeline in Figure 6 shows the implementation of the changes to the controls chronologically:

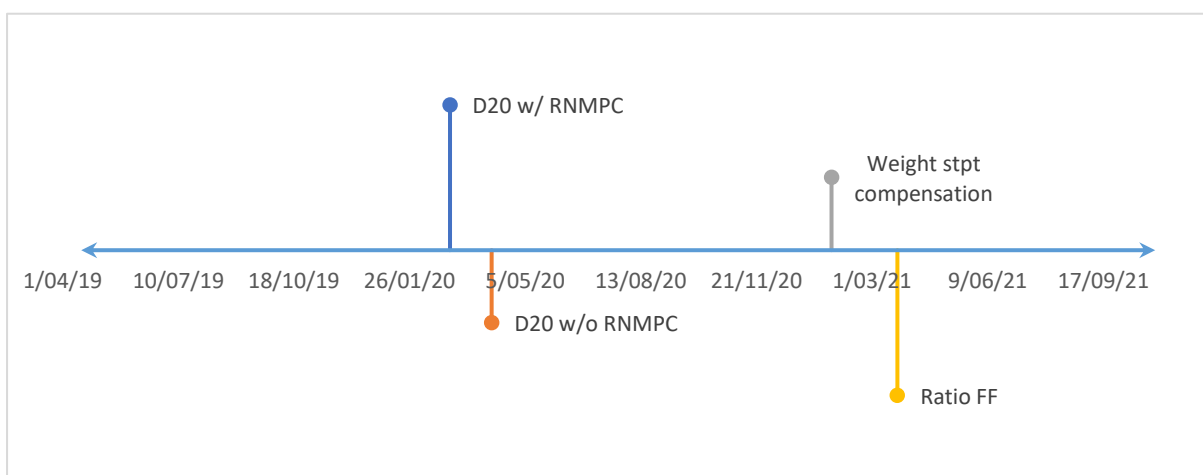


Figure 6 - Timeline to illustrate control change implementations

As the torque was the main concern, the ability to control the torque was evaluated at each stage. The following chart shows the torque measurement over a two-year period, sampled at ten-minute intervals. Times when the mill was not running have been excluded from the dataset. The five

intervals listed, marking the five major distinct control strategy implementations have been illustrated [A, B, C, D, E] on the chart in Figure 7. No other data filtering has taken place on this chart.

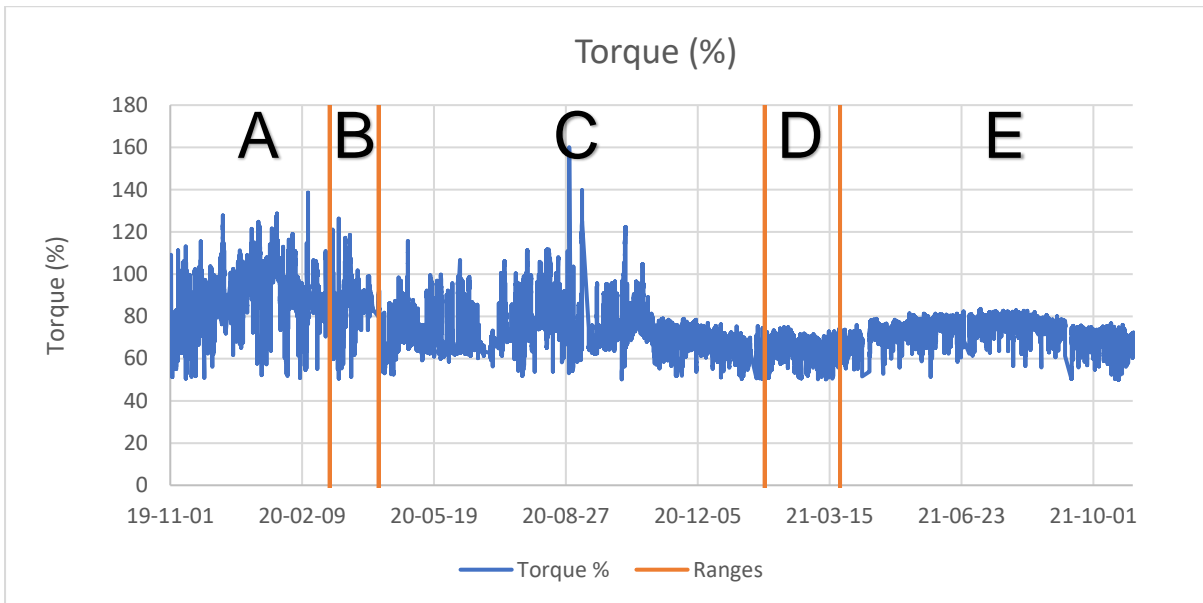


Figure 7 - Plot of SAG mill torque measurement over a 2-year period

Figure 8 aims to quantify the number of times the torque limit on the SAG mill was exceeded (> 80%) and the severity of each violation. A rolling sum of the violations over 80% torque has been plotted on Figure 8 (the data set is the same as the ten-minute sampled data from Figure 7). It can be seen that during period A and B, a high number of severe events occurred, which drastically reduce in period C and have all but gone in period D and E.

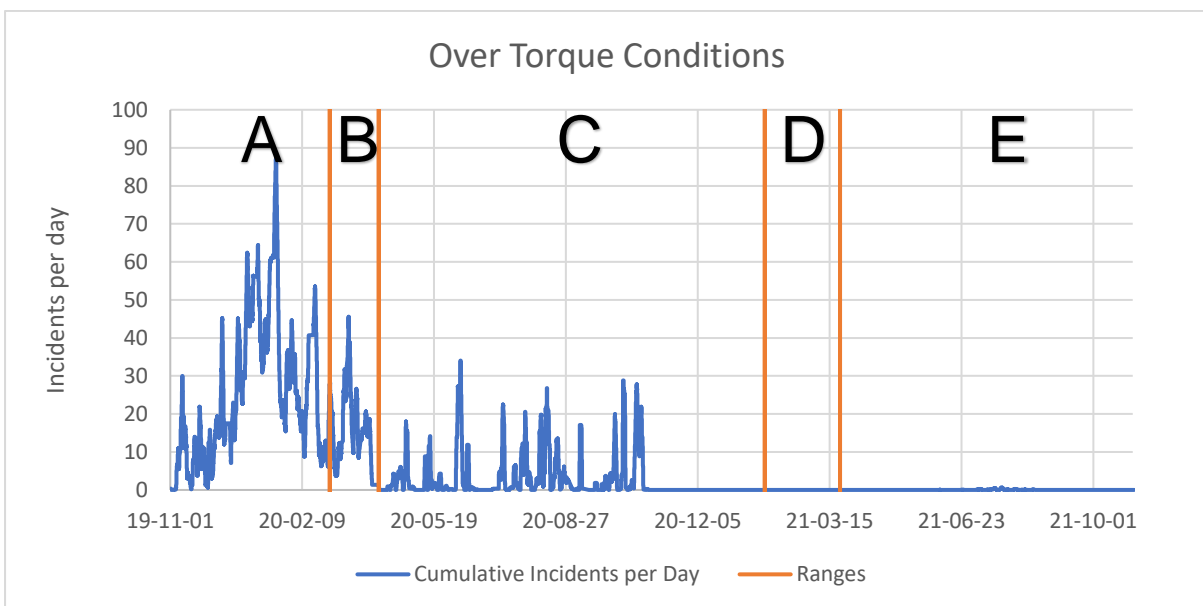


Figure 8 - Time series plot of the cumulative weighted over torque incidents per day

As can be seen from Figure 8, the number of over torque events has greatly reduced due to the improvements in the control and control of the grinding media content. Quite noticeable is the further reduction of high torque even occurrences during the C period. This is attributed to continual review and tuning of the controllers, not to a fundamental change in the control philosophy. Plotting the normal distributions for the torque measurement over the same periods (shown in Figure 9), shows that after the final control changes, the mill is operating far closer to its torque limit and the data quoted illustrates that the number of over torque events has considerably subsided. These two factors indicate that the control of the SAG mill has greatly improved.

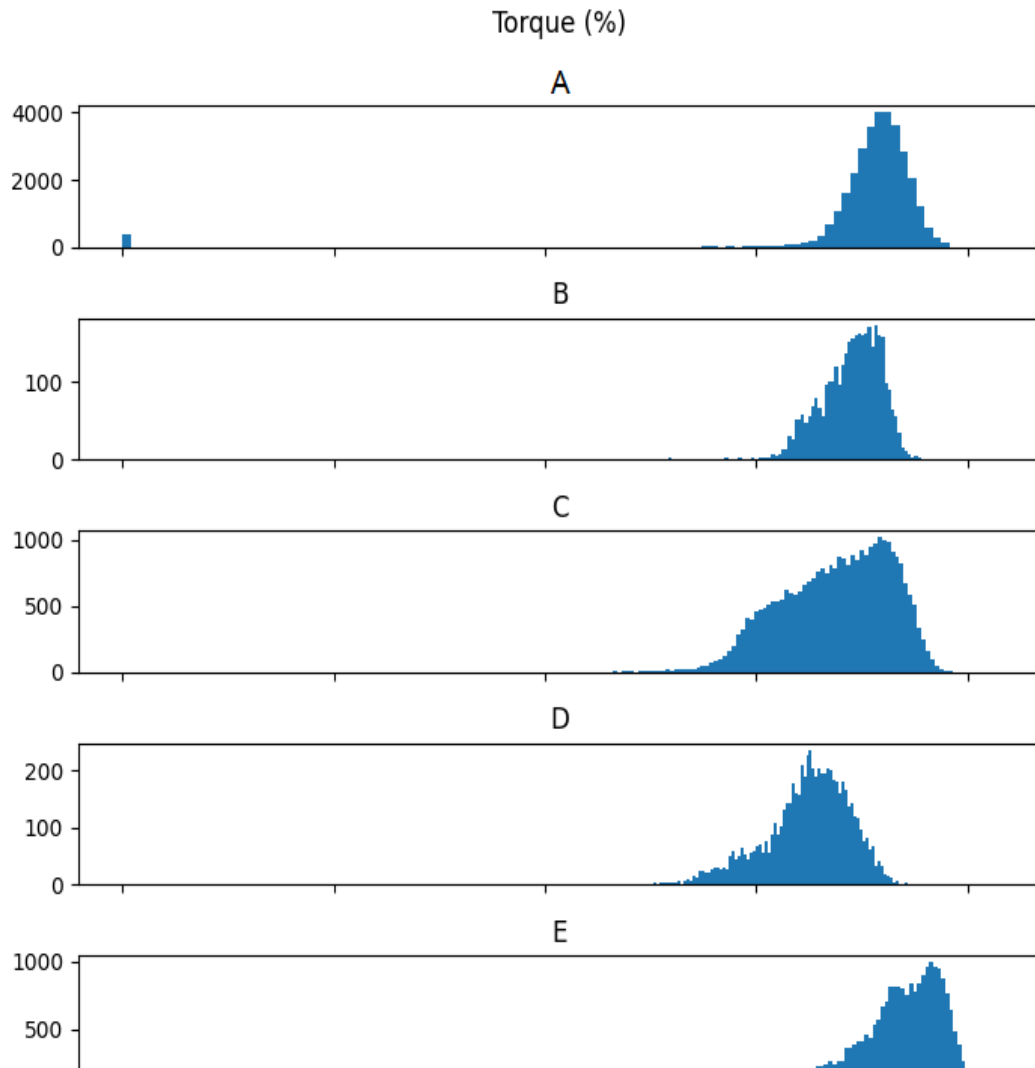


Figure 9 - Normal distribution of SAG mill torque measurement

Improvement to the control can further be highlighted by plotting the error in the SAG mill weight control as shown in Figure 10. The narrowing of the error band in the following plots shows that the mill is better able to hold setpoint and less susceptible to disturbances in the system.

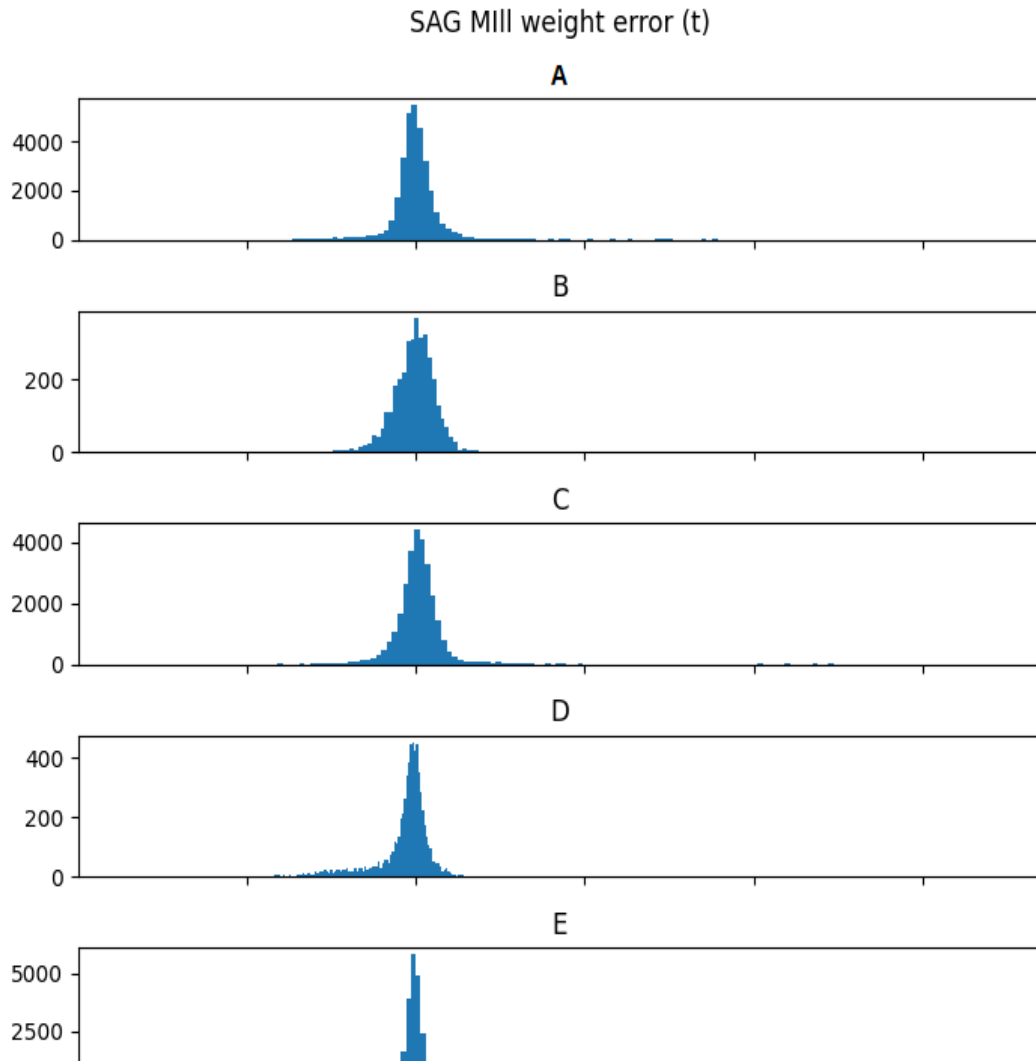


Figure 10 - Normal distribution of the SAG mill weight error (setpoint - process variable)

The mill work index was plotted over the same periods, with the combined mill work index showing a decrease in the energy required for grinding as shown in Figure 11.

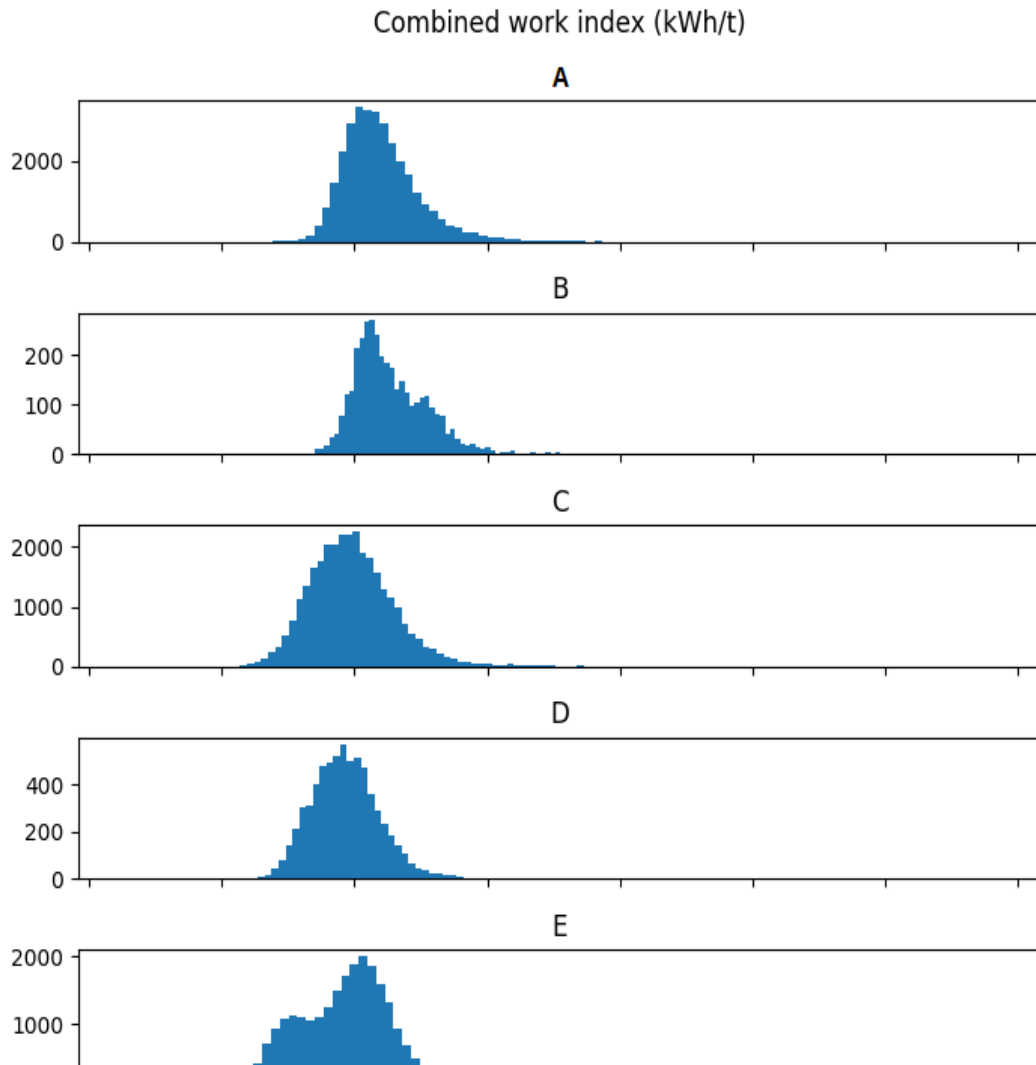


Figure 11 - Normal distribution of the combined work index for the grinding circuit

As previously mentioned in this paper the feed to the plant is quite variable. This means that the mill work index may be associated with variations in the orebody. Plotting the normal distribution for the Ni feed grade does reveal a large variation in the ore. However, one can see that the distribution of %Ni feed grades for periods A and E are quite similar in Figure 12. This shows that the improvements in the SAG mill control are not primarily due to changes in the ore.

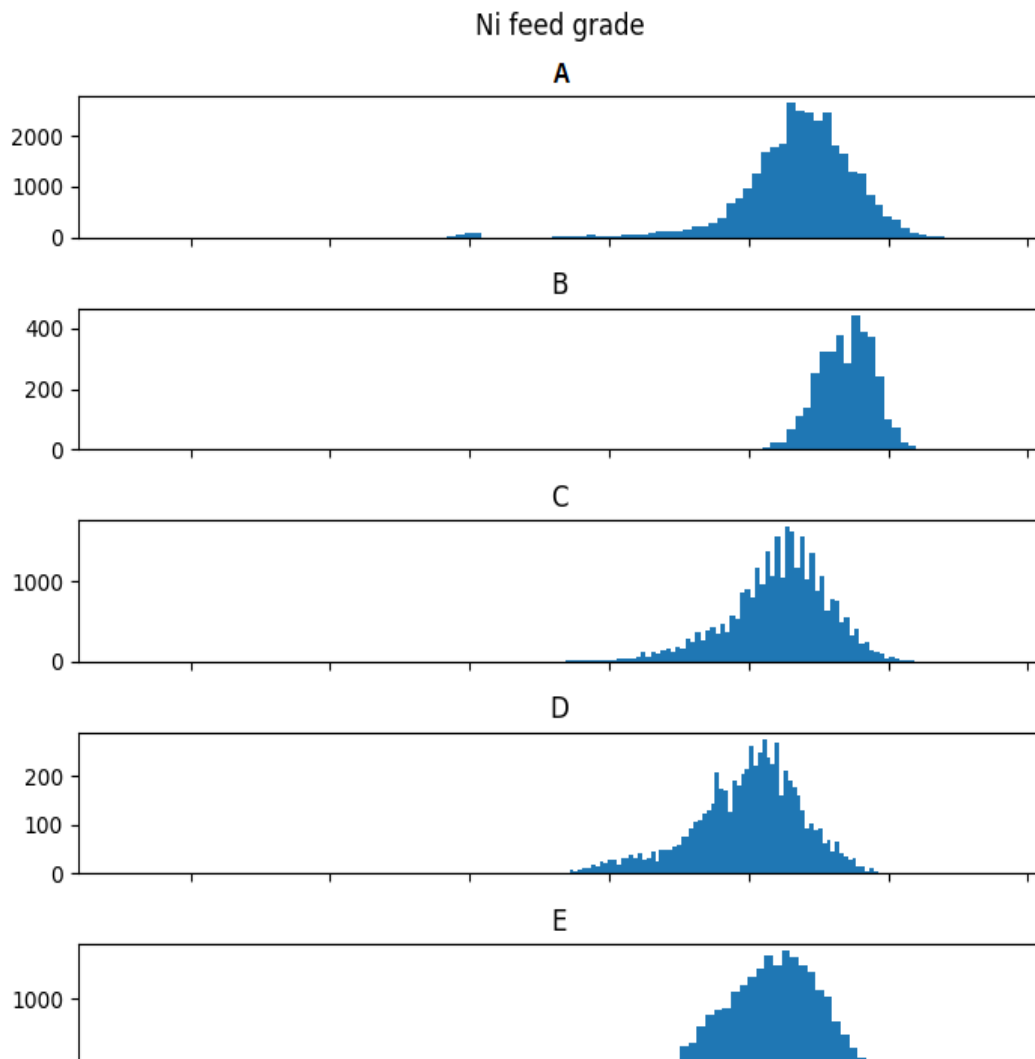


Figure 12 - Distribution plot showing the %Ni in the feed to the circuit

3DPM ANALYSER ON/OFF TRIALS

The effect of the 3DPM feed forward D20 signal on SAG mill weight control and specific energy consumption was investigated using data obtained from on/off trials conducted at Nova. These trials involved turning off the forward D20 used as part of the SAG weight/speed control scheme for two periods of week on and two periods of week off.

Results showed that the 3DPM signal being part of the control "tightens up" weight control around the SAG weight setpoint, as evidenced by a statistically significant lower standard deviation of weight error. Additionally, the feed forward D20 signal reduces the SAG specific energy consumption as a result of better weight control. This is due to less time spent either over or under filled, both of which result in inefficient grinding.

To observe the control improvement, the data had to be analysed at 30-second intervals as the dynamics of SAG weight control are shorter than the one-hour or ten-minute intervals that were first analysed.

A potential confounding factor in this result is Ni head grade and ore hardness. It was observed that during the on periods, the average Ni head grade was higher. Previous studies have shown that SAG mill specific energy stays fairly constant as head grade increases within the normal range of

operation; very high head grades approaching 3% result in a reduced SAG specific energy as shown in Figure 15. The measured reduction in SAG specific energy during the 3DPM on periods is therefore attributed to the improved weight control.

Histograms and descriptive statistics of this trial are shown in Figure 13, Figure 14, Figure 15 and Table 2.

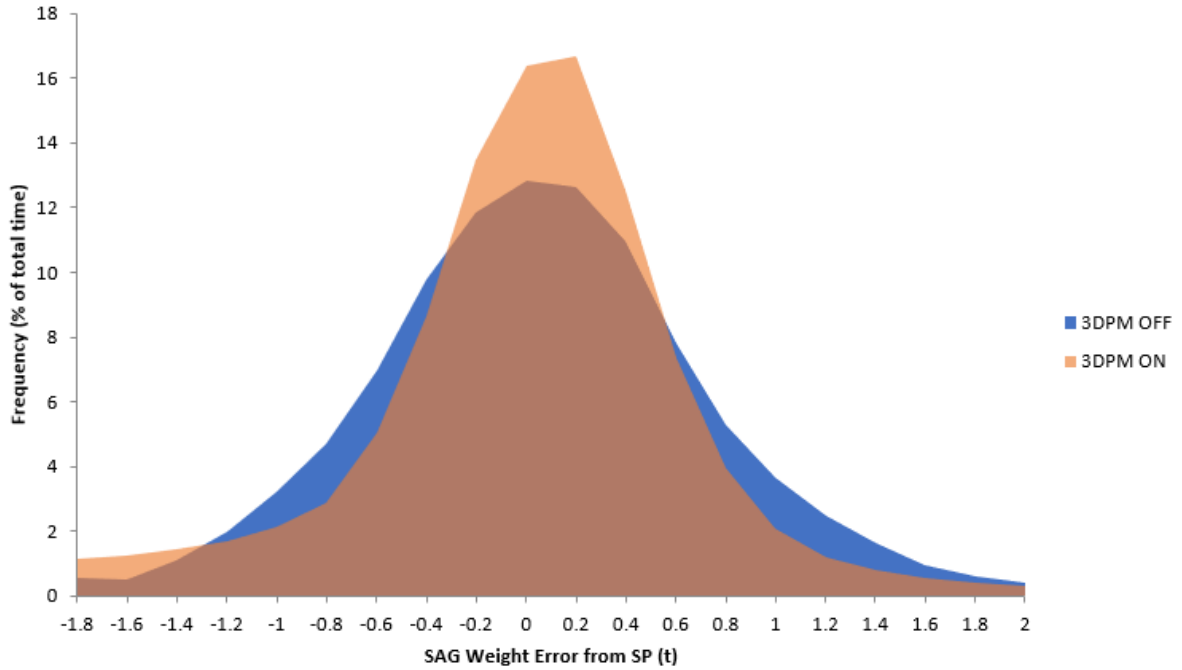


Figure 13 - 3DPM trial histogram of SAG weight control

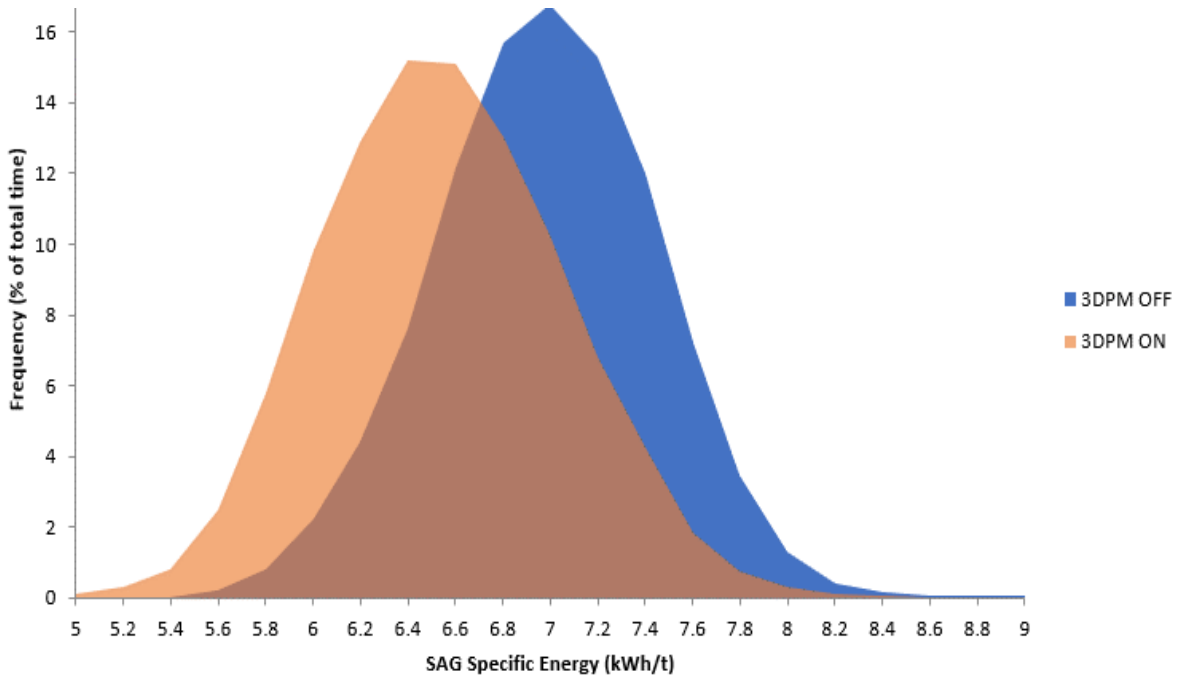


Figure 14 - 3DPM trial histogram of SAG specific energy

Table 2 - 3DPM trial descriptive statistics

Parameter	Unit	3DPM on	3DPM off
Throughput average	t/h	198.22	192.88
Throughput std dev	t/h	9.57	10.61
Ni grade average	%	2.12	1.69
SAG SE average	kWh/t	6.45	6.88
SAG SE std dev	kWh/t	0.51	0.47
SAG SE 2 sample test for different means	P(T=t) two tail	0.0000	
SAG weight error average	tonnes	-0.09	-0.05
SAG weight error std dev	tonnes	0.61	0.66
SAG weight F test for 2 sample variances	P(F<=f) one tail	0.0000	

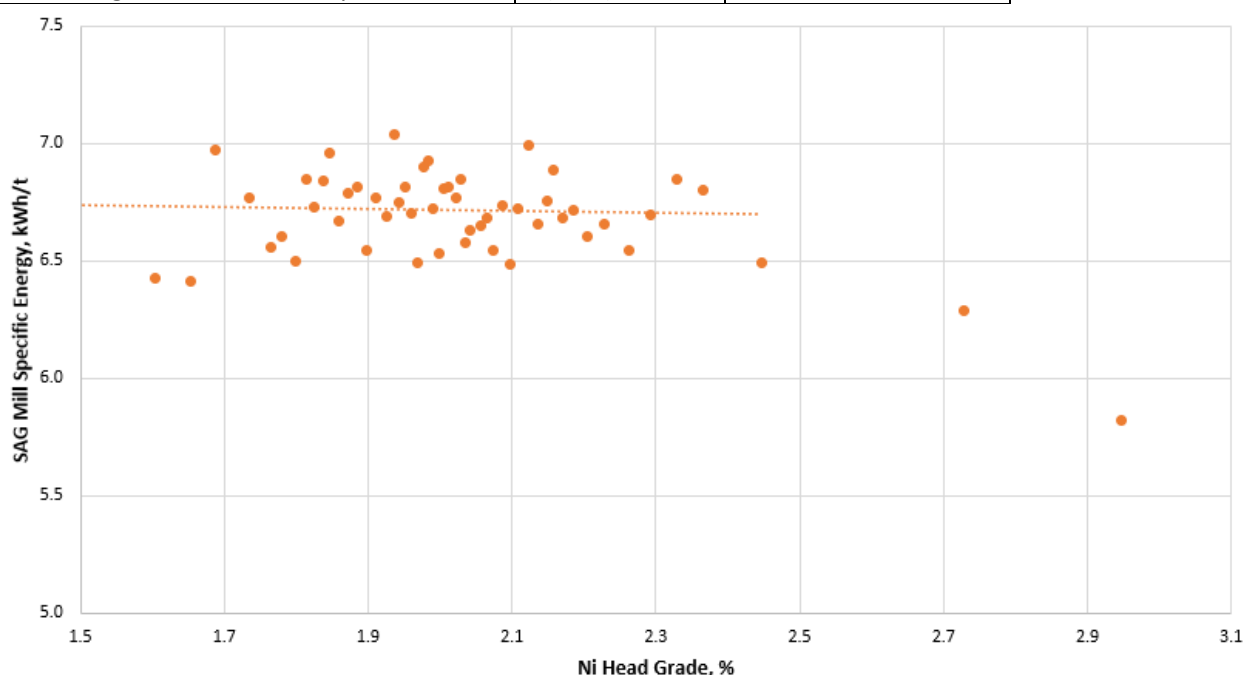


Figure 15 - Plot of SAG specific energy vs Ni head grade

CONCLUSIONS

The grinding circuit efficiency and stability greatly improved when comparing the first half of the dataset (12 months from 01/11/2019 to 01/11/2020) to the last half (12 months from 01/11/2020 to 01/11/2021). These improvements are attributed to the sum of several improvement initiatives including the introduction and use of a rock size analyser, predictive controllers and improved control of grinding media addition and SAG mill fill volume.

The methodology followed implemented control strategies in a systematic and modular manner to build on improvements. This allowed the improvements to be reviewed to determine their benefit. From these reviews some systems were excluded from the final system, such as the exclusion of the “ball loading” trigger and removal of the MPC control of the SAG mill weight controller. Even though the MPC control has shown to be highly effective on other parts of the circuit such as the feed controller to the SAG mill and discharge of the grinding circuit, it was not well adapted at maintaining the SAG mill weight. This is likely due to the non-linearities in the system. The approach of determining the ore characteristics and the effect on the SAG mill weight allowed for a simpler and more effective feed forward controller to be implemented.

Overall, the project was successful and reduced the number of over torque conditions that were

experienced on the mill. Additionally, the liner wear of the mill has decreased, and the work index of the grinding circuit is lower by an average of 0.43 kwh/t.

ACKNOWLEDGEMENTS

The authors would like to thank IGO for granting permission to publish this paper. A special thanks to the metallurgical team at Nova for their contributions to the control system and their willingness and support in trying new strategies.

REFERENCES

- Baas, D. and Mikhael, G.L. (2018). Developing Flotation Circuit Control and Automation for the Phu Kham Copper-Gold Operation Concentrator. In: Back to Basics 2018: Proceedings of the 2018 Mill Operators' Conference, The Australasian Institute of Mining and Metallurgy, Melbourne, pp. 55-76.
- Gomes-Sebastião, G.A., Hearne, Z., Lam, S., van der Spuy, D., Thompson, M., and Vines, N. (2018). Nova Copper-Nickel Project Optimization of the Copper Rougher-Scavenger Circuit through Advanced Measurement and Control. In: Back to Basics 2018: Proceedings of the 2018 Mill Operators' Conference, The Australasian Institute of Mining and Metallurgy, Melbourne, pp. 77-92.
- Thurley, M.J., Degerfeldt, D., Nystrom, J., Nordenskjold, R. and Lindqvist, L. (2018). Automated, online measurement of bulk material size distribution on conveyor using 3D profile imaging at Boliden Mines, in Proceedings 14th AusIMM Mill Operators' Conference 2018, August 2018, Brisbane, Australia, pp 641-652 (The Australasian Institute of Mining and Metallurgy: Melbourne)
- Napier-Munn, T. J., Morrell, S., Morrison, R. D., & Kojovic, T. (1996). Mineral Comminution Circuits: Their Operation and Optimisation. Indooroopilly, Qld Australia: Julius Kruttschnitt Mineral Research Centre, University of Queensland.

The Future of Hybrid Lining for Large Diameter AG/SAG and Ball Mills

S Yaver Imam¹, J Bustamante², V Grover³, S Abhishek⁴, M Sherman⁵

1. Global Director Product Development, Tega Industries, Kolkata, India; yaver.imam@tegaindustries.com
2. Global Product Manager, Tega Industries, Santiago, Chile; juan.bustamante@tegaindustries.cl
3. Global Business Head, Tega Industries, Sudbury, Canada; vinay.grover@tegaindustries.com
4. Global Product Head, Tega Industries, Kolkata, India; abhishek.sinha@tegaindustries.com
5. Technical Director Mining & Metals, Vancouver, Canada; mark.sherman@fluor.com

ABSTRACT

Since the introduction of large diameter semi autogenous (SAG) Mills in comminution circuits, the conventional all steel liner has been favoured as the proven wear material. However, over the last few years, the use of hybrid liners (a composite of steel and rubber) in large diameter SAG Mills, eg 34 ft in diameter or larger, has increased in popularity due to the advantages of reduced liner weight, fewer liner pieces, and increased liner toughness. This allows hybrid liners to withstand higher levels of impact, thereby eliminating cracks and premature failure when compared with conventional steel liners. These advantages have improved the hybrid liners' reliability and has reduced safety risks during mill re-lines via the bolting of hybrid liners from the outside. The elimination of liner failure plus reduced SAG mill reline time has increased mill run-time and improved reline crew safety.

Operators have reported that use of hybrid liners has generated two major advantages compared with steel liners. Firstly, the hybrid liners' ability to resist large and frequent impacts without cracking allows mill operation at full speed from day one of liner installation, thereby eliminating the several weeks ramp-up period, which has been required for the last approximately 20 years to protect the traditional all-steel liner designs. The ability to operate at high speed immediately after re-line results in SAG mill power draw increasing by approximately 3% to 5% over the life of the liners, thereby allowing additional tonnes to be milled over the full life cycle.

Secondly it was observed that the hybrid liner's rolled steel inserts (400 - 550 BHN) embedded in the rubber matrix, wore at a lower rate when compared with the all-steel liners (300 - 350 BHN), with the difference being almost 30% lower wear rate in the last weeks of service life. This allowed the hybrid liner to operate with a steeper average face angle, generating better charge lift that achieved a 1.5% to 2% increase in average mill power draw over liner life. This contributed to the additional tonnes milled over the life of the liner set.

This paper presents the effects of changing from all steel liners to hybrid liners on two different Chilean SAG Mills (36 ft and 40 ft diameter) and a Peruvian 27 ft diameter ball mill. It demonstrates the significant impact that switching from traditional steel liners to Tega's Dyna Prime hybrid liners has had on these large diameter mills in terms of Specific Grinding Energy (SGE) consumption and mill productivity, and the journey through the steps of problem analysis, solution identification, validation, and field trials to produce the world's 'best practice' liner design for the toughest application in the largest diameter SAG and ball mills.

INTRODUCTION

During the second half of the 1990s, large diameter SAG mills, eg 36 ft in diameter and greater, began to proliferate in the industry, with examples including KCGM, St Ives, Alumbrera, Ernest Henry

and Batu Hijau SAG mills. The first of the 38 ft mills entered service at the Antamina operation in the late 1990s followed almost immediately by the first of the 40 ft SAG mills at Cadia. This era also ushered in the shift from what was then the typical 'rail bar' SAG mill liner, Figure , to the now common top hat (or Sombrero) design, Figure 2, made possible by Professor Rajamani's seminal trajectory modelling work at the University of Utah's Comminution Centre (Rajamani, 1996). The change from rail bar to top hat design was driven by the premature failure of the rail bar liners in the larger diameter SAG mills which caused significant unplanned mill downtime and compromised mill production.



Figure 1: the typical 1990s rail bar SAG shell liner

Shortly after the introduction of the top hat liners, some operators started using larger grinding media, e.g. 140 mm and 152 mm diameter steel balls, instead of the typical 125 mm steel balls, in their pursuit of increased throughput rates and reduced milling costs. Although the diameter of the typical steel ball only increased by approximately 22%, the mass of the grinding ball increased by nearly 60%, e.g., 14 kg for a 152 mm ball vs 9 kg for a 125 mm ball.



Figure 2: the first top hat, or sombrero, SAG shell liners, Alumbreira, Argentina, 1997

The combination of larger balls being dropped from a greater height increased the amount of energy carried by grinding balls. When directed into the mill charge this increased the amount of impact breakage in the mill. However, if the ball struck the mill liners instead of the mill charge, then this continued ball strikes at higher energy led to liner failure. As a result, industry confidence in the reliability of conventional steel liners, which had been in use for several decades, began to wane.

Some operations attempted to reduce the risk of liner failure by starting the mill at a lower mill speed after a re-line, e.g., 68% critical speed when the lifter height and leading face angle were at their maximum. By operating at a lower mill speed, the trajectory of the steel balls was less aggressive and the risk of a large ball striking an unprotected liner was minimised. Over several weeks, as the lifter height and leading lifter face angle wore down, the mill speed was incrementally increased up to the more typical operating speed of 76% critical. The widespread adoption of impact meters also provided an additional tool for monitoring ball strikes against the unprotected shell liners. It is now common practice to control SAG mill speed based on the impact monitor's output. Even with these management tools in place, steel liners still suffer from premature failure, requiring unplanned downtime to replace them.

In addition to the introduction of larger mill diameters and larger ball diameters, another SAG milling development over the last two decades is the use of partial or full secondary crushing of the SAG mill feed. In general terms, mill operators have found that SAG mills are most productive, and easier to control, when operated with a high ball charge, e.g., 18% to >20% combined with a relatively low rock charge of 4% to 8% of mill volume respectively, arguably making this the most demanding SAG shell liner application.

The desire to maximise SAG mill run time has also seen mill operators seek liners that are faster and easier to replace. The industry has responded in several ways, with some operators choosing to

instal fewer but larger pieces, and some operators using twin-boom reline machines to allow concurrent replacement of liners on opposite sides of the mill to reduce SAG mill reline time. The concept of larger pieces has necessitated the use of composite liners, i.e. a combination of steel and rubber, to keep liner mass within the current limits of liner handling capabilities, as well as to reduce the effects of inconsistent steel properties that become more pronounced as steel liner mass and volume increased.

This paper covers the challenges faced by the operators of two large diameter SAG mills in Chile. The first SAG mill, a 40 ft diameter mill lined with chrome-moly steel liners, processes 4300 t/h and is charged with 158 mm (6¼in) steel balls. It suffered major mill downtime due to significant discharge end mill shell liner failures from cracked lifter bars, frequent bolt breakages, excessive peening, and excessive wear on certain parts of the liner. The frequent unplanned shutdowns reduced the availability of the SAG mill thereby reducing the tonnes of copper produced. A detailed analysis of the historical pattern of failure and operating data was performed by Tega, including typical milling parameters, the charge motion inside mill, liner geometry, and the materials of liner construction. Various computational tools, eg Discrete Element Modelling (DEM), Finite Element Modelling (FEM), and fracture mechanics, were used to develop a thorough understanding of the mechanisms that promoted liner failure. This resulted in Tega developing a hybrid lining system – the Dyna Prime liner, which consists of rolled steel housed in a rubber matrix which has surpassed the 40 ft SAG mill operators' expectations in terms of liner life and milling performance.

Subsequent plant trials at a second Chilean hard rock SAG milling operation (36 ft diameter mill) that had previously used a different composite lining system, have also been successful, resulting in increased liner life with no liner failures recorded. A trial of the ball mill version of the hybrid lining system in a 27 ft diameter ball mill in Peru also reported increased liner life and a small reduction in the specific grinding energy consumed by the ball mill.

This paper presents the key findings from the journey through the steps of problem analysis, solution identification, validation, and field trials to produce the world's 'best practice' liner design for the toughest application in the largest diameter SAG and Ball mills.

Liner Wear & Failure Analysis

The assumptions for mill utilisation for large SAG mills reflect the increasing mill diameter:

- smaller diameter SAG mills, eg less than 36 ft, would typically operate at run-times of 94% or more, as demonstrated by operations such as Northparkes in Australia (28 ft diameter and 32 ft diameter SAG mills) circa mid 1990s and the Ok Tedi 32 ft SAG mills in Papua New Guinea circa 2005 to 2008
- however, recent projects that propose to use 40 ft diameter SAG mills are typically designed for 92% run-time.

The reduction in mill utilisation rate reflects the time taken to the mill as well as the increased frequency of having to replace liners that have prematurely failed in service. In general terms, there are four major wear types that have the potential to affect metal liner service life:

- fatigue wear
- abrasion wear
- adhesive wear (e.g. metal surfaces sliding across each other i.e. unoiled bearing surfaces); and
- corrosion wear.

Tega's analysis of the most common liner failure mode identified that fatigue wear, in the form of adiabatic shear cracks, occurs in the steel liner due to high impact force imparted by large ball sizes. Some steel liner suppliers responded by supplying a more malleable liner which allowed the liner to

deform instead of cracking, however this material wore faster from abrasion. These more malleable alloys also suffered from 'cold welding', the result of liner edges flowing into each other and then being pounded together by the steel balls impacts. This made liner removal a tedious and time-consuming task, thereby increasing reline time significantly. Ultimately, operators have to choose between risking increased frequency of liner failure from fatigue cracking from ball strikes, or choosing a softer alloy less prone to cracking but that wears faster, resulting in inferior ball trajectories and liners that take longer to remove from the mill.

Tega recognised that the mill operators wanted fewer, larger liner pieces to reduce re-line time. However, Tega also recognised that this would challenge manufacturers to produce castings with homogenous properties throughout the lifter section during heat treatment, due to the different geometries of the lifter and plate sections. In addition, larger castings can suffer from other quality issues attributable to micro-segregations and non-metallic inclusions.

Hybrid Liner Development

The first hybrid / composite liner technology was installed in a Chilean 28 ft x 14 ft fixed-speed SAG mill in 1998. The liner was a hybrid design of shell plate (rubber and steel bonded together) combined with a metal lifter. The design produced very good results for many years, resulting in the hybrid lining being used at several other mines with varying results. In the early stages of hybrid liner development, some composite liners (rubber and rolled steel bonded together) experienced bonding failures. The failures occurred because of the inadequate bond strength between the rubber and the steel member and because of the low stiffness modulus of the system to handle large deformation due to impact loading. Some designs also experienced cracking in the rolled steel (despite the right blend of stiffness and damping modulus) due to hydrogen embrittlement from incorrect steel cutting procedure.

Other hybrid liner manufacturers trialled hybrid liners in larger SAG mills (>34 ft in diameter) to overcome the cracking of all-steel liners, however inappropriate proportions of steel in the rubber matrix did not provide the desired stiffness and damping coefficients which were required to sustain the high energy impacts and achieve the desired liner service life. These liners failed under the impact loading because the liner design could not sustain the large amount of deformation encountered in service.

Recognising the past failures of hybrid liners in large diameter SAG mill, Tega's more than 40 years expertise in rubber compounding, bonding capability between metal and rubber, mill process parameter analysis, and liner design development provided the confidence to pursue the development of a composite lining design that Tega believed offered the mill operators the best combination of wear and impact resistance. This would offer SAG mill operators increased liner life and elimination of liner failures.

Liner modelling

High impact forces, generated by steel balls or large ore lumps (a 180 mm spherical lump of ore has the same mass as a 125 mm steel ball) on the liner surface can occur over a wide range of incident velocities. Tega recognised that both the velocity of impact (low-speed and high-speed) and the angle of impact are important to determine the minimum threshold stiffness and damping modulus for design. Therefore, Tega used DEM formulations to map the contact events and calculate the impact energy distributions for the different zones of the liner surface throughout the SAG mill's rotation (both high energy and low energy impact), shown in Figure 3.

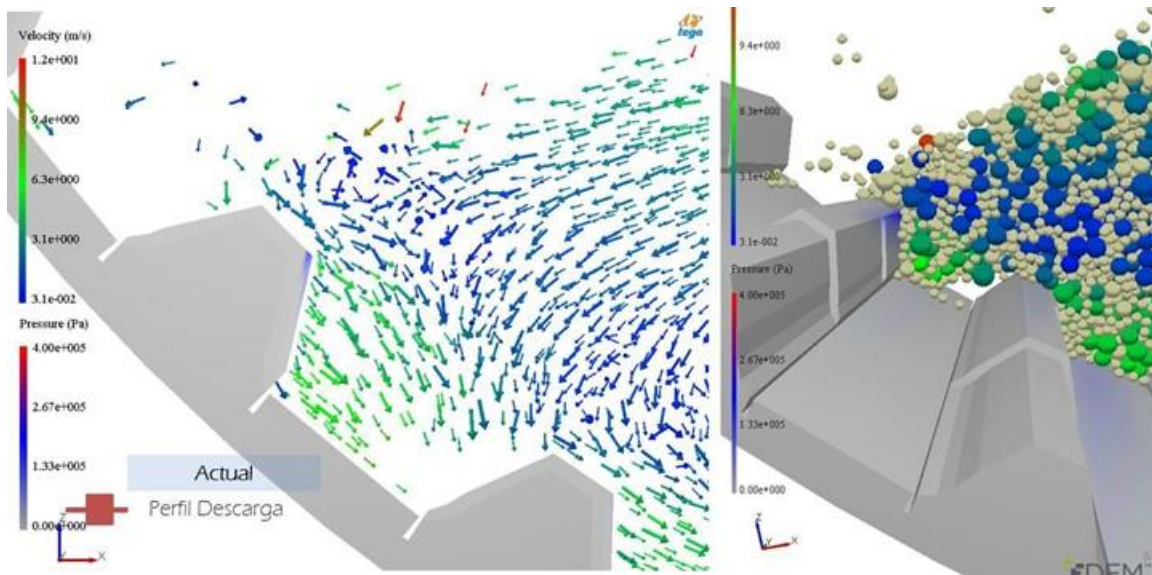


Figure 3: DEM Model output for SAG Mill ore and steel ball velocities

Tega also used an FEM approach to determine the dynamic response of mill liners against the rapidly changing impact loading (time dependent loading). An explicit dynamics approach allowed analysis of non-linearities including large deformations, large strains, plasticity, hyper-elasticity and material failure as shown in Figure 4. The material description used in design calculations included finite deformations, strain hardening, thermal softening, rate sensitivity frictional contact, heat generation due to plastic working, and friction. The use of DEM and FEM techniques helped to minimise design risk and improve the reliability of the design predictions.

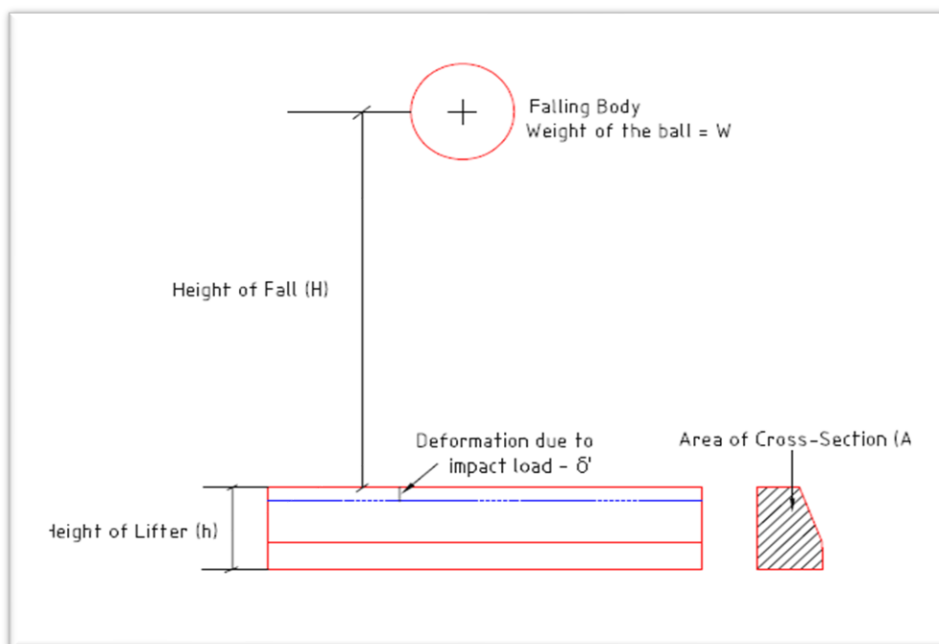


Figure 4: Example of Finite Element Calculation Approach

Tega proposes that contact duration and the contact area during any impact event are the criteria which determine contact force and therefore the onset of the adiabatic shear bands in the steel liner. Pressure distribution under the contact area also changes at different instants of impact (which is a restitution period). Elastic deformation develops until yielding initiates after which plastic deformation alters the pressure distribution through the steel.

These same two parameters, i.e., contact duration and contact area, depend on the material damping and stiffness coefficients. Tega designed the new Dyna Prime liner using multilayers of steel inserts in a matrix of hyper-elastic polymeric material with the objective of using the damping properties of the polymeric material to reduce the overall contact force, thereby eliminating adiabatic shearing of the steel. Use of multi layers of abrasion resistant steels maintained the desired level of stiffness and rubber between the steel surfaces, which helped to damp the impact force. The resultant normal and tangential components of the forces were found to be much lower in Tega's hybrid design compared with the original steel liners shown in Figure 5.

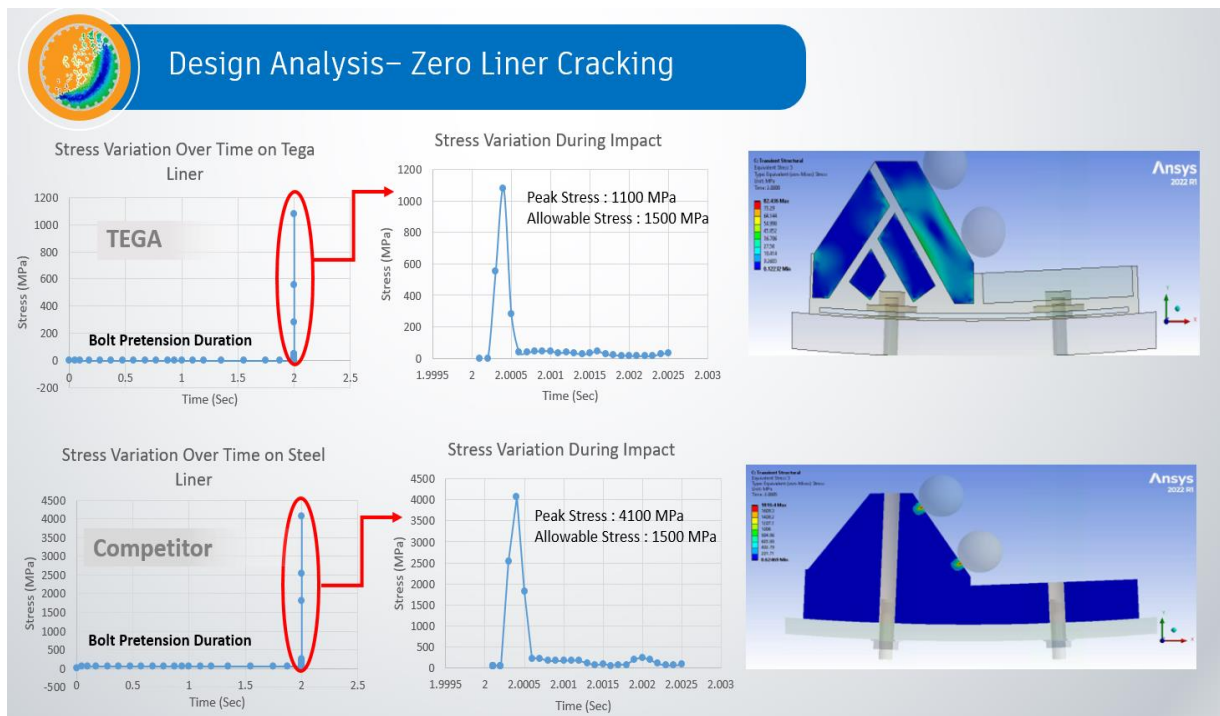


Figure 5: Conceptual comparison Tega Dyna Prime Liner vs steel casting

Figure 6 shows that the peak stress developed during impact would be greater in cast steel liners compared with the hybrid liners. This suggests that the hybrid design construction will have better impact strength resistance if designed with right blend of stiffness and damping coefficients compared with the cast steel liners.

Tega proposed that the improved hybrid design comprised of multiple layers of hard steel heat treated to produce a superior wear resistant metallurgical structure, interspersed with multi layers of rubber and polyurethane, would be expected to improve both the reliability and service of the liners.

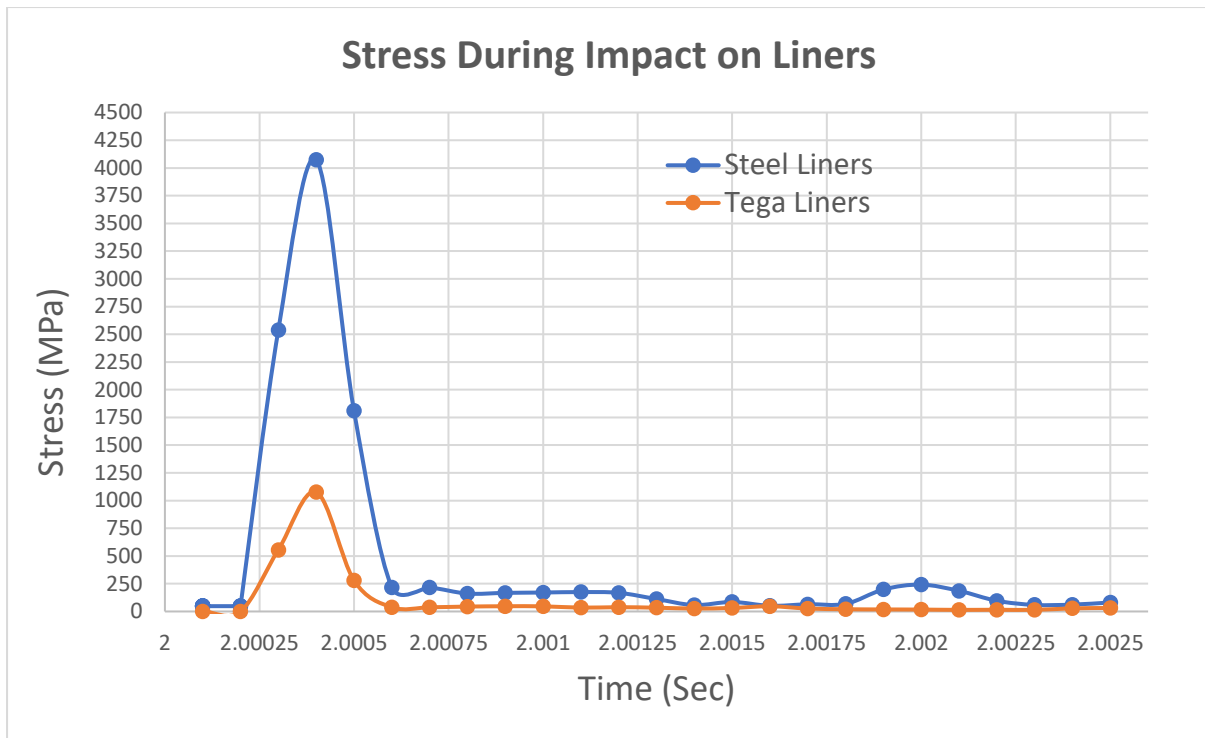
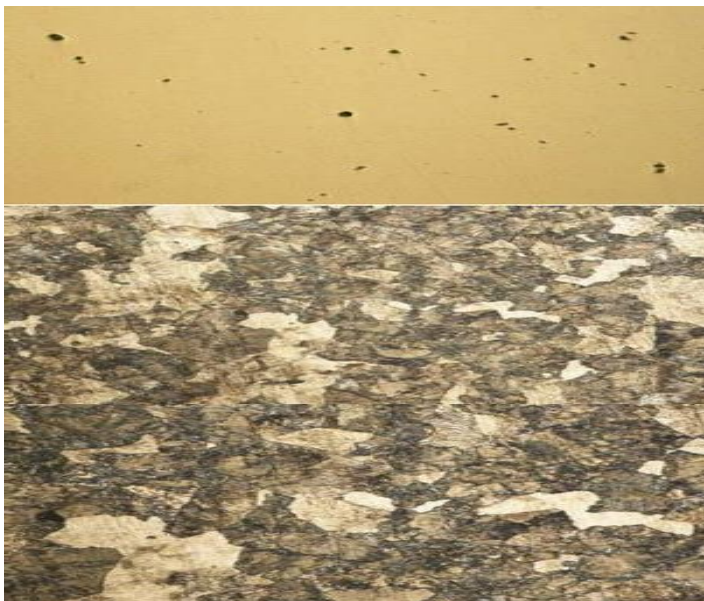


Figure 6: Stress vs time, Tega Dyna Prime liner vs steel casting

Liner metallurgy

TEGA developed a special chrome - molybdenum alloy for use in the hybrid liners proposed for trial in a 40 ft diameter SAG Mill, charged with 6¼ inch balls with the aim to balance impact and abrasion wear resistance. This was achieved by producing a fine pearlite microstructure, shown in Figure 7. The heat treatment studies to achieve this structure were conducted with a sample with the same cross-section of the lifter design. This developed a special heat treatment cycle that minimised variability in the hardness profile across the lifter's steel sections per Figure 8.



Prepared as per ASTM E3, and the micro etching as per ASTM E407. According to ASTM E-45, the piece has metallic inclusions level 2, type A (Sulfide type) and D (Globular type oxide).

This microstructure is fine pearlite. According to ASTM E112, it is possible to determine that the grain size is 6 to 7 micron, which improved the toughness of the lifter. By obtaining a completely pearlitic microstructure, work hardening is favoured, which improves the resistance to wear as the lifter is impacted.

Figure 7: Microstructure of Tega's hybrid liner steel

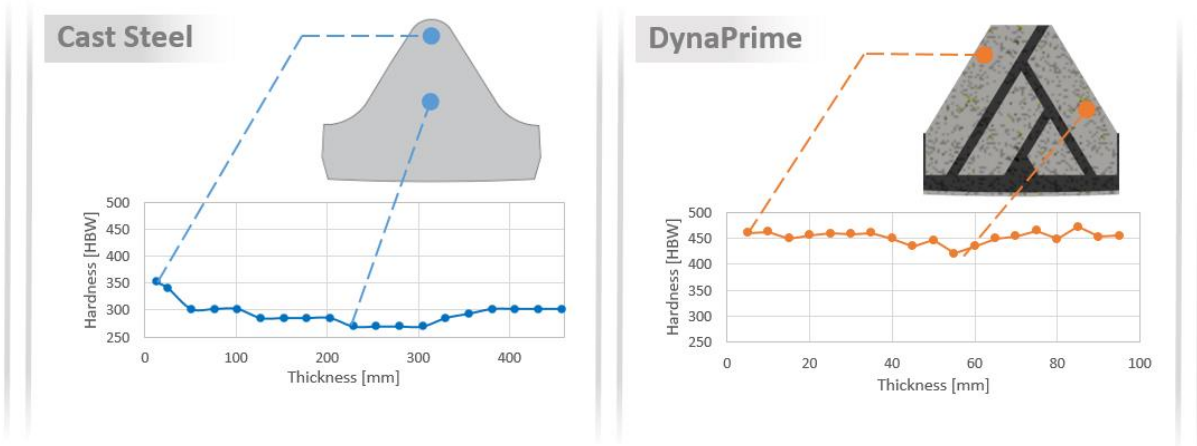


Figure 8: Hardness profile comparison cast steel vs Tega hybrid liner

The final piece of the SAG liner survivability puzzle was the issue of broken liner bolts. Tega utilised a bolting from the outside approach, using a different fixing method, that suggested reduced bolt strain, Figure 9.

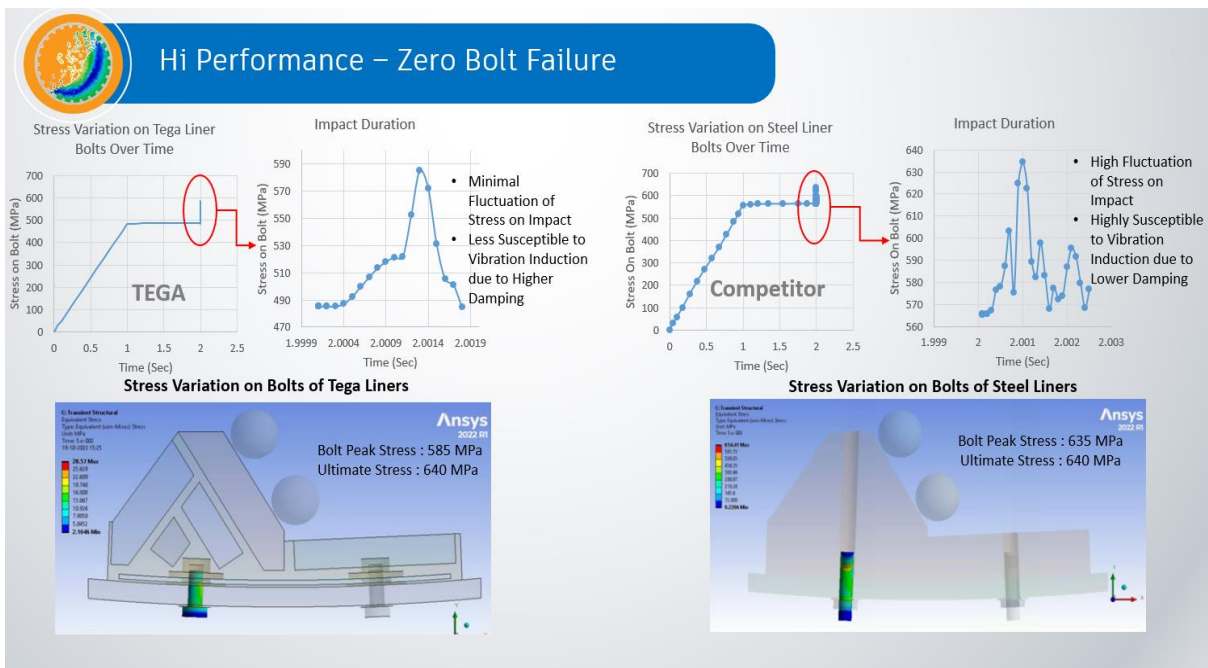


Figure 9: Tega's outside bolting system

Tega's DynaPrime Liner

The final task was to combine these design elements into a complete lining system. The various design elements of the Dyna Prime SAG Mill Shell Lining System:

- Hybrid Liners, rings 1 and 2 in this three-ring design, are bolted from the outside
- Liner ring 3, i.e., the liners closest to the grates, is a chrome-moly casting, contained within a polyurethane dampening system for improved impact force adsorption. The shell portion of the liners consists of AR steel (red), embedded within a rubber matrix, which both absorbs impact and resists adiabatic shear and or cracking.

The Dyna Prime lining system was now ready for plant trial in a 40 ft SAG mill charged with 6¼ inch balls.

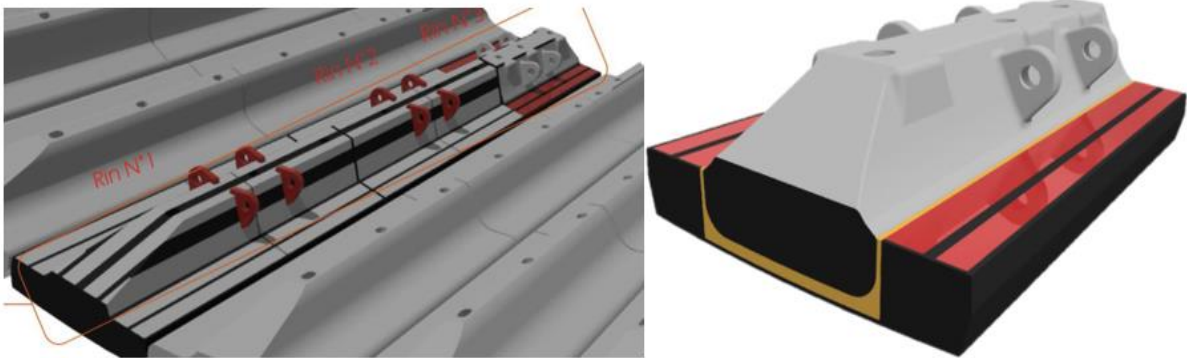


Figure 10: Tega's Dyna Prime Lining system for large diameter SAG mills

Plant Trials

Several Dyna Prime field trials were conducted to determine if the lining system achieved its design objectives of increased liner service life and no liner failures.

Plant Trial 1: 40 ft diameter SAG Mill

A Chilean 40 ft diameter SAG mill processing 4300 t/h charged with 6¼ inch balls was experiencing unexpected downtime events due to the premature failure of steel shell liners. Several design modifications were implemented but none resolved the liner failure issues, Figure 11 and Figure 12.



Figure 11: Hybrid steel liner failure

Figure 11 shows the typical failure mode of an alternative supplier's composite liner due to impact. The shell plate portion consisted of a combination of abrasion-resistant (AR) steel welded to a bottom plate, interspersed with rubber spacers. Failure occurred due to the AR steel cracking and welding failure due to heavy impact. The design construction could not resist the impact magnitude, due to improper stiffness and damping coefficients used in the design.

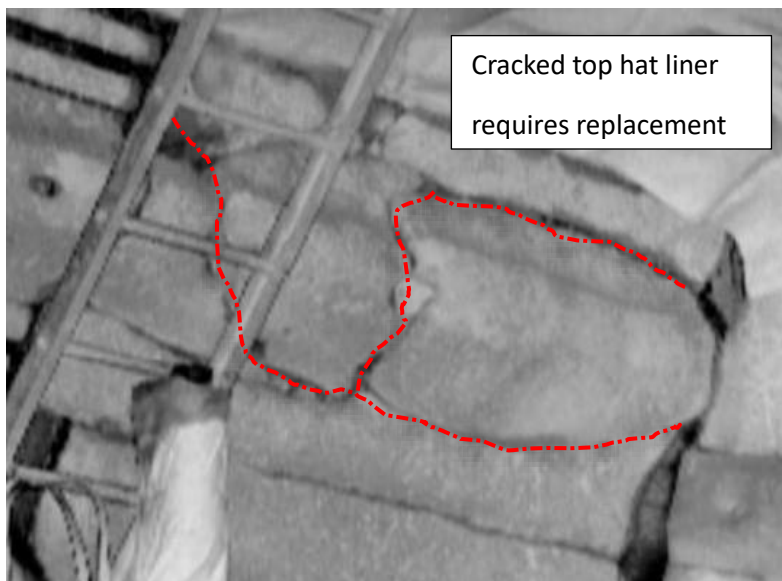


Figure 12: Steel casting failure requiring replacement

Figure 12 shows a typical failure of the cast steel top hat (Sombrero) liner. These liners were installed alongside the alternative supplier's hybrid design to allow a side-by-side comparison of liner performance in the same impact environment. Tega's interpretation of the mode of failure for the top hat cast liner design is that due to the cross-sectional area change of the cast liner, a different temperature gradient is present in the shell and lifter portion of the casting, which produces different microstructures that causes brittleness in the transition zone and residual stress after heat treatment.

The Dyna Prime Liner's condition in the same SAG mill is presented in Figure 13. The alternative liner

supplier's hybrid liner design, left hand side, failed before 90 days service. The Dyna Prime Liner shown in Figure 13 is after 180 days service. Based on the wear profile, Tega estimated that the liner would have provided another 40 days of service life.

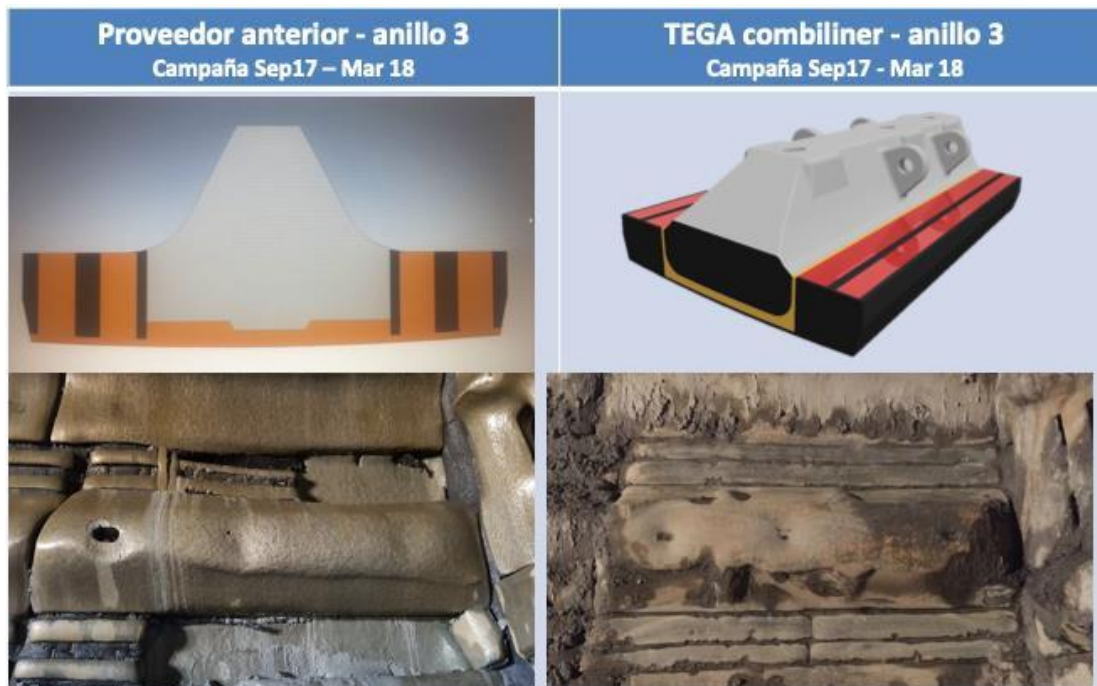


Figure 13: Failed hybrid liner after 90 days, left, vs Tega Liner after 180 days service, right

Plant Trial 2: 36 ft Diameter SAG Mill

A second plant trial was undertaken in a 36 ft diameter SAG mill processing a blend of primary and secondary crushed hard ore. This mill had been using hybrid liners for several years, with operating practice showing that liner performance was most reliable when operating at speeds ranging from around 8.6 rev/min (66% critical) after a reline and then slowly rising to an operating maximum of approximately 9.1 rev/min (70% critical), Figure 14. A review of SAG mill performance had identified that use of relatively slow mill speeds after mill reline was restricting throughput rate, however previous attempts to increase SAG mill speed resulted in a significant increase in liner failure. The time lost to unplanned replacement of failed liners resulted in a net loss in SAG mill production. Therefore an improvement in SAG liner performance would be required before increasing mill's speed to increase throughput.

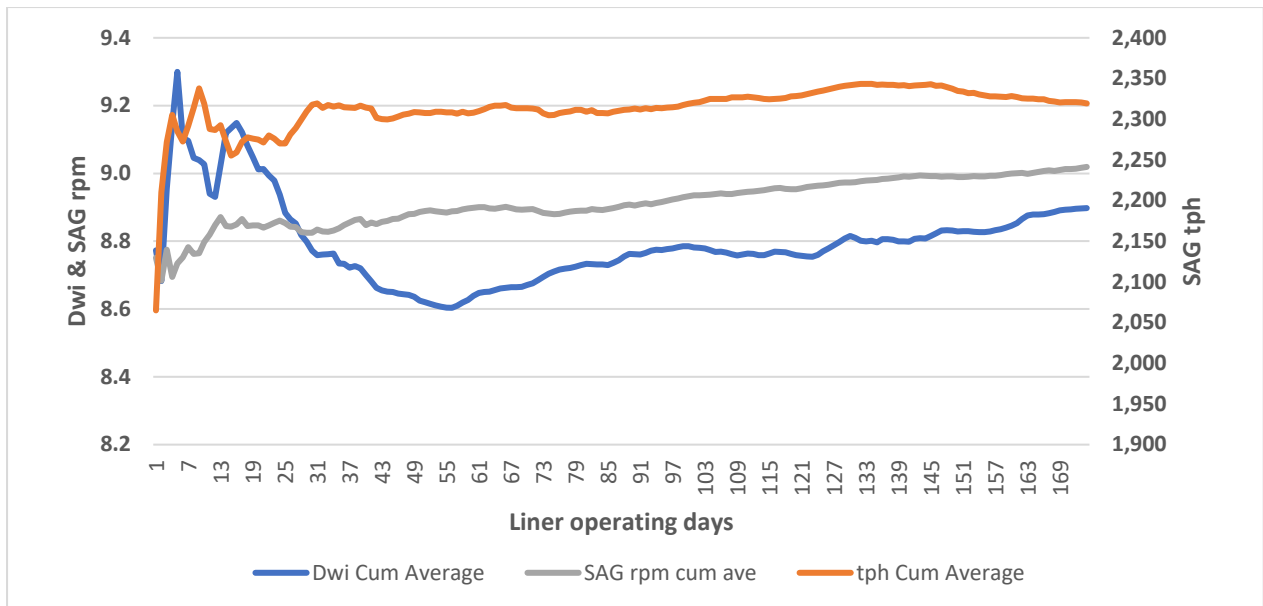


Figure 14: Cumulative averages for SAG feed hardness (Dwi) vs mill speed rev/min vs SAG mill treatment rate t/h

Recent plant trial data showed that Tega's Dyna Prime liner:

- Did not fail in service. No cracks or excessive wear rates were recorded for the steel components, and the rubber was found to be in good condition at the end of the scheduled eight month trial, during which time 11 Mt of ore were milled;
- Analysis of lifter wear identified that the discharge end liners, which are exposed to the highest impact forces and wear rates, indicated a projected liner service life of approximately 14 months, Figure 15.

Figure 16 presents the difference in lifter face angle wear rates between the steel (Acero) and the Tega liner during the plant trial. This data demonstrated that Tega's concept of using a fine pearlitic structure chrome-moly steel alloy was successful in reducing the wear rate of the steel. The ability to maintain a steeper face angle for longer would enable the mill to draw more power and process more tonnes over the life of the liner set.

Note that only three discharge end, and two feed end hybrid liners, were installed in the mill to assess the hybrid liner's survivability, so data to compare against Figure 14 could not be generated. However, given the success of the hybrid liner in this arduous application (high ball charge and low rock charge), further trials are scheduled for the coming year.

Fecha de instalación: 08/01/2022
 Inspección nº 07: 06/09/2022
 Tiempo de operación: 241 días [8 Meses]
 Tonelaje procesado: 11 Mton

Anillo 2 [Lado Descarga]

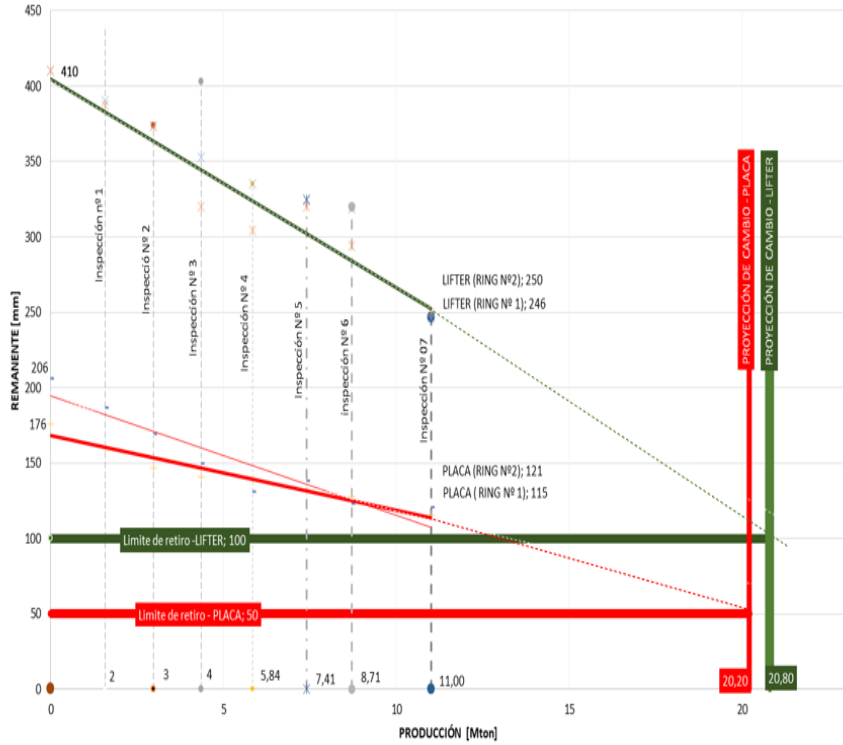
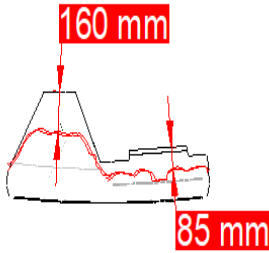


Figure 15: Wear rate recorded for Tega Liner

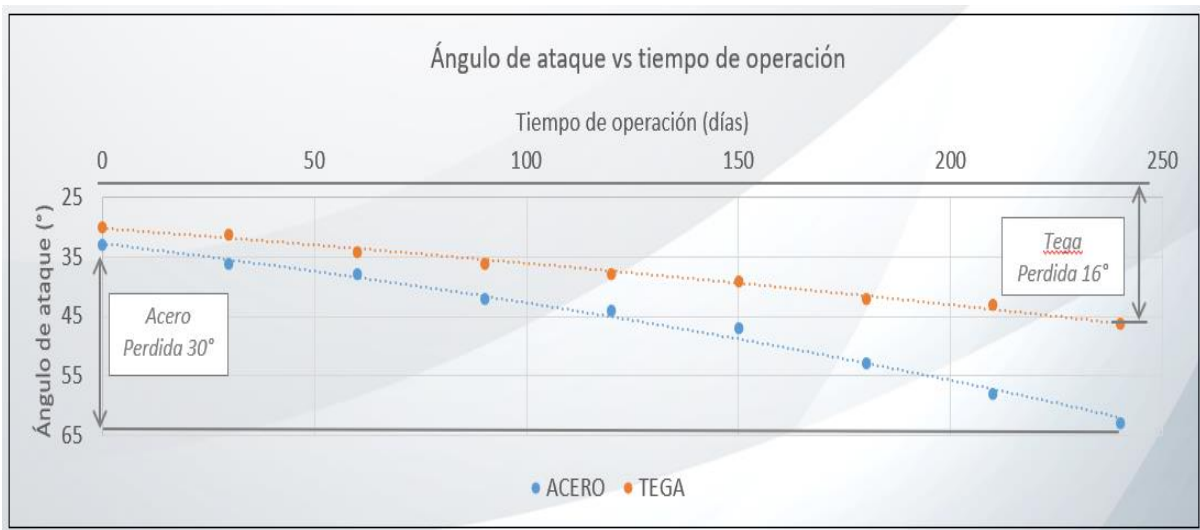


Figure 16: Lifter face angle wear rates – Tega vs Steel

Notes:

- Angulo de ataque = leading lifter face angle
- Acero = steel
- Tiempo de operacion (dias) – liner service life (days)
- Acero Perdida 300 = steel worn by 30 degrees
- Tega Perdida 160 = Tega liner worn by 16 degrees

The results of the two SAG mill trials, one being a 40 ft high-throughput rate mill, with the second being a 36 ft SAG operating with one of the most aggressive milling conditions (i.e. a blend of primary and secondary crushed hard ore), demonstrated that Tega has produced a SAG mill liner that has not failed in service and offers superior wear rates compared with the traditional all steel liner. The superior wear rates allow the Tega lifter face angle to be maintained at a steeper angle over the service life of the lifter, which offers the operators:

- the opportunity to draw more SAG mill power and potentially mill more tonnes; and
- operate the mill with greater confidence knowing that the risk of failed liners has been significantly diminished, if not eliminated.

Trial 3: 27 ft diameter Ball Mill

Tega liners were installed in one of six parallel lines of 27 ft of ball mills, ML501, on 25th Feb 2022. These ball mills process a tertiary crushed feed, where high pressure grinding rolls (HPGR) are used as the tertiary crusher. Table 1, copied from an independent consultant's report (J Consultores Ltda. 2023) presents the average operating results for all six ball mills.

Table 1: Key Ball Mill Metrics

	Valores Promedio					
	MB 101	MB 201	MB 301	MB 401	MB 501	MB 601
% +65#	11.66	11.21	11.36	11.12	11.53	11.69
%	101.1	97.2	98.5	96.4	100.0	101.4
TPH	2356	2397	2331	2352	2392	2333
%	98.5	100.2	97.5	98.3	100.0	97.5
MW	20.70	20.74	20.80	20.65	20.52	20.01
%	100.9	101.1	101.4	100.6	100.0	97.5
kWh/t	8.78	8.65	8.93	8.78	8.58	8.58
%	102.4	100.9	104.0	102.3	100.0	100.0
Wio	11.44	11.10	11.53	11.23	11.04	11.05
%	103.7	100.6	104.5	101.8	100.0	100.1

Notes:

- Valores Promedio = average values
- +65# = mesh of grind, which is the North American method of describing grind size. In this case, the mass of material that is coarser than 65 mesh, equivalent to 88.5% passing 210 μ m
- TPH = short tons per hour
- MW = average ball mill power draw
- kWh/t = kilowatt hours consumed per short ton milled (i.e. specific grinding energy)
- Wio = Operational Work Index, an indicator of ore hardness

The data in Table 1 shows that the mill fitted with Tega's hybrid liners is operating at peak power efficiency, i.e., consuming only 8.58 kWh/t. While Mill 601 is operating at the same kWh/t, the mill fitted with the hybrid liners operated at 2.5% higher throughput rate. Based on these results, the operator has decided to reline a second ball mill with the hybrid liners.

Future Developments

Mill sizes will continue to grow: a 42 ft SAG mill, manufactured approximately ten years ago, is transitioning from storage to delivery to a site in South America. A second 42 ft SAG mill is expected to be ordered before year end. Options for a 44 ft diameter mill have already been discussed by mill vendors and it is believed that some 44 ft shells are now available for delivery from China. It is worth noting, however, that 40 ft SAG mills already present significant challenges to the industry:

- A 40 ft SAG mill is only 10% greater in diameter than a 36 ft SAG mill; however
- because the diameter is 10% greater, the cross-sectional area of the SAG mill is 21% larger ($1.1^2 = 1.21$); and therefore
- lifter height must increase to pick up the same proportion of the mill charge as for 36 ft diameter mill, Figure 17.

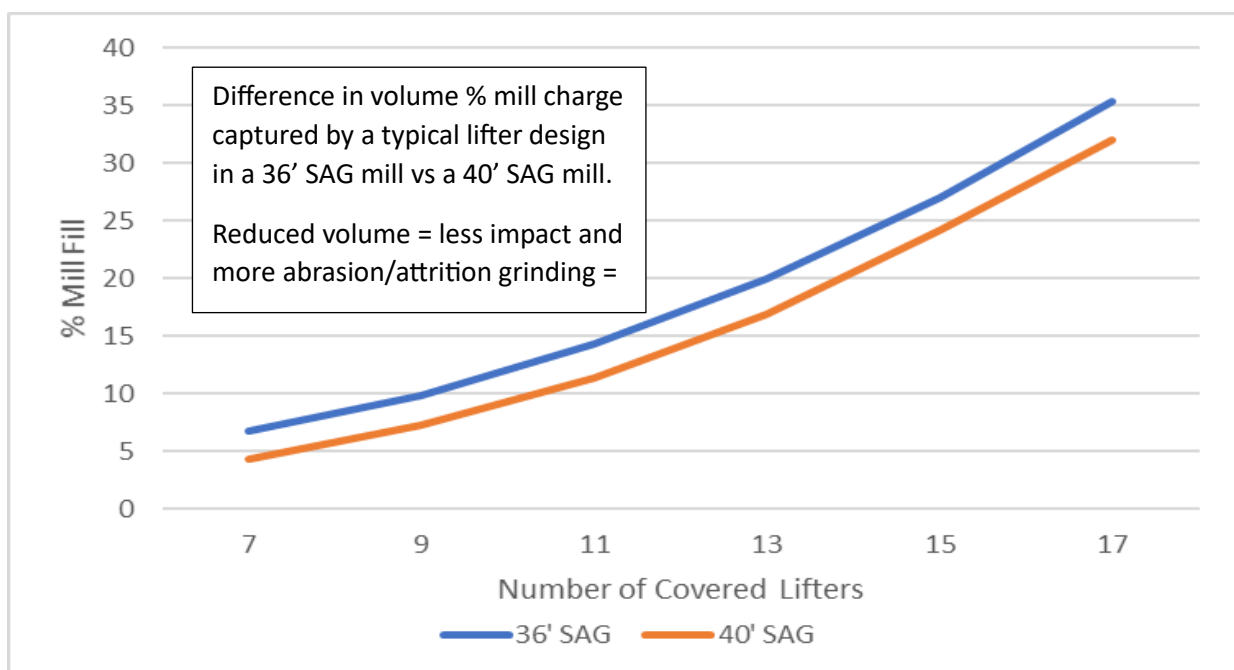


Figure 17: Volume % of mill charge captured by a 250 mm tall lifter on top of a 150 mm shell plate

Increasing the height of the lifter will challenge the industry for the same reasons as outlined earlier in this paper:

- traditional steel lifters will suffer from inconsistent hardness through the casting, resulting in accelerated wear rates once the heat treated harder outer skin is worn through. This results in a rapid loss of face angle and decline in milling performance in the last stages of liner service life; and
- increasing height means increasing liner mass, which will require development of liner handling machines capable of moving the increased liner mass.

Given that SAG mills are tasked with milling as much material as possible, increasing mill diameters present unique challenges for SAG mill liner manufacturers, as already evidenced by the decrease in mill utilisation rates compared with previous decades. Tega proposes that the use of hybrid liner designs can provide solutions to the challenges of increased impact and increased abrasion wear rates. This will become more important since future ores will, in general, be lower grade, harder and more abrasive, than ores being milled to date. Therefore, an increase in SAG mill run time will

become even more important.

The ability of the hybrid liner to survive the high impact SAG milling environment also allows the SAG mill to start at full speed after a re-line. For the operator of Plant 2, Tega has proposed a trial that, when fully lined with Tega's hybrid liners, would allow the SAG mill to start at approx. 73% critical speed, rather than the 66% - 68% critical speed that has been used in the past, Figure 18. The faster ramp-up has been estimated to increase SAG mill power draw by 3.5% over the life of the liner set, which has the potential to increase throughput by a similar amount.

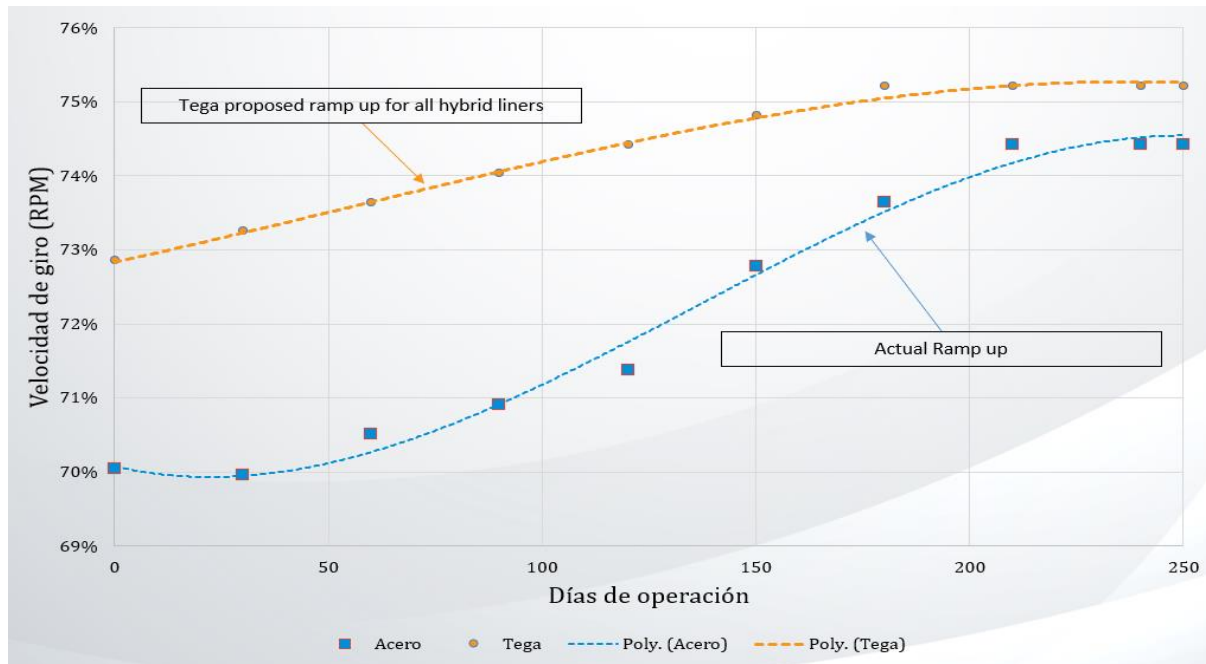


Figure 18: Proposed ramp-up schedule for SAG mill fully lined with Tega Liners

The ultimate goal is to start the mill immediately after a reline at what most operators would consider to be full SAG mill speed, i.e. 78% - 80% critical.

CONCLUSIONS

Substantial efforts have been expended by steel liner manufacturers over the last two decades to improve a cast steel liner's ability to withstand the harsh conditions in large diameter SAG mills. However, these efforts haven't translated into operating benefits, with modern plant designs choosing to typically specify SAG mill run times of 92%, which is 2% to 3% lower than the SAG mill run times achieved approximately 30 years ago. This has resulted from a SAG milling environment with larger diameter mills, larger diameter steel balls, and the use of aggressive ball and rock load combinations to optimise the milling of secondary crushed feeds. All of these factors have produced significant increases in the impact forces in the mill, which increases the frequency of broken liners. When combined with the significant amounts of time required to re-line the larger SAG mills, the end result has been a decrease in mill availability.

Tega has developed the technical tools and computational approach to predict the behaviour of liners under different SAG milling environments. Combined with Tega's more than 40 years' expertise in rubber compounding and optimising the bonding between metal and rubber, Tega has developed a composite lining design that offers mill operators the best combination of wear and impact resistance.

This paper presented the results from three plant trials that demonstrated that Tega's approach produced a superior liner when compared with both the traditional steel liner and other hybrid lining systems, via:

- no liner failures
- extended liner life; and
- improved mill power utilisation (via reduced lifter face angle wear rates)

This results in improved mill performance.

The future of SAG milling will see an increase in mill diameter and the milling of harder and more abrasive ores. Tega's hybrid liners have demonstrated that they are ideally placed to meet the challenges of the current and future SAG milling applications.

ACKNOWLEDGEMENTS

The authors would like to acknowledge the many parties that have facilitated the improvement in liner design, and especially the leadership teams of the mines who have undertaken trials of the new technology.

REFERENCES

J Consultores Ltda., 2023. Personal Communication. June.

Rajamani, R K, and Mishra B K, 1996. Dynamics of Ball and Rock Charge in SAG Mills, in *Proceedings of an International Conference on Autogenous and Semi-Autogenous Grinding Technology 1996*, Volume 2, pp 700 – 712 (University of British Columbia: Vancouver)

Designing Grinding Plants to Maximise Mill Availability During Relining

J Bohorquez¹, J Hodges², S Gwynn-Jones³ and P Van Rooyen⁴

1. MRD Team Leader, Russell Mineral Equipment Pty Ltd, Glenvale Australia, Joel.Bohorquez@rmeglobal.com
2. Applications Design Engineer, Russell Mineral Equipment Pty Ltd, Glenvale Australia, Jordan.Hodges@rmeglobal.com
3. Global Applications Engineering Manager, Russell Mineral Equipment Pty Ltd, Glenvale Australia, Stephen.Gwynn-Jones@rmeglobal.com
4. Regional Applications Engineering Team Leader, Russell Mineral Equipment Pty Ltd, Glenvale Australia, Pierre.VanRooyen@rmeglobal.com

ABSTRACT

Grinding mill relining typically represents between two (2%) and five (5%) percent of lost mill availability annually in the experience of the authors. With ever increasing production demands there is ever increasing production pressure, making it highly beneficial to reduce relining duration to achieve higher mill availability.

While grinding mill maintenance often dictates the plant shut duration, it is rarely made a priority when designing concentrator plants. Other important factors such as mill geometry, drive selection, other processing equipment and costs tend to have the largest influence on plant features that can negatively impact relining and other maintenance activity durations. Mill availability is a direct function of relining and other maintenance activity durations as they require the mill and associated equipment to be taken out of service for said activities. Further to this, cost and project schedule constraints encourage plant design features to be copied with little to no time to study the impact on relining and maintenance activities and durations. However, mine owners who insist on optimising relining and other maintenance activities see benefits in both faster relines and reduced safety risks to the relining crew.

Russell Mineral Equipment (RME) has engineered over 550 Mill Relining Machines (MRMs) since 1990, with a large portion of these machines going to Greenfield and Brownfield expansion projects. RME assists many end users and designers to understand which plant design aspects facilitate relining best practices and ultimately lead to increased mill availability. In one example, RME has supported a mine owner's engineering team to increase their mill availability by almost 2.2% through plant design improvements that facilitate faster and safer relines.

This paper provides advice on the best practice in plant design for relining and contains:

- Examples of reduced mill availability when sites did not consider and implement mill relining best practices
- The relationship between the mills charge height and the platform height around the outside of the mill and its impact on relining performance and safety
- Examples of good and poor space around the mill to facilitate relining activities such as MRM insertion, feed chute removal, liner staging zones and bolt knock-in activities.
- A case study showing the impacts of implementing the topics within this paper and how an additional 2% of mill availability can be achieved for a 36' Semi-Autonomous Grinding (SAG) mill.

INTRODUCTION

Designing grinding plants to facilitate best practice relining and maintenance activities provides an excellent return on investment. Not only is mill availability increased, but safety is improved by reductions in relining times and the elimination of hazards. In recent years, two papers, one from a mine owner, and another from a plant designer, have highlighted the safety and performance benefits of designing for relining at Carrapateena and Gruyere.

The authors recognise that many projects must minimise CAPEX in order to secure financing. However, many CAPEX-constrained projects still model their financial performance assuming 8000 hours of annual mill operation. This requires some consideration of relining at the plant design stage in order to achieve.

This paper aims to provide plant designers with additional insights on the benefits of optimising the plant design for relining, and tools that help operators achieve and exceed their annual mill availability targets. This paper is separated into two distinct parts: liner optimisation and plant design, and will discuss the following topics; liner design, mill deck layout, liner supply system, the relationship of charge and deck levels knock in systems and dual versus single sided relining.

An overview of the mill relining process is described below:

1. The mill is prepared for relining by stopping the feed but continuing to rotate the mill to 'grind out', lowering the charge level. Once this is completed the mill is stopped and the drive isolated and locked out. The feed chute and guarding around the mill is removed to enable access for relining. New liners are placed on the mill deck ready for the reline, in addition to the other relining equipment, fasteners and consumables.
2. The feed chute transporter is moved from its parked position, extracts and lifts the feed chute, and relocates it to somewhere that will enable feed chute maintenance and will not interfere with other relining activities. The feed conveyor discharge box is sealed up.
3. The mill relining machine is driven from its parked position into the entry of the mill, manoeuvring through the plant to avoid any obstacles such as columns or other equipment.
4. The reline crew remove the accessible nuts securing the liners and use hammers to knock-in the bolts and then the liners onto the charge inside the mill. No reliners are able to enter the mill until all of the accessible liners and bolts are knocked-in.
5. The reline crew enters the mill to install slings or specialised lifting tools to the worn liners, which are then lifted by the mill relining machine and removed from the mill. A forklift is used to collect the liners from the rear of the machine and place them on the mill deck.
6. Once all of the worn liners are removed, the forklift collects new liners from the mill deck and places them onto the rear of the machine. Simultaneously, the worn liners on the deck are transported off the mill deck with a second forklift to clear the space.
7. The new liners are placed by the mill relining machine against the mill shell, and reline crew members inside of the mill insert the liner bolts. The reline crew outside of the mill connect the nuts to the bolts and secure them with rattle guns. All of the accessible liners and bolts are placed in this manner.
8. The reline crew exits the mill and the mill drive is de-isolated. The reline crew carefully rotate (aka 'inch') the mill until a new set of liners is accessible. Once the mill has been rotated it is isolated. During this period new liners are conveyed to the mill deck by forklifts.
9. Steps four (4) to eight (8) are repeated until all of the liners have been replaced.
10. The mill relining machine is removed from the mill and relocated to the parked position. An original equipment manufacturer (OEM) service technician completes an audit on the machine to identify any maintenance needs in advance of the next reline.
11. The feed chute and guarding is reinstalled, and the mill drive is de-isolated. The mill is then ready to resume operation.

12. After a short period of operation, the mill is stopped and all of the liner bolts are re-torqued to manufacturer specifications.

LINER OPTIMISATION FOR FASTER MILL RELINING

To improve mill relining efficiency when designing a grinding plant, it is important to understand the requirements of the mill liners due to their impact on plant layout and structural requirements. While RME is not a liner supplier, the company collaborates with all OEMs in the liner supplier market globally. This experience has deepened the author's understanding of relevant liner design concepts as they link to other plant design topics.

In general, a new greenfield plant's first liner set are likely to be a simple, low-cost design for the initial warranty period. After a few campaigns when the initial stock of OEM liners is spent, the liner design will be changed in order to increase mill availability and throughput. A good plant design will ensure that the site is able to optimise the design of the liners to achieve availability and productivity targets, without jeopardising the safety of maintenance practises.

In brief, liner optimisation falls into three categories; grinding performance geometry, liner life and liner piece count. Whilst the first two categories specifically address mill operational performance, the third category has an impact on mill downtime and subsequently, annual mill availability.

Liner Grinding Performance Geometry

Liner grinding performance geometry improvements are about making changes to the shape of the liners in order to affect the way the ore is processed or conveyed within the mill. This can include the tailoring of liner quantity, face angle and the height of the shell liner lifter bars to achieve certain grinding performance, based on the circuit design and ore characteristics (Powell et al., 2018). Faulkner et al. (2019) presented a case study on a large copper mine in Kazakhstan which optimised grinding performance geometry for a 40ft SAG mill. In this case, pulp lifters were changed to a vortex design to improve discharge efficiency and reduce mill power consumption. The result was a 28.5% improvement to throughput during the testing period.

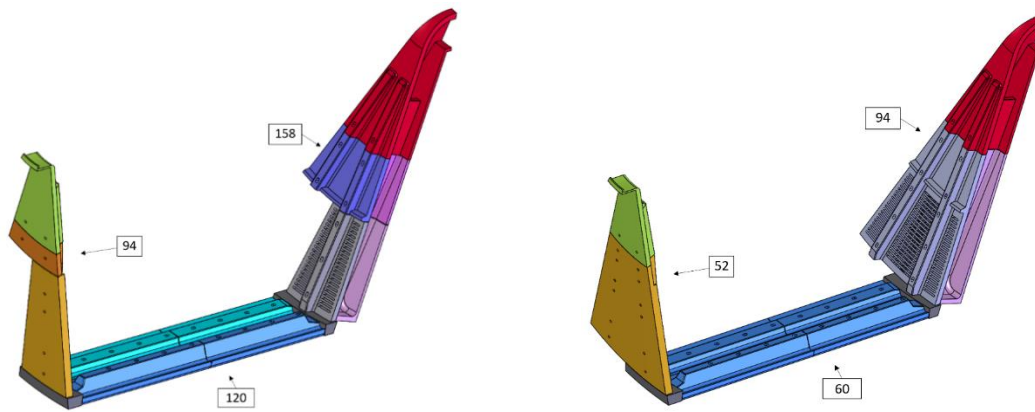
Liner Life

Liner life is affected by a range of factors including but not limited to: specified mill design operating parameters, liner construction materials, manufacturing methods, and the geometry of the liner itself. However, mine sites will often need to achieve specific intervals between reline events, so they can align shutdowns with other necessary maintenance activities. To achieve this, it is common practice to increase thickness in the areas of highest wear in order to extend liner life. This could be, for example, increasing the thickness of shell liner lifters for more wear allowance, before the lifter geometry becomes insufficient to lift the charge.

Liner Piece Count

The third liner design optimisation category directly addresses relining maintenance activities. Reducing the total liner piece count can result in shorter relines, simply because the number of liners handled during a reline is reduced. In the 40 ft SAG mill examples discussed by Faulkner et al. (2019) a design change reduced the number of shell liners by 33.3%.

For instance, as seen in Figure 1, a non-optimised liner set for a 36 ft x 21 ft SAG mill typically consists of a total piece count of 372 liners, each with a maximum mass of 2 486 kg. Whereas an optimised liner set can have a total piece count of 206 liners, each with a maximum mass of 5 268 kg. This reduces the liner piece count by 45% which can result in a similar reduction for reline duration.



Non-optimised liners (372 liners)

Optimised liners (206 liners)

Figure 1 – Illustration of liner piece count reduction through optimisation

Consequences of Liner Optimisation for Plant Design

Each of the before-mentioned liner optimisations have consequences for liner size and weight, and ultimately plant design. Firstly, increasing the size or weight of liners can require the implementation of a larger capacity liner handler. Liner handlers vary in lifting capacity from 1 000 kg to 8 000 kg. The selection of a larger liner handler can impact plant layout and structural requirements due to increases to machine size and operating and transport loads. However, when this is considered at the plant design stage, the cost of the larger liner handler is minimal compared to the plant retrofits needed to accommodate it after the plant has been built. Secondly, the weight and size of the liners needs to be considered when designing the plant's liner laydown areas, as discussed later in the paper.

PLANT DESIGN CONSIDERATIONS

Concentrator plants should be designed to facilitate fast and safe relining practices for maximum mill availability. The following interdependent plant design principles play a significant role in relining performance.

Mill Deck Layout

Liner staging and handling

The mill deck must have appropriate space to efficiently store (stage) new liners before they are installed into the mill, as well as efficient space to store worn liners that have been removed. As shown in Figure 2, having dedicated new and old liner storage areas close to the mill relining machine ensures the machine is never waiting for liners to be inserted or extracted from the mill. This will keep overall relining duration as short as possible.

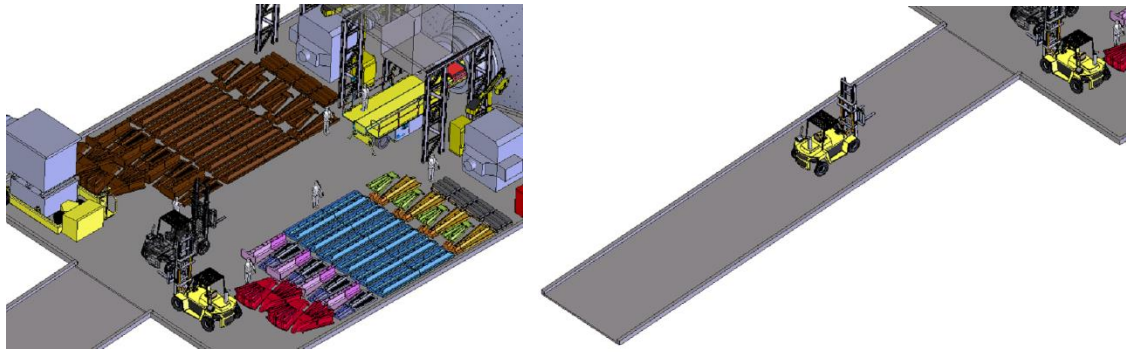


Figure 2 – Left: Example of new and old mill liner lay areas.
Right: CAD plant model showing ramp to mill deck

Mill relining machine and feed chute transporter

The mill deck must also be sized appropriately in order to park, maintain, manoeuvre and insert the mill relining machine into the mill for a reline efficiently. Similarly, the feed chute transporter needs space to be maintained, stored, maneuvered into position to extract the feed chute, and parked in an appropriate location during a reline. Figure 3 is an example of the clear trajectory space required to manoeuvre a mill relining machine to the mill from a parked location. Note that for both machines, the turning radius space required is larger than that of the parked position, which impacts the recommended deck length. Previous papers have outlined the importance of considering the impact of relining equipment on plant structural design, particularly in reference to equipment operating and transport loads.

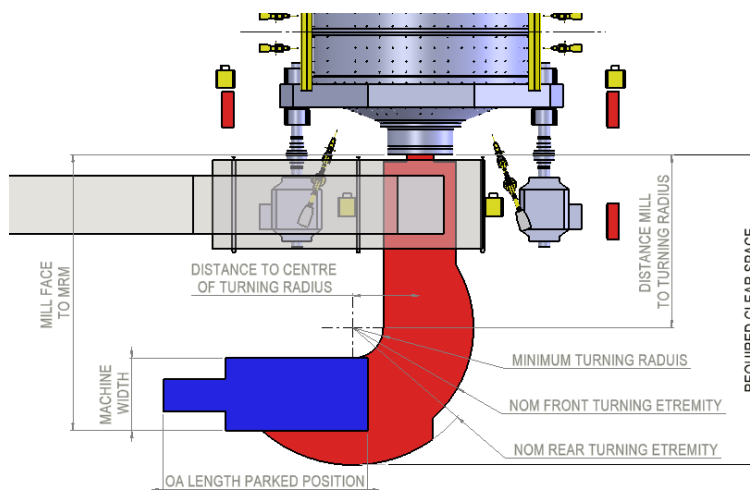


Figure 3 – Space requirements for a mill relining machine to complete a 90 degree turn into a mill

Mill deck access

Almost all grinding mill decks are at a level above the natural ground level, making access to the deck a challenge. It is RME's experience that it is common for plant designers to debate the cost-benefit of adding a ramp at the plant design stage. The authors have observed that grinding operations and maintenance personnel who have experienced sites with and without a ramp become vehement advocates for the inclusion of ramps. This is because the ramp also benefits a range of other operational and maintenance activities. RME recommends that a ramp is included on every mill deck,

where it is possible to do so. From a relining efficiency perspective, a ramp enables multiple forklifts to deliver new liners and ancillary items onto the mill deck liner installation. Similarly, they can also be used to quickly remove the old worn liners off the mill deck.

Feed Chute Removal

An important plant design consideration is the method for removing and storing the mill feed chute during relining and maintenance. Sites often choose to keep one or more spare feed chutes, so that feed chute liner maintenance can be conducted independently of the mill reline, which is good practise. While the feed chute itself is typically included in the equipment scope of the mill manufacturer, the system for feed chute removal can be split out to a specialised equipment provider.

Broadly, there are three methods of removing a feed chute as shown in Figure 4: a winch-based system, a powered rail base solution and a rubber-tyred solution.



Figure 4 – Examples of different feed chute removal methods. Left: Winch with one-directional rail base. Middle: Powered two-directional rail base. Right: Rubber-tyred transporter

An important consideration when designing the method for feed chute removal, is that feed chute bases are often partially buried in ore and product from the feed system or overhead cyclones. This means that any drives or rail bearings can be difficult to access for maintenance until the mill shutdown has commenced, and the feed chute removed from the mill. This can lead to delays in the removal process.

Another factor to consider is that the feed chute often needs to be removed when it is choked (full). This therefore is the weight condition that drives the selection of feed chute removal equipment capacity.

In 2021, RME conducted a trade-off study comparing two feed chute removal systems for a nickel producer. The site had a constrained plant footprint, so the feed chute removal system needed to increase the space available on the mill deck for other relining activities. The Engineering, Procurement and Construction Management (EPCM) contractor had initially selected a two-directional rail base system which limited forklift access to one side of the small mill deck. This design meant there was insufficient space on the mill deck for liner laydown, which was expected to prolong the reline duration. After a review of options, the EPCM changed to a rubber-tyred feed chute removal solution. This removed the need for floor rails, and allowed the feed chute to be positioned in a different location that did not impede the speed of relining and maintenance. This change greatly improved the space available for liner laydown, ensuring the best use of the plant design's limited space.

Liner Supply System

The liner supply system refers to the method of disposing worn liners from the mill relining machine to their disposal location and the supply of new liners from their mill deck or yard location to the machine for installation. The liner supply system is a common bottleneck in the relining process when it is not considered during plant design stage. On such sites, it is common to observe relining activities stopping and waiting for forklifts or other equipment finishing their tasks to deliver a new liner, or collect a worn liner from the liner handler liner cart so that another liner can be removed. Such an observation indicates a need to optimise the liner supply system to reduce relining duration.

Various methods of supplying and disposing liners from the liner handler to their laydown areas are used in the industry. The most common method, and one of the most simple and efficient, is the use of mobile equipment such as forklifts and mobile equipment. However, there are also other methods that are even less efficient and more likely to create bottlenecks in milling buildings. For example, the use of telehandlers or cranes to bring liners from the yard to the mill deck, and liner slide ramps to lower liners from the mill deck to the yard.

The design of the concentrator building, mill deck layout, and access to it from the yard, may restrict the liner supply and disposal system that can be used, as described in Table 1. An ideal liner supply system is formed by a combination of:

1. A sufficiently large allocation of space in front of the mill to laydown liners and other parts (e.g. liner fasteners, relining tools, feed chutes storage), and;
2. Using two or more forklifts (or other mobile equipment) to move new and worn liners between the yard laydown, the mill deck laydown, and the mill relining machine. This system has the added benefit of leaving the overhead crane available for other critical tasks during the shutdown.

Table 1 – Main factors affecting mill deck size

Factor	Design Goal	Design Challenges
Mill relining machine trajectory	Ensures efficient insertion of the mill relining machine into mill with minimal obstacles. Ideally, space is allocated for a set of 'maintenance tie downs' in the parked position to allow for mill relining testing.	The deck needs to be of sufficient size to accommodate a long mill relining machine with a large turning circle. Plant support columns are often placed in the trajectory path and tight manoeuvres can be time consuming.
Feed chute transporter trajectory and feed chute extraction	Ensures efficient trajectory to the feed chute, extraction of the feed chute, and transporting the feed chute to an appropriately defined storage and maintenance area.	The feed chute must be stored in a position which does not obstruct the mill relining machine from being maneuvered from its storage area to the mill and back. High wheel loads can affect deck structural design.
Scope of relines and maximum pieces replaced per inch	A large laydown area for a full scope relining ensures the mill relining machine is not waiting for liners to be transported from ground level.	To provide enough dedicated clear space on the mill deck for the storage of new liners and a waiting area for the old liners to be removed from the mill.
System of liners to mill relining machine	By designing an efficient liner delivery system it ensures the mill relining machine will never wait for new liners to arrive on the deck or old liners to be removed off the deck.	Providing sufficient space for forklift operation to prevent relining delays. Providing sufficient space for liner laydown on the deck, that considers at a minimum the number of liners moved per inch.

Factor	Design Goal	Design Challenges
System of liners to mill deck from the storage yard	An efficient system of transporting liners between yard and mill deck will require less space for liners on the mill deck. This could be a second forklift or a crane moving batches.	A system which cannot keep pace with the relining machine will require a large laydown area on the mill deck or it will bottleneck the mill relining machine from completing liner replacement cycles.
Knock-in system	The knock-in system dictates how long the cycle time is to remove old worn liners from the mill. A well-designed plant layout considers the operating space requirements for the selected knock-in system.	Recoilless hammer selection is a function of liner mass. A hammer that is too small will have a tougher time knocking-in liner bolts. The suspension method and position is critical in ensuring a recoilless hammer can be used effectively. Jibs have a large footprint and need to be able to rotate without hitting obstructions such as columns.
Dual-sided relining	Has the potential to drastically reduce reline times via a reduction in inching cycles.	Drive type and layout considerations and limitations impact the success of dual-sided relining.
Access routes for personnel and plant	Ensures personnel can safely move around the mill deck to access necessary areas and equipment without being exposed to hazards.	Liner laydown areas should not block personnel or forklift access routes to other parts of the plant. Forklift access routes to other mills should not pass directly behind a mill relining machine if two mills are being relined simultaneously to avoid forklift traffic delays.

Platforms and charge levels

The height of external reline platforms relative to the mill centreline has an influence on the coordination and ergonomics of reline activities between 'outside' and 'inside' crew members. Having the charge and work platform elevations during a reline positioned, such that optimal working ranges are aligned in all zones, results in safer and more efficient work conditions for all personnel. As shown in Figure 5, when the mill relining deck is matched to the charge height, the relining crew members inside and outside the mill are able to coordinate relining activities in an ergonomic and efficient manner.

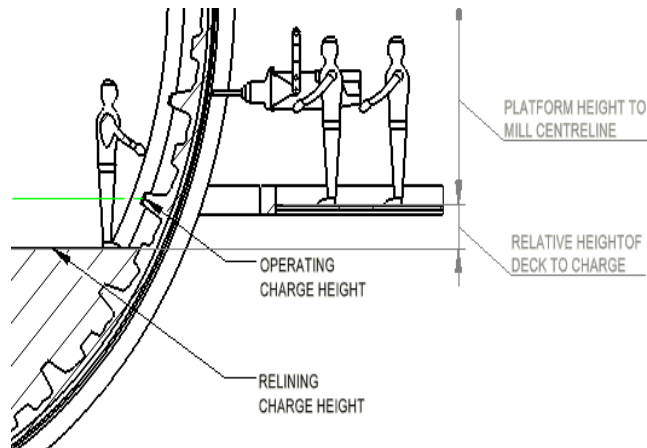


Figure 5 – Mill deck to charge level relationship

When designing plants for efficient relining, the first step when deciding on platform heights is to ascertain the range of charge heights that can be achieved on the project’s mills. This is something that can be partly controlled by grinding out the mill, but is also predetermined by the initial fill volume and the percentage of grinding media. Figure 6 shows that at over 100 relines, which RME has attended, fill volumes during relining can vary between 35% and 10%. The takeaway message from this data is that in order to determine optimal platform heights, it is necessary to request information from the process engineers about the operating specific fill volumes of the mills on the current project.

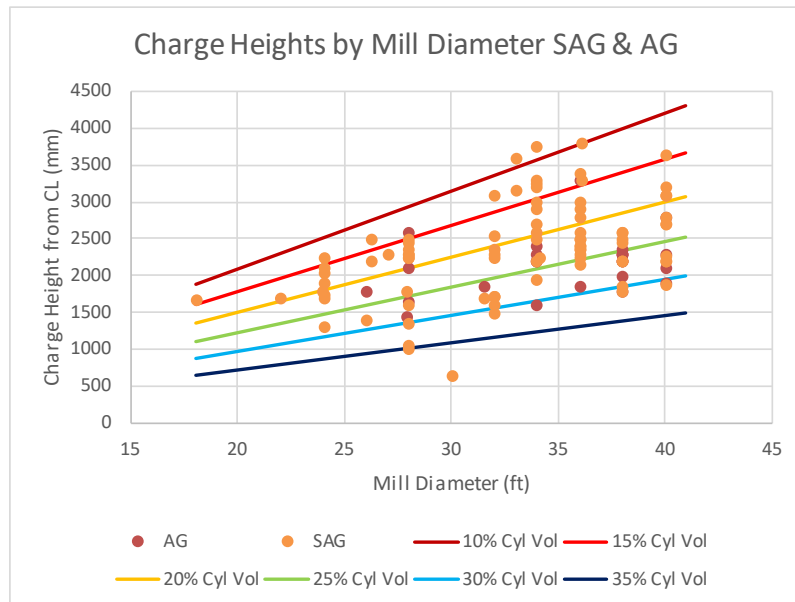


Figure 6 – Charge height for a range of SAG mills from data collected from over 100 RME-attended relines photos

In the lead up to a SAG/AG mill reline shutdown, typically the mill operator will attempt to ‘grind out’ product to reduce the volume of ore and slurry within the mill, such that the charge reaches a level

similar to the external relining platforms. Grinding out is difficult to control, and it is common for the reline crew to realise that the charge is still too high when the chute is first retracted. This requires the start of the shutdown to be delayed while grinding out continues. Similarly, the crew can realise the charge has been ground out too far. A good level of alignment between the charge and external reline platforms ensures that the external crew can knock-in and secure bolts at elevations that the internal crew can safely access, and vice versa.

A very high or very low mill centreline height can make it difficult to match the reline charge height to the relining platforms, as shown in Figure 7. The consequence is that the accessibility of the crew is limited in one area, and it can lead to additional hazards from working at heights. Alternatively, the crew will be required to inch the mill more frequently, increasing the reline duration.

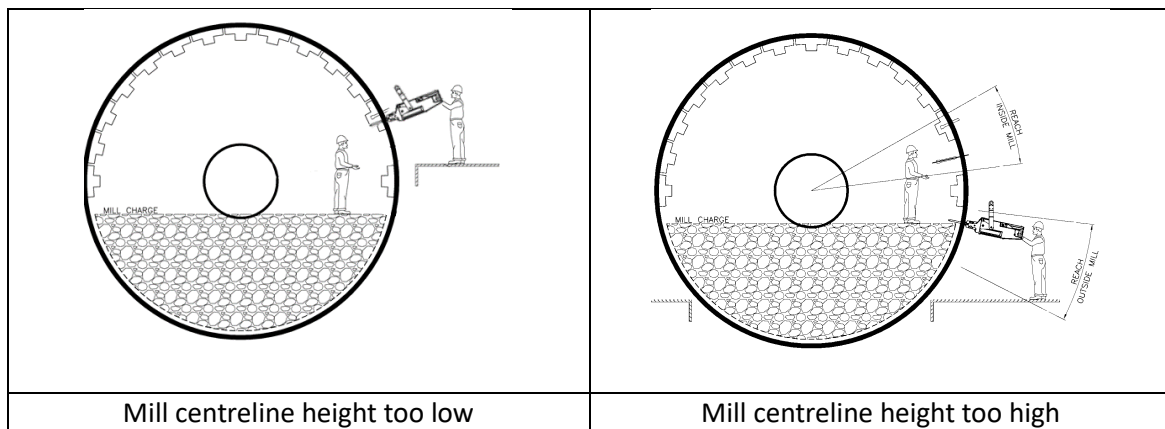


Figure 7 – Mill centreline relative to charge level for an overflow mill

For optimal mill relining, it is preferable that the deck in front of the mill is the same height as the access platforms around the mill. Thus, RME recommends that the charge height is considered even before deciding the relative height of the mill itself in relation to the mill building. For larger SAG mills, this can lead to the mill centreline being 2.5-2.8 meters above the mill deck (noting that above 2.8 meters can cause challenges for mill relining machine design due to machine balance considerations).

Knock in systems

An important consideration in grinding plant design is the system for knocking-in the liner bolts from the outside of the mill during the worn liner removal phase of relining. Some examples of the equipment sites use for knock-in is shown in Figure 8.



Sledgehammer

Battering ram

Hydraulic recoilless hammer

Figure 8 – Examples of knock-in system equipment

A significant portion of the reline can be attributed to the time spent loosening the nuts and washers, and then using a combination of manual and mechanised solutions for ‘knocking-in’ the bolts and liners from the outside of the mill. As a rule of thumb, the knock-in phase of a reline can take between 15-35% of the total time spent relining. Some examples of this are included in Figure 9 for relines RME has captured. By optimising the plant design to consider the knock-in system, and by selecting the correct quantity and type of equipment, it is possible to significantly improve the speed and safety of this activity, leading to increased mill availability.

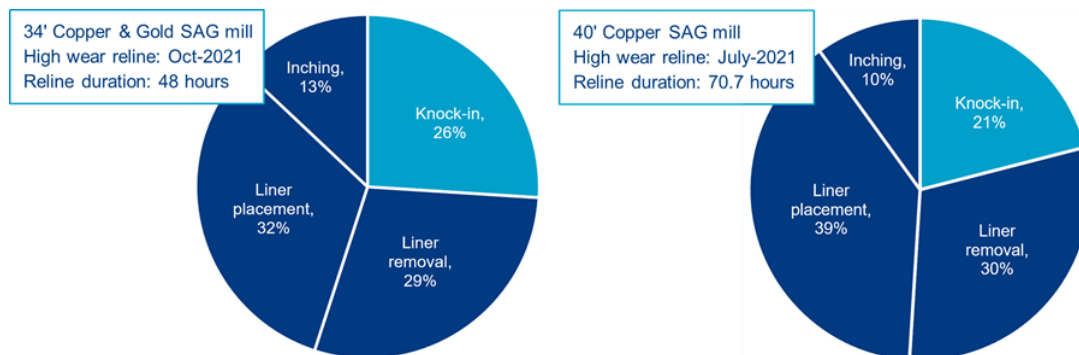


Figure 9 – Knock-in phase as a percentage of total reline duration [8]

The difficulty of bolt knock-in and liner knock-in is something that can vary between sites based on a number of factors. Sites that experience more difficult bolt knock-in will spend longer in the knock-in phase. Difficult bolt knock-in and increased difficulty of dislodging liners are usually not observed until the reline operation has commenced and is typically connected with the following symptoms:

- Fragments of grinding media and ore plugging the liner bolt holes inside the mill
- Misalignment of the hole in the liner and the hole in the mill shell
- Accumulation of slurry between the mill shell and liner
- Distortion of holes in the mill shell from missed hammer blows
- Adjacent liners being stuck together from peening or metal flow

- Bolt nuts needing to be cut off with an oxyacetylene torch rather than removed using a rattle gun

These symptoms are often attributed to the following causes:

- Variation in ore hardness and competency
- Campaign mill operational practices
- Level of liner wear at the time of the reline
- Liner design features (e.g. liner geometry between adjacent liners susceptible to metal flow from impact)
- Manufacturing methods and/or material selection of fasteners
- Inadequate liner sealing arrangement leading to wetting of fasteners with leakage of slurry

At the early stages of plant design it can be difficult to predict the impact of the above factors. The recommended approach is to identify other operating sites with similar mills, liners and ore properties, and use their existing equipment as a guide for the selection of the future project's knock-in equipment.

The design of the knock-in system has the potential to affect the space requirements around the mills, particularly the positions of nearby columns, and the floor spacing requirements in between multiple mills.

Another factor affecting the selection of the knock-in equipment is the difficulty encountered when 'breaking-in', which is the activity to knock-in the first row of liners. This can take several times longer than any other knock-in phase due to these liners being stuck in place due to circumferential forces and potential liner peening. Sometimes the knock-in equipment needs to be selected specifically to focus on this aspect of relining.

The knock-in system includes multiple pieces of equipment:

- Hammers and rams used for liner bolt knock-in – refer to Table 2 for additional details on the options available and the impact on plant design
- Suspension system for recoilless hammers and rams – refer to Table 2 on the options available for suspension equipment and the impact on plant design
- Working at heights equipment – in most sites there is a space between the mill and the platform that is large enough to fall between, and so the crew needs to be equipped with fall prevention or fall arrest equipment.
- Impact wrenches (aka 'rattle guns') for nut removal – the benefit of correct selection and quantity of impact wrenches on reline time is not to be underestimated. Removal of the nuts is a critical path activity and most sites can improve relining speed by simply adding additional impact wrenches or replacing unreliable old units.
- Oxy-fuel cutting equipment for stuck nut removal – unfortunately it is common practise for sites to be forced into cutting the nuts off if they cannot be removed by an impact wrench. Sites often benefit from having multiple kits available to avoid the time delay in transporting one unit around the mill during a reline. Due to the slow speed and hot work risks of oxy cutting the nuts, and delays moving the equipment, it is the authors' opinion that it is better to engage a specialist to eliminate the root cause of nuts becoming seized to reduce reline time.

Table 2 – Comparison of knock-in methods

Hammer/ram type	Benefits	Challenges
Sledgehammers	<ul style="list-style-type: none"> • An overhead swing with good technique can deliver up to 200 Joules of blow energy 2-5 seconds. • Multiple reline personnel can use sledgehammers in the same area. • Low cost. • Can access bolts in hard to reach places – with lower power. 	<ul style="list-style-type: none"> • It is common for reline personnel to experience minor injuries to hands and repetitive strain injuries. • The rate and power in sledgehammer blows reduces noticeably as the crew becomes tired during a shift. • It can be difficult to swing a sledgehammer when there is other equipment nearby – blow energy is often limited to less than 100 Joules. • Not very effective against stuck bolts due to low blow energy. • Unable to knock-in liners onto the charge. • At high altitudes reline personnel will experience fatigue due to the lack of oxygen.
Battering ram suspended by crane	<ul style="list-style-type: none"> • Can deliver 300-600 Joules of blow energy every 10-20 seconds. 	<ul style="list-style-type: none"> • Often relies on the use of an overhead crane, which can be busy with other tasks during a reline. This leads to delays while the crew waits for the crane to arrive. • Cannot be used on bolts close to the ground. • It is difficult to aim, and can damage the mill shell over time. • Requires careful management of risk. • Requires a large operating area around the mill.
Hydraulic recoilless hammers	<ul style="list-style-type: none"> • Can deliver between 750-2000 Joules of blow energy at speeds of one blow every 0.5-1 seconds. • Delivers same blow energy regardless of the bolt position. • Can be used to knock-in the bolts, and also the liners. 	<ul style="list-style-type: none"> • Requires multiple reline crew members to operate safely. • Works best with a suspension system that is designed specifically to suit the application. • Requires space around the mill to manoeuvre into position for each bolt.

In general, it is recommended that the plant design accommodates hydraulic recoilless hammers on all zones of the mill (feed, shell and discharge) as seen in Figure 10. This will ensure that the site is able to relocate recoilless hammers to any the zone of the mill when a stuck bolt or liner is encountered. On several recent new projects supported by RME, this assessment of the hammer working zones has required the following plant design changes:

- Changing the mill drive configuration to be ‘outboard’ to create space for the recoilless hammers to operate on both sides of the mill (refer to the separate section below on relining on both sides)
- Extending the floor adjacent to the mill to provide between 3-3.5 meters of flat working area for the crew operating the recoilless hammers (often there is an uneven floor in this area caused by the mill concrete plinths)

- Repositioning pipework, valve banks and electrical control panels away from the recoilless hammer's operating zones
- Repositioning of columns near the feed end of the mill for supporting the overhead access for the feed conveyors and feed chute inspection points
- Repositioning the columns for the monorail system to avoid clashes with the recoilless hammers during operation

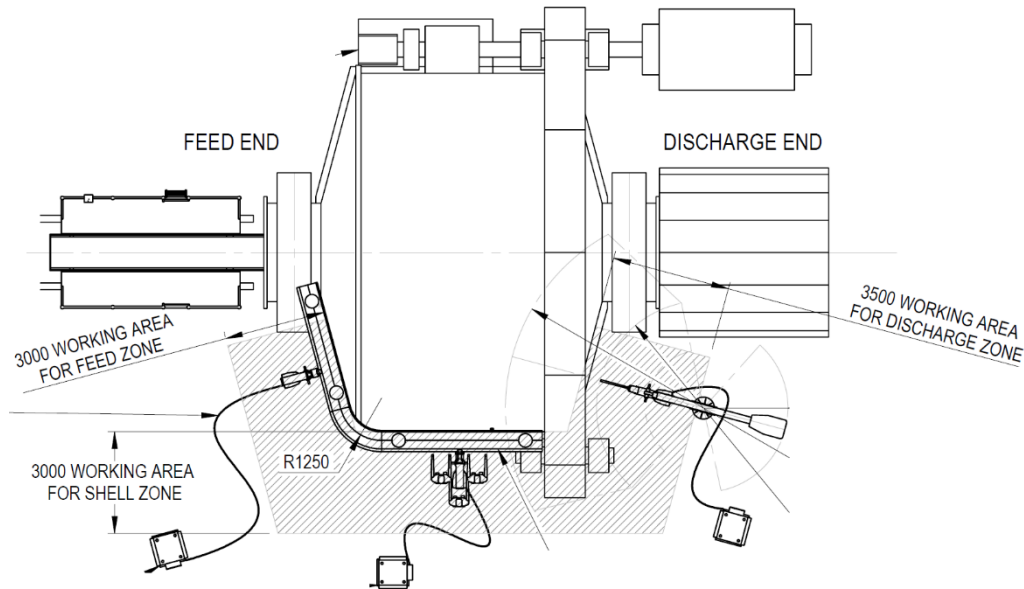


Figure 10 – Working area to operate hydraulic recoilless hammers on a SAG mill with mill drive on one side

Separate from the recoilless hammer itself, the selection of the hammer suspension equipment can impact the plant layout. There are broadly three options: overhead crane, monorails and jibs. In practise, the optimal suspension system is usually a combination of monorails and jibs on different zones of a mill.

- **Overhead crane:** An overhead crane is typically selected for convenience because it is already factored into the plant design, but it comes with major limitations to the relining process. It prevents the use of multiple hammers and introduces a 'wait time' delay into almost every knock-in phase, as the overhead crane is used for other maintenance activities. It is therefore not recommended to use an overhead crane for recoilless hammer suspension.
- **Monorails:** Monorails are selected because they allow the hammer to be quickly repositioned between bolts on a long section of mill shell. Twin tube monorails have a second smaller tube to support the impact wrench and other tools to further improve relining ergonomics. An important design consideration with monorails is that the performance of the recoilless hammer also depends on the hammer having sufficient preload against the bolt, which is a function of gravity and the hanging angle of the hammer from the monorail. Since monorails are a fixed structure, it is critical that during the plant design process the monorails be positioned specifically to suit the mill and plant geometry to achieve the required design preloads for all bolt positions. Failure to consider this when positioning the monorails can lead to poor hammer performance, crew fatigue and increase risk of hammer damage from dry firing.

- **Jib cranes:** Jibs that are specifically designed for recoilless hammer suspension are typically the most flexible option from a plant designer’s perspective, and in most cases deliver performance that is equal to or superior to monorails. To achieve optimal hammer preload the jib can telescope the boom forward and backward as the bolt is knocked-in. Recoilless hammers will often have on-board controls to control the jib’s telescoping function. The position of the jib within the plant layout needs to be assessed at an early stage. A mobile jib can be lifted into place with an overhead crane and will have a larger baseplate footprint for stabilisation. A fixed jib on the other hand, while having a smaller baseplate, will demand more attention to the swing angles during plant design to ensure it does not clash with adjacent columns.
 - The only exception where monorails are superior to jibs are typically long ball mill shell zones.

Dual vs single-sided relining

Dual-sided or single-sided relining is an important consideration that needs to be evaluated during the design phase of a plant. Dual-sided relining has the potential to drastically reduce overall relining time by achieving two main goals. The first is by directly reducing the overall inching time by reducing the number of inches required, which can be a saving of between 20-60 minutes per inch. The second is that dual-sided relining enables more activities to be completed in parallel (e.g. knock-in and bolt torque-up can be completed on both sides simultaneously). In order to realise the full benefit, dual-sided relining requires the appropriate recoilless hammer selection and sufficient additional hammers in each zone. The mill drive type (geared vs gearless) and location is almost always the key deciding factor if dual-sided relining is possible. If dual-sided relining is selected, the knock-in and suspension system that has been selected for the mill will typically be replicated or mirrored on both sides of the mill.

Broadly speaking there are two main drive methods of a grinding mill, a Ring Gear Drive (RGD) and a Gearless Motor Drive (GMD). In Figure 11, a GMD and common RGDs configurations are shown which consisting of the ring gear, a motor and sometimes a gearbox configuration, this is known as the driveline.

With RGD mills the driveline can be placed either inboard or outboard of the grinding mill. Inboard implying the driveline is located next to the mill shell, whereas an outboard-located driveline sits ‘past’ the mill’s feed or discharge end. A GMD can be placed on the feed or discharge end of a mill shell.

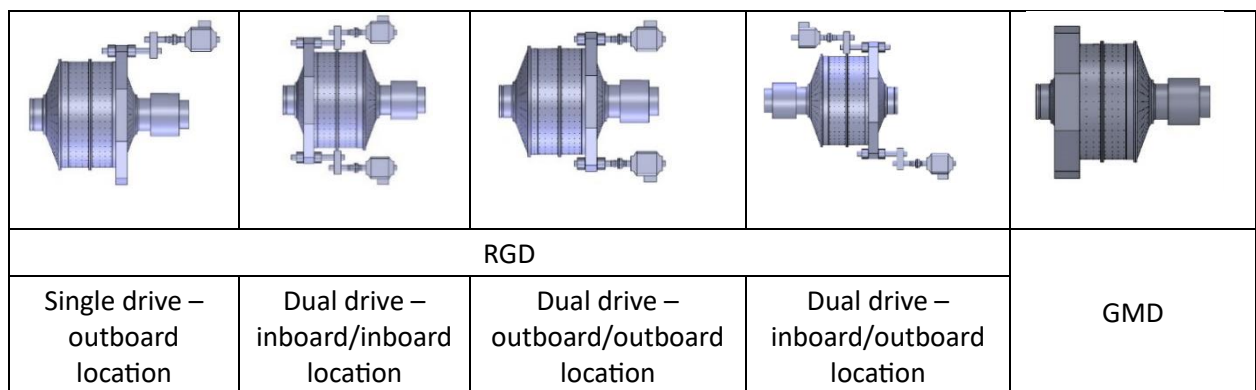


Figure 11 – Drive configurations

In the case of RGDs, if the drivelines are located outboard, then dual-sided relining is possible. However, as covered in the preceding section, specific consideration will be needed for the suspension method. If, however, an inboard driveline location is selected, dual-sided relining will not be possible due to the lack of access to the mill shell on the side where the drive is located. It must be noted a dual drive with an inboard/inboard driveline configuration is a poor layout and will significantly impact relining performance and safety due to its tight spaces and ergonomic aspects, refer to Table 3.

GMDs offer the most space to easily perform dual-sided relining, due to the wrap-around-motor style of the drive without the need for reduction gearboxes, large electric drive motors and inching drives.

Table 3 – Summary of how RGD type affects relining access

RGD type	Inboard configuration	Outboard configuration	Dual In/Outboard config.
Single Drive	Single-sided relining is possible. Dual-sided relining would involve compromises and working at height.	Both dual- and single-sided relining is possible.	NA
Dual Drive	Both dual- and single-sided relining would involve compromises and working at height.	Both dual- and single sided relining is possible.	Single-sided relining is possible. Dual-sided relining would involve compromises and working at height.

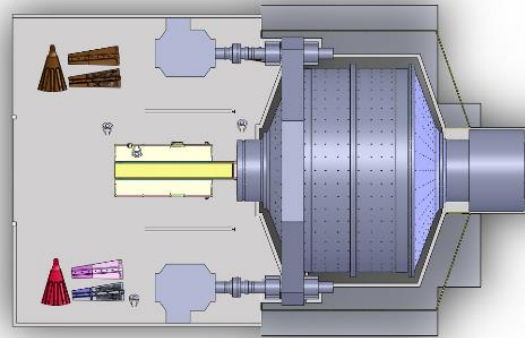
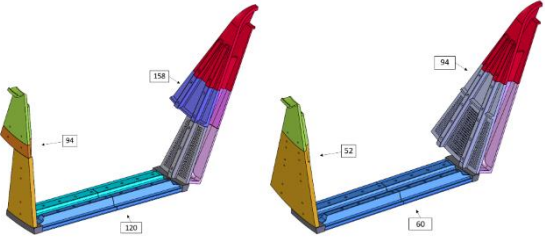
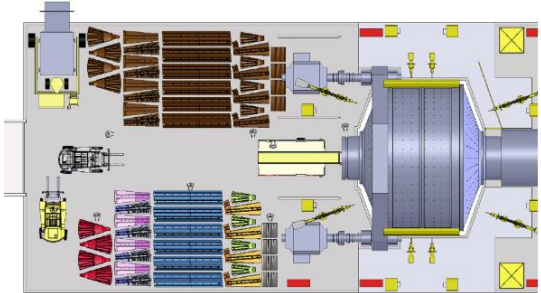
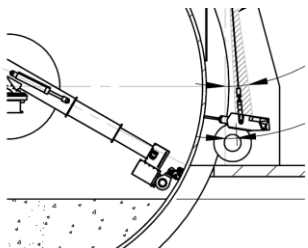
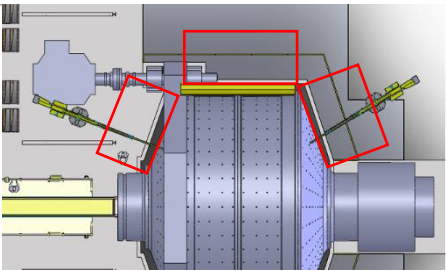
CASE STUDY

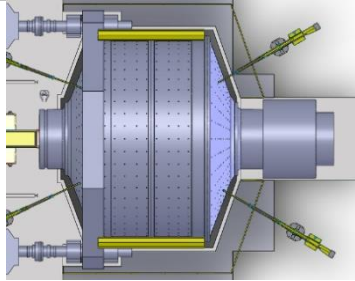
It can be difficult to quantify the impact of plant design changes on the speed of mill relining and maintenance. However, RME has developed in-house discrete event simulation technology for mill relining trade-off studies called MILL RELINE DIRECTOR (MRD). In order to quantify the mill availability benefits of each of the recommendations in this paper, a 36ft X 21ft SAG mill was analysed using typical industry performance data as captured by RME.

MRD Model Scenarios

Calculating annual mill availability assumes typical industry values for liner life. A high wear reline scope is assumed to include replacement of shell liners, grates, outer feed end and occurs every six months. A full scope reline includes additional liners such as filler rings, mid plates on discharge and feed end are replaced every 12 months, while pulp lifters and dischargers are replaced every 24 months. Table 4 summarises each plant design improvement scenario as discussed earlier.

Table 4 – Scenarios considered for 36ft SAG mill case study

Scenario	Description	Reference Image
Reference Case	<ul style="list-style-type: none"> • Undersized mill deck design • Crane for liner supply to deck • Sledgehammers • Poorly optimised deck height – extra inches required • 2500 kg mill relining machine capacity • Slow to remove feed chute and install mill relining machine 	
Scenario 1 Small mill deck with reduced liner quantity	<p>Same as Reference Case with the following changes:</p> <ul style="list-style-type: none"> • Increased mill relining machine capacity from 2500 kg to 6000 kg • Liner piece count reduced from 372 to 206 pieces 	
Scenario 2 Optimised deck size and liner supply system	<p>Same as Scenario 1 with the following changes:</p> <ul style="list-style-type: none"> • Optimised mill deck size • Ramp access to deck • Forklifts for liner supply to deck • Normal speed to remove feed chute and install mill relining machine due to space 	
Scenario 3 Optimised mill deck platform heights	<p>Same as Scenario 2 with the following changes:</p> <ul style="list-style-type: none"> • Mill deck height position optimised compared to charge levels during relining 	
Scenario 4 Single-sided knock-in equipment	<p>Same as Scenario 3 with the following changes:</p> <ul style="list-style-type: none"> • Added recoilless hydraulic hammers on one side with sufficient space to operate • Jib and monorails for hammer suspension on each zone 	

Scenario	Description	Reference Image
Scenario 5 Dual-sided knock-in equipment	Same as Scenario 4 with the following changes: <ul style="list-style-type: none"> • Added recoilless hydraulic hammers on both sides with sufficient space to operate • Mirrored suspension solutions onto both sides of the mill 	

Results and discussions

Figure 12 demonstrates the annual mill availability benefits associated with each plant design improvement scenario for the case study 36 ft X 21 ft SAG mill. These benefits are the result of optimised relining as shown in Table 4. Each scenario improves mill availability from between 0.6% to 0.3%, leading to a combined improvement that reduces annual downtime lost to relining from 3.7% to only 1.5%. This equates to a 60% reduction in annual reline time.

Globally, there are 73 x 36 ft SAG mills operating. The average value of the contained metal produced from these mills is US\$80 000 /h according to current London Metal Exchange (LME) pricing. Implementing all of the recommendations in this paper mill would lead to an additional US\$15 M of metal production per annum (\$80 k x 190 hours) for the average 36 ft SAG mill. This assumes that all of the additional mill availability from faster relining can be converted to mill utilisation, which is site dependent.

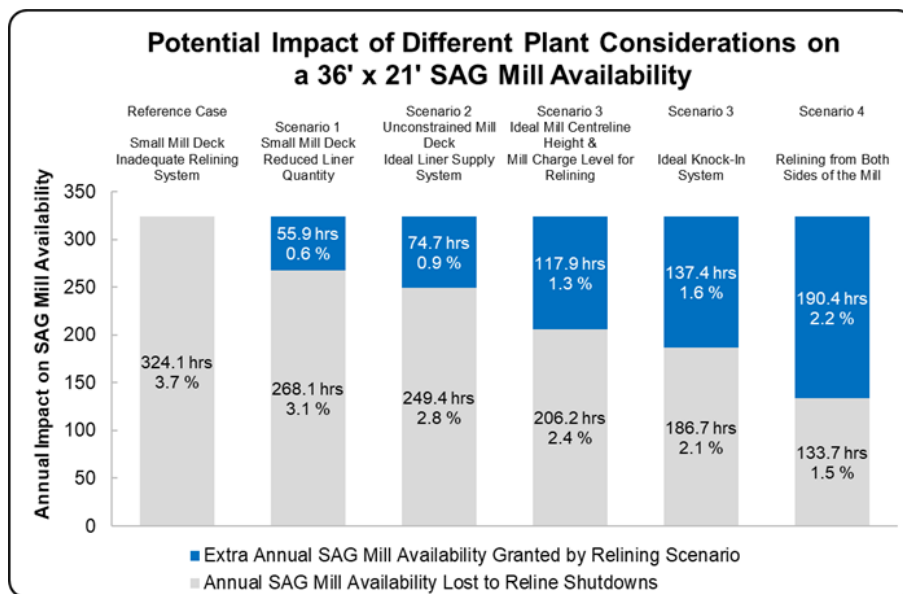


Figure 12 – Comparison of scenario results

Improving relining performance will also deliver safety benefits due to reduced relining duration. Considering relining duration and the number of relining crew members, a person-hour risk exposure value can be calculated per scenario. Each plant design improvement scenario had an impact on the person-hour risk exposure time as seen in Figure 13.

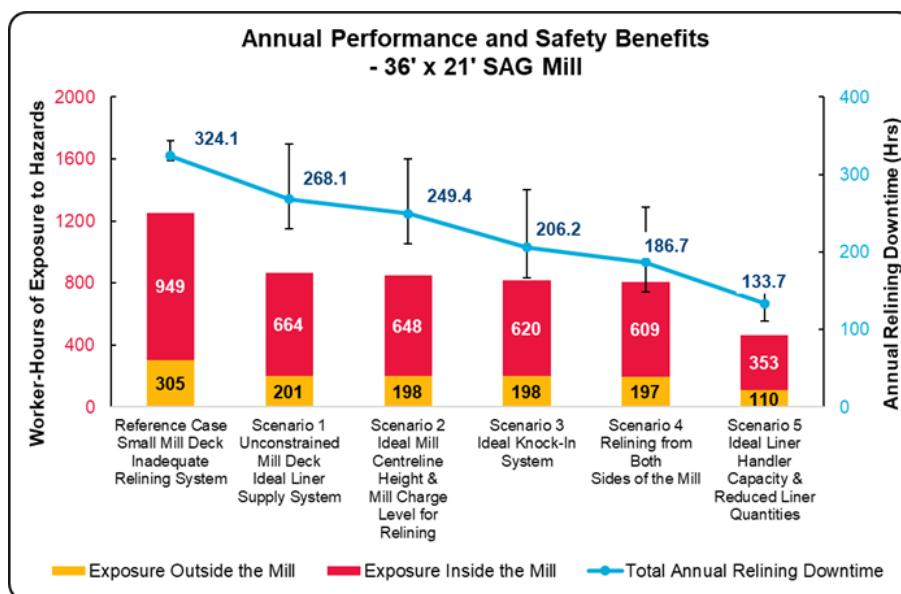


Figure 13 – Comparison of worker-hour exposure scenarios

In order to unlock additional mill availability, production and reduced person-hour risk exposure time, it is imperative that plant design factors for optimised relining are considered during project pre-feasibility stage when CAPEX estimates are being established. This provides the opportunity for a trade-off study like the one presented in this report. RME can assist with project-specific trade-off studies.

CONCLUSION

This paper has provided an overview of the benefits of designing a grinding plant for relining. By implementing the recommendations in this paper, a case study on a 36 ft SAG mill found it could be possible to increase mill availability by up to 2.2%, which translates to 190 h/y. Based on an average value of processed metal of US\$80 000 /h, this yields an increase in production value of up to US\$15 000 000 /y. The person-hour exposure time is also improved by 271% or 791 h/y.

The authors recommend that during the pre-feasibility phase of a concentrator project, the plant design factors that impact relining are considered, and a total cost of ownership analysis is performed to understand how relining performance directly impacts mill availability and the associated mill value per annum. RME can be engaged to provide quantitative analysis services using discrete event simulation to assist with trade-off studies. In this paper's appendix, a plant design checklist has been developed to assist engineers consider these aspects of relining.

REFERENCES

- Smith D. (2008) 'Designing and Planning For Maximum Grinding Mill Availability – A Team Approach' MetPlant Conference, Perth, Australia
- Powell M., Yahyaei M., Geronimo J., Yussupova Z., Kumar P. (2018) 'The Designed Approach to Mill Liner Optimisation – Experience at Pustynnoye Mine, Kazakhstan' Mill Operators' Conference 2018, Brisbane, Australia
- Faulkner C., Lozovoy N., Kumar S., Lee J. (2019) 'Increased Throughput from Liner Design Initiatives in the Aktogay 40 ft. SAG Mill' SAG 2019 conference, Vancouver, Canada

Taghimohammadi M., Grignon J., Sherman M., Virani I. (2019) 'Continuous Improvement in SAG Mill Liner Design to Increase Hard Rock Throughput' SAG 2019 conference, Vancouver, Canada

Coker R. (2007) 'Productivity Gains Through Faster and Safer Mill Relining Technologies and Methods' Crushing and Grinding Conference

Weidenbach M., Baade B., Seppelt J., Lane G., Stephenson D. (2019) 'Grinding Circuit Design for the Carrapateena Concentrator' MetPlant Conference, Perth, Australia

Radford R., Lovatt I., Putland B., Becker M. (2021) 'Gruyere Gold Project Western Australia, part 1 – from design to commissioning' Mill Operators' Conference, Brisbane, Australia

Bohorquez J., Gwynn-Jones S. (2021) 'The Knock-in Effect – Quantifying the Knock-in Effect of THUNDERBOLT MAGNUM Recoilless Hammer technology on reline duration and mill availability.' RUSSELL MINERAL EQUIPMENT whitepaper

Rubie P., Russell J., O'Shannassy G., Yap F. (2015) 'Simulation as a Tool to Enable World's Best Relining Practice – A Sense-making Tool for Decision Makers' SAG 2015 conference, Vancouver, Canada

APPENDIX

The checklist in Table 5 is included to assist plant designers and mine owners in auditing the suitability of a plant's design to maximise mill availability through efficient relining.

Table 5 – Plant design for relining checklist

Topic	Areas to Inspect	Notes/Tips
MILL DECK LAYOUT AND STRUCTURE	<ul style="list-style-type: none"> • Efficient installation and removal of mill relining machine. • Efficient extraction and storage of feed chute with a feed chute transporter. • Space for liner laydown for one inch of new and worn liners. • Space for other equipment and maintenance activities to take place. • Understand which, if any liners, either new or worn, can be stacked on the deck. • If the machine must reach multiple mills, then ensure there is space to reach each mill. 	<ul style="list-style-type: none"> • Request proposal drawings of feed chute transporter and mill relining machine highlighting overall dimensions and trajectory requirements. • Ensure structural columns do not impede trajectory. • Understand floor loading limits for transport and liner storage.
FEED CHUTE REMOVAL	<ul style="list-style-type: none"> • Chocked capacity of feed chute is significantly greater than that of the empty and nominally full chute, this impacts the feed chute removal process • Feed chute base structure needs to accommodate transporter pickup points 	<ul style="list-style-type: none"> • Often feed chutes require their own maintenance, implying the chutes should be stored in areas well clear of mill relining activities.
LINER SUPPLY SYSTEM	<ul style="list-style-type: none"> • The size of the mill and largest scope relines dictate how much space is needed for liner lay, this directly impacts the liner supply system. • Can a ramp be installed to access the mill deck? • What other maintenance activities can benefit from a ramp? 	<ul style="list-style-type: none"> • A lower piece count of liners can sometimes be less dependent on costly ramps. • Understanding the average liner delivery rate onto and off the deck.
RELINING PLATFORM HEIGHTS AND CHARGE LEVELS	<ul style="list-style-type: none"> • What is the expected charge level of the mill and what is the client strategy around grinding out? • Can the mill position with a mill centreline height that aligns the relining platform with the charge level? • How many liners or row of bolts can be reached both inside and outside the mill? As this will influence the total number of inches required per reline. 	<ul style="list-style-type: none"> • Mills that are too low are also problematic for items such as feed chutes. • Mills that are too high are problematic for mill relining machines. • Inching cycles are time consuming activities and should ideally be kept to a minimum per reline.

Topic	Areas to Inspect	Notes/Tips
KNOCK-IN SYSTEM	<ul style="list-style-type: none"> • Are hammers and ancillaries selected to suit bolt difficulty and sizing to prioritise speed or power? • What drive type has been selected? • What is the mass of the liners? • Does the client expect excessive peening of the liners? • Have special tools been selected to assist with the worn liner removal process? 	<ul style="list-style-type: none"> • Different suspension systems are better suited to various drive types. • Ensure the hammers are able to provide sufficient power and momentum for break-in.
DUAL-SIDED RELINING VS SINGLE-SIDED RELINING	<ul style="list-style-type: none"> • What is the intended drive type and where the driveline will be positioned? • Is there space on both sides of the mill to install knock-in and suspension equipment? • Dual-sided relining may require increased mill deck space due to increased demand in liners per inch. 	<ul style="list-style-type: none"> • If there is more than one mill on the mill deck, ensure they have sufficient space between them for concurrent relines.
LINER OPTIMISATION	<ul style="list-style-type: none"> • Reducing liner count to improve reline speeds result in heavier larger liners, requiring higher capacity mill relining machines – which can feedback into plant design through forklift capacity, deck size requirements and structural loadings. • To future-proof the mill relining machine selection, it is prudent to assume liners will be manufactured from steel and not always in a poly-met form. 	<ul style="list-style-type: none"> • The mill relining deck to charge level becomes increasingly important as larger liners require a greater reach.

Unlocking Increased Paste Production at Prominent Hill through Debottlenecking of the Belt Filter

N Curtis¹, O Whatnall², S Wilson³, J Sum⁴ and C Samuel⁵

1. Metallurgist- Paste Fill, BHP, 2 Harma Drive, nicole.curtis1@bhp.com
2. General Manager, Jord International Inc., Denver, CO, owhatnall@jord.com.au
3. Mechanical Engineer, Jord International, 63 Knutsford Avenue, swilson@jord.com.au
4. Metallurgy Superintendent, BHP, 2 Harma Drive, jo.sum@bhp.com
5. Aftermarket & Reliability Engineer, Jord International, St Leonards, NSW, csamuel@jord.com.au

ABSTRACT

The Prominent Hill copper-gold concentrator treats a combination of open pit and underground ore. As the open pit ore reserves deplete, Prominent Hill is undergoing the Wira Shaft Expansion Project, targeted at increasing the capacity of its underground mine. With this expansion, there is an increased demand for paste to fill underground voids. In 2020, the Malu Paste Plant (MPP) was commissioned with the intent of increasing paste production to meet current and future demand by upgrading the existing cemented hydraulic fill plant (CHF).

The new belt filter, a major component in the process flow at the MPP, was identified as a significant bottleneck to achieving increased paste production.

This paper discusses the identification of the limitations associated with the belt filter and details the subsequent design modifications and implementation of solutions which have put the MPP on track to meet current and future demands of the underground mine. Data is presented to quantify the outcomes which include a marked increase in throughput and improved process control, leading to enhanced autonomous operation of the MPP.

INTRODUCTION

To facilitate the expansion of the Malu underground mine at Prominent Hill, an upgrade of the existing cemented hydraulic fill (CHF) to the Malu Paste Plant (MPP) was required. The design intent of this upgrade was to increase reliability of paste and overall production rates from an average of 125 m³/h to design of 215 m³/h at 60% utilisation. The MPP flow sheet (shown in Figure) consists of the CHF cyclone circuit, with the addition of a belt filter, paste mixer and upgraded binder system. Plant tailings are deslimed through hydrocyclones then dewatered by the belt filter. The filter cake is mixed in the paste mixer with water, non-classified tailings and binder to produce the optimum blend required to fill a particular void underground.

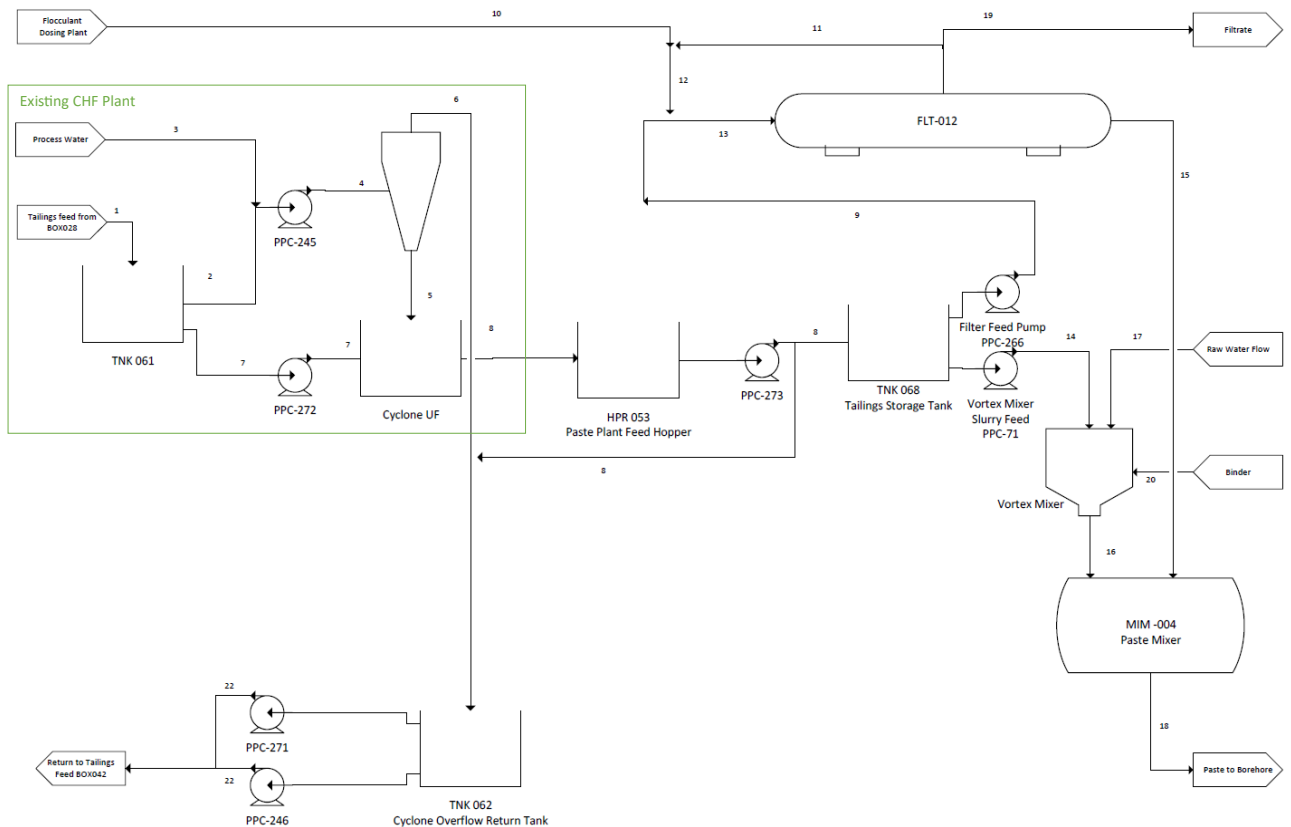


Figure 1: Malu Paste Plant process flow diagram

The MPP is a batch operation where both production rate and utilisation are critical in meeting the mine production targets. When the MPP was commissioned in 2020 it was not able to sustain production rates of 215 m³/h at 60% utilisation. The inability to achieve these targets resulted from a combination of unplanned downtime and process instability.

Analysis of the MPP conducted in 2021 determined that the belt filter was the cause of the reduced production rate and the major cause of downtime and process instability. With the expertise of Jord International (Jord), three upgrades were identified which collectively improved utilisation, process stability and production rate. These upgrades involved replacing the original feed distributor with a two-stage feed system, redesign of the wear plate throat and increased seal belt water.

This paper provides a brief overview of the belt filter, followed by an explanation of each of the bottlenecks and their corresponding rectification proposed by Jord. Finally, it details the improvements in the belt filter performance since the implementation of these upgrades.

BELT FILTER – OVERVIEW

The belt filter is a horizontal vacuum filter designed for continuous operation of high-capacity filtration. The filtration area of the belt is 4.25 m wide and 36 m long with a total area of 156 m². There are five major components that make up the belt filter: feed slurry distributor, filter cloth, carrier belt, vacuum box and a large number of rollers of differing functions. These components are highlighted in Figure 2.



Figure 2: Belt Filter

Brief Functional Description

Slurry is fed onto the horizontal vacuum belt filter at the tail end through the feed slurry distributor, onto a filter cloth which separates the solids while allowing liquid to pass. An endless carrier belt, with curbing on both sides to contain slurry, supports the cloth that rests on top of it. To help encourage even flow across the width of the filter cloth a rubber plate is used after the feed distributor to form a dam of slurry on the filter cloth. Density, volumetric flow of the slurry and belt speed determine the height of the feed dam. These parameters are controlled to ensure an adequate feed dam level is maintained. A high-level event will allow slurry to spill over the sides of the carrier belt onto rollers and ancillary belt filter components.

Grooves across the width of the carrier belt allow filtrate to flow under the cloth towards a row of holes on the side of the belt. The holes align with a side mounted vacuum box through which a vacuum is applied. It is important that these holes align with the vacuum box to ensure consistent vacuum pressure, allowing for uniform drying of the filter cake. Misalignment of these holes can cause process instability due to changes in moisture content of the filter cake.

An effective vacuum is achieved by a seal between the stationary vacuum box and the moving carrier belt via a pair of seal belts, one on each side of the filtrate holes. Seal belts slide over replaceable plastic wear plates as they are drawn along by the carrier belt. Water is pumped through the wear plates, lubricating and cooling the seal belts. Insufficient water can lead to high friction between the carrier belt and the vacuum box. This can cause belt filter breakdowns when this friction forces the carrier belt to track to one side or if the seal belts melt from the increased temperature caused by the friction.

TWO-STAGE FEED SYSTEM UPGRADE

Bottleneck

The original feed system was identified as a bottleneck in both production and utilisation. It allowed feed to flow from a single inlet into a feed pot which distributed the feed through four mining hoses and into the feed distributor onto the cloth. A combination of the feed travelling at a high velocity, 90-degree bends and unlined pipework in this part of the circuit, led to increased wear. The wear and subsequent buildup of material led to warping of the metal distributor and uneven distribution

of the feed. This resulted in variations in the cake thickness leading to process instability as well as downtime due to wear in the feed system.

The original feed system had a rubber plate installed to create a feed dam with the intent of better distributing the feed across the cloth. This feed dam became a bottleneck and restricted the belt filter production rate. At steady state operation during 2021, with the design feed density of 55% solids and a filter feed of 240 m³/h (389 t/h) the dam would consistently overflow. The image in **Error! Reference source not found.** illustrates a high feed dam event. It was observed that spillage over the side of the carrier belt was resulting in increased roller failures which at the time was contributing to 16% of the belt filter downtime.



Figure 3: High feed dam level

To reduce spillage, a minimum feed density of 58% solids was targeted giving a maximum maintainable filter feed flow rate of 240 m³/h (400 t/h). At these rates the feed dam operated just below the spillage limit. Though the feed dam was high, it was evident by cracking of the filter cake at the discharge of the belt that the filter would have greater filtration capacity if more feed was available. By restricting feed density and consequently the throughput to the belt filter for improved utilisation, the belt filter dam level became a constraint on overall plant production rate.

Rectification

Jord's standard feed system depicted in Figure 4 was retrofitted onto the current belt filter at the MPP. The new system reduced the velocity in the feed pipework by splitting it in two with a sacrificial y-joint. These two streams are then distributed into four separate feed chambers. Two feed chambers are directed forward and the other two backwards, towards the feed dam, reducing the volumetric flow to the dam by 50%. Since the upgrade of the feed system there has not been a high feed dam event, the filter cake has been well distributed across the filter and, due to the robust design, very little wear has been observed.



Figure 4: Two-Stage Feed System

WEAR PLATE REDESIGN

Bottleneck

For effective drying of the filter cake and consistent vacuum pressure, alignment of the filtrate holes in the carrier belt with the vacuum box is necessary to ensure there is a pathway for the filtrate to flow through the seal belt system into the vacuum box. There was a tight tolerance in the wear plate throat on the original wear plates resulting in regular misalignment between the filtrate holes and the vacuum box, particularly during minor process upsets and start-ups. Without this path for filtrate to flow, the slurry on the cloth didn't dewater, causing variations in filter cake moisture, impacting process stability.

Rectification

A complete redesign of the wear plates was conducted to increase the size of the throat to ensure the filtrate holes in the carrier belt consistently aligned with the vacuum box. As part of the upgrade, the entire seal belt and vacuum box system underwent a comprehensive overhaul, this included replacing all the components in the seal belt system and re-leveling the vacuum box. After the implementation of this upgrade the carrier belt holes operate in constant alignment with the vacuum box, improving filter cake consistency and eliminating this process instability.

SEAL BELT WATER RECTIFICATION

Bottleneck

Typical industry flowrates for seal water for a horizontal belt filter of this size are in the range of 400-600 L/min, depending on the belt speed. The original seal belt flowrate was 12 L/min which is an order of magnitude lower than industry standard. Jord observed that this low water input was

causing carrier belt tracking and seal belt failure which were two of the main reasons for the unplanned belt filter downtime.

The MPP carrier belt would regularly track towards the vacuum box side of the filter and ride over the guide rollers. These events would occur without notice and cause a substantial amount of downtime as the process to track the 4.25 m rubber belt back in place was exceedingly difficult. Belt tracking during operation was caused by high friction between the carrier belt and the vacuum box due to poor performance from the seal belt system.

Seal belts must be well supplied with seal water for lubrication and cooling. Without sufficient water, friction melts the plastic of the wear plate and shreds the rubber and fabric of the seal belt. Shreds of melted material then start to block the seal water galleries, further reducing supply and increasing friction. MPP seal belts were consistently undersupplied with seal water and experienced regular failures.

Rectification

The low seal belt water flow was rectified by increasing the flow to 485 L/min. To facilitate these changes and ensure adequate distribution of the increased water flow, extra water addition points were added to the wear plates and the feed pump impeller was upgraded to meet the new demand. The increased water has ensured the seal belt system is consistently lubricated and cooled, resulting in the extended life of the seal belts. These were historically changed on average every two months and now have not been replaced since the water increase in October 2022. The carrier belt performance has also benefited from ample lubrication and there have been no reported tracking events since the upgrade.

RESULTS

Since the implementation of all three upgrades, there has been a significant improvement in the overall operation of the belt filter. The redirection of half the feed via the two-stage feed system has successfully prevented the feed dam overflowing. Additionally, the increased water to the seal belt system has eliminated belt tracking issues and extended seal belt life. Furthermore, the large wear plate throat has improved belt alignment, leading to enhanced process stability.

The upgrades have enabled a marked improvement in production rates and utilisation of the belt filter. As highlighted in Table , there has been a 40 m³/h increase of the filter feed flowrate and a reduction of 17 hours per month of unplanned downtime. There has also been an observed improvement in process stability with consistent filter cake thickness and moisture.

Table 1: Belt Filter Improvements

	Before upgrades	After upgrades	%Diff
Belt Filter Volumetric Flow [m ³ /h]	240	280	17%
Belt Filter Downtime [h/month]	24	7	-243%

CONCLUSIONS

Prominent Hill has successfully unlocked increased paste production at the MPP by debottlenecking the belt filter. Through identification of the belt filter bottlenecks and execution of subsequent design modifications the MPP has seen an increase in belt filter production, enhanced process stability and a reduction in downtime. Debottlenecking the belt filter has put the MPP on track to meet the current and future demands of the underground mine.

ACKNOWLEDGEMENTS

The authors would like to thank BHP and Jord International for permission to publish this paper.

A special acknowledgement is made to the many people who contributed to the successful troubleshooting, optimisation and execution of the MPP upgrades including the Prominent Hill Engineering and Maintenance teams, Baylev, Paul Von Stanke, Stephen Viney and Jord International.

Concentrate Filter Cake Washing for Chloride Removal at Carrapateena

R Jones¹, J Reinhold², K Affleck³ and F Burns⁴

1. Senior Metallurgist - Projects, BHP Carrapateena, Pernatty, South Australia, 5173. Email: rhys.jones@bhp.com
2. Senior Metallurgist - Plant, BHP Carrapateena, Pernatty, South Australia, 5173. Email: jacqueline.reinhold@bhp.com
3. Metallurgist - Plant, BHP Carrapateena, Pernatty, South Australia, 5173. Email: kathryn.affleck@bhp.com
4. Superintendent - Metallurgy, BHP Carrapateena, Pernatty, South Australia, 5173. Email: fraser.burns@bhp.com

ABSTRACT

Carrapateena is an iron-oxide-copper-gold (IOCG) mine located in the Gawler Craton, South Australia, owned and operated by BHP. The ore is processed by a conventional sulfide flotation concentrator producing a copper silver gold (Cu-Au-Ag) concentrate. Ultrafine grinding of rougher concentrate to a 15-20 µm P80 target liberates deleterious non sulfide gangue (NSG) from sulfide minerals prior to cleaning. The resulting copper concentrate is thickened and reports to the concentrate filter, a Metso VPA 2040-32 filter press.

Raw water for use in the milling and flotation processes is sourced from borefields located within an 80km radius of the Carrapateena site. This water is hypersaline, containing >20,000ppm Chlorine (Cl). Fresh water, containing <500ppm Cl, is produced onsite from the bore water via an energy intensive reverse osmosis (RO) process.

Chlorides are present in the copper concentrate due to the use of the hypersaline process water. Chlorine is considered a deleterious element and is removed from the concentrate during filtration by washing the filter cake with fresh water. Cake washing occurs during a dedicated step in the filter cycle.

The as-commissioned filter press inconsistently achieved the required chloride removal, at the desired throughput rate. A key challenge was poor cake permeability imparted by its ultrafine particle size distribution.

This paper outlines the modifications to the filter press and its control strategies that were required to achieve satisfactory removal of chlorides, whilst minimising the volume of fresh water utilised, without compromising final cake moisture content, and maximising throughput.

INTRODUCTION

Carrapateena is a copper-gold deposit, located 460 km north of Adelaide in the Gawler Craton, South Australia. The deposit is currently mined using the sub-level cave (SLC) mining method, with future mining to transition to a block cave footprint beneath the SLC.

The copper mineralogy present at Carrapateena is chalcopyrite and bornite, hosted in an iron oxide breccia; and is typical of IOCG deposits also located in South Australia. A sulfide flotation concentrator produces a Cu-Au-Ag concentrate for sale to copper smelters. Construction of the concentrator was completed in late 2019, slurry commissioning began in Q4 2019 with the first concentrate produced and filtered in December the same year.

Effective operation of the dewatering processes at Carrapateena is essential to ensure final concentrate quality requirements are achieved.

Process water at Carrapateena is sourced from a borefield surrounding the mine and is hypersaline in nature, containing up to 70 000 ppm of dissolved chlorides. Washing of the filtered concentrate with lower chloride water is essential to decrease the chloride content of the wet cake from notionally 70 000 ppm chloride to below the concentrate specification for customers of 350 ppm chloride. Fresh water produced from a reverse osmosis plant, usually 500 ppm Cl, is utilised as the low chloride water source to displace the process water during a cake washing step thus improving the final concentrate cake quality.

Due to the nature of the Carrapateena operation utilising an offsite analytical laboratory, analytical results for the final cake quality would be delayed by 24 or 48 hours from production, resulting in reduced ability to respond to an increased Cl content. A vertical plate pressure filter (Metso VPA 2040-32 filter press) is employed to further dewater the thickened concentrate to produce the final saleable concentrate. Initial operation of the filter press yielded concentrates with chloride concentrations which exceeded the concentrate sales specification. A range of improvements were identified and implemented to further guarantee that the quality requirements are met. This paper discusses the improvements made to the operation of the filter to reduce the chloride content of the resulting filter cake.

PROCESS PLANT DESCRIPTION

Sub-level cave ore is primary crushed underground to nominal P80 of 100 mm. Primary crushed product is conveyed to the surface where it is stockpiled. The grinding circuit is a conventional Semi Autogenous And Ball Milling Circuit (SABC) that nominally produces a flotation feed at P80 of 75 μm at a rate of 500 t/h, since expanded to circa 700 t/h.

The flotation circuit commences with a roughing stage of five conventional float cells. Rougher tails report to the final tailings thickener. Rougher concentrate proceeds to the regrind circuit where a hydrocyclone pack cuts at a nominal 20 μm . Underflow proceeds to a single regrind High Intensity Grinding Mill (HIG) producing a nominal mill product size of 80% passing 20 μm with capacity down to 15 μm .

The regrind mill product, combined with the hydrocyclone overflow, feeds a Jameson Cell in a Cleaner Scalper duty. Cleaner Scalper concentrate reports directly to the final concentrate. Cleaner Scalper tailings proceed to numerous stages of conventional mechanical cleaning in Cleaner One, Cleaner One Scavenger, Cleaner Two and Cleaner Three Scavenger respectively. A Cleaner One Scavenger is operated in an open-circuit configuration, with tailings reporting to final tailings. Cleaners Two and Three Scavenger are operated in a closed-circuit configuration, with the tailings of each reporting back to the proceeding stage. The concentrate from Cleaner Two and Cleaner Three Scavenger feed an additional Jameson Cell, as Cleaner Three. The two Jameson concentrates combine to produce the final concentrate. The high slimes proportion, up to 35% present as sub 7 μm , a result of the fine grind, presents significant challenges for dewatering.

Flotation tailings are dewatered first by a high-rate thickener, to nominal density of 60% w/w solids. A pumping train transfers the thickened tailings slurry between 7.5 km and 11.8 km to sub-aerial discharge spigots within a dedicated tailing storage facility.

The copper concentrate is dewatered first by a high-rate thickener to nominal underflow density of 55% w/w. A concentrate storage tank provides 24-hour surge capacity between the thickener and filter press, a Metso VPA2040-32/40 vertical plate filter. The transportable moisture limit (TML) is

regularly monitored at approximately 11-12% moisture. Concentrate is hauled by road train to Whyalla for shipment of concentrate to customers.

Filter Press

The filter press, Metso VPA2040-32/40 vertical plate filter was initially installed as 32 plates with the capacity to expand as plant throughput increased. VPA stands for “Vertical Press Airblow” and refers to the compressed air filtration and drying used by the unit.

The filter consists of a rectangular frame formed by a fixed press head with a moving press head running along the side rails controlled by four hydraulic cylinders working in parallel. Moving filter chambers are located between the press heads. These chambers contain filter clothes on either side allowing for filtration on both sides of the chamber and are suspended from tubular supports. Spray water and motorised vibrators are used to wet and clean the cloths. A diagram with the major components is given in Figure 2.

Specifications for the filter feed, cake and operational specifications as determined by the OEM and supplier are provided in Tables 1, 2 and 3.

Table 1: Filter Feed Solution Specifications As Per The Supplier Process Design Criteria And Concentrate Filter Data Sheet

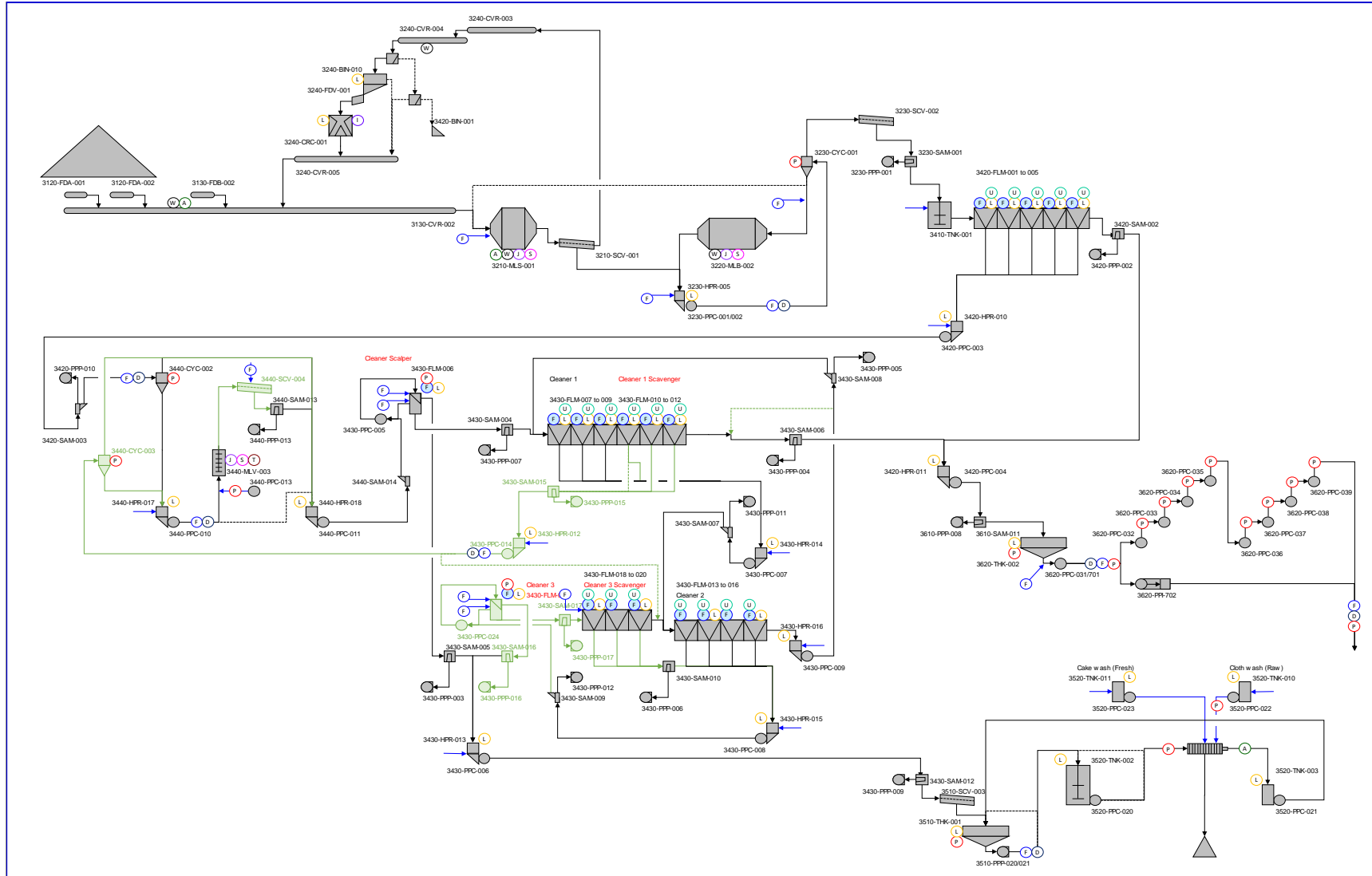
Variable	Filter Feed Specifications
Percent Solids (% w/w)	65
Particle Size P80 (µm)	20
Feed Chloride Concentration (ppm)	51 000

Table 2: Filter Cake Specifications As Per Supplier Issued Process Design Criteria And Concentrate Filter Data Sheet

Variable	Filter Cake Specifications
Cake Moisture Design (%)	8.9
Total Moisture Limit (%)	11.6
Maximum Wet Cake Chloride Concentration (ppm)	300

Table 3: Filter Specifications As Per The Supplier Process Design Criteria And Concentrate Filter Calculations

Variable	Filter Operational Specifications
Specific Throughput Rate (dmt/h)	52.4
Cycle Time (min)	12.3
Tonnes Per Cycle (dmt)	10.76
Fresh Water Ratio Usage (m ³ /dmt)	0.8



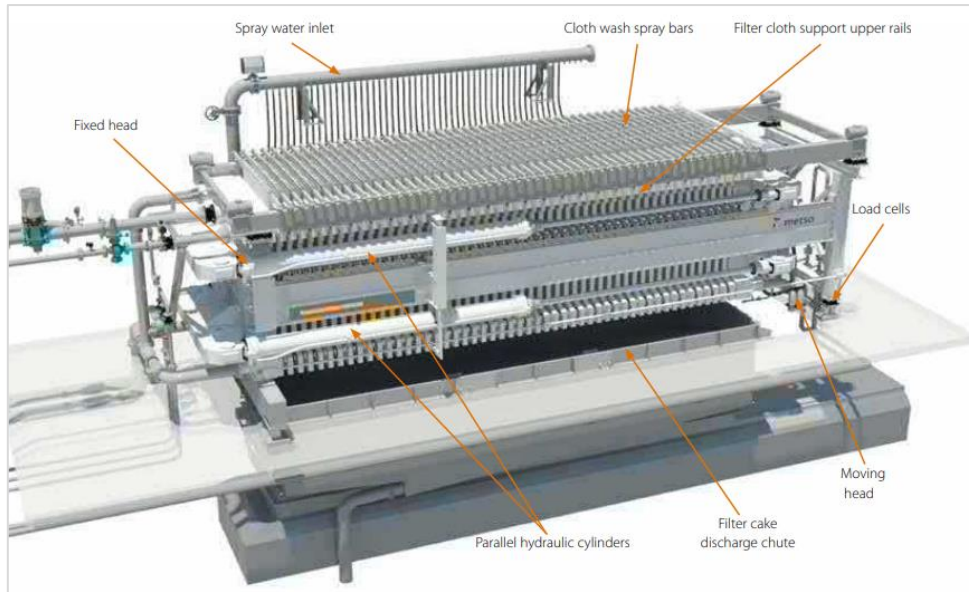


Figure 2: Metso VPA filter press major components.

Borefield and RO Plant

Water for Carrapateena is sourced from two borefields; northern and radial. The bore water is hypersaline, and the quality varies greatly between the two sources. The water from the northern borefield is used as process water in the milling and flotation circuits because of the high chloride and total dissolved solids content. Water from the dewatering process and the decant return from the tailing's storage facility top up the process water. Water from the radial borefield is used to feed the Reverse Osmosis (RO) plant as its of higher quality than the northern borefield. Water composition of all these streams is included in Table 4.

The RO Plant for the Carrapateena project was designed to produce up to 1310 m³/d of potable water. The plant was designed by MAK Water and includes ultrafiltration pre-treatment, followed by reverse osmosis to remove dissolved minerals. Chloride is added to the potable water to meet drinking water requirements. The potable water is left unchlorinated for use in reagent make up, cooling water systems, safety shower systems and in the filter. The fresh water produced contains less than 500 ppm of dissolved chlorides.

Table 4: Water composition as sampled in 2020.

	Process Stream	Process Water	Northern Borefield Water	Radial Borefield Water	Fresh Water (RO Product)
Variable	Chlorides (ppm)	59 400	37 700	14 900	210
	Total Dissolved Solids (ppm)	124 000	73 000	49 300	568
	pH	7.42	7.16	7.25	7.60

FILTER PRESS OPERATION AS INSTALLED

The VPA filter press was received with operating logic from Metso. As received, the filter press did not meet the operational specifications or filter cake performance indicated in the project design criteria. Table 5 details the performance of the filter following commissioning. The following section details the operating logic as received and the areas for improvements identified.

Table 5: Filter Press Commissioning Performance Compared to Design Criteria

	Cake Moisture, %	Cake Chloride Concentration, ppm	Filter Specific Throughput (dmt/h)	Fresh Water Usage, m³/t
As commissioned	12.3 ± 0.7	2100 ± 280	32.1 ± 0.8	0.42 ± 0.01
Design	8.9	< 300	52.4	0.8

Feeding and Filtration

Slurry feed into the filter occurs in four steps. The first three steps are designed to build a solids bed prior to injecting slurry at high pressure to prevent cloth breakages. The feed pump initially speeds up to 65% until a 0.8 bar pressure is achieved in the slurry feed line. The feed pump then ramps to 82% speed. The fourth and concluding step in filling stage can be run through a “feed by time” or “feed by derivative” process.

During “feed by time” slurry is fed into the filter for a set time – as set by operator. A minimum feed weight will trigger an alarm if the filter does not fill sufficiently within the given timeframe. Due to variances in feed density, particle size distribution and feed volume because of changing driving head in the filter feed tank over time, this method was deemed unproductive in the Carrapateena filter press.

During “feed by derivative”, the end of the step is determined by the rate of change in load cell reading as a function of time. The filter continues to fill until the weight change observed is no more than 50 kg over a given time - as set by the operator. Although this method performed better with variances in feed density fed into the filter than the “feed by time”, it also resulted in large variations in cake mass, thickness, and compaction. As discussed in a later section, compaction specifically has a significant impact on the efficiency of subsequent steps, particularly cake wash.

An improvement opportunity was identified to ensure suitable filter filling without over compaction.

Turbidity sensors are installed on the filtrate discharge ports designed to identify higher than standard solids content in the filtrate indicating a damaged cloth. The turbidity sensors initially installed were ineffective at identifying these conditions. A redesign of the filtrate sampling and sensor would be required to obtain relevant and accurate data to cloth damage.

Membrane Pressing

The VPA pressing cycle was originally designed with one membrane press stage with the facility to add in another. During the pressing cycle, the rubber membrane on one side of the cake is inflated using high pressure air. Membrane step one, after filling, is designed to begin the dewatering process and is run to a set time limit. The use of the first step, however, can seem counter intuitive. The step starts the dewatering process, then the sequence adds more water during a later cake wash step then an air drying to re-dewater the cake.

The second optional membrane press follows the cake wash step for further dewatering prior to air drying. The operation of the membrane press at high pressure can result in over compaction of the cake. Greater cake compaction reduces the efficiency of the cake wash and air-dry cycles. As the water or air progresses through the cake, it cracks creating paths of least resistance, enabling air

and water to channel through small pockets of cake rather than equally across the cake bed.

An improvement opportunity was identified to reduce over compaction because of the membrane presses and improve the step sequencing.

Cake Wash

The VPA filter press was installed with an optional cake wash step. The cake wash is one of the primary reasons why the VPA filter press was chosen for Carrapateena. During the cake wash step, the process water entrained within the concentrate voids is displaced with fresh water. The fresh water, of notably lower chloride content than process water, reduces the final cake chloride content.

As received, the cake wash step washes the pressed concentrate for a set time – as set by the operator. Washing to a set time was unfavourable to the Carrapateena concentrate requirements due to variations in slurry and water quality and concentrate compaction. It was observed at this stage the cake chloride content was not proportional to cake wash time or the water delivered.

A greater wash time resulted in a lower chloride content but resulted in a reduced throughput rate of the filter below the design criteria and what would be required in future.

Additionally, the equipment supplied made it difficult to control cake wash water supply pressure. A higher cake wash pressure, whilst resulting in a higher flow and lower step duration, combined with concerns of compaction, resulted in cake cracking, which creates a path of least resistance for the water and air in a future step, making both ineffective.

Attempts to control the were made by using the installed filter feed pressure gauge. However, the water would have already fed through the cake by the time it reached this gauge and often still resulted in over pressurising and cake cracking. A fixed cake wash pump speed also resulted in the same outcome.

Multiple improvement opportunities were identified to improve the effectiveness of the cake wash process and improve the final cake quality. These include:

1. Filling low pressure
2. Filling medium pressure
3. Filling high pressure
4. Cake Build
5. Membrane Press indirectly with air inflation
6. Air Drying with compressed air
7. Water wash displacement
8. Air drying
9. Cake Discharge
10. Plate cleaning
11. Cycle repeats

Air Drying

There are two available air-drying stages on the VPA filter press – before or after the cake wash. One or both can be utilised.

The air-drying step ran for a set time – as set by the operator. The pressure used in the air drying is also less than that used in the membrane press. Due to the variance in filling and compaction, this

was deemed ineffective at achieving the small target range for cake moisture content. A greater dry time resulted in a lower moisture content but resulted in a reduced throughput rate of the filter below the design criteria and what would be required in future.

A series of steps follow air dry that discharge the cake, vibrate and wash the cloths, and then the sequence repeats. Further utilisation and optimisation of the air-drying steps was identified as an improvement opportunity.

Initial Optimisation

An initial optimisation program was implemented on the concentrate filter in the weeks immediately following commissioning. This program focused on utilising the filter sequence and logic as provided by Metso and altering the fixed step timers across all key filter operations to maintain both filter cake moisture and Cl content within required specifications.

Table 6: Filter Press Performance After Initial Optimisation

	Cake Moisture, %	Cake Cl, ppm	Filter Specific Throughput (dmt/h)	Wash Water Requirement, m³/dmt
As commissioned	12.3 ± 0.7	2100 ± 280	32.1 ± 0.8	0.42 ± 0.01
Initial optimisation <i>Adjusting step timers and pressure regulators to target cake Cl and moisture</i>	9.6 ± 0.9	240 ± 160	30.1 ± 1.7	0.72 ± 0.01

The results of this program were well controlled cake moisture and Cl content at the expense of filter throughput and increased RO wash water demand.

The following limitations towards further optimisation via this approach were identified as follows:

1. Filter sequence as commissioned implemented a dewatering step (membrane press) ahead of cake wash, leading to a tradeoff between dewatering and cake wash efficiency.
2. Natural variability in filter feed slurry properties necessitated running extended step timers to ensure well controlled cake quality across all encountered feeds.

Further optimisation of the filter cycles were performed to improve the performance of the filter to allow it to produce filter cake with low chloride and high throughput.

FILTER PRESS ADVANCED OPTIMISATION AND OPERATIONAL CHANGES

The various improvement opportunities identified during initial optimisation were driven by automation and/or sequencing. An advanced optimisation program was developed to investigate these opportunities to increase the filter throughput without impacting on cake chloride or moisture content. The focus of this program was to define a measurable end state for each major step of the filter sequence, and identify opportunities to either better utilise existing

instrumentation on the filter, or add existing instrumentation such that the defined end point of each step could be triggered by instrumentation rather than a fixed step timer.

In the midst of this work, an expansion of the filter to 40 plates was completed in February of 2021.

Closing

An initial change implemented that covers both automation and sequencing, whilst not directly related to cake chloride or moisture content, instead aimed to improve the accuracy, and understanding of filter throughput. An automating tare step was implemented after the close of the filter. The tare is completed and deemed successful if the filter weight is ± 50 kg of zero for five seconds. If the filter weight and time do not satisfy these conditions, then an alarm is triggered. This prevented any remnant cake from the previous cycle or change in conditions of the cloths, from altering the final drop weight of that cycle.

A regular comparison was completed that compared the filter drop weight and the same mass over a certified weighbridge. The auto tare enabled an accuracy of the filter weight between $\pm 5\%$.

Feeding And Filtration

Numerous alterations were made to the feed and filtration stages of the filter press. The method utilised was the “feed by derivative” with conditions added. The feed pump runs at a constant 70% until a pressure of 0.8 bar is achieved. After this, a P&ID controller takes over the pump speed with a slurry feed pressure set point of 4.5 bar. A minimum filter weight of 13 500 kg must be achieved. Feeding ends when the filter weight does not vary by more than 10 kg over 30 seconds.

Whilst still maintaining protection for the filter cloths with a middling speed until a bed is formed as indicated by the 0.8 bar pressure, these conditions removed the filter feed tank level and driving head as a factor that dictated cycle time, whilst also enabling consistent cake thickness and limiting compaction. The improved tare function for the load cells also enabled a finer control to mark the end of the “feed by derivative” step.

Further improvements in this step are to install a flow meter on the slurry feed line. This will enable further understanding and control of the feed into the filter without relying on the pressure feed pressure.

Membrane Compression

A range of sequence alterations were made around membrane compression as shown in Figure 3. Firstly, the initial membrane press was to provide stabilisation for the cake only, and not as a dewatering step. This was achieved by the inflation of the membranes to a minimum time to achieve full inflation and at a minimum pressure required for equipment protection. Additional interlocks were put in place to ensure the sequence could not proceed to the cake wash step without the membranes being pressurised to further protect the equipment. Secondly, was to utilise the optional second membrane press which enabled two steps of dewatering, a membrane press and air drying, after cake wash, to ensure the final concentrate cake met the product specifications. This did require installation of valving and regulators that were not initially supplied.

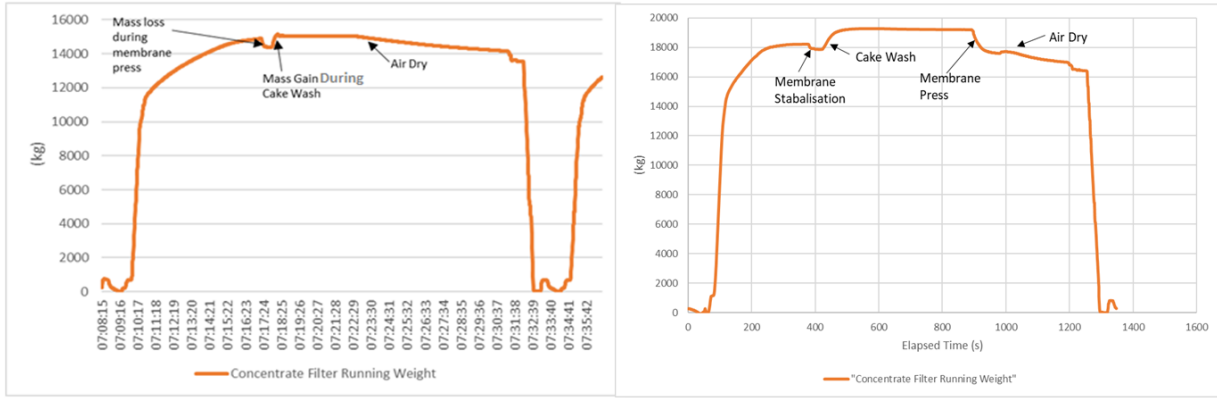


Figure 3: Membrane Compression Sequencing Changes

For the second membrane press, further automation was implemented that used a derivative control, like that of the “feed by derivative”. The high-pressure membrane press does not have a set time, instead the step continues until the weight change observed by the filter load cells is less than 20 kg over a 15 s, indicating no further dewatering by compressions is available. It was observed that that as the time of the step increased the mass loss curve flattened as displayed in Figure 4 which provided the data required for the derivative control implementation. It also indicated that if membrane press two is allowed to extend for too long it will switch from dewatering the cake to compaction. Ensuring the second membrane press stopped at an appropriate time, ensured maximum efficiency of the dewatering step whilst optimising the sequence duration to achieve the concentrate cake moisture content and reducing the risk of cake compaction.

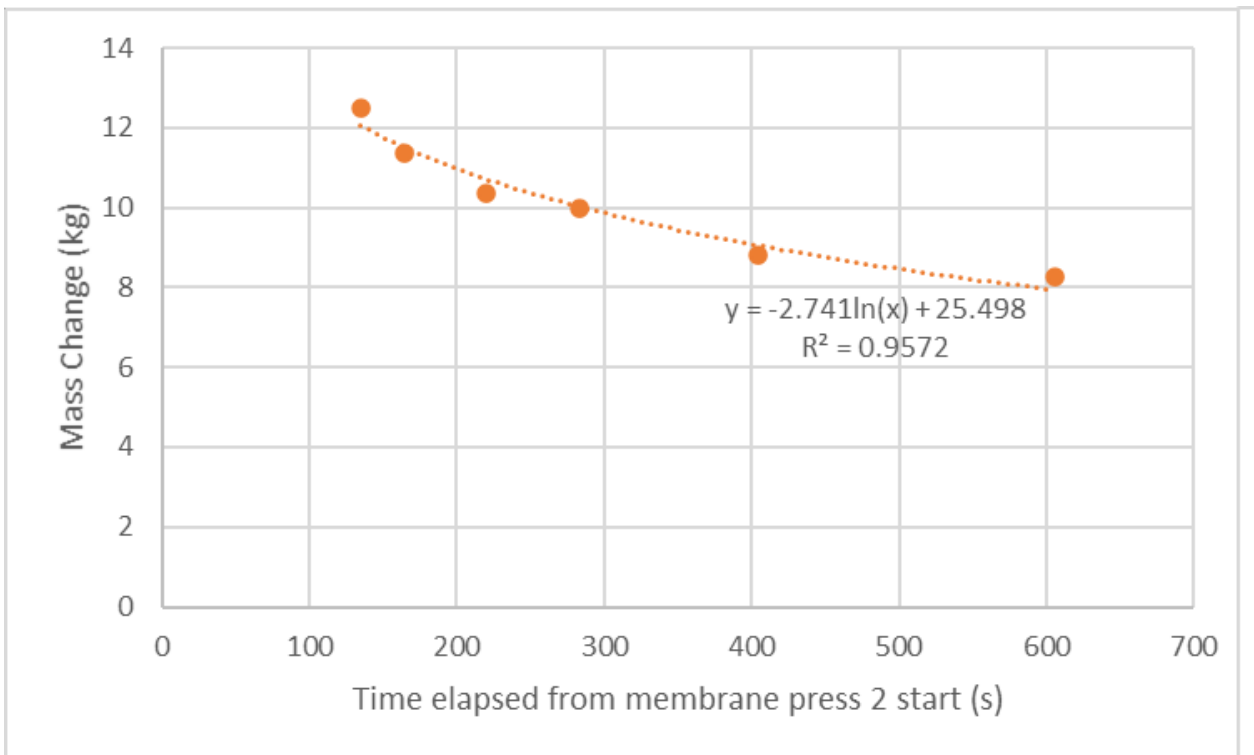


Figure 4: Mass change versus membrane press two times.

Cake Washing

During early operation, a flow meter and pressure gauge was installed on the discharge of the cake wash pump which allowed further automation and control of the supply. This resulted in a constant pressure and more time within the cake wash step at the desired operational pressure reducing overall step time.

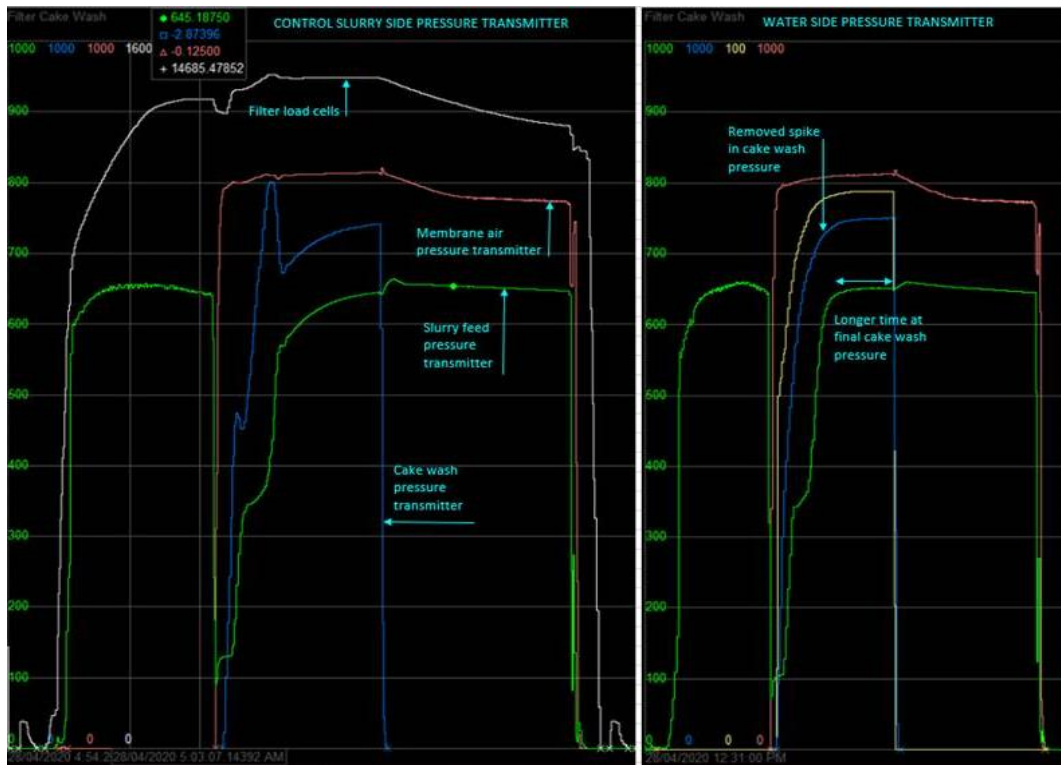


Figure 5: Cake wash pressure control.

An investigation was conducted into the filtrate conductivity and cake chloride content. The filtrate conductivity is related to the chloride content in the filtrate as presented in Figure 6. The same relationship was found with the resultant chloride content in filter cake.

Conductivity probes were installed on the filtrate port to monitor the filtrate conductivity as an implied filtrate chloride content. Further automation was then added to the cake wash step whereby the conductivity of the filtrate must drop below a given value before the sequence can progress to the next step. The final iteration of the cake wash step saw a permissive type of approach. The cake wash step operates to minimum volume, then until the filtrate conductivity is below a set target or until a maximum time has been reached. This ensures competing priorities are considered, filter cake quality whilst not compromising on using excessive water. Should the filter not reach the conductivity target and instead the maximum time is reached, an investigation is run into the recent calibration of the conductivity probes or potentially poor freshwater quality. Ultimately controlling the cake wash duration to conductivity makes the step adaptable to changing slurry and water properties while reducing freshwater usage.

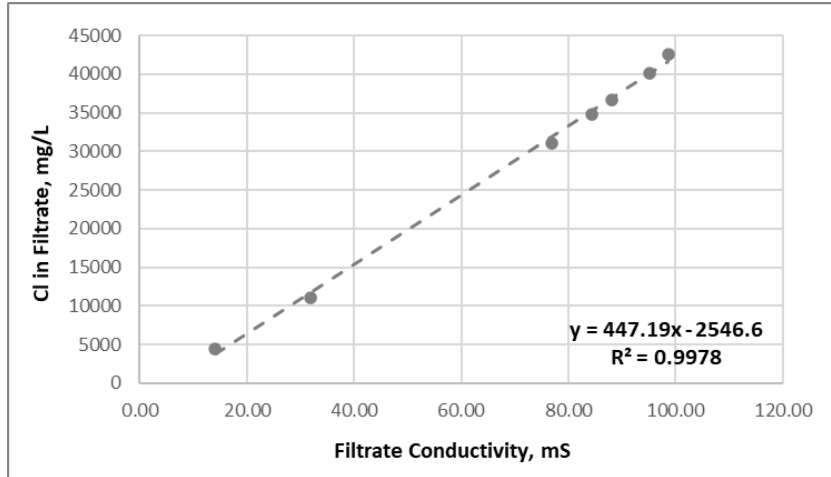


Figure 6: Filtrate Chloride Grade Compared to Filtrate Conductivity

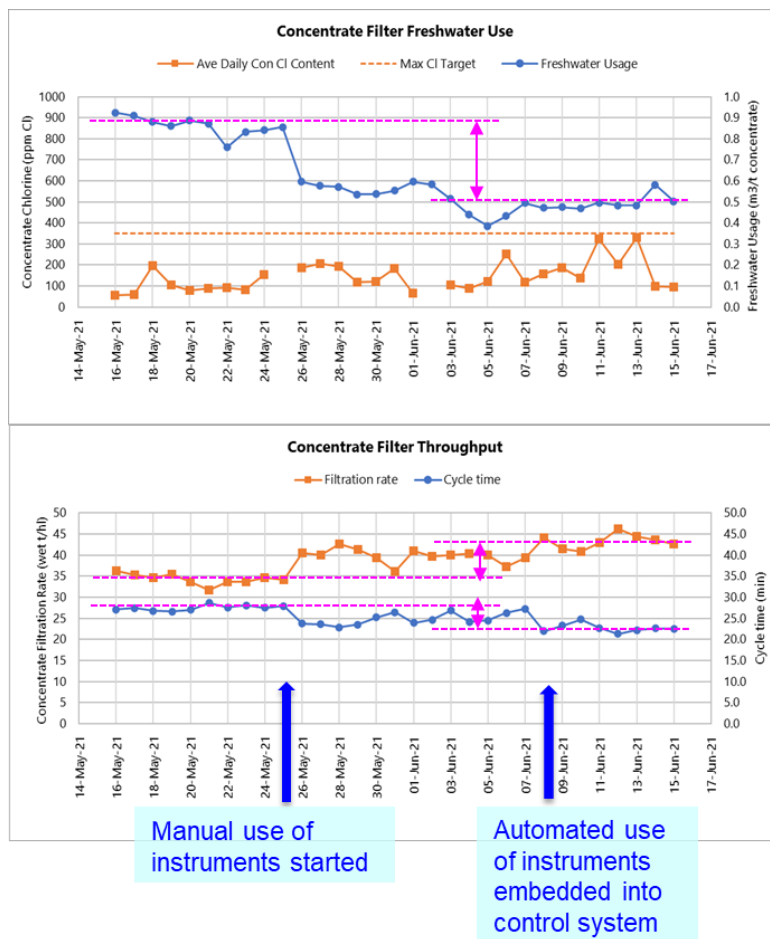


Figure 7: Implementation of filtrate conductivity instruments for filter control

Air Dry

Tests were conducted to measure how cake moisture changed with respect to other variables. This data looked at the moisture content as a function of both membrane press two and air dry time. The results showed that cake moisture was not linear to drying time or air volume and was greatly influenced by slurry properties. The cake moisture, however, was linear to the mass loss in these two steps.

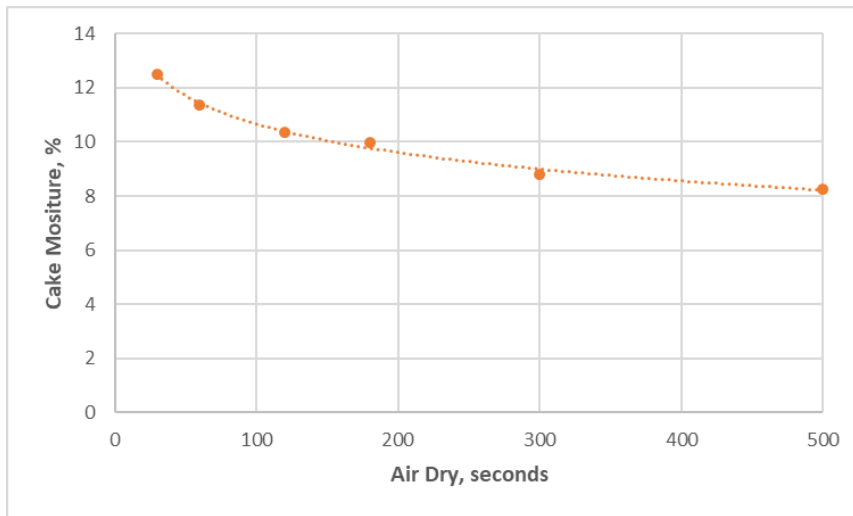


Figure 8: Cake Moisture as a function of air dry time

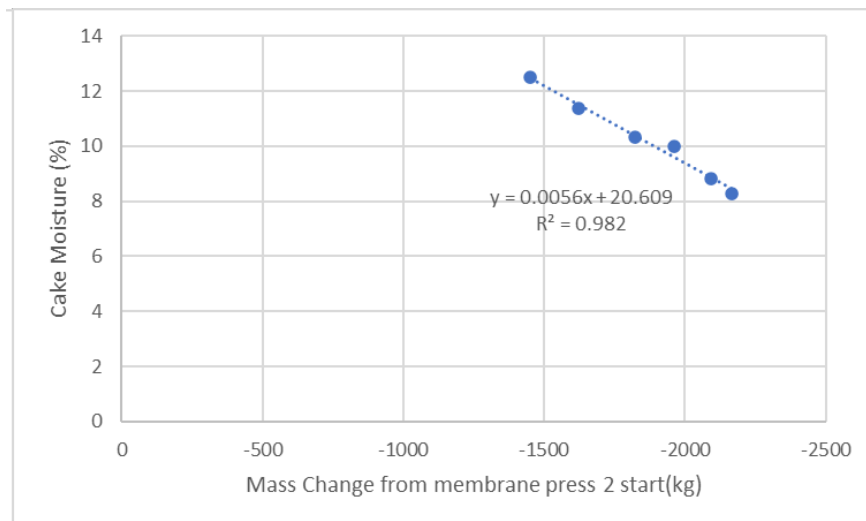


Figure 9 - Cake moisture versus mass change from start of membrane press (membrane press two plus drying step).

An automation change was implemented that allowed for two methods of air drying to be selected between by the operator - “fixed time” and “fixed mass drop”. If “fixed time” is selected the air-drying step operates as initially designed whilst if “fixed mass drop” is selected the air dry will continue until the filter mass has decreased by 2 100 kg – as entered by the operator.

CONCLUSIONS

An advanced optimisation approach has been applied to Carrapateena concentrate filter.

Advanced optimisation of the filter press has allowed for a 15% increase in filter press throughput as compared to initial optimisation (30% including expansion of the press) without compromising on cake quality requirements.

Table 7: Filter Press Performance After Advanced Optimisation

	Cake Moisture, %	Cake Cl, ppm	Filter Specific Throughput (dmt/h)	Wash Water Requirement, m³/dmt
Design?	?	?	?	?
As commissioned	12.3 ± 0.7	2100 ± 280	32.1 ± 0.8	0.42 ± 0.01
Initial optimisation <i>Adjusting step timers and pressure regulators to target cake Cl and moisture</i>	9.6 ± 0.9	240 ± 160	30.1 ± 1.7 <i>34.7 (adjusted for 40 plate expansion)</i>	0.72 ± 0.01
Enhanced optimisation	9.0 ± 0.4	250 ± 70	39.0 ± 0.7 <i>15% Increase from initial optimisation</i> <i>30% increase with inclusion of press expansion</i>	0.45 ± 0.03 <i>38% reduction from initial optimisation</i>

The focus of advanced optimisation was to define a measurable end state for each major step of the filter sequence, and to utilise instrumentation to trigger the end of each step rather than rely on a fixed step timer.

As well as increasing the filter throughput, advanced optimisation was able to unlock a 38% saving in costly RO water usage through the concentrate filter.

The optimisation process is ongoing with further opportunities for enhanced operation through use of instrumentation still underway.

Pumping for Profit

R Doyle¹

1. Pump Specialist, Audax Enterprises Pty Ltd, 19 Welbourne Heights, Parmelia, 6167 WA
roger.doyle@audaxenterprises.com.au

ABSTRACT

Slurry pumps consume much of the power used in processing plants and a large portion of the maintenance budget. Millions of dollars' worth of production is lost annually due to unplanned outages caused by pump failures, yet few sites have staff who understand the complexities of slurry pumping.

Slurry pumps, with their large performance envelopes, are the heart of most processing plants but in the absence of an engineering evaluation of changes that are made to the system, pump failures will continue to cause extended plant shutdowns and companies will suffer the associated production losses.

Slurry pumps are selected to address the unique conditions that are predicted to exist within the circuit for which they are selected. Subsequent alterations to the process rarely involve an appropriate analysis of the revised conditions that the pump needs to meet.

Numerous decisions are made by various departments within an operation that alter the performance of slurry circuits. The anonymous examples of the cost to the business, by decisions of the different departments, are provided out of the author's 15-years of involvement with a variety of mineral processing sites during the author's employment by four different pump manufacturers.

None of these implementations followed an appropriate analysis of the effects that the changes would have on the efficiency and wear life of the pump.

As an example, the author conducted an engineering evaluation of a circuit in which the production from a previous process upgrade had exceeded expectation and was reported to be 'working well' apart from occasional bogging of the pump. Raising the pump speed by 110 rev/min increased zircon concentrate production at the site by 11 t/d, valued at an additional \$3.2 M/y, for a cost of less than \$5000.

This paper identifies areas where increased pumping costs are being incurred in the absence of engineering consideration of the effects of changes to slurry circuits. Operating and maintenance costs can be reduced when appropriately trained on-site staff are supported by systems that provide the data on which the effective evaluation of slurry pumping circuits depends.

The only winners at present are the pump-spares suppliers who are called upon to supply replacements for both the fully worn and the partially worn parts that are discarded following the maintenance of poorly operating pumps.

INTRODUCTION

Many decisions that influence slurry pump performance are being made in the absence of any engineering analysis and often lead to reduced efficiency, reduced wear life and unplanned downtime. The one common key performance indicator (KPI) through all departments seems to be cost minimisation, while the financial loss to a site of unplanned down time, which can amount to many thousands of dollars per hour, rarely seems to appear in the KPIs of any department.

It is the **System Curve** that indicates the total head (static head plus the change in friction head) as the volume and composition of the flow through a system changes. The system curve for every installation is unique as it is developed from the flow requirements for the process, the size and

physical arrangement of the pipework and the slurry parameters.

The appropriate pump is then selected to meet the predicted flow and head requirement.

It is the system curve that changes when factors within a circuit are altered while the pump curve remains the same.

The **Pump Curve** displayed in Figure 1, shows that, when pumping water, efficiency can vary from 50% to 73% while power requirement can vary from 5 kW to 140 kW without exceeding the performance envelope of the pump.

The duty point for the selected pump is identified as the point where the pump curve is intersected by the system curve but will move when there is any change in the flow, pipework, or slurry composition. Any change in these parameters will change the efficiency and wear life of the pump.

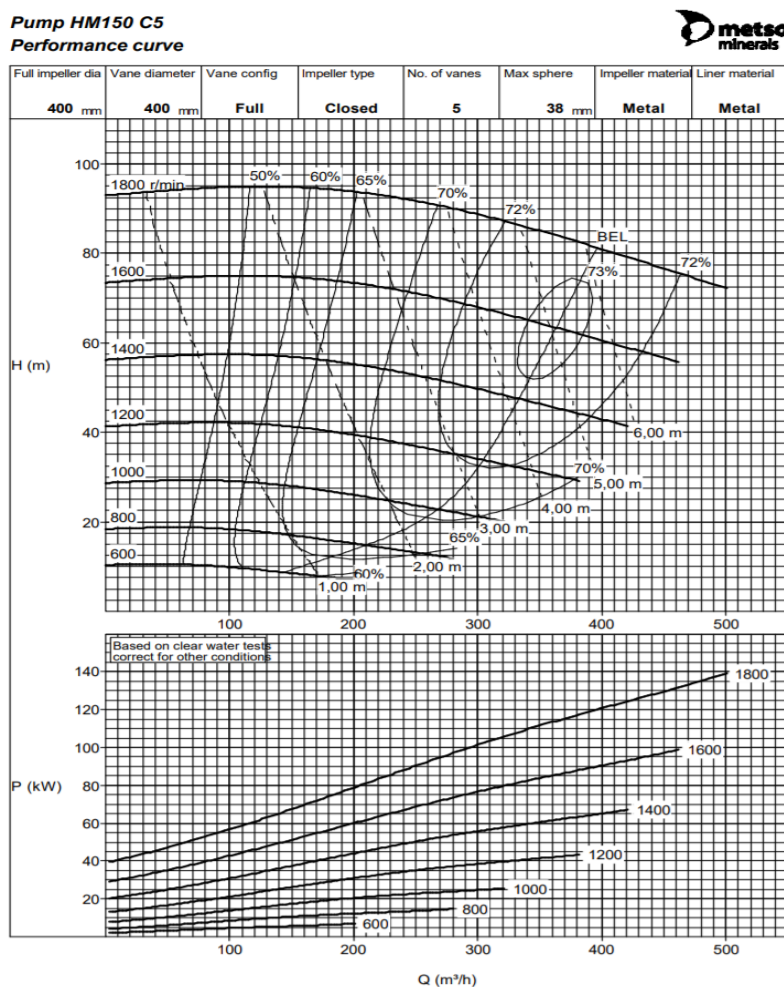


Figure 1. Example of a Metso pump curve.

The annual total ownership cost of slurry pumps in many cases exceed their purchase price and the cost minimisation efforts of the different departments, in the absence of appropriate pump engineering evaluation, often leads to an increase in the total ownership cost of the pump. Decisions that affect the performance and efficiency of the pumps are made as the different departments focus on achieving their individual KPIs. In the absence of the on-site skills to appropriately evaluate the effect of changes that are made along with a clear determination of the change that has caused the plant down time, decisions will continue to be made that reduce plant productivity.

The data collection systems in most processing plants are primarily installed for the monitoring of production parameters. Comprehensive monitoring of the factors that influence the individual slurry circuits is rarely included in the design and escalating unrecognised operating costs can continue to mount. In most cases, challenges with a circuit are only addressed when the pump displays performance or maintenance issues, so the pump becomes the focus, but the issue is generally created by unmonitored changes in the circuit or the slurry composition.

Though there may be several pumps with an identical build within the plant, efficiency and wear life of the pumps will differ, as no two slurry circuits are the same. Personnel who are appropriately trained to evaluate slurry pumping systems, supported by systems that record the performance and maintenance of each individual circuit, is the only way to minimise slurry pumping costs.

PROCESSING PLANT DESIGN CHALLENGES

In a recent evaluation of a plant with oversized pumps, the author identified a potential saving of \$750 000 in power costs, purely due to efficiency improvements had more appropriately sized pumps had been installed. Maintenance costs for the more appropriately sized pumps would have also been reduced but as both oversized and undersized pumps suffer from increased wear, the spare parts suppliers were happy.

Most mineral processing sites are developed by specialist 'design and construct' organisations, to meet the production goals required by the end user, sometimes within performance limits set by the client.

Process calculations determine the flow requirement between each stage of the process while small sample analysis provides the estimates for the slurry composition that each stage of the process will be required to handle. The inlet and discharge elevations determine the static head in each slurry circuit, while the slurry characteristics along with the flow rate, the pipe internal diameter and length of run along with the style and number of fittings, determines the increasing friction losses as the flow rate increase and are represented by the predicted system curve. The total head at the required flow rate identifies the duty point for which the selected pump is selected.

Component selection decisions

The value of lost production due to unplanned pump maintenance requirements in most cases exceeds the cost of installing duty/standby pumps arrangements which would enable production to continue following a pump failure. This arrangement can also allow pumps to be run to failure, which can maximise the benefit gained from the expensive spare parts. It also enables the pump to be repaired to a consistent standard by the on-site maintenance teams rather than by labor hire during planned shuts.

Design and construct organisations maximise their profits by minimising their costs and smaller components offer lower CAPEX but suffer higher OPEX throughout their life.

Smaller pipes and pipe fittings are cheaper to purchase but operate at higher velocities, which increases both wear rate and the power required by the pump to overcome the additional resistance to flow.

To meet a particular flow rate, an impeller with a small diameter requires a higher speed than an impeller with a larger diameter, but power requirement will remain very similar. The higher the speed of the impeller the higher the wear rate and potentially the greater the OPEX due to the more frequent maintenance downtime required.

It is generally the pump supplier who selects the size and build for their chosen pump and there will often be two alternatives available for the single duty point, as is shown in Figure 2.

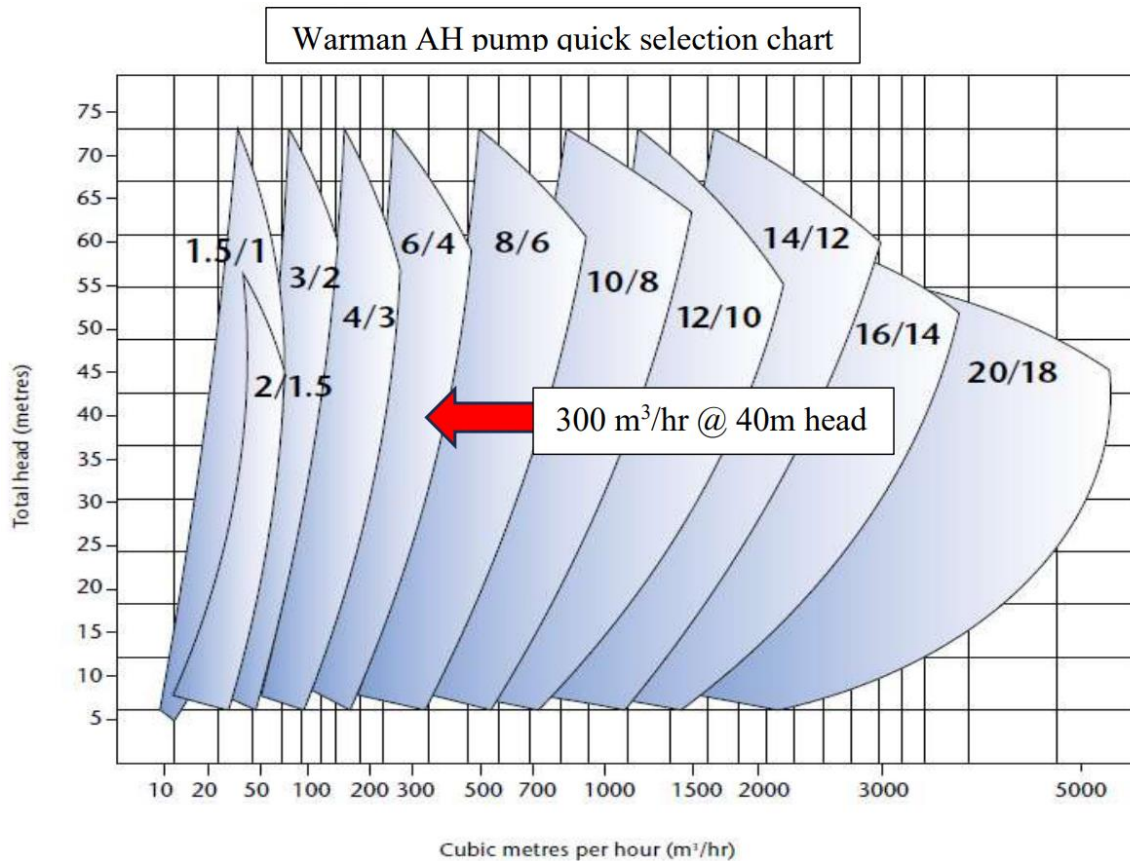


Figure 2. Both the 6/4 AH and the 8/6AH can meet the required duty.

Historically, it was recommended that for improved slurry flow, the suction between a tank or hopper and the pump should be angled down. Because this is a more expensive connection than a horizontal spigot, in today's economic environment it is rarely designed into a plant. Many plants are operated above the design name-plate capacity and the site-works costs of increasing pump size in installations with a horizontal spigot is an additional barrier to upsizing the pump to improved efficiency and reduce wear.

INSTALLATION CHALLENGES

The positioning of process components does not always consider the maintainability of the component with instances where components weighing 300 kg that require regular maintenance, exceed the reach capacity of the on-site crane. Repeated mobilisation of appropriate lifting equipment to remote sites not only costs many thousands of dollars but can also extend plant downtime when unscheduled failures occur.

Installation does not always exactly represent the designed layout that was used to calculate the system resistance curve upon which the duty point for the pump was predicted. While minimising pipe and cable runs will minimise installation costs, the ongoing cost and time implications on the subsequent maintenance of the pump that is caused by reduced access can be very costly.

Maintenance costs for the pump shown in Figures 3 and 4 are more expensive than for a free-standing pump because each rebuild requires an additional two to three hours for the crane, the crane operator and two fitters. In addition to these costs, identified safety concerns require the attention of a rigger who is trained to an intermediate level.

All the site inductions that the author has attended place engineering controls above Administrative Controls and PPE but are too often missed out at the design and installation stages with subsequent

engineering re-designs being deemed “too expensive”.



Figure 3. Actuator above pump centre-line Figure 4. Overhead pipework prevents vertical lift.

COMMISSIONING CHALLENGES

Slurry pumps operate with varying levels of efficiency within very large operating envelopes, with speed adjustment being the simplest method to match the pump to the required duty point. The adoption of variable speed drives (VSDs) for pumps has simplified the balancing of flows in the individual circuits within the plant, to meet changes in the system curve. In some situations, the scale of the changes may require a change in the pulley ratios for a pump to meet the desired duty or an impeller change to overcome some unpredicted slurry characteristics. Not only are these material changes during commissioning not always passed on, which results in subsequent stock availability issues, but shows that not all the differences between the estimated design flows and operating reality can be overcome within the adjustments available with the VSD.

More importantly, in the absence of appropriate slurry and pump monitoring equipment in each slurry circuit, the simple VSD adjustments hide the difference between the reality of the situation in the plant and the values developed from the small sample tests on which the design of the plant was based. Many sites commence operations with pumps that would not have been selected had the actual operating conditions been known. The ‘design’ system curve, which determined where on the pump curve the selected pump would be operating, was estimated by a combination of the **Static Head** (vertical height between the centre of the pump and the point of discharge), and the **Friction Head** (estimated from small sample slurry trials and proposed circuit design and estimated tank operating level). In an operating plant all these parameters can be accurately measured. Tank level can be monitored and pressure readings at the discharge of the pump and at the point of discharge from the pipework, combined with the actual density of the slurry, provides the **Total Head** against which the pump is working. Add in the flow rate and you have the operating duty point.

The lack of monitoring to defines the operating duty point and accuracy of the predicted system curve which was developed for the original pump selection, means that any potential to upgrade the circuit to a more efficient one, can neither be identified nor costed out.

PROCESS CHANGE CHALLENGES

Many plants are operated at above their design capacity, with the installed pumps drawing more power and wearing out faster because they are having to work harder to overcome the increased friction head through the system. If the settling velocity of the slurry is considered it can often be the case that a larger diameter pipe will maintain flow rates above the settling velocity and reduce the power requirement and wear rate of both the pump parts and the pipeline. Once the plant is running it is possible to accurately determine all these parameters and it is much simpler to obtain this information if the appropriate monitoring facilities have been included in the design. Any changes to the slurry flow will alter the performance and wear life of the pump but until process changes are subjected to a comprehensive review of the whole circuit for optimum efficiency and performance, operating costs cannot be minimised.

The benefit of slurry circuit evaluation

To maximise recovery in a mineral processing wet plant, an additional Kelsey Jig was installed to increase recovery of zircon concentrate to 2.1 t/h. The upgrade exceeded expectations, but it was found that the concentrate pump bogged when recovery exceeded 2.5 t/h. To avoid the downtime caused by the bogged pump, the Jig parameters were adjusted so that production did not exceed the pump's capacity. Following an engineering assessment of the whole circuit, the author suggested increasing pump speed by 110 rev/min, which required increasing the motor size from 5 kW to 7.5 kW. This minor change saw an 11 t/d reduction in the zircon concentrate reporting to the tails stream with an annual value of \$3.2 M.

PROCUREMENT ISSUES

The price that slurry pump manufacturers charge for their spare parts has been an issue for as long as the author has been in the industry, with many sites turning to suppliers of reverse engineered components that are cheaper to purchase. While claims are made that they are equivalent to the manufacturer's parts and the parts may show equivalent performance when first installed, total ownership costs can be higher.

Where cost savings reduced profit.

One of the key performance indicators for the stores on a site was to minimise stock value and the decision had been made to use parts from an alternative supplier who offered a significant reduction in purchase price and would reduce the cost of the on-site inventory. A trial was set up to compare the performance of impellers in two identical pumps, run at the same speed, supplied out of the same hopper, discharging to the same point.

The author had requested to attend site during any maintenance activity and received a call that the pump containing the OEM's impeller was vibrating badly and had failed. (See Figure 5.) Investigations showed that the urethane (dark material) had been stripped from one of the pumping veins, exposing the internal skeleton (brown colour) which had worn rapidly and unbalanced the impeller. Despite site staff reporting that the replicator's impeller was still 'performing well', the author insisted that as it was a trial, the replicator's impeller should also be inspected. (See Figure 6.)



Figure 5. OEM impeller Figure 6. Replicator impeller

Analysis of the performance of the two impellers revealed that although the purchase price of the impeller from the replicator showed a small saving, the increase in power that was required to match the performance of the OEM impeller during its operating life, greatly exceeded the saving achieved by its purchase. An effectively monitored trial saved the increase in operating costs that the “cheaper” alternative would have imposed.

MAINTENANCE CHALLENGES

The author has met and worked with numerous fitters on many sites, but few have displayed an understanding of the critical adjustments that influence pump wear, or the design features that provide for more accurate assembly and adjustment. In the absence of appropriate training or maintenance procedures, the variable maintenance standards of pumps by individual fitters, results in inconsistent wear life of pumps. The primary driver for maintenance frequency is varied but, in an effort to minimise unplanned down time, management sometimes reduces the maintenance intervals to meet the life achieved by poor maintenance operations.

Component replacement issues

The fear of unplanned pump failure has seen the practice of replacing all the wet-end components in a pump, at each maintenance interval, has become the standard in all the plants to which the author has had access. The ‘Close to failure’ assessment that is made by staff when the pump is opened is very arbitrary with the actual wear of the failing component seldom being accurately assessed. The lack of wear assessment and recording of the remaining life of each of the wet-end components means that few sites truly get their money’s worth from the parts they install. Figure 7 shows an impeller that did provide value for money. While it had not physically failed, it could no longer meet the required flow within the speed adjustment available with the VSD.



Figure 7. Two views of the worn impeller that was no longer able to maintain the required flow.

The ‘replace-all’ practice has seen millions of dollars’ worth of partially worn but usable components disposed of without consideration of the environmental legacy this creates. Using partially worn components in low wearing, non-critical pumps can reduce costs, while building up and resurfacing some components is a cost saving option implemented on some sites.

Upgrading all the wet-end components to the same ‘improved wear’, more expensive material will not change the relative wear and there will be an even greater financial loss in the components that are discarded with useable wear life remaining. The ultimate goal with a slurry pump is to have all the wet-end components close to failure at predictable intervals. While the potential wear life of each individual component is not established, it is not possible to select components that have wear lives that are a multiple of the life of the fastest wearing component. Minimising component costs will never be achieved if all the components are upgraded to a single, more expensive but more wear-resistant material.

RECORD KEEPING CHALLENGES

Every slurry pump works in a unique slurry circuit and the performance will be determined by a combination of the pump build, the configuration of the pipework and the slurry parameters. Slurry pump efficiency cannot be maximised when the slurry parameters for the original pump selection, that were derived from small sample testing, are not validated in the operating plant, nor analysed for their effect on the pump during subsequent process alterations.

Pump records

The only changes in a pump curve that the pump creates are the changes due to wear and variations in the assembly during maintenance. Rebuilding pumps to a predetermined standard, measuring the wear life potential of all components and keeping photographic records of the wear patterns, can assist with making the appropriate adjustments to maximise efficiency and minimise environmental degradation. Any slight changes in impeller design will change the wear causing vortices in a pump which are pump speed, impeller clearances and slurry characteristic dependent. Changing to an alternate supplier for spare parts may reduce the inventory costs but may provide variable wear results on different wet-end components in the various pumps into which they are fitted. When impellers from different suppliers with the same claimed performance are stocked under the same stock code, and randomly installed in pumps, predicting the meantime before failure becomes impossible.

The different design of the pump-out vanes on the two impellers in Figure 8 will generate different vortices and the wear patterns on the liners, throat-bush and impeller are likely to vary considerably.



Figure 8. Two impellers for the same pump with claimed equivalent performance.

Slurry records

The original pump selection required numerous details including flow, discharge head, particle size distribution, solids concentration, slurry specific gravity, particle shape, slurry pH, temperature and site elevation. Any variation in these parameters from those used to calculate the system curve for the original pump selection will alter the influences on the pump and may reveal that there is a more appropriate build or size of pipe or pump, available to meet the changed conditions. The ongoing measurement and analysis of these parameters, as the plant feed and process changes, would enable the system curve to be updated and the suitability of the pump and pipework to be optimised.

Pipework records

The maximum internal diameter for the original pipework is determined by estimating the settling velocity of the slurry within each circuit. Smaller pipes and fittings are generally lower in cost but increase the friction head that the pump needs to overcome. Any alteration in pipework or fittings will change the system curve. Measurement of the elevation difference and pressure drop over the length of the discharge circuit provides the only accurate determination of the true friction head.

CONCLUSIONS

Slurry pumps expose the challenges that exist or have developed in the slurry circuits that they service. Very few of the people who alter different components of a slurry circuit have received any training that identifies the effect on the performance of the pump that the proposed changes will have. Maximising the efficiency of a slurry circuit is a complex issue that requires the ongoing analysis of all the changes that are made to the circuit. Until sites develop the capacity to measure,

record and appropriately analyse their slurry circuits, their bottom line will continue to suffer. Automatic control of the flow through mineral processing plants is a dream for many, but will remain a dream until the appropriate data is recorded and available to be analysed.

ACKNOWLEDGEMENTS

The author would like to acknowledge Weir Minerals, Keto Pumps, Metso, FFF and the 7D Team for the experiences and opportunities that they provided, which enabled the author to offer appropriate support to customers who were searching for answers to better understand and improve their pumping operations.

The author would especially like to thank those colleagues and on-site staff who appreciated the support that was offered.

Slurry Pump Safety Considerations in Mineral Processing Plants

A Varghese^{1,4}, S Martins², E Lessing³, G Hassan⁵ and A Karrech⁶

1. Metso Corporation, Product Manager – Digital Products, Metso Outotec Australia Ltd, 1110 Hay Street, West Perth, 6005 WA, Australia, alan.varghese@mogroup.com
2. Metso Corporation, Research & Development Engineer, Metso Outotec Canada Inc., 795 George V Ave, Lachine, QC H8S 2R9, Canada, sudarshan.martins@mogroup.com
3. Metso Corporation, Vice President – Engineering, Pumps, Metso Oyj Finland, Rauhalanpuisto 9, 02230, Espoo, Finland, evert.lessing@mogroup.com
4. University of Western Australia, PhD candidate, University of Western Australia, 35 Stirling Highway, Crawley, 6009 WA, Australia, alan.varghese@research.uwa.edu.au
5. University of Western Australia, Senior Lecturer, University of Western Australia, 35 Stirling Highway, Crawley, 6009 WA, Australia, ghulam.hassan@uwa.edu.au
6. University of Western Australia, Professor, University of Western Australia, 35 Stirling Highway, Crawley, 6009 WA, Australia, ali.karrech@uwa.edu.au

ABSTRACT

Slurry pumps are used in a wide range of industries, including mining, agriculture, and wastewater treatment. They are designed to handle abrasive and corrosive materials, making them an essential part of many industrial processes. However, due to the nature of their operation, slurry pumps can be hazardous if not used and maintained properly. Incorrect operation of slurry pumps can result in explosion, injuries or even fatalities, property damage and loss of production.

Slurry pumps, unlike the clean water pumps, can be bogged, particularly when pumping very thick slurry at speeds too close to the settling velocity. If the suction and discharge lines of the pump become closed or blocked, and the impeller continues to spin in the volute, the resulting energy input to the liquid may cause the liquid to heat up and generate steam that is at pressures greater than the casing burst pressure, which can trigger an explosion.

This paper presents a collection of global case examples of safety incidents involving pumps, offering insights into their causes and subsequent effects. Additionally, it evaluates the existing solutions implemented across the industry to mitigate safety incidents, considering various stages from design to operation. Through this evaluation, significant shortcomings in the current methods are identified and validated.

Furthermore, the advent of digitalisation has revolutionised pump monitoring and maintenance practices, promising significant improvements in pump safety. Using sensors and monitoring systems, pumps can undergo continuous surveillance to detect any potential failures. This proactive approach enables timely maintenance and repairs, thereby preventing catastrophic failure from occurring.

INTRODUCTION

Slurry pumps play a pivotal role in numerous industries, such as mining, agriculture, and wastewater treatment, due to their ability to handle abrasive and corrosive substances. These pumps are specifically engineered to withstand and effectively manage challenging materials, making them indispensable in various industrial processes. Given the paramount importance of safety in industrial settings, it is crucial that the equipment employed meets stringent safety standards to ensure its suitability for the intended purpose. Where the equipment is continuously monitored it is closer to meeting the safety standards in vigour. Digitalisation brings equipment significantly closer to meeting those safety standards.

Various methodologies have been developed to assist Original Equipment Manufacturers (OEM) ensuring safety in their designs for intended use. One such method involves adopting a life cycle perspective, which involves considering the required safety-related aspects throughout each phase of the equipment's lifespan (Rausand & Utne 2009). A product's life cycle encompasses its conception, development, operation, and eventual disposal (Hammer 1993).

In broad terms, the life cycle model, seen from a manufacturer's point of view, can be broken down into three stages, namely pre-development (Stage I), development (Stage II), and post-development (Stage III). At each stage, the relevant safety legislation and applicable safety standards are taken into consideration. Moreover, all risk assessments are carried out taking into account the consequences of identified hazards and their associated probabilities of occurrence.

In this article the emphasis is on Stage III, which can be broken into several sub-phases (ISO 12100-1). The key sub-phases involve transport, assembly, installation, commissioning, use and decommissioning. In particular the sub-phase "use" includes the setting, teaching/programming or process changeover, operation, cleaning, fault identification and maintenance. Similarly, with the decommissioning sub-phase, the process entails the careful dismantling and, with a focus on safety, the proper disposal of the equipment. More specifically, the focus here is on the Operation sub-phase of the Stage III, Post-development – Use of the pump. During this phase, the associated explosion risk of running a pump with blockages in the suction and discharge is highlighted. Published case studies are reviewed with the objective to identifying common causes and proposing ways to mitigate them.

Since these blockages are not caused by the pump itself, but rather by the system in which the pump operates, all pump OEM's highlight this risk very clearly in their Installation, Operations and Maintenance Manuals. However, the authors contend that the proliferation of cost-affordable sensors and the dawning of the Digitalisation era opens doors to greatly improve pump operational safety.

PUMP FAILURES—EXPLOSIONS

Why do simultaneous blockage of both the suction and discharge of a pump lead to a potential explosion risk when the pump continues to run?

When the flow rate is zero, the continued energy input builds up as heat in the fluid trapped within the pump. If this heat cannot be conducted out fast enough, typically through the pump's casing, then fluid will continue to heat up, with a commensurate increase in pressure inside the pump. If left unchecked, the pressure can reach a level higher than the burst pressure of the pump case. Once this happens, the release will cause the internal pressure to drop below the liquid's boiling point, resulting in a sudden conversion of the liquid into a rapidly expanding gas (Kevin G. Stricklin, Neal H. Merrifield & Linda F. Zeiler 2011). This is known as a Boiling Liquid Expanding Vapor Explosion (BLEVE). An exploded casing of a slurry pump is shown in Figure 1A.

Water hammering is another cause of explosive pump failures. This failure arises from abrupt velocity changes experienced by the fluid flowing through the pump (Kevin G. Stricklin, Neal H.

Merrifield & Linda F. Zeiler 2011). The energy release in such an explosion can be quite significant and violent, carrying a high probability of causing serious harm or even fatality. Water hammer pressure surge is known to release far less energy than the burst of a pump case due to over pressure. A water hammer event on slurry pump is illustrated in Figure 1B.

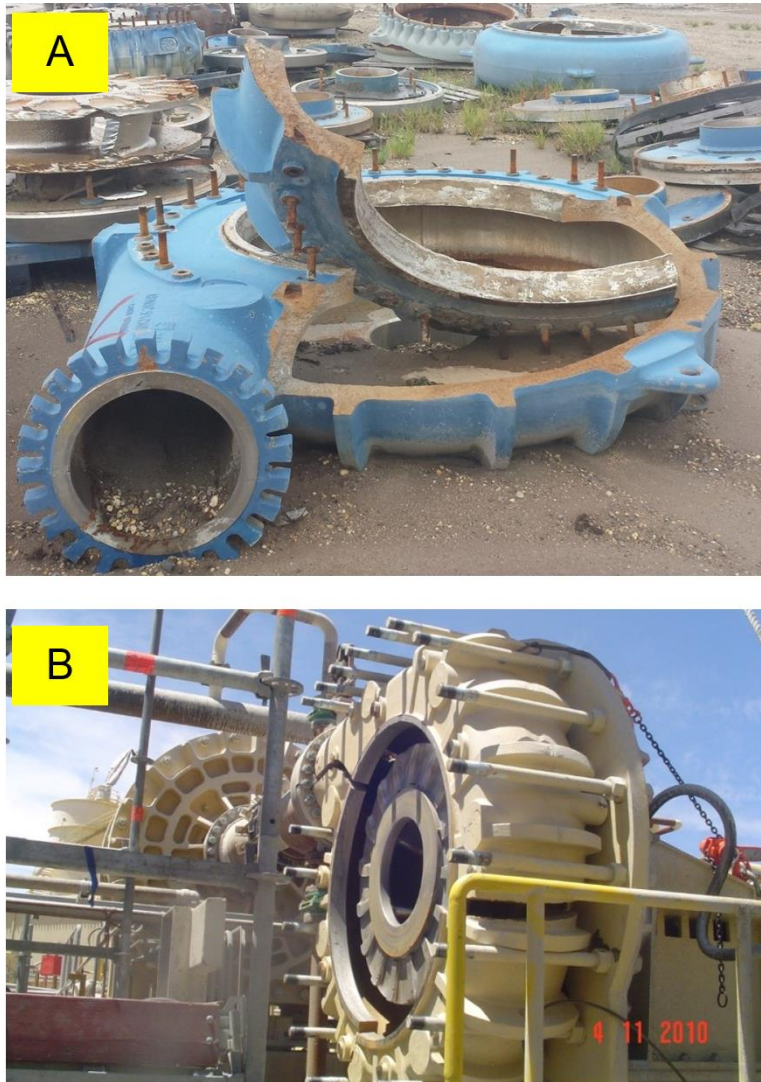






Figure 1: (a) slurry pump exploded casing (GIW Industries 2017) and (b) 20 x 18 MillMax HP pump after water hammer event (Crawford & Bessett 2019)




Case Studies


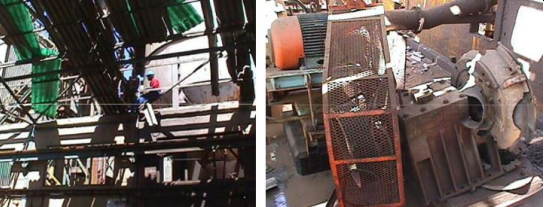

In this section, a number of pump failure cases are described in Table 1. When possible, the consequences and causes of the failures are highlighted. The data was obtained from published incidents and from internal Metso documentation and covers a period of 1999-2022.



Table 1: Global examples of pump failures, their effects and causes



No.	Pump type	Country	Description	Injury	Damage	Root Cause	Photos	Reference
1	Slurry	Australia	Modification to the PLC code incorrectly allowed the pump to continue running outside its designated automatic start/stop sequence, with suction and discharge valves closed. The slurry inside got superheated and resulted in an explosion.		x	Operator Error & Blockage		(Queensland Government 2017)
2	Slurry	Australia	Hot water sprayed the operator when he went to remove the outlet hose due to the pump not operating correctly. A possible cause was the inlet foot valve was buried in fine material, which blocked the inlet. Any blockage to the flow into any pump impeller will cause its contents to heat. Operator received 2 nd degree burns to both thighs and wrists.	x	x	Blockage		(Sneddon 1999)
3	Water	Australia	A worker was seriously burnt from hot water when a hose blew off due the closing of a remotely operated controlled valve. Water heated up due to the system design that kept water recirculating through the pump.	x		Blockage		(Regan 2002)



No.	Pump type	Country	Description	Injury	Damage	Root Cause	Photos	Reference
4	Slurry	Australia	A 200 mm inlet pump, in multistage operation, burst.		x			
5	Slurry	Australia	A water hammer incident on a multistage application, where pressure spikes were a risk. The spikes were greater than the maximum pressure capacity of pump.		x	Water hammer		



No.	Pump type	Country	Description	Injury	Damage	Root Cause	Photos	Reference
6	Slurry	Brazil	A 150mm inlet slurry pump exploded after running against a blocked discharge for over an hour.		x	Blockage		
7	Slurry	France	A combination of flange loading, and a water hammer incident were identified as causes.		x	Water hammer		
8	Slurry	Jamaica	The slurry pump operated against closed valve.	x	x	Blockage		
9	Slurry	Liberia	A 14/12 rubber lined slurry pump exploded, shattering the pump house roof.		x			(Connor 2003; Keto Pumps 2017; O'Connor

No.	Pump type	Country	Description	Injury	Damage	Root Cause	Photos	Reference
								2006)
10	Slurry	Kazakhstan	A pump was operated with a closed valve or blocked discharge pipe for 2.5 hours. Slurry in the casing would have superheated above boiling point.		x	Blockage		
11	Slurry	Namibia	A large sand transfer pump exploded. Pieces of the pump was found more than 100m from the building, the roof of which shattered. The force ripped the pump pedestal off its base.		x			(Connor 2003; Keto Pumps 2017; O'Connor 2006)
12	Slurry	Namibia	A slimes transfer pump exploded at the Namdeb diamond mine		x			(Connor 2003; Keto Pumps 2017; O'Connor 2006)
13	General	South Africa	The mill return pump exploded when the suction was blocked by a piece of conveyor belting used to line the feed sump.		x	Blockage		(Connor 2003; Keto Pumps 2017; O'Connor 2006)

No.	Pump type	Country	Description	Injury	Damage	Root Cause	Photos	Reference
14	General	South Africa	The cyanide transfer pump exploded after the operator started the pump without checking the status of the suction and the discharge valves, which were closed.		x	Blockage		(Connor 2003; Keto Pumps 2017; O'Connor 2006)
15	General	South Africa	A calcine water pump exploded when it was started with both suction and discharge valves closed. The incident was after power failure, and it was a simple case of the operator starting the wrong pump. The force of explosion ripped the pump body off its base and fractured the rear half of casing.		x	Blockage		(Connor 2003; Keto Pumps 2017; O'Connor 2006)
16	Slurry	South Africa	A carbon transfer pump was started with both suction and discharge lines choked with carbon. The bolts holding the casing failed. As a result, the casing opened up. An engineering apprentice working nearby was hit in the face and arms with hot carbon particles.	x	x	Blockage		(Connor 2003; Keto Pumps 2017; O'Connor 2006)
17	Slurry	South Africa	UG2 transfer pump exploded. The operator, standing on the flange of the discharge line, lost three toes.	x	x			(Connor 2003; Keto Pumps 2017; O'Connor 2006)

No.	Pump type	Country	Description	Injury	Damage	Root Cause	Photos	Reference
								
18	General	Tanzania	The explosion occurred as operators had closed the suction and discharge valves on a standby pump without tagging out the unit. Control started the standby pump remotely, not knowing that the valves were shut.		x	Blockage		(Connor 2003; Keto Pumps 2017; O'Connor 2006)
19	General	USA	A chilled water circuit brine pump at a US Nuclear defence facility was inadvertently started with valves closed. Within two hours, it exploded.	x	x	Blockage		(Connor 2003; Keto Pumps 2017; O'Connor 2006)
20	Slurry	USA	A sand pump exploded when the suction and discharge were blocked. A miner standing 10m away was seriously injured.	x	x	Blockage		(Connor 2003; Keto Pumps 2017; O'Connor 2006)

No.	Pump type	Country	Description	Injury	Damage	Root Cause	Photos	Reference
21	Slurry	USA	A fine coal transfer pump became blocked after standing for two days. It was started without gland service water and quickly overheated. When the operator stopped the pump, the gland service water entered the red-hot all-metal casing creating steam. The resulting explosion killed the operator.	x	x			(Connor 2003; Keto Pumps 2017; O'Connor 2006)
22	General	USA	An unspecified incident occurred at an underground mine that caused an explosion. The explosion was felt 280m away. 80kg of the pump material could not be found during the clean-up operation.		x			(Connor 2003; Keto Pumps 2017; O'Connor 2006)
23	Slurry	USA	A 350mm inlet slurry pump exploded, hitting the roof. Pieces were found far away.		x			

No.	Pump type	Country	Description	Injury	Damage	Root Cause	Photos	Reference
24	Sludge		The pump was started remotely, without a proper field check against closed valves.		x	Blockage	 Figure 6. Close-up of Damaged Head	(Giles & Lodal 2001)
25	Condensate		The pump was operated with both suction and discharge valve in the closed position.		x	Blockage	 Figure 7. Damaged Motor and Baseplate	(Giles & Lodal 2001)

Observations

From the previously described case studies, it is evident that incorrect operation of pump systems can result in explosions, causing damage to property, loss of production and in some cases might potentially even lead to severe injury or even loss of life. All explosions where BLEVE events occurred were caused by obstruction of both the suction and discharge sides of the pumps. One of the root causes of this obstruction is the inadvertent closing of both the intake and discharge valves. With the high level of automation of plants these days it is therefore critical to make sure automated valves are properly interlocked preventing starting pumps remotely against closed valves. However specific to slurry pumps, unlike clear liquid pumps, this obstruction can also be caused by blockage. This blockage can occur in a slurry pipeline from operation of the pipeline at sub critical velocity or with high solids concentration above design, large debris, pipeline starting and stopping, pipe liner collapse, reducing pump speed to a level that causes particles to settle in pipelines (Burgess 2005). It is therefore important to consider this blocking especially due to increasing use of variable speed drives where control of speed is possible and if speed is reduced to an extent where flow stops or plugs the line. In addition, use of mechanical seals in lieu of gland packing that has burst pressure exceeding casing burst pressure hence, transferring the weak link to pump (Keto Pumps 2017).

To contextualise the gathered data in a meaningful way; the authors decided to use the data and carry out a Risk Assessment to determine the Level of Risk using a typical generic Risk Matrix shown in Figure 2, as is commonly used in best practise safety systems. For clarity, the process and rating decided on is briefly described forthwith:

- The level of risk is determined by evaluating both the Consequence of the identified hazard (pump suction and discharge obstruction, leading to a pump explosion) and the Probability of the hazard happening.
- Probability: The data gathered identifies 23 explosion cases over 23 years. The period in question is very long and captures major events but it establishes that not all cases are documented. For example, the work of O'Connor (2006) states an average of one explosion per year at an AngloGold Metallurgical operation in South Africa. However, these specific cases are not listed in the previous tables, nor are there any recorded explosions in countries such as China or India in nearly a quarter of a century. This supports the claim that the explosion rate of pumps is greater than 1 per year. Notably, the analysis excludes the two cases attributed to water hammer incidents. Furthermore, it is about how safe the operation wants to be. A single fatality is Extreme. Many fatalities become catastrophic. While the probability of fatality may appear low if it is evaluated over the total number of pumps. The probability grows considerably if evaluated over the number of pumps with blockages. Therefore, the probability of an explosion occurring is significant and one can even argue that these incidents are not rare or unlikely, and fortunately they are not common, leaving only two options: Possible and Likely.
- Consequence: There is no doubt, considering the recorded fatalities and serious injuries (including limb losses) indicated in Table 1, that the consequences must be categorised as Major, at the very least.

The resulting Risk Level identified is Extreme. It is clear that the consequences of pump explosion should not be taken lightly and further efforts are needed to identify measures that prioritise the safety of individuals.

Risk Matrix					
PROBABILITY (How Often?)	Consequence or Hazard Effect RISK RATING				
	INSIGNIFICANT	MINOR	MODERATE	MAJOR	CATASTROPHIC
Almost Certain	M	H	H	E	E
Likely	M	M	H	E	E
Possible	L	M	M	E	E
Unlikely	L	L	M	H	E
Rare	L	L	M	H	H
Level of Risk	Low	Medium	High	Extreme	
Loss Type	Insignificant	Minor	Moderate	Major	Catastrophic
Harm to People (Safety / Health)	First aid Exposure to minor health risk	Medical treatment Exposure to major health risk	Lost time Reversible impact on health	Single Fatality Loss of quality of life Irreversible impact on health	Multiple fatalities Impact on health ultimately fatal
Environmental Impact	Insignificant environmental harm*	Minor environmental harm*	Moderate environmental harm*	Major environmental harm*	Catastrophic environmental harm*
Probability	Almost certain	Likely	Possible	Unlikely	Rare
	Expected to occur	Will occur occasionally	May occur	Not expected to occur	Requires unusual chain of events



Figure 2: Slurry pump explosion case risk rating

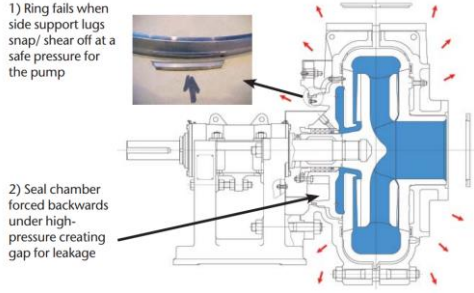
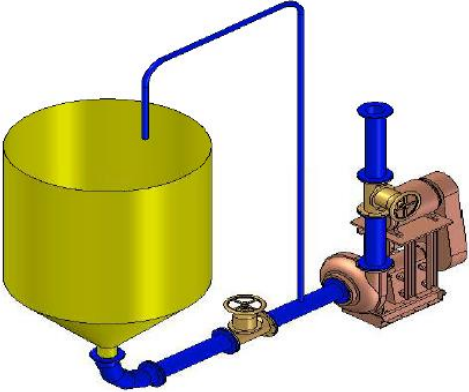
SOLUTIONS

The number of pump safety incidents has led many engineers and researchers to investigate and develop possible solution to eliminate or, at least, reduce the risk of further occurrences. Connor (2003) and O'Connor (2006) conducted multiple investigations, ranging from current detection, pressure sensing, temperature monitoring, strain gauges, pressure relief valves, rupture discs, fusible plugs, graphite bursting discs and standpipe or flow bypass pipeline. Also, Burgess (2005) reviewed and developed pump designs to incorporate a thermal cut-out device and pressure relief failure ring, with a focus on processes that use high temperature slurries. A list of identified solutions is presented in Table 2.

Table 2: Pump safety solutions

No	Detection means	Description	Limitation	Reliability	Reference
1	Current detection	It is assumed that the motor current drops when the valves are closed or the pump is blocked. Upon testing on various sizes, the current draw varied from pump to pump, with no apparent relationship.	Technical	Poor	(Connor 2003; O'Connor 2006)
2	Pressure sensor	The use of pressure switches, fitted at the suction and discharge pipes. This solution if acceptable for clear and process water, however slurry, carbon, acids, and other chemicals introduce problems such as sensor port blockage. The cost is also a factor.	Technical, cost & susceptible to damage	Poor	(Burgess 2005; Connor 2003; O'Connor 2006)

No	Detection means	Description	Limitation	Reliability	Reference
3	Temperature sensor	Probes are installed to measure the temperature. The probes carry the risk that the slurry will block them, but they are a better option than pressure sensors due to their faster response when valves are closed. The cost can be factor.	Cost & susceptible to damage	Poor	Connor 2003; O'Connor 2006)
4	Thermal cut-out	A thermal cut-out device can be mounted through the pump outer casing. They measure the temperature on the outside of the metal liner or case. They can be set to cut-off the power supply to the motor when the temperature exceeds a safe critical level. By design, the pressure remains below dangerous levels, even at the set critical temperature.	Metal only	Good for metal lined pumps	(Burgess 2005)
5	Rupture disc	Rupture discs are mechanical safety devices for pressure relief. They are used in petrochemical industries. Their fragile construction and high cost are factors limiting their use. 	Cost & fragile	Poor	Connor 2003; O'Connor 2006)
6	Fusible plugs	Fusible plugs are devices that offer relief when a set temperature is exceeded. The lowest response temperature was 80 °C and is much too close to the boiling temperatures. As for the pressure plugs, they are like rupture discs.	Cost, availability & fragile	Poor	Connor 2003; O'Connor 2006)
7	Graphite bursting discs	These are graphite discs, with a centre machined out to give the desired pressure rating. The bursting discs should be located on the suction line, as close to the pump inlet as possible. Problems during installation can cause them to fail below their rated pressure. 	Fragile	Poor or medium	(Burgess 2005; Connor 2003; O'Connor 2006)
8	Strain gauges	Strain gauges are added to the casing to monitor deformation, which are a precursor to an explosion. They were not suitable as the casings are cast iron and have non-linear stress/strain relationship.	Technical	Poor	(Connor 2003)
9	Pressure relief valve	Used in process industries where every boiler has one fitted to 10% above the maximum working pressure. This can be very reliable solution as they can handle	Cost	Poor or medium	(Burgess 2005; O'Connor 2006)

No	Detection means	Description	Limitation	Reliability	Reference
		both temperature and pressure. However, they come at a high cost.			
10	Pressure relief failure ring	<p>A ring is designed to fail in shear at a pressure approximately 20% greater than the maximum allowable working pressure. This allows fluid, steam and slurry to escape out the back of the pump. This material is contained within the pump by guarding and is discharged downwards to the ground between the casing and the base.</p> 	Cost & metal only	Good	(Burgess 2005)
11	Sandpipe	<p>For simple installations, where the pump is fed from a tank or hopper, a 50mm standpipe can be welded into the suction pipe. It is placed immediately before the pump so it can relieve directly back to the tank in cases of over-pressure.</p> 	Scalability	Poor or medium	(Burgess 2005; Connor 2003; O'Connor 2006)
12	Vibration sensor	The operating characteristics of a blocked pump are assumed to differ from that of a normal operating pump. Consequently, the vibrational signatures are assumed to be different and measurable.	Technical	Good	
13	Flow meter	Flow meters directly measure the rate of material flowing through the pumps. If the rate falls below a set value, the operator can be warned of the possible onset of a dangerous pressure condition.	Technical & cost	Good	
14	Pump power	Monitoring pump power can identify a zero-flow condition where the shut head pump	Technical & Cost	Medium	

No	Detection means	Description	Limitation	Reliability	Reference
		power shows greatly reduced power consumption than normal.			

The catastrophic failures described in the cases studies can be mitigated by directly detecting the root causes: blockages and water hammering. The root causes can be detected by using the solutions proposed in Table 2. Although many options are presented, the US Mine Safety and Health Administration recommends using either (1) direct flow measurements, (2) pump motor current measurements, and/or (3) pump temperature measurement to identify dangerous pump conditions (Kevin G. Stricklin, Neal H. Merrifield & Linda F. Zeiler 2011)

Digitalisation

Digitalisation has transformed the monitoring and maintenance of pumps, promising advancements in pump safety. By leveraging sensors and monitoring systems, pumps can now be subject to continuous monitoring to detect any potential failures. This enables proactive actions, effectively preventing catastrophic failures from taking place.

Considering this, it is suggested to:

1. Add sensors such as flow, current or temperature sensors,
2. Consume as much of the data as possible. If you measure it, use it. The data is valuable enough for it to have been measured.
3. Define relevant metrics and derived quantities such as safety alerts defined from exceeded temperatures, insufficient flows, etc.
4. Define a decision framework where action can be triggered by the actionable information. The actions are defined interventions meant to keep the pump safe.
5. Assign champions for all the information. Who is the custodian for the safety alerts?

Nazari and Cristonffanini (2019) have explored digitalisation to identify pipe sanding in a gold mineral processing plant in North America. The authors created a digital twin of a Hydrocyclone Feed Pump and Thickener Underflow Pump using virtual densitometer and compare it with a physical densitometer in the line. When sudden deviation between physical and virtual readings occurs, it indicates development of pipe sanding and advance process control can increase pump speed to temporarily wash out the precipitated slurry. This saves from complete blockage of suction or discharge line and an explosion event (Canadian Institute of Mining 2018; Schug et al. 2019).

As the adage goes, “you can’t control what you can’t measure” (DeMarco 1982). The indication is there a significant gap in what can be measured and what is presently measured. That is why these incidents persist even though the ability to identify them exists. This is especially true for the pump’s operational phase, where there is a continual struggle to get good verifiable data—Big Data remains a myth in this case. It is not an impossibility. With adequate resources, an appropriate measurement system mated to a proper digital infrastructure can protect the pump and its operator. Moreover, the data can inform the Design phase, enhancing the continual improvement of the pump, as illustrated in Figure 3.

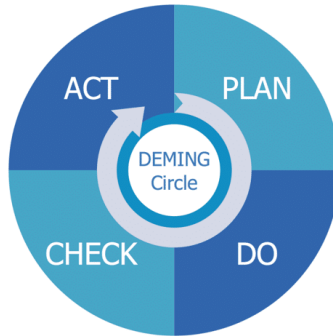


Figure 3: Continual pump improvement model

CONCLUSIONS

This paper provides a general overview of safety incidents involving pumps, and exploring the causes and effects of their explosion. It includes a brief evaluation of current solutions employed in the industry to mitigate safety incidents throughout the design and operation phases. Although shortcomings in the current methods are identified, practical recommendations are provided to improve slurry pump safety. Since digitalisation is revolutionising the way pumps are monitored and maintained, it can be leveraged to enhance pump safety. Using sensors and monitoring systems, pumps can be continuously monitored for potential failures, allowing for proactive maintenance and repairs before catastrophic failures occur.

ACKNOWLEDGEMENTS

The authors are grateful for the support from many individuals and organisations who have contributed to this research. In particular, Metso Corporation and the University of Western Australia for their collaboration. Special thanks to Alan Dennis from Metso plant solutions team for providing good practices in design of mineral processing plants, and to pump sales and service team members in Metso who collected various case examples over the years.

REFERENCES

- Burgess, KE 2005, 'Centrifugal Slurry Pump Design for Safety', paper presented to International Conference on Engineering Design, ICED 05 Melbourne, <https://www.designsociety.org/publication/22997/Centrifugal+Slurry+Pump+Design+for+Safety>.
- Canadian Institute of Mining, MaP 2018, *Digital twins in mining and mineral processing - Sohail Nazari presents at McEwen Mining*, Canadian Institute of Mining, Metallurgy and Petroleum, McEwen Mining, https://www.youtube.com/watch?v=R_O8f9bSfio&ab_channel=CanadianInstituteofMining%2CMetallurgyandPetroleum.
- Connor, BPO 2003, 'Centrifugal Pump Explosions', *Rise of the Machines - The 'State of the Art' in Mining Mechanisation, Automation, Hydraulic Transportation and Communications*, <http://www.saimm.co.za/Conferences/RiseOfMachines/022-O'Connor.pdf>.
- Crawford, J & Bessett, N 2019, 'Development of centrifugal slurry pumps in tailings disposal and comparison with positive displacement pumps', *Proceedings of the 22nd International Conference on Paste, Thickened and Filtered Tailings*.
- DeMarco, T 1982, *Controlling Software Projects: Management, Measurement & Estimation*, Yourdon Press.

Giles, DS & Lodal, PN 2001, 'Case histories of pump explosions while running isolated', *Process Safety Progress*, vol. 20, no. 2, pp. 152-6.

GIW Industries 2017, *Catastrophic Slurry Pump Cavitation — and How to Avoid It*, KSB, <<https://giw.ksb.com/blog/catastrophic-slurry-pump-cavitation>>.

Hammer, W 1993, *Product Safety Management and Engineering*, 2 edn, American Society of Safety Engineers, Des Plaines, Ill.

ISO 2010, *ISO 12100:2010 Safety of machinery — General principles for design — Risk assessment and risk reduction*, ISO, <<https://www.iso.org/standard/51528.html>>.

Keto Pumps 2017, 'Centrifugal Pump Explosions', *Green Paper*, <<https://www.ketopumps.com/media/1342/keto-green-paper-centrifugal-pump-explosions.pdf>>.

USDo Labor 2011, *Potential Safety Hazard Related to Explosion of Pumps*, by Kevin G. Stricklin, Neal H. Merrifield & Linda F. Zeiler, U.S. Department of Labor, <<https://arlweb.msha.gov/regs/complian/PIB/2011/pib11-32.asp>>.

Nazari, S & Cristonffanini, C 2019, 'Digital Twin in Mineral Processing', paper presented to 51st Annual Canadian Mineral Processors Operators Conference, Ottawa, Ontario, January 22-24, <<https://www-onemine-org.ezproxy.library.uwa.edu.au/document/document.cfm?docid=242895&docorgid=15>>.

O'Connor, BP 2006, 'Centrifugal Pump Explosions', *"Rise of the machines"*, <file:///C:/Users/alanj/Downloads/Centrifugal%20Pump%20Explosions.pdf>.

Sa Health 2017, *Slurry Pump Explosion*, by Queensland Government, 1 edn, Queensland Government, <<https://www.dnrme.qld.gov.au/business/mining/safety-and-health/alerts-and-bulletins/mines-safety/slurry-pump-explosion>>.

Rausand, M & Utne, IB 2009, 'Product safety – Principles and practices in a life cycle perspective', *Safety science*, vol. 47, no. 7, pp. 939-47.

MRNS Wales 2002, *Hot water from pump burns quarry worker*, by Regan, R, New South Wales, <http://www.dpi.nsw.gov.au/_data/assets/pdf_file/0003/66918/Safety-Alert-02-09-Hot-Water-from-Pump-Burns-Quarry-Worker.pdf>.

Schug, B, Anderson, C, Nazari, S & Cristoffanini, C 2019, 'Real world improvement through virtual instrumentation at OceanaGold Haile', paper presented to Technology, 03 February 2021, <<https://www-onemine-org.ezproxy.library.uwa.edu.au/document/document.cfm?docid=247528&docorgid=10>>.

SE Mine 1999, *Serious Accident Involving a Pump*, by Sneddon, N, Mineral Resources New South Wales, <https://resourcesandgeoscience.nsw.gov.au/_data/assets/pdf_file/0003/67026/Safety-Alert-99-02-Serious-accident-involving-a-pump.pdf>.

Filtered Tailings – a Copper Experience.

L. Vimercati¹ and R. Williams²

1. Process Engineer, DiefenbachSrl, Bergamo Italy 24020. Email: l.vimercati@diefenbachsrl.com
2. Business Development Manager, McLanahan Corp, Wangara WA6023, Australia: Email: rwilliams@mclanahan.com.au

ABSTRACT

Filtered tailings are becoming more common across several operations and commodities (including copper, bauxite, nickel, gold and iron ore) and is often a key expectation of the communities in which the resources sector operates.

A wrong filter press sizing can create a bottleneck on the plant line, causing problems that can affect both the upstream and downstream processes.

During the selection phase, smaller filtration equipment may be considered however when filtering tailings the volumes are normally very high and variable. The filtration of concentrates is relatively easy in comparison due to more consistent mineralogy and size distribution, whereas all the gangue ends up in tailings making the filtration of tailings more variable.

INTRODUCTION

Transitioning to a greener future requires the resources sector to adopt more sustainable practices.

Filtered tailings are become a key expectation of the communities we operate in and are growing in a number of mining commodities including copper, bauxite, nickel, gold and iron ore.

The filtration technologies required range from dewatering screens to vacuum and pressure filters. Particular challenges faced in copper applications include large scale which means several units of large size are often required. In addition, a high specific gravity that cause sedimentation issues and a high abrasion index make demands on achieving filter availability levels above 90%.

To ensure the proper process plant operations a correct equipment sizing is essential. While seeming obvious the key equipment is sometimes considered a smaller item and can be subject to “value engineering” optimisation. A wrong filter press sizing can create a bottleneck on the plant line, causing problems that can affect both the upstream and downstream processes.

The accessories required and often supplied with the filter have to be sized in order to be suitable for the filtration target. A filter press is able to reach very high performance in terms of cake dryness however a number of variables need to be assessed and considered to reach optimal efficiency.

These include:

- Chamber thickness;
- Feed pressure;
- Membrane or recessed chamber;
- Cloths wash pressure and frequency;
- Cake wash requirements;
- Cloth type.

It is important to carry out testing to select the most appropriate combination of all these process parameters.

Once the key process requirements are established: machine availability, layout and power consumption must then be considered key points to be able to economically hit the target that is the tailings flow rate treated to obtain a product that can be dry stacked.

There are a series of selection criteria that can have impact on both capital and operating costs.

The following should all be considered:

1. Filter press designs commonly come in overhead beam or side beam configurations. A major advantage of the overhead beam style is the ability to hang a large number of plates (over 200) off the robust central support. This, combined with a single plate opening device, provides very high filtration area in a compact footprint reducing building costs. Side beam filters can offer a faster opening mechanism to allow reduction on cycle times but this can bring about additional opex through faster filter wear.
2. Throughput considerations will affect the selection of both number of chambers and the plate size. Due to larger volumes tailings filters typically utilise 1500, 2000 or 2500mm sized plates and while most filter press manufacturers are designing for larger units, these have not yet proven a cost-effective alternative.
3. The requirement (or not) to provide cake drying via compressed air can offer an advantage over the use of membrane plates but the power consumption of large air compressors can be an additional opex burden.
4. A key requirement is the selection of the filter feeding pump. This is a challenging duty requiring initially high-flow low-head but as the cycle advances this changes to a low-flow high-head one.
5. Another main factor is the necessity of a high-pressure cloth wash system. The high-pressure cloth wash installation will affect the initial cost for the equipment but decrease the opex related to the changing of cloths. If a spare filter press is not available then extra capacity has to be considered in order to make up for the time lost during the wash cycles. This option reduces the cloths change frequency and associated costs.
6. Linked to the cloth washing described, cloths change is an important aspect. There are different types of cloth installation systems, the target is to enable a fast installation type also on overhead beam filter presses in order to decrease maintenance time and any downtime caused by cloths failure.

This paper describes how these considerations were assessed for a specific case in a copper plant in Dominican Republic shown in aerial view in Figure 1.



Figure 4 Aerial view of the Dominican Republic filtration plant

CASE STUDY - Copper tailings dewatering and stacking plant

The copper tailings plant for this case study is in the Dominican Republic, the start-up was in 2021. The plant includes three filter presses 1500 x 1500 with 110 plates installed, suitable to treat almost 230 tph of dry solids, shown in Figure 2.



Figure 5 Filter presses installation for copper tailings treatment.

In addition to the filters the plant includes:

- Cloths washing skid, one in common with three filters;
- Drip trays;
- Inlet flow meters;
- Feed pumps and flushing systems;

- Filtrate and core blow discharge buffer tank and booster pump;
- Slurry thickener.

FILTER SIZING

Filter sizing was made starting from the requirements of the customer to treat 228 tph and from information obtained from lab tests:

- Slurry solids % [w/w]: 50%;
- Slurry solids % [v/v]: 22%;
- Solid SG [g/cm³]: 3.57;
- Liquid SG [kg/dm³]: 1.00;
- Slurry SG [kg/dm³]: 1.56;
- Overall cycle time [hh.mm.ss]: 00:16:12;
- Final cake moisture % [w/w]: 16%;
- Wet cake density [kg/dm³]: 2.55;
- Dry cake density [kg/dm³]: 2.15 (after cake drying).

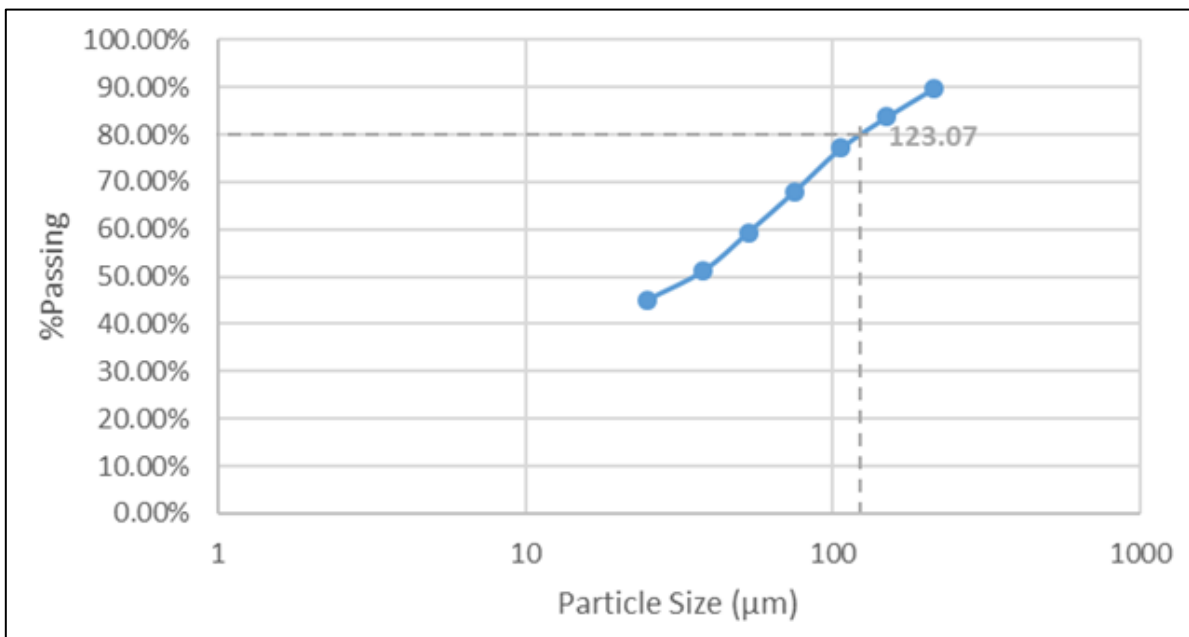


Figure 6 Slurry PSD.

Laboratory and pilot test

The slurry test includes two different scales: lab and pilot.

The lab test requires a low quantity of product and can frame all main parameters as:

- Slurry
 - Specific weight;
 - Solids concentration;
 - pH;

- Temperature;
- Particle Size Distribution (PSD) as shown in Figure 3.
- Process
 - Chamber thickness;
 - Chamber type;
 - Filtration pressure;
 - Cake washing water quantity and efficiency;
 - Cake blowing air quantity and pressure;
 - Squeezing coefficient and pressure;
 - Cloths selection;
 - Phase times;
 - Slurry conditioning.
- Cake and filtrate
 - Specific weight;
 - Final moisture;
 - Filtrate quality.

Results obtained from the lab skid shown in Figure 5 are scalable and data obtained can be used for industrial sizing.

All data obtained from a lab test can be verified at pilot scale.



Figure 7 Laboratory skid and pilot skid.

Using the information provided in this paper and considering some sizing factors the necessary filter presses total volume was 28.75 m³.

- Cake volume for each filter: 9,583 m³;
- Total wet cake for each cycle: 73.31 tonne;
- Total dry cake for each cycle: 61.58 tonne.

An important parameter for filling and filtration time is slurry flowrate.

This slurry has two main physical characteristics which are in conflict with each other:

- High abrasion level;
- High density.

These two conditions mean that an equilibrium condition must be found so that the solids do not settle in the pipes and, at the same time, the wear of the parts in contact with the slurry is reduced.

The identified value was between 2.65 and 3.00 m/s, avoiding having solids settling and reducing wear on pumps, piping, valves and cloths.

The maximum flowrate reached during the filling and filtering phase was between 160-180 m³/h for each filter, considering an inlet diameter for each feeding side of DN150.

In this case the inlet diameter was set by filter plates that have a DN150 hole but flowrate could be increased with a different plate design.

With this setting the cloths lifetime can be extended and opex reduced.



Figure 8 Slurry feeding pumps and flushing systems.

Slurry pump design data was:

- Maximum flowrate: 160-180 m³/h
- Maximum pressure: 13-15 bar
- Installed power: 55 kW



Figure 10 Operating cloth washer.

Considering 1.5 min per plate the overall washing cycle is about 2.75 hours for each filter.

The HP washing cycle is not performed every cycle, usually once or twice per week (some special cases may need one cycle per day).

Considering the washing cycle time, the design filter press volume is higher to be able to treat the inlet flowrate in less time. This increased capex cost is justified by the decreased opex cloths cost:

- Cloth lifetime about 1500-2000 cycles
- Cloth costs about 150-220 euro each
- About 25 000 euro for a set of cloths for one filter.

The high performance of the washer device and its skid can guarantee a good restoration of cloths filtering efficiency and an increase of their lifetime.

Design data

The washing skid shown in Figure 8 has the following data:

- Pump flow rate: 170 l/min
- Number of nozzles installed on washer arm: 46
- Water pressure: 100 bar
- Water tank: 1500 L
- Installed power: 37 kW

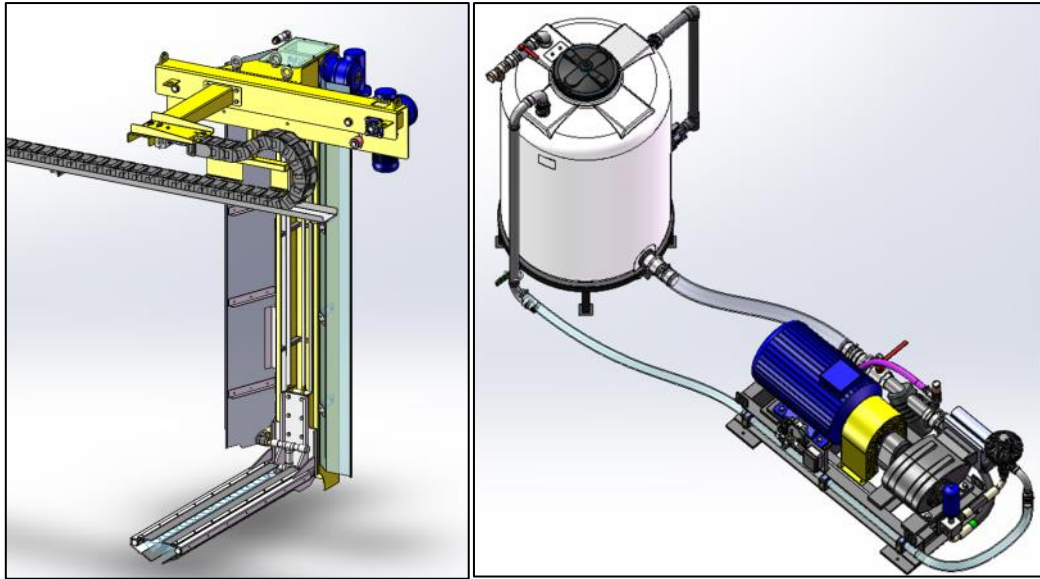


Figure 11 Cloths washing device and skid.

Cake discharge system

System installed on overhead beam is a “one by one”.

There are two different types, one with a trolley which moves inside the beam (7 sec/plate opening time) and one with hooks that grabs plates continuously (2.5 – 3 sec/plate).

The system installed on these filter presses is a continuous type with an average opening time of 2.7 sec/plate.

On new filters, following a detailed study we are now able to lower the opening time to 1.5 sec/plate on new filters. This improvement also provides a new cloth washer control logic.



Figure 12 Cake discharge.

COMMISSIONING

During commissioning the optimisation of variable parameters, also of items out of scope, was a key phase.

The first variable was the feeding pump, trying to save time during filling and flowrate the initial set point was too high with a filling flowrate higher than 180 m³/h. The wear on the cloths was acceptable but the high specific weight of the slurry (higher than declared) caused pumping issues.

To be able to reach filtration pressure with a good flowrate a more powerful motor would have been more suitable. A correct equilibrium was found by adjusting pump ramp-up with new values in terms of speed and pressure settings.



Figure 13 Cake discharged during commissioning.

Filter cloths were another key point. In order to hit the target the choice of the right cloth is critical. In this case, during commissioning, it was noticed that a cloths upgrade could improve performance. An increase of permeability would have a big impact on cake consistency and filtration time (Figure 10). A new set of cloths has been provided however at time of writing no performance data was available.

CONCLUSIONS

Dewatering by pressure filtration and dry stacking is expensive and is generally only adopted when less costly options are not available. The biggest challenge is to develop and improve filtering plants in order to minimise the costs optimizing utilities consumptions without losing sight of the goal and ensuring maximum reliability.

Practical experience has demonstrated pressure filtration to be viable for copper tailings. One of the key lessons learnt from this experience is to design the equipment taking into account the high abrasion anticipated. Neglecting this key aspect will lead to excessive operating costs.

Constant monitoring of the parameters and continuous research can lead to continuous optimisation of the operation of the plant and consequently to an improvement of the output product.

Real-Time Monitoring and Control of Gold Processing Plants

N Grigg¹, M Ntombela², B Wraith³ and A Lewis-Gray⁴

1. General Manager – Global Sales and Solutions, Gekko Systems, 321 Learmonth Road, Ballarat, VIC, NigelG@gekkos.com
2. Senior Process Engineer, Gekko Systems, 321 Learmonth Road, Ballarat, VIC, MxolisiN@gekkos.com
3. Senior Process Engineer, Gekko Systems, 321 Learmonth Road, Ballarat, VIC, Ben.Wraith@gekkos.com
4. Technical Director, Gekko Systems, 321 Learmonth Road, Ballarat, VIC, SandyG@gekkos.com

ABSTRACT

A range of real-time instruments for use in gold processing circuits has been developed in collaboration with Gekko Systems. These instruments, the OnLine Gold Analyser (OLGA) and Carbon Scout (CS) are used to measure and monitor metallurgical process parameters, including such as gold concentration, carbon concentration, slurry density, pH, dissolved oxygen, and gold loading on carbon in real-time. The output process data are mapped, visualised, and fed into process control platforms, enabling process plant operators and metallurgists to monitor and track critical operating factors. Installed in processing plants globally, these real-time instruments have been proven to benefit operators in plant performance and safety.

The OLGA, by measuring gold concentration and slurry density in real-time, provides operators with a quicker and more frequent turnaround time, enabling expedient metallurgical process control reactions. The CS, by monitoring and tracking carbon concentration in adsorption tanks, helps prevent adverse occurrences such as carbon leakage and provides more frequent and periodic gold-in-circuit data that would otherwise occur weekly or monthly. Additionally, the X-Ray Fluorescence (XRF) analyser on the CS creates opportunities for operators to track carbon loading in the circuit to maximise gold loading prior to elution.

This paper discusses installations where these real-time monitoring instruments have been in operation, providing notable value and benefits to the operators.

WHY REAL-TIME INSTRUMENTS?

Sensing, data artificial intelligence (AI), and automation in the mining industry is being introduced at a ramp-up rate. To help address these challenges, the automobile industry developments can provide lessons from its experience, to accelerate the application of digital capabilities, analysis, AI, and automation in the mining industry. It is critical particularly as access to skilled human resources becomes more difficult (Gray, 2022).

Instruments for process monitoring and control are common in mineral processing plants. These instruments include flow meters, pressure and temperature sensors, level sensors, pH and dissolved oxygen sensors, weightometers, load cells, and many other chemical and physical process instruments such as cyanide analysers and particle size distribution (PSD) analysers. While these provide real-time measurements of some parameters, the core critical measurements within the process are often not captured in real-time. Daily, shift, and/or periodic samples are often manually collected by operators and analysed at an on-site or off-site laboratory using common analytical assaying methods, leading to significant delays in obtaining data.

Carbon management, feed grade, and gold loading on carbon are examples of circuit data amongst many that are key and critical to an adequately operated gold processing plant. Operators often

sample the pulp and carbon at intervals that often vary across sites, while composite samples provide daily or shift results used partly for metal accounting and for process control. Staunton et al, 2017, discussed the optimisation of carbon-in-pulp/carbon-in-leach (CIP/CIL) circuits where the condition and management of carbon in these circuits are key factors prominent in circuit optimisation.

The CS samples slurry from the leach and adsorption tanks to measure carbon concentration (g/L), slurry density (%w/w or kg/L), slurry pH, dissolved oxygen (DO) levels (ppm), and gold loading on carbon (Au ppm). The consistent sample depth, large sample volume, frequent sampling cycle intervals, and easily accessible sampling and analysis stations offer superior returns to operators. Operators' safety is enhanced via the reduced frequency of on-tank activities (less exposure to the HCN⁻ environment) and the minimised number of manual handling tasks. Financial benefits include, but are not limited to, reduced gold solution losses due to improved carbon movement and carbon management across the adsorption circuit.

The OLGA measures gold concentration (Au ppm) and slurry density (%w/w or kg/L) on a slurry or solution stream and is well-suited for both leaching and flotation circuits. The online measurement is updated every 10 minutes as a 1-hour rolling average. This enables proactive process control towards reagent control, grade and impurities insights (e.g. arsenic content), and more importantly monitoring of untimely excursions.

Real-time instruments (RTI) provide outputs that are used in a process plant. These output measurements are used to control the process to ultimately optimise the process or a part of it; illustrated in Figure .



Figure 1 - Basic process control cycle

The concept of automating the leaching, adsorption, and flotation circuits is illustrated in Figure 2. Reagent addition, carbon movement, and plant feed rates are easily controlled using stream and circuit data from the RTIs. These measurements should be able to supplement, and in some cases replace, the manual sampling practices currently used.

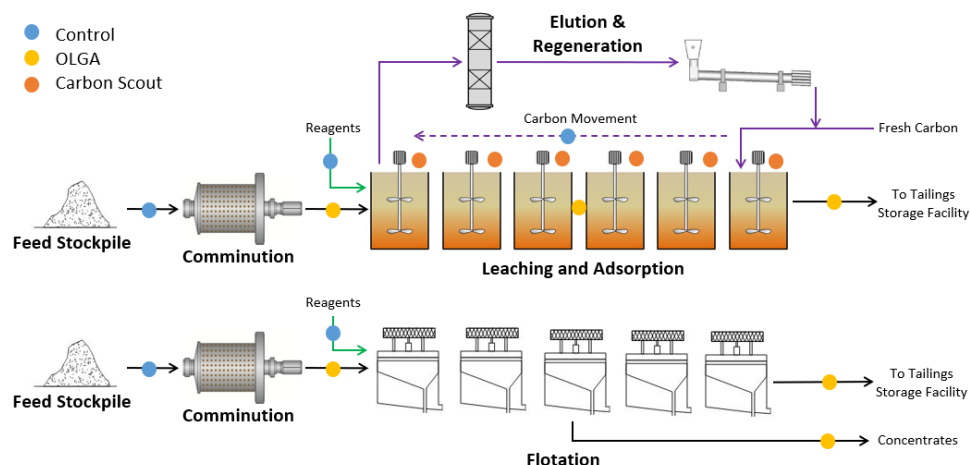


Figure 2 - Locations for OLGA and CS sampling and analysis points in leaching-adsorption and flotation circuits

Both the CS and OnLine Gold Analyser are examples of how real-time instruments can be utilised in gold processing plants, as sensing technologies, coupled together with Gekko Systems' Neon Analytics digital platform to achieve a fully automated real-time gold processing system (Gray, 2022). Figure 3 illustrates an example of one mining operation in Australia.



Figure 3 - Example of Neon Analytics platform pages for CS (top) and Carbon Movement Automation (bottom)

CARBON SCOUT

The CS was developed by Curtin University's Gold Processing Technology Group and commercialised by Gekko Systems. The CS measures gold concentration, slurry density, pH, dissolved oxygen (DO), and gold loading on carbon. An XRF analyser is used to measure gold loading after screening and cleaning a carbon sample. These measurements are reported across the CIL or CIP tank train and are provided typically every 30 to 60 minutes for each tank.

Figure 4 shows the typical CS instrument and operating schematic.

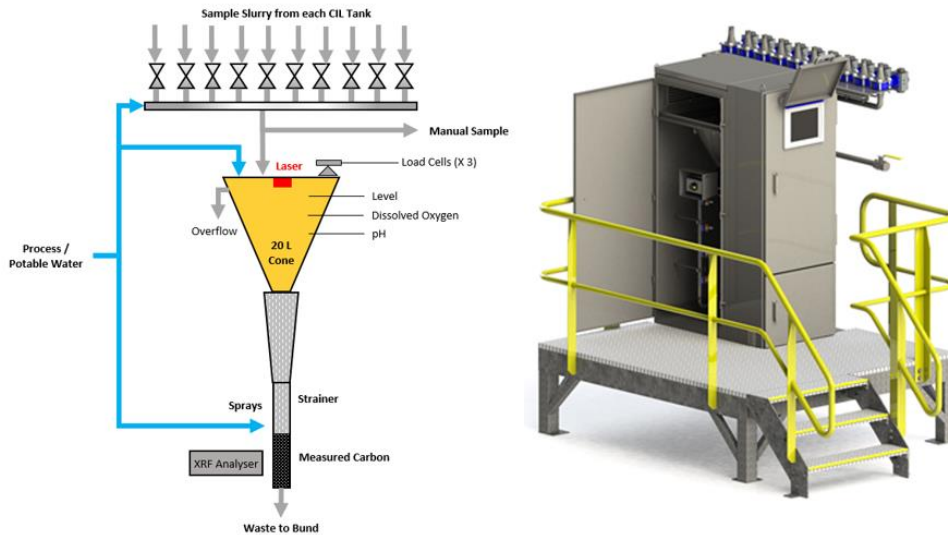


Figure 4 - CS analytical engine concept (left) and module on a platform (right)

Two case studies are detailed in this paper, one at Alkane Resources' Tomingley Gold Operations in New South Wales, and the second at Gold Fields and Gold Road Resources joint-venture Gruyere Mine in Western Australia.

At Tomingley Gold Operations, the CS analysed 5758 samples in one month (April 2022) alone. With each sample producing more data than just carbon concentration, over 70 000 discrete sample characteristics are provided. This is compared with a maximum of 1440 data points in a month when manually sampling the slurry by plant operators. This increase in reliable, consistent, and more frequent data has helped plant personnel at Tomingley to make better-informed decisions on how best to operate their plant.

At Gruyere Mine, the operational team has partially eliminated manual samples for carbon concentration, reducing the risk of manual handling injuries and minimising personnel exposure time on top of the tanks. Current work includes a gold-in-circuit (GIC) sampling station to enable more frequent, easily accessible (ground level), and consistent sampling for their monthly GIC surveys. Figure 5 shows recent (mid-2022) carbon concentration results from the CS.

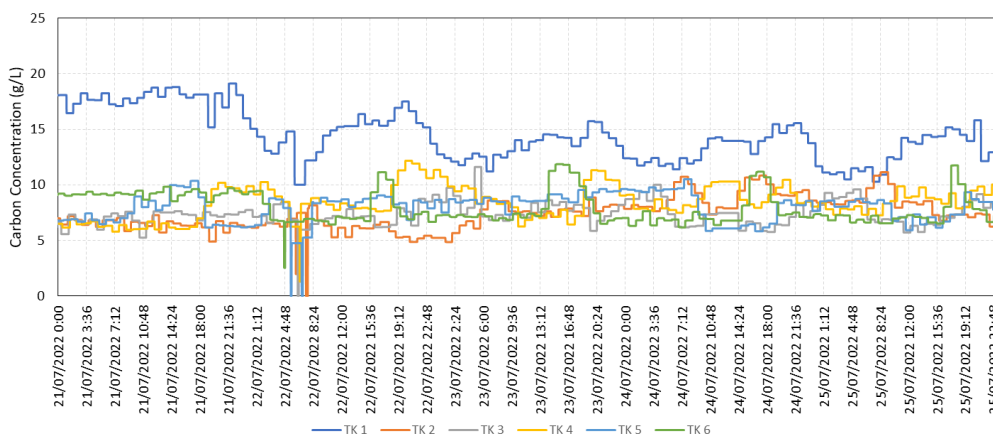


Figure 5 - Carbon concentration at Gruyere JV as measured by the CS over a five-day period

Further, gold loading on carbon is measured on each tank sample using the XRF analyser within the CS package, as illustrated in Figure 6. Ongoing XRF model baselining and calibration is part of the project to ensure that the model correctly represents the actual gold loadings measured by validation sample analysis. This also ensures that all design, operational, automation, and maintenance aspects of the XRF analyser are adequately captured and communicated within the project team.

A benefit of real-time gold loading measurements is in the optimisation of carbon stripping in the elution circuit. It is commonly accepted that elution strips are more efficiently operated with the highest possible carbon loading (gold grade on loaded carbon) to minimise the number of elutions required. If a gold plant can recover more gold with fewer strips while maintaining or bettering production targets, any additional elution strip at month-end becomes a bonus to production.

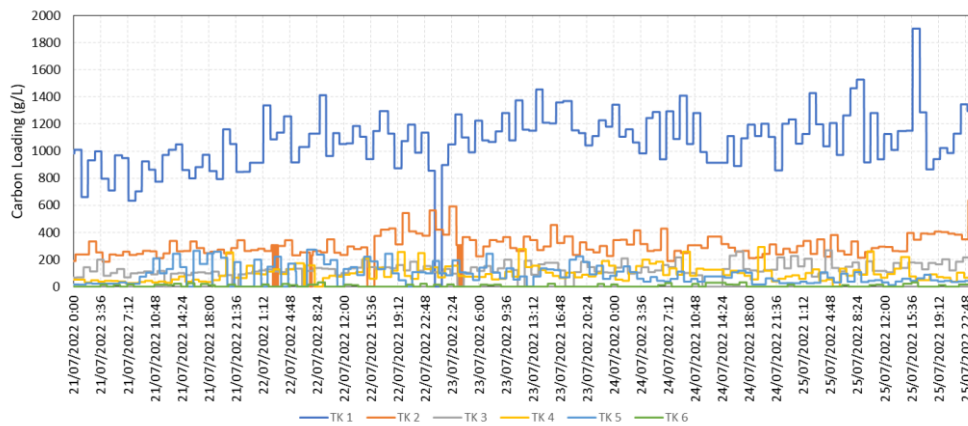


Figure 6 - Carbon loading at Gruyere Mine as measured by the CS’s XRF analyser over a 5-day period

In another processing plant in Australia, a 13% reduction (Figure 7) in solution losses was achieved through automated carbon movement by the CS, delivering an approximate AUD\$1.1 million in savings per annum. Staunton et al, 2017, state that to improve on the typical soluble gold loss of 0.01 ppm target, which has not changed in 30 years, circuit operation requires to be in “such a way to maximise the efficiency of carbon adsorption”. The automated carbon movement was driven using the CS for tank-by-tank carbon concentration monitoring. Figure 7 graphically illustrates the potential benefit if all other conditions remain constant.

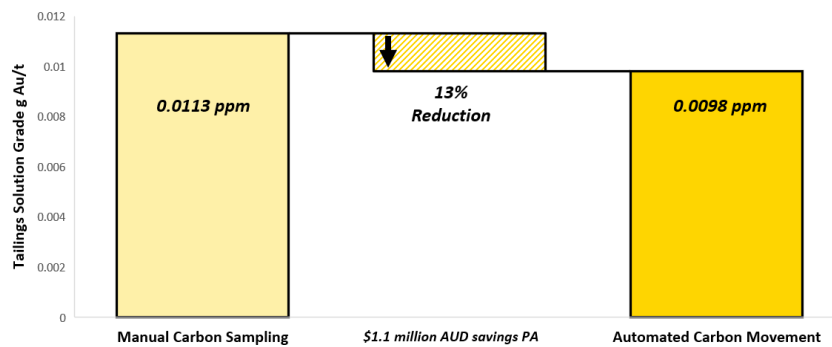


Figure 7 - Effect of automating carbon movement on solution grades

In the case of the CS installed at a gold processing site in South America, the CS measurements demonstrate the significance of automated sample measurements. Figure 8 illustrates the before and after scenarios on CIL Tank 3 and Tank 4 of the circuit. No carbon concentration measurements were collected for a period where Tank 3's carbon concentration drops while Tank 4's carbon concentration increased over the day. Upon resumption of CS measurements, a more stable and controlled carbon concentration was observed. While the event was mainly due to an out-of-service carbon transfer pump, the ability to detect this in real-time is a great advantage providing the operators and control room personnel with real-time feedback on carbon concentration measurements, and therefore tank-by-tank carbon inventories. And the consequence of such an event may manifest itself as a significant excursion in solution losses.

Although this was not the case at this specific site, it is a demonstrable example of how a holed screen in an upstream tank (Tank 3) can leak carbon into the downstream tank (Tank 4) without detection. In such cases, the CS is able to detect such events within an hour of occurrence as it cycles through the tanks in the circuit.

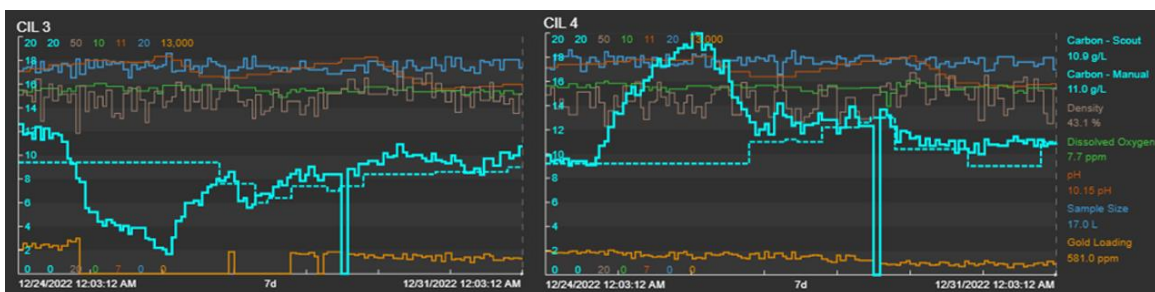


Figure 8: CIL Tank 3 and Tank 4 CS Measurements at a site in South America over a 7-day period.

ONLINE GOLD ANALYSER

The OLGA was developed in a collaboration between Gekko Systems and the Commonwealth Scientific and Industrial Research Organisation (CSIRO). The OLGA continuously measures total gold concentration in process slurry or solution streams using XRF technology. The output is updated every ten minutes on a 60-minute rolling average and enables streamlined process monitoring and control which often informs sitewide metal accounting, reagent addition, and control. Site no longer must wait hours, shifts, or days to receive assay results of feed, tails, or concentrate streams. The OLGA has been installed in two operating mines in Australia, a flotation circuit since late 2018, and a leaching circuit since early 2021.

Case study one was at Mt Carlton Operations, located approximately 150 km south of Townsville in Queensland, a 45 000 to 50 000 oz/y operation. Trials were undertaken on both the flotation feed and tails streams. Figure 9 (Cervellin et al, 2021) illustrates the OLGA measurements, shift composite samples and grab (validation) samples are compared.

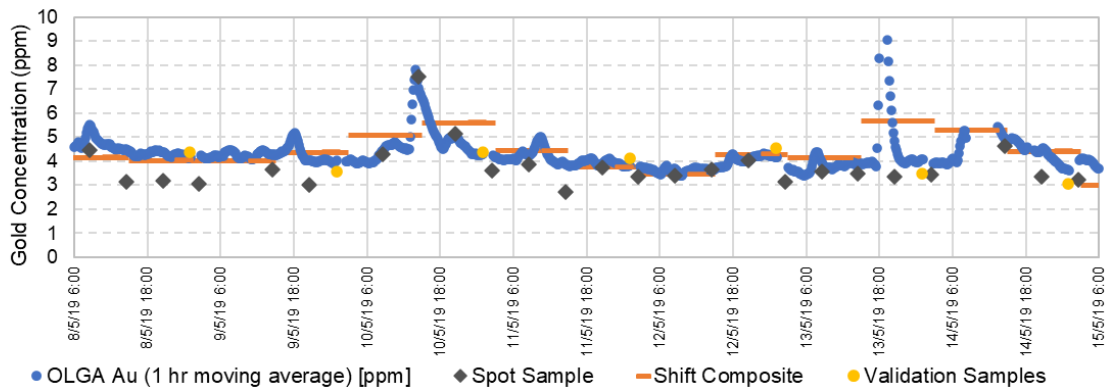


Figure 9 - Day production sample tracker between OLGA, validation, and spot samples at Mt Carlton

A trial on the flotation tails stream was also conducted, with this indicating further calibration work and testing was required for this low-grade stream). However, as the original intent of the OLGA was to measure the flotation feed stream, the OGLA was permanently reinstated on the flotation feed stream (Cervellin et al, 2021).

Figure 10 illustrates the scatter plot of the OLGA-validation sample pairs over the trial period (Cervellin et al, 2021) with reasonable validation.

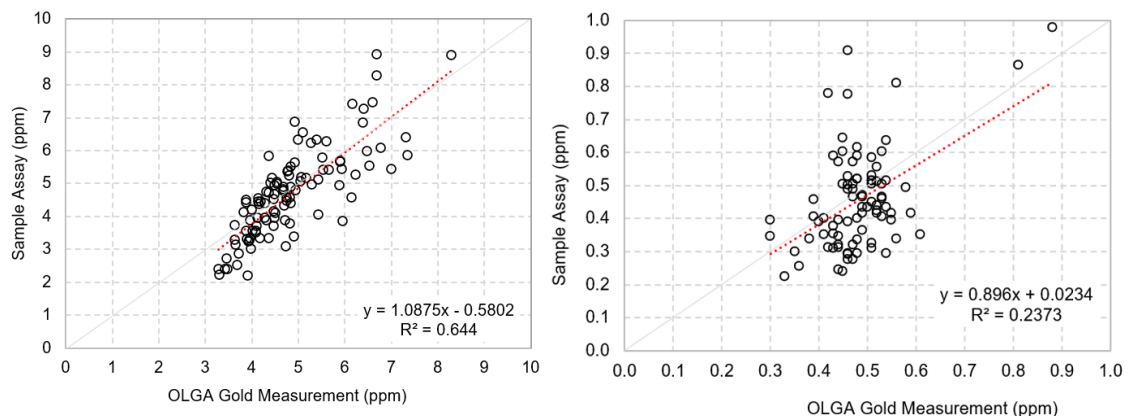


Figure 10 - OLGA versus validation sample data for flotation feed (left) and flotation tails (right)

An added benefit of the Mt Carlton OLGA was that it provided arsenic content on the flotation feed stream, which often assisted site staff with timely insights required for the safety aspects related to arsenic dust and hygiene monitoring in the plant.

Case study two explores the concept of online and real-time gold measurements when integrated into a wider project. Gruyere Mine, a 1000 t/h gold producing mine operated by Gold Fields as part of their joint venture with Gold Road Resources installed the OLGA. This METS Ignited industry-funded project included the OLGA, CS, and integration with the online remote monitoring platform, MillROC. Figure 11 shows the instruments installed on site.



Figure 11 - OLGA and CS installation at the Gruyere Mine

The OLGA at Gruyere was installed in February-March 2021 and commissioned in April 2021. Sampling from the leach feed stream, some of the initial work involved distinguishing between gold in solution and gold in solids as OLGA measures total gold in the stream. The raw gold X-ray spectra values are then normalised using solids content (%w/w) to achieve total gold in the sample and then converted using the calibration model into gold concentration.

A challenge encountered was the residual cyanide and residual gold in solution present in the recycled process water contributing to the total gold “seen” by the OLGA, and that gold in solution signal appeared to distort the overall total gold concentration. This issue was further complicated by the OLGA sample extraction point being at the same location as the circuit’s initial cyanide dosing location, resulting in gold already leached into solution before reaching the OLGA downstream. Subsequently, the OLGA sample extraction point was relocated ahead of cyanide addition, and this change improved measurements. Figure 12 shows the comparative data for the solution, solid and total slurry phases and illustrates the gold in solution effect against the validation samples.

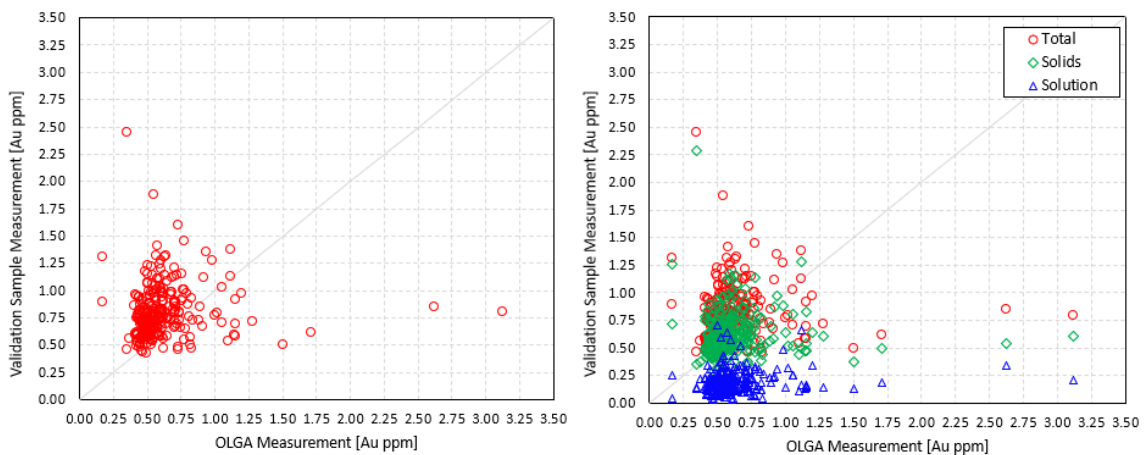


Figure 12 - Gruyere OLGA versus validation sample gold readings classified as total slurry (left) and solid, solution and total slurry (right)

A time-trend over a four-day period in July 2022 (Figure 13) indicates how the OLGA's real-time gold measurement are visualised on the site's online monitoring platform. This data provides valuable insights into the gold grades feeding the leach circuit.

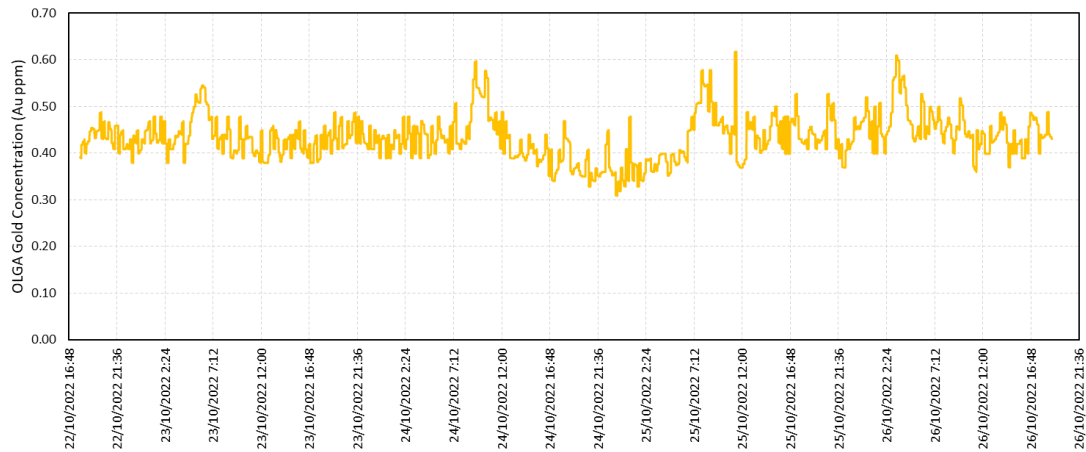


Figure 13 - OLGA gold measurements trend over a 4-day period at Gruyere Mine

WHAT DOES THE GOLD PLANT OF THE FUTURE ENTAIL?

Various integrated packages of remote and in-situ sensors are available to the processing industry. Many packages focus on one part or section of the process plant. For example, some sensors monitor remote ore tracking from blasting, stockpiles and muckpiles all the way into the primary crushing circuit. Some sensors focus on the comminution circuit to track and optimise the grinding mills and associated classification cyclones. Other packages focus on the leaching and adsorption circuit excluding the elution and carbon regeneration circuit.

Ideally, the whole gold process plant should integrate real-time instruments and sensors with the overall objective of automating process aspects amenable to automation. Optimisation and improved value must be the focus and goal, as without this, the project may fall into stagnation and suppress benefits.

The authors' initial and possible ultimate vision for the "gold plant of the future" encompasses meaningful, directed and value-driven real-time instrumentation that must aim to give value-driven insights into the process and, ultimately the products. The inclusion of the various instruments into a single platform enables a better-integrated system that draws all control and automation aspects through a single control point, operating under an integrated value-based control philosophy. The overarching objectives towards achieving this are summarised in Table and displayed graphically in Figure 15.

Table 1 - Selected outcomes from improved circuit control in gold process plants

Circuit / Unit Process	Control Aspect	Outcome
Stockpiling	Feed Rate; Ore Blend; Particle Size Distribution	Efficient process
Comminution	Mill power	Energy efficient process
Reagents	Addition and Consumption	Lower operating costs
Leaching	Gold leaching	Improved recoveries
Adsorption	Carbon Management	Reduced solution losses
Elution	Carbon Loading; Optimum No of Strips	Lower operating costs
Regeneration	Carbon Health	Reduced solution losses
Cyanide Detoxification	Reagent Control	Lower operating costs

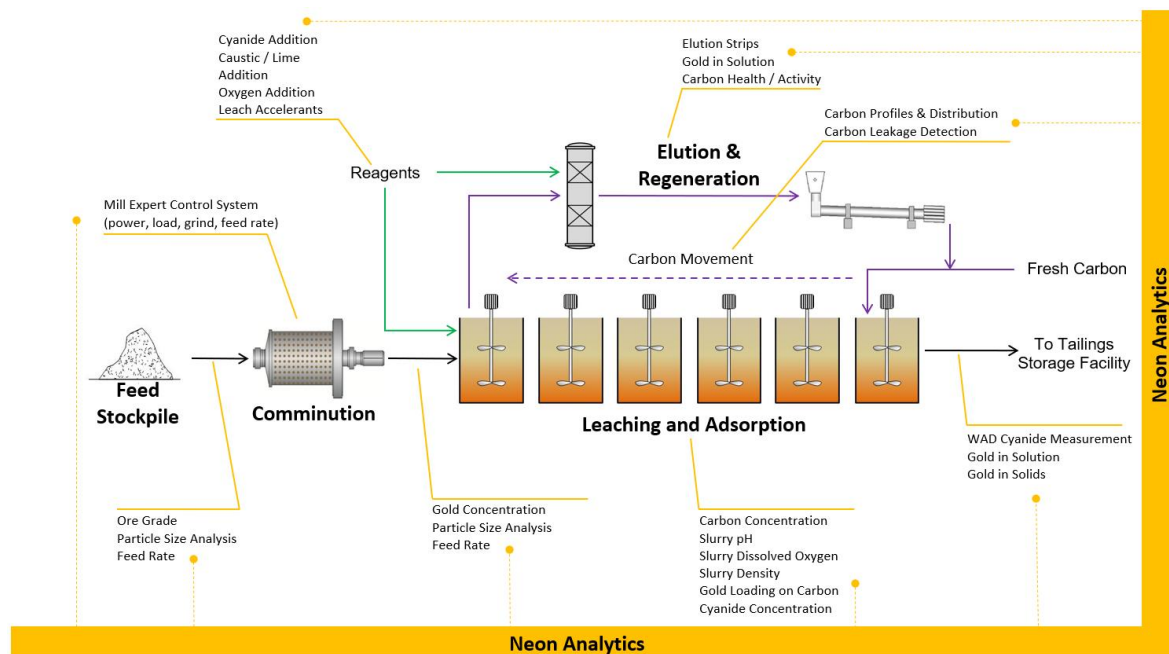


Figure 14 - Automation of a gold processing plant, integrated through a single or multi-faceted platform

An application (Neon Analytics) is currently under development and in trial for modules that cover the CS. This platform enables the process team to draw access aspects of plant control into a single visual tool while enabling benchmarking data to guide and inform the site on their relative position across industry peers.

COLLABORATION, CULTURE AND DIGITAL TRANSFORMATION

It is a key necessity that industry players with various unique capabilities and resources to collaborate, partner and offer sustainable technological solutions to the mining industry. These partnerships must include institutions that conduct research and development, academia, government organisations, equipment manufacturers, data handling and analytics within the broader minerals processing sector.

Automation and control of gold processing plants involve different hardware and software platforms, needing robustness to account for all aspects of the plant's operational, maintenance, performance, and ultimately value delivery aspects. Collaboration within the industry sectors delivers strong returns to all stakeholders, achieving shorter turnaround times from concept to operational results.

The case of the Gruyere Mine project is a testament to a direct and collaborative approach from various mining industry players, including:

- Gekko Systems
- Gold Fields Australia
- METS Ignited
- CSIRO
- Curtin University – Gold Technology Group
- Orway IQ and Process IQ (now Molycop).

CONCLUSIONS

Gold processing plants with instruments such as the CS, OLGA, and others, stand to gain significant and real benefits such as improved safety, increased recoveries, reduced gold solution losses, and lower operational costs amongst others.

A critical outcome is often the elimination or significant reduction of excursions that signify certain events occurring in the process. Together with excursions, the detection of some events in real-time offers the operators highly regarded insights that are often left for days or weeks before detection.

It is therefore critical that these real-time instruments are robust, reliable, sufficiently accurate for the purpose and less demanding on maintenance. It is obvious and realistic that in their infancy these technologies will continue to be improved, updated, and developed with feedback received from the operators and maintenance personnel on mine sites. This creates a continuous improvement environment that integrates both the suppliers and users on an ongoing basis, and such feedback has been used towards the update of the CS into the current Mk6 version in the market. Partnering with the CSIRO, the OLGA is taken forward in its development as work on the Beta version is ongoing.

It has been demonstrated through several projects that collaboration amongst minerals industry partners is key to enabling faster product development and rollout to mine sites. The slow uptake of new technology in the mining industry, relative to certain other industries such as manufacturing, automotive, and petrochemicals, brings about an opportune objective towards collaborative partnerships for technology development.

With all the examples presented in this paper of OLGA and CS applications in use, gold process plants must be moving toward full automation in the near future. This does not imply functions performed by operators are completely eliminated but are instead complemented and supported by these real-time instruments.

ACKNOWLEDGEMENTS

The extent of the knowledge, experience, skills, and resources from all these collaborators brought about a project that encompasses a significant number of elements found in gold leaching and adsorption, including real-time and remote monitoring. The authors would like to acknowledge and thank the Gruyere Mine for the supportive and structured approach under which the OLGA and CS project is guided, executed, and managed.

REFERENCES

Cervellin, A, Robinson, J, Sia, A, Craig, E, Killer, L. Online gold analysis at Evolution Mining Mt Carlton. *Mill Operators Conference, Perth, Australia, 2021.*

Gray, S, Sensors and automation – a unique opportunity to leverage real-time gold recovery data through data analysis and automation in gold processing. IMPC Asia-Pacific 2022, Melbourne, Australia, 22-24 August 2022.

Staunton, W P, Barbetti, K, Optimising the Management of CIP/CIL Circuits. COM2017 The Conference of Metallurgists, Vancouver, Canada, 2017.

Gekko Systems. Alkane and Carbon Scout Case Study, 2022.

Gekko Systems. Final Technical Report – GFO Real Time Gold Solution Project, 2022.

Ravenswood Gold Mine Expansion from 3.2 to 12 Mt/y

G Ballantyne¹, M Pyle², G Lane³, A Lawry⁴, V Jayawardana⁵, D Jeffery⁶, J Marx⁷, T Mitchell⁸, and

E McLean⁹

1. Director Technical Solutions, Ausenco, 189 Grey St, South Bank, Brisbane, grant.ballantyne@Ausenco.com
2. Director Technical Solutions, Ausenco, 189 Grey St, South Bank, Brisbane, matt.pyle@Ausenco.com
3. Chief Technical Officer, Ausenco, 189 Grey St, South Bank, Brisbane, greg.lane@Ausenco.com
4. General Manager Projects, Ravenswood Gold Pty Ltd, 307 Queen Street, Brisbane, andrew.lawry@ravenswoodgold.com
5. Senior Process Engineer, Ausenco, 189 Grey St, South Bank, Brisbane, viren.jayawardana@Ausenco.com
6. Lead Process Engineer, Ausenco, 189 Grey St, South Bank, Brisbane, david.jeffery@Ausenco.com
7. Project Director, Ausenco, 189 Grey St, South Bank, Brisbane, john.marx@Ausenco.com
8. Project Metallurgist, Ravenswood Gold Pty Ltd, Macrossan Street, Ravenswood, timothy.mitchell@ravenswoodgold.com
9. Manager Minerals Consulting Ausenco, 189 Grey St, South Bank, Brisbane, eddie.mclean@ausenco.com

ABSTRACT

Ravenswood has a long history of gold production with more than 4 Moz mined since 1868. Ravenswood Gold currently owns the deposit with another 4 Moz still in resource. Ausenco was approached in 2020 to explore expansion opportunities to increase the annual capacity from 3.2 Mt/y to 12 Mt/y, and a fast-tracked project was commenced. In only 30 months, the project progressed from initial scoping to gold pour. The expansion scope included a new crushing and screening plant, expanded milling circuit, gold leaching circuit, and gold room, additional tails thickener, upgraded water and power services.

The new Ravenswood Gold processing plant can be operated efficiently across a range of capacities (between 5-12 Mt/y). Preconcentration is used to selectively upgrade the ore efficiently early in the process, helping improve the operation's economics while significantly reducing water and energy consumption. Quick, accurate decision making was a priority in the initial scoping and concept development phase of the project and techno-economic modelling was used to aid in this.

This paper explores the approach used to fast-track the design, construction and commissioning of the expanded plant and presents examples of when the approach was effective in determining the size and number of new leaching tanks; the optimum grind size; the mill size and configuration, and the rejection rate of coarse waste.

INTRODUCTION

In Quarter 1 of 2020, representatives from Ravenswood and Ausenco met to discuss the expansion options for Ravenswood gold mine. At the initial meeting a strategy was agreed and the Ravenswood expansion project commenced. The strategy considered a staged expansion from 3.2 Mt/y to 12 Mt/y with a very tight schedule driving the project.

Prior to the expansion, the existing operations at Ravenswood treated up to 3.2 Mt/y of mineralised waste dumps (MWD) in the existing Nolans crushing and milling circuits (see simple block flow diagram Figure). This circuit was a standard three-stage crushing circuit with the ability to reject low-grade coarse waste following the secondary crusher. The MWD ore was low grade and the gold

deported to the fines following blasting and crushing due to the fracture characteristics of the less competent mineralised rock.

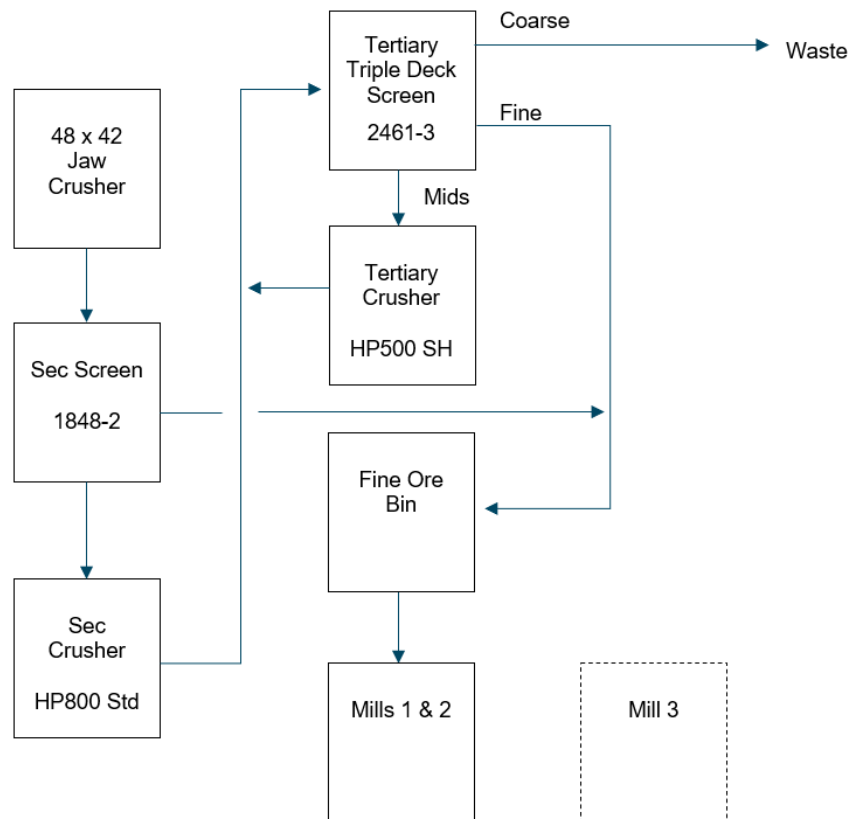


Figure 1 Block diagram of the operating (2022) Nolans crushing and milling circuits

The decision was made to expand the Ravenwood crushing, grinding and leaching circuits to process 12 Mt/y using a staged approach which aligned with the processing of different ore sources:

- Stage 1: circuit expanded to process 5.0 Mt/y of Buck Reef West (BRW) ore
- Stage 2: circuit expansion to process 7.1 Mt/y of BRW ore
- Stage 3: increase primary crusher throughput to treat 12 Mt/y of Sarsfield ore followed by 40% rejection of coarse screened, low-grade material with 7.1 Mt/y of beneficiated and upgraded ore to grinding and downstream leaching.

Multiple options were considered for each of these stages to define a capital cost efficient approach that considered operator preferences, development schedule, plant layout, the overall power constraint and performance.

This paper outlines the process design, delivery, commissioning and early operation of the expanded project. The key successes and challenged of this project are outlined in the paper, including:

1. the speed with which the project progressed from design through delivered and commissioning
2. the continuous operation of the existing processing plant during construction and the minimal downtime during commissioning

- the delivery of a project during the disruptions of a global pandemic.

PROCESS DESIGN

Stage 1: 5 Mt/y plant

Stage 1 consisted of upgrading the crushing and leaching circuits to increase the throughput to 5 Mt/y. As the existing Nolans crushing plant had insufficient capacity, a stand-alone crushing circuit was designed that would meet Stage 3 capacity requirements.

The Stage 1 crushing circuit consists of three-stage crushing with gyratory primary crusher, a secondary cone crusher and two tertiary cone crushers to provide a P_{80} of 9 mm at 5 t/y. The existing Fine Ore Stockpile (FOS) was deemed sufficient for operation at 5.0 Mt/y. The existing milling circuit could process 5.0 Mt/y with a feed F_{80} of 9 mm to a product P_{80} of 220 μm .

Stage 1 included the following works downstream of cyclone overflow grinding product to accommodate the increased volumetric capacity and to retain 24-hours residence time:

- Two new trash screens with provision for one additional screen to be installed in Stage 2.
- Three new leach tanks, each 5100 m³ live volume, with provision for three additional tanks of the same capacity to be installed in Stage 2.
- Provision of cyanide addition, HCN detectors, down-shaft oxygen injection from the existing pressure swing adsorption (PSA) plant to the three new leach tanks.
- Conversion of an existing 2500 m³ leach tank to a carbon adsorption tank with installation of two intertank screens and a carbon recovery pump.
- Installation of one additional intertank screen in the existing 2500 m³ tank used for adsorption duty and redirection of carbon flow from this tank to the modified upstream adsorption tank.
- Conversion of the seven CIP tanks (approximately 1200 m³) to a series-parallel arrangement in which the first tank with two intertank screens is in series with the modified two upstream adsorb tanks followed by parallel trains of three CIP adsorb tanks, each with existing one intertank screen.
- The AARL stripping circuit has two 5 tonne batch columns. Thirteen strips per week are required for elution duty.

Stage 2: 7.1 Mt/y plant

Options explored to determine the best strategy for expanding the crushing and milling circuit to 7.1 Mt/y included:

- Two- and three-stage crushing (Options 1A and 1B) followed by SAG milling.
- Retaining the Nolan's crushing plant and optimising the capital costs for a three-stage crushing circuit (Option 2).
- A three-stage crushing circuit feeding HPGR closed with a dry screen (Option 3).

Option 2, which retained the Nolan's crushing circuit, was selected because:

- it utilised existing equipment
- it leveraged from existing work and maintenance practices

- no new grinding equipment (SAG mill) or other process technology (HPGR) were introduced
- engineering, procurement and delivery occurred in the shortest time frame
- it provided for the least redundancy of existing and temporary facilities.

Prior to expansion, the existing milling circuit consisted of three mills:

- Mill 1: originally a grate discharge ball mill, 5.5 m IS ϕ x 5.8 m EGL x 3250 kW, configured in open circuit that was being converted to overflow to remove the flow constraint.
- Mill 2: an overflow ball mill, 4.5 m IS ϕ x 9.2 m EGL x 3250 kW, configured in closed circuit and fed by Mill 1 product.
- Mill 3: a grate discharge mill, 5.0 m IS ϕ x 7.9 m EGL x 4000 kW, which operated in closed circuit in parallel to Mill 1 and Mill 2.

In Stage 2, additional milling capacity was required to process the increased solids throughput and to achieve a finer grind product size, P80 106 μ m. As a result of a trade-off study to determine the optimum grind size and circuit configuration, a new 7.3 m IS ϕ x 11.0 m EGL x 12 000 kW primary ball mill (Mill 4) was selected. This mill was configured in closed-circuit to deliver the required transfer size to Mill 3.

To feed Mill 4, the FOS was expanded and a new reclaim was constructed, all while the existing stockpile and reclaim was operational (**Error! Reference source not found.**).

Figure 2 Schematic of upgrade to fine ore stockpile (FOS)

Stage 2 included the following works downstream of cyclone overflow grinding product to accommodate the increased volumetric capacity and to retain 24-hours residence time:

- One additional trash screen installed in Stage 2.
- A further three new leach tanks were installed, each 5100 m³ live volume, the same tank capacity as installed for Stage 1.
- Provision of cyanide addition, HCN detectors, down-shaft oxygen injection.
- No further work to adsorption circuit as the modifications made in Stage 1 were sized to accommodate the flow rates and duty for Stage 2.
- The AARL stripping circuit has two 5 t batch columns. Tankage and electrowinning cells were

increased to enable 18 strip cycles per week based on a 16-hour electrowinning time. Existing acid wash and regeneration systems were retained.

Stage 3: 12 Mt/y plant

From characterisation testing, the Sarsfield ore exhibited the same beneficiation ability as the MWD material. In operation at the existing Nolans plant on MWD, typically 40% of the mass was rejected from the tertiary screen oversize at a size of 35 mm (Figure 3). Therefore, to maintain a milling throughput of 7.1 Mt/y, the primary and secondary crushing circuits capacity was increased to 12 Mt/y.

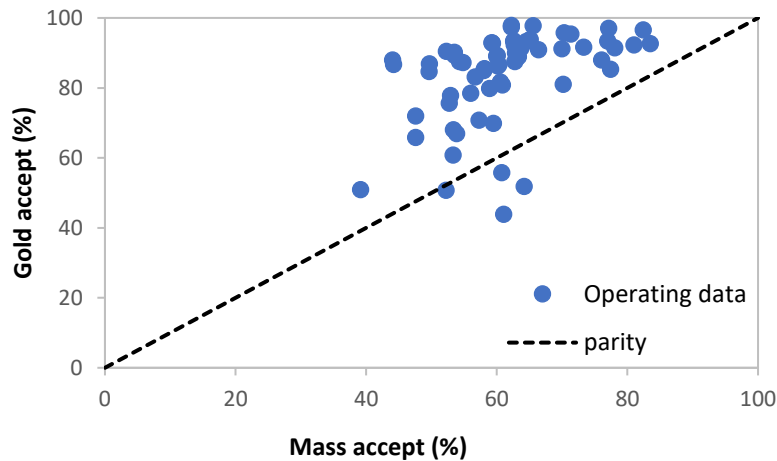


Figure 3 Release analysis of operating data from the Nolan's plant prior to expansion.

The leaching, adsorption, elution and electrowinning upgrades for Stage 3 were completed in Stage 2.

The crushing circuit flow sheet with the Stage 2 upgrade to the FOS and the Stage 3 integration of beneficiation rejection are shown in Figure 4.

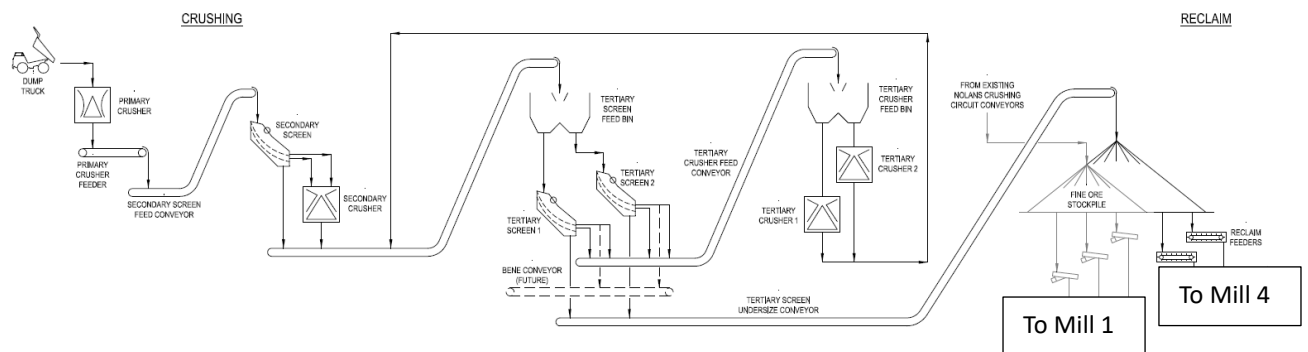


Figure 4 Crushing circuit flow sheet

The flow sheet for the new Mill 4 in closed circuit with the existing Mill 3 and the additional gravity and intensive cyanidation reactor are shown in Figure 5.

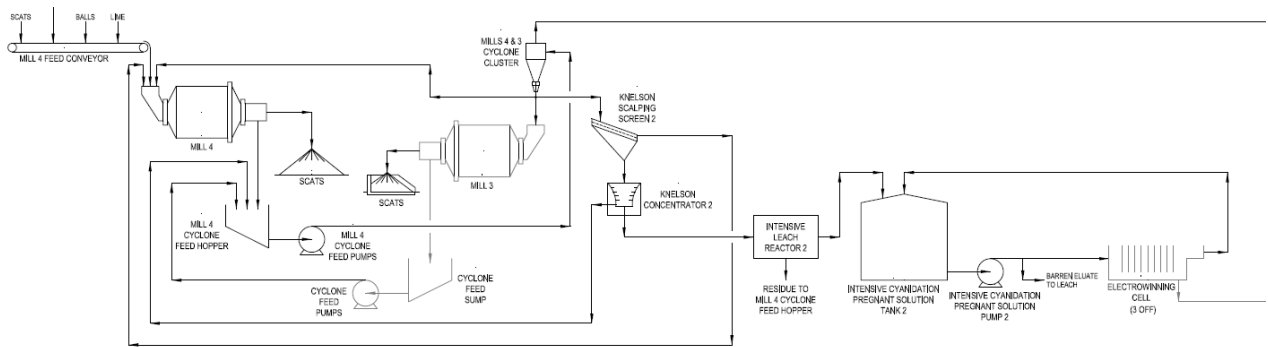


Figure 5 Mill 3/4 circuit flow sheet

The upgrades to the leaching and adsorption circuit are shown in Figure 6, including the additional leaching tanks and the additional thickener. No changes to the AARL elution, electrowinning, regeneration and smelting circuits were made – only additional equipment and repurposing tankage and electrowinning cells were implemented.

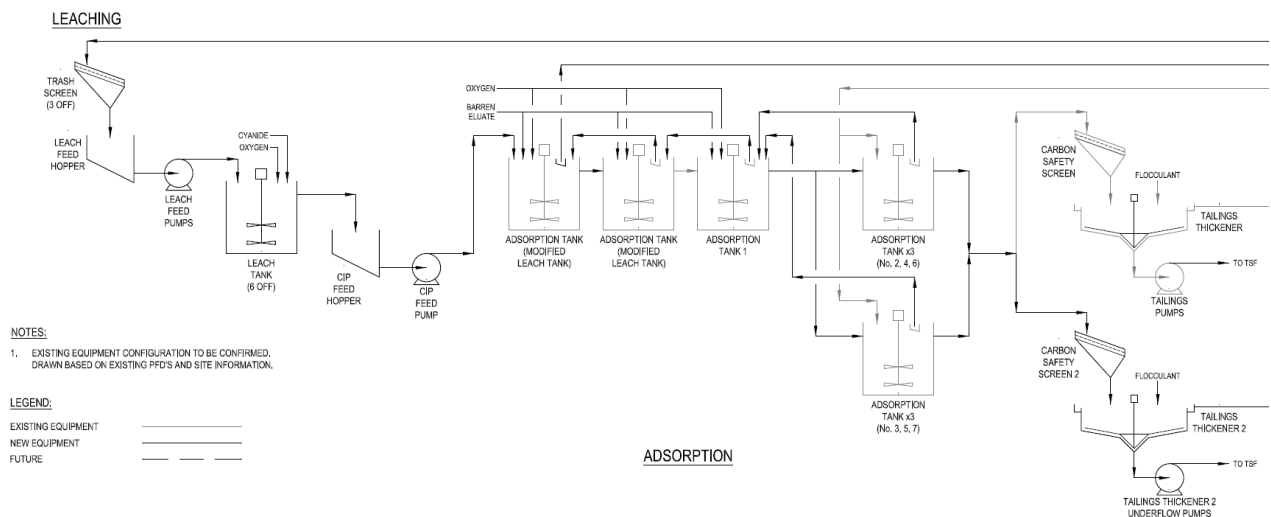


Figure 6 Upgrades to the leaching and adsorption circuit

PROJECT DELIVERY

The Ravenswood Gold Expansion Project was delivered on a fast-tracked schedule. This required staged construction, commissioning and handover to the owner's operations team. This approach allowed Ravenswood Gold to bring forward gold sales and improve NPV to capital cost ratio across the project. Achieving the fast-track timeline required Ausenco to draw on past design experience and maintain an agile construction delivery approach, utilising opportunities as they arose throughout construction.

Construction and commissioning schedules were developed to align with the staged handover of the new plant. Early in the process, it was determined that Stage 1 would only include the leaching circuit expansion, and exclude the new crushing circuit to align with the project schedule. Constructability reviews during early stages of the design ensured construction efficiency was not hampered by the staged approach. The strategy included:

- Independent MCCs for each stage which tied into the overall site distribution network once commissioned, allowing subsequent stage MCCs to be constructed without any energised components.

- Site layout that ensured physical segregation of construction and operating work areas that were progressively changed as the project progressed.

Construction

Site access was granted to the bulk earthworks contractors in November 2020. Detailed excavations and civil works commenced in February 2021. Key delivery dates for hand-over to operations were:

- Stage 1 (leaching circuit) in July 2021.
- Stage 2 (crushing circuit) in July 2022.
- Stage 3 (milling circuit with reagents and gold room) in September 2022.

The global pandemic impacted fabrication, manufacturing, logistics and construction activities requiring elevated levels of change management and remote support. The staged handover approach was only achieved by selecting local manufacturers for the early construction activities, including structural steel fabrication, platework and tank fabrication. This mitigated the macro logistic delays associated with overseas fabrication. The project also took advantage of the availability of second-hand secondary and tertiary crushers to improve delivery times and reduce the impact of the unpredictable and unreliable global shipping timeframes.

Overseas manufacturing could not be avoided for critical components of the plant, including the primary crusher, the ball mill and its associated components. In-person inspections of the equipment was not able to take place, as travel was prohibited and many factories were in lock-down preventing third party inspections by local representatives. Factory Acceptance Testing was performed via video conferencing, principally by mobile phone which allowed roaming and up-close inspections of requested equipment.

Onsite construction activities were impacted by the availability of local, suitably qualified construction personnel. Construction resources could only be sourced from within the state, as borders were shut between Queensland neighboring states and territories. The resource constraint impacts were compounded by the volume of construction work in progress within the state during this period. Multiple strategies were implemented during this period to attract the required resources to the project, including adjusting working rosters, introducing additional contractors and subcontractors who brought core construction teams with them, and introducing project performance incentives.

Government regulated COVID-19 reporting, testing and quarantine measures evolved throughout the project. To allow construction activities to continue throughout the entire pandemic period, personnel were regularly tested for the COVID-19 virus. If found to be positive, the individual could not travel home and would instead isolate in approved quarantine hotels in the neighboring towns. Return to site was only permitted once a negative rapid-antigen test was provided at the site entrance.

Progressive design development and agile change-management allowed construction schedule reduction opportunities to be realised throughout the project. One example was a reduction of over 4 km of electrical cabling, achieved by changing to a more direct cable route between the crushing MCC and the primary crushing structure. The cable was buried underground, implementing long term preservation measures like mechanical protection and termite control. These approaches saved two weeks in the construction schedule. This opportunity was raised and able to be implemented within a fortnight.

Another opportunity employed during the project was to make minor strategic alterations to the structural design to allow significant pre-assembly of structures and conveyor modules. This reduced the work on site and allowed for installation of components like cable trays, handrails and pipework at ground level, prior to installation.

Specialist commissioning teams were mobilised at the relevant stages of the project to ensure the construction team could progress without distraction of commissioning effort.

Commissioning

The Project allowed for progressive commissioning and handover of the new plant in three stages. This staged-approach allowed the owner to realise the financial benefits of the completed sections at the earliest possible time. Operational familiarisation of the new equipment was also able to be completed while the project team were still available on site for support. The site project commissioning and operations teams coordinated the planning and execution of pre-commissioning and process commissioning of the staged expansion circuits. A collaborative approach was taken to planning tie-ins and shutdowns and reducing interruptions to production, while maintaining project timelines.

Stage 1 (leach expansion) and Stage 2 (crushing expansion) were brought online with minimal impact on the existing plant operation. The impact on the mills of intermittent operation during ore commissioning and ramp up of the Stage 2 crushing circuit was mitigated by utilising feed from the existing crushing circuits.

Stage 3 commissioning included more complex interactions with the existing plant. The Stage 3 expansion featured a new grinding and classification circuit with gravity gold recovery and intensive leaching, new tailings thickening and pumping, and additional electrowinning cells and pregnant liquor tank. Once the new or modified equipment and circuits were tied-in, the production was contingent upon quick, successful commissioning to maintain continuous operation.

The Stage 3 grinding circuit design included a new stockpile reclaim and conveying system to the new 12 MW ball mill (Mill 4), while the existing ball mill (Mill 3) became a secondary ball mill treating a portion of cyclone underflow from the new Mill 4 classification cyclones. The existing stockpile feed conveyor system to Mill 3 was to be demolished, as were the classification cyclones servicing Mill 3. Discharge from Mill 3 was diverted to be combined in the new Mill 4 discharge hopper for classification in the new Mill 4 cyclones.

One impact after the tie-in to enable ore commissioning was that no production was possible from the existing Mill 3 without the new Mill 4 circuit in operation. Whilst this was an efficient design, making use of existing Mill 3 grinding power and improved classification efficiency, the impact on production during ore commissioning of the new Mill 4 was a risk. Ore commissioning of a new grinding mill included significant downtime, both planned (e.g., critical fastener checks, drive train alignments, inspections, and liner retorques on the new ball mill after nominated periods of operation) and unplanned (e.g., typical operating and maintenance issues arising when the new plant sees design operating conditions for the first time).

The site project team identified a better way to improve operating flexibility and allow parallel operation of the existing Mill 3 and new Mill 4 as standalone circuits, until the Mill 4 circuit was reliable and the final integration with Mill 3 was possible. This was achieved in Mill 3 and Mill 4 circuit piping design modifications which allowed:

- The ability to retain the Mill 3 feed conveyor system and option to continue to use Mill 3 as a primary mill, in addition to being fed cyclone underflow from the new Mill 4 cyclones when

operating as a secondary ball mill.

- Simultaneous feed to the leach circuit from both the new Mill 4 and the existing Mill 3 cyclones.
- Quick changeover of Mill 3 discharge pump piping for the option to combine Mill 3 discharge with Mill 4 discharge for classification by Mill 4 cyclones (per design), or to continue using the original Mill 3 classification cyclones independent of the Mill 4 circuit in the event that Mill 4 was offline.

With the support of the operations team, the circuit modifications were implemented during a planned shutdown. The improved design provided flexibility to quickly reinstate Mill 3 as an independent primary ball mill circuit if issues arose with the new Mill 4, and vice versa. This minimised the impact on production during Mill 4 commissioning and ramp up and allowed the final design configuration to be implemented when operating conditions and equipment availability permitted. This flexibility paid further dividends when an unexpected failure of the Mill 4 motor subsequently occurred.

Another pressure point in Stage 3 was the tie in and commissioning of the new electrowinning and expanded gold room circuit. The existing electrowinning circuit treating pregnant solution from both elution and intensive leaching of gravity concentrates was to be repurposed to treat only existing and new gravity intensive leach solutions. Three new electrowinning cells and a new pregnant liquor tank and pumping were installed. Modifications were made to the existing pregnant and barren liquor tanks and pumps to provide three parallel electrowinning circuits to treat pregnant solution from the existing elution circuit. The additional electrowinning capacity was required to allow more carbon strips from the existing elution circuit to match the increased plant throughput. Due to the complexity of the piping and equipment tie ins and constraints of working within the footprint of the existing electrowinning and gold room area, the previous piping options were unavailable.

The project and operations teams again collaborated to plan and execute a significant number of complex tie ins to the existing electrowinning and gold recovery circuit during a two-day shutdown. The first batch of pregnant liquor from elution was treated through one of the new electrowinning cells the day after the shutdown. Aside from the mechanical, electrical, piping, and instrumentation tie-ins, there were several complex control system modifications to be made where pumps, control valves, interlocks, and sequences from the previous configurations needed to be reprogrammed to suit the new installation.

Programming and automation updates were completed quickly and within a week of the shutdown and tie-in works, all the new electrowinning cells were in production, and the existing electrowinning cells were being used to treat pregnant solution from the existing and new intensive leach reactors. The safe and effective commissioning of the expanded desorption and recovery circuit was achieved due to the combined efforts of the Ravenswood Gold operations team and project team.

OPERATION

Stage 1 – Leaching

The new leach circuit was commissioned in July 2021. Table presents a summary of leach performance in the month prior to, and post commissioning of Stage 1. The 30-day periods were to limit the impacts of different ores types and their leach characteristics.

Table 1 Performance statistics in the month prior to and following Stage 1.

Date (2021)	Throughput (t/d)	Throughput (Mt/y)	Leach feed grade (Au g/t)	Solid tail grade (Au g/t)	Leach extraction (%)
11-6 to 10-7	13,911	5.1	0.45	0.06	86.4
11-7 to 9-8	13,408	4.9	0.51	0.04	91.4

All data is a 30-day average

The leach extraction increase of 5% (absolute) and the decrease in solids tail grade were consistent with design expectations.

Stage 2 – Crushing

The new crushing circuit (Buck Reef crusher) was commissioned during June and July 2022 with the first ore feed on 24 July 2022. The beneficiation section was operational by February 2023.

A steady improvement in throughput solids rate towards the design rate of 1200 t/h (closed circuit) and more recently towards 1960 t/h in beneficiation mode (bene mode) is shown in Figure 7. The main issue with ramp up was poor run time due to numerous mechanical issues. The main mechanical issues included:

- primary crusher mantle and hydraulic issues since start-up caused by installation of the incorrect hydroset and undersized accumulator; these are now largely resolved
- main belt feeder (CV501) failure caused by allowing the vault to run empty causing damage (April 23)
- primary crusher eccentric and gear drive misalignment due to incorrect installation (April 23)
- secondary crusher eccentric bearing failure (second-hand unit) (June 23).

Since commencement, the highest run time was date 402 h (November 2022) compared to the design of 510 h per month. Despite this low monthly run time, the design daily closed-circuit throughput has been exceeded, as shown in Table 2. Bene mode is where coarse waste is rejected in the crushing circuit; closed circuit is without rejection of coarse waste.

Table 2 Daily and monthly performance of the crushing circuit.

Plant	Unit	Design	Achieved
Daily – bene mode	kt/d	34	31
Daily – closed circuit	kt/d	19	28
Monthly – closed circuit	kt/month	592	534

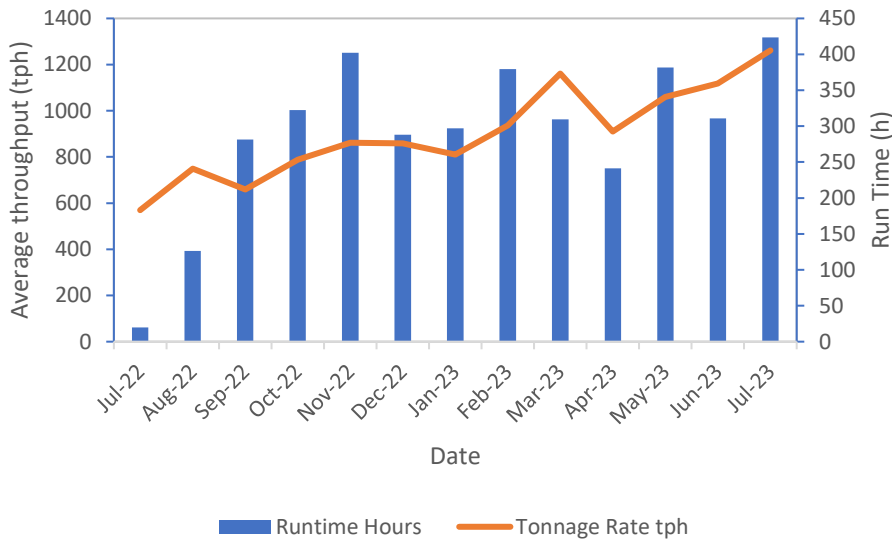


Figure 7 Buck Reef crushing performance

Stage 3 – Milling

The new milling circuit (Mill 4) was commissioned during August and September 2022 with first feed on 30 September. The mill ran for a period of 54-days after which one of the dual drive motors experienced an electrical failure most likely caused by workmanship (quality) issues during the Covid period. Inspection of the second motor revealed that it was also damaged and near failure. Although the initial prognosis was that both motors were beyond repair, these motors were successfully repaired in two workshops in Brisbane to the credit of those involved. Both motors continue to operate (to July 2023). Warranty replacement motors are expected in August 2023.

The mill was returned to operation after 71-days of downtime in February 2023 and continues to ramp up. Additional mechanical failures in the mill gear lube system were experienced during March, April and May 2023 most likely caused by oil contamination and/or a pump failure. Debottlenecking some of the original sections of the plant such as adsorption tank flowrates are also impairing throughput and work continues there.

Figure 8 indicates the erratic Mill 4 throughput affected by motor and mechanical failures but also shows a general improvement in total tonnes processed. Grind size from the two milling circuits is also erratic but shows an overall improvement, decreasing from an average P_{80} of 195 μm in Aug/Sep 2022 to 130 μm in Jun/Jul 2023).

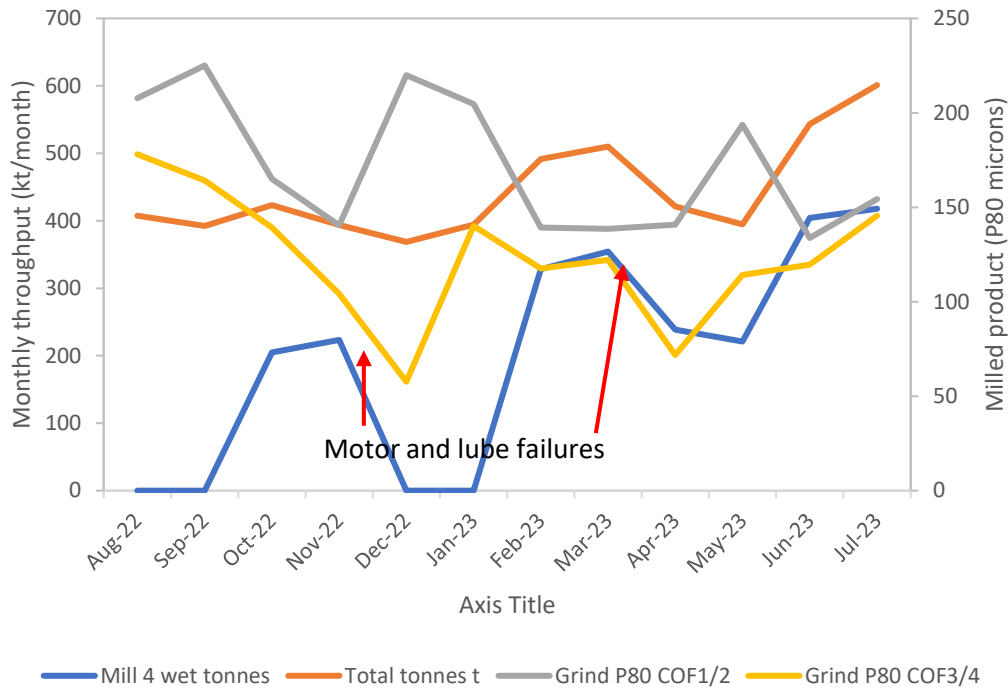


Figure 8 Monthly throughput and milled product size

Table 3 shows the site targets which exceeded the corresponding design throughput.

Table 3 Milling circuit performance against design

Plant	Unit	Design parameter	Achieved
Milled product – daily	kt	19	22
weekly	Kt	137	148
monthly	kt	592	601

CONCLUSIONS

The design and construction of the Ravenswood expansion achieved the design objectives with a staged approach.

The Ravenswood plant now operates at or above the target daily throughput rate for Stage 2 operation.

The beneficiation and rejection of coarse waste is now in operation and the circuit is ramping up to Stage 3 throughput rates.

The delivery of this project during the Covid pandemic, and with a very tight schedule, was a challenge, but the project's success demonstrated what was possible.

Ramp-up to consistent performance has been negatively impacted by mill motor and mechanical failures, in both the crusher and milling circuits caused by design and quality issues. Ravenswood's operations and maintenance staff, with OEM support, continue to focus on resolving mechanical issues and runtimes to improve the performance, availability and throughput rate of the operations.

The key to the success of this project was the speed with which the project was progressed from design through to construction and commissioning with minimal downtime. This was achieved with

a collaborative relationship between Ravenswood and Ausenco to drive the project forward with singular focus.

ACKNOWLEDGEMENTS

The authors would like to thank Ravenswood and Ausenco for the support in publishing this paper. The success of this project is due to the professional, innovative, diligent and co-operative work from Ravenswood's project and operations teams, Ausenco's study, project, construction and commissioning teams, and the support of OEMs.

Evaluation of High-Shear Leach Reactor at IMK Gold Mine

D Prananta¹, A Dhayanto², W Padmonobo³, R Schultz⁴, S Flatman⁵, M Battersby⁶

1. PERHAPI, General Manager/KTT, PT Pelsart Tambang Kencana – Indonesia, Sungai Durian, Kabupaten Kotabaru, Kalimantan Selatan Province, dadang.prananta@imkgold.co.id
2. PERHAPI, Plant Manager, PT Indo Muro Kencana – Indonesia, Dirung, Dirung Lingkin, Tanah Siang Sel., Kabupaten Murung Raya, Kalimantan Tengah 73971, alex.dhayanto@imkgold.co.id
3. PERHAPI FAusIMM, SEAP Representative, Maelgwyn Mineral Services Ltd – Jakarta – Indonesia, Nifarro Park, ITS Tower 6 floor, Jalan Raya Pasar Minggu 18, South Jakarta, wiku24@gmail.com
4. Project Metallurgical Engineer, Maelgwyn Mineral Services Ltd – Cardiff – United Kingdom, Ty Maelgwyn, 1A Gower Road, Cathays, Cardiff CF24 4PA, rschultz@maelgwyn.com
5. C.Eng Pr Eng FSAIMM, General Manager, Maelgwyn Mineral Services Ltd – Cardiff – United Kingdom, Ty Maelgwyn, 1A Gower Road, Cathays, Cardiff CF24 4PA, sflatman@maelgwyn.com
6. C.Eng FAusIMM MIMMM SME, Managing Director, Maelgwyn Mineral Services Ltd – Cardiff – United Kingdom, Ty Maelgwyn, 1A Gower Road, Cathays, Cardiff CF24 4PA, MBattersby@maelgwyn.com

ABSTRACT

Various types of aerators and spargers have been trialled in gold and silver processing since the late 1980s. Initially, simply to inject oxygen or air into pulps to increase dissolved oxygen levels and improve leaching kinetics with cyanide. These basic designs have been enhanced by the incorporation of high shear, pressure hold-up and ultra-fine bubble generation systems. Essentially the aerator has become a low-pressure leach reactor. There are now over 80 of these reactors in operation worldwide treating a range of ore types and achieving significant increases in gold and silver recovery and leach kinetics combined with reductions in reagent consumption.

The PT Indo Muro Kencana gold mine in Indonesia identified serious challenges in maintaining production performance due to variations in the ore properties at the mine. The changes in ore characteristics resulted in a reduction of recoveries of approximately 4% for gold and 7% for silver despite the addition of hydrogen peroxide to compensate for the lowering of the dissolved oxygen levels in the leach to below 10 ppm. To overcome these issues, a high-shear leach reactor was installed and trialled for one year under different operating conditions. The trial proved successful, improving oxygen utilisation with significantly higher dissolved oxygen levels above 20 ppm, which allowed the stoppage of the hydrogen peroxide addition. Importantly, the recovery of gold and silver improved by 1.30% and 4.90%, respectively. This paper presents the development and theory behind the high shear reactor technology together with details of the installation and operating strategy of the reactor at the mine. Finally, the technical and economical evaluation of the case study will be reported that led to the permanent acceptance of technology.

INTRODUCTION

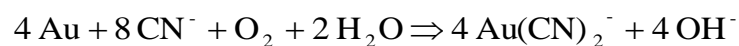
Whilst there are many lixivants for gold and silver, cyanide has been and remains the most widely used lixiviant for the leaching of these precious metals. Such leaching takes place in a high pH environment where a supply of oxygen is necessary for the reaction to proceed. Historically, where most ores were considered “free milling” the oxygen was supplied simply by flowing air through the leaching tanks. With the introduction of Carbon-In-Leach (CIL) technology for the extraction of gold (DeMent and King, 1982) and the increasing complexity of mineralogy of gold ores being mined various methods of improving the supply of oxygen have been developed. This paper details one such modern development using a high shear leach reactor and its application at the PT Indo Muro Kencana gold mine in Indonesia.

Chemistry of cyanidation

To be able to determine the potential suitability of an oxygen addition device to improve cyanidation it is necessary to have a basic understanding of the cyanidation reaction itself, the factors driving it, and importantly the role of oxygen. Simply raising dissolved oxygen (DO) levels without considering mineralogy and importantly surface passivation will not necessarily improve recoveries.

Mineralogical considerations

Whilst cyanide is one of the major drivers if not the major driver of gold dissolution it cannot be viewed in isolation particularly in respect of the relationship between cyanide and oxygen derived from the well-known Elsner’s equation (Elsner, 1846).



From the above, it is apparent that both cyanide and oxygen are required in an aqueous solution to leach gold. For the leaching of pure gold, the stoichiometry of Elsner’s reaction gives the required molar ratio of free cyanide to oxygen as 8:1 (or 6.5:1 when expressed as a mass ratio). As cyanide is the more expensive reagent, it is desirable from a financial point of view to ensure that cyanide is the rate-limiting reagent (Vorster and Flatman, 2001). It is important to note that the rate of dissolution of gold in alkaline cyanide solutions is controlled by the rate of dissolution of oxygen from the bulk solution to the metal surface.

For a gold ore with a 10 ppm head grade, 0.4 ppm of oxygen in 50% solids by weight slurry should theoretically be sufficient for gold dissolution alone. However, in practice significantly more oxygen is required to maintain gold dissolution due to numerous competing side reactions that also take place consuming oxygen and so potentially “starving” the leach of oxygen. The net effect of this can be to slow down leach kinetics or even, potentially bring the leach to a halt unless there is an efficient means of raising dissolved oxygen levels. Many of these undesirable side reactions have kinetics faster than the gold dissolution reaction and so take precedence ahead of the gold dissolution. The reactions consuming oxygen (and often cyanide as well) can be categorised in terms of increasing oxygen demand into two basic groupings namely solution and solid species.

Solution species oxidation

Some of the mineralogical phases might dissolve and react in the comminution circuit ahead of the main leach circuit and thus lead to solution species prone to oxidation. The circuit process water might also contribute to these species. The more important of these include:

- **Ferrous iron:** the oxidation of Ferrous to Ferric (Fe^{2+} to Fe^{3+}) requires $\frac{1}{4} \text{ O}_2$ for each iron in solution to be oxidised (Lotz *et al*, 2015). Hence, without the further addition of oxygen, a 50 ppm Fe^{2+} in solution could consume the entire mass of oxygen contained at usual equilibrium values. Therefore, at Fe^{2+} levels exceeding 10-20 ppm, it is advisable to apply pre-oxidation to reduce the oxygen consumption

during the leach and prevent ferro-cyanide formation at the same time. The mass of oxygen required is relatively low and addition could be achieved using lances or other low efficiency mass transfer devices.

- **Sulfur species:** unstable products of sulfide dissolution may also consume oxygen to form thiosulfate or poly-thionates. The oxygen consumption for these species is higher than the iron oxidation, but the kinetics tend to be slower. Where fresh meta-stable sulfur compounds are present in solution, more aggressive pre-oxidation might be advisable to try and convert them away from thiocyanate forming species. The oxygen mass requirements are still relatively moderate.

Solid, mineral phase components to be oxidised

Whilst solution species oxidation largely prevents the slowdown of gold leach kinetics due to inadequate oxygen levels as well as limiting cyanide consumption due to iron or sulfur, the solid phase oxidation may be unavoidable, desired and targeted, or best restricted. Minerals such as pyrrhotite (Fe_7S_8) are very easily oxidised and would consume nearly the same mass of oxygen to be transformed to sulfate and ferric hydroxide. Hence for each 1 kg of sulfide oxidised in the leach feed approximately 1 kg of oxygen would be required if the oxidation reaction were to advance to completion. It will be appreciated that even at modest sulfur dissolution levels the oxygen requirement will be expressed in tons per day rather than kilograms.

Similarly, arsenopyrite (FeAsS) would consume oxygen equating to half the mass of arsenopyrite to be oxidised. The oxidation kinetics of this reaction are reasonably fast. Lastly, pyrite (FeS_2) would consume the same mass of oxygen for each mass equivalent FeS_2 transformation to sulfate and ferric hydroxide. However, the kinetics of this reaction are significantly slower than the two aforementioned ones (pyrrhotite and arsenopyrite) (Lotz et al, 2015).

Pyrrhotite may fall into the category of unavoidable oxidations and must be accommodated to a degree whether the mineral is gold barren or not. Arsenopyrite and pyrite are often associated with gold and hence the dissolution of these matrix minerals might be deliberately targeted through oxidation to release encapsulated gold.

Surface passivation consideration (film boundary layer effect)

Whether it is the dissolution of relatively coarse free gold, the oxidation of gold containing sulfides or the diffusion of either oxygen or cyanide to the solid interface (or the diffusion of $\text{Au}(\text{CN})_2^-$ from the solid interface into the bulk solution phase) – the reaction kinetics are driven by the film boundary layers. With less agitation or shear, the layer will be thicker than under conditions of raised shear. This is illustrated in Figure 1:

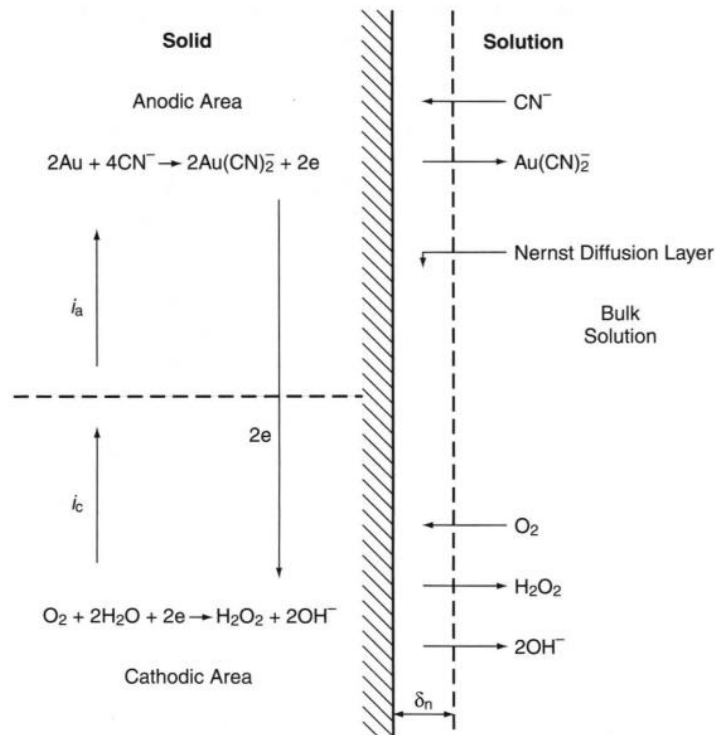


Figure 1 – Mass control across the film boundary layer – solid to solution (Marsden and House, 1992)

A reduction in film boundary layers can increase the gold dissolution reaction rates significantly. This can be achieved via a shear reactor, which has the benefit of the shear removing mineral species that may be coating or passivating the desired mineral surface and effectively rendering it temporarily refractory to cyanide. This is an additional benefit when compared with the use of lances and other low efficiency addition devices.

Developments in improving oxygen addition in the leaching of gold

Overall History

There have been various developments in the addition of oxygen to the leach that range from the simple introduction of air with lances to the addition of oxygen directly with complex high shear leach reactors. Some initial developments were centred around the goldfields of Western Australia in the 1990s. The oxide ores mostly encountered gave problems in increasing the dissolved oxygen levels of the leach. There were two reasons for this:

- firstly, the oxide ores contained appreciable amounts of clay materials that made slurries in the leach tanks highly viscous.
- secondly, the very high levels of Total Dissolved Salts (TDS), up to 300,000 mg/L, encountered in the goldfields, buffered the slurries resulting in pH levels buffering out at around pH 9.5 or below (NICNAS, 2010).

Both factors led to reductions in dissolved oxygen (DO) levels in the leach to below levels required to satisfy the Elsner equation. To increase the DO levels some operations introduced pure oxygen, rather than air, into the leach.

Over time various methods of more efficient oxygen distribution with aerators were developed. The Filblast aerator (Seracini, 1995) and the Multi-Mix oxygen blaster (Ellis *et al*, 2002), (Ellis and Senanayake, 2004) were trialled extensively in Western Australia with some success. However, the abrasive nature of pumped mineral slurries resulted in high wear of the aerators, requiring constant maintenance and replacement with resulting downtime.

The oxygen suppliers also offered different solutions for more efficient oxygen dissolution that they had been using in other industries and processes. Air Liquide offered the BICONE (Air Liquide Standard Application Equipment, 2022) and British Oxygen Company (BOC), now part of the Linde group, offers the EDR oxygenator as part of the Goldox process. The EDR is a type of ring system distributor located in the pulp (British Oxygen Company, 2023). It is thought that EDR stands for “Eddies Doughnut Ring” to reflect the inventor and the method of distribution.

Aachen high shear leach reactor history

The development of the Aachen high shear leach reactor followed somewhat a similar development to the above-mentioned oxygen aerators, in having its basis in the West Australian goldfields. One of the co-inventors was operating a gold plant that could not achieve satisfactory DO levels. At the same time the other co-inventor had developed a novel aerator for flotation bubble generation (Imhof, 1987). The Aachen high shear leach reactor was formulated based on merging the application requirements with the advanced design. Early installations were at the Emperor gold mine, Fiji (1997); Mines d'Or de Salsigne, France (1998) and Kanowna Belle, Australia (1999). Whilst successful, it was quickly realised that at these operations where reactive sulfides were present there was more to efficient leaching than just raising the DO levels to the stoichiometric requirement. The role that high shear played in counteracting the boundary layer effect was recognised. The Aachen high shear leach reactor went through many design iterations with the aim of increasing fine bubble generation, increasing shear across the reactor, and then improving the wear resistance to handle the changing pressures, velocities, and turbulence in the unit due to the increased shear.

High shear leach reactors have proven themselves to be a major contributor to increase gold recoveries at many operations. There are currently over eighty Aachen high shear leach reactors in operation world-wide. They have been incorporated into proprietary processes for gold recovery (Flatman *et al*, 2010), (McMahon *et al*, 2016). Their importance in gold processing was demonstrated by the reactors being the successful basis of the design for two, Tier One gold plants in Africa belonging to Randgold Resources, now Barrick Gold Inc. (Mahlangu *et al*, 2019), with both operations designed to produce over 500,000 oz Au/Annum.

History of mining and processing at PT Indo Muro Kencana gold mine

PT Indo Muro Kencana gold mine (IMK) is located in the Central Kalimantan Region within the Indonesian portion of Borneo Island. The mine site has had three stages of ownership. The initial operators were from 1994 until 2002 (PT IMK 1st Operators). Followed by the second operators from 2004 until 2013 (PT IMK 2nd Operators). Then in 2016 the current operators PT IMK Now took over the operation.

Processing at IMK has modified over time by the various operators due to mining different ore bodies, ore types and the drive for process improvements i.e., increasing recovery and lowering reagent consumptions:

- ore type and ore bodies: this variation was related to the depth of the various mining zones or ore bodies, where proportions of eluvial ore were higher at the beginning years of the operation and processing was performed in a particular manner to maximise throughput or recovery. This has changed as the mine has grown older with mining depths or ore bodies changing, and with gold and silver feed grades decreasing.
- process improvements: some processing variations may be seen between PT IMK 1st Operators and PT IMK 2nd Operators, but the most significant processing variations have been performed during the operation of PT IMK Now. A list of the four largest processing variations:
 - recovery circuit was converted in 2017 and upgraded in 2018 & 2022 from Merrill

Crowe to Electrowinning, to increase production capacity.

- cyanide destruction in the tailings circuit was converted from the INCO Detox process to a ReCYN Plant.
- on-site thickener was converted from a clarification thickener to a tailings thickener to finally a pre-leach thickener.
- improvements in leaching to optimise cyanide (CN) usage, through balance of optimised DO levels & shear to achieve maximum recovery.

These points are illustrated further in the ore type variation trend and the basic flow sheet diagrams shown in Figures 2 through 5:

- changes between PT IMK 1st Operators and PT IMK 2nd Operators basic flow sheet diagrams are indicated in red.
- changes between PT IMK 2nd Operators and PT IMK Now basic flow sheet diagrams are indicated in blue.

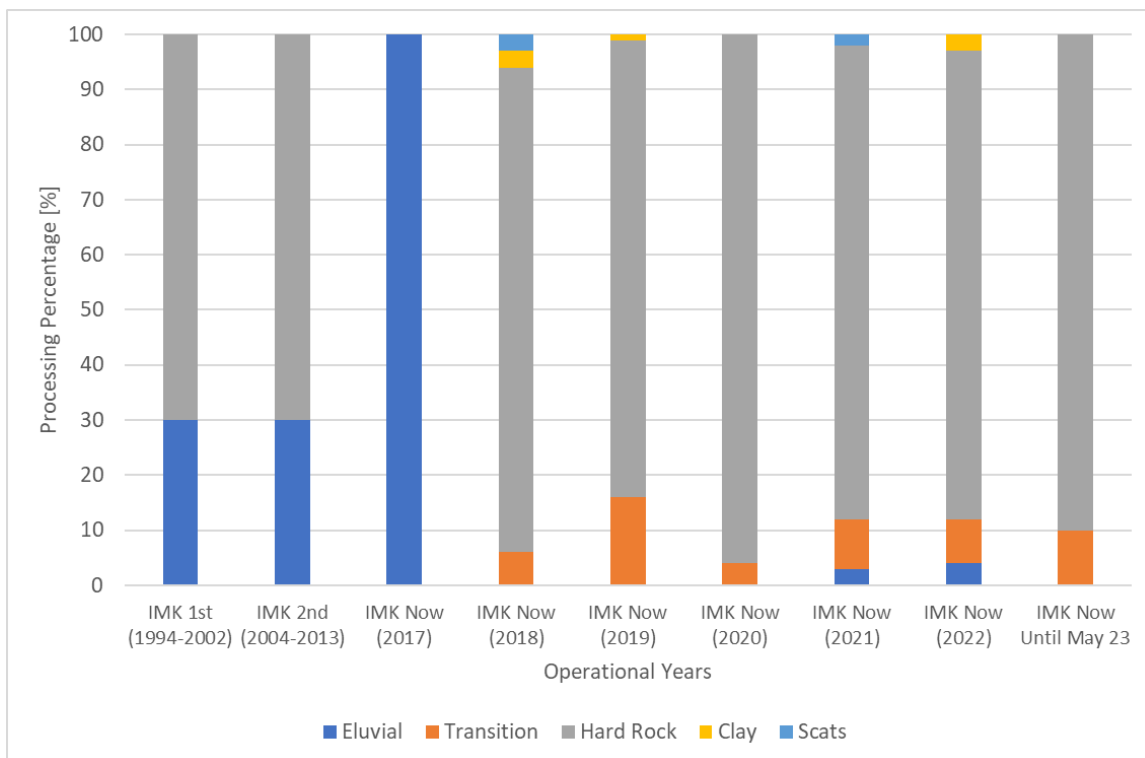


Figure 2 – Ore type variation history trend

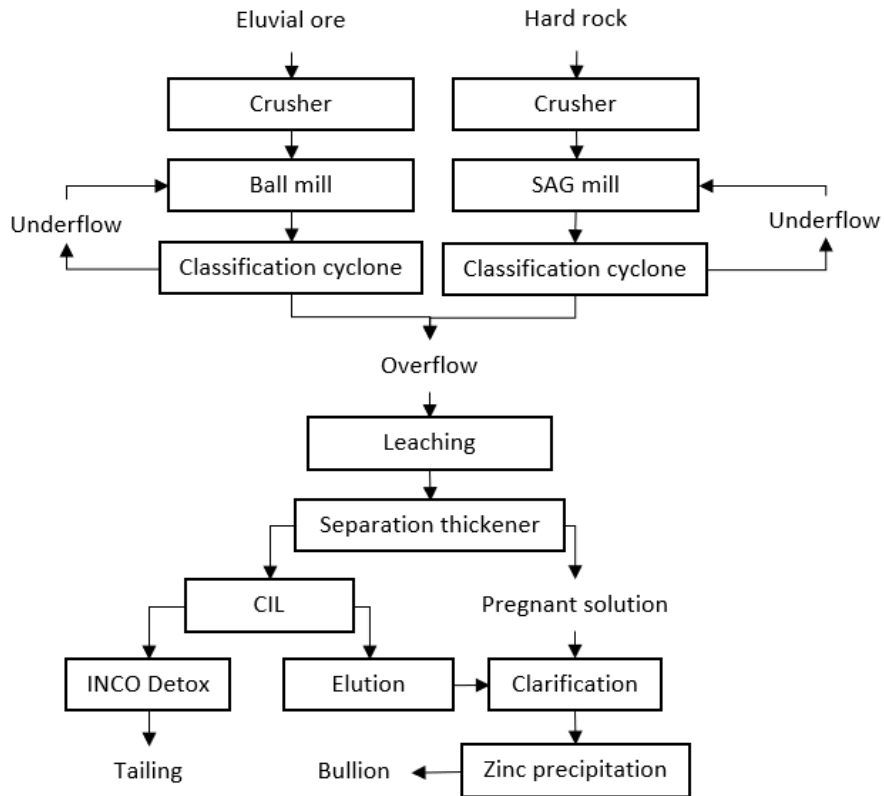


Figure 3 – Basic flow sheet diagram during PT IMK 1st Operators ownership

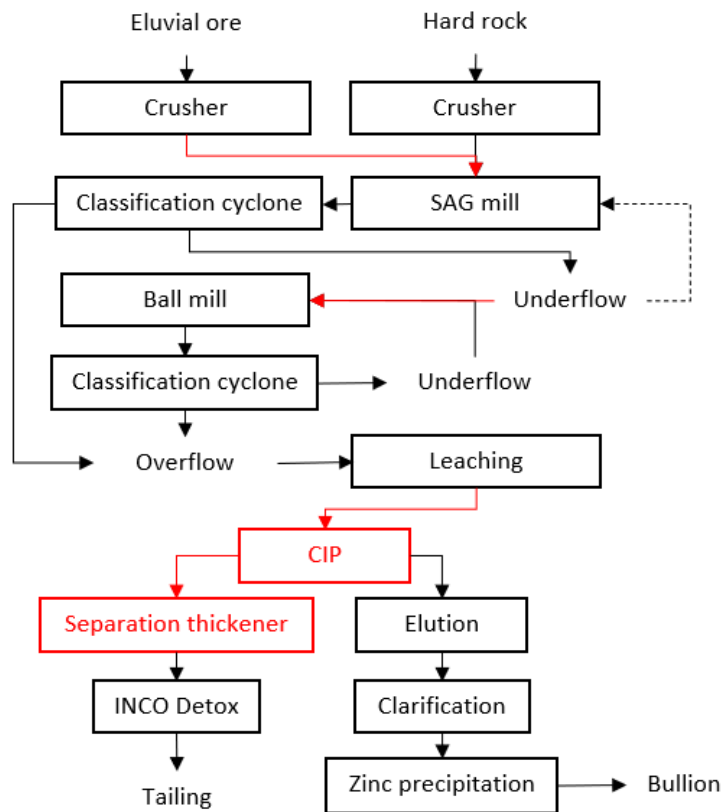


Figure 4 – Basic flow sheet diagram during PT IMK 2nd Operators ownership

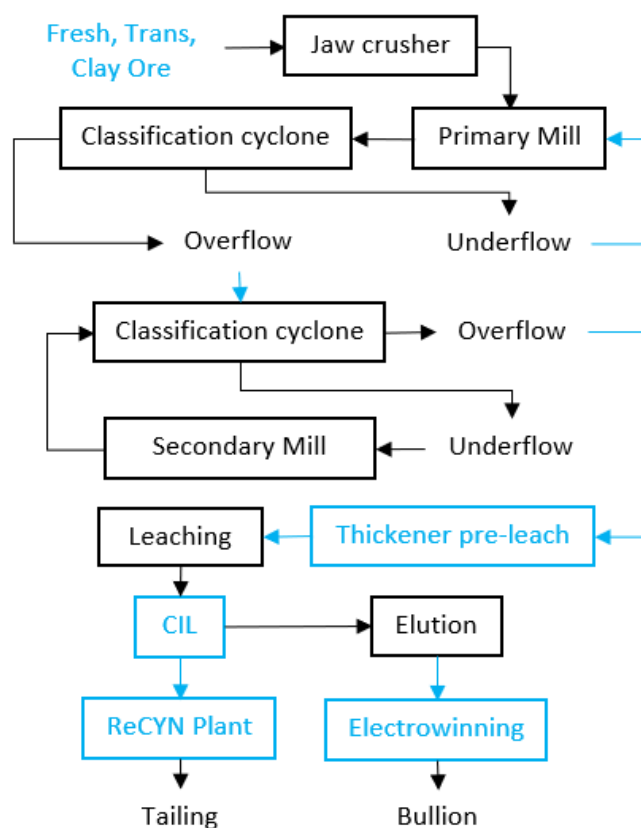


Figure 5 – Current basic flow sheet diagram during PT IMK Now ownership

THE PLANT TRIAL

Processing background

The Life of Mine (LOM) of PT Indo Muro Kencana gold mine is based primarily on two ore bodies – Bantain and Serujan. A few other ore bodies have been mined and processed in the past, but the Bantain and Serujan ore bodies make up a vast majority of the mining and processing that has taken place to date.

Based on historical processing information from PT IMK 1st Operators and some of their own initial processing, it was indicated to PT IMK Now that whilst mineralogy of the two ore bodies varied, the Bantain ore body was more refractory in nature:

- higher clay content in the ore leading to increased slurry viscosities in the leach requiring lowering % solids in the leach and reducing plant throughput.
- higher reagent consumptions or finer grinding required to maintain Au and Ag recoveries.
- additionally measured total sulfur content was on average 30% higher for the Bantain ore body than the Serujan ore body and similarly measured total sulfide sulfur content was on average 43% higher too.

This led to the decision of PT IMK Now to initially focus on primarily mining and processing the Serujan ore body, whilst performing metallurgical testing and evaluation on the Bantain ore body. This led to the implementation of modifications to the processing plant, to allow the plant to better process the Bantain ore body once the Serujan ore body was depleted in April 2022.

The mining and processing of the Bantain and Serujan ore bodies over time during the operation of PT IMK Now is illustrated further in the monthly and yearly ore body feed proportion percentage

trends (Figures 6 and 7). These figures indicate the transverse of the more refractory Bantain ore body from 10%-30%, between 2018 and 2021, to 100% during 2022 to current.

A timeline list of the processing improvements implemented by PT IMK Now to assist with the processing of the Bantain ore body. Originally the PT IMK processing plant leaching circuit was made up of four 2500 m³ leach tanks followed by ten 500 m³ CIP tanks:

- a) 2018 – 4th leach tank was converted from a leach tank to a CIL tank which improved leaching kinetics. Additionally, the ReCYN plant was installed, by converting the last three CIP tanks to RIL tanks, to allow for higher CN levels to be run through the leach by capturing and recycling CN that would have originally gone through detoxification and sent to tailings.
- b) 2019 – oxygen plant utilisation was improved by installing specialised lances in the first two leach tanks, which improved dissolved oxygen levels in the leach but not to the required levels.
- c) 2020 – 3rd leach tank was converted from a leach tank to a CIL tank which improved leaching kinetics further. Additionally, the on-site thickener was converted to a pre-leach thickener, which improved leach reagent consumption and increased plant throughput.
- d) 2021 – hydrogen peroxide dosage was started on 1st leach tank, which improved dissolved oxygen levels further.
- e) 2022 – high-shear leach reactor installed to improve leach kinetics and reagent utilisation, leading to a significant increase in dissolved oxygen levels.

The positive effects of these processing improvements on the production figures of PT Indo Muro Kencana gold mine, increasing throughput while increasing or maintaining gold and silver recoveries is illustrated in the operational data summary table (Table 1).

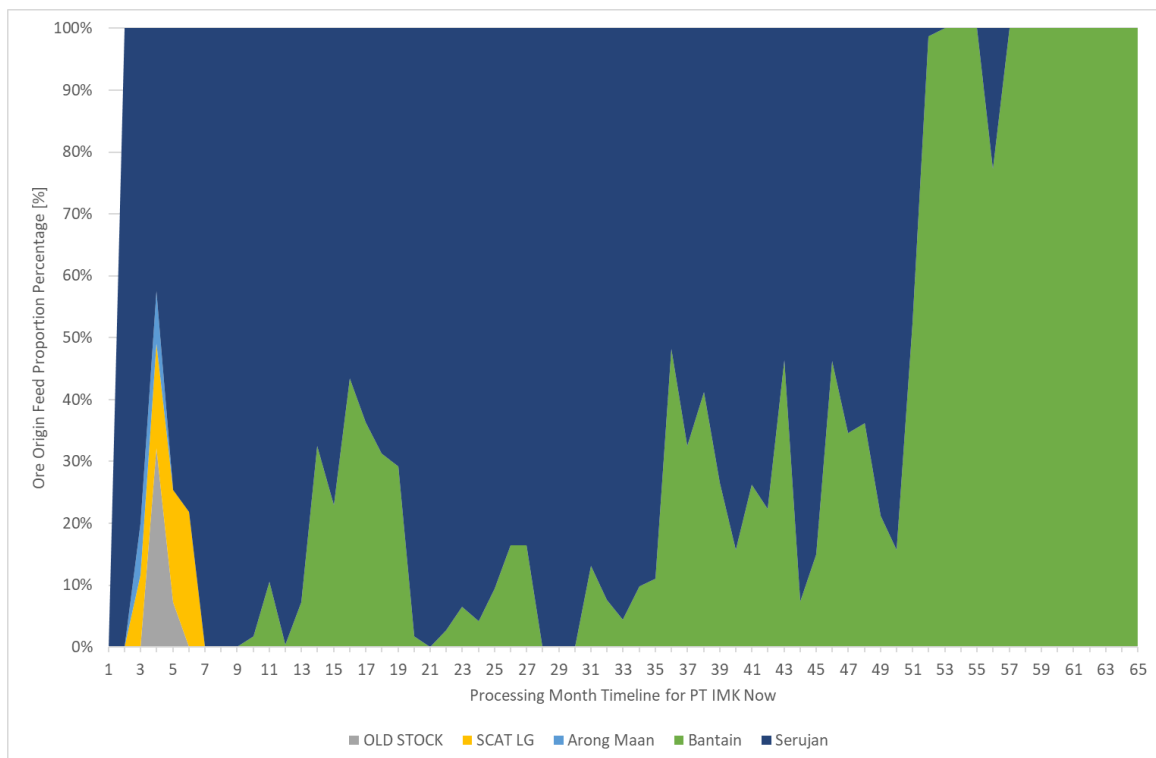


Figure 6 – Monthly PT IMK Now ore body feed proportion percentage trend

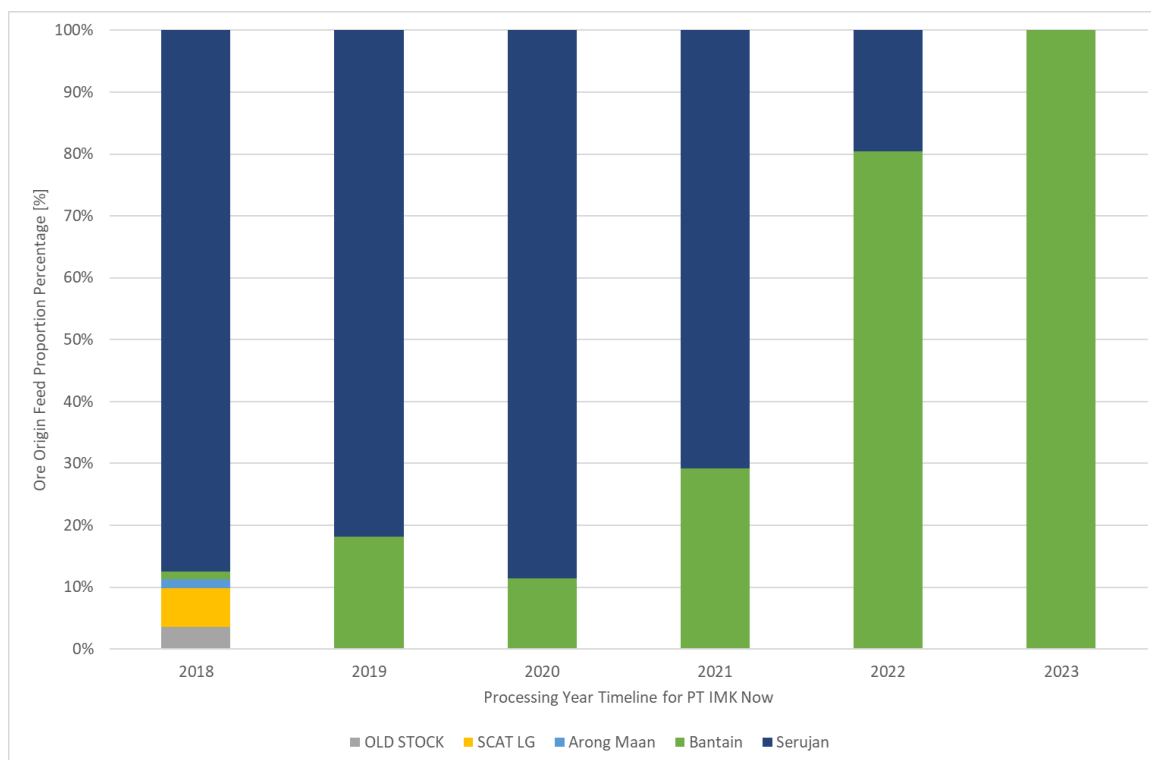


Figure 7 – Yearly PT IMK Now ore body feed proportion percentage trend

Table 1 – Operational data summary table

KPI	PT IMK 1st (1994-2002)	PT IMK 2nd (2004-2013)	PT IMK Now						
			2017	2018	2019	2020	2021	2022	Until May 23
Ore Milled (dmt)	11,227,389	4,531,585	267,889	547,944	1,098,781	1,315,155	1,348,562	1,520,851	555,024
Throughput (dt/h)	150	80	60	120	140	170	170	180	200
Au feed grade (g/t)	3.80	2.32	0.88	1.71	1.92	1.63	1.76	1.33	1.37
Au recovery (%)	95	92	77	95	95	96	97	96	97
Ag feed grade (g/t)	99.00	30.30	13.38	45.50	56.20	41.85	50.56	41.92	27.93
Ag recovery (%)	71	70	33	73	75	79	76	79	78

High shear leach reactor installation

PT IMK Now were approached and made aware of the benefits of high-shear leach reactor technology in the second quarter of 2021. Through collaboration between the processing and equipment supplier teams and by analysing historical processing data, the potential improvements in leach kinetics and reagent utilisations were seen and explained to the PT IMK Now processing team.

The normal route for the installation of such technology would be the laboratory testing of suitable plant samples to demonstrate the potential improvements, before the client commits to the investment of installing industrial plant size units.

However, due to the PT IMK Now wanting to install this technology before the depletion of the Serujan ore body in the second quarter of 2022 and the equipment supplier team seeing the potential process improvement through the analysing of historical processing data, it was agreed, between both parties, that the lab scale phase test work would be bypassed and instead one plant scale high-shear leach reactor would be installed and trialed for one year, monitoring the unit's performance with processing the more challenging Bantain ore body.

Through discussions held between the PT IMK Now process, maintenance & projects teams, and the equipment supplier team, it was decided that initially one high-shear leach reactor would be installed as a bund area structure installation adjacent to the 1st leach tank. Constant collaboration between the above teams allowed for the PT IMK Now projects team to fast track the engineering drawings and bill of materials for the installation. The concrete, structure, piping, pump, motor, electrical cabinets, and cabling were purchased by the PT IMK Now team themselves, through their own suppliers, where the PT IMK Now team made a special request to purchase the valves, instrumentation, and control cabinet through the equipment supplier team direct.

The one-year trial was commissioned, after the build and installation were performed by the PT IMK Now team's projects and maintenance personnel. Once commissioned, three visits took place during the one-year trial, to perform maintenance on the unit, if required and to assist the site team with operating and maximising the performance of the technology together with the overall improvement in their processing. In addition, remote support was continuously provided during the trial.

The completed build is shown Figures 8a, 8b & 8c.



Figure 8a, 8b & 8c – Images of some portions of the high shear leach reactor installation at PT IMK

Trial analysis

The original agreement for the trial was for the first four months to be dedicated towards the PT IMK Now team to become familiar with the operation of the high-shear leach reactor and to continuously optimise the unit, to maximise its performance and efficiency, to benefit the leaching circuit of the operation. This was achieved through continuous consultation with the equipment supplier team, where balance was achieved between unit throughput, unit part wear and oxygen supply.

The remainder of the trial would involve operating and monitoring the performance of the unit, to assist the mine site with processing the more challenging Bantain ore body.

Due to LOM requirements, the high-shear leach reactor commissioning coincided with feeding 100% of the more refractory Bantain ore body to the processing plant, with minimal Serujan ore body (April 2022 / Month 52). As can be seen in Figure 6, the PT IMK Now team did not have historical operating data where high levels of Bantain ore body were fed to the processing plant.

Therefore, the performance of the high-shear leach reactor, towards metal recovery, could not be assessed by comparing the operational data of the plant before and after the high-shear leach reactor was commissioned. A different approach was required. A test work campaign was decided through consultation between the PT IMK Now team and equipment supplier team. This comparison analysis methodology for the test work campaign is described:

- ten laboratory scale leach tests were performed in total and were performed when three portions of the Bantain ore body were blended and fed to the processing plant (Bantain zones 3-1, 5-9 & 6-1). This blend was a good starting position to analyse the effectiveness of the high-shear leach reactor against the difficult to process Bantain ore body.
- the plan was to take samples at two locations in the leaching circuit, after sodium cyanide (NaCN) had been dosed, and these samples would be taken to the plant's met lab, where the leaching process would be replicated at lab scale on these samples, where different means of oxygen injection would be applied:
 - oxygen injection means: A / pure oxygen (O₂) = ordinary oxygen bubbling in the lab leach tank to achieve the DO target (15 - 20 ppm).
 - oxygen injection means: B / hydrogen peroxide (PRX) = hydrogen peroxide dosage in the lab leach tank to achieve the DO target (15 – 20 ppm).
 - oxygen injection means: C / Aachen Assisted Leaching (AAL) = oxygen injection through the high-shear leach reactor initially (first 7 h of the leach) and then maintained at the DO target with ordinary oxygen bubbling in the lab leach tank (15 – 20 ppm).
- the two locations for the samples would be at the feed to the 1st leach tank (before the high-shear leach reactor) and at the discharge of the 1st leach tank (after the high-shear leach reactor). These samples would be taken at a duration of 7 h apart, with the feed to the 1st leach tank being the first sample (sample one) and the discharge of the 1st leach tank being the second sample (sample two). The 7 h duration is the calculated residence time of the 1st leach tank.
- sample one, once taken would be split into three subsamples. Two subsamples would be placed into a 5 L lab scale leach tank each and agitated at 250 rpm. These two subsamples would each follow the oxygen injection means of A & B (O₂ & PRX respectively).
- the third subsample would be used for head grade analysis by analysing the solid and solution for Au and Ag content. The NaCN content of the sample was also determined at this point.
- sample two, once taken 7 h after sample one, would be placed into its own lab scale 5L leach reactor and agitated at 250 rpm. This sample would follow the oxygen injection means of C

(AAL). As this sample has already been leaching for 7 h in the 1st leach tank, it would slot into the same leach timescale of the other two samples (oxygen injection means A & B).

- oxygen injection means A & B underwent kinetic leach sampling after 2, 4, 8, 24, 32 and 48 h marks, where both solids and solution were analysed for Au and Ag content. The DO, pH and NaCN content was also measured or determined at each of these kinetic points and recorded.
- oxygen injection means C underwent the same kinetic leach sampling as oxygen injection means A & B, except for the 2 and 4 h marks, due to the sample only being taken from the 1st leach tank discharge 7 h into the leach.
- carbon addition at 10 g/L was added to all three oxygen injections means (A, B & C) after the 22 h mark and was analysed for Au and Ag content at the 48 h mark.

The test work plan was repeated ten times on different days where it was still ensured that the ore blend was still of Bantain ore body and of the three zones of Bantain zones 3-1, 5-9 & 6-1.

As processing experience of Bantain ore body, in relation to processing parameters (pH and DO) and reagent consumptions (lime, NaCN and hydrogen peroxide), are known to PT IMK Now, through historical processing information from PT IMK 1st Operators and some of their own initial processing, the performance of the high-shear leach reactor, in relation to these criteria, could be assessed by comparing the operational data of the plant before and after the high-shear leach reactor was commissioned.

RESULTS AND DISCUSSION

Metal recovery

The metal recovery analysis was determined twice from the test work campaign. Once on the 32 h leach kinetic sampling point and the other on the 48 h leach kinetic sampling point:

- the 32 h leach kinetic sampling point was a representation of the actual leach residence time at the PT IMK gold mine.
- while the 48 h leach kinetic sampling point was an indication to the PT IMK Now processing team, which was to measure the effects of increasing the leach residence time by an additional 16 h. An internal investigation was undertaken to see the effects of the potential installation of two additional 2500 m³ leach tanks.

The results are in relation to the three Oxygen Injection Means, as described in the previous section (the plant trial – trial analysis): A = O₂, B = PRX & C = AAL.

Metal recovery – 32 h leach kinetic sampling point

The test results for Au and Ag recovery for the 32 h leach kinetic sampling point are shown in Figure 9 and 10, where the median Au recovery for O₂ was 94.4%, while PRX and AAL were 95.3% and 96.6%, respectively. Similarly, the median Ag recovery for O₂ was 72.8%, while PRX and AAL were 75.0% and 79.9%, respectively.

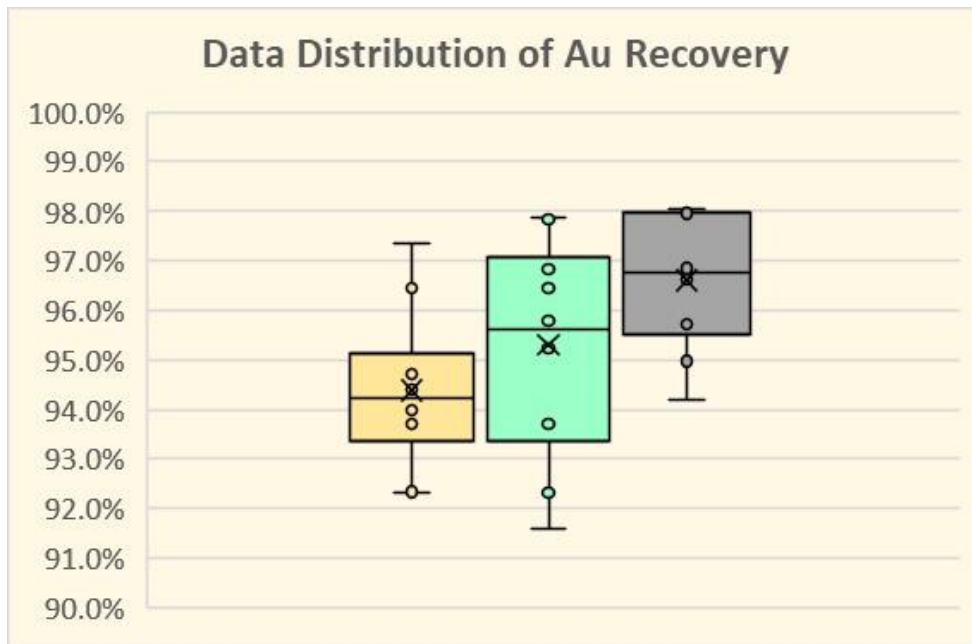


Figure 9 – Au recovery results for 32 h leach kinetic sample point for O₂, PRX and AAL

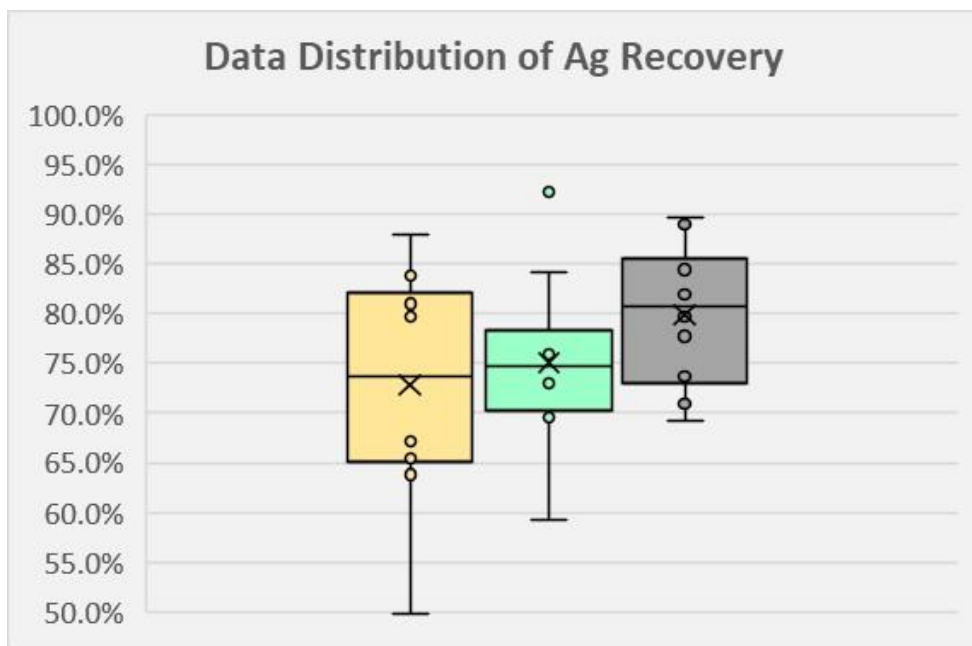


Figure 10 – Ag recovery results for 32 h leach kinetic sample point for O₂, PRX and AAL

The box plot diagram displayed in Figure 9, also indicated that Au recovery was consistently higher for AAL when compared to O₂, as indicated by comparing the range and median of the metal recovery results in the trends. However, this was not the same when comparing the range of the boxes in the trend between PRX and AAL, where PRX and AAL may have sometimes overlapped. However, the median for AAL was higher than the median for PRX.

As for silver recovery, sometimes the recovery of AAL was lower than both O₂ and PRX, indicated by the potential overlap of the range of the boxes in the box plot diagram in Figure 10. However, the median of AAL was higher than both O₂ and PRX for silver recovery also.

Since the sample of this test work represents the whole slurry being processed in PT IMK processing plant, a hypothetical t-Test analysis was conducted to predict the whole population behaviour, in this case: plant slurry. The analysis result is shown in Table 2:

Table 2 – Au and Ag recovery t-test analysis of O₂ vs AAL & PRX vs AAL for 32 h leach kinetic sampling point

Criteria	Au Recovery		Ag Recovery		Au Recovery		Ag Recovery	
	O ₂	AAL	O ₂	AAL	PRX	AAL	PRX	AAL
Mean (%)	94.4	96.6	72.8	79.9	95.3	96.6	75.0	79.9
Variance (%)	0.02	0.02	1.40	0.50	0.05	0.02	0.77	0.50
Observations	10	10	10	10	10	10	10	10
Pearson Correlation	0.63		0.30		0.54		0.46	
df	9		9		9		9	
t Stat	-5.54		-1.90		-2.25		-1.84	
P(T<=t) one-tail	0.000		0.045		0.025		0.049	
t Critical one-tail	1.83		1.83		1.83		1.83	
P(T<=t) two-tail	0.00		0.09		0.05		0.10	
t Critical two-tail	2.26		2.26		2.26		2.26	

The following two hypotheses were chosen related to the t-test analysis for each of the columns within Table 2:

- a null hypothesis (H0) that stated there was no statistically significant difference between the means of O₂ or PRX when compared to AAL.
- and an alternative hypothesis (H1) that stated there was a statistically significant difference between the means of O₂ or PRX when compared to AAL.

For the null hypothesis (H0) to be acceptable, the P one-tail value, from Table 2, needed to be greater than the significance level of 0.05, which was not the case for all four columns and therefore the null hypothesis (H0) may have been rejected.

This therefore indicated there was a statically significant difference between the means of the Au and Ag recovery results between AAL and O₂ or PRX, which suggested that the difference between the calculated and measured means was unlikely to have occurred by chance, for the 32 h leach kinetic sampling point.

Metal recovery – 48 h leach kinetic sampling point

The test results on Au and Ag recovery for the 48 h leach kinetic sampling point are shown in Figure 11 and 12, where the average Au recovery for O₂ was 95.6%, while PRX and AAL were 94.9% and 96.9%, respectively. Similarly, the average Ag recovery for O₂ was 74.7%, while PRX and AAL were 76.9% and 84.3%, respectively.

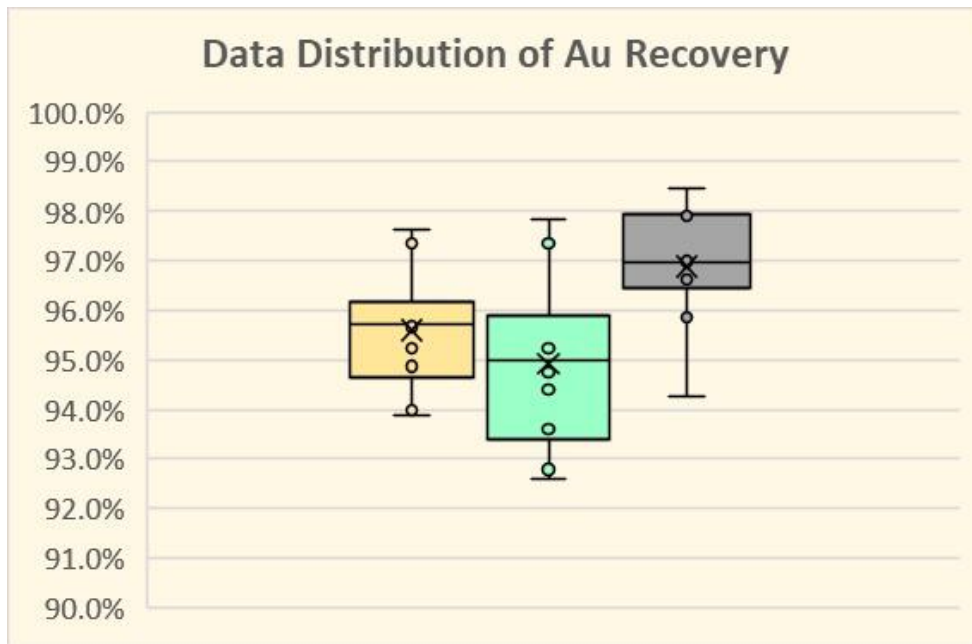


Figure 11 – Au recovery results for 48 h leach kinetic sample point for O₂, PRX and AAL

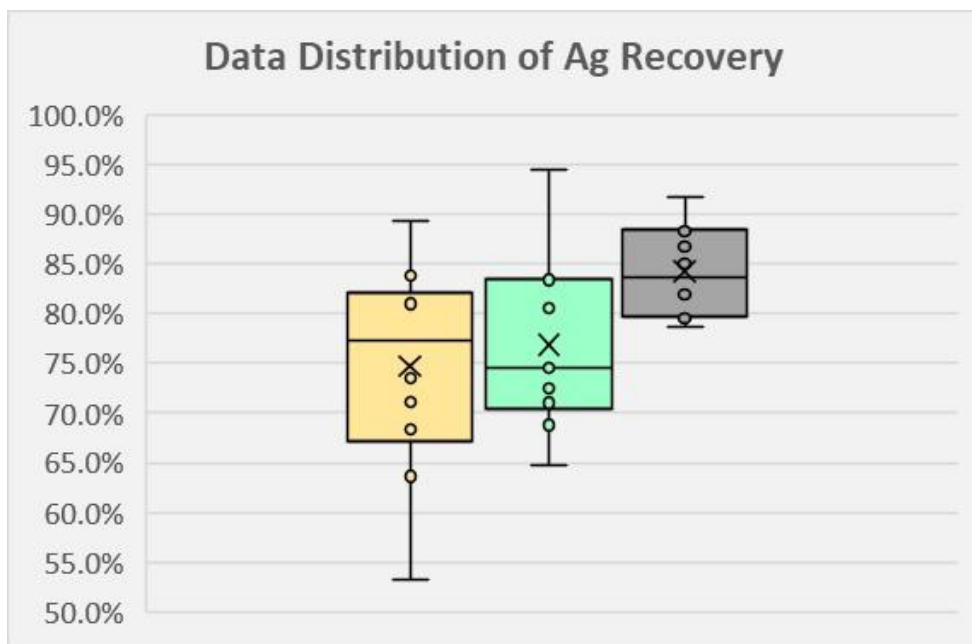


Figure 12 – Ag recovery results for 48 h leach kinetic sample point for O₂, PRX and AAL

The box plot diagram displayed in Figure 11, also indicated that Au recovery was consistently higher for AAL when compared to O₂ and PRX, as indicated by comparing the range and median of the metal recovery results in the trend.

As for silver recovery, sometimes the recovery of AAL was lower than both O₂ and PRX, indicated by the potential overlap of the range of the boxes in the trend of Figure 12. However, the median of AAL was higher than both O₂ and PRX for silver recovery also. Additionally, the range of the recovery results for AAL was the narrowest when compared to O₂ and PRX, which indicated the effectiveness of AAL to reach a narrower specific range of recovery results.

Once again, since the sample of this test work represents the whole slurry being processed in PT IMK processing plant, a hypothetical t-Test analysis was conducted to predict the whole population behaviour, in this case: plant slurry. The analysis result is shown in Table 3:

Table 3 – Au and Ag recovery t-test analysis of O₂ vs AAL & PRX vs AAL for 48 h leach kinetic sampling point

Criteria	Au Recovery		Ag Recovery		Au Recovery		Ag Recovery	
	O ₂	AAL	O ₂	AAL	PRX	AAL	PRX	AAL
Mean (%)	95.6	96.9	74.7	84.3	94.9	96.9	76.9	84.3
Variance (%)	0.02	0.01	1.18	0.21	0.03	0.01	0.77	0.21
Observations	10	10	10	10	10	10	10	10
Pearson Correlation	0.25		0.27		-0.14		0.25	
df	9		9		9		9	
t Stat	-2.75		-2.86		-2.79		-2.65	
P(T<=t) one-tail	0.01		0.01		0.01		0.01	
t Critical one-tail	1.83		1.83		1.83		1.83	
P(T<=t) two-tail	0.02		0.02		0.02		0.03	
t Critical two-tail	2.26		2.26		2.26		2.26	

In the same way as the 32 h leach kinetic sampling point, the following two hypotheses were chosen related to the t-test analysis for each of the columns within Table 3:

- a null hypothesis (H0) that stated there was no statistically significant difference between the means of O₂ or PRX when compared to AAL.
- and an alternative hypothesis (H1) that stated there was a statistically significant difference between the means of O₂ or PRX when compared to AAL.

Again, for the null hypothesis (H0) to be acceptable, the P one-tail value, from Table 3, needed to be greater than the significance level of 0.05, which was not the case for all four columns and therefore the null hypothesis (H0) may have been rejected.

This therefore indicated there was also a statically significant difference between the means of the Au and Ag recovery results between AAL and O₂ or PRX, which suggested that the difference between the calculated and measured means was unlikely to have also occurred by chance, for the 48 h leach kinetic sampling point.

Metal recovery – 32 h and 48 h leach kinetic sampling points comparison

When comparing the Au recovery results, between the 32 h and 48 h leach kinetic sampling points, O₂ had the biggest increase of 1.2%, but was still 1.3% lower than AAL.

However, when comparing the Ag recovery results, between the 32 h and 48 h leach kinetic sampling points, AAL had a large increase of 4.4%. This was quite a significant increase for an additional 16 h of leaching residence time.

This is illustrated further in Table 4:

Table 4 – Au and Ag recovery comparison between 32 h and 48 h leach kinetic sampling points

Sampling time	Au Recovery (%)			Ag Recovery (%)		
	O ₂	PRX	AAL	O ₂	PRX	AAL
32 h Mean	94.4	95.3	96.6	72.8	75.0	79.9
48 h Mean	95.6	94.9	96.9	74.7	76.9	84.3
Difference	1.2	-0.4	0.3	1.9	1.9	4.4

Leaching process parameters and reagent consumption rates

As the installation and commissioning of the high shear leach reactor was completed at the start of April 2022 and it was agreed that the first four months of the trial (April – July 2022) would be dedicated towards the PT IMK Now team becoming familiar with the operation of the high shear leach reactor and to continuously optimise the unit, through continuous consultation with the equipment supplier team.

As a result, the optimum point of operating the high shear leach reactor was achieved where a balance was found between unit throughput, unit part wear and oxygen supply. This then allowed the PT IMK Now team to maximise the performance and efficiency benefits of the leaching circuit.

Therefore, apart from the improved metal recoveries, additional benefits / improvements were also seen in maintaining higher DO in the leaching circuit, while optimising reagent dosage efficiency, allowing for reduction and even stoppage of some reagent consumptions.

Three timescales were chosen to indicate these above-mentioned benefits / improvements and are listed:

- After Aachen = a set duration after the high-shear leach reactor was commissioned.
- Before Aachen = the first three months of 2022, before the installation of the high-shear leach reactor.
- 2021 = the yearly average for the entire year of 2021.

In relation to DO levels in the leach and oxygen enhancement reagents, higher levels of DO were achieved during the After Aachen timescale, where oxygen injection was added to the leach through the high-shear leach reactor alone. This was better than the 2021 timescale, where conventional oxygen injection was mainly done through lances in the leach tanks. This was also better than the Before Aachen timescale, where both conventional oxygen injection was done through lances in the leach tanks and additional injection was done through the dosing of hydrogen peroxide at the start of the leach tanks.

The PT IMK Now team's minimum DO target in their first two leach tanks was 20ppm, which was only achieved during the After Aachen timescale. This maintaining of the DO level target in the leach, during the After Aachen timescale, was so consistently high, that the PT IMK Now team were confident to stop dosing hydrogen peroxide at the start of the leach tanks daily and instead only dose when maintenance or inspections were required to be performed on the high-shear leach reactor.

These benefits / improvements are illustrated further in Figures 13 & 14.

In relation to lime addition before the leach, lower levels of lime were required to be added before the leach, during the After Aachen timescale, to maintain pH leach targets. This was better than both the 2021 timescale and the Before Aachen timescale.

These benefits / improvements are illustrated further in Figures 14.

In relation to cyanide addition in the leach, lower levels of NaCN were required to be added to the leach, during the After Aachen timescale, to maintain free NaCN and metal recovery targets. This was better than both the 2021 timescale and the Before Aachen timescale.

This benefit / improvement is illustrated further in Figure 14.

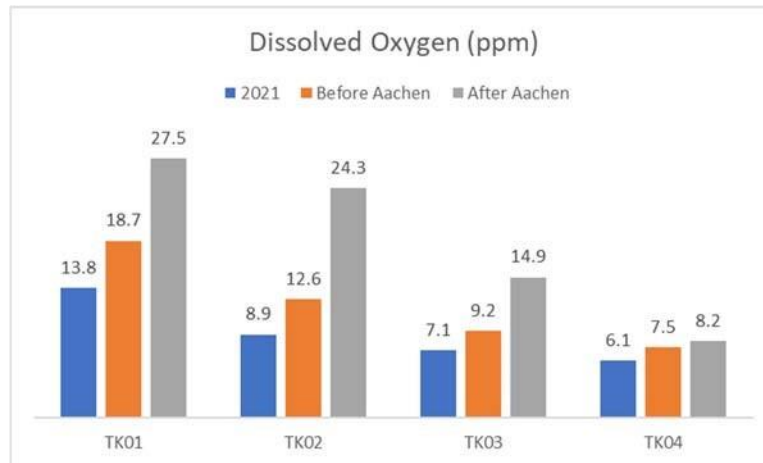


Figure 13 – Average DO levels within the first four leach tanks for the three chosen timescales

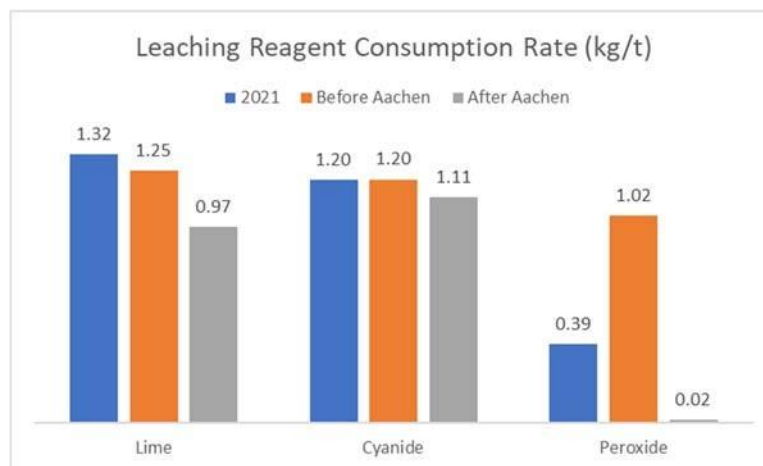


Figure 14 – Average leach reagent consumption rates for the three chosen timescales

Through historical processing information from PT IMK 1st Operators and some of PT IMK Now's own initial processing, during 2019, 2020 & 2021 (Figure 6 & 7), plus metallurgical testing that was performed by the PT IMK Now team, it was understood by the team that the Bantain ore body would not be as easy to process as the first mined ore body of Serujan (Figure 6 & 7).

Therefore, it was unexpected, by the PT IMK Now team, for the above performance of the leach, during the timescale of when the high-shear leach reactor was operating (After Aachen), to be the best of the three chosen timescales, as the After Aachen timescale was when the Bantain ore body was predominantly mined and fed to the PT IMK processing plant. The other two timescales, 2021

and Before Aachen was when the Serujan ore body was predominantly mined and fed to the PT IMK processing plant.

ECONOMIC EVALUATION

The previous section (results and discussion) has shown that the installation of the high shear leach reactor, at the PT IMK processing plant, had positive improvements in metal recovery (for Au and Ag) and in the reduction of leach reagents consumption rates (for hydrogen peroxide, sodium cyanide and lime).

It was therefore decided to determine a basic economic evaluation calculation to give an indication of the estimated value the PT IMK Now team have experienced since the installation of the high shear leach reactor.

For ease, the calculation has used the difference between the PRX and AAL oxygen injection means for the metal recovery, as hydrogen peroxide addition was occurring in the leach before the installation of the high shear leach reactor. For the reduction of leach reagents consumption rates, the difference between the Before Aachen and After Aachen timescales was used for the calculation, due to these timescales indicating leach reagents consumption rates, before and after the installation of the high shear leach reactor respectively.

The values used for the basic economic evaluation calculations were:

- a 1.30% increase in Au recovery and a 4.90% increase in Ag recovery.
- a 98.4% decrease in hydrogen peroxide, a 7.3% decrease in sodium cyanide, and a 22.4% decrease in lime consumptions.
- an estimated monthly total operational expenditure (Opex) cost for the high shear leach reactor was also used in the basic economic evaluation calculation. This cost included the monthly rental for the high shear leach reactor, with sufficient spares, continuous remote site support and actual site visits for commissioning + incremental (3, 6 & 12 month respectively) - to perform maintenance if required and site assistance with improving technology and processing performance.
- additionally, the estimated monthly total Opex cost also included the power costs and maintenance costs for the axillary equipment needed to assist the operation of the high shear leach reactor (pump, motor, etc.).
- lastly, the estimated total capital expenditure (Capex) cost for the installation of the high shear leach reactor was obtained and used in the basic economic evaluation calculation to see the payback period for the PT IMK Now team.

The results from the basic economic evaluation indicated that:

- the estimated additional revenue for the PT IMK Now team from the positive improvements in metal recovery was equivalent to 273 210 USD/month.
- the estimated total reagent saving for the PT IMK Now team from the reduction of leach reagents consumptions rates was equivalent to 121 864 USD/month.
- the estimated total monthly Opex cost for operating the high shear leach reactor was equivalent to 23 500 USD/month.
- the estimated total Capex cost for the installation of the high shear leach reactor was equivalent to 184 296 USD/month.

This then gave the estimated value, the PT IMK Now team have experienced since the installation of the high shear leach reactor, of around 370 000 USD/month and a payback period of just over 14 days. Additional information on how the above benefits and costs were calculated are indicated in Table 5, 6, 7 and 8.

Table 5 – Estimated monthly additional revenue from improved metal recovery

Criteria	Value	Unit
Avg Current Ore Processed	135 000	t/month
Avg Current Au Feed Grade	1.30	g/t
Avg Current Ag Feed Grade	35	g/t
Au Improve Recovery (PRX to AAL)	1.30	%
Ag Improve Recovery (PRX to AAL)	4.90	%
Au Improve Recovered	74	oz
Ag Improve Recovered	7397	oz
Avg Au price	1,700	USD/oz
Avg Ag price	20	USD/oz
Estimated Additional Revenue	273 210	USD/month

Table 6 – Estimated monthly total reagent saving from reduced leach reagents consumption rates

Criteria	Value	Unit
Hydrogen Peroxide		
Consumption Reduction (from Before Aachen to After Aachen)	1.01	L/t
Avg Current Ore Processed	135 000	t/month
Reduced consumption	136 350	L/month
Avg price	0.63	USD/L
Estimated Saving	85 900	USD/month
Sodium Cyanide		
Consumption Reduction (from Before Aachen to After Aachen)	0.09	kg/t
Avg Current Ore Processed	135 000	t/month
Reduced consumption	12 150	kg/month
Avg price	2.12	USD/kg
Estimated Saving	25 758	USD/month
Lime		
Consumption Reduction (from Before Aachen to After Aachen)	0.28	kg/t
Avg Current Ore Processed	135 000	t/month
Reduced Consumption	37 800	kg/month
Avg price	0.27	USD/kg
Estimated Saving	10 206	USD/month

Estimated Total Reagent Saving	121 864	USD/month
---------------------------------------	----------------	------------------

Table 7 – Estimated monthly value since the installation of the high shear leach reactor

Criteria	Value (USD/month)
Monthly Savings / Additional Revenue	
Estimated Total Reagent Saving	121 864
Estimated Additional Revenue	273 210
Subtotal	395 074
Monthly Cost for Monthly Savings / Additional Revenue	
Estimated Total Opex Cost for high shear leach reactor	23 500
Subtotal	23 500
Estimated Additional Value	371 574

Table 8 – Estimated payback period for the installation of the high shear leach reactor

Criteria	Value	Unit
Monthly Additional Value		
Estimated Additional Value	371 574	USD/month
Subtotal	371 574	USD/month
Capex Cost for installation of high shear leach reactor		
Estimated Capex Cost for slurry pump	36 801	USD
Estimated Capex Cost for civil works (performed by IMK)	25 000	USD
Estimated Capex Cost for piping and fittings	15 000	USD
Estimated Capex Cost for valves and instrumentation	27 495	USD
Estimated Capex Cost for personnel (performed by IMK)	10 000	USD
Estimated Shipping Cost	15 000	USD
Estimated Import Duty & Taxes	55 000	USD
Subtotal	184 296	USD
Total Number of Days in a Working Month	30	days
Estimated Payback Period	14.88	days

CONCLUSIONS

As indicated in all the previous sections, the installation of the high shear leach reactor at PT IMK gold mine was a success and has led to the permanent acceptance of the technology by the PT IMK Now team. The main reasons for this acceptance are listed here:

- an improved level of maintaining DO within the first four leach tanks and maintaining the PT IMK Now teams target of higher than 20ppm within the first two leach tanks was achieved after the installation of the high shear leach reactor. This was believed to be due to the fine

bubble generation and increased shear across the high shear leach reactor, which allowed for better utilisation of the oxygen supplied to the unit from the plant. This utilisation efficiency boost was good enough to allow the PT IMK Now team to stop dosing hydrogen peroxide almost completely. This led to a reagent saving of around 85 900 USD/month.

- an increased level in measuring of free NaCN in the leach was experienced after the installation of the high shear leach reactor. This was believed to be due to the increased shear across the high shear leach reactor, which allowed for better utilisation of the free NaCN within the leach. This utilisation efficiency improvement allowed the lowering of the addition of fresh NaCN in the leach to still maintain free NaCN and in turn metal recovery targets. This reduction led to a reagent saving of around 25 750 USD/month.
- an increased level in measuring pH in the leach was experienced after the installation of the high shear leach reactor. This was believed to be due to the increased shear across the high shear leach reactor, which allowed for any residual unreacted lime to be reacted, improving the utilisation of the lime within the leach. This utilisation efficiency improvement allowed the lowering of the addition of fresh lime in the leach to still maintain pH targets. This reduction led to a reagent saving of around 10 200 USD/month.
- an improved metal recovery of 1.30% for Au and 4.90% for Ag was achieved after the installation of the high shear leach reactor. This was believed to be due to the increased kinetics experienced in the leach due to the improved level of DO and better reagent utilisation, boosting the reaction of the desired metal particles, when it was passing through the high shear leach reactor. This led to additional revenue of around 273 000 USD/month.
- a combination of the above three estimated savings and additional revenue, less the estimated total monthly Opex cost for operating the high shear leach reactor of around 23 500 USD/month, gave an estimated value of around 370 000 USD/month.
- with an estimated total Capex cost for the installation of the high shear leach reactor of around 185 000 USD, gave a payback period of just over 14 days.

An additional benefit that has been implemented by the PT IMK Now team, since the permanent acceptance of the high shear leach reactor technology, was that the boost in leach kinetics throughout the plant, believed from the technology, had allowed the PT IMK Now team to increase the throughput of the processing plant by 17.65% (from 170 dtph to 200 dtph), while still maintaining Au and Ag recoveries at 98% and 78% respectively.

An ongoing investigation is the potential modifications to the plant to allow for the increased Au and Ag recoveries, seen when completing the leach tests for an additional 16 h longer, than the current plant residence leach time of around 32 h. These improvements were 0.3% for Au and 4.4% for Ag, which would be equivalent to an estimated additional revenue of 59% or 162 000 USD/month, on top of the estimated additional revenue seen since the installation of the high shear leach reactor. The two methods being investigated is the additional installation of more leach tanks versus the additional installation of more high shear leach reactors, where the additional installation of more high shear leach reactors would be the easiest and cheaper option and is currently being investigated.

ACKNOWLEDGEMENTS

The authors would like to acknowledge the IMK Site and Head Office team for all the hard work contributed to the importation & installation of the high shear leach reactor and the dedication & drive to assisting with sampling, data analyses, and interpretations to show the effectiveness of the technology.

REFERENCES

- Air Liquide Standard Application Equipment, 2022. Injector-BICONE, [online]. Available from: https://uk.airliquide.com/statics/2022-09/nexelia_wt_mem_injector-bicone_sheet_en_lr.pdf?VersionId=0_3Yx92m_EoB257Yqd.aQ4NYAGk6LyG5 [Accessed: 21 August 2023].
- British Oxygen Company, 2023. GOLDOX Processes, [online]. Available from: <https://www.boc-gas.com.au/en/applications/goldox/index.html> [Accessed: 21 August 2023].
- Dement, E R and King, N D, 1982. Merrill-Crowe / Carbon-In-Pulp An Economic Evaluation, in *Carbon-In-Pulp Technology for the Extraction of Gold 1982*, pp 89-106 (The Australasian Institute of Mining and Metallurgy: Melbourne).
- Ellis, S, Andrezza, J and Senanyake, G, 2002. The Influence of a Pipe Reactor to Improve Pre-Oxidation and Gold Recovery and Lower Cyanide Consumption, in *Metallurgical Plant Design and Operating Strategies (MetPlant) 2002* (The Australasian Institute of Mining and Metallurgy: Melbourne).
- Ellis, S and Senanayake, G, 2004. The effects of dissolved oxygen and cyanide dosage on gold extraction from a pyrrhotite-rich ore, *Elsevier Hydrometallurgy*, Volume 72 Issues 1-2: 39-50.
- Elsner, L, 1846. On the Behaviour of Various Metals in an Aqueous Solution of Potassium Cyanide, in *J. Prakt. Chem.* 37, pp 441-446.
- Flatman, S, Battersby, M, Imhof, R, Battersby, R M and Ibrayev, S, 2010. The Leachox™ Refractory Gold Process - The Testing, Design, Installation and Commissioning of a Large Scale Plant at the VASGOLD Gold Mine, Kazakhstan, in *Proceedings of Precious Metals '10 2010* (Minerals Engineering International: Falmouth).
- Imhof, R M, 1987. A device for dispersing a gas into a liquid, Germany Patent DE3741843.
- Lotz, P, van der Merwe, J, Mogashoa, S, Flatman, S and Imhof, R, 2015. Aachen Reactors™, a proven system to realize hidden economic potentials, in *Proceedings World Gold 2015* (The Southern African Institute of Mining and Metallurgy: Johannesburg).
- Mahlangu T, Sumaili, F A, Ayizi, D N, Sindani, B M, Mande, P, du Toit, G, Verster, M, Mogashoa, S M, and Lotz, P W, 2019. Kibali Gold Mine sulfide concentrate treatment – understanding the preoxidation of sulfide concentrates, in *Proceedings World Gold 2019*, pp 488-503 (The Australasian Institute of Mining and Metallurgy: Melbourne).
- Marsden, J O and House, C I, 1992. *The Chemistry of Gold Extraction Second Edition*, pp 242 (Society of Mining, Metallurgy and Exploration Inc., Colorado, United States of America).
- McMahon, M, Seaman, D R, Sharman, P, Adamson, B and Seaman, B A, 2016. Optimising the Telfer Pyrite Regrind Circuit - Effect of Dissolved Oxygen Demand, in *Proceedings 13th AusIMM Mill Operators' Conference 2016*, pp 51-58 (The Australasian Institute of Mining and Metallurgy: Melbourne).
- NICNAS, 2010. Sodium Cyanide, *Priority Existing Chemical Assessment Report No.31*, 23.
- Seracini, B J S, 1995. The Filblast Cyanidation Process, in *Randol Gold Forum Perth 1995*, pp 245-250 (Randol International Ltd: Colorado).

Vorster, B J and Flatman, S R, 2001. Cyanide Control in the Metallurgical Process of Gold Extraction in Anglogold (S.A.), in *Cyanide: Social, Industrial and Economic Aspects*, pp 535-547 (The Minerals, Metals & Materials Society: Pittsburgh).

Refractory Gold Concentrate Treatment Hub for Toll Treating

L. McDonnell¹, R. McKechnie², K. Roche³, P. Bullock⁴, S. Nikolic⁵

1. Senior Metallurgist, Glencore Technology, Level 29, 180 Ann street, Brisbane, Qld 4000, laurie.mcdonnell@glencore.com.au
2. Metallurgist, Glencore Technology, Level 29, 180 Ann street, Brisbane, Qld 4000, rebecca.mckechnie@glencore.com.au
3. Senior Metallurgist, Glencore Technology, Level 29, 180 Ann street, Brisbane, Qld 4000, kelvin.roche@glencore.com.au
4. Principal Metallurgist, Glencore Technology, Level 29, 180 Ann street, Brisbane, Qld 4000, paul.bullock1@glencore.com.au
5. Manager - Technology, Glencore Technology, Level 29, 180 Ann street, Brisbane, Qld 4000, stanko.nikolic@glencore.com.au

ABSTRACT

Gold hosted in refractory sulfides has historically been overlooked in preference of easily recoverable gold which requires less upfront capital. However, as reserves of these ores become depleted in the face of continuously increasing gold demand, opportunities arise for forward-looking companies to capitalise on the requirement for pre-treatment of sulfide-hosted gold.

Gold hosted in refractory sulfides requires pre-treatment to oxidise the sulfide minerals, releasing the gold and making it amenable to recovery via traditional Carbon-In-Leach processes. Several established options exist to liberate sulfide hosted gold, but the key to maximising this opportunity lies in the selection of an approach that is sufficiently flexible to manage variations in feed whilst still achieving high recoveries.

This paper focuses on Glencore Technology's Albion Process™ as a robust pre-treatment solution for refractory gold feeds that may vary significantly in their throughput and mineralogy and contain high levels of impurities such as arsenic. The Albion Process uses a combination of mechanical and chemical liberation of the gold via ultrafine mineral grinding and oxidative leaching at atmospheric pressure. The simplicity of this process combined with the tight size distribution achieved using the IsaMill™ and high oxygen utilisation afforded by the HyperSparge™ and OxiLeach™ reactor designs allows for significant variability in the feed to any Albion Process plant without compromising recovery. This opens the door for an Albion Process plant refractory gold treatment hub capable of toll treating concentrates produced from a multitude of external ore bodies. Real world examples are used to demonstrate how one Albion Process plant can accept significant variation in feed composition and rate and still achieve high gold recoveries.

INTRODUCTION

Gold hosted within refractory sulfides is often perceived as too difficult to extract and recover and is therefore overlooked in favour of easily recoverable free milling gold. As reserves of free milling gold become depleted in the face of increasing gold demand, the requirement to treat these deposits is also increasing. The cost associated with the construction of a processing plant to treat refractory sulfides can be significant. Facilities that are able to deal with variable feed characteristics can unlock opportunities for both process plant operators by maximising available feed and essentially prolonging the life of the operation, as well as for other mining operations who may be unable to treat their sulfide material, by providing an opportunity to sell concentrate.

The Albion Process is an ideal technology for this scenario as it provides flexibility in terms of mineralogy, throughput, oxidation extent and residence time. The features of the Albion Process that underpin this flexibility will be outlined in this paper along with real world projects which

demonstrate how an Albion Process plant is intended to be used as a processing hub.

THE ALBION PROCESS

The Albion Process was developed by Glencore in 1994 and is a globally patented technology comprising two steps. The first step is ultra-fine grinding using the IsaMill (Figure). The ultrafine sizing is the key to leaching of at atmospheric pressure. For coarser particles a passivating surface layer stops prevents leaching of the mineral matrix; for ultrafine particles the passivating layer itself represents most of the particle.



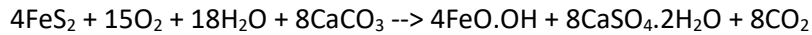
Figure 1: Model of IsaMill Plant

The second step comprises oxidative leaching of the finely ground sulfide concentrate utilising finely dispersed oxygen injection (HyperSparge) in an auto thermal atmospheric leach tank such as Glencore Technology's Oxidative Leach Reactors (OxiLeach, Figure 2).



Figure 2: OxiLeach Reactor Train

The oxidative leach can be operated under a range of pH conditions, varying from acidic to neutral and has been commercialised in zinc and gold with five plants currently in operation. These have been reported on extensively (Hourn & Turner, 2010; Hourn & Turner, 2012; Voigt, Hourn, & Mallah, 2016; Senshenko, Aksenov, Vasiliev, & Seredkin, 2016). Albion Process oxidative leaching under conditions closer to neutral (pH 5.5) is optimal for the oxidation of pyrite, arsenopyrite and other gold bearing minerals, to break down the sulfide matrix and render the precious metals amenable to downstream cyanidation. In order to maintain the leach at the target pH of 5.5, limestone is dosed into each reactor to neutralise the acid generated by the pyrite oxidation reaction:



During this process, any arsenic that may be present will coprecipitate with iron, forming a stable ferroarsenate (predominantly scorodite). As such the Albion Process is capable of handling high arsenic feeds and yields a residue with arsenic species that are inert and safe for tailings.

When Albion Process leaching occurs under acidic conditions, base metal sulfides are oxidised and the target metals simultaneously leached into solution. Gold bearing sulfide minerals such as pyrite will also oxidise according to the above reaction, albeit at a slower rate compared to those exhibited at the higher pH of a 'neutral' leach. On completion of the acidic leach, a neutralisation stage remove iron and arsenic from solution via the dosing of limestone to coprecipitate them. As the precious metals remain in the solid residue, a subsequent thickening stage directs the leach solution to downstream processing (SX/EW, precipitation, etc.) for base metals recovery, while the precious metals in the residue are directed to the cyanide leach.

The ability to operate at different chemistries, handle variation in feeds and to process high arsenic concentrates makes the Albion Process ideal for treating precious metal concentrates or complex polymetallic concentrates in which precious metals are finely disseminated in base metal sulfides.

HYPERSPARGE

The HyperSparge is a proven and cost-effective sparging system for delivering air, oxygen, or other gases for leaching or oxidation processes and is a key component of the Albion Process Oxicleach reactors. The system uses an alloy steel injection lance fitted with a hard-wearing ceramic nozzle to inject a concentrated supersonic jet of gas into the process solution or slurry. The supersonic gas jet enters the process stream at velocities exceeding of 400 m/s, creating a region of very high local shear and fine bubbles, resulting in efficient oxygen mass transfer and therefore high gas utilisation.

PROCESSING HUB PHILOSOPHY

Historically, processing of refractory sulfides has been overlooked in favour of the easier to process gold hosted in oxides. As the oxide portion of their deposits are depleted and operations begin to move into the transition and sulfide regions of an ore body, gold recoveries decline since refractory gold is typically not amenable to direct cyanidation. This is often the point at which operations will cease or the operator's focus moves to another deposit. As reserves of free milling gold are progressively depleted, the viability of treating sulfide deposits needs to increase to meet demand. .

However, circuits to treat sulfide deposits are more complex than their simpler oxide counterparts, and the capital associated with building (or retrofitting) a plant to treat sulfide ores can be prohibitive, particularly for junior mining companies. This may present a unique opportunity for forward looking companies who have the capacity to undertake larger projects. The robustness of the Albion Process would enable the design of a processing plant for a specific deposit with sufficient flexibility installed to allow for the treatment of third-party feeds from other deposits. This flexibility is achieved across both stages of the Albion Process. In the first stage, ultra-fine grinding, the IsaMill affords flexibility because it can be adjusted to target both finer and coarser grind sizes depending on the requirements of individual concentrates.

In the second stage of the Albion Process, oxidative leaching, the leach reactors (e.g., OxiLeach) can be configured as either an acid or neutral Albion Process depending on whether there are base and precious metals present or just precious metals. For periods of decreased throughput or for concentrates that require lower residence time, up to half of the leach train can be bypassed, decreasing equipment wear. Alternatively, leach train can easily be expanded with the addition of extra reactors, a change that is not always achievable with some alternative technologies such as pressure leaching. The opportunity to target residence time coupled with an efficient sparging system (e.g., HyperSparge) also allows sulfide oxidation targets to be adjusted to suit specific feeds.

These features mean that the Albion Process is well suited for a hub-style processing plant capable of treating various concentrates from particular regions, reinforcing the opportunity for both the company who constructs the plant, and the companies who would then have a path to sell concentrate. As the Albion Process is capable of treating relatively 'dirty' or 'low grade' concentrates, it provides the added benefit of lowering the cut-off point for what might be considered a 'saleable' concentrate for other mines that may not have the processing capabilities to produce final metal.

The following sections provide examples of gold processing hub projects that are currently being undertaken by JSC Altynalmas (Altynalmas).

NEUTRAL HUB – PUSTYNNOYE PROJECT

Altynalmas has been developing a number of gold deposits in Kazakhstan and are progressing two Albion Process projects. The first of these is the Pustynnoye Neutral Albion Process Hub. The processing plant for this project has been designed to treat concentrates from four precious metal deposits; Pustynnoye, Kariernoye, Aksu and Sayak. Characterisation results for the individual concentrates generated from each of these deposits exhibited significant variation, summarised here:

Gold:	15.2 – 57.5 g/t
Silver:	1.9 – 94 g/t
Iron:	18.2 – 35.3%
Sulfur:	11.9 – 38.2%

As expected, the gold hosting minerals pyrite and arsenopyrite also varied greatly between concentrates with ranges as follows:

Pyrite:	2.0 – 70%
Arsenopyrite:	3.5 – 65%

For this project, the optimum grind size was determined to be 80% passing 8 μm . Although this is at the finer end of what would typically be required for high recoveries in the Albion Process, sizing the IsaMill for this fine grind size was logical to allow the plant to accept highly variable concentrate feeds. The test work was conducted on two separate master composite blends of the concentrates labelled as 'Pustynnoye blend' and 'Kariernoye blend'. Extensive test work was undertaken to optimise conditions and confirm the recovery results after the Albion Process. Despite the variability between the two composites, gold recoveries increased from 45.4% (untreated concentrate) to 93.2% and 91.9% after oxidative leaching for the two blends, respectively. The results along with the recovery post ultrafine grinding alone are summarised in Figure 3.

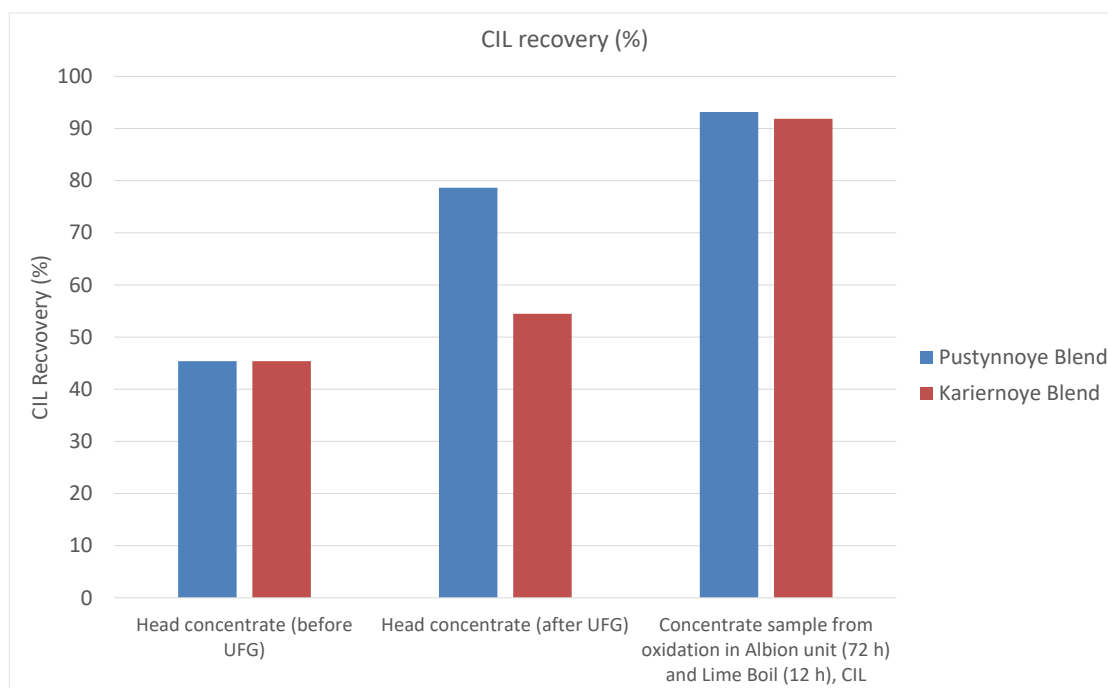


Figure 3: CIL Recoverable Gold for Pustynnoye Project

The consistency in gold recovery despite the notable differences in feed characteristics reinforced the flexibility of the Albion Process with regard to significant feed variation, making it an ideal option for meeting the project objective of treating feeds from four different deposits. The two blends treated represent samples from 4 deposits. It also de-risked the option of developing further deposits, which is currently underway with drilling being conducted in the Akbakai mine cluster which consists of another three refractory ore bodies.

ACID HUB – MIZEK PROJECT

In addition to the Pustynnoye Neutral Albion Process Hub, Altynalmas are also progressing the Mizek Acid Albion Process Hub. The purpose of this hub is to process the polymetallic concentrates that contain both base and precious metals. The initial hub design has been based on the Mizek concentrate which contains copper, zinc, gold, and silver. The Mizek concentrate specifications used in the design of the processing plant are as follows:

Gold:	16.2 g/t
Silver:	52.4 g/t
Iron:	29.3%
Sulfur:	39.8%
Copper:	7.0%
Zinc:	16.0%

With the metals predominantly hosted in the following minerals:

Pyrite:	57%
Sphalerite:	22%

Chalcopyrite: 9%

The optimum grind size target for this project was determined to be 80% passing 8 μm , since sizing the mill for the finest required grind size enhances flexibility to accept a wider range of feeds and variability. Extensive test work was undertaken to optimise leach conditions and confirm the gold recoveries achievable via the Albion Process. After oxidative leaching, CIL gold and silver recoveries increased from 28.9% as received to 95.2% for gold and from 25.3% to 95.4% for silver.

These results along with the recovery post ultrafine grinding alone are summarised in Figure 4.

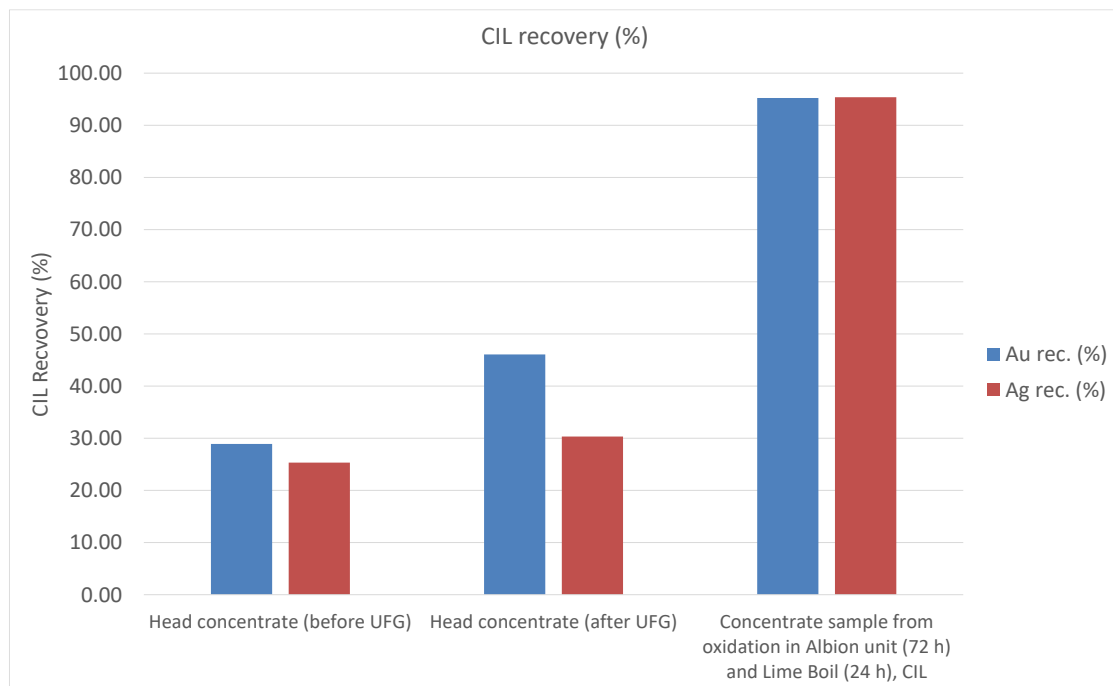


Figure 4: CIL Recoverable Gold and Silver for the Mizek Project

Test work for base metals also indicated that Albion Process leaching achieved excellent zinc recoveries (99.5%) and high copper recoveries (91.8%) at a sulfur oxidation of 96.7% (Figure 5).

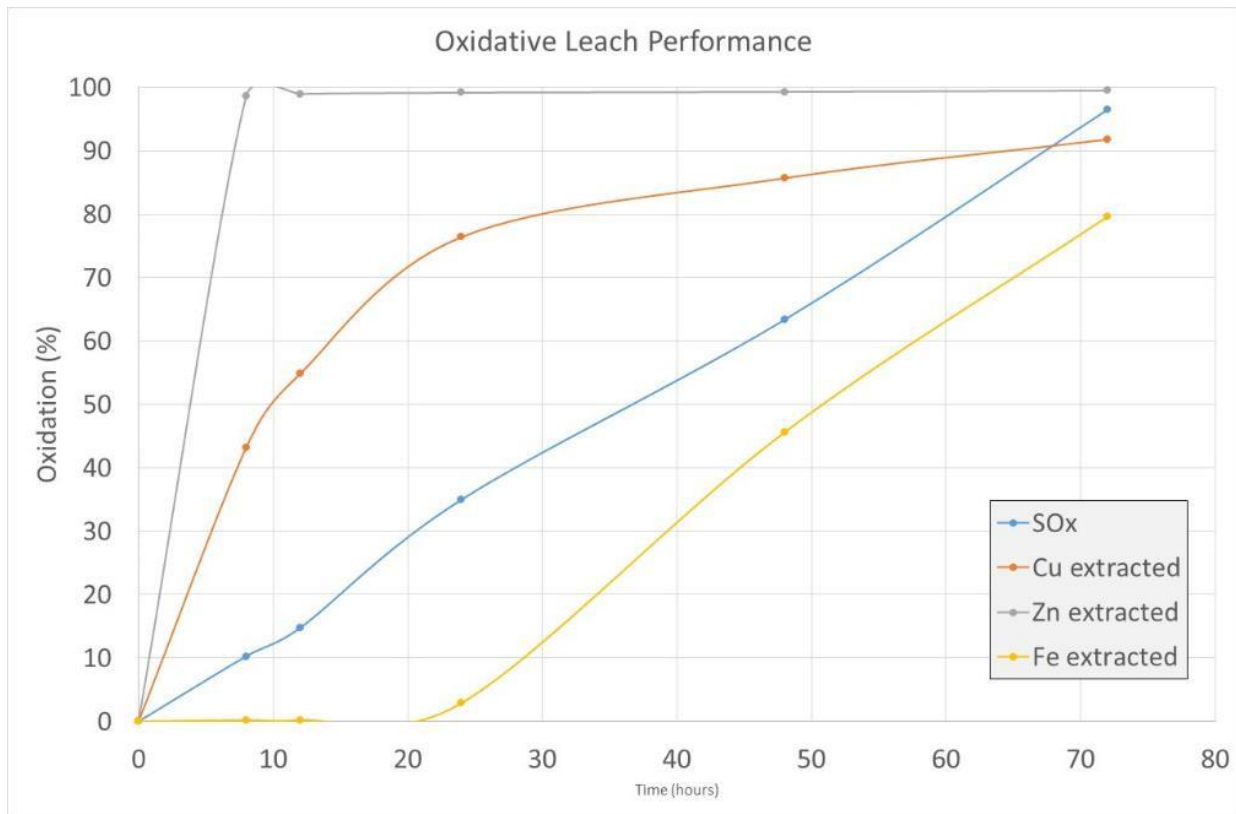


Figure 5: Oxidative Leach Performance for Mizek Project

The Sayak deposit is also being considered as feed for the Acid Albion Process Hub and has the following specifications:

Gold:	46.2 g/t
Silver:	23.1 g/t
Iron:	26.1%
Sulfur:	18.3%
Copper:	0.61%
Cobalt:	0.84%

Differently from the Mizek Cu-Zn deposit (upon which the processing hub has been designed) the primary base metals to be targeted in Sayak are copper and cobalt. As precipitation was selected as the downstream base metal processing option, the precipitation stages can be modified to target different base metals. This will allow for copper and zinc products to be produced initially from Mizek, before changing to produce copper and cobalt products at a later stage when the feed changes to Sayak.

The overall Mizek Acid Albion Process Hub is shown in Figure 6 with the IsaMill and base metals thickening and filtration located on the left, the OxLeach reactors and two stages of base metal precipitation in the middle section, and iron control filtration and lime boil areas on the right.

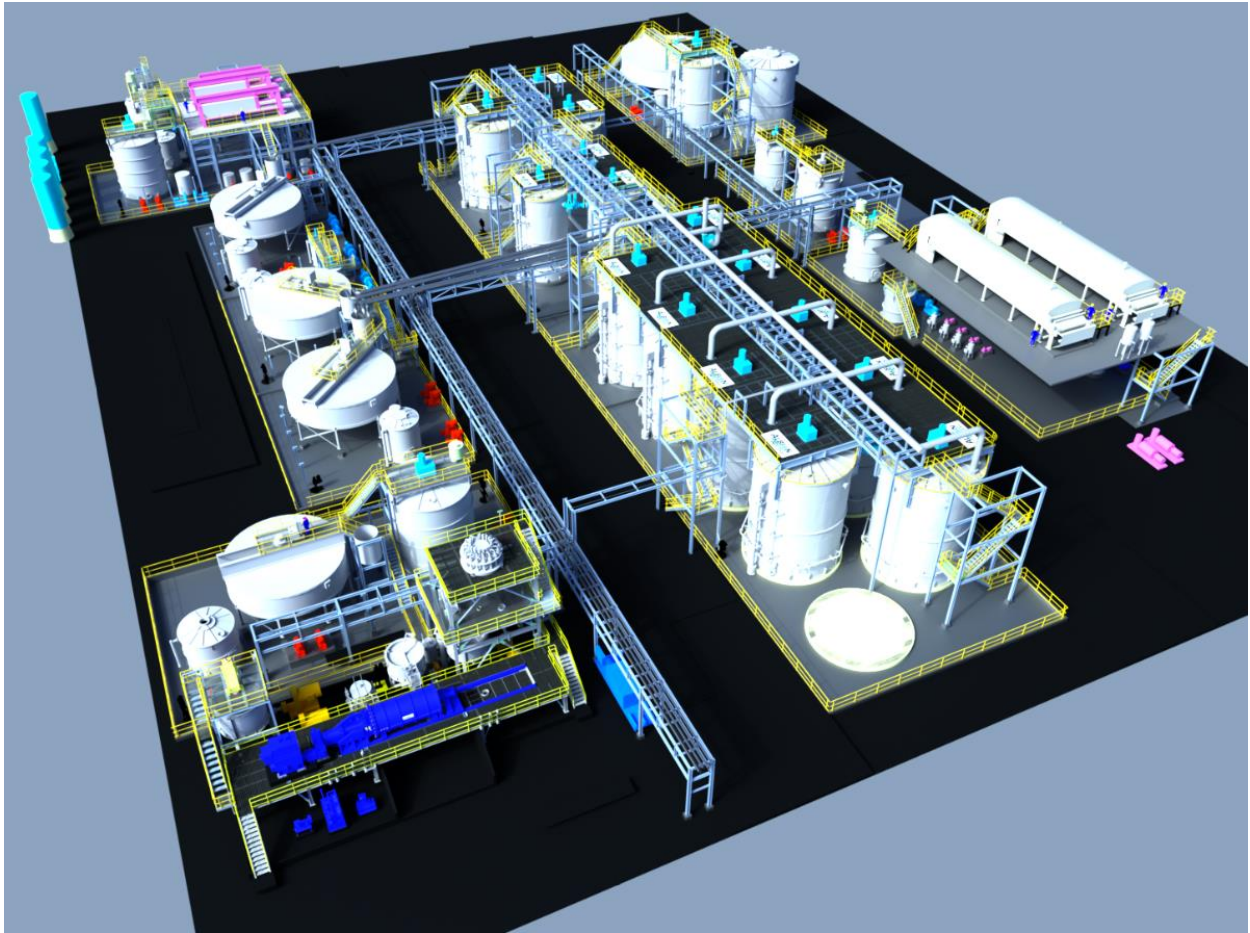


Figure 6: Mizek Acid Albion Process Layout

BENEFITS OF THE ALBION PROCESS

The Albion Process offers several advantages over other leaching technologies due to the nature in which it operates. Previous investigations have indicated a lower oxygen consumption for the Albion Process when compared with medium temperature pressure oxidation (MT-POX) (SNC Lavalin, 2009). This is due to the opportunity to target the extent of the sulfur oxidation required for high metal recoveries in the Albion Process, whereas in MT-POX 100% of sulfides are oxidised. Additionally, the HyperSparge and impeller design in the OxiLeach reactors afford high oxygen usage efficiency. This results in lower capital cost associated with the oxygen plant as well as lower ongoing operating costs.

As the Albion Process operates auto thermally and at atmospheric pressure, power input is also decreased compared with POX (Alymore, 2012), improving costs and lowering environmental impact. Adding to the environmental benefit, the Albion Process has also been shown to use significantly less water than MT-POX (SNC Lavalin, 2009). The autothermal and atmospheric nature of the operation has the additional benefit of not needing any pressure reduction or heat removal. This contributes to a more stable process that simpler to operate.

Albion Process availability is also very high due to:

- The oxidative leaching train consists of multiple reactors in series which are interconnected with launders, each with a bypass. This launder system allows individual reactors to be taken out of operation while online.
- The HyperSparge design allows removal and replacement while online.

These features give the ability to maximise throughput even during periods of maintenance.

CONCLUSIONS

This paper outlines how the Albion Process can be set up as a hub style processing plant and used to treat multiple feeds, whether they be for precious metal, base metal, or polymetallic feeds. The key to this flexibility is the ability to adjust operation of the IsaMill and OxiLeach stages, where required, to suit varying feeds. As discussed, the oxidative leaching capacity can be expanded by simply adding more reactors to the train.

This hub style design allowing toll treating of different feeds provides benefit for both the operator of the plant because it maximises the available feed for their plant, and other miners who may have sulfide deposits that they are unable to process alone and would be able to supply the concentrates to feed the plant.

ACKNOWLEDGEMENTS

The authors would like to thank JSC Altynalmas for allowing to publication of this paper. Thanks also goes to the Institute TOMS for completing the test work that was reported on in this document and everyone within Glencore Technology that has worked on these projects to date.

REFERENCES

- Alymore, M. 2012. Evaluating Process Options for Treating some Refractory Ores. ALTA Conference Proceedings. Perth.
- SNC Lavalin. 2009. Concentrate Treatment Options Scoping Study.
- Hourn, M., & Turner, D. (2010). Albion Process for treatment of refractory ores. ALTA Conference Proceedings. Perth.
- Hourn, M., & Turner, D. (2012). Commercialisation of the Albion Process. ALTA Conference Proceedings. Perth.
- Voigt, P., Hourn, M., & Mallah, D. (2016). Treatment of Low Grade Materials. Proceedings of MINEX. Moscow.
- Senshenko, A., Aksenov, A., Vasiliev, A., & Seredkin, Y. (2016). Technology for Processing of Refractory Gold-Containing Concentrates Based on Ultrafine Grinding and Atmospheric Oxidation. Proceedings of IMPC Conference. Montreal.

Application of Stirred Milling in the Expansion of Martabe Gold Mine

M Liu¹, R Tanio², J Herrin³ and B Neilson⁴

1. Sulfide Resources Metallurgical Specialist, PT Agincourt Resources, Perth WA, Michael.Liu@agincourtresources.com
2. Director Engineering Management, PT Agincourt Resources, Sumatera Utara Indonesia, Ruli.Tanio@agincourtresources.com :
3. Papua Region Account Manager, Metso, Jakarta, Indonesia John.Herrin@mogroup.com :
4. Vice President, Stirred Mills and HPGR, Metso, Perth, Australia Bjorn.Nielsen@mogroup.com

ABSTRACT

The Martabe Gold Expansion project was an upgrade project designed to increase throughput with the existing plant while utilising minimal footprint and the fewest significant modifications to site possible.

As the Martabe project has developed and optimised, plant capacity has increased to well above the original design point and the P80 feeding the leach plant has gradually become coarser as the capacity has expanded. Additional milling capacity has been added to the plant to return to that optimal product size and further increase capacity.

Site conditions create unique challenges including limited footprint, seismic hazards, coarse product size targets, and hard, competent ore. To meet these challenges, Metso has supplied a VTM-4500-C for the application. The VTM-4500-C is the largest Vertimill® installed in the Asia-Pacific region. The mill operates in closed circuit with hydrocyclones and has been designed to minimise the footprint of the expansion while offering the maximum throughput increase.

This paper discusses the design philosophy, machine selections, challenges of commissioning, and progress through the ramp-up period. In addition, the paper discusses the impact on the overall comminution circuit and changes required to the operational philosophy to incorporate the new machine into the plant.

INTRODUCTION

MARTABE GOLD MINE

The Martabe Gold Mine is in the district of Batang Toru in the Province of North Sumatra, approximately 40 km southeast of the coastal town of Sibolga. Figure 1 shows the mining area contract of work. The mine is currently managed by PT Agincourt Resources which is part of PT Pamapersada Nusantara, a part of the Astra group.

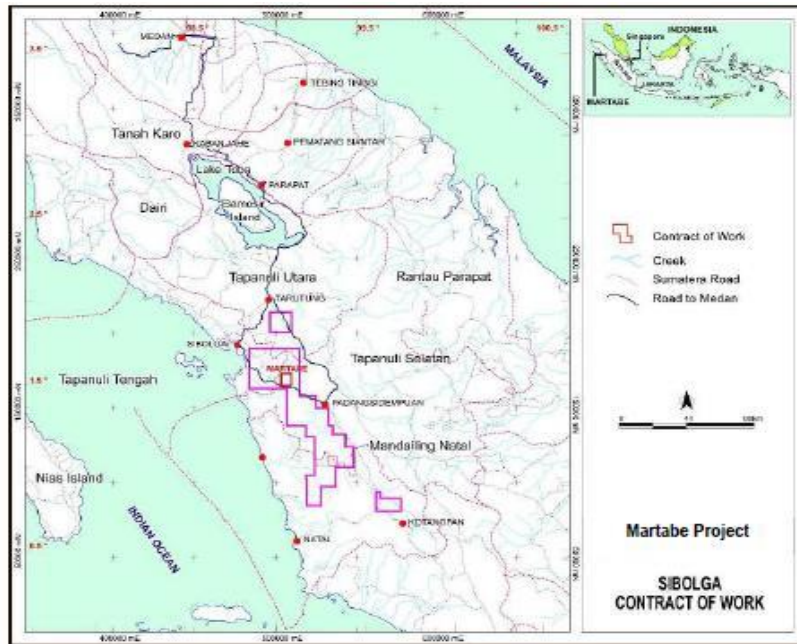


Figure 1 - Location of Martabe Gold Mine

Martabe gold mine has been in operation since July 2012. The plant was designed by Ausenco with a design nameplate capacity of 4.5 Mt/y but with provision for an expansion of up to 6.6 Mt/y through the addition of secondary crushing and screening and pebble crushing.

Overview of Martabe CIP Plant

Run-of-mine (ROM) ore enters the plant in the dump hopper and then travels over a vibrating grizzly to scalp fines. The grizzly oversize is crushed by a Metso C200 jaw crusher. The original design capacity for the crusher was 675 t/h with a closed side setting (CSS) of 150 mm. Crushed material is then sent either to the coarse ore stockpile or to the secondary crushing station. Material is then reclaimed from the stockpile and fed to a SABC (SAG, ball mill, pebble crusher) circuit to generate a final ball mill hydrocyclone overflow product of 80% passing 150 μm . The SAG mill was identified as the early circuit bottleneck so it was decided to move forward with the design and installation of the secondary crushing circuit. A schematic diagram of the Martabe comminution circuit is shown in Figure 2 and a full process description follows.

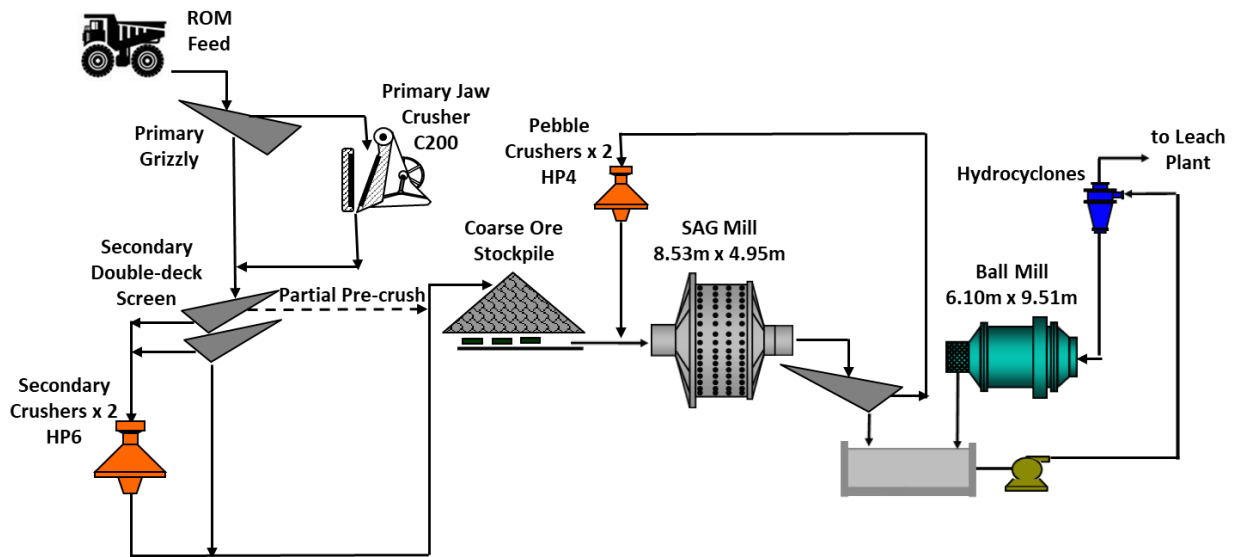


Figure 2 – Schematic of Martabe comminution circuit

The secondary crushing circuit was installed in 2015 and operational by late 2016. The secondary crushing station consists of a primary double-deck screen, which receives primary crushed material and grizzly undersize. It has been configured to allow for either a partial or full pre-crush of the SAG feed by crushing material either from both screen decks or from the second screen deck only. Fines from the screen are directed to the coarse ore stockpile along with crushed material and, if operating as a partial pre-crush, the coarse uncrushed material. The secondary crushers have been designed to operate in duty/standby mode but can be operated concurrently. The secondary crushers are Metso HP6 cone crushers and operate, primarily, as a partial pre-crush treating only the oversize from the second screen deck. With the inclusion of the secondary crushing design capacity was increased to 790 t/h for the plant.

Crushed ore is reclaimed from the stockpile by two reclaim feeders, each with a variable speed drive. The apron feeders are designed to treat 910 t/h each. The stockpile has a live capacity of 16 hours. The apron feeders discharge ore onto the reclaim conveyor, which conveys ore to the SAG mill feed conveyor and into the SAG mill.

The grinding circuit is a standard SABC circuit. The Metso SAG mill is rated at 6.5 MW with a variable speed drive. The high aspect ratio SAG mill has an inside shell diameter of 8.53 m with an effective grinding length (EGL) of 4.95 m. The SAG mill discharges onto a single deck wet screen with 12 mm slotted screen apertures. Oversize from the screen feeds a set of duty/standby HP4 Metso cone crushers. Undersize from the screen goes to the ball mill hydrocyclone feed sump box.

The secondary grinding circuit consists of a fixed speed 6.10 m x 9.51 m EGL Metso Ball mill rated at 6.5 MW operating in closed circuit with a set of 16 Krebs 20 in primary cyclones. The cyclone overflow product has a design P80 of 150 µm with a pulp density ranging between 45-50% solids for direct feed to the leaching circuit. The cyclone underflow feeds the ball mill and the ball mill trommel undersize is sent to the ball mill hydrocyclone feed sump box.

Secondary (Ball) Milling Bottleneck

With the previously outlined comminution circuit arrangement and the recent inclusion of the secondary crushing circuit, the throughput bottleneck has shifted from being SAG mill to the secondary (Ball) mill. Figures 3, 4, and 5 show mill operating data dating from 2014 through to 2019.

The gradual increase in milling throughput over the period has caused a gradual decrease in percent passing 150 µm as no additional grinding power had been added to the plant. The monthly average percent passing 150 µm dropped from 84% passing to 76% passing as throughput rates increased from 470 t/h to 730 t/h.

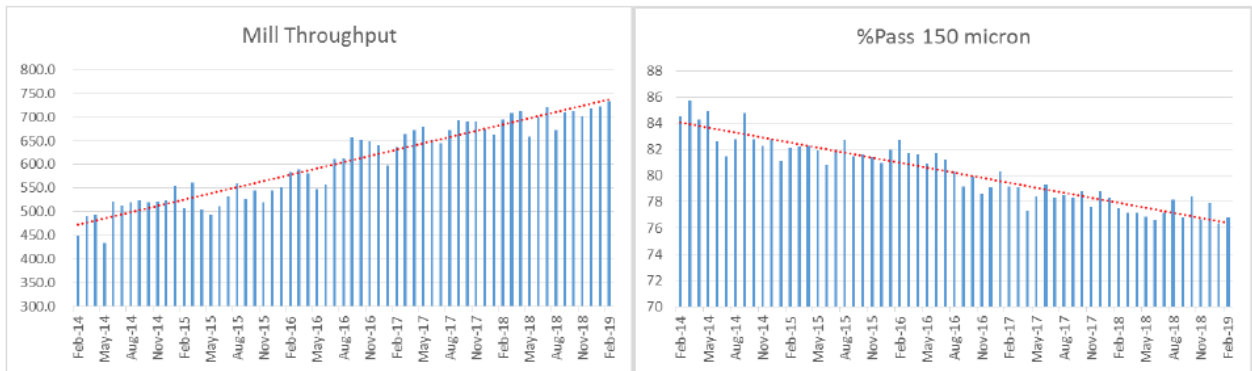


Figure 3 – Historical mill throughput

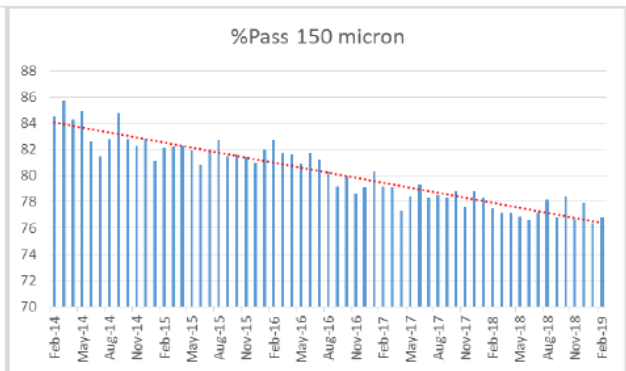


Figure 4 – leach feed % -150 µm by month

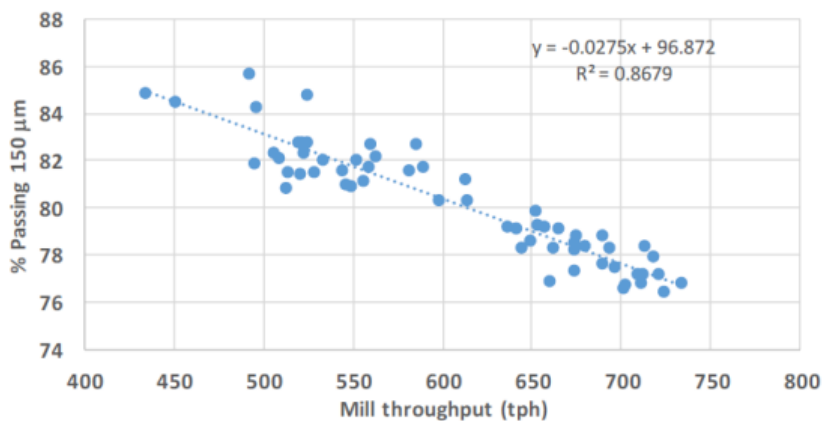


Figure 5 - Mill throughput t/h vs % Passing 150 µm by month 2014-19

To alleviate the secondary milling constraint and further expand throughput, an upgrade or expansion to the grinding capacity was investigated. Preliminary high-level evaluation made by the project metallurgy team suggested that the best option to upgrade for secondary milling is to add a vertical mill rather than second ball mill. The key driver for the selection was the reduced footprint relative to the ball mill making inclusion into the plant easier.

PROCESS SIMULATION AND MODELLING

To determine the best circuit configuration and equipment selection for upgrading the secondary milling circuit, a mineral processing consultant was engaged to conduct process simulation and modelling to confirm and optimise the solution. A grinding circuit survey was carried out in February 2019 by site personnel with inputs from the consultant regarding circuit sampling and data requirements. The data was then sent for analysis and modelling to determine the additional grinding equipment required to maximise the circuit throughput.

Modelling results and simulation work indicated that the maximum mill tonnage of 800 t/h can be achieved from the existing grinding circuit where the SAG mill speed will be operating at 75% critical

speed (11 r/m) at 14% ball charge and near maximum power/motor capacity (6020 kW). The ball mill power draw was already near maximal utilisation so no further gains could come from the installed mill. The grinding product size under those operating conditions was 180 μm .

To achieve that 800 t/h, approximately 40% of the mass flow would need to be crushed by the secondary crusher to produce a SAG feed size of F_{80} 98.8 mm. The utilisation of the secondary crushing circuit along with the generation of a finer feed size fraction has improved throughput but cannot be further used to unload the secondary milling circuit. The modelling showed that the additional grinding power required to attain the target P_{80} 150 μm at 800 t/h maximum throughput rate will be approximately 1300 kW (excluding losses to the drive train). Table 1 summarises the design parameters utilised in consultant simulations.

Table 1 - Power Utilisation based on Simulation and Modelling

Parameter	Units	Simulation Results
Ore Parameters		
Cwi	kWh/t	16.7
Bwi	kWh/t	17.1
SMC Axb		45.2
Percentage Sec Crushing	%	40.7
Grinding Circuit		
SAG Mill Feed Rate	dry t/h	800
Mill Feed Size F_{80}	mm	98.8
Grinding Product Size P_{80}	μm	180
Pebble Recycle Rate	t/h	417
SAG Mill Power Draw	kW	6020
Ball Mill Power Draw	kW	6212
Pebble Crusher Power Draw	kW	45.7
SAG Mill Pinion Power	kW	5570
Ball Mill Pinion Power	kW	5746
Pebble Crusher Net Power	kW	30
Power Utilisation		
SAG Mill Specific Energy	kWh/t	7
Ball Mill Specific Energy	kWh/t	7.2
Pebble Crusher Specific Energy	kWh/t	0.04
Total Specific Energy	kWh/t	14.2
Additional Power Required		
P_{80} 150 μm	kW	1294

Due to the footprint constraints in the grinding area, a vertical mill was recommended as the

preferred technology to provide the additional power required to achieve the target throughput and grind. To increase secondary milling capacity, the additional milling could be added in parallel with the existing secondary mill or added as a tertiary grinding step treating the ball mill hydrocyclone overflow. The recommended flow sheet to maximise vertical mill efficiency was to coarsen the cyclone overflow and feed that to the new tertiary milling circuit. The other option would be to feed the vertical mill the ball mill hydrocyclone underflow directly. If treating ball mill hydrocyclone underflow, pre-screening would be required to remove +2 mm material to prevent vertical mill overloads. The additional screen added circuit complexity, cost, and footprint making it unattractive.

In addition to the simplicity of the circuit, there were other benefits to the larger circuit with the tertiary milling approach. With minimal modification, a split can be added to the ball mill hydrocyclone overflow to allow the circuit to either feed the vertical mill circuit or feed the leach plant as per the current design. The vertical mill circuit can then easily be added to the plant with no downtime impact on the operating mills. Further, if required, the mill can easily be removed from service without impacting the downtime of the whole grinding circuit. Finally, if the ball mill is off-line there is the option to operate the SAG mill together with the vertical mill by diverting the cyclone underflow back to the SAG mill. The entire grinding plant gains significant redundancy and flexibility to optimise power utilisation.

The initial concept was to operate the vertical mill in open circuit but after simulation and investigation that plan was also changed. Due to the low reduction ratio and small required additional circuit specific grinding energy (1.6 kWh/t), the slurry velocity through the mill was quite high. To avoid a high “up-flow” velocity through the Vertimill an open circuit was initially selected.

Metso was consulted with respect to “up-flow” velocity limitations and received feedback that the concerns around flow velocity are minimal with references showing other sites operating at flows more than 2000 m³/h without issue. The mill would have better efficiency operating in closed circuit and with that feedback, the team at Martabe decided to opt for the closed-circuit configuration. The other added benefit with the closed-circuit configuration is the reduction of one pump box and pump arrangement from the system. The consultant recommended installation of a Metso VTM-3000-WB Vertimill (VTM) with a 2240 kW motor treating the VTM cyclone underflow to achieve the required milling rate and grind size. Additional simulation work showed a reduction in grind size at P80 122 µm is achievable with the VTM-4500-C unit at 3016 kW motor power. Closed and Open circuit VTM configurations are shown in Figures 6 and 7 respectively:

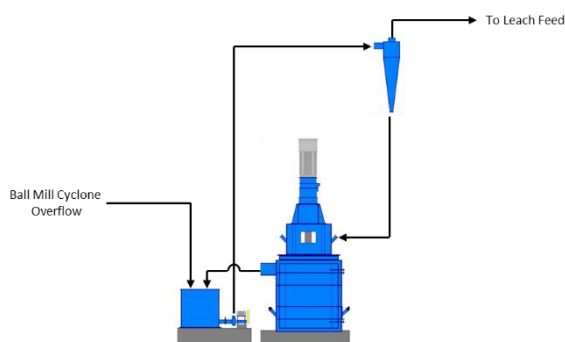


Figure 6 - VTM closed circuit

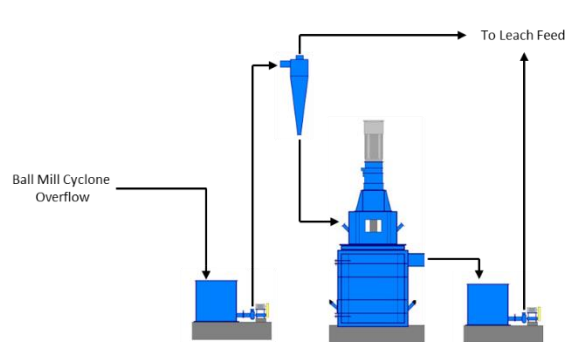


Figure 7 –VTM open circuit

DESIGN AND CONSTRUCTION

Ausenco Detail Engineering and Design

Ausenco was engaged to conduct front end engineering design (FEED) and detailed engineering including design of the tertiary grinding circuit commencing in June 2020 with an estimated completion period of six months. Key deliverables included:

- Project and engineering design of the process facilities, plant services /equipment and supporting infrastructure.
- Procurement package on equipment and bulk supply and materials.
- Issue for construction material take-offs, equipment list and all engineering discipline (earthworks, concrete, mechanical and electrical).
- Provide OPEX and CAPEX cost estimates on the vertical mill expansion circuit.

The Martabe team reviewed other available stirred milling technologies. There were other inherent between the alternate technologies and the Metso machine. The Metso VTM utilises a magnetic lining rather than a grid liner, utilises a top feed system rather than a pumped bottom fed system, and utilises a bolted segment design rather than welded segments. In addition to the differences in the features, the VTM had several mills of this sizes already in operation and was able to offer a large enough mill for the application in a single unit. Given such options, the team at Martabe selected the Metso design. There were six VTM-4500-C units installed at the time of the evaluation but none in a location easily accessible for the Martabe team.

The Metso VTM-4500-C with a 3350 kW motor was selected as the preferred model as opposed to the 2230 kW, VTM-3000-WB. The immediate target throughput for the upgrade was 825 t/h, up from 730 t/h, which required approximately 1500 kW. After this expansion there would be no further potential for expansion due to the lack of footprint. To ensure the maximal return, the mill selection was not based on the short-term capacity target but rather long-term target of 950 t/h with the intention being to upgrade other sections of the plant as bottlenecks shift from ball milling to SAG milling, crushing, or leaching and detox.

In addition to future throughput increases, the possible transition to sulfide ore and the need for flotation may require a finer grind so the extra grinding power could prove beneficial to flotation performance. The incremental increase in equipment cost for the upgraded unit was sensible as well as the 150% increase in power only came at about a 10-15% increase in equipment cost and minimal increases to the overall installed cost. Finally, there was an existing VTM-4500-C from a previous cancelled project available for Martabe. Although some refurbishment was required, the availability of this existing unit minimised the lead time and improved project net present value.

The process design criteria for the Vertimill was based on achieving 825 t/h (nominal) throughput with the VTM-4500-C unit in closed circuit with the regrind cyclones at a maximum recirculating load of 200% and a leach feed density at 50% solids w/w. Forged carbon steel balls with a seasoned charge and 25 mm top size were specified for the initial charge and a media wear rate of 85 g/kW h was used as for budgeting and CAPEX/OPEX estimation purposes.

General arrangement of the proposed upgraded secondary milling circuit is shown in Figure 8.



Figure 8 - General Arrangement of Vertimill Circuit

The following existing key plant equipment had to be upgraded to accommodate the increase in mill throughput rates:

- Cyclone Feed Pumps – replaced Krebs MillMax 16/14-39 MMD 750 kW with 450 M150 MCR 900 kW
- Leach Feed Pumps – replaced 12/10 Warman EE-M 150 kW replaced with 12/10 Warman F-M 260 kW
- Vertimill circuit Process Water Pump – New ISO Pro 200x140 75 kW Southern Cross
- New high voltage switchgear, transformer, motor control centre, and switch room.
- New overhead 11 kV high voltage power line and substation

To save in CAPEX the replaced cyclone feed pumps Krebs Millmax 16/14-39 MMD 750 kW were used in the regrind cyclone feed pumps application along with its electrical drives and VVVF. The estimated OPEX for the Vertimill circuit was at \$0.65/t. Table 2 shows a summary of those costs.

Table 2 - OPEX Breakdown Vertimill

Summary Vertimill OPEX	
Description	Unit Cost (\$/t)
Labour	-
Reagents & Consumables	0.20
Power	0.36
Maintenance Materials	0.09
Total	0.65

Note:

- 1) Labour cost – no additional operators required
- 2) Based on mill rate 825 t/h

- 3) Mill operating time is 93%

The Martabe project team carried out the tendering, procurement and expediting services for the project. At completion, total project cost was under budget by approximately 8%.

Major equipment packages with long lead periods such as the mill, pumps, cyclones and electrical equipment were finalised by November 2020. Major construction packages ready for Issue For Construction (IFC) were finalised by November 2020.

Construction and Commissioning

Construction of the expansion plant commenced in January 2021 and was completed by December 2021 inclusive of commissioning. There was a two-month delay in the schedule due to temporary work interruption caused by COVID-19 restrictions.

Through the course of the project there were several challenges with mill construction. Metso provided on-site support with local field service engineering resources but supervisory level support was only available remotely from Metso USA. Minor fit issues proved difficult to solve as remote communication of issues proved challenging and COVID restrictions made rapid procurement of tools extremely challenging.

The scope of the project also expanded as the project progressed. When adding new gland seal water lines for the new pumps, issues with existing system were discovered. The gland water supply and pressure were low due to scaling of delivery lines. Several lines had to be replaced entirely and, eventually, it was decided to upgrade the gland water pump to provide additional pressure and flow. These seal water delivery issues led to delays in commissioning of several slurry pumps.

Dry commissioning was relatively smooth with the main challenge being integration of PLC and SCADA programming between the existing Martabe system and the new expansion system. Due to COVID restrictions, the overseas design engineers were unable to reach site for commissioning. A local commissioning PLC systems engineer was engaged, which took significant time and effort for familiarisation with the system. Once the PLC SCADA issues were resolved, water commissioning proceeded well and took approximately 7 days to complete. Figure 9 shows the milling circuit nearing its completion.



Figure 9 - VTM-4500-C circuit during construction

Slurry commissioning was completed in the first week of December 2021 with all equipment performing as per design. The circuit ramped up to normal milling rates over the following several weeks to ensure any newly identified plant bottlenecks would not present a problem. There were several minor punch-list items still being resolved during the handover with site’s operations team. Local Metso mechanical, electrical, and commissioning technical support was available onsite, providing guidance on construction and mill operation staff throughout the commissioning process.

The standby primary cyclone feed pump and leach feed pumps commenced its change over and upgrade shortly after successful operation of the Vertimill circuit. Good pump maintenance and planning allowed no interruptions or stoppages during the transition period whilst the circuit was in preparation for the upgrade with only the duty pump in operation. Full performance testing of the Vertimill whereby the tonnage and power draw will be ramped up to maximum capacity will be conducted in the future as other main bottlenecks within the plant are resolved (crusher capacity and CIL volumetric flow rate).

OPERATIONAL EXPERIENCES

Initial Ramp-up and Performance Testing

The initial ramp-up phase for the project progressed from December 2021 through February 2022 with the first round of performance testing in the middle of February. The initial ramp up in throughput occurred over two to three weeks with daily increases to throughput. Through that process there were several days where production had to be limited due to downstream constraints. Figure 10 shows the immediate impact on product sizing. After achieving the 825 t/h target throughput, the product from the mill remained significantly finer than the target of 80% passing 150 µm so target mill operating power target was reduced. As mill power has reduced, the circulating load has gradually increased with minimal impact on P80 indicating the product curve from the mill has not only gotten finer but also sharper with less ultrafine material.

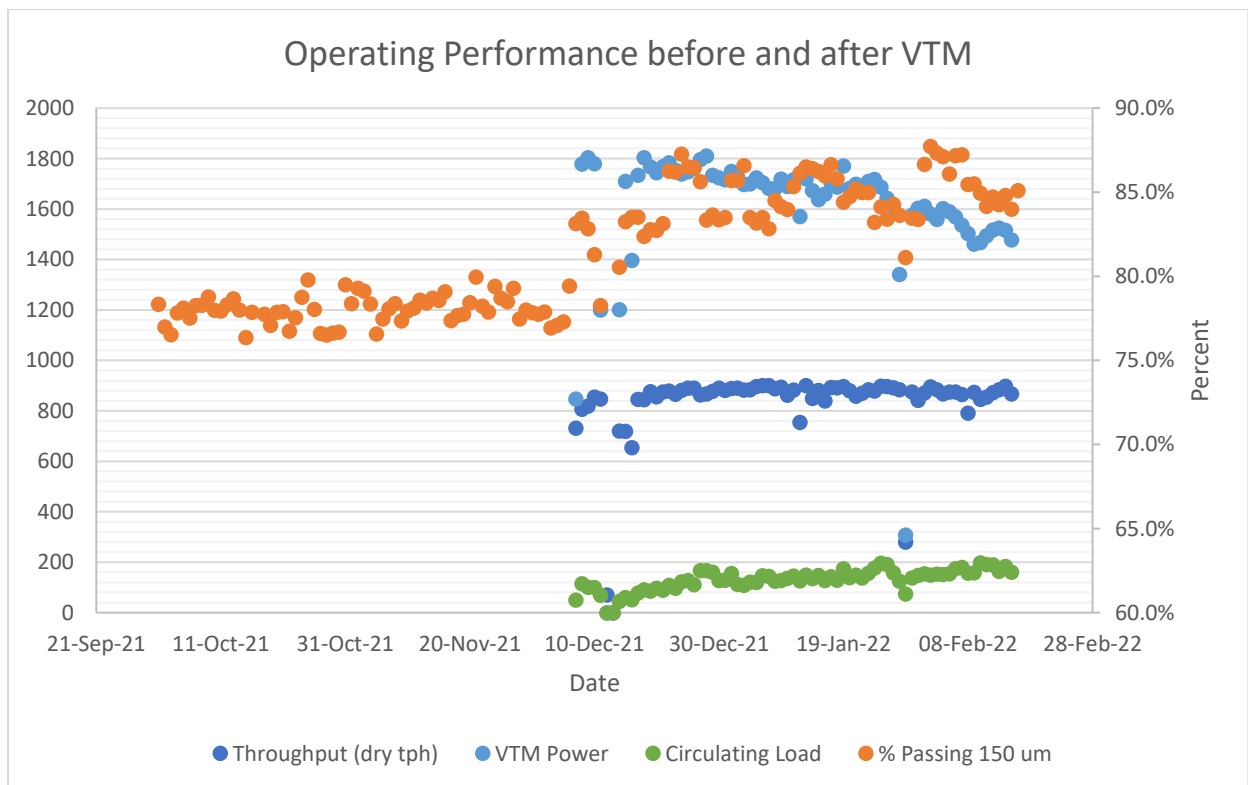


Figure 10 - Impact of Vertimill start-up on product fineness

In terms of circuit qualitative performance, early observations from the mill start-up showed significant improvement in the trash screen performance. Previously, coarse ore was continually reporting to trash screen oversize, causing issues in the inter-tank screens in the leaching area, and causing issues with resin separation and premature wear in the RECYN cyanide recovery system on site. With the start-up of the new mill, these issues disappeared almost instantaneously providing a general improvement in the operability of the plant.

In February 2022 performance testing was performed on the mill to determine the milling efficiency and compare to the original design parameters. The plant was able to operate with stability at 825 t/h so the decision was made to proceed with a two-hour sampling campaign of the milling circuit. Composite samples were collected at 20-minute intervals during the period. Samples were collected for the ball mill hydrocyclone overflow, Vertimill discharge, and Vertimill hydrocyclone feed, overflow, and underflow. For Vertimill hydrocyclone feed samples, one of the overflow pipes from the hydrocyclones was removed prior to the survey period and blanked so that when the feed valve was opened 100% of the material discharged from the cyclone underflow. At the completion of the survey period, the feed belt was stopped, and a belt cut was taken in order to perform a Bond Ball Mill Work Index.

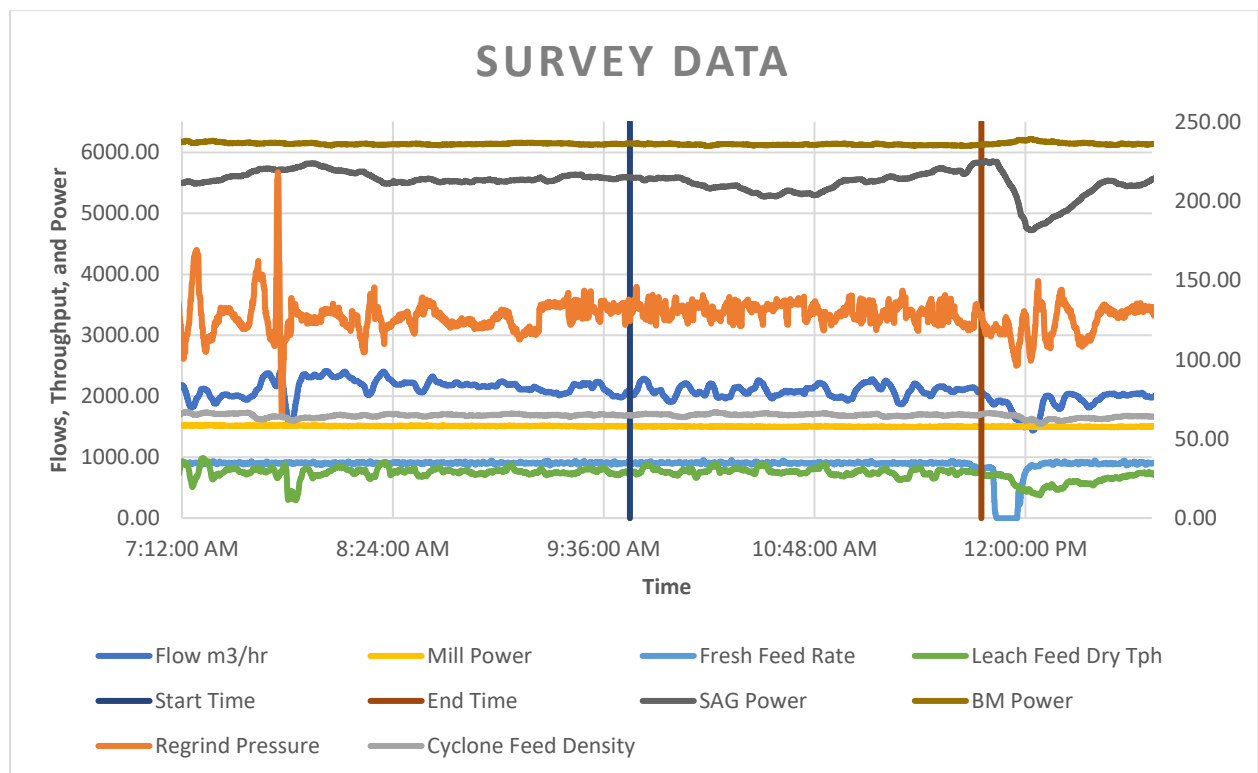


Figure 11 - Vertical mill circuit performance data

Figure 11 shows the operating data for the circuit during the survey period. Mill powers, solids densities, and slurry flows were quite steady during the period. Table 3 shows the average values and standard deviations for the circuit performance data during the survey period.

Table 3 - Circuit key performance data during survey

Stream	Ball Mill Power kW	SAG Mill Power kW	SAG Milling Water m3/h	Total Milling Water m3/h	Wet Plant Feed t/h	Dry plant feed t/h	Leach Feed Flow m3/h	Leach Feed Density %	Leach Feed t/h
Average	6126.27	5511.31	205.22	644.12	902.49	838.23	1014.64	51.15	757.23
Standard Deviation	9.77	135.97	3.51	7.87	16.46	15.29	64.62	1.70	49.88
% of Average	0	2	2	1	2	2	6	3	7
Stream	VTH Cyc Feed Flow m3/h	Vertimill Power kW	VTH Cyc Feed Pump Speed %	VTH Cyc Feed Sump Level %	BM Cyc Feed Pressure kPa	VTH Cyc Feed Pressure kPa	VTH Cyc Feed Density % Solids w/w	VTH Cyc Feed Sump Dilution water m3/h	Leach Feed Water m3/h
Average	2091.72	1502.19	85.08	64.98	86.29	130.38	65.24	30.01	730.42
Standard Deviation	90.13	4.38	0.72	1.27	9.32	5.04	0.57	0.24	53.05
% of Average	4	0	1	2	11	4	1	1	7

Samples were analysed for percent solids and particle size. Particle sizes and material flows from the operating data were then combined and balanced. Figure 12 shows the raw and balanced particle size distributions.

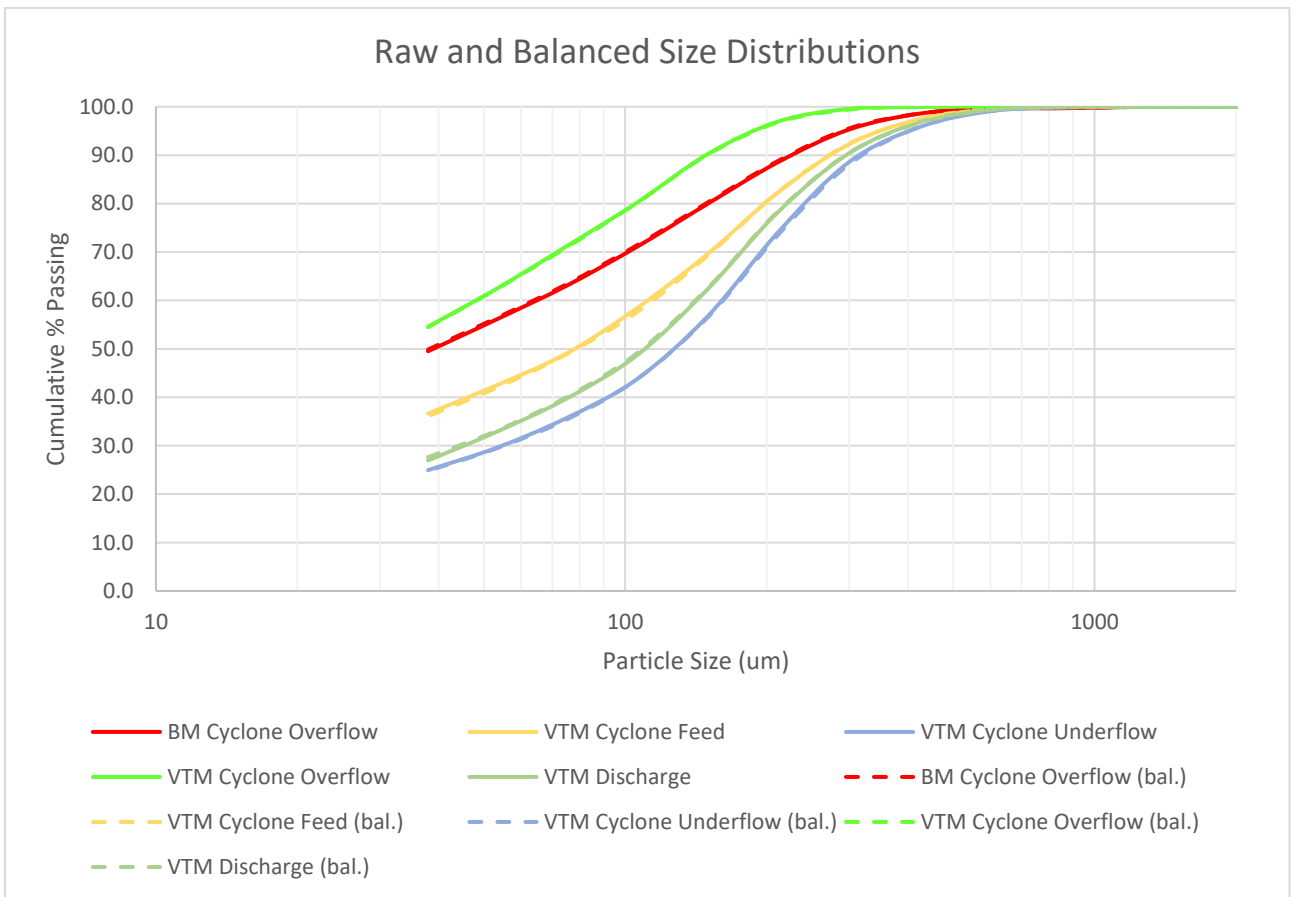


Figure 12 - Mass balanced particle size distributions from Vertimill circuit

The SAG feed sample was sent to a metallurgical testing laboratory in Jakarta to perform a Bond Ball Mill Work Index test. The results are summarised in Table 4. The ore being processed through the plant proved to be softer than the ore treated during the 2019 survey. The mine plan indicated roughly similar ore for the coming weeks so in lieu of postponing performance testing, it was decided that performance testing would proceed but with the performance parameters adjusted based upon the ore characteristics of the material processed during the survey.

Table 4 - Results of Bond Ball Mill Work Index test

Sample Name	JK BBM Data					
	Aperture μm	F80 μm	P80 μm	Grindability g/rev	Work Index (Wi) kWh/t	Mib
Martabe VTM Performance Testing 2022-02-14	212	2422	171	1.596	15.3	17.5
Martabe VTM Performance Testing 2022-02-14 Dup	150	2442	106	1.357	15.0	18.9

The mill is operating in a tertiary grinding stage treating whole ore and was designed using the Bond Ball Mill Work Index approach to equipment selection. The sizing approach uses the Rowland Modified Bond (Rowland, 1980) approach to estimating the required specific energy for a ball mill application then applying an additional Vertimill Efficiency Factor to estimate the required power for a Vertimill in the application. The throughput and feed size used in the calculation were estimated by utilising a phantom cyclone with an assumed hydrocyclone efficiency and assumed feed and product distributions. Table 5 shows a summary of the calculated energy requirements. The original design calculations included a safety factor but the analysis of the operating data does not.

Of critical import is whether the approach to design compares well with the operating data. Utilising the same methodology as in the design step but with the operating mill data, the Vertimill efficiency factor should be 0.714. The Vertimill Efficiency factor estimated from the operating data was 0.717 indicating the parameters used in the design methodology accurately reflect operating performance.

Table 5: Summary of milling efficiency calculations

	Original Design	Feb 2022 With Design	Feb 2022 Actual Operating
Material	Whole Ore	Whole Ore	Whole Ore
Stage	Tertiary	Tertiary	Tertiary
Mill Type	VTM	VTM	VTM
Throughput (t/h)	825.0	830.3	830.3
F80 (µm)	180	148.59	148.59
P80 (µm)	150	105	105
Work Index (kWh/t)	17.1	15	15
Classifier Efficiency (%)	55%	61%	61%
Estimated Bypass (%)	49.14	49.96	49.96
F80 adj (µm)	209	192	192
Corrected Feed Rate (t/h)	419.6	415.5	415.5
Reduction Ratio	1.4	1.8	1.8
Safety Factor	1.12	1	1
EF7	2.00	1.28	1.28
VTM Efficiency Factor	0.75	0.714	0.717
Uncorrected Bond Specific Energy (kWh/t)	2.15	3.79	3.79
Corrected Specific Energy (kWh/t)	3.62	3.45	3.46
Grinding Process Power Required (kW)	1517	1434	1439
Drivetrain Losses (%)	5.0	4.1	4.1
Operating Motor Power (kW)	1597	1496	1501
Percent of VTM-4500-C Motor Power Used (%)	47.6	44.6	44.7

In the original design, the expected circulating load was approximately 150% with a design maximum value of 200%. During the survey period, the circulating load was 163% so the performance was quite close to the original projections. During the survey, eight Cavex 400 mm hydrocyclones, of the 18 installed, were in operation with an operating pressure of 130 kPa. The efficiency in the target product range of 150 µm to 106 µm was 60-65% so performance was acceptable during the sampling period. The cyclones were able to achieve that efficiency operating at extremely high feed densities of 63-65% solids.

Based upon the current operational efficiency, the Vertimill will not be a bottleneck in achieving the long-term target of 950 t/h throughput.

Wear Life

Since the start-up of the mill, there has been one wear inspection and one liner change. For the Vertimill the normal approach to tracking wear is by measuring the ball charge height inside the mill and by tracking operating hours or kWh. Physical inspections of the liners are possible, but the

downtime associated with performing an inspection essentially takes the same time as doing a liner change so normally that is only done with the first liner set.

With new liners, the mill will draw full power with a media charge height of approximately 280 to 300 cm from the base plate. As the liners wear, the charge level inside the mill increases to compensate for the reduction in liner size and charge activity. As a rule of thumb, liners can be considered fully worn when the height has increased between 40-60 cm. Charge height measurements can only be considered accurate ± 10 cm because of how the charge height is affected by screw position when the mill is shut down. The charge height can only be measured when the mill is shut down and so is not measured frequently. Figure 13 shows the results of the first charge measurement performed on January 28. The height had increased by approximately 10 cm in 52 days. This initial charge measurement indicated the liners would be fully worn somewhere between May and July.

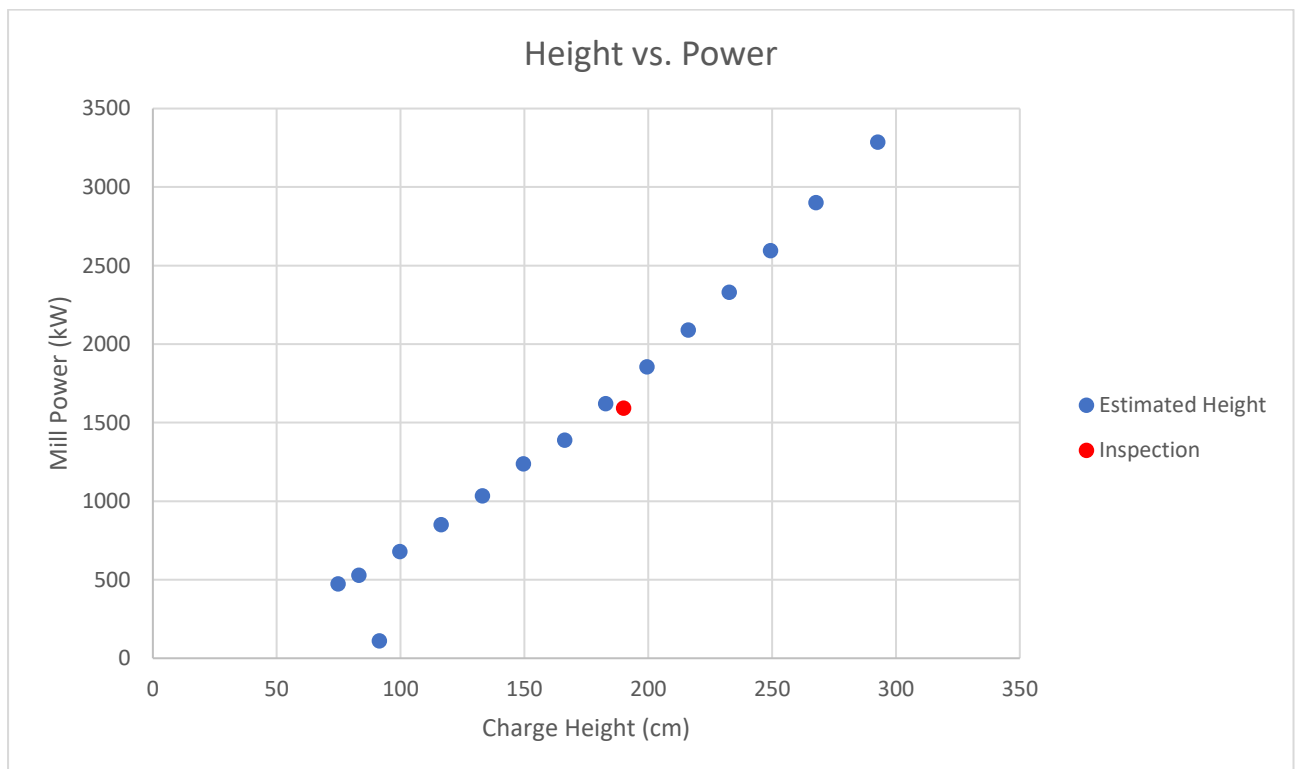


Figure 13: Initial wear measurements

To minimise downtime, shutdowns for the Vertimill were to coincide with the shutdowns for the SAG and Ball mill. The first shutdown after mill start-up was scheduled for March 9, 2022. The next shutdown was to happen in June 2022 so at the March shutdown the liners were going to be inspected with the plan to take measurements, estimate remaining life, and replace if required.

During the shutdown, the liners were inspected and found to have substantial life remaining, however the end liners had to be replaced. Figure 14 shows pictures of the worn liners and the replacement process. The wear measurements indicated that the liners would have lasted until late April into early May or roughly 3000 hours, and hence would not have lasted until the June 2022 shutdown. For the duration of the operational period, the mill was operating at relatively low power, as evidenced by the lack of wear on the upper liners. The end liner wear rate is expected to be similar when operating at full power as the end liners were fully covered. As the power target increases, the wear rate will increase on the upper liners. An improved liner design is being considered to help the site align the Vertimill shutdown with the upstream SAG mill and Ball mill shutdowns, increase Vertimill uptime, and hence overall plant performance.

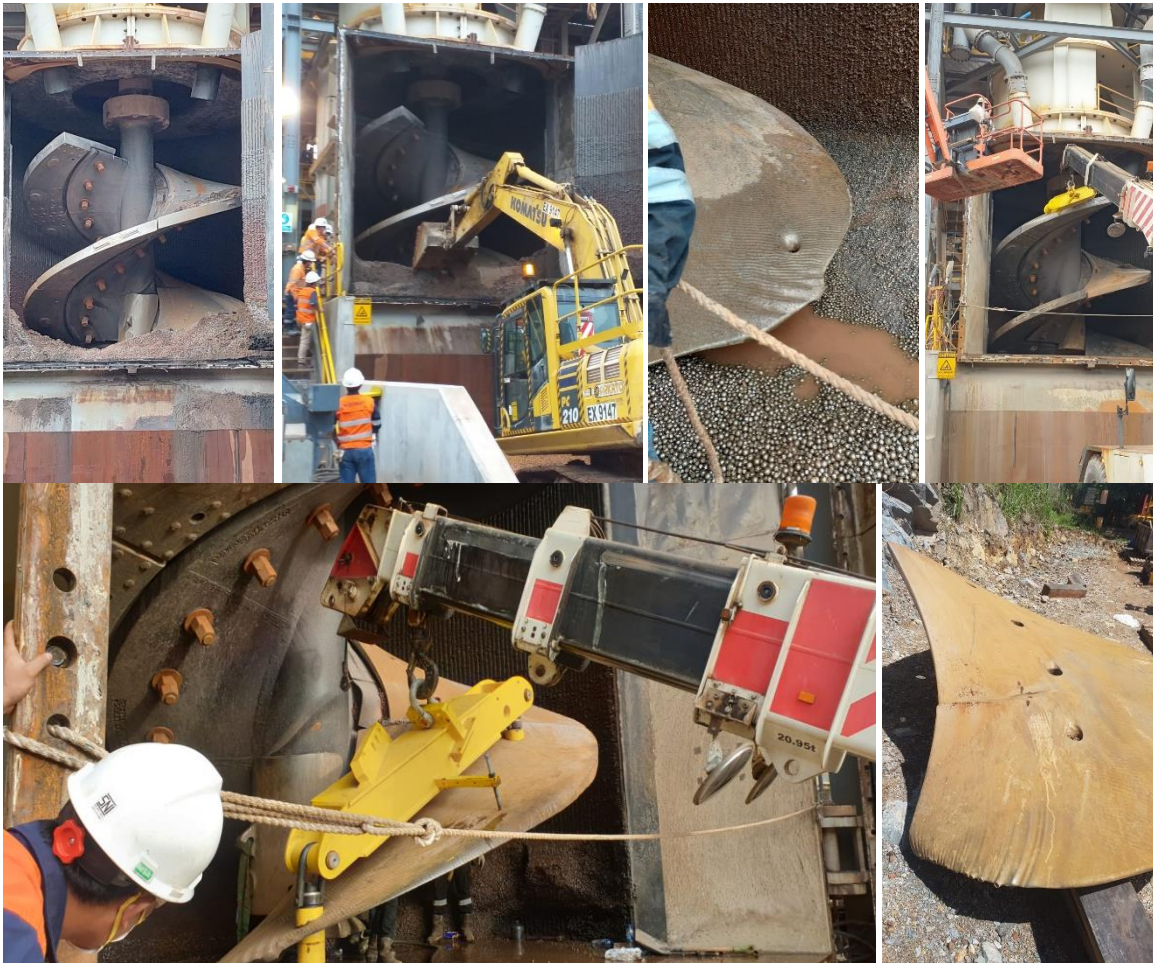


Figure 14 - Inspection and replacement of end liners

CONCLUSIONS

The execution and installation of the Vertimill VTM 4500 at Martabe gold mine was deemed to be a success as the following key objectives were met:

- Design milling throughput rate at 825 t/h was achieved at target grind size of $P_{80} 112 \mu\text{m}$.
- Well executed engineering, designing and planning despite the challenges with existing plant footprint constraints Integration with equipment and services from existing brown field plant was implemented to plan.
- Despite challenges with site access during the pandemic, the Vertimill was successfully commissioned with minimal interruptions to schedule and production.
- Operating milling unit cost has reduced by \$0.55/t. A further reduction of \$0.55/t in G&A unit cost resulting in a total reduction in unit cost of \$1.12/t is expected. This is due to the increase in milling throughput rates as a result of the Vertimill upgrade. With the reduction in unit cost \$/t an increase in ore reserves is facilitated as lower cut-off grade (previously deemed marginal) are now economically viable.

Several notable key improvements within the process plant have been noticed whilst operating the Vertimill at the finer grind:

- Significant reduction of coarse and grit material resulting in improved screening efficiency within the trash screen area. The linear screen which was installed to provide additional trash screen capacity prior to the Vertimill upgrade is now frequently unused despite the increase in volumetric flowrate.
- The trash screen bund previously received significant coarse particle carry-over but now receives almost none.
- Fineness in grind size also led to less grit particles reporting to the elution circuit and has helped with improved solution flow through both acid and elution columns with less blockages and restrictions.
- The CIL inter-tank screens are pegging less with better hydraulic and volumetric flow.
- Less grit in the circuit also improves operations of the cyanide RECYN circuit as previously the coarse grit was impeding on resin transfer and movement throughout the loading and stripping circuit.

ACKNOWLEDGEMENTS

The authors would like to acknowledge PT. Agincourt Resources for allowing the publishing of this paper. The authors would also like to acknowledge PT. Geoservices for performing the test work.

REFERENCES

Rowland C.A., Kjos D.M. Rod and Ball mills, in Mineral Processing Plant Design, SME of AIME, New York (1980), p. 239-278

